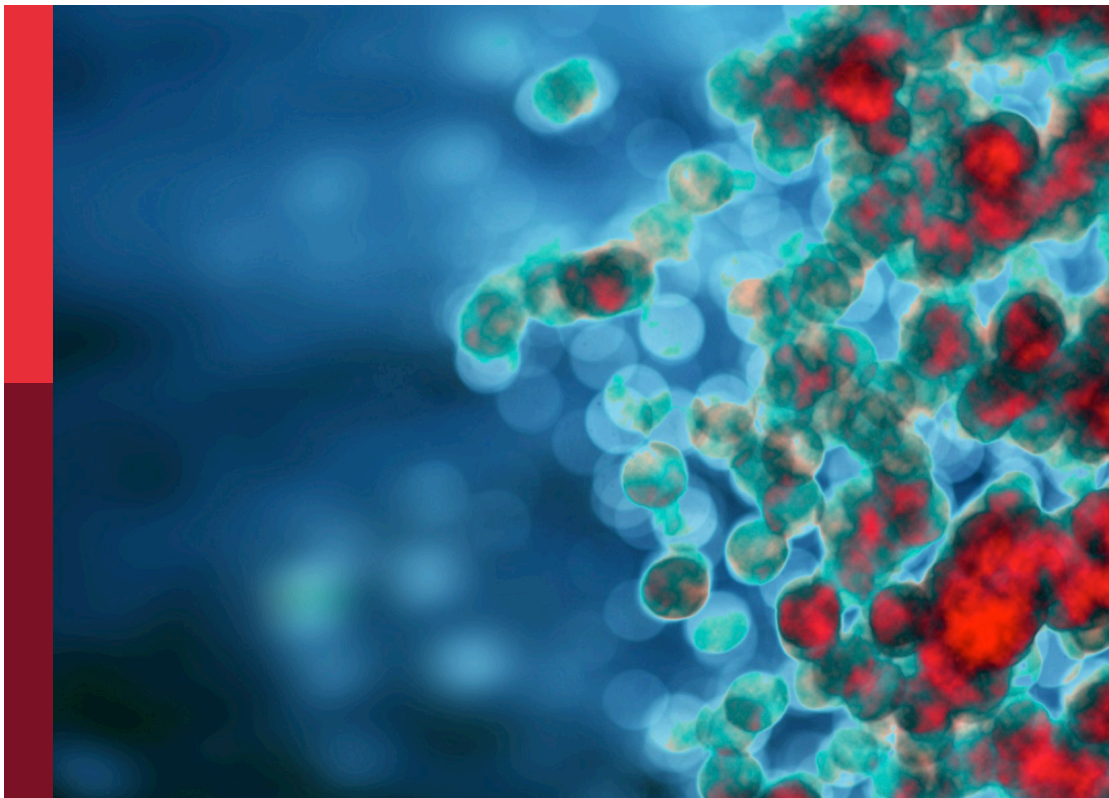
frontiers | Research Topics

Novel insights into inflammatory roles of mast cells and basophils

Edited by
Satoshi Tanaka and Frans J. Van Overveld

Published in
Frontiers in Immunology



FRONTIERS EBOOK COPYRIGHT STATEMENT

The copyright in the text of individual articles in this ebook is the property of their respective authors or their respective institutions or funders. The copyright in graphics and images within each article may be subject to copyright of other parties. In both cases this is subject to a license granted to Frontiers.

The compilation of articles constituting this ebook is the property of Frontiers.

Each article within this ebook, and the ebook itself, are published under the most recent version of the Creative Commons CC-BY licence. The version current at the date of publication of this ebook is CC-BY 4.0. If the CC-BY licence is updated, the licence granted by Frontiers is automatically updated to the new version.

When exercising any right under the CC-BY licence, Frontiers must be attributed as the original publisher of the article or ebook, as applicable.

Authors have the responsibility of ensuring that any graphics or other materials which are the property of others may be included in the CC-BY licence, but this should be checked before relying on the CC-BY licence to reproduce those materials. Any copyright notices relating to those materials must be complied with.

Copyright and source acknowledgement notices may not be removed and must be displayed in any copy, derivative work or partial copy which includes the elements in question.

All copyright, and all rights therein, are protected by national and international copyright laws. The above represents a summary only. For further information please read Frontiers' Conditions for Website Use and Copyright Statement, and the applicable CC-BY licence.

ISSN 1664-8714
ISBN 978-2-83252-121-2
DOI 10.3389/978-2-83252-121-2

About Frontiers

Frontiers is more than just an open access publisher of scholarly articles: it is a pioneering approach to the world of academia, radically improving the way scholarly research is managed. The grand vision of Frontiers is a world where all people have an equal opportunity to seek, share and generate knowledge. Frontiers provides immediate and permanent online open access to all its publications, but this alone is not enough to realize our grand goals.

Frontiers journal series

The Frontiers journal series is a multi-tier and interdisciplinary set of open-access, online journals, promising a paradigm shift from the current review, selection and dissemination processes in academic publishing. All Frontiers journals are driven by researchers for researchers; therefore, they constitute a service to the scholarly community. At the same time, the *Frontiers journal series* operates on a revolutionary invention, the tiered publishing system, initially addressing specific communities of scholars, and gradually climbing up to broader public understanding, thus serving the interests of the lay society, too.

Dedication to quality

Each Frontiers article is a landmark of the highest quality, thanks to genuinely collaborative interactions between authors and review editors, who include some of the world's best academicians. Research must be certified by peers before entering a stream of knowledge that may eventually reach the public - and shape society; therefore, Frontiers only applies the most rigorous and unbiased reviews. Frontiers revolutionizes research publishing by freely delivering the most outstanding research, evaluated with no bias from both the academic and social point of view. By applying the most advanced information technologies, Frontiers is catapulting scholarly publishing into a new generation.

What are Frontiers Research Topics?

Frontiers Research Topics are very popular trademarks of the *Frontiers journals series*: they are collections of at least ten articles, all centered on a particular subject. With their unique mix of varied contributions from Original Research to Review Articles, Frontiers Research Topics unify the most influential researchers, the latest key findings and historical advances in a hot research area.

Find out more on how to host your own Frontiers Research Topic or contribute to one as an author by contacting the Frontiers editorial office: frontiersin.org/about/contact

Novel insights into inflammatory roles of mast cells and basophils

Topic editors

Satoshi Tanaka — Kyoto Pharmaceutical University, Japan

Frans J. Van Overveld — University College Roosevelt, Netherlands

Citation

Tanaka, S., Van Overveld, F. J., eds. (2023). *Novel insights into inflammatory roles of mast cells and basophils*. Lausanne: Frontiers Media SA.

doi: 10.3389/978-2-83252-121-2

Table of contents

07 Editorial: Novel insights into inflammatory roles of mast cells and basophils
Satoshi Tanaka and Frans J. Van Overveld

09 Immunoprofiling Reveals Novel Mast Cell Receptors and the Continuous Nature of Human Lung Mast Cell Heterogeneity
Elin Rönnberg, Daryl Zhong Hao Boey, Avinash Ravindran, Jesper Säfholm, Ann-Charlotte Orre, Mamdoh Al-Ameri, Mikael Adner, Sven-Erik Dahlén, Joakim S. Dahlin and Gunnar Nilsson

19 Inhibition of Orai Channel Function Regulates Mas-Related G Protein-Coupled Receptor-Mediated Responses in Mast Cells
Shaswati Chaki, Ibrahim Alkanfari, Saptarshi Roy, Aetas Amponnawarat, Yvonne Hui, Carole A. Oskeritzian and Hydar Ali

30 Autocrine/Paracrine Loop Between SCF^{+}/c-Kit^{+} Mast Cells Promotes Cutaneous Melanoma Progression
Tiziana Annese, Roberto Tamma, Mariella Bozza, Alfredo Zito and Domenico Ribatti

41 The Inhibitory Receptor Siglec-8 Interacts With FcεRI and Globally Inhibits Intracellular Signaling in Primary Mast Cells Upon Activation
Wouter Korver, Alan Wong, Simon Gebremeskel, Gian Luca Negri, Julia Schanin, Katherine Chang, John Leung, Zachary Benet, Thuy Luu, Emily C. Brock, Kenneth Luehrsen, Alan Xu and Bradford A. Youngblood

52 A Critical Function for the Transcription Factors GLI1 and GLI2 in the Proliferation and Survival of Human Mast Cells
Guido Hernan Falduto, Annika Pfeiffer, Qunshu Zhang, Yuzhi Yin, Dean Darrel Metcalfe and Ana Olivera

69 Elastase- and LPS-Exposed Cpa3$^{Cre/+}$ and ST2$^{-/-}$ Mice Develop Unimpaired Obstructive Pulmonary Disease
Eduardo I. Cardenas, Perla A. Alvarado-Vazquez, Erika Mendez-Enriquez, Erik A. Danielsson and Jenny Hallgren

81 Ataxin-3, The Spinocerebellar Ataxia Type 3 Neurodegenerative Disorder Protein, Affects Mast Cell Functions
Anna S. Sowa, Eva Haas, Jeannette Hübener-Schmid and Axel Lorentz

91 Novel Insights Into the Immune-Regulatory Functions of Mast Cells in the Cutaneous Immune Response
Tetsuya Honda and Yuki Honda Keith

97 The Potential Role of Basophils in Urticaria
Riko Takimoto-Ito, Ni Ma, Izumi Kishimoto, Kenji Kabashima and Naotomo Kambe

102 Differential Effects of Alarmins on Human and Mouse Basophils
Adriana R. Gambardella, Remo Poto, Valentina Tirelli, John T. Schroeder, Gianni Marone, Fabrizio Mattei, Gilda Varricchi and Giovanna Schiavoni

115 Role of Basophils in a Broad Spectrum of Disorders
Kensuke Miyake, Junya Ito and Hajime Karasuyama

129 IgG Autoantibodies Against IgE from Atopic Dermatitis Can Induce the Release of Cytokines and Proinflammatory Mediators from Basophils and Mast Cells
Remo Poto, Isabella Quinti, Gianni Marone, Maurizio Taglialatela, Amato de Paulis, Vincenzo Casolaro and Gilda Varricchi

141 Uncovering the Mast Cell Response to *Mycobacterium tuberculosis*
Ivonne Torres-Atencio, Ariadne Campble, Amador Goodridge and Margarita Martin

149 Regulatory Roles of Phospholipase A_2 Enzymes and Bioactive Lipids in Mast Cell Biology
Yoshitaka Taketomi and Makoto Murakami

164 Spatiotemporal Patterns of Substance P-Bound MRGPRX2 Reveal a Novel Connection Between Macropinosome Resolution and Secretory Granule Regeneration in Mast Cells
Pia Lazki-Hagenbach, Elisabeth Kleeblatt, Hydar Ali and Ronit Sagi-Eisenberg

177 CT-M8 Mice: A New Mouse Model Demonstrates That Basophils Have a Nonredundant Role in Lupus-Like Disease Development
John Tchen, Quentin Simon, Léa Chapart, Christophe Pellefigues, Hajime Karasuyama, Kensuke Miyake, Ulrich Blank, Marc Benhamou, Eric Daugas and Nicolas Charles

189 Immunological Changes of Basophil Hyperreactivity to Sweat in Patients With Well-Controlled Atopic Dermatitis
Tomofumi Numata, Shunsuke Takahagi, Kaori Ishii, Satoshi Morioke, Takanobu Kan, Hayato Mizuno, Yuhki Yanase, Tomoko Kawaguchi, Akio Tanaka and Michihiro Hide

197 Mast Cell and Basophil Granule Proteases - *In Vivo* Targets and Function
Lars Hellman, Srinivas Akula, Zhirong Fu and Sara Wernersson

213 Allergen-Specific IgA Antibodies Block IgE-Mediated Activation of Mast Cells and Basophils
Yasmeen S. El Ansari, Cynthia Kanagaratham, Oliver T. Burton, Jenna V. Santos, Brianna-Marie A. Hollister, Owen L. Lewis, Harald Renz and Hans C. Oettgen

224 Roles of Mast Cells in Cutaneous Diseases
Takafumi Numata, Kazutoshi Harada and Susumu Nakae

236 STAT3 gain-of-function is not responsible for low total IgE levels in patients with autoimmune chronic spontaneous urticaria
Merle Sauer, Jörg Scheffel, Stefan Frischbutter, Niklas Mahnke, Marcus Maurer, Thomas Burmeister, Karoline Krause and Martin Metz

243 Development of mouse model for oral allergy syndrome to identify IgE cross-reactive pollen and food allergens: ragweed pollen cross-reacts with fennel and black pepper
Anna Kamei, Kumi Izawa, Tomoaki Ando, Ayako Kaitani, Risa Yamamoto, Akie Maehara, Takuma Ide, Hiromichi Yamada, Mayuki Kojima, Hexing Wang, Koji Tokushige, Nobuhiro Nakano, Toshiaki Shimizu, Hideoki Ogawa, Ko Okumura and Jiro Kitaura

258 The Number of MRGPRX2-Expressing Cells Is Increased in Skin Lesions of Patients With Indolent Systemic Mastocytosis, But Is Not Linked to Symptom Severity
Polina Pyatilova, Tameem Ashry, Yanyan Luo, Jiajun He, Hanna Bonnekoh, Qingqing Jiao, Sherezade Moñino-Romero, Man Hu, Jörg Scheffel, Stefan Frischbutter, Maud A. W. Hermans, Bradford A. Youngblood, Marcus Maurer, Frank Siebenhaar and Pavel Kolkhir

267 Evidence for histamine release in chronic inducible urticaria – A systematic review
Kanokvalai Kulthanan, Martin K. Church, Eva Maria Grekowitz, Tomasz Hawro, Lea Alice Kiefer, Kanyalak Munprom, Yanisorn Nanchaipruek, Chuda Rujitharanawong, Dorothea Terhorst-Molawi and Marcus Maurer

277 Mast cell tissue heterogeneity and specificity of immune cell recruitment
Peter W. West and Silvia Bulfone-Paus

288 Dynamically upregulated mast cell CPA3 patterns in chronic obstructive pulmonary disease and idiopathic pulmonary fibrosis
Premkumar Siddhuraj, Jimmie Jönsson, Manar Alyamani, Pavan Prabhala, Mattias Magnusson, Sandra Lindstedt and Jonas S. Erjefält

306 Multifunctional regulation of VAMP3 in exocytic and endocytic pathways of RBL-2H3 cells
Satomi Mishima, Marin Sakamoto, Hikaru Kioka, Yuka Nagata and Ryo Suzuki

320 Mast cells and tryptase are linked to itch and disease severity in mycosis fungoides: Results of a pilot study
Dorothea Terhorst-Molawi, Katharina Lohse, Katharina Ginter, Viktoria Puhl, Martin Metz, Man Hu, Marcus Maurer and Sabine Altrichter

330 Utilizing mast cells in a positive manner to overcome inflammatory and allergic diseases
Zhongwei Zhang, Peter B. Ernst, Hiroshi Kiyono and Yosuke Kurashima

343 The exon-skipping oligonucleotide, KitStop, depletes tissue-resident mast cells *in vivo* to ameliorate anaphylaxis
Barry A. Hedgespeth, Douglas B. Snider, Katie J. Bitting and Glenn Cruse

frontiers | Frontiers in Immunology

TYPE Editorial
PUBLISHED 24 March 2023
DOI 10.3389/fimmu.2023.1186264

Check for updates

OPEN ACCESS

EDITED AND REVIEWED BY
Pietro Ghezzi,
University of Urbino Carlo Bo, Italy

*CORRESPONDENCE
Satoshi Tanaka
tanaka-s@mb.kyoto-phu.ac.jp

SPECIALTY SECTION
This article was submitted to Inflammation, a section of the journal Frontiers in Immunology

RECEIVED 14 March 2023
ACCEPTED 20 March 2023
PUBLISHED 24 March 2023

CITATION
Tanaka S and Van Overveld FJ (2023) Editorial: Novel insights into inflammatory roles of mast cells and basophils. *Front. Immunol.* 14:1186264. doi: 10.3389/fimmu.2023.1186264

COPYRIGHT
© 2023 Tanaka and Van Overveld. This is an open-access article distributed under the terms of the Creative Commons Attribution License (CC BY). The use, distribution or reproduction in other forums is permitted, provided the original author(s) and the copyright owner(s) are credited and that the original publication in this journal is cited, in accordance with accepted academic practice. No use, distribution or reproduction is permitted which does not comply with these terms.

Editorial: Novel insights into inflammatory roles of mast cells and basophils

Satoshi Tanaka[1]* and Frans J. Van Overveld[2]

[1]Department of Pharmacology, Division of Pathological Sciences, Kyoto Pharmaceutical University, Kyoto, Japan, [2]Department of Science, University College Roosevelt, Middelburg, Netherlands

KEYWORDS

mast cell, basophil, inflammation, urticaria, IgE, c-kit, atopic dermatitis

Editorial on the Research Topic
Novel insights into inflammatory roles of mast cells and basophils

Mast cells and basophils share some phenotypic characteristics, such as the expression of a high-affinity membrane receptor for IgE, FcεRI, and the granule storage of inflammatory mediators including histamine. Mast cells are found to be resident in nearly all vascularized tissues, whereas basophils migrate into the inflamed tissues from the circulation.

Accumulating evidence suggests that cutaneous mast cells play critical roles in chronic spontaneous urticaria (CSU) and that there are several promising therapeutic approaches (1). Sauer et al. verified the involvement of STAT3 in type IIb autoimmune CSU. The roles of histamine in chronic inducible urticaria were reviewed by Kulthanan et al., Takimoto-Ito et al. reported a case in which activated basophils remained in circulation during treatment with omalizumab. Miyake et al. summarized recent findings of human and murine basophils, including their roles in immune tolerance. The regulatory roles of mast cells were also discussed by Zhang et al. and Honda and Honda Keith. Poto et al. and Numata et al. investigated, respectively, the actions of autoantibodies against IgE and sweat antigen-induced chronic activation of basophils in patients with atopic dermatitis. Kamei et al. demonstrated an IgE-dependent murine model of oral allergy syndrome. El Ansari et al. found that allergen-specific IgA could suppress the IgE-mediated activation of mast cells.

MRGPRX2 has received attention as a novel therapeutic target of chronic urticaria and drug-induced anaphylaxis, because its agonists have been found to have a structural diversity (2) (McNeil). In this topic, signal transduction and regulation of intracellular localization of MRGPRX2 were investigated (Chaki et al.; Lazki-Hagenbach et al.). West and Bulfone-Paus discussed the heterogeneity of tissue mast cells, with special attention given to the expression of MRGPRX2. Numata et al. summarized the roles of mast cells in cutaneous diseases. In indolent systemic mastocytosis, an increased number of mast cells expressing MRGPRX2 was found in the skin but was not linked to symptom severity (Pyatilova et al.).

Mast cells have also been found to play important roles in allergic asthma and COPD (3). Rönnberg et al. characterized human lung mast cell populations with a novel approach. Cardenas et al. and Gambardella et al. investigated the effects of alarmins, including IL-33,

on mast cells and basophils. Siddhuraj et al. demonstrated the upregulation of CPA3 in lung mast cells upon chronic inflammation. Hellman et al. summarized the *in vivo* functions of mast cell/basophil granule proteases including CPA3. Torres-Atencio et al. reviewed the roles of mast cells in Mycobacterium tuberculosis infection.

Annese et al. and Terhorst-Molawi et al. investigated the roles of mast cells during tumor progression. The proliferation and functions of mast cells are regulated by various factors, including transcription factors, enzymes, and membrane proteins (Sowa et al.; Falduto et al.; Teketomi et al.; Korver et al.; Mishima et al.). Novel murine experimental models for the depletion of mast cells and basophils were also introduced here (Tchen et al.; Hedgespeth et al.).

We hope that this topic encourages and accelerates the research of mast cells and basophils.

Author contributions

All authors listed have made a substantial, direct, and intellectual contribution to the work and approved it for publication.

Acknowledgments

We wish to convey our appreciation to all the authors who have participated in this Research Topic and all the reviewers for their insightful comments.

Conflict of interest

The authors declare that the research was conducted in the absence of any commercial or financial relationships that could be construed as a potential conflict of interest.

Publisher's note

All claims expressed in this article are solely those of the authors and do not necessarily represent those of their affiliated organizations, or those of the publisher, the editors and the reviewers. Any product that may be evaluated in this article, or claim that may be made by its manufacturer, is not guaranteed or endorsed by the publisher.

References

1. Kaplan A, Lebwohl M, Giménez-Arnau A, Hide M, Armstrong AW, Maurer M. Chronic spontaneous urticaria: Focus on pathophysiology to unlock treatment advances. *Allergy*. (2022) 78:389–401. doi: 10.1111/all.15603

2. Kühn H, Kolkhir P, Babina M, Düll M, Frischbutter S, Fok JS, et al. Mas-related G protein-coupled receptor X2 and its activators in dermatologic allergies. *J Allergy Clin Immunol* (2021) 147:456–69. doi: 10.1016/j.jaci.2020.08.027

3. Virk H, Arthur G, Bradding P. Mast cells and their activation in lung disease. *Transl Res* (2016) 174:60–76. doi: 10.1016/j.trsl.2016.01.005

frontiers in Immunology

ORIGINAL RESEARCH
published: 04 January 2022
doi: 10.3389/fimmu.2021.804812

Immunoprofiling Reveals Novel Mast Cell Receptors and the Continuous Nature of Human Lung Mast Cell Heterogeneity

Elin Rönnberg[1,2], Daryl Zhong Hao Boey[1,2], Avinash Ravindran[1,2], Jesper Säfholm[2,3], Ann-Charlotte Orre[4], Mamdoh Al-Ameri[4], Mikael Adner[2,3], Sven-Erik Dahlén[2,3], Joakim S. Dahlin[1,2] and Gunnar Nilsson[1,2,5]**

[1] Division of Immunology and Allergy, Department of Medicine Solna, Karolinska Institutet, and Karolinska University Hospital, Clinical Immunology and Transfusion Medicine, Stockholm, Sweden, [2] Centre for Allergy Research, Karolinska Institutet, Stockholm, Sweden, [3] Unit for Experimental Asthma and Allergy Research, The Institute of Environmental Medicine, Karolinska Institutet, Stockholm, Sweden, [4] Thoracic Surgery, Department of Molecular Medicine and Surgery, Karolinska Institutet, and Karolinska University Hospital, Stockholm, Sweden, [5] Department of Medical Sciences, Uppsala University, Uppsala, Sweden

OPEN ACCESS

Edited by:
Frans J. Van Overveld, University College Roosevelt, Netherlands

Reviewed by:
Laura Sánchez-Muñoz, Servicio de Salud de Castilla La Mancha, Spain
Timotheus You Fu Halim, University of Cambridge, United Kingdom

***Correspondence:**
Gunnar Nilsson
gunnar.p.nilsson@ki.se
Elin Rönnberg
elin.ronnberg.hockerlind@ki.se

Specialty section:
This article was submitted to Inflammation, a section of the journal Frontiers in Immunology

Received: 29 October 2021
Accepted: 06 December 2021
Published: 04 January 2022

Citation:
Rönnberg E, Boey DZH, Ravindran A, Säfholm J, Orre A-C, Al-Ameri M, Adner M, Dahlén S-E, Dahlin JS and Nilsson G (2022) Immunoprofiling Reveals Novel Mast Cell Receptors and the Continuous Nature of Human Lung Mast Cell Heterogeneity. Front. Immunol. 12:804812. doi: 10.3389/fimmu.2021.804812

Background: Immunohistochemical analysis of granule-associated proteases has revealed that human lung mast cells constitute a heterogeneous population of cells, with distinct subpopulations identified. However, a systematic and comprehensive analysis of cell-surface markers to study human lung mast cell heterogeneity has yet to be performed.

Methods: Human lung mast cells were obtained from lung lobectomies, and the expression of 332 cell-surface markers was analyzed using flow cytometry and the LEGENDScreen™ kit. Markers that exhibited high variance were selected for additional analyses to reveal whether they were correlated and whether discrete mast cell subpopulations were discernable.

Results: We identified the expression of 102 surface markers on human lung mast cells, 23 previously not described on mast cells, of which several showed high continuous variation in their expression. Six of these markers were correlated: SUSD2, CD49a, CD326, CD34, CD66 and HLA-DR. The expression of these markers was also correlated with the size and granularity of mast cells. However, no marker produced an expression profile consistent with a bi- or multimodal distribution.

Conclusions: LEGENDScreen analysis identified more than 100 cell-surface markers on mast cells, including 23 that, to the best of our knowledge, have not been previously described on human mast cells. The comprehensive expression profiling of the 332 surface markers did not identify distinct mast cell subpopulations. Instead, we demonstrate the continuous nature of human lung mast cell heterogeneity.

Keywords: human lung mast cells, heterogenity, chymase (CMA1), carboxypeptidase A3 (CPA3), SUSD2, CD38, FcεRI

INTRODUCTION

Heterogeneity among mast cells has been known for a long time and was first attributed to differential expression of proteoglycans in rodent mast cells, which gave them distinct staining patterns (1). This led to the division of rodent mast cells into connective tissue mast cells and mucosal mast cells. In humans, mast cell heterogeneity has been based on the expression of mast cell proteases, i.e., cells expressing tryptase only (MC_T) and those expressing both tryptase and chymase (MC_{TC}) as well as carboxypeptidase A (2, 3). These subtypes have been defined using immunohistochemistry, a method that produced binary results, that is, the absence or presence of expression. The MC_{TC} subtype is more predominant in connective tissues such as the skin, while the MC_T subset is more prevalent in mucosal surfaces such as the airways and gastrointestinal tract (4).

Mast cells are found in the human lungs in all different compartments, i.e., under the epithelium, in smooth muscle bundles, around pulmonary vessels, in the parenchyma and in close proximity to sensory nerves (5). Human lung mast cells (HLMCs) have several important functions in health and diseases, such as host defense, induction of acute inflammatory responses, vascular regulation, bronchoconstriction and tissue remodeling (6–9). The heterogeneity of HLMCs was first suggested to be related to differences in their size and function (10), where a heterogeneity in the response to secretagogues also was reported (11). It was described that the protease expression within HLMCs differ, with the MC_T being the predominant subtype except around pulmonary vessels, where the MC_T and MC_{TC} subtypes are found in equal numbers (2). However, the heterogeneity among HLMCs goes beyond size and protease expression, as demonstrated by the differential expression of certain mast cell-related markers (FcεRI, IL-9R, 5-LO, LTC_4S, etc.) among the MC_T and MC_{TC} populations in different lung compartments (12).

Mast cell heterogeneity has primarily been studied in a binary manner using immunohistochemistry, describing the absence or presence of a given marker. Here, we used a quantitative flow cytometry-based approach to study HLMC heterogeneity, profiling the expression of 332 surface markers and intracellular staining of the proteases tryptase, chymase and CPA3. None of these markers distinctly divided the HLMCs studied into subpopulations. However, several markers showed a high degree of variation within the mast cell population with a nonclustered gradient expression pattern. Six of these markers correlated with each other, revealing the continuous nature of HLMC heterogeneity rather than separation into distinct subpopulations.

MATERIALS AND METHODS

Ethical Approval

The local ethics committee approved the collection of lung tissue from patients undergoing lobectomy, and all patients provided informed consent (Regionala Etikprövningsnämnden Stockholm, 2010/181-31/2).

Cell Preparation

Single-cell suspensions were obtained from macroscopically healthy human lung tissue as previously described (13). Briefly, human lung tissue was cut into small pieces and enzymatically digested for 45 min with DNase I and collagenase. Thereafter, the tissue was mechanically disrupted by plunging through a syringe, the cells were washed, and debris was removed by 30% Percoll centrifugation. After preparation, the cells were stained and analyzed by flow cytometry.

Flow Cytometry

The following antibodies were used: anti-CD45-V500 (Clone HI30, BD Biosciences, San Jose, CA, USA), anti-CD14-APC-Cy7 (clone M5E2, BioLegend, San Diego, CA, USA), anti-CD117-APC (clone 104D2, BD Biosciences), anti-FcεRI-FITC (clone CRA1, Miltenyi Biotec, Bergisch Gladbach, Germany), anti-FcεRI-PE (clone CRA1, BioLegend), anti-SUSD2-PE (clone W3D5, BioLegend), anti-CD63- FITC (clone H5C6, BD Biosciences), anti-CD49a-BV786 (clone SR84, BD Biosciences), anti-CD66a/c/e-A488 (clone ASL-32, BioLegend), anti-CD326-BV650 (clone 9C4, BioLegend), anti-CD34-BV421 (clone 581, BD Biosciences), anti-HLA-DR-PE/Cy5 (clone L243, BioLegend), anti-CD344-PE/Vio770 (clone CH3A4A7, Miltenyi Biotec), anti-CD38-BV421 (clone HIT2, BD Biosciences), anti-tryptase (clone G3, Millipore, Burlington, MA, USA) conjugated in-house with an Alexa Fluor 647 monoclonal antibody labeling kit (Thermo Fisher Scientific, Waltham, MA, USA), anti-CPA3 antibodies (clone CA5, a kind gift from Andrew Walls, Southampton, UK) conjugated in-house with an Alexa Fluor™ 488 antibody labeling kit (Thermo Fisher Scientific) and chymase (clone B7, Millipore) conjugated in-house with a PE Conjugation Kit (Abcam, Cambridge, UK). Surface staining was performed by incubation for 30 min at 4 degrees with the antibodies in PBS+ 2% FBS, followed by washing with PBS+ 2% FBS. When using the LEGENDScreen™ human cell screening kit, which contains 332 markers and 10 isotype controls, conjugated to PE (Cat. 70001, BioLegend) that are detailed in **Supplementary Table S1**, cells were first stained with anti-CD45, anti-CD117, anti-CD14 and anti-FcεRI antibodies for 30 min, followed by washing. Thereafter, the cells were stained with the kit reagents according to the manufacturer's instructions. The cells from each donor were not sufficient to run an entire screen. Therefore, each kit was run using several donors, and a total of 10 donors were used to run three Legendscreens kits. The presence of anti- FcεRI antibody in the backbone panel did not result in mast cell activation, as measured by surface CD63 expression (data not shown). For intracellular staining, cells were fixed with 4% paraformaldehyde (PFA) and permeabilized using 0.1% saponin in PBS with 0.01 M HEPES (PBS-S buffer). Nonspecific binding was blocked using blocking buffer (PBS-S with 5% dry milk and 2% fetal calf serum (FCS)). The cells were thereafter

stained intracellularly over-night with the antibodies in blocking buffer, thereafter washed with PBS-S buffer and PBS+ 2% FBS. The cells were analyzed using a BD FACSCanto (BD, Franklin Lakes, NJ, USA) or BD LSRFortessa, and FlowJo software version 10 (FlowJo LLC, Ashland, OR, USA) was used for flow cytometry data analysis. Fluorescent minus one (FMO) controls (extracellular) or isotype controls (intracellular) were used to establish gates for positive staining (**Supplementary Figure S1**).

Statistical Analysis

Statistical analyses were performed with GraphPad Prism software version 7.0b (**Figures 1C**, **2** and **4**) or the Python environment (3.7) with the following packages: statsmodels (0.10.1), seaborn (0.9.0), scipy (1.4.1), pandas (1.1.0), numpy (1.18.1), and matplotlib (3.1.3) (**Figure 1D**). The specific methods used are detailed in the figure legends. * $p < 0.05$; ** $p < 0.01$; *** $p<0.001$; **** $p<0.0001$.

RESULTS

Expression of Mast Cell Proteases

The classic division into distinct human mast cell subpopulations is based on the presence or absence of granule-associated antigens, i.e., the proteases tryptase, chymase and CPA3. We therefore first performed intracellular staining of lung cells and used a flow cytometry-based readout to accurately characterize the mast cell population with respect to the expression of tryptase, chymase and CPA3. Flow cytometry analysis identified $CD45^{+}CD14^{low}CD117^{high}$ HLMCs with the characteristic expression of tryptase (**Figures 1A, B**). The HLMC population showed a high variation of chymase and CPA3 expression between individual cells and the degree of CPA3 and chymase double positive cells varied considerably from donor to donor (**Figure 1C**). However, no distinct subpopulations were discernable, instead there was a continuous spectrum of expression levels.

Immunoprofiling of HLMCs

Whereas intracellular antigens failed to discriminate distinct subpopulations, we set out to perform an extensive mapping of cell surface antigens on HLMCs to potentially identify distinct subpopulations and novel markers. Flow cytometry analysis characterized the expression of 332 surface markers on HLMCs, using a LEGENDScreen™ human cell screening kit. Since many of the markers are broadly expressed we used $CD14^{+}$ cells as a reference to selectively enrich for lineage-specific antigens in HLMCs (**Figure 1D**). Well-known monocyte markers such as CD11b, CD11c, and HLA-DR were highly expressed on $CD14^{+}$ cells, verifying the validity in enriching for lineage-characteristic markers. In analogy, HLMCs expressed high levels of CD117 and FcεRI. Markers with the most significant differences between the HLMCs and $CD14^{+}$ cells included CD9, CD59, CD274 and CD226 (**Figure 1D**). CD9 is a broadly expressed tetraspanin with a wide variety of functions; in mast cells, it is abundantly expressed and has been implicated in chemotaxis and activation (14). CD59 can prevent complement-induced cytolytic cell death by preventing assembly of the complement membrane attack complex and has also been implicated in T cell activation (15). CD274 is also known as programmed death ligand-1 (PD-L1) and can cause blockade of T cell activation (16). CD226 has received increasing interest in recent years and can play a role in many immunological processes (17), including enhancement of FcεRI-mediated activation in mast cells (18).

Of the 332 markers analyzed, HLMCs showed significant expression of 102 markers (**Figure 2**), of which 23, to the best of our knowledge, have not been described on (non-neoplastic) human MCs before (**Table 1**).

Heterogeneous Expression of the High-Affinity IgE Receptor FcεRI

One of the principal markers for MCs is the expression of the high-affinity IgE-receptor FcεRI. FcεRI expression on HLMCs has been shown to differ among compartments in the lungs, as well as between healthy and diseased tissues. HLMCs from healthy individuals present in the parenchyma are negative for FcεRI, while patients with concurrent asthma show higher expression of the receptor (12, 19). In our study, the expression varied considerably between donors and there was no clear separation between the negative and positive FcεRI populations but rather a continuous spectrum of expression and approximately 50% of the donors expressed FcεRI on virtually all MCs (**Figures 3A–C**).

Heterogeneous Expression of Cell-Surface Markers With a Continuous Distribution

The heterogeneity of HLMCs has primarily been studied using immunohistochemistry in a binary manner and they have been divided into the MC_T and MC_{TC} subtypes (2, 3). How this heterogeneity is reflected by the heterogeneous expression of cell-surface markers has barely been investigated. None of the surface markers investigated in this study, using quantitative flow cytometry, did distinctly and consistently divide the HLMCs into subpopulations (data not shown). However, several markers were expressed with a considerable continuous variation within the HLMC population (**Table 2**). Co- stainings of nine of these markers revealed that expression of six of the markers, SUSD2, CD49a, CD326, CD34, CD66 and HLA-DR correlated ($r > 0.4$) (**Figures 4A–H**). The correlations seen between markers was not due to autofluorescence since there was no correlations in the FMO controls (**Supplementary Figures S1A–E**). In addition, the HLMCs showed no significant staining with the 10 isotype controls (**Figure 2**).

We next investigated if the expression of these markers correlated to the classical mast cell subsets using intracellular staining for CPA3 as a marker for MC_{TC}. Expression of neither SUSD2, CD38 (**Figures 4I, J**) nor CD344 (data not shown) correlated with CPA3 expression.

Since the expression of SUSD2, a marker for stem/progenitor cells (20), correlated to CD34, that is expressed on circulating

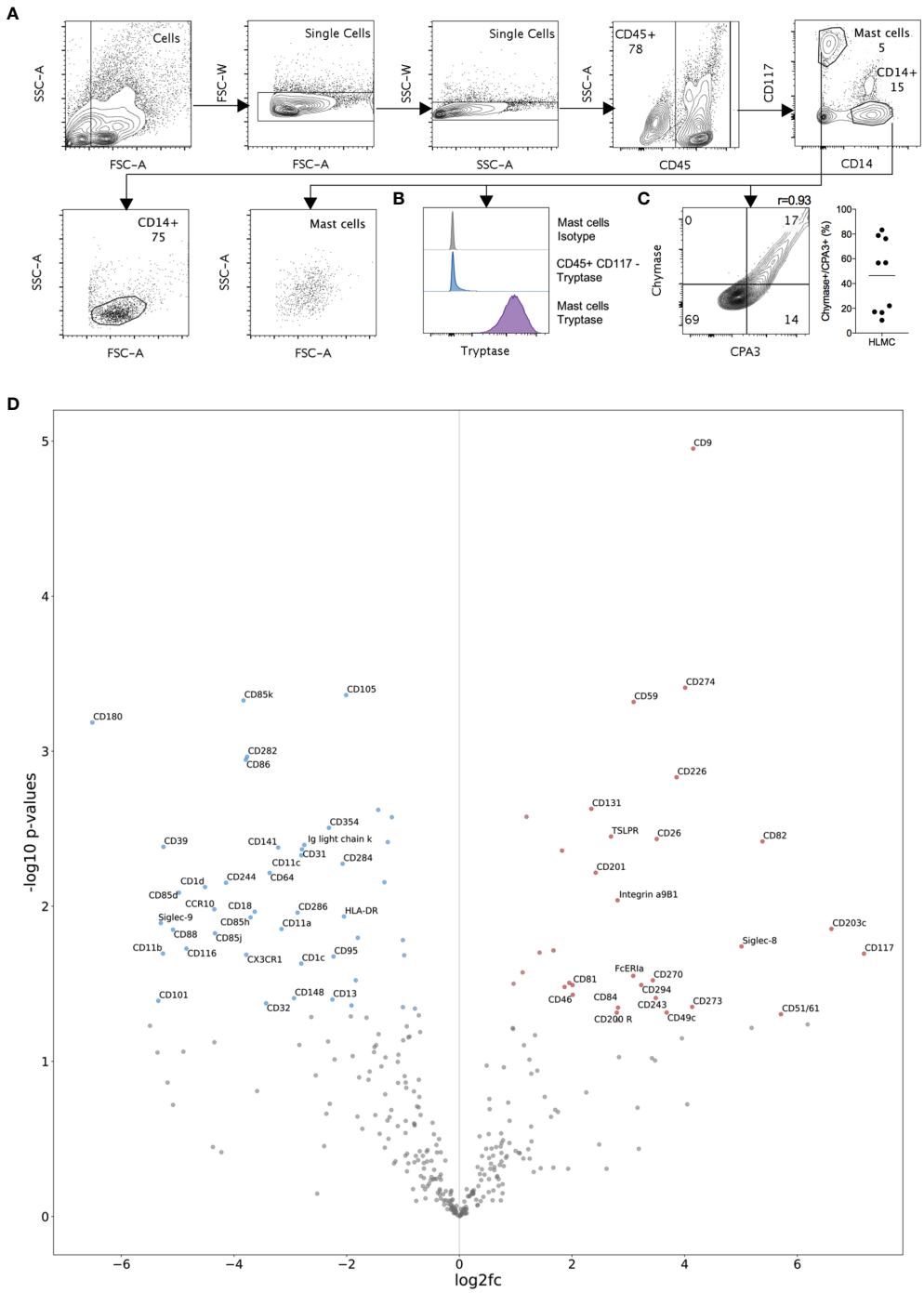


FIGURE 1 | Protease expression and LEGENDScreen analysis of HLMC. **(A)** Representative gating strategies for HLMCs and CD14$^+$ cells are shown. **(B)** Intracellular tryptase-, **(C)** chymase- and CPA3- stained HLMCs and quantification of CPA3$^+$/Chymase$^+$ cells n = 9. **(D)** Comparison of marker expression included in the LEGENDScreen kit between mast cells and CD14$^+$ cells. Volcano plot showing log2-fold change in mast cells divided by CD14$^+$ cells (normalized MFI values with the plate-matched FMO subtracted) against -log10 p-values (independent 2-sided t-test) of mast cells against CD14$^+$ cells. Markers are annotated only if abs(log2fc) => 2 and p-value < 0.05. n = 3.

mast cell progenitors (21), we investigated if the expression of these markers could identify MCs in different stages of maturation. When mast cells mature they become larger with an increasing number of granules (22). We therefore gated SUSD2 low, intermediate and high cells and compared the FSC and SSC values that reflect the size and granularity of the cells. However, SUSD2high cells had higher FSC and SSC then SUSD2low cells (**Figures 4K–M**), suggesting that they were

Marker	%	MFI	
CD1a	6	1	
CD1b	8	1	
CD1c	5	1	
CD1d	8	1	
CD2	52	2	
CD3	25	1	
CD4	76	3	**
CD5	9	1	
CD6	12	1	
CD7	22	1	
CD8a	16	1	
CD9	100	11	****
CD10	53	3	*
CD11a	73	4	****
CD11b	51	3	*
CD11b act	31	1	
CD11c	85	4	****
CD13	97	5	****
CD14	26	1	
CD15	3	0	
CD16	35	2	
CD18	94	5	****
CD19	2	0	
CD20	5	0	
CD21	10	1	
CD22	99	5	****
CD23	2	0	
CD24	21	1	
CD25	8	0	
CD26	92	5	****
CD27	3	0	
CD28	31	1	
CD29	100	7	****
CD30	35	2	
CD31	74	4	****
CD32	56	3	*
CD33	100	7	****
CD34	58	2	
CD35	22	1	
CD36	68	4	***
CD38	68	4	***
CD39	41	2	
CD40	33	2	
CD41	58	3	*
CD42b	2	0	
CD43	100	6	****
CD44	100	11	****
CD45	92	5	****
CD45RA	86	4	****
CD45RB	40	2	
CD45RO	90	5	****
CD46	100	8	****
CD47	100	9	****
CD48	99	6	****
CD49a	47	2	
CD49c	99	6	****
CD49d	97	5	****
CD49e	92	5	****
CD49f	54	2	
CD50	81	4	****
CD51	100	6	****
CD51/61	100	6	****
CD52	92	5	****
CD53	98	5	****
CD54	99	6	****
CD55	100	6	****
CD56	3	0	
CD57	3	0	
CD58	100	7	****
CD59	100	10	****
CD61	90	4	****
CD62E	5	1	
CD62L	6	0	
CD62P	35	2	
CD63	100	7	****
CD64	55	3	**
CD66a/c/e	67	3	*
CD66b	4	0	
CD69	99	6	****
CD70	5	1	
CD71	66	3	**
CD73	42	2	
CD74	55	3	*
CD79b	25	1	
CD80	18	1	
CD81	100	8	****

Marker	%	MFI	
CD82	100	10	****
CD83	56	3	**
CD84	100	7	****
CD85a	12	1	
CD85d	10	1	
CD85g	5	1	
CD85h	13	1	
CD85j	34	2	
CD85k	26	1	
CD86	9	1	
CD87	12	1	
CD88	9	1	
CD89	8	0	
CD90	17	1	
CD93	5	0	
CD94	2	0	
CD95	28	1	*
CD96	3	0	
CD97	100	5	****
CD99	100	6	****
CD100	32	2	*
CD101	3	0	
CD102	26	1	
CD103	1	0	
CD104	6	0	
CD105	5	1	
CD106	2	0	
CD107a	80	3	****
CD108	6	1	
CD109	2	0	
CD111	30	1	*
CD112	13	1	
CD114	5	1	
CD115	40	2	***
CD116	6	0	
CD117	100	5	****
CD119	55	2	***
CD122	1	0	
CD123	8	1	
CD124	5	1	
CD126	6	1	
CD127	2	0	
CD129	4	0	
CD131	65	2	****
CD132	17	1	
CD134	4	0	
CD135	2	0	
CD137	4	0	
CD137L	12	1	
CD138	18	1	
CD140a	2	0	
CD140b	5	1	
CD141	25	1	
CD143	33	1	*
CD144	3	0	
CD146	23	1	
CD148	56	2	***
CD150	2	0	
CD152	20	1	
CD154	5	0	
CD155	26	1	*
CD156c	94	4	****
CD158a/h	2	0	
CD158b	5	0	
CD158d	34	1	
CD158e1	2	0	
CD158f	2	0	
CD161	2	0	
CD162	92	4	****
CD163	18	1	
CD164	100	5	****
CD165	2	0	
CD166	88	3	****
CD167a	13	1	
CD169	2	0	
CD170	71	2	****
CD172a	74	3	****
CD172b	11	1	
CD172g	5	1	
CD178	33	1	
CD179a	9	1	
CD179b	2	0	
CD180	1	0	
CD181	6	0	
CD182	1	0	
CD183	7	0	

Marker	%	MFI	
CD184	4	0	
CD193	2	0	
CD195	4	0	
CD196	4	0	
CD197	3	0	
CD200	6	1	
CD200 R	100	5	****
CD201	36	1	*
CD202b	2	0	
CD203c	98	4	****
CD205	39	1	*
CD206	5	1	
CD207	2	0	
CD209	1	0	
CD210	3	0	
CD213a2	3	0	
CD215	19	1	
CD218a	4	0	
CD220	2	0	
CD221	8	1	
CD226	88	3	****
CD229	1	0	
CD231	7	1	
CD235ab	4	0	
CD243	77	3	**
CD244	2	0	
CD245	18	1	
CD252	3	0	
CD253	2	0	
CD254	1	0	
CD255	2	0	
CD257	7	1	
CD258	3	0	
CD261	2	0	
CD262	5	0	
CD263	2	0	
CD266	2	0	
CD267	2	0	
CD268	1	0	
CD270	100	5	****
CD271	2	0	
CD273	63	2	*
CD274	93	3	***
CD275	17	1	
CD276	93	4	****
CD277	91	3	***
CD278	2	0	
CD279	1	0	
CD282	1	0	
CD284	2	0	
CD286	2	0	
CD290	1	0	
CD294	24	1	
CD298	100	7	****
CD300e	28	1	
CD300F	96	4	****
CD301	4	1	
CD303	2	0	
CD304	30	1	
CD307	2	0	
CD307d	2	0	
CD314	3	0	
CD317	95	3	****
CD318	13	1	
CD319	5	1	
CD324	3	1	
CD325	2	0	
CD326	45	2	
CD328	65	3	**
CD334	1	0	
CD335	5	0	
CD336	1	0	
CD337	2	0	
CD338	1	0	
CD340	1	0	
CD344	55	2	*
CD351	2	0	
CD352	12	1	
CD354	15	1	
CD355	2	0	
CD357	4	1	
CD360	2	0	
B2M	100	9	****
BTLA	2	0	
C3AR	50	2	
C5L2	5	1	

Marker	%	MFI	
CCR10	30	1	
CLEC12A	92	3	***
CLEC9A	2	0	
CX3CR1	1	0	
CXCR7	2	0	
OPRD	2	0	
DLL1	3	0	
DLL4	1	0	
DR3	14	1	
EGFR	4	0	
erbB3	1	0	
FcεRIα	41	2	
FcRL6	2	0	
Galectin-9	4	0	
GARP	3	0	
HLA-A,B,C	99	7	****
HLA-A2	35	3	*
HLA-DQ	46	2	
HLA-DR	84	4	****
HLA-E	38	2	
HLA-G	9	1	
IFNGR2	2	0	
Ig light chain κ	26	1	
Ig light chain λ	36	2	
IgD	1	0	
IgM	1	0	
IL-28RA	2	0	
Integrin αvβ1	77	3	****
Integrin B5	7	1	*
Integrin B7	11	1	***
Jagged 2	6	1	
LAP	1	0	
LT-B R	8	1	****
Mac- 2	3	0	
MAIR- II	11	1	****
MICA/MICB	1	0	
SUSD2 (W3D5)	45	2	****
SUSD2 (W5C5)	46	2	****
W7C6	2	0	
W4A5	53	2	****
MSCA-1	1	0	
NKp80	0	0	
Notch 1	2	1	
Notch 2	2	1	
Notch 3	1	0	
Notch 4	1	0	
NPC (57D2)	3	0	
Podoplanin	7	1	
Pre- BCR	2	0	
PSMA	6	0	
Siglec-10	25	2	****
Siglec-8	82	3	****
Siglec-9	18	1	****
SSEA-1	1	0	
SSEA-3	1	0	
SSEA-4	1	0	
SSEA-5	22	1	****
TCR γ/σ	3	0	
TCR Vβ13,2	1	0	
TCR Vβ23	2	0	
TCR Vβ8	1	0	
TCR Vβ9	0	0	
TCR Vσ2	1	0	
TCR Vγ9	1	0	
TCR Vα24-Jα18	6	1	
TCR Vα7,2	1	0	
TCR a/B	2	0	
Tim-1	1	0	
Tim-3	30	2	****
Tim-4	1	0	
TLT-2	0	0	
TRA-1-60-R	1	0	
TRA-1-81	1	0	
TSLPR	10	1	****
Ms IgG1 κ	1	0	
Ms IgG2a κ	4	1	
Ms IgG2b	1	0	
Ms IgG3 κ	2	0	
Ms IgM κ	0	0	
Rat IgG1	1	0	
Rat IgG2a	2	0	
Rat IgG2b	1	0	
Rat IgM κ	0	0	
AH IgG	1	0	

FIGURE 2 | Expression of cell-surface antigens on HLMCs. HLMCs stained with the LEGENDScreen human cell screening kit. Mast cells were gated as $CD45^{+}CD14^{low}CD117^{high}$ cells. Shown are the percent positive (%) for each marker, the MFI (normalized to the plate-matched FMO control and log_{10} transformed) and the stars represents the significance of the MFI of the marker compared to that of the FMO control (one-way ANOVA with Dunnett's multiple comparisons test). *$p < 0.05$, **$p < 0.01$, ***$p < 0.001$, ****$p < 0.0001$. n = 3.

TABLE 1 | Novel antigens identified on HLMCs.

Marker (clone)	Description
CD36	Receptor binding a broad range of lipids
CD45RO	Isoform of CD45
CD66a/c/e	Adhesion molecules
CD74	Involved in MHC class II antigen processing and a receptor for macrophage migration inhibitory factor
CD111	Adhesion molecule
CD115	Receptor for M-CSF and IL-34
CD131	Common β subunit of the IL-3, IL-5 and GM-CSF receptors
CD143	Metallopeptidase
CD148	Tyrosine phosphatase involved in signal transduction
CD164	Sialomucin involved in cell adhesion and proliferation
CD166	Glycoprotein involved in cell adhesion and migration
CD205	Endocytic receptor involved in antigen uptake and processing
CD243	Involved in transportation of molecules across cell membranes
CD270	Receptor for TNFSF14, BTLA, LTA and CD160
CD277	Regulate T cell responses
CD317	Blocks the release of certain viruses from infected cells
CD344 (Frizzled-4)	Receptor for Wnt proteins and norrin
CLEC12A/CD371	C-type lectin-like receptor with an immunoreceptor tyrosine-based inhibitory motif (ITIM) domain
Integrin α9β1	Integrin mediating cell adhesion and migration
SUSD2 (W3D5, W5C5)	Potentially involved in cell adhesion as this transmembrane protein contains functional domains associated with adhesion molecules
(W4A5)	Antigen has yet to be described
Siglec-9	Lectin that binds sialic acid and has ITIM domains
SSEA-5	A glycan

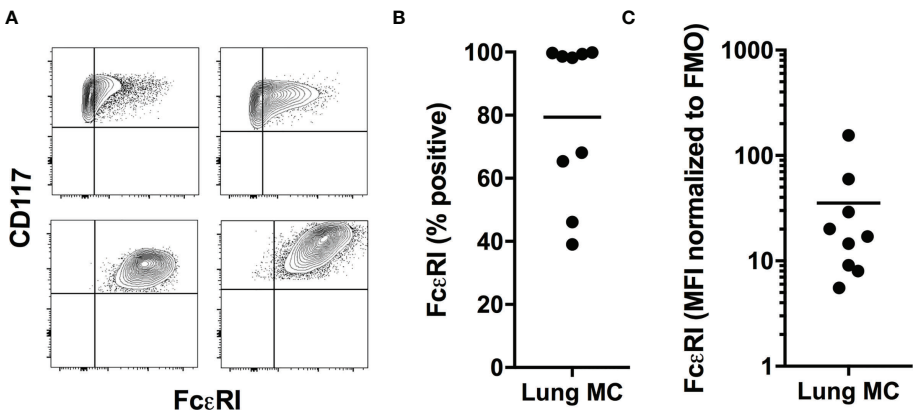


FIGURE 3 | FcεRI expression on HLMCs. Examples of CD117/FcεRI expression on HLMCs gated as $CD45^{+}CD14^{low}CD117^{high}$ cells from four donors **(A)**. Quantification of the percent positive for FcεRI **(B)** and the MFI of FcεRI normalized to that of the matched FMO control **(C)**. n = 9.

larger with a higher granularity and therefore unlikely to be immature MCs.

SUSD2 has been linked to proliferation in cancer cells (23), why we investigated the proliferation status of the cells with the proliferation marker Ki-67. However, in agreement with the fact that mast cells are long-lived cells with low turnover (24), no staining was observed (**Supplementary Figure S2**).

DISCUSSION

HLMCs have been shown to be heterogeneous; classically, they have been studied using immunohistochemistry in a binary manner, and they have been divided into the MC_T and MC_{TC} subtypes based on whether the mast cell proteases chymase and CPA3 are detectable (2, 3). By using a quantitative flow cytometry based method we indeed found high variation in chymase and CPA3 expression but no distinct subpopulations were discernable (**Figure 1C**). The apparent discrepancy between our study and previous immunohistochemical studies is probably due to the fact that we have studied the expression in a quantitative manner using flow cytometry, thus finding that there is a spectrum of different expression levels. In contrast, in previous studies the cells have been classified into MC_T/MC_{TC} cells in a binary manner depending on the detection limit of the immunohistochemical technique.

Although attempts have been made to map cell-surface antigens on HLMCs (25–30), extensive mapping including the

TABLE 2 | The 10 markers from the LEGENDScreen analysis with the highest robust coefficient of variation (robust CV).

Marker	Robust CV
SUSD2 (W5C5)	264
SUSD2 (W3D5)	246
CD344	172
CD49a	160
CD326	155
CD66a/c/e	153
CD34	134
HLA-DR	133
SSEA-5	131
CD63	124
CD38	123

heterogeneity of cell-surface antigen expression has not been carried out. In this study, we identified significant expression of 102 markers on the HLMC surface (**Figure 2**), of which, to the best of our knowledge, 23 are novel mast cell markers (**Table 1**). Several of these markers, including SSEA-5, SUSD2, W4A5, CD243, CD111, CD131 and CD164, are described as markers expressed on stem cells. The expression of stem cell markers on mast cells is in accordance with results from the FANTOM5 consortium, in which skin mast cells exhibited similarities with stem cells (31). In some cases, our results are in disagreement with previously published data; for example, CD4, CD10, CD36 and CD74 were previously shown to not be expressed by HLMCs (26, 27). This discrepancy might be explained by differences in the procedures, as in contrast to published data, we did not purify or culture the studied mast cells prior to analysis (25, 27, 29, 30). Culturing mast cells has been shown to alter their phenotype and expression of cell-surface receptors (31, 32). Furthermore, although macroscopically healthy tissue distal from the tumor was used for our analysis, one cannot rule out the possibility that also this part of the tissue is affected by the disease and can have an impact on the results.

The expression of FcεRI has been shown to differ in different compartments of the lung, with mast cells present in the parenchyma being negative for FcεRI (12). We have investigated single cell suspensions from lung tissues without separation of the parenchymal cells. However, we did not observe distinct FcεRI positive and negative mast cell populations but rather a continuous spectrum of expression levels (**Figure 3A**). Additionally, in about 50% of the donors virtually all mast cells stained positive for FcεRI, meaning that we cannot detect any FcεRI negative parenchymal mast cell population in these individuals (**Figure 3A**). This discrepancy is again likely to be due to the different techniques used, immunohistochemistry and flow cytometry, and the different detection limits of the techniques. We also observed a large variation in expression of FcεRI among individuals (**Figures 3A–C**), and in line with our results, this has previously been shown also for human skin mast cells (33). The reasons for this variation could be manifold, as the surface expression of FcεRI can be regulated in many different ways. FcεRI is, for example, upregulated by IL-4 and stabilized on the cell surface by the binding of IgE antibodies (34). Furthermore, it was described recently that IL-33 downregulates the expression of FcεRI (35, 36), indicating that the state of inflammation in the tissue can influence FcεRI expression.

Heterogeneous expression of cell-surface markers on mast cells has scarcely been investigated. We investigated the heterogeneity of cell-surface markers in a quantitative manner using flow cytometry and did not find any markers that distinctly and consistently divided the studied mast cells into subpopulations with a bi- or multimodal distribution (data not shown). We did, however, find several markers with considerable continuous variation in expression within the mast cell populations (**Table 2**), and co-stainings revealed that six of these markers, SUSD2, CD49a, CD326, CD34, CD66 and HLA-DR, were correlated (**Figure 4**). To investigate whether these markers are correlated with the classic mast cell subpopulations MC_T and MC_{TC}, we costained for SUSD2 and CPA3, but no correlation was detected, ruling out the possibility that these markers are extracellular markers of the classic mast cell subtypes (**Figure 4I**). Recently, CD38 was demonstrated to be differentially expressed in human nasal polyp mast cells where $CD38^{low}$ were of the MC_{TC} subtype, while $CD38^{high}$ MCs were a heterogenous pool of both MC_T and MC_{TC} cells (37). In our study, CD38 did not distinctly separate the HLMCs into subpopulations and did not correlate with CPA3; i.e., in HLMCs CD38 could not be used to distinguish the MC_T and MC_{TC} subtypes (**Figure 4J**). CD344 did not correlate with the MC_T or MC_{TC} profile either (data not shown). Another marker suggested to be expressed on MC_{TC} is the complement 5a receptor CD88 (38). However, we did not detect significant expression of CD88 on HLMCs (**Figure 2**). Thus, we were unable to find an extracellular marker that distinguishes the classical mast cell subsets.

One of the markers that showed high continuous variation in the HLMCs, CD63, is used as a surrogate marker for mast cell activation (39), i.e., degranulation. However, CD63 did not correlate to any of the other eight markers investigated, including the 6 markers that show correlation to each other SUSD2, CD49a, CD326, CD34, CD66 or HLA-DR indicating that these markers do not reflect varying degree of activation (**Figure 4G** and data not shown).

Since two of our six heterogeneity markers that correlate, CD34 and SUSD2, is expressed on stem/progenitor cells (20, 21, 40), we wondered whether these markers could identify cells in different stages of mast cell maturation. However, if that was the case, one would expect cells with high expression of SUSD2/CD34 to be small and contain few granules similar to mast cell progenitors (21). In contrast, the cells with high expression of SUSD2 had relatively high FSC and SSC values (**Figures 4K–M**), suggesting that they were relatively large and granular and therefore unlikely to be immature mast cells. In this context, it is worth noting that mature murine mast cells also express CD34 (41), and in these cells, CD34 inhibits adhesion and is required for optimal migration (42).

SUSD2 is also expressed in certain cancers, in which it has been linked to proliferation (23); thus, one could imagine that

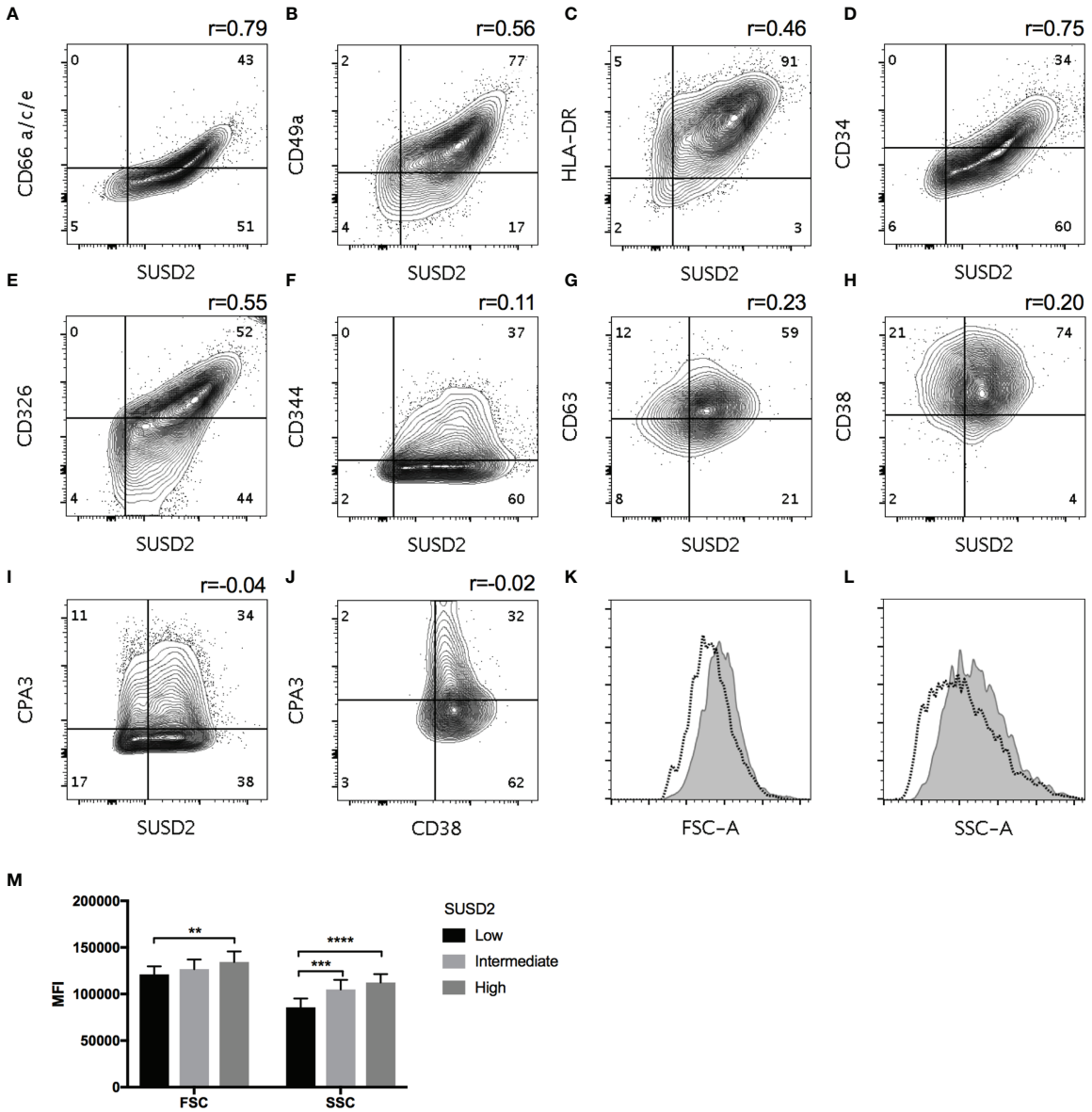


FIGURE 4 | Co-staining of HLMCs with indicated markers. Pearson correlations in each donor was calculated and the average r is shown (n = 3-4) **(A–J)**. SUSD2low, intermediate and high cells were gated, and the FSC **(K)** and SSC **(L)** values of the SUSD2low (dotted line) and SUSD2high (filled gray) populations are shown. Quantification of FSC and SSC is shown in **(M)**, mean ± SEM, n = 5. Two-way ANOVA with Bonferroni's multiple comparisons test was performed. **p < 0.01; ***p < 0.001; ****p < 0.0001.

cells with high SUSD2 expression are proliferating. However, we could not detect any staining for the proliferation marker Ki67 in HLMCs (**Supplementary Figure S2**).

In summary, we have identified the expression of 102 cell-surface antigens on HLMCs, of which 23 have not been described previously on MCs. Several of these antigens had a high continuous variability in their expression within the HLMC population. The expression of six of these markers correlated to each other and the size and granularity of the cells. Further studies are needed to determine how these cells differ functionally. None of the markers correlated with the intracellular protease expression. Thus, in contrast to the dogma of distinct mast cell subtypes, we demonstrate the continuous nature of HLMC heterogeneity.

DATA AVAILABILITY STATEMENT

The original contributions presented in the study are included in the article/**Supplementary Material**. Further inquiries can be directed to the corresponding authors.

ETHICS STATEMENT

The studies involving human participants were reviewed and approved by Regionala Etikprövningsnämden, Stockholm. The patients/participants provided their written informed consent to participate in this study.

AUTHOR CONTRIBUTIONS

ER, JD, and GN conceived and designed the studies. ER, JD, and AR designed and performed the experiments. ER, DZ, and JD analyzed the data. JS, A-CO, MA-A, MA, and S-ED provided samples. ER, GN, and JD wrote the manuscript draft. All authors reviewed, critically revised, and approved the final manuscript.

FUNDING

This study was supported by grants from the Swedish Research Council (2018-02070 and 2020-01693); the Heart-Lung Foundation; The Swedish Cancer Society; the Ellen, Walter and Lennart Hesselman Foundation; the Tore Nilsson Foundation; the Lars Hierta Memorial Foundation; the Konsul Th C Bergh Foundation; the Tornspiran Foundation; the O. E. and Edla Johanssons Foundation; the Swedish Society for Medical Research; The Centre for Allergy Research Highlights Asthma Markers of Phenotype (ChAMP) consortium funded by the Swedish Foundation for Strategic Research; the AstraZeneca & Science for Life Laboratory Joint Research Collaboration; and the Karolinska Institutet. The funding sources were not involved in the study design, collection and interpretation of data, writing the report or the decision to submit the article for publication.

ACKNOWLEDGMENTS

We thank Andrew Walls for the generous gift of the anti-CPA3 antibody.

SUPPLEMENTARY MATERIAL

The Supplementary Material for this article can be found online at: https://www.frontiersin.org/articles/10.3389/fimmu.2021.804812/full#supplementary-material

REFERENCES

1. Enerback L. Mast Cells in Rat Gastrointestinal Mucosa. 2. Dye-Binding and Metachromatic Properties. *Acta Pathol Microbiol Scand* (1966) 66:303–12. doi: 10.1111/apm.1966.66.3.303
2. Irani AA, Schechter NM, Craig SS, Deblois G, Schwartz LB. Two Types of Human Mast Cells That Have Distinct Neutral Protease Compositions. *Proc Natl Acad Sci USA* (1986) 83:4464–8. doi: 10.1073/pnas.83.12.4464.
3. Irani AM, Goldstein SM, Wintroub BU, Bradford T, Schwartz LB. Human Mast Cell Carboxypeptidase. Selective Localization to MCTC Cells. *J Immunol* (1991) 147:247–53.
4. Metcalfe DD, Baram D, Mekori YA. Mast Cells. *Physiol Rev* (1997) 77:1033–79. doi: 10.1152/physrev.1997.77.4.1033
5. Balzar S, Fajt ML, Comhair SA, Erzurum SC, Bleecker E, Busse WW, et al. Mast Cell Phenotype, Location, and Activation in Severe Asthma. Data From the Severe Asthma Research Program. *Am J Respir Crit Care Med* (2011) 183:299–309. doi: 10.1164/rccm.201002-0295OC
6. Holgate ST, Hardy C, Robinson C, Agius RM, Howarth PH. The Mast Cell as a Primary Effector Cell in the Pathogenesis of Asthma. *J Allergy Clin Immunol* (1986) 77:274–82. doi: 10.1016/S0091-6749(86)80104-X
7. Bradding P, Walls AF, Holgate ST. The Role of the Mast Cell in the Pathophysiology of Asthma. *J Allergy Clin Immunol* (2006) 117:1277–84. doi: 10.1016/j.jaci.2006.02.039
8. Erjefalt JS. Mast Cells in Human Airways: The Culprit? *Eur Respir Rev* (2014) 23:299–307. doi: 10.1183/09059180.00005014
9. Arthur G, Bradding P. New Developments in Mast Cell Biology: Clinical Implications. *Chest* (2016) 150:680–93. doi: 10.1016/j.chest.2016.06.009
10. Schulman ES, Kagey-Sobotka A, Macglashan DW Jr, Adkinson NF Jr, Peters SP, Schleimer RP, et al. Heterogeneity of Human Mast Cells. *J Immunol* (1983) 131:1936–41.
11. Lowman MA, Rees PH, Benyon RC, Church MK. Human Mast Cell Heterogeneity: Histamine Release From Mast Cells Dispersed From Skin, Lung, Adenoids, Tonsils, and Colon in Response to IgE-Dependent and Nonimmunologic Stimuli. *J Allergy Clin Immunol* (1988) 81:590–7. doi: 10.1016/0091-6749(88)90199-6
12. Andersson CK, Mori M, Bjermer L, Lofdahl CG, Erjefalt JS. Novel Site-Specific Mast Cell Subpopulations in the Human Lung. *Thorax* (2009) 64:297–305. doi: 10.1136/thx.2008.101683
13. Ravindran A, Ronnberg E, Dahlin JS, Mazzurana L, Safholm J, Orre AC, et al. An Optimized Protocol for the Isolation and Functional Analysis of Human Lung Mast Cells. *Front Immunol* (2018) 9:2193. doi: 10.3389/fimmu.2018.02193
14. Brosseau C, Colas L, Magnan A, Brouard S. CD9 Tetraspanin: A New Pathway for the Regulation of Inflammation? *Front Immunol* (2018) 9:2316. doi: 10.3389/fimmu.2018.02316
15. Venneker GT, Asghar SS. CD59: A Molecule Involved in Antigen Presentation as Well as Downregulation of Membrane Attack Complex. *Exp Clin Immunogenet* (1992) 9:33–47.
16. Qin W, Hu L, Zhang X, Jiang S, Li J, Zhang Z, et al. The Diverse Function of PD-1/PD-L Pathway Beyond Cancer. *Front Immunol* (2019) 10:2298. doi: 10.3389/fimmu.2019.02298
17. Huang Z, Qi G, Miller JS, Zheng SG. CD226: An Emerging Role in Immunologic Diseases. *Front Cell Dev Biol* (2020) 8:564. doi: 10.3389/fcell.2020.00564
18. Bachelet I, Munitz A, Mankutad D, Levi-Schaffer F. Mast Cell Costimulation by CD226/CD112 (DNAM-1/Nectin-2): A Novel Interface in the Allergic Process. *J Biol Chem* (2006) 281:27190–6. doi: 10.1074/jbc.M602359200
19. Andersson CK, Tufvesson E, Aronsson D, Bergqvist A, Mori M, Bjermer L, et al. Alveolar Mast Cells Shift to an FcepsilonRI-Expressing Phenotype in Mild Atopic Asthma: A Novel Feature in Allergic Asthma Pathology. *Allergy* (2011) 66:1590–7. doi: 10.1111/j.1398-9995.2011.02723.x
20. Sivasubramaniyan K, Harichandan A, Schumann S, Sobiesiak M, Lengerke C, Maurer A, et al. Prospective Isolation of Mesenchymal Stem Cells From Human Bone Marrow Using Novel Antibodies Directed Against Sushi Domain Containing 2. *Stem Cells Dev* (2013) 22:1944–54. doi: 10.1089/scd.2012.0584
21. Dahlin JS, Malinovschi A, Ohrvik H, Sandelin M, Janson C, Alving K, et al. Lin- CD34hi CD117int/hi FcepsilonRI+ Cells in Human Blood Constitute a Rare Population of Mast Cell Progenitors. *Blood* (2016) 127:383–91. doi: 10.1182/blood-2015-06-650648
22. Dahlin JS, Ekoff M, Grootens J, Lof L, Amini RM, Hagberg H, et al. KIT Signaling is Dispensable for Human Mast Cell Progenitor Development. *Blood* (2017) 130:1785–94. doi: 10.1182/blood-2017-03-773374
23. Umeda S, Kanda M, Miwa T, Tanaka H, Tanaka C, Kobayashi D, et al. Expression of Sushi Domain Containing Two Reflects the Malignant Potential of Gastric Cancer. *Cancer Med* (2018) 7:5194–204. doi: 10.1002/cam4.1793

24. Kiernan JA. Production and Life Span of Cutaneous Mast Cells in Young Rats. *J Anat* (1979) 128:225–38.
25. Sperr WR, Agis H, Czerwenka K, Klepetko W, Kubista E, Boltz-Nitulescu G, et al. Differential Expression of Cell Surface Integrins on Human Mast Cells and Human Basophils. *Ann Hematol* (1992) 65:10–6. doi: 10.1007/BF01715119
26. Agis H, Fureder W, Bankl HC, Kundi M, Sperr WR, Willheim M, et al. Comparative Immunophenotypic Analysis of Human Mast Cells, Blood Basophils and Monocytes. *Immunology* (1996) 87:535–43. doi: 10.1046/j.1365-2567.1996.493578.x
27. Ghannadan M, Baghestanian M, Wimazal F, Eisenmenger M, Latal D, Kargul G, et al. Phenotypic Characterization of Human Skin Mast Cells by Combined Staining With Toluidine Blue and CD Antibodies. *J Invest Dermatol* (1998) 111:689–95. doi: 10.1046/j.1523-1747.1998.00359.x
28. Wimazal F, Ghannadan M, Muller MR, End A, Willheim M, Meidlinger P, et al. Expression of Homing Receptors and Related Molecules on Human Mast Cells and Basophils: A Comparative Analysis Using Multi-Color Flow Cytometry and Toluidine Blue/Immunofluorescence Staining Techniques. *Tissue Antigens* (1999) 54:499–507. doi: 10.1034/j.1399-0039.1999.540507.x
29. Ghannadan M, Hauswirth AW, Schernthaner GH, Muller MR, Klepetko W, Schatzl G, et al. Detection of Novel CD Antigens on the Surface of Human Mast Cells and Basophils. *Int Arch Allergy Immunol* (2002) 127:299–307. doi: 10.1159/000057747
30. Florian S, Sonneck K, Czerny M, Hennersdorf F, Hauswirth AW, Buhring HJ, et al. Detection of Novel Leukocyte Differentiation Antigens on Basophils and Mast Cells by HLDA8 Antibodies. *Allergy* (2006) 61:1054–62. doi: 10.1111/j.1398-9995.2006.01171.x
31. Motakis E, Guhl S, Ishizu Y, Itoh M, Kawaji H, De Hoon M, et al. Redefinition of the Human Mast Cell Transcriptome by Deep-CAGE Sequencing. *Blood* (2014) 123:e58–67. doi: 10.1182/blood-2013-02-483792
32. Guhl S, Neou A, Artuc M, Zuberbier T, Babina M. Skin Mast Cells Develop non-Synchronized Changes in Typical Lineage Characteristics Upon Culture. *Exp Dermatol* (2014) 23:933–5. doi: 10.1111/exd.12558
33. Babina M, Guhl S, Artuc M, Trivedi NN, Zuberbier T. Phenotypic Variability in Human Skin Mast Cells. *Exp Dermatol* (2016) 25:434–9. doi: 10.1111/exd.12924
34. Kraft S, Kinet JP. New Developments in FcepsilonRI Regulation, Function and Inhibition. *Nat Rev Immunol* (2007) 7:365–78. doi: 10.1038/nri2072
35. Babina M, Wang Z, Franke K, Guhl S, Artuc M, Zuberbier T. Yin-Yang of IL-33 in Human Skin Mast Cells: Reduced Degranulation, But Augmented Histamine Synthesis Through P38 Activation. *J Invest Dermatol* (2019) 139 (7):1516–25. doi: 10.1016/j.jid.2019.01.013
36. Ronnberg E, Ghaib A, Ceriol C, Enoksson M, Arock M, Safholm J, et al. Divergent Effects of Acute and Prolonged Interleukin 33 Exposure on Mast Cell IgE-Mediated Functions. *Front Immunol* (2019) 10:1361. doi: 10.3389/fimmu.2019.01361
37. Dwyer DF, Ordovas-Montanes J, Allon SJ, Buchheit KM, Vukovic M, Derakhshan T, et al. Human Airway Mast Cells Proliferate and Acquire Distinct Inflammation-Driven Phenotypes During Type 2 Inflammation. *Sci Immunol* (2021) 6(56):eabb7221. doi: 10.1126/sciimmunol.abb7221
38. Oskeritzian CA, Zhao W, Min HK, Xia HZ, Pozez A, Kiev J, et al. Surface CD88 Functionally Distinguishes the MCTC From the MCT Type of Human Lung Mast Cell. *J Allergy Clin Immunol* (2005) 115:1162–8. doi: 10.1016/j.jaci.2005.02.022
39. Redegeld FA, Yu Y, Kumari S, Charles N, Blank U. Non-IgE Mediated Mast Cell Activation. *Immunol Rev* (2018) 282:87–113. doi: 10.1111/imr.12629
40. Bredenkamp N, Stirparo GG, Nichols J, Smith A, Guo G. The Cell-Surface Marker Sushi Containing Domain 2 Facilitates Establishment of Human Naive Pluripotent Stem Cells. *Stem Cell Rep* (2019) 12:1212–22. doi: 10.1016/j.stemcr.2019.03.014
41. Drew E, Merkens H, Chelliah S, Doyonnas R, Mcnagny KM. CD34 is a Specific Marker of Mature Murine Mast Cells. *Exp Hematol* (2002) 30:1211–8. doi: 10.1016/S0301-472X(02)00890-1
42. Drew E, Merzaban JS, Seo W, Ziltener HJ, Mcnagny KM. CD34 and CD43 Inhibit Mast Cell Adhesion and are Required for Optimal Mast Cell Reconstitution. *Immunity* (2005) 22:43–57. doi: 10.1016/j.immuni.2004.11.014

Conflict of Interest: S-ED reports personal fees from AstraZeneca, Cayman Chemicals, GSK, Novartis, Regeneron, Sanofi, and Teva, for consultancies outside the submitted work.

The remaining authors declare that the research was conducted in the absence of any commercial or financial relationships that could be construed as a potential conflict of interest.

Publisher's Note: All claims expressed in this article are solely those of the authors and do not necessarily represent those of their affiliated organizations, or those of the publisher, the editors and the reviewers. Any product that may be evaluated in this article, or claim that may be made by its manufacturer, is not guaranteed or endorsed by the publisher.

Copyright © 2022 Rönnberg, Boey, Ravindran, Säfholm, Orre, Al-Ameri, Adner, Dahlén, Dahlin and Nilsson. This is an open-access article distributed under the terms of the Creative Commons Attribution License (CC BY). The use, distribution or reproduction in other forums is permitted, provided the original author(s) and the copyright owner(s) are credited and that the original publication in this journal is cited, in accordance with accepted academic practice. No use, distribution or reproduction is permitted which does not comply with these terms.

frontiers in Immunology

ORIGINAL RESEARCH
published: 20 January 2022
doi: 10.3389/fimmu.2021.803335

Inhibition of Orai Channel Function Regulates Mas-Related G Protein-Coupled Receptor-Mediated Responses in Mast Cells

Shaswati Chaki[1], *Ibrahim Alkanfari*[1,2], *Saptarshi Roy*[1], *Aetas Amponnawarat*[1,3], *Yvonne Hui*[4], *Carole A. Oskeritzian*[4] *and Hydar Ali*[1]*

[1] Department of Basic and Translational Sciences, University of Pennsylvania School of Dental Medicine, Philadelphia, PA, United States, [2] Faculty of Dentistry, King AbdulAziz University, Jeddah, Saudi Arabia, [3] Department of Family and Community Dentistry, Faculty of Dentistry, Chiang Mai University, Chiang Mai, Thailand, [4] Department of Pathology, Microbiology and Immunology, University of South Carolina School of Medicine, Columbia, SC, United States

OPEN ACCESS

Edited by:
Frans J. Van Overveld, University College Roosevelt, Netherlands

Reviewed by:
Zane Orinska, Forschungszentrum Borstel, Germany
Frank A. Redegeld, Utrecht University, Netherlands

***Correspondence:**
Hydar Ali
alih@upenn.edu

Specialty section:
This article was submitted to Inflammation, a section of the journal Frontiers in Immunology

Received: *27 October 2021*
Accepted: *28 December 2021*
Published: *20 January 2022*

Citation:
Chaki S, Alkanfari I, Roy S, Amponnawarat A, Hui Y, Oskeritzian CA and Ali H (2022) Inhibition of Orai Channel Function Regulates Mas-Related G Protein-Coupled Receptor-Mediated Responses in Mast Cells. Front. Immunol. 12:803335. doi: 10.3389/fimmu.2021.803335

Mast cells (MCs) are tissue resident immune cells that play important roles in the pathogenesis of allergic disorders. These responses are mediated *via* the cross-linking of cell surface high affinity IgE receptor (FcεRI) by antigen resulting in calcium (Ca^{2+}) mobilization, followed by degranulation and release of proinflammatory mediators. In addition to FcεRI, cutaneous MCs express Mas-related G protein-coupled receptor X2 (MRGPRX2; mouse ortholog MrgprB2). Activation of MRGPRX2/B2 by the neuropeptide substance P (SP) is implicated in neurogenic inflammation, chronic urticaria, mastocytosis and atopic dermatitis. Although Ca^{2+} entry is required for MRGPRX2/B2-mediated MC responses, the possibility that calcium release-activated calcium (CRAC/Orai) channels participate in these responses has not been tested. Lentiviral shRNA-mediated silencing of Orai1, Orai2 or Orai3 in a human MC line (LAD2 cells) resulted in partial inhibition of SP-induced Ca^{2+} mobilization, degranulation and cytokine/chemokine generation (TNF-α, IL-8, and CCL-3). Synta66, which blocks homo and hetero-dimerization of Orai channels, caused a more robust inhibition of SP-induced responses than knockdown of individual Orai channels. Synta66 also blocked SP-induced extracellular signal-regulated kinase 1/2 (ERK1/2) and Akt phosphorylation and abrogated cytokine/chemokine production. It also inhibited SP-induced Ca^{2+} mobilization and degranulation in primary human skin MCs and mouse peritoneal MCs. Furthermore, Synta66 attenuated both SP-induced cutaneous vascular permeability and leukocyte recruitment in mouse peritoneum. These findings demonstrate that Orai channels contribute to MRGPRX2/B2-mediated MC activation and suggest that their inhibition could provide a novel approach for the modulation of SP-induced MC/MRGPRX2-mediated disorders.

Keywords: Calcium release-activated calcium (CRAC), Orai, Mast cells, Mas-related G protein-coupled receptor X2 (MRGPRX2), Mas-related G protein-coupled receptor B2 (MrgprB2), Substance P

INTRODUCTION

Mast cells (MCs) are tissue resident immune cells best known for their roles in anaphylaxis and atopic disorders, which result from FcεRI/IgE-mediated histamine release and the generation of lipid mediators and cytokines (1). It is well documented that the release of calcium (Ca^{2+}) from intracellular stores and its subsequent influx through store-operated calcium (SOC) channels are required for IgE-mediated release of newly synthesized mediators (2). Human and murine MCs express the endoplasmic reticulum (ER)-resident protein stromal interaction molecule-1 and -2 (STIM-1/2) that sense the depletion of intracellular Ca^{2+}, resulting in the activation of calcium release-activated calcium (CRAC) channels such as CRACM1, CRACM2 and CRACM3 (also known as Orai1, Orai2 and Orai3) (3–6). Utilization of gene silencing and pharmacological approaches has demonstrated that Orai channels contribute to IgE-mediated degranulation in human lung MCs *in vitro* and bronchoconstriction *ex vivo* (6–8).

While all MCs are characterized by the expression of cell surface FcεRI, cutaneous MCs highly expresses a newly identified G protein-coupled receptor (GPCR) known as Mas-related GPCR-X2 (MRGPRX2, mouse counterpart MrgprB2) (9). Activation of this receptor by an increasing list of cationic ligands contributes to host defense, pseudoallergy and a number of chronic inflammatory diseases (9–11). Substance P (SP)-mediated activation of human skin MCs *via* MRGPRX2 is implicated in the pathogenesis of chronic urticaria and mastocytosis (12, 13). Moreover, activation of murine MCs by SP *via* MrgprB2 contributes to experimental neurogenic inflammation, pain, and atopic dermatitis (14, 15). Although both anti-IgE and SP cause intracellular increase in Ca^{2+} concentration, the kinetics of Ca^{2+} mobilization varies for different stimuli. Stimulation of human peripheral blood-derived cultured MCs (PBCMCs) with anti-IgE causes more sustained Ca^{2+} mobilization compared to SP. This is correlated with IgE-dependent progressive degranulation with larger granule size while SP stimulation results in faster degranulation with smaller granule size (16). However, the mechanism *via* which SP activates MRGPRX2 to cause Ca^{2+} mobilization and mediator release is unknown.

The purpose of this study was to determine if Orai channels contribute to SP-induced signaling and mediator release in human and murine MCs *in vitro* and MrgprB2-mediated inflammation *in vivo*. We utilized complementary approaches, namely, shRNA-mediated knockdown of Orai1, Orai2 and Orai3 in human MCs line, LAD2 and an Orai inhibitor, Synta66, in human skin-derived MCs and mouse peritoneal MCs for *in vitro* studies. We also tested the effects of Synta66 on SP-induced cutaneous vascular permeability and leukocyte recruitment in mouse peritoneum. This study provides novel insights on the role of Orai channels on MC activation by SP with potential implications for modulating MRGPRX2-mediated disorders.

Abbreviations: CRAC, calcium release-activated calcium; FITC, fluorescein isothiocyanate; GPCR, G Protein-coupled receptor; IL-8, interleukin-8; TNF-α, Tumor Necrosis Factor-alpha; LAMP-1, lysosomal-associated membrane protein-1; MCs, mast cells; MFI, mean fluorescent intensity; MrgprB2, Mas-related G protein-coupled receptor B2; MRGPRX2, Mas-related G protein-coupled receptor X2; PE, phycoerythrin; PMCs, peritoneal mast cells; STIM-1, stromal interaction molecule-1; SOC, store-operated calcium; SP, substance P; WT, wild-type.

MATERIALS AND METHODS

Reagents

All cell culture reagents were purchased from Invitrogen (Carlsbad, CA, USA); recombinant human stem cell factor (rhSCF), mouse interleukin-3 (mIL-3), and mouse stem cell factor (mSCF) were from PeproTech (Rocky Hill, NJ, USA); p-nitrophenyl-N-acetyl-β-D-glucosamine (PNAG) was from Sigma-Aldrich (St. Louis, MO, USA) and Fura-2 acetoxymethyl ester was from Abcam (Cambridge, MA, USA). Substance P (SP) was from AnaSpec (Fremont, CA, USA). Phycoerythrin-conjugated anti-MRGPRX2, FITC-conjugated anti LAMP-1 and all other flow cytometry antibodies were from Biolegends (San Diego, CA, USA). Rabbit anti-Orai1, Orai2 and Orai3 antibodies from Alomone lab (Rockville, MD, USA), anti-ERK1/2, anti-phospho-ERK1/2 (Thr-202/Tyr-204), anti-phospho-Akt (Ser-473), anti-Akt, β-Actin and goat anti-rabbit IgG-HRP were obtained from Cell Signaling Technology (Danvers, MA, USA). SuperSignal West Pico Maximum Sensitivity Substrate was from Thermo Scientific (Rockford, IL, USA). Synta66 (3-fluoro-pyridine-4-carboxylic acid (2,5-dimethoxy-biphenyl-4-yl)-amide) was purchased from Calbiochem (San Diego, CA, USA). ELISA kits for mouse TNF-α, and human TNF-α, IL-8, CCL-3 were obtained from R&D system (Minneapolis, MN, USA). BCA Protein Assay Kit was obtained from Pierce Biotechnology (Rockford, IL, USA).

Mice

C57BL/6 (WT) mice were obtained from the Jackson Laboratory (Bar Harbor, ME, USA). $MrgprB2^{-/-}$ mice were generated *via* CRISPR/Cas9 by CRISPR core of University of Pennsylvania (17). All mice were housed under specific pathogen-free conditions on autoclaved hardwood bedding. Both male and female mice (8–10 weeks old) were used for experiments. All experiments were approved by the Institutional Animal Care and Use Committee at University of Pennsylvania.

Cell Line Cultures

The human MC line LAD2 was provided by Dr. A. Kirshenbaum and Dr. D. Metcalfe (Laboratory of Allergic Diseases, National Institute of Allergy and Infectious Diseases, National Institutes of Health, Bethesda, MD, USA) and was maintained in complete StemPro-34 medium supplemented with L-glutamine (2 mM), penicillin (100 IU/ml), streptomycin (100 μg/ml), and rhSCF (100 ng/ml). Hemidepletion was performed weekly with media containing rhSCF (18).

Human Skin-Derived Primary Mast Cell Isolation and Culture

Human skin surgical sample was collected from the Cooperative Human Tissue Network of the National Cancer Institute, as

approved by the Internal Review Board at the University of South Carolina. Skin MCs were harvested and cultured as previously described (18, 19). Briefly, subcutaneous fat was removed by blunt dissection, and residual tissue was cut into 1 to 2 mm fragments and digested with type 2 collagenase (1.5 mg/ml), hyaluronidase (0.7 mg/ml), and DNase I (0.3 mg/ml) in Hank's Balanced Salt Solution (HBSS) for 2 h at 37°C. The dispersed cells were collected by filtering through a 70-μm cell strainer and resuspended in HBSS containing 1% fetal calf serum (FCS) and 10 mM HEPES to stop the reaction. Cells were resuspended in HBSS and layered over 75% Percoll in a HBSS cushion and centrifuged at 800×*g* at room temperature for 20 min. Nucleated cells were collected from the buffer/Percoll interface. Percoll gradient-enriched cells were resuspended at a concentration of 1×10^6 cells/ml in serum-free X-VIVO 15 medium containing 100 ng/ml rhSCF. MCs were used after 6–10 weeks of culture, when purity was nearly 100%, as confirmed with toluidine blue staining.

Isolation of Mouse Peritoneal MCs

Mouse peritoneal cells were isolated by intraperitoneal lavage from 8 to 10 weeks old C57BL/6 and MrgprB2$^{-/-}$ mice weighing ~20 g as described previously (20). Briefly, the peritoneal cavity was lavaged with 10 ml sterile cold HBSS supplemented with 3% FCS and 10 mM HEPES, pH 7.2. The cells were cultured in Roswell Park Memorial Institute (RPMI 1640) medium supplemented with 10% FCS, murine IL-3 (10 ng/ml), and murine SCF (30 ng/ml). After 48 h, non-adherent cells were removed, and adherent cells were cultured in fresh medium for an additional 4–6 weeks. Suspension cells were used for experiments as peritoneal MCs (PMCs).

Generation and Purification of Scramble shRNA, Orai1 shRNA, Orai2 shRNA and Orai3 shRNA and Knockdown in LAD2 Cells Using Lentiviral Transduction

To inhibit Orai1, Orai2, and Orai3 protein expression in human MCs, lentiviral shRNA-mediated knockdown was performed in LAD2 cells. Orai1, Orai2, and Orai3 targeted Mission shRNA lentiviral plasmids were purchased from Sigma-Aldrich. The clone that gave highest knockdown efficacy for Orai1 (TRCN0000413611), Orai2 (TRCN0000166201), and Orai3 (TRCN0000165405) were used for the study. A nontargeted scramble vector (SHC002) was used as a control. Nontargeted control or respective Orai knockdown plasmids were packaged into virus particle using HEK293T cells. Targeted shRNA plasmid (4.5 μg) along with helper plasmid pCMV-VSV-G (Addgene# 8454, 0.57 μg) and pCMV-dR8.2 (Addgene# 8455, 4.5 μg) were transfected in HEK293T cells (6×10^6 cells/transfection) in T75 flask. After 72 h, viral particles were harvested, filtered through 0.45 μm filter and concentrated using Lenti-X^{TM} concentrator (Takara Bio Inc, Japan). Cell transduction was performed by mixing 1.5 ml of concentrated virus particles with 3.5 ml of LAD2 (10×10^6) cells. After 8 h incubation in 37°C and 5% CO_2, medium was changed to complete StemPro34 media and antibiotic puromycin (2 μg/ml; Sigma) was added after 16 h (21). Western blotting was performed to confirm knockdown and experiments were performed 4 days after initiation of puromycin selection.

Degranulation Measured by β-Hexosaminidase Release Assay

The degranulation was measured by β-hexosaminidase release as described previously (21). Briefly, LAD2 cells (1×10^4), human skin-derived MCs (5×10^3), and PMCs (1×10^4) were seeded into a 96-well, white, clear-bottom cell culture plate in HEPES buffer containing 0.1% bovine serum albumin (BSA) and stimulated with differing concentrations of SP for 30 min at 37°C. Cells without treatment were designated as control. To determine the total β-hexosaminidase content, unstimulated cells were lysed in 50 μl of 0.1% Triton X-100. Aliquots (20 μl) of supernatants or cell lysates were incubated with 20 μl of 1 mM p-nitrophenyl-*N*-acetyl-β-*D*-glucosamine (PNAG) for 1.15 h at 37°C. The reaction was stopped by adding 250 μl of stop solution (0.1 M Na_2CO_3/0.1 M $NaHCO_3$). For assays using CRAC inhibitor (Synta66), cells were incubated for 5 min with the suitable dose of inhibitor prior to agonist stimulations. The absorbance was measured with a microplate reader at a wavelength of 405 nm using Versamax microplate spectrophotometer (Molecular Devices, San Jose, CA, USA). Data was represented as percent degranulation by diving the β-hexosaminidase release in sample with total β-hexosaminidase release.

Degranulation Measured by the Surface Expression of Lysosomal-Associated Membrane Protein 1 (LAMP-1)

Degranulation was also assessed by flow cytometric measurement of the surface expression of LAMP-1 (20). Murine PMCs (3×10^5) were stimulated with SP (100 μM) for 10 min in HEPES buffer containing 0.1% BSA, washed and exposed to FITC-conjugated anti-LAMP-1 antibody in FACS buffer (PBS containing 2% FCS and 0.02% sodium azide) for 30 min on ice in dark. For experiments involving inhibitors, PMCs were incubated with Synta66 (10 μM) for 5 min prior to SP stimulation. Cell surface expression of LAMP-1 was measured by flow cytometry using a BD LSR II flow cytometer (San Jose, CA) and analyzed with the FlowJo software version 10.7.2 (Tree Star Inc., Ashland, OR). The adjusted mean fluorescent intensity (MFI) was calculated as a ratio of the MFI of sample to the MFI of isotype control.

Calcium Mobilization

LAD2 (0.3×10^6 cells) cells were loaded with 1 μM Fura-2 acetoxymethyl ester in Ca^{2+}-free HEPES-buffered saline containing 0.1% BSA for 30 min in the dark at 37°C, followed by de-esterification for additional 15 min at room temperature. Cells were washed, resuspended in Ca^{2+}-free buffer and Ca^{2+} mobilization was measured for 25 min with addition of SP at 100 s and reintroduction of Ca^{2+} at 400 s. For assay with inhibitor, cells were loaded with Fura-2 acetoxymethyl ester (Fura-2AM) and incubated with 10 μM of Synta66 for 30 min in Ca^{2+}-free buffer prior to ligand stimulation. Calcium signals

was determined using a Hitachi F-2700 Fluorescence Spectrophotometer with dual excitation wavelength of 340 and 380 nm, and an emission wavelength of 510 nm at every 2 s (22). For the assay with human skin MCs, cells (0.2×10^6) were loaded with Fura-2 acetoxymethyl ester similarly in presence and absence of Synta66, and Ca^{2+} mobilization was measured in Varioskan LUX Multimode Microplate Reader (ThermoScientific, Waltham, MA, USA).

Western Blotting

Western blotting was performed as described previously (17). Briefly, control and Orai shRNA transduced LAD2 cells (1×10^6) were lysed in radioimmunoprecipitation assay buffer (1× RIPA) with protease inhibitor cocktail, and the protein concentration was measured by the BCA protein assay. Twenty five micrograms of protein samples were applied to 10% sodium dodecyl sulfate-polyacrylamide gel electrophoresis (SDS-PAGE) and subsequently transferred to PVDF membrane. After brief blocking (5% skim milk, 1 h), blots were incubated with antibodies against Orai1 (1:500), Orai2 (1:500), Orai3 (1:500) and β-Actin (1:1,000) at 4°C overnight. Blots were incubation with specific horseradish peroxidase (HRP)-conjugated secondary antibodies for another hour, followed by incubation with an HRP substrate for ECL and image captured on iBRIGHT 1500 (ThermoFisher, Waltham, MA, USA). Signal quantitation was carried out after normalization to β-Actin loading controls, as indicated. For the assay with Orai inhibitor, LAD2 cells (2×10^6) were preincubated with Synta66 (10 μM) for 30 min, stimulated with SP (1 μM) for different time intervals (0, 5, 15 and 30 min) and cell lysates were prepared. Protein samples were run in SDS-PAGE, incubated with anti-phospho-pERK1/2 (1:2,000), anti-phospho-Akt (1:1,000), anti-ERK1/2 (1:2,000), and anti-Akt (1:1,000) antibodies and processed similarly.

ELISA (Enzyme-Linked Immunosorbent Assay)

ELISAs were performed according to the manufacturer's protocol (DuoSet ELISA kits, R&D systems) to quantify the release of murine TNF-α and human TNF-α, IL-8 and CCL-3. Briefly, LAD2 cells were washed once in serum-free Stem-Pro™-34 medium, suspended in complete medium and seeded in 24-well sterile plate (0.3×10^6 cells/well) with appropriate concentration of agonist stimulation for 24 h. For experiments involving Synta66, cells were preincubated with inhibitor for 30 min prior to agonist stimulation. After 24 h, cells were centrifuged, and supernatants were collected to measure cytokines by ELISA. The expression of mTNF-α was measured in serum samples from mice untreated or treated with Synta66 and SP.

Murine Evans Blue Dye Extravasation Model

Evans blue extravasation studies were performed on male and female C57BL/6 mice (8–10 weeks of age and weighing 20–25 g). Mice were anesthetized using Ketamine : Xylazine and intraperitoneally (i.p) injected with Synta66 (10 mg/kg in 50 μl DMSO) following intravenous (i.v.) injection with 0.1 ml of 1% Evans blue in saline. After 1 h, intradermal injection of SP (50 μM in 20 μl saline) was performed into the one ear, while vehicle was injected in other side. After 30 min, mice were euthanized; ear tissues were harvested, weighed, immersed in 500 μl of formamide and incubating overnight at 56°C. Each tissue solution was centrifuged at 10,000 rpm for 10 min; Evans blue dye extravasation was determined by collecting 200 μl of the supernatant and the OD values were measured at 650 nm using Versamax microplate spectrophotometer (20).

In Vivo Murine Peritonitis Model

In short, 8–10 weeks old C57BL/6 mice (male and female) were intraperitoneally (i.p) injected with 50 μl of Synta66 (10 mg/kg in DMSO) or vehicle. After 1 h, peritonitis was induced by intraperitoneal injection of SP (50 μl of 200 μM SP in saline) or vehicle. Three hours later, all mice were euthanized and peritoneal exudate was collected by flushing the peritoneal cavity with 10 ml of sterile cold 1× PBS and centrifuged at 400×*g* for 10 min at 4°C. Pellet-containing cells were processed for flow cytometric analysis and serum prepared from blood collected by cardiac puncture for cytokine measurement by ELISA (23, 24).

Flow Cytometry Assay

To quantify the leukocyte recruitment, we performed flow cytometry as described previously (15). Following induction of peritonitis by SP injection, peritoneal lavage was collected and cells were washed with FACS buffer. Peritoneal cells were treated with CD16/32 Fc block (clone93, cat#101320) for 15 min followed by anti-CD45-FITC (clone 30-F11; cat #103108), CD11b-PerCP-Cy5.5 (clone M1/70, cat#101227), and Ly6G-BV421 (clone 1AB, cat#127628) for 45 min to stain neutrophils. Live versus Dead cells were stained using Zombie Yellow™ Fixable viability dye (Biolegend, CA). The data were acquired with BD LSR II flow cytometer (San Jose, CA) and analyzed by FlowJo software version 10.7.2 (Tree Star Inc., Ashland, OR). Neutrophils were gated as $CD45^+CD11b^+Ly6G^+$ live cells.

Statistical Analysis

Statistical analyses were performed using GraphPad PRISM software version 9.0.1 (San Diego, CSA). Results were expressed as mean ± standard error of the mean (SEM) values derived from at least three independent experiments. Differences between groups were analyzed by analysis of variance (ANOVA) following by Dunnett's, Sidak's and Tukey's multiple comparisons tests. A p-value less than or equal to 0.05 was considered to be significant.

RESULTS

Knockdown of Orai1/2/3 Partially Inhibit SP/MRGPRX2-Mediated Ca^{2+} Influx and Degranulation in LAD2 Cells

All three known Orai isoforms are expressed in human lung MCs and participate in FcεRI-mediated activation (6). Moreover, in a

human MC line, LAD2 cells, shRNA-mediated silencing of STIM-1 results in significant decrease in MRGPRX2-mediated Ca^{2+} mobilization and degranulation (25). Given that STIM-1 couples to Orai1 for Ca^{2+} influx (26), we hypothesized that this CRAC channel contributes to SP-induced responses in human MCs. To test this possibility, we used lentiviral shRNA to individually silence the expression of Orai1, Orai2, and Orai3 in LAD2 cells, which endogenously express MRGPRX2. As shown in **Figures 1A, B**, transduction of LAD2 cells with lentiviral Orai1 resulted in >80% reduction of protein expression when compared to scrambled shRNA control, as determined by western blotting. This was associated with ~50% decrease in SP-induced Ca^{2+} influx (**Figure 1C**) and degranulation (**Figure 1D**). We found that although Orai2 silencing resulted in ~50% reduction in protein expression (**Figures 1A, B**), this was associated with significant inhibition of Ca^{2+} influx (**Figure 1E**) with small reduction in degranulation (**Figure 1F**). Knockdown of Orai3 in LAD2 cells resulted in ~50% decrease in protein expression (**Figures 1A, B**). This was associated with a small but significant reduction in SP-induced Ca^{2+} influx (**Figure 1G**) and degranulation (**Figure 1H**).

SP-Induced Cytokine/Chemokine Production is Substantially Inhibited in Orai Knockdown LAD2 Cells

In addition to degranulation, Orai-mediated Ca^{2+} influx regulates the activities of the transcription factors NFAT and NF-κB, which are required for cytokine/chemokine induction in immune cells (27, 28). We therefore sought to determine the effects Orai1, Orai2 or Orai3 knockdown on SP-induced TNF-α, IL-8, and CCL-3 generation in LAD2 cells. Despite the fact that individual Orai1 and Orai3 knockdown resulted in ~50% inhibition SP-induced Ca^{2+} influx and degranulation (**Figure 1**), this resulted in substantial inhibition of SP-induced cytokine/chemokine generation (**Figures 2A–C**). By contrast, knockdown of Orai2 had variable effects on SP-induced TNF-α, IL-8, and CCL-3 generation (**Figures 2A–C**).

CRAC Channel Inhibitor Synta66 Inhibits SP-Induced Responses in LAD2 Cells

Synta66 is a CRAC inhibitor that inhibits the formation of Orai1:Orai1, Orai1:Orai2, and Orai1:Orai3 dimers (29). Therefore, we used Synta66 to determine the combined role of Orai channels

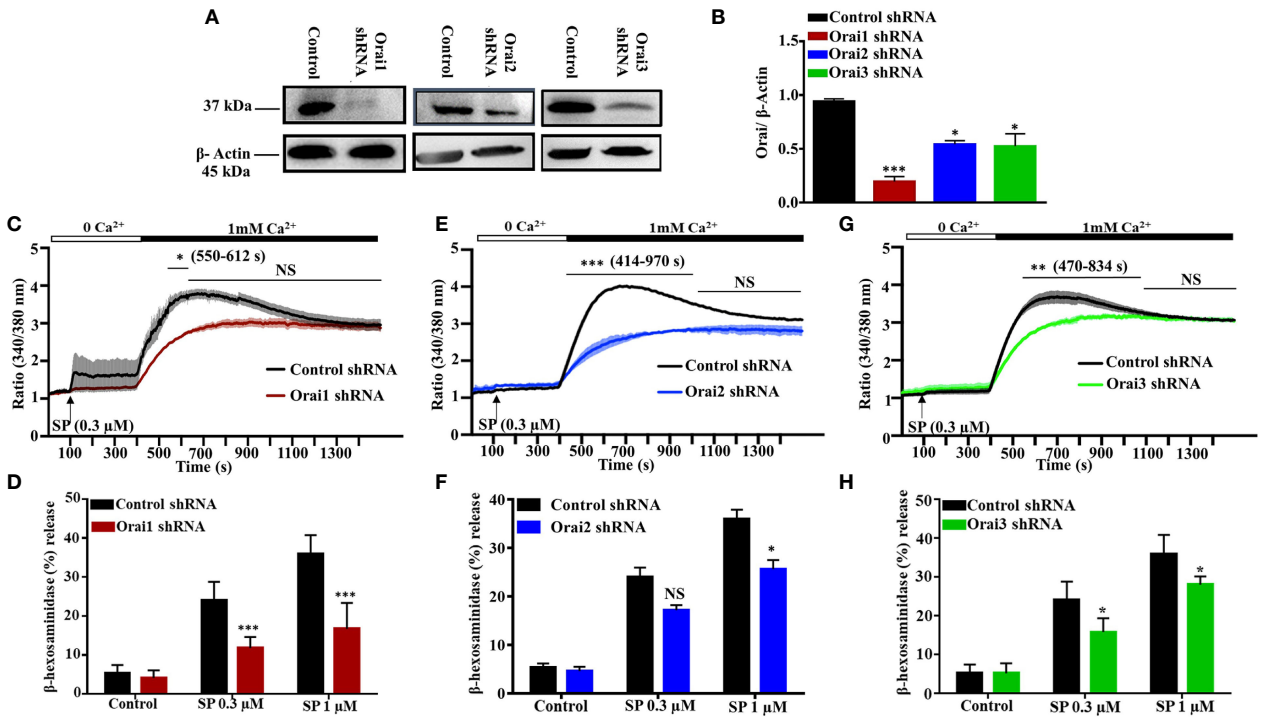


FIGURE 1 | Lentiviral shRNA-Mediated Knockdown of Orai1, Orai2, and Orai3 Reduces SP-Induced Responses in LAD2 Cells. **(A)** Knockdown efficiency of each Orai channel was determined by western blotting in cells transduced with non-targeted (control) or Orai-specific shRNA and a representative blot is shown. **(B)** Quantification of Orai knockdown is represented as bar graph of relative intensities of Orai protein bands normalized to respective β-Actin. **(C, E, G)** Cells were loaded with Fura-2AM, resuspended in Ca^{2+}-free buffer (1.5 ml) and measurement of intracellular Ca^{2+} mobilization was initiated *via* the addition of SP (0.3 μM, at 100s). At 400 s, Ca^{2+} concentration of the buffer was increased to 1 mM *via* the addition of 1.5 μl of 1 M calcium and influx was measured for additional 18 min. **(D, F, H)** Effects of Orai knockdown on SP-induced degranulation, as measured by β-hexosaminidase release. Data presented are mean ± SEM of N = 4 experiments. Statistical significance was determined by two-way ANOVA with Tukey's multiple comparisons at a value ***p < 0.001, **p < 0.01, *p < 0.05, and NS, "not significant".

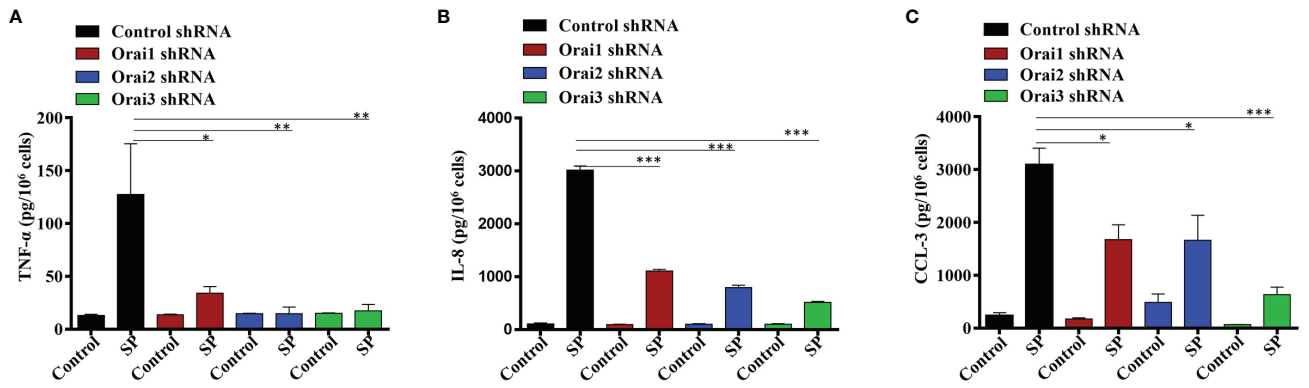


FIGURE 2 | Orai1, Orai2, and Orai3 contribute to SP-Induced Cytokines Generation in LAD2 Cells. LAD2 cells with shRNA-mediated knockdown of each Orai channel or non-targeted (control) cells were exposed to SP (1 μM, for 24 h). Culture supernatants were used to quantitate **(A)** TNF-α, **(B)** IL-8 and **(C)** CCL-3 by ELISA. Data presented are mean ± SEM of N = 3 experiments. Statistical significance was determined by one-way ANOVA with Tukey's multiple comparisons at a value ***$p < 0.001$, **$p < 0.01$ and *$p < 0.05$.

on SP-induced Ca^{2+} influx, degranulation and cytokine/chemokine production. Pretreatment of LAD2 cells with Synta66 (10 μM) resulted in substantial reduction of SP-induced Ca^{2+} influx (**Figure 3A**) but complete inhibition of degranulation (**Figure 3B**), TNF-α, IL-8 and CCL-3 generation (**Figures 3C–E**). Involvement of extracellular signal-regulated kinases 1/2 (ERK1/2) and Akt pathways in cytokine production in MCs are well documented (30, 31). Furthermore, MRGPRX2-mediated MC activation leads to increased ERK1/2 and Akt phosphorylation (32, 33). STIM-1 inhibitor SKF pretreatment caused inhibition of ERK1/2 and Akt phosphorylation in LL-37 stimulated MCs *via* MRGPRX2 (25). We therefore sought to determine the effects of Synta66 on ERK1/2 and Akt phosphorylation in LAD2 cells. As shown in **Figures 3F–H**, SP stimulation resulted in time dependent enhanced ERK1/2 and Akt (Ser473) phosphorylation, which were significantly inhibited by Synta66.

Synta66 Inhibits SP-Induced Ca^{2+} Influx and Degranulation in Primary Human Skin MCs

In addition to LAD2 cells, SP causes degranulation in human skin MCs *via* MRGPRX2 (24, 34). To determine the biological relevance of studies with LAD2 cells, we tested the effect of Synta66 on SP-induced Ca^{2+} influx and degranulation in primary human skin-derived MCs isolated from three different donors. Initially, cell surface expression of MRGPRX2 in skin MCs was tested by flow cytometry. Representative flow cytometry traces for MRGPRX2 expression in skin MCs from three healthy donors are shown in **Supplementary Figure 1**. We found that SP triggered Ca^{2+} influx and degranulation in skin-derived MCs in all three donors (**Figures 4A–F**). Stimulation of human skin-derived MCs with SP resulted in Ca^{2+} mobilization from both intracellular stores as well as Ca^{2+} influx from the extracellular medium (**Figures 4A, C, E**). Synta66 (10 μM) specifically blocked Ca^{2+} influx with no effect on intracellular Ca^{2+} release (**Figures 4A, C, E**). Synta66 also caused significant inhibition in SP-induced degranulation in skin-derived MCs (**Figures 4B, D, F**).

Synta66 Attenuates SP-Induced Degranulation in Mouse PMCs *In Vitro* and Vascular Permeability and Peritonitis *In Vivo*

Our next goal was to determine the effect of Synta66 on MrgprB2-mediated responses in primary mouse PMCs *in vitro* and biological responses *in vivo*. First, we used PMCs from wild-type (WT) and $MrgprB2^{-/-}$ mice to confirm that SP causes degranulation in PMCs *via* MrgprB2. As shown in **Supplementary Figure 2**, SP caused degranulation in WT-PMCs which is completely abrogated in $MrgprB2^{-/-}$ PMCs. Furthermore, we found that Synta66 (10 μM) ablated SP-induced degranulation in mouse PMCs, as measured by both β-hexosaminidase release and cell surface expression of LAMP-1 by flow cytometry (**Figures 5A, B**). Gating strategy for LAMP-1 expression by flow cytometry was shown in **Supplementary Figure 3**. To determine the effect of blocking Orai channels on mouse cutaneous MCs degranulation *in vivo*, we administered Synta66 or vehicle intraperitoneally (i.p) followed by Evans blue dye injection through intravenous route. SP was then injected into one ear and vehicle into the other. The data presented in **Figure 5C** clearly demonstrate that, consistent with its effect on human skin MCs (**Figure 4**), Synta66 inhibited murine cutaneous MC degranulation *in vivo* as determined by a significant reduction in SP-induced Evans blue dye extravasation.

We also sought to determine if Synta66 inhibits cytokine production and the recruitment of inflammatory cells *in vivo*. Mice were injected (i.p) with Synta66 prior to intraperitoneal injection with SP or vehicle. Three hours later, serum TNF-α concentration and neutrophil recruitment in peritoneal lavage ($CD45^+CD11b^+Ly6G^+$ live cells) were quantitated. As shown in

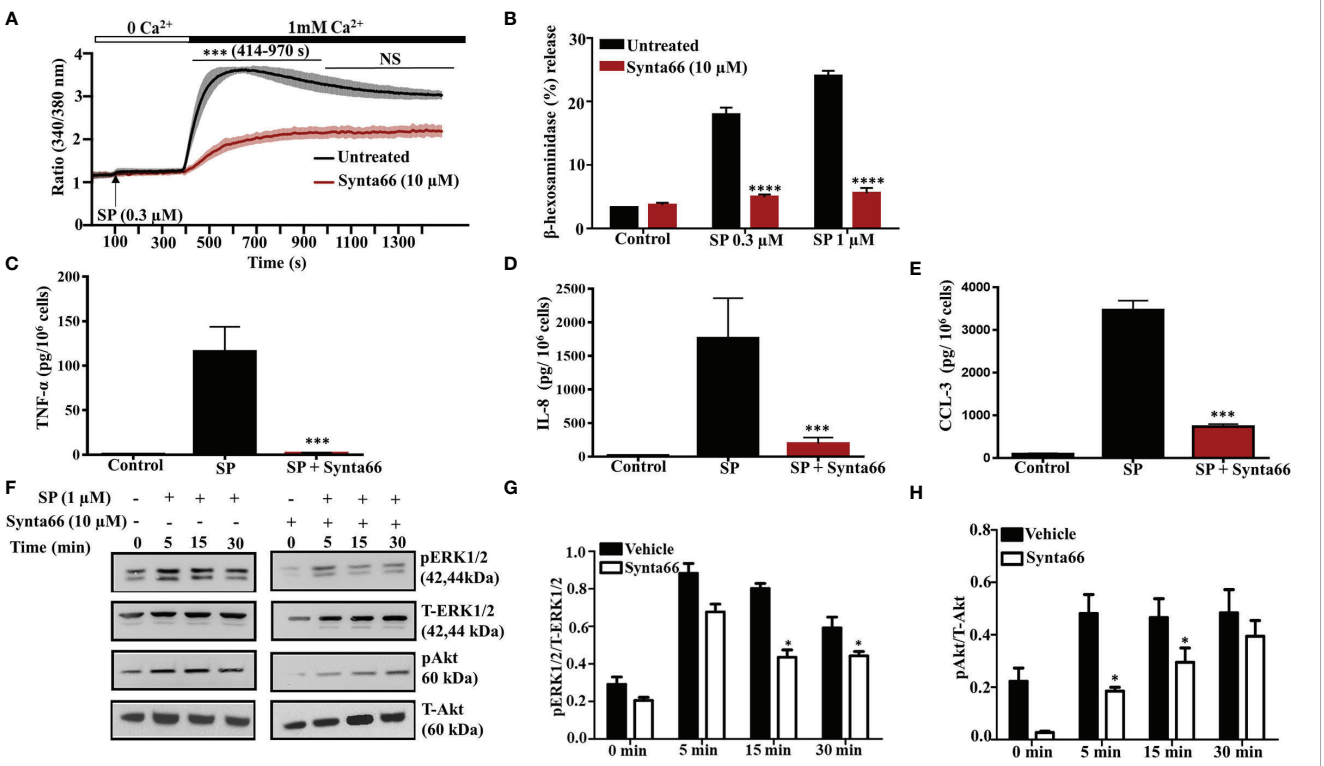


FIGURE 3 | Synta66 Causes Substantial Inhibition of SP-Induced Responses in LAD2 Cells. **(A)** Fura-2AM-loaded LAD2 cells were preincubated with Synta66 (10 µM, 30 min) in Ca^{2+}-free buffer and the measurement of intracellular Ca^{2+} mobilization was initiated *via* the addition of SP (0.3 µM) at 100 s. After 400 s, Ca^{2+} concentration of the buffer was increased to 1 mM and Ca^{2+} measurement was continued for additional 18 min **(B)** LAD2 cells were preincubated with Synta66 (10 µM, 5 min), stimulated with the indicated concentrations of SP and β-hexosaminidase release was determined. **(C–E)** Cells were preincubated with Synta66 (10 µM, 30 min) and stimulated with SP (1 µM for 24 h) and culture supernatants were used to measure TNF-α, IL-8 and CCL-3. **(F)** Synta66-preincubated cells were stimulated with SP for different time points and western blotting was performed on cell lysate with anti-pERK1/2, anti-pAkt, total anti-ERK1/2 and total anti-Akt antibodies. **(G, H)** Bar graphs represent relative intensities of bands of phosphoproteins normalized to respective total proteins. Data presented are mean ± SEM of N = 3 experiments. Statistical significance comparing multiple groups was determined by one-way ANOVA with Tukey's multiple comparisons at a value ****p <0.0001, ***p <0.001, and NS, "not significant" **(A–E)**. Statistical significance was determined by Student's t-test at a value *p < 0.05 **(G, H)**.

Figure 5D, serum TNF-α level was significantly reduced in Synta66-treated mice. SP injection caused recruitment of inflammatory cells at peritoneal cavity and Synta66 substantially inhibited SP-induced leukocyte recruitment especially neutrophils (**Figures 5E–G** and **Supplementary Figure 4**).

DISCUSSION

Ca^{2+} is an indispensable second messenger signaling for agonist induced MC activation and mediator release (35). FcεRI and MRGPRX2-mediated signaling utilize both shared and distinct pathways that lead to Ca^{2+} mobilization and degranulation. Both FcεRI and MRGPRX2 mediated signaling caused comparable level of Ca^{2+} mobilization, however there is marked differences in spatiotemporal pattern of granule exocytosis and mediator content (16). Moreover, FcεRI stimulation cause PLCγ dependent Ca^{2+} influx while MRGPRX2 couples to Gαq to promote Ca^{2+} influx (35, 36). Identification of Ca^{2+} channel in FcεRI-mediated signaling is well characterized and Orai plays a crucial role in antigen-IgE-dependent MC activation (6–8, 37, 38). However, the possibility that MC activation *via* MRGPRX2/MrgprB2 requires Orai channels has not been determined. Using shRNA-mediated knockdown of Orai1/Orai2/Orai3 and a pharmacological inhibitor, we provide the first demonstration that Orai channels are involved in MRGPRX2/MrgprB2-mediated MC activation *in vitro* and vascular permeability and leukocytes recruitment *in vivo*.

Ashmole et al. demonstrated that transcripts of all three known Orai channels are expressed in human lung MCs. Moreover, Orai1 mRNA is most abundant isoform in human lung MCs (6). However, our data showed comparable expression of all three Orai proteins in LAD2 cells which suggests there might be variable level expression of Orai isoforms in different MC lineage. Knockdown of Orai1 resulted in inhibition of FcεRI-dependent Ca^{2+} influx and mediator release (7). Similarly, we found that Orai1 significantly contributes to MRGPRX2-mediated Ca^{2+} influx and mediator release in LAD2 cells. Tsvilovskyy et al., recently showed that absence of Orai2 in mouse PMCs results in enhanced FcεRI and MrgprB2-mediated

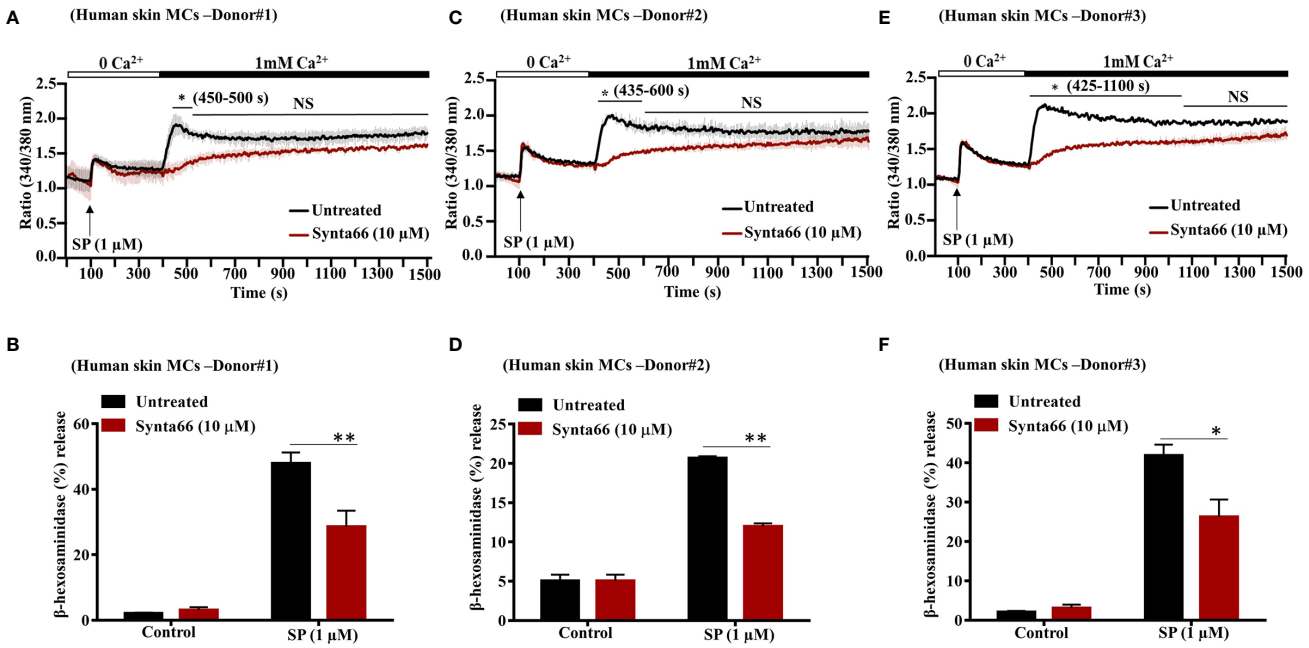


FIGURE 4 | Synta66 inhibits SP-induced Ca^{2+} influx and degranulation in Human Skin Derived MCs. **(A, C, E)** MCs from three donors were pretreated with Synta66 (10 µM, 30 min) and intracellular Ca^{2+} influx was determined in **(B, D, F)**. MCs were preincubated with Synta66, stimulated with SP (1 µM) and β-hexosaminidase release was determined. Data shown are mean ± SEM of three individual experiments from three donors. Statistical significance was determined by two-way ANOVA with Tukey's multiple comparisons at a value **p < 0.01, *p < 0.05, and NS, "not significant".

Ca^{2+} mobilization and degranulation when compared to control cells (38). Based on this finding, it was proposed that Orai2 serves as a negative regulator for MCs degranulation *via* two possible mechanisms. One involving the formation of a heterodimer with Orai1 and thus preventing its activation and the other resulting in the formation of Orai2-STIM-1 complex rendering insufficient STIM-1 available for Orai1 activation. However, shRNA-mediated downregulation of Orai2 in human lung MCs has marginal inhibitory effects on IgE-mediated Ca^{2+} mobilization and degranulation (7). Our data demonstrated that although Orai2 knockdown caused significant reduction in Ca^{2+} mobilization, it has minimum effect on degranulation. The reason for the difference is not clear but could reflect differences in the expression level of Orai1 and Orai2 in human and rodent MCs. Thus, while human lung MCs and LAD2 cells express Orai1 at >10-fold higher than that of Orai2, rodent MCs express both proteins at similar levels (8, 39). In addition, unlike Orai1, majority of the Orai2 is found in intracellular sites in rat basophilic leukemia (RBL-2H3) cells and the possibility that intracellular Orai2 could modulate Ca^{2+} influx has been suggested but the mechanism is not clear (39). Ashmole et al., successfully utilized adenoviral shRNA to silence the expression of Orai1 and Orai2 but not Orai3 in human lung MCs (7). However, our attempt to knockdown Orai3 in LAD2 cells using lentiviral shRNA was more successful and resulted in partial reduction in SP-induced Ca^{2+} influx and degranulation.

Given that Orai1 and Orai3 are expressed at similar levels in human primary MCs and LAD2 cells, it is possible that Orai1:Orai3 dimer contributes to SP-induced signaling and mediator release (8). Because we were unable to silence the expression of Orai3 to >50% in LAD2 cells, it was not feasible to simultaneously reduce the expression both Orai1 and Orai3. Synta66 is an established pharmacological inhibitor that blocks homo- and heterodimer formation of Orai channel (29). Furthermore, Synta66 causes substantial inhibition of IgE-mediated degranulation in human lung MCs and LAD2 cells and blocks allergen-induced bronchial smooth muscle contraction *ex vivo* (6, 7). However, because Orai2 is expressed at low level in MCs and found predominantly in the cytoplasm, any inhibitory effect of Synta66 likely reflects its ability to target Orai1 and Orai3 (8, 39). Here, we also found that Synta66 caused complete inhibition of SP-induced Ca^{2+} influx and degranulation, indicating probable involvement of Orai1:Orai3 dimer in MRGPRX2-mediated MC activation. Along with cultured MCs, Synta66 exhibited similar inhibitory effect on primary human skin-derived MCs indicating its biological relevance.

Calcium influx initiates a cascade of downstream signaling that lead to calmodulin–calcineurin dependent NFAT1 and NF-κβ activation resulted in transcription of cytokine genes (40, 41). Calcium-dependent NFAT activation caused IL-17 and TNF-α secretion associated with autoimmune disease rheumatoid arthritis (42). Orai1 also modulates Th1 and Th17 responses in experimental autoimmune encephalomyelitis (43). Moreover, Orai also contributes FcεRI-mediated release of an array of inflammatory cytokines such as TNF-α, IL-5, IL-6, IL-8, and IL-13 from human lung MCs (8). The data presented herein

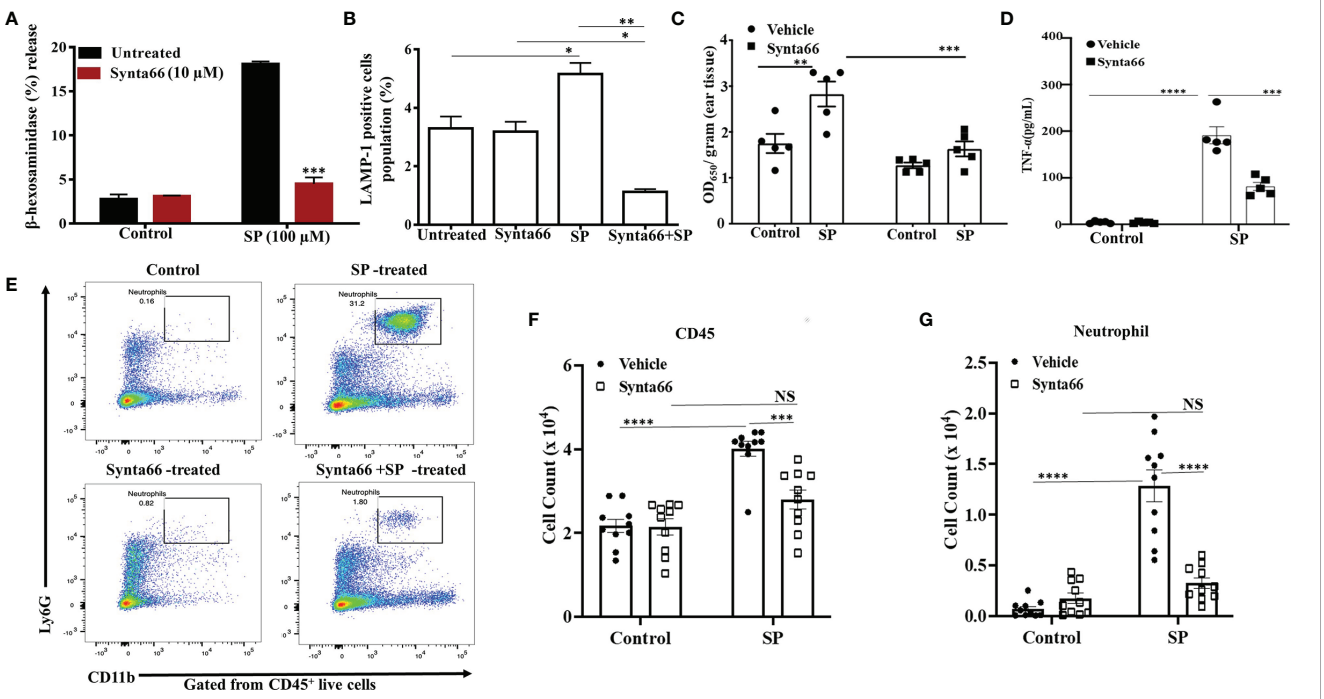


FIGURE 5 | Synta66 Attenuates SP-Induced Murine MC Responses *in vitro* and *in vivo*. SP-induced **(A)** β-hexosaminidase release (N = 4) and **(B)** LAMP-1 expression as determined by flow cytometry on PMCs (N = 3). **(C)** Synta66 or vehicle was administered *via* i.p. injection prior to SP injection in one ear and the buffer control in the other. Vascular permeability was quantified by measuring Evans blue extravasation. Synta66-treated or untreated mice were injected (i.p) with SP. After 3 h, blood and peritoneal lavage fluid was collected (N = 5). **(D)** Serum TNF-α was determined by ELISA, N = 5. **(E)** Representative FACS images showing neutrophil recruitment and numbers indicate the percentage of $CD45^+CD11b^+$ $Ly6G^+$ live cells in peritoneal cavity. The absolute number of immune cells was calculated from the flow cytometry profile for each mouse based on gated (50,000 cells) population **(F)** Total $CD45^+$ cells, and **(G)** Total neutrophil counts. Data presented are mean ± SEM of N = 10. Statistical significance was determined by two-way ANOVA with Sidak's multiple comparisons at a value ****$p < 0.0001$, ***$p < 0.001$, **$p < 0.01$, *$p < 0.05$ and NS, "not significant".

demonstrate that knockdown of individual Orai channel significantly reduce proinflammatory cytokine/chemokine secretion. Blocking of Orai channel using pharmacological inhibitor showed complete ablation of cytokine/chemokine generation which may be due to its inhibitory effect on multiple Orai isoforms. In agreement with the cytokine production Synta66 pretreatment caused inhibition of ERK1/2 and Akt phosphorylation.

As for human MCs, rodent MCs also express all three Orai family members (44). Orai1 plays a predominant role in Ca^{2+} signaling in murine T-cells *in vitro* and *in vivo*. Nonfunctional Orai1 knock-in mice showed impaired Ca^{2+} influx *in vitro* and reduced delayed hypersensitivity and colitis *in vivo* (45). Although mutation in Orai1 in human patient has no major phenotypic effect, $Orai1^{-/-}$ mice cannot survive (46–48). Therefore, use of pharmacological inhibitor for Orai could overcome the lethality associated with genetic deletion of Orai1 *in vivo*. Our data on isolated peritoneal MCs demonstrated complete inhibition of SP-induced degranulation by Synta66. MC degranulation is associated with enhanced vascular permeability and cutaneous anaphylaxis. Synta66 pretreatment inhibited SP-induced vascular permeability (early MC response) and reduced immune cell recruitment and cytokine production (delayed MC response).

In conclusion, we have utilized gene-silencing and pharmacological strategies to show that multiple Orai/CRAC channels contribute to SP-induced MRGPRX2-mediated Ca^{2+} influx, degranulation, TNF-α, IL-8 and CCL-3 generation in MCs *in vitro*. Most importantly, we found that SP-induced increased vascular permeability and neutrophil recruitment, which are mediated *via* MrgprB2, are blocked by Synta66. These findings suggest that Orai channel inhibitors could serve as a novel strategy for the modulation of neurogenic inflammation, pain, chronic urticaria, mastocytosis and atopic dermatitis.

DATA AVAILABILITY STATEMENT

The original contributions presented in the study are included in the article/**Supplementary Material**. Further inquiries can be directed to the corresponding author.

ETHICS STATEMENT

The studies involving human participants were reviewed and approved by the Internal Review Board at the University of South

Carolina. The patients/participants provided their written informed consent to participate in this study. The animal study was reviewed and approved by the Institutional Animal Care and Use Committee at University of Pennsylvania.

AUTHOR CONTRIBUTIONS

HA contributed to conception, supervision and funding acquisition of the study. SC, IA, SR, and AA performed experiments and analyzed the data. SC, SR, and HA wrote the first draft of the manuscript. YH and CO provided human skin MCs for the study. All authors contributed to the article and approved the submitted version.

FUNDING

This work was supported by the National Institutes of Health grants R01-AI124182, R01-AI143185 and R01-AI149487 to HA, and R21-AR067996 and P20 GM-103641 to CO.

ACKNOWLEDGMENTS

We thank the FACS core facility of the School of Dental Medicine, University of Pennsylvania, for flow cytometry data acquisition and analysis. We also thank Drs. Arnold Kirshenbaum and Dean Metcalfe (NIAID/NIH) for providing a human MC line LAD2 cells.

SUPPLEMENTARY MATERIAL

The Supplementary Material for this article can be found online at: https://www.frontiersin.org/articles/10.3389/fimmu.2021.803335/full#supplementary-material

Supplementary Figure 1 | Cell Surface Expression of MRGPRX2 in Human Skin MCs from Three Donors. Skin MCs were incubated with PE-conjugated anti-MRGPRX2 antibody (blue histograms) or isotype control antibody (grey histograms) and receptor expression was assessed by flow cytometry N=3.

Supplementary Figure 2 | SP Induces Degranulation in Mouse PMCs *via* MrgprB2. Peritoneal MCs from WT and MrgprB2$^{-/-}$ mice were exposed to SP and β-hexosaminidase release was determined. Data presented are mean ± SEM of N=3 experiments. Statistical significance was determined by two-way ANOVA with Tukey's multiple comparisons at a value ***$p < 0.001$.

Supplementary Figure 3 | Flow Cytometry Gating Strategy of LAMP1 Expression in PMCs N=3.

Supplementary Figure 4 | Flow cytometry gating strategy of peritoneal lavage immune cells. Numbers indicate the percentage of cells pre-gated on viability. Debris- cells, single cells, CD45$^+$ live cells, CD45$^+$CD11b$^+$Ly6G$^+$ live cells (neutrophils).

REFERENCES

1. Galli SJ, Gaudenzio N, Tsai M. Mast Cells in Inflammation and Disease: Recent Progress and Ongoing Concerns. *Annu Rev Immunol* (2020) 38:49–77. doi: 10.1146/annurev-immunol-071719-094903
2. Shaw PJ, Feske S. Physiological and Pathophysiological Functions of SOCE in the Immune System. *Front Biosci* (2012) 4:2253–68. doi: 10.2741/e540
3. Prakriya M, Feske S, Gwack Y, Srikanth S, Rao A, Hogan PG. Orai1 Is an Essential Pore Subunit of the CRAC Channel. *Nature* (2006) 443(7108):230–3. doi: 10.1038/nature05122
4. Derler I, Jardin I, Romanin C. Molecular Mechanisms of STIM/Orai Communication. *Am J Physiol Cell Physiol* (2016) 310(8):C643–62. doi: 10.1152/ajpcell.00007.2016
5. Vig M, DeHaven WI, Bird GS, Billingsley JM, Wang H, Rao PE, et al. Defective Mast Cell Effector Functions in Mice Lacking the CRACM1 Pore Subunit of Store-Operated Calcium Release-Activated Calcium Channels. *Nat Immunol* (2008) 9:89–96. doi: 10.1038/ni1550
6. Ashmole I, Duffy SM, Leyland ML, Morrison VS, Begg M, Bradding P. CRACM/Orai Ion Channel Expression and Function in Human Lung Mast Cells. *J Allergy Clin Immunol* (2012) 129:1628–35.e2. doi: 10.1016/j.jaci.2012.01.070
7. Ashmole I, Duffy SM, Leyland ML, Bradding P. The Contribution of Orai (CRACM)1 and Orai(CRACM)2 Channels in Store-Operated Ca2+ Entry and Mediator Release in Human Lung Mast Cells. *PloS One* (2013) 8:e74895. doi: 10.1371/journal.pone.0074895
8. Wajdner HE, Farrington J, Barnard C, Peachell PT, Schnackenberg CG, Marino JP Jr, et al. Orai and TRPC Channel Characterization in Fcεri-Mediated Calcium Signaling and Mediator Secretion in Human Mast Cells. *Physiol Rep* (2017) 5(5):e13166. doi: 10.14814/phy2.13166
9. Roy S, Chalatip CAN, Thapaliya M, Deepak V, Ali H. Multifaceted MRGPRX2: New Insight Into the Role of Mast Cells in Health and Disease. *J Allergy Clin Immunol* (2021) 148(2):293–308. doi: 10.1016/j.jaci.2021.03.049
10. Amponnawarat A, Chalatip CAN, Ali H. Murepavadin, A Small Molecule Host Defense Peptide Mimetic, Activates Mast Cells *via* MRGPRX2 and Mrgprb2. *Front Immunol* (2021) 12:689410. doi: 10.3389/fimmu.2021.689410
11. Van der Does AM, Bergman P, Agerberth B, Lindbom L. Induction of the Human Cathelicidin LL-37 as a Novel Treatment Against Bacterial Infections. *J Leukoc Biol* (2012) 92(4):735–42. doi: 10.1189/jlb.0412178
12. Brzezinska-Blaszczyk E, Zalewska A. *In Vitro* Reactivity of Mast Cells in Urticaria Pigmentosa Skin. *Arch Dermatol Res* (1998) 290:14–7. doi: 10.1007/s004030050270
13. Deepak V, Komarow HD, Alblaihess AA, Carter MC, Metcalfe DD, Ali H. Expression of MRGPRX2 in Skin Mast Cells of Patients With Maculopapular Cutaneous Mastocytosis. *J Allergy Clin Immunol Pract* (2021) 9(10):3841–3.e1. doi: 10.1016/j.jaip.2021.05.042
14. Serhan N, Basso L, Sibilano R, Petitfils C, Meixiong J, Bonnart C, et al. House Dust Mites Activate Nociceptor-Mast Cell Clusters to Drive Type 2 Skin Inflammation. *Nat Immunol* (2019) 20:1435–43. doi: 10.1038/s41590-019-0493-z
15. Green DP, Limjunyawong N, Gour N, Pundir P, Dong X. A Mast-Cell-Specific Receptor Mediates Neurogenic Inflammation and Pain. *Neuron* (2019) 101:412–20.e3. doi: 10.1016/j.neuron.2019.01.012
16. Gaudenzio N, Sibilano R, Marichal T, Starkl P, Reber LL, Cenac N, et al. Different Activation Signals Induce Distinct Mast Cell Degranulation Strategies. *J Clin Invest* (2016) 126:3981–98. doi: 10.1172/JCI85538
17. Alkanfari I, Freeman KB, Roy S, Jahan T, Scott RW, Ali H. Small-Molecule Host-Defense Peptide Mimetic Antibacterial and Antifungal Agents Activate Human and Mouse Mast Cells *via* Mas-Related GPCRs. *Cells* (2019) 8:311. doi: 10.3390/cells8040311
18. Chalatip CAN, Amponnawarat A, Roy S, Carol AO, Ali H. MRGPRX2 Activation by Rocuronium: Insight From Studies With Human Skin Mast Cells and Missense Variants. *Cells* (2021) 10:156. doi: 10.3390/cells10010156
19. Kambe N, Kambe M, Kochan JP, Schwartz LB. Human Skin-Derived Mast Cells can Proliferate While Retaining Their Characteristic Functional and

Protease Phenotypes. *Blood* (2001) 97(7):2045–52. doi: 10.1182/blood.V97.7.2045
20. Roy S, Gupta K, Ganguly A, Ali H. β-Arrestin2 Expressed in Mast Cells Regulates Ciprofloxacin-Induced Pseudoallergy and IgE-Mediated Anaphylaxis. *J Allergy Clin Immunol* (2019) 144(2):603–6. doi: 10.1016/j.jaci.2019.04.024
21. Roy S, Ganguly A, Haque M, Ali H. Angiogenic Host Defense Peptide AG-30/5C and Bradykinin B2 Receptor Antagonist Icatibant Are G Protein Biased Agonists for MRGPRX2 in Mast Cells. *J Immunol* (2019) 202:1229–38. doi: 10.4049/jimmunol.1801227
22. Chalatip CAN, Roy S, Alkanfari I, Ganguly A, Ali H. Identification of Gain and Loss of Function Missense Variants in MRGPRX2's Transmembrane and Intracellular Domains for Mast Cell Activation by Substance P. *Int J Mol Sci* (2019) 20:5247. doi: 10.3390/ijms20215247
23. Luissint AC, Williams HC, Kim W, Flemming S, Azcutia V, Hilgarth RS, et al. Macrophage-Dependent Neutrophil Recruitment Is Impaired Under Conditions of Increased Intestinal Permeability in JAM-Adeficient Mice. *Mucosal Immunol* (2019) 12:668–78. doi: 10.1038/s41385-019-0143-7
24. Fujisawa D, Kashiwakura J, Kita H, Kikukawa Y, Fujitani Y, Sasaki-Sakamoto T, et al. Expression of Mas-Related Gene X2 on Mast Cells Is Upregulated in the Skin of Patients With Severe Chronic Urticaria. *J Allergy Clin Immunol* (2014) 134:622–33.e9. doi: 10.1016/j.jaci.2014.05.004
25. Occhiuto CJ, Kammala AK, Yang C, Nellutla R, Garcia M, Gomez G, et al. Store-Operated Calcium Entry *via* STIM1 Contributes to MRGPRX2 Induced Mast Cell Functions. *Front Immunol* (2019) 10:3143. doi: 10.3389/fimmu.2019.03143
26. Baraniak JHJr., Zhou Y, Nwokonko RM, Jennette MR, Kazzaz SA, Stenson JM, et al. Orai Channel C-Terminal Peptides Are Key Modulators of STIM-Orai Coupling and Calcium Signal Generation. *Cell Rep* (2021) 35:109322. doi: 10.1016/j.celrep.2021.109322
27. Berry CT, May MJ, Freedman BD. STIM- and Orai-Mediated Calcium Entry Controls NF-KappaB Activity and Function in Lymphocytes. *Cell Calcium* (2018) 74:131–43. doi: 10.1016/j.ceca.2018.07.003
28. Yoast RE, Emrich SM, Zhang X, Xin P, Johnson MT, Fike AJ, et al. The Native ORAI Channel Trio Underlies the Diversity of Ca(2+) Signaling Events. *Nat Commun* (2020) 11:2444. doi: 10.1038/s41467-020-16232-6
29. Zhang X, Xin P, Yoast RE, Emrich SM, Johnson MT, Pathak T, et al. Distinct Pharmacological Profiles of ORAI1, ORAI2, and ORAI3 Channels. *Cell Calcium* (2020) 91:102281. doi: 10.1016/j.ceca.2020.102281
30. Subramanian H, Gupta K, Parameswaran N, Ali H. Regulation of Fc∈RI Signaling in Mast Cells by G Protein-Coupled Receptor Kinase 2 and Its RH Domain. *J Biol Chem* (2014) 289:20917–27. doi: 10.1074/jbc.M113.523969
31. Xie G, Wang F, Peng X, Liang Y, Yang H, Li L. Modulation of Mast Cell Toll-Like Receptor 3 Expression and Cytokines Release by Histamine. *Cell Physiol Biochem* (2018) 46(6):2401–11. doi: 10.1159/000489646
32. Kiatsurayanon C, Niyonsaba F, Chieosilapatham P, Okumura K, Ikeda S, Ogawa H. Angiogenic Peptide (AG)-30/5C Activates Human Keratinocytes to Produce Cytokines/Chemokines and to Migrate and Proliferate *via* MrgX Receptors. *J Dermatol Sci* (2016) 83:190–9. doi: 10.1016/j.jdermsci.2016.05.006
33. Salzer S, Kresse S, Hirai Y, Koglin S, Reinholz M, Ruzicka T, et al. Cathelicidin Peptide LL-37 Increases UVB-Triggered Inflammasome Activation: Possible Implications for Rosacea. *J Dermatol Sci* (2014) 76:173–9. doi: 10.1016/j.jdermsci.2014.09.002
34. Wang Z, Franke K, Zuberbier T, Babina M. Cytokine Stimulation *via* MRGPRX2 Occurs With Lower Potency Than FceRI-Aggregation But With Similar Dependence on the ERK1/2 Module in Human Skin Mast Cells. *J Invest Dermatol* (2021) S0022–202X(21)01655-9. doi: 10.1016/j.jid.2021.07.153
35. Holowka D, Calloway N, Cohen R, Gadi D, Lee J, Smith NL, et al. Roles for Ca (2+) Mobilization and Its Regulation in Mast Cell Functions. *Front Immunol* (2012) 3:104. doi: 10.3389/fimmu.2012.00104
36. Robas N, Mead E, Fidock M. MrgX2 Is a High Potency Cortistatin Receptor Expressed in Dorsal Root Ganglion. *J Biol Chem* (2003) 278(45):44400–4. doi: 10.1074/jbc.M302456200
37. Solís-López A, Kriebs U, Marx A, Mannebach S, Liedtke WB, Caterina MJ, et al. Analysis of TRPV Channel Activation by Stimulation of Fcεri and MRGPR Receptors in Mouse Peritoneal Mast Cells. *PloS One* (2017) 12(2):e0171366. doi: 10.1371/journal.pone.0171366
38. Tsvilovskyy V, Solis-Lopez A, Schumacher D, Medert R, Roers A, Kriebs U, et al. Deletion of Orai2 Augments Endogenous CRAC Currents and Degranulation in Mast Cells Leading to Enhanced Anaphylaxis. *Cell Calcium* (2018) 71:24–33. doi: 10.1016/j.ceca.2017.11.004
39. Ikeya M, Yamanoue K, Mochizuki Y, Konishi H, Tadokoro S, Tanaka M, et al. Orai-2 Is Localized on Secretory Granules and Regulates Antigen-Evoked Ca (2)(+) Mobilization and Exocytosis in Mast Cells. *Biochem Biophys Res Commun* (2014) 451:62–7. doi: 10.1016/j.bbrc.2014.07.060
40. Dolmetsch RE, Lewis RS, Goodnow CC, Healy JI. Differential Activation of Transcription Factors Induced by Ca2+ Response Amplitude and Duration. *Nature* (1997) 386(6627):855–8. doi: 10.1038/386855a0
41. Gwack Y, Feske S, Srikanth S, Hogan PG, Rao A. Signalling to Transcription: Store-Operated Ca^{2+} Entry and NFAT Activation in Lymphocytes. *Cell Calcium* (2007) 42:145–56. doi: 10.1016/j.ceca.2007.03.007
42. Miskin JE, Abrams CC, Goatley LC, Dixon LK. A Viral Mechanism for Inhibition of the Cellular Phosphatase Calcineurin. *Science* (1998) 281:562–5. doi: 10.1126/science.281.5376.562
43. Kaufmann U, Shaw PJ, Kozhaya L, Subramanian R, Gaida K, Unutmaz D, et al. Selective ORAI1 Inhibition Ameliorates Autoimmune Central Nervous System Inflammation by Suppressing Effector But Not Regulatory T Cell Function. *J Immunol* (2016) 196:573–85. doi: 10.4049/jimmunol.1501406
44. Clemens RA, Lowell CA. CRAC Channel Regulation of Innate Immune Cells in Health and Disease. *Cell Calcium* (2019) 78:56–65. doi: 10.1016/j.ceca.2019.01.003
45. McCarl CA, Khalil S, Ma J, Oh-hora M, Yamashita M, Roether J, et al. Store-Operated Ca^{2+} Entry Through ORAI1 Is Critical for T Cell-Mediated Autoimmunity and Allograft Rejection. *J Immunol* (2010) 185(10):5845–58. doi: 10.4049/jimmunol.1001796
46. Feske S. ORAI1 and STIM1 Deficiency in Human and Mice: Roles of Storeoperated Ca2+ Entry in the Immune System and Beyond. *Immunol Rev* (2009) 231:189–209. doi: 10.1111/j.1600-065X.2009.00818.x
47. Braun A, Varga-Szabo D, Kleinschnitz C, Pleines I, Bender M, Austinat M, et al. Orai1 (CRACM1) Is the Platelet SOC Channel and Essential for Pathological Thrombus Formation. *Blood* (2009) 113:2056–63. doi: 10.1182/blood-2008-07-171611
48. Bergmeier W, Oh-Hora M, McCarl CA, Roden RC, Bray PF, Feske S. R93W Mutation in Orai1 Causes Impaired Calcium Influx in Platelets. *Blood* (2009) 113:675–8. doi: 10.1182/blood-2008-08-174516

Conflict of Interest: The authors declare that the research was conducted in the absence of any commercial or financial relationships that could be construed as a potential conflict of interest.

Publisher's Note: All claims expressed in this article are solely those of the authors and do not necessarily represent those of their affiliated organizations, or those of the publisher, the editors and the reviewers. Any product that may be evaluated in this article, or claim that may be made by its manufacturer, is not guaranteed or endorsed by the publisher.

Copyright © 2022 Chaki, Alkanfari, Roy, Amponnawarat, Hui, Oskeritzian and Ali. This is an open-access article distributed under the terms of the Creative Commons Attribution License (CC BY). The use, distribution or reproduction in other forums is permitted, provided the original author(s) and the copyright owner(s) are credited and that the original publication in this journal is cited, in accordance with accepted academic practice. No use, distribution or reproduction is permitted which does not comply with these terms.

frontiers in Immunology

ORIGINAL RESEARCH
published: 24 January 2022
doi: 10.3389/fimmu.2022.794974

Autocrine/Paracrine Loop Between SCF$^+$/c-Kit$^+$ Mast Cells Promotes Cutaneous Melanoma Progression

Tiziana Annese[1], *Roberto Tamma*[1], *Mariella Bozza*[2], *Alfredo Zito*[2] *and Domenico Ribatti*[1]*

[1] Department of Basic Medical Sciences, Neurosciences and Sensory Organs, University of Bari Medical School, Bari, Italy,
[2] Istituto di Ricovero e Cura a Carattere Scientifico (IRCCS) Istituto Tumori Giovanni Paolo II, Bari, Italy

c-Kit, or mast/stem cell growth factor receptor Kit, is a tyrosine kinase receptor structurally analogous to the colony-stimulating factor-1 (CSF-1) and platelet-derived growth factor (PDGF) CSF-1/PDGF receptor Tyr-subfamily. It binds the cytokine KITLG/SCF to regulate cell survival and proliferation, hematopoiesis, stem cell maintenance, gametogenesis, mast cell development, migration and function, and it plays an essential role in melanogenesis. SCF and c-Kit are biologically active as membrane-bound and soluble forms. They can be expressed by tumor cells and cells of the microenvironment playing a crucial role in tumor development, progression, and relapses. To date, few investigations have concerned the role of SCF$^+$/c-Kit$^+$ mast cells in normal, premalignant, and malignant skin lesions that resemble steps of malignant melanoma progression. In this study, by immunolabeling reactions, we demonstrated that in melanoma lesions, SCF and c-Kit were expressed in mast cells and released by themselves, suggesting an autocrine/paracrine loop might be implicated in regulatory mechanisms of neoangiogenesis and tumor progression in human melanoma.

Keywords: angiogenesis, mast cells, melanoma, tumor progression, tumor microenevironment

OPEN ACCESS

Edited by:
Frans J. Van Overveld, University College Roosevelt, Netherlands

Reviewed by:
Antonella Naldini, University of Siena, Italy
Pawan Kumar Raghav, University of California, San Francisco, United States

***Correspondence:**
Domenico Ribatti
domenico.ribatti@uniba.it

Specialty section:
This article was submitted to Inflammation, a section of the journal Frontiers in Immunology

Received: *14 October 2021*
Accepted: *05 January 2022*
Published: *24 January 2022*

Citation:
Annese T, Tamma R, Bozza M, Zito A and Ribatti D (2022) Autocrine/Paracrine Loop Between SCF$^+$/c-Kit$^+$ Mast Cells Promotes Cutaneous Melanoma Progression. Front. Immunol. 13:794974. doi: 10.3389/fimmu.2022.794974

INTRODUCTION

Stem cell factor (SCF) is a mast cell growth factor (1) involved in mast cell survival and migration (2). One of the main chemoattractant factors released by tumor cells is SCF (2–4). c-Kit (CD 117) is a member of class III transmembrane receptor tyrosine kinases (RTKs), linked to the platelet-derived growth factor (PDGF)/colony-stimulating factor-1 (CSF-1) subfamily (5), and acts as a natural receptor of SCF (6). c-Kit is expressed in mast cells and is involved in their growth and development (7). Mice lacking c-Kit or its ligand result in the absence of mast cells and exhibit several other kit-dependent phenotypic abnormalities (8, 9). Inhibition of the SCF/c-Kit axis inhibits the migration of mouse bone marrow-derived cultured mast cells to tumors in a transplanted tumor model in mice (2), and mutations in c-Kit have been associated with the development of gastrointestinal stromal tumors, various forms of mastocytosis, and mast cell leukaemia (10).

SCF exists as two alternatively spliced variants, the membrane-anchored protein and the soluble one differing in exon 6. Both isoforms are initially membrane-anchored and are composed of an extracellular domain, a transmembrane portion and an intracellular domain, which is not present in

the membrane-anchored form of SCF (11). The isoform that retains the exon 6 is rapidly cleaved to generate the soluble protein (12–14). Both isoforms, with some differences, have a role in c-Kit activation.

c-Kit exists as four isoforms that differ for four amino acid residues of the extracellular domain (15). The full-length membrane-anchored one activates the intracellular signalling pathways in response to SCF binding, while the soluble one retains only the extracellular domain (16, 17).

SCF binding to the c-Kit extracellular domain induces its dimerization and follow the activation of its intrinsic tyrosine kinase activity that couples with a set of cytoplasmic signalling pathways including mitogen-activated protein kinase pathways (MAPK), fosfoinositide 3-kinase (PI3K) and Src family kinases, resulting in cell proliferation, migration and malignant transformation associated with different genetic diseases and cancers (18, 19).

Mast cells are numerous in tissues and organs exposed to the external environment, including the skin, the lung, and the gut, and are often located near to potential targets of their mediators, such as glands and blood vessels (20, 21). Mast cells are attracted in the tumor microenvironment and promote tumor angiogenesis and lymphangiogenesis by releasing vascular endothelial growth factor (VEGF), fibroblast growth factor-2 (FGF-2), and proteases (22). In addition, mast cells support tumor invasiveness by their immunosuppressive activity, releasing tumor necrosis factor-alpha (TNF-α), histamine, and interleukin-10 (IL-10) and suppressing T cells and natural killer (NK) that in turn induce immune tolerance mediated by regulatory T cells (Treg) (22). Tissue-derived mast cells from human skin secrete several angiogenic molecules, including VEGF, granulocyte-macrophage colony-stimulating factor (GM-CSF), interleukin-8 (IL-8) monocyte chemoattractant protein-1 (MCP-1), and require SCF for their secretion (23).

Given the complexity of the SCF/c-Kit pathway and the multiple cells and physiological/pathological conditions in which it can be activated, the complete understanding of the biological roles of SCF/c-Kit is still an issue that deserves a thorough investigation. In this study, we have evaluated the expression of SCF and c-Kit in mast cells located near to the blood vessels and skin glands, during the tumor progression of human melanoma and we have correlated their expression with microvascular density.

MATERIALS AND METHODS

Patients and Tissue Collection

This retrospective monocentric study included formaldehyde fixed and paraffin-embedded (FFPE) skin biopsies from 35 normal, premalignant lesions and melanoma patients who underwent curative resection (**Table 1**). Full-thickness skin samples containing epidermis, dermis, and hypodermis were collected from the archive of the Unità Operativa Complessa di Anatomia Patologica, IRCCS, Istituto Tumori "Giovanni Paolo II", Bari, Italy. The study was approved by the local institutional Ethics Committees and followed the Helsinki Declaration of 1964 and later versions. All patients agreed to participate in the study and signed written informed consent. Skin biopsies were divided into four histological subgroups, namely normal skin (NS; n=5), common nevi (CN; n=10), dysplastic nevi (DN; n=10), melanomas at different stages (M; n=10).

CD31, VEGFA, c-Kit, and SCF Immunolabelling

FFPE blocks were cooled on ice and serially sectioned using a standard microtome. Three μm thickness tissue sections were dewaxed by oven-dried at 60°C for 1 hour and then immersed two times in fresh xylene for 5 minutes. Before starting staining protocols, the slides were rehydrated in an alcohol scale, rinsed for 10 min in Tris-buffered saline solution (TBS), and heated in a solution of sodium citrate pH 6.0 (ref. S1700, Agilent Dako) at 98°C in a water bath for 30 min. After cooling at room temperature for 30 min, the slides were rinsed in distilled water two times and one time in TBS for 1 min each. Then, tissue sections were washed in TBS + 0.025 Triton X-100 (TBS-Tr), and the endogenous phosphatases and peroxidases were blocked in an enzyme-blocking (ref. S2003, Agilent Dako) for 10 min. Afterwards, the sections were incubated with primary antibodies rabbit polyclonal IgG to CD31 (diluted 1:60; ref. ab28364, Abcam), or rabbit polyclonal IgG to VEGFA (diluted 1:200; ref. AB-90010, Immunological Sciences) or mouse monoclonal IgG1 to c-Kit (diluted 1:500; ref. AMAB90901, ATLAS Antibodies), or rabbit polyclonal IgG to SCF (diluted 1:1000; ref. ab64677, Abcam) for 30 min at room temperature. The sections were rinsed in TBS-Tr, incubated with biotinylated polymer for 15 min (ref. K5005, Agilent Dako), streptavidin-AP for 15 min (ref. K5005, Agilent Dako), and finally, the immunodetection was performed with a red chromogen for 20 min at room temperature (ref. K5005, Agilent Dako). In the end, all the sections were washed in distillate water, counterstained with Gill's hematoxylin (ref. GHS132-1L, Sigma-Aldrich), and mounted in Glycergel (ref. C0563, Agilent Dako). As negative controls for primary antibodies specificity and nonspecific binding of the secondary antibodies, primary antibodies were omitted, or isotype-specific immunoglobulins at the same protein concentration as the primary antibody replacing the primaries antibodies were added.

Morphometric Analysis

Immunolabeled slides were scanned using the whole-slide scanning platform Aperio ScanScope CS (Leica Biosystems, Nussloch, Germany) at 40x magnification, stored as high-resolution digital images, and analysed using the Aperio Positive Pixel Count algorithm or the counter tool embedded in the ImageScope v.11.2.0.780 (Leica Biosystems). Morphometric analysis was performed on three randomly selected fields/biopsy at 20x or 40x magnification using the rectangle tools to determine the specific areas of interest.

The analyses were performed in the same section area for all the staining by transferring the annotated region of interest across semi-serial slides.

TABLE 1 | Clinical and histological information on patients.

	Normal skin[a]			
Average age (year)	46			
Men/women	1/4			
	Common nevi			
Average age (year)	37			
Men/women	4/6			
	Dysplastic nevi[b]			
Average age (year)	56			
Men/women	2/8			
	Melanomas			
Average age (year)	64			
Men/women	4/6			
Subclassification	*(n=4)*	*(n=2)*	*(n=2)*	*(n=2*
AJCC stage	*IIA*	*IB*	*IIB*	*IIIC*
Breslow Depth	*T3a (2-3mm)*	*T2a (2 mm)*	*T3b (4 mm)*	*T4a (5 mm)*
Clark level	*IV*	*IV*	*IV*	*IV*
Ulceration	*absent*	*absent*	*present (1/2)*	*absent*
Growth Phase	*vertical*	*radial and vertical*	*vertical*	*radial and vertical*
Mitoses/mm^2	*2-3*	*4-5*	*18-20*	*8-9*
Tumoral lymphocytic infiltration	*present (2/4)*	*present*	*absent*	*present*
Peritumoral lymphocytic infiltration	*present*	*present*	*present*	*present*
Vascular invasion	*absent*	*present*	*absent*	*absent*
Overall	**35**			

[a]*All normal skin sections were from patients who underwent surgery for suspect breast cancer.*
[b]*All dysplastic nevi showed severe atypia but negative margins. AJCC, American Joint Committee on Cancer.*

The negative pen tool was used to draw negative free areas not to be analysed with the Aperio Positive Pixel Count algorithm in order to include data corresponding only to MCs in the analysis. In addition, for SCF$^+$/c-Kit$^+$ MCs counts, the other cell types were excluded based on morphology (see results paragraph and **Figure 1**).

Statistical Analysis

Statistical analyses were performed using one-way ANOVA with Tukey's multiple comparisons test, and proteins expression correlation was calculated assumed data sampled from no Gaussian distribution by Spearman nonparametric correlation analysis using the GraphPad Prism 6.01. Statistical significance was set at $P \leq 0.05$, and results are given as mean ± SD.

RESULTS

Mast Cells and Tumor Cells Express SCF and c-Kit in Normal, Premalignant, and Malignant Skin Lesions

To unequivocally quantify SCF/c-Kit of mast cells, we discriminate tumor cells based on their peculiar morphology. As shown in **Figure 1**, mast cells were identified as mononuclear cells containing many dense secretory granules covering the nucleus (**Figure 1** arrowhead), or cells with a dense red-positive plasma membrane signal as a crown (**Figure 1B**, arrowhead in the centre), or degranulated cells (**Figure 1A** arrowhead, see the soluble form of SCF; **Figure 1E**, see the soluble form of c-Kit), or elongated cells (**Figure 1F**). On the contrary, tumor cells appear to be pigmentated or not, faintly labelled for both SCF o c-Kit and with nucleolated nuclei (**Figures 1A, D** arrow). Based on these morphological profiles and employing the negative pen tool embedded in the ImageScope, we remove from the selected regions of interest the area of signals not related to mast cells.

SCF$^+$/c-Kit$^+$ Mast Cells Distribution Around Microvessels in Normal, Premalignant, and Malignant Skin Lesions

In this study, we evaluate angiogenesis in normal, premalignant, and malignant skin lesions, which resemble steps of malignant melanoma progression, in relation to mast cells infiltrate around microvessels with the aim to identify a possible relation to mast cells distribution, SCF/c-Kit expression by mast cells, and microvessel formation.

In agreement with the literature, our CD31 immunohistological staining showed a higher number of transversely or longitudinally cut blood vessels with an appreciable lumen in melanoma than normal skin, compound and dysplastic nevi (**Figures 2A–D**). The CD31 immunolabelling positivity and the number of CD31$^+$ microvessels progressively increased from normal skin to melanoma (**Figures 2M, N**; **Table 2** for raw data), highlighting a significative involvement of angiogenesis in melanoma progression.

Neo-angiogenesis mechanisms are related to the expression of angiogenic cytokines such as VEGFA. Its expression is usually absent in normal skin and nevi, but heterogeneous, ranging from negative to strongly positive, in melanomas (24, 25). To explore the angiogenic profile in our samples, we performed immunohistochemical analysis of VEGFA expression by tumor cells and cells surrounding the blood vessel. We found that VEGFA immunolabelling positivity progressively increased from normal skin to melanoma (**Figures 2E–L, O** and **Table 2** for raw data), and its expression amount, by both tumor cell or cell

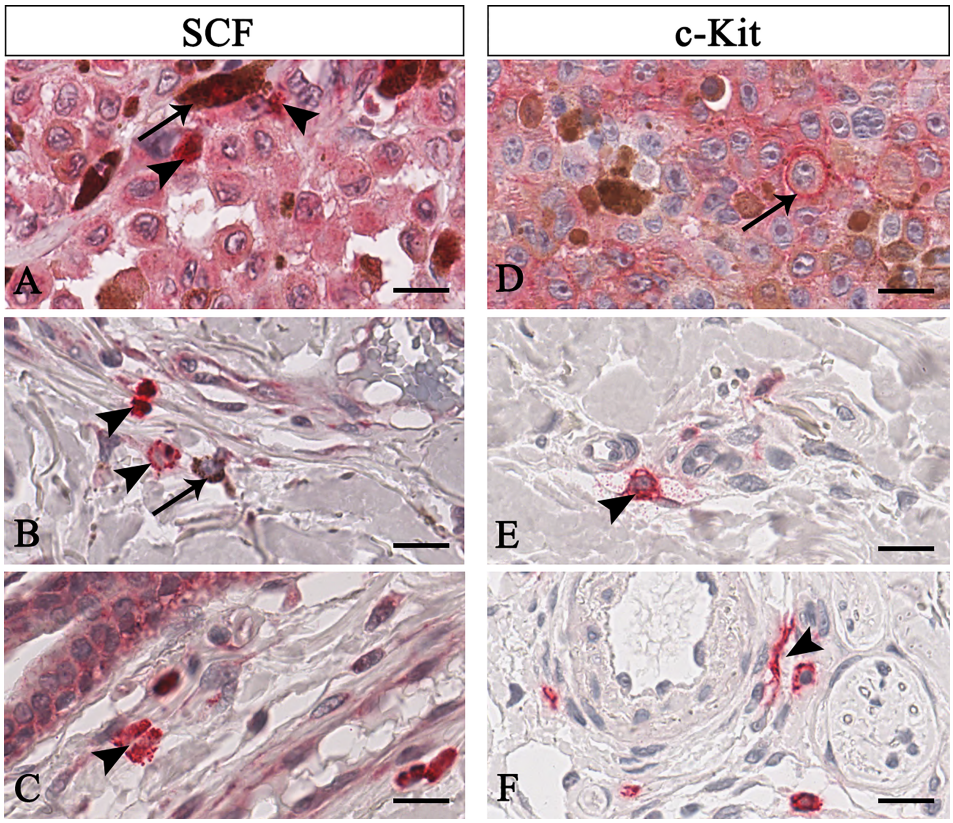


FIGURE 1 | Representative immunohistochemistry of SCF **(A–C)** or c-Kit **(D–F)** in the melanomas tissue sections. Micrographs show pigmented tumor cells (**A**, arrow) or not-pigmented tumor cells but with nucleolated nuclei (**D**, arrow) labelled for both SCF or c-Kit. Instead, SCF$^+$/c-Kit$^+$ mast cells are rounded-shape and hyperchromatic cells with positive granules in the cytoplasm (**B**, arrowhead) or secreted (**A, C, E** arrowhead). Some mast cells are spindle-shaped, thus resembling fibroblasts (**F**, arrowhead). Scale bar: 60 μm.

surrounding blood vessel, significative positive correlate with CD31 expression (**Figure 2P**). These results confirmed CD31 and VEGFA as good indicators of angiogenic changes in melanocytic lesions essential to multistep tumorigenesis.

Among cells of the microenvironment, mast cells take part in angiogenesis, tissue repair, and tissue remodelling that occurs in many tumor settings (26). Here, in normal, premalignant, and malignant skin lesions, we evaluate mast cells distribution in the connective tissue around CD31$^+$ blood vessels as SCF$^+$ or c-Kit$^+$ cells with a masked nucleus, or cells with granules in the cytoplasm, or on the membrane, or outside the cells (as discerned in **Figure 1**). The analyses, conducted in the same region of interest on serial tissue sections for all the three markers, demonstrated an increased number of mast cells close to microvessels in melanoma lesions compared to premalignant ones and normal skin (**Figure 3**). The SCF or c-Kit immunolabelling positivity and the number of SCF$^+$/c-Kit$^+$ mast cells progressively increased from normal skin to melanoma (**Figures 3M, N**; **Table 2** for raw data). Moreover, correlation analysis of SCF$^+$/c-Kit$^+$ MCs and CD31$^+$ microvessels and correlation analysis of SCF and c-Kit by linear regression showed significative positive correlations for both (**Figures 3O, P**).

SCF$^+$/c-Kit$^+$ Mast Cells Distribution Around Cutaneous Glands in Normal, Premalignant, and Malignant Skin Lesions

Here, we examined SCF$^+$/c-Kit$^+$ mast cells distribution and location around the cutaneous gland in normal, premalignant, and malignant skin lesions by immunohistochemical staining because we observed that they not only surrounded the microvessels but also preferred to locate at extracellular matrix around the cutaneous glands. The analysis of immunolabeling reactions, conducted in the same region of interest on serial tissue sections for SCF and c-Kit, demonstrated an increased number of mast cells close to cutaneous glands in melanoma lesions than premalignant ones and normal skin (**Figure 4**). The number of SCF$^+$/c-Kit$^+$ mast cells progressively increased from normal skin to melanoma (**Figures 4I, J**; **Table 3** for raw data). Moreover, correlation analysis of SCF and c-Kit by linear regression showed significative positive correlations for both (**Figure 4K**). Overall, these results show a possible cross-talk between mast cells and gland epithelium mediated by the SCF/c-Kit pathway and involved in melanoma progression. As shown in **Figure 4** by SCF immunolabelling, the glandular epithelium cells can express SCF, which can bind the c-Kit express by the surrounded mast cells to sustain their proliferation, the pro-

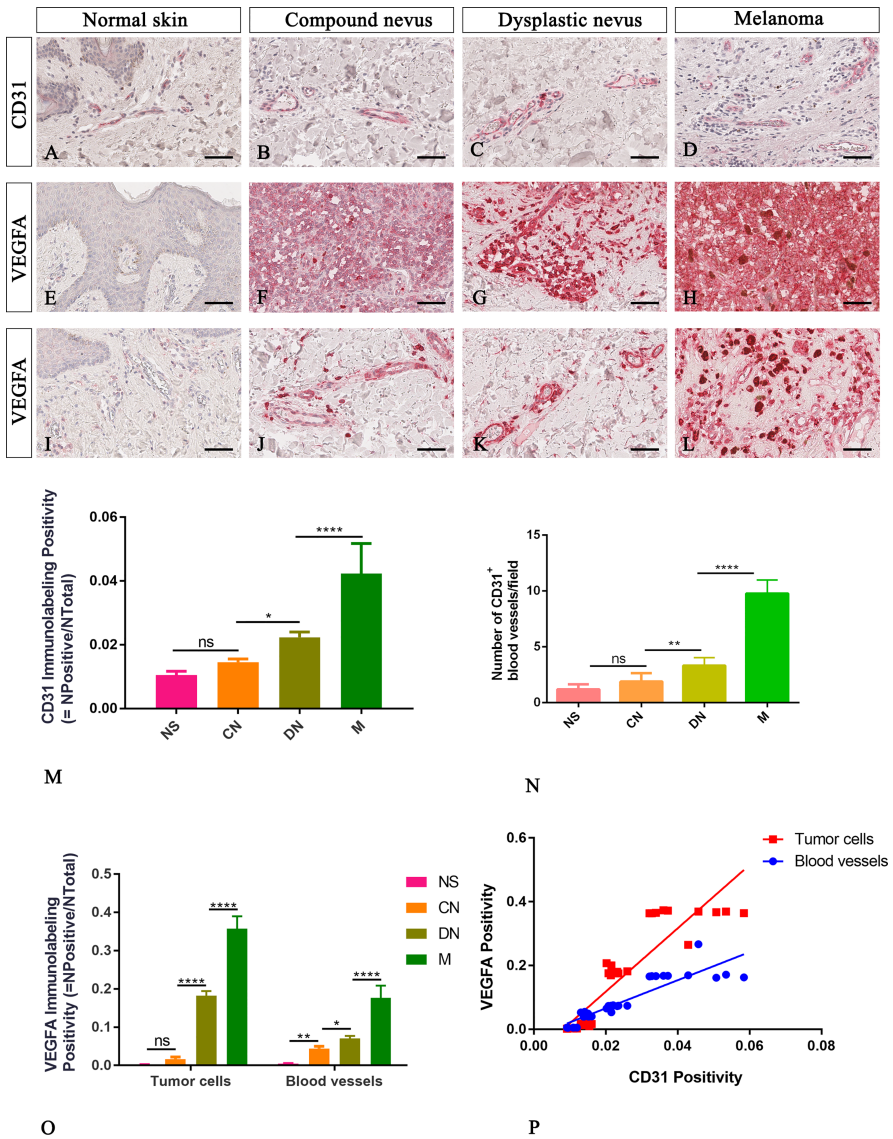


FIGURE 2 | Representative immunohistochemistry of CD31 or VEGFA in the normal skin **(A, E, I)**, compound nevi **(B, F, J)**, dysplastic nevi **(C, G, K)**, and melanomas **(D, H, L)** tissue sections. Micrographs **(A–D)** and morphometric analysis **(M, N)** show a significative gradual increased microvascular density calculated as both percentages of CD31 immunolabeling positivity and the number of the CD31$^+$ blood vessels in melanoma lesions compared to premalignant ones and normal skin. Micrographs **(E–L)** and morphometric analysis **(O)** show a significative gradual increased VEGFA expression in both cells of tumor mass **(E–H)** and surrounding blood vessels **(I–L)** in melanoma lesions compared to premalignant ones and normal skin. The lack of VEGFA expression is evident by the epidermis cells in the normal skin **(E)**, while a faint signal is present around the blood vessels **(I)**. Linear regression analysis shows positive relationships between VEGFA expression by tumor cells or by cells surrounding blood vessels and CD31 **(P)** [For VEGFA by tumor cells: y=9.929x-0.08029; R2 = 0.8095; p ≤ 0.0001. For VEGFA expression by cells surrounded blood vessels: y=4.407x-0.0225; R2 = 0.8117; p ≤ 0.0001]. Data are reported as means ± SD, and Tukey post-test was used to compare all groups after one-way ANOVA. Statistical significance: ns, not significative; *p ≤ 0.05; **p≤ 0.01; ****p ≤ 0.0001. Scale bar: 60 μm.

inflammatory microenvironment, therefore tumor maintenance and progression as tumor growth-promoting loop (27–29).

DISCUSSION

In this study, we have demonstrated that in melanoma lesions, SCF and c-Kit are expressed in mast cells and released by themselves, suggesting an autocrine/paracrine loop might be implicated in regulatory mechanisms of neoangiogenesis and tumor progression in human melanoma.

SCF/c-Kit pathway activation regulates normal melanocytes, germ cells, and hematopoietic cells (included mast cells) proliferation and/or differentiation. SCF binding to the c-Kit monomer in its extracellular region induces dimerisation (30). The dimerised c-Kit acts as both enzyme and substrate through

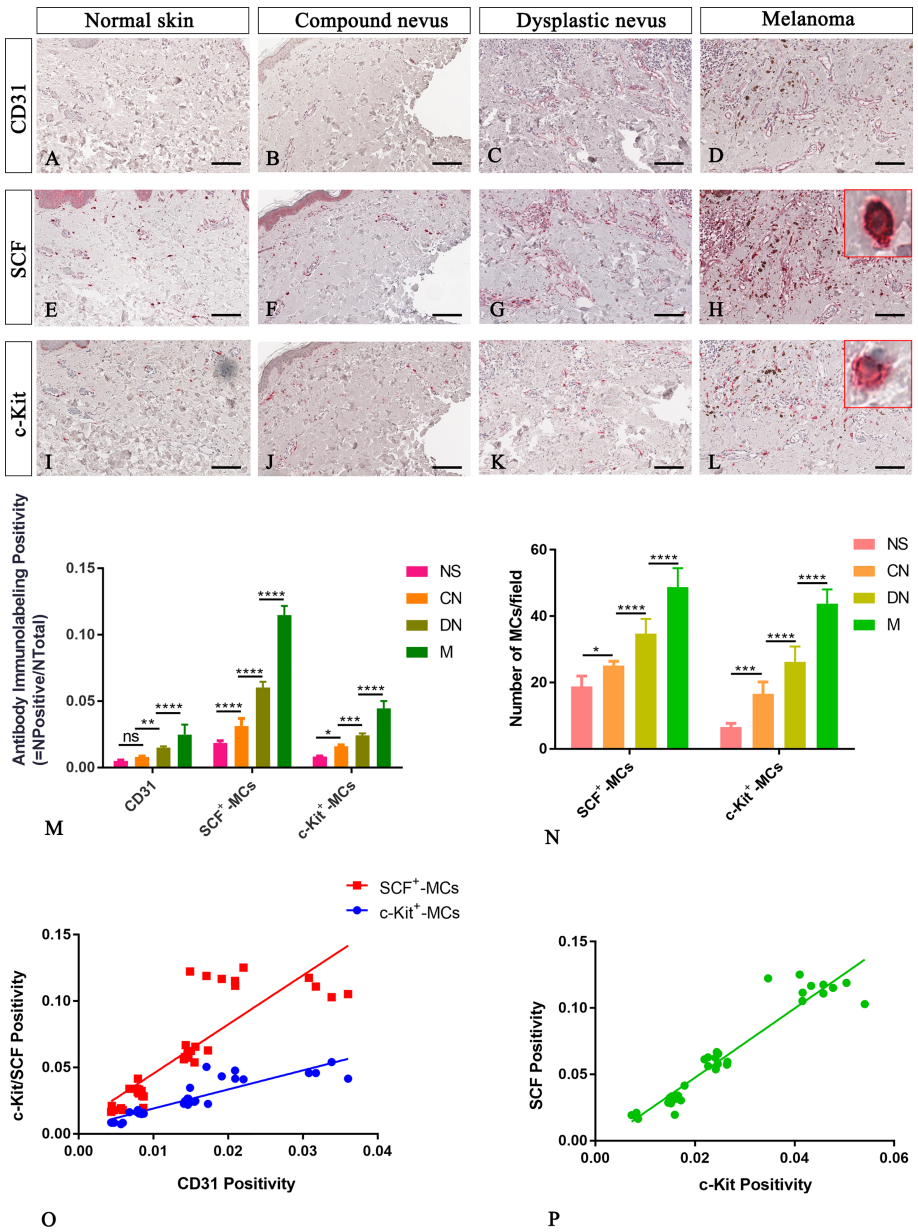


FIGURE 3 | Representative immunohistochemistry of SCF or c-Kit on the same area of interest around CD31+ blood vessels in the normal skin **(A, E, I)**, compound nevi **(B, F, J)**, dysplastic nevi **(C, G, K)**, and melanomas **(D, H, L)** tissue sections. The micrographs show a significative gradual increased CD31, SCF, and c-Kit expression in malignant melanoma lesions compared to premalignant ones and normal skin **(A–L)**. The SCF- or c-Kit-positive mast cells appear mostly with a strong red-granulous membranous and moderate cytoplasmic staining in all the samples (see the inserts in the red rectangles; scale bar: 10 μm). The morphometric analysis performed on the same region of interest for all three markers confirmed an increased SCF+/c-Kit+ mast cell infiltrate around blood vessels in melanoma compared to normal skin, compound nevi, and dysplastic ones, both in percentages of immunolabeling positivity and number of positive cells **(M, N)**. Linear regression analysis shows positive relationships between SCF or c-Kit and CD31**(O)**, and between SCF and c-Kit **(P)** [**(O)** For SCF: y=3.698x+0.008438; R2 = 0.7048; $p \leq 0.0001$. **(O)** For c-Kit: y=1.435x+0.004774; R2 = 0.792; $p \leq 0.0001$. **(P)** y=2.61x-0.004682; $R^2 = 0.9123$; $p \leq 0.0001$]. Data are reported as means ± SD, and Tukey post-test was used to compare all groups after one-way ANOVA. Statistical significance: ns, not significative; *$p \leq 0.05$; **$p \leq 0.01$; ***$p \leq 0.001$; ****$p \leq 0.0001$. Scale bar: 200 μm.

phosphorylation of its specific amino acid residues (pTyr) in the intracellular juxtamembrane region. Phosphorylated c-Kit tyrosine residues recruit signal trasduction protein-containing Src homology 2 (SH2) domains and pTyr-binding (PTB) domains (31). These downstream effector molecules have different biological effects: inhibit proliferation, or induce c-Kit degradation, cell proliferation, differentiation, survival, and migration (32). These effects will depend on total binding

TABLE 2 | Summary of the morphometric analysis performed to evaluate c-Kit+/SCF+ mast cells around blood vessels.

Analysis	EXPERIMENTAL GROUPS						
	NS	***vs***	**CN**	***vs***	**DN**	***vs***	**M**
CD31+ blood vessels immunolabeling positivity at 40x magnification	0.010496 ± 0.001164	ns	0.014543 ± 0.000963	*	0.022343 ± 0.001654	****	0.042335 ± 0.009406
Number of CD31+ blood vessels/field at 40x magnification	1 ± 0.5	ns	2 ± 1	**	3 ± 1	****	10 ± 1
VEGFA+ tumor cells immunolabeling positivity at 40x magnification	0.002165 ± 0.000317	ns	0.017022 ± 0.005223	****	0.182269 ± 0.011900	****	0.357288 ± 0.032636
VEGFA+ cells surrounding blood vessels immunolabeling positivity at 40x magnification	0.005185 ± 0.000186	**	0.044378 ± 0.005987	*	0.070713 ± 0.0006719	****	0.176649 ± 0.031862
CD31+ blood vessels immunolabeling positivity at 20x magnification	0.005016 ± 0.000720	ns	0.008073 ± 0.000556	**	0.014986 ± 0.000965	****	0.024751 ± 0.007599
SCF+ mast cells immunolabeling positivity at 20x magnification	0.018520 ± 0.001716	****	0.031347 ± 0.005586	****	0.060341 ± 0.004191	****	0.114667 ± 0.007065
c-Kit+ mast cells immunolabeling positivity at 20x magnification	0.008168 ± 0.000506	*	0.016015 ± 0.001027	***	0.024208 ± 0.001522	****	0.0444600 ± 0.005451
Number of SCF+ mast cells/field at 20x magnification	19 ± 3	*	25 ± 1	****	35 ± 4	****	49 ± 6
Number of c-Kit+ mast cells/field at 20x magnification	7 ± 1	***	17 ± 4	****	26 ± 5	****	44 ± 4

The morphometric values are expressed as mean ± SD (n= 5 for normal skin (NS) group and n=10 for the others) and have been utilised for the graphs in ***Figures 2–4****. Tukey's post-test was used to compare all groups after One-way ANOVA and Spearman for correlation (ns, not significative; *p ≤ 0.05; **p ≤ 0.01; ***p ≤ 0.001; ****p ≤ 0.0001).*

affinities and the number of recruitment sites (33). So this is why different cells show different phenotypes despite employing the same core sets of cell-signalling proteins. For instance, in the erythroleukemic K562 cell line and megakaryoblastic cell line MO7e, which expresses c-Kit and the phosphatases SHP-1/SHP-2 mRNA, under SCF stimuli and the inhibition of protein tyrosine phospahatase SHP-1/SHP-2 by the inhibitor NSC87877, increased cell proliferation, *via* PI3K-DAG-PKC signalling pathway was demonstrated through an increased c-Kit phosphorylation (32, 34).

The SCF/c-Kit pathway also plays a crucial role in tumor development, progression, and relapses (35). In epithelial ovarian cancer (EOC), the SCF/c-Kit autocrine/paracrine loop promotes cancer stem cell (CSC) survival, the leading cause of EOC initiation and relapse (36). In EOC, tumor cells (less amount) and c-Kit+ CSCs express the only membrane-anchored isoform of SCF, while tumor-associated macrophages (TAMs) and tumor-associated fibroblasts (TAFs) express even the secreted isoform (36).

Controversial is the literature concerning SCF/c-Kit transcript and protein level expression by tumor cells during melanoma progression. Some authors reported the loss of c-Kit expression during malignant transformation of melanocytes, but others, later in tumor progression, in invasive melanoma, compared to *in situ* lesions (37–40). Not only tumor cells but also cells of the microenvironment can express these molecules as secreted and/or membrane-bound isoforms for both (36, 41).

Human malignant melanoma is an aggressive and highly metastatic tumor with a poor prognosis and high drug resistance. Malignant melanoma progresses through different steps from common nevi, dysplastic nevi, *in situ* melanoma, radial growth phase melanoma, vertical growth phase melanoma, and metastatic melanoma (42). In parallel with tumor progression and dissemination, melanoma cells, in concert with microenvironment cells, orchestrate the angiogenic switch that favours tumor cell growth, extravasation and metastases (43, 44).

Tissue distribution and localisation of mast cells are intimately connected to their physiological and pathological functions, such as allergic immune reactions, innate and adaptive immunity, and fibrosis (45, 46). Tumor cells are surrounded by an infiltrate of inflammatory cells, such as lymphocytes, neutrophils, macrophages and mast cells. It is well known that mast cells accumulate at the periphery of melanomas and nevi, especially around the microvasculature, where have a pivotal role in neo-angiogenesis and metastasis mechanisms (47, 48). We have previously demonstrated a correlation between tumor vascularity and mast cell density and poor prognosis in melanoma (49), we have investigated the pattern of mast cells around the blood vessels in melanoma, and we have demonstrated that a higher number of mast cells can be observed in melanoma as compared with samples from common acquired nevi (50).

In this study, we have confirmed that CD31 immunolabelling positivity and the number of CD31+ microvessels in parallel to

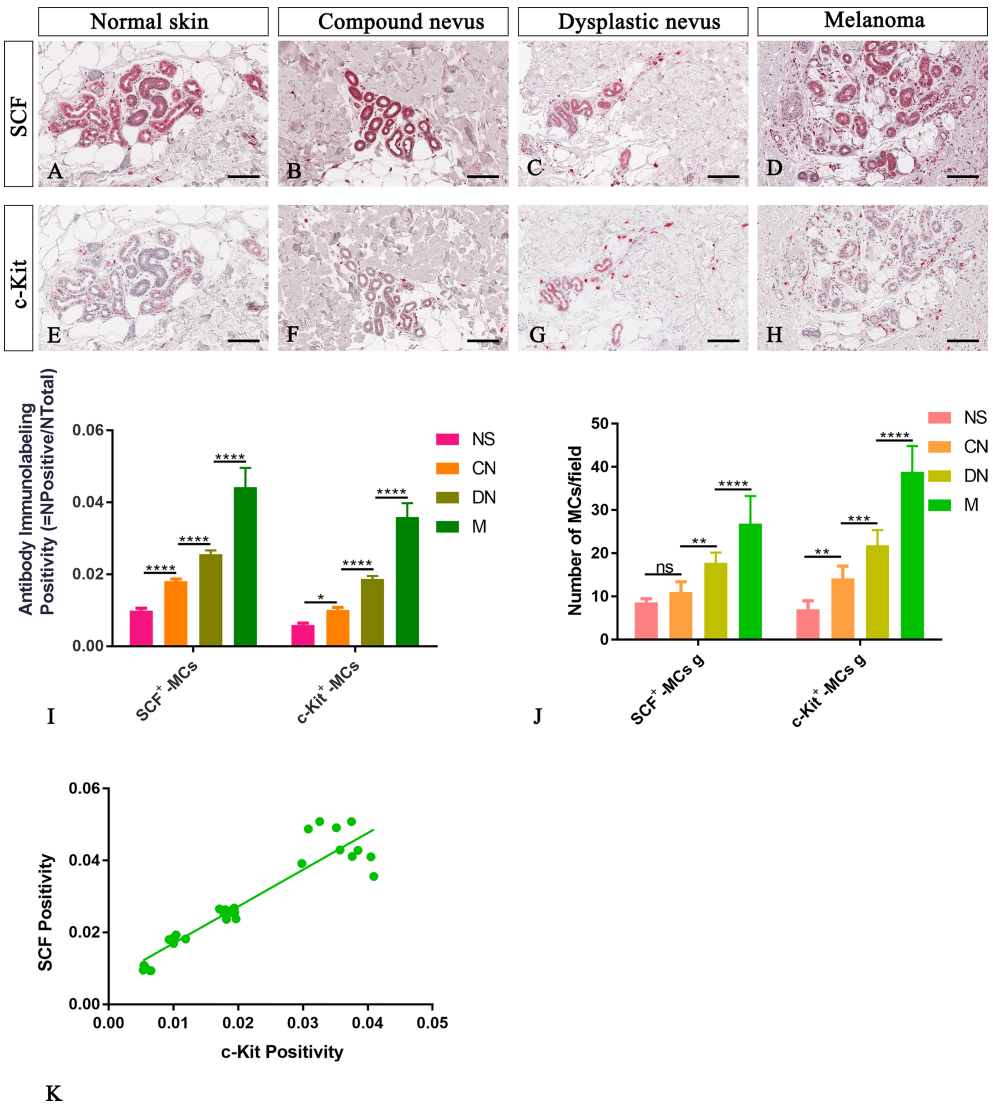


FIGURE 4 | Representative immunohistochemistry of SCF or c-Kit on the same area of interest around glands in the normal skin **(A, E)**, compound nevi **(B, F)**, dysplastic nevi **(C, G)**, and melanomas **(D, H)** tissue sections. The micrographs show a significative gradual increased SCF and c-Kit expression in malignant melanoma lesions compared to premalignant ones and normal skin **(A–H)**. The morphometric analysis performed on the same region of interest for both markers confirmed an increased SCF$^+$/c-Kit$^+$ mast cell infiltrate around glands in melanoma compared to normal skin, compound nevi, and dysplastic nevi, both as percentages of immunolabeling positivity and as number of positive cells **(I, J)**. Linear regression analysis shows the positive relationships between **(K)** SCF and c-Kit [**(K)** y=1.023+0.006766; R^2 = 0.8848; p ≤ 0.0001]. Data are reported as means ± SD, and Tukey post-test was used to compare all groups after one-way ANOVA. Statistical significance: ns, not significative; *p ≤ 0.05; **p ≤ 0.01; ***p ≤ 0.001; ****p ≤ 0.0001. Scale bar: 200 μm.

VEGFA expression by both tumor cells or cells surrounding blood vessels progressively increased from normal skin to melanoma, highlighting a significative involvement of angiogenesis in melanoma progression. Moreover, we have focused our attention on the role of mast cells positive to SCF/c-Kit in the initiation and progression of cutaneous melanoma. SCF is one of the principal growth factors responsible for the early development of CD34$^+$/c-Kit$^+$ mast cell progenitors and the development and function of melanocytes (51–54). SCF bind to the c-Kit tyrosine kinase receptor regulates mast cell development, survival, and function (35, 55). We have demonstrated that the number of SCF$^+$/c-Kit$^+$ mast cells progressively increased from normal skin to melanoma. In agreement with these results, also in pancreatic carcinoma, an increase in the number of chymase$^+$/tryptase$^+$ or SCF$^+$/c-Kit$^+$ mast cells in normal and tumor pancreatic tissue biopsies and cell lines was shown with a higher expression in the latter (56). Previous studies have reported the negative impact of SCF on c-Kit expression, demonstrating that a high SCF amount decreases the expression of c-Kit but does not affect the c-Kit phosphorylation (34, 57, 58). The immunohistochemistry on FFPE biopsy sections allows us to evaluate the biological

TABLE 3 | Summary of the morphometric analysis performed to evaluate c-Kit+/SCF+ mast cells around glands.

Analysis	EXPERIMENTAL GROUPS						
	NS	***vs***	**CN**	***vs***	**DN**	***vs***	**M**
SCF+ mast cells immunolabeling positivity at 20x magnification	0.009901 ± 0.000678	****	0.018071 ± 0.000614	****	0.025568 ± 0.001080	****	0.044227 ± 0.005330
c-Kit+ mast cells immunolabeling positivity at 20x magnification	0.005852 ± 0.000549	*	0.010092 ± 0.000707	****	0.018666 ± 0.000847	****	0.03912 ± 0.003842
Number of SCF+ mast cells/field at 20x magnification	9 ± 1	ns	11 ± 2	**	18 ± 2	****	27 ± 6
Number of c-Kit+ mast cells/field at 20x magnification	7 ± 2	**	14 ± 3	***	22 ± 3	****	39 ± 6

The morphometric values are expressed as mean ± SD (n= 5 for normal skin (NS) group and n=10 for the others) and have been utilised for the graphs in ***Figures 2–4****. Tukey's post-test was used to compare all groups after One-way ANOVA and Spearman for correlation (ns, not significative; * $p \leq 0.05$; ** $p \leq 0.01$; *** $p \leq 0.001$; **** $p \leq 0.0001$).*

phenomena in a context closer to the physiological one without overstating our data. Furthermore, it is very likely that in our study, the maintenance of a high expression of c-Kit is also attributable to other molecules and pathways active by other cells of the microenvironment. Zhang et al. (4) provided evidence that SCF released by tumor cells modulated tumor angiogenesis by regulating mast cells. These Authors used sense or anti-sense SCF cDNA to overexpress or deplete SCF expression in rat mammary tumor cells. Depletion of SCF significantly decreased mast cell infiltration and vascularisation, whereas the opposite effects were observed in SCF-overexpressing tumors.

Keratinocytes secrete SCF (4). SCF induces melanoblasts to differentiate into melanocytes and is mitogenic for melanocytes *in vivo* and *in vitro* (59). Injection of SCF into the human skin results in local accumulation of mast cells (60). c-Kit is a growth factor for melanocyte migration and proliferation and is massively involved in the tumorigenesis of cutaneous malignancies, being immunohistochemically densely expressed in dysplastic nevi and in melanoma. Melanocytes from metastatic melanoma lose the expression of c-Kit and an inverse correlation between c-Kit and tumor progression has been demonstrated in melanoma (61). In metastatic malignant melanoma, c-Kit staining was lower than in primary malignant melanoma (62).

In this context, we suggest that SCF+/c-Kit+ mast cells may be involved in the angiogenic response occurring during tumor progression in human melanoma. Mast cells are involved in an autocrine/paracrine loop that could stimulate the endothelial cell proliferation to sustain neo-angiogenesis, and the releasing of pro-inflammatory mediators and pro-angiogenic cytokines by themselves, which, in turn, sustain proliferation and activation of mast cells and tumor progression.

DATA AVAILABILITY STATEMENT

The raw data supporting the conclusions of this article will be made available by the authors, without undue reservation.

ETHICS STATEMENT

The studies involving human participants were reviewed and approved by Istituto Tumori Giovanni Paolo II, Bari. The patients/participants provided their written informed consent to participate in this study.

AUTHOR CONTRIBUTIONS

TA and DR conceived, planned, and write the work. TA, RT, MB, and AZ performed the experimental work. All authors contributed to the article and approved the submitted version.

REFERENCES

1. Anderson DM, Lyman SD, Baird A, Wignall JM, Eisenman J, Rauch C, et al. Molecular Cloning of Mast Cell Growth Factor, a Hematopoietin That Is Active in Both Membrane Bound and Soluble Forms. *Cell* (1990) 63(1):235–43. doi: 10.1016/0092-8674(90)90304-w
2. Huang B, Lei Z, Zhang GM, Li D, Song C, Li B, et al. SCF-Mediated Mast Cell Infiltration and Activation Exacerbate the Inflammation and Immunosuppression in Tumor Microenvironment. *Blood* (2008) 112 (4):1269–79. doi: 10.1182/blood-2008-03-147033
3. Bellone G, Smirne C, Carbone A, Buffolino A, Scirelli T, Prati A, et al. KIT/ Stem Cell Factor Expression in Premalignant and Malignant Lesions of the Colon Mucosa in Relationship to Disease Progression and Outcomes. *Int J Oncol* (2006) 29(4):851–9. doi: 10.3892/ijo.29.4.851
4. Zhang W, Stoica G, Tasca SI, Kelly KA, Meininger CJ. Modulation of Tumor Angiogenesis by Stem Cell Factor. *Cancer Res* (2000) 60(23):6757–62.
5. Besmer P, Murphy JE, George PC, Qiu FH, Bergold PJ, Lederman L, et al. A New Acute Transforming Feline Retrovirus and Relationship of its Oncogene V-Kit With the Protein Kinase Gene Family. *Nature* (1986) 320(6061):415–21. doi: 10.1038/320415a0
6. Martin FH, Suggs SV, Langley KE, Lu HS, Ting J, Okino KH, et al. Primary Structure and Functional Expression of Rat and Human Stem Cell Factor Dnas. *Cell* (1990) 63(1):203–11. doi: 10.1016/0092-8674(90)90301-t
7. Yarden Y, Kuang WJ, Yang-Feng T, Coussens L, Munemitsu S, Dull TJ, et al. Human Proto-Oncogene C-Kit: A New Cell Surface Receptor Tyrosine

Kinase for an Unidentified Ligand. *EMBO J* (1987) 6(11):3341–51. doi: 10.1002/j.1460-2075.1987.tb02655.x
8. Reber LL, Marichal T, Galli SJ. New Models for Analyzing Mast Cell Functions. *vivo Trends Immunol* (2012) 33(12):613–25. doi: 10.1016/j.it.2012.09.008
9. Ribatti D, Crivellato E, Nico B, Guidolin D, Gassmann M, Djonov V. Mast Cells and Macrophages in Duodenal Mucosa of Mice Overexpressing Erythropoietin. *J Anat* (2009) 215(5):548–54. doi: 10.1111/j.1469-7580.2009.01131.x
10. Valent P, Akin C, Sperr WR, Mayerhofer M, Fodinger M, Fritsche-Polanz R, et al. Mastocytosis: Pathology, Genetics, and Current Options for Therapy. *Leuk Lymphoma* (2005) 46(1):35–48. doi: 10.1080/10428190400010775
11. Lu HS, Clogston CL, Wypych J, Fausset PR, Lauren S, Mendiaz EA, et al. Amino Acid Sequence and Post-Translational Modification of Stem Cell Factor Isolated From Buffalo Rat Liver Cell-Conditioned Medium. *J Biol Chem* (1991) 266(13):8102–7. doi: 10.1016/S0021-9258(18)92947-9
12. Heissig B, Hattori K, Dias S, Friedrich M, Ferris B, Hackett NR, et al. Recruitment of Stem and Progenitor Cells From the Bone Marrow Niche Requires MMP-9 Mediated Release of Kit-Ligand. *Cell* (2002) 109(5):625–37. doi: 10.1016/s0092-8674(02)00754-7
13. Longley BJ, Tyrrell L, Ma Y, Williams DA, Halaban R, Langley K, et al. Chymase Cleavage of Stem Cell Factor Yields a Bioactive, Soluble Product. *Proc Natl Acad Sci U S A* (1997) 94(17):9017–21. doi: 10.1073/pnas.94.17.9017
14. Kawaguchi M, Hearing VJ. The Roles of Adams Family Proteinases in Skin Diseases. *Enzyme Res* (2011) 2011:482498. doi: 10.4061/2011/482498
15. Cardoso HJ, Figueira MI, Correia S, Vaz CV, Socorro S. The SCF/C-KIT System in the Male: Survival Strategies in Fertility and Cancer. *Mol Reprod Dev* (2014) 81(12):1064–79. doi: 10.1002/mrd.22430
16. Ronnstrand L. Signal Transduction via the Stem Cell Factor Receptor/C-Kit. *Cell Mol Life Sci* (2004) 61(19-20):2535–48. doi: 10.1007/s00018-004-4189-6
17. Turner AM, Bennett LG, Lin NL, Wypych J, Bartley TD, Hunt RW, et al. Identification and Characterization of a Soluble C-Kit Receptor Produced by Human Hematopoietic Cell Lines. *Blood* (1995) 85(8):2052–8. doi: 10.1182/blood.V85.8.2052.bloodjournal8582052
18. Reber L, Da Silva CA, Frossard N. Stem Cell Factor and its Receptor C-Kit as Targets for Inflammatory Diseases. *Eur J Pharmacol* (2006) 533(1-3):327–40. doi: 10.1016/j.ejphar.2005.12.067
19. Lennartsson J, Ronnstrand L. Stem Cell Factor Receptor/C-Kit: From Basic Science to Clinical Implications. *Physiol Rev* (2012) 92(4):1619–49. doi: 10.1152/physrev.00046.2011
20. Galli SJ, Kalesnikoff J, Grimbaldeston MA, Piliponsky AM, Williams CM, Tsai M. Mast Cells as "Tunable" Effector and Immunoregulatory Cells: Recent Advances. *Annu Rev Immunol* (2005) 23:749–86. doi: 10.1146/annurev.immunol.21.120601.141025
21. Wilgus TA, Wulff BC. The Importance of Mast Cells in Dermal Scarring. *Adv Wound Care (New Rochelle)* (2014) 3(4):356–65. doi: 10.1089/wound.2013.0457
22. Ribatti D. Mast Cells and Macrophages Exert Beneficial and Detrimental Effects on Tumor Progression and Angiogenesis. *Immunol Lett* (2013) 152(2):83–8. doi: 10.1016/j.imlet.2013.05.003
23. McHale C, Mohammed Z, Gomez G. Human Skin-Derived Mast Cells Spontaneously Secrete Several Angiogenesis-Related Factors. *Front Immunol* (2019) 10:1445. doi: 10.3389/fimmu.2019.01445
24. Einspahr JG, Thomas TL, Saboda K, Nickolof BJ, Warneke J, Curiel-Lewandrowski C, et al. Expression of Vascular Endothelial Growth Factor in Early Cutaneous Melanocytic Lesion Progression. *Cancer* (2007) 110(11):2519–27. doi: 10.1002/cncr.23076
25. Massi D, Landriscina M, Piscazzi A, Cosci E, Kirov A, Paglierani M, et al. S100A13 Is a New Angiogenic Marker in Human Melanoma. *Mod Pathol* (2010) 23(6):804–13. doi: 10.1038/modpathol.2010.54
26. Ribatti D, Crivellato E. Mast Cells, Angiogenesis, and Tumour Growth. *Biochim Biophys Acta* (2012) 1822(1):2–8. doi: 10.1016/j.bbadis.2010.11.010
27. Meininger CJ, Yano H, Rottapel R, Bernstein A, Zsebo KM, Zetter BR. The C-Kit Receptor Ligand Functions as a Mast Cell Chemoattractant. *Blood* (1992) 79(4):958–63. doi: 10.1182/blood.V79.4.958.bloodjournal794958
28. Nocka K, Buck J, Levi E, Besmer P. Candidate Ligand for the C-Kit Transmembrane Kinase Receptor: KL, a Fibroblast Derived Growth Factor Stimulates Mast Cells and Erythroid Progenitors. *EMBO J* (1990) 9(10):3287–94. doi: 10.1002/j.1460-2075.1990.tb07528.x
29. Tsai M, Takeishi T, Thompson H, Langley KE, Zsebo KM, Metcalfe DD, et al. Induction of Mast Cell Proliferation, Maturation, and Heparin Synthesis by the Rat C-Kit Ligand, Stem Cell Factor. *Proc Natl Acad Sci U S A* (1991) 88(14):6382–6. doi: 10.1073/pnas.88.14.6382
30. Lemmon MA, Pinchasi D, Zhou M, Lax I, Schlessinger J. Kit Receptor Dimerization is Driven by Bivalent Binding of Stem Cell Factor. *J Biol Chem* (1997) 272(10):6311–7. doi: 10.1074/jbc.272.10.6311
31. Wagner MJ, Stacey MM, Liu BA, Pawson T. Molecular Mechanisms of SH2- and PTB-Domain-Containing Proteins in Receptor Tyrosine Kinase Signaling. *Cold Spring Harb Perspect Biol* (2013) 5(12):a008987. doi: 10.1101/cshperspect.a008987
32. Raghav PK, Singh AK, Gangenahalli G. Stem Cell Factor and NSC87877 Synergism Enhances C-Kit Mediated Proliferation of Human Erythroid Cells. *Life Sci* (2018) 214:84–97. doi: 10.1016/j.lfs.2018.09.055
33. Leung KK, Hause RJJr., Barkinge JL, Ciaccio MF, Chuu CP, Jones RB. Enhanced Prediction of Src Homology 2 (SH2) Domain Binding Potentials Using a Fluorescence Polarization-Derived C-Met, C-Kit, Erbb, and Androgen Receptor Interactome. *Mol Cell Proteomics* (2014) 13(7):1705–23. doi: 10.1074/mcp.M113.034876
34. Raghav PK, Singh AK, Gangenahalli G. Stem Cell Factor and NSC87877 Combine to Enhance C-Kit Mediated Proliferation of Human Megakaryoblastic Cells. *PLoS One* (2018) 13(11):e0206364. doi: 10.1371/journal.pone.0206364
35. Metz M, Grimbaldeston MA, Nakae S, Piliponsky AM, Tsai M, Galli SJ. Mast Cells in the Promotion and Limitation of Chronic Inflammation. *Immunol Rev* (2007) 217:304–28. doi: 10.1111/j.1600-065X.2007.00520.x
36. Mazzoldi EL, Pavan S, Pilotto G, Leone K, Pagotto A, Frezzini S, et al. A Juxtacrine/Paracrine Loop Between C-Kit and Stem Cell Factor Promotes Cancer Stem Cell Survival in Epithelial Ovarian Cancer. *Cell Death Dis* (2019) 10(6):412. doi: 10.1038/s41419-019-1656-4
37. Takahashi H, Saitoh K, Kishi H, Parsons PG. Immunohistochemical Localisation of Stem Cell Factor (SCF) With Comparison of its Receptor C-Kit Proto-Oncogene Product (C-KIT) in Melanocytic Tumours. *Virchows Arch* (1995) 427(3):283–8. doi: 10.1007/BF00203396
38. Giehl KA, Nagele U, Volkenandt M, Berking C. Protein Expression of Melanocyte Growth Factors (Bfgf, SCF) and Their Receptors (FGFR-1, C-Kit) in Nevi and Melanoma. *J Cutan Pathol* (2007) 34(1):7–14. doi: 10.1111/j.1600-0560.2006.00569.x
39. Slipicevic A, Herlyn M. KIT in Melanoma: Many Shades of Gray. *J Invest Dermatol* (2015) 135(2):337–8. doi: 10.1038/jid.2014.417
40. Welker P, Schadendorf D, Artuc M, Grabbe J, Henz BM. Expression of SCF Splice Variants in Human Melanocytes and Melanoma Cell Lines: Potential Prognostic Implications. *Br J Cancer* (2000) 82(8):1453–8. doi: 10.1054/bjoc.1999.1076
41. Dahlen DD, Lin NL, Liu YC, Broudy VC. Soluble Kit Receptor Blocks Stem Cell Factor Bioactivity. *vitro Leuk Res* (2001) 25(5):413–21. doi: 10.1016/s0145-2126(00)00122-3
42. Breslow A. Thickness, Cross-Sectional Areas and Depth of Invasion in the Prognosis of Cutaneous Melanoma. *Ann Surg* (1970) 172(5):902–8. doi: 10.1097/00000658-197011000-00017
43. Ria R, Reale A, Castrovilli A, Mangialardi G, Dammacco F, Ribatti D, et al. Angiogenesis and Progression in Human Melanoma. *Dermatol Res Pract* (2010) 2010:185687. doi: 10.1155/2010/185687
44. Novikova IA, Maksimova NA, Ulianova EP, Maksimova MI, Shulgina OG, Grankina A, et al. Some Immunohistochemical Markers of Angiogenesis in Melanocytic Skin Neoplasms. *J Clin Oncol* (2017) 35(15_suppl):e21067–e. doi: 10.1200/JCO.2017.35.15_suppl.e21067
45. Krystel-Whittemore M, Dileepan KN, Wood JG. Mast Cell: A Multi-Functional Master Cell. *Front Immunol* (2015) 6:620. doi: 10.3389/fimmu.2015.00620
46. Hugle T. Beyond Allergy: The Role of Mast Cells in Fibrosis. *Swiss Med Wkly* (2014) 144:w13999. doi: 10.4414/smw.2014.13999
47. Dvorak AM, Mihm MCJr., Osage JE, Dvorak HF. Melanoma. An Ultrastructural Study of the Host Inflammatory and Vascular Responses. *J Invest Dermatol* (1980) 75(5):388–93. doi: 10.1111/1523-1747.ep12523627

48. Varricchi G, Galdiero MR, Marone G, Granata F, Borriello F, Marone G. Controversial Role of Mast Cells in Skin Cancers. *Exp Dermatol* (2017) 26 (1):11–7. doi: 10.1111/exd.13107
49. Ribatti D, Ennas MG, Vacca A, Ferreli F, Nico B, Orru S, et al. Tumor Vascularity and Tryptase-Positive Mast Cells Correlate With a Poor Prognosis in Melanoma. *Eur J Clin Invest* (2003) 33(5):420–5. doi: 10.1046/j.1365-2362.2003.01152.x
50. Guidolin D, Crivellato E, Nico B, Andreis PG, Nussdorfer GG, Ribatti D. An Image Analysis of the Spatial Distribution of Perivascular Mast Cells in Human Melanoma. *Int J Mol Med* (2006) 17(6):981–7. doi: 10.3892/ijmm.17.6.981
51. Rennick D, Hunte B, Holland G, Thompson-Snipes L. Cofactors are Essential for Stem Cell Factor-Dependent Growth and Maturation of Mast Cell Progenitors: Comparative Effects of Interleukin-3 (IL-3), IL-4, IL-10, and Fibroblasts. *Blood* (1995) 85(1):57–65. doi: 10.1182/blood.V85.1.57.bloodjournal85157
52. Broudy VC. Stem Cell Factor and Hematopoiesis. *Blood* (1997) 90(4):1345–64. doi: 10.1182/blood.V90.4.1345
53. Galli SJ. New Insights Into "the Riddle of the Mast Cells": Microenvironmental Regulation of Mast Cell Development and Phenotypic Heterogeneity. *Lab Invest* (1990) 62(1):5–33.
54. Galli SJ, Tsai M, Wershil BK, Tam SY, Costa JJ. Regulation of Mouse and Human Mast Cell Development, Survival and Function by Stem Cell Factor, the Ligand for the C-Kit Receptor. *Int Arch Allergy Immunol* (1995) 107(1-3):51–3. doi: 10.1159/000236928
55. Orfao A, Garcia-Montero AC, Sanchez L, Escribano L. Rema. Recent Advances in the Understanding of Mastocytosis: The Role of KIT Mutations. *Br J Haematol* (2007) 138(1):12–30. doi: 10.1111/j.1365-2141.2007.06619.x
56. Esposito I, Kleeff J, Bischoff SC, Fischer L, Collecchi P, Iorio M, et al. The Stem Cell Factor-C-Kit System and Mast Cells in Human Pancreatic Cancer. *Lab Invest* (2002) 82(11):1481–92. doi: 10.1097/01.lab.0000036875.21209.f9
57. Baghestanian M, Agis H, Bevec D, Bankl HC, Hofbauer R, Kress HG, et al. Stem Cell Factor-Induced Downregulation of C-Kit in Human Lung Mast Cells and HMC-1 Mast Cells. *Exp Hematol* (1996) 24(12):1377–86.
58. Konig A, Corbacioglu S, Ballmaier M, Welte K. Downregulation of C-Kit Expression in Human Endothelial Cells by Inflammatory Stimuli. *Blood* (1997) 90(1):148–55. doi: 10.1182/blood.V90.1.148.148_148_155
59. Grichnik JM, Burch JA, Burchette J, Shea CR. The SCF/KIT Pathway Plays a Critical Role in the Control of Normal Human Melanocyte Homeostasis. *J Invest Dermatol* (1998) 111(2):233–8. doi: 10.1046/j.1523-1747.1998.00272.x
60. Costa JJ, Demetri GD, Harrist TJ, Dvorak AM, Hayes DF, Merica EA, et al. Recombinant Human Stem Cell Factor (Kit Ligand) Promotes Human Mast Cell and Melanocyte Hyperplasia and Functional Activation *in Vivo*. *J Exp Med* (1996) 183(6):2681–6. doi: 10.1084/jem.183.6.2681
61. Natali PG, Nicotra MR, Winkler AB, Cavaliere R, Bigotti A, Ullrich A. Progression of Human Cutaneous Melanoma is Associated With Loss of Expression of C-Kit Proto-Oncogene Receptor. *Int J Cancer* (1992) 52(2):197–201. doi: 10.1002/ijc.2910520207
62. Isabel Zhu Y, Fitzpatrick JE. Expression of C-Kit (CD117) in Spitz Nevus and Malignant Melanoma. *J Cutan Pathol* (2006) 33(1):33–7. doi: 10.1111/j.0303-6987.2006.00420.x

Conflict of Interest: The authors declare that the research was conducted in the absence of any commercial or financial relationships that could be construed as a potential conflict of interest.

Publisher's Note: All claims expressed in this article are solely those of the authors and do not necessarily represent those of their affiliated organizations, or those of the publisher, the editors and the reviewers. Any product that may be evaluated in this article, or claim that may be made by its manufacturer, is not guaranteed or endorsed by the publisher.

Copyright © 2022 Annese, Tamma, Bozza, Zito and Ribatti. This is an open-access article distributed under the terms of the Creative Commons Attribution License (CC BY). The use, distribution or reproduction in other forums is permitted, provided the original author(s) and the copyright owner(s) are credited and that the original publication in this journal is cited, in accordance with accepted academic practice. No use, distribution or reproduction is permitted which does not comply with these terms.

frontiers in Immunology

ORIGINAL RESEARCH
published: 28 January 2022
doi: 10.3389/fimmu.2022.833728

The Inhibitory Receptor Siglec-8 Interacts With FcεRI and Globally Inhibits Intracellular Signaling in Primary Mast Cells Upon Activation

*Wouter Korver[1], Alan Wong[1], Simon Gebremeskel[1], Gian Luca Negri[2], Julia Schanin[1], Katherine Chang[1], John Leung[1], Zachary Benet[1], Thuy Luu[1], Emily C. Brock[1], Kenneth Luehrsen[1], Alan Xu[1] and Bradford A. Youngblood[1]**

[1] Allakos Inc., Redwood City, CA, United States, [2] LM Biostat Consulting Inc., Victoria, BC, Canada

OPEN ACCESS

Edited by:
Frans J. Van Overveld,
University College Roosevelt,
Netherlands

Reviewed by:
Zane Orinska,
Leibniz-Zentrum für Medizin und Biowissenschaften,
Forschungszentrum Borstel, Germany
Jesse Goyette,
University of New South Wales,
Australia

***Correspondence:**
Bradford A. Youngblood
byoungblood@allakos.com

Specialty section:
This article was submitted to Inflammation, a section of the journal Frontiers in Immunology

Received: 12 December 2021
Accepted: 11 January 2022
Published: 28 January 2022

Citation:
Korver W, Wong A, Gebremeskel S, Negri GL, Schanin J, Chang K, Leung J, Benet Z, Luu T, Brock EC, Luehrsen K, Xu A and Youngblood BA (2022) The Inhibitory Receptor Siglec-8 Interacts With FcεRI and Globally Inhibits Intracellular Signaling in Primary Mast Cells Upon Activation. Front. Immunol. 13:833728. doi: 10.3389/fimmu.2022.833728

Immunomodulation of mast cell (MC) activity is warranted in allergic and inflammatory diseases where MCs have a central role in pathogenesis. Targeting Siglec-8, an inhibitory receptor on MCs and eosinophils, has shown promising activity in preclinical and clinical studies. While the intracellular pathways that regulate Siglec-8 activity in eosinophils have been well studied, the signaling mechanisms that lead to MC inhibition have not been fully elucidated. Here, we evaluate the intracellular signaling pathways of Siglec-8-mediated inhibition in primary MCs using an anti-Siglec-8 monoclonal antibody (mAb). Phospho-proteomic profiling of FcεRI-activated MCs revealed Siglec-8 mAb-treatment globally inhibited proximal and downstream kinases, leading to attenuated MC activation and degranulation. In fact, Siglec-8 was found to directly interact with FcεRI signaling molecules. Siglec-8 inhibition was dependent on both cytoplasmic immunoreceptor tyrosine-based inhibitory motifs (ITIMs) that interact with the SH2 containing protein phosphatase Shp-2 upon Siglec-8 phosphorylation. Taken together, these data support a model in which Siglec-8 regulates proximal FcεRI-induced phosphorylation events through phosphatase recruitment and interaction with FcεRIγ, resulting in global inhibition of MCs upon Siglec-8 mAb engagement.

Keywords: mast cells, IgE receptor, Siglec-8, intracellular signaling, proteomics

INTRODUCTION

Mast cells (MCs) are found at the internal and external interfaces of the body, in particular at mucosal surfaces, surrounding blood vessels, and directly interacting with peripheral nerves. They respond to a broad array of both IgE-dependent and -independent activating signals, including allergens, cytokines, complement proteins, Toll-like receptor (TLR) ligands, and neuropeptides (1). Upon stimulation, MCs secrete a broad range of inflammatory mediators that can cause anaphylactic responses and drive acute and chronic inflammation (2). Because of the myriad inflammatory mediators they release, and their ability to recruit and activate other immune cells and respond to their environment, MCs are considered key drivers of pathology in gastrointestinal, ophthalmic, dermatologic, respiratory, and proliferative diseases (3).

Sialic-acid-binding immunoglobulin-like lectin (Siglec)-8 is an inhibitory receptor selectively expressed on human MCs and eosinophils (4, 5). Since Siglec-8 does not have a true functional orthologue in non-primates, studies on receptor function in MCs rely on transgenic mice or *ex vivo* assessments of human cells (6). Targeting Siglec-8 with a monoclonal antibody (mAb) has shown promising inhibitory activity in both pre-clinical and clinical studies (6). Multiple studies have evaluated the intracellular pathways of Siglec-8-mediated cell death in IL-5-primed eosinophils and have demonstrated a role for CD11b/CD18 integrin-mediated adhesion, Src family kinases, Syk, and SHIP1 (7, 8). However, unlike the activity seen in eosinophils, Siglec-8 does not induce death of MCs, suggesting the intracellular pathways of Siglec-8 signaling in eosinophils and MCs are different (9). Like many inhibitory receptors, Siglec-8 contains two immunoreceptor tyrosine-based inhibitory motifs (ITIMs) in its cytoplasmic domain that are thought to participate in negative regulation of MC activation (10, 11). Indeed, Siglec-8 mAbs have been shown to inhibit both IgE-dependent and -independent MC activation *in vivo*, including systemic anaphylaxis in humanized mice and IL-33- and Substance P-mediated MC activation in Siglec-8 transgenic mice (12–14). Similarly, nanoparticles displaying allergen and Siglec-8 ligands have been shown to suppress phosphorylation of kinases activated by high affinity IgE receptor (FcεRI) signaling and reduce IgE-mediated murine anaphylaxis (15). Consistent with Siglec-8 functioning as an inhibitory receptor, the membrane proximal ITIM was shown to be required for Siglec-8 mAb-mediated inhibition of FcεRI-dependent calcium flux and secretory responses in MCs (9). Despite these studies identifying specific components of Siglec-8 signaling in MCs, the intracellular mechanisms that contribute to Siglec-8-mediated inhibition of MCs have not been comprehensively evaluated.

In the current study, we investigate the inhibitory effects of Siglec-8 on FcεRI intracellular signaling in primary MCs using a Siglec-8 mAb. Through phospho-proteome profiling of FcεRI-activated MCs, we find that Siglec-8 mAb treatment globally inhibits intracellular phosphorylation events, including inhibition of the kinases involved in initiating the FcεRI signaling cascade. We demonstrate that both cytoplasmic ITIMs confer Siglec-8 mediated MC inhibition and are required for Shp-2 recruitment. Consistent with broad FcεRI-mediated inhibition, we demonstrate that Siglec-8 directly interacts with FcεRI machinery. Collectively, these data provide additional mechanistic insight into the intracellular signaling pathways that contribute to Siglec-8-mediated MC inhibition.

MATERIALS AND METHODS

Bone Marrow Mast Cell Generation

Bone marrow from the femurs and tibias of wild-type C57BL/6 mice or Siglec-8 transgenic mice (16) was cultured in complete medium (DMEM supplemented with 10% FBS (Cytiva), 2 mM L-glutamine (Gibco), 1% antibiotic-antimycotic solution (Gibco), 50 μM β-mercaptoethanol (Gibco) in the presence of 10ng/mL mIL-3, Stemcell Technologies). After 2 days of culture, cells in suspension were transferred to a new flask and fresh culture medium was added two times per week with the cell count maintained between 0.5-1x10^6/mL for 6-8 weeks prior to use. MC maturity was monitored using flow cytometry staining with antibodies against CD45 (clone 30-F11, Biolegend), and MC markers CD117 (clone 2B8, eBiosciences) and FcεRIα (clone MAR-1, Biolegend). Siglec-8 expression was monitored using PE conjugated antibody from R&D Systems (clone 837535). Bone marrow mast cells are referred to as BMMC (from C57BL/6 wild-type mice) and S8-BMMC (from Siglec-8 transgenic mice).

Methods for human MC generation and activation can be found in the **Supplementary Material**.

FcεRI-Mediated Bone Marrow Mast Cell Activation and Siglec-8 mAb Treatment

S8-BMMC were plated in 96-well round bottom tissue culture plates at 5x10^4 per well and centrifuged for 2 min at 400g prior to resuspending with biotinylated anti-FcεRI (clone MAR-1, Biolegend) at 250ng/mL plus biotinylated isotype-control mouse antibody (MOPC21, mouse IgG1, Allakos) or biotinylated Siglec-8 mAb (2E2, mouse IgG1, Allakos) at 5μg/mL at 4°C for 2 min. Cells were washed in PBS and then incubated in PBS with 10μg/mL neutravidin (Thermo) for 2 min. After an additional PBS wash, cells were resuspended in 200μl 37°C complete medium and incubated for 20 min at 37°C for flow analysis or for 1 or 6 hours for analysis of histamine or cytokine levels in the supernatant. For flow cytometry, cells were resuspended in 100μl cold FACS buffer (PBS/1%BSA) containing 100ng anti-CD63-PE/Cy7 antibody (clone NVG-2, Biolegend), 100ng anti-CD107a-PE (clone 1D4B, Biolegend), 3μl 7-AAD (Becton Dickinson) as viability marker and 0.2μl mouse Fc block (BD). The percent of CD63 and CD107a expressing cells was determined by flow cytometry on a Novocyte Quanteon (Agilent). For cytokine quantification, 25μl of supernatant was analyzed using Meso Scale Discovery's U-plex kit (customized for the quantification of the indicated cytokines). Histamine levels were determined using an enzyme immunoassay kit (Beckman Coulter).

Transfections, Immunoprecipitation and Western Blotting

BMMCs (2x10^6) were transfected with 10μg plasmid expressing wild-type or mutant full-length Siglec-8 fused with an N-terminal FLAG tag. In addition to the wild-type sequence, plasmids containing ITIM mutants of Siglec-8 were generated by changing the tyrosine residue at position 447 of the proximal motif (wild-type=LHYATL) to phenylalanine (Y447F=LHFATL) and the tyrosine at position 470 of the distal motif (wild-type=SEYSEIK) to phenylalanine (Y470F= SEFSEIK). The double mutant contains both mutations (Y447F+Y470F). For all transfections, plasmid DNA (10 μg) was added to 2x10^6 cells and transfected using the 4D-Nucleofector (Lonza) with P3 nucleofector solution and Supplement 1 and program DS-130. Transfection efficiency of BMMC was consistently between 80-95% under these conditions. Cells were incubated at 37°C in complete medium for 6 hours for lysis for IP/WB or 16 hours for functional assays (FcεRI cross-linking). A fresh 30mM stock solution of pervanadate was prepared by adding 150μl of 200mM sodium orthovanadate (FivePhoton/

Fisher) to 844µl PBS, plus 6.1µl 30% H_2O_2 (Sigma) and incubated for 20 min at room temperature prior to addition to cells at the indicated final concentrations to inhibit phosphatases.

Cells were lysed in Pierce IP lysis buffer (Thermo) with HALT protease and phosphatase inhibitors (Thermo). Lysates were used directly for Western Blotting or immunoprecipitation by adding 25µl Pierce anti-FLAG or anti-HA magnetic agarose beads (Thermo) for 30 min at room temperature while rotating. Siglec-8 IPs were performed using anti-Siglec-8 polyclonal rabbit antibody (Thermo, PA5-28846) at 10µg/mL for 30 min followed by addition of Magnetic Protein A/G beads (Pierce). After 4 washes with TBS-T, proteins were eluted by incubation at 70°C for 10 min in 1xLB with reducing agent added (Thermo), separated by SDS-PAGE and subjected to Western Blot analysis. 5% milk (Bio-Rad) in TBS-0.1%Tween-20 was used for blocking. Anti-FLAG antibody was from Sigma; anti-HA, anti-Lyn (clone LYN-01) and anti-Siglec-8 from Thermo; anti-Shp-2 (clone D50F2) from Cell Signaling Technologies; 4G10 from Millipore/Sigma. Anti-FLAG and anti-4G10 antibodies for Western blotting were directly conjugated to HRP, other primary antibodies were detected using HRP conjugated mouse anti-rabbit IgG, light chain specific (Jackson ImmunoResearch 211-032-171) at 1:2,000 dilution in TBS-T/5% milk. Western blots were developed using Immobilon Forte western HRP substrate (Millipore) and imaged using the iBright imaging system (Thermo).

Mass Spectrometry

Detailed methods for MS and proteomics analysis can be found in the **Supplementary Material**.

Confocal Microscopy

S8-BMMC were stained in PBS/1% BSA on ice for 30 min with anti-S8-AF647 (Allakos), anti-FcεRI-PE (clone MAR-1, Biolegend) and fixed in 2% PFA. For crosslinking, S8-BMMC were treated as described under 'FceRI-Mediated Bone Marrow Mast Cell Activation and Siglec-8 mAb Treatment' and subsequently fixed in 2% PFA. Fixed cells were spun onto poly-D-lysine (50µg/mL for 1 hour, GIBCO) coated 96-well glass plates (Cellvis) at 2,000g for 5 min and covered in 200ul PBS with 1µg/mL DAPI for nuclear staining. Cells were imaged on a Leica Stellaris 5 confocal microscope using a 63x objective with oil immersion. Images were analyzed using ImageJ. Briefly, cells were identified manually as ROIs. Within ROIs, bright foci greater than 0.6 µm in diameter were defined as punctae. Intensity of PE was then determined by averaging the fluorescent intensity within each punctae mask.

RESULTS

Bone Marrow Mast Cells From Transgenic Mice Express Functional Siglec-8 and Respond to FcεRI-Mediated Activation

To interrogate MC activation and inhibition *in vitro*, we developed a system using MCs derived from the bone marrow of Siglec-8 transgenic mice (S8-BMMCs) (16). Upon differentiation after about 6 weeks of culture, these MCs displayed a mature phenotype, including expression of MC phenotypic markers and Siglec-8 (**Figure 1A**).

Stimulation of S8-BMMCs with an agonistic anti-FcεRI antibody in the presence of an isotype control antibody (ISO), induced degranulation as detected by the upregulation of degranulation markers CD63 and CD107a on mast cells (**Figure 1B**). In addition, FcεRI-mediated activation significantly induced histamine secretion (**Figure 1C**, measured after 1 hour), and TNFα, IL-6 and CCL2 cytokine secretion (**Figure 1D**, at 6 hours) compared to unstimulated cells. In the presence of a Siglec-8 mAb, both degranulation and mediator release by activated S8-BMMCs were strongly inhibited compared to isotype control treatment (**Figures 1B–D**). Siglec-8 mAb-mediated inhibition of MC degranulation was concentration dependent: a statistically significant reduction in the upregulation of CD63 and CD107a compared to isotype control treatment was observed with Siglec-8 mAb concentrations of 80ng/mL and higher (**Figure 1E**). To determine if the presence of FcεRI-bound IgE affected Siglec-8 mAb activity, we cultured S8-BMMCs in the presence of titrating concentrations of IgE. While the level of FcεRI-mediated activation was lower in the presence of a high IgE concentration, the inhibition by Siglec-8 mAb was not affected (**Supplementary Figure 1A**). These data demonstrate that S8-BMMCs respond to FcεRI-mediated activation *in vitro* and express functional Siglec-8. To confirm natively expressed Siglec-8 functioned similarly, we evaluated Siglec-8 mAb-mediated inhibition in human primary MCs derived from peripheral blood $CD34^+$ cells activated with agonistic anti-human FcεRI antibody CRA-1. Similar levels of Siglec-8 mAb-inhibition were seen in human MCs compared to S8-BMMCs, demonstrating transgenic expression of Siglec-8 in BMMCs is reflective of human function (**Supplementary Figures 1B, C**).

Siglec-8 mAb Treatment Globally Inhibits FcεRI-Induced Intracellular Signaling

Inhibition of MCs through Siglec-8 has been described previously (9, 12, 13, 16), but the intracellular signaling pathways have not been fully elucidated. To investigate this, we profiled phospho-proteomes of S8-BMMCs that were stimulated in the absence or presence of Siglec-8 mAb by mass spectrometry. Three treatment conditions were evaluated in duplicate: 1) unstimulated S8-BMMCs, and S8-BMMCs activated by cross-linking of the FcεR1 receptor for 2 min in the presence 2) or absence 3) of Siglec-8 mAb. Proteomes were labeled by Tandem Mass Tag (TMT) and enriched for phospho-serine, -threonine and -tyrosine peptides prior to analysis by mass spectrometry and subsequent quantification of phospho-peptides (**Figure 2A**).

In the FcεRI stimulated MCs, 348 unique phosphosites were identified as differentially phosphorylated by more than 2-fold, of which 41 were upregulated more than 4-fold relative to unstimulated control MCs (adjusted p-value < 0.05; **Figure 2B**). Strikingly, in the presence of a Siglec-8 mAb the number of differential phosphosites decreased to 71 (2-fold) and 7 (4-fold),

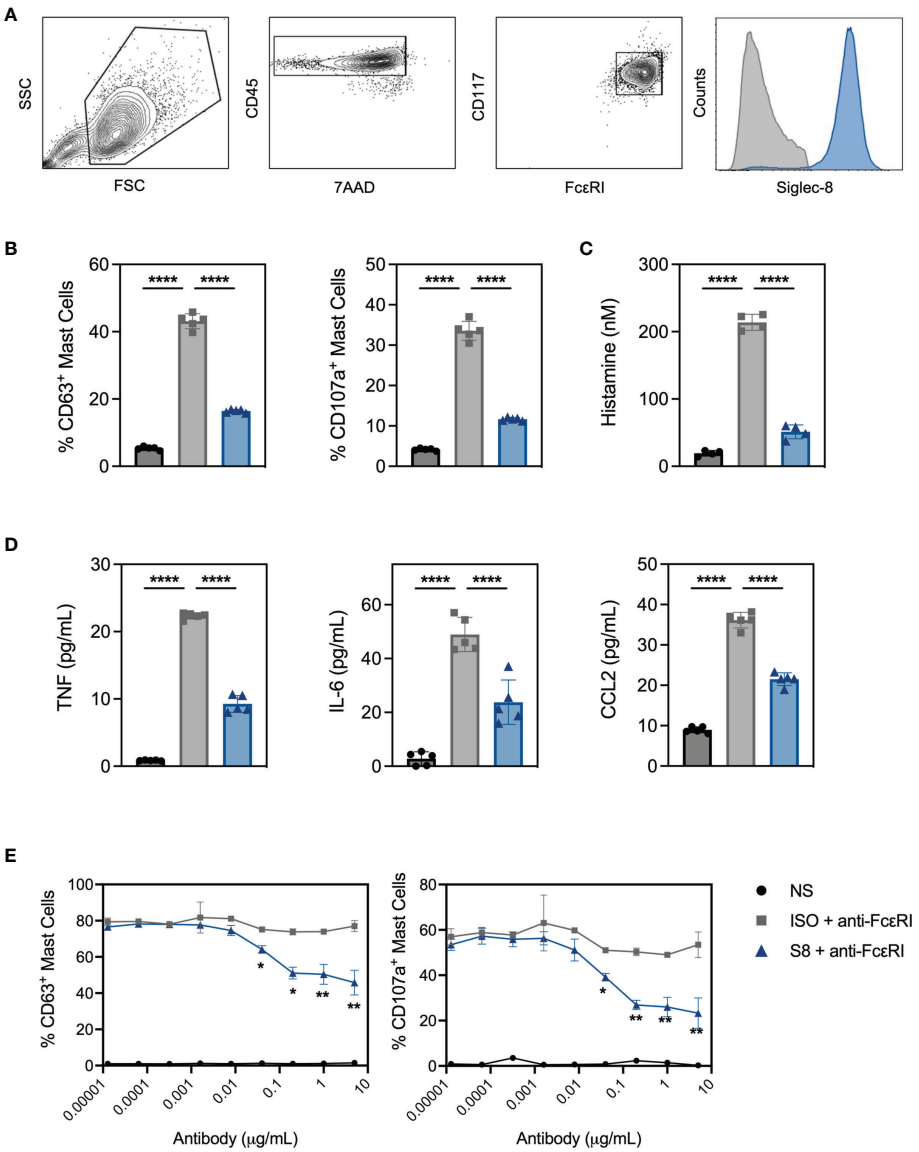


FIGURE 1 | BMMC from transgenic mice respond to FcεRI activation and express functional Siglec-8. **(A)** BMMC-S8 flow cytometry gating strategy. Right panel represents Siglec-8 staining (blue) and FMO stain (grey) **(B)** Levels of surrogate degranulation markers CD63 and CD107a on the cell surface of unstimulated MC (NS; black bars), when cross-linked with the anti-FcεRI antibody MAR-1 for 15 min (ISO + anti-FcεRI, grey bars) or co-cross-linked with MAR-1 and Siglec-8 mAb (S8 + anti-FcεRI, blue bars). **(C)** Histamine concentrations in the culture medium of MC collected 1 hour after stimulation as in **(B)**. **(D)** Cytokine concentrations in the culture medium of MC collected 6 hours after stimulation. **(E)** Titration of isotype control mAb and Siglec-8 mAb in combination with anti-FcεRI-mediated (MAR-1) activation. Left panel: % of CD63 positive MC. Right panel: % of CD107a positive MC. Data are plotted as mean ± SEM (n=5) and are representative of 5 experiments. *p < 0.05, **p < 0.01, ****p < 0.0001 by one-way ANOVA test **(B–D)** or unpaired t test **(E)**.

respectively. A heatmap representing differential phosphorylation events further confirmed that the majority of the FcεRI-induced phosphorylation events were reduced in the presence of Siglec-8 mAb (**Figure 2C**). Many of the abundantly phosphorylated peptides that were decreased represented key proteins known to be immediately downstream of FcεRI signaling (17–19), including the kinase Syk, adaptor molecules Gab2 and Dapp1, and the more downstream kinases protein kinase C and Akt (**Figure 2C**). In addition, Siglec-8 mAb-treatment inhibited signaling molecules phosphorylated upon activation such as Erk, the phosphatase Ship1, scaffold proteins Wipf1, Ahnak and Lat2 and the gamma subunit of FcεRI itself (**Figure 2C** and **Supplementary Figure 2**). The induction and inhibition of global p-Tyr phosphorylation (**Supplementary Figure 3A**) and specific phosphorylation events for p-Syk and p-Erk were confirmed by Western blot and intracellular flow cytometry analysis (**Supplementary Figures 3B–D**).

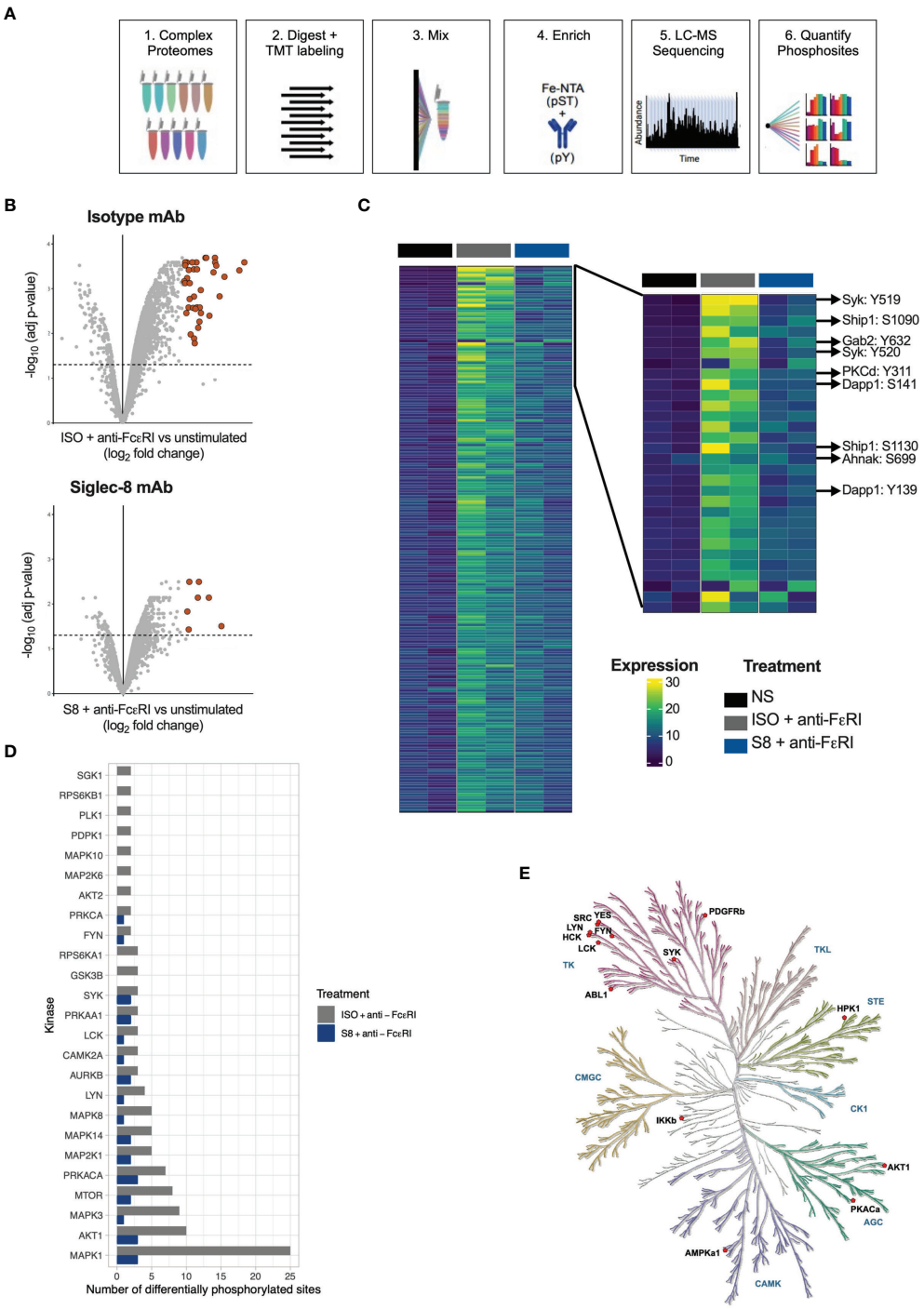


FIGURE 2 | Phospho-proteome of FcεRI-stimulated and Siglec-8-inhibited S8-BMMCs. **(A)** Schematic of the process for determining phospho-proteomes of MCs. **(B)** Volcano plots of Log2 fold change against statistical significance of the abundance of phospho-peptides 2 min after FcεRI crosslinking in the presence of isotype control antibody (top panel) or Siglec-8 mAb (bottom panel). Highlighted are the peptides upregulated more than 4-fold. **(C)** Heatmap of quantified phospho-peptides. Each line represents a unique phospho-peptide with the first two columns representing the unstimulated MCs in two independent experiments, the next two columns the phospho-proteome from MCs activated through FcεRI and the last two columns represent activation in the presence of a Siglec-8 mAb. The heatmap is ranked from top to bottom by fold induction upon activation averaged over the two experiments. Right panel: zoom in on the top sections of the heatmap in **(C)**. **(D)** Bar graph representing the number of phosphosites predicted to be phosphorylated by the indicated kinase in the FcεRI stimulated conditions. **(E)** Kinase tree highlighting the kinases that are known to modify sites that showed differential phosphorylation between the isotype and Siglec-8 mAb conditions upon FcεRI activation.

Siglec-8 Inhibits Proximal Kinase Activity Upon FcεRI-Mediated Mast Cell Activation

Using the integrative PhosphoSitePlus database (20), we mapped phosphorylation sites to annotated kinases to identify differences in kinase activity between Siglec-8 mAb *vs* isotype conditions. We identified proximal kinases known to be associated with FcεRI activation (Lyn, Syk, Fyn) as well as kinases involved in downstream pathways (e.g., MAPK family members) (**Figure 2D**). FcεRI-activated MCs treated with a Siglec-8 mAb had fewer phosphorylated sites for all predicted kinases compared to activated MCs treated with an isotype control antibody (**Figure 2D**). The kinase tree in **Figure 2E** highlights the kinases known to modify the sites that showed differential phosphorylation (1.2 fold) between isotype and Siglec-8 mAb conditions, including the tyrosine kinases that function at the top of the FcεRI signaling cascade (Syk, Lyn) as well as those downstream (Ikkb). These data demonstrate that Siglec-8 mediates global inhibition of FcεRI signaling in primary MCs by regulating FcεRI-mediated kinase activity upon mAb engagement.

Both Siglec-8 ITIMs Are Involved in the Inhibition of FcεRI-Induced Degranulation and Phosphatase Recruitment

Siglec-8 contains two ITIMs in its cytosolic tail (**Figure 3A**). The motif nearest to the membrane was previously demonstrated to be required for Siglec-8 mediated inhibition in rat basophilic leukemia cell activation (9), but whether a single or both tyrosines in the ITIMs of the intracellular domain of Siglec-8 are critical for inhibitory activity in primary MC is unknown. Expression constructs were generated for mutant versions of Siglec-8, in which the tyrosine residues were replaced with phenylalanine residues, either separately (Y447F and Y470F) or combined to generate a double mutant (Y447F+Y470F). BMMCs transfected with each of the wild-type or mutant Siglec-8 constructs were activated *via* anti-FcεRI agonist antibody MAR-1 (ISO+anti-FcεRI). FcεRI activation was inhibited in the presence of a Siglec-8 mAb for BMMCs transfected with wild-type or single-mutant Siglec-8 (**Figure 3B**), although inhibitory function was partially attenuated in BMMCs transfected with the membrane proximal ITIM mutant (Y447F), but not the membrane distal ITIM mutant (Y470F). However, BMMCs expressing the double ITIM mutant lost almost all Siglec-8-mediated inhibition. The percent inhibition calculated from these data obtained for each Siglec-8 variant is plotted in **Figure 3C**. These data demonstrate that both functional ITIMs are required for Siglec-8 mediated inhibition in FcεRI-activated primary BMMCs.

Src-homology 2 (SH2) domain containing protein tyrosine phosphatases have been shown to be critical for inhibition of immune cells through Siglec family members and other ITIM containing receptors (10, 21). We detected Shp-1 at low levels in BMMCs and did not observe an interaction with Siglec-8 (data not shown). In T cells, mechanistic and single cell imaging studies of programmed cell death 1 (PD-1) demonstrated that Shp-2 is required for inhibition (22, 23). Since the ITIMs were required for Siglec-8 mediated inhibition in BMMCs (**Figure 3B**), we assessed if Shp-2 physically interacted with Siglec-8 in BMMCs transfected with FLAG-tagged Siglec-8 (wild-type or double-mutant) in the presence or absence of the phosphatase inhibitor pervanadate (PVD). In the absence or in the presence of 0.1mM concentrations of PVD, Shp-2 did not co-immunoprecipitate with Siglec-8 despite the presence of Shp-2 protein in whole cell lysates under all conditions (**Figure 3D**, panel 1 + 2). Incubation with a high concentration of PVD (1mM) resulted in Shp-2 co-immunoprecipitating with wild-type Siglec-8, but not with the double ITIM mutant (**Figure 3D**, panels 2 + 3). To evaluate if the Shp-2/Siglec-8 interaction was dependent on Siglec-8 ITIM phosphorylation, we probed with a pan-tyrosine phosphorylation antibody (**Figure 3D**, panel 4). Indeed, wild-type but not the double ITIM mutant Siglec-8 was tyrosine phosphorylated at the high PVD concentration (**Figure 3D**, panel 5). These data strongly suggest that Siglec-8 phosphorylation within the ITIM motifs is required for Shp-2 interaction.

Siglec-8 Interacts With Proximal FcεRI Signaling Machinery

The inhibition of FcεRI-mediated proximal signaling events led us to hypothesize that Siglec-8 may directly interact with FcεRI signaling components. We investigated potential physical interactions of Siglec-8 with FcεRI and associated signaling molecules using BMMCs transfected with FLAG-tagged Siglec-8. Surprisingly, Siglec-8 co-immunoprecipitated with FcεRIγ from lysates of unstimulated MC, demonstrating that these proteins can co-exist in a complex (**Figure 4A**). Since the Src kinase Lyn is immediately activated upon IgE cross-linking of FcεRI (24–26), and its predicted level of phosphorylation was decreased in Siglec-8 mAb-treated MCs (**Figures 2D, E**), we evaluated if Lyn also interacted with Siglec-8. Indeed, we detected Lyn in the immunoprecipitate of Siglec-8, demonstrating that Lyn also can interact in complex with Siglec-8 (**Figure 4B**).

Next, we investigated if Siglec-8 colocalized with FcεRI in S8-BMMCs using confocal microscopy. We observed a relatively homogeneous distribution of Siglec-8 and the FcεRI receptor complex on the membrane of unstimulated S8-BMMCs, suggesting they may partially co-localize, in line with the immunoprecipitation data (**Figure 4C**, top panels). Co-cross-linking of both FcεRI and Siglec-8 resulted in large membrane associated structures (punctae) (**Figure 4C**, bottom panels), in which Siglec-8 and FcεRI co-resided. Interestingly, co-localization of both receptors was reduced when only FcεRI was engaged with mAb (**Figure 4C**, middle panels). Quantification of the confocal images confirmed a significant increase in the number of punctae and the presence of Siglec-8 within these punctae when FcεRI and Siglec-8 were both co-cross-linked compared to unstimulated or FcεRI only engagement (**Figure 4D**). The level of Siglec-8 present in complex with FcεRI was trending lower when FcεRI was crosslinked by itself compared to unstimulated cells. Taken together, these data demonstrate that Siglec-8 interacts with FcεRI and its signaling components and suggest the existence of

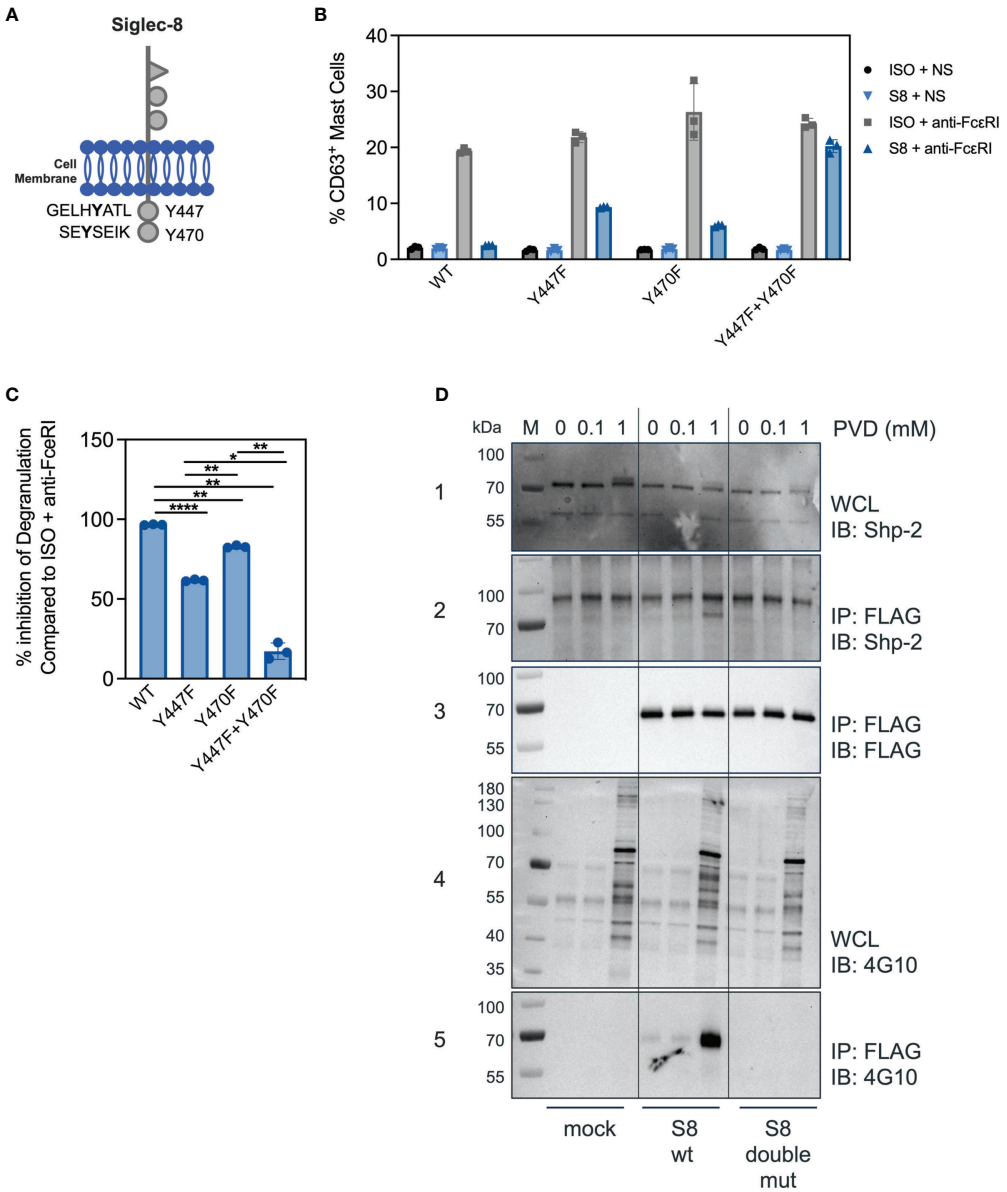


FIGURE 3 | Both ITIM motifs are required for Siglec-8 mediated inhibition. **(A)** Schematic of the Siglec-8 receptor with its two tyrosine residues in the context of ITIM motifs indicated. **(B)** Percent of CD63 positive MC in unstimulated (ISO + NS, S8 + NS), stimulated (ISO + anti-FcεRI) and inhibited (S8 + anti-FcεRI) MC after transfection of the indicated wild-type or mutant Siglec-8 expression constructs Data are plotted as mean ± SEM (n=3) and are representative of 3 experiments. **(C)** Percent inhibition of Siglec-8 mAb-treatment for each Siglec-8 expression construct was calculated compared to ISO condition. *p < 0.05, **p < 0.01, ****p < 0.0001 by one-way ANOVA test. **(D)** Western blot analysis of Siglec-8-Shp2 interaction. Immunoblot (IB) of whole cell lysates (WCL) or FLAG immunoprecipitations (IP) from primary MC mock transfected or with expression constructs for wild-type Siglec-8-FLAG or ITIM double mutant Siglec-8-FLAG. Cells were subjected to PVD treatment for two min and WCL were analyzed for presence of Shp-2 (panel 1) and p-Tyr (panel 4). Anti-FLAG IPs were analyzed for presence of Shp-2 (panel 2), Siglec-8-FLAG (panel 3) and p-Tyr (panel 5). Experiments were performed 2-3 times for confirmation.

multi-protein complexes where activating and inhibitory receptors interact with multiple proximal signaling mediators. We propose a model whereby recruitment of sufficient levels of Siglec-8 to FcεRI complexes results in increased phosphatase activity that inhibits proximal kinase activity leading to broad attenuation of intracellular signaling and subsequent degranulation in MCs (**Figure 5**).

DISCUSSION

In recent years, our understanding of the interplay between activating and inhibitory receptors in immune cells has greatly increased through large scale expression and proteomics studies. As key effector cells in acute and chronic allergic and inflammatory responses, MC numbers and activation state

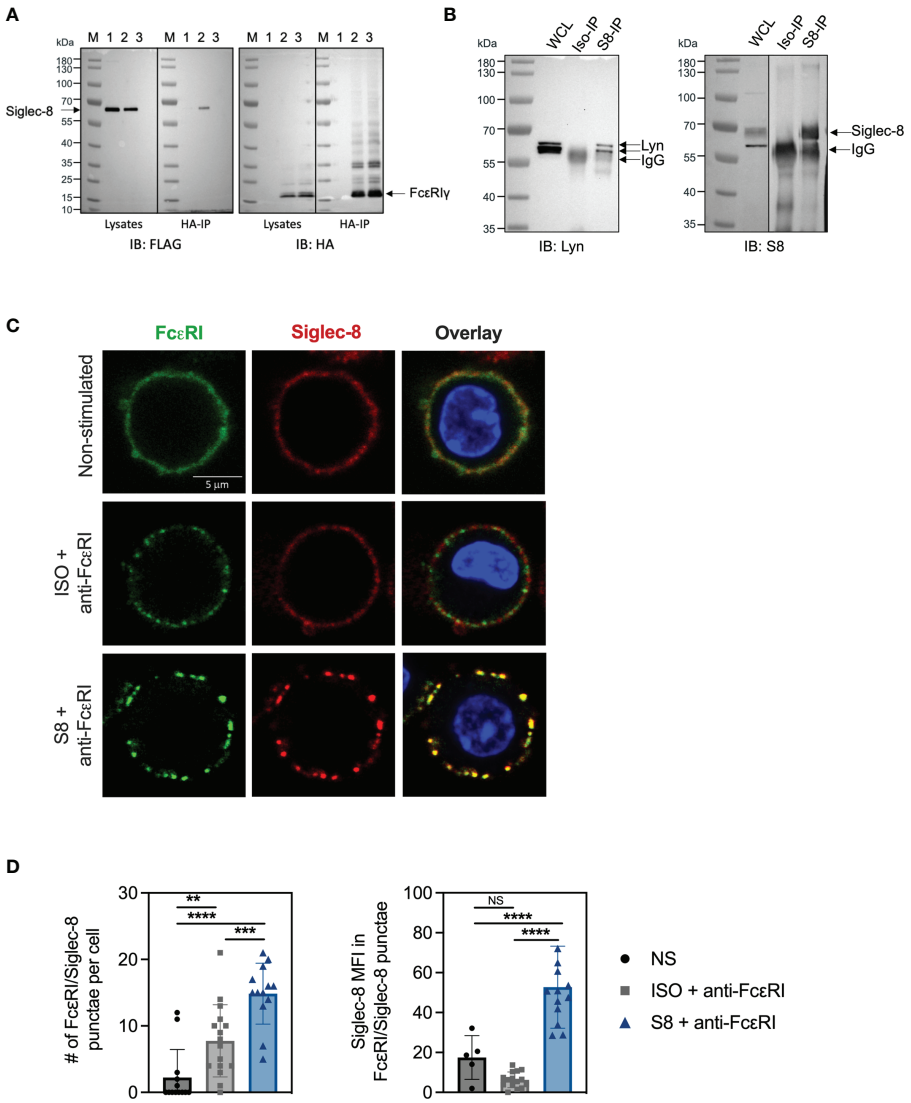


FIGURE 4 | Siglec-8 interacts with FcεRI machinery components. **(A)** Western blot analysis of Siglec-8-FcεRIγ interaction. Immunoblot (IB) of whole cell lysates (WCL) or HA immunoprecipitations (IP) from primary MC transfected with expression constructs for Siglec-8-FLAG (lane 1) or FcεRIγ-HA (lane 3) or both (lane 2). Blots were developed with anti-FLAG (left panel) and anti-HA (right panel). **(B)** Western blot analysis of Siglec-8-Lyn interaction. WCL, isotype IP or S8 IP from S8-BMMC were developed using anti-Lyn or anti-Siglec-8 antibodies. **(C)** Confocal microscopy imaging of Siglec-8 (red) and FcεRI (green) in S8-BMMC. **(D)** Quantification of confocal images. Left panel: number of FcεRI punctae per cell (PE channel). Right panel: Siglec-8 median fluorescence intensity within FcεRI/Siglec-8 punctae (AF647 channel). Experiments were performed 2-3 times. NS, not significant, $^{**}p < 0.01$, $^{***}p < 0.001$, $^{****}p < 0.0001$ by one-way ANOVA test.

have been shown to be aberrantly increased in several diseases (3, 27, 28). The inhibitory receptor Siglec-8 has emerged as a promising drug target in MC-driven diseases and the work described herein was carried out to study in detail the effects of Siglec-8 engagement on intracellular signaling upon MC activation through FcεRI.

While inhibition of FcεRI-mediated activation of MC through Siglec-8 engagement has been demonstrated previously (9, 15, 16), the consequences of this inhibition on intracellular signaling have not been thoroughly investigated. Here we present the first comprehensive evaluation of phosphoproteomes from FcεRI-activated and Siglec-8-engaged MCs. Our data support the conclusion that broad inhibition of proximal anti-FcεRI-induced phosphorylation events in primary MCs results in attenuated degranulation and mediator release in the presence of Siglec-8 mAb.

The inhibition by a Siglec-8 mAb is contingent on the presence of intracellular tyrosine residues within the ITIM domains, as has been described for other Siglec family members (9, 29, 30). We provide evidence that both ITIM domains in Siglec-8 participate in inhibiting FcεRI-induced activation in primary S8-BMMCs. This is analogous to the observed requirement for inhibition through CD22 (Siglec-2) in B cells, which was shown to depend on all three of its ITIMs

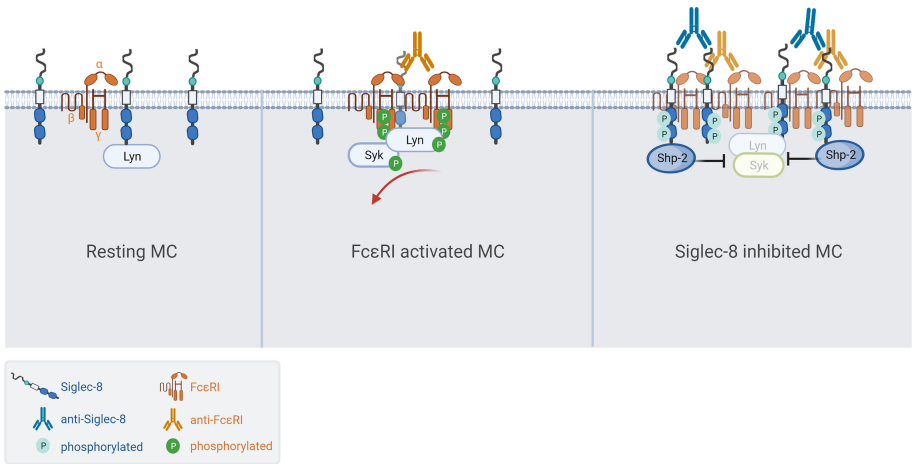


FIGURE 5 | Model of Siglec-8 mediated inhibition of FcεRI signaling in MCs. (Left) Siglec-8 and FcεRI are distributed along the membrane of resting MC while partially colocalizing. (Middle) Cross-linking with MAR-1 anti-FcεRI results in high density clusters of FcεRI resulting in phosphorylation at the ITAM, subsequent MC activation/degranulation and partial exclusion of Siglec-8 from the activating complexes. (Right) In the presence of Siglec-8 mAb, phosphatases like Shp-2 are recruited to large complexes of activating (FcεRI) and inhibitory (Siglec-8) receptors resulting in potent inhibition of intracellular signaling.

for fully efficient inhibition (30). In contrast, data from studies with Siglec-7 and Siglec-9 demonstrated only the most proximal of two ITIMs to be critical for inhibitory activity (29). The differences between the requirements of ITIM motifs for inhibition may depend on 1) the origin of the cell type used, whether it is a primary cell or immortalized line, 2) the expression of downstream signaling molecules in these cells, particularly SH2 containing protein tyrosine phosphatases Shp-1 and Shp-2 and 3) the conformation/dimerization of the receptors. In structural studies, Shp-2 was found to require both of its SH2 domains for binding to phosphorylated ITIMs (31), which may be achieved by engaging with two motifs on the same receptor or through dimerization of receptors. While Shp-1 was detected at low levels in BMMCs, we cannot rule out a role for Shp-1 similar to Shp-2 based on our data.

In contrast to the cell death-inducing activity mediated by Siglec-8 mAb antibodies in eosinophils (12, 32), our *in vitro* assessments of Siglec-8 mediated MC activity revealed little evidence of inhibition by a Siglec-8 mAb in the absence of FcεRI-induced activation. These data suggest that a close physical association of activating and inhibitory receptors is required for inhibition and are consistent with recent work studying CD33 (Siglec-3) and Siglec-8 (15, 33). The authors demonstrate that FcεRI and Siglec-8/CD33 are not entirely co-localized in the same membrane microdomain and active recruitment of the inhibitory receptor to the lipid rafts containing the IgE-FcεRI complex is required. However, Siglec-8 mAbs have also been shown to inhibit non-ITAM-mediated activation of MCs, including stimulation through cytokine receptors, GPCRs, and TLRs (13, 14, 28). These data suggest that Siglec-8 could modulate intracellular signaling pathways differently depending on the mode of MC activation. In support of this, transcriptomic profiling of peritoneal MCs stimulated with IL-33 and treated with a Siglec-8 mAb showed significantly increased expression of genes associated with TLR inhibition, MyD88 signaling, and other ITIM-containing receptors (13). Additional studies are needed to elucidate how Siglec-8 and its engagement inhibits IgE-independent MC activation.

Interaction of Siglec-8 with FcεRIγ was detected in co-immunoprecipitation and imaging experiments (**Figures 4A, C**), which suggests that at least subsets of these two proteins are in the same protein complex in resting MC. Recent high precision microscopy studies demonstrated, in accordance with our model, subtle changes in location and organization in the plasma membrane between resting and stimulated states, with lipid-based and protein-based interactions leading to suprathreshold phosphorylation by facilitating access of kinase and exclusion of phosphatase activity (34). Collectively, our data provide novel mechanistic insight into intracellular signaling pathways that contribute to Siglec-8 mediated MC inhibition and suggest that Siglec-8 can influence the complex orchestration of activating and inhibitory activities by regulating upstream kinases and phosphatases upon stimulation through FcεRI.

DATA AVAILABILITY STATEMENT

The original contributions presented in the study are publicly available. This data can be found here: ProteomeXchange, PXD030820 link: http://proteomecentral.proteomexchange.org/cgi/GetDataset?ID=PXD030820

ETHICS STATEMENT

Ethical review and approval was not required for the animal study because the involvement of animals was solely for the

harvesting of cells for culturing and *in vitro* experiments. This study was conducted in accordance with the ethical conduct in the care and use of animals and in compliance with ARRIVE guidelines.

AUTHOR CONTRIBUTIONS

WK, JS, BY designed experiments. WK, AW, SG, JS, KC, JL, ZB, TL, EB, KL conducted experiments. GN analyzed proteomics data and provided bioinformatics support. WK, BY wrote the manuscript. All authors contributed to manuscript revision, read, and approved the submitted version.

ACKNOWLEDGMENTS

Editing support was provided by Jocelyn Hybiske, PhD, a professional medical writer, funded by Allakos. The model was created with biorender.com. We thank Drs Bruce Bochner and Bob Schleimer for critical reading of the manuscript.

SUPPLEMENTARY MATERIAL

The Supplementary Material for this article can be found online at: https://www.frontiersin.org/articles/10.3389/fimmu.2022.833728/full#supplementary-material

REFERENCES

1. Komi DEA, Mortaz E, Amani S, Tiotiu A, Folkerts G, Adcock IM. The Role of Mast Cells in IgE-Independent Lung Diseases. *Clin Rev Allergy Immunol* (2020) 58(3):377–87. doi: 10.1007/s12016-020-08779-5
2. Moon TC, Befus AD, Kulka M. Mast Cell Mediators: Their Differential Release and the Secretory Pathways Involved. *Front Immunol* (2014) 5:569. doi: 10.3389/fimmu.2014.00569
3. Krystel-Whittemore M, Dileepan KN, Wood JG. Mast Cell: A Multi-Functional Master Cell. *Front Immunol* (2015) 6:620. doi: 10.3389/fimmu.2015.00620
4. Kikly KK, Bochner BS, Freeman SD, Tan KB, Gallagher KT, D'Alessio KJ, et al. Identification of SAF-2, a Novel Siglec Expressed on Eosinophils, Mast Cells, and Basophils. *J Allergy Clin Immunol* (2000) 105(6 Pt 1):1093–100. doi: 10.1067/mai.2000.107127
5. Floyd H, Ni J, Cornish AL, Zeng Z, Liu D, Carter KC, et al. Siglec-8. A Novel Eosinophil-Specific Member of the Immunoglobulin Superfamily. *J Biol Chem* (2000) 275(2):861–6. doi: 10.1074/jbc.275.2.861
6. Youngblood BA, Leung J, Falahati R, Williams J, Schanin J, Brock EC, et al. Discovery, Function, and Therapeutic Targeting of Siglec-8. *Cells* (2020) 10 (1):19. doi: 10.3390/cells10010019
7. Carroll DJ, O'Sullivan JA, Nix DB, Cao Y, Tiemeyer M, Bochner BS. Sialic Acid-Binding Immunoglobulin-Like Lectin 8 (Siglec-8) is an Activating Receptor Mediating Beta2-Integrin-Dependent Function in Human Eosinophils. *J Allergy Clin Immunol* (2018) 141(6):2196–207. doi: 10.1016/j.jaci.2017.08.013
8. Carroll DJ, Cao Y, Bochner BS, O'Sullivan JA. Siglec-8 Signals Through a Non-Canonical Pathway to Cause Human Eosinophil Death In Vitro. *Front Immunol* (2021) 12:737988. doi: 10.3389/fimmu.2021.737988
9. Yokoi H, Choi OH, Hubbard W, Lee HS, Canning BJ, Lee HH, et al. Inhibition of FcepsilonRI-Dependent Mediator Release and Calcium Flux From Human Mast Cells by Sialic Acid-Binding Immunoglobulin-Like Lectin 8 Engagement. *J Allergy Clin Immunol* (2008) 121(2):499–505 e1. doi: 10.1016/j.jaci.2007.10.004
10. Crocker PR, Paulson JC, Varki A. Siglecs and Their Roles in the Immune System. *Nat Rev Immunol* (2007) 7(4):255–66. doi: 10.1038/nri2056
11. Duan S, Paulson JC. Siglecs as Immune Cell Checkpoints in Disease. *Annu Rev Immunol* (2020) 38:365–95. doi: 10.1146/annurev-immunol-102419-035900
12. Youngblood BA, Brock EC, Leung J, Falahati R, Bryce PJ, Bright J, et al. AK002, a Humanized Sialic Acid-Binding Immunoglobulin-Like Lectin-8 Antibody That Induces Antibody-Dependent Cell-Mediated Cytotoxicity Against Human Eosinophils and Inhibits Mast Cell-Mediated Anaphylaxis in Mice. *Int Arch Allergy Immunol* (2019) 180(2):91–102. doi: 10.1159/000501637
13. Schanin J, Gebremeskel S, Korver W, Falahati R, Butuci M, Haw TJ, et al. A Monoclonal Antibody to Siglec-8 Suppresses non-Allergic Airway Inflammation and Inhibits IgE-Independent Mast Cell Activation. *Mucosal Immunol* (2021) 14(2):366–76. doi: 10.1038/s41385-020-00336-9
14. Gebremeskel S, Davis T, Wong A, Brock E, Leung J, Schanin J, et al. A Siglec-8 Antibody Reduces Substance P-Induced Inflammation by Inhibiting MRGPR-Mediated Mast Cell Activation. *Allergy* (2020) 75(Suppl. 109):5–99. doi: 10.1111/all.14504
15. Duan S, Arlian BM, Nycholat CM, Wei Y, Tateno H, Smith SA, et al. Nanoparticles Displaying Allergen and Siglec-8 Ligands Suppress IgE-FcepsilonRI-Mediated Anaphylaxis and Desensitize Mast Cells to Subsequent Antigen Challenge. *J Immunol* (2021) 206(10):2290–300. doi: 10.4049/jimmunol.1901212
16. Youngblood BA, Brock EC, Leung J, Falahati R, Bochner BS, Rasmussen HS, et al. Siglec-8 Antibody Reduces Eosinophils and Mast Cells in a Transgenic Mouse Model of Eosinophilic Gastroenteritis. *JCI Insight* (2019) 4(19): e126219. doi: 10.1172/jci.insight.126219
17. Cao L, Yu K, Banh C, Nguyen V, Ritz A, Raphael BJ, et al. Quantitative Time-Resolved Phosphoproteomic Analysis of Mast Cell Signaling. *J Immunol* (2007) 179(9):5864–76. doi: 10.4049/jimmunol.179.9.5864
18. Kambayashi T, Koretzky GA. Proximal Signaling Events in Fc Epsilon RI-Mediated Mast Cell Activation. *J Allergy Clin Immunol* (2007) 119(3):544–52; quiz 553-4. doi: 10.1016/j.jaci.2007.01.017
19. Oettgen HC, Burton OT. IgE and Mast Cells: The Endogenous Adjuvant. *Adv Immunol* (2015) 127:203–56. doi: 10.1016/bs.ai.2015.03.001
20. Hornbeck PV, Zhang B, Murray B, Kornhauser JM, Latham V, Skrzypek E. PhosphoSitePlus, 2014: Mutations, PTMs and Recalibrations. *Nucleic Acids Res* (2015) 43(Database issue):D512–20. doi: 10.1093/nar/gku1267
21. Macauley MS, Crocker PR, Paulson JC. Siglec-Mediated Regulation of Immune Cell Function in Disease. *Nat Rev Immunol* (2014) 14(10):653–66. doi: 10.1038/nri3737
22. Yokosuka T, Takamatsu M, Kobayashi-Imanishi W, Hashimoto-Tane A, Azuma M, Saito T. Programmed Cell Death 1 Forms Negative Costimulatory Microclusters That Directly Inhibit T Cell Receptor Signaling by Recruiting Phosphatase SHP2. *J Exp Med* (2012) 209(6):1201–17. doi: 10.1084/jem.20112741
23. Patsoukis N, Duke-Cohan JS, Chaudhri A, Aksoylar HI, Wang Q, Council A, et al. Interaction of SHP-2 SH2 Domains With PD-1 ITSM Induces PD-1 Dimerization and SHP-2 Activation. *Commun Biol* (2020) 3(1):128. doi: 10.1038/s42003-020-0845-0
24. Scharenberg AM, Kinet JP. Initial Events in Fc Epsilon RI Signal Transduction. *J Allergy Clin Immunol* (1994) 94(6 Pt 2):1142–6. doi: 10.1016/0091-6749(94)90323-9
25. Nunomura S, Gon Y, Yoshimaru T, Suzuki Y, Nishimoto H, Kawakami T, et al. Role of the FcepsilonRI Beta-Chain ITAM as a Signal Regulator for Mast Cell Activation With Monomeric IgE. *Int Immunol* (2005) 17(6):685–94. doi: 10.1093/intimm/dxh248
26. Okayama Y, Kashiwakura JI, Matsuda A, Sasaki-Sakamoto T, Nunomura S, Yokoi N, et al. The Interaction Between Lyn and FcepsilonRIbeta is Indispensable for FcepsilonRI-Mediated Human Mast Cell Activation. *Allergy* (2012) 67(10):1241–9. doi: 10.1111/j.1398-9995.2012.02879.x.
27. Wang Q, Lepus CM, Raghu H, Reber LL, Tsai MM, Wong HH, et al. IgE-Mediated Mast Cell Activation Promotes Inflammation and Cartilage Destruction in Osteoarthritis. *Elife* (2019) 8:e39905. doi: 10.7554/eLife.39905
28. Gebremeskel S, Schanin J, Coyle KM, Butuci M, Luu T, Brock EC, et al. Mast Cell and Eosinophil Activation Are Associated With COVID-19 and TLR-Mediated Viral Inflammation: Implications for an Anti-Siglec-8 Antibody. *Front Immunol* (2021) 12:650331. doi: 10.3389/fimmu.2021.650331
29. Avril T, Floyd H, Lopez F, Vivier E, Crocker PR. The Membrane-Proximal Immunoreceptor Tyrosine-Based Inhibitory Motif Is Critical for the

Inhibitory Signaling Mediated by Siglecs-7 and -9, CD33-Related Siglecs Expressed on Human Monocytes and NK Cells. *J Immunol* (2004) 173 (11):6841–9. doi: 10.4049/jimmunol.173.11.6841

30. Muller J, Obermeier I, Wohner M, Brandl C, Mrotzek S, Angermuller S, et al. CD22 Ligand-Binding and Signaling Domains Reciprocally Regulate B-Cell Ca2+ Signaling. *Proc Natl Acad Sci USA* (2013) 110(30):12402–7. doi: 10.1073/pnas.1304888110
31. Hof P, Pluskey S, Dhe-Paganon S, Eck MJ, Shoelson SE. Crystal Structure of the Tyrosine Phosphatase SHP-2. *Cell* (1998) 92(4):441–50. doi: 10.1016/S0092-8674(00)80938-1
32. Nutku E, Aizawa H, Hudson SA, Bochner BS. Ligation of Siglec-8: A Selective Mechanism for Induction of Human Eosinophil Apoptosis. *Blood* (2003) 101 (12):5014–20. doi: 10.1182/blood-2002-10-3058
33. Duan S, Koziol-White CJ, Jester WFJr., Smith SA, Nycholat CM, Macauley MS, et al. CD33 Recruitment Inhibits IgE-Mediated Anaphylaxis and Desensitizes Mast Cells to Allergen. *J Clin Invest* (2019) 129(3):1387–401. doi: 10.1172/JCI125456
34. Bag N, Wagenknecht-Wiesner A, Lee A, Shi SM, Holowka DA, Baird BA. Lipid-Based and Protein-Based Interactions Synergize Transmembrane Signaling Stimulated by Antigen Clustering of IgE Receptors. *Proc Natl Acad Sci USA* (2021) 118(35):e2026583118. doi: 10.1073/pnas.2026583118

Conflict of Interest: WK, AW, SG, JS, KC, JL, ZB, TL, EB, KL, AX and BY were employed by Allakos Inc. GN was employed by LM Biostat Consulting Inc.

The authors declare that this study received funding from Allakos Inc. The funder had the following involvement with the study: data collection, analysis, interpretation, study design, and writing of this article.

Publisher's Note: All claims expressed in this article are solely those of the authors and do not necessarily represent those of their affiliated organizations, or those of the publisher, the editors and the reviewers. Any product that may be evaluated in this article, or claim that may be made by its manufacturer, is not guaranteed or endorsed by the publisher.

Copyright © 2022 Korver, Wong, Gebremeskel, Negri, Schanin, Chang, Leung, Benet, Luu, Brock, Luehrsen, Xu and Youngblood. This is an open-access article distributed under the terms of the Creative Commons Attribution License (CC BY). The use, distribution or reproduction in other forums is permitted, provided the original author(s) and the copyright owner(s) are credited and that the original publication in this journal is cited, in accordance with accepted academic practice. No use, distribution or reproduction is permitted which does not comply with these terms.

frontiers in Immunology

ORIGINAL RESEARCH
published: 16 February 2022
doi: 10.3389/fimmu.2022.841045

A Critical Function for the Transcription Factors GLI1 and GLI2 in the Proliferation and Survival of Human Mast Cells

Guido Hernan Falduto, Annika Pfeiffer, Qunshu Zhang, Yuzhi Yin, Dean Darrel Metcalfe† and Ana Olivera†*

Mast Cell Biology Section, Laboratory of Allergic Diseases, National Institute of Allergy and Infectious Diseases, National Institutes of Health, Bethesda, MD, United States

OPEN ACCESS

Edited by:
Satoshi Tanaka, Kyoto Pharmaceutical University, Japan

Reviewed by:
Zou Xiang, Hong Kong Polytechnic University, Hong Kong SAR, China
Christian Kosan, Friedrich Schiller University Jena, Germany

***Correspondence:**
Ana Olivera
ana.olivera@nih.gov

†These authors share senior authorship

Specialty section:
This article was submitted to Inflammation, a section of the journal Frontiers in Immunology

Received: *21 December 2021*
Accepted: *27 January 2022*
Published: *16 February 2022*

Citation:
Falduto GH, Pfeiffer A, Zhang Q, Yin Y, Metcalfe DD and Olivera A (2022) A Critical Function for the Transcription Factors GLI1 and GLI2 in the Proliferation and Survival of Human Mast Cells. Front. Immunol. 13:841045. doi: 10.3389/fimmu.2022.841045

Mast cell hyperactivity and accumulation in tissues are associated with allergy and other mast cell-related disorders. However, the molecular pathways regulating mast cell survival in homeostasis and disease are not completely understood. As glioma-associated oncogene (GLI) proteins are involved in both tissue homeostasis and in the hematopoietic system by regulating cell fate decisions, we sought to investigate the role for GLI proteins in the control of proliferation and survival of human mast cells. GLI1 transcripts were present in primary human mast cells and mast cell lines harboring or not activating mutations in the tyrosine kinase receptor KIT (HMC-1.1 and HMC-1.2, and LAD2 cells, respectively), while GLI2 transcripts were only present in HMC-1.1 and HMC-1.2 cells, suggesting a role for oncogenic KIT signaling in the regulation of GLI2. Reduction in GLI activity by small molecule inhibitors, or by shRNA-mediated knockdown of GLI1 or GLI2, led to increases in apoptotic cell death in both cultured human and murine mast cells, and reduced the number of peritoneal mast cells in mice. Although GLI proteins are typically activated *via* the hedgehog pathway, steady-state activation of GLI in mast cells occurred primarily *via* non-canonical pathways. Apoptosis induced by GLI silencing was associated with a downregulation in the expression of KIT and of genes that influence p53 stability and function including USP48, which promotes p53 degradation; and iASPP, which inhibits p53-induced transcription, thus leading to the induction of p53-regulated apoptotic genes. Furthermore, we found that GLI silencing inhibited the proliferation of neoplastic mast cell lines, an effect that was more pronounced in rapidly growing cells. Our findings support the conclusion that GLI1/2 transcription factors are critical regulators of mast cell survival and that their inhibition leads to a significant reduction in the number of mast cells *in vitro* and *in vivo*, even in cells with constitutively active KIT variants. This knowledge can potentially be applicable to reducing mast cell burden in mast cell-related diseases.

Keywords: mast cell, GLI, hedgehog signaling pathway, KIT, apoptosis, proliferation

INTRODUCTION

Mast cells are immune cells of the myeloid lineage with key roles in the initiation of allergic reactions and in the regulation of chronic inflammation. Activated mast cells mediate these functions through the release of a vast variety of vasoactive and immune-modulatory molecules (1). The severity of mast cell-mediated reactions generally depends on the extent and duration of mast cell responses, and it is influenced by the number of mast cells in tissues (2).

Mast cells terminally differentiate in tissues, where they take up long-term residence. Mast cell numbers are increased in allergic disorders such as asthma, allergic rhinitis, food allergy and atopic dermatitis (2, 3), partly due to enhanced recruitment of mast cell progenitors to the affected sites followed by their maturation (1, 4, 5). Abnormal increases in mast cells are also seen in other mast cell disorders such as mastocytosis, where clonal expansion of mast cells occurs in organs such as the skin, bone marrow and the gastrointestinal tract among others, in association with somatic activating mutations in the tyrosine kinase receptor KIT (CD117) (6, 7). Indeed, KIT enhances the survival, proliferation and function of mast cells and plays an important role in tissue mast cell homeostasis *in vivo* (8) as evidenced also by the lack of tissue mast cells in mice with a deficiency in KIT or its ligand (9), and the observed decrease in mast cell counts after blocking KIT activity in humans (10, 11). However, the regulatory mechanisms balancing mast cell survival (via KIT or other microenvironmental signals) and cell death to maintain mast cell homeostasis in health and disease are not well understood. Knowledge of these mechanisms may be relevant for strategies to reduce mast cells numbers and activity in mast cell-related disorders (2, 12, 13).

Glioma-associated oncogene family (GLI) transcription factors regulate the expression of various genes critical for proliferation, survival, genetic stability, and cell determination, during embryonic development and later in life. One of these target genes is *KIT*, whose promoter region contains two GLI consensus-binding sites (14) and its expression can be negatively or positively regulated depending on the GLI isoforms (14–16). GLI transcription factors consist of three family members, namely GLI1, GLI2 and GLI3. The canonical pathway for the activation of GLI is the hedgehog pathway (HH), although increasing evidence demonstrates that transcriptional expression and post-translational modifications leading to the activation of GLI also occur by non-canonical mechanisms (17). In the canonical HH-pathway (**Figure 1A**), the 12-pass transmembrane receptor Patched 1 (PTCH1) is activated by the HH ligands sonic (SHH), Indian (IHH), and desert HH (DHH). In their absence, PTCH1 inhibits the 7-pass transmembrane G protein-coupled receptor smoothened (SMO), leading to the partial proteasomal degradation of GLI3 and to a much lesser extent of GLI2, to form transcriptional repressor forms (GLI^R). In the presence of HH ligands, PTCH1 stops the inhibition of SMO, proteolysis of GLI is blocked and thus active, full length GLI activator forms (GLI^A) accumulate and translocate into the nucleus to induce gene transcription. Unlike GLI2 and GLI3, GLI1 is not subject to proteolysis, and its levels are mainly regulated by induction of transcription, which is the reason why GLI1 is used as a reliable reporter of HH activity (18, 19). Overall, GLI1 acts exclusively and GLI2 primarily as transcriptional activators (GLI^A), while GLI3 acts as the main transcriptional repressor due to its proteolytic processing (20, 21). The GLI proteins are also regulated by sequestration with suppressor of fused (SUFU), which prevents them from entering the nucleus, until activation mechanisms dissociate the complex (**Figure 1A**) (22).

Dysregulation of GLI^A and GLI^R has been linked to hematological malignancies such as chronic and acute myeloid leukemia among other types of cancer (23, 24). More recently, in a subset of patients with congenital aggressive mastocytosis, a germline mutation causing reduced $GLI3^R$ compared to $GLI3^A$ was identified, which was associated with mast cell transformation (16). Considering these associations, the role of GLI proteins in cell fate decisions, and their reported regulatory role in KIT expression, we aimed to investigate a potential involvement of GLI transcription factors and the HH-pathway in the proliferation and survival of normal and neoplastic human mast cells. By using inhibitors of GLI and components of the HH-pathway and by shRNA-mediated approaches, we show that homeostatic regulation of GLI1 and GLI2, largely through non-canonical pathways, plays an important role in the survival of human and mouse mast cells *in vitro* and *in vivo*, as well as in the proliferation and survival of neoplastic mast cells carrying or not oncogenic KIT variants. As will be shown, such data provides relevant information on the function of GLI proteins in mast cell biology and tissue homeostasis, and on the molecular underpinnings for this regulation, which includes the regulation of KIT and p53. Furthermore, these additions to the understanding of the molecular pathways that regulate mast cell proliferation, survival and death have relevance in developing novel pharmacological strategies to decrease mast cell numbers, and in the treatment of mast cell-associated disorders.

Abbreviations: GLI, Glioma-associated oncogene family; HH, hedgehog pathway; SHH, sonic HH ligand; SAG, SMO agonist; GLI^A, GLI activator forms; GLI^R, GLI repressor forms; ATO, arsenic trioxide/A_2O_3; BMMC, bone marrow-derived mast cells; hMC, primary human mast cells.

MATERIALS AND METHODS

Inhibitors and Agonists

The tyrosine kinase inhibitor (TKI) dasatinib, SMO agonist (SAG)- hydrochloride, GLI1/2 inhibitor GANT61, and SMO antagonist vismodegib (GDC-0449) were purchased from Selleckchem (Houston, TX). GLI1/2 inhibitor HPI-1, PI3Kα/δ/β inhibitor LY-294002 hydrochloride, and MEK1/2 inhibitor U0126 were purchased from Tocris (Minneapolis, MN). High activity recombinant Human Sonic Hedgehog (SHH) Protein was purchased from R&D Systems (Minneapolis, MN) and arsenic trioxide (A_2O_3 or ATO) from Millipore Sigma (Burlington, MA).

Animal Studies

$Ptch1^{+/-}$ mice ($Ptch1^{tm1Mps}$/J; Stock No: 003081) were obtained from The Jackson Laboratory (Bar Harbor, ME) (25) and bred to

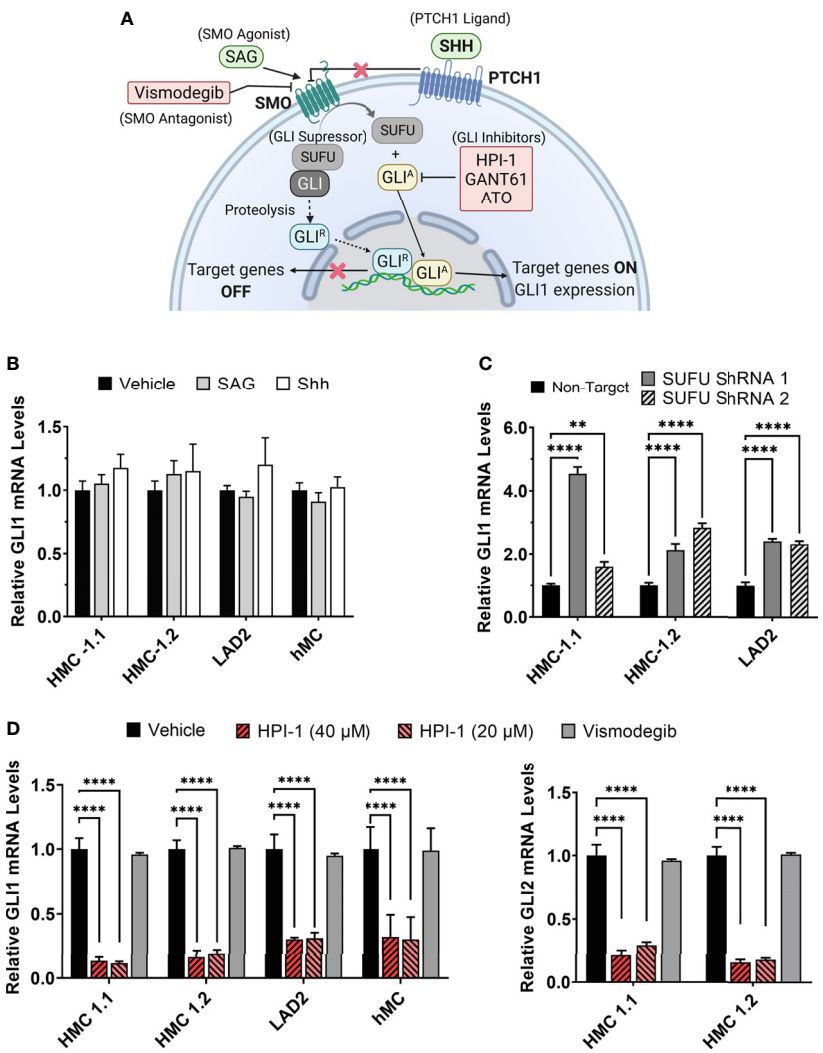


FIGURE 1 | Modulation of GLI1/2 expression in human mast cells. **(A)** Simplified illustration of the canonical hedgehog signaling pathway and some of the small molecules used for its activation or inhibition. **(B)** Relative GLI1 mRNA levels ($2^{-\Delta\Delta Cq}$) in human mast cell lines (HMC-1.1, HMC-1.2, LAD2) and primary human mast cells (hMC) after 20 h incubation with the SMO agonist SAG (200 nM) or the PTCH1 ligand SHH (500 ng/mL). **(C)** Relative GLI1 mRNA levels ($2^{-\Delta\Delta Cq}$) in mast cells transduced with lentiviral particles containing two separate shRNA constructs to knockdown SUFU (see **Supplementary Figure 2**). **(D)** Relative GLI1 and GLI2 mRNA levels ($2^{-\Delta\Delta Cq}$) after 5 h culture with the GLI1/2 inhibitor HPI-1 (20 or 40 μM) or with the SMO inhibitor vismodegib (40 μM). Results are expressed as Mean ± SD of three independent experiments. GAPDH and ACTB were used for normalization. Each individual experiment was done in triplicate. Two-way ANOVA followed by Dunnet multiple comparisons test was used for statistical analysis. $^{**}p < 0.01$; $^{****}p < 0.0001$.

obtain Wt and Ptch1$^{+/-}$ littermates in AAALAC-accredited NIAID animal facilities. C57BL/6J mice were obtained from the Jackson Laboratory and injected every other day with GLI1/2 inhibitors for a total of 7 injections. Mice were randomly divided into three groups (n=4/group) and injected intraperitoneally (150 μL) with either saline vehicle control (PBS : EtOH; 95:5%), HPI-1 (2 mg/kg), or GANT61 (2 mg/kg). Two days after the last injection, mice were euthanized, peritoneal lavage was performed, and mast cell percentages (FcεRI$^+$ Kit$^+$ cells) were obtained by FACS analysis. Cells were resuspended at 10^7 cells/mL in PBS plus LIVE/DEAD™ Fixable Green Dead Cell Stain Kit (Thermo Fisher Scientific, Waltham, MA) according to the manufacturer's instructions. Cells were then washed, resuspended in FACS buffer (PBS + 3% FBS + 2mM EDTA), and Fcγ receptors blocked with anti-CD16/CD32 (clone 2.4G2, BD Biosciences, Franklin Lakes, NJ). Cells were stained with an optimal amount of anti-Kit-PE (clone ACK2, eBioscience) and anti-FcεRI-APC (clone MAR-1, Biolegend, San Diego, CA). Data acquisition was performed on a LSRFortessa™ (BD Biosciences) and analyzed using FlowJo software (Tree Star, Ashland, OR). These experiments with live mice were performed under an animal study proposal (LAD2E) approved by the NIAID-DIR-Animal Care and Use Committee, in accordance with federal regulatory requirements and ethical standards under the guidance of the Office of Animal Care and Use of the National Institutes of Health.

Cell Culture

Mouse bone marrow-derived mast cells (BMMC) were differentiated from the marrow of tibias and femurs of Wt and Ptch1$^{+/-}$ littermate mice and cultured for at 6-8 weeks in RPMI 1640 supplemented with 10% FBS, HEPES (1M), penicillin (100 U/mL), streptomycin, 4 mM L-glutamine (100 µg/mL), sodium pyruvate (1 mM), 2-mercaptoethanol (50 µM), and IL-3 (30 ng/mL, R&D Systems). Cultures were analyzed by flow cytometry and BMMC were identified as FcεRI and Kit double positive cells as described above. Degranulation assays of BMMC were performed as described (26).

HMC-1.1 and HMC-1.2 cell lines were cultured in Iscove's Modified Dulbecco's Medium supplemented with 10% FBS, L-Glutamine (2 mM), penicillin (100 U/ml), streptomycin (100 µg/ml). LAD2 cells were cultured in StemPro-34™ supplemented with StemPro-34™ Nutrient Supplement (Gibco), L-Glutamine (2 mM), penicillin (100 U/ml), streptomycin (100 µg/ml), and SCF (100 ng/ml, R&D Systems).

Primary human mast cell cultures (hMC) were derived from CD34+ lymphocytapheresis progenitors obtained from healthy volunteers following informed consent under a protocol (NCT00001756) approved by the National Institutes of Health Internal Review Board. Cells were cultured as described (27) and used between 7–9 weeks of culture when >95% were mast cells identified as KIT and FcεRI double positive cells.

Growth Assays

The growth of HMC-1.1 and HMC-1.2 cells was quantified using CyQUANT™ Direct Cell Proliferation Assay (Thermo Fisher Scientific). Cells ($3x10^4$) were seeded in 100 µL in 96-well black/clear bottom plates (Corning Inc., Corning, NY) and cultured for 72 h in the presence of inhibitors of GLI or agonists/antagonist of the hedgehog pathway activators as indicated in the figures. Vehicle controls (up to 0.1% DMSO for HPI-1, 0.08% ethanol for GANT61, and PBS for ATO), and control samples containing no vehicle were included in all experiments. These vehicles did not affect growth of the cells. Cells were stained with the Cyquant dye following the manufacturer's instructions. The relative fluorescence units (RFU) were determined using a Spark® microplate reader (TECAN, Männedorf, Switzerland). For LAD2 cells, $6x10^5$ cells were seeded in 6-well plates (2 mL) and cultured for 7 days in the presence or absence of inhibitors. Viable cells were counted using a Acridine Orange/Propidium Iodide (AO/PI) cell viability kit using a LUNA-FL™ Dual Fluorescence Cell Counter (Logos Biosystems, Gyeonggi-do, South Korea).

Proliferation Assays

To identify proliferating cells, mast cell lines were stained with 5 µM of Cell Trace Violet (Thermo Fischer Scientific) in PBS following manufacturer's guidelines. After washing, $5x10^5$ cells were plated in 6 well plates (2 mL/well) with or without the indicated concentrations of inhibitors and cultured for 72 h (HMC-1.1 and HMC-1.2) or 7 days (LAD2) in culture media. To determine viability, cells were collected and stained with a LIVE/DEAD™ Fixable Green Dead Cell Stain Kit (Thermo Fischer Scientific) in PBS for 10 min on ice. Data acquisition was performed on a LSRFortessa™ and analyzed using FlowJo software. After gating out dead cells (LIVE/DEAD™ stained), generations of proliferating cells were recognized by diminishing fluorescence intensity. Cultures of BMMC were stained with 5 µM of Cell Trace Violet (CTV), plated in 6-well plates ($5x10^5$ cells in 2 mL) and after 6 days, proliferation and cell viability were analyzed as described above. Cultures of hMC differentiated for 7-9 weeks were plated in 24-well plates ($2.5x10^5$ cells in 1 mL) in growth media with or without the indicated concentrations of inhibitors, and cell viability was analyzed after 5 days as described above.

Apoptosis Assays

To identify cells undergoing apoptosis, expression of surface phosphatidylserine was determined by annexin V staining. Cells ($5x10^5$) were cultured in 6-well plates (2 mL) for 48 h (HMC-1.1 and HMC-1.2), 6 days (LAD2), or 4 days (hMC) in the presence or absence of the indicated concentrations of inhibitors and stained using Pacific Blue™ Annexin V/SYTOX™ AADvanced™ Apoptosis Kit (Thermo Fischer Scientific) following the manufacturer's instructions. Cells were analyzed for annexin V expression in a LSRFortessa™.

In some experiments, apoptosis was further demonstrated by quantifying caspase-3/7 activity using CellEvent™ Caspase-3/7 Green Detection Reagent (Thermo Fischer Scientific), a specific substrate for caspase 3/7 that becomes fluorescent after cleavage. HMC-1.1 or HMC-1.2 cells ($5x10^5$) were cultured with or without various treatments for 48 h in 96-well black/clear bottom plates (100 µL), following the manufacturer's instructions, and RFU were measured in a Spark® microplate reader.

ShRNA-Mediated Knockdown

Knockdown of GLI1 and GLI2 was conducted by transducing cells with GLI-specific ShRNA constructs. Bacterial glycerol stocks containing the pLKO.1-puro plasmid shRNA constructs were obtained from Millipore Sigma: TRCN0000020486 (construct 1) and TRCN0000232063 (construct 2) for GLI1; and TRCN0000033329 (construct 1) and TRCN0000033330 (construct 2) for GLI2. Plasmid DNA was isolated from individual carbenicillin-resistant colonies using Qiaprep Spin Miniprep Kit (Qiagen). As a non-target control, we used a pLKO.1-puro non-Mammalian shRNA Control Plasmid DNA (SHC002). Lentiviral particles were produced by following the manufacturer's protocol. Briefly, the packaging lentiviral genes and viral envelop gene (Mission Lentiviral packaging mix, Millipore Sigma) along with plasmid DNA (3.4 µg) were co-transfected into HEK 293T cells (70% confluency in T75 flask) using FuGENE6 transfection reagent (Roche, Indianapolis, IN) to produce lentiviral particles containing the shRNA constructs. The transfected 293T cells were grown in Dulbecco modified Eagle medium that contained FBS (10%) and L-glutamine (4 mM). At 16 h post-transfection, the media was removed and replaced with fresh Dulbecco modified Eagle medium that included penicillin (100 U/mL) and streptomycin (100 mg/mL) and 10% FBS. Supernatants containing viral particles were collected at 40-44 h and 66-70 h post-transfection and

combined. Viral particle titer was quantified by using HIV Type 1 p24 Antigen ELISA (ZeptoMetrix Corporation, Buffalo, NY). Cells plated in 6-well plates were transduced with the supernatants containing lentivirus, using approximately 5-10 transduction units (TU)/cell. After 20 h, transduced cells were changed to virus-free medium and selected by adding 2 μg/mL puromycin (*In vivo*gen, San Diego, CA) for HMC-1.2 cells or 0.5 μg/mL puromycin for LAD2 cells. After 5 days of selection, cells were changed to puromycin-free medium and used for experiments.

To knockdown SUFU, lentiviral transduction particles TRCN0000019464 (construct 1), TRCN0000358840 (construct 2) for HMC-1.1 and HMC-1.2, TRCN0000358906 (construct 1), TRCN0000358838 (construct 2) for LAD2, and non-Target ShRNA control were purchased from Millipore Sigma. Cells were transduced as described above, except that no selection was conducted, and RNA was extracted at 96 h post-transduction.

Quantitative Real-Time PCR

Total RNA from 1-3 × 10^6 cells, treated as specified in the figure legends, was extracted using RNeasy plus mini kit (Qiagen, Valencia, CA). Reverse transcription and real time qPCR reactions to quantify various gene transcripts were performed in one step using iTaq Universal Probes One-Step Kit (Bio-Rad, Hercules, CA). The following PrimePCR™ probe sets were also purchased from Bio-Rad: SHH (qHsaCEP0040459) PTCH1 and Ptch1 (qHsaCEP0055042 and qMmuCEP0053013), SMO and Smo (qHsaCEP0051485 and qMmuCIP0032784), GLI1 and Gli1 (qHsaCEP0050608 and qMmuCEP0054131), GLI2 (qHsaCEP0057630), GLI3 (qHsaCEP0050421), SUFU (qHsaCEP0058238), KIT (qHsaCIP0026913), PPP1R13L (iASPP) (qHsaCEP0057704), and USP48 (qHsaCEP0049878). GAPDH and Gapdh (qHsaCEP0041396 and qMmuCEP0039581) and ACTB (qHsaCEP0036280) were used as reference genes.

For gene expression profiling of differentially expressed genes within the mitochondrial apoptotic pathway, we used predesigned 96-well panels with probes for 24 genes (Human, Catalog# 10025095, from Bio-Rad). cDNA (25 ng/reaction) obtained from cells after various treatments and using iScript cDNA synthesis Kit (Bio-Rad), were distributed on the plates and amplified using SYBR® Green. All the PCR reactions were conducted in CFX96 Touch Real-Time PCR Detection System (Bio-Rad).

Western-Blot

Cell lysates were obtained by lysing 4-8x10^6 cells, treated as specified in the figure legends, in 200-400 μL of RIPA Buffer (Cell Signaling Technologies, Danvers, MA) containing Protease/Phosphatase Inhibitor Cocktail (Roche) for 25 min on ice. Samples were incubated for 10 min at 70°C and separated by electrophoresis on 4–12% NuPage Bis-Tris gels (Thermo Fisher Scientific). Proteins were transferred to nitrocellulose membranes (0.2 μm pore size) using Trans-Blot Turbo Transfer Packs (Bio-Rad) followed by blocking in TBS Intercept blocking buffer (LI-COR Biosciences, Lincoln, NE). Blots were incubated with the primary antibodies purchased from Cell Signaling Technologies (KIT clone Ab81, polyclonal phospho-KIT (Tyr823, #77522), p53 clone DO-7, β-Actin clone 13E5 or polyclonal #4967, GLI1 clone L42B10, GLI2 clone E7R1N) overnight or 1 h for β-Actin at 4°C on a shaker. Bands were detected using infrared-labeled secondary antibodies and imaging of the bands was performed using an Odyssey CLx Infrared Imaging System (LI-COR Biosciences). Quantification of infrared fluorescence was conducted using Image Studio Lite (version 5.2).

Statistical Analysis

Statistical analysis was conducted using GraphPad Prism (GraphPad, San Diego, CA, version 9.1.1). The following significance scale was used on the graphs (* $p<0.05$, ** $p<0.01$, *** $p<0.001$, **** $p<0.0001$).

RESULTS

Expression of HH Signaling Pathway Components and Modulation of GLI1/2 in Human Mast Cells

Activation of GLI proteins usually occurs downstream of the PTCH1/HH-pathway (**Figure 1A**), and which has not been explored in detail in mast cells. Thus, we first determined the level of mRNA expression of the main HH-pathway components in hMC and mast cell lines expressing normal (LAD2) or oncogenic KIT variants (HMC-1.1 and HMC-1.2). As shown in **Table 1**, PTCH1 mRNA was present in all human mast cell types but the key transducer of the HH-pathway, SMO, was not

TABLE 1 | Relative mRNA expression in human mast cells of the main genes involved in the Hedgehog signal transduction pathway.

	HMC-1.1		HMC-1.2		LAD2		hMC	
	Mean ± SD	*N*	*Mean ± SD*	*N*	*Mean ± SD*	*N*	*Mean ± SD*	*N*
SHH	ND	3	ND	3	ND	3	–	–
PTCH1	1.77 ± 0.40	3	1.78 ± 0.66	3	0.24 ± 0.010	2	3.02 ± 1.15	3
GLI1	0.49 ± 0.12	5	0.43 ± 0.28	6	0.37 ± 0.14	6	0.44 ± 0.19	5
GLI2	7.69 ± 0.23	4	15.72 ± 0.42	3	ND	3	ND	2
GLI3	0.020 ± 0.003	3	0.027 ± 0.012	3	0.027 ± 0.012	3	0.057 ± 0.021	3
SUFU	3.66 ± 0.48	2	4.68 ± 0.26	2	2.48 ± 0.96	3	6.73 ± 1.04	2
SMO	ND	3	ND	3	ND	3	ND	3

Mean values are normalized expression by GAPDH and ACTB ($2^{-\Delta Cq}$). Mean and SD values are expressed as value x 10^3. ND, Non-detected.

detectable in any cell type (Cq >39). The levels of the activator GLI1 were similar in all studied human mast cells, while the mRNA levels of GLI3 were barely detectable (Cq values of approximately 34). Notably, GLI2 mRNA was only expressed in the cell lines with KIT variants (HMC-1.1 and HMC-1.2 cells) and at higher levels than GLI1, suggesting a role for oncogenic KIT signaling in the regulation of GLI levels, particularly of GLI2. Related to such regulation, we found that inhibition of KIT, the downstream PI3K pathway, or particularly the MEK/ERK1/2 pathway, reduced GLI2 expression (**Supplementary Figure 1A**). The presence of GLI1 and GLI2 proteins, in accordance with the mRNA levels (**Table 1**), was confirmed by western-blot (**Supplementary Figure 1B**).

Since the levels of SMO mRNA (**Table 1**) and protein (not shown) were under the limit of detection, we questioned whether the canonical HH-pathway was functional in mature mast cells. As enhanced GLI1 expression is a main reporter assay for the activation of the HH-pathway (19, 28), we tested the effect of the PTCH1 agonist SHH or a pharmacological activator of SMO (SAG) (see **Figure 1A**) on GLI1 mRNA levels in hMC and mast cell lines. Neither of these approaches had significant effects on GLI1 mRNA levels after 6 h (not shown) or 20 h in hMC or mast cell lines (**Figure 1B**), consistent with the conclusion that the HH-pathway is not inducible in these cells under our experimental conditions.

SUFU is a key suppressor of GLI1 activity that can be regulated by SMO or by non-canonical pathways. Since SUFU was abundantly expressed in mast cells (**Table 1**), we used shRNA-mediated silencing of SUFU aiming to activate GLI bypassing upstream pathways. This approach resulted in 40 to 65% reduction in SUFU mRNA levels (**Supplementary Figure 2**) and led to an increase in GLI1 mRNA expression in all cell lines (**Figure 1C**), suggesting that the reduction of SUFU and thus SUFU/GLI complexes, allows GLI to enter the nucleus and further induce its own expression. The increased expression of GLI1 by silencing of SUFU implicates a role for SUFU in the regulation of GLI1 in mast cells and demonstrates that GLI1 is functionally active and capable of inducing its own expression, an outcome not seen by activation of PTCH1 or SMO (**Figure 1B**). This observation also suggests that SUFU/GLI may be mainly regulated *via* non-canonical pathways or that the induction of the canonical pathway is obscured by its homeostatic activation, although we did not detect SHH mRNA in these cells (**Table 1**).

Conversely to the knockdown of SUFU, the inhibition of GLI activation by a small molecule inhibitor, HPI-1, markedly reduced GLI1 and GLI2 mRNA expression in human mast cells, while no effect was observed with the SMO inhibitor vismodegib (**Figure 1D**). These data suggest that in cultured human mast cells, GLI transcription factors are active and regulated under steady state conditions by mechanisms other than the canonical HH-pathway.

Homeostatic Activation of the HH-Pathway and Gli Activity Promotes Differentiation and Proliferation of Murine Mast Cells

To further investigate the potential consequences of homeostatic activation of the HH- pathway, we used a mouse model of haploinsufficiency of Ptch1. Ptch1 inhibits Smo in a catalytic manner, in that one molecule of Ptch1 can regulate about 50 molecules of Smo (29). Therefore, Ptch1 downregulation can result in significantly less Smo repression and in turn, enhanced activation of Gli1 (25, 30) (**Figure 1A**), representing some level of constitutive activation of the HH-pathway. We confirmed that $Ptch1^{+/-}$ bone marrow cells and BMMC cultured for 7 weeks had significantly lower Ptch1 mRNA levels due to the lack of one allele (**Figure 2A**).

Although $Ptch1^{+/-}$ BMMC developed into mast cells with similar appearance, expression of FcεRI and Kit, and degranulation responses as Wt BMMC (**Supplementary Figure 3A, B**), we observed that mast cells developed slightly faster (note a significantly higher proportion of mast cells determined as $FcεRI^{+}$ Kit^{+} cells by 4 weeks; **Figure 2B**), and that the total number of $Ptch1^{+/-}$ BMMC by the end of the culture was also significantly greater than in Wt BMMC (**Figure 2C**). We then tested the proliferation of mast cells during early development and in differentiated mast cells. By 2-3 weeks, when mast cells represent 20-30% of the cell culture, gated $Ptch1^{+/-}$ BMMC showed, on average, a significant 3-fold reduction in CTV fluorescence intensity (due to dye dilution as cells proliferate) compared to gated Wt BMMC, while by 6 weeks, when mast cells represent >95% of the culture, the reduction in CTV fluorescence intensity in $Ptch1^{+/-}$ cells was no more than 1.5 over Wt cells and did not reach statistical significance (**Figure 2D**). The trend towards reduced CTV in mature $Ptch1^{+/-}$ BMMC cultures was however mirrored by a modest but statistically significant increase in cell numbers compared to Wt BMMC (**Supplementary Figure 3C**). This suggests that early in the development of mast cells, increased Ptch1/HH-pathway activity can promote mast cell differentiation and proliferation but the effect in proliferation diminishes in differentiated mast cells coinciding with a drop in the expression of Smo (**Figure 2A**), and reminiscent of the undetectable SMO expression in human mast cells (**Table 1**). In agreement with these data, the Smo agonist (SAG) had no effect on the proliferation of 6-week-old Wt or $Ptch1^{+/-}$ BMMC (**Figure 2E**). In contrast, in the same 6-week-old cultures, inhibition of Gli1/2 by GANT61 reduced the proliferation of BMMC (**Figure 2E**) and caused a prominent increase in cell death (**Figure 2F**), potentially implicating Gli proteins in these processes.

Altogether, the data obtained from the haploinsufficiency Ptch1 mouse model system and inhibitors of the HH-pathway in BMMC are consistent with the conclusion that this pathway may contribute to the proliferation and differentiation of mast cells during early stages of development, but that the constitutive activation of the HH-pathway plays only a minor role in the proliferation of already differentiated mast cells. Of note, we did not detect differences in the numbers of tissue mast cells in these mice although the numbers trended to be slightly higher in $Ptch1^{+/-}$ mice, suggesting that haploinsufficiency in the HH-pathway does not significantly affect mast cell homeostasis *in vivo* (**Supplementary Figure 3D**). Our findings also suggest that Gli activity, mostly conferred by non-canonical pathways and perhaps to a lesser extent through homeostatic Ptch1/Smo, may represent an important regulator of survival in differentiated mast cells.

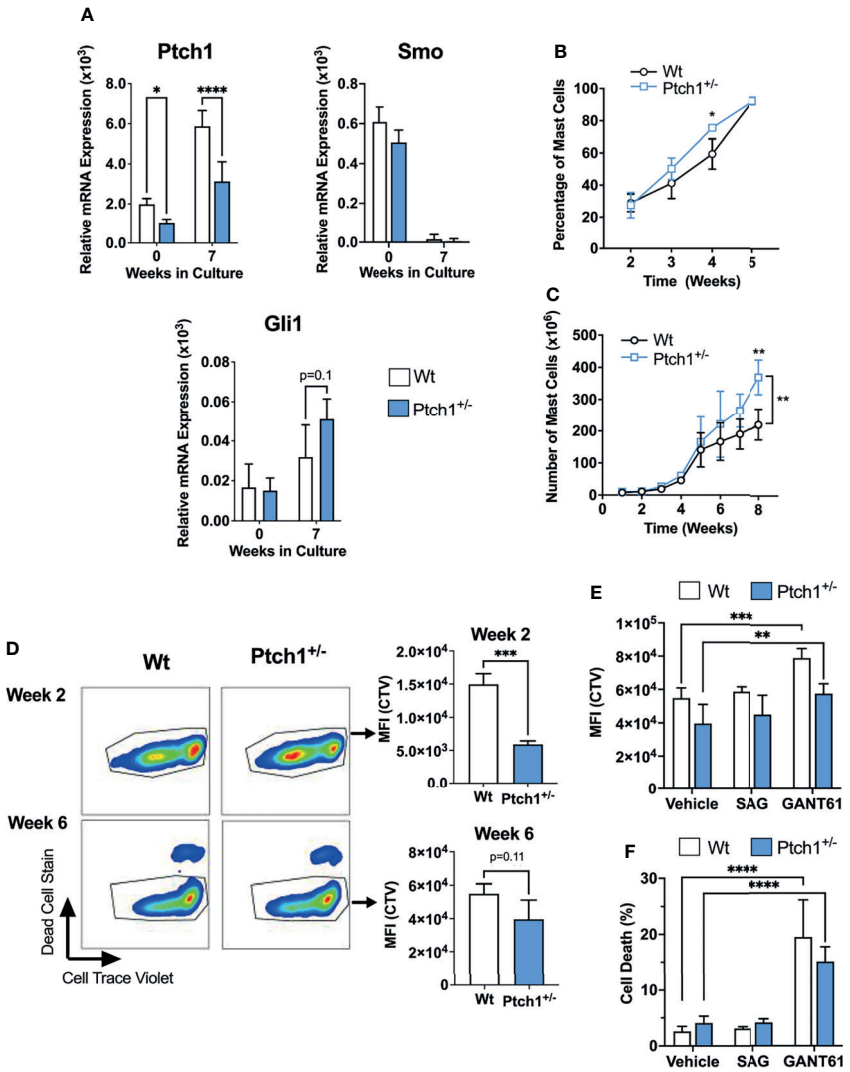


FIGURE 2 | Ptch1 haploinsufficiency provides a proliferative advantage in mouse BMMC. **(A)** Relative mRNA levels ($2^{-\Delta Cq}$) of Ptch1, Smo, and Gli1 in fresh bone marrow cells and after 7 weeks in culture, when >98% of cells are mast cells. Gapdh was used for normalization. **(B, C)** Percentage of mast cells (Kit^+ $Fc\varepsilon RI^+$ cells) **(B)** and total mast cell numbers **(C)** at the indicated times after initiation of the bone marrow culture (n=3 mice/group). Similar results were obtained in additional sets of cultures. The bracket in C indicates statistical significance between the two curves using 2-way ANOVA. The SD bars are not visible in some of the points due to the low variability between those cultures. **(D)** Proliferation assay using Cell Trace Violet (CTV) by FACS. BMMC were stained with the dye, at week 2 or 6 of culture. After washing, they were placed in culture media, and 6 days later, analyzed for CTV intensity and cell death staining. Representative dot-plots in $Fc\varepsilon RI^+$ Kit^+ gated cells are shown on the left. On the right, the average of CTV median intensity in cultures is shown (n=3 mice/group). **(E, F)** CTV staining **(E)** and dead cell staining **(F)** of 6-week-old BMMC in the presence of the Smo agonist SAG (200 nM) or the Gli1/2 antagonist GANT61 (20 μM) for 6 days (n=3 mice/group). Results are shown as Mean ± SD. Unpaired t test or 2-way ANOVA followed by Dunnet multiple comparisons test were used for statistical analysis. *p < 0.05; **p < 0.01; ***p < 0.001; ****p < 0.0001.

GLI1/2 Inhibition Reduces Human Mast Cell Growth by Downregulating Proliferation and Viability

Given these results and the regulation of GLI1 in human mast cells by the reduction in SUFU expression (**Figure 1C** and **Supplementary Figure 2**), we next focused on understanding the role of GLI proteins, particularly GLI1 and GLI2, in the regulation of human mast cell proliferation and survival. We employed the widely used GLI inhibitors GANT61 and ATO (31–33), and the new generation inhibitor HPI-1 (34), which as shown in **Figure 1D**, effectively downregulated both GLI1 and GLI2 mRNA expression, a readout of pathway inhibition.

All GLI inhibitors markedly reduced (by 40 to 95%) the growth of neoplastic human mast cells in culture (**Figure 3A**) in a concentration-dependent manner (**Figure 3A**). We used concentrations ranging from 5 to 40 μM of GANT61 and HPI-1, or up to 10 μM of ATO, as these were within the range of the reported IC_{50} for the corresponding inhibitors in several cell line

models (31, 34–36). Concentrations greater than 40 μM for HPI-1 and GANT61, or greater than10 μM for ATO were not tested due to concerns of potential off-target effects. The reductions in cell growth were observed at 72 h in HMC-1.1 and HMC-1.2 cells (**Figure 3A**, left and middle panels), while in the slower growing LAD2 cells, a reduction of about 50% in cell number was observed after 7 days in culture (**Figure 3A**, right panel). In contrast, vismodegib, an FDA-approved antagonist of SMO, did not show a significant effect in either GLI1 mRNA expression (**Figure 1D**) or cell growth of either cell line (**Figure 3A**).

Using flow cytometry assays on LAD2 and HMC-1.2 cells as examples of neoplastic cells without or with oncogenic KIT variants, we were able to demonstrate that GLI inhibition by 20 μM GANT61 or HPI-1, a concentration near the approximated IC50 (**Figure 3A**), not only reduced cell proliferation (indicated by the higher median CTV fluorescence intensity), but also caused a prominent 3-to-26-fold increase in cell death (**Figure 3B** and **Supplementary Figure 4**), similarly to our results in BMMC (**Figures 2E, F**). In contrast, vismodegib did not show any noticeable effects on cell proliferation or cell death (**Figure 3B**). Although primary human mast cells do not proliferate after 5 weeks in culture (and thus proliferation could not be tested), their survival was also significantly reduced after GLI inhibition but not after SMO inhibition (**Figure 3C** and **Supplementary Figure 4**). Altogether, these results suggest that in normal or neoplastic mast cells, GLI transcription factors play a key homeostatic role in the proliferation and/or survival of mast cells largely *via* non-canonical pathways.

To demonstrate that growth inhibition was not due to off-target effects of these drugs, we also performed GLI1 or GLI2 specific shRNA-mediated silencing in HMC-1.2 and LAD2 cells, using at least two independent constructs for each. We did not target GLI2 in LAD2 cells since GLI2 expression was not detected

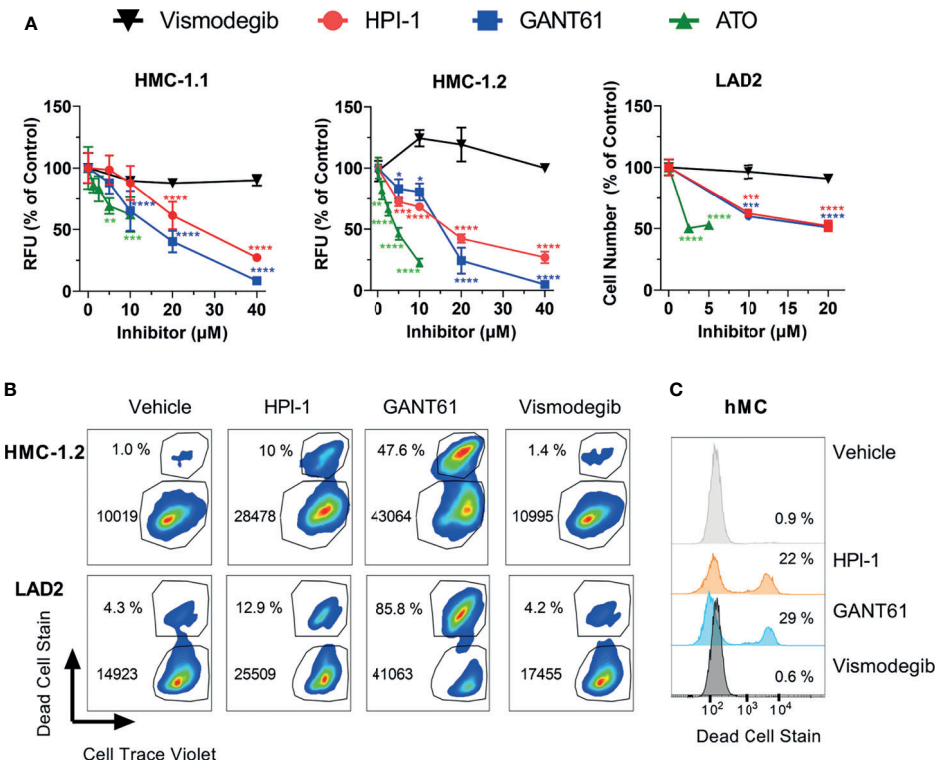


FIGURE 3 | GLI1/2 inhibitors reduce human mast cell growth by decreasing viability and proliferation. **(A)** HMC-1.1 (left panel), HMC-1.2 (middle panel), and LAD2 (right panel) cells were cultured for 72 h (HMC-1.1 and HMC-1.2 cells) or 7 days (LAD2 cells) with increasing concentrations of the indicated inhibitors of GLI1/2 (HPI-1, GANT61 and ATO) or SMO (vismodegib). Cell growth was assessed by measuring relative units of fluorescence (RFU) that represent viable cells using a Cyquant assay; or counting viable cells with a cell counter (LAD2 cells). Results were normalized to vehicle control (represented as concentration 0 μM) and are expressed as Mean ± SD of three independent experiments. Two-way ANOVA followed by Dunnet multiple comparisons test (compared to vehicle) were used for statistical analysis. Approximated IC_{50} values, estimated using a non-linear fit between the inhibitor concentration and the normalized response (variable slope) with GraphPad Prism 9, were for HPI-1: 25 μM in HMC-1.1 and 16 μM in HMC1.2; and for GANT61: 15 μM in HMC-1.1 and 14 μM in HMC1.2**. (B)** Representative dot-plots of three independent experiments in which HMC-1.2 and LAD2 were cultured for 72 h or 7 days, respectively, in the presence of the indicated inhibitors (20 μM). Cells were stained with Cell Trace Violet (CTV) before the incubation and at the end of the experiment stained with green dead cell stain. The percentage of dead cells and median fluorescence intensity (MFI) for CTV is shown in each dot-plot. **(C)** Representative histograms of primary human mast cells (hMC; 1 healthy donor out of 2) cultured for 5 days with the indicated inhibitors (20 μM) and stained with green dead cell stain. Averages of CTV MFI and percentages of dead cells in three independent experiments are shown in **Supplementary Figure 4**. *p < 0.05; **p < 0.01; ***p < 0.001; ****p < 0.0001.

in these cells (**Table 1**). It is worth noting that a correlation between the reduction in GLI mRNA and the functional effects may not be linear because cells with a more efficient reduction in GLI1 or GLI2 are more likely to die during the course of the experiments (when knockdown efficiency was assessed), while those cells where the knockdown was less efficient may remain alive. Nevertheless, effective GLI1 or GLI2 silencing (by about 50%; **Figure 4A**) reduced the growth of HMC-1.2 cells by more than 50% (**Figure 4B**, left panel) in 72 h. Similarly, knockdown of GLI1 in LAD2 cells (**Figure 4A**) reduced cell numbers by 50% in 7 days (**Figure 4B**, right panel). Using flow cytometry assays, GLI silencing reduced both the proliferation and survival of HMC-1.2 as well as the survival of LAD2 cells (**Figure 4C** and **Supplementary Figure 5**), confirming a specific role for GLI1/2 in these biological processes.

GLI1/2 Inhibitors Induce Apoptosis and Regulate p53 in Human Mast Cells

We next used annexin V staining and flow cytometry to assess the type of death induced by the loss of GLI activity. The increase in annexin V staining after GLI1/2 inhibition indicated cell death by apoptosis (**Figure 5A**), a finding that was confirmed by directly measuring caspase 3/7 activity in cultures 48 h after treatment with GLI1/2 inhibitors (**Figure 5B**). Unlike HPI-1 and GANT61, vismodegib did not affect either annexin V staining (**Figure 5A**) or the activity of caspase 3/7 (**Figure 5B**),

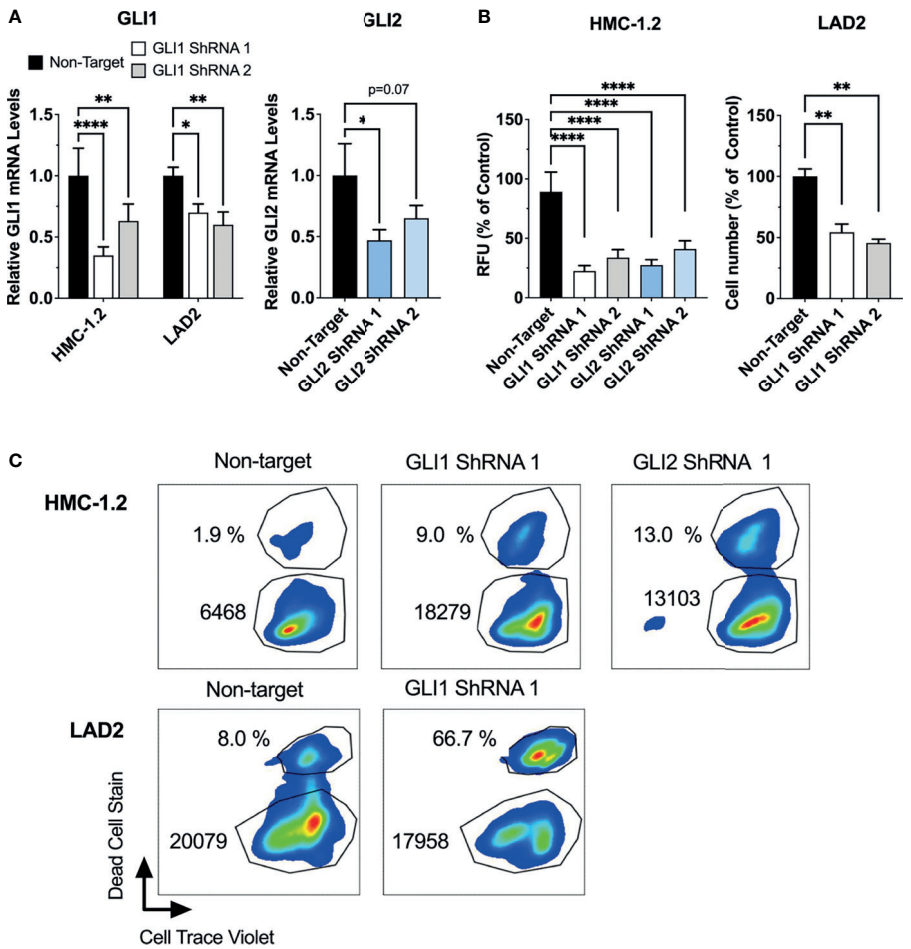


FIGURE 4 | ShRNA-mediated silencing of GLI1/2 reduces human mast cell growth by decreasing viability and proliferation. **(A)** HMC-1.2 and LAD2 cells were transduced with lentiviral particles containing GLI1 or GLI2 shRNA constructs (two independent constructs for each). After proper selection, relative GLI1 and GLI2 mRNA levels ($2^{-\Delta\Delta Cq}$) were quantified by qPCR. GAPDH and ACTB were used for normalization. **(B)** After proper selection numbers of viable HMC-1.2 (left) and LAD2 (right) cells were assessed using the Cyquant assay (relative fluorescence units, RFU) or a cell counter, respectively. Cell numbers were assessed after 72 h in HMC-1.2 cells and after 7 days in LAD2 cells. Results are expressed as Mean ± SD of three independent experiments. One-way or 2-way ANOVA followed by Dunnet multiple comparisons test were used for statistical analysis. **(C)** After proper selection, cell proliferation and cell death were assessed as described in **Figure 3**. Representative dot-plots of two independent experiments are shown. The percentage of dead cells and median fluorescence intensity (MFI) of Cell Trace Violet (CTV) fluorescence within the live cells gate are shown in each dot-plot. Averages of CTV MFI and percentages of dead cells in two independent experiments are shown in **Supplementary Figure 5**. *$p < 0.05$; **$p < 0.01$; ****$p < 0.0001$.

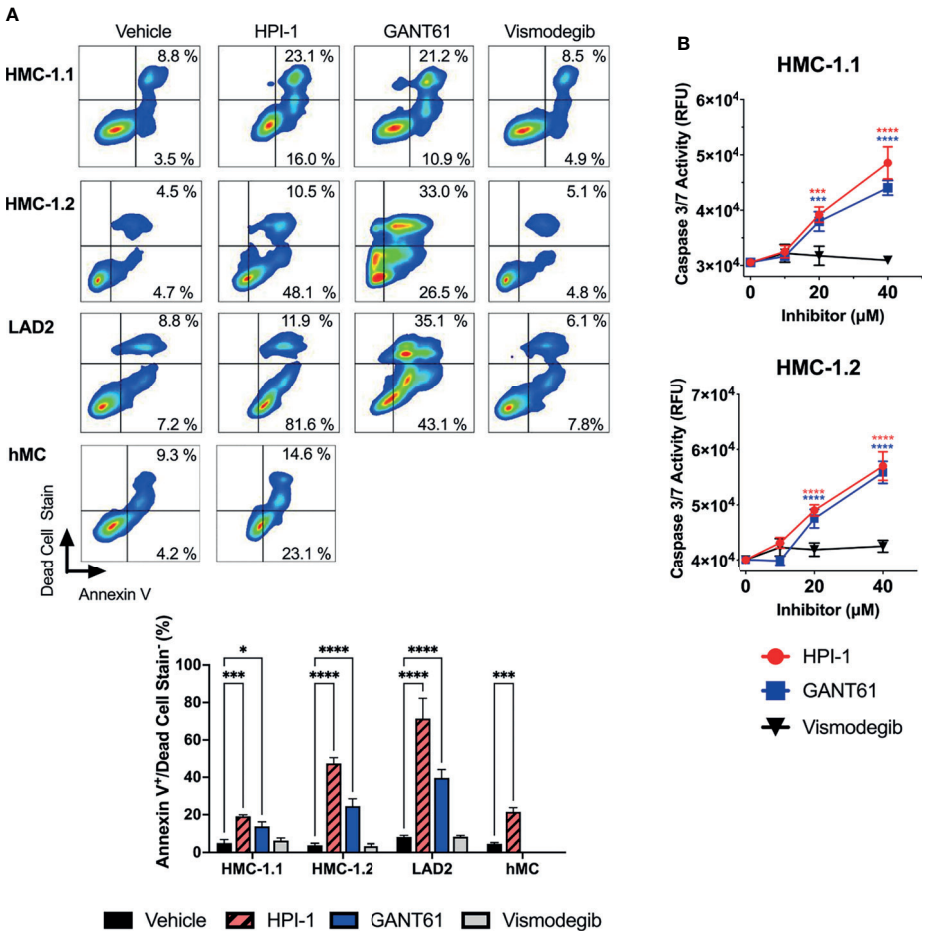


FIGURE 5 | GLI1/2 inhibition causes apoptosis in human mast cells. **(A)** HMC-1.1, HMC-1.2, LAD2, and primary human mast cells (hMC) were cultured in the presence of HPI-1, GANT61, or vismodegib (20 μM) for 48 h (HMC-1.1 and HMC-1.2 cells), 6 days (LAD2 cells) and 4 days (hMC). The percentages of annexin V positive and dead cells were quantified by flow cytometry. Representative dot-plots from one of three independent experiments are shown. The bar graph represents the average percentage of apoptotic cells (annexinV$^+$/dead cell stain$^-$) in three independent experiments using the indicated cells and treatments. **(B)** Caspase 3/7 activity was quantified by measuring relative units of fluorescence (RFU) of a caspase 3/7 substrate in HMC-1.1 and HMC 1.2 after 48h incubation with increasing concentrations of inhibitors, vehicle control is represented as concentration 0 μM. Results expressed as Mean ± SD of three independent experiments. Two-way ANOVA followed by Dunnet multiple comparisons test (compared to vehicle) were used for statistical analysis. *p < 0.05; ***p < 0.001; ****p < 0.0001.

underlining a function for GLI proteins in mast cell survival that is largely independent of SMO regulation.

In addition, we performed gene expression profile arrays of apoptotic pathways in the aggressive neoplastic HMC-1.2 mast cell line. The arrays showed that inhibition of GLI activity by HPI-1 and GANT or by GLI1 silencing *via* shRNA caused an upregulation of genes involved in the mitochondrial or intrinsic apoptotic pathway. Ingenuity Pathway Analysis of the genes upregulated in these expression arrays indicated activation of p53 as one potential upstream regulator of the apoptotic process (**Figure 6A**, right). Indeed, BBC3 (PUMA), BCL2L11 (BIM), and BAX, and to some extent APAF1, FAS and BAK1, all reported transcriptional targets of p53 (37, 38), were generally increased with all or most of the treatments with GANT61, HPI-1 or GLI1-ShRNA construct (**Figure 6A**), suggesting an upregulation of p53 function by loss of GLI activity.

An increase in p53 protein levels after inhibition of GLI was then corroborated by immunoblotting (**Figure 6B**). GLI1/2 proteins have been reported in other cells to induce the transcription of the deubiquitinase USP48 (39), which can bind and stabilize Mdm2 leading to the degradation of p53 (40), and of iASPP, an inhibitor of p53-induced transcription (41). Next, we analyzed the gene expression of these antiapoptotic proteins after GLI1/2 inhibition. Treatment of HMC-1.1, HMC-1.2 or LAD2 cells with HPI-1 caused a 50% reduction in the mRNA levels of USP48 and iASPP (**Figure 6C**), suggesting that homeostatic GLI activity regulates p53 stability and transcriptional activity by regulating respectively USP48 and iASSP, and that loss of GLI activity causes an increase in p53-mediated apoptotic cell death, thus linking transcriptional regulatory function of GLI to the control of mast cell apoptosis (see illustration in **Figure 6C**).

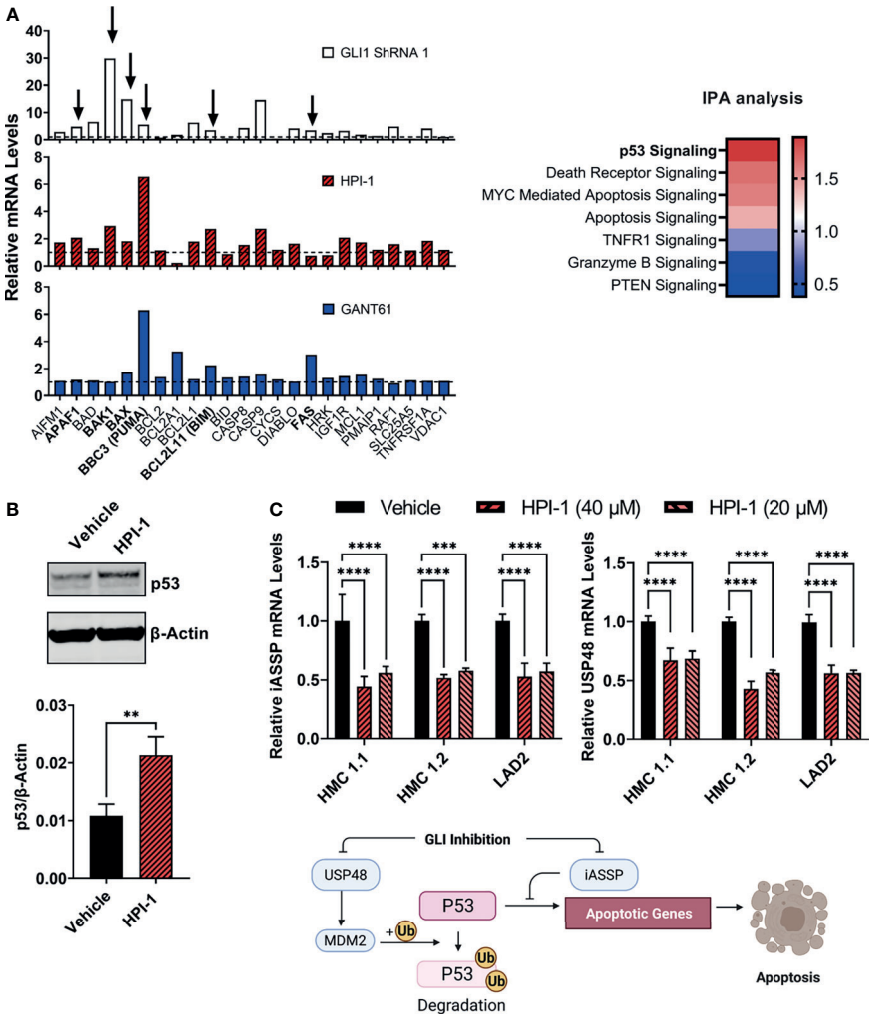


FIGURE 6 | GLI1 inhibition stabilizes p53 and alters the gene expression of pro-apoptotic proteins. **(A)** Gene expression profiling of differentially expressed genes ($2^{-\Delta\Delta Cq}$) within the mitochondrial apoptotic pathway (p53-regulated genes are marked by arrows and in bold). RNA from HMC-1.2 cells was extracted after an overnight incubation with HPI-1 or GANT61 (40 μM) or after proper selection of GLI1 shRNA (construct 1)-transduced cells. Vehicle and non-target mRNA levels are represented by dotted lines. Z-scores heatmap of the top seven canonical pathways modulated in GLI1 ShRNA (construct 1)-transduced cells, determined by using an IPA analysis. **(B)** HMC-1.2 cells were incubated overnight in the presence of HPI-1 (40 μM), cell lysates were obtained and p53 was quantified by western blot. β-actin was used as a loading control. The western blot shows a representative experiment and the average quantification of p53 protein expression, normalized to β-actin, in 3 independent experiments, are shown in the bar graph (Mean ± SD). Full-length blots are shown in **Supplementary Figure 6A**. **(C)** RNA from human mast cell lines was obtained after incubation for 5 h with HPI-1 (20 or 40 μM) and relative mRNA levels ($2^{-\Delta\Delta Cq}$) of iASSP and USP48 was determined by qPCR. GAPDH and ACTB were used for normalization. Results are expressed as Mean ± SD of three independent experiments. Illustration represents the regulation of p53 levels and function by iASSP and USP48. Unpaired t test or 2-way ANOVA followed by Dunnet multiple comparisons test were used for statistical analysis. **p < 0.01; ***p < 0.001; ****p < 0.0001.

GLI1 Inhibition Downregulates KIT Expression in Human Mast Cells

The HH-pathway and GLI3 have been implicated in the regulation of KIT expression (14). In agreement, inhibition of GLI1 *via* HPI-1 or GLI1 shRNA reduced KIT mRNA in the human mast cell lines and primary mast cell cultures (**Figure 7A**), with accompanying reductions in KIT protein levels (**Figure 7B**). It is important to note that the reduction in KIT occurred regardless of the presence of oncogenic KIT variants in mast cells, and the constitutive phosphorylation of KIT in HMC-1.2 cells, harboring V560G and D816V, was also prominently reduced (**Figure 7B**), making targeting of GLI1/2 another potential avenue for controlling mast cell numbers even in dysplastic diseases with aggressive KIT mutations.

Gli1/2 Inhibitors Reduce Mast Cell Numbers *In Vivo*

To demonstrate that the effects of Gli1/2 inhibition were not restricted to mast cells in culture, we determined the numbers of peritoneal mast cells in mice after successive injections with HPI-

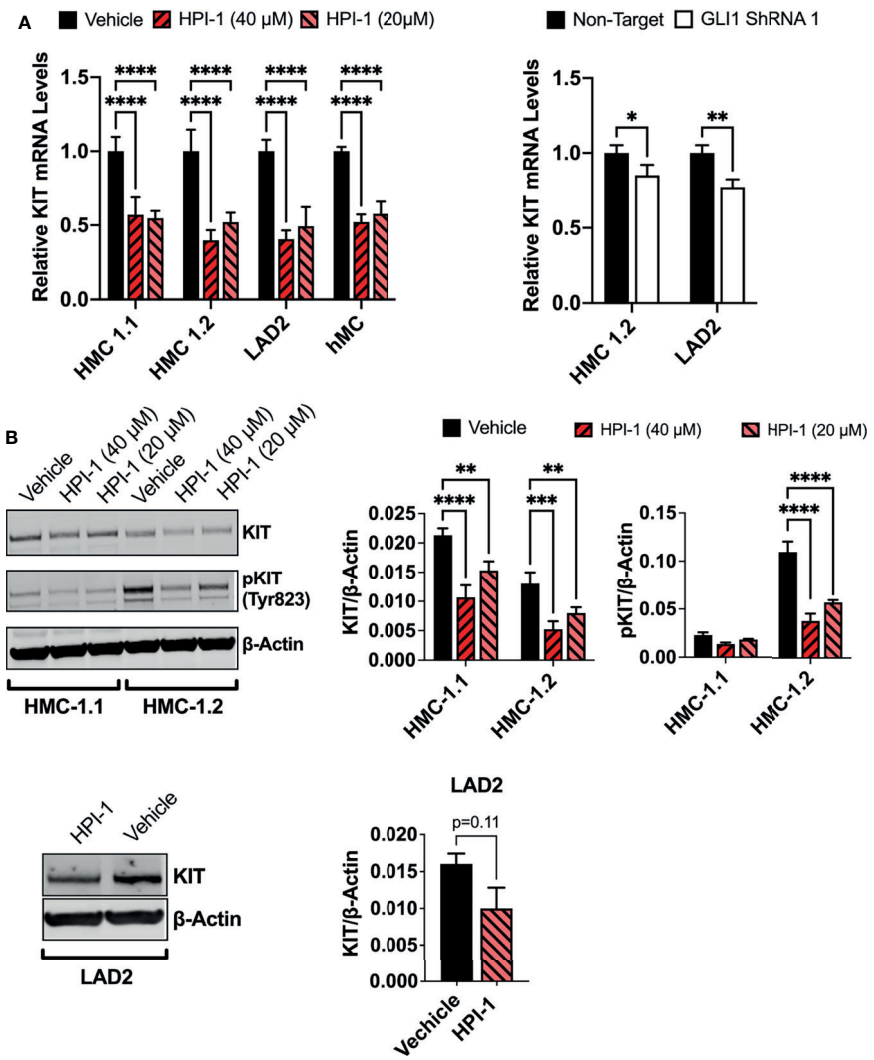


FIGURE 7 | GLI1 inhibition downregulates KIT expression and phosphorylation in human mast cells. **(A)** Relative KIT mRNA levels ($2^{-\Delta\Delta Cq}$) in mast cell lines or primary human mast cells (hMC) after 5h incubation with HPI-1 (20 or 40 μM) or 48h after transduction with lentiviral particles containing GLI1 shRNA (construct 1), no puromycin selection was conducted. Results are expressed as Mean ± SD of three independent experiments. GAPDH and ACTB were used for normalization. **(B)** HMC-1.1, HMC-1.2 and LAD2 cells were cultured overnight with HPI-1 (20 or 40μM) and lysed. Proteins were resolved in SDS-PAGE. KIT and phosphorylated-KIT (pKIT) were quantified by western-blot. β-actin was used as a loading control. The blots show representative images, and the bar graphs are the average relative band intensities of KIT and phospho-KIT (normalized by β-actin) in 2 independent experiments (Mean ± SD). Unpaired t test or 2-way ANOVA followed by Dunnet multiple comparisons test were used for statistical analysis. *p < 0.05; **p < 0.01; ***p < 0.001; ****p < 0.0001. Full-length blots are shown in **Supplementary Figure 6B**.

1 or GANT61 (**Figure 8A**). These inhibitors, used at concentrations 10 to 37 times lower (2 mg/Kg) than those used in xenograph *in vivo* models (20-75 mg/kg) (42–44), significantly reduced the number of peritoneal mast cells identified as FcεRI$^+$/Kit$^+$ cells (**Figures 8B** left, and **8C**). In contrast, the total number of peritoneal cells were not significantly changed (**Figure 8B** right). These results provide proof of principle that GLI proteins have a function in the survival of mast cells in tissue and offer GLI pathway components as potential targets for mast cell depletion in tissues. Further characterization of the effects on specific cell populations is warranted when considering the use of these drugs for specific depletion of mast cells *in vivo*.

DISCUSSION

Mast cells are effector cells in allergic inflammation and play important roles in immune surveillance. In normal tissue, the numbers of mast cells are maintained constant but can increase significantly in disease conditions and contribute to mast cell-related symptoms. Although mast cell replenishment and expansion can occur by differentiation from mast cell precursors in tissue (45–47), their numbers are also determined by signals from growth factor and cytokine receptors that regulate mature mast cell proliferation and death (3). The understanding of these fundamental processes and the

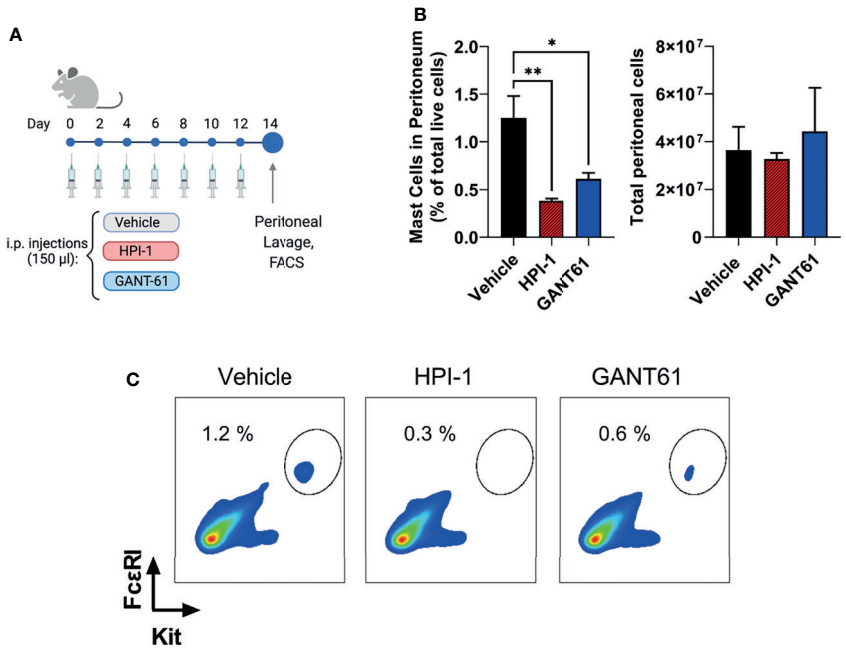


FIGURE 8 | Gli1/2 inhibitors reduce peritoneal mast cell numbers *in vivo*. **(A)** Scheme illustrating the protocol for treatment of mice with the indicated Gli1/2 inhibitors. **(B)** Peritoneal lavage was obtained 2 days after the last injection with vehicle control (PBS : EtOH; 95:5%), HPI-1 (2 mg/Kg), or GANT61 (2 mg/Kg). Cells were stained with anti-FcεRI and anti-Kit antibodies and separated by FACS. Percentages of mast cell ($FcεRI^+$ Kit^+ cells) among total live peritoneal cells for each treatment are shown (left). The number of viable cells in the peritoneal lavage after these treatments was measured using a cell counter (right panel). Results are expressed as Mean ± SD (n=4 mice/group). One-way ANOVA followed by Dunnet multiple comparisons test were used for statistical analysis. **(C)** Representative dot-plots from one mouse per group are shown. *$p < 0.05$; **$p < 0.01$.

intracellular regulatory components of mast cell homeostasis remain incomplete (2, 3). In this study, we demonstrate that GLI1/2 family members are critical transcription factors that reduce apoptotic signals and heighten proliferation of human and mouse mast cells in culture and regulate mast cell homeostasis *in vivo*. Our findings also provide insight into the underlying mechanisms for GLI actions and offer targets for potential development of therapies to control dysregulated mast cells.

Among the transcription factors known to regulate mast cell numbers *in vitro* and *in vivo*, GATA2 and MITF are notable in mast cell lineage specification and function (48–50), while STAT5 is known to regulate proliferation and survival of mast cells (3, 51). Here, we implicate the transcription factors GLI1 and GLI2 as additional key players in the steady-state regulation of the proliferation and survival of normal and transformed mast cells. This conclusion is based on the findings that inhibition of GLI1/2 by small molecules or by single shRNA-mediated knockdown effectively and markedly reduced the growth of human mast cell lines, particularly the aggressive, highly proliferative HMC-1.1 and HMC-1.2 cell lines and caused a marked drop in mast cell viability that was common to primary and neoplastic human mast cells. Furthermore, Gli1/2 inhibitors, when injected peritoneally into mice, also significantly diminished peritoneal mast cell numbers, indicating a function for Gli in the survival of mouse mast cells *in situ*.

The effect of GLI1/2 suppression on reduced human mast cell viability was accompanied by an increase in apoptotic markers. Analysis of gene expression arrays followed by western-blot assays, led us to associate the apoptotic process with an increase in the levels and activity of the tumor suppressor p53. Some reports have implicated p53 in GLI-mediated regulation of proliferation and apoptosis (41, 52–54), while in others, GLI1/2 inhibition induced p53-independent apoptosis (55, 56). In human mast cells, the increase in p53 activity induced by GLI inhibition was associated with a downregulation of two antiapoptotic proteins known to impact p53 stability and function: USP48 and iASSP, respectively (see illustration in **Figure 6C**). USP48 binds MDM2 to promote MDM2-mediated p53 ubiquitination and degradation (40), while iASPP is a p53 cofactor that inhibits p53 ability to transactivate pro-apoptotic target genes (57). In support for a cause-effect relationship between GLI inhibition and the reduction in USP48 and iASSP mRNA levels, USP48 was found to be a direct transcriptional target of GLI1 in glioblastoma cells (39), and iASPP to be induced by GLI1/2 activation *via* E2F1 in melanoma cells (39, 41). Cytokines that suppress mast cell growth and survival such as TGF-β, IL-4 and IL-10 (58) and drugs that induce mast cell apoptosis (59, 60) often require p53 activation and expression of apoptotic proteins (PUMA, APAF, BIM and BAX) that counteract the antiapoptotic BCL2 family members (Bcl2, Bclxl and MCL1), which are known

to extend mast cell survival (13, 61–63). This underscores the importance of p53 regulation in mast cell biology. Our data is consistent with the conclusion that GLI proteins, in standard cell culture media conditions, and in the absence of additional exogenous stimuli, act as negative modulators of p53 by controlling the expression of USP48 and iASPP, which offers mechanistic insights for p53 regulation in mast cells as well as potential targets to induce mast cell depletion.

Thus, the steady-state action of GLI acts as a gatekeeper to repress p53, therefore favoring mast cell survival. The activity of GLI proteins is usually studied in the context of the canonical HH signaling, although GLI can also be activated by non-canonical pathways (17, 19, 64, 65). Our data overall does not advocate a major role for a canonical activation of GLI. Autocrine pathway induction *via* constitutive production of HH ligands is unlikely since we did not find mRNA for the most broadly expressed HH ligand, SHH, in any of the human mast cells. The canonical HH-pathway involves activation of PTCH1 which allows for the required translocation of SMO to the primary cilium and consequent GLI activation (66). The primary cilium is a sensory organelle considered to be present in most vertebrate cells (67) except for lymphoid and myeloid cells (68). In support, hematopoietic-specific deletion of Ptch1 did not lead to activation of the HH signaling pathway (69). In another report, however, primary cilia were documented to be present in most human blood and bone marrow cells, although their lineage was not determined (70). It is currently unknown whether mast cells, of myeloid origin, have a primary cilium to support this pathway. Nonetheless, our results altogether contradict the presence of a functional canonical HH-pathway in these cells: 1) SMO expression was not detectable in differentiated mast cells; 2) activation of the pathway by a PTCH1 ligand or a SMO agonist (SAG) did not result in GLI expression or affected human mast cell proliferation and survival; and 3) GLI expression and these biological functions were not altered by inhibition of SMO with the antagonist vismodegib.

This conclusion differs from a recent report that describes a haploinsufficient heterozygous mutation in GLI3 in a subpopulation of congenital mastocytosis with Greig cephalopolysyndactyly syndrome and implicates the canonical HH-pathway in aggressive mastocytosis and cultured neoplastic mast cells (16). In contrast to our work, this study found that SMO antagonists, particularly sonidegib, reduced the growth of neoplastic HMC-1.1 and HMC-1.2 cells. These effects were seen in longer times than the 3 days we used in our experiments, when cells have further expanded. A possible explanation for this discrepancy might be the confluency of the cells in the two studies, since other reports have shown that cultured cells only express cilia and become HH responsive when they are confluent (71, 72). In addition, it is important to keep in mind potential off target effects of these drugs after prolonged treatments. Nevertheless, our study agrees with that of Polivka et al. (16) in that the activation of GLI in human mast cells includes a prominent non-canonical component resulting in mast cell growth/survival. Further studies are needed to determine if the canonical pathway can be induced *in vivo* or under particular experimental conditions, and how exactly GLI activity is maintained and regulated in human mast cells by non-canonical pathways.

Related to the canonical pathway, our experiments using a mouse model of Ptch1 haploinsufficiency that can achieve some level of constitutive HH-pathway activation, showed that a reduction in Ptch1 expression provides a proliferative advantage to BMMC before the culture reaches full maturity. However, the functional effect of Ptch1 haploinsufficiency was minimal in differentiated BMMC, consistent with our data in human mast cells that argues against a role for the canonical HH-pathway. Since early cultures contain mixed cell lineages, these experiments cannot discern whether the HH-pathway is intrinsically important for differentiation and proliferation of mouse mast cell progenitors, or it is secondary to the activation of this pathway on other cell types. This later view is supported by a report where only deletion of Ptch1 in non-hematopoietic cells, but not deletion of Ptch1 in hematopoietic cells, caused dramatic hematopoietic phenotypes including increased circulating myeloid progenitors (69). Polivka et al. (16) also showed the presence of SHH in biopsies of the skin, digestive tract, and bone marrow of patients with mastocytosis, environments where mast cells were present and thus the HH-pathway could also affect mast cells or mast cell progenitors *via* mast cell-extrinsic mechanisms.

Many transcription factors that regulate mast cell homeostasis, including MITF, GATA2 and STAT5 influence the expression of KIT. Conversely, KIT regulate the expression/activation status of these transcription factors (3, 48–51, 73). KIT is a central receptor providing positive signals for mast cell survival and proliferation. Previous reports have shown or suggested that GLI transcription factors regulate KIT expression (14, 16). We provide confirmation that GLI1/2 inhibition suppressed KIT expression at the mRNA and protein levels in human mast cells, regardless of oncogenic mutations, an effect that may also represent a cause for the drop in viability and proliferation in the cells. Reciprocally to GLI regulating KIT expression, KIT signals were described to regulate GLI expression (16). Although we did not explore this possibility, our results showed that the expression of GLI2 (only detected in HMC-1.1 and HMC-1.2 cells) is regulated by KIT oncogenic signals, mainly the MEK/ERK1/2 pathway and to some extent the PI3K pathway (**Supplementary Figure 1A**) suggesting positive feedback loops between KIT and GLI. The increase in GLI2 expression in the rapidly growing neoplastic HMC-1.1 and HMC-1.2 cells (**Table 1** and **Supplementary Figure 1**) is consistent with findings that increased expression of GLI^A can lead to transformation (18, 19).

In summary, the data presented here support a role for GLI transcription factors as molecular rheostats of mast cell preservation. Homeostatic GLI function, modulated in cultures mainly by non-canonical pathways, controls p53 function and KIT expression, resulting in suppression of apoptosis and promoting proliferation of mast cells, thus contributing to mast cell number maintenance in steady-state and possibly in disease conditions with mast cell-related presentations, as shown

in mastocytosis (16). Future studies are warranted to gain a better understanding of GLI regulation in mast cells in their local environment and to develop targeted intracellular delivery mechanisms for inhibitors of GLI and its targets to control mast cell numbers when needed.

DATA AVAILABILITY STATEMENT

The original contributions presented in the study are included in the article/**Supplementary Material**. Further inquiries can be directed to the corresponding author.

ETHICS STATEMENT

The studies involving human participants were reviewed and approved by National Institutes of Health Internal Review Board, protocol# NCT00001756. The patients/participants provided their written informed consent to participate in this study. The animal study (under protocol LAD2E) was reviewed and approved by NIAID-DIR-Animal Care and Use Committee.

AUTHOR CONTRIBUTIONS

GF designed and conducted experiments, analyzed data, prepared figures, and drafted the manuscript. AP, QZ, and YY performed experiments and analyzed data. AO supervised the study, designed and helped with experiments, prepared figures, and wrote the manuscript. DM supervised the study, wrote the manuscript, and provided funding. All authors approved the manuscript.

FUNDING

This work was supported by the Division of Intramural Research of the National Institutes of Health (NIH), National Institute of Allergy and Infectious Diseases (NIAID).

ACKNOWLEDGMENTS

We thank all MCBS members for their valuable intellectual contributions. Illustrations were created with BioRender.com (2020). **Figure 1A** was adapted from the template "Hedgehog signaling pathway") (https://app.biorender.com/biorender-templates)

SUPPLEMENTARY MATERIAL

The Supplementary Material for this article can be found online at: https://www.frontiersin.org/articles/10.3389/fimmu.2022.841045/full#supplementary-material

REFERENCES

1. Falduto GH, Pfeiffer A, Luker A, Metcalfe DD, Olivera A. Emerging Mechanisms Contributing to Mast Cell-Mediated Pathophysiology With Therapeutic Implications. *Pharmacol Ther* (2021) 220:107718. doi: 10.1016/j.pharmthera.2020.107718
2. Piliponsky AM, Levi-Schaffer F. Regulation of Apoptosis in Mast Cells. *Apoptosis* (2000) 5(5):435–41. doi: 10.1023/a:1009680500988
3. Caslin HL, Kiwanuka KN, Haque TT, Taruselli MT, MacKnight HP, Paranjape A, et al. Controlling Mast Cell Activation and Homeostasis: Work Influenced by Bill Paul That Continues Today. *Front Immunol* (2018) 9:868. doi: 10.3389/fimmu.2018.00868
4. Dahlin JS, Hallgren J. Mast Cell Progenitors: Origin, Development and Migration to Tissues. *Mol Immunol* (2015) 63(1):9–17. doi: 10.1016/j.molimm.2014.01.018
5. Bankova LG, Dwyer DF, Liu AY, Austen KF, Gurish MF. Maturation of Mast Cell Progenitors to Mucosal Mast Cells During Allergic Pulmonary Inflammation in Mice. *Mucosal Immunol* (2015) 8(3):596–606. doi: 10.1038/mi.2014.91
6. Valent P, Akin C, Metcalfe DD. Mastocytosis: 2016 Updated WHO Classification and Novel Emerging Treatment Concepts. *Blood* (2017) 129 (11):1420–7. doi: 10.1182/blood-2016-09-731893
7. Cruse G, Metcalfe DD, Olivera A. Functional Deregulation of KIT: Link to Mast Cell Proliferative Diseases and Other Neoplasms. *Immunol Allergy Clin North Am* (2014) 34(2):219–37. doi: 10.1016/j.iac.2014.01.002
8. Jensen BM, Akin C, Gilfillan AM. Pharmacological Targeting of the KIT Growth Factor Receptor: A Therapeutic Consideration for Mast Cell Disorders. *Br J Pharmacol* (2008) 154(8):1572–82. doi: 10.1038/bjp.2008.204
9. Reber LL, Marichal T, Galli SJ. New Models for Analyzing Mast Cell Functions *In Vivo*. *Trends Immunol* (2012) 33(12):613–25. doi: 10.1016/j.it.2012.09.008
10. Cahill KN, Katz HR, Cui J, Lai J, Kazani S, Crosby-Thompson A, et al. KIT Inhibition by Imatinib in Patients With Severe Refractory Asthma. *N Engl J Med* (2017) 376(20):1911–20. doi: 10.1056/NEJMoa1613125
11. Cerny-Reiterer S, Rabenhorst A, Stefanzl G, Herndlhofer S, Hoermann G, Mullauer L, et al. Long-Term Treatment With Imatinib Results in Profound Mast Cell Deficiency in Ph+ Chronic Myeloid Leukemia. *Oncotarget* (2015) 6 (5):3071–84. doi: 10.18632/oncotarget.3074
12. Paivandy A, Pejler G. Novel Strategies to Target Mast Cells in Disease. *J Innate Immun* (2021) 13(3):131–47. doi: 10.1159/000513582
13. Ekoff M, Nilsson G. Mast Cell Apoptosis and Survival. *Adv Exp Med Biol* (2011) 716:47–60. doi: 10.1007/978-1-4419-9533-9_4
14. Tang CM, Lee TE, Syed SA, Burgoyne AM, Leonard SY, Gao F, et al. Hedgehog Pathway Dysregulation Contributes to the Pathogenesis of Human Gastrointestinal Stromal Tumors *via* GLI-Mediated Activation of KIT Expression. *Oncotarget* (2016) 7(48):78226–41. doi: 10.18632/oncotarget.12909
15. Cain JE, Islam E, Haxho F, Blake J, Rosenblum ND. GLI3 Repressor Controls Functional Development of the Mouse Ureter. *J Clin Invest* (2011) 121 (3):1199–206. doi: 10.1172/JCI45523
16. Polivka L, Parietti V, Bruneau J, Soucie E, Madrange M, Bayard E, et al. The Association of Greig Syndrome and Mastocytosis Reveals the Involvement of Hedgehog Pathway in Advanced Mastocytosis. *Blood* (2021) 138(23):2396–407. doi: 10.1182/blood.2020010207
17. Pietrobono S, Gagliardi S, Stecca B. Non-Canonical Hedgehog Signaling Pathway in Cancer: Activation of GLI Transcription Factors Beyond Smoothened. *Front Genet* (2019) 10:556. doi: 10.3389/fgene.2019.00556
18. Iriana S, Asha K, Repak M, Sharma-Walia N. Hedgehog Signaling: Implications in Cancers and Viral Infections. *Int J Mol Sci* (2021) 22 (3):1042. doi: 10.3390/ijms22031042
19. Carballo GB, Honorato JR, de Lopes GPF, Spohr T. A Highlight on Sonic Hedgehog Pathway. *Cell Commun Signal* (2018) 16(1):11. doi: 10.1186/s12964-018-0220-7

20. Schrader EK, Harstad KG, Holmgren RA, Matouschek A. A Three-Part Signal Governs Differential Processing of Gli1 and Gli3 Proteins by the Proteasome. *J Biol Chem* (2011) 286(45):39051–8. doi: 10.1074/jbc.M111.274993
21. Pan Y, Wang B. A Novel Protein-Processing Domain in Gli2 and Gli3 Differentially Blocks Complete Protein Degradation by the Proteasome. *J Biol Chem* (2007) 282(15):10846–52. doi: 10.1074/jbc.M608599200
22. Tukachinsky H, Lopez LV, Salic A. A Mechanism for Vertebrate Hedgehog Signaling: Recruitment to Cilia and Dissociation of SuFu-Gli Protein Complexes. *J Cell Biol* (2010) 191(2):415–28. doi: 10.1083/jcb.201004108
23. Khan AA, Harrison CN, McLornan DP. Targeting of the Hedgehog Pathway in Myeloid Malignancies: Still a Worthy Chase? *Br J Haematol* (2015) 170 (3):323–35. doi: 10.1111/bjh.13426
24. Lau BW, Huh K, Madero-Marroquin R, De Marchi F, Lim Y, Wang Q, et al. Hedgehog/GLI1 Activation Leads to Leukemic Transformation of Myelodysplastic Syndrome *In Vivo* and GLI1 Inhibition Results in Antitumor Activity. *Oncogene* (2019) 38(5):687–98. doi: 10.1038/s41388-018-0431-9
25. Goodrich LV, Milenkovic L, Higgins KM, Scott MP. Altered Neural Cell Fates and Medulloblastoma in Mouse Patched Mutants. *Science* (1997) 277 (5329):1109–13. doi: 10.1126/science.277.5329.1109
26. Kulinski JM, Proia RL, Larson EM, Metcalfe DD, Olivera A. S1P(4) Regulates Passive Systemic Anaphylaxis in Mice But Is Dispensable for Canonical IgE-Mediated Responses in Mast Cells. *Int J Mol Sci* (2018) 19(5):1279. doi: 10.3390/ijms19051279
27. Yin Y, Bai Y, Olivera A, Desai A, Metcalfe DD. An Optimized Protocol for the Generation and Functional Analysis of Human Mast Cells From CD34(+) Enriched Cell Populations. *J Immunol Methods* (2017) 448:105–11. doi: 10.1016/j.jim.2017.06.003
28. Lee J, Platt KA, Censullo P, Ruiz i Altaba A. Gli1 is a Target of Sonic Hedgehog That Induces Ventral Neural Tube Development. *Development* (1997) 124 (13):2537–52. doi: 10.1242/dev.124.13.2537
29. Taipale J, Cooper MK, Maiti T, Beachy PA. Patched Acts Catalytically to Suppress the Activity of Smoothened. *Nature* (2002) 418(6900):892–7. doi: 10.1038/nature00989
30. Wetmore C, Eberhart DE, Curran T. The Normal Patched Allele is Expressed in Medulloblastomas From Mice With Heterozygous Germ-Line Mutation of Patched. *Cancer Res* (2000) 60(8):2239–46.
31. Bacelar Sacramento de Araujo T, de Oliveira Siquara da Rocha L, Torres Andion Vidal M, Cerqueira Coelho PL, Galvao Dos Reis M, Solano de Freitas Souza B, et al. GANT61 Reduces Hedgehog Molecule (GLI1) Expression and Promotes Apoptosis in Metastatic Oral Squamous Cell Carcinoma Cells. *Int J Mol Sci* (2020) 21(17):6076. doi: 10.3390/ijms21176076
32. Li B, Giambelli C, Tang B, Winterbottom E, Long J, Jin K, et al. Arsenic Attenuates GLI Signaling, Increasing or Decreasing its Transcriptional Program in a Context-Dependent Manner. *Mol Pharmacol* (2016) 89 (2):226–32. doi: 10.1124/mol.115.100867
33. Beauchamp EM, Ringer L, Bulut G, Sajwan KP, Hall MD, Lee YC, et al. Arsenic Trioxide Inhibits Human Cancer Cell Growth and Tumor Development in Mice by Blocking Hedgehog/GLI Pathway. *J Clin Invest* (2011) 121(1):148–60. doi: 10.1172/JCI42874
34. Hyman JM, Firestone AJ, Heine VM, Zhao Y, Ocasio CA, Han K, et al. Small-Molecule Inhibitors Reveal Multiple Strategies for Hedgehog Pathway Blockade. *Proc Natl Acad Sci USA* (2009) 106(33):14132–7. doi: 10.1073/pnas.0907134106
35. Mahindroo N, Connelly MC, Punchihewa C, Yang L, Yan B, Fujii N. Amide Conjugates of Ketoprofen and Indole as Inhibitors of Gli1-Mediated Transcription in the Hedgehog Pathway. *Bioorg Med Chem* (2010) 18 (13):4801–11. doi: 10.1016/j.bmc.2010.05.001
36. Tse WP, Cheng CH, Che CT, Lin ZX. Arsenic Trioxide, Arsenic Pentoxide, and Arsenic Iodide Inhibit Human Keratinocyte Proliferation Through the Induction of Apoptosis. *J Pharmacol Exp Ther* (2008) 326(2):388–94. doi: 10.1124/jpet.107.134080
37. Fischer M. Census and Evaluation of P53 Target Genes. *Oncogene* (2017) 36 (28):3943–56. doi: 10.1038/onc.2016.502
38. Aubrey BJ, Kelly GL, Janic A, Herold MJ, Strasser A. How Does P53 Induce Apoptosis and How Does This Relate to P53-Mediated Tumour Suppression? *Cell Death Differ* (2018) 25(1):104–13. doi: 10.1038/cdd.2017.169
39. Zhou A, Lin K, Zhang S, Ma L, Xue J, Morris SA, et al. Gli1-Induced Deubiquitinase USP48 Aids Glioblastoma Tumorigenesis by Stabilizing Gli1. *EMBO Rep* (2017) 18(8):1318–30. doi: 10.15252/embr.201643124
40. Cetkovska K, Sustova H, Uldrijan S. Ubiquitin-Specific Peptidase 48 Regulates Mdm2 Protein Levels Independent of its Deubiquitinase Activity. *Sci Rep* (2017) 7:43180. doi: 10.1038/srep43180
41. Pandolfi S, Montagnani V, Lapucci A, Stecca B. HEDGEHOG/GLI-E2F1 Axis Modulates iASPP Expression and Function and Regulates Melanoma Cell Growth. *Cell Death Differ* (2015) 22(12):2006–19. doi: 10.1038/cdd.2015.56
42. Lauth M, Bergstrom A, Shimokawa T, Toftgard R. Inhibition of GLI-Mediated Transcription and Tumor Cell Growth by Small-Molecule Antagonists. *Proc Natl Acad Sci U S A* (2007) 104(20):8455–60. doi: 10.1073/pnas.0609699104
43. Zhang KQ, Chu XD. GANT61 Plays Antitumor Effects by Inducing Oxidative Stress Through the miRNA-1286/RAB31 Axis in Osteosarcoma. *Cell Biol Int* (2021) 45(1):61–73. doi: 10.1002/cbin.11467
44. Fu J, Rodova M, Roy SK, Sharma J, Singh KP, Srivastava RK, et al. GANT-61 Inhibits Pancreatic Cancer Stem Cell Growth *In Vitro* and in NOD/SCID/IL2R Gamma Null Mice Xenograft. *Cancer Lett* (2013) 330(1):22–32. doi: 10.1016/j.canlet.2012.11.018
45. Gentek R, Ghigo C, Hoeffel G, Bulle MJ, Msallam R, Gautier G, et al. Hemogenic Endothelial Fate Mapping Reveals Dual Developmental Origin of Mast Cells. *Immunity* (2018) 48(6):1160–71.e5. doi: 10.1016/j.immuni.2018.04.025
46. Dahlin JS, Malinovschi A, Ohrvik H, Sandelin M, Janson C, Alving K, et al. Lin- CD34hi CD117int/hi FcepsilonRI+ Cells in Human Blood Constitute a Rare Population of Mast Cell Progenitors. *Blood* (2016) 127(4):383–91. doi: 10.1182/blood-2015-06-650648
47. Dahlin JS, Heyman B, Hallgren J. Committed Mast Cell Progenitors in Mouse Blood Differ in Maturity Between Th1 and Th2 Strains. *Allergy* (2013) 68 (10):1333–7. doi: 10.1111/all.12223
48. Desai A, Sowerwine K, Liu Y, Lawrence MG, Chovanec J, Hsu AP, et al. GATA-2-Deficient Mast Cells Limit IgE-Mediated Immediate Hypersensitivity Reactions in Human Subjects. *J Allergy Clin Immunol* (2019) 144(2):613–617 e14. doi: 10.1016/j.jaci.2019.05.007
49. Lee YN, Brandal S, Noel P, Wentzel E, Mendell JT, McDevitt MA, et al. KIT Signaling Regulates MITF Expression Through miRNAs in Normal and Malignant Mast Cell Proliferation. *Blood* (2011) 117(13):3629–40. doi: 10.1182/blood-2010-07-293548
50. Shahlaee AH, Brandal S, Lee YN, Jie C, Takemoto CM. Distinct and Shared Transcriptomes are Regulated by Microphthalmia-Associated Transcription Factor Isoforms in Mast Cells. *J Immunol* (2007) 178(1):378–88. doi: 10.4049/jimmunol.178.1.378
51. Harir N, Boudot C, Friedbichler K, Sonneck K, Kondo R, Martin-Lanneree S, et al. Oncogenic Kit Controls Neoplastic Mast Cell Growth Through a Stat5/PI3-Kinase Signaling Cascade. *Blood* (2008) 112(6):2463–73. doi: 10.1182/blood-2007-09-115477
52. Stecca B, Ruiz i Altaba A. A GLI1-P53 Inhibitory Loop Controls Neural Stem Cell and Tumour Cell Numbers. *EMBO J* (2009) 28(6):663–76. doi: 10.1038/emboj.2009.16
53. Kang HN, Oh SC, Kim JS, Yoo YA. Abrogation of Gli3 Expression Suppresses the Growth of Colon Cancer Cells *via* Activation of P53. *Exp Cell Res* (2012) 318(5):539–49. doi: 10.1016/j.yexcr.2011.12.010
54. Ho L, Stojanovski A, Whetstone H, Wei QX, Mau E, Wunder JS, et al. Gli2 and P53 Cooperate to Regulate IGFBP-3- Mediated Chondrocyte Apoptosis in the Progression From Benign to Malignant Cartilage Tumors. *Cancer Cell* (2009) 16(2):126–36. doi: 10.1016/j.ccr.2009.05.013
55. Matsumoto T, Tabata K, Suzuki T. The GANT61, a GLI Inhibitor, Induces Caspase-Independent Apoptosis of SK-N-LO Cells. *Biol Pharm Bull* (2014) 37 (4):633–41. doi: 10.1248/bpb.b13-00920
56. Mazumdar T, Devecchio J, Agyeman A, Shi T, Houghton JA. Blocking Hedgehog Survival Signaling at the Level of the GLI Genes Induces DNA Damage and Extensive Cell Death in Human Colon Carcinoma Cells. *Cancer Res* (2011) 71(17):5904–14. doi: 10.1158/0008-5472.CAN-10-4173
57. Bergamaschi D, Samuels Y, Sullivan A, Zvelebil M, Breyssens H, Bisso A, et al. iASPP Preferentially Binds P53 Proline-Rich Region and Modulates Apoptotic Function of Codon 72-Polymorphic P53. *Nat Genet* (2006) 38 (10):1133–41. doi: 10.1038/ng1879
58. Ryan JJ, Kashyap M, Bailey D, Kennedy S, Speiran K, Brenzovich J, et al. Mast Cell Homeostasis: A Fundamental Aspect of Allergic Disease. *Crit Rev Immunol* (2007) 27(1):15–32. doi: 10.1615/critrevimmunol.v27.i1.20

59. Bandara G, Munoz-Cano R, Tobio A, Yin Y, Komarow HD, Desai A, et al. Targeting Sphingosine Kinase Isoforms Effectively Reduces Growth and Survival of Neoplastic Mast Cells With D816V-KIT. *Front Immunol* (2018) 9:631. doi: 10.3389/fimmu.2018.00631
60. Paez PA, Kolawole M, Taruselli MT, Ajith S, Dailey JM, Kee SA, et al. Fluvastatin Induces Apoptosis in Primary and Transformed Mast Cells. *J Pharmacol Exp Ther* (2020) 374(1):104–12. doi: 10.1124/jpet.119.264234
61. Aichberger KJ, Mayerhofer M, Gleixner KV, Krauth MT, Gruze A, Pickl WF, et al. Identification of MCL1 as a Novel Target in Neoplastic Mast Cells in Systemic Mastocytosis: Inhibition of Mast Cell Survival by MCL1 Antisense Oligonucleotides and Synergism With PKC412. *Blood* (2007) 109(7):3031–41. doi: 10.1182/blood-2006-07-032714
62. Hazzan T, Eberle J, Worm M, Babina M. Apoptotic Resistance of Human Skin Mast Cells is Mediated by Mcl-1. *Cell Death Discov* (2017) 3:17048. doi: 10.1038/cddiscovery.2017.48
63. Mekori YA, Gilfillan AM, Akin C, Hartmann K, Metcalfe DD. Human Mast Cell Apoptosis is Regulated Through Bcl-2 and Bcl-Xl. *J Clin Immunol* (2001) 21(3):171–4. doi: 10.1023/a:1011083031272
64. Nolan-Stevaux O, Lau J, Truitt ML, Chu GC, Hebrok M, Fernandez-Zapico ME, et al. GLI1 is Regulated Through Smoothened-Independent Mechanisms in Neoplastic Pancreatic Ducts and Mediates PDAC Cell Survival and Transformation. *Genes Dev* (2009) 23(1):24–36. doi: 10.1101/gad.1753809
65. de la Roche M, Ritter AT, Angus KL, Dinsmore C, Earnshaw CH, Reiter JF, et al. Hedgehog Signaling Controls T Cell Killing at the Immunological Synapse. *Science* (2013) 342(6163):1247–50. doi: 10.1126/science.1244689
66. Bangs F, Anderson KV. Primary Cilia and Mammalian Hedgehog Signaling. *Cold Spring Harb Perspect Biol* (2017) 9(5):a028175. doi: 10.1101/cshperspect.a028175
67. Anvarian Z, Mykytyn K, Mukhopadhyay S, Pedersen LB, Christensen ST. Cellular Signalling by Primary Cilia in Development, Organ Function and Disease. *Nat Rev Nephrol* (2019) 15(4):199–219. doi: 10.1038/s41581-019-0116-9
68. Wheatley DN. Primary Cilia in Normal and Pathological Tissues. *Pathobiology* (1995) 63(4):222–38. doi: 10.1159/000163955
69. Siggins SL, Nguyen NY, McCormack MP, Vasudevan S, Villani R, Jane SM, et al. The Hedgehog Receptor Patched1 Regulates Myeloid and Lymphoid Progenitors by Distinct Cell-Extrinsic Mechanisms. *Blood* (2009) 114(5):995–1004. doi: 10.1182/blood-2009-03-208330
70. Singh M, Chaudhry P, Merchant AA. Primary Cilia are Present on Human Blood and Bone Marrow Cells and Mediate Hedgehog Signaling. *Exp Hematol* (2016) 44(12):1181–7.e2. doi: 10.1016/j.exphem.2016.08.009
71. Bailey EC, Milenkovic L, Scott MP, Collawn JF, Johnson RL. Several PATCHED1 Missense Mutations Display Activity in Patched1-Deficient Fibroblasts. *J Biol Chem* (2002) 277(37):33632–40. doi: 10.1074/jbc.M202203200
72. Quarmby LM, Parker JD. Cilia and the Cell Cycle? *J Cell Biol* (2005) 169 (5):707–10. doi: 10.1083/jcb.200503053
73. Li Y, Qi X, Liu B, Huang H. The STAT5-GATA2 Pathway is Critical in Basophil and Mast Cell Differentiation and Maintenance. *J Immunol* (2015) 194(9):4328–38. doi: 10.4049/jimmunol.1500018

Conflict of Interest: The authors declare that the research was conducted in the absence of any commercial or financial relationships that could be construed as a potential conflict of interest.

Publisher's Note: All claims expressed in this article are solely those of the authors and do not necessarily represent those of their affiliated organizations, or those of the publisher, the editors and the reviewers. Any product that may be evaluated in this article, or claim that may be made by its manufacturer, is not guaranteed or endorsed by the publisher.

Copyright © 2022 Falduto, Pfeiffer, Zhang, Yin, Metcalfe and Olivera. This is an open-access article distributed under the terms of the Creative Commons Attribution License (CC BY). The use, distribution or reproduction in other forums is permitted, provided the original author(s) and the copyright owner(s) are credited and that the original publication in this journal is cited, in accordance with accepted academic practice. No use, distribution or reproduction is permitted which does not comply with these terms.

frontiers | Frontiers in Immunology

ORIGINAL RESEARCH
published: 13 April 2022
doi: 10.3389/fimmu.2022.830859

Elastase- and LPS-Exposed Cpa3$^{Cre/+}$ and ST2$^{-/-}$ Mice Develop Unimpaired Obstructive Pulmonary Disease

Eduardo I. Cardenas[1,2], *Perla A. Alvarado-Vazquez*[1], *Erika Mendez-Enriquez*[1], *Erik A. Danielsson*[1,3] *and Jenny Hallgren*[1]*

[1] Department of Medical Biochemistry and Microbiology, Uppsala University, Uppsala, Sweden, [2] Division of Lung and Airway Research, Institute of Environmental Medicine, Karolinska Institute, Stockholm, Sweden, [3] Department of Surgical Sciences, Uppsala University Hospital, Uppsala, Sweden

OPEN ACCESS

Edited by:
Frans J. Van Overveld, University College Roosevelt, Netherlands

Reviewed by:
Jeffrey Louis Curtis, University of Michigan, United States
Mark Wilson, Genentech, Inc., United States

***Correspondence:**
Jenny Hallgren
Jenny.hallgren@imbim.uu.se
orcid.org/0000-0002-3685-5364

Specialty section:
This article was submitted to Inflammation, a section of the journal Frontiers in Immunology

Received: *07 December 2021*
Accepted: *23 March 2022*
Published: *13 April 2022*

Citation:
Cardenas EI, Alvarado-Vazquez PA, Mendez-Enriquez E, Danielsson EA and Hallgren J (2022) Elastase- and LPS-Exposed Cpa3$^{Cre/+}$ and ST2$^{-/-}$ Mice Develop Unimpaired Obstructive Pulmonary Disease. Front. Immunol. 13:830859. doi: 10.3389/fimmu.2022.830859

IL-33 and its receptor ST2, as well as mast cells and their mediators, have been implicated in the development of chronic obstructive pulmonary disease (COPD). However, whether mast cells and the ST2 receptor play a critical role in COPD pathophysiology remains unclear. Here, we performed repeated intranasal administrations of porcine pancreatic elastase and LPS for four weeks to study COPD-like disease in wildtype, ST2-deficient, and Cpa3$^{Cre/+}$ mice, which lack mast cells and have a partial reduction in basophils. Alveolar enlargement and changes in spirometry-like parameters, e.g. increased dynamic compliance and decreased expiratory capacity, were evident one day after the final LPS challenge and worsened over time. The elastase/LPS model also induced mild COPD-like airway inflammation, which encompassed a transient increase in lung mast cell progenitors, but not in mature mast cells. While ST2-deficient and Cpa3$^{Cre/+}$ mice developed reduced pulmonary function uninterruptedly, they had a defective inflammatory response. Importantly, both ST2-deficient and Cpa3$^{Cre/+}$ mice had fewer alveolar macrophages, known effector cells in COPD. Elastase/LPS instillation *in vivo* also caused increased bronchiole contraction in precision cut lung slices challenged with methacholine *ex vivo*, which occurred in a mast cell-independent fashion. Taken together, our data suggest that the ST2 receptor and mast cells play a minor role in COPD pathophysiology by sustaining alveolar macrophages.

Keywords: COPD - chronic obstructive pulmonary disease, pulmonary function, airway hyperresposiveness, mast cell (MC), ST2, IL-33

Abbreviations: COPD, Chronic obstructive pulmonary disease; Cdyn, Dynamic compliance; FEV_{100}, Forced expiratory volume in 100 milli sec; FVC, Forced vital capacity; H&E, Hematoxylin & Eosin stain; LPS, Lipopolysaccaride; Lin, Lineage; OCT, Optimal cutting temperature compound; PBS, Phosphate buffered saline; PCLS, Precision cut lung slices; TLC, Total lung capacity.

INTRODUCTION

Chronic obstructive pulmonary disease (COPD) is an inflammatory disease of the airways predominantly caused by long-term tobacco smoking, and characterized by progressive and irreversible airflow obstruction. Lack of effective treatments and an increasing prevalence among aging populations make COPD a major health problem, and one of the main causes of death worldwide (1, 2). COPD diagnosis relies on pulmonary function testing to evaluate specific lung alterations. COPD patients often exhibit alveolar enlargement (i.e., emphysema), which causes an increase in their total lung capacity (TLC). The chronic inflammation associated with COPD damages the elastic properties of the airways, which is detected as an increase in dynamic compliance (C_{dyn}). COPD patients also have an overall decrease in their expiratory capacity (measured as forced expiratory volume in 1 s/forced vital capacity: FEV1/FVC) due to the ongoing airway inflammation, mucus hypersecretion, emphysema, and loss of elastic recoil. The development of COPD appears to be mainly driven by neutrophils, macrophages, and $CD8^+$ and $CD4^+$ (Th1/Th17) T cells (3). However, the inflammatory response associated with COPD involves several other mediators and cell types such as IL-33 and mast cells (MCs) whose contributions to COPD pathophysiology have not been fully elucidated.

IL-33 is an alarmin predominantly released by the airway epithelium in response to infection and inhaled irritants such as pollution and allergens. IL-33 acts *via* the ST2 receptor on immune cells and structural cells to induce activation and production of proinflammatory mediators, leading to cellular recruitment to the lung and expansion of innate and adaptive immune cells (4). The IL-33/ST2 axis has been most studied in the context of asthma, where IL-33 both enhances allergic responses and plays a pivotal role in antigen-independent responses. Interestingly, expression of IL-33 and the ST2 receptor is increased in lung, serum, and plasma samples from COPD patients (5–7). The increase in IL-33 and ST2 correlates with reduced pulmonary function and higher eosinophil counts in blood, and is more frequent in patients with chronic bronchitis or severe COPD (5, 7). Moreover, an IL-33 gene polymorphism is associated with impaired pulmonary function and early onset of COPD (8). In mice, short-term exposure to cigarette smoke upregulates epithelial IL-33 expression, downregulates ST2 on type 2 innate lymphoid cells, and enhances ST2 expression on macrophages and NK cells, thereby amplifying type 1 immune responses toward influenza infection (5). Although cigarette smoke-induced models of COPD are relevant to human disease, they require long-term exposures to induce the alterations in lung function associated with COPD. In contrast, changes in lung function that recapitulate human COPD can be induced rapidly over a few weeks by administering elastase to the lung (9). Interestingly, intratracheal injection of elastase also induces higher levels of lung IL-33 in mice (10). However, IL-33-deficiency enhances murine emphysema caused by intratracheal administrations of elastase or cigarette smoke extract (10).

MCs are rare ST2-expressing tissue-resident immune cells that release proteases and proinflammatory mediators upon activation by IL-33 (11, 12). Moreover, experimental studies suggest that IL-33-induced activation of MCs participates in key features of asthma (13). For example, IL-33 has been shown to enhance antigen-induced bronchoconstriction *via* MC activation (14), and to induce IL-13-dependent airway hyperresponsiveness *in vivo*, possibly *via* MC activation and release of IL-13 (15). However, MCs activated by IL-33 have also been shown to induce regulatory T cell differentiation and suppression of inflammation in a model of Papain-induced allergic airway inflammation (16). Importantly, MCs have also been implicated in smoke-dependent models of COPD. Mice lacking the MC-specific proteases mMCP-6 or Prss31, which are the mouse homologs of human β- and γ-tryptase, respectively, have less airway inflammation and histological evidence of emphysema (17, 18). There is also evidence of MC-involvement in the human disease. COPD patients have a higher proportion of tryptase- and chymase-expressing MCs (MC_{TC}) in the lung and increased tryptase activity in sputum and plasma, all of which correlates with reduced pulmonary function and enhanced disease severity (19, 20). MC numbers are increased in lung biopsies from patients with centrilobular emphysema (21) and chronic bronchitis (22), and MC mediators such as histamine and tryptase are elevated in bronchoalveolar lavage fluid (BALF) from long-term cigarette smokers (23). Altogether, these data indicate that MCs and the IL-33/ST2 axis might be relevant to COPD pathophysiology, but whether they contribute to the impaired pulmonary function that defines COPD has not been thoroughly examined.

In the present study, we investigated how the absence of MCs or the ST2 receptor impacted two key features of COPD: airway inflammation and reduced pulmonary function. For this purpose, ST2-deficient and $Cpa3^{Cre/+}$ mice, which lack MCs and have a partial reduction in basophils, were subjected to a model of COPD induced by repeated intranasal administrations of porcine pancreatic elastase (henceforth elastase) and LPS. While ST2-deficient and $Cpa3^{Cre/+}$ mice had a defective inflammatory response, both strains developed COPD-like impaired pulmonary function. In addition, analysis of precision-cut lung slices (PCLS) revealed that MCs were dispensable for the development of airway hyperresponsiveness (AHR) in elastase/LPS-induced COPD-like disease.

MATERIALS AND METHODS

Mice

$Cpa3^{Cre/+}$ (24) and $ST2^{-/-}$ (25) mice on Balb/c background were originally provided by Hans-Reimer Rodewald and Andrew McKenzie, respectively. These strains and Balb/c JBomTac mice were bred and maintained at the Swedish National Veterinary Institute (Uppsala). All experiments were performed in age- and weight-matched female mice, and conducted in accordance with the ethical permit approved by the Uppsala animal ethics committee (5.8.18-05248/2018).

Elastase-Dependent COPD Models

Mice (8 ± 1 weeks old, 20 ± 1 g) received porcine pancreatic elastase (1.2 U in 50 µl phosphate buffer saline [PBS] i.n.) on day 1 and LPS from *Escherichia coli* O26:B6 (7 µg in 50 µl PBS i.n., both from Sigma-Aldrich) on day 4 for four consecutive weeks as shown in **Figure 1A**. Control mice received the same volume of PBS on the indicated days. All administrations were performed under isoflurane anesthesia, and pulmonary function, airway inflammation, emphysema development and AHR were evaluated 1, 4 or 7 days after the final LPS administration. Alternatively, mice received a single dose of elastase (1.2 U in 50 µl PBS i.n.) or PBS (50 µl i.n.) as shown in **Supplementary Figure 2A**, and pulmonary function was evaluated 21 days later.

Pulmonary Function Testing

Mice were anesthetized (100 mg/kg ketamine, 20 mg/kg xylazine, and 3 mg/kg acepromazine i.p.), tracheotomized, and connected to a Buxco pulmonary function test system (Data Sciences International; DSI). Because pulmonary function measurements are influenced by size (26), only weight-matched mice were compared. We report the average of 3 consecutive measurements for each parameter evaluated.

Flow Cytometry

To assess airway inflammation by flow cytometry, mice were euthanized and BALF obtained by flushing and aspiration of 1 ml of PBS through a tracheal cannula. Lungs were perfused through the right ventricle (PBS, 10 ml), excised, cut in small pieces, and digested on a gentle MACS Octo Dissociator using a mouse lung digestion kit (both from Miltenyi Biotec). Undigested debris was removed from the lung cell suspension *via* 44% Percoll (Sigma-Aldrich) centrifugation (400 g, 20 min). For residual red blood cell elimination, lung cells were incubated in lysis buffer (1 min; 150 mM NH_4Cl, 9.5 mM $NaHCO_3$, 1.2 mM EDTA) on ice before extensive washing. Isolated BALF and lung cells were counted in a hemocytometer using trypan-blue exclusion and stained with the antibodies listed in **Supplementary Table 1**. Alveolar macrophages ($CD45^+$ Siglec-F^+ $CD11c^+$), eosinophils ($CD45^+$ Siglec-F^+ $CD11c^-$), neutrophils ($CD45^+$ Siglec-$F^{-/lo}$ $CD11c^{-/lo}$ $CD11b^+$ $Ly6G^+$), and $CD4^+$ ($CD45^+$ Siglec-$F^{-/lo}$ $CD11c^{-/lo}$ $CD11b^{-/lo}$ $Ly6G^{-/lo}$ $CD3^+$ $CD4^+$) and $CD8^+$ ($CD45^+$ Siglec-$F^{-/lo}$ $CD11c^{-/lo}$ $CD11b^{-/lo}$ $Ly6G^{-/lo}$ $CD3^+$ $CD8^+$) T cells were identified in BALF as shown in **Supplementary Figure 1**. Mature MCs ($CD45^+$ lineage [Lin]$^-$ c-kit^{hi} $ST2^+$ $Fc\varepsilon RI^+$ $CD16/32^+$ Integrin $\beta7^{lo}$) and MC progenitors ($CD45^+$ Lin^- c-kit^{hi} $ST2^+$ $Fc\varepsilon RI^+$ $CD16/32^+$ Integrin $\beta7^{hi}$) were identified in lung tissue as shown in **Supplementary Figures 3, 4**. Lin was defined as: $B220^+$ $CD3^+$ $CD4^+$ $CD8b^+$ Gr-1^+ TER-119^+ $CD11b^+$. Basophils ($CD45^+$ Lin^- c-kit^- $Fc\varepsilon RI^+$ $CD49b^+$) were identified in lung tissue as shown in **Supplementary Figure 4**. Gating of $Fc\varepsilon RI^+$ and $ST2^+$ cells were set using fluorophore-matched isotype controls. Flow cytometry was performed on a LSRFortessa™, and data was analysed using FlowJo™ (both from BD Biosciences).

Histology

To qualitatively assess emphysema development, mice were euthanized, and their lungs filled manually using a 2 ml syringe (1.5 ml optimal cutting temperature [OCT] compound). After fixation (4% PFA in PBS), they were cryoprotected (20% sucrose in PBS), and embedded in OCT compound. Cryosections (8 µm) were stained with hematoxylin and eosin (H&E) and imaged with a Nikon Eclipse 90i Upright microscope (Nikon Instruments).

Preparation of PCLS and AHR Determination

PCLS were prepared as described previously (27). In brief, mice were euthanized, tracheotomized, and their lungs filled with pre-warmed (37°C) low-melting point agarose (4% w/v in PBS; SeaPrep). Whole mice were immersed on ice until agarose solidified, and PCLS (200 µm) were prepared from the left lobe using a vibratome (VT1000 S; Leica Biosystems). Individual PCLS were incubated (37°C, 5% CO_2) in 1 ml of MEM without phenol red (Gibco), and media was changed every 30 min for the first 2 h, and every h for the next 2 h to remove agarose. Following overnight incubation (37 °C, 5% CO_2) in 1 ml of RPMI-1640 without FCS (Sigma-Aldrich), individual PCLS were placed in 2 ml MEM and immobilized using a nylon thread attached to a platinum rod. Bronchioles surrounded by a smooth muscle layer (observed as a grey shadow) were time lapse-imaged every 10 s with a Nikon Eclipse Ti2-E inverted microscope. The first min was used as baseline, and the contraction in response to methacholine (100 µM), and subsequently to KCl (60 mM) was recorded for 3 min each. Bronchioles that failed to respond to at least one of these reagents were considered dead and excluded from the final analysis. Bronchial lumen area for each image was calculated using FIJI/ImageJ and changes in lumen area were expressed as fold decrease from baseline. Bronchioles were divided according to their lumen area at baseline into three groups: small (< 5000 μm^2), medium (5000-15000 μm^2), and large (15000-40000 μm^2), and comparisons were performed among similar-sized bronchioles.

Statistical Analysis

Multiple comparisons were performed by one-way ANOVA followed by Dunnett's *post hoc* test. Comparisons between two groups were done by two-tailed unpaired Student's t-test or Mann-Whitney U test (for values that were not normally distributed). All analyses were carried out in GraphPad Prism 9.1.

RESULTS

Elastase/LPS-Treated Mice Develop COPD-Like Airway Inflammation and Reduced Pulmonary Function

To induce COPD-like disease, weight- and age-matched female mice received alternating intranasal administrations of elastase and LPS for four weeks (**Figure 1A**). Mice subjected to this model developed larger lung volumes (increased TLC), higher C_{dyn}, and decreased expiratory capacity (lower FEV_{100}/FVC) than the control mice, which only received PBS (**Figures 1B–D**). This impaired pulmonary function was apparent one day after

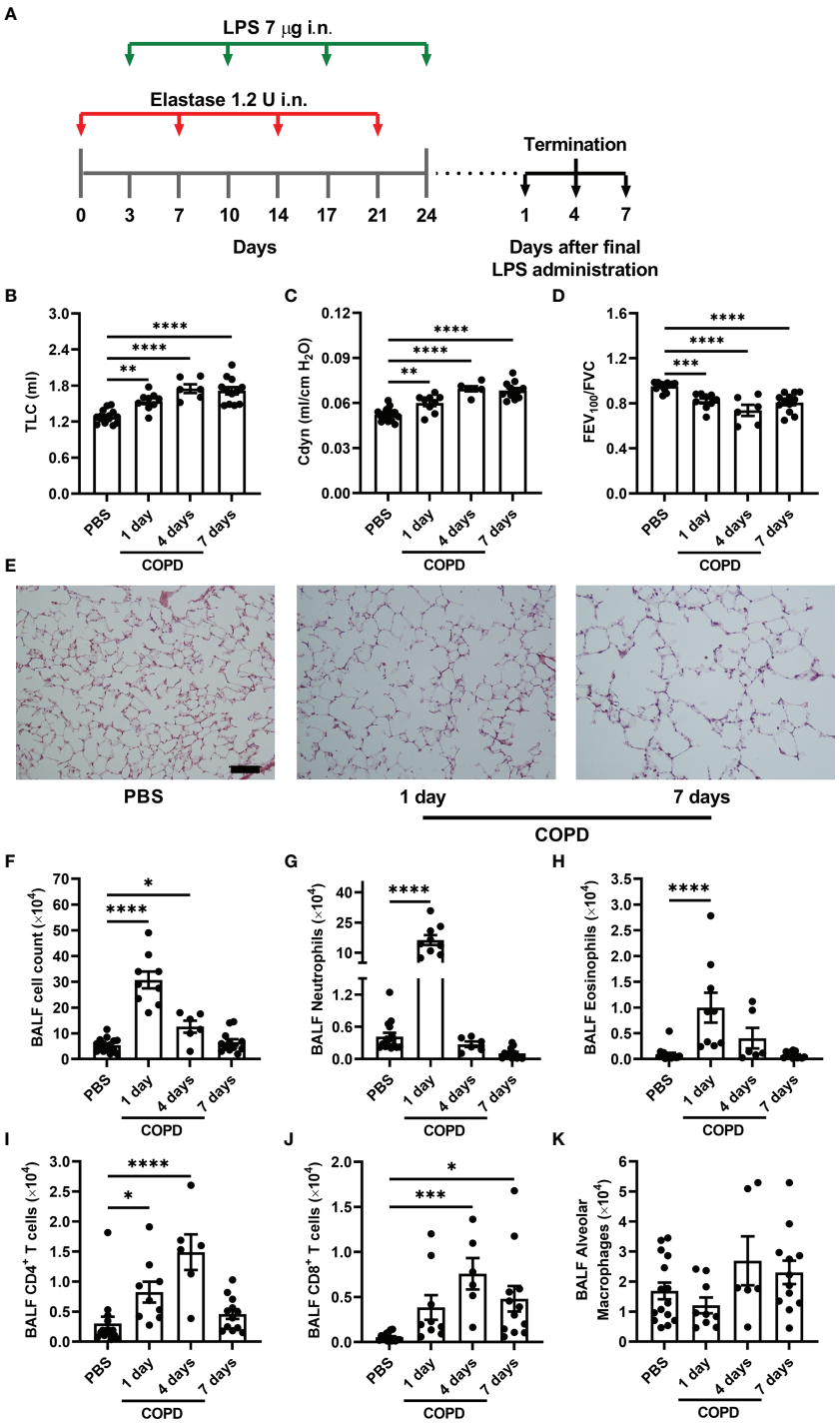


FIGURE 1 | Elastase/LPS instillation causes COPD-like impaired lung function, emphysema, and airway inflammation. **(A)** Wildtype Balb/c mice received alternating intranasal (i.n.) administrations of elastase and LPS for four weeks, and were analyzed one, four or seven days after the final LPS administration. Control mice received PBS instead. **(B)** TLC **(C)** Cdyn, **(D)** FEV_{100}/FVC were measured *in vivo*. **(E)** Representative H&E-stained lung sections selected to visualize emphysema development. Scale bar = 200 μm. **(F)** Total cells, **(G)** neutrophils, **(H)** eosinophils, **(I)** $CD4^+$ T cells, **(J)** $CD8^+$ T cells, and **(K)** alveolar macrophages were quantified in BALF. Data were obtained from 6-15 mice per group pooled from 2-3 individual experiments and shown as means ± SEM. Statistical significance was tested by one-way ANOVA followed by Dunnett's *post hoc* test to compare each group against the control. *p < 0.05, **p < 0.005, ***p < 0.0005, ****p < 0.0001.

the final LPS administration, worsened over the next days, and was accompanied by histological evidence of alveolar enlargement (i.e. emphysema) (**Figure 1E**).

To characterize the inflammatory populations associated with elastase/LPS-induced COPD-like disease, cells in BALF were analyzed by flow cytometry (**Supplementary Figure 1**). A major increase in inflammatory cells in BALF was found one day after the final LPS administration, which partly resolved over the following days (**Figure 1F**). The inflammatory cells in BALF consisted primarily of neutrophils, accompanied by a smaller increase in eosinophils, one day after the final LPS administration (**Figures 1G, H**). A small peak in the number of $CD4^+$ and $CD8^+$ T cells was found four days after the final LPS administration (**Figures 1I, J**). The elastase/LPS treatment did not significantly change the number of alveolar macrophages (**Figure 1K**). Altogether, our data suggest that the elastase/LPS model induces a transient inflammation that is not sustained.

The ST2 Receptor Plays a Minor Role in Elastase/LPS-Induced COPD-Like Airway Inflammation

Given that both clinical and animal studies have implicated the IL-33/ST2 axis in COPD, we hypothesized that the IL-33 receptor ST2 would play a role in elastase/LPS-induced COPD-like disease. However, when ST2-deficient mice ($ST2^{-/-}$) and their wildtype littermates ($ST2^{+/+}$) were subjected to this model, no differences were found between the pulmonary function outcomes (TLC, C_{dyn}, and FEV_{100}/FVC) of each group, neither at one nor at seven days after the final LPS administration (**Figures 2A–C**). Nevertheless, quantification of inflammatory cells in BALF revealed that ST2-deficient mice had fewer eosinophils (**Figure 2D**), $CD4^+$ T cells (**Figure 2E**), $CD8^+$ T cells (**Figure 2F**), and alveolar macrophages (**Figure 2G**) than $ST2^{+/+}$ mice seven days after the final LPS administration. In contrast, ST2 deficient mice had similar neutrophil numbers and overall BALF cell count as their wildtype littermates (**Figures 2H, I**).

Recently, Morichika et al. used a less severe model of COPD (a single dose of elastase) to show that IL-33-deficiency enhanced emphysema development in mice (10). We adopted this model, and evaluated pulmonary function 21 days later (**Supplementary Figure 2A**). Elastase alone did not induce increased TLC (**Supplementary Figure 2B**) but caused slightly higher C_{dyn} (**Supplementary Figure 2C**) and decreased FEV_{100}/FVC (**Supplementary Figure 2D**). Still, $ST2^{-/-}$ and $ST2^{+/+}$ mice developed similar C_{dyn} and FEV_{100}/FVC after a single dose of elastase (**Supplementary Figures 2E, F**). To summarize, our data suggest that the ST2 receptor is redundant for the development of elastase- and elastase/LPS-induced COPD-like impaired pulmonary function. Nonetheless, the ST2 receptor is required for an intact elastase/LPS-induced airway inflammation.

Elastase/LPS-Treated $Cpa3^{Cre/+}$ Mice Have Fewer Alveolar Macrophages

We have previously shown that viral and allergic airway inflammation induce the recruitment of MC progenitors to the lung, which precedes the accumulation of lung MCs (28–30). To determine whether MCs and their progenitors accumulate in elastase/LPS-induced COPD-like disease, cells from dissociated lung tissue were analyzed by flow cytometry (**Supplementary Figure 3**). Elastase/LPS-treated mice had increased total cell numbers in lung tissue one and seven days after the final LPS administration (**Figure 3A**). Although the number of mature MCs did not change, there was a transient 2-fold increase in MC progenitors one day after the final LPS administration that was lost over time (**Figures 3B, C**).

To investigate whether MCs play a crucial role in elastase/LPS-induced COPD-like disease, $Cpa3^{Cre/+}$ mice, which lack mature MCs due to the carboxypeptidase A3 (Cpa3)-dependent genotoxic overexpression of Cre recombinase (24), were used to model MC deficiency. Using flow cytometry (**Supplementary Figure 4**), we confirmed that $Cpa3^{Cre/+}$ mice with COPD-like disease lacked mature MCs in the lung (**Figure 4A**). However, they had equal numbers of lung MC progenitors as their wildtype littermates (**Figure 4B**). Similar to what was previously reported in naïve and other disease models (24, 27, 31), $Cpa3^{Cre/+}$ mice with COPD-like disease had a 73% reduction in basophil numbers at both time points (**Figure 4C**). $Cpa3^{Cre/+}$ and $Cpa3^{+/+}$ mice developed similar impaired pulmonary function after elastase/LPS treatments (**Figures 4D–F**). Still, $Cpa3^{Cre/+}$ mice had a reduction in total BALF cell count seven days after the final LPS administration (**Figure 4G**), which was at least partly due to a decrease in the number of alveolar macrophages (**Figure 4H**). Nonetheless, BALF neutrophil, eosinophil and T cell numbers were similar in $Cpa3^{Cre/+}$ and $Cpa3^{+/+}$ mice with COPD-like disease (**Figures 4I–L**).

Recently, Shibata et al. showed that emphysema development required basophil-derived IL-4 in a single dose of elastase model (32). In our study, $Cpa3^{Cre/+}$ mice were not protected from developing impaired pulmonary function caused by a single dose of elastase (**Supplementary Figures 5A, B**). To conclude, $Cpa3^{Cre/+}$ mice developed unimpaired elastase- and elastase/LPS-induced COPD-like reduced pulmonary function, but had a reduced inflammatory response following elastase/LPS-instillation.

Elastase/LPS-Treated Mice Develop AHR Independently of MCs

AHR affects one in four patients with mild-to-moderate COPD and is a good indicator of disease progression and mortality (33). To determine whether mice with elastase/LPS-induced COPD-like disease develop AHR, methacholine-induced bronchiole contraction in PCLS was evaluated *ex vivo* seven days after the final LPS administration. Large bronchioles (PBS: 22685 ± 1223 μm^2, COPD: 24707 ± 1822 μm^2 lumen area at baseline) from elastase/LPS-treated mice showed stronger contraction (33% ± 0.05 average maximum reduction in airway lumen area from baseline) than those from PBS control mice (**Figures 5A–C**). No differences in contraction in response to methacholine were found when analyzing small- and medium-sized bronchioles (**Supplementary Figure 6**). To test whether MCs contributed

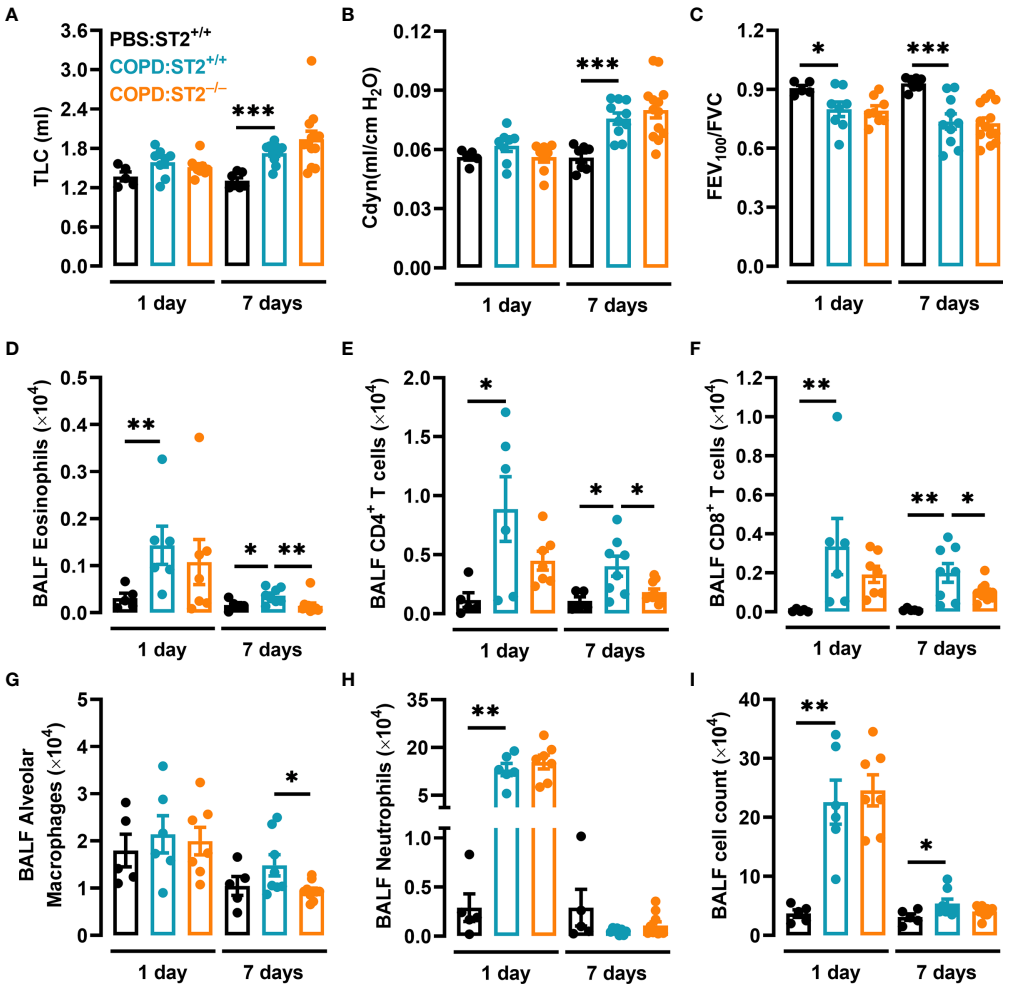


FIGURE 2 | The ST2 receptor is redundant for the development of COPD-like reduced pulmonary function but required for the induction of an intact inflammatory response. $ST2^{+/+}$ and $ST2^{-/-}$ mice were subjected to elastase/LPS-induced COPD-like disease and analyzed one and seven days after the final LPS administration. Control mice received PBS instead. **(A)** TLC, **(B)** Cdyn, and **(C)** FEV_{100}/FVC were assessed *in vivo*. **(D)** Eosinophils, **(E)** $CD4^+$ T cells, **(F)** $CD8^+$ T cells, **(G)** alveolar macrophages, **(H)** neutrophils, and **(I)** total cells were quantified in BALF. For the 1-day time point, data were obtained in **(A-C)** from 5-8 mice per group pooled from 5 individual experiments, and in **(D-I)** from 5-7 mice per group pooled from 4 individual experiments. For the 7-day time point, data were obtained in **(A-C)** from 7-13 mice per group pooled from 5 individual experiments, and in **(D-I)** from 8-10 mice per group pooled from 4 individual experiments. Data is shown as means ± SEM. Statistical significance was tested by Mann-Whitney U test. *$p < 0.05$, **$p < 0.005$, ***$p < 0.0005$.

to AHR in this model, large bronchioles from elastase/LPS-treated $Cpa3^{+/+}$ (22231 ± 1223 μm^2) and $Cpa3^{Cre/+}$ (21850 ± 1350 μm^2) mice were analyzed. However, they showed a similar contraction pattern in response to methacholine (**Figures 5D, E**).

DISCUSSION

The pathological mechanisms behind COPD development are still under investigation. Due to ethical reasons, experimental research on COPD requires animal models. While cigarette smoke-based models are relevant to the human disease, induction of COPD-like disease in mice requires daily cigarette smoke exposure for up to six months, and results in mild non-progressive disease (9). Elastase-instillation, on the other hand, causes severe and progressive emphysema in mice in less than one month (9). By exposing mice to repeated intranasal instillations of elastase and LPS for four weeks, Sajjan et al. established a model in which C57BL/6 mice developed COPD-like airway inflammation and impaired pulmonary function (as determined by a Flexivent system) seven days after the final LPS administration (34). As elastase (10) or LPS alone can induce IL-33 expression in macrophages and epithelial cells (35, 36), we thought that the elastase/LPS model would be relevant to study mechanisms of COPD in mice. In our study, Balb/c mice subjected to the elastase/LPS model developed alveolar enlargement. However, the histological assessment of alveolar enlargement was not quantified and represents a limitation of our study. Instead, emphysema development was quantified by pulmonary function testing, which detected impaired

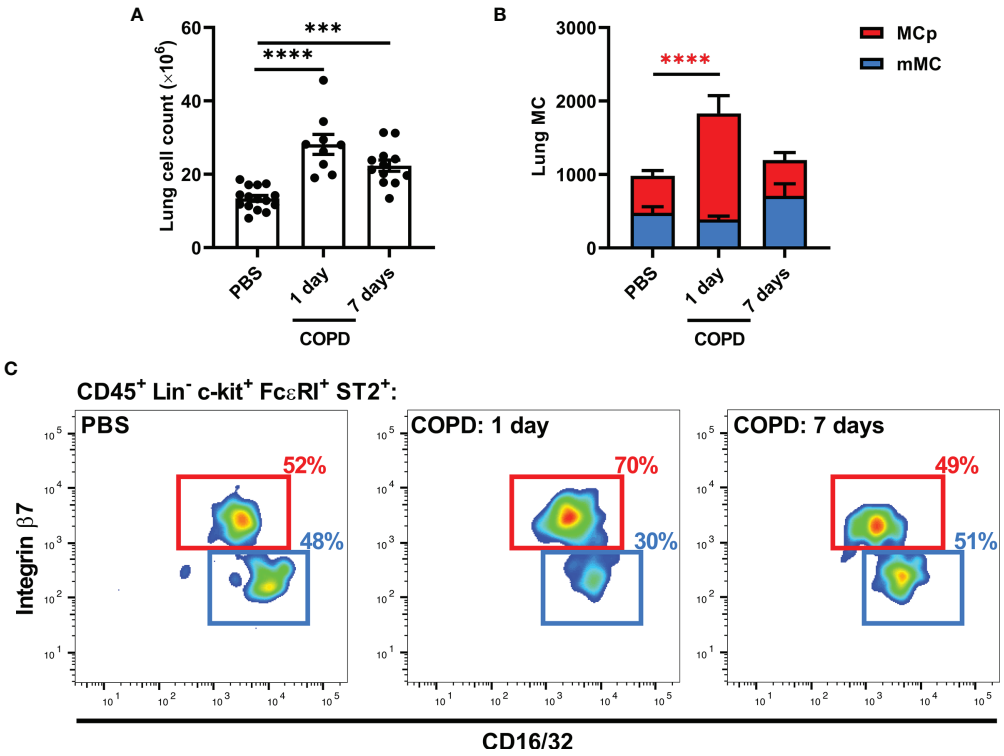


FIGURE 3 | Elastase/LPS instillation induces an increase in lung MC progenitors. **(A-C)** Wildtype Balb/c mice were subjected to elastase/LPS-induced COPD-like disease and analyzed one or seven days after the final LPS administration. **(A)** Total lung cells and **(B)** lung MCs [mature MCs (mMC) and MC progenitors (MCp)] were quantified in lung. **(C)** Representative pseudo-color plots showing the final gates for MCp and mMC, which express different levels of CD16/32 and integrin β7. Data in **(A, B)** were obtained from 9-15 mice per group pooled from 2-3 individual experiments. Data are shown as means ± SEM. Statistical significance was tested in **(A, B)** by one-way ANOVA followed by Dunnett's *post hoc* test to compare each group against the control. ***$p < 0.0005$, ****$p < 0.0001$.

spirometry-like measurements as early as one day after the final LPS administration. Moreover, we confirmed that the elastase/LPS protocol induced mild airway inflammation, with a peak in total BALF cells one day after the last LPS administration, which consisted primarily of neutrophils, followed by a later increase in $CD4^+/CD8^+$ T cells and a gradual decline in total BALF cell numbers.

The IL-33/ST2 axis has been implicated in COPD, and exposure to cigarette smoke or elastase instillation upregulate IL-33 and ST2 in mice (5, 10, 37). However, we did not find a role for the ST2 receptor in the decline in pulmonary function caused by elastase/LPS treatment, nor 21 days after a single elastase instillation. In contrast, IL-33-deficient mice had enhanced static compliance and alveolar enlargement 21 days after a single elastase administration (10). But Morichika et al. also found that antibody-blocking of ST2 could not replicate the increased compliance observed in elastase-treated IL-33-deficient mice (10). Thus, IL-33 may have effects in this setting that are not mediated by the canonical IL-33 receptor ST2.

ST2-deficient mice have impaired type 2 responses, produce less type 2 cytokines (e.g. IL-4 and IL-5) (25), and absence of the ST2 receptor has been shown to impact eosinophil, macrophage, and $CD4^+$ and $CD8^+$ T cell differentiation (38–41). In agreement with these and other studies that position the IL-33/ST2 axis as key player for the induction of airway inflammation across various settings, ST2-deficient mice subjected to elastase/LPS administrations had fewer BALF eosinophils, alveolar macrophages, and $CD4^+$ and $CD8^+$ T cells than their wildtype littermates. We speculate that the decline in pulmonary function observed in the elastase/LPS model is largely due to the direct action of elastase alone, and that the mild airway inflammation associated with this model had little impact on pulmonary function. This could potentially explain why the reduced airway inflammation in ST2-deficient mice after elastase/LPS treatment did not lead to an improved pulmonary function. Alternatively, the method used to measure pulmonary function may not be sensitive enough to pick up small differences.

MCs express ST2, and are activated by IL-33 to produce a wide array of mediators that could potentially participate in COPD pathophysiology (42). However, $Cpa3^{Cre/+}$ mice, which lack MCs and have a partial reduction in basophils, developed a similar decline in pulmonary function as their wildtype littermates after elastase alone, or elastase/LPS treatment. Interestingly, Shibata et al. found that diphtheria toxin-injected $Mcpt8^{DTR}$ mice, which have a complete lack of basophils, developed significantly less elastase-induced emphysema (32). This discrepancy can have (at least) two explanations: 1) MCs are redundant for the development of elastase- and elastase/LPS-

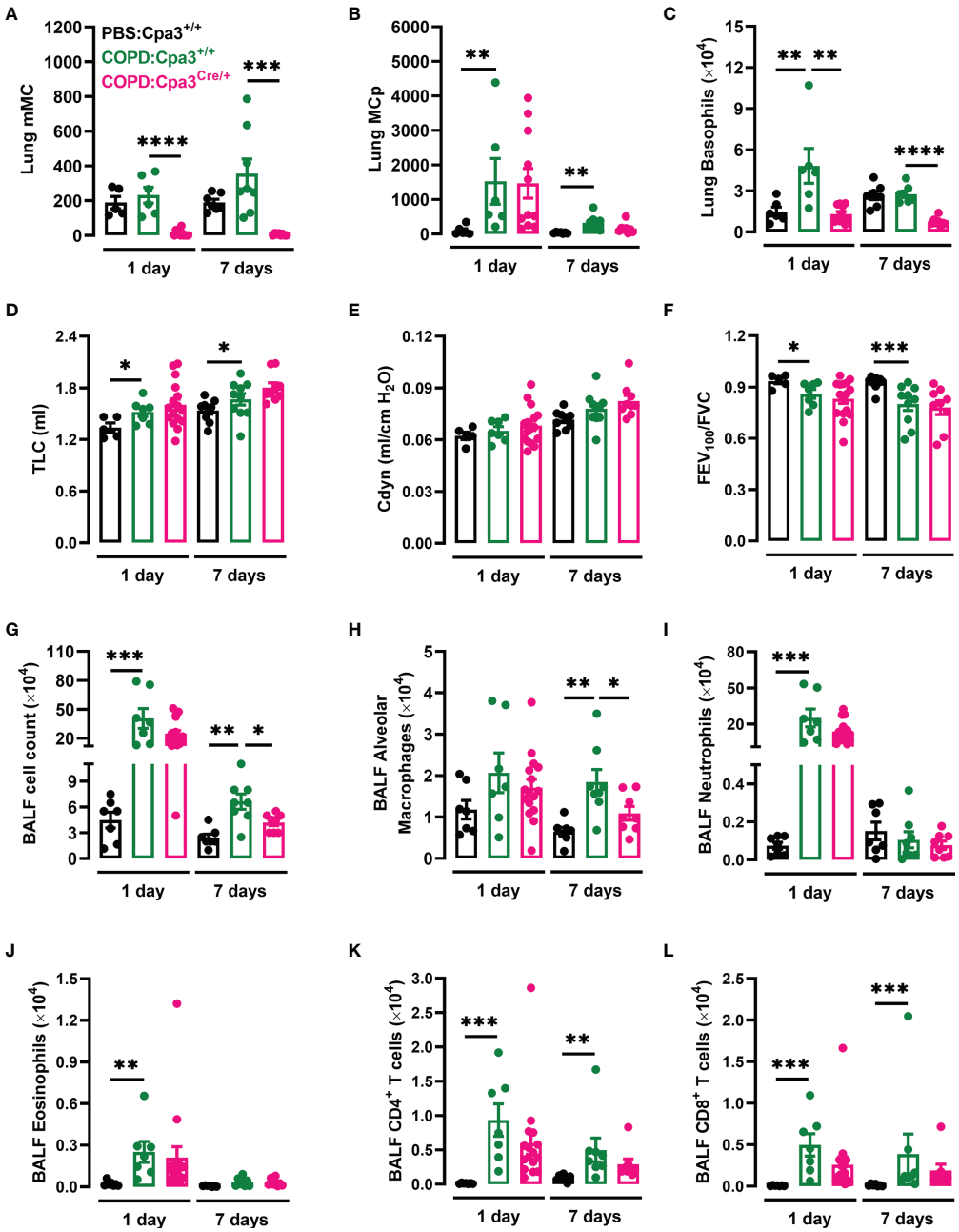


FIGURE 4 | Cpa3$^{Cre/+}$ mice have a defective inflammatory response upon elastase/LPS treatment. Cpa3$^{+/+}$ and Cpa3$^{Cre/+}$ mice were subjected to elastase/LPS-induced COPD-like disease and analyzed one or seven days after the final LPS administration. Control mice received PBS instead. **(A)** Mature MCs (mMC), **(B)** MC progenitors (MCp), and **(C)** basophils were quantified in lung. **(D)** TLC **(E)** Cdyn, and **(F)** FEV_{100}/FVC were determined *in vivo*. **(G)** Total cells, **(H)** alveolar macrophages, **(I)** neutrophils, **(J)** eosinophils, **(K)** CD4$^+$ T cells, and **(L)** CD8$^+$ T cells were quantified in BALF. For the 1-day time point, data in **(A–C)** were obtained from 6-11 mice per group pooled from 3 individual experiments, and in **(D–L)** from 7-16 mice per group pooled from 4 individual experiments. For the 7-day time point, data in **(A–C, G–L)** were obtained from 8 mice per group pooled from 4 individual experiments, and in **(D-F)** from 9-10 mice per group pooled from 5 individual experiments. Statistical significance was tested by Mann-Whitney U test. *p < 0.05, **p < 0.005, ***p < 0.0005, ****p < 0.0001.

induced COPD-like emphysema and the partial reduction in basophils observed in Cpa3$^{Cre/+}$ mice is not enough to recapitulate the findings of Shibata and colleagues, or 2) the absence of MCs in Cpa3$^{Cre/+}$ mice is pathological and compensates for the protection granted by having fewer basophils. On the other hand, Mcpt8 gene expression is not completely restricted to basophils. El Hachem et al. identified Mcpt8 expression in granulocyte-monocyte progenitors, which

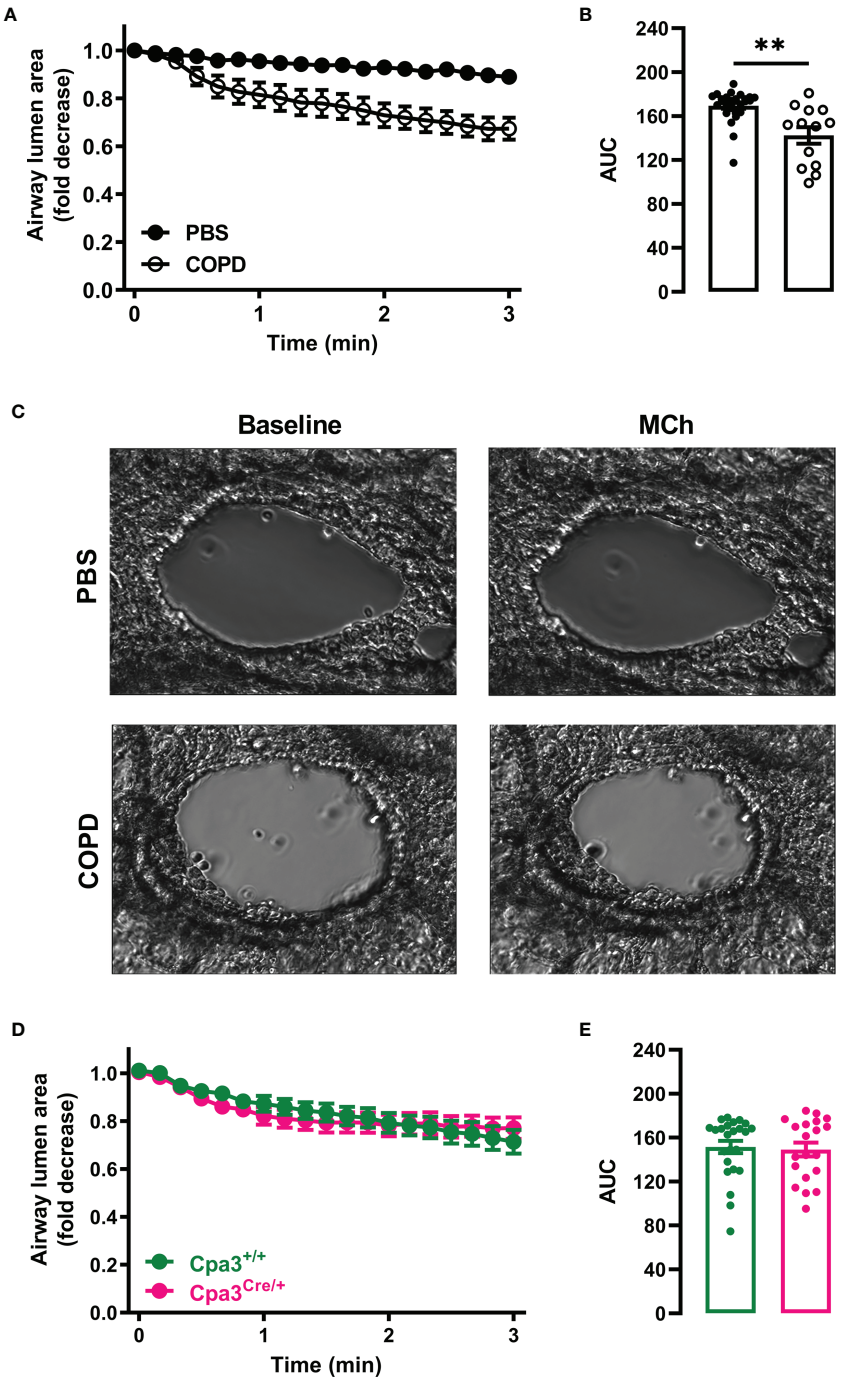


FIGURE 5 | Elastase/LPS instillation causes AHR in large bronchioles independently of MCs. PCLS were obtained from **(A–C)** wildtype Balb/c and **(D, E)** $Cpa3^{+/+}$ and $Cpa3^{Cre/+}$ mice with elastase/LPS-induced COPD-like disease seven days after the final LPS (or PBS) administration. Time-lapse images of individual bronchioles were recorded every 10 s for 1 min before challenge with methacholine (MCh) and recorded for 3 more min. **(A, D)** Airway narrowing after MCh challenge determined as fold decrease from baseline. **(B, E)** Area under the curve (AUC) was calculated for each individual bronchiole. **(C)** Representative images of lung bronchioles before and after MCh challenge. Data in **(A, B, D, E)** are shown as means ± SEM from **(A, B)** 13-27 PCLS per group obtained from 5 PBS and 5 COPD mice pooled from four individual experiments, and **(D, E)** 20-24 PCLS per group obtained from 4 $Cpa3^{+/+}$ and 3 $Cpa3^{Cre/+}$ mice pooled from three individual experiments. Statistical significance in **(B, E)** was tested by unpaired Student's t-test. ** $p < 0.005$.

caused depletion of additional cell lineages such as eosinophils and neutrophils in diphtheria toxin-treated Mcpt8^{DTR} mice (43). Furthermore, Mcpt8-driven Cre-mediated recombination was also detected in <25% of peritoneal MCs, and <10% of other cell lineages in Basoph8 x iDTR mice (44). Future research is needed to dissect the specific contributions of MCs and basophils in COPD.

Since MCs play a major role in AHR in house dust mite-induced allergic airway inflammation (27), we determined whether they could also play a role in AHR in elastase/LPS-induced COPD-like disease. Previously, Van Dijk et al. demonstrated that incubating PCLS from naïve mice with elastase caused AHR *in vitro* (45). In our study, PCLS prepared from mice with elastase/LPS-induced COPD-like disease had increased contraction in response to methacholine *ex vivo* when large bronchioles were assessed. However, Cpa3$^{Cre/+}$ mice developed AHR to methacholine to a similar degree as their wild type littermates. Of note, the average maximum contraction of these bronchioles (33 ± 0.05%) was approximately half of the contraction observed in PCLS from mice with house dust mite-induced allergic airway inflammation (57 ± 5%) (27). It is possible that the mild AHR observed *ex vivo* in PCLS from elastase/LPS-treated mice could explain why Sajjan et al. were unable to detect AHR *in vivo* after elastase/LPS instillation (34). Alternatively, the difference in AHR induction could be due to the use of different mouse strains.

MCs accumulate in the airway smooth muscle of patients with centrilobular emphysema, and those with higher MC number at this location also had increased AHR (21). Other studies found changes in MC distribution and phenotype, and higher sputum tryptase levels that were associated with increased COPD severity (19, 20). In mouse models of allergic airway inflammation, MCs accumulate due to the recruitment and expansion of MC progenitors, which is required for full-blown AHR (27). However, in the current study, elastase/LPS instillation induced only a small increase in MC progenitors, which was not sustained and did not give rise to an increase in mature MCs in the lung. Furthermore, the levels of the MC-specific protease mMCP-1 and trypsin-like activity (as a surrogate marker of MC tryptase) in BALF were similar in mice with elastase/LPS-induced COPD-like disease and PBS controls (results not shown). To conclude, although our data suggest that MCs are dispensable for the development of AHR and COPD-like reduced pulmonary function in elastase/LPS-treated mice, the model failed to recapitulate the MC-related changes that occur in COPD patients. Thus, further studies are needed to find even better mouse models of COPD.

Alveolar macrophages are thought to play a pivotal role in COPD, and disease progression is associated with an increase in macrophages (46). We found that the number of alveolar macrophages in BALF was reduced after elastase/LPS instillation in Cpa3$^{Cre/+}$ mice. This is in line with studies of mice lacking the MC-specific mediators mMCP-6 or Prss31, which had fewer neutrophils and macrophages in BALF following exposure to cigarette smoke (17, 18). Together, these data suggest that MCs promote expansion of alveolar macrophages in COPD-like disease. Mechanistically, this is in line with a recent publication demonstrating that MCs activated *via* IL-33/ST2 release macrophage-attracting factors, including GM-CSF (CSF2), which promote tumor-associated macrophages responsible for tumor cell proliferation and angiogenesis in a preclinical model of gastric cancer (47). Given that GM-CSF is required for the development of monocyte-derived alveolar macrophages (48), we speculate that the decreased alveolar macrophage numbers in Cpa3$^{Cre/+}$ and ST2$^{-/-}$ mice with COPD-like disease may be explained by a loss of ST2-mediated MC release of such factors. However, as basophils are also reduced in Cpa3$^{Cre/+}$ mice, we cannot exclude the involvement of basophils in the induction of alveolar macrophages.

A limitation of our study is that the experiments were performed exclusively in female mice. Male mice (and their airways) grow faster than females, which has challenging consequences. First, it is difficult to breed enough weigh-matched males to start an experiment, and secondly, they continue to grow differently during the experiment, resulting in mice with unequal size at the end of the experiment. Given that differences in size/weight impact lung function outcomes (26), we decided to use female mice for our study. Future research should evaluate potential sex differences.

To conclude, repeated elastase/LPS instillation caused COPD-like impaired pulmonary function, emphysema, and mild AHR in ST2-deficient, Cpa3$^{Cre/+}$, and their wildtype littermates. However, ST2$^{-/-}$ and Cpa3$^{Cre/+}$ mice had a defective inflammatory response in this model, especially regarding alveolar macrophages, which were reduced in both strains. Given that MCs become activated and release pro-inflammatory mediators in response to ST2 stimulation, it seems possible that MCs stimulated *via* IL-33/ST2 contribute to the expansion of alveolar macrophages that occurs in COPD patients. To the best of our knowledge, this is the first time that the roles of MCs and the ST2 receptor were investigated in a mouse model of elastase/LPS-induced COPD-like disease. Our results complement previous findings in cigarette smoke-induced COPD models, and highlight the need for better mouse models.

DATA AVAILABILITY STATEMENT

The original contributions presented in the study are included in the article/**Supplementary Material**. Further inquiries can be directed to the corresponding author.

ETHICS STATEMENT

The animal study was reviewed and approved by Uppsala animal ethics committee (5.8.18-05248/2018).

AUTHOR CONTRIBUTIONS

EC and JH designed the project. EC performed all *in vivo* experiments, lung function analyses, and flow cytometry. PA-V performed the histological analysis. EM-E performed the tryptase assay and supervised the set-up of precision cut lung slice-experiments. ED helped with some of the initial experiments as part of his master degree project. EC analyzed and compiled the collected data, and performed the statistical analyses. JH interpreted and supervised the data and statistical analyses. EC and JH wrote the paper. All authors read, contributed to and approved the final manuscript.

FUNDING

The present study was funded by grants to JH by the Swedish Research Council, Swedish Heart-Lung Foundation, Knut and Alice Wallenberg Foundation, Agnes and Mac Rudberg Foundation, Malin and Lennart Philipson Foundation, Apotekare Hedberg Foundation, Konsul ThC Bergh Foundation, Mats Kleberg Foundation, and Axel and Signe Lagerman Foundation; and to EIC by the Gustaf Adolf Johansson Foundation, Agnes and Mac Rudberg Foundation, and P. O. Zetterling Foundation.

ACKNOWLEDGMENTS

We thank Thorsten Feyerabend and Hans-Reimer Rodewald, as well as Andrew McKenzie, for kindly providing the Cpa3$^{Cre/+}$ and ST2 (Il1rl1)-deficient mice, respectively. Flow cytometry was performed at BioVis, Uppsala University.

SUPPLEMENTARY MATERIAL

The Supplementary Material for this article can be found online at: https://www.frontiersin.org/articles/10.3389/fimmu.2022.830859/full#supplementary-material

REFERENCES

1. Adeloye D, Chua S, Lee C, Basquill C, Papana A, Theodoratou E, et al. Global and Regional Estimates of COPD Prevalence: Systematic Review and Meta-Analysis. *J Glob Health* (2015) 5(2):20415. doi: 10.7189/jogh.05-020415
2. World Health Organization. *The Top 10 Causes of Death* (2019). Available at: https://www.who.int/news-room/fact-sheets/detail/the-top-10-causes-of-death.
3. Barnes PJ. Inflammatory Mechanisms in Patients With Chronic Obstructive Pulmonary Disease. *J Allergy Clin Immunol* (2016) 138(1):16–27. doi: 10.1016/j.jaci.2016.05.011
4. Donovan C, Hansbro PM. IL-33 in Chronic Respiratory Disease: From Preclinical to Clinical Studies. *ACS Pharmacol Transl Sci* (2020) 3(1):56–62. doi: 10.1021/acsptsci.9b00099
5. Kearley J, Silver JS, Sanden C, Liu Z, Berlin AA, White N, et al. Cigarette Smoke Silences Innate Lymphoid Cell Function and Facilitates an Exacerbated Type I Interleukin-33-Dependent Response to Infection. *Immunity* (2015) 42(3):566–79. doi: 10.1016/j.immuni.2015.02.011
6. Xia J, Zhao J, Shang J, Li M, Zeng Z, Zhao J, et al. Increased IL-33 Expression in Chronic Obstructive Pulmonary Disease. *Am J Physiol Lung Cell Mol Physiol* (2015) 308(7):L619–27. doi: 10.1152/ajplung.00305.2014
7. Kim SW, Rhee CK, Kim KU, Lee SH, Hwang HG, Kim YI, et al. Factors Associated With Plasma IL-33 Levels in Patients With Chronic Obstructive Pulmonary Disease. *Int J Chron Obstruct Pulmon Dis* (2017) 12:395–402. doi: 10.2147/COPD.S120445
8. Sun BB, Ma LJ, Qi Y, Zhang GJ. Correlation of IL-33 Gene Polymorphism With Chronic Obstructive Pulmonary Disease. *Eur Rev Med Pharmacol Sci* (2019) 23(14):6277–82. doi: 10.26355/eurrev_201907_18449
9. Wright JL, Cosio M, Churg A. Animal Models of Chronic Obstructive Pulmonary Disease. *Am J Physiol Lung Cell Mol Physiol* (2008) 295(1):L1–15. doi: 10.1152/ajplung.90200.2008
10. Morichika D, Taniguchi A, Oda N, Fujii U, Senoo S, Itano J, et al. Loss of IL-33 Enhances Elastase-Induced and Cigarette Smoke Extract-Induced Emphysema in Mice. *Respir Res* (2021) 22(1):150. doi: 10.1186/s12931-021-01705-z
11. Allakhverdi Z, Smith DE, Comeau MR, Delespesse G. Cutting Edge: The ST2 Ligand IL-33 Potently Activates and Drives Maturation of Human Mast Cells. *J Immunol* (2007) 179(4):2051–4. doi: 10.4049/jimmunol.179.4.2051
12. Komai-Koma M, Brombacher F, Pushparaj PN, Arendse B, McSharry C, Alexander J, et al. Interleukin-33 Amplifies IgE Synthesis and Triggers Mast Cell Degranulation *via* Interleukin-4 in Naive Mice. *Allergy* (2012) 67(9):1118–26. doi: 10.1111/j.1398-9995.2012.02859.x
13. Mendez-Enriquez E, Hallgren J. Mast Cells and Their Progenitors in Allergic Asthma. *Front Immunol* (2019) 10:821. doi: 10.3389/fimmu.2019.00821
14. Sjoberg LC, Gregory JA, Dahlen SE, Nilsson GP, Adner M. Interleukin-33 Exacerbates Allergic Bronchoconstriction in the Mice *via* Activation of Mast Cells. *Allergy* (2015) 70(5):514–21. doi: 10.1111/all.12590
15. Kaur D, Gomez E, Doe C, Berair R, Woodman L, Saunders R, et al. IL-33 Drives Airway Hyper-Responsiveness Through IL-13-Mediated Mast Cell: Airway Smooth Muscle Crosstalk. *Allergy* (2015) 70(5):556–67. doi: 10.1111/all.12593
16. Morita H, Arae K, Unno H, Miyauchi K, Toyama S, Nambu A, et al. An Interleukin-33-Mast Cell-Interleukin-2 Axis Suppresses Papain-Induced Allergic Inflammation by Promoting Regulatory T Cell Numbers. *Immunity* (2015) 43(1):175–86. doi: 10.1016/j.immuni.2015.06.021
17. Beckett EL, Stevens RL, Jarnicki AG, Kim RY, Hanish I, Hansbro NG, et al. A New Short-Term Mouse Model of Chronic Obstructive Pulmonary Disease Identifies a Role for Mast Cell Tryptase in Pathogenesis. *J Allergy Clin Immunol* (2013) 131(3):752–62. doi: 10.1016/j.jaci.2012.11.053
18. Hansbro PM, Hamilton MJ, Fricker M, Gellatly SL, Jarnicki AG, Zheng D, et al. Importance of Mast Cell Prss31/transmembrane Tryptase/Tryptase-Gamma in Lung Function and Experimental Chronic Obstructive Pulmonary Disease and Colitis. *J Biol Chem* (2014) 289(26):18214–27. doi: 10.1074/jbc.M114.548594
19. Andersson CK, Mori M, Bjermer L, Lofdahl CG, Erjefalt JS. Alterations in Lung Mast Cell Populations in Patients With Chronic Obstructive Pulmonary Disease. *Am J Respir Crit Care Med* (2010) 181(3):206–17. doi: 10.1164/rccm.200906-0932OC
20. Zhang X, Zheng H, Ma W, Wang F, Zeng X, Liu C, et al. Tryptase Enzyme Activity Is Correlated With Severity of Chronic Obstructive Pulmonary Disease. *Tohoku J Exp Med* (2011) 224(3):179–87. doi: 10.1620/tjem.224.179
21. Ballarin A, Bazzan E, Zenteno RH, Turato G, Baraldo S, Zanovello D, et al. Mast Cell Infiltration Discriminates Between Histopathological Phenotypes of Chronic Obstructive Pulmonary Disease. *Am J Respir Crit Care Med* (2012) 186(3):233–9. doi: 10.1164/rccm.201112-2142OC
22. Pesci A, Rossi GA, Bertorelli G, Aufiero A, Zanon P, Olivieri D. Mast Cells in the Airway Lumen and Bronchial Mucosa of Patients With Chronic Bronchitis. *Am J Respir Crit Care Med* (1994) 149(5):1311–6. doi: 10.1164/ajrccm.149.5.8173772
23. Kalenderian R, Raju L, Roth W, Schwartz LB, Gruber B, Janoff A. Elevated Histamine and Tryptase Levels in Smokers' Bronchoalveolar Lavage Fluid. Do

Lung Mast Cells Contribute to Smokers' Emphysema? *Chest* (1988) 94 (1):119–23. doi: 10.1378/chest.94.1.119
24. Feyerabend TB, Weiser A, Tietz A, Stassen M, Harris N, Kopf M, et al. Cre-Mediated Cell Ablation Contests Mast Cell Contribution in Models of Antibody- and T Cell-Mediated Autoimmunity. *Immunity* (2011) 35 (5):832–44. doi: 10.1016/j.immuni.2011.09.015
25. Townsend MJ, Fallon PG, Matthews DJ, Jolin HE, McKenzie AN. T1/ST2-Deficient Mice Demonstrate the Importance of T1/ST2 in Developing Primary T Helper Cell Type 2 Responses. *J Exp Med* (2000) 191(6):1069–76. doi: 10.1084/jem.191.6.1069
26. Alvarado-Vazquez PA, Mendez-Enriquez E, Hallgren J. Use of Spirometry-Like Measurements to Monitor House Dust Mite-Induced Experimental Asthma in Mice. *Allergy* (2021) 76(7):2204–7. doi: 10.1111/all.14681
27. Mendez-Enriquez E, Alvarado-Vazquez PA, Abma W, Simonson OE, Rodin S, Feyerabend TB, et al. Mast Cell-Derived Serotonin Enhances Methacholine-Induced Airway Hyperresponsiveness in House Dust Mite-Induced Experimental Asthma. *Allergy* (2021) 76(7):2057–69. doi: 10.1111/all.14748
28. Zarnegar B, Mendez-Enriquez E, Westin A, Soderberg C, Dahlin JS, Gronvik KO, et al. Influenza Infection in Mice Induces Accumulation of Lung Mast Cells Through the Recruitment and Maturation of Mast Cell Progenitors. *Front Immunol* (2017) 8:310. doi: 10.3389/fimmu.2017.00310
29. Zarnegar B, Westin A, Evangelidou S, Hallgren J. Innate Immunity Induces the Accumulation of Lung Mast Cells During Influenza Infection. *Front Immunol* (2018) 9:2288. doi: 10.3389/fimmu.2018.02288
30. Abonia JP, Hallgren J, Jones T, Shi T, Xu Y, Koni P, et al. Alpha-4 Integrins and VCAM-1, But Not MAdCAM-1, Are Essential for Recruitment of Mast Cell Progenitors to the Inflamed Lung. *Blood* (2006) 108(5):1588–94. doi: 10.1182/blood-2005-12-012781
31. Feyerabend TB, Gutierrez DA, Rodewald HR. Of Mouse Models of Mast Cell Deficiency and Metabolic Syndrome. *Cell Metab* (2016) 24(1):1–2. doi: 10.1016/j.cmet.2016.06.019
32. Shibata S, Miyake K, Tateishi T, Yoshikawa S, Yamanishi Y, Miyazaki Y, et al. Basophils Trigger Emphysema Development in a Murine Model of COPD Through IL-4-Mediated Generation of MMP-12-Producing Macrophages. *Proc Natl Acad Sci USA* (2018) 115(51):13057–62. doi: 10.1073/pnas.1813927115
33. Tkacova R, Dai DLY, Vonk JM, Leung JM, Hiemstra PS, van den Berge M, et al. Airway Hyperresponsiveness in Chronic Obstructive Pulmonary Disease: A Marker of Asthma-Chronic Obstructive Pulmonary Disease Overlap Syndrome? *J Allergy Clin Immunol* (2016) 138(6):1571–1579.e10. doi: 10.1016/j.jaci.2016.04.022
34. Sajjan U, Ganesan S, Comstock AT, Shim J, Wang Q, Nagarkar DR, et al. Elastase- and LPS-Exposed Mice Display Altered Responses to Rhinovirus Infection. *Am J Physiol Lung Cell Mol Physiol* (2009) 297(5):L931–44. doi: 10.1152/ajplung.00150.2009
35. Jin R, Xu J, Gao Q, Mao X, Yin J, Lu K, et al. IL-33-Induced Neutrophil Extracellular Traps Degrade Fibronectin in a Murine Model of Bronchopulmonary Dysplasia. *Cell Death Discov* (2020) 6:33. doi: 10.1038/s41420-020-0267-2
36. Ohno T, Oboki K, Kajiwara N, Morii E, Aozasa K, Flavell RA, et al. Caspase-1, Caspase-8, and Calpain Are Dispensable for IL-33 Release by Macrophages. *J Immunol* (2009) 183(12):7890–7. doi: 10.4049/jimmunol.0802449
37. Qiu C, Li Y, Li M, Li M, Liu X, McSharry C, et al. Anti-Interleukin-33 Inhibits Cigarette Smoke-Induced Lung Inflammation in Mice. *Immunology* (2013) 138(1):76–82. doi: 10.1111/imm.12020
38. Johnston LK, Hsu CL, Krier-Burris RA, Chhiba KD, Chien KB, McKenzie A, et al. IL-33 Precedes IL-5 in Regulating Eosinophil Commitment and Is Required for Eosinophil Homeostasis. *J Immunol* (2016) 197(9):3445–53. doi: 10.4049/jimmunol.1600611
39. Dagher R, Copenhaver AM, Besnard V, Berlin A, Hamidi F, Maret M, et al. IL-33-ST2 Axis Regulates Myeloid Cell Differentiation and Activation Enabling Effective Club Cell Regeneration. *Nat Commun* (2020) 11(1):4786. doi: 10.1038/s41467-020-18466-w
40. Alvarez F, Fritz JH, Piccirillo CA. Pleiotropic Effects of IL-33 on CD4(+) T Cell Differentiation and Effector Functions. *Front Immunol* (2019) 10:522. doi: 10.3389/fimmu.2019.00522
41. Baumann C, Frohlich A, Brunner TM, Holecska V, Pinschewer DD, Lohning M. Memory CD8(+) T Cell Protection From Viral Reinfection Depends on Interleukin-33 Alarmin Signals. *Front Immunol* (2019) 10:1833. doi: 10.3389/fimmu.2019.01833
42. Redegeld FA, Yu Y, Kumari S, Charles N, Blank U. Non-IgE Mediated Mast Cell Activation. *Immunol Rev* (2018) 282(1):87–113. doi: 10.1111/imr.12629
43. El Hachem C, Hener P, Kirstetter P, Li J, Chan S, Li M. Treatment of MCPT8 (DTR) Mice With High- or Low-Dose Diphtheria Toxin Leads to Differential Depletion of Basophils and Granulocyte-Macrophage Progenitors. *Eur J Immunol* (2018) 48(5):861–73. doi: 10.1002/eji.201747351
44. Pellefigues C, Mehta P, Prout MS, Naidoo K, Yumnam B, Chandler J, et al. The Basoph8 Mice Enable an Unbiased Detection and a Conditional Depletion of Basophils. *Front Immunol* (2019) 10:2143. doi: 10.3389/fimmu.2019.02143
45. Van Dijk EM, Culha S, Menzen MH, Bidan CM, Gosens R. Elastase-Induced Parenchymal Disruption and Airway Hyper Responsiveness in Mouse Precision Cut Lung Slices: Toward an *Ex Vivo* COPD Model. *Front Physiol* (2016) 7:657. doi: 10.3389/fphys.2016.00657
46. Hogg JC, Chu F, Utokaparch S, Woods R, Elliott WM, Buzatu L, et al. The Nature of Small-Airway Obstruction in Chronic Obstructive Pulmonary Disease. *N Engl J Med* (2004) 350(26):2645–53. doi: 10.1056/NEJMoa032158
47. Eissmann MF, Dijkstra C, Jarnicki A, Phesse T, Brunnberg J, Poh AR, et al. IL-33-Mediated Mast Cell Activation Promotes Gastric Cancer Through Macrophage Mobilization. *Nat Commun* (2019) 10(1):2735. doi: 10.1038/s41467-019-10676-1
48. Guilliams M, De Kleer I, Henri S, Post S, Vanhoutte L, De Prijck S, et al. Alveolar Macrophages Develop From Fetal Monocytes That Differentiate Into Long-Lived Cells in the First Week of Life *via* GM-CSF. *J Exp Med* (2013) 210 (10):1977–92. doi: 10.1084/jem.20131199

Conflict of Interest: The authors declare that the research was conducted in the absence of any commercial or financial relationships that could be construed as a potential conflict of interest.

Publisher's Note: All claims expressed in this article are solely those of the authors and do not necessarily represent those of their affiliated organizations, or those of the publisher, the editors and the reviewers. Any product that may be evaluated in this article, or claim that may be made by its manufacturer, is not guaranteed or endorsed by the publisher.

Copyright © 2022 Cardenas, Alvarado-Vazquez, Mendez-Enriquez, Danielsson and Hallgren. This is an open-access article distributed under the terms of the Creative Commons Attribution License (CC BY). The use, distribution or reproduction in other forums is permitted, provided the original author(s) and the copyright owner(s) are credited and that the original publication in this journal is cited, in accordance with accepted academic practice. No use, distribution or reproduction is permitted which does not comply with these terms.

frontiers | Frontiers in Immunology

ORIGINAL RESEARCH
published: 26 April 2022
doi: 10.3389/fimmu.2022.870966

Ataxin-3, The Spinocerebellar Ataxia Type 3 Neurodegenerative Disorder Protein, Affects Mast Cell Functions

Anna S. Sowa[1], *Eva Haas*[2], *Jeannette Hübener-Schmid*[2*] *and Axel Lorentz*[1*]

[1] *Institute of Nutritional Medicine, University of Hohenheim, Stuttgart, Germany,* [2] *Institute of Medical Genetics and Applied Genomics, University of Tübingen, Tübingen, Germany*

Spinocerebellar ataxia type 3 (SCA3), also known as Machado-Joseph Disease, is a progressive neurodegenerative disorder characterized by loss of neuronal matter due to the expansion of the CAG repeat in the *ATXN3/MJD1* gene and subsequent ataxin-3 protein. Although the underlying pathogenic protein expansion has been known for more than 20 years, the complexity of its effects is still under exploration. The ataxin-3 protein in its expanded form is known to aggregate and disrupt cellular processes in neuronal tissue but the role of the protein on populations of immune cells is unknown. Recently, mast cells have emerged as potential key players in neuroinflammation and neurodegeneration. Here, we examined the mast cell-related effects of ataxin-3 expansion in the brain tissues of 304Q ataxin-3 knock-in mice and SCA3 patients. We also established cultures of mast cells from the 304Q knock-in mice and examined the effects of 304Q ataxin-3 knock-in on the immune responses of these cells and on markers involved in mast cell growth, development and function. Specifically, our results point to a role for expanded ataxin-3 in suppression of mast cell marker CD117/c-Kit, pro-inflammatory cytokine TNF-α and NF-κB inhibitor IκBα along with an increased expression of the granulocyte-attracting chemokine CXCL1. These results are the beginning of a more holistic understanding of ataxin-3 and could point to the development of novel therapeutic targets which act on inflammation to mitigate symptoms of SCA3.

Keywords: ataxin-3, MJD, SCA3, mast cell, cytokine, neurodegeneration, inflammation

OPEN ACCESS

Edited by:
Frans J. Van Overveld, University College Roosevelt, Netherlands

Reviewed by:
Claudia Gonzalez-Espinosa, Centro de Investigación y de Estudios Avanzados del Instituto Politécnico Nacional, Mexico
Jiro Kitaura, Juntendo University, Japan

****Correspondence:***
Jeannette Hübener-Schmid
Jeannette.Huebener@med.uni-tuebingen.de
Axel Lorentz
lorentz@uni-hohenheim.de

Specialty section:
This article was submitted to Inflammation, a section of the journal Frontiers in Immunology

Received: *07 February 2022*
Accepted: *23 March 2022*
Published: *26 April 2022*

Citation:
Sowa AS, Haas E, Hübener-Schmid J and Lorentz A (2022) Ataxin-3, The Spinocerebellar Ataxia Type 3 Neurodegenerative Disorder Protein, Affects Mast Cell Functions. Front. Immunol. 13:870966. doi: 10.3389/fimmu.2022.870966

INTRODUCTION

Spinocerebellar ataxia type 3 (SCA3), also known as Machado-Joseph disease (MJD), belongs to the group of neurodegenerative disorders known as polyglutamine (polyQ) disease associated with a polyQ expansion in the protein expressed by the corresponding causative gene (1). In SCA3, the polyQ-expanded protein is known as ataxin-3 and patients carry an expansion between 61 and 87 repeats on the affected allele resulting in the observed phenotype characterized by a disturbance of movement coordination (cerebellar ataxia), bulbar, pyramidal and extrapyramidal signs, and a possible occurrence of peripheral neuropathy or ophthalmoplegia (2). Currently, there is no cure or no therapy mitigating disease progression available for SCA3.

Although in the 20 years since the discovery of the ataxin-3 protein large strides have been made to understand the cellular dysfunction underlying the disease such as, mitochondrial and autophagic disturbances, as well as the protein cleavage and aggregation (3), the full mechanisms behind neuronal death are still unknown. The newly developed 304Q ataxin-3 knock-in mouse model is an important promising tool to further reveal the pathologic effects of ataxin-3 expansion (4). These knock-in mice express 304Q instead of the 6Q normally present in either one or both of the murine ataxin-3 alleles. With twelve months of age these heterozygous and homozygous mice show a significant weight reduction compared to wild type (WT) mice. Despite a very mild motor phenotype, they already show massive SDS-insoluble ataxin-3 and ubiquitin-positive aggregates throughout the brain supporting a strong positive correlation between the polyQ expansion and a toxic function of ataxin-3 related to neurons (4).

Mast cells are important players in the immune system and exert their effects *via* expression and release of mediators involved in physiological functions of the body including innate and adaptive immune response, tissue healing, angiogenesis, and normal neuronal growth (5). The best-known activation of mast cells occurs during type I allergic reactions through crosslinking of immunoglobulin (Ig) E bound FcεRI receptors by antigens. Degranulation occurs a few seconds after crosslinking and results in release of granules stored mediators attracting leukocytes such as eosinophils, neutrophils, or Th2 lymphocytes and increasing permeability of the blood vessels to allow immune cell passage (5, 6). In addition to the FcεRI, mast cells express a variety of receptors such as other Fc receptors, receptors for chemokines and cytokines, or receptors for pathogen associated molecular patterns such as Toll-like receptors, all involved in mast cell activation and immune response (5, 6). In the last decade, mast cells have gained traction in their role in neurodegeneration. They are incredibly potent and considered the first responders able to initiate and magnify immune responses in the brain partly due to their capacity to access neuronal tissue and to affect the blood brain barrier (7). Although mast cells are important immune cells, their role in SCA3 remains to be discovered. It is still unclear if mast cells could play a pathogenic role as mediators of ataxin-3 activity.

The role of ataxin-3 in cell autonomous inflammatory pathways is only beginning to be examined (8). Therefore, we analyzed the effects of ataxin-3 expansion in the brain tissues of the 304Q ataxin-3 knock-in mice and the cerebellar post-mortem brain tissue of SCA3 patients on markers involved in mast cell growth, development and function. For these studies, we also established cultures of mast cells from the 304Q ataxin-3 knock-in mice. Our results point to a role for expanded ataxin-3 in suppression of mast cell marker CD117/c-Kit, pro-inflammatory cytokine TNF-α and NF-κB inhibitor IκBα along with an increased expression of the granulocyte-attracting chemokine CXCL1. This is the first report to describe an immune cell phenotype for SCA3 and a mast cell-specific phenotype for neurodegenerative conditions.

Abbreviations: ATXN3, ataxin-3 gene/protein; BMMC, bone marrow-derived mast cells; CD117, proto-oncogene c-KIT; ERK, extracellular signal-regulated kinases; LPS, lipopolysaccharide; NF-κB, nuclear factor kappa B; PMA, Phorbol-12-myristat-13-acetat; SCA3, spinocerebellar ataxia type 3; MJD, Machado Joseph Disease; TNF-α, tumor necrosis factor alpha; IL, interleukin; DNP, 2,4-dinitrophenyl; GAPDH, glyceraldehyde 3-phosphate dehydrogenase; CXCL, C-X-C motif chemokine ligand; WT, wild type.

MATERIALS AND METHODS

Generation of 304Q Ataxin-3 Knock-In Mice

This study was carried out in strict accordance with the recommendations presented in the Guide for Care and Use of Laboratory Animals of the University of Tübingen, Germany. The protocols were approved by the Institutional Animal Care and Use Committee (IACUC) of the University of Tübingen, Germany. Ataxin-3 knock-in C57Bl/6 mice with 304Q were generated using zinc finger technologies and providing a donor vector with (CAACAGCAG)48 as described (4). One out of three founders integrated up to 304 CAGs into the *ataxin-3* gene. 304Q ataxin-3 knock-in mice used in the current study were either heterozygous or homozygous. Mouse housing and genotyping were described earlier (4). For qRT-PCR 3 mice per genotype at the age of 2 and 12 months and western blot analyses 4 mice per genotype were analyzed at the age of 3 and 12 months.

Histological Analysis of Tissue Mast Cells

Formalin-fixed tissue samples were embedded in paraffin. After deparaffinization and rehydration, 5 µM thick sections were stained with toluidine blue (Carl Roth, Karlsruhe, Germany) for visualization of mast cells. Mast cells were counted at 200-400x magnification. Microscopic analysis was performed using AxioVision software (Carl Zeiss Microscopy, Jena, Germany).

Generation and Culture of Bone Marrow-Derived Mast Cells (BMMC)

Bone marrow cells were collected from femurs of homozygous (304Q/304Q) and heterozygous (WT/304Q) 12 month old 304Q ataxin-3 knock-in and wild type (WT/WT) mice and cultured in RPMI (Gibco, Thermo Fisher Scientific, Waltham, MA), supplemented with 10% fetal bovine serum, penicillin/streptomycin (Biochrom, Berlin, Germany), plus 30 ng/mL mouse IL-3 (PeproTech, Hamburg, Germany). Cells were cultured in 6 well plates, incubated at 37°C in a humidified incubator under 5% (v/v) CO2. Starting after 3 days, half of the medium was changed once a week every week. In addition, starting after 3 weeks, medium was changed completely once a week every week by transferring the non-adherent cells in fresh medium into a new plate. After culture for 9 weeks, cells were used for functional assays. For each genotype, several lines were generated. Maturity and purity of the BMMC were examined on cytospins stained with May-Grünwald/Giemsa (Carl Roth). We did not detect differences in the staining of pure BMMC from

304Q/304Q mice compared to BMMC from WT/WT mice (not shown).

Treatment and Analyses of BMMC

To detect release of β-hexosaminidase, BMMC were loaded with 2,4-dinitrophenyl (DNP)-specific IgE for 90 min and stimulated with 0.1 μg/ml DNP (Thermo Fisher Scientific), for 90 min. To analyze phosphorylation status of signaling molecules, BMMC were stimulated with DNP/IgE or with 1 μM phorbol ester PMA and 1 μM ionomycin (*In vivo*Gen, San Diego, USA) for 10 min or with 1 μg/ml lipopolysaccharide (LPS) from Escherichia coli 0111:B4 (Sigma-Aldrich, Munich, Germany) for 30 min. To analyze cytokine expression and release, BMMC were stimulated for 90 min or for 6 h and culture supernatants were tested by ELISA (R&D systems, MN) in accordance with the manufacturer's instructions. Degranulation of BMMC was quantified by determining the amount of released β-hexosaminidase in the supernatant by color enzyme assay (9). The percent degranulation of mast cells was estimated by the following formula: (β-hexosaminidase activity in the supernatant fraction/total β-hexosaminidase activity in the cellular and supernatant fraction) ×100.

RNA Preparation and Real-Time RT-PCR

For analysis of BMMC, total RNA was prepared by using EXTRACTME RNA isolation kit (7Bioscience, Hartheim, Germany). Real-time RT-PCR was performed using SsoFastTM EVAGreen Supermix (Bio Rad Laboratories, Munich, Germany) and as described (10). To analyze data, a relative quantification method was performed by using the housekeeping gene of glyceraldehyde 3-phosphate dehydrogenase (*Gapdh*) or *β-actin* as a reference for expression of the target gene. The CFX Manager 2.1 software of BioRad Laboratories was used. For analysis of human and murine brain tissue, total RNA was prepared using AllPrep DNA/RNA/microRNA Universal Kit (Qiagen, Hilden, Germany) as described earlier (4). 500 ng purified RNA was transcribed into cDNA using QuantiTect Reverse Transcription Kit (Qiagen) Real-time RT-PCR was performed using SYBR Green PCR Master Mix (Qiagen) as described. qRT-PCR was run on the LightCycler 480 II (Roche, Mannheim, Germany). Relative gene expression quantification was performed by normalization to the housekeeping genes *Sdha*, *Pdh*, *mActb* and *Tbp* using LightCycler 480 SW 1.5.1 software (Roche). Specific sense/anti-sense primers: human *ACTB*: 5' AAA GAC CTG TAC GCC AAC AC/5' CTC AGG AGG AGC AAT GAT CT, human *CD117*: 5' GCC CAA TAT AAA AGG CAA AT/5' AGT GCA AAT GGT TAC TTC CA, human *IL-3RA*: 5' CCT CCT TTG GCT CAC GCT G/5' GCC CAC TCG GAC GGT GTA G, human *TNF*: 5' CAG ATA GAT GGG CTC ATA CCA GGG/5' GCC CTC TGG CCC AGG CAG TCA G, human *CXCL8*: 5' CTG AGA GTG ATT GAG AGT GG/5' ACA ACC CTC TGC ACC CAG TT, mouse *Gapdh*: 5' TGT TCC TAC CCC CAA TGT GT/5' AGA GTG GGA GTT GCT GTT GA, mouse *Cd117*: 5' CTG GTG GTT CAG AGT TCC ATA GAC/5' TCA ACG ACC TTC CCG AAG G, mouse *Il-3rα chain*: 5' TGG AGG AAG TCG CTG CTC TA/5' CGT CAC CTC GCA GTC TTC AA, mouse *Tnf*: 5' GGA GGC AAC AAG GTA GAG/5' TGT CCA TTC CTG AGT TCT G, mouse *Cxcl1*: 5' TAG GGT GAG GAC ATG TGT G/5' GCC CTA CCA ACT AGA CAC AA, mouse *Sdha*: 5' GCA GCA CAG GGA GGT ATC A/5' CTC AAC CAC AGA GGC AGG A, mouse *Pdh*: 5' GTA GAG GAC ACG GGC AAG AT/5' TGA AAA CGC CTC TTC AGC A, mouse *mActb*: 5' CCA CAC CCG CCA CCA GTT CG/5' TAC AGC CCG GGG AGC ATC GT, mouse *Tbp*: 5' TCT ATT TTG GAA GAG CAA CAA AGA C/5' GAG GCT GCT GCA GTT GCT A

Western Blot Analysis

Western blot analysis of BMMC was performed as described previously (11) and murine brain lysates as described in Haas et al. (4). Shortly, frozen brain tissue was homogenized in TES buffer (4% Tris Base pH 7.5, 0.1 mM EDTA, 100 mM Na2Cl) containing protease inhibitor complete EDTA-free protease inhibitor cocktail (Roche). Afterwards, TNES (TES-buffer plus 10% Igepal CA-630) was added in a relation of 1:10 and homogenates incubated on ice for 30 min. Homogenates were centrifuged at 13.200 g for 25 min at 4°C and to supernatants glycerol to a final concentration of 10% were added. For Western blot analyses, 4x LDS sample buffer (1 M Tris base pH 8.5, 2 mM EDTA, 8% LDS, 40% glycerol, 0.025% phenol red) and 100 mM 1,4-dithiothreitol (MerckMillipore) was added to 30 μg of protein lysates and heat-denatured at 70°C for 10 min. Protein samples were separated electrophoretically using 8% Bis-Tris gel and MOPS (50 mM MOPS, 50 mM Tris base pH 7.3, 3.5 mM SDS, 1 mM EDTA) electrophoresis buffer. Proteins were transferred on 0.2 um nitrocellulose membrane (GE Healthcare) using a Bicine/Bis-Tris transfer buffer (25 mM Bicine, 25 mM Bis-Tris pH 7.2, 1 mM EDTA, 15% methanol). After membrane blocking with 5% skimmed milk powder (Sigma-Aldrich), membranes were incubated with the respective primary antibody at 4°C overnight. For visualization of proteins of brain lysates, membranes were incubated with fluorescence tagged secondary antibodies (IRdye 800CW goat anti-mouse IgG (H+L), LI-COR or IRdye 800CW goat anti-rabbit IgG (H+L) LI-COR) for 1.5 hours at room temperature and fluorescence signal detection was performed on the LI-COR ODYSSEY FC (LI-COR). Visualization of proteins of BMMC was performed by the secondary antibodies anti-mouse IgG or anti-rabbit IgG HRP-linked (Cell Signaling Technology®) and Super Signal® West Dura Extended Duration Substrate (Thermo Fisher Scientific, Waltham, MA). The obtained signals were measured by bioimaging analyzer (Alpha Innotech Corporation, San Leandro, CA). The membranes were stripped and used for a second or third staining. Membranes were probed with phospho-ERK (MAPK)-1/2 (12D4) mouse mAb, IκBα (44D4) rabbit mAb, CD117 (D13A2) rabbit mAb (all from Cell Signaling Technology®, Frankfurt, Germany), TNF alpha (EPR19147) rabbit mAb (from Abcam), β-Actin (AC-15) mouse mAb (Sigma Aldrich), GAPDH (D-6) mouse mAb (from Santa Cruz Biotechnology, Dallas, TX). β-Actin or GAPDH labeling was used as loading control for normalization.

Statistics

Data expressed as mean ± SEM. Unpaired t-test was used to analyze differences between two groups. Two-way analysis of variance was used to analyze differences between genotypes and stimulation conditions with Bonferroni multiple comparisons. A value of $p < 0.05$ was considered to be statistically significant.

RESULTS

Brain Tissues of 304Q Ataxin-3 Knock-In Mice and Post-Mortem SCA3 Patients Show an Effect of Expanded Ataxin-3 on the Expression of Mast Cell Markers and Inflammatory Cytokines

In order to elucidate the effects of polyglutamine expansion of ataxin-3 on mast cells we chose to analyze the mRNA expression levels of the mast cell markers CD117/c-Kit and IL-3 receptor α-chain (IL-3Rα) using 304Q ataxin-3 knock-in mice. The 304Q ataxin-3 knock-in mouse model represents the human patient phenotype on a neuropathological, behavioral, and transcriptomic levels in a more complete manner than any existing SCA3 mouse. CD117 is a mast/stem cell receptor for growth factor SCF important in the mast cell development and function, while IL-3R is a potent receptor involved in the stimulation of mast cell growth in response to IL-3 produced by activated T cells (12). There was both a significant down-regulation of *Cd117* expression and a significant up-regulation of *mKc/Cxcl1* expression in the brains of 12-month-old 304Q/304Q and WT/304Q mice compared to WT/WT mice (**Figures 1B, D**). Also, the brains of 304Q ataxin-3 knock-in mice were tested for expression of the cytokine gene *Tnf* and the chemokine *mKc/Cxcl1*. *Tnf* is well known to participate in an acute inflammation and *mKc/Cxcl1* (homologue to human *IL-8/CXCL8*) is involved in pro-inflammatory chemotaxis of mast cells. The *Cxcl1* expression was reliably increased, but no changes in the levels of *Tnf* expression were detected in 304Q ataxin-3 knock-in mice relative to WT/WT mice. The housekeeping genes *Sdha*, *Pdh*, *mActb*, and *Tbp* were not affected (**Figures 1A, C**).

In order to demonstrate the relevance of our findings in the SCA3 mouse model to human disease, we tested the expression of *IL3RA*, *TNF* and *CXCL8* in the post-mortem brain tissues of human SCA3 patients. Noteworthy, we found a tendency towards an increased expression of *CXCL8* associated with a significantly decreased expression of *CD117* compared to controls consistent with our observations in 304Q ataxin-3 knock-in mice (**Figure 1E**).

To confirm the findings for gene expression on protein level, we analyzed the expression of CD117 and TNF-α in brain tissues by Western blot. A significant down-regulation of both CD117 and TNF-α was detected in the 12-month-old 304Q/304Q and WT/304Q mice compared to WT/WT mice (**Figure 2**). We have not established mast cell staining in the available brain tissues, but we have stained mast cells in intestinal tissues. There was a trend towards lower mast cell numbers in duodenal and jejunal tissues of 304Q/304Q ataxin-3 knock-in mice compared to WT controls (**Supplementary Figure S1**).

PolyQ-Expanded Ataxin-3 Modulates Expression of CD117 and Cytokines in BMMC

Next, we aimed to analyze the effect of ataxin-3 directly in mast cells. Thus, we generated cultures of BMMC from the 12-month-old WT/WT, WT/304Q, or 304Q/304Q ataxin-3 knock-in mice. Interestingly, culturing bone marrow cells from 304Q/304Q ataxin-3 knock-in the presence of IL-3 for 6 weeks resulted in 71 ± 9.5% mature BMMC compared to 91 ± 1.3 and 97 ± 2% from WT/WT or WT/304Q mice, respectively. Pure BMMC were found in all cases following 9 weeks of culture. Recovery was 406 ± 159% of BMMC from WT/WT mice compared to 234 ± 33% and 225 ± 82% of BMMC from WT/304Q or 304Q/304Q ataxin-3 knock-in mice. No differences concerning size and degree of granulation were observed between mature BMMC derived from WT/WT, WT/304Q, or 304Q/304Q ataxin-3 knock-in mice.

Expression levels of *Cd117*, *Tnf* and *Cxcl1* mRNA were determined before and after stimulation of BMMC with IgE/2,4-dinitrophenyl (DNP), ionomycin/phorbol-12-myristat-acetate (PMA) or lipopolysaccharide (LPS). The *Cd117* expression was strongly reduced in BMMC from homozygous and, to a lesser extent, heterozygous 304Q ataxin-3 knock-in mice compared to cells from WT/WT mice (**Figure 3A**). This finding could be confirmed on protein level by Western blot, which showed a significantly lower expression of CD117 in BMMC from 304Q/304Q ataxin-3 knock-in compared to cells from WT/WT mice (**Figure 3E**). *Tnf* expression in response to ionomycin/PMA stimulation was substantially reduced in cells from 304Q/304Q and WT/304Q mice compared to WT/WT controls (**Figure 3B**). In contrast, a marked increase of mRNA expression for the proinflammatory chemokine gene *Cxcl1* was detected in BMMC from 304Q/304Q mice relative to WT/WT mice in response to LPS stimulation (**Figure 3C**). These observations are in accordance with our findings in mouse and human SCA3 brain tissues.

304Q Ataxin-3 Modulates Cytokine Release by BMMC

BMMC from 12-month-old 304Q ataxin-3 knock-in mice were stimulated with either IgE/DNP or ionomycin/PMA for 90 min and the release of pre-stored β-hexosaminidase as marker of degranulation was measured (**Figure 3D**). In both cases the stimulated BMMC demonstrated robust degranulation; however, there was no difference between the responses of BMMC from 304Q ataxin-3 knock-in mice compared to WT/WT mice demonstrating that the expanded 304Q ataxin-3 did not influence the capacity of BMMC to degranulate (**Figure 3D**).

To analyze the release of *de novo* synthesized cytokines, BMMC from 12-month-old 304Q ataxin-3 knock-in mice were stimulated with either IgE/DNP, ionomycin/PMA, or LPS for 6 h. The amount of released TNF-α protein measured by ELISA showed a strong decrease upon ionomycin/PMA stimulation in BMMC from 304Q/304Q mice compared to WT/WT mice (**Figure 3F**) in agreement with the gene expression data. The release of CXCL1 also correlated to the measured mRNA levels, with a strong increase in CXCL1 levels in BMMC from 304Q/304Q mice (**Figure 3G**).

304Q Ataxin-3 Modulates Activation of NF-κB Signaling Pathway in BMMC

Further, we aimed to analyze the signaling pathways altered in BMMC from 304Q ataxin-3 knock-in 3 mice compared to BMMC from WT/WT mice to observe which proteins could be responsible for the transcriptional changes in cytokine production. We analyzed two main signaling pathways

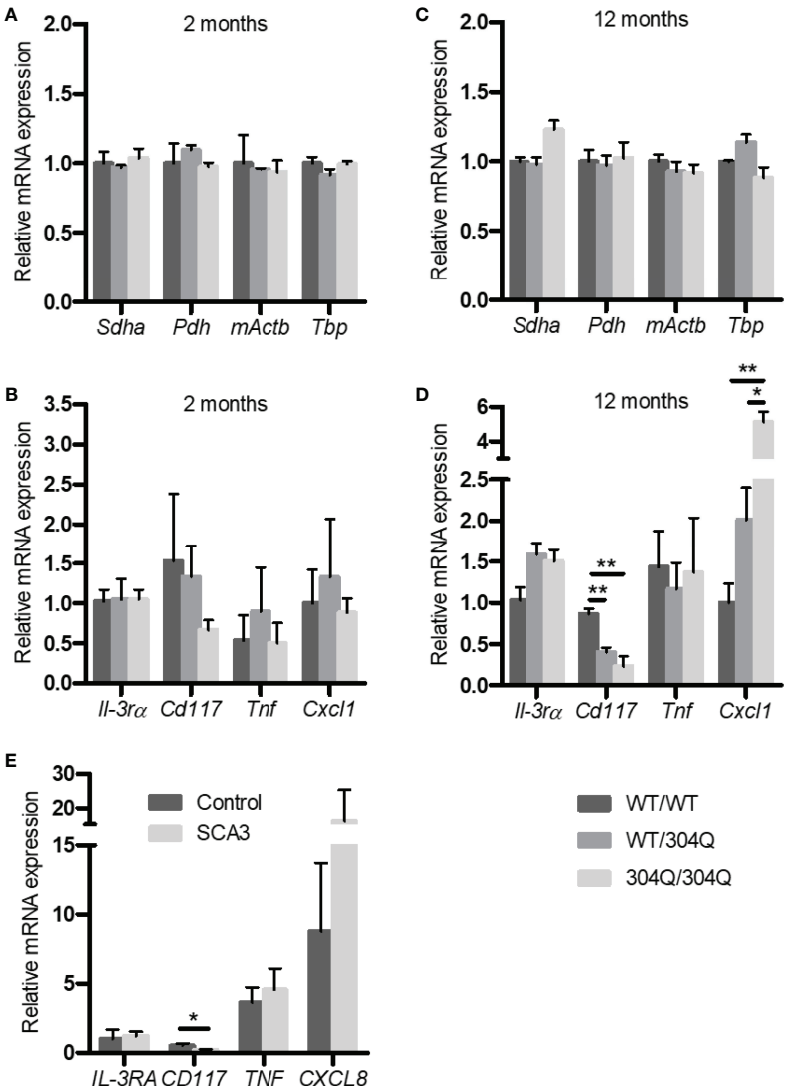


FIGURE 1 | Expression of *Il-3rα*, *Cd117*, *Tnf*, and *Cxcl1/mKc* as well as the housekeeping genes *Sdha*, *Pdh*, *mActb* and *Tbp* mRNA in brain tissue from 2-month-old **(A, B)** and from 12-month-old **(C, D)** WT/WT, WT/304Q, and 304Q/304Q ataxin-3 knock-in mice. Unpaired t test shows statistically significant differences, n = 3, Values are mean ± SEM, *p < 0.05, **p < 0.01. Expression of *CD117*, *IL-3RA*, *TNF*, and *CXCL8* mRNA in cerebellar brain tissue of SCA3 patients normalized using *β-actin* **(E)**. Total RNA was extracted, reverse-transcribed and analyzed by quantitative real-time PCR, n = 4-6. Values are mean ± SEM, p values were calculated by unpaired t-test, *p < 0.05.

involved in mast cell cytokine expression, the MAPK pathway ERK1/2 and the NF-κB pathway.

We did not observe significant differences in phosphorylation of ERK1/2 (**Figure 4A**). However, we found a significant increase of the NF-κB inhibitor IκBα in BMMC from homozygous 304Q/Q304 ataxin-3 knock-in mice (**Figure 4B**). The increase of IκBα could be responsible for a decreased expression of TNF-α as a consequence of a decreased NF-κB activity.

DISCUSSION

Ataxin-3, a causative protein of SCA3, is ubiquitously expressed throughout different organs, tissues and cells, including the brain and the immune system (13). Since the discovery of the polyQ-expanded ataxin-3 in patients with SCA3 (1) it was reported that this protein causes a complex pattern of gene expression changes in transgenic SCA3 cell lines and human SCA3 pontine neurons (14). Various molecular mechanisms have been proposed to explain the toxic function of polyQ expansion, including dysregulation of transcription, impairment of the ubiquitin–proteasome system, mitochondrial dysfunction, dysregulation of intracellular $Ca2^{+}$ homeostasis, impairment of axonal transport and genotoxic stress (15). These single-cause hypotheses are not entirely satisfactory and, taken together, indicate that the disease pathogenesis might not be exclusive to one particular structure or dysfunction. Therefore, further

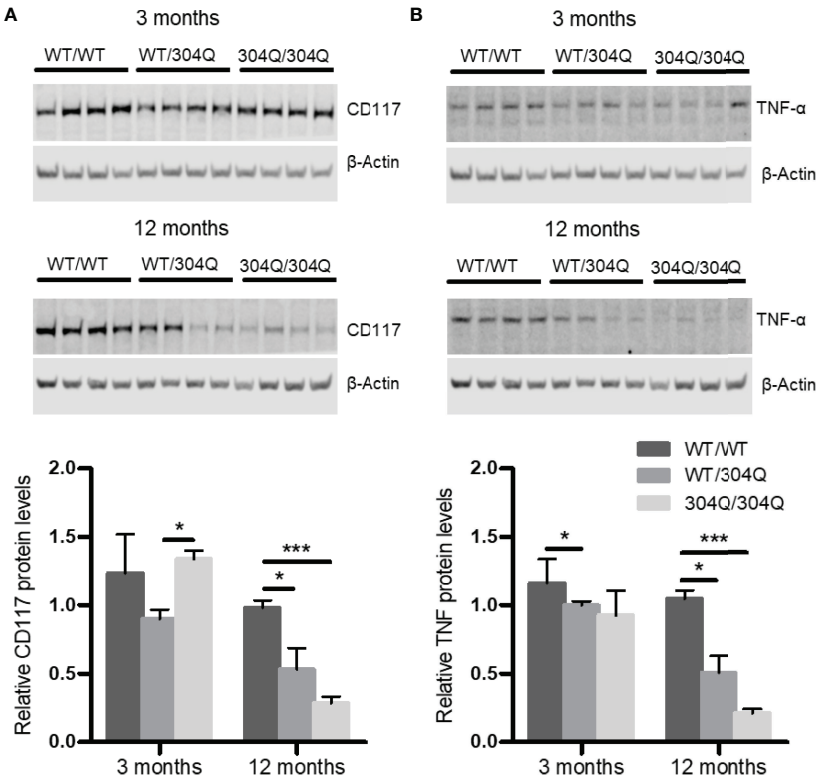


FIGURE 2 | CD117 and TNF-α are down-regulated in cerebellar brain tissue of 304Q/304Q ataxin-3 knock-in mice. Protein levels of CD117 **(A)** and TNF-α **(B)** in relation to β-actin in brain tissue from 3-month-old and from 12-month-old WT/WT, WT/304Q, or 304Q/304Q ataxin-3 knock-in mice. Unpaired t test shows statistically significant differences, n = 4. Values are mean ± SEM, *p < 0.05, ***p < 0.001.

studies are required to evaluate the implications of a polyQ expansion in SCA3 toxicity.

Mast cells were recently implicated as agents of neurodegeneration in several disease (16). Mast cells are potent activators and regulators of the peripheral immune system with access to neuronal tissue. They are able to affect the blood-brain barrier and thus could be involved in CNS pathology. Mast cells are involved in a multitude of conditions including cancer, allergy, psoriasis, multiple sclerosis, Parkinson's disease, stroke, autism, migraines, sleep disorders, stress and inflammation (17). Brain mast cells are crucial mediators of sleep and fundamental neurobehavior which are all involved in ataxia and similar neurodegenerative disorders (18).

In this study we evaluated the hypothesis of mast cell contribution to SCA3. For this purpose, we tested the mRNA and protein expression levels of the inflammatory mast cell marker CD117/c-Kit and IL-3Rα in the brains of normal and 304Q ataxin-3 knock-in mice. CD117/c-Kit signaling network plays an important role in several cell functions including proliferation, survival, apoptosis, motility, adhesion and angiogenesis (19). We found that the expression of CD117, but not of IL-3Rα, was reduced in comparison with healthy controls. In order to analyze the effect of expanded ataxin-3 directly in mast cells we established the BMMC cultures from homozygous and heterozygous 304Q ataxin-3 knock-in mice. In agreement with the brain data, expression levels of CD117 in BMMC from 304Q ataxin-3 knock-in mice were reduced compared to cells from WT/WT mice in stimulated and unstimulated cells. We conclude that mast cells are negatively regulated by the expanded ataxin-3. Analyses of post-mortem brain samples from the SCA3 patients corroborate this conclusion.

Consistently, we found that maturation of BMMC from 304Q/304Q ataxin-3 knock-in mice takes longer than from homozygous WT and heterozygous 304Q ataxin-3 knock-in mice. However, these findings need to be confirmed in future studies by more quantitative techniques such as flow cytometry or transmission electron microscopy. Furthermore, the cell recovery/proliferation of pure mature BMMC from 304Q/304Q ataxin-3 knock-in mice was lower compared to BMMC from WT controls. Interestingly, expression of mutant huntingtin, the disease protein in Huntington´s disease (HD), was also shown to affect maturation of BMMC (20). This finding combined with our observation suggests a significant impairment in mast cells maturation in polyQ-associated neurodegenerative conditions such as SCA3 and HD.

In general, mast cells exert their effects *via* expression and release of mediators involved in physiological functions of the body through the intracellular activation of tyrosine kinases (5).

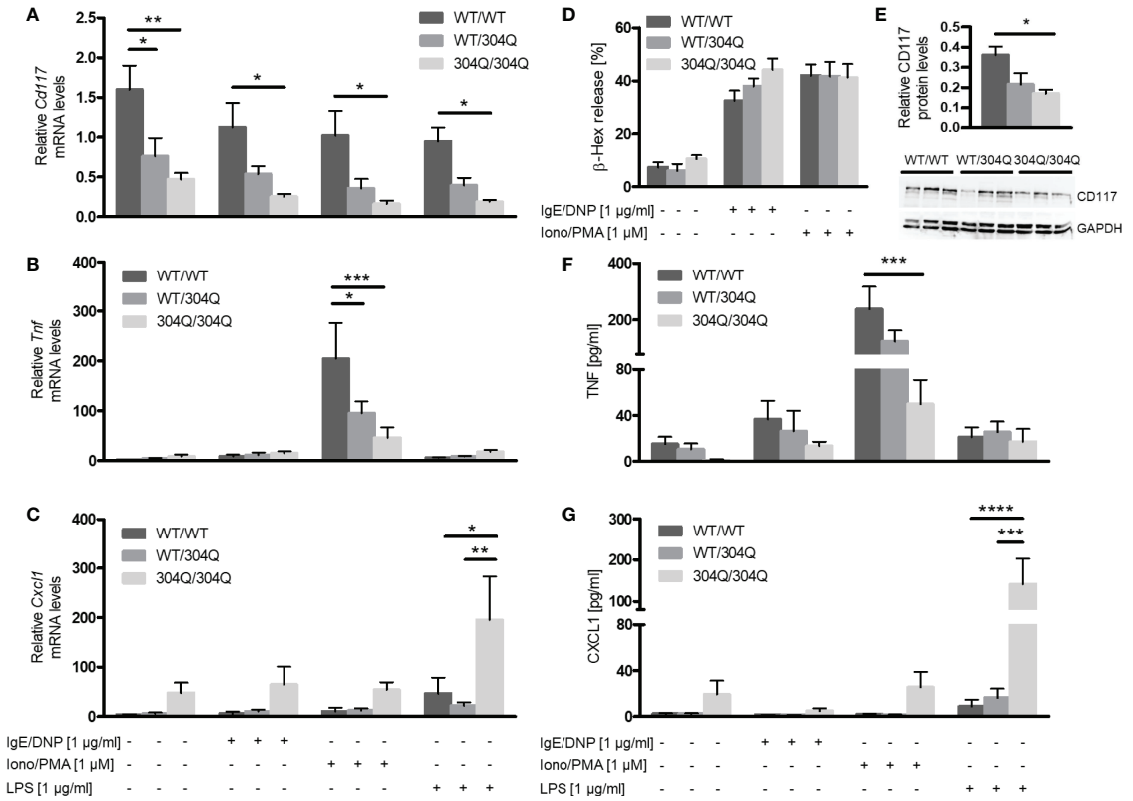


FIGURE 3 | Expression of *Cd117* and *Tnf* is down-regulated and expression of *Cxcl1* is upregulated in BMMC from 304Q/304Q ataxin-3 knock-in mice. *Cd117* **(A)**, *Tnf* **(B)**, and *Cxcl1* **(C)** mRNA levels were determined following stimulation of BMMC from WT/WT, WT/304Q, or 304Q/304Q ataxin-3 knock-in mice with IgE/DNP, ionomycin/PMA or LPS for 90 min. Release of β-hexosaminidase (β-Hex) **(D)** as a marker of degranulation was measured following stimulation with IgE/DNP or ionomycin/PMA. Protein levels of CD117 in relation to GAPDH were measured in BMMC from WT/WT, WT/304Q, or 304Q/304Q ataxin-3 knock-in mice **(E)**. Release of cytokines TNF-α **(F)** and CXCL1 **(G)** in supernatants of BMMC from 304Q ataxin-3 knock-in mice were measured following stimulation with IgE/DNP, ionomycin/PMA or LPS for 6h Unpaired t test **(E)** and two-way ANOVA **(A–D, F, G)** show statistically significant differences, n = 3-5. Values are mean ± SEM, *p < 0.05, **p < 0.01, ***p < 0.001, ****p < 0.0001.

The best-known activation of mast cells occurs during type-I allergic reactions through crosslinking of IgE bound to FcεRI receptors by antigens (6). However, no effect of 304Q ataxin-3 on degranulation was found in our experiments with BMMC judging by the amounts of released β-hexosaminidase following stimulation with IgE/DNP or ionomycin/PMA. We conclude that the mast cell signaling involved in degranulation is not targeted by the expanded ataxin-3.

Along with the reduced expression of CD117, we detected a suppressive effect of expanded ataxin-3 on the mRNA and protein expression of the proinflammatory TNF-α both in the cerebellar brain regions and supernatants of ionomycin/PMA-stimulated BMMC. TNF-α expression in response to FcεRI cross-linking was low compared to ionomycin/PMA stimulation. This may be due to different time courses and the strength of the ionomycin/PMA stimulation which skips receptor-mediated signals and directly induces PKC phosphorylation and calcium concentration elevation, respectively (21). TNF-α is a pleiotropic cytokine. Activation of signaling by TNF-α initiates a variety of potential outcomes, including cell proliferation, gene activation or cell death (22). The intracellular signaling pathways induced by this cytokine in SCA3 along with the role of ataxin-3 are only beginning to be examined (8).

In contrast to CD117 and TNF-α, the mRNA and protein levels of CXCL1 were found stimulated by the expanded ataxin-3 both in the brains and BMMC. Mast cells, like macrophages, have the capacity to newly synthesize CXCL1, making detectable amounts within 1 hour of LPS treatment (23). CXCL1 is a mouse homologue to human IL-8/CXCL8 involved in a number of pro-inflammatory activities, including the chemotaxis of neutrophils to the site of injury thereby aggravating the ongoing inflammatory response. CXCL1 is also shown to display a neuroprotective function (24). Future work will reveal the specific role for the mast cell-released CXCL1 stimulation in response to expanded ataxin-3 in the mechanism of SCA3.

The modulation of transcription of TNF-α and CXCL1 in BMMC expressing the expanded 304Q ataxin-3 compared to the healthy controls prompted us to test if this process involves NF-κB which is a protein complex that controls transcription,

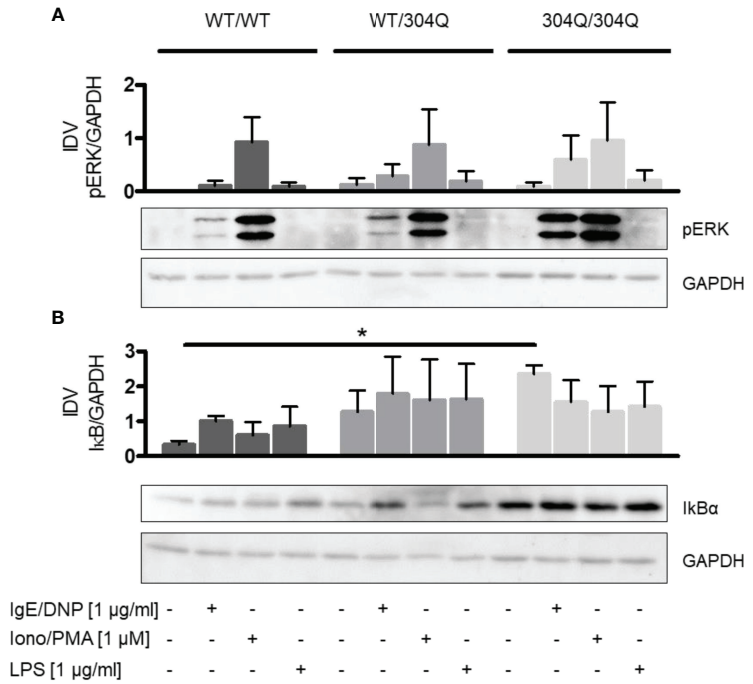


FIGURE 4 | ERK1/2 and NF-κB signaling in BMMC from WT/WT, WT/304Q, or 304Q/304Q ataxin-3 knock-in mice. **(A)** BMMC from WT/WT, WT/304Q, and 304Q/304Q ataxin-3 knock-in mice stimulated or unstimulated with IgE/DNP, ionomycin/PMA or LPS for 10 min. Supernatants of BMMC cultures were analyzed by Western blot for ERK1/2 phosphorylation **(A)** and IkBα **(B)** relative to GAPDH. Representative pictures and densitometric analyses as integrated density values (IDV) are shown. Unpaired t test shows statistically significant differences, n = 3. Values are mean ± SEM, *p < 0.05.

cytokine/chemokine production and cell survival. NF-κB is found in almost all animal cell types and is involved in cellular responses to diverse stimuli. Canonically, TNF-α is one of the major inducers of NF-κB activity (25) which in turn is expected to activate expression of CXCL1 (26). Therefore, the reduced expression of TNF-α in the BMMC from 304Q ataxin-3 knock-in mice is consistent with the increased expression of the NF-κB inhibitor, IκBα, but not with the increased expression of CXCL1 we observed. Moreover, CXCL1 binding to its receptors CXCR1/2 is supposed to activate the downstream extracellular signal-regulated kinases 1 and 2 (ERK1/2) (27). However, we did not observe significant differences in phosphorylation of ERK1/2. This conundrum points out to the profound interference of the polyQ-expanded ataxin-3 with the normal transcriptional and signaling responses of mast cells. The exploration of alternative pathways is warranted to clarify this point further.

Ataxin-3 is a deubiquitylating enzyme that removes and disassembles ubiquitin chains from specific substrates (28). NF-κB signaling consists of a series of positive and negative regulatory elements. Inducing stimuli trigger IKK activation leading to phosphorylation, ubiquitination, and degradation of IκB proteins, resulting in release of NF-κB, its nuclear translocation and ultimately induction of NF-κB target genes (29). However, a direct interaction of NF-κB pathway and the deubiquitinase ataxin-3 has not yet been shown. A possible pathway that activates NF-κB signaling in context of expanded ataxin-3 could be *via* the U-box E3 ligase CHIP, which has been identified as a direct interaction partner of ataxin-3. Thereby, ataxin-3 and CHIP interact and regulate each other's activity (28). On the other side, CHIP was shown to promote the activation of NF-κB signaling (30). Additionally, an siRNA-based drug screen in mammalian cells expressing expanded ataxin-3 identified 15 genes which are related to TNF/NF-κB and ERK1/2 pathways and concluded that expanded ataxin-3 can be regulated by these pro-inflammatory and cell death/survival pathways (31). Moreover, ataxin-3 may be involved in deubiquitination of several signaling molecules and it is hard to predict how expanded ataxin-3 may affect certain modifications and thus the behavior or fate of such proteins.

Recently, expression of mutant huntingtin (mHtt) was shown to affect toll-like receptor 4 (TLR-4) intracellular trafficking and cytokine production in BMMC (20). Similar to our findings in BMMC with the expanded ataxin-3, expression of TNF-α was reduced while the release of β-hexosaminidase was not affected in mHtt-expressing BMMC. Besides NF-κB several transcription factors such as AP-1, SP1, ETS-1, ELK-1, and NFAT have been found to be involved in TNF-α mRNA production (32). Pérez-Rodríguez et al. report that the ERK-ELK-c-Fos signaling axis, but not NF-κB, participate in TNF-α gene transcription in BMMCs in response to LPS stimulation *via* TLR-4. We found the highest induction of TNF-α in response to stimulation with ionomycin/PMA, which is known to cause PKC activation and

an increase in intracellular calcium (21). Consistently, we found a strong activation of the downstream signaling molecules ERK1/2 in response to ionomycin/PMA stimulation. Thus, TNF-α expression in response to ionomycin/PMA also appears to depend on ERK1/2-related transcription factors such as ELK-1. However, different from the findings in BMMC expressing mutant huntingtin, we observed no significant differences in the phosphorylation of ERK1/2 in BMMC with expanded ataxin-3 compared to wild type BMMC. Further investigations are needed to identify all signaling molecules involved and all effects of ataxin-3 in mast cells.

In summary, we identified for the first time the mast cell target genes transcriptionally dysregulated by the polyQ-expanded ataxin-3. Future work will reveal the pathogenic mechanisms behind these observations and will examine the previous hypothesis that transcriptional dysregulation appears to represent a unifying feature of polyQ disorders (14).

DATA AVAILABILITY STATEMENT

The original contributions presented in the study are included in the article/**Supplementary Material**. Further inquiries can be directed to the corresponding authors.

ETHICS STATEMENT

The studies involving human participants were reviewed and approved by Ethics Committee Tübingen. The patients/participants provided their written informed consent to participate in this study. The animal study was reviewed and approved by Institutional Animal Care and Use Committee (IACUC) of the University of Tübingen.

AUTHOR CONTRIBUTIONS

AS and AL contributed to conception and design of the study. AS, EH, JH-S, and AL performed experiments and data analyses. AS wrote the first draft of the manuscript. All authors contributed to manuscript revision, read, and approved the submitted version.

ACKNOWLEDGMENTS

We would like to thank Yvonne Soltow, Chrisovalantou Huridou and Teresa Braun for excellent technical assistance. We would also like to thank Serguei Popov for his assistance with this manuscript. We also acknowledge support by the Open Access Publishing Fund of the University of Tübingen.

SUPPLEMENTARY MATERIAL

The Supplementary Material for this article can be found online at: https://www.frontiersin.org/articles/10.3389/fimmu.2022.870966/full#supplementary-material

REFERENCES

1. Kawaguchi Y, Okamoto T, Taniwaki M, Aizawa M, Inoue M, Katayama S, et al. CAG Expansions in a Novel Gene for Machado-Joseph Disease at Chromosome 14q32.1. *Nat Genet* (1994) 8:221–28. doi: 10.1038/ng1194-221
2. Matos CA, de Almeida LP, Nóbrega C. Machado-Joseph Disease/Spinocerebellar Ataxia Type 3: Lessons From Disease Pathogenesis and Clues Into Therapy. *J Neurochem* (2019) 148:8–28. doi: 10.1111/jnc.14541
3. Weber JJ, Sowa AS, Binder T, Hübener J. From Pathways to Targets: Understanding the Mechanisms Behind Polyglutamine Disease. *BioMed Res Int* (2014) 2014:701758. doi: 10.1155/2014/701758
4. Haas E, Incebacak RD, Hentrich T, Huridou C, Schmidt T, Casadei N, et al. A Novel SCA3 Knock-In Mouse Model Mimics the Human SCA3 Disease Phenotype Including Neuropathological, Behavioral, and Transcriptional Abnormalities Especially in Oligodendrocytes. *Mol Neurobiol* (2021) 59:495–522. doi: 10.1007/s12035-021-02610-8
5. Krystel-Whittemore M, Dileepan KN, Wood JG. Mast Cell: A Multi-Functional Master Cell. *Front Immunol* (2016) 6:620. doi: 10.3389/fimmu.2015.00620
6. Lorentz A, Baumann A, Vitte J, Blank U. The SNARE Machinery in Mast Cell Secretion. *Front Immunol* (2012) 3:143. doi: 10.3389/fimmu.2012.00143
7. Hendriksen E, van Bergeijk DA, Oosting RS, Redegeld RA. Mast Cells in Neuroinflammation and Brain Disorders. *Neurosci Biobehav Rev* (2017) 83:774. doi: 10.1016/j.neubiorev.2017.10.030
8. Sowa AS, Popova TG, Harmuth T, Weber JJ, Pereira Sena P, Schmidt J, et al. Neurodegenerative Phosphoprotein Signaling Landscape in Models of SCA3. *Mol Brain* (2021) 14:57. doi: 10.1186/s13041-020-00723-0
9. Schwartz LB, Austen KF, Wasserman SI. Immunologic Release of Beta-Hexosaminidase and Beta-Glucuronidase From Purified Rat Serosal Mast Cells. *J Immunol* (1979) 123:1445–50.
10. Hagenlocher Y, Feilhauer K, Schäffer M, Bischoff SC, Lorentz A. Citrus Peel Polymethoxyflavones Nobiletin and Tangeretin Suppress LPS- and IgE-Mediated Activation of Human Intestinal Mast Cells. *Eur J Nutr* (2017) 56:1609–20. doi: 10.1007/s00394-016-1207-z
11. Feuser K, Feilhauer K, Staib L, Bischoff SC, Lorentz A. Akt Cross-Links IL-4 Priming, Stem Cell Factor Signaling, and IgE-Dependent Activation in Mature Human Mast Cells. *Mol Immunol* (2011) 48:546–52. doi: 10.1016/j.molimm.2010.10.010
12. Stone KD, Prussin C, Metcalfe DD. IgE, Mast Cells, Basophils, and Eosinophils. *J Allergy Clin Immunol* (2010) 125(2 Suppl 2):S73. doi: 10.1016/j.jaci.2009.11.017
13. Uhlén M, Fagerberg L, Hallström BJ, Lindskog C, Oksvold P, Mardinoglu A, et al. Proteomics. Tissue-Based Map of the Human Proteome. *Science* (2015) 347(6220):1260419. doi: 10.1126/science.1260419
14. Evert BO, Vogt IR, Vieira-Saecker AM, Ozimek L, de Vos RA, Brunt ER, et al. Gene Expression Profiling in Ataxin-3 Expressing Cell Lines Reveals Distinct Effects of Normal and Mutant Ataxin-3. *J Neuropathol Exp Neurol* (2003) 62:1006–18. doi: 10.1093/jnen/62.10.1006
15. Takahashi T, Katada S, Onodera O. Polyglutamine Diseases: Where Does Toxicity Come From? What Is Toxicity? Where Are We Going? *J Mol Cell Biol* (2010) 2:180–91. doi: 10.1093/jmcb/mjq005
16. Jones MK, Nair A, Gupta M. Mast Cells in Neurodegenerative Disease. *Front Cell Neurosci* (2019) 13:171. doi: 10.3389/fncel.2019.00171
17. Skaper SD, Facci L, Giusti L. Mast Cells, Glia and Neuroinflammation: Partners in Crime? *Immunology* (2014) 141:314–27. doi: 10.1111/imm.12170

18. Chikahisa S, Kodama T, Soya A, Sagawa Y, Ishimaru Y, Séi H, et al. Histamine From Brain Resident MAST Cells Promotes Wakefulness and Modulates Behavioral States. *PloS One* (2013) 8:e78434. doi: 10.1371/journal.pone.0078434
19. Stankov K, Popovic S, Mikov M. C-KIT Signaling in Cancer Treatment. *Curr Pharm Des* (2014) 20:2849–80. doi: 10.2174/13816128113199990593
20. Pérez-Rodríguez MJ, Ibarra-Sánchez A, Román-Figueroa A, Pérez-Severiano F, González-Espinosa C. Mutant Huntingtin Affects Toll-Like Receptor 4 Intracellular Trafficking and Cytokine Production in Mast Cells. *J Neuroinflamm* (2020) 17:95. doi: 10.1186/s12974-020-01758-9
21. Chang YY, Hsu WH, Pan TM. Monascus Secondary Metabolites Monascin and Ankaflavin Inhibit Activation of RBL-2H3 Cells. *J Agric Food Chem* (2015) 63:192–9. doi: 10.1021/jf504013n
22. Gough P, Myles IA. Tumor Necrosis Factor Receptors: Pleiotropic Signaling Complexes and Their Differential Effects. *Front Immunol* (2020) 11:585880. doi: 10.3389/fimmu.2020.585880
23. De Filippo K, Dudeck A, Hasenberg M, Nye E, van Rooijen N, Hartmann K, et al. Mast Cell and Macrophage Chemokines CXCL1/CXCL2 Control the Early Stage of Neutrophil Recruitment During Tissue Inflammation. *Blood* (2013) 121:4930–37. doi: 10.1182/blood-2013-02-486217
24. Omari KM, Lutz SE, Santambrogio L, Lira SA, Raine CS. Neuroprotection and Remyelination After Autoimmune Demyelination in Mice That Inducibly Overexpress CXCL1. *Am J Pathol* (2009) 174:164–76. doi: 10.2353/ajpath.2009.080350
25. Hayden MS, Ghosh S. Regulation of NF-KappaB by TNF Family Cytokines. *Semin Immunol* (2014) 26:253–66. doi: 10.1016/j.smim.2014.05.004
26. Burke SJ, Lu D, Sparer TE, Masi T, Goff MR, Karlstad MD, et al. NF-κb and STAT1 Control CXCL1 and CXCL2 Gene Transcription. *Am J Physiol Endocrinol Metab* (2014) 306:E131–49. doi: 10.1152/ajpendo.00347.2013
27. Bolitho C, Hahn MA, Baxter RC, Marsh DJ. The Chemokine CXCL1 Induces Proliferation in Epithelial Ovarian Cancer Cells by Transactivation of the Epidermal Growth Factor Receptor. *Endocr Relat Cancer* (2010) 17:929–40. doi: 10.1677/ERC-10-0107
28. Winborn BJ, Travis SM, Todi SV, Scaglione KM, Xu P, Williams AJ, et al. The Deubiquitinating Enzyme Ataxin-3, a Polyglutamine Disease Protein, Edits Lys63 Linkages in Mixed Linkage Ubiquitin Chains. *J Biol Chem* (2008) 283:26436–43. doi: 10.1074/jbc.M803692200
29. Hayden MS, Ghosh S. Shared Principles in NF-kappaB Signaling. *Cell* (2008) 132:344–62. doi: 10.1016/j.cell.2008.01.020
30. Liu Y, Sun Y, Han S, Guo Y, Tian Q, Ma Q, et al. CHIP Promotes the Activation of NF-κb Signaling Through Enhancing the K63-Linked Ubiquitination of TAK1. *Cell Death Discov* (2021) 7:246. doi: 10.1038/s41420-021-00637-3
31. Ashraf NS, Sutton JR, Yang Y, Ranxhi B, Libohova K, Shaw ED, et al. Druggable Genome Screen Identifies New Regulators of the Abundance and Toxicity of ATXN3, the Spinocerebellar Ataxia Type 3 Disease Protein. *Neurobiol Dis* (2020) 137:104697. doi: 10.1016/j.nbd.2019.104697
32. Falvo JV, Tsytsykova AV, Goldfeld AE. Transcriptional Control of the TNF Gene. *Curr Dir Autoimmun* (2010) 11:27–60. doi: 10.1159/000289196

Conflict of Interest: The authors declare that the research was conducted in the absence of any commercial or financial relationships that could be construed as a potential conflict of interest.

Publisher's Note: All claims expressed in this article are solely those of the authors and do not necessarily represent those of their affiliated organizations, or those of the publisher, the editors and the reviewers. Any product that may be evaluated in this article, or claim that may be made by its manufacturer, is not guaranteed or endorsed by the publisher.

Copyright © 2022 Sowa, Haas, Hübener-Schmid and Lorentz. This is an open-access article distributed under the terms of the Creative Commons Attribution License (CC BY). The use, distribution or reproduction in other forums is permitted, provided the original author(s) and the copyright owner(s) are credited and that the original publication in this journal is cited, in accordance with accepted academic practice. No use, distribution or reproduction is permitted which does not comply with these terms.

frontiers | Frontiers in Immunology

MINI REVIEW
published: 12 May 2022
doi: 10.3389/fimmu.2022.898419

Novel Insights Into the Immune-Regulatory Functions of Mast Cells in the Cutaneous Immune Response

Tetsuya Honda[1*] *and Yuki Honda Keith*[2]

[1] *Department of Dermatology, Hamamatsu University School of Medicine, Hamamatsu, Japan,* [2] *Department of Dermatology, Kyoto University Graduate School of Medicine, Kyoto, Japan*

Skin is a frontline organ that is continuously exposed to external stimuli, including pathogens. Various immune cells reside in the skin under physiological conditions and protect the body from the entry of pathogens/antigens by interacting with each other and orchestrating diverse cutaneous immune responses. To avoid unnecessary inflammation and tissue damage during the elimination of external pathogens and antigens, skin possesses regulatory systems that fine-tune these immune reactions. Mast cells (MCs) are one of the skin-resident immune cell populations that play both effector and regulatory functions in the cutaneous immune response. So far, the interleukin-10-mediated mechanisms have mostly been investigated as the regulatory mechanisms of MCs. Recent studies have elucidated other regulatory mechanisms of MCs, such as the maintenance of regulatory T/B cells and the programmed cell death protein-1/programmed cell death-ligand 1-mediated inhibitory pathway. These regulatory pathways of MCs have been suggested to play important roles in limiting the excessive inflammation in inflammatory skin diseases, such as contact and atopic dermatitis. The regulatory functions of MCs may also be involved in the escape mechanisms of antitumor responses in skin cancers, such as melanoma. Understanding and controlling the regulatory functions of skin MCs may lead to novel therapeutic strategies for inflammatory skin diseases and skin cancers.

Keywords: mast cell, IL-10, PD-1, regulatory T cells (Tregs), regulatory B cells (Bregs)

OPEN ACCESS

Edited by:
Satoshi Tanaka, Kyoto Pharmaceutical University, Japan

Reviewed by:
Carole A. Oskeritzian, University of South Carolina, United States

***Correspondence:**
Tetsuya Honda
hontetsu@hama-med.ac.jp

Specialty section:
This article was submitted to Inflammation, a section of the journal Frontiers in Immunology

Received: *17 March 2022*
Accepted: *19 April 2022*
Published: *12 May 2022*

Citation:
Honda T and Keith YH (2022) Novel Insights Into the Immune-Regulatory Functions of Mast Cells in the Cutaneous Immune Response. Front. Immunol. 13:898419. doi: 10.3389/fimmu.2022.898419

INTRODUCTION

Skin is the outermost organ separating the body from the outer environment. As the skin is constantly exposed to various external stimuli, such as pathogens and physical/chemical trauma, it has sophisticated barrier systems that protect the body from such stimuli. One such barrier system includes the immunological barrier, in which skin-resident or infiltrated immune cells exhibit effector functions to eliminate the pathogens (1). To form this barrier, the immune cells perform effector functions by interacting with each other and producing various cytokines/chemokines, leading to inflammation. While inflammation is necessary for efficient protection of the body from external stimuli such as pathogens and antigens, excess of it can cause undesired tissue damage. To

minimize tissue damage, multiple regulatory systems must precisely control the effector functions of immune cells.

Among the immune cells in the skin, mast cells (MCs) are one of the most abundant skin-resident immune cells, accounting for approximately 10% of all hematopoietic cells in the skin (2). Skin MCs consist in connective tissue-type MCs (CTMCs) in mice and tryptase-positive, chymase-positive MC_{TC} in humans and are considered to be derived from the bone marrow, yolk sac, and the aorta-gonad-mesonephros region (3–6). Under physiological conditions, MCs are localized in the hypodermis and dermis, mainly around blood vessels, nerve fibers, and hair follicles (7, 8). Several studies have been performed to elucidate the roles of MCs in the skin under steady and diseased conditions. MCs play both facilitating and regulatory roles in a context-dependent manner (9–13). So far, the interleukin (IL)-10-mediated mechanisms have mostly been investigated as the regulatory mechanisms of MCs. However, recent studies have revealed several IL-10-independent regulatory functions of MCs.

In this review, we discuss the recent findings on the immunoregulatory functions of skin MCs and their underlying mechanisms in the context of inflammatory skin diseases and skin cancers, focusing on contact dermatitis, atopic dermatitis (AD), and malignant melanoma (**Table 1**).

CONTACT DERMATITIS

Contact dermatitis, such as metal allergy and plant allergy, is a prototypic Th1/Type 1 $CD8^+$ T cells (Tc1)-type immune response of the skin (1). Mouse contact hypersensitivity (CHS) is one of the most frequently used animal models of contact dermatitis (22). Small molecules (<500 Da), called haptens, bind to self-proteins and become antigens to induce CHS. When foreign antigens invade the skin, they are captured by the skin dendritic cells (DCs), mainly dermal DCs, which subsequently migrate to the skin-draining lymph nodes (LNs) and undergo maturation. The migrated DCs then present the antigens to naive T cells in an antigen-specific manner and promote their differentiation into effector T cells (sensitization). When the same antigens enter the skin, the skin DCs present the antigens to skin-infiltrated effector T cells *in situ* and activate them to produce cytokines and cytotoxic molecules, such as interferon-γ and granzyme B, which lead to antigen-specific immune responses (elicitation). MCs play a role in CHS regulation *via* multiple mechanisms.

Promotion of CHS by MCs

During the sensitization phase in CHS, MCs play promoting role by interacting with or recruiting immune cells in the skin. Upon hapten exposure, MCs release tumor necrosis factor (TNF) and promote the maturation/migration of dermal DC s to the LNs, leading to the facilitation of sensitization (23, 24). MC-derived exosome may also be involved in DC maturation (25). Furthermore, MCs facilitate sensitization by amplifying the infiltration of neutrophils into the hapten exposed skin, a key step for sensitization (26, 27), by releasing TNF and histamine (26). Recruitment of neutrophils by MCs are also important for the promotion of elicitation (23, 28). In addition, MCs present antigens to T cells by acquiring major histocompatibility complex class II (MHCII) from DCs, and can facilitate elicitation (29). However, in the elicitation phase, negative regulatory functions of MCs have also been elucidated as illustrated below.

IL-10-Dependent Regulation of CHS

Previous studies have investigated the role of skin MCs in CHS using MC-deficient mice, such as WBB6F1-$Kit^{W/Wv}$ ($Kit^{W/Wv}$) and C57BL/6-$Kit^{W\text{-}sh/W\text{-}sh}$ ($Kit^{W\text{-}sh/W\text{-}sh}$) mice (Kit-dependent, constitutive MC deficiency) (9). In these mice, both facilitating and regulatory roles of MCs have been reported in CHS. For example, Norman et al. reported that CHS responses in $Kit^{W/Wv}$ mice are reduced when it is induced by low-concentration hapten (oxazolone) and elevated when it is induced by high-concentration hapten, suggesting that MCs are necessary for the development of CHS and to limit the excess inflammation (30). Grimbaldeston et al. also reported exacerbated oxazolone-induced CHS responses in $Kit^{W/Wv}$ and $Kit^{W\text{-}sh/W\text{-}sh}$ mice. This exacerbation was eliminated by the transfer of wild-type (WT) mouse-derived MCs, but not IL-10-deficient ($IL\text{-}10^{-/-}$) mouse-derived MCs, suggesting that MCs limit inflammation in CHS in an IL-10-dependent manner (14). Using IL-10 reporter mice, it was later confirmed that MCs produce IL-10 most abundantly in the skin one day after the elicitation in oxazolone-induced CHS, whereas MCs produce minimal IL-10 when CHS was induced with low concentrations of oxazolone (15).

Because Kit-dependent MC-deficient mice have various hematological abnormalities other than MC deficiency, it has been debated whether the exacerbated CHS response in these mice is solely attributable to MC deficiency. However, exacerbated CHS responses have also been observed in Kit-independent MC-deficient mice (9, 11), and MC-specific depletion of IL-10 ($Mcpt5\text{-}Cre^{+}Il10^{f/f}$ mice) recapitulated the exacerbated CHS phenotype in MC-deficient mice (15). These results indicate that MCs play a suppressive role in eliciting oxazolone-induced CHS *via* IL-10 production. In contrast, these regulatory functions of MCs were not observed by Dudeck et al., in which MC-deficient mice (both Kit-dependent and Kit-independent MC-deficient mice) were treated with 2-4-dinitrofluorobenzene-induced CHS, and showed attenuated CHS responses. Furthermore, MC-specific depletion of IL-10 did not affect the CHS response (23). Thus, MCs seem to change their roles depending on the type and concentration of haptens, although the molecular mechanisms underlying the switch of MC function in each context remain unclear. CHS protocol (e.g. interval between sensitization and elicitation, skin site of sensitization), the parameter used to measure inflammation, and the timing of analysis after the elicitation (e.g. early versus late phase) are other potential variables that would influence the functions of MCs or phenotype of MC-deficient mice in CHS. In the early phase, MCs may facilitate CHS by releasing inflammatory mediators such as TNF and histamine (23), while in the late phase, MCs may limit CHS by producing anti-inflammatory mediators such as IL-10 (15).

TABLE 1 | A summary of references regarding the regulatory functions of mast cells in the skin.

Mouse model	Regulatory mechanisms (reference)
Contact hypersensitivity	Production of IL-10 (14, 15)
	Maintenance of Bregs via IL-5 (16)
	Reduction of T_{RM}s by degradation of IL-15 (17)
	PD-1/PD-L1 signaling (18)
Atopic dermatitis	Maintenance of Tregs via IL-2 (19)
Malignant melanoma	Recruitment of Tregs (20)
	Induction of M2 macrophages by histamine (21)

Maintenance of Regulatory B cells

In addition to MCs, IL-10 is produced by several cell populations, such as regulatory T cells (Tregs) and regulatory B cells (Bregs). Both cell populations play crucial roles in the termination of the CHS response (22, 31). Kim et al. reported that MCs inhibit CHS responses by maintaining the IL-10^+ Breg number in skin-draining LNs in an IL-5-dependent manner (16). In oxazolone-induced CHS, *Kit*$^{W\text{-}sh/W\text{-}sh}$ mice showed an augmented CHS response, which was accompanied by a reduced IL-10^+ Breg number in the skin-draining LNs. Reconstitution with MCs restored the population of IL-10^+ Bregs in *Kit*$^{W\text{-}sh/W\text{-}sh}$ mice and suppressed the CHS response. The level of IL-5 was markedly decreased in the LNs of *Kit*$^{W\text{-}sh/W\text{-}sh}$ mice and was restored by reconstitution of MCs. This recovery of Breg number and IL-5 level in LNs was diminished under reconstitution with IL-$5^{-/-}$ MCs. Based on these results, it has been proposed that MCs perform regulatory functions in CHS by maintaining Breg number in LNs (16). MCs may increase IL-10 levels in peripheral tissues by producing IL-10 themselves and by maintaining IL-10-producing cell populations, such as Bregs.

Maintenance of Resident Memory T Cells

Skin-resident memory T (T_{RM}) cells are a subset of memory T cells that provide local surveillance and do not migrate out of the skin (32). Upon inflammation, effector T cells infiltrate the skin, and some of them become T_{RM} cells, mostly $CD8^+$ T_{RM} cells. IL-7, IL-15, and transforming growth factor (TGF)-β are pivotal cytokines that generate the skin T_{RM} cells (32). Skin T_{RM} cells protect the body from the invasion of pathogens; however, they are also involved in the development of various inflammatory skin diseases, including contact dermatitis.

Using oxazolone-induced CHS, Gimenez-Rivera et al. examined the relationship between MCs and $CD8^+$ T_{RM} cells in skin (17). The authors modified CHS *via* repeated elicitation at long intervals (elicitation at 30 days and 60 days after the 1st elicitation), which led to the accumulation of antigen-specific T_{RM} cells in the elicited skin. Under these conditions, the CHS response was significantly increased in *Kit*$^{W\text{-}sh/W\text{-}sh}$ and *Mcpt5-Cre*$^+$*iDTR* mice. The number of $CD8^+$ T_{RM} cells was significantly higher in MC-deficient mice than in control WT mice. In addition, the expression levels of IL-15, but not IL-7 and TGF-β, were upregulated in MC-deficient mice. *In vitro*, the MC proteases such as chymase and carboxypeptidase degraded IL-15. These results suggest that MCs limit skin inflammation in CHS by regulating the T_{RM} cell number *via* IL-15 degradation (17).

Programmed Cell Death Protein-1/ Programmed Cell Death-Ligand 1 Signaling

The abovementioned regulatory functions of MCs are exhibited in a contact-independent manner *via* cytokine production. However, MCs can also exhibit regulatory functions by direct contact *via* the programmed cell death-1 (PD-1, CD279)/ programmed cell death-ligand 1 (PD-L1, CD274) pathway (18). The PD-1/PD-L1 pathway is a negative regulator that coordinates the balance between T cell activation and tolerance (33). PD-1 expressed on effector T cells binds to PD-L1 expressed on various tissue-resident and antigen-presenting cells and transduces signals that inhibit the proliferation of T cells and their effector functions.

To investigate the mechanisms by which the PD-1/PD-L1 pathway regulates T cell activation in CHS, we induced CHS in *Pdl1*$^{-/-}$ mice and found that *Pdl1*$^{-/-}$ and WT mice treated with the anti-PD-L1 antibody exhibited an exacerbated CHS response, indicating that the PD-1/PD-L1 pathway is important for the negative regulation of the CHS response. However, the effect of the anti-PD-L1 antibody on the CHS response was abolished in MC-deficient mice, suggesting that MCs are involved in PD-1/ PD-L1-mediated negative regulation of effector T cells. Skin MCs highly express PD-L1 in both mice and humans. MCs interact with T cells in the skin, as revealed by two-photon microscopic observations. In a co-culture system of effector T cells and MCs, effector T cell activation was induced by WT MCs, which was further enhanced by *Pdl1*$^{-/-}$ MCs or *via* the blockade of the PD-1/ PD-L1 pathway by the anti-PD-L1 antibody. These results suggest that MCs directly contact effector T cells in the skin and negatively regulate their activation *via* the PD-1/PD-L1 pathway (18).

ATOPIC DERMATITIS

Atopic dermatitis (AD) is a common chronic inflammatory skin disease. Type 2 cytokines, especially IL-4 and IL-13, are central mediators that induce various symptoms in AD, such as pruritus and skin barrier defects (34). The number of MCs is significantly increased in the skin lesions of AD, suggesting the involvement of MCs in the establishment of AD. Similar to the studies on CHS, both pro- and anti-inflammatory functions of MCs have been reported in the AD model, which may be dependent on the model used in the study.

Regulatory Function of MCs in AD: Maintenance of Tregs (Oxazolone-Induced AD Model)

As mentioned in section 1, oxazolone is a representative hapten to induce CHS, a type 1 immune response in the skin. Single time application of oxazolone following the sensitization (at intervals of 5-7 days) induces CHS. However, repeated and frequent application of oxazolone (5-10 times at intervals of a few days) causes type 2 cytokine-shifted inflammation in the skin and is used as an AD model (35). *Kit*$^{W\text{-}sh/W\text{-}sh}$ mice exhibited exacerbated dermatitis, whereas adoptive transfer of WT MCs

into $Kit^{W\text{-}sh/W\text{-}sh}$ mice decreased the inflammatory response, indicating that MCs play a suppressive role in this AD model (19). The suppressive effects of MC reconstitution were not observed in $Il2^{-/-}$ MCs, suggesting that MC-derived IL-2 is involved in the suppression mechanism. Since the ratio of activated T cells to Tregs in the skin was significantly higher in $Kit^{W\text{-}sh/W\text{-}sh}$ mice reconstituted with $Il2^{-/-}$ MCs than in those reconstituted with WT MCs, it was concluded that MCs inhibit dermatitis by maintaining Tregs *via* IL-2 production (19). Exacerbated phenotypes in $Kit^{W\text{-}sh/W\text{-}sh}$ mice have also been reported in the MC903-induced AD model (36), but the underlying mechanisms by which MCs suppress inflammation in this model remain unclear.

Pro-Inflammatory Function of MCs in AD (House Dust Mite/Staphylococcal Enterotoxin B -Induced AD Model)

Repeated treatment with *Dermatophagoides farinae* (house dust mite: HDM) extract and staphylococcal enterotoxin B (SEB) induces skin inflammation that mimics AD (37). Clinical scores were significantly lower in $Kit^{W\text{-}sh/W\text{-}sh}$ mice and Kit-independent MC-deficient mice (*Cpa3-Cre*$^{+}$*Mcl-1f/f*) than in the corresponding WT mice, indicating that MCs are required for maximal skin inflammation in this model (38). Since the Fc receptor for IgE-deficient ($FcεRI^{-/-}$) mice also showed reduced skin inflammation in this model, the authors speculated that MCs facilitate atopic skin inflammation *via* FcεRI-dependent mechanisms. In another study using the same HDM/SEB-induced AD model, Serhan et al. revealed that MCs promote atopic skin inflammation by interacting with the nociceptive sensory neurons (nociceptors) (39). HDM directly activates nociceptors, which produce substance P. Substance P induces the activation of MCs surrounding nociceptors *via* the Mas-related G protein-coupled receptor B (MRGPRB), a receptor for cationic molecules from the MRGPR family. These results suggest that after exposure to HDM allergens, nociceptors sense the allergens and induce MC degranulation *via* the activation of MRGPRB on MCs, leading to the initiation of type 2 inflammation.

Therefore, in AD lesions, MCs may play facilitating roles *via* the release of various chemical mediators by degranulation, which may induce both IgE-dependent (FcεRI-mediated) and independent (MRGPRB-mediated) responses. In contrast, MCs may play regulatory roles in AD by maintaining Treg number and suppressing Th2 cell activation.

MALIGNANT MELANOMA

Malignant melanoma (MM) is one of the most malignant types of skin cancer (40). Previous studies on the involvement of MCs in MM development have mostly been based on histological analysis investigating the number of MCs surrounding the MM and its relation to prognosis. Some reports have shown a correlation between tumor progression and the number of MCs surrounding the tumors (41, 42), whereas others have shown a decrease in the number of MCs in advanced MM (43, 44); therefore, the results have not been consistent. Recent studies using mouse MM models have shown both beneficial and detrimental roles of MCs in MM development (20, 45).

Kaesler et al. reported the beneficial role of MCs in the antitumor response in MM (45). The authors first identified that patients exhibiting better responses to anti-cytotoxic T-lymphocyte antigen 4 (CTLA4) antibody treatment developed colitis as an immune-mediated adverse effect with a systemic lipopolysaccharide (LPS) signature. In a mouse model of MM using the B16 melanoma cell line, LPS treatment reduced the tumor volume. MC-deficient mice (*Mcpt5-cre*$^{+}$ R-$DTA^{fl/fl}$) showed increased tumor volume compared to control WT mice, and the suppressive effect of LPS treatment on tumor volume was not observed in MC-deficient mice. Based on these results, the authors concluded that the effective immune control of MM by the anti-CTLA4 antibody was dependent on LPS-activated MCs, which recruit tumor-infiltrating effector T cells *via* secretion of C-X-C motif chemokine ligand 10 (45).

In contrast, Somasundaram et al. reported an association between MCs and resistance to anti-PD-1 therapy in MM (20). Using humanized mice and melanomas from human patients, the authors first examined the immune cell changes in tumors after treatment with anti-PD-1 antibodies. Immunohistochemical and flow cytometric analyses revealed that MC numbers were increased in the group resistant to anti-PD-1 antibodies. Furthermore, RNA sequence analysis of tumors from patients with MM before and after anti-PD-1 antibody treatment showed an increase in MC number after treatment, especially in the non-responder group. Meanwhile, the elimination of MCs with sunitinib enhanced the therapeutic effects of the anti-PD1 antibody in the humanized MM model. Mechanistically, numerous Treg infiltrations were observed around the MCs at tumor sites, correlating with decreased MHC class I expression in the surrounding tumors. These findings suggest that MCs may promote tumor progression by downregulating tumor MHC class I expression by recruiting Tregs, either directly or indirectly. Histamine from MCs may contribute to tumor promotion by enhancing peritumoral M2 macrophage differentiation and suppressing $CD8^{+}$ T cell activity (21). These results suggest that the depletion of MCs or downregulation of MC function can be used as potential therapeutic strategies for MM.

DISCUSSION

As described above, MCs perform immunosuppressive functions *via* diverse mechanisms, at least in mice (**Table 1**). At the initial stage of inflammation or when the extent of inflammation is low, MCs may play a role in promoting inflammation. However, at the late stage of inflammation or when inflammation becomes excessive, MCs may switch their role from pro- to anti-inflammatory and fine-tune inflammation to avoid undesired tissue damage (11, 15). In the cancer environment, where the activation of innate and acquired immune systems is necessary for the elimination of tumors, such regulatory functions by MCs may become deleterious to the host.

However, many open questions are unanswered. For example, signals that induce the regulatory functions of skin MCs are not yet fully understood. As for the signals that induce IL-10 production from skin MCs, a few pathways, such as vitamin D receptor signaling-dependent pathway and the IgE signaling-dependent pathway, have been reported (12, 46). Analysis of the signal-transducing molecules in those pathways may become a clue to understand the molecular mechanisms by which MCs acquire regulatory functions. Besides, skin MCs may be heterogenous populations as reported in MCs in other organs such as lung (47) and esophagus (48), and MCs with regulatory functions, such as IL-10-producing MCs, may be a particular MC subset in the skin. Indeed, while skin MCs under physiological state are maintained by local proliferation in adult skin (5, 6), bone marrow-derived MCs appear in the skin in inflammatory state (49, 50), suggesting that skin MCs may be heterogenous populations (skin resident MCs versus bone marrow-derived MCs). We are currently investigating the functional differences between those MC populations. In addition, since there are various discrepancies in the pathogenesis of human diseases and mouse disease models, elucidating the physiological significance of MCs in human diseases remains a challenge. Skin organoids/human skin equivalent systems as intermediates between mouse disease models and human patients constitute a promising strategy that will likely lead to a better understanding of the role of MC in skin diseases. Human cutaneous MCs produce minimal IL-10 (51, 52); therefore, whether IL-10-mediated regulation by MCs, as revealed by mouse studies, is actually involved in human diseases remains to be verified. Nevertheless, elucidation of the molecular mechanisms that control MC function may lead to the development of novel therapeutic strategies for inflammatory skin diseases and skin cancers.

AUTHOR CONTRIBUTIONS

All authors listed have made a substantial, direct, and intellectual contribution to the work and approved it for publication.

FUNDING

This work was supported by the Japan Society for the Promotion of Science KAKENHI (JP19K08790, JP15H05906 [T.H.], Japan Science, Japan Agency for Medical Research and Development (AMED) (19ek0410062s0201) [T.H.], Kose Cosmetology Research Foundation [T.H.], Lydia O'leary Memorial Pias Dermatological Foundation [T.H.]

REFERENCES

1. Kabashima K, Honda T, Ginhoux F, Egawa G. The Immunological Anatomy of the Skin. *Nat Rev Immunol* (2019) 19(1):19–30. doi: 10.1038/s41577-018-0084-5
2. Dwyer DF, Barrett NA, Austen KF. Immunological Genome Project C. Expression Profiling of Constitutive Mast Cells Reveals a Unique Identity Within the Immune System. *Nat Immunol* (2016) 17(7):878–87. doi: 10.1038/ni.3445
3. Kitamura Y, Shimada M, Hatanaka K, Miyano Y. Development of Mast Cells From Grafted Bone Marrow Cells in Irradiated Mice. *Nature* (1977) 268 (5619):442–3. doi: 10.1038/268442a0
4. Hallgren J, Gurish MF. Pathways of Murine Mast Cell Development and Trafficking: Tracking the Roots and Routes of the Mast Cell. *Immunol Rev* (2007) 217:8–18. doi: 10.1111/j.1600-065X.2007.00502.x
5. Gentek R, Ghigo C, Hoeffel G, Bulle MJ, Msallam R, Gautier G, et al. Hemogenic Endothelial Fate Mapping Reveals Dual Developmental Origin of Mast Cells. *Immunity* (2018) 48(6):1160–71.e5. doi: 10.1016/j.immuni.2018.04.025
6. Li Z, Liu S, Xu J, Zhang X, Han D, Liu J, et al. Adult Connective Tissue-Resident Mast Cells Originate From Late Erythro-Myeloid Progenitors. *Immunity* (2018) 49(4):640–53.e5. doi: 10.1016/j.immuni.2018.09.023
7. Elieh Ali Komi D, Wohrl S, Bielory L. Mast Cell Biology at Molecular Level: A Comprehensive Review. *Clin Rev Allergy Immunol* (2020) 58(3):342–65. doi: 10.1007/s12016-019-08769-2
8. Honda Y, Ono S, Honda T, Kataoka TR, Egawa G, Kitoh A, et al. Murine Neonatal Skin Mast Cells Are Phenotypically Immature and Minimally Sensitized With Transplacentally Transferred Ige. *J Allergy Clin Immunol* (2019) 144(2):617–20.e5. doi: 10.1016/j.jaci.2019.05.011
9. Galli SJ, Gaudenzio N, Tsai M. Mast Cells in Inflammation and Disease: Recent Progress and Ongoing Concerns. *Annu Rev Immunol* (2020) 38:49–77. doi: 10.1146/annurev-immunol-071719-094903
10. Zhang Z, Kurashima Y. Two Sides of the Coin: Mast Cells as a Key Regulator of Allergy and Acute/Chronic Inflammation. *Cells* (2021) 10(7):1615–33. doi: 10.3390/cells10071615
11. Gaudenzio N, Marichal T, Galli SJ, Reber LL. Genetic and Imaging Approaches Reveal Pro-Inflammatory and Immunoregulatory Roles of Mast Cells in Contact Hypersensitivity. *Front Immunol* (2018) 9:1275. doi: 10.3389/fimmu.2018.01275
12. Nagata K, Nishiyama C. Il-10 in Mast Cell-Mediated Immune Responses: Anti-Inflammatory and Proinflammatory Roles. *Int J Mol Sci* (2021) 22 (9):4972–87. doi: 10.3390/ijms22094972
13. Voss M, Kotrba J, Gaffal E, Katsoulis-Dimitriou K, Dudeck A. Mast Cells in the Skin: Defenders of Integrity or Offenders in Inflammation? *Int J Mol Sci* (2021) 22(9):4589–619. doi: 10.3390/ijms22094589
14. Grimbaldeston MA, Nakae S, Kalesnikoff J, Tsai M, Galli SJ. Mast Cell-Derived Interleukin 10 Limits Skin Pathology in Contact Dermatitis and Chronic Irradiation With Ultraviolet B. *Nat Immunol* (2007) 8(10):1095–104. doi: 10.1038/ni1503
15. Reber LL, Sibilano R, Starkl P, Roers A, Grimbaldeston MA, Tsai M, et al. Imaging Protective Mast Cells in Living Mice During Severe Contact Hypersensitivity. *JCI Insight* (2017) 2(9). doi: 10.1172/jci.insight.92900
16. Kim HS, Lee MB, Lee D, Min KY, Koo J, Kim HW, et al. The Regulatory B Cell-Mediated Peripheral Tolerance Maintained by Mast Cell Il-5 Suppresses Oxazolone-Induced Contact Hypersensitivity. *Sci Adv* (2019) 5(7):eaav8152. doi: 10.1126/sciadv.aav8152
17. Gimenez-Rivera VA, Siebenhaar F, Zimmermann C, Siiskonen H, Metz M, Maurer M. Mast Cells Limit the Exacerbation of Chronic Allergic Contact Dermatitis in Response to Repeated Allergen Exposure. *J Immunol* (2016) 197 (11):4240–6. doi: 10.4049/jimmunol.1600236
18. Hirano T, Honda T, Kanameishi S, Honda Y, Egawa G, Kitoh A, et al. Pd-L1 on Mast Cells Suppresses Effector Cd8(+) T-Cell Activation in the Skin in Murine Contact Hypersensitivity. *J Allergy Clin Immunol* (2021) 148(2):563–73.e7. doi: 10.1016/j.jaci.2020.12.654
19. Hershko AY, Suzuki R, Charles N, Alvarez-Errico D, Sargent JL, Laurence A, et al. Mast Cell Interleukin-2 Production Contributes to Suppression of Chronic Allergic Dermatitis. *Immunity* (2011) 35(4):562–71. doi: 10.1016/j.immuni.2011.07.013
20. Somasundaram R, Connelly T, Choi R, Choi H, Samarkina A, Li L, et al. Tumor-Infiltrating Mast Cells Are Associated With Resistance to Anti-Pd-1 Therapy. *Nat Commun* (2021) 12(1):346. doi: 10.1038/s41467-020-20600-7
21. Li H, Xiao Y, Li Q, Yao J, Yuan X, Zhang Y, et al. The Allergy Mediator Histamine Confers Resistance to Immunotherapy in Cancer Patients *Via*

Activation of the Macrophage Histamine Receptor H1. *Cancer Cell* (2022) 40 (1):36–52.e9. doi: 10.1016/j.ccell.2021.11.002
22. Honda T, Egawa G, Grabbe S, Kabashima K. Update of Immune Events in the Murine Contact Hypersensitivity Model: Toward the Understanding of Allergic Contact Dermatitis. *J Invest Dermatol* (2013) 133(2):303–15. doi: 10.1038/jid.2012.284
23. Dudeck A, Dudeck J, Scholten J, Petzold A, Surianarayanan S, Kohler A, et al. Mast Cells Are Key Promoters of Contact Allergy That Mediate the Adjuvant Effects of Haptens. *Immunity* (2011) 34(6):973–84. doi: 10.1016/j.immuni.2011.03.028
24. Otsuka A, Kubo M, Honda T, Egawa G, Nakajima S, Tanizaki H, et al. Requirement of Interaction Between Mast Cells and Skin Dendritic Cells to Establish Contact Hypersensitivity. *PloS One* (2011) 6(9):e25538. doi: 10.1371/journal.pone.0025538
25. Skokos D, Botros HG, Demeure C, Morin J, Peronet R, Birkenmeier G, et al. Mast Cell-Derived Exosomes Induce Phenotypic and Functional Maturation of Dendritic Cells and Elicit Specific Immune Responses *in Vivo*. *J Immunol* (2003) 170(6):3037–45. doi: 10.4049/jimmunol.170.6.3037
26. Weber FC, Nemeth T, Csepregi JZ, Dudeck A, Roers A, Ozsvari B, et al. Neutrophils Are Required for Both the Sensitization and Elicitation Phase of Contact Hypersensitivity. *J Exp Med* (2015) 212(1):15–22. doi: 10.1084/jem.20130062
27. Moniaga CS, Watanabe S, Honda T, Nielsen S, Hara-Chikuma M. Aquaporin-9-Expressing Neutrophils Are Required for the Establishment of Contact Hypersensitivity. *Sci Rep* (2015) 5:15319. doi: 10.1038/srep15319
28. Biedermann T, Kneilling M, Mailhammer R, Maier K, Sander CA, Kollias G, et al. Mast Cells Control Neutrophil Recruitment During T Cell-Mediated Delayed-Type Hypersensitivity Reactions Through Tumor Necrosis Factor and Macrophage Inflammatory Protein 2. *J Exp Med* (2000) 192(10):1441–52. doi: 10.1084/jem.192.10.1441
29. Dudeck J, Medyukhina A, Frobel J, Svensson CM, Kotrba J, Gerlach M, et al. Mast Cells Acquire Mhcii From Dendritic Cells During Skin Inflammation. *J Exp Med* (2017) 214(12):3791–811. doi: 10.1084/jem.20160783
30. Norman MU, Hwang J, Hulliger S, Bonder CS, Yamanouchi J, Santamaria P, et al. Mast Cells Regulate the Magnitude and the Cytokine Microenvironment of the Contact Hypersensitivity Response. *Am J Pathol* (2008) 172(6):1638–49. doi: 10.2353/ajpath.2008.070559
31. van de Veen W, Stanic B, Wirz OF, Jansen K, Globinska A, Akdis M. Role of Regulatory B Cells in Immune Tolerance to Allergens and Beyond. *J Allergy Clin Immunol* (2016) 138(3):654–65. doi: 10.1016/j.jaci.2016.07.006
32. Tokura Y, Phadungsaksawasdi P, Kurihara K, Fujiyama T, Honda T. Pathophysiology of Skin Resident Memory T Cells. *Front Immunol* (2020) 11:618897. doi: 10.3389/fimmu.2020.618897
33. Keir ME, Butte MJ, Freeman GJ, Sharpe AH. Pd-1 and Its Ligands in Tolerance and Immunity. *Annu Rev Immunol* (2008) 26:677–704. doi: 10.1146/annurev.immunol.26.021607.090331
34. Honda T, Kabashima K. Reconciling Innate and Acquired Immunity in Atopic Dermatitis. *J Allergy Clin Immunol* (2020) 145(4):1136–7. doi: 10.1016/j.jaci.2020.02.008
35. Kitagaki H, Ono N, Hayakawa K, Kitazawa T, Watanabe K, Shiohara T. Repeated Elicitation of Contact Hypersensitivity Induces a Shift in Cutaneous Cytokine Milieu From a T Helper Cell Type 1 to a T Helper Cell Type 2 Profile. *J Immunol* (1997) 159(5):2484–91.
36. Svanberg S, Li Z, Ohlund P, Roy A, Abrink M. Mast Cells Limit Ear Swelling Independently of the Chymase Mouse Mast Cell Protease 4 in an Mc903-Induced Atopic Dermatitis-Like Mouse Model. *Int J Mol Sci* (2020) 21 (17):6311–28. doi: 10.3390/ijms21176311
37. Kawakami Y, Yumoto K, Kawakami T. An Improved Mouse Model of Atopic Dermatitis and Suppression of Skin Lesions by an Inhibitor of Tec Family Kinases. *Allergol Int* (2007) 56(4):403–9. doi: 10.2332/allergolint.O-07-486
38. Ando T, Matsumoto K, Namiranian S, Yamashita H, Glatthorn H, Kimura M, et al. Mast Cells Are Required for Full Expression of Allergen/Seb-Induced Skin Inflammation. *J Invest Dermatol* (2013) 133(12):2695–705. doi: 10.1038/jid.2013.250
39. Serhan N, Basso L, Sibilano R, Petitfils C, Meixiong J, Bonnart C, et al. House Dust Mites Activate Nociceptor-Mast Cell Clusters to Drive Type 2 Skin Inflammation. *Nat Immunol* (2019) 20(11):1435–43. doi: 10.1038/s41590-019-0493-z
40. Curti BD, Faries MB. Recent Advances in the Treatment of Melanoma. *N Engl J Med* (2021) 384(23):2229–40. doi: 10.1056/NEJMra2034861
41. Ribatti D, Ennas MG, Vacca A, Ferreli F, Nico B, Orru S, et al. Tumor Vascularity and Tryptase-Positive Mast Cells Correlate With a Poor Prognosis in Melanoma. *Eur J Clin Invest* (2003) 33(5):420–5. doi: 10.1046/j.1365-2362.2003.01152.x
42. Ribatti D, Vacca A, Ria R, Marzullo A, Nico B, Filotico R, et al. Neovascularisation, Expression of Fibroblast Growth Factor-2, and Mast Cells With Tryptase Activity Increase Simultaneously With Pathological Progression in Human Malignant Melanoma. *Eur J Cancer* (2003) 39 (5):666–74. doi: 10.1016/s0959-8049(02)00150-8
43. Biswas A, Richards JE, Massaro J, Mahalingam M. Mast Cells in Cutaneous Tumors: Innocent Bystander or Maestro Conductor? *Int J Dermatol* (2014) 53 (7):806–11. doi: 10.1111/j.1365-4632.2012.05745.x
44. Siiskonen H, Poukka M, Bykachev A, Tyynela-Korhonen K, Sironen R, Pasonen-Seppanen S, et al. Low Numbers of Tryptase+ and Chymase+ Mast Cells Associated With Reduced Survival and Advanced Tumor Stage in Melanoma. *Melanoma Res* (2015) 25(6):479–85. doi: 10.1097/CMR.0000000000000192
45. Kaesler S, Wolbing F, Kempf WE, Skabytska Y, Koberle M, Volz T, et al. Targeting Tumor-Resident Mast Cells for Effective Anti-Melanoma Immune Responses. *JCI Insight* (2019) 4(19). doi: 10.1172/jci.insight.125057
46. Biggs L, Yu C, Fedoric B, Lopez AF, Galli SJ, Grimbaldeston MA. Evidence That Vitamin D(3) Promotes Mast Cell-Dependent Reduction of Chronic Uvb-Induced Skin Pathology in Mice. *J Exp Med* (2010) 207(3):455–63. doi: 10.1084/jem.20091725
47. Derakhshan T, Samuchiwal SK, Hallen N, Bankova LG, Boyce JA, Barrett NA, et al. Lineage-Specific Regulation of Inducible and Constitutive Mast Cells in Allergic Airway Inflammation. *J Exp Med* (2021) 218(1). doi: 10.1084/jem.20200321
48. Ben-Baruch Morgenstern N, Ballaban AY, Wen T, Shoda T, Caldwell JM, Kliewer K, et al. Single-Cell Rna Sequencing of Mast Cells in Eosinophilic Esophagitis Reveals Heterogeneity, Local Proliferation and Activation That Persists in Remission. *J Allergy Clin Immunol* (2022). doi: 10.1016/j.jaci.2022.02.025
49. Weitzmann A, Naumann R, Dudeck A, Zerjatke T, Gerbaulet A, Roers A. Mast Cells Occupy Stable Clonal Territories in Adult Steady-State Skin. *J Invest Dermatol* (2020) 140(12):2433–41.e5. doi: 10.1016/j.jid.2020.03.963
50. Sonoda T, Tsuyama K, Kitamura Y, Tanooka H. Different Effects of Dimethylbenz(Alpha)Anthracene and Tetradecanoylphorbol Acetate on Differentiation of Mast Cells in the Skin of Mice. *Am J Pathol* (1982) 106 (3):312–7.
51. Motakis E, Guhl S, Ishizu Y, Itoh M, Kawaji H, de Hoon M, et al. Redefinition of the Human Mast Cell Transcriptome by Deep-Cage Sequencing. *Blood* (2014) 123(17):e58–67. doi: 10.1182/blood-2013-02-483792
52. Rennick D, Hunte B, Holland G, Thompson-Snipes L. Cofactors Are Essential for Stem Cell Factor-Dependent Growth and Maturation of Mast Cell Progenitors: Comparative Effects of Interleukin-3 (Il-3), Il-4, Il-10, and Fibroblasts. *Blood* (1995) 85(1):57–65. doi: 10.1182/blood.V85.1.57.bloodjournal85157

Conflict of Interest: The authors declare that the research was conducted in the absence of any commercial or financial relationships that could be construed as a potential conflict of interest.

Publisher's Note: All claims expressed in this article are solely those of the authors and do not necessarily represent those of their affiliated organizations, or those of the publisher, the editors and the reviewers. Any product that may be evaluated in this article, or claim that may be made by its manufacturer, is not guaranteed or endorsed by the publisher.

Copyright © 2022 Honda and Keith. This is an open-access article distributed under the terms of the Creative Commons Attribution License (CC BY). The use, distribution or reproduction in other forums is permitted, provided the original author(s) and the copyright owner(s) are credited and that the original publication in this journal is cited, in accordance with accepted academic practice. No use, distribution or reproduction is permitted which does not comply with these terms.

frontiers | Frontiers in Immunology

MINI REVIEW
published: 17 May 2022
doi: 10.3389/fimmu.2022.883692

The Potential Role of Basophils in Urticaria

Riko Takimoto-Ito[1], *Ni Ma*[2], *Izumi Kishimoto*[2], *Kenji Kabashima*[1] *and Naotomo Kambe*[1,2*]

[1] Department of Dermatology, Kyoto University Graduate School of Medicine, Kyoto, Japan, [2] Department of Dermatology, Kansai Medical University, Hirakata, Japan

Urticaria is a symptom of acute skin allergies that is not clearly understood, but mast cell histamine is hypothesized to cause swelling and itching. Omalizumab, an anti-human IgE antibody that traps IgE and prevents its binding to high-affinity IgE receptors, is effective in treating urticaria. We recently experienced a case of urticaria refractory to antihistamine therapy in which the peripheral-blood basophil count responded to omalizumab therapy and its withdrawal. Furthermore, the peripheral-blood basophils showed an unexpected increase in the expression of a cell surface activation marker. This phenomenon has been reported by other analyses of basophil and mast cell dynamics during omalizumab treatment. Here, we analyze these observations and formulate a hypothesis for the role of basophils in urticaria. Specifically, that activated basophils migrate to the local skin area, lowering peripheral-blood counts, omalizumab therapy alters basophilic activity and causes their stay in the peripheral blood. We hope that our analysis will focus urticaria research on basophils and reveal new aspects of its pathogenesis.

Keywords: basophil, urticaria, mast cell, IgE, omalizumab

OPEN ACCESS

Edited by:
Satoshi Tanaka,
Kyoto Pharmaceutical University, Japan

Reviewed by:
Bettina Wedi,
Hannover Medical School, Germany

***Correspondence:**
Naotomo Kambe
nkambe@kuhp.kyoto-u.ac.jp

Specialty section:
This article was submitted to Inflammation, a section of the journal Frontiers in Immunology

Received: *25 February 2022*
Accepted: *20 April 2022*
Published: *17 May 2022*

Citation:
Takimoto-Ito R, Ma N, Kishimoto I, Kabashima K and Kambe N (2022) The Potential Role of Basophils in Urticaria. Front. Immunol. 13:883692. doi: 10.3389/fimmu.2022.883692

INTRODUCTION

Urticaria is a common skin disease characterized by itchy, red, raised bumps or hives. It is generally classified based on its duration, acute (≦ 6 weeks) or chronic (>6 weeks), and the relevance of eliciting factors, spontaneous (no specific eliciting factor involved) or inducible (specific eliciting factor involved) (1). Based on these classifications, chronic spontaneous urticaria (CSU) is diagnosed based a duration of over 6 weeks and the absence of identifiable eliciting factors.

The etiology and pathogenesis of CSU remain largely unexplored. However, there is a consensus that cutaneous mast cells play a major role by releasing histamine, which acts on blood vessels and nerves to cause swelling and provoke itching, respectively. Antihistamine is the standard treatment for urticaria and antihistamine-resistant patients are well-controlled with omalizumab, an anti-human IgE antibody, which reconfirms that IgE is important in the pathology of urticaria, even in CSU with unknown triggers.

PERIPHERAL BLOOD BASOPHIL COUNTS AND THE DISEASE ACTIVITY OF CSU

We recently reported a case with a 6-year history of severe CSU, whose peripheral basophil count was persistently low (almost zero cells per μL) for more than 1 year (2). Upon urticaria resolution by omalizumab administration, we noticed that the peripheral basophil count had increased. When the patient discontinued omalizumab, the peripheral blood basophil count again dropped to zero and urticaria recurred. Restarting omalizumab rescued the peripheral blood basophil count and improved the skin rash. Before our observation, this inverse correlation with basophil count and urticarial activity has been confirmed by clinical trials of omalizumab (3) in which they quantified peripheral-blood basophils using blood histamine levels and flow cytometry. The study authors found that both parameters increased with omalizumab treatment and clinical CSU improvement.

The contribution of basophils to allergic reactions, acquired immunity, and autoimmune diseases is better understood (4, 5), though it was long ignored or confused with that of tissue-resident mast cells. This may be because basophils account for less than 1% of granulocytes in the peripheral blood and are phenotypically similar to mast cells. Both cell types have basophilic granules in their cytoplasm, high-affinity IgE receptors (FcεRI) on their surface, and release histamine and other chemical mediators.

The fact that basophils express FcεRI and release histamine, together with observation that the basophils in peripheral blood inversely correlate with urticarial rash severity, suggests that basophils play a role in CSU. Indeed, as omalizumab has become more frequently used in the treatment of CSU refractory to antihistamine therapy, a number of reports have examined potential predictors of its efficacy (6–10). Many studies have demonstrated that low total IgE levels are an essential marker for discriminating the efficacy of omalizumab. Fok et al. (9) found that low IgE levels in CSU patients did not respond to omalizumab or had only a weak effect, but there was no evidence to suggest which marker was effective. Aghdam et al. (10) evaluated whole blood leukocytes responses in CSU patients treated with omalizumab to elucidate the effect of omalizumab on different FcεRI-bearing leukocytes, only percentage of basophil increased after omalizumab treatment, but other white blood cells remain stable. As for baseline characteristics of CSU patients, Johal et al. (6) reported higher symptom scores and slower symptom improvement with omalizumab treatment in those with decreased peripheral blood basophils than in those without, which is consistent with previous studies focusing on basopenia as a marker of disease severity (11). Rijavec et al. (7) reported that a very low number of absolute basophil count in the circulation (1.7 basophils/μL) is predictive of a poor response to omalizumab. Furthermore, low circulating basophils count significantly correlated with very low densities of FcεRI and IgE on basophils. They also confirmed the basopenia using the low expression of basophil-related genes in the whole-blood genes, including *FCER1A* that codes α-chain of FcεRI, *CPA3* that codes carboxypeptidase A3, and *HDC* that involves histamine synthesis.

The phenomenon that basophils are inversely correlated with CSU severity is not specific to omalizumab treatment, as it was also observed in CSU patients treated with antihistamines (12). This report measured symptom severity using the daily baseline urticaria activity score; the more severe the symptoms, the lower the peripheral blood basophil count. Thus, the relationship between peripheral-blood basophils and urticaria severity is not treatment-method dependent.

In clinical practice, basophils account for a very small percentage of peripheral blood cells, which makes it difficult to define an expected value. However, basophil fluctuations can indicate urticaria activity, at least on a patient-by-patient basis.

A BASOPHIL ACTIVATION MARKER INCREASED AFTER THE INITIATION OF OMALIZUMAB

Not only did omalizumab treatment affect peripheral-blood basophil levels (2), it also increased their surface expression of CD203c, which reflects the activation state of basophils (13). It seems a paradoxical phenomenon where peripheral circulating basophils appear to express more CD203c after successful omalizumab treatment. Of course, it is important to consider that CD203c expression is not equivalent to CD63 expression and is not a specific marker for degranulation. Its expression can be driven by IL-3 at least *in vitro* (14), besides IgE-FcεRI cross-linking (15). Therefore, some reports suggest that CD203c expression is not a suitable index for assessing basophil activation in patients with CSU (14).

However, omalizumab has also been reported to enhance sensitivity of human basophils to IgE-mediated stimulation (16–21). Basophils collected from the patients with the sensitivity to cat allergens showed 3- to 125-fold more sensitive to antigen-driven secretion after the treatment with omalizumab (17). Nevertheless, the lack of change in responsiveness to non-IgE-mediated stimuli, e.g., to N-formyl-methionyl-leucyl-phenylalanine, may be worth considering (18).

To explain this, we hypothesized that activated basophils migrate locally to the skin while patients experience CSU symptoms, and inactive or immature basophils unable to show sufficient activity in response to IgE-mediated stimulation remain in the peripheral blood (**Figure 1**, step 1). Once the CSU symptoms are relieved, the basophils with the ability to become fully activated in response to stimuli stay in the peripheral blood, increasing the frequency of peripheral blood basophils that express cell-surface CD203c.

BASOPHIL INFILTRATION OF CSU LESIONS

The BB1 antibody against human basophils has detected basophil infiltration into skin lesions (22–24). In CSU patients, the number of mast cells in autologous serum-induced wheals remains constant

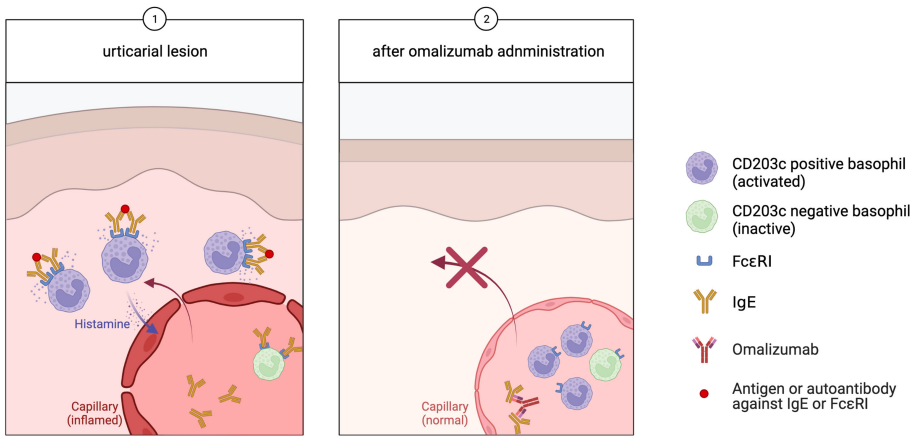


FIGURE 1 | In urticaria, (Step 1) activated basophils migrate to the skin lesions, while inactive basophils remain in the peripheral blood. (Step 2) Omalizumab binds free IgE, which prevents further basophilic activity and a corresponding decrease in FcεRI expression. Activated CD203c-positive basophils stay in the peripheral blood, leading to an increase of the peripheral blood basophil population.

from about 30 minutes to 48 hours after development. However, the number of basophils was high at baseline compared to healthy skin and further increased by about 30 minutes after onset (23). Moreover, the immunohistochemistry analysis of autologous wheals revealed overlapping trends of IL-4 (possibly expressed by activated basophils) and the chemokine receptor CCR3, which are primarily associated with type 2 immune responses. The presence of these molecules peaked at 30 minutes, then began to decline, which suggests that these recruiting mechanisms might attract basophils early in the reaction (23).

The relationship between blood and tissue basophil counts has not been studied in detail. However, given the finding that blood basopenia is frequently observed in CSU patients (25), these reports of the identification of basophils at sites of inflammatory lesions suggest that the decrease in basophils is probably the result of migration of basophils from the circulation to the tissues.

DISCUSSION

Unfortunately, the mechanism for omalizumab efficacy in urticaria is not clear (16). FcεRI are also expressed on dendritic cells (DCs), potent antigen presenting cells, and eosinophils, and there are reports that omalizumab treatment actually deregulates FcεRI expression on DCs (21), but it is assumed that mast cells and basophils are the main cells involved in the pathogenesis of CSU. Another evidence, as well, indicated that DCs do not play a principal role in CSU. Although a reduction in FcεRI expression of CD1c in DCs after omalizumab treatment could be observed (10), this reduction did not correlate with clinical changes. It is well known that the expression of FcεRI on the cell surface of mast cells is regulated by the amount of external IgE (26, 27). The same is true for basophils. This theory is supporting evidence that allergic reactions occur more quickly and severely upon a second exposure than it did after the first. The prevailing hypothesis is that omalizumab binds free IgE, which reduces FcεRI expression on mast cells and basophils.

In atopic dermatitis patients, the omalizumab-dependent reduction of free IgE in the circulating blood is followed by the downregulation of basophilic FcεRI expression as early as 3 days after the first dose (28). In allergic rhinitis patients, the FcεRI expression on basophils had decreased by 88% on day 7 of omalizumab treatment, which is also when the acute allergen wheal size decreased (29). In CSU, and other allergic diseases, the mean basophil-bound IgE and basophil FcεRI expression were noticeably reduced 7 days after initiating omalizumab treatment. These data corresponded with the onset of symptom relief, and basophilic activity remained suppressed throughout the omalizumab treatment period (30).

Our severe CSU patient responded similarly to omalizumab treatment (2). CRA1 antibody confirmed that the amount of FcεRI expressed on basophils decreased, reflecting the result of IgE neutralization by omalizumab. CRA2 antibodies, which recognize the IgE–FcεRI binding site, can measure unbound FcεRI but did not detect any free FcεRI on peripheral-blood basophils before omalizumab administration. These results mean that all the IgE receptors on peripheral-blood basophils are in a state of IgE binding. Flow cytometry confirmed that CRA2-positive basophils appeared only after external IgE was neutralized by omalizumab.

Interestingly, the reduction of FcεRI expression on cutaneous mast cells is much slower than for basophils (**Figure 2**). A previous report indicated that it takes 70 days after omalizumab administration for mast-cell FcεRI expression to be significantly reduced (29). The phenotypic change in cutaneous mast cells observed with omalizumab treatment offers novel insights into the time required for tissue responses and mast cell behavior to shift in CSU (16). The same is observed in cell cultures; when human mast cells, purified from the skin are cultured *in vitro*, the FcεRI expression does not decrease even IgE has been withdrawn for 4 to 8 weeks (31). Unlike peripheral-blood basophils, once skin mast cells have acquired FcεRI expression, its expression does not immediately change when external IgE levels decrease. This difference may be related to the lifespan length of the two cells.

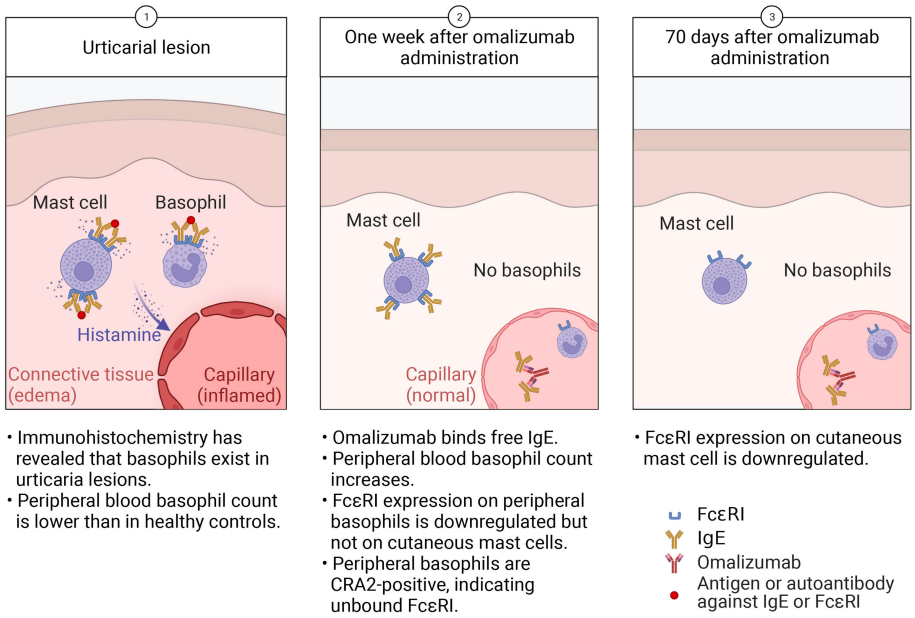


FIGURE 2 | In urticaria, (Step 1) activated cutaneous mast cells and basophils release histamine, which acts on blood vessels to cause swelling. Activated basophils are recruited to the skin lesion, lowering the peripheral-blood basophil count. (Step 2) Within a week of omalizumab administration, the reduction in free IgE leads to decreased FcεRI expression on basophils but not cutaneous mast cells. Activated, $CD203c^{+}$ basophils stay in the peripheral blood. (Step 3) After 70 days of omalizumab treatment, mast-cell FcεRI expression decreases but they remain in the skin.

In basophils, further studies are needed to determine whether the amount of IgE receptors on the same cell can change depending on the amount of external IgE, or whether new cells are mobilized from the bone marrow each time, resulting only in expressing FcεRI dependent on the amount of external IgE.

Thus, that the early (within 7 days) onset of omalizumab's therapeutic effects mirrors basophil dynamics and corresponds with changes in the basophil population leads us to hypothesize that basophils play a large role in CSU pathology (**Figure 2**). Although there is much to learn about urticaria, we expect that focusing on basophils will reveal new aspects of its pathogenesis.

AUTHOR CONTRIBUTIONS

RT-I, IK, NM, KK and NK contributed to conception and design of the study. RT-I and NK wrote the first draft of the manuscript. All authors contributed to manuscript revision, read, and approved the submitted version.

FUNDING

This study was supported by a Grant-in-Aid for Young Scientists (B) to IK (Grant No. 20K17364).

ACKNOWLEDGMENTS

This study was conducted in collaboration with Professor H. Karasuyama and Dr. K. Miyake at the Tokyo Medical and Dental University. Figures were created with BioRender software, ©biorender.com.

REFERENCES

1. Zuberbier T, Abdul Latiff AH, Abuzakouk M, Aquilina S, Asero R, Baker D, et al. The International EAACI/GA(2)LEN/EuroGuiDerm/APAAACI Guideline for the Definition, Classification, Diagnosis, and Management of Urticaria. *Allergy* (2022) 77(3):734–66. doi: 10.1111/all.15090
2. Kishimoto I, Kambe N, Ly NTM, Nguyen CTH, Okamoto H. Basophil Count Is a Sensitive Marker for Clinical Progression in a Chronic Spontaneous Urticaria Patient Treated With Omalizumab. *Allergol Int* (2019) 68(3):388–90. doi: 10.1016/j.alit.2019.02.002
3. Saini SS, Omachi TA, Trzaskoma B, Hulter HN, Rosen K, Sterba PM, et al. Effect of Omalizumab on Blood Basophil Counts in Patients With Chronic Idiopathic/Spontaneous Urticaria. *J Invest Dermatol* (2017) 137(4):958–61. doi: 10.1016/j.jid.2016.11.025
4. Karasuyama H, Miyake K, Yoshikawa S, Yamanishi Y. Multifaceted Roles of Basophils in Health and Disease. *J Allergy Clin Immunol* (2018) 142(2):370–80. doi: 10.1016/j.jaci.2017.10.042
5. Yamanishi Y, Miyake K, Iki M, Tsutsui H, Karasuyama H. Recent Advances in Understanding Basophil-Mediated Th2 Immune Responses. *Immunol Rev* (2017) 278(1):237–45. doi: 10.1111/imr.12548
6. Johal KJ, Chichester KL, Oliver ET, Devine KC, Bieneman AP, Schroeder JT, et al. The Efficacy of Omalizumab Treatment in Chronic Spontaneous Urticaria Is Associated With Basophil Phenotypes. *J Allergy Clin Immunol* (2021) 147(6):2271–80.e8. doi: 10.1016/j.jaci.2021.02.038

7. Rijavec M, Kosnik M, Koren A, Kopac P, Selb J, Vantur R, et al. A Very Low Number of Circulating Basophils Is Predictive of a Poor Response to Omalizumab in Chronic Spontaneous Urticaria. *Allergy* (2021) 76(4):1254–7. doi: 10.1111/all.14577
8. MacGlashan D Jr, Saini S, Schroeder JT. Response of Peripheral Blood Basophils in Subjects With Chronic Spontaneous Urticaria During Treatment With Omalizumab. *J Allergy Clin Immunol* (2021) 147(6):2295–304.e12. doi: 10.1016/j.jaci.2021.02.039
9. Fok JS, Kolkhir P, Church MK, Maurer M. Predictors of Treatment Response in Chronic Spontaneous Urticaria. *Allergy* (2021) 76(10):2965–81. doi: 10.1111/all.14757
10. Alizadeh Aghdam M, Knol EF, van den Elzen M, den Hartog Jager C, van Os-Medendorp H, Knulst AC, et al. Response of FcepsilonRI-Bearing Leucocytes to Omalizumab in Chronic Spontaneous Urticaria. *Clin Exp Allergy* (2020) 50 (3):364–71. doi: 10.1111/cea.13566
11. Huang AH, Chichester KL, Saini SS. Association of Basophil Parameters With Disease Severity and Duration in Chronic Spontaneous Urticaria (CSU). *J Allergy Clin Immunol Pract* (2020) 8(2):793–5.e6. doi: 10.1016/j.jaip.2019.08.004
12. Grattan CE, Dawn G, Gibbs S, Francis DM. Blood Basophil Numbers in Chronic Ordinary Urticaria and Healthy Controls: Diurnal Variation, Influence of Loratadine and Prednisolone and Relationship to Disease Activity. *Clin Exp Allergy* (2003) 33(3):337–41. doi: 10.1046/j.1365-2222.2003.01589.x
13. Buhring HJ, Seiffert M, Giesert C, Marxer A, Kanz L, Valent P, et al. The Basophil Activation Marker Defined by Antibody 97A6 Is Identical to the Ectonucleotide Pyrophosphatase/Phosphodiesterase 3. *Blood* (2001) 97 (10):3303–5. doi: 10.1182/blood.v97.10.3303
14. Gentinetta T, Pecaric-Petkovic T, Wan D, Falcone FH, Dahinden CA, Pichler WJ, et al. Individual IL-3 Priming Is Crucial for Consistent *In Vitro* Activation of Donor Basophils in Patients With Chronic Urticaria. *J Allergy Clin Immunol* (2011) 128(6):1227–34.e5. doi: 10.1016/j.jaci.2011.07.021
15. Kalm F, Mansouri L, Russom A, Lundahl J, Nopp A. Adhesion Molecule Cross-Linking and Cytokine Exposure Modulate IgE- and Non-IgE-Dependent Basophil Activation. *Immunology* (2021) 162(1):92–104. doi: 10.1111/imm.13268
16. Kaplan AP, Gimenez-Arnau AM, Saini SS. Mechanisms of Action That Contribute to Efficacy of Omalizumab in Chronic Spontaneous Urticaria. *Allergy* (2017) 72(4):519–33. doi: 10.1111/all.13083
17. Macglashan DW Jr, Saini SS. Omalizumab Increases the Intrinsic Sensitivity of Human Basophils to IgE-Mediated Stimulation. *J Allergy Clin Immunol* (2013) 132(4):906–11.e1-4. doi: 10.1016/j.jaci.2013.04.056
18. Zaidi AK, Saini SS, Macglashan DWJr. Regulation of Syk Kinase and FcRbeta Expression in Human Basophils During Treatment With Omalizumab. *J Allergy Clin Immunol* (2010) 125(4):902–8.e7. doi: 10.1016/j.jaci.2009.12.996
19. MacGlashan DW Jr, Savage JH, Wood RA, Saini SS. Suppression of the Basophil Response to Allergen During Treatment With Omalizumab Is Dependent on 2 Competing Factors. *J Allergy Clin Immunol* (2012) 130 (5):1130–5.e5. doi: 10.1016/j.jaci.2012.05.038
20. Palacios T, Stillman L, Borish L, Lawrence M. Lack of Basophil CD203c-Upregulating Activity as an Immunological Marker to Predict Response to Treatment With Omalizumab in Patients With Symptomatic Chronic Urticaria. *J Allergy Clin Immunol Pract* (2016) 4(3):529–30. doi: 10.1016/j.jaip.2015.11.025
21. Prussin C, Griffith DT, Boesel KM, Lin H, Foster B, Casale TB. Omalizumab Treatment Downregulates Dendritic Cell FcepsilonRI Expression. *J Allergy Clin Immunol* (2003) 112(6):1147–54. doi: 10.1016/j.jaci.2003.10.003
22. Ito Y, Satoh T, Takayama K, Miyagishi C, Walls AF, Yokozeki H. Basophil Recruitment and Activation in Inflammatory Skin Diseases. *Allergy* (2011) 66 (8):1107–13. doi: 10.1111/j.1398-9995.2011.02570.x
23. Caproni M, Giomi B, Volpi W, Melani L, Schincaglia E, Macchia D, et al. Chronic Idiopathic Urticaria: Infiltrating Cells and Related Cytokines in Autologous Serum-Induced Wheals. *Clin Immunol* (2005) 114(3):284–92. doi: 10.1016/j.clim.2004.10.007
24. Ying S, Kikuchi Y, Meng Q, Kay AB, Kaplan AP. TH1/TH2 Cytokines and Inflammatory Cells in Skin Biopsy Specimens From Patients With Chronic Idiopathic Urticaria: Comparison With the Allergen-Induced Late-Phase Cutaneous Reaction. *J Allergy Clin Immunol* (2002) 109(4):694–700. doi: 10.1067/mai.2002.123236
25. Rorsman H. Basopenia in Urticaria. *Acta Allergol* (1961) 16:185–215. doi: 10.1111/j.1398-9995.1961.tb02894.x
26. Yamaguchi M, Sayama K, Yano K, Lantz CS, Noben-Trauth N, Ra C, et al. IgE Enhances Fc Epsilon Receptor I Expression and IgE-Dependent Release of Histamine and Lipid Mediators From Human Umbilical Cord Blood-Derived Mast Cells: Synergistic Effect of IL-4 and IgE on Human Mast Cell Fc Epsilon Receptor I Expression and Mediator Release. *J Immunol* (1999) 162(9):5455–65.
27. Yamaguchi M, Lantz CS, Oettgen HC, Katona IM, Fleming T, Miyajima I, et al. IgE Enhances Mouse Mast Cell Fc(epsilon)RI Expression *In Vitro* and *In Vivo*: Evidence for a Novel Amplification Mechanism in IgE-Dependent Reactions. *J Exp Med* (1997) 185(4):663–72. doi: 10.1084/jem.185.4.663
28. MacGlashan DWJr., Bochner BS, Adelman DC, Jardieu PM, Togias A, McKenzie-White J, et al. Down-Regulation of Fc(epsilon)RI Expression on Human Basophils During *In Vivo* Treatment of Atopic Patients With Anti-IgE Antibody. *J Immunol* (1997) 158(3):1438–45.
29. Beck LA, Marcotte GV, MacGlashan D, Togias A, Saini S. Omalizumab-Induced Reductions in Mast Cell Fce Psilon RI Expression and Function. *J Allergy Clin Immunol* (2004) 114(3):527–30. doi: 10.1016/j.jaci.2004.06.032
30. Metz M, Staubach P, Bauer A, Brehler R, Gericke J, Kangas M, et al. Clinical Efficacy of Omalizumab in Chronic Spontaneous Urticaria Is Associated With a Reduction of FcepsilonRI-Positive Cells in the Skin. *Theranostics* (2017) 7 (5):1266–76. doi: 10.7150/thno.18304
31. Kambe N, Kambe M, Kochan JP, Schwartz LB. Human Skin-Derived Mast Cells can Proliferate While Retaining Their Characteristic Functional and Protease Phenotypes. *Blood* (2001) 97(7):2045–52. doi: 10.1182/blood.v97.7.2045

Conflict of Interest: The authors declare that the research was conducted in the absence of any commercial or financial relationships that could be construed as a potential conflict of interest.

Publisher's Note: All claims expressed in this article are solely those of the authors and do not necessarily represent those of their affiliated organizations, or those of the publisher, the editors and the reviewers. Any product that may be evaluated in this article, or claim that may be made by its manufacturer, is not guaranteed or endorsed by the publisher.

Copyright © 2022 Takimoto-Ito, Ma, Kishimoto, Kabashima and Kambe. This is an open-access article distributed under the terms of the Creative Commons Attribution License (CC BY). The use, distribution or reproduction in other forums is permitted, provided the original author(s) and the copyright owner(s) are credited and that the original publication in this journal is cited, in accordance with accepted academic practice. No use, distribution or reproduction is permitted which does not comply with these terms.

frontiers | Frontiers in Immunology

ORIGINAL RESEARCH
published: 26 May 2022
doi: 10.3389/fimmu.2022.894163

Differential Effects of Alarmins on Human and Mouse Basophils

Adriana R. Gambardella[1,2†‡], Remo Poto[1,2,3,4†‡], Valentina Tirelli[5†], John T. Schroeder[6†], Gianni Marone[2,3,4,7†], Fabrizio Mattei[1†], Gilda Varricchi[2,3,4,7†] and Giovanna Schiavoni[1*†]*

[1] Department of Oncology and Molecular Medicine, Istituto Superiore di Sanità (ISS), Rome, Italy, [2] Department of Translational Medical Sciences, University of Naples Federico II, Naples, Italy, [3] Center for Basic and Clinical Immunology Research (CISI), University of Naples Federico II, Naples, Italy, [4] World Allergy Organization (WAO) Center of Excellence, Naples, Italy, [5] Core Facilities, Istituto Superiore di Sanità (ISS), Rome, Italy, [6] Division of Allergy and Clinical Immunology, Department of Medicine, Johns Hopkins University School of Medicine, Baltimore, MD, United States, [7] Institute of Experimental Endocrinology and Oncology (IEOS), National Research Council, Naples, Italy

Epithelial-derived alarmins (IL-33, TSLP, and IL-25) play an upstream role in the pathogenesis of asthma. Basophil-derived cytokines are a pivotal component of allergic inflammation. We evaluated the *in vitro* effects of IL-33, TSLP, and IL-25, alone and in combination with IL-3 on purified peripheral blood human basophils (hBaso) and bone marrow-derived mouse basophils (mBaso) in modulating the production of IL-4, IL-13, CXCL8 or the mouse CXCL8 equivalents CXCL1 and CXCL2. IL-3 and IL-33, but not TSLP and IL-25, concentration-dependently induced IL-4, IL-13, and CXCL8 release from hBaso. IL-3 synergistically potentiated the release of cytokines induced by IL-33 from hBaso. In mBaso, IL-3 and IL-33 rapidly induced IL-4 and IL-13 mRNA expression and protein release. IL-33, but not IL-3, induced CXCL2 and CXCL1 from mBaso. Differently from hBaso, TSLP induced IL-4, IL-13, CXCL1 and CXCL2 mRNA expression and protein release from mBaso. IL-25 had no effect on IL-4, IL-13, and CXCL1/CXCL2 mRNA expression and protein release even in the presence of IL-3. No synergism was observed between IL-3 and either IL-25 or TSLP. IL-3 inhibited both TSLP- and IL-33-induced CXCL1 and CXCL2 release from mBaso. Our results highlight some similarities and marked differences between the effects of IL-3 and alarmins on the release of cytokines from human and mouse basophils.

Keywords: allergy, asthma, basophils, IL-4, IL-13, IL-25, IL-33, TSLP

OPEN ACCESS

Edited by:
Satoshi Tanaka, Kyoto Pharmaceutical University, Japan

Reviewed by:
Jiro Kitaura, Juntendo University, Japan
Joakim Dahlin, Karolinska Institutet (KI), Sweden

***Correspondence:**
Gilda Varricchi
gildanet@gmail.com
Giovanna Schiavoni
giovanna.schiavoni@iss.it

***ORCID:**
Adriana R. Gambardella
orcid.org/0000-0002-5335-8650
Remo Poto
orcid.org/0000-0002-4723-0167
Valentina Tirelli
orcid.org/0000-0001-6021-0833
John T. Schroeder
orcid.org/0000-0002-5263-7850
Gianni Marone
orcid.org/0000-0002-9849-4701
Fabrizio Mattei
orcid.org/0000-0002-5357-7773
Gilda Varricchi
orcid.org/0000-0002-9285-4657
Giovanna Schiavoni
orcid.org/0000-0001-9135-0556

‡These authors share first authorship

Specialty section:
This article was submitted to Inflammation, a section of the journal Frontiers in Immunology

Received: *11 March 2022*
Accepted: *14 April 2022*
Published: *26 May 2022*

Citation:
Gambardella AR, Poto R, Tirelli V, Schroeder JT, Marone G, Mattei F, Varricchi G and Schiavoni G (2022) Differential Effects of Alarmins on Human and Mouse Basophils. Front. Immunol. 13:894163. doi: 10.3389/fimmu.2022.894163

INTRODUCTION

The epithelium represents a pivotal component of the innate immune system, providing a physical and immune barrier that is a first line of defense against environmental insults (1, 2). Damaged epithelial cells release a range of proinflammatory mediators causing barrier dysfunction and tissue remodeling (3, 4). Allergens, cytokines, microbial products, cigarette smoke extracts and physical stimuli induce the release of epithelium-derived alarmins including interleukin (IL)-33, thymic

Abbreviations: ACK, Ammonium-Chloride-Potassium; BM, Bone marrow; BSA, Bovine serum albumin; CDBA, culture-derived human basophils; FACS, Fluorescence-activated cell sorter; FCS, Fetal calf serum; hBaso, Human basophils; HSA, Human serum albumin; IL, Interleukin; IMDM, Iscove modified Dulbecco media; mBaso, Mouse basophils; OD, Optical density; qRT-PCR, Quantitative reverse transcription-PCR; rmIL, recombinant mouse interleukin; TSLP, Thymic stromal lymphopoietin; VEGF, Vascular endothelial growth factor.

stromal lymphopoietin (TSLP) and IL-25 (3–7), also known as IL-17E (8). Although these alarmins possess some common characteristics, they markedly differ in immunological and biochemical characteristics (9–11). IL-33, an IL-1 superfamily member cytokine (9, 12), functions *via* IL-1RL1 (ST2)-mediated activation of several immune cells (12–14). TSLP is an IL-2 family member that activates the heterodimeric receptor TSLPR : IL-7Rα on a wide range of immune and non-immune cells (10, 15). IL-25/IL-17E is an unusual member of the IL-17 family of cytokines that binds, as a dimer, to the heterodimeric receptor IL-17RA : IL-17RB present on some immune cells (8). The upstream role of these epithelial alarmins has identified TSLP (16–18) and IL-33 (19, 20) as potential therapeutic targets for the treatment of T2-high and presumably also for T2-low asthma (20–22).

Although basophils account for 0.5% - 1% of all leukocytes in bone marrow and peripheral blood (23, 24), these cells play critical roles in clearing pathogens (25, 26), and initiating inflammatory processes in allergy (27–30), autoimmunity (31–34), immunodeficiencies (35, 36), and cancer (37–40). Most of these studies have been conducted in humans using peripheral blood basophils (hBaso) and often using mouse bone marrow-derived basophils (mBaso) as a model system. Since the beginning of these studies, there has been a debate regarding whether mouse basophils were indeed similar to human basophils (41, 42). It is now becoming evident that hBaso differ from mBaso with respect to cytokine and chemokine produced (43–46), surface receptors (47–49), responsiveness to immunological (46, 47, 49) and pharmacological stimuli (50). For instance, activated hBaso release a specific profile of cytokines (e.g., IL-3, IL-4, IL-13, CXCL8, VEGF-A) (36, 51–58), whereas mBaso express a wider spectrum of cytokines/chemokines (e.g., IL-3, IL-4, IL-6, IL-13, TNF-α, CXCL1, CXCL2, CXCL4) (43–45, 59, 60). Moreover, there has been controversy regarding the functional expression of TSLP receptor on human versus mouse basophils (46, 47, 49, 61). Finally, human and mouse basophils release IL-3 (58, 62). Therefore, there is the possibility of an autocrine priming mediated by IL-3 of basophils for functional response to alarmins.

Taken together, much remains to be learned about immunological differences between hBaso and mBaso. Accordingly, in this study we explored the *in vitro* effects of IL-33, TSLP, and IL-25, alone and in combination with IL-3 on the release of cytokines from highly purified human peripheral blood basophils and bone marrow-derived mouse basophils.

MATERIALS AND METHODS

Reagents and Buffers

Bovine serum albumin (BSA), human serum albumin (HSA), [piperazine-N,N' -bis (2-ethanesulfonic acid) (Pipes)] (Sigma-Aldrich, Milan, Italy), L-glutamine, antibiotic-antimycotic solution (10,000 IU penicillin, 10 mg/mL streptomycin, and 25 μg/mL amphotericin B), fetal calf serum (FCS), Iscove modified Dulbecco medium (IMDM) and Hanks' balanced salt solution (GIBCO, Grand Island, NY, USA), RPMI 1640 with 25 mM HEPES buffer, Eagle's minimum essential medium (Flow Laboratories, Irvine, UK), Percoll (Pharmacia Fine Chemicals, Uppsala, Sweden), rhIL-3, rhIL-33, rhIL-25, and rhTSLP (R& D System, Minneapolis, MN, USA), CD117 MicroBead (Miltenyi Biotech, Bologna, Italy), and $HClO_4$ (Baker Chemical Co., Deventer, Netherlands) were commercially purchased. The Pipes (P) buffer was a mixture of 25 mM Pipes, 110 mM NaCl, 5 mM KCl, pH 7.37, referred to as P. P2CG, contains, in addition to P, 2 mM $CaCl_2$ and 1 g/L dextrose (63); pH was titrated to 7.4 with sodium bicarbonate.

Purification and Stimulation of Human Basophils

The study involving the use of human blood cells was approved by the Ethics Committee of the University of Naples Federico II (198/18), and written informed consent was obtained from all subjects involved in the study according to the recommendations from the Declaration of Helsinki. Basophils were purified from peripheral blood of healthy volunteers, aged 18-42 years, undergoing hemapheresis within the Immunohematology Unit at the University of Naples Federico II. Buffy coats were subjected to double-Percoll density centrifugation, which produced basophil-depleted cell and basophil-enriched cell suspensions (46). Basophils were purified from the basophil-enriched cell suspensions using the Basophil Isolation Kit II (Miltenyi, Biotec, Bologna, Italy). Basophils, with purity ~ 99% assessed by Alcian blue staining (64), were incubated at 37°C for 18 hours (52) in IMDM in the presence of increasing concentrations (1, 10, or 100 ng/ml) of the following cytokines: rhIL-3, rhIL-33, rhIL-25, and rhTSLP (R&D, Minneapolis, MN, USA). In some experiments, hBaso were stimulated with a combination of rhIL-3 (10 ng/ml) plus either rhIL-33 (10 ng/ml), rhTSLP (10 ng/ml) or rhIL-25 (10 ng/ml). At the end of these incubations, the cell-free supernatants were harvested and stored at -20°C for subsequent assay of IL-4, IL-13 and CXCL8 by ELISA.

Differentiation and Purification of Bone Marrow-Derived Mouse Basophils

C57Bl/6 female mice were purchased from Charles River Laboratories (Calco, Italy) and housed in the animal facility at Istituto Superiore di Sanità (Rome, Italy), according to the current Italian law guidelines (D.Lgs.vo 26/14: Authorization no. 243/2016-PR, Prot. D9997.13). Bone marrow (BM) was collected from tibiae and femurs of 6-10 week old female C57BL/6 mice and cells were disaggregated by gently pipetting with RPMI 1640 culture medium (EuroClone, Pero, Milan, Italy) containing 10% FCS, 1% penicillin, 1% fungizone, 1% streptomycin. To eliminate the erythrocytes, the BM cell suspension was incubated with 4 ml of ammonium-chloride-potassium (ACK) lysis buffer for 4 minutes at 22°C. BM cells (30×10^6) were cultured in complete RPMI 1640 supplemented with 1% of sodium pyruvate (Basophil medium) plus 2 ng/ml of recombinant mouse IL-3 (rmIL-3; R&D Systems, Minneapolis, MN, USA). At days 4 and 7 of differentiation, non-adherent cells

were harvested, centrifuged (5 minutes at 400 x g, 4°C) and re-seeded in a new flask containing fresh Basophil medium and 2 ng/ml of rmIL-3. At day 10, cells were harvested and stained with the following monoclonal antibodies (mAbs) for flow cytometry analyses: PE anti-mouse CD49b (clone DX5, Miltenyi Biotec), FITC anti-mouse FcεR1 (clone MAR-1), PE-Cy7 anti-mouse CD117/c-kit (clone 2B8), APC anti-mouse CD11c (clone N418) or APC anti-mouse CD200R (clone Ba13) (all from Biolegend, San Diego, CA, USA). Mouse basophils ($FcεR1^+$ $CD11c^-$ $c\text{-}kit^-$) were purified by fluorescence activated cell sorting (FACS) using a MoFlo Astrios EQ cell sorter (Beckman Coulter, Brea, CA, USA). The obtained mBaso population was routinely > 98% pure (see **Figure S1**).

Stimulation of Mouse Basophils

Sorted mBaso were incubated (10^6 cells/ml) for various times at 37°C with graded concentrations (1, 10, or 100 ng/ml) of the following cytokines: rmIL-3, rmIL-33 (BioLegend, San Diego, CA, USA), rmIL-25 and rmTSLP (R&D Systems, Minneapolis, MN, USA). In some experiments, mBaso were stimulated with a combination of rmIL-3 (1 ng/ml) plus either rmIL-33 (1 or 10 ng/ml), rmTSLP (1 or 10 ng/ml) or rmIL-25 (1 or 10 ng/ml). Cells and culture supernatants were harvested at 4 h and 24 h for further analyses.

Gene Expression Analysis With qRT-PCR

Total RNA was extracted from mBaso by using TRIsure reagent (Bioline, London, UK). Messenger RNA was reverse transcribed by means of Tetro cDNA Synthesis Kit (Bioline). Quantitative reverse transcription-PCR (qPCR) was performed using Sensimix Plus SYBR Kit containing the fluorescent dye SYBR Green (Bioline) and by means of an ABI 7500 Real-time PCR system (Applied Biosystems, Thermo Fisher Scientific, Waltham, MA, USA). Forward and reverse primers (**Table SI**) were purchased from Eurofin Genomics (Ebersberg, Germany). Triplicates were performed for each experimental point and data were normalized to HPRT (2-ΔCt method).

ELISA Assays

Human IL-4, IL-13 and CXCL8 were assessed in duplicate samples using ELISA kits according to the manufacturer's instructions (Quantikine ELISA Kit) (R&D Systems, Minneapolis, MN, USA). The ELISA detection range was 31-2,000 pg/ml (IL-4), 125-4,000 pg/ml (IL-13) and 31-2,000 pg/ml (CXCL8). mBaso were cultured in 48 multiwells at 10^6 cells/ml with single or combined cytokines, as described above. Supernatants were collected after 24 hours to perform ELISA assays by using specific kits to evaluate the production of murine IL-4 (Biolegend), IL-13 (Thermo Fisher Scientific), CXCL1 and CXCL2 (R&D Systems, Minneapolis, MN, USA). The ELISA detection range was 2-125 pg/ml (mIL-4), 7.8-500 pg/ml (mIL-13) 15.6- 1,000 pg/ml (mCXCL1), 7.8- 500 pg/ml (mCXCL2).

Flow Cytometry of IL-33, IL-25 and TSLP Receptors

mBaso were cultured for 24 hours alone (untreated) or in the presence of IL-3 at graded concentrations (1, 10 or 100 ng/ml). Cells were then stained with PE-Cy7 anti-mouse ST2 (clone RMST2-2; Thermo Fisher Scientific), PE anti-mouse TSLPR (clone 22H9; BD Biosciences, Franklin Lakes, NJ) and APC anti-mouse IL-25R/IL-17RB (clone 9B19) (Biolegend, San Diego, CA, USA) and analyzed by flow cytometry.

Statistical Analysis

All data were analyzed for statistical significance by means of Prism 8 (GraphPad software). Values from groups were compared by Student's *t*-test based on the parametric or nonparametric distribution of the continuous variables. One-way ANOVA analysis of variance was performed to compare means among multiple groups, followed by *post hoc* testing (Tukey test). Values were considered significant when the probability was below the 5% confidence level ($p < 0.05$).

RESULTS

Effects of IL-3 and Alarmins on Cytokine Release from Human Basophils

In a first series of experiments we evaluated the effects of incubation (20 h at 37°C) with IL-3 on purified basophils from healthy donors (hBaso). **Figure 1A** shows that IL-3 (1 to 100 ng/ml) concentration-dependently induced the secretion of IL-13 and CXCL8 and, to a lesser extent, of IL-4 from five different preparations of hBaso. We also investigated the effects of alarmins (IL-33, TSLP, and IL-25) on the production of cytokines from hBaso. **Figure 1B** indicates that IL-33 (1 to 100 ng/ml) caused a concentration-dependent release of IL-4, IL-13, and CXCL8.

The heterodimeric receptor for TSLP, composed of TSLPR and IL-7Rα, has not been found on basophils from healthy donors and allergic subjects (47) and the activating property of TSLP on human basophils has been apparently conflicting (46, 47, 49, 61, 65). In all our four independent experiments, we found that TSLP (0.1 to 100 ng/ml) did not induce the release of detectable levels of IL-4, IL-13, and CXCL8 from purified basophils obtained from healthy donors (**Figure 1C**). IL-25 (IL-17E) is an alarmin which belongs to the IL-17 family and activates the heterodimeric receptor IL-17RA : IL-17RB (8). **Figure 1D** shows the results of four independent experiments, indicating that IL-25 (0.1 to 100 ng/ml) did not cause the release of IL-4, IL-13, and CXCL8 from hBaso.

Effects of IL-3 on Alarmin-Induced Cytokine Release from Human Basophils

Human basophils express the heterodimeric IL-3 receptor composed of the IL-3Rα (CD123) and the βc chain (61, 66). IL-3 is best known for its ability to mediate priming effects when combined with a variety of different co-stimuli (58, 67–70). As also shown in **Figure 1**, IL-33 (10 ng/ml) and IL-3 (10 ng/ml) caused IL-4 release from hBaso. Incubation of hBaso with IL-3 (10 ng/ml) and IL-33 (10 ng/ml) synergistically potentiated IL-4 release from hBaso ($p < 0.001$). IL-3 and IL-33 induced the secretion of both IL-13 and CXCL8 from hBaso. **Figure 2A** also

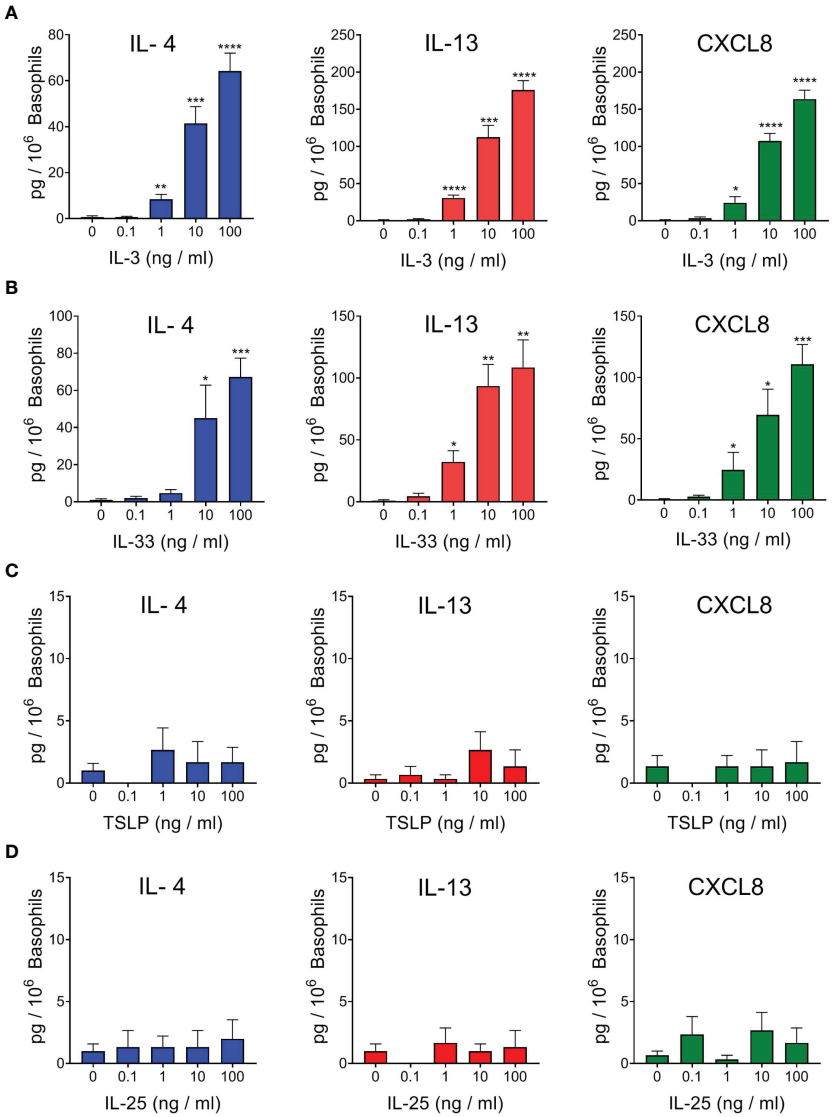


FIGURE 1 | Effects of increasing concentrations of rhIL-3 **(A)**, rhIL-33 **(B)**, rhTSLP **(C)**, and rhIL-25 **(D)** on IL-4, IL-13, and CXCL8 release from different preparations of human basophils (n=5). Basophils were incubated (18 hours at 37°C) with the indicated concentrations of cytokines. At the end of incubations, cell-free supernatants were collected and analyzed for IL-4, IL-13, and CXCL8 protein by ELISA. *$p < 0.05$; **$p < 0.01$; ***$p < 0.001$; ****$p < 0.0001$.

shows that incubation of hBaso with IL-3 synergistically potentiated the capacity of IL-33 to induce IL-13 ($p < 0.001$) and CXCL8 ($p < 0.001$).

Similar experiments were performed to investigate the possible interactions between IL-3 and TSLP or IL-25 on the release of cytokines from hBaso. **Figure 2B** shows the results of four independent experiments performed with different preparations of hBaso, indicating that the lack of activating effect of TSLP on the release of cytokines (IL-4, IL-13, and CXCL8) was not modified by co-incubation with IL-3 (10 ng/ml). Similarly, hBaso were essentially unresponsive to IL-25 even when cells were co-incubated with IL-3 (10 ng/ml) (**Figure 2C**).

Effects of IL-3 and Alarmins on Cytokine Release from Mouse Basophils

To evaluate the effects of IL-3 and alarmins on cytokine release by mBaso we employed highly purified BM-derived basophils. After 10 days of differentiation in the presence of IL-3 (71), basophils were FACS-sorted as FcεR1$^+$ CD11c$^-$ kit$^-$ to remove contaminating mast cells (FcεR1$^+$, c-kit$^+$) and dendritic cells (CD11c$^+$), yielding more than 95% pure population (**Figure S1**). Sorted mBaso were cultured in the presence of graded concentrations of IL-3, IL-33, TSLP or IL-25. Cytokine and chemokine expression was evaluated after 4 h and 24 h, while the protein release in the culture supernatants was measured

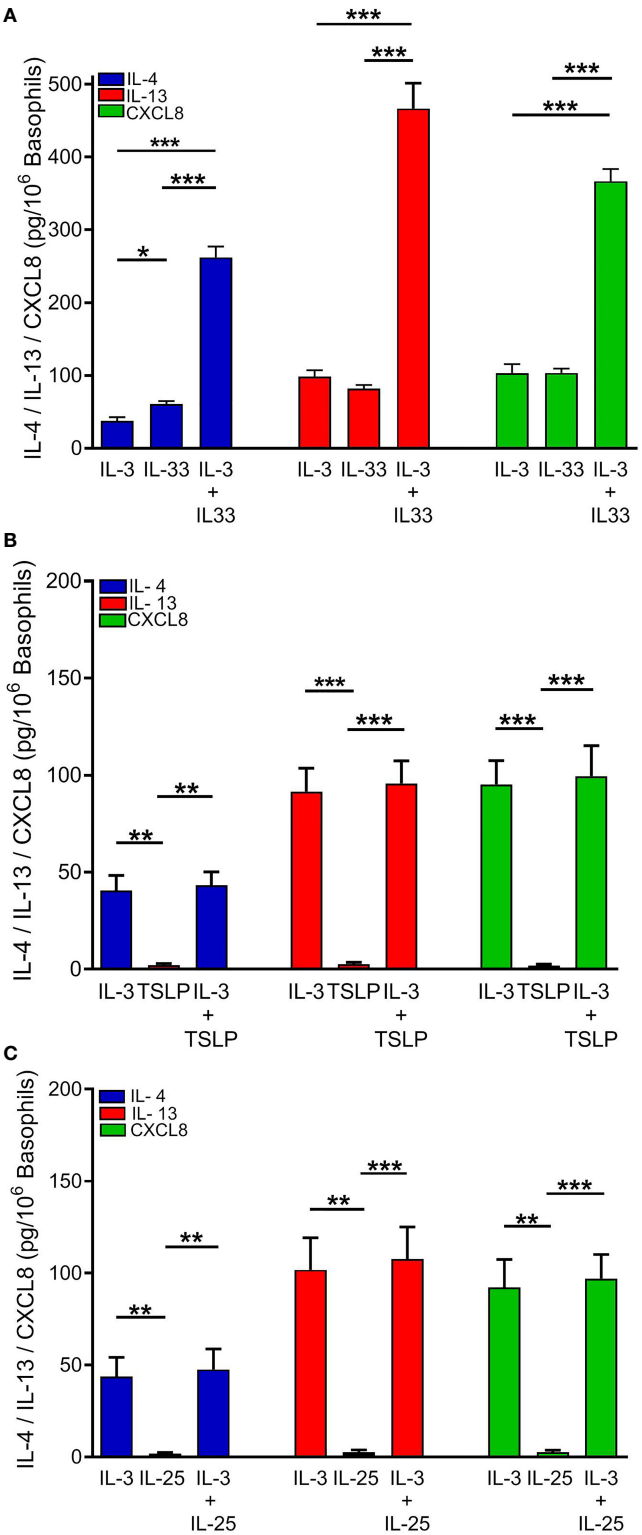


FIGURE 2 | Effects of rhIL-3 (10 ng/ml), alone and in combination with **(A)** rhIL-33 (10 ng/ml), **(B)** rhTSLP (10 ng/ml), or **(C)** rhIL-25 (10 ng/ml), on IL-4, IL-13, and CXCL8 released from different preparations of human basophils (n = 4). Basophils were incubated (18 hours at 37°C) with the indicated concentrations of cytokines. At the end of incubations, cell-free supernatants were collected and analyzed for IL-4, IL-13, and CXCL8 protein by ELISA. *$p < 0.05$; **$p < 0.01$; ***$p < 0.001$.

after 24 h of incubation. IL-3 induced both mRNA expression (**Figures 3A** and **S2A** for statistical analysis) and protein release (**Figure 3C**) of IL-4 and IL-13 in similar amounts and a concentration-dependent manner, with maximum efficacy at 10 ng/ml. Stimulation of mBaso with IL-33 also induced concentration-dependent expression (**Figures 3A** and **S2B**) and production (**Figure 3D**) of IL-4 and IL-13, the latter released in notably higher amounts (~ 5-fold) with respect to IL-4 (**Figure 3D**). Of note, TSLP induced low but significant increases in the expression of IL-4 and IL-13 mRNA (**Figures 3A** and **S2C**) and secretion of protein (**Figure 3E**) levels in mBaso stimulated with just 1 ng/ml. In contrast, IL-25 failed to induce any of these cytokines by mBaso at all concentrations tested (**Figures 3A, F** and **S2D**). We also measured the expression and release of the chemokines CXCL1 and CXCL2, two mouse functional homologues of human

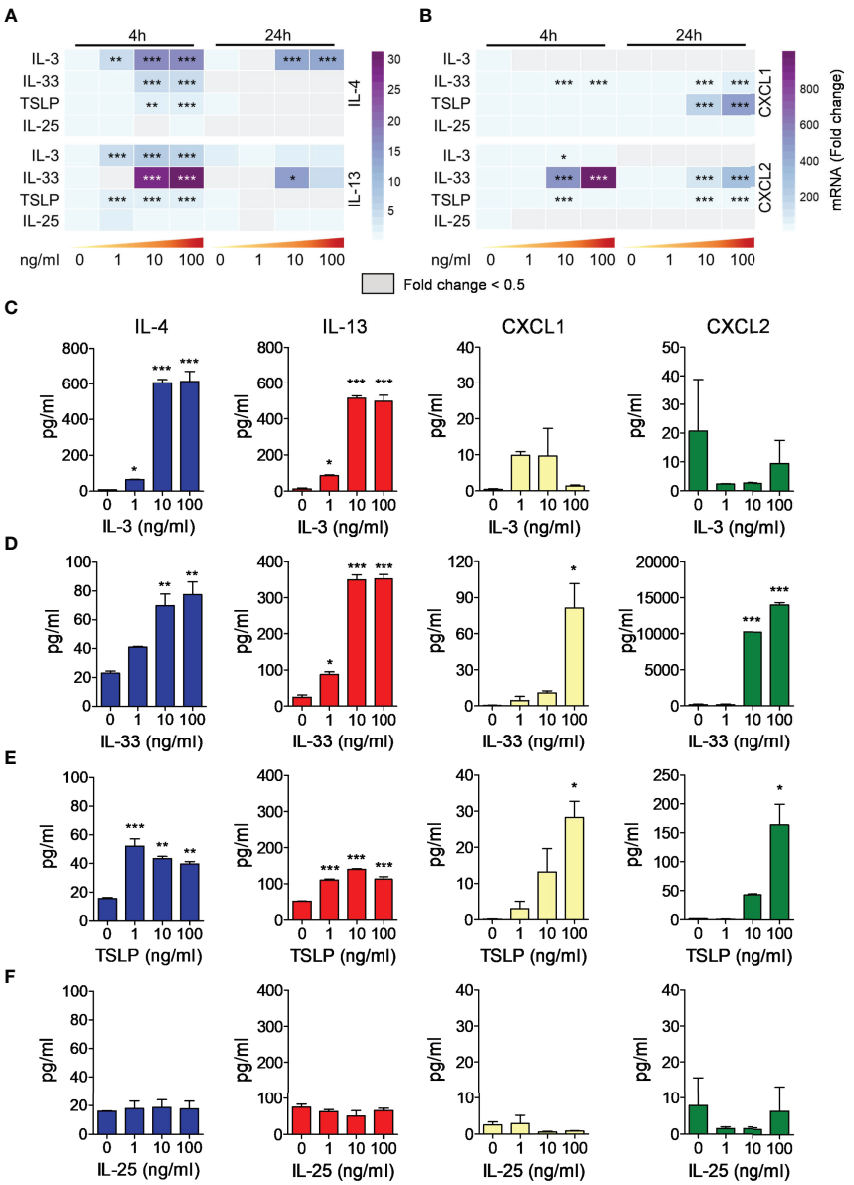


FIGURE 3 | Effects of rmIL-3, rmIL-33, rmTSLP, or rmIL-25 on cytokine (IL-4, IL-13) and chemokine (CXCL1, CXCL2) mRNA expression and protein release by mBaso. Purified mBaso (10^6 cells/ml) were stimulated with the indicated concentrations of rmIL-3, rmIL-33, rmTSLP, or rmIL-25. Expression of IL-4 and IL-13 **(A)**, CXCL1 and CXCL2 **(B)** mRNAs after 4 and 24 hours of stimulation was assessed by qRT-PCR. Data in heatmap represent the mean fold increase of mRNA normalized to HPRT and with respect to untreated (NT) controls at 4 h +/- SD. Concentrations of IL-4, IL-13, CXCL1 and CXCL2 in culture supernatants of mBaso incubated (24 hours at 37°C) with the indicated concentrations of rmIL-3 **(C)**, rmIL-33 **(D)**, rmTSLP **(E)**, or rmIL-25 **(F)** were measured by ELISA. Data represent the mean amount of released cytokines +/- SD in culture triplicates. One representative experiment out of at least three replicates is shown. *$p < 0.05$; **$p < 0.01$; ***$p < 0.001$.

CXCL8 (72). IL-3 did not increase the expression of CXCL1 and CXCL2 in mBaso (**Figures 3B** and **S2A**). Both IL-33 and TSLP could induce these two chemokines in mBaso. In fact, TSLP dose-dependently enhanced the expression (**Figures 3B** and **S2C**) and production (**Figure 3E**) of both chemokines, while IL-33 showed a greater capacity to induce CXCL2, compared to CXCL1, both at mRNA (**Figures 3B** and **S2B**) and protein level (**Figure 3D**). In contrast, stimulation with IL-25 failed to induce either CXCL1 or CXCL2 expression (**Figures 3B** and **S2D**) and protein release (**Figure 3F**) in mBaso.

Effects of IL-3 on Alarmin-Induced Cytokine Release from Mouse Basophils

Next, we analyzed whether IL-3 could synergistically increase the response of mBaso to alarmin stimulation. To this end, we cultured mBaso with a suboptimal dose of IL-3 (1 ng/ml) in combination with an optimal dose of IL-33 (10 ng/ml), TSLP (10 ng/ml) or IL-25 (10 ng/ml). IL-3 strongly synergized with IL-33 in inducing IL-4 and IL-13 mRNA expression (**Figures 4A** and **S3A** for statistical analysis) and protein secretion (**Figure 4B**) by mBaso. In contrast, IL-3 decreased the expression (**Figures 4A** and **S3A** for statistical analysis) and production (**Figure 4B**) of CXCL1 and CXCL2 induced by IL-33. Combination of IL-3 (1 ng/ml) with TSLP (10 ng/ml) did not enhance IL-4 and IL-13 production while it inhibited the expression (**Figures 4C** and **S3B** for statistical analysis) and release (**Figure 4D**) of CXCL1 and CXCL2 with respect to TSLP alone. IL-3 (1 ng/ml) failed to prime mBaso to IL-25 (10 ng/ml) stimulation, with regard to cytokine and chemokine secretion (**Figure 4F**). Moreover, this combined treatment resulted in a slight but significant reduction in the levels of IL-13 secreted compared to those seen with IL-3 alone (**Figures 4E, F** and **S3C** for statistical analysis). Although we found a synergistic effect of IL-3 and IL-25 in inducing the mRNA expression of CXCL1 at 24 h (**Figures 4E** and **S3C**), the levels of released CXCL1 were not significantly higher compared to those from mBaso exposed to the single cytokines or left untreated (**Figure 4F**).

Modulation of Alarmin Receptor Expression in mBaso by IL-3

We asked whether the effects of IL-3 in modulating the response of mBaso to alarmins could be attributable to its differential capacity to modulate the expression of membrane receptors for these alarmins. Thus, we stimulated mBaso with graded concentrations of IL-3 and analyzed the expression of the specific subunits of each alarmin, namely ST2, TSLPR and IL-17RB, by qRT-PCR and flow cytometry. We observed a IL-3 (1-100 ng/ml) concentration-dependent increase in the mRNA (**Figure 5A**) and membrane protein (**Figure 5B**) of ST2 and TSLPR, but this did not affect the expression of IL-25R. Overall, these data indicate that IL-3 may enhance the responsiveness of mBaso to stimulation with IL-33 at least in part by increasing the expression of its specific receptor on basophil membranes.

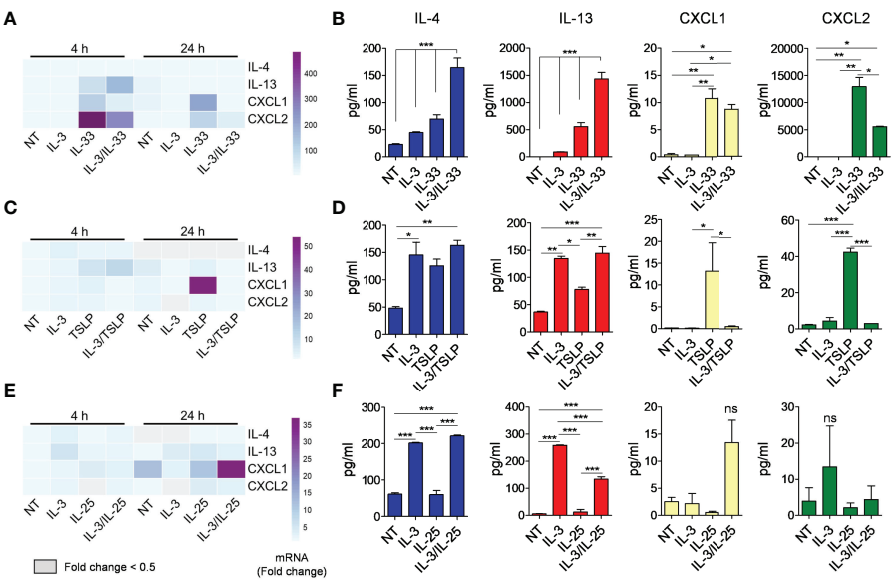


FIGURE 4 | Effects of rmIL-3 alone and in combination with rmIL-33, rmTSLP, or rmIL-25 on cytokine (IL-4, IL-13) and chemokine (CXCL1, CXCL2) mRNA expression and release from mBaso. Purified mBaso (10^6 cells/ml) were stimulated with rmIL-3 (1 ng/ml) alone and in combination with **(A, B)** rmIL-33 (10 ng/ml), **(C, D)** rmTSLP (10 ng/ml) or **(E, F)** rmIL-25 (10 ng/ml). **(A, C, E)** mRNA expression was assessed by qRT-PCR after 4 and 24 hours of stimulation. Data in heatmap represent the mean fold increase of mRNA normalized to HPRT and with respect to untreated (NT) controls at 4 h +/- SD. **(B, D, F)** Concentrations of IL-4, IL-13, CXCL1 and CXCL2 in culture supernatants of mBaso incubated (24 h at 37°C) with the indicated combinations were measured by ELISA. NT: not stimulated. Data represent the mean amount of released cytokines +/- SD in culture triplicates. One representative experiment out of at least two replicates is shown. *$p < 0.05$; **$p < 0.01$; ***$p < 0.001$ ns, Not Significant.

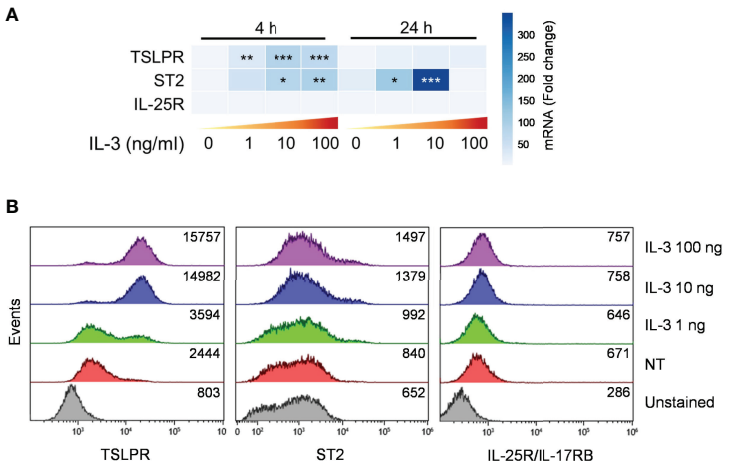


FIGURE 5 | Expression of alarmin receptors by murine basophils. Sorted mBaso (10^6 cells/ml) were cultured (24 hours at 37°C) alone (NT) or in the presence of the indicated concentrations of rmIL-3. Cells were then analyzed for expression of ST2, TSLPR and IL-25/IL-17RG by **(A)** qRT-PCR and **(B)** flow citometry. **(A)** Data in heatmap represent the mean fold mRNA increase normalized to HPRT and with respect to untreated (0) controls at 4 h +/- SD. **(B)** Numbers inside each plot represent mean fluorescence intensity values. One representative experiment out of two is shown. *$p < 0.05$; **$p < 0.01$; ***$p < 0.001$.

DISCUSSION

Increasing evidence supports the concept that the epithelium constitutes a key component of the innate immune system, providing a physical and immune-modulatory barrier that is a first line of defense against environmental insults (1, 2). Alarmins (TSLP, IL-33, IL-25/IL-17E), constitutively expressed in epithelial cells, are the first reactors to immunologic, infectious, neoplastic and traumatic insults and rapidly initiate innate and adaptive immune responses (11, 14, 73). In this study, we have analyzed the *in vitro* effects of IL-33, TSLP, and IL-25, alone and in combination with IL-3, on the production of cytokines from highly purified peripheral blood human basophils and bone marrow-derived mouse basophils. Our results showed some similarities and several qualitative and quantitative differences between the effects of these alarmins on human and mouse basophils.

IL-3, at all concentrations tested, markedly induced IL-13 and CXCL8 secretion from hBaso, whereas it has less effect on IL-4, consistent with previous reports (46, 54, 74). By contrast, IL-3 concentration-dependently caused a rapid and long-lasting increase in both IL-4 and IL-13 mRNA expression and in the secretion of these cytokines from mBaso.

Another striking difference between human and mouse basophils was the response to TSLP. We confirmed the recent results by other investigators (46, 47) by showing that a wide spectrum of TSLP did not induce the release of cytokines IL-4 and IL-13 from hBaso. We also extended the previous findings by showing that TSLP did not cause CXCL8 release from hBaso. In contrast, TSLP caused IL-4, IL-13, CXCL1 and CXCL2 mRNA expression and the release of these cytokines from mBaso. The latter findings support a role of TSLP in the differentiation and activation of basophils, as previously demonstrated in different mouse models (37, 75–77).

The distinct effects of TSLP on cytokine release from hBaso and mBaso could be explained by different methods of cell preparations. hBaso purified from peripheral blood of normal donors are not exposed to IL-3, while mBaso are obtained from bone marrow-derived precursors differentiated in the presence of IL-3. For the above reasons, we recently examined the effects of TSLP, alone and in presence of IL-3, on culture-derived human basophils (CDBA) (61). CDBA were obtained by culturing $CD34^+$ precursor cells in the presence of IL-3. In these experiments, IgE-sensitized and non IgE-sensitized basophils stimulated with TSLP alone or in combination with IL-3 did not release IL-4 and IL-13 (61).

The activating effects of IL-33 on hBaso and mBaso were qualitatively similar but presented some quantitative differences. This alarmin induced the secretion of similar amounts of IL-4 and IL-13 from hBaso but higher levels of IL-13 compared to IL-4 in mBaso. CXCL8 in hBaso was induced by IL-33 at similar levels as CXCL1 in mBaso. In mBaso, IL-33 induced massive amounts of CXCL2. Accordingly, a recent report has shown that IL-33 induces similar amounts of mRNA and protein expression of the neutrophil-attracting mediators CXCL1 and CXCL2 by bone marrow-derived basophils in a mouse model of skin inflammation (60).

IL-25/IL-17E is a member of the IL-17 cytokine family and is known to activate a limited number of immune cells (11). As previously reported (46), a wide range of concentrations of IL-25 did not induce the release of IL-4 and IL-13 from hBaso. Our results extend on these findings in showing that IL-25 displayed no capacity to induce CXCL8 secretion from basophils purified from unselected healthy volunteers. The current and previous results (46) indicate that IL-25 does not induce the release of several cytokines from basophils purified from peripheral blood of healthy volunteers. IL-25 also failed to induce IL-4, IL-13, CXCL1 and CXCL2 mRNA expression in mBaso or to stimulate

the production of these cytokines. Notably, we observed that IL-25 even inhibits the release of IL-13 induced by IL-3 from mBaso. It should be noted that in different experimental models it has been reported that IL-25 inhibits the activating property of IL-22 (78) and of Poly I:C (79).

IL-3 is well known for its ability to synergize with a wide range of immunological stimuli to augment the release of several mediators from human basophils (51, 54, 58, 74, 80). Consistent with the results previously published (57, 58, 80), we found that exposure of hBaso to IL-3 synergistically potentiated the activating effects of IL-33 for the production of IL-13, IL-4, and CXCL8 from these cells. The synergistic interaction between IL-3 and IL-33 was more marked with respect to IL-13 secretion compared to IL-4 release from hBaso. These findings are explained, in part, by evidence that IL-3 significantly induces the expression of ST2 – the IL-33 receptor on human basophils (80, 81). These findings might have translational relevance in various immune disorders. Human and mouse basophils release IL-3 (58, 62). Therefore, the synergistic interaction between IL-3 and certain alarmins on the release of immunomodulatory cytokines from hBaso and mBaso might be relevant in the pathophysiology of different basophil-mediated disorders such as allergic diseases (27–30), parasitic infections (82, 83), autoimmunity (31–34), and cancer (37–40).

To the best of our knowledge, it had never been demonstrated whether a similar priming effect of IL-3 is also exerted on mBaso activated by different stimuli. In this study we have examined the possible interactions between IL-3 and three alarmins on the production of cytokines from mBaso. Incubation of mBaso with low-dose (1 ng/ml) of IL-3 synergistically potentiated the releasing activity of IL-33 (10 ng/ml) on the secretion of both IL-4 and IL-13. The relevance of these findings is supported by the observation that IL-3 and IL-33 synergize *in vivo* to produce IL-4 from mBaso (84). Interestingly, the observation that IL-3 increased the expression of ST2 on mBaso suggests that IL-3 may amplify IL-33 responsiveness through up-regulation of ST2. On the other hand, the finding that IL-3 inhibited the production of CXCL1 and CXCL2 induced by IL-33 suggests the involvement of downstream modulation pathways.

It has been reported that IL-3 induces the expression of TSLPR but not of IL-7Rα on human basophils (47). In the latter study, basophils were unresponsive to TSLP. In keeping with this, IL-3 markedly upregulated the expression of TSLPR on mBaso, both mRNA and cell surface protein, but did not enhance their response to TSLP. Interestingly, incubation of mBaso with low-dose (1 ng/ml) IL-3 inhibited the production of CXCL1 and CXCL2 from mBaso stimulated by TSLP, as observed with IL-33. Incubation of hBaso with IL-3 did not modify the lack of response to IL-25 of these cells. Similar to hBaso, IL-25 had no effect on IL-3-stimulated mBaso with respect to IL-4/IL-13 mRNA expression and protein level and this correlated with failure by IL-3 to increase IL-17RB expression on mBaso.

Collectively, our results highlight different levels of complexity when examining the effects of alarmins (TSLP, IL-33, and IL-25) on the production of different cytokines from hBaso and mBaso. In particular, IL-33 appears to have comparable activating effects on both human and mouse basophils. By contrast, TSLP is a more selective activator of mBaso, but not of hBaso. Moreover, IL-25 seemingly does not activate mouse or human basophils. The above information appear of translational relevance for efforts at elucidating the complex immunological functions of alarmins in allergic disorders. It is commonly thought that epithelial-derived alarmins (IL-33, TSLP, IL-25) play an upstream role in the pathogenesis of asthma (2, 10, 15, 73) where basophil-derived cytokines are a pivotal component of allergic inflammation (26, 67, 85). Our results suggest that individual alarmins, which have different and specific roles in the activation of basophils, presumably play distinct roles in the pathogenesis of allergic disorders.

We also found quantitative differences in the activating properties of IL-3 and alarmins. For instance, the IL-3 and IL-3 plus IL-33 conditions markedly increased IL-13 more than IL-4 production from hBaso, but had similar effects on the release of these cytokines from mBaso. Another striking difference between human and mouse basophils was found when examining the synergism between IL-3 and alarmins. IL-3 synergistically potentiated the release of several cytokines induced by IL-33 in human and murine basophils. In contrast, combination of IL-3 with either IL-33 or TSLP caused an inhibitory effect in mBaso, but not in hBaso, in the production of neutrophil-attracting chemokines. Finally, IL-3 and IL-25 had no synergistic or additive effect in both human and murine basophils.

The prominent differences in the activating properties of IL-3 and of the three alarmins examined in this study are not surprising. IL-3, together with IL-5 and GM-CSF, belongs to the β common chain (βc) cytokine family (61). IL-33 is an IL-1 family member that activates the ST2 receptor enabling the recruitment of the co-receptor IL-1RAcP (86). TSLP is a member of the IL-2 family of helical cytokines, which binds to the heterodimeric TSLPR, namely the IL-7Rα receptor chains (10). IL-25/IL-17E is an unusual member of the IL-17 family of cytokines which binds as a disulphide-linked dimer to IL-17RA-IL-17RB receptor chains (11). Moreover, IL-3 and the three alarmins activate distinct signaling and transcription factors (11, 50, 87). Therefore, it is not surprising that these different cytokines produce distinct physiological effects on human and mouse basophils.

Bone marrow-derived murine basophils are often used as a model system for studies of the role of these cells in human health and disease (37, 45, 50, 59, 60, 62). Our results illustrate several differences in the release of some key cytokines induced by IL-3 and alarmins, alone and in combination, from hBaso and mBaso. Although mouse basophils represent useful models for understanding the role of these cells in different experimental disorders, our findings suggest caution when making generalizations to human disease.

Another important technical issue is the purity of cells with which one works. Basophils account for 0.5% - 1% of all leukocytes in bone marrow and peripheral blood (23, 24) and are difficult to purify to the homogeneity. Our experiments were carefully executed with highly purified human and mouse basophils in order to exclude the possibility that contaminating cells, in particular IgE^+ dendritic cells (47, 88), may have influenced the expression and production of cytokines. However, we cannot exclude the possibility that during the purification procedures to obtain highly purified

basophils we could have lost a small percentage of cells responsive to some of the examined alarmins (e.g., TSLP, IL-25).

Our study has some limitations that should be pointed out. First, mouse basophils were generated by culturing murine bone marrow cells for 14 days with IL-3. Murine basophils generated in this manner have an activated phenotype (82, 89) and differ from naïve primary mature basophils (50). Therefore, bone marrow-derived mBaso cannot be directly compared to mature hBaso obtained from peripheral blood. Another technical issue stems from the purification procedures to obtain highly purified human and mouse basophils. We used flow cytometry to purify mBaso and there is a possibility that this procedure might have activated murine basophils. Finally, Gonzales and collaborators have recently identified four phenotypically distinct subpopulations of human peripheral blood basophils (90) and Pellefigues and coworkers have provided some evidence of the existence of mBaso functional heterogeneity (50). In our study, we did not address the emerging issue of possible existence of human and mouse basophil heterogeneity. Another obvious question is if mBaso from other tissues are similar to bone marrow-derived mBaso. There is preliminary evidence that mBaso can acquire distinct characteristics depending on the different tissue locations (50). Collectively, these observations highlight the intrinsic complexity of analyzing and comparing the *in vitro* functions of human versus mouse basophils.

In conclusion, our study highlights some similarities and several differences in response to alarmins between hBaso and bone marrow-derived mBaso. The results of this study can thereby serve as a reference guide for scientists of basophil biology to interpret the results obtained with human basophils versus those of mouse. Such information appears of translational relevance for efforts aimed at elucidating the complex biological functions of both alarmins and basophils in health and disease.

DATA AVAILABILITY STATEMENT

The original contributions presented in the study are included in the article/**Supplementary Material**. Further inquiries can be directed to the corresponding authors.

ETHICS STATEMENT

The study involving the use of human blood cells was approved by the Ethics Committee of the University of Naples Federico II (198/18), and written informed consent was obtained from all subjects involved in the study according to the recommendations from the Declaration of Helsinki. The patients/participants provided their written informed consent to participate in this study. C57Bl/6 female mice were housed in the animal facility at Istituto Superiore di Sanità (Rome, Italy), according to the current Italian law guidelines (D.Lgs.vo 26/14: Authorization no. 243/2016-PR, Prot. D9997.13).

AUTHOR CONTRIBUTIONS

ARG, RP, VT, JTS, GM, GV, GS designed and conducted laboratory studies. ARG, GM, FM, GV, GS designed and performed data analysis. ARG, RP, JTS, GM, FM, GV, GS interpreted data. ARG, RP, GM, FM, GV, GS drafted the manuscript and interpreted data. ARG, JTS, GM, GV, GS edited the manuscript. All the authors approved the manuscript.

FUNDING

This work was supported in part by grants from the CISI-Lab Project (University of Naples Federico II), TIMING Project and Campania Bioscience (Regione Campania) to GM, GV, AIRC (IG 21366) to GS, and by grant R01 AI141486 [National Institute of Allergy and Infectious Diseases (NIAID), National Institutes of Health (NIH)] to JS.

ACKNOWLEDGMENTS

The authors thank Dr. Gjada Criscuolo for her excellent managerial assistance in preparing this manuscript and the administrative staff (Dr. Roberto Bifulco, Dr. Anna Ferraro and Dr. Maria Cristina Fucci), without whom it would not be possible to work as a team.

SUPPLEMENTARY MATERIAL

The Supplementary Material for this article can be found online at: https://www.frontiersin.org/articles/10.3389/fimmu.2022.894163/full#supplementary-material

REFERENCES

1. Cayrol C, Duval A, Schmitt P, Roga S, Camus M, Stella A, et al. Environmental Allergens Induce Allergic Inflammation Through Proteolytic Maturation of IL-33. *Nat Immunol* (2018) 19:375–85. doi: 10.1038/s41590-018-0067-510.1038/s41590-018-0067-5
2. Akdis CA. Does the Epithelial Barrier Hypothesis Explain the Increase in Allergy, Autoimmunity and Other Chronic Conditions? *Nat Rev Immunol* (2021) 21:739–51. doi: 10.1038/s41577-021-00538-710.1038/s41577-021-00538-7
3. Weng CM, Wang CH, Lee MJ, He JR, Huang HY, Chao MW, et al. Aryl Hydrocarbon Receptor Activation by Diesel Exhaust Particles Mediates Epithelium-Derived Cytokines Expression in Severe Allergic Asthma. *Allergy* (2018) 73:2192–204. doi: 10.1111/all.13462
4. Kato A, Favoreto SJr., Avila PC, Schleimer RP. TLR3- and Th2 Cytokine-Dependent Production of Thymic Stromal Lymphopoietin in Human Airway

Epithelial Cells. *J Immunol* (2007) 179:1080–7. doi: 10.4049/jimmunol.179.2.1080
5. Kouzaki H, O'Grady SM, Lawrence CB, Kita H. Proteases Induce Production of Thymic Stromal Lymphopoietin by Airway Epithelial Cells Through Protease-Activated Receptor-2. *J Immunol* (2009) 183:1427–34. doi: 10.4049/jimmunol.0900904jimmunol.0900904
6. Lee HC, Headley MB, Loo YM, Berlin A, Gale MJr., Debley JS, et al. Thymic Stromal Lymphopoietin Is Induced by Respiratory Syncytial Virus-Infected Airway Epithelial Cells and Promotes a Type 2 Response to Infection. *J Allergy Clin Immunol* (2012) 130:1187–1196 e1185. doi: 10.1016/j.jaci.2012.07.031S0091-6749(12)01218-3
7. Uller L, Leino M, Bedke N, Sammut D, Green B, Lau L, et al. Double-Stranded RNA Induces Disproportionate Expression of Thymic Stromal Lymphopoietin Versus Interferon-Beta in Bronchial Epithelial Cells From Donors With Asthma. *Thorax* (2010) 65:626–32. doi: 10.1136/thx.2009.12593065/7/626
8. McGeachy MJ, Cua DJ, Gaffen SL. The IL-17 Family of Cytokines in Health and Disease. *Immunity* (2019) 50:892–906. doi: 10.1016/j.immuni.2019.03.021
9. Cayrol C, Girard JP. Interleukin-33 (IL-33): A Nuclear Cytokine From the IL-1 Family. *Immunol Rev* (2018) 281:154–68. doi: 10.1111/imr.12619
10. Varricchi G, Pecoraro A, Marone G, Criscuolo G, Spadaro G, Genovese A. Thymic Stromal Lymphopoietin Isoforms, Inflammatory Disorders, and Cancer. *Front Immunol* (2018) 9:1595. doi: 10.3389/fimmu.2018.01595
11. Borowczyk J, Shutova M, Brembilla NC, Boehncke WH. IL-25 (IL-17E) in Epithelial Immunology and Pathophysiology. *J Allergy Clin Immunol* (2021) 148:40–52. doi: 10.1016/j.jaci.2020.12.628
12. Martin NT, Martin MU. Interleukin 33 Is a Guardian of Barriers and a Local Alarmin. *Nat Immunol* (2016) 17:122–31. doi: 10.1038/ni.3370ni.3370
13. Brusilovsky M, Rochman M, Rochman Y, Caldwell JM, Mack LE, Felton JM, et al. Environmental Allergens Trigger Type 2 Inflammation Through Ripoptosome Activation. *Nat Immunol* (2021) 22:1316–26. doi: 10.1038/s41590-021-01011-210.1038/s41590-021-01011-2
14. Afferni C, Buccione C, Andreone S, Galdiero MR, Varricchi G, Marone G, et al. The Pleiotropic Immunomodulatory Functions of IL-33 and Its Implications in Tumor Immunity. *Front Immunol* (2018) 9:2601. doi: 10.3389/fimmu.2018.02601
15. Gauvreau GM, Sehmi R, Ambrose CS, Griffiths JM. Thymic Stromal Lymphopoietin: Its Role and Potential as a Therapeutic Target in Asthma. *Expert Opin Ther Targets* (2020) 24:777–92. doi: 10.1080/14728222.2020.1783242
16. Menzies-Gow A, Corren J, Bourdin A, Chupp G, Israel E, Wechsler ME, et al. Tezepelumab in Adults and Adolescents With Severe, Uncontrolled Asthma. *N Engl J Med* (2021) 384:1800–9. doi: 10.1056/NEJMoa2034975
17. Gauvreau GM, O'Byrne PM, Boulet LP, Wang Y, Cockcroft D, Bigler J, et al. Effects of an Anti-TSLP Antibody on Allergen-Induced Asthmatic Responses. *N Engl J Med* (2014) 370:2102–10. doi: 10.1056/NEJMoa1402895
18. Corren J, Parnes JR, Wang L, Mo M, Roseti SL, Griffiths JM, et al. Tezepelumab in Adults With Uncontrolled Asthma. *N Engl J Med* (2017) 377:936–46. doi: 10.1056/NEJMoa1704064
19. Kelsen SG, Agache IO, Soong W, Israel E, Chupp GL, Cheung DS, et al. Astegolimab (Anti-ST2) Efficacy and Safety in Adults With Severe Asthma: A Randomized Clinical Trial. *J Allergy Clin Immunol* (2021) 148:790–8. doi: 10.1016/j.jaci.2021.03.044
20. Wechsler ME, Ruddy MK, Pavord ID, Israel E, Rabe KF, Ford LB, et al. Efficacy and Safety of Itepekimab in Patients With Moderate-To-Severe Asthma. *N Engl J Med* (2021) 385:1656–68. doi: 10.1056/NEJMoa2024257
21. Diver S, Khalfaoui L, Emson C, Wenzel SE, Menzies-Gow A, Wechsler ME, et al. Effect of Tezepelumab on Airway Inflammatory Cells, Remodelling, and Hyperresponsiveness in Patients With Moderate-to-Severe Uncontrolled Asthma (CASCADE): A Double-Blind, Randomised, Placebo-Controlled, Phase 2 Trial. *Lancet Respir Med* (2021) 9:1299–312. doi: 10.1016/S2213-2600(21)00226-5
22. Marone G, Spadaro G, Braile M, Poto R, Criscuolo G, Pahima H, et al. Tezepelumab: A Novel Biological Therapy for the Treatment of Severe Uncontrolled Asthma. *Expert Opin Investig Drugs* (2019) 28:931–40. doi: 10.1080/13543784.2019.1672657
23. Galli SJ, Tsai M. IgE and Mast Cells in Allergic Disease. *Nat Med* (2012) 18:693–704. doi: 10.1038/nm.2755nm.2755
24. Gauvreau GM, Denburg JA. Hemopoietic Progenitors: The Role of Eosinophil/Basophil Progenitors in Allergic Airway Inflammation. *Expert Rev Clin Immunol* (2005) 1:87–101. doi: 10.1586/1744666X.1.1.87
25. Galli SJ. Mast Cells and Basophils. *Curr Opin Hematol* (2000) 7:32–9. doi: 10.1097/00062752-200001000-00007
26. Siracusa MC, Kim BS, Spergel JM, Artis D. Basophils and Allergic Inflammation. *J Allergy Clin Immunol* (2013) 132:789–801. doi: 10.1016/j.jaci.2013.07.046S0091-6749(13)01295-5
27. Varricchi G, Raap U, Rivellese F, Marone G, Gibbs BF. Human Mast Cells and Basophils-How Are They Similar How Are They Different? *Immunol Rev* (2018) 282:8–34. doi: 10.1111/imr.12627
28. Spadaro G, Giurato G, Stellato C, Marone G, Casolaro V. Basophil Degranulation in Response to IgE Ligation Is Controlled by a Distinctive Circadian Clock in Asthma. *Allergy* (2020) 75:158–68. doi: 10.1111/all.14002
29. Miyake K, Shibata S, Yoshikawa S, Karasuyama H. Basophils and Their Effector Molecules in Allergic Disorders. *Allergy* (2021) 76:1693–706. doi: 10.1111/all.14662
30. MacGlashan DJr., Saini S, Schroeder JT. Response of Peripheral Blood Basophils in Subjects With Chronic Spontaneous Urticaria During Treatment With Omalizumab. *J Allergy Clin Immunol* (2021) 147:2295–304. e2212. doi: 10.1016/j.jaci.2021.02.039
31. Sharma M, Bayry J. Autoimmunity: Basophils in Autoimmune and Inflammatory Diseases. *Nat Rev Rheumatol* (2015) 11:129–31. doi: 10.1038/nrrheum.2014.199nrrheum.2014.199
32. Lamri Y, Vibhushan S, Pacreau E, Boedec E, Saidoune F, Mailleux A, et al. Basophils and IgE Contribute to Mixed Connective Tissue Disease Development. *J Allergy Clin Immunol* (2021) 147:1478–89. e1411. doi: 10.1016/j.jaci.2020.12.622
33. Charles N, Hardwick D, Daugas E, Illei GG, Rivera J. Basophils and the T Helper 2 Environment Can Promote the Development of Lupus Nephritis. *Nat Med* (2010) 16:701–7. doi: 10.1038/nm.2159nm.2159
34. Pellefigues C, Dema B, Lamri Y, Saidoune F, Chavarot N, Loheac C, et al. Prostaglandin D2 Amplifies Lupus Disease Through Basophil Accumulation in Lymphoid Organs. *Nat Commun* (2018) 9:725. doi: 10.1038/s41467-018-03129-810.1038/s41467-018-03129-8
35. Marone G, Varricchi G, Loffredo S, Galdiero MR, Rivellese F, de Paulis A. Are Basophils and Mast Cells Masters in HIV Infection? *Int Arch Allergy Immunol* (2016) 171:158–65. doi: 10.1159/000452889000452889
36. Patella V, Florio G, Petraroli A, Marone G. HIV-1 Gp120 Induces IL-4 and IL-13 Release From Human Fc Epsilon RI+ Cells Through Interaction With the VH3 Region of IgE. *J Immunol* (2000) 164:589–95. doi: 10.4049/jimmunol.164.2.589
37. Hayes MD, Ward S, Crawford G, Seoane RC, Jackson WD, Kipling D, et al. Inflammation-Induced IgE Promotes Epithelial Hyperplasia and Tumour Growth. *Elife* (2020) 9:e51862. doi: 10.7554/eLife.51862e51862]51862
38. Marone G, Gambardella AR, Mattei F, Mancini J, Schiavoni G, Varricchi G. Basophils in Tumor Microenvironment and Surroundings. *Adv Exp Med Biol* (2020) 1224:21–34. doi: 10.1007/978-3-030-35723-8_2
39. De Monte L, Wormann S, Brunetto E, Heltai S, Magliacane G, Reni M, et al. Basophil Recruitment Into Tumor-Draining Lymph Nodes Correlates With Th2 Inflammation and Reduced Survival in Pancreatic Cancer Patients. *Cancer Res* (2016) 76:1792–803. doi: 10.1158/0008-5472.CAN-15-1801-T0008-5472.CAN-15-1801-T
40. Lavin Y, Kobayashi S, Leader A, Amir ED, Elefant N, Bigenwald C, et al. Innate Immune Landscape in Early Lung Adenocarcinoma by Paired Single-Cell Analyses. *Cell* (2017) 169:750–65. e717. doi: 10.1016/j.cell.2017.04.014
41. Dvorak AM. The Mouse Basophil, A Rare and Rarely Recognized Granulocyte. *Blood* (2000) 96:1616–7. doi: 10.1182/blood.V96.4.1616
42. Lee JJ, McGarry MP. When Is a Mouse Basophil Not a Basophil? *Blood* (2007) 109:859–61. doi: 10.1182/blood-2006-06-027490
43. Sokol CL, Chu NQ, Yu S, Nish SA, Laufer TM, Medzhitov R. Basophils Function as Antigen-Presenting Cells for an Allergen-Induced T Helper Type 2 Response. *Nat Immunol* (2009) 10:713–20. doi: 10.1038/ni.1738ni.1738
44. Cohen M, Giladi A, Gorki AD, Solodkin DG, Zada M, Hladik A, et al. Lung Single-Cell Signaling Interaction Map Reveals Basophil Role in Macrophage Imprinting. *Cell* (2018) 175:1031–1044 e1018. doi: 10.1016/j.cell.2018.09.009

45. Piliponsky AM, Shubin NJ, Lahiri AK, Truong P, Clauson M, Niino K, et al. Basophil-Derived Tumor Necrosis Factor Can Enhance Survival in a Sepsis Model in Mice. *Nat Immunol* (2019) 20:129–40. doi: 10.1038/s41590-018-0288-710.1038/s41590-018-0288-7
46. Schroeder JT, Bieneman AP. Activation of Human Basophils by A549 Lung Epithelial Cells Reveals a Novel IgE-Dependent Response Independent of Allergen. *J Immunol* (2017) 199:855–65. doi: 10.4049/jimmunol.1700055jimmunol.1700055
47. Salabert-Le Guen N, Hemont C, Delbove A, Poli C, Braudeau C, Fantou A, et al. Thymic Stromal Lymphopoietin Does Not Activate Human Basophils. *J Allergy Clin Immunol* (2018) 141:1476–9. e1476. doi: 10.1016/j.jaci.2017.11.012
48. Daeron M. Innate Myeloid Cells Under the Control of Adaptive Immunity: The Example of Mast Cells and Basophils. *Curr Opin Immunol* (2016) 38:101–8. doi: 10.1016/j.coi.2015.12.004S0952-7915(15)00170-3
49. Salter BM, Oliveria JP, Nusca G, Smith SG, Watson RM, Comeau M, et al. Thymic Stromal Lymphopoietin Activation of Basophils in Patients With Allergic Asthma Is IL-3 Dependent. *J Allergy Clin Immunol* (2015) 136:1636–44. doi: 10.1016/j.jaci.2015.03.039
50. Pellefigues C, Mehta P, Chappell S, Yumnam B, Old S, Camberis M, et al. Diverse Innate Stimuli Activate Basophils Through Pathways Involving Syk and IkappaB Kinases. *Proc Natl Acad Sci USA* (2021) 118:e2019524118. doi: 10.1073/pnas.2019524118 2019524118
51. Rivellese F, Suurmond J, de Paulis A, Marone G, Huizinga TW, Toes RE. IgE and IL-33-Mediated Triggering of Human Basophils Inhibits TLR4-Induced Monocyte Activation. *Eur J Immunol* (2014) 44:3045–55. doi: 10.1002/eji.201444731
52. Genovese A, Borgia G, Bjorck L, Petraroli A, de Paulis A, Piazza M, et al. Immunoglobulin Superantigen Protein L Induces IL-4 and IL-13 Secretion From Human Fc Epsilon RI+ Cells Through Interaction With the Kappa Light Chains of IgE. *J Immunol* (2003) 170:1854–61. doi: 10.4049/jimmunol.170.4.1854
53. Patella V, Giuliano A, Bouvet JP, Marone G. Endogenous Superallergen Protein Fv Induces IL-4 Secretion From Human Fc Epsilon RI+ Cells Through Interaction With the VH3 Region of IgE. *J Immunol* (1998) 161:5647–55.
54. Redrup AC, Howard BP, MacGlashan DWJr., Kagey-Sobotka A, Lichtenstein LM, Schroeder JT. Differential Regulation of IL-4 and IL-13 Secretion by Human Basophils: Their Relationship to Histamine Release in Mixed Leukocyte Cultures. *J Immunol* (1998) 160:1957–64.
55. MacGlashan DJr., White JM, Huang SK, Ono SJ, Schroeder JT, Lichtenstein LM. Secretion of IL-4 From Human Basophils. The Relationship Between IL-4 mRNA and Protein in Resting and Stimulated Basophils. *J Immunol* (1994) 152:3006–16.
56. de Paulis A, Prevete N, Fiorentino I, Rossi FW, Staibano S, Montuori N, et al. Expression and Functions of the Vascular Endothelial Growth Factors and Their Receptors in Human Basophils. *J Immunol* (2006) 177:7322–31. doi: 10.4049/jimmunol.177.10.7322
57. Smithgall MD, Comeau MR, Yoon BR, Kaufman D, Armitage R, Smith DE. IL-33 Amplifies Both Th1- and Th2-Type Responses Through Its Activity on Human Basophils, Allergen-Reactive Th2 Cells, iNKT and NK Cells. *Int Immunol* (2008) 20:1019–30. doi: 10.1093/intimm/dxn060dxn060
58. Schroeder JT, Chichester KL, Bieneman AP. Human Basophils Secrete IL-3: Evidence of Autocrine Priming for Phenotypic and Functional Responses in Allergic Disease. *J Immunol* (2009) 182:2432–8. doi: 10.4049/jimmunol.0801782182/4/2432
59. Schneider E, Petit-Bertron AF, Bricard R, Levasseur M, Ramadan A, Girard JP, et al. IL-33 Activates Unprimed Murine Basophils Directly *In Vitro* and Induces Their *In Vivo* Expansion Indirectly by Promoting Hematopoietic Growth Factor Production. *J Immunol* (2009) 183:3591–7. doi: 10.4049/jimmunol.0900328jimmunol.0900328
60. Hsu CL, Chhiba KD, Krier-Burris R, Hosakoppal S, Berdnikovs S, Miller ML, et al. Allergic Inflammation Is Initiated by IL-33-Dependent Crosstalk Between Mast Cells and Basophils. *PloS One* (2020) 15:e0226701. doi: 10.1371/journal.pone.0226701PONE-D-19-24853
61. Varricchi G, Poto R, Marone G, Schroeder JT. IL-3 in the Development and Function of Basophils. *Semin Immunol* (2022) 54:101510. doi: 10.1016/j.smim.2021.101510
62. Rignault-Bricard R, Machavoine F, Mecheri S, Hermine O, Schneider E, Dy M, et al. IL-3-Producing Basophils Are Required to Exacerbate Airway Hyperresponsiveness in a Murine Inflammatory Model. *Allergy* (2018) 73:2342–51. doi: 10.1111/all.13480
63. Patella V, de Crescenzo G, Marino I, Genovese A, Adt M, Gleich GJ, et al. Eosinophil Granule Proteins Activate Human Heart Mast Cells. *J Immunol* (1996) 157:1219–25.
64. Gilbert HS, Ornstein L. Basophil Counting With a New Staining Method Using Alcian Blue. *Blood* (1975) 46:279–86. doi: 10.1182/blood.V46.2.279.279
65. Varricchi G, Poto R, Criscuolo G, Marone G, de Paulis A, Spadaro G, et al. The Pleiotropic Functions of Thymic Stromal Lymphopoietin in Allergic Inflammation. *Global J Pathol Microbiol* (2021) 9:10–25. doi: 10.31437/2310-8703.2021.09.2
66. MacDonald SM, Schleimer RP, Kagey-Sobotka A, Gillis S, Lichtenstein LM. Recombinant IL-3 Induces Histamine Release From Human Basophils. *J Immunol* (1989) 142:3527–32.
67. Schroeder JT. Basophils: Emerging Roles in the Pathogenesis of Allergic Disease. *Immunol Rev* (2011) 242:144–60. doi: 10.1111/j.1600-065X.2011.01023.x
68. Bischoff SC, de Weck AL, Dahinden CA. Interleukin 3 and Granulocyte/Macrophage-Colony-Stimulating Factor Render Human Basophils Responsive to Low Concentrations of Complement Component C3a. *Proc Natl Acad Sci USA* (1990) 87:6813–7. doi: 10.1073/pnas.87.17.6813
69. Ochensberger B, Tassera L, Bifrare D, Rihs S, Dahinden CA. Regulation of Cytokine Expression and Leukotriene Formation in Human Basophils by Growth Factors, Chemokines and Chemotactic Agonists. *Eur J Immunol* (1999) 29:11–22. doi: 10.1002/(SICI)1521-4141(199901)29:01<11::AID-IMMU11>3.0.CO;2-B
70. Miura K, MacGlashan DWJr. Dual Phase Priming by IL-3 for Leukotriene C4 Generation in Human Basophils: Difference in Characteristics Between Acute and Late Priming Effects. *J Immunol* (2000) 164:3026–34. doi: 10.4049/jimmunol.164.6.3026
71. Yoshimoto T, Nakanishi K. Generation and Characterization of Mouse Basophils From Bone Marrow and Purification of Basophils From Spleen. *Curr Protoc Immunol* (2012) Chapter 3, Unit 3 24. doi: 10.1002/0471142735.im0324s98
72. Hol J, Wilhelmsen L, Haraldsen G. The Murine IL-8 Homologues KC, MIP-2, and LIX are Found in Endothelial Cytoplasmic Granules But Not in Weibel-Palade Bodies. *J Leukoc Biol* (2010) 87:501–8. doi: 10.1189/jlb.0809532jlb.0809532
73. Hong H, Liao S, Chen F, Yang Q, Wang DY. Role of IL-25, IL-33, and TSLP in Triggering United Airway Diseases Toward Type 2 Inflammation. *Allergy* (2020) 75:2794–804. doi: 10.1111/all.14526
74. Ochensberger B, Daepp GC, Rihs S, Dahinden CA. Human Blood Basophils Produce Interleukin-13 in Response to IgE-Receptor-Dependent and -Independent Activation. *Blood* (1996) 88:3028–37. doi: S0006-4971(20)61543-9 doi: 10.1182/blood.V88.8.3028.bloodjournal8883028
75. Siracusa MC, Saenz SA, Hill DA, Kim BS, Headley MB, Doering TA, et al. TSLP Promotes Interleukin-3-Independent Basophil Haematopoiesis and Type 2 Inflammation. *Nature* (2011) 477:229–33. doi: 10.1038/nature10329nature10329
76. Noti M, Wojno ED, Kim BS, Siracusa MC, Giacomin PR, Nair MG, et al. Thymic Stromal Lymphopoietin-Elicited Basophil Responses Promote Eosinophilic Esophagitis. *Nat Med* (2013) 19:1005–13. doi: 10.1038/nm.3281nm.3281
77. Giacomin PR, Siracusa MC, Walsh KP, Grencis RK, Kubo M, Comeau MR, et al. Thymic Stromal Lymphopoietin-Dependent Basophils Promote Th2 Cytokine Responses Following Intestinal Helminth Infection. *J Immunol* (2012) 189:4371–8. doi: 10.4049/jimmunol.1200691jimmunol.1200691
78. Min HK, Won JY, Kim BM, Lee KA, Lee SJ, Lee SH, et al. Interleukin (IL)-25 Suppresses IL-22-Induced Osteoclastogenesis in Rheumatoid Arthritis *via* STAT3 and P38 MAPK/IkappaBalpha Pathway. *Arthritis Res Ther* (2020) 22:222. doi: 10.1186/s13075-020-02315-810.1186/s13075-020-02315-8
79. Xu G, Zhang L, Wang DY, Xu R, Liu Z, Han DM, et al. Opposing Roles of IL-17A and IL-25 in the Regulation of TSLP Production in Human Nasal Epithelial Cells. *Allergy* (2010) 65:581–9. doi: 10.1111/j.1398-9995.2009.02252.xALL2252
80. Pecaric-Petkovic T, Didichenko SA, Kaempfer S, Spiegl N, Dahinden CA. Human Basophils and Eosinophils Are the Direct Target Leukocytes of the

Novel IL-1 Family Member IL-33. *Blood* (2009) 113:1526–34. doi: 10.1182/blood-2008-05-157818S0006-4971(20)37722-3
81. Suzukawa M, Iikura M, Koketsu R, Nagase H, Tamura C, Komiya A, et al. An IL-1 Cytokine Member, IL-33, Induces Human Basophil Activation *via* its ST2 Receptor. *J Immunol* (2008) 181:5981–9. doi: 10.4049/jimmunol.181.9.5981
82. Voehringer D. Basophil Modulation by Cytokine Instruction. *Eur J Immunol* (2012) 42:2544–50. doi: 10.1002/eji.201142318
83. Eberle JU, Voehringer D. Role of Basophils in Protective Immunity to Parasitic Infections. *Semin Immunopathol* (2016) 38:605–13. doi: 10.1007/s00281-016-0563-310.1007/s00281-016-0563-3
84. Yoshikawa S, Oh-Hora M, Hashimoto R, Nagao T, Peters L, Egawa M, et al. Pivotal Role of STIM2, But Not STIM1, in IL-4 Production by IL-3-Stimulated Murine Basophils. *Sci Signal* (2019) 12:eaav2060. doi: 10.1126/scisignal.aav206012/576/eaav2060
85. Mali SS, Bautista DM. Basophils Add Fuel to the Flame of Eczema Itch. *Cell* (2021) 184:294–6. doi: 10.1016/j.cell.2020.12.035
86. Schmitz J, Owyang A, Oldham E, Song Y, Murphy E, McClanahan TK, et al. IL-33, an Interleukin-1-Like Cytokine That Signals *via* the IL-1 Receptor-Related Protein ST2 and Induces T Helper Type 2-Associated Cytokines. *Immunity* (2005) 23:479–90. doi: 10.1016/j.immuni.2005.09.015
87. Li X, Bechara R, Zhao J, McGeachy MJ, Gaffen SL. IL-17 Receptor-Based Signaling and Implications for Disease. *Nat Immunol* (2019) 20:1594–602. doi: 10.1038/s41590-019-0514-y10.1038/s41590-019-0514-y
88. Maggi L, Rossettini B, Montaini G, Matucci A, Vultaggio A, Mazzoni A, et al. Omalizumab Dampens Type 2 Inflammation in a Group of Long-Term Treated Asthma Patients and Detaches IgE From FcepsilonRI. *Eur J Immunol* (2018) 48:2005–14. doi: 10.1002/eji.201847668
89. Sharma M, Das M, Stephen-Victor E, Galeotti C, Karnam A, Maddur MS, et al. Regulatory T Cells Induce Activation Rather Than Suppression of Human Basophils. *Sci Immunol* (2018) 3:eaan0829. doi: 10.1126/sciimmunol.aan08293/23/eaan0829
90. Vivanco Gonzalez N, Oliveria JP, Tebaykin D, Ivison GT, Mukai K, Tsai MM, et al. Mass Cytometry Phenotyping of Human Granulocytes Reveals Novel Basophil Functional Heterogeneity. *iScience* (2020) 23:101724. doi: 10.1016/j.isci.2020.101724S2589-0042(20)30921-4

Conflict of Interest: The authors declare that the research was conducted in the absence of any commercial or financial relationships that could be construed as a potential conflict of interest.

Publisher's Note: All claims expressed in this article are solely those of the authors and do not necessarily represent those of their affiliated organizations, or those of the publisher, the editors and the reviewers. Any product that may be evaluated in this article, or claim that may be made by its manufacturer, is not guaranteed or endorsed by the publisher.

Copyright © 2022 Gambardella, Poto, Tirelli, Schroeder, Marone, Mattei, Varricchi and Schiavoni. This is an open-access article distributed under the terms of the Creative Commons Attribution License (CC BY). The use, distribution or reproduction in other forums is permitted, provided the original author(s) and the copyright owner(s) are credited and that the original publication in this journal is cited, in accordance with accepted academic practice. No use, distribution or reproduction is permitted which does not comply with these terms.

frontiers | Frontiers in Immunology

REVIEW
published: 27 May 2022
doi: 10.3389/fimmu.2022.902494

Role of Basophils in a Broad Spectrum of Disorders

*Kensuke Miyake**, *Junya Ito and Hajime Karasuyama*

Inflammation, Infection and Immunity Laboratory, Advanced Research Institute, Tokyo Medical and Dental University (TMDU), Tokyo, Japan

Basophils are the rarest granulocytes and have long been overlooked in immunological research due to their rarity and similarities with tissue-resident mast cells. In the last two decades, non-redundant functions of basophils have been clarified or implicated in a broad spectrum of immune responses, particularly by virtue of the development of novel analytical tools for basophils. Basophils infiltrate inflamed tissues of patients with various disorders, even though they circulate in the bloodstream under homeostatic conditions. Depletion of basophils results in the amelioration or exaggeration of inflammation, depending on models of disease, indicating basophils can play either beneficial or deleterious roles in a context-dependent manner. In this review, we summarize the recent findings of basophil pathophysiology under various conditions in mice and humans, including allergy, autoimmunity, tumors, tissue repair, fibrosis, and COVID-19. Further mechanistic studies on basophil biology could lead to the identification of novel biomarkers or therapeutic targets in a broad range of diseases.

Keywords: basophils, allergy, IL-4, tissue repair, fibrosis, autoimmune diseases, tumor, COVID-19

OPEN ACCESS

Edited by:
Satoshi Tanaka, Kyoto Pharmaceutical University, Japan

Reviewed by:
Hans Oettgen, Boston Children's Hospital and Harvard Medical School, United States
Kazushige Obata-Ninomiya, Benaroya Research Institute, United States

****Correspondence:***
Kensuke Miyake
miyake.mbch@tmd.ac.jp

Specialty section:
This article was submitted to Inflammation, a section of the journal Frontiers in Immunology

Received: *23 March 2022*
Accepted: *04 May 2022*
Published: *27 May 2022*

Citation:
Miyake K, Ito J and Karasuyama H (2022) Role of Basophils in a Broad Spectrum of Disorders. Front. Immunol. 13:902494. doi: 10.3389/fimmu.2022.902494

1 INTRODUCTION

Basophils are the least common granulocytes, representing ~0.5% of peripheral blood leukocytes in both mice and humans. Basophils have long been regarded erroneously as the blood-circulating mast cells, due to their phenotypic similarities with tissue-resident mast cells, including the surface expression of the high-affinity IgE receptor (FcεRI), and the release of histamine in response to various stimuli. Actually, in clinical settings, basophils are frequently used as a surrogate for tissue-resident mast cells for allergy diagnosis. Nevertheless, basophils and mast cells differ from each other in several aspects. Basophils usually circulate in the blood, while mast cells reside in peripheral tissues. Basophils have much shorter lifespan than mast cells. Moreover, the gene expression profile is quite distinct between basophils and mast cells in both mice and humans (1, 2), implying that basophils have unique roles distinct from those played by mast cells.

In the last two decades, a series of analytical tools for basophils have been developed, including basophil-depleting antibodies (3, 4), genetically engineered mice which specifically lack basophils (5–11), basophil-reporter mice (7, 11, 12), and basophil-specific Cre-expressing mice (7, 13, 14). Studies using these powerful tools have identified non-redundant roles of basophils in Th2-type immune responses, including the allergic inflammation (15–17) and protective immunity against parasitic infections (18–20). Basophils are also shown to play important roles in other types of responses, such as autoimmunity (21), tissue repair (22), fibrosis (23), cancer (24–26), and possibly COVID-19

pathogenesis (27). In this review, we summarize the recent developments on the contribution of basophils to the pathogenesis of a variety of inflammatory disorders, based on research findings published mainly during the past 5 years. Regarding inflammatory responses associated with parasitic infections, we highly recommend readers to refer recent review articles (18–20).

2 ROLE OF BASOPHILS IN ALLERGIC INFLAMMATION

2.1 Basophils as a Tool for Allergy Diagnosis

Basophils isolated from patients' blood are often used for allergy testing in clinical settings. The basophil activation test (BAT) is a representative assay, in which patient's blood is incubated with suspected allergens, and the activation of basophils in the blood is assessed by the upregulation of CD63 and/or CD203c on their cell surface (28, 29). BAT is useful for the diagnosis of a wide variety of allergic disorders, including allergy to food, drug, or venom as well as allergic rhinitis and asthma. BAT is also utilized to monitor allergy therapeutics, such as allergen immunotherapy and anti-IgE therapy (30–32).

Approximately 10-15% of individuals have basophils that are non-responsive to anti-IgE antibody or allergen stimulation, known as non-responder or non-releaser basophils (33). The non-responder basophil phenotype is associated with downregulation of spleen tyrosine kinase (Syk), even though the functional significance of non-responder basophils remains elusive. The presence of non-responder basophils is a challenge when using BAT for allergy diagnosis.

BAT is a potential diagnostic tool for hypersensitivity reactions against COVID-19 mRNA vaccines, but its usefulness for predicting allergic reactions to the mRNA vaccines remains controversial. Troelnikov et al. recruited three patients with a history of polyethylene glycol (PEG) allergy and found that all three patients displayed a positive skin intradermal test and BAT for a PEG-containing mRNA vaccine, while all of them displayed negative BAT for PEG itself (34). Basophils from these patients were also activated by PEGylated liposomal doxorubicin, suggesting that PEGylated lipid nanoparticles, but not PEG itself, are the cause of their hypersensitivity reactions. Warren et al. recruited patients with a previous history of allergic reactions against mRNA vaccines (35). Only 1 of 11 patients displayed a positive skin prick test for the mRNA vaccines, even though all patients clinically underwent allergic reactions to the mRNA vaccines. In contrast, 10 of 11 patients displayed a positive BAT against PEG alone while all 11 patients had a positive BAT against the mRNA vaccines, even though PEG-specific IgE could not be detected in these patients. This suggests a role for non-IgE-mediated allergic reactions against the COVID-19 mRNA vaccines. Interestingly, Labella et al. reported that 50% of persons with a history of SARS-CoV-2 infection displayed positive BAT against the mRNA vaccine, irrespective of their vaccination status (36). Therefore, a positive BAT result against the mRNA vaccines may be attributed to either a PEG allergy or a previous SARS-CoV2 infection.

Additional allergy tests using basophils have been proposed. McKenzie et al. established a method for detecting allergen specific IgE on basophils, designated as CytoBas (37). Qi et al. reported that upon activation, basophils and mast cells release $CD203c^+$ extracellular vesicles, and the presence of such vesicles has strong diagnostic value in patients with drug allergies (38).

2.2 Skin Allergy

2.2.1 Cutaneous Basophils Hypersensitivity

In the 1970s, basophils attracted attention since massive infiltration of basophils into the skin lesion was observed in certain forms of delayed-type hypersensitivity reactions triggered by the injection of foreign antigens (39, 40). It is called cutaneous basophil hypersensitivity (CBH) and mainly studied in guinea pigs. This reaction clinically and histologically resembles Jones-Mote responses to rabbit serum proteins in humans. CBH is hardly elicited in mice, and the functional role of basophils in CBH remains to be clarified. Skin allergic reactions against COVID-19 mRNA vaccination clinically resemble Jones-Mote reactions (41) characterized by erythematous and indurated skin reactions. Although it remains unclear whether basophils are indeed recruited to the site of the mRNA vaccination, it would be possible that basophils are potentially involved in the hypersensitivity reactions against COVID-19 mRNA vaccines since some reports indicate the IgE-independent basophil activation by mRNA vaccines (34, 35).

2.2.2 Atopic Dermatitis

The infiltration of basophils in the skin has been described in several inflammatory skin disorders, including atopic dermatitis (AD), bullous pemphigoid, prurigo, Henoch-Shönlein purpura, eosinophilic pustular folliculitis (Ofuji's disease), and urticaria (42, 43). Of note, peripheral blood basophils from patients with AD display upregulated expression of activation markers such as CD63 and CD203c on the cell surface, compared with those from healthy controls (44, 45). This suggests a possible role for basophils in the pathogenesis of AD. As discussed below, studies from mouse AD models demonstrated that basophils contribute to the allergic inflammation, pruritus, and barrier dysfunction in AD, three key features that contribute to the pathogenesis of AD (46) (**Figure 1**).

2.2.2.1 Allergic Inflammation in AD

Basophils play important roles in the induction of skin allergic inflammation in multiple models of AD, including IgE-dependent chronic allergic inflammation (IgE-CAI) (47, 48), the MC903-induced model (42), the oxazolone-induced model (49, 50), and the IL-33-transgenic mouse model (51). In IgE-CAI, mice are first sensitized with hapten trinitrophenol-specific IgE, followed by an intradermal challenge of corresponding allergens in ear skin, which results in severe ear swelling and infiltration of inflammatory cells, including eosinophils, macrophages, neutrophils, and basophils. IgE-CAI can be elicited even in the absence of mast cells. On the other hand, depletion of basophils almost completely abolishes ear swelling

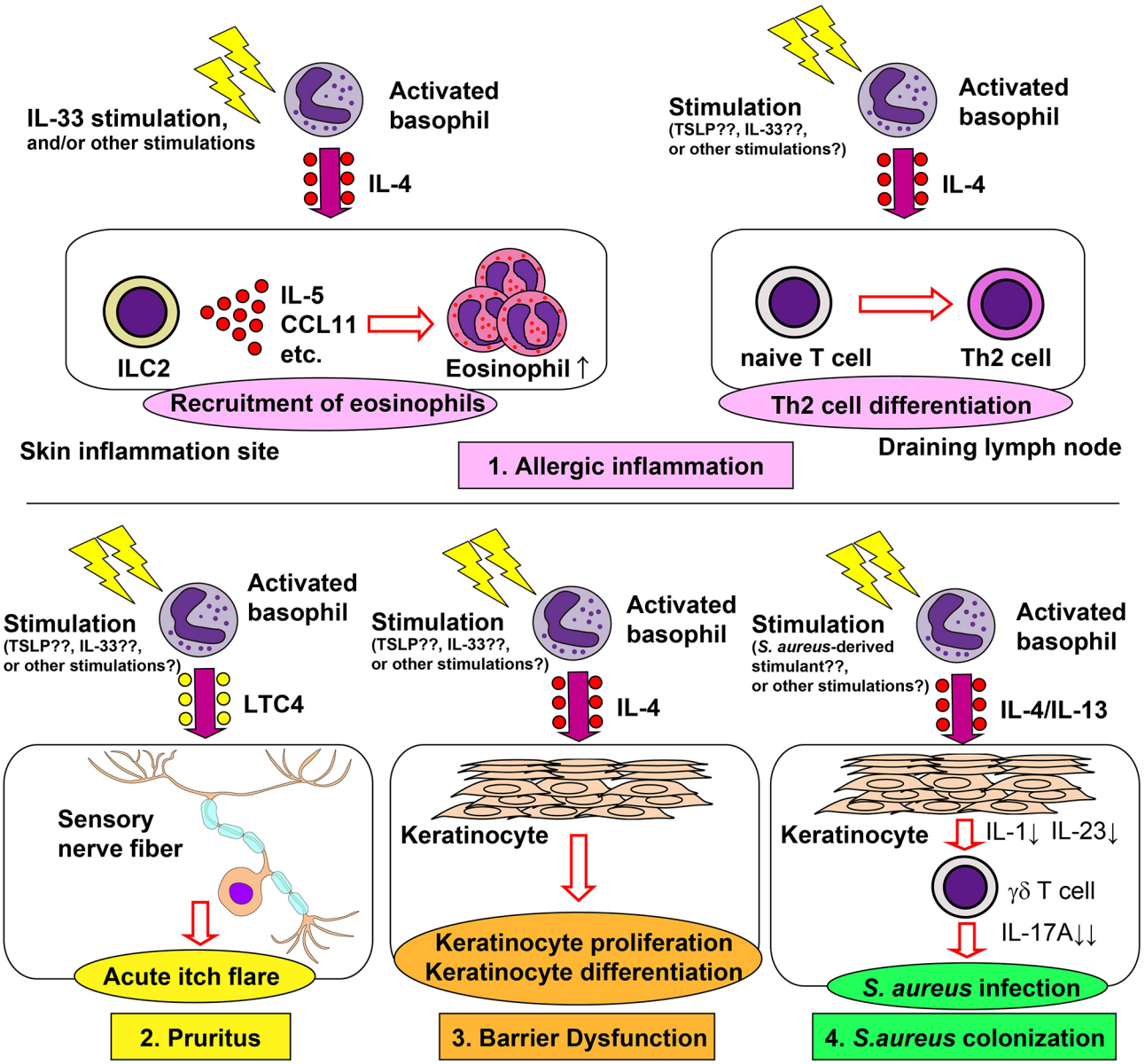


FIGURE 1 | Role of basophils in the pathogenesis of atopic dermatitis. Basophils contribute to allergic inflammation, pruritus, barrier dysfunction and *Staphylococcus aureus* colonization in atopic dermatitis (AD). 1) Basophil-derived interleukin (IL)-4 stimulates group 2 innate lymphoid cells (ILC2s) to enhance the production of IL-5 and CCL11, leading to enhanced recruitment of eosinophils to the skin lesion (upper left panel). Basophil-derived IL-4 also augments the differentiation of naïve T cells into Th2 cells in draining lymph nodes (upper right panel). 2) Basophil-derived leukotriene C4 (LTC4) acts on CysLTR2$^+$ sensory neurons, inducing acute itch flares in AD (lower left panel). 3) Basophil-derived IL-4 promotes proliferation and differentiation of keratinocyte (lower middle panel). 4) Basophil-derived IL-4 suppresses the IL-1 and IL-23 production by keratinocytes, leading to reduced production of IL-17A by γδ T cells and, therefore, increased susceptibility to *S. aureus* infection (lower right panel).

and cellular infiltration (3, 6, 48), illustrating an essential role for basophils in the induction of IgE-CAI. Serine proteases released by basophils play critical roles in the development of IgE-CAI (52). Moreover, basophil-derived interleukin (IL)-4 plays a key role in the recruitment of eosinophils to the skin lesion, and thus promotes cutaneous inflammation (53). In an IgE-dependent skin allergic inflammation model similar to IgE-CAI, basophil-derived IL-4 promotes the expression of adhesion molecules, resulting in the enhanced recruitment of eosinophils (54). Basophil-derived IL-4 also plays an important role in the development of AD induced by repetitive topical application of hapten oxazolone (50). In this model, basophils are the major source of IL-4 in the skin lesion, consistent with recent single-cell RNA-seq data (55). Depletion of basophils ameliorates eczematous skin inflammation with crusts and scales, suggesting the role of basophil-derived IL-4 in the formation of

lichenized skin lesions. Basophil-derived IL-4 also plays key roles in other AD models. In a topical MC903 application model, basophil-derived IL-4 acts on skin-resident group 2 innate lymphoid cells (ILC2s), leading to enhanced proliferation of ILC2s and AD-like skin inflammation (42). Similarly, in the IL-33-transgenic mouse model, basophils promote the proliferation of ILC2s, possibly through the production of IL-4 (51). Thus, basophil-derived IL-4 appears to contribute to AD pathogenesis in the mouse models. In moderate-to-severe AD patients, the treatment with dupilumab, a human monoclonal antibody against IL-4Rα, rapidly improves the disease (56), suggesting the involvement of IL-4 and IL-13 in the pathogenesis of human AD. Given that human basophils can produce a large amount of IL-4 in response to various stimuli (57), it is likely that basophils contribute to the pathogenesis of certain types of AD in humans.

Several reports indicate that basophils contribute to Th2 cell differentiation in mouse AD models (12, 49, 58). Infiltration of basophils into skin draining lymph nodes is observed in some AD models, including the MC903-induced and oxazolone-induced models (12, 49), suggesting that basophils can provide IL-4 required for the differentiation of naive $CD4^+$ T cells into Th2 cells. Moreover, basophils are capable of presenting antigens to naïve T cells, leading to the induction of Th2 cell differentiation (59–61). However, this role of basophils remains controversial, since some reports argued that basophils are incapable of processing and presenting antigens to naïve T cells (62, 63). Miyake et al. revisited this issue and found that basophils acquire peptide-MHC-II complexes from dendritic cells (DCs) through trogocytosis and can present antigens to naïve T cells, promoting their differentiation into Th2 cells (35). Therefore, the functional significance of basophils in Th2 cell differentiation may differ, depending on experimental settings, determined in part by the extent of the basophil-DC interaction in draining lymph nodes.

2.2.2.2 Pruritus in AD

AD is characterized by chronic and intense itch, which can be mediated by both histaminergic and non-histaminergic pathways (64). Th2 cytokines including IL-4, IL-13, and IL-31 interact with sensory neurons to provoke chronic itch in the context of AD (65, 66). Basophils can produce a large amount of IL-4 in response to various stimuli (57), and are the major source of IL-4 in the skin lesions of multiple AD models (48, 50, 67). Moreover, basophils can produce IL-31 in response to anti-IgE and N-formyl-methionyl-leucyl-phenylalanine stimulation (68). Therefore, it is probable that basophils play a role in pruritus in AD.

Approximately 50% of patients with AD experience acute itch flares, which is the exacerbation of intense itch, within 2 months. Wang et al. showed that basophils contribute to acute itch flares by interacting with sensory neurons *via* leukotriene C4 (LTC4) in a mouse model. Mice were first topically sensitized with MC903 and allergens (ovalbumin; OVA) on ear skin for 10 days, followed by an intradermal OVA challenge at a separate skin site, leading to acute itch flares at the challenge site, and chronic itch at the sensitization site (44). Basophil depletion significantly reduced the occurrence of acute itch flares, whereas mast cell-deficiency had no effect. Moreover, chemogenic activation of basophils induced acute itch flares, suggesting the critical roles of basophils in acute itch flares. Importantly, pharmacological inhibition of LTC4 significantly reduced the occurrence of acute itch flares, and LTC4 levels in the skin lesion were partly dependent on basophils. These results indicate the possible involvement of the basophil-LTC4 axis in acute itch flares.

2.2.2.3 Skin Barrier Dysfunction in AD

Skin barrier dysfunction is considered critical for the pathogenesis of AD. Damaged epithelial cells produce cytokines such as thymic stromal lymphopoietin (TSLP) and IL-33, leading to the promotion of Th2 immunity (69). Th2 immunity in turn promotes further disruption of the skin barrier (70). Consistent with this, the *in vitro* treatment of keratinocytes with either IL-4 or IL-13 induced the reduction of barrier-related genes (71, 72). Of note, the treatment of AD patients with dupilumab significantly increased epidermal barrier-related genes (73), suggesting that IL-4 and/or IL-13 promote skin barrier dysfunction in AD patients. In accordance with this, in a MC903-induced AD model, basophil depletion decreased the expression of IL-4 and IL-13 in skin lesion, reduced epidermal hyperplasia and keratinocyte proliferation and significantly reduced trans-epidermal water loss (67), indicating the involvement of basophils in skin barrier dysfunction through the IL-4 and IL-13 production.

2.2.2.4 Staphylococcus aureus Infection in AD

Skin colonization of *S. aureus* is frequently observed in patients with AD and is involved in the pathogenesis of AD (74, 75). In mice, the intradermal injection of lipoteichoic acid, a principal cell wall component of *S. aureus*, enhances skin recruitment of basophils in a TSLP-dependent manner (76). Moreover, basophil-derived IL-4 promoted cutaneous *S. aureus* infection in a mouse model of *S. aureus* infection. The tape stripping-induced skin barrier disruption triggered the recruitment of basophils to the skin and facilitated cutaneous *S. aureus* colonization (77). Either basophil depletion or basophil-specific IL-4/IL-13 deficiency protected mice from enhanced *S. aureus* infection. Basophil-derived IL-4/IL-13 suppresses IL-1 and IL-23 production by keratinocytes. This leads to reduced IL-17A expression by γδ T cells and impaired production of neutrophil-attracting chemokines in the skin, resulting in enhanced *S. aureus* infection. Callewaert et al. reported that the dupilumab treatment reduces *S. aureus* colonization in patients with AD (78), suggesting that basophil-derived IL-4/IL-13 may also promote cutaneous *S. aureus* infections in AD patients.

2.2.2.5 Resolution of AD

Basophils reportedly contribute to the resolution of allergic inflammation through the generation of M2 macrophages. In the IgE-CAI model, basophil-derived IL-4 promotes the differentiation of inflammatory monocytes into anti-inflammatory M2 macrophages, leading to the resolution of skin allergic inflammation (48). Pellefigues et al. identified two distinct roles for basophils during an allergic inflammation in another AD model, in which mice were topically applied with MC903 for 4 consecutive days only. Mice developed continual aggravation of ear swelling and skin barrier dysfunction for

approximately 9-10 days (inflammation phase), followed by the resolution of skin inflammation after 10 days (resolution phase). Depletion of basophils in the inflammation phase resulted in the improvement of barrier dysfunction, indicating the proinflammatory role of basophils. By contrast, either basophil-specific macrophage colony-stimulating factor (M-CSF)-deficiency or IL-4 neutralization resulted in aggravated ear swelling and skin barrier dysfunction in the resolution phase. Considering that IL-4 and M-CSF are important for the generation of anti-inflammatory M2 macrophages, basophil-derived IL-4 and M-CSF likely cooperate together to promote M2 macrophage differentiation, leading to the resolution of AD. In line with this, basophil-depletion at the resolution phase resulted in the impaired generation of $CD206^{hi}$ macrophages and reduced efferocytosis (phagocytosis of apoptotic cells) capacity in macrophages.

2.2.3 Chronic Spontaneous Urticaria

Chronic spontaneous urticaria (CSU) is characterized by itchy hives or angioedema which lasts for at least 6 weeks. Several lines of evidence have suggested the role of basophils in the pathogenesis of CSU (79–81). Ito et al. demonstrated the recruitment of basophils to skin lesions in patients with CSU (43). Extreme basopenia in the blood is commonly observed in patients with CSU (82, 83), and blood basopenia is associated with disease severity (84, 85). Omalizumab, a humanized monoclonal anti-IgE antibody, has been approved for the treatment of CSU (86, 87). Notably, the omalizumab therapy rapidly increases the blood basophil number (88–90), whereas the number of $Fc\varepsilon RI^{+}$ cells in skin lesions is decreased by omalizumab treatment (88). These results indicate the possibility that blood basopenia mirrors the recruitment of basophils to the skin lesion.

In some patients with CSU, IgG autoantibodies against IgE and FcεRI are detected (91–93), which is considered to be a cause of CSU (94). A recent study revealed that blood basopenia is strongly associated with the presence of autoantibodies against IgE or FcεRI (95). Furthermore, blood basopenia combined with autoantibodies is a predictor for slower response to omalizumab therapy (96). Nonetheless, how basopenia is associated with autoantibody and poor therapeutic responses against omalizumab remains unclear. Autoantibody-mediated activation of basophils may promote basophil recruitment to the skin lesion resulting in basopenia in the blood. It is also postulated that patients bearing autoantibodies display resistance to omalizumab therapy, possibly due to the inability of anti-IgE antibody to interfere with IgG autoantibody-mediated basophil activation.

2.3 Respiratory Allergy

In patients with moderate-to-severe asthma, the treatment with dupilumab, an anti-IL-4Rα antibody, efficiently reduces severe exacerbation and improves lung functions (97), suggesting the involvement of IL-4 and/or IL-13 in the pathogenesis of asthma. In line with this, several animal studies demonstrated the therapeutic effect of IL-4 and IL-13 inhibition on type 2 lung inflammation (98–100). Basophils are a potent source of IL-4 and IL-13 (50) and therefore may contribute to the development of lung inflammation in patients with asthma. Indeed, histopathological analysis revealed basophil infiltration in the lungs of asthmatic patients, especially in fatal cases (101, 102). Sputum basophils from asthmatic patients display increased expression of activation markers such as CD63 and CD203c, compared with blood basophils (103). Notably, the treatment of asthma patients with benralizumab, a human monoclonal antibody against IL-5Rα, significantly reduces the count of not only eosinophils but also basophils in the blood (104–106). This suggests that the therapeutic effect of benralizumab can be attributed in part to the basophil depletion.

The frequency of basophils in the sputum of patients is higher in eosinophilic asthma than in non-eosinophilic asthma and healthy controls (103, 107) and positively correlated with that of sputum eosinophils, implying a possible role of basophils in eosinophil recruitment to inflamed lungs. In accordance with this, the expression of basophil/mast cell-related genes in sputum is associated with lung eosinophilic inflammation (108). In a papain-induced asthma model, activated basophils produce IL-4 which promotes the proliferation of ILC2, enhances the production of IL-5 and CCL11 from TSLP-activated ILC2s, and facilitates recruitment of eosinophils into the lungs (109, 110). Matsuyama et al. reported that the long-acting muscarinic antagonist acts on muscarinic M3 receptor expressed by basophils to suppress IL-4 production. Therefore, it inhibits activation and proliferation of ILC2s, leading to the reduced eosinophil infiltration and airway inflammation. Unlike basophils, mast cells rather suppress papain-induced lung allergic inflammation by promoting regulatory T cell expansion (111).

Infiltration of basophils is observed in nasal polyps in patients with chronic rhinosinusitis (112–114). Recent study suggested the role of basophils in aspirin-exacerbated respiratory disease (AERD) (114), which is characterized by the triad of chronic rhinosinusitis, namely nasal polyps (CRSwNP), asthma and intolerance to cyclooxygenase-1 inhibitors. Patients with AERD displayed increased basophil numbers in nasal polyps and peripheral blood, compared to patients with CRSwNP alone. Basophils from nasal polyps of AERD patients displayed an activated phenotype and increased rates of degranulation, as assessed by the loss of staining with 2D7, a basophil granule-specific antibody. Frequency of basophil degranulation was positively correlated with disease severity, suggesting the possible contribution of basophils to the pathogenesis of AERD.

2.4 Gastrointestinal Allergy

As mentioned earlier, basophils are extensively utilized for the diagnosis of food allergies. Besides their usefulness in the diagnosis, basophils are implicated in the pathogenesis of peanut allergy in a human study (115). In mouse models of epicutaneous allergen sensitization, basophils promote the production of allergen-specific IgE, leading to the development of food allergies (116–119). Basophils also play a key role in the effector phase of food allergies (120). After repeated intragastric challenge with allergens, basophils infiltrated the jejunum, and the depletion of basophils reduced the incidence of diarrhea, concurrent with the reduction of $mMCP\text{-}1^{+}$

mast cells in the jejunum. In this model, IL-4 produced by basophils plays a key role in the food allergy pathogenesis. Given that IL-4Rα on mast cells plays a critical role in this model (121), it can be assumed that basophil-derived IL-4 acts on mast cells to aggravate food allergies.

Recent studies have identified the role of basophils in the pathogenesis of eosinophilic esophagitis (EoE), a food allergy-related chronic and inflammatory esophageal disorder (122, 123). Infiltration of basophils into the esophagus is observed in patients with active EoE, and the frequency of basophils in the esophagus is positively correlated with eosinophil infiltration in the esophagus (122). In mice, EoE-like esophageal inflammation can be triggered by epicutaneous sensitization and subsequent challenge with food allergens (122, 123). Basophil depletion or TSLP neutralization significantly reduces the esophageal infiltration of eosinophils, highlighting the roles of TSLP and basophils in the pathogenesis of the mouse EoE model. In another mouse model of EoE, the IL-33 receptor on basophils plays a key role in the recruitment of basophils to the esophagus and esophageal eosinophilic inflammation (123).

2.5 Systemic Anaphylaxis

Basophils reportedly contribute to IgG1-mediated anaphylaxis through the release of the platelet-activating factor (PAF) in a mouse model (124). In a food allergy model, mice deficient for the inhibitory receptor Allergin-1 showed systemic anaphylaxis in a basophil-dependent manner (125). Human studies also indicated the possible involvement of basophils in systemic anaphylaxis. In patients with acute anaphylaxis, blood basophil numbers decreased in the acute phase and recovered in the convalescent phase (126–128). Concurrently, the intracellular histamine content of basophils significantly decreased in patients with anaphylaxis (128). Serum levels of CCL2 significantly increased in the acute phase, as compared with healthy controls or with the convalescent phase (126, 127). Further *in vitro* experiments revealed that the serum from patients with acute phase anaphylaxis promoted basophil chemotaxis in a CCL2-depedent manner, suggesting the role of CCL2-mediated basophil chemotaxis during systemic anaphylaxis (127).

2.6 Functional Significance of CD15s Expressed on Human Basophils in Allergic Inflammation

Puan et al. reported that single nucleotide polymorphisms (SNPs) in the fucosyltransferase 6 (*FUT6*) gene locus are associated with the surface expression of CD15s (sialyl Lewis x) in human basophils (129). *In vitro* experiments showed that CD15s on basophils is functionally important for the rolling on E-selectin-coated surfaces. Indeed, patients with *FUT6* null mutations had higher basophil numbers in the blood and lower itch sensitivity against mosquito bites. Furthermore, *FUT6*-deficiency significantly reduced serum concentration of total IgE and house dust mite (HDM)-specific IgE and decreased skin prick responses against HDM antigens. These results highlight the role of basophils in HDM-induced allergy and itch sensitivity against insect bites.

3 ROLE OF BASOPHILS IN TISSUE REPAIR AND FIBROSIS

3.1 Resolution of Inflammation and Tissue Repair

Following acute and chronic inflammation, an integrated resolution process takes place, which results in the reduction of cellular infiltration and tissue damage repair (130). As mentioned earlier, basophils promote the generation of anti-inflammatory M2 macrophages, leading to the resolution of allergic inflammation (48, 67). This beneficial role of basophils was also demonstrated in liver tissue repair after *Listeria monocytogenes* (Lm) infection (131). Lm infection induced necroptosis of liver-resident Kupffer cells, which triggered IL-33 production from hepatocytes and IL-4 production from recruited basophils. Recruited monocytes were alternatively activated by basophil-derived IL-4, leading to the replacement of ablated Kupffer cells with monocyte-derived macrophages. This was also the case when healing after myocardial infarction (MI) (22). In an animal model of MI, basophils infiltrated heart tissue, and basophil depletion or basophil-specific IL-4/IL-13-deficiency resulted in the deterioration of cardiac functions and increased the infarct region. Moreover, basophil-specific IL-4/IL-13-deficiency increased the infiltration of inflammatory $Ly6C^{hi}$ monocytes and reduced $Ly6C^{lo}$ reparative macrophage numbers, suggesting the involvement of basophil-derived IL-4/IL-13 in the phenotypic transition from inflammatory monocytes to reparative macrophages (22, 132). Stimulation of basophils by IPSE/α-1 significantly enhanced cardiac functions, demonstrating the important role of activated basophils in post-MI tissue repair. In patients with acute MI, low blood basophil counts were associated with increased scar size and poor outcomes, which raises the possibility that basophils contribute to the tissue repair process. Thus, basophil-derived IL-4 and IL-13 contributes to a variety of tissue repair responses (**Figure 2** upper panel).

Basophil-derived amphiregulin is also involved in UVB-induced suppression of cutaneous inflammation (133). Inclan-Rico et al. revealed that basophils contributed to the resolution of lung inflammation by inhibiting ILC2 activation in a helminth infection model (134). Lung-infiltrated basophils stimulate ILC2s to enhance the expression of the receptor for the neuropeptide neuromedin B, and neuromedin B-mediated signals inhibit exaggerated activation of ILC2s and prevent excess lung inflammation.

3.2 Tissue Fibrosis and Emphysema

Type 2 immunity promotes tissue repair whereas the dysregulated or chronic tissue repair program leads to tissue fibrosis (135). In an allograft heart transplantation model, basophil-derived IL-4 was involved in tissue fibrosis (23). Donor-derived basophils infiltrated allograft heart and produced IL-4, while basophil depletion reduced the number of α-SMA^{+} myofibroblasts and hence inhibits allograft fibrosis. In accordance with this, an IL-4 receptor-deficient graft heart was resistant to tissue fibrosis. In this model, IL-3 played a role in the recruitment and activation of basophils (136). Therefore, it can be assumed that IL-3-activated basophils produce IL-4 which in

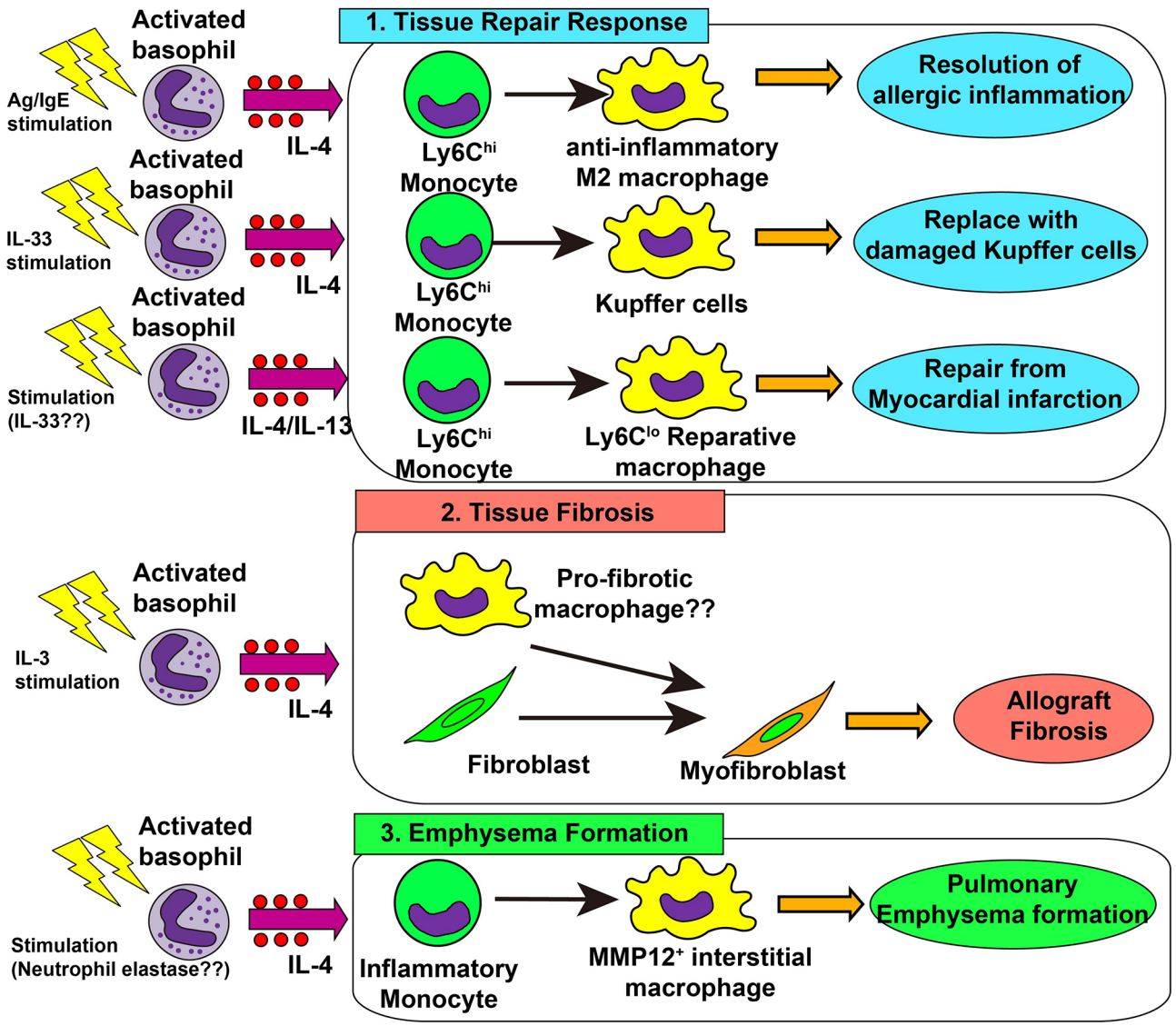


FIGURE 2 | Role of basophils in tissue repair responses, tissue fibrosis and emphysema formation. 1) In skin allergy, basophil-derived interleukin (IL)-4 promotes the differentiation of inflammatory monocytes into anti-inflammatory M2 macrophages, leading to the resolution of allergic inflammation. In the liver infected with *Listeria monocytogenes*, basophil-derived IL-4 promotes monocyte differentiation into M2 macrophages which replace damaged Kupffer cells, promoting healing of liver damage. In myocardial infarction, basophil-derived IL-4 and/or IL-13 promotes the generation of reparative Ly6C^{lo} macrophages which enhances post-infarction tissue repair. 2) In allograft heart transplantation, basophil-derived IL-4 promotes tissue fibrosis, possibly by acting on tissue-resident macrophages or fibroblasts, leading to the generation of myofibroblasts and deposition of collagen fibers. 3) In a chronic obstructive lung disease (COPD) model, basophil-derived IL-4 promotes the generation of MMP-12^{+} interstitial macrophages which promote the destruction of alveolar walls and emphysema formation.

turn acts on heart-resident macrophages and fibroblasts to promote the generation of myofibroblasts and deposition of collagens (**Figure 2** middle panel).

A recent report implicated basophils in IgG4-related diseases (IgG4-RD) (137). IgG4-RD is characterized by elevated IgG4 levels in serum, storiform fibrosis, and marked infiltration of IgG4-producing plasma cells in multiple organs, including the pancreas, kidney, and salivary glands. Basophils expressing both TLR2 and TLR4 infiltrated pancreatic tissues in patients with type 1 autoimmune pancreatitis, a pancreatic manifestation of IgG4-RD (138). Furthermore, LPS-stimulated basophils produced IL-13 and B cell-activating factor (BAFF), which induced IgG4 production by B cells (139), suggesting that basophils may contribute to IgG4 production in patients with IgG4-RD.

Dysregulated tissue repair responses can cause pulmonary emphysema (140). Shibata et al. revealed that basophils contribute to the pathogenesis of pulmonary emphysema in an elastase-induced mouse model of chronic obstructive lung disease (COPD) (13). Basophil-derived IL-4 promoted the generation of emphysema-prone MMP12^{+} interstitial macrophages,

contributing to lung emphysema formation (**Figure 2** lower panel). On the other hand, genetically engineered mast cell-deficient mice ($Cpa3^{Cre/+}$ mice) developed pulmonary emphysema as much as observed in mast cell-sufficient mice, even though these mice showed partial reduction of basophils (141). A recent report showed basophil infiltration in the inflamed lung tissue of patients with COPD, especially in severe cases (142), suggesting the possible contribution of basophils for COPD development in humans.

4 ROLE OF BASOPHILS IN AUTOIMMUNE DISEASES

4.1 Systemic Lupus Erythematosus

Autoreactive IgE antibodies are frequently detected in patients with systemic lupus erythematosus (SLE), and the serum level of autoreactive IgE is associated with disease activity and active nephritis (143–147). In phase Ib clinical trial, omalizumab therapy showed some efficacy on disease activity in SLE patients with elevated level of serum autoreactive IgE antibody (148), which indicates the role of autoreactive IgE in the pathogenesis of SLE. Moreover, patients with SLE displayed blood basopenia, and their basophils had upregulated expression of activation markers such as CD63 and CD203c, compared with basophils from healthy controls (144, 149). Additionally, patient serum induced basophil activation in an IgE-dependent manner (149). These observations suggest the role of autoreactive IgE antibodies and basophils in SLE. In line with this, basophils play critical roles in animal models of lupus nephritis, including *Lyn*-deficient mice, MRL-*lpr/lpr* lupus prone mice, and a pristane-induced SLE model (144, 149, 150). The presence of a feedback-loop is proposed for the pathogenesis of mouse SLE models and patients (149, 151) (**Figure 3**). In SLE models, basophils are recruited to secondary lymphoid organs, display an activated phenotype, and produce IL-4, IL-13, and BAFF to promote autoantibody production. The formation of immune complexes of IgE autoantibodies and autoantigens further activates blood-circulating basophils to enhance the expression of CD62L, which in turn facilitates the homing of basophils into secondary lymphoid organs. Prostaglandin D2 (PGD2) is involved in the recruitment of basophils to secondary lymphoid organs (152). PGD2, possibly produced by activated basophils, enhances surface expression of CXCR4 in basophils, promoting the migration of basophils into secondary lymphoid organs. In accordance with this, basophils from patients with SLE display high CXCR4 expression on their cell surface, which is positively correlated with disease activity.

4.2 Other Autoimmune Diseases

Lamri et al. reported that basophils contributed to the pathogenesis of mixed connective tissue disease (MCTD) (153). Patients with MCTD displayed blood basopenia and upregulated expression of CD203c, CD63 and CXCR4 on the surface of basophils. In a mouse MCTD-like lung inflammation model, the infiltration of activated basophils was observed in lung draining lymph nodes. Depletion of basophils or IgE-deficiency prevented the development of lung MCTD-like inflammation. Yuk et al. showed that basophil-derived IL-6 potentiated T cell differentiation into Th17 cells, thus promoting the development of experimental autoimmune encephalomyelitis (154).

5 ROLE OF BASOPHILS IN CANCER

Several lines of evidence have indicated the possible role of basophils in the development of cancer (24). In pancreatic ductal adenocarcinoma (PDAC), basophils infiltrate tumor draining lymph nodes and express *IL4*. A higher number of infiltrating basophils is associated with reduced PDAC patient survival. In a mouse model of pancreatic cancer, basophils recruited to tumor draining lymph nodes were activated by T cell-derived IL-3 to produce IL-4, promoting Th2 cell and M2 macrophage differentiation which favors pancreatic cancer development. Similarly, basophil infiltration in the tumor microenvironment was a predictor for poor human gastric cancer prognosis (155).

Basophils reportedly contribute to the pathogenesis of chronic myeloid leukemia (CML) (25). Blood basophilia is frequently observed in patients with CML and is associated with poor prognosis of CML. In a mouse model of CML, basophils produced large amount of CCL3 in the bone marrow, which inhibits the functions of normal hematopoietic stem cells and supports the proliferation of leukemia cells (156).

Intriguingly, basophils played a rather protective role in a mouse melanoma model. The depletion of regulatory T cells resulted in substantial infiltration of basophils and $CD8^+$ T cells in the tumor microenvironment achieving complete rejection of transplanted melanoma (157). Tumor-infiltrating basophils produce CCL3 and CCL4 to promote the recruitment of $CD8^+$ T cells into the tumor microenvironment enhancing tumor rejection. In patients with ovarian cancer, the activated basophil phenotype was predicative of better prognosis (158).

Taken together, these data show that basophils play either deleterious or protective roles in a context-dependent manner. In accordance with this, the opposite roles of basophils were reported in mutagen-induced skin carcinogenesis in mice. On one hand, Crawford et al. demonstrated the protective role of basophils (159). Repetitive application of DNA-damaging xenobiotics DMBA resulted in the production of autoreactive IgE and accumulation of IgE^+ basophils in the skin. Deficiency of IgE or FcεRIα promotes tumorigenesis and tumor growth, suggesting the contribution of basophils in the inhibition of epithelial carcinogenesis. On the other hand, Hayes et al. showed that basophils and IgE rather enhanced tumor growth in an inflammation-induced skin carcinogenesis model (160) in which mice were first topically treated with DMBA and subsequently with TPA (protein kinase C activator). This led to the production of natural IgE and the accumulation of IgE^+ basophils in the skin. IgE-deficiency or basophil depletion abolished epithelial hyperplasia. Basophil-derived histamine is thought to promote epithelial hyperplasia, thus promoting TPA-induced tumor growth.

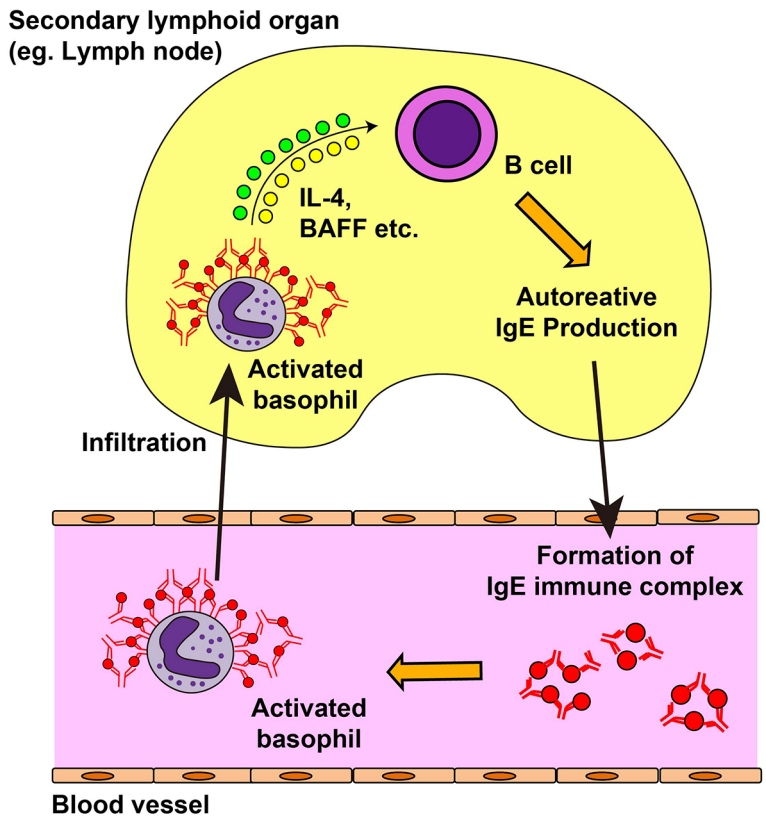


FIGURE 3 | Feedback loop for the exacerbation of systemic lupus erythematosus. In the mouse model of systemic lupus erythematosus (SLE) and in patients with SLE, autoreactive IgE antibodies can be detected in the blood. Autoreactive IgE antibodies form immune complexes with corresponding autoantigens and activate blood-circulating basophils. Activated basophils upregulate the surface expression of CD62L and CXCR4 and infiltrate into lymph nodes. They produce interleukin (IL)-4, IL-13, and B cell-activating factor (BAFF) which in turn induces autoantibody production from B cells, resulting in the deposit of immune complexes in the kidney and in disease progression.

6 POSSIBLE ROLES OF BASOPHILS IN COVID-19

Emerging evidence suggests a possible role for basophils in COVID-19 (27). Mass-cytometry analysis revealed that the blood basophil number decreases during the acute phase and is restored in the recovery phase (161). In line with this, several studies demonstrated that the blood basophil number is significantly lower in severe COVID-19 patients, compared with less-severe patients or non-COVID-19 patients (162–167). Therefore, lower blood basophil counts would be a risk factor predicting a poor COVID-19 prognosis (162, 168). Notably, the plasma level of anti-SARS-CoV2 IgG correlated positively with the number of blood-circulating basophils (161), suggesting the possible role for basophils in IgG responses against SARS-CoV2.

Surface expression profiles of blood basophils are also altered in COVID-19 patients, especially in severe cases (164, 167). Basophils showed upregulated expression of activation markers such as CD63 and CD11b in severe cases (167). In line with this, *in vitro* co-culture of basophils with SARS-CoV2 led to the production of IL-4 and IL-13 by basophils (169). Further mechanistic studies will be required to identify whether basophils play protective or deleterious roles in COVID-19.

7 CONCLUSION AND PERSPECTIVES

Basophils have long been neglected from immunological studies, partly due to their similarity to tissue-resident mast cells, even though they have been evolutionally conserved in many animal species. We now appreciate that basophils have non-redundant roles distinct from those played by mast cells in a variety of immune and inflammatory responses, including IgE-CAI, papain-induced asthma, and elastase-induced COPD models. Studies of animal models identified that basophils infiltrate either the sites of inflammation or the draining lymph nodes and regulate immune responses by interacting with various types of cells, including macrophages, T cells, ILCs and sensory neurons. Recent human studies, including the treatments of patients with therapeutic antibodies (e.g. omalizumab, benralizumab and dupilumab), have advanced our understanding of human basophil pathophysiology. Further mechanistic studies would

identify novel roles for basophils in an even broader range of disorders and promote the development of novel strategies for the treatment of such diseases by targeting basophils and their products.

AUTHOR CONTRIBUTIONS

All authors listed have made a substantial, direct and intellectual contribution to the work and approved it for publication.

FUNDING

This work was supported by research grants from the Japanese Ministry of Education, Culture, Sports, Science and Technology [20K16277(KM), 19H01025 (HK), 22K07115 (KM), 21K18255 (HK), 22H02845 (HK)], SENSHIN Medical Research Foundation (KM), Takeda Science Foundation (KM), KANAE Foundation for the Promotion of Medical Science (KM), The Uehara Memorial Foundation (KM), The Naito Foundation (KM), and Ohyama Health Foundation (KM).

REFERENCES

1. Dwyer DF, Barrett NA, Austen KF. Immunological Genome Project C. Expression Profiling of Constitutive Mast Cells Reveals a Unique Identity Within the Immune System. *Nat Immunol* (2016) 17(7):878–87. doi: 10.1038/ni.3445
2. Motakis E, Guhl S, Ishizu Y, Itoh M, Kawaji H, de Hoon M, et al. Redefinition of the Human Mast Cell Transcriptome by Deep-CAGE Sequencing. *Blood* (2014) 123(17):e58–67. doi: 10.1182/blood-2013-02-483792
3. Obata K, Mukai K, Tsujimura Y, Ishiwata K, Kawano Y, Minegishi Y, et al. Basophils Are Essential Initiators of a Novel Type of Chronic Allergic Inflammation. *Blood* (2007) 110(3):913–20. doi: 10.1182/blood-2007-01-068718
4. Denzel A, Maus UA, Rodriguez Gomez M, Moll C, Niedermeier M, Winter C, et al. Basophils Enhance Immunological Memory Responses. *Nat Immunol* (2008) 9(7):733–42. doi: 10.1038/ni.1621
5. Wada T, Ishiwata K, Koseki H, Ishikura T, Ugajin T, Ohnuma N, et al. Selective Ablation of Basophils in Mice Reveals Their Nonredundant Role in Acquired Immunity Against Ticks. *J Clin Invest* (2010) 120(8):2867–75. doi: 10.1172/JCI42680
6. Ohnmacht C, Schwartz C, Panzer M, Schiedewitz I, Naumann R, Voehringer D. Basophils Orchestrate Chronic Allergic Dermatitis and Protective Immunity Against Helminths. *Immunity* (2010) 33(3):364–74. doi: 10.1016/j.immuni.2010.08.011
7. Sullivan BM, Liang HE, Bando JK, Wu D, Cheng LE, McKerrow JK, et al. Genetic Analysis of Basophil Function *in vivo*. *Nat Immunol* (2011) 12(6):527–35. doi: 10.1038/ni.2036
8. Sawaguchi M, Tanaka S, Nakatani Y, Harada Y, Mukai K, Matsunaga Y, et al. Role of Mast Cells and Basophils in IgE Responses and in Allergic Airway Hyperresponsiveness. *J Immunol* (2012) 188(4):1809–18. doi: 10.4049/jimmunol.1101746
9. Mukai K, BenBarak MJ, Tachibana M, Nishida K, Karasuyama H, Taniuchi I, et al. Critical Role of P1-Runx1 in Mouse Basophil Development. *Blood* (2012) 120(1):76–85. doi: 10.1182/blood-2011-12-399113
10. Matsuoka K, Shitara H, Taya C, Kohno K, Kikkawa Y, Yonekawa H. Novel Basophil- or Eosinophil-Depleted Mouse Models for Functional Analyses of Allergic Inflammation. *PloS One* (2013) 8(4):e60958. doi: 10.1371/journal.pone.0060958
11. Pellefigues C, Mehta P, Prout MS, Naidoo K, Yumnam B, Chandler J, et al. The Basoph8 Mice Enable an Unbiased Detection and a Conditional Depletion of Basophils. *Front Immunol* (2019) 10:2143. doi: 10.3389/fimmu.2019.02143
12. Miyake K, Shiozawa N, Nagao T, Yoshikawa S, Yamanishi Y, Karasuyama H. Trogocytosis of Peptide-MHC Class II Complexes From Dendritic Cells Confers Antigen-Presenting Ability on Basophils. *Proc Natl Acad Sci U.S.A.* (2017) 114(5):1111–6. doi: 10.1073/pnas.1615973114
13. Shibata S, Miyake K, Tateishi T, Yoshikawa S, Yamanishi Y, Miyazaki Y, et al. Basophils Trigger Emphysema Development in a Murine Model of COPD Through IL-4-Mediated Generation of MMP-12-Producing Macrophages. *Proc Natl Acad Sci USA* (2018) 115(51):13057–62. doi: 10.1073/pnas.1813927115
14. Yoshikawa S, Oh-Hora M, Hashimoto R, Nagao T, Peters L, Egawa M, et al. Pivotal Role of STIM2, But Not STIM1, in IL-4 Production by IL-3-Stimulated Murine Basophils. *Sci Signal* (2019) 12(576):eaav2060. doi: 10.1126/scisignal.aav2060
15. Nakashima C, Otsuka A, Kabashima K. Recent Advancement in the Mechanism of Basophil Activation. *J Dermatol Sci* (2018) 91(1):3–8. doi: 10.1016/j.jdermsci.2018.03.007
16. Varricchi G, Raap U, Rivellese F, Marone G, Gibbs BF. Human Mast Cells and Basophils-How Are They Similar How Are They Different? *Immunol Rev* (2018) 282(1):8–34. doi: 10.1111/imr.12627
17. Miyake K, Shibata S, Yoshikawa S, Karasuyama H. Basophils and Their Effector Molecules in Allergic Disorders. *Allergy* (2021) 76(6):1693–706. doi: 10.1111/all.14662
18. Eberle JU, Voehringer D. Role of Basophils in Protective Immunity to Parasitic Infections. *Semin Immunopathol* (2016) 38(5):605–13. doi: 10.1007/s00281-016-0563-3
19. Karasuyama H, Miyake K, Yoshikawa S. Immunobiology of Acquired Resistance to Ticks. *Front Immunol* (2020) 11:601504. doi: 10.3389/fimmu.2020.601504
20. Peng J, Siracusa MC. Basophils in Antihelminth Immunity. *Semin Immunol* (2021) 53:101529. doi: 10.1016/j.smim.2021.101529
21. Poddighe D, Dossybayeva K, Bexeitov Y, Mukusheva Z. Basophils in Autoimmunity: Systemic Lupus Erythematosus and More? *Autoimmun Rev* (2021) 20(4):102790. doi: 10.1016/j.autrev.2021.102790
22. Sicklinger F, Meyer IS, Li X, Radtke D, Dicks S, Kornadt MP, et al. Basophils Balance Healing After Myocardial Infarction *via* IL-4/IL-13. *J Clin Invest* (2021) 131(13):e136778. doi: 10.1172/JCI136778
23. Schiechl G, Hermann FJ, Rodriguez Gomez M, Kutzi S, Schmidbauer K, Talke Y, et al. Basophils Trigger Fibroblast Activation in Cardiac Allograft Fibrosis Development. *Am J Transplant* (2016) 16(9):2574–88. doi: 10.1111/ajt.13764
24. Marone G, Schroeder JT, Mattei F, Loffredo S, Gambardella AR, Poto R, et al. Is There a Role for Basophils in Cancer? *Front Immunol* (2020) 11:2103. doi: 10.3389/fimmu.2020.02103
25. Mukaida N, Tanabe Y, Baba T. Cancer non-Stem Cells as a Potent Regulator of Tumor Microenvironment: A Lesson From Chronic Myeloid Leukemia. *Mol BioMed* (2021) 2(1):7. doi: 10.1186/s43556-021-00030-7
26. Chauhan J, Stavraka C, Grandits M, Palhares L, Josephs DH, Lacy KE, et al. Clinical and Translational Significance of Basophils in Patients With Cancer. *Cells* (2022) 11(3):438. doi: 10.3390/cells11030438
27. Murdaca G, Di Gioacchino M, Greco M, Borro M, Paladin F, Petrarca C, et al. Basophils and Mast Cells in COVID-19 Pathogenesis. *Cells* (2021) 10(10):2754. doi: 10.3390/cells10102754
28. Hemmings O, Kwok M, McKendry R, Santos AF. Basophil Activation Test: Old and New Applications in Allergy. *Curr Allergy Asthma Rep* (2018) 18(12):77. doi: 10.1007/s11882-018-0831-5
29. Santos AF, Alpan O, Hoffmann HJ. Basophil Activation Test: Mechanisms and Considerations for Use in Clinical Trials and Clinical Practice. *Allergy* (2021) 76(8):2420–32. doi: 10.1111/all.14747
30. Tsai M, Mukai K, Chinthrajah RS, Nadeau KC, Galli SJ. Sustained Successful Peanut Oral Immunotherapy Associated With Low Basophil Activation and Peanut-Specific IgE. *J Allergy Clin Immunol* (2020) 145(3):885–96 e6. doi: 10.1016/j.jaci.2019.10.038
31. Schmid JM, Wurtzen PA, Siddhuraj P, Jogdand P, Petersen CG, Dahl R, et al. Basophil Sensitivity Reflects Long-Term Clinical Outcome of Subcutaneous

Immunotherapy in Grass Pollen-Allergic Patients. *Allergy* (2021) 76 (5):1528–38. doi: 10.1111/all.14264
32. MacGlashan DWJr., Saini SS. Syk Expression and IgE-Mediated Histamine Release in Basophils as Biomarkers for Predicting the Clinical Efficacy of Omalizumab. *J Allergy Clin Immunol* (2017) 139(5):1680–2.e10. doi: 10.1016/j.jaci.2016.12.965
33. Puan KJ, Andiappan AK, Lee B, Kumar D, Lai TS, Yeo G, et al. Systematic Characterization of Basophil Anergy. *Allergy* (2017) 72(3):373–84. doi: 10.1111/all.12952
34. Troelnikov A, Perkins G, Yuson C, Ahamdie A, Balouch S, Hurtado PR, et al. Basophil Reactivity to BNT162b2 Is Mediated by PEGylated Lipid Nanoparticles in Patients With PEG Allergy. *J Allergy Clin Immunol* (2021) 148(1):91–5. doi: 10.1016/j.jaci.2021.04.032
35. Warren CM, Snow TT, Lee AS, Shah MM, Heider A, Blomkalns A, et al. Assessment of Allergic and Anaphylactic Reactions to mRNA COVID-19 Vaccines With Confirmatory Testing in a US Regional Health System. *JAMA Netw Open* (2021) 4(9):e2125524. doi: 10.1001/jamanetworkopen.2021.25524
36. Labella M, Cespedes JA, Dona I, Shamji MH, Agache I, Mayorga C, et al. The Value of the Basophil Activation Test in the Evaluation of Patients Reporting Allergic Reactions to the BNT162b2 mRNA COVID-19 Vaccine. *Allergy* (2021). doi: 10.1111/all.15148
37. McKenzie CI, Varese N, Aui PM, Wines BD, Hogarth PM, Thien F, et al. CytoBas: Precision Component-Resolved Diagnostics for Allergy Using Flow Cytometric Staining of Basophils With Recombinant Allergen Tetramers. *Allergy* (2021) 76(10):3028–40. doi: 10.1111/all.14832
38. Qi Z, Xue Q, Wang H, Cao B, Su Y, Xing Q, et al. Serum CD203c+ Extracellular Vesicle Serves as a Novel Diagnostic and Prognostic Biomarker for Succinylated Gelatin Induced Perioperative Hypersensitive Reaction. *Front Immunol* (2021) 12:732209. doi: 10.3389/fimmu.2021.732209
39. Dvorak HF. Cutaneous Basophil Hypersensitivity. *J Allergy Clin Immunol* (1976) 58(1 pt. 2):229–40. doi: 10.1016/0091-6749(76)90159-7
40. Katz SI. Recruitment of Basophils in Delayed Hypersensitivity Reactions. *J Invest Dermatol* (1978) 71(1):70–5. doi: 10.1111/1523-1747.ep12544415
41. Askenase PW. Rare Skin Reactions After mRNA Vaccination, Similar to Jones-Mote Basophil Responses. *N Engl J Med* (2021) 385(18):1720–1. doi: 10.1056/NEJMc2111452
42. Kim BS, Wang K, Siracusa MC, Saenz SA, Brestoff JR, Monticelli LA, et al. Basophils Promote Innate Lymphoid Cell Responses in Inflamed Skin. *J Immunol* (2014) 193(7):3717–25. doi: 10.4049/jimmunol.1401307
43. Ito Y, Satoh T, Takayama K, Miyagishi C, Walls AF, Yokozeki H. Basophil Recruitment and Activation in Inflammatory Skin Diseases. *Allergy* (2011) 66(8):1107–13. doi: 10.1111/j.1398-9995.2011.02570.x
44. Wang F, Trier AM, Li F, Kim S, Chen Z, Chai JN, et al. A Basophil-Neuronal Axis Promotes Itch. *Cell* (2021) 184(2):422–40.e17. doi: 10.1016/j.cell.2020.12.033
45. Imamura S, Washio K, Mizuno M, Oda Y, Fukunaga A, Nishigori C. Activated Steady Status and Distinctive FcepsilonRI-Mediated Responsiveness in Basophils of Atopic Dermatitis. *Allergol Int* (2021) 70 (3):327–34. doi: 10.1016/j.alit.2021.01.005
46. Kabashima K. New Concept of the Pathogenesis of Atopic Dermatitis: Interplay Among the Barrier, Allergy, and Pruritus as a Trinity. *J Dermatol Sci* (2013) 70(1):3–11. doi: 10.1016/j.jdermsci.2013.02.001
47. Mukai K, Matsuoka K, Taya C, Suzuki H, Yokozeki H, Nishioka K, et al. Basophils Play a Critical Role in the Development of IgE-Mediated Chronic Allergic Inflammation Independently of T Cells and Mast Cells. *Immunity* (2005) 23(2):191–202. doi: 10.1016/j.immuni.2005.06.011
48. Egawa M, Mukai K, Yoshikawa S, Iki M, Mukaida N, Kawano Y, et al. Inflammatory Monocytes Recruited to Allergic Skin Acquire an Anti-Inflammatory M2 Phenotype *via* Basophil-Derived Interleukin-4. *Immunity* (2013) 38(3):570–80. doi: 10.1016/j.immuni.2012.11.014
49. Otsuka A, Nakajima S, Kubo M, Egawa G, Honda T, Kitoh A, et al. Basophils are Required for the Induction of Th2 Immunity to Haptens and Peptide Antigens. *Nat Commun* (2013) 4:1739. doi: 10.1038/ncomms2740
50. Yamanishi Y, Mogi K, Takahashi K, Miyake K, Yoshikawa S, Karasuyama H. Skin-Infiltrating Basophils Promote Atopic Dermatitis-Like Inflammation *via* IL-4 Production in Mice. *Allergy* (2020) 75(10):2613–22. doi: 10.1111/all.14362
51. Imai Y, Yasuda K, Nagai M, Kusakabe M, Kubo M, Nakanishi K, et al. IL-33-Induced Atopic Dermatitis-Like Inflammation in Mice Is Mediated by Group 2 Innate Lymphoid Cells in Concert With Basophils. *J Invest Dermatol* (2019) 139(10):2185–94.e3. doi: 10.1016/j.jid.2019.04.016
52. Iki M, Tanaka K, Deki H, Fujimaki M, Sato S, Yoshikawa S, et al. Basophil Tryptase mMCP-11 Plays a Crucial Role in IgE-Mediated, Delayed-Onset Allergic Inflammation in Mice. *Blood* (2016) 128(25):2909–18. doi: 10.1182/blood-2016-07-729392
53. Eberle JU, Radtke D, Nimmerjahn F, Voehringer D. Eosinophils Mediate Basophil-Dependent Allergic Skin Inflammation in Mice. *J Invest Dermatol* (2019) 139(9):1957–65.e2. doi: 10.1016/j.jid.2019.03.1129
54. Cheng LE, Sullivan BM, Retana LE, Allen CD, Liang HE, Locksley RM. IgE-Activated Basophils Regulate Eosinophil Tissue Entry by Modulating Endothelial Function. *J Exp Med* (2015) 212(4):513–24. doi: 10.1084/jem.20141671
55. Liu Y, Cook C, Sedgewick AJ, Zhang S, Fassett MS, Ricardo-Gonzalez RR, et al. Single-Cell Profiling Reveals Divergent, Globally Patterned Immune Responses in Murine Skin Inflammation. *iScience* (2020) 23(10):101582. doi: 10.1016/j.isci.2020.101582
56. Beck LA, Thaci D, Hamilton JD, Graham NM, Bieber T, Rocklin R, et al. Dupilumab Treatment in Adults With Moderate-to-Severe Atopic Dermatitis. *N Engl J Med* (2014) 371(2):130–9. doi: 10.1056/NEJMoa1314768
57. Yamanishi Y, Karasuyama H. Basophil-Derived IL-4 Plays Versatile Roles in Immunity. *Semin Immunopathol* (2016) 38(5):615–22. doi: 10.1007/s00281-016-0568-y
58. Leyva-Castillo JM, Hener P, Michea P, Karasuyama H, Chan S, Soumelis V, et al. Skin Thymic Stromal Lymphopoietin Initiates Th2 Responses Through an Orchestrated Immune Cascade. *Nat Commun* (2013) 4:2847. doi: 10.1038/ncomms3847
59. Sokol CL, Chu NQ, Yu S, Nish SA, Laufer TM, Medzhitov R. Basophils Function as Antigen-Presenting Cells for an Allergen-Induced T Helper Type 2 Response. *Nat Immunol* (2009) 10(7):713–20. doi: 10.1038/ni.1738
60. Perrigoue JG, Saenz SA, Siracusa MC, Allenspach EJ, Taylor BC, Giacomin PR, et al. MHC Class II–Dependent Basophil–CD4+ T Cell Interactions Promote TH2 Cytokine–Dependent Immunity. *Nat Immunol* (2009) 10 (7):697–705. doi: 10.1038/ni.1740
61. Yoshimoto T, Yasuda K, Tanaka H, Nakahira M, Imai Y, Fujimori Y, et al. Basophils Contribute to TH2-IgE Responses *In Vivo via* IL-4 Production and Presentation of Peptide-MHC Class II Complexes to CD4+ T Cells. *Nat Immunol* (2009) 10(7):706–12. doi: 10.1038/ni.1737
62. Hammad H, Plantinga M, Deswarte K, Pouliot P, Willart MA, Kool M, et al. Inflammatory Dendritic Cells–Not Basophils–Are Necessary and Sufficient for Induction of Th2 Immunity to Inhaled House Dust Mite Allergen. *J Exp Med* (2010) 207(10):2097–111. doi: 10.1084/jem.20101563
63. Tang H, Cao W, Kasturi SP, Ravindran R, Nakaya HI, Kundu K, et al. The T Helper Type 2 Response to Cysteine Proteases Requires Dendritic Cell-Basophil Cooperation *via* ROS-Mediated Signaling. *Nat Immunol* (2010) 11 (7):608–17. doi: 10.1038/ni.1883
64. Yang TB, Kim BS. Pruritus in Allergy and Immunology. *J Allergy Clin Immunol* (2019) 144(2):353–60. doi: 10.1016/j.jaci.2019.06.016
65. Cevikbas F, Wang X, Akiyama T, Kempkes C, Savinko T, Antal A, et al. A Sensory Neuron-Expressed IL-31 Receptor Mediates T Helper Cell-Dependent Itch: Involvement of TRPV1 and TRPA1. *J Allergy Clin Immunol* (2014) 133(2):448–60. doi: 10.1016/j.jaci.2013.10.048
66. Oetjen LK, Mack MR, Feng J, Whelan TM, Niu H, Guo CJ, et al. Sensory Neurons Co-Opt Classical Immune Signaling Pathways to Mediate Chronic Itch. *Cell* (2017) 171(1):217–28.e13. doi: 10.1016/j.cell.2017.08.006
67. Pellefigues C, Naidoo K, Mehta P, Schmidt AJ, Jagot F, Roussel E, et al. Basophils Promote Barrier Dysfunction and Resolution in the Atopic Skin. *J Allergy Clin Immunol* (2021) 148(3):799–812.e10. doi: 10.1016/j.jaci.2021.02.018
68. Raap U, Gehring M, Kleiner S, Rudrich U, Eiz-Vesper B, Haas H, et al. Human Basophils are a Source of - and Are Differentially Activated by - IL-31. *Clin Exp Allergy* (2017) 47(4):499–508. doi: 10.1111/cea.12875
69. Yang G, Seok JK, Kang HC, Cho YY, Lee HS, Lee JY. Skin Barrier Abnormalities and Immune Dysfunction in Atopic Dermatitis. *Int J Mol Sci* (2020) 21(8):2867. doi: 10.3390/ijms21082867
70. Furue M. Regulation of Filaggrin, Loricrin, and Involucrin by IL-4, IL-13, IL-17a, IL-22, AHR, and NRF2: Pathogenic Implications in Atopic Dermatitis. *Int J Mol Sci* (2020) 21(15):5382. doi: 10.3390/ijms21155382

71. Kim BE, Leung DY, Boguniewicz M, Howell MD. Loricrin and Involucrin Expression is Down-Regulated by Th2 Cytokines Through STAT-6. *Clin Immunol* (2008) 126(3):332–7. doi: 10.1016/j.clim.2007.11.006
72. Howell MD, Kim BE, Gao P, Grant AV, Boguniewicz M, DeBenedetto A, et al. Cytokine Modulation of Atopic Dermatitis Filaggrin Skin Expression. *J Allergy Clin Immunol* (2009) 124(3 Suppl 2):R7–R12. doi: 10.1016/j.jaci.2009.07.012
73. Guttman-Yassky E, Bissonnette R, Ungar B, Suarez-Farinas M, Ardeleanu M, Esaki H, et al. Dupilumab Progressively Improves Systemic and Cutaneous Abnormalities in Patients With Atopic Dermatitis. *J Allergy Clin Immunol* (2019) 143(1):155–72. doi: 10.1016/j.jaci.2018.08.022
74. Kobayashi T, Glatz M, Horiuchi K, Kawasaki H, Akiyama H, Kaplan DH, et al. Dysbiosis and Staphylococcus Aureus Colonization Drives Inflammation in Atopic Dermatitis. *Immunity* (2015) 42(4):756–66. doi: 10.1016/j.immuni.2015.03.014
75. Nakatsuji T, Chen TH, Two AM, Chun KA, Narala S, Geha RS, et al. Staphylococcus Aureus Exploits Epidermal Barrier Defects in Atopic Dermatitis to Trigger Cytokine Expression. *J Invest Dermatol* (2016) 136(11):2192–200. doi: 10.1016/j.jid.2016.05.127
76. Brauweiler AM, Goleva E, Leung DYM. Staphylococcus Aureus Lipoteichoic Acid Initiates a TSLP-Basophil-IL4 Axis in the Skin. *J Invest Dermatol* (2020) 140(4):915–7 e2. doi: 10.1016/j.jid.2019.09.004
77. Leyva-Castillo JM, Das M, Kane J, Strakosha M, Singh S, Wong DSH, et al. Basophil-Derived IL-4 Promotes Cutaneous Staphylococcus Aureus Infection. *JCI Insight* (2021) 6(21):e149953. doi: 10.1172/jci.insight.149953
78. Callewaert C, Nakatsuji T, Knight R, Kosciolek T, Vrbanac A, Kotol P, et al. IL-4ralpha Blockade by Dupilumab Decreases Staphylococcus Aureus Colonization and Increases Microbial Diversity in Atopic Dermatitis. *J Invest Dermatol* (2020) 140(1):191–202.e7. doi: 10.1016/j.jid.2019.05.024
79. Saini SS. Basophil Responsiveness in Chronic Urticaria. *Curr Allergy Asthma Rep* (2009) 9(4):286–90. doi: 10.1007/s11882-009-0040-3
80. Kaplan AP, Gimenez-Arnau AM, Saini SS. Mechanisms of Action That Contribute to Efficacy of Omalizumab in Chronic Spontaneous Urticaria. *Allergy* (2017) 72(4):519–33. doi: 10.1111/all.13083
81. Poddighe D, Vangelista L. Effects of Omalizumab on Basophils: Potential Biomarkers in Asthma and Chronic Spontaneous Urticaria. *Cell Immunol* (2020) 358:104215. doi: 10.1016/j.cellimm.2020.104215
82. Rauber MM, Pickert J, Holiangu L, Mobs C, Pfutzner W. Functional and Phenotypic Analysis of Basophils Allows Determining Distinct Subtypes in Patients With Chronic Urticaria. *Allergy* (2017) 72(12):1904–11. doi: 10.1111/all.13215
83. Kishimoto I, Kambe N, Ly NTM, Nguyen CTH, Okamoto H. Basophil Count is a Sensitive Marker for Clinical Progression in a Chronic Spontaneous Urticaria Patient Treated With Omalizumab. *Allergol Int* (2019) 68(3):388–90. doi: 10.1016/j.alit.2019.02.002
84. Huang AH, Chichester KL, Saini SS. Association of Basophil Parameters With Disease Severity and Duration in Chronic Spontaneous Urticaria (CSU). *J Allergy Clin Immunol Pract* (2020) 8(2):793–5.e6. doi: 10.1016/j.jaip.2019.08.004
85. Rijavec M, Kosnik M, Koren A, Kopac P, Selb J, Vantur R, et al. A Very Low Number of Circulating Basophils Is Predictive of a Poor Response to Omalizumab in Chronic Spontaneous Urticaria. *Allergy* (2021) 76(4):1254–7. doi: 10.1111/all.14577
86. Maurer M, Rosen K, Hsieh HJ, Saini S, Grattan C, Gimenez-Arnau A, et al. Omalizumab for the Treatment of Chronic Idiopathic or Spontaneous Urticaria. *N Engl J Med* (2013) 368(10):924–35. doi: 10.1056/NEJMoa1215372
87. Kaplan A, Ferrer M, Bernstein JA, Antonova E, Trzaskoma B, Raimundo K, et al. Timing and Duration of Omalizumab Response in Patients With Chronic Idiopathic/Spontaneous Urticaria. *J Allergy Clin Immunol* (2016) 137(2):474–81. doi: 10.1016/j.jaci.2015.08.023
88. Metz M, Staubach P, Bauer A, Brehler R, Gericke J, Kangas M, et al. Clinical Efficacy of Omalizumab in Chronic Spontaneous Urticaria Is Associated With a Reduction of FcepsilonRI-Positive Cells in the Skin. *Theranostics* (2017) 7(5):1266–76. doi: 10.7150/thno.18304
89. Saini SS, Omachi TA, Trzaskoma B, Hulter HN, Rosen K, Sterba PM, et al. Effect of Omalizumab on Blood Basophil Counts in Patients With Chronic Idiopathic/Spontaneous Urticaria. *J Invest Dermatol* (2017) 137(4):958–61. doi: 10.1016/j.jid.2016.11.025
90. Akdogan N, Demirel Ogut N, Dogan S, Atakan N. Long-Term Effects of Omalizumab on Peripheral Blood Cells and C-Reactive Protein Levels in Patients With Chronic Spontaneous Urticaria. *Dermatol Ther* (2019) 32(4):e12966. doi: 10.1111/dth.12966
91. MacGlashan D. Autoantibodies to IgE and FcepsilonRI and the Natural Variability of Spleen Tyrosine Kinase Expression in Basophils. *J Allergy Clin Immunol* (2019) 143(3):1100–7.e11. doi: 10.1016/j.jaci.2018.05.019
92. Asero R, Marzano AV, Ferrucci S, Lorini M, Carbonelli V, Cugno M. Co-Occurrence of IgE and IgG Autoantibodies in Patients With Chronic Spontaneous Urticaria. *Clin Exp Immunol* (2020) 200(3):242–9. doi: 10.1111/cei.13428
93. Altrichter S, Zampeli V, Ellrich A, Zhang K, Church MK, Maurer M. IgM and IgA in Addition to IgG Autoantibodies Against FcvarepsilonRIalpha are Frequent and Associated With Disease Markers of Chronic Spontaneous Urticaria. *Allergy* (2020) 75(12):3208–15. doi: 10.1111/all.14412
94. Bracken SJ, Abraham S, MacLeod AS. Autoimmune Theories of Chronic Spontaneous Urticaria. *Front Immunol* (2019) 10:627. doi: 10.3389/fimmu.2019.00627
95. MacGlashan DJr., Saini S, Schroeder JT. Response of Peripheral Blood Basophils in Subjects With Chronic Spontaneous Urticaria During Treatment With Omalizumab. *J Allergy Clin Immunol* (2021) 147(6):2295–304 e12. doi: 10.1016/j.jaci.2021.02.039
96. Johal KJ, Chichester KL, Oliver ET, Devine KC, Bieneman AP, Schroeder JT, et al. The Efficacy of Omalizumab Treatment in Chronic Spontaneous Urticaria Is Associated With Basophil Phenotypes. *J Allergy Clin Immunol* (2021) 147(6):2271–80.e8. doi: 10.1016/j.jaci.2021.02.038
97. Castro M, Corren J, Pavord ID, Maspero J, Wenzel S, Rabe KF, et al. Dupilumab Efficacy and Safety in Moderate-to-Severe Uncontrolled Asthma. *N Engl J Med* (2018) 378(26):2486–96. doi: 10.1056/NEJMoa1804092
98. Russkamp D, Aguilar-Pimentel A, Alessandrini F, Gailus-Durner V, Fuchs H, Ohnmacht C, et al. IL-4 Receptor Alpha Blockade Prevents Sensitization and Alters Acute and Long-Lasting Effects of Allergen-Specific Immunotherapy of Murine Allergic Asthma. *Allergy* (2019) 74(8):1549–60. doi: 10.1111/all.13759
99. Le Floc'h A, Allinne J, Nagashima K, Scott G, Birchard D, Asrat S, et al. Dual Blockade of IL-4 and IL-13 With Dupilumab, an IL-4Ralpha Antibody, Is Required to Broadly Inhibit Type 2 Inflammation. *Allergy* (2020) 75(5):1188–204. doi: 10.1111/all.14151
100. Conde E, Bertrand R, Balbino B, Bonnefoy J, Stackowicz J, Caillot N, et al. Dual Vaccination Against IL-4 and IL-13 Protects Against Chronic Allergic Asthma in Mice. *Nat Commun* (2021) 12(1):2574. doi: 10.1038/s41467-021-22834-5
101. Koshino T, Arai Y, Miyamoto Y, Sano Y, Itami M, Teshima S, et al. Airway Basophil and Mast Cell Density in Patients With Bronchial Asthma: Relationship to Bronchial Hyperresponsiveness. *J Asthma* (1996) 33(2):89–95. doi: 10.3109/02770909609054536
102. Kepley CL, McFeeley PJ, Oliver JM, Lipscomb MF. Immunohistochemical Detection of Human Basophils in Postmortem Cases of Fatal Asthma. *Am J Respir Crit Care Med* (2001) 164(6):1053–8. doi: 10.1164/ajrccm.164.6.2102025
103. Suzuki Y, Wakahara K, Nishio T, Ito S, Hasegawa Y. Airway Basophils are Increased and Activated in Eosinophilic Asthma. *Allergy* (2017) 72(10):1532–9. doi: 10.1111/all.13197
104. Lommatzsch M, Marchewski H, Schwefel G, Stoll P, Virchow JC, Bratke K. Benralizumab Strongly Reduces Blood Basophils in Severe Eosinophilic Asthma. *Clin Exp Allergy* (2020) 50(11):1267–9. doi: 10.1111/cea.13720
105. Numata T, Miyagawa H, Nishioka S, Okuda K, Utsumi H, Hashimoto M, et al. Efficacy of Benralizumab for Patients With Severe Eosinophilic Asthma: A Retrospective, Real-Life Study. *BMC Pulm Med* (2020) 20(1):207. doi: 10.1186/s12890-020-01248-x
106. Pelaia C, Crimi C, Benfante A, Caiaffa MF, Calabrese C, Carpagnano GE, et al. Therapeutic Effects of Benralizumab Assessed in Patients With Severe Eosinophilic Asthma: Real-Life Evaluation Correlated With Allergic and Non-Allergic Phenotype Expression. *J Asthma Allergy* (2021) 14:163–73. doi: 10.2147/JAA.S297273

107. Brooks CR, van Dalen CJ, Hermans IF, Gibson PG, Simpson JL, Douwes J. Sputum Basophils Are Increased in Eosinophilic Asthma Compared With Non-Eosinophilic Asthma Phenotypes. *Allergy* (2017) 72(10):1583–6. doi: 10.1111/all.13185
108. Winter NA, Qin L, Gibson PG, McDonald VM, Baines KJ, Faulkner J, et al. Sputum Mast Cell/Basophil Gene Expression Relates to Inflammatory and Clinical Features of Severe Asthma. *J Allergy Clin Immunol* (2021) 148 (2):428–38. doi: 10.1016/j.jaci.2021.01.033
109. Motomura Y, Morita H, Moro K, Nakae S, Artis D, Endo TA, et al. Basophil-Derived Interleukin-4 Controls the Function of Natural Helper Cells, a Member of ILC2s, in Lung Inflammation. *Immunity* (2014) 40(5):758–71. doi: 10.1016/j.immuni.2014.04.013
110. Kabata H, Flamar AL, Mahlakoiv T, Moriyama S, Rodewald HR, Ziegler SF, et al. Targeted Deletion of the TSLP Receptor Reveals Cellular Mechanisms That Promote Type 2 Airway Inflammation. *Mucosal Immunol* (2020) 13 (4):626–36. doi: 10.1038/s41385-020-0266-x
111. Morita H, Arae K, Unno H, Miyauchi K, Toyama S, Nambu A, et al. An Interleukin-33-Mast Cell-Interleukin-2 Axis Suppresses Papain-Induced Allergic Inflammation by Promoting Regulatory T Cell Numbers. *Immunity* (2015) 43(1):175–86. doi: 10.1016/j.immuni.2015.06.021
112. Mahdavinia M, Carter RG, Ocampo CJ, Stevens W, Kato A, Tan BK, et al. Basophils are Elevated in Nasal Polyps of Patients With Chronic Rhinosinusitis Without Aspirin Sensitivity. *J Allergy Clin Immunol* (2014) 133(6):1759–63. doi: 10.1016/j.jaci.2013.12.1092
113. Kagoya R, Kondo K, Baba S, Toma-Hirano M, Nishijima H, Suzukawa K, et al. Correlation of Basophil Infiltration in Nasal Polyps With the Severity of Chronic Rhinosinusitis. *Ann Allergy Asthma Immunol* (2015) 114(1):30–5. doi: 10.1016/j.anai.2014.09.017
114. Stevens WW, Staudacher AG, Hulse KE, Poposki JA, Kato A, Carter RG, et al. Studies of the Role of Basophils in Aspirin-Exacerbated Respiratory Disease Pathogenesis. *J Allergy Clin Immunol* (2021) 148(2):439–49.e5. doi: 10.1016/j.jaci.2021.02.045
115. Savage JH, Courneya JP, Sterba PM, Macglashan DW, Saini SS, Wood RA. Kinetics of Mast Cell, Basophil, and Oral Food Challenge Responses in Omalizumab-Treated Adults With Peanut Allergy. *J Allergy Clin Immunol* (2012) 130(5):1123–9.e2. doi: 10.1016/j.jaci.2012.05.039
116. Noti M, Kim BS, Siracusa MC, Rak GD, Kubo M, Moghaddam AE, et al. Exposure to Food Allergens Through Inflamed Skin Promotes Intestinal Food Allergy Through the Thymic Stromal Lymphopoietin-Basophil Axis. *J Allergy Clin Immunol* (2014) 133(5):1390–9, 9 e1-6. doi: 10.1016/j.jaci.2014.01.021
117. Muto T, Fukuoka A, Kabashima K, Ziegler SF, Nakanishi K, Matsushita K, et al. The Role of Basophils and Proallergic Cytokines, TSLP and IL-33, in Cutaneously Sensitized Food Allergy. *Int Immunol* (2014) 26(10):539–49. doi: 10.1093/intimm/dxu058
118. Han H, Thelen TD, Comeau MR, Ziegler SF. Thymic Stromal Lymphopoietin-Mediated Epicutaneous Inflammation Promotes Acute Diarrhea and Anaphylaxis. *J Clin Invest* (2014) 124(12):5442–52. doi: 10.1172/JCI77798
119. Hussain M, Borcard L, Walsh KP, Pena Rodriguez M, Mueller C, Kim BS, et al. Basophil-Derived IL-4 Promotes Epicutaneous Antigen Sensitization Concomitant With the Development of Food Allergy. *J Allergy Clin Immunol* (2018) 141(1):223–34.e5. doi: 10.1016/j.jaci.2017.02.035
120. Kashiwakura JI, Ando T, Karasuyama H, Kubo M, Matsumoto K, Matsuda T, et al. The Basophil-IL-4-Mast Cell Axis Is Required for Food Allergy. *Allergy* (2019) 74(10):1992–6. doi: 10.1111/all.13834
121. Burton OT, Darling AR, Zhou JS, Noval-Rivas M, Jones TG, Gurish MF, et al. Direct Effects of IL-4 on Mast Cells Drive Their Intestinal Expansion and Increase Susceptibility to Anaphylaxis in a Murine Model of Food Allergy. *Mucosal Immunol* (2013) 6(4):740–50. doi: 10.1038/mi.2012.112
122. Noti M, Wojno ED, Kim BS, Siracusa MC, Giacomin PR, Nair MG, et al. Thymic Stromal Lymphopoietin-Elicited Basophil Responses Promote Eosinophilic Esophagitis. *Nat Med* (2013) 19(8):1005–13. doi: 10.1038/nm.3281
123. Venturelli N, Lexmond WS, Ohsaki A, Nurko S, Karasuyama H, Fiebiger E, et al. Allergic Skin Sensitization Promotes Eosinophilic Esophagitis Through the IL-33-Basophil Axis in Mice. *J Allergy Clin Immunol* (2016) 138(5):1367–80 e5. doi: 10.1016/j.jaci.2016.02.034
124. Tsujimura Y, Obata K, Mukai K, Shindou H, Yoshida M, Nishikado H, et al. Basophils Play a Pivotal Role in Immunoglobulin-G-Mediated But Not Immunoglobulin-E-Mediated Systemic Anaphylaxis. *Immunity* (2008) 28 (4):581–9. doi: 10.1016/j.immuni.2008.02.008
125. Lin YH, Tahara-Hanaoka S, Nagai K, Yoshikawa S, Kubo M, Shibayama S, et al. Selective Suppression of Oral Allergen-Induced Anaphylaxis by Allergin-1 on Basophils in Mice. *Int Immunol* (2020) 32(3):213–9. doi: 10.1093/intimm/dxz075
126. Korosec P, Turner PJ, Silar M, Kopac P, Kosnik M, Gibbs BF, et al. Basophils, High-Affinity IgE Receptors, and CCL2 in Human Anaphylaxis. *J Allergy Clin Immunol* (2017) 140(3):750–8.e15. doi: 10.1016/j.jaci.2016.12.989
127. Vantur R, Rihar M, Koren A, Rijavec M, Kopac P, Bidovec-Stojkovic U, et al. Chemokines During Anaphylaxis: The Importance of CCL2 and CCL2-Dependent Chemotactic Activity for Basophils. *Clin Transl Allergy* (2020) 10 (1):63. doi: 10.1186/s13601-020-00367-2
128. Yamaga S, Yanase Y, Ishii K, Ohshimo S, Shime N, Hide M. Decreased Intracellular Histamine Concentration and Basophil Activation in Anaphylaxis. *Allergol Int* (2020) 69(1):78–83. doi: 10.1016/j.alit.2019.05.009
129. Puan KJ, San Luis B, Yusof N, Kumar D, Andiappan AK, Lee W, et al. FUT6 Deficiency Compromises Basophil Function by Selectively Abrogating Their Sialyl-Lewis X Expression. *Commun Biol* (2021) 4(1):832. doi: 10.1038/s42003-021-02295-8
130. Schett G, Neurath MF. Resolution of Chronic Inflammatory Disease: Universal and Tissue-Specific Concepts. *Nat Commun* (2018) 9(1):3261. doi: 10.1038/s41467-018-05800-6
131. Bleriot C, Dupuis T, Jouvion G, Eberl G, Disson O, Lecuit M. Liver-Resident Macrophage Necroptosis Orchestrates Type 1 Microbicidal Inflammation and Type-2-Mediated Tissue Repair During Bacterial Infection. *Immunity* (2015) 42(1):145–58. doi: 10.1016/j.immuni.2014.12.020
132. Prabhu SD, Frangogiannis NG. The Biological Basis for Cardiac Repair After Myocardial Infarction: From Inflammation to Fibrosis. *Circ Res* (2016) 119 (1):91–112. doi: 10.1161/CIRCRESAHA.116.303577
133. Meulenbroeks C, van Weelden H, Schwartz C, Voehringer D, Redegeld FAM, Rutten V, et al. Basophil-Derived Amphiregulin Is Essential for UVB Irradiation-Induced Immune Suppression. *J Invest Dermatol* (2015) 135 (1):222–8. doi: 10.1038/jid.2014.329
134. Inclan-Rico JM, Ponessa JJ, Valero-Pacheco N, Hernandez CM, Sy CB, Lemenze AD, et al. Basophils Prime Group 2 Innate Lymphoid Cells for Neuropeptide-Mediated Inhibition. *Nat Immunol* (2020) 21(10):1181–93. doi: 10.1038/s41590-020-0753-y
135. Gieseck RL3rd, Wilson MS, Wynn TA. Type 2 Immunity in Tissue Repair and Fibrosis. *Nat Rev Immunol* (2018) 18(1):62–76. doi: 10.1038/nri.2017.90
136. Balam S, Schiechl-Brachner G, Buchtler S, Halbritter D, Schmidbauer K, Talke Y, et al. IL-3 Triggers Chronic Rejection of Cardiac Allografts by Activation of Infiltrating Basophils. *J Immunol* (2019) 202(12):3514–23. doi: 10.4049/jimmunol.1801269
137. Watanabe T, Minaga K, Kamata K, Kudo M, Strober W. Mechanistic Insights Into Autoimmune Pancreatitis and IgG4-Related Disease. *Trends Immunol* (2018) 39(11):874–89. doi: 10.1016/j.it.2018.09.005
138. Yanagawa M, Uchida K, Ando Y, Tomiyama T, Yamaguchi T, Ikeura T, et al. Basophils Activated *via* TLR Signaling may Contribute to Pathophysiology of Type 1 Autoimmune Pancreatitis. *J Gastroenterol* (2018) 53(3):449–60. doi: 10.1007/s00535-017-1390-6
139. Watanabe T, Yamashita K, Sakurai T, Kudo M, Shiokawa M, Uza N, et al. Toll-Like Receptor Activation in Basophils Contributes to the Development of IgG4-Related Disease. *J Gastroenterol* (2013) 48(2):247–53. doi: 10.1007/s00535-012-0626-8
140. Kulkarni T, O'Reilly P, Antony VB, Gaggar A, Thannickal VJ. Matrix Remodeling in Pulmonary Fibrosis and Emphysema. *Am J Respir Cell Mol Biol* (2016) 54(6):751–60. doi: 10.1165/rcmb.2015-0166PS
141. Cardenas EI, Alvarado-Vazquez PA, Mendez-Enriquez E, Danielsson Erik A, Hallgren J. Elastase- and LPS-Exposed Cpa3Cre/+ and ST2-/- Mice Develop Unimpaired Obstructive Pulmonary Disease. *Front Immunol* (2022) 13:830859. doi: 10.3389/fimmu.2022.830859
142. Jogdand P, Siddhuraj P, Mori M, Sanden C, Jonsson J, Walls AF, et al. Eosinophils, Basophils and Type 2 Immune Microenvironments in COPD-Affected Lung Tissue. *Eur Respir J* (2020) 55(5):1900110. doi: 10.1183/13993003.00110-2019

143. Atta AM, Santiago MB, Guerra FG, Pereira MM, Sousa Atta ML. Autoimmune Response of IgE Antibodies to Cellular Self-Antigens in Systemic Lupus Erythematosus. *Int Arch Allergy Immunol* (2010) 152 (4):401–6. doi: 10.1159/000288293
144. Charles N, Hardwick D, Daugas E, Illei GG, Rivera J. Basophils and the T Helper 2 Environment can Promote the Development of Lupus Nephritis. *Nat Med* (2010) 16(6):701–7. doi: 10.1038/nm.2159
145. Dema B, Charles N, Pellefigues C, Ricks TK, Suzuki R, Jiang C, et al. Immunoglobulin E Plays an Immunoregulatory Role in Lupus. *J Exp Med* (2014) 211(11):2159–68. doi: 10.1084/jem.20140066
146. Dema B, Pellefigues C, Hasni S, Gault N, Jiang C, Ricks TK, et al. Autoreactive IgE is Prevalent in Systemic Lupus Erythematosus and is Associated With Increased Disease Activity and Nephritis. *PloS One* (2014) 9(2):e90424. doi: 10.1371/journal.pone.0090424
147. Charles N. Autoimmunity, IgE and Fcεri-Bearing Cells. *Curr Opin Immunol* (2021) 72:43–50. doi: 10.1016/j.coi.2021.03.003
148. Hasni S, Gupta S, Davis M, Poncio E, Temesgen-Oyelakin Y, Joyal E, et al. Safety and Tolerability of Omalizumab: A Randomized Clinical Trial of Humanized Anti-IgE Monoclonal Antibody in Systemic Lupus Erythematosus. *Arthritis Rheumatol* (2019) 71(7):1135–40. doi: 10.1002/art.40828
149. Pan Q, Gong L, Xiao H, Feng Y, Li L, Deng Z, et al. Basophil Activation-Dependent Autoantibody and Interleukin-17 Production Exacerbate Systemic Lupus Erythematosus. *Front Immunol* (2017) 8:348. doi: 10.3389/fimmu.2017.00348
150. Dema B, Lamri Y, Pellefigues C, Pacreau E, Saidoune F, Bidault C, et al. Basophils Contribute to Pristane-Induced Lupus-Like Nephritis Model. *Sci Rep* (2017) 7(1):7969. doi: 10.1038/s41598-017-08516-7
151. Sharma M, Bayry J. Autoimmunity: Basophils in Autoimmune and Inflammatory Diseases. *Nat Rev Rheumatol* (2015) 11(3):129–31. doi: 10.1038/nrrheum.2014.199
152. Pellefigues C, Dema B, Lamri Y, Saidoune F, Chavarot N, Loheac C, et al. Prostaglandin D2 Amplifies Lupus Disease Through Basophil Accumulation in Lymphoid Organs. *Nat Commun* (2018) 9(1):725. doi: 10.1038/s41467-018-03129-8
153. Lamri Y, Vibhushan S, Pacreau E, Boedec E, Saidoune F, Mailleux A, et al. Basophils and IgE Contribute to Mixed Connective Tissue Disease Development. *J Allergy Clin Immunol* (2021) 147(4):1478–89.e11. doi: 10.1016/j.jaci.2020.12.622
154. Yuk CM, Park HJ, Kwon BI, Lah SJ, Chang J, Kim JY, et al. Basophil-Derived IL-6 Regulates TH17 Cell Differentiation and CD4 T Cell Immunity. *Sci Rep* (2017) 7:41744. doi: 10.1038/srep41744
155. He X, Cao Y, Gu Y, Fang H, Wang J, Liu X, et al. Clinical Outcomes and Immune Metrics in Intratumoral Basophil-Enriched Gastric Cancer Patients. *Ann Surg Oncol* (2021) 28(11):6439–50. doi: 10.1245/s10434-021-09815-0
156. Baba T, Tanabe Y, Yoshikawa S, Yamanishi Y, Morishita S, Komatsu N, et al. MIP-1alpha/CCL3-Expressing Basophil-Lineage Cells Drive the Leukemic Hematopoiesis of Chronic Myeloid Leukemia in Mice. *Blood* (2016) 127 (21):2607–17. doi: 10.1182/blood-2015-10-673087
157. Sektioglu IM, Carretero R, Bulbuc N, Bald T, Tuting T, Rudensky AY, et al. Basophils Promote Tumor Rejection *via* Chemotaxis and Infiltration of CD8 + T Cells. *Cancer Res* (2017) 77(2):291–302. doi: 10.1158/0008-5472.CAN-16-0993
158. Bax HJ, Chauhan J, Stavraka C, Khiabany A, Nakamura M, Pellizzari G, et al. Basophils From Cancer Patients Respond to Immune Stimuli and Predict Clinical Outcome. *Cells* (2020) 9(7):1631. doi: 10.3390/cells9071631
159. Crawford G, Hayes MD, Seoane RC, Ward S, Dalessandri T, Lai C, et al. Epithelial Damage and Tissue Gammadelta T Cells Promote a Unique Tumor-Protective IgE Response. *Nat Immunol* (2018) 19(8):859–70. doi: 10.1038/s41590-018-0161-8
160. Hayes MD, Ward S, Crawford G, Seoane RC, Jackson WD, Kipling D, et al. Inflammation-Induced IgE Promotes Epithelial Hyperplasia and Tumour Growth. *Elife* (2020) 9:e51862. doi: 10.7554/eLife.51862
161. Rodriguez L, Pekkarinen PT, Lakshmikanth T, Tan Z, Consiglio CR, Pou C, et al. Systems-Level Immunomonitoring From Acute to Recovery Phase of Severe COVID-19. *Cell Rep Med* (2020) 1(5):100078. doi: 10.1016/j.xcrm.2020.100078
162. Laing AG, Lorenc A, Del Molino Del Barrio I, Das A, Fish M, Monin L, et al. A Dynamic COVID-19 Immune Signature Includes Associations With Poor Prognosis. *Nat Med* (2020) 26(10):1623–35. doi: 10.1038/s41591-020-1038-6
163. Kazancioglu S, Bastug A, Ozbay BO, Kemirtlek N, Bodur H. The Role of Haematological Parameters in Patients With COVID-19 and Influenza Virus Infection. *Epidemiol Infect* (2020) 148:e272. doi: 10.1017/S095026882000271X
164. Vitte J, Diallo AB, Boumaza A, Lopez A, Michel M, Allardet-Servent J, et al. A Granulocytic Signature Identifies COVID-19 and Its Severity. *J Infect Dis* (2020) 222(12):1985–96. doi: 10.1093/infdis/jiaa591
165. Ten-Caten F, Gonzalez-Dias P, Castro I, Ogava RLT, Giddaluru J, Silva JCS, et al. In-Depth Analysis of Laboratory Parameters Reveals the Interplay Between Sex, Age, and Systemic Inflammation in Individuals With COVID-19. *Int J Infect Dis* (2021) 105:579–87. doi: 10.1016/j.ijid.2021.03.016
166. Alnor A, Sandberg MB, Toftanes BE, Vinholt PJ. Platelet Parameters and Leukocyte Morphology is Altered in COVID-19 Patients Compared to non-COVID-19 Patients With Similar Symptomatology. *Scand J Clin Lab Invest* (2021) 81(3):213–7. doi: 10.1080/00365513.2021.1894601
167. Lourda M, Dzidic M, Hertwig L, Bergsten H, Palma Medina LM, Sinha I, et al. High-Dimensional Profiling Reveals Phenotypic Heterogeneity and Disease-Specific Alterations of Granulocytes in COVID-19. *Proc Natl Acad Sci USA* (2021) 118(40):e2109123118. doi: 10.1073/pnas.2109123118
168. Sun Y, Zhou J, Ye K. White Blood Cells and Severe COVID-19: A Mendelian Randomization Study. *J Pers Med* (2021) 11(3):195. doi: 10.3390/jpm11030195
169. Bonam SR, Chauvin C, Levillayer L, Mathew MJ, Sakuntabhai A, Bayry J. SARS-CoV-2 Induces Cytokine Responses in Human Basophils. *Front Immunol* (2022) 13:838448. doi: 10.3389/fimmu.2022.838448

Conflict of Interest: The authors declare that the research was conducted in the absence of any commercial or financial relationships that could be construed as a potential conflict of interest.

Publisher's Note: All claims expressed in this article are solely those of the authors and do not necessarily represent those of their affiliated organizations, or those of the publisher, the editors and the reviewers. Any product that may be evaluated in this article, or claim that may be made by its manufacturer, is not guaranteed or endorsed by the publisher.

Copyright © 2022 Miyake, Ito and Karasuyama. This is an open-access article distributed under the terms of the Creative Commons Attribution License (CC BY). The use, distribution or reproduction in other forums is permitted, provided the original author(s) and the copyright owner(s) are credited and that the original publication in this journal is cited, in accordance with accepted academic practice. No use, distribution or reproduction is permitted which does not comply with these terms.

frontiers | Frontiers in Immunology

ORIGINAL RESEARCH
published: 31 May 2022
doi: 10.3389/fimmu.2022.880412

Check for updates

OPEN ACCESS

Edited by:
Satoshi Tanaka,
Kyoto Pharmaceutical University,
Japan

Reviewed by:
Jorge Sánchez,
University of Antioquia, Colombia
Donald W. MacGlashan,
Johns Hopkins University,
United States

***Correspondence:**
Gilda Varricchi
gildanet@gmail.com
Vincenzo Casolaro
vcasolaro@unisa.it

†ORCID:
Remo Poto
orcid.org/0000-0002-4723-0167
Isabella Quinti
orcid.org/0000-0002-3328-7584
Gianni Marone
orcid.org/0000-0002-9849-4701
Maurizio Taglialatela
orcid.org/0000-0002-8202-0560
Amato de Paulis
orcid.org/0000-0003-0347-2540
Vincenzo Casolaro
orcid.org/0000-0001-9810-0488
Gilda Varricchi
orcid.org/0000-0002-9285-4657

Specialty section:
This article was submitted to Inflammation, a section of the journal Frontiers in Immunology

Received: 21 February 2022
Accepted: 27 April 2022
Published: 31 May 2022

Citation:
Poto R, Quinti I, Marone G, Taglialatela M, de Paulis A, Casolaro V and Varricchi G (2022) IgG Autoantibodies Against IgE from Atopic Dermatitis Can Induce the Release of Cytokines and Proinflammatory Mediators from Basophils and Mast Cells. Front. Immunol. 13:880412. doi: 10.3389/fimmu.2022.880412

IgG Autoantibodies Against IgE from Atopic Dermatitis Can Induce the Release of Cytokines and Proinflammatory Mediators from Basophils and Mast Cells

Remo Poto [1,2,3†], Isabella Quinti [4†], Gianni Marone [1,2,3,5†], Maurizio Taglialatela [6†], Amato de Paulis [1,2,3†], Vincenzo Casolaro [7†] and Gilda Varricchi [1,2,3,5*†]*

[1] Department of Translational Medical Sciences, University of Naples Federico II, Naples, Italy, [2] Center for Basic and Clinical Immunology Research (CISI), University of Naples Federico II, Naples, Italy, [3] World Allergy Organization (WAO) Center of Excellence, Naples, Italy, [4] Department of Molecular Medicine, Sapienza University of Rome, Rome, Italy, [5] Institute of Experimental Endocrinology and Oncology (IEOS), National Research Council (CNR), Naples, Italy, [6] Department of Neuroscience, University of Naples Federico II, Naples, Italy, [7] Department of Medicine, Surgery and Dentistry 'Scuola Medica Salernitana', University of Salerno, Baronissi, Italy

IgE-mediated release of proinflammatory mediators and cytokines from basophils and mast cells is a central event in allergic disorders. Several groups of investigators have demonstrated the presence of autoantibodies against IgE and/or FcεRI in patients with chronic spontaneous urticaria. By contrast, the prevalence and functional activity of anti-IgE autoantibodies in atopic dermatitis (AD) are largely unknown. We evaluated the ability of IgG anti-IgE from patients with AD to induce the *in vitro* IgE-dependent activation of human basophils and skin and lung mast cells. Different preparations of IgG anti-IgE purified from patients with AD and rabbit IgG anti-IgE were compared for their triggering effects on the *in vitro* release of histamine and type 2 cytokines (IL-4, IL-13) from basophils and of histamine and lipid mediators (prostaglandin D_2 and cysteinyl leukotriene C_4) from human skin and lung mast cells. One preparation of human IgG anti-IgE out of six patients with AD induced histamine release from basophils, skin and lung mast cells. This preparation of human IgG anti-IgE induced the secretion of cytokines and eicosanoids from basophils and mast cells, respectively. Human monoclonal IgE was a competitive antagonist of both human and rabbit IgG anti-IgE. Human anti-IgE was more potent than rabbit anti-IgE for IL-4 and IL-13 production by basophils and histamine, prostaglandin D_2 and leukotriene C_4 release from mast cells. Functional anti-IgE autoantibodies rarely occur in patients with AD. When present, they induce the release of proinflammatory mediators and cytokines from basophils and mast cells, thereby possibly contributing to sustained IgE-dependent inflammation in at least a subset of patients with this disorder.

Keywords: allergy, anti-IgE, atopic dermatitis, basophils, IL-4, IL-13, mast cells

INTRODUCTION

Mast cells and basophils are important cells of the immune system (1–3) and play critical roles in several allergic (4–9) and autoimmune disorders (10–12), infections (13, 14), cardiovascular diseases (15–17), immunodeficiencies (18), and cancer (19–22). The secretion of preformed mediators (e.g. histamine) and *de novo* synthesis of lipid mediators (e.g. leukotriene C_4, prostaglandin D_2) and various cytokines following FcεRI cross-linkage plays key roles in diverse IgE-mediated allergic conditions, including atopic dermatitis (AD) (23), chronic spontaneous urticaria (CSU) (24, 25), asthma (5, 26, 27), allergic rhinitis (28), food allergies (29), and anaphylaxis (30–32).

Human mast cells and basophils express a complete ($\alpha\beta\gamma2$), high-affinity receptor for IgE (FcεRI) (33). The interaction of IgE with its receptor is characterized by a very slow dissociation rate ($K_{off} < 10^{-5}$/s), accounting for its uniquely high affinity, the highest reported for a human immunoglobulin (Ig) to any of its receptors (34, 35). Aggregation of FcεRI bound to IgE by multivalent antigens, anti-IgE antibodies generated in rabbit or goat (36, 37), or superantigens (38–41) leads to mast cell and basophil activation and mediator release.

Several studies have reported the presence of spontaneously occurring autoantibodies to IgE (36, 42–45), FcεRI (46–49), or both in diverse allergic (36, 42–46, 48, 50–52) and autoimmune disorders (47, 53). Most of these studies have focused on the ability of anti-IgE/FcεRI autoantibodies isolated from patients with CSU to activate peripheral blood basophils (36, 42, 46–48). However, most anti-IgE/FcεRI antibodies isolated from patients with CSU (36), asthma (50), or AD (44) are ineffective basophil secretagogues, which might explain some of the controversies in the field (50, 54). These controversial findings do not necessarily rule out the ability of some of these autoantibodies to activate human tissue mast cells. In any instance, the recent documentation of IgE autoantibodies against eosinophil peroxidase and eosinophil cationic protein in some patients with CSU and AD further reinforce the notion that shared, dysregulated immune functions may differentially contribute to the pathogenesis of these conditions (55).

Even though basophils account for approximately 1% of circulating peripheral blood leukocytes, analysis of basophil activation *in vitro* has become a mainstay of research in allergy and immunology for some compelling reasons. First, these cells can play critical roles in the activation of type 2 immune responses through the production of such Th2-like cytokines as IL-4 and IL-13 (38, 39, 56–62); second, basophils have the propensity to migrate into the sites of allergic inflammation (63–65); last, but not least, these cells are much more readily available for analysis than human tissue-resident mast cells.

The purpose of this study was four-fold. First, we examined the presence of functional IgG anti-IgE autoantibodies in patients with AD and compared their functions to rabbit IgG anti-IgE and to human polyclonal IgG. Second, we evaluated the effects of functional IgG anti-IgE on the release of Th2-like cytokines (IL-4 and IL-13) from human basophils. Third, we investigated whether human monoclonal IgE is a competitive antagonist of human and rabbit IgG anti-IgE. Finally, we examined the ability of functional human IgG anti-IgE to activate human primary skin and lung mast cells.

MATERIALS AND METHODS

Reagents and Buffers

Bovine serum albumin, human serum albumin, piperazine-N,N'-bis (2-ethanesulfonic acid) (Pipes), L-glutamine, antibiotic-antimycotic solution (10,000 IU penicillin, 10 mg/mL streptomycin, and 25 μg/mL amphotericin B), collagenase (Worthington Biochemical Corp., Lakewood, NJ, USA), Hanks' balanced salt solution, fetal calf serum (FCS) (Thermo-Fisher, Grand Island, NY, USA), pronase (Merck Millipore, Burlington, CA, USA), RPMI 1640 with 25 mM HEPES buffer, Eagle's minimum essential medium (Fuji Film, Research Triangle Park, NC, USA), Percoll (Pharmacia Fine Chemicals, Uppsala, Sweden), CD117 MicroBeads (Miltenyi Biotech, Bologna, Italy), Iscove modified Dulbecco Medium (IMDM) (Fuji Film, Research Triangle Park, NC, USA), $HClO_4$ (Baker Chemical Co., Deventer, Netherlands), hyaluronidase, chymopapain, elastase type I, cysteinyl leukotriene C_4 (LTC_4), and prostaglandin D_2 (PGD_2) (Sigma Chemical Co., St. Louis, MO), deoxyribonuclease I (Merck Millipore, Burlington, CA, USA), (^{3}H)-LTC_4 and (^{3}H)-PGD_2 (New England Nuclear, Boston, MA) were commercially purchased. Rabbit IgG anti-IgE antibody, produced by rabbit immunization with the Fc fragment of a human IgE myeloma (patient PS) and then absorbed with the IgE Fab as previously described (37), was kindly donated by Drs. Kimishige and Teruko Ishizaka (La Jolla Institute for Allergy and Immunology, La Jolla, CA). Rabbit anti-LTC_4 and anti-PGD_2 antibodies were a gift of Dr. Lawrence M. Lichtenstein (The Johns Hopkins University, Baltimore, MD). The Pipes buffer used in these experiments was a mixture of 25 mM Pipes, 110 mM NaCl, 5 mM KCl, pH 7.37, referred to as P. P2CG contains, in addition to P, 2 mM $CaCl_2$ and 1 g/L dextrose (66); pH was titrated to 7.4 with $NaHCO_3$.

Atopic Dermatitis Patients

The study was approved by the Ethics Committee of the University of Naples Federico II, School of Medicine (Prot. 198/18), and informed consent was obtained from all participants prior to collection of blood according to recommendations from the Declaration of Helsinki. Serum samples from six patients with AD (aged 5 to 17 years) and six normal donors (aged 6 to 22 years) were collected and stored at -20°C. Patients with AD had similar clinical pictures, characterized by a chronic, pruritic skin eruption marked by erythema, papules, or lichenification of flexural areas of the extremities, face and neck (67). Serum samples were obtained from these patients after not taking any drug for at least one week.

Purification of Human Monoclonal IgE

IgE myeloma protein was purified from a myeloma patient (68) by gel filtration on Sepharose G-200 followed by elution through

a Sepharose CL-4B column. Analysis by sodium dodecyl-sulfate polyacrylamide gel electrophoresis of purified human monoclonal IgE proteins demonstrated a single protein with a m.w. of 180,000-200,000 D. Analysis by radioimmunoassay showed no IgG, IgM, or IgA contamination (38, 69, 70).

Purification of Human Polyclonal IgG

Human IgG were purified by precipitation of human serum with 50% saturated NH_4SO_4 followed by chromatography on a DEAE-cellulose column equilibrated with 0.01 M phosphate buffer (pH 7.9), as previously described (70, 71).

Purification of Human IgG Anti-IgE Antibody

Comparable levels of IgG anti-IgE antibodies were detected in serum samples from the six AD patients studied, which averaged 1,020 ng/ml (± 135 ng/ml), much higher than in nonatopic controls (< 50 ng/ml) (45). For affinity purification of these autoantibodies, sera (3 ml for each run) were passed through an immunosorbent Sepharose 4B column (1.2 x 5 cm) coated with IgE purified from ADZ (45). Immunosorbent-bound Ig with anti-IgE activity were eluted with glycine HCl buffer 0.2 M (pH 2.8), and the pH was rapidly readjusted by the addition of 2 M NaOH. The total content of immunoglobulins of the eluted fraction was measured by radioimmunoassay. Anti-IgE activity belonged to the IgG isotype. IgE content was less than 0.05 U/ml. The specificity and activity of IgG anti-IgE were tested as described elsewhere (45).

Purification of Human Basophils

Basophils were purified from peripheral blood of healthy volunteers, aged 19-45 years, undergoing hemapheresis within the Immunohematology Unit at the University of Naples Federico II. Buffy coats were subjected to double-Percoll density centrifugation, which produced basophil-depleted and basophil-enriched cell suspensions (72). Basophils were purified from the basophil-enriched cell suspensions using the Basophil Isolation Kit II (Miltenyi, Biotec, Bologna, Italy). Basophils, with purity ≥ 95%, assessed by Alcian blue staining, were incubated in IMDM in the presence of activating stimuli for 4 hours (IL-4 secretion) or 18 hours (IL-13 secretion) at 37°C (38). At the end of these incubations, the cell-free supernatants were stored at -20°C for subsequent assay of IL-4 and IL-13.

Isolation of Human Skin Mast Cells

The study was approved by the Ethics Committee of the University of Naples Federico II (Protocol: Human MC No. 7/19) and informed consent was obtained from all donors. Skin obtained from patients undergoing either mastectomy for breast cancer or elective cosmetic surgery was separated from the subcutaneous fat by blunt dissection. The tissue was finely cut into 1- to 2-mm fragments and dispersed into single-cell suspension as previously described (73). Yields with this technique ranged between 0.1 and 0.9 × 10^6 mast cells/g of wet tissue, and purity was between 5 and 10%. Human skin mast cells (HSMCs) were further purified using a CD117 MicroBead kit cell sorting system (Miltenyi Biotec, Bologna, Italy) according to the manufacturer's instructions. Mast cell purity using this technique ranged from 36 to 71% as assessed by Alcian blue staining.

Isolation of Human Lung Mast Cells

Human lung mast cells (HLMCs) were purified from macroscopically normal lung tissue obtained from patients [hepatitis C virus (HCV−), hepatitis B surface Ag (HBsAg−), HIV−] affected by lung adenocarcinoma undergoing thoracic surgery (74, 75). Freshly resected lung tissue was obtained intraoperatively and was minced finely with scissors and washed extensively with Pipes buffer over Nytex cloth (120-µm pore size) (Tetko, Elmsford, NY, USA). The cells were suspended (10^6 cells/mL) in RPMI 1640 with 5% FCS, 2 mM L-glutamine, and 1% antibiotic-antimycotic solution and incubated in 24-well plates (Falcon, Becton Dickinson, Milan, Italy). The enzymatic tissue dispersion yielded ≈5 × 10^5 mast cells/gram of lung tissue and purity ranged from 4% to 19% (40). HLMCs were further purified using a CD117 MicroBead kit cell sorting system (Miltenyi Biotec, Bologna, Italy) according to the manufacturer's instructions (40). Mast cell purity using this technique ranged from 58% to 82% as assessed by Alcian blue staining.

Histamine Release From Human Basophils

Whole blood samples were processed immediately after collection to obtain leukocyte-enriched preparations (76, 77). Duplicate leukocyte aliquots were incubated (45 minutes at 37°C) in P2CG buffer with increasing concentrations of rabbit IgG anti-human IgE myeloma (patient PS; anti-IgE) or human IgG anti-IgE. Cell-free supernatants were collected and stored at −20°C for subsequent assay of histamine content using an automated fluorometric technique (78). Histamine release (HR) was expressed as percent of the total content assessed in parallel samples lysed by addition of 2% $HClO_4$, minus the basal, or spontaneous release (77). Percent HR values were the means of duplicate determinations, differing by <5%. Basophil reactivity, that is, the maximal percent histamine release (HR_{MAX}), and threshold sensitivity (HR_{SENS}), that is, 100x the inverse of the secretagogue concentration inducing half-maximal HR (EC_{50}), were calculated as described (76, 79–81).

Histamine Release From Mast Cells

HSMCs or HLMCs (≈3 × 10^4 mast cells per tube) were resuspended in P2CG. 0.3 mL of the cell suspensions were placed in 12 × 75 mm polyethylene tubes. 0.2 mL of each prewarmed releasing stimulus was added, and incubation was continued at 37°C for 45 min (40, 41). At the end of incubation, cells were centrifuged (1000× g, 4°C, 5 min) and supernatants were stored at −20°C for subsequent assay of histamine content. Histamine was measured in duplicate determinations with an automated fluorometric technique (78).

IL-4 and IL-13 ELISA

IL-4 and IL-13 were assessed in duplicate samples using ELISA kits according to manifacturer's instructions (Quantikine ELISA Kit) (R&D Systems, Minneapolis, MN, USA). The ELISA detection range was 31-2,000 pg/ml (IL-4) and 125-4,000 pg/ml (IL-13).

Immunoassay of LTC_4 and PGD_2

LTC_4 and PGD_2 were measured in duplicate samples by radioimmunoassay (40, 82). The anti-LTC_4 and anti-PGD_2 antibodies are highly selective, with less than 1% cross-reactivity to other eicosanoids (82, 83).

Statistical Analysis

Data were analyzed with the GraphPad Prism 8 software package (GraphPad Software, La Jolla, CA, USA). Values were expressed as mean ± SEM (standard error of the mean). Statistical analysis was performed using Student's t-test or one-way analysis of variance. Values were considered significant when the probability was below the 5% confidence level ($p < 0.05$).

RESULTS

Effects of Human and Rabbit IgG Anti-IgE on Histamine Release From Human Basophils

In a first group of experiments, we compared the effects of increasing concentrations of human IgG anti-IgE purified from the sera of six patients with AD, rabbit IgG anti-IgE and human polyclonal IgG on HR from human basophils. **Figure 1A** shows that increasing concentrations (10^{-4} to 3 x 10^{-2} µg/ml) of human IgG anti-IgE isolated from only one out of six AD patients, as previously described (44), induced the release of substantial amounts of histamine from basophils isolated from six different normal donors. Shown for comparison is the concentration-dependent release of histamine induced by higher concentrations of rabbit IgG anti-IgE (10^{-3} to 3 x 10^{-1} µg/ml) in parallel experiments with the same basophil preparations (**Figure 1B**). Similarly, in the same experiments, non-functional human IgG anti-IgE purified from the other five AD patients did not induce HR from basophils (**Figure 1C**). In these experiments, human polyclonal IgG (10^{-3} to 3 µg/ml) purified from six healthy donors failed to induce mediator release from basophils (**Figure 1D**). Basophil reactivity, that is the maximal percent HR (HR_{MAX}) in response to human IgG anti-IgE (70.0% ± 3.80%), was similar to basophil reactivity to rabbit IgG anti-IgE (65.8% ± 3.68%). By contrast, the secretagogue concentration inducing half-maximal histamine release (EC_{50}) induced by the functionally active human anti-IgE preparation (2.4 x 10^{-3} ± 5 x 10^{-4} µg/ml) was significantly lower than the corresponding concentration of rabbit anti-IgE (4 x 10^{-2} ± 1 x 10^{-2} µg/ml), hence resulting in significantly higher HR_{SENS} ($p < 0.05$).

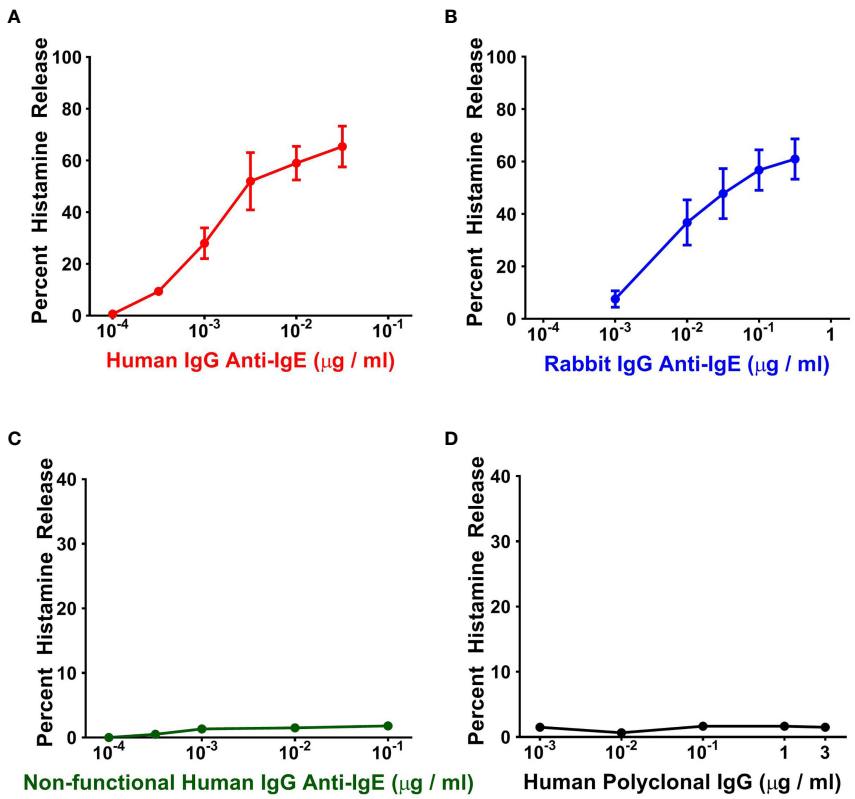


FIGURE 1 | Effects of increasing concentrations of human IgG anti-IgE **(A)** and rabbit IgG anti-IgE **(B)** on HR from basophils obtained from six normal donors. Neither non-functional human IgG anti-IgE obtained from the other five atopic dermatitis donors **(C)** nor human polyclonal, pooled from six nonatopic donors, IgG induced mediator release from basophils **(D)**. Each point represents the mean ± SEM percent HR in six different preparations of basophils. Error bars are not shown when graphically too small.

These results indicate that one preparation of the human IgG anti-IgE preparations tested was active on human basophils. This preparation of human IgG anti-IgE is from now on referred to as "human anti-IgE".

Effects of Human and Rabbit Anti-IgE on Cytokine Production by Human Basophils

IgE cross-linking induced by rabbit or goat anti-IgE (57, 58, 60, 61, 72, 84–87) or superantigens (38, 39, 59) can induce the production of IL-4 and IL-13 from human basophils. In a series of parallel experiments, we compared the effects of human and rabbit anti-IgE on the release of IL-4 and IL-13 from peripheral blood basophils purified (> 95%) from healthy donors. **Figure 2** shows the results of five independent experiments in which we examined the effects of increasing concentrations (10^{-3} to 10^{-1} μg/ml) of human and rabbit anti-IgE. In these experiments, basophils were incubated 4 hours at 37°C to evaluate IL-4 release, whereas they were incubated 18 hours at 37°C to examine IL-13 production, as previously reported (38, 39, 60, 72). Both preparations of anti-IgE induced a concentration-dependent release of IL-4 (**Figure 2A**) and IL-13 (**Figure 2B**). However, human anti-IgE, at all tested concentrations, was more effective than the corresponding concentrations of rabbit anti-IgE in inducing the release of both IL-4 and IL-13 from basophils. IgG with anti-IgE activity obtained from the other five AD patients did not cause IL-4 and IL-13 release from human basophils (data not shown). Similarly, human polyclonal IgG obtained from six normal donors did not induce cytokine release from basophils (data not shown).

Effects of Human Monoclonal IgE on Human or Rabbit Anti-IgE-Induced Mediator Release From Human Basophils

The ability of human and rabbit anti-IgE to trigger basophil mediator release suggested that it might interact with basophil-bound IgE. To test this hypothesis we conducted experiments to verify whether soluble human monoclonal IgE purified from a myeloma patient (68) (70) might inhibit the mediator response to human and rabbit anti-IgE. To this end, basophils were preincubated (10 min at 37°C) with increasing concentrations of human IgE and the cells were incubated for an additional 30 min at 37°C in the presence of increasing concentrations of human or rabbit anti-IgE. **Figure 3** illustrates the results of typical experiments showing that preincubation with increasing concentrations of human monoclonal IgE concentration-dependently shifted to the right effects on basophil HR of both human (**Figure 3A**) and rabbit anti-IgE (**Figure 3B**). Preincubation (10 min at 37°C) of human basophils with tenfold higher concentrations of human polyclonal IgG did not interfere with either human (**Figure 3C**) or rabbit anti-IgE effects (**Figure 3D**). Similar results were obtained in three additional experiments. The parallel shift to the right of the HR curve caused by increasing concentrations of human monoclonal IgE on both human and rabbit anti-IgE, without changes in maximal efficacy, suggested that it might act as a competitive inhibitor.

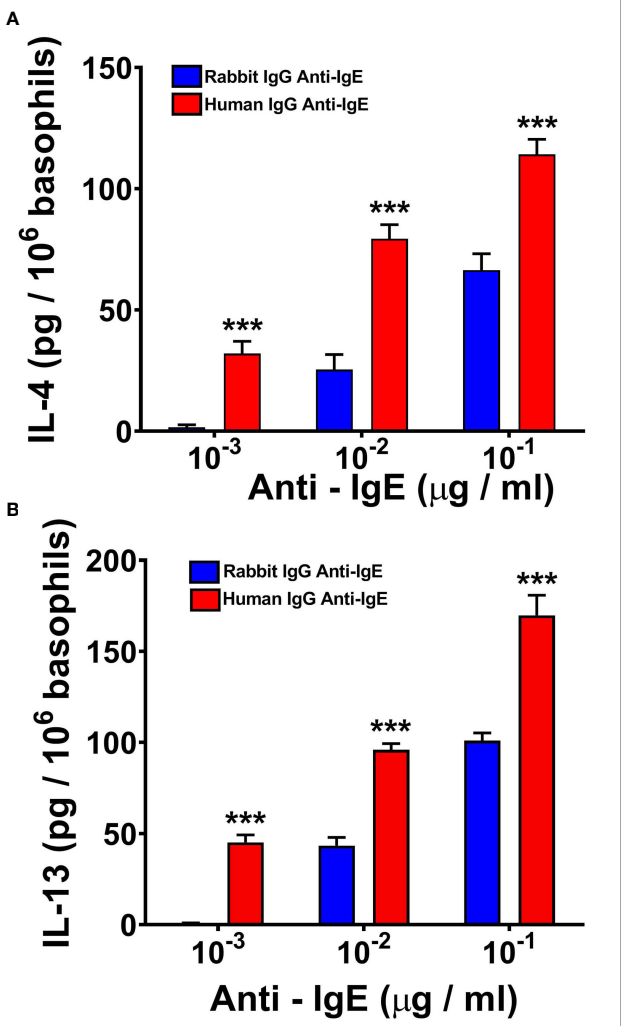


FIGURE 2 | Effects of increasing concentrations of human IgG anti-IgE (red bars) and rabbit IgG anti-IgE (blue bars) on IL-4 **(A)** and IL-13 **(B)** release from human basophils obtained from five donors. Basophils were incubated with secretagogues for 4 hours (IL-4) or 18 hours (IL-13) at 37°C. Each bar represents the mean ± SEM in five parallel experiments. Error bars are not shown when graphically too small. ***$p < 0.001$ when compared to the corresponding value obtained with rabbit IgG anti-IgE.

Effects of Human and Rabbit Anti-IgE on Histamine Release and *De Novo* Synthesis of PGD_2 From Human Skin Mast Cells

In five parallel experiments, we compared the activating properties of human and rabbit anti-IgE on HR (**Figure 4A**) and *de novo* synthesis of PGD_2 by HSMCs (**Figure 4B**). The maximal percent HR caused by human anti-IgE (17.8 ± 0.91%) was similar to that induced by rabbit anti-IgE (20.2 ± 2.8%). Similarly, the maximal production of PGD_2 induced by human anti-IgE (31.1 ± 3.7 ng/10^6 cells) was comparable to that caused by rabbit anti-IgE (30.5 ± 2.6 ng/10^6 cells). By contrast, the secretagogue concentration inducing half-maximal histamine release (EC_{50}) for histamine release was significantly lower (5 x

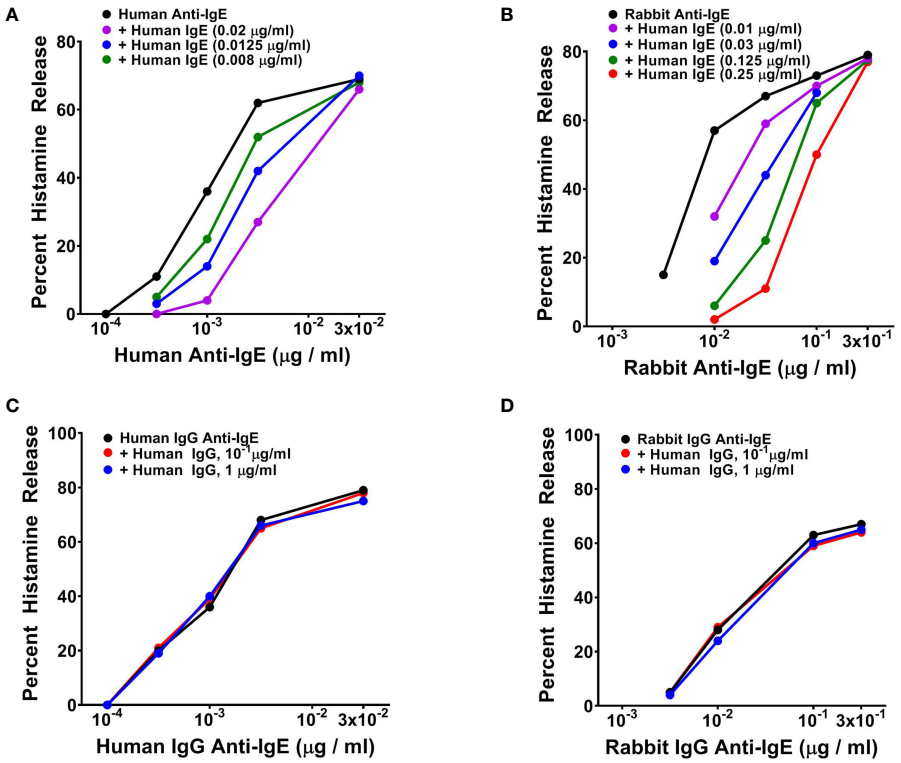


FIGURE 3 | **(A)** Effects of increasing concentrations of human monoclonal IgE on human IgG anti-IgE-induced HR from human basophils. Cells were preincubated (10 minutes, 37°C) with the indicated concentrations of IgE and then challenged with the indicated concentrations of human IgG anti-IgE for an additional 30 minutes at 37°C. Each value is the mean of duplicate determinations in a typical experiment out of three similar experiments. **(B)** Effects of increasing concentrations of human monoclonal IgE on rabbit IgG anti-IgE-induced HR from human basophils. Cells were preincubated (10 minutes, 37°C) with increasing concentrations of IgE and then challenged with the indicated concentrations of rabbit IgG anti-IgE for an additional 30 minutes at 37°C. Each value is the mean of duplicate determinations in a typical experiment out of four. **(C)** Effect of increasing concentrations of human polyclonal IgG purified from a healthy donor on human IgG anti-IgE-induced HR from human basophils. Cells were preincubated (10 minutes, 37°C) with increasing concentrations of human polyclonal IgG and then challenged with the indicated concentrations of human IgG anti-IgE for an additional 30 minutes at 37°C. **(D)** Effect of increasing concentrations of human polyclonal IgG purified from a healthy donor on rabbit IgG anti-IgE-induced HR from human basophils. Cells were preincubated (10 minutes, 37°C) with increasing concentrations of human polyclonal IgG and then challenged with the indicated concentrations of rabbit IgG anti-IgE for an additional 30 minutes at 37°C. Each value is the mean of duplicate determinations in a typical experiment out of four.

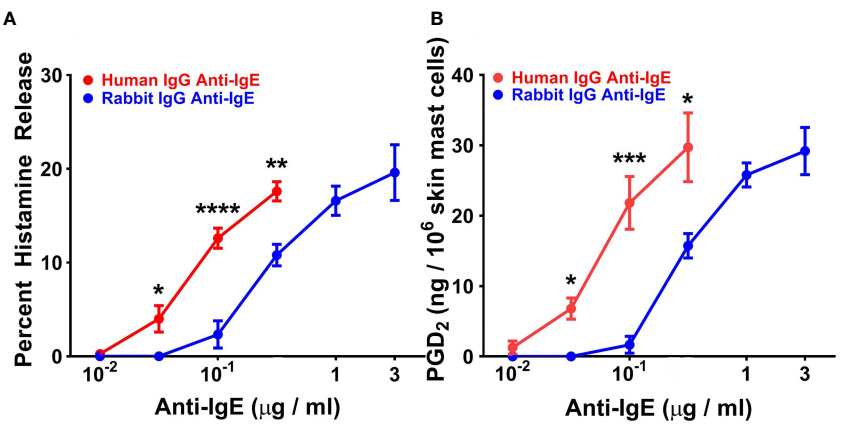


FIGURE 4 | Effects of increasing concentrations of human IgG anti-IgE and rabbit IgG anti-IgE on HR **(A)** and the *de novo* synthesis of PGD_2 **(B)** from HSMCs obtained from five different donors. HSMCs were incubated (45 min at 37°C) in the presence of the indicated concentrations of human IgG anti-IgE or rabbit IgG anti-IgE. Each point shows the mean ± SEM. **** $p < 0.0001$, *** $p < 0.001$, ** $p < 0.01$, * $p < 0.05$ when compared to the corresponding value. Error bars are not shown when graphically too small.

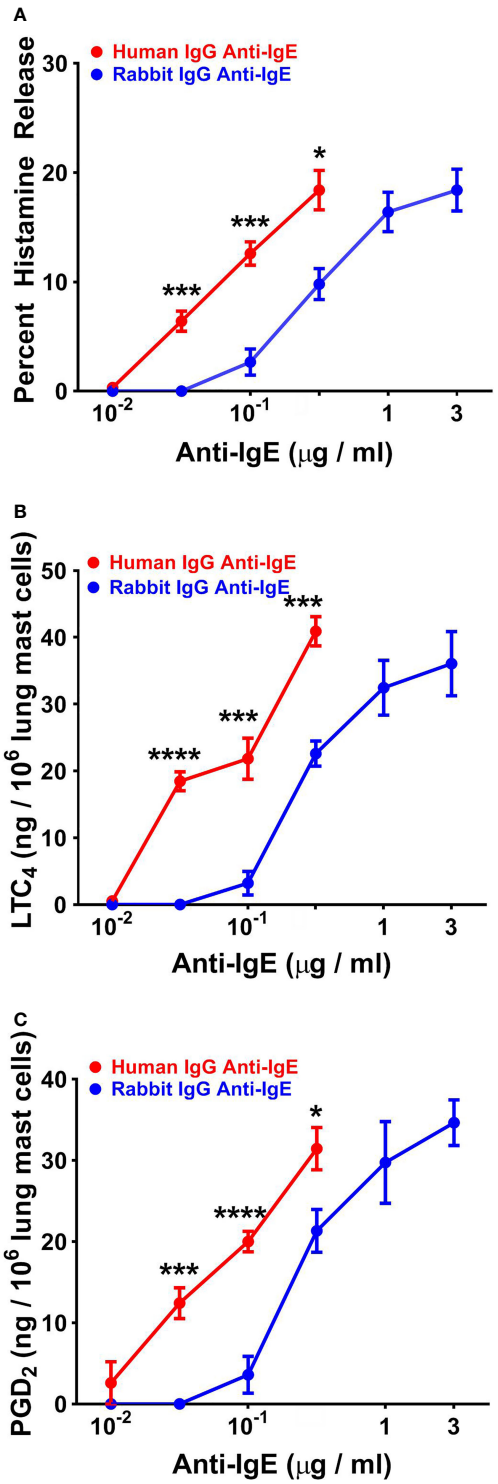


FIGURE 5 | Effects of increasing concentrations of human IgG anti-IgE and rabbit IgG anti-IgE on HR **(A)** and the de novo synthesis of LTC_4 **(B)** and PGD_2 **(C)** from HLMCs obtained from five different donors. HLMCs were incubated (45 min at 37°C) in the presence of the indicated concentrations of human IgG anti-IgE or rabbit IgG anti-IgE. Each point shows the mean ± SEM. **** $p < 0.0001$, *** $p < 0.001$, * $p < 0.05$ when compared to the corresponding value. Error bars are not shown when graphically too small.

10^{-2} ± 1 x 10^{-2} μg/ml) for human anti-IgE compared to rabbit anti-IgE (2.5 x 10^{-1} ± 6 x 10^{-2} μg/ml) ($p < 0.05$), indicating a comparably higher HR_{SENS}. Similarly, the EC_{50} for PGD_2 production caused by human anti-IgE (7.2 x 10^{-2} ± 2.1 x 10^{-3} μg/ml) was significantly lower than that of rabbit anti-IgE (2.9 x 10^{-1} ± 3 x 10^{-2} μg/ml) ($p < 0.05$).

Effects of Human and Rabbit Anti-IgE on Histamine Release and *De Novo* Synthesis of Lipid Mediators From Human Lung Mast Cells

In five experiments, we compared the effects of increasing concentrations of human and rabbit anti-IgE on HR and *de novo* synthesis of LTC_4 and PGD_2 from HLMCs. Increasing concentrations (10^{-2} to 3x10^{-1} μg/ml) of human or rabbit anti-IgE (10^{-1} to 3 μg/ml) caused a concentration-dependent release of histamine from HLMCs (**Figure 5A**). The maximal percent HR in response to human anti-IgE (18.4% ± 1.8%) was similar to HLMC reactivity to rabbit anti-IgE (20.2% ± 1.2%). By contrast, the EC_{50} was significantly lower (4.6 x 10^{-2} ± 4 x 10^{-3} μg/ml) for human compared to rabbit anti-IgE (3.4 x 10^{-1} ± 8 x 10^{-2} μg/ml) ($p < 0.01$). In these experiments, we also compared the effects of human and rabbit anti-IgE on the *de novo* synthesis of LTC_4 and PGD_2 from HLMCs. **Figure 5B** shows that the maximal production of LTC_4 by HLMCs exposed to human anti-IgE (40.9 ± 2.2 ng/10^6 cells) was similar to that caused by rabbit anti-IgE (42.5 ± 2.0 ng/10^6 cells). By contrast, the concentration of human anti-IgE inducing half-maximal LTC_4 release was significantly lower (4.0 x 10^{-2} ± 4 x 10^{-3} μg/ml) than the EC_{50} for rabbit anti-IgE (2.5 x 10^{-1} ± 6 x 10^{-2} μg/ml) ($p < 0.05$). Similarly, HLMC reactivity to human anti-IgE (31.4 ± 2.6 ng/10^6 cells) was similar to rabbit anti-IgE (38.9 ± 3.0 ng/10^6 cells) with respect to PGD_2 production (**Figure 5C**). The EC_{50} for PGD_2 production caused by human anti-IgE (4.2 x 10^{-2} ± 1 x 10^{-3} μg/ml) was significantly lower than that of rabbit anti-IgE (2.8 x 10^{-1} ± 8 x 10^{-2} μg/ml) ($p < 0.05$).

DISCUSSION

Our results indicate that although autoantibodies against IgE can be found in some patients with AD, these can rarely induce the activation of human basophils and mast cells. We have detected functional IgG anti-IgE in one out of six patients with AD and characterized its ability to trigger mediator release from human basophils and mast cells. This human IgG anti-IgE is a more potent secretagogue than rabbit IgG anti-IgE, and human monoclonal IgE appears to act as a competitive antagonist of either antibody. A novel finding emerging from this study is the ability of human anti-IgE from AD to induce the release of IL-4 and IL-13 from human basophils. Another novel aspect is the observation that human anti-IgE activates not only human basophils, but also skin and lung mast cells to release histamine and arachidonic acid metabolites.

The role of naturally occurring anti-IgE/FcεRI autoantibodies in allergic and non allergic disorders is still a fascinating and unsettled issue, as recently discussed by Galli (54). Several investigators have found these autoantibodies in CSU (42, 46–49, 88–91) and in asthma (43, 50, 92). By contrast, anti-IgE autoantibodies have been inconsistently found in AD patients (43–45, 47, 52). Anti-IgE/FcεRI autoantibodies of the IgG class have been found in most of these studies (43–48, 88, 90, 91, 93, 94), while IgM (42, 49), and/or IgA autoantibodies have been only documented in rare instances (49). In most cases the autoantibodies found in patients with CSU or AD lacked the capacity to activate human basophils *in vitro* (36, 44, 47). While in some studies human IgE-specific IgG autoantibodies were able to activate human basophils (44, 47), in others they even inhibited basophil activation (36, 50).

A limitation in most of these functional studies was that they only examined the potential effects of autoantibodies to IgE or FcεRI on HR from human peripheral blood basophils (36, 42, 46–48, 88, 90, 91). The above results, while contrasting, do not necessarily rule out the hypothesis that these naturally occurring autoantibodies can activate human basophils to release cytokines (e.g., IL-4, IL-13) or tissue mast cells to produce arachidonic acid metabolites.

In this study, we found that only one preparation of human IgG anti-IgE out of six patients with AD had the ability to activate peripheral blood basophils purified from normal donors and mast cells isolated from human skin or lung tissue. Although the sample size examined in this study is too small to conclusively estimate the prevalence of functional anti-IgE autoantibodies in AD patients, these results allow to raise a few points. The apparent low prevalence of functional autoantibodies to IgE might explain, at least in part, the controversial results on the presence of functional such autoantibodies in AD patients (43–45, 47, 52). Moreover, our findings are in line with the systematic, aptly controlled observations by MacGlashan demonstrating that the autoantibodies to IgE and/or FcεRI from the vast majority of patients with CSU lacked the capacity to activate human basophil mediator release (36).

Our results provide some information on the functional potency of the IgG anti-IgE isolated from a patient with AD. Although basophil reactivity, that is the maximal HR in response to human anti-IgE, was similar to that induced by rabbit anti-IgE, the potency of human anti-IgE was significantly higher than that of rabbit anti-IgE. Similar results were obtained when comparing the reactivity and threshold sensitivity of human skin and lung mast cells to human and rabbit anti-IgE in experiments looking not only at the HR but also the *de novo* synthesis of lipid mediators (*i.e.*, PGD_2, and LTC_4). Collectively, these results indicate that human anti-IgE, when it is functionally present, can be significantly more potent than rabbit anti-IgE preparations commonly used in experimental or diagnostic *in vitro* protocols for IgE-dependent activation of human $FcεRI^+$ cells.

We also provide some clues on the immunologic mechanism of activation of human basophils by human IgG anti-IgE. We found that preincubation of human basophils with increasing concentrations of human monoclonal IgE purified from a myeloma patient (68, 70) concentration-dependently interfered with the activating properties of both human and rabbit anti-IgE. The specificity of this response was confirmed by the observation

that preincubation of basophils with tenfold higher concentrations of human polyclonal IgG did not antagonize the ability of both human and rabbit to trigger mediator release anti-IgE.

A novel finding of this study is the ability of human IgG anti-IgE to induce the release of Th2-like cytokines (e.g., IL-4, IL-13) from human basophils. The vast majority of studies exploring the functional activity of human anti-IgE and anti-FcεRI have evaluated the ability of these autoantibodies to induce HR from human basophils (36, 42, 47, 48, 50, 88, 90, 91). To the best of our knowledge, we provide the first evidence that a functional preparation of human IgG anti-IgE can also induce the release of IL-4 and IL-13 from human basophils. Also in this case, we observed that only IgG anti-IgE obtained from one out of six AD donors could cause cytokine release from basophils.

Our findings may have some translational relevance. AD is characterized by robust Th2-mediated immune responses to numerous environmental stimuli (95). The Th2 cytokines IL-4 and IL-13 are believed to play pivotal roles in the pathogenesis of AD (96, 97). Consistent with these findings, dual IL-4 and IL-13 blockade with the IL-4Rα antagonist, dupilumab showed unprecedented efficacy in adult AD patients (98, 99). Moreover, recent evidence indicates that LTC_4 plays a role in a mouse model of AD (100). The observation that human IgG anti-IgE is a potent stimulus for the production of IL-4/IL-13 from basophils and LTC_4 from mast cells suggests that these autoantibodies may play a role in the onset and progression of at least a subset of AD patients.

Human basophils and mast cells are key contributors to allergic disorders (1, 13, 26), including AD (67). A closer understanding of their roles in allergies has been marked by the considerable heterogeneity of these cells, whereby distinct morphologic and functional properties can not only be appreciated between mast cells and basophils (26) but also between cells located in different tissues and districts (40, 101–104). In this study, we demonstrated that human IgG anti-IgE is a potent stimulus for the production of Th2-like cytokines, hinting at a possible role in the upstream control of allergic responses, including IgE synthesis. Further, the agonist effects on prostanoids secretion from skin mast cells, mediators found at substantial levels in AD lesions (105), might have important clinical implications in AD.

In conclusion, our results extend previous findings (36, 44) indicating that only a minority of IgG anti-IgE isolated from patients with AD activates human $FcεRI^+$ cells. Our data show that when functional autoantibodies to IgE are present, these can be more potent than rabbit IgG anti-IgE in inducing the release of histamine, cytokines (IL-4, IL-13) and lipid mediators (PGD_2, and LTC_4) from human basophils and/or mast cells. Further studies in larger cohorts of patients with different phenotypes of AD are needed to more conclusively assess the prevalence of functional autoantibodies to IgE or FcεRI and their possible contribution to disease pathogenesis and the response to current and prospective therapeutic strategies.

DATA AVAILABILITY STATEMENT

The raw data supporting the conclusions of this article will be made available by the authors, without undue reservation.

ETHICS STATEMENT

The studies involving human participants were reviewed and approved by the Ethics Committee of the University of Naples Federico II, School of Medicine (Prot. 198/18), and informed consent was obtained from all participants prior to collection of blood according to recommendations from the Declaration of Helsinki. Written informed consent to participate in this study was provided by the participants' legal guardian/next of kin.

AUTHOR CONTRIBUTIONS

RP, IQ, GM, VC, and GV designed the research. RP, IQ, AP, and VC did the experiment. RP, GM, MT, VC, and GV analyzed the data and wrote the manuscript. All authors listed have made a substantial, direct, and intellectual contribution to the work and approved it for publication.

FUNDING

This work was supported in part by grants from the CISI-Lab Project (University of Naples Federico II) and TIMING Project and Campania Bioscience (Regione Campania).

ACKNOWLEDGMENTS

The authors would like to thank Dr. Gjada Criscuolo for her excellent managerial assistance in preparing it and the administrative staff (Dr. Roberto Bifulco, Dr. Anna Ferraro and Dr. Maria Cristina Fucci), without whom it would not be possible to work as a team.

REFERENCES

1. Galli SJ, Gaudenzio N, Tsai M. Mast Cells in Inflammation and Disease: Recent Progress and Ongoing Concerns. *Annu Rev Immunol* (2020) 38:49–77. doi: 10.1146/annurev-immunol-071719-094903
2. Hamey FK, Lau WWY, Kucinski I, Wang X, Diamanti E, Wilson NK, et al. Single-Cell Molecular Profiling Provides a High-Resolution Map of Basophil and Mast Cell Development. *Allergy* (2021) 76:1731–42. doi: 10.1111/all.14633
3. Miyake K, Shibata S, Yoshikawa S, Karasuyama H. Basophils and Their Effector Molecules in Allergic Disorders. *Allergy* (2021) 76:1693–706. doi: 10.1111/all.14662
4. Schroeder JT. Basophils: Emerging Roles in the Pathogenesis of Allergic Disease. *Immunol Rev* (2011) 242:144–60. doi: 10.1111/j.1600-065X.2011.01023.x

5. Marone G, Borriello F, Varricchi G, Genovese A, Granata F. Basophils: Historical Reflections and Perspectives. *Chem Immunol Allergy* (2014) 100:172–92. doi: 10.1159/000358734
6. Siracusa MC, Saenz SA, Hill DA, Kim BS, Headley MB, Doering TA, et al. TSLP Promotes Interleukin-3-Independent Basophil Haematopoiesis and Type 2 Inflammation. *Nature* (2011) 477:229–33. doi: 10.1038/nature10329
7. Siracusa MC, Wojno ED, Artis D. Functional Heterogeneity in the Basophil Cell Lineage. *Adv Immunol* (2012) 115:141–59. doi: 10.1016/B978-0-12-394299-9.00005-9
8. Bradding P, Arthur G. Mast Cells in Asthma–State of the Art. *Clin Exp Allergy* (2016) 46:194–263. doi: 10.1111/cea.12675
9. Galli SJ, Kalesnikoff J, Grimbaldeston MA, Piliponsky AM, Williams CM, Tsai M. Mast Cells as "Tunable" Effector and Immunoregulatory Cells: Recent Advances. *Annu Rev Immunol* (2005) 23:749–86. doi: 10.1146/annurev.immunol.21.120601.141025
10. Rivellese F, Nerviani A, Rossi FW, Marone G, Matucci-Cerinic M, de Paulis A, et al. Mast Cells in Rheumatoid Arthritis: Friends or Foes? *Autoimmun Rev* (2017) 16:557–63. doi: 10.1016/j.autrev.2017.04.001
11. Maurer M, Altrichter S, Schmetzer O, Scheffel J, Church MK, Metz M. Immunoglobulin E-Mediated Autoimmunity. *Front Immunol* (2018) 9:689. doi: 10.3389/fimmu.2018.00689
12. Lamri Y, Vibhushan S, Pacreau E, Boedec E, Saidoune F, Mailleux A, et al. Basophils and IgE Contribute to Mixed Connective Tissue Disease Development. *J Allergy Clin Immunol* (2021) 147:1478–89.e1411. doi: 10.1016/j.jaci.2020.12.622
13. Eberle JU, Voehringer D. Role of Basophils in Protective Immunity to Parasitic Infections. *Semin Immunopathol* (2016) 38:605–13. doi: 10.1007/s00281-016-0563-3
14. Yamanishi Y, Miyake K, Iki M, Tsutsui H, Karasuyama H. Recent Advances in Understanding Basophil-Mediated Th2 Immune Responses. *Immunol Rev* (2017) 278:237–45. doi: 10.1111/imr.12548
15. Shi GP, Bot I, Kovanen PT. Mast Cells in Human and Experimental Cardiometabolic Diseases. *Nat Rev Cardiol* (2015) 12:643–58. doi: 10.1038/nrcardio.2015.117
16. Varricchi G, Marone G, Kovanen PT. Cardiac Mast Cells: Underappreciated Immune Cells in Cardiovascular Homeostasis and Disease. *Trends Immunol* (2020) 41:734–46. doi: 10.1016/j.it.2020.06.006
17. Sicklinger F, Meyer IS, Li X, Radtke D, Dicks S, Kornadt MP, et al. Basophils Balance Healing After Myocardial Infarction *via* IL-4/IL-13. *J Clin Invest* (2021) 131:e136778. doi: 10.1172/JCI136778
18. Marone G, Varricchi G, Loffredo S, Galdiero MR, Rivellese F, de Paulis A. Are Basophils and Mast Cells Masters in HIV Infection? *Int Arch Allergy Immunol* (2016) 171:158–65. doi: 10.1159/000452889
19. Varricchi G, Galdiero MR, Loffredo S, Marone G, Iannone R, Granata F. Are Mast Cells MASTers in Cancer? *Front Immunol* (2017) 8:424. doi: 10.3389/fimmu.2017.00424
20. Sektioglu IM, Carretero R, Bulbuc N, Bald T, Tuting T, Rudensky AY, et al. Basophils Promote Tumor Rejection *via* Chemotaxis and Infiltration of CD8+ T Cells. *Cancer Res* (2017) 77:291–302. doi: 10.1158/0008-5472.CAN-16-0993
21. Hayes MD, Ward S, Crawford G, Seoane RC, Jackson WD, Kipling D, et al. Inflammation-Induced IgE Promotes Epithelial Hyperplasia and Tumour Growth. *Elife* (2020) 9:e51862. doi: 10.7554/eLife.51862
22. De Monte L, Wormann S, Brunetto E, Heltai S, Magliacane G, Reni M, et al. Basophil Recruitment Into Tumor-Draining Lymph Nodes Correlates With Th2 Inflammation and Reduced Survival in Pancreatic Cancer Patients. *Cancer Res* (2016) 76:1792–803. doi: 10.1158/0008-5472.CAN-15-1801-T
23. Serhan N, Basso L, Sibilano R, Petitfils C, Meixiong J, Bonnart C, et al. House Dust Mites Activate Nociceptor-Mast Cell Clusters to Drive Type 2 Skin Inflammation. *Nat Immunol* (2019) 20:1435–43. doi: 10.1038/s41590-019-0493-z
24. Rauber MM, Pickert J, Holiangu L, Mobs C, Pfutzner W. Functional and Phenotypic Analysis of Basophils Allows Determining Distinct Subtypes in Patients With Chronic Urticaria. *Allergy* (2017) 72:1904–11. doi: 10.1111/all.13215
25. Vasagar K, Vonakis BM, Gober LM, Viksman A, Gibbons SPJr., Saini SS. Evidence of *In Vivo* Basophil Activation in Chronic Idiopathic Urticaria. *Clin Exp Allergy* (2006) 36:770–6. doi: 10.1111/j.1365-2222.2006.02494.x
26. Varricchi G, Raap U, Rivellese F, Marone G, Gibbs BF. Human Mast Cells and Basophils-How are They Similar How are They Different? *Immunol Rev* (2018) 282:8–34. doi: 10.1111/imr.12627
27. Galli SJ, Tsai M. IgE and Mast Cells in Allergic Disease. *Nat Med* (2012) 18:693–704. doi: 10.1038/nm.2755
28. Zhai GT, Wang H, Li JX, Cao PP, Jiang WX, Song J, et al. IgD-Activated Mast Cells Induce IgE Synthesis in B Cells in Nasal Polyps. *J Allergy Clin Immunol* (2018) 142:1489–1499.e1423. doi: 10.1016/j.jaci.2018.07.025
29. Macchia D, Melioli G, Pravettoni V, Nucera E, Piantanida M, Caminati M, et al. Guidelines for the Use and Interpretation of Diagnostic Methods in Adult Food Allergy. *Clin Mol Allergy* (2015) 13:27. doi: 10.1186/s12948-015-0033-933
30. Leyva-Castillo JM, Galand C, Kam C, Burton O, Gurish M, Musser MA, et al. Mechanical Skin Injury Promotes Food Anaphylaxis by Driving Intestinal Mast Cell Expansion. *Immunity* (2019) 50:1262–75.e1264. doi: 10.1016/j.immuni.2019.03.023
31. Choi HW, Suwanpradid J, Kim IH, Staats HF, Haniffa M, MacLeod AS, et al. Perivascular Dendritic Cells Elicit Anaphylaxis by Relaying Allergens to Mast Cells *via* Microvesicles. *Science* (2018) 362:eaao0666. doi: 10.1126/science.aao0666
32. Dispenza MC, Krier-Burris RA, Chhiba KD, Undem BJ, Robida PA, Bochner BS. Bruton's Tyrosine Kinase Inhibition Effectively Protects Against Human IgE-Mediated Anaphylaxis. *J Clin Invest* (2020) 130:4759–70. doi: 10.1172/JCI138448
33. Blank U, Huang H, Kawakami T. The High Affinity IgE Receptor: A Signaling Update. *Curr Opin Immunol* (2021) 72:51–8. doi: 10.1016/j.coi.2021.03.015
34. Garman SC, Wurzburg BA, Tarchevskaya SS, Kinet JP, Jardetzky TS. Structure of the Fc Fragment of Human IgE Bound to its High-Affinity Receptor Fc epsilonRI Alpha. *Nature* (2000) 406:259–66. doi: 10.1038/35018500
35. Kulczycki AJr., Metzger H. The Interaction of IgE With Rat Basophilic Leukemia Cells. II. Quantitative Aspects of the Binding Reaction. *J Exp Med* (1974) 140:1676–95. doi: 10.1084/jem.140.6.1676
36. MacGlashan D. Autoantibodies to IgE and FcepsilonRI and the Natural Variability of Spleen Tyrosine Kinase Expression in Basophils. *J Allergy Clin Immunol* (2019) 143:1100–1107.e1111. doi: 10.1016/j.jaci.2018.05.019
37. Ishizaka T, Ishizaka K, Johansson SG, Bennich H. Histamine Release From Human Leukocytes by Anti-Gamma E Antibodies. *J Immunol* (1969) 102:884–92.
38. Genovese A, Borgia G, Bjorck L, Petraroli A, de Paulis A, Piazza M, et al. Immunoglobulin Superantigen Protein L Induces IL-4 and IL-13 Secretion From Human Fc Epsilon RI+ Cells Through Interaction With the Kappa Light Chains of IgE. *J Immunol* (2003) 170:1854–61. doi: 10.4049/jimmunol.170.4.1854
39. Patella V, Florio G, Petraroli A, Marone G. HIV-1 Gp120 Induces IL-4 and IL-13 Release From Human Fc Epsilon RI+ Cells Through Interaction With the VH3 Region of IgE. *J Immunol* (2000) 164:589–95. doi: 10.4049/jimmunol.164.2.589
40. Cristinziano L, Poto R, Criscuolo G, Ferrara AL, Galdiero MR, Modestino L, et al. IL-33 and Superantigenic Activation of Human Lung Mast Cells Induce the Release of Angiogenic and Lymphangiogenic Factors. *Cells* (2021) 10:145. doi: 10.3390/cells10010145
41. Marone G, Rossi FW, Pecoraro A, Pucino V, Criscuolo G, Paulis A, et al. HIV Gp120 Induces the Release of Proinflammatory, Angiogenic, and Lymphangiogenic Factors From Human Lung Mast Cells. *Vaccines (Basel)* (2020) 8:208. doi: 10.3390/vaccines8020208
42. Gruber BL, Baeza ML, Marchese MJ, Agnello V, Kaplan AP. Prevalence and Functional Role of Anti-IgE Autoantibodies in Urticarial Syndromes. *J Invest Dermatol* (1988) 90:213–7. doi: 10.1111/1523-1747.ep12462239
43. Nawata Y, Koike T, Hosokawa H, Tomioka H, Yoshida S. Anti-IgE Autoantibody in Patients With Atopic Dermatitis. *J Immunol* (1985) 135:478–82.
44. Marone G, Casolaro V, Paganelli R, Quinti I. IgG Anti-IgE From Atopic Dermatitis Induces Mediator Release From Basophils and Mast Cells. *J Invest Dermatol* (1989) 93:246–52. doi: 10.1111/1523-1747.ep12277582
45. Quinti I, Brozek C, Wood N, Geha RS, Leung DY. Circulating IgG Autoantibodies to IgE in Atopic Syndromes. *J Allergy Clin Immunol* (1986) 77:586–94. doi: 10.1016/0091-6749(86)90350-7
46. Niimi N, Francis DM, Kermani F, O'Donnell BF, Hide M, Kobza-Black A, et al. Dermal Mast Cell Activation by Autoantibodies Against the High Affinity IgE Receptor in Chronic Urticaria. *J Invest Dermatol* (1996) 106:1001–6. doi: 10.1111/1523-1747.ep12338544

47. Fiebiger E, Hammerschmid F, Stingl G, Maurer D. Anti-FcepsilonRIalpha Autoantibodies in Autoimmune-Mediated Disorders. Identification of a Structure-Function Relationship. *J Clin Invest* (1998) 101:243–51. doi: 10.1172/JCI511
48. Hide M, Francis DM, Grattan CE, Hakimi J, Kochan JP, Greaves MW. Autoantibodies Against the High-Affinity IgE Receptor as a Cause of Histamine Release in Chronic Urticaria. *N Engl J Med* (1993) 328:1599–604. doi: 10.1056/NEJM199306033282204
49. Altrichter S, Zampeli V, Ellrich A, Zhang K, Church MK, Maurer M. IgM and IgA in Addition to IgG Autoantibodies Against FcvarepsilonRIalpha are Frequent and Associated With Disease Markers of Chronic Spontaneous Urticaria. *Allergy* (2020) 75:3208–15. doi: 10.1111/all.14412
50. Chan YC, Ramadani F, Santos AF, Pillai P, Ohm-Laursen L, Harper CE, et al. "Auto-Anti-IgE": Naturally Occurring IgG Anti-IgE Antibodies may Inhibit Allergen-Induced Basophil Activation. *J Allergy Clin Immunol* (2014) 134:1394–1401 e1394. doi: 10.1016/j.jaci.2014.06.029
51. Nawata Y, Koike T, Yanagisawa T, Iwamoto I, Itaya T, Yoshida S, et al. Anti-IgE Autoantibody in Patients With Bronchial Asthma. *Clin Exp Immunol* (1984) 58:348–56.
52. Czech W, Stadler BM, Schopf E, Kapp A. IgE Autoantibodies in Atopic Dermatitis–Occurrence of Different Antibodies Against the CH3 and the CH4 Epitopes of IgE. *Allergy* (1995) 50:243–8. doi: 10.1111/j.1398-9995.1995.tb01141.x
53. Gruber BL, Kaufman LD, Marchese MJ, Roth W, Kaplan AP. Anti-IgE Autoantibodies in Systemic Lupus Erythematosus. Prevalence and Biologic Activity. *Arthritis Rheum* (1988) 31:1000–6. doi: 10.1002/art.1780310810
54. Galli SJ. Complexities in Analyzing Human Basophil Responses to Autoantibodies to IgE or FcepsilonRI. *J Allergy Clin Immunol* (2019) 143:932–4. doi: 10.1016/j.jaci.2018.12.998
55. Sanchez J, Sanchez A, Munera M, Garcia E, Lopez JF, Velasquez-Lopera M, et al. Presence of IgE Autoantibodies Against Eosinophil Peroxidase and Eosinophil Cationic Protein in Severe Chronic Spontaneous Urticaria and Atopic Dermatitis. *Allergy Asthma Immunol Res* (2021) 13:746–61. doi: 10.4168/aair.2021.13.5.746
56. Galeotti C, Stephen-Victor E, Karnam A, Das M, Gilardin L, Maddur MS, et al. Intravenous Immunoglobulin Induces IL-4 in Human Basophils by Signaling Through Surface-Bound IgE. *J Allergy Clin Immunol* (2019) 144:524–535.e528. doi: 10.1016/j.jaci.2018.10.064
57. Rivellese F, Suurmond J, de Paulis A, Marone G, Huizinga TW, Toes RE. IgE and IL-33-Mediated Triggering of Human Basophils Inhibits TLR4-Induced Monocyte Activation. *Eur J Immunol* (2014) 44:3045–55. doi: 10.1002/eji.201444731
58. Silver MR, Margulis A, Wood N, Goldman SJ, Kasaian M, Chaudhary D. IL-33 Synergizes With IgE-Dependent and IgE-Independent Agents to Promote Mast Cell and Basophil Activation. *Inflammation Res* (2010) 59:207–18. doi: 10.1007/s00011-009-0088-5
59. Patella V, Giuliano A, Bouvet JP, Marone G. Endogenous Superallergen Protein Fv Induces IL-4 Secretion From Human Fc Epsilon RI+ Cells Through Interaction With the VH3 Region of IgE. *J Immunol* (1998) 161:5647–55.
60. Redrup AC, Howard BP, MacGlashan DWJr., Kagey-Sobotka A, Lichtenstein LM, Schroeder JT. Differential Regulation of IL-4 and IL-13 Secretion by Human Basophils: Their Relationship to Histamine Release in Mixed Leukocyte Cultures. *J Immunol* (1998) 160:1957–64.
61. Ochensberger B, Daepp GC, Rihs S, Dahinden CA. Human Blood Basophils Produce Interleukin-13 in Response to IgE-Receptor-Dependent and -Independent Activation. *Blood* (1996) 88:3028–37.
62. MacGlashan DJr., White JM, Huang SK, Ono SJ, Schroeder JT, Lichtenstein LM. Secretion of IL-4 From Human Basophils. The Relationship Between IL-4 mRNA and Protein in Resting and Stimulated Basophils. *J Immunol* (1994) 152:3006–16.
63. Ito Y, Satoh T, Takayama K, Miyagishi C, Walls AF, Yokozeki H. Basophil Recruitment and Activation in Inflammatory Skin Diseases. *Allergy* (2011) 66:1107–13. doi: 10.1111/j.1398-9995.2011.02570.x
64. Guo CB, Liu MC, Galli SJ, Bochner BS, Kagey-Sobotka A, Lichtenstein LM. Identification of IgE-Bearing Cells in the Late-Phase Response to Antigen in the Lung as Basophils. *Am J Respir Cell Mol Biol* (1994) 10:384–90. doi: 10.1165/ajrcmb.10.4.7510984
65. Irani AM, Huang C, Xia HZ, Kepley C, Nafie A, Fouda ED, et al. Immunohistochemical Detection of Human Basophils in Late-Phase Skin Reactions. *J Allergy Clin Immunol* (1998) 101:354–62. doi: 10.1016/S0091-6749(98)70248-9
66. Patella V, de Crescenzo G, Marino I, Genovese A, Adt M, Gleich GJ, et al. Eosinophil Granule Proteins Activate Human Heart Mast Cells. *J Immunol* (1996) 157:1219–25.
67. Nomura T, Kabashima K. Advances in Atopic Dermatitis in 2019-2020: Endotypes From Skin Barrier, Ethnicity, Properties of Antigen, Cytokine Profiles, Microbiome, and Engagement of Immune Cells. *J Allergy Clin Immunol* (2021) 148:1451–62. doi: 10.1016/j.jaci.2021.10.022
68. Maisonpierre PC, Suri C, Jones PF, Bartunkova S, Wiegand SJ, Radziejewski C, et al. Angiopoietin-2, a Natural Antagonist for Tie2 That Disrupts *In Vivo* Angiogenesis. *Science* (1997) 277:55–60. doi: 10.1126/science.277.5322.55
69. Romagnani S, Damiani G, Giudizi MG, Biagiotti R, Almerigogna F, Delprete GF, et al. *In Vitro* Production of IgE by Human Peripheral Blood Mononuclear Cells. III. Demonstration of a Circulating IgE-Bearing Cell Involved in the Spontaneous IgE Biosynthesis. *Clin Exp Immunol* (1982) 49:176–84.
70. Marone G, Tamburini M, Giudizi MG, Biagiotti R, Almerigogna F, Romagnani S. Mechanism of Activation of Human Basophils by Staphylococcus Aureus Cowan 1. . *Infect Immun* (1987) 55:803–9. doi: 10.1128/iai.55.3.803-809.1987
71. Romagnani S, Giudizi MG, del Prete G, Maggi E, Biagiotti R, Almerigogna F, et al. Demonstration on Protein A of Two Distinct Immunoglobulin-Binding Sites and Their Role in the Mitogenic Activity of Staphylococcus Aureus Cowan I on Human B Cells. *J Immunol* (1982) 129:596–602.
72. Schroeder JT, Bieneman AP. Activation of Human Basophils by A549 Lung Epithelial Cells Reveals a Novel IgE-Dependent Response Independent of Allergen. *J Immunol* (2017) 199:855–65. doi: 10.4049/jimmunol.1700055
73. de Paulis A, Stellato C, Cirillo R, Ciccarelli A, Oriente A, Marone G. Anti-Inflammatory Effect of FK-506 on Human Skin Mast Cells. *J Invest Dermatol* (1992) 99:723–8. doi: 10.1111/1523-1747.ep12614216
74. Staiano RI, Loffredo S, Borriello F, Iannotti FA, Piscitelli F, Orlando P, et al. Human Lung-Resident Macrophages Express CB1 and CB2 Receptors Whose Activation Inhibits the Release of Angiogenic and Lymphangiogenic Factors. *J Leukoc Biol* (2016) 99:531–40. doi: 10.1189/jlb.3HI1214-584R
75. Ferrara AL, Galdiero MR, Fiorelli A, Cristinziano L, Granata F, Marone G, et al. Macrophage-Polarizing Stimuli Differentially Modulate the Inflammatory Profile Induced by the Secreted Phospholipase A2 Group IA in Human Lung Macrophages. *Cytokine* (2021) 138:155378. doi: 10.1016/j.cyto.2020.155378
76. Casolaro V, Spadaro G, Marone G. Human Basophil Releasability. VI. Changes in Basophil Releasability in Patients With Allergic Rhinitis or Bronchial Asthma. *Am Rev Respir Dis* (1990) 142:1108–11. doi: 10.1164/ajrccm/142.5.1108
77. Spadaro G, Giurato G, Stellato C, Marone G, Casolaro V. Basophil Degranulation in Response to IgE Ligation is Controlled by a Distinctive Circadian Clock in Asthma. *Allergy* (2020) 75:158–68. doi: 10.1111/all.14002
78. Siraganian RP. An Automated Continuous-Flow System for the Extraction and Fluorometric Analysis of Histamine. *Anal Biochem* (1974) 57:383–94. doi: 10.1016/0003-2697(74)90093-1
79. MacGlashan DWJr. Basophil Activation Testing. *J Allergy Clin Immunol* (2013) 132:777–87. doi: 10.1016/j.jaci.2013.06.038
80. Dahlen B, Nopp A, Johansson SG, Eduards M, Skedinger M, Adedoyin J. Basophil Allergen Threshold Sensitivity, CD-Sens, is a Measure of Allergen Sensitivity in Asthma. *Clin Exp Allergy* (2011) 41:1091–7. doi: 10.1111/j.1365-2222.2011.03763.x
81. Glaumann S, Nopp A, Johansson SG, Rudengren M, Borres MP, Nilsson C. Basophil Allergen Threshold Sensitivity, CD-Sens, IgE-Sensitization and DBPCFC in Peanut-Sensitized Children. *Allergy* (2012) 67:242–7. doi: 10.1111/j.1398-9995.2011.02754.x
82. de Paulis A, Cirillo R, Ciccarelli A, de Crescenzo G, Oriente A, Marone G. Characterization of the Anti-Inflammatory Effect of FK-506 on Human Mast Cells. *J Immunol* (1991) 147:4278–85.
83. Patella V, Casolaro V, Bjorck L, Marone G. Protein L. A Bacterial Ig-Binding Protein That Activates Human Basophils and Mast Cells. *J Immunol* (1990) 145:3054–61.

84. Gibbs BF, Haas H, Falcone FH, Albrecht C, Vollrath IB, Noll T, et al. Purified Human Peripheral Blood Basophils Release Interleukin-13 and Preformed Interleukin-4 Following Immunological Activation. *Eur J Immunol* (1996) 26:2493–8. doi: 10.1002/eji.1830261033
85. Smithgall MD, Comeau MR, Yoon BR, Kaufman D, Armitage R, Smith DE. IL-33 Amplifies Both Th1- and Th2-Type Responses Through its Activity on Human Basophils, Allergen-Reactive Th2 Cells, iNKT and NK Cells. *Int Immunol* (2008) 20:1019–30. doi: 10.1093/intimm/dxn060
86. Chen K, Xu W, Wilson M, He B, Miller NW, Bengten E, et al. Immunoglobulin D Enhances Immune Surveillance by Activating Antimicrobial, Proinflammatory and B Cell-Stimulating Programs in Basophils. *Nat Immunol* (2009) 10:889–98. doi: 10.1038/ni.1748
87. Sharma M, Das M, Stephen-Victor E, Galeotti C, Karnam A, Maddur MS, et al. Regulatory T Cells Induce Activation Rather Than Suppression of Human Basophils. *Sci Immunol* (2018) 3:eaan0829. doi: 10.1126/sciimmunol.aan0829
88. Eckman JA, Hamilton RG, Gober LM, Sterba PM, Saini SS. Basophil Phenotypes in Chronic Idiopathic Urticaria in Relation to Disease Activity and Autoantibodies. *J Invest Dermatol* (2008) 128:1956–63. doi: 10.1038/jid.2008.55
89. Sabroe RA, Francis DM, Barr RM, Black AK, Greaves MW. Anti-Fc (episilon)RI Auto Antibodies and Basophil Histamine Releasability in Chronic Idiopathic Urticaria. *J Allergy Clin Immunol* (1998) 102:651–8. doi: 10.1016/s0091-6749(98)70283-0
90. Grattan CE, Francis DM, Hide M, Greaves MW. Detection of Circulating Histamine Releasing Autoantibodies With Functional Properties of Anti-IgE in Chronic Urticaria. *Clin Exp Allergy* (1991) 21:695–704. doi: 10.1111/j.1365-2222.1991.tb03198.x
91. Soundararajan S, Kikuchi Y, Joseph K, Kaplan AP. Functional Assessment of Pathogenic IgG Subclasses in Chronic Autoimmune Urticaria. *J Allergy Clin Immunol* (2005) 115:815–21. doi: 10.1016/j.jaci.2004.12.1120
92. Ritter C, Battig M, Kraemer R, Stadler BM. IgE Hidden in Immune Complexes With Anti-IgE Autoantibodies in Children With Asthma. *J Allergy Clin Immunol* (1991) 88:793–801. doi: 10.1016/0091-6749(91)90187-s
93. Marone G, Spadaro G, Palumbo C, Condorelli G. The Anti-IgE/anti-FcepsilonRIalpha Autoantibody Network in Allergic and Autoimmune Diseases. *Clin Exp Allergy* (1999) 29:17–27. doi: 10.1046/j.1365-2222.1999.00441.x
94. Paganelli R, Quinti I, D'Offizi GP, Papetti C, Nisini R, Aiuti F. Studies on the *In Vitro* Effects of Auto-Anti-IgE. Inhibition of Total and Specific Serum IgE Detection by a Human IgG Autoantibody to IgE. *J Clin Lab Immunol* (1988) 26:153–7.
95. Gittler JK, Shemer A, Suarez-Farinas M, Fuentes-Duculan J, Gulewicz KJ, Wang CQ, et al. Progressive Activation of T(H)2/T(H)22 Cytokines and Selective Epidermal Proteins Characterizes Acute and Chronic Atopic Dermatitis. *J Allergy Clin Immunol* (2012) 130:1344–54. doi: 10.1016/j.jaci.2012.07.012
96. Eichenfield LF, Tom WL, Chamlin SL, Feldman SR, Hanifin JM, Simpson EL, et al. Guidelines of Care for the Management of Atopic Dermatitis: Section 1. Diagnosis and Assessment of Atopic Dermatitis. *J Am Acad Dermatol* (2014) 70:338–51. doi: 10.1016/j.jaad.2013.10.010
97. Oetjen LK, Mack MR, Feng J, Whelan TM, Niu H, Guo CJ, et al. Sensory Neurons Co-Opt Classical Immune Signaling Pathways to Mediate Chronic Itch. *Cell* (2017) 171:217–228.e213. doi: 10.1016/j.cell.2017.08.006
98. Beck LA, Thaci D, Hamilton JD, Graham NM, Bieber T, Rocklin R, et al. Dupilumab Treatment in Adults With Moderate-to-Severe Atopic Dermatitis. *N Engl J Med* (2014) 371:130–9. doi: 10.1056/NEJMoa1314768
99. Thaci D, Simpson EL, Beck LA, Bieber T, Blauvelt A, Papp K, et al. Efficacy and Safety of Dupilumab in Adults With Moderate-to-Severe Atopic Dermatitis Inadequately Controlled by Topical Treatments: A Randomised, Placebo-Controlled, Dose-Ranging Phase 2b Trial. *Lancet* (2016) 387:40–52. doi: 10.1016/S0140-6736(15)00388-8
100. Voisin T, Perner C, Messou MA, Shiers S, Ualiyeva S, Kanaoka Y, et al. The CysLT2R Receptor Mediates Leukotriene C4-Driven Acute and Chronic Itch. *Proc Natl Acad Sci USA* (2021) 118:1031-44.e18. doi: 10.1073/pnas.2022087118182022087118
101. Cohen M, Giladi A, Gorki AD, Solodkin DG, Zada M, Hladik A, et al. Lung Single-Cell Signaling Interaction Map Reveals Basophil Role in Macrophage Imprinting. *Cell* (2018) 175:1031–1044 e1018. doi: 10.1016/j.cell.2018.09.009
102. Pellefigues C, Mehta P, Chappell S, Yumnam B, Old S, Camberis M, et al. Diverse Innate Stimuli Activate Basophils Through Pathways Involving Syk and IkappaB Kinases. *Proc Natl Acad Sci USA* (2021) 118:e2019524118. doi: 10.1073/pnas.2019524118
103. Varricchi G, Loffredo S, Borriello F, Pecoraro A, Rivellese F, Genovese A, et al. Superantigenic Activation of Human Cardiac Mast Cells. *Int J Mol Sci* (2019) 20:1828. doi: 10.3390/ijms20081828
104. Vivanco Gonzalez N, Oliveria JP, Tebaykin D, Ivison GT, Mukai K, Tsai MM, et al. Mass Cytometry Phenotyping of Human Granulocytes Reveals Novel Basophil Functional Heterogeneity. *iScience* (2020) 23:101724. doi: 10.1016/j.isci.2020.101724
105. Sawada Y, Honda T, Nakamizo S, Nakajima S, Nonomura Y, Otsuka A, et al. Prostaglandin E2 (PGE2)-EP2 Signaling Negatively Regulates Murine Atopic Dermatitis-Like Skin Inflammation by Suppressing Thymic Stromal Lymphopoietin Expression. *J Allergy Clin Immunol* (2019) 144:1265–1273 e1269. doi: 10.1016/j.jaci.2019.06.036

Conflict of Interest: The authors declare that the research was conducted in the absence of any commercial or financial relationships that could be construed as a potential conflict of interest.

Publisher's Note: All claims expressed in this article are solely those of the authors and do not necessarily represent those of their affiliated organizations, or those of the publisher, the editors and the reviewers. Any product that may be evaluated in this article, or claim that may be made by its manufacturer, is not guaranteed or endorsed by the publisher.

Copyright © 2022 Poto, Quinti, Marone, Taglialatela, de Paulis, Casolaro and Varricchi. This is an open-access article distributed under the terms of the Creative Commons Attribution License (CC BY). The use, distribution or reproduction in other forums is permitted, provided the original author(s) and the copyright owner(s) are credited and that the original publication in this journal is cited, in accordance with accepted academic practice. No use, distribution or reproduction is permitted which does not comply with these terms.

frontiers | Frontiers in Immunology

MINI REVIEW
published: 02 June 2022
doi: 10.3389/fimmu.2022.886044

Uncovering the Mast Cell Response to *Mycobacterium tuberculosis*

Ivonne Torres-Atencio[1,2], *Ariadne Campble*[2], *Amador Goodridge*[2*] *and Margarita Martin*[3,4]

[1] Departamento de Farmacología, Facultad de Medicina, Universidad de Panamá, Panama, Panama, [2] Tuberculosis Biomarker Research Unit, Centro de Biología Molecular y Celular de Enfermedades (CBCME) – Instituto de Investigaciones Científicas y Servicios de Alta Tecnología (INDICASAT-AIP), Ciudad Del Saber, Panama, [3] Biochemistry Unit, Biomedicine Department, Faculty of Medicine, University of Barcelona, Barcelona, Spain, [4] Laboratory of Clinical and Experimental Respiratory Immunoallergy, August Pi i Sunyer Biomedical Research Institute (IDIBAPS), Barcelona, Spain

The immunologic mechanisms that contribute to the response to *Mycobacterium tuberculosis* infection still represent a challenge in the clinical management and scientific understanding of tuberculosis disease. In this scenario, the role of the different cells involved in the host response, either in terms of innate or adaptive immunity, remains key for defeating this disease. Among this coordinated cell response, mast cells remain key for defeating tuberculosis infection and disease. Together with its effector's molecules, membrane receptors as well as its anatomical locations, mast cells play a crucial role in the establishment and perpetuation of the inflammatory response that leads to the generation of the granuloma during tuberculosis. This review highlights the current evidences that support the notion of mast cells as key link to reinforce the advancements in tuberculosis diagnosis, disease progression, and novel therapeutic strategies. Special focus on mast cells capacity for the modulation of the inflammatory response among patients suffering multidrug resistant tuberculosis or in co-infections such as current COVID-19 pandemic.

Keywords: tuberculosis, mast cells, disease control, histamine, co-infection, biomarker, anti-TB therapy, disease progression

OPEN ACCESS

Edited by:
Satoshi Tanaka,
Kyoto Pharmaceutical University, Japan

Reviewed by:
Rosa Muñoz Cano,
Hospital Clínic de Barcelona, Spain
Rommel Chacon-Salinas,
Instituto Politécnico Nacional, Mexico

***Correspondence:**
Amador Goodridge
agoodridge@indicasat.org.pa

Specialty section:
This article was submitted to Inflammation, a section of the journal Frontiers in Immunology

Received: *28 February 2022*
Accepted: *02 May 2022*
Published: *02 June 2022*

Citation:
Torres-Atencio I, Campble A, Goodridge A and Martin M (2022) Uncovering the Mast Cell Response to Mycobacterium tuberculosis. Front. Immunol. 13:886044. doi: 10.3389/fimmu.2022.886044

MINI REVIEW

Mycobacterium tuberculosis (MTB) is the bacterium that causes tuberculosis (TB), which surpasses Human Immunodeficiency Virus (HIV) as the leading cause of death by an infectious agent. According to the World Health Organization (WHO), in 2019, approximately 10 million people became ill with active tuberculosis, and 1.2 million died from this disease (1). It is estimated that one third of the world population is infected with this bacterium but remains asymptomatic. Before the coronavirus (COVID-19) pandemic, TB was the leading cause of death from a single infectious agent (1).

Despite advances made over the past 20 years in understanding the mechanisms that contribute to protective immunity against MTB, there are still major gaps in scientific and clinical knowledge regarding TB. One of these gaps is TB latency, specifically the mechanisms that allow MTB to remain clinically latent and how the infection is reactivated, and disease development occurs. Another crucial point that remains unclear is the individual roles of the different immune cells participating in the host response to the bacilli. The existence of multi-drug resistant strains adds yet another layer of complexity to understanding interactions between the bacilli and genetically

distinct hosts. These represent the main obstacles to developing treatments directed at latent infections as a means to prevent disease (2).

Under the current COVID-19 pandemic conditions, another cause for concern is possible co-infection with MTB and SARS-CoV-2 virus. In addition to co-infected patients presenting more severe respiratory symptoms, the cellular mediators released during acute COVID-19 infection increase the risk of latent tuberculosis reactivation (3). Mast cells are among these cellular mediators and play a role in mast cell activation syndrome (MCAS) (4). While MCAS could be exacerbated with multiple pathogen infections, no major MCAS among patients with triple infections of TB, HIV, and SARS-CoV-2 has been noticed (5, 6). Rivas et al. reported two unusual cases of patients with triple infections of SARS-CoV-2, MTB, and HIV. Following treatment with supplemental oxygen and initiation of antituberculosis and antiretroviral therapies, both patients demonstrated clinical improvement and recovery from COVID-19. Thus, the effect of multiple infection on mast cell response requires a deeper revision to denote differences between clinical observations and the cellular and molecular level of MCAS.

Host resistance to MTB infection requires a coordinated effort between cells of the innate and adaptive immune systems (7). Various lung immune cell populations respond to MTB, and while their functions offer host protection, they can also result in potentially damaging inflammation. For example, although CD4+ T cells are mainly responsible for containing the infection through specific antigen recognition, these T cells are also major contributors to disease at different stages of infection (8). Macrophages, neutrophils, dendritic cells, NK, and B lymphocytes have also been shown to play an important role in the MTB infection response (9). Thus, the participation of both adaptative and innate immune branches remains key for defense against tuberculosis.

While the roles of these immune cells have been determined, the role of mast cells (MC) remains unclear. This minireview aims to consolidate the knowledge available on the host's MC response to MTB. Special focus will be directed to the cellular and clinical aspects related to this interaction.

MCs FUNCTION

MCs' versatility results from several elements that characterize their immune protection skills. First, MCs store a variety of mediators in their granules and express a diverse population of receptors on the cell membrane. Second, MCs are strategically distributed throughout the body in sites whose function complements the immune system. Specifically, MCs are found in skin and gastrointestinal and respiratory tissues and mucous membranes (10). The diversity of MC receptors, their signaling pathways and products make MCs central effector cells in the pathogenesis of many respiratory diseases, particularly diseases with underlying inflammatory and allergic pathologies (11).

In addition to the role mast cells play in allergenic processes, increasing evidence points to the participation of these cells in other pathologies ranging from autoimmune disorders, infectious diseases to cancer. In these processes, MCs have deleterious effects. Understanding how MCs cause damage as well as finding strategies to limit these effects is an important area of research (10).

MCs are further classified into two subtypes according to their protease content. Those found in skin are mostly chymase-tryptase positive (MC_{TC}), while those located in mucosa, such as bronchial epithelium, are tryptase positive (MC_T). In addition to the MC subtype, the increase in the number of MCs is also important in inflammatory processes (12). The major activation pathway is through the FcεRI and its interaction with IgE. Other MC receptors have a sentinel response to lipopolysaccharides or peptidoglycans generated by bacteria. For example, upon activation, Toll-Like Receptors (TLRs) induce the synthesis and up-regulation of cytokines including GM-CSF, IL-6, IL-8, and IL-10 (13). The precise cytokine profile depends on the activation route within the mast cell. To facilitate this interaction, MCs are located at the host-environment interface, proximal to both blood and lymphatic vessels. In addition, MCs are present along nerve fibers and close to tissue-resident immune cells (i.e. dendritic cells) (14).

Advancements in our understanding of MC biology have identified an abundance of checkpoints for potential therapeutic intervention. For example, the introduction of antihistamines more than 80 years ago led to the discovery of the different histamine receptors, one of the major inflammatory mediators stored in MCs (15). H1-antihistamines represent the cornerstone of treatment in patients with pruritus, allergic rhinitis, or allergic conjunctivitis, and this receptor is abundantly expressed on MCs (15).

MC ANTIMICROBIAL ACTIVITY

MCs demonstrate antimicrobial activity against bacteria, fungi, and viruses (14). These functions are executed following pathogen recognition *via* pattern recognition receptors (PRRs), and Fc receptors. At the beginning of an infection, MCs signal the pathogen's presence to innate and adaptive immune cells present near the infection site or distally in the draining lymph nodes (14). Mouse models of infectious pathogens have demonstrated increased pathogen clearance in animals with sufficient MCs compared to MC-deficient mice (16).

MCs have unique features that make their functions crucial for host defense. First, they are preponderant in the skin and mucosal sites, which is where most pathogens initiate infection, and they are among the first cells to encounter pathogens along with other innate immune cells, such as dendritic cells and macrophages. Second, MCs can recognize three targets: the pathogens directly, host molecules that opsonize pathogens, and/or signals released by infected cells in the vicinity. Third, after activation, MCs release inflammatory mediators and antimicrobial peptides that contribute to immune cell recruitment and the clearance of the invading pathogen (14).

Moreover, MCs can both initiate and sustain the inflammatory response due to *de novo* synthesis of mediators and their ability to

undergo multiple regranulation-degranulation cycles. One remarkable feature that distinguishes MCs from all other granulated cell types (e.g. neutrophils) is that cellular degranulation is not automatically associated with cell death. Instead, early studies suggest that MCs not only survive this process but possess the ability to recover, replenish their granules and participate in another round of degranulation (17). This special ability of regranulation makes sense considering the longevity and high time and energy investment in terms of weeklong development and maturation of MCs (18). On the other hand the ability of MCs to independently phagocytize and kill bacteria has also been discussed and remains controversial (19). In recent years, an additional antimicrobial mechanism, known as mast extracellular traps (MECT), has been proposed (20).

MICROBIAL SIGNALS THAT ACTIVATE MCs: PAMPS AND DAMPS

MCs activation mechanisms differ according to the pathogen. Depending on the stimuli perceived by MCs, they release a panel of inflammatory mediators for the type of pathogen detected (21). For example, in one study, MCs secreted proinflammatory cytokines when challenged by respiratory syncytial virus, they secreted anti-viral type 1 IFN (22). This differential response results from the characteristics of the MC surface receptors that are engaged and the signals released by those receptors.

MCs express a wide array of pattern recognition receptors (PRRs). The PRRs are a class of germ line-encoded receptors that recognize both extra- and intracellular pathogens as well as pathogen-derived products and pathogen-associated molecular patterns (PAMPS) (23). Among these PRRs, TLR expression in MCs from various origins has been well documented. Human MCs have been shown to express TLR1, TLR2, TLR3, TLR4, TLR5, TLR6, TLR7, TLR8, and TLR9 at different levels depending on the literature consulted (24–26).

The best-characterized receptors are TLR2, TLR4, and TLR5, which recognize the following bacterial products: peptidoglycan, lipopolysaccharide (LPS), and Flagelin, respectively (14). Cytokine and chemokine production and secretion are the common functional outcomes of TLR signaling in MCs, but this signaling can also induce calcium influx and degranulation (e.g. peptidoglycan stimulation through TLR2) (27).

MTB can be recognized by MC PRRs, as is the case with TLR2 (28). In addition, MCs can respond to danger signals (DAMPS), such as IL-33, released by neighboring infected host cells, which activates proinflammatory cytokine secretion by MCs to resolve infection (29). Previous exposure to pathogens/TLR-ligands enhances IgE-dependent release of several inflammatory mediators in MCs, which suggests that infections might magnify the severity of allergic reactions (30). In addition to the PPRs, other molecules, such as the glycosylphosphatidylinositol-anchored proteins (GPI) receptor CD48, can bind pathogens and trigger MC degranulation and microbe uptake (31). Complement receptors (CR3, CR4, C3aR, and C5aR) and immunoglobulin receptors (FcεRI, FcγRI, FcγRII, and Fcγ RIII) have also been reported to mediate the MC response to other pathogens, including bacteria and parasites (32).

MCs INNATE RESPONSE TO PATHOGENS: RELEASE OF PREFORMED AND *DE NOVO* MEDIATORS

The MC response to invading pathogens includes the release of mediators that regulate vascular flow, permeability, and cell chemotaxis. MCs can upregulate adhesion molecules on vascular endothelium, facilitating cellular recruitment from circulation into infection sites. MC-derived TNF recruits neutrophils to sites of bacterial infection (33). MC-derived eotaxin (CCL11) or IL-8 recruits eosinophils or cytotoxic cells after parasitic or viral infection, respectively (34). Eicosanoid pathways are also activated by pathogens. Leukotrienes and prostaglandins contribute to permeability, neutrophil chemotaxis and mucus production (14).

In addition, MCs can clear pathogens by releasing compounds with bactericidal activity, such as cathelicidins or β-defensins (35). Cathelicidins are host antimicrobial peptides that can be constitutively produced or induced by TLR2 signals in MCs; these peptides act in two ways: by killing pathogens and inducing MCs to migrate to the infection site (36).

MICROBE UPTAKE AND INTRACELLULAR AND EXTRACELLULAR KILLING

The precise role of the phagocytic capability of MCs in the host defense against bacteria remains under debate. Available evidence suggest that this role probably has a minor impact compared with the bacterial killing mediated by professional phagocytes. Recently, a review updated the knowledge about MCs phagocytic capabilities of (37). These authors compiled evidences to support the notion that several MCs membrane receptors bind free and/or opsonized pathogens. We believe that such capabilities highlight the enormous MCs versatility in controlling infectious disease during the early innate immune responses.

MCs have several mechanisms available to kill microbes they come in contact with. One of these mechanisms results from the recognition of opsonized microbes by the complement or IgG receptors. Following their binding, pathogens are internalized *via* a route involving the endosome-lysosome pathway, similar to that of phagocytes (19). However, microbe uptake can proceed without cytosolic degradation, leading to the formation of pathogen reservoirs. For most pathogens, these reservoirs have adverse effects on the host (19, 31), but other pathogens undergo intracellular degradation within MCs.

The other mechanism MCs use to kill microbes is Mast Extracellular Traps (MECT). These are antimicrobial structures that support extracellular killing of bacteria that have not been efficiently phagocytized. MECTs act through a combination of

direct killing of entrapped pathogens and/or physical retention so that phagocytic cells recruited to the infection site can then eliminate the pathogen (38). These structures were first described in other cell types, including neutrophils (39).

This antimicrobial strategy implies a disruption of the nuclear membrane and a release of nuclear and granular components, which cause cell death. Some studies suggest that this process is an active and regulated event where the presence of microbes induces MECT, and the production of reactive oxygen species (ROS) leads to cell death (40).

The major components of MECTs are DNA, histones, granule proteins, such as tryptase, and antimicrobial peptides. The role of MECTs still requires further investigation; however, a possible explanation of its physiological relevance in MCs can be derived from the fact that this action is restricted to the same physical space that demonstrates MC activity. The antimicrobial action is observed locally, avoiding uncontrolled MC activation and the undesirable spread of proinflammatory mediators after an overwhelming infection to the tissue, which could lead to vascular leakage and further enhance inflammation and tissue damage (20).

MCs IN LUNG DISEASES

MC activity is involved in the maintenance of healthy lungs, contributing to defense against several respiratory pathogens, including *Mycobacterium tuberculosis, Staphylococcus aureus, Francisella tularensis, Streptococcus pyogenes, Klebsiella pneumoniae, Listeria monocytogenes, Pseudomona aeruginosa*, and *Streptococcus pneumoniae* (41). However, inappropriate or chronic activation of MCs by IL-9 may lead to pathologic inflammation and remodeling of tissue structures, including fibrosis during uncontrolled infections (42). There is strong evidence of MC number increase and activation in lung diseases, such as atopic and nonatopic asthma (43), while changes in the phenotypes of the MCs present in the airway (44) have been observed for pulmonary fibrosis (45) and pulmonary hypertension, which is characterized by increased pulmonary vascular resistance and remodeling (46). Mast cell activation may also play a role in acute respiratory distress syndrome (ARDS) (47) and chronic obstructive pulmonary disease (COPD) (48). Associations between MC infiltration and lung cancer prognosis give contradictory results; the differential contributions of MCs to tumor angiogenesis and tumor cytotoxicity according to the microenvironment may explain the lack of consistent conclusions (49).

SARS-CoV-2 infection in mice model have revealed the effects MCs humoral mediators. The histamine from MCs granules increases the expression of cytokines, such as IL-6, and chemokines, such as IL-8; which favor the hyperinflammatory state observed at severe stages of viral infection. The cytokines and chemokines also degrade the extracellular matrix and the hyaline membrane of the intra-alveolar space, which can lead to thrombosis (50). On the other hand, the lungs of COVID-19 patients show a diffuse alveolar damage (DAD) with suppression of MCs proliferation (51). A plausible explanation is that the high interferon levels in the early phase of COVID-19 might cause this suppression observed in DAD (51). DAD is also observed in lungs of patients ADRS, acute hypersensitivity pneumonitis, idiopathic acute interstitial pneumonia, drug abuse, toxic inhalants, ingestants, connective tissue disease, viral and bacterial infections including some acute forms of tuberculosis (52, 53). In addition, the levels of serum anti-SARS-CoV-2–spike S1 protein-specific IgE (SP-IgE) and anti-SARS-CoV-2 nucleocapsid protein-specific IgE (NP-IgE) appear to be significantly higher in patients suffering severe COVID-19; and SP-IgE levels correlated with the total lung severity scores and the ratio of arterial oxygen partial pressure to fractional inspired oxygen (PaO_2/FiO_2) (54). Post-acute sequalae COVID-19 patients report significantly higher expression in serum of IL-6 and CXCL1; whereas no difference was observed on serum levels of IL-8, TNF, CCL2, CCL3, IL-17A, IL-33, and VEGF (55). Taken all together these initial evidences warrant separate review to accurately compile the natural history of MCs during SARS-CoV-2 infection, disease and resolution.

TUBERCULOSIS

Members of the *Mycobacterium tuberculosis* complex, which include *MTB*, *M. caprae, M. microti, M. pinnipedii*, *M. africanum*, and *M. canettii* (the latter two are responsible for a small number of cases in Africa), are responsible for TB. The first three species mainly affect humans, while *M. bovis*, which is also part of the *MTB* complex group, is involved primarily in cattle infections. Mycobacteria other than tuberculosis (MOTT) can cause pulmonary TB in humans. These are also known as non-tuberculous mycobacteria (NTM) and affect mainly immunocompromised patients as well as the elderly.

The first contact between the bacilli and the patient occurs when the patient inhales microdroplets containing the bacilli, which constitutes the pulmonary transmission of TB. After this primary contact, the infection can go unnoticed for several weeks, and at this point, there are three possible outcomes. First, the infection may be controlled by the human immune cells; second, the bacilli can remain in a latent state and third, the patient may present with symptoms. Once the infection is established, granulomas, which are aggregates of infected macrophages surrounded by different immune cells, begin to form (56).

The initial MTB infection is asymptomatic. Despite symptoms initiation is variable, after approximately 4 to 6 weeks, the patient starts to present hypersensitivity to tuberculin (57). Symptoms that a patient with pulmonary TB may present include cough, fever, night sweats, weight loss, and hemoptysis.

MTB can establish either an acute infection of the lung tissue or a chronic infection where it remains inside the immune system cells. The bacteria can reside inside alveolar macrophages after entering through a phagocytotic process with the help of the complement fraction (8). However, there are other cells involved in recognizing MTB after it enters the body, as well as modulating the immune response. For example, previous studies have

demonstrated that in addition to residing in macrophages, MTB infects different cell types in the lungs, including dendritic cells and neutrophils; moreover, the dominant infected cell population varies at the different stages of infection (58, 59). Pahari et al. reviewed MTB interactions using a mononuclear phagocyte system and highlighted the mechanisms involved in reversing the immune suppression induced by MTB infection (60).

TB is diagnosed by isolating and identifying MTB on sputum samples from ill patients. This can be completed by observing the bacilli under a microscope, culturing the bacilli, or by PCR (61). Other laboratory tests can also be performed, such as the tuberculin test (TST) and the Interferon Gamma test (IGRA).

For example, the TST is not completely specific, because patients that have been vaccinated with the Bacillus Calmette Guerin (BCG) vaccine will show a positive result (62). On the other hand, the IGRA tests have yielded high rates of conversions between positive and negative latent tuberculosis infection (LTBI), mainly due to the cutoff values (63). Although these tests are highly accepted, they are not foolproof and represent a challenge when trying to correctly diagnose patients. For these reasons, it is important to evaluate other methods for diagnosing patients with TB, especially patients with LTBI.

MCs AND TUBERCULOSIS

The first evidence of MCs' role in TB came from various studies performed over previous decades. First, Ratnam et al. studied rodent lungs after MTB infection and reported the presence of "cells containing many electron-dense intracytoplasmic granules" which were determined to be from MCs (64, 65). Later, Muñoz et al. demonstrated that MTB could activate MCs *in vitro*, resulting in MCs degranulation and production of the inflammatory cytokines TNFα and IL-6 (66). *In vivo* experimentation showed an increase in MCs after MTB infection in rodent lungs (65). Also, MC-derived TNFα may play a role in the early steps of infection since it is stored in granules and can be immediately released after infection. TNFα has an initial impact in neutrophil recruitment and leads to the differentiation of circulant monocytes to macrophages in addition to playing an important role in granuloma maintenance. An experimental animal TB model that excluded TNFα showed an increase in IL-6 production (67).

Muñoz and colleagues showed CD48 recognizes and mediates MTB uptake into MCs (66). The same authors found that MTB can also enter the MCs through lipid rafts (68). TLR2 has also been proposed to play a role in MCs after MTB infection. Transfer of $TLR2^{+/+}$ MCs into $TLR^{-/-}$MTB-infected mice showed diminished lung bacterial growth and an increase in proinflammatory cytokine release that contributes to granuloma maintenance (69). More recently, a study by Naqvi et al. demonstrated a massive increase in MC numbers in the infected lung of BCG infected animals (70). They also showed that *in vitro* co-culture of BCG and rodent Rat Basophilic Leukaemia (RBL-2H3) MCs led to significant killing of BCG, phagocytosis of BCG, take up BCG-derived antigens by macropinocytosis, generation of Reactive Oxygen Species (ROS) and degranulation. All together these evidences suggest that MCs play a significant protective role during tuberculosis infection and disease.

MC-mediated innate immunity usually promotes timely resolution of acute infection; however, paradoxically, this same response can also promote chronic infections and exacerbate pathologies. In the TB context, MTB uptake through raft membrane domains might also allow the bacteria to bypass the lysosome degradation route, thereby resulting in intracellular MTB survival (68). During lung mycobacterial infection, MCs are involved in the development of granulomas, which may also protect bacteria from total clearance (71). On the other hand, MTB can use additional strategies to evade the immune response; for example, MTB can produce catalase, which degrades hydrogen peroxide, thereby preventing the release of mast cells' extracellular traps (MCETS) (72).

Experiments using recombinant MTB antigens provide further insights into the MC response triggered by MTB. These antigens are present in a group of proteins actively produced by MTB during its growth. The recombinant MTB antigens MTSA-10, MPT-63, and ESAT-6 were found to induce the release of inflammatory mediators (66). MCs also respond specifically to MTB lipids increasing calcium influx and degranulation (73). In contrast, such immune response have been tested as therapeutic strategy for chronic diseases such as chronic spontaneous urticaria (CSU) (74). Yan and colleagues demonstrated that the use of BCG polysaccharide nucleic acid (BCG-PSN) significantly reduced the recovery time of patients suffering CSU (74). They supported this finding by showing *in-vitro* data that revealed BCG-PSN also inhibited the hexosaminidase release rates in IgE-sensitized RBL-2H3 cells. Taken all together, the modulating role of Mycobacteria promises a novel therapeutic strategy for targeting chronic autoimmune diseases. Molecular mechanisms of MCs and MTB interaction now warrant a multidisciplinary effort to generate new fundamental basis that depict the MC´s microbial intake (**Figure 1**).

The precise lipids involved and the exact MC receptors that are triggered remain unknown. Determining this is further complicated by the fact that MTB's lipid composition varies throughout the infection process. There is a lipid profile that dampens or enhances immune responses resulting in bacterial persistence or clearance (75). This differential expression may be key in determining the clinical fate of infection. It would be key to assess MCs activation mechanisms in those scenarios. A better understanding of lipid interactions with MCs could lead to the development of immunomodulators distinct from the traditional protein antigen-based vaccines. Moreover, it would be useful to determine if MCs play a role in the establishment and perpetuation of the granuloma, as well as identify a molecule that can be used as a biomarker to classify patients in the different stages of infection.

There are also clinical evidences that support the role of MC´s in the MTB clearance during TB. An earlier study investigated the MC density on tissue sections of 45 people suffering tuberculous lymphadenitis. They found lymph node to have a significant increase of MC´s with greater granuloma involvement and multinucleated giant cell formation (76). In contrast, during

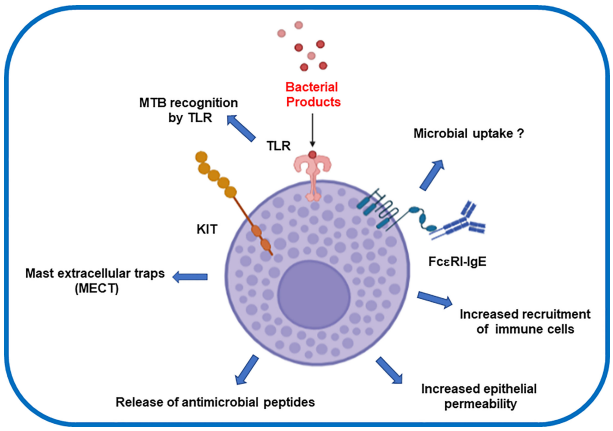


FIGURE 1 | Effector inflammatory response after mast cells interaction with *Mycobacterium tuberculosis*.

tuberculous pleurisy, there is no significant increase in MC´s when compared to individuals with nonspecific pleuritis (77). When studying more severe pulmonary TB among patients admitted to the intensive care units, it was observed that these patients have an increased MCs in lung tissue (78). In fact, a recent study analyzed fibrotic tissue from post-mortem lung tissue microarrays from individuals with pulmonary TB and healthy control subjects (79). They demonstrated that MCs were localized at pneumonic areas, in the granuloma periphery and particularly abundant. Similarly, non-tuberculosis mycobacteria trigger MCs response. Emerging evidences show MCs within leprosy lesions, including collagen increase and tryptase-rich mast cell density (80, 81). Taken all together, these early clinical evidences support the notion of MCs playing a role during MTB infection and disease.

CONCLUSION

The role of MCs in infectious processes, including TB infection, supports their potential use as biomarkers to predict disease severity. MCs should also be considered a therapeutic target for treating patients that do not respond as expected to anti-TB therapies. These therapies usually result in the modulation of immune cell populations, including mast cells. Without this modulation, the mycobacteria evade the immune response through the decomposition of hydrogen peroxide, which is an essential trigger for MCET induction. There is emerging *in vivo* and clinical evidences that highlight some other roles of MCs during TB. Further studies are warranted to fully characterize the complete MCs contribution not only during disease, but also during latent TB infection stage as well as clearance after anti-TB therapy.

AUTHOR CONTRIBUTIONS

Conceptualization: AG and IT-A; Investigation: AG, AC, MM, and IT-A; Resources: AG and MM; Writing – original draft preparation: AG, AC, MM, and IT-A; Writing – review and editing: AG, MM, and IT-A; Funding acquisition: AG, MM and IT-A. All authors contributed to the article and approved the submitted version.

FUNDING

This research was partially funded by the National Secretariat of Science and Technology of Panama (SENACYT) through the Sistema Nacional de Investigadores. AG is funded by the Sistema Nacional de Investigadores SNI de Panamá de la Secretaría Nacional de Ciencia, Tecnología e Innovación (SENACYT), grant No. 22-2020. IT-A is funded by Vicerrectoría de Investigación y Postgrada, Universidad de Panamá.

ACKNOWLEDGMENTS

The authors thank Maria Joao Amorim and Colleen Goodridge for their critical review of the manuscript. Figures were done using https://app.biorender.com/biorender-templates.

REFERENCES

1. WHO. *Global Tuberculosis Report*. Geneve, Switzerland: W.H. Organization (2021).
2. Keshavjee S, Amanullah F, Cattamanchi A, Chaisson R, Dobos KM, Fox GJ, et al. Moving Toward Tuberculosis Elimination. Critical Issues for Research in Diagnostics and Therapeutics for Tuberculosis Infection. *Am J Respir Crit Care Med* (2019) 199(5):564–71. doi: 10.1164/rccm.201806-1053PP
3. Crisan-Dabija R, Grigorescu C, Pavel CA, Artene B, Popa IV, Cernomaz A, et al. Tuberculosis and COVID-19: Lessons From the Past Viral Outbreaks and Possible Future Outcomes. *Can Respir J* (2020) p:1401053. doi: 10.1155/2020/1401053

4. Afrin LB, Weinstock LB, Molderings GJ. Covid-19 Hyperinflammation and Post-Covid-19 Illness may be Rooted in Mast Cell Activation Syndrome. *Int J Infect Dis* (2020) 100:327–32. doi: 10.1016/j.ijid.2020.09.016
5. Rivas N, Espinoza M, Loban A, Luque O, Jurado J, Henry-Hurtado N, et al. Case Report: COVID-19 Recovery From Triple Infection With Mycobacterium Tuberculosis, HIV, and SARS-CoV-2. *Am J Trop Med Hyg* (2020) 103(4):1597–9. doi: 10.4269/ajtmh.20-0756
6. Piliponsky AM, Acharya M, Shubin NJ. Mast Cells in Viral, Bacterial, and Fungal Infection Immunity. *Int J Mol Sci* (2019) 20(12):1–15. doi: 10.3390/ijms20122851
7. Garcia-Rodriguez KM, Goenka A, Alonso-Rasgado MT, Hernandez-Pando R, Bulfone-Paus S. The Role of Mast Cells in Tuberculosis: Orchestrating Innate Immune Crosstalk? *Front Immunol* (2017) 8:1290. doi: 10.3389/fimmu.2017.01290
8. Scriba TJ, Carpenter C, Pro SC, Sidney J, Musvosvi M, Rozot V, et al. Differential Recognition of Mycobacterium Tuberculosis-Specific Epitopes as a Function of Tuberculosis Disease History. *Am J Respir Crit Care Med* (2017) 196(6):772–81. doi: 10.1164/rccm.201706-1208OC
9. Bozzano F, Marras F, De Maria A. Immunology of Tuberculosis. *Mediterr J Hematol Infect Dis* (2014) 6(1):e2014027. doi: 10.4084/mjhid.2014.027
10. Paivandy A, Pejler G. Novel Strategies to Target Mast Cells in Disease. *J Innate Immun* (2021) 13(3):131–47. doi: 10.1159/000513582
11. Thangam EB, Jemima EA, Singh H, Baig MS, Khan M, Mathias CB, et al. The Role of Histamine and Histamine Receptors in Mast Cell-Mediated Allergy and Inflammation: The Hunt for New Therapeutic Targets. *Front Immunol* (2018) 9:1873. doi: 10.3389/fimmu.2018.01873
12. Mendez-Enriquez E, Hallgren J. Mast Cells and Their Progenitors in Allergic Asthma. *Front Immunol* (2019) 10:821. doi: 10.3389/fimmu.2019.00821
13. Komi DEA, Khomtchouk K, Santa Maria PL. A Review of the Contribution of Mast Cells in Wound Healing: Involved Molecular and Cellular Mechanisms. *Clin Rev Allergy Immunol* (2020) 58(3):298–312. doi: 10.1007/s12016-019-08729-w
14. Abraham SN, St John AL. Mast Cell-Orchestrated Immunity to Pathogens. *Nat Rev Immunol* (2010) 10(6):440–52. doi: 10.1038/nri2782
15. Simons FE, Simons KJ. Histamine and H1-Antihistamines: Celebrating a Century of Progress. *J Allergy Clin Immunol* (2011) 128(6):1139–50:e4. doi: 10.1016/j.jaci.2011.09.005
16. Dawicki W, Marshall JS. New and Emerging Roles for Mast Cells in Host Defence. *Curr Opin Immunol* (2007) 19(1):31–8. doi: 10.1016/j.coi.2006.11.006
17. Wernersson S, Pejler G. Mast Cell Secretory Granules: Armed for Battle. *Nat Rev Immunol* (2014) 14(7):478–94. doi: 10.1038/nri3690
18. Gurish MF, Austen KF. Developmental Origin and Functional Specialization of Mast Cell Subsets. *Immunity* (2012) 37(1):25–33. doi: 10.1016/j.immuni.2012.07.003
19. Feger F, Varadaradjalou S, Gao Z, Abraham SN, Arock M. The Role of Mast Cells in Host Defense and Their Subversion by Bacterial Pathogens. *Trends Immunol* (2002) 23(3):151–8. doi: 10.1016/S1471-4906(01)02156-1
20. Mollerherm H, von Kockritz-Blickwede M, Branitzki-Heinemann K. Antimicrobial Activity of Mast Cells: Role and Relevance of Extracellular DNA Traps. *Front Immunol* (2016) 7:265. doi: 10.3389/fimmu.2016.00265
21. St John AL, Abraham SN. Innate Immunity and its Regulation by Mast Cells. *J Immunol* (2013) 190(9):4458–63. doi: 10.4049/jimmunol.1203420
22. Al-Afif A, Alyazidi R, Oldford SA, Huang YY, King CA, Marr N, et al. Respiratory Syncytial Virus Infection of Primary Human Mast Cells Induces the Selective Production of Type I Interferons, CXCL10, and CCL4. *J Allergy Clin Immunol* (2015) 136(5):1346–54 e1. doi: 10.1016/j.jaci.2015.01.042
23. Kawai T, Akira S. The Role of Pattern-Recognition Receptors in Innate Immunity: Update on Toll-Like Receptors. *Nat Immunol* (2010) 11(5):373–84. doi: 10.1038/ni.1863
24. Kulka M, Alexopoulou L, Flavell RA, Metcalfe DD. Activation of Mast Cells by Double-Stranded RNA: Evidence for Activation Through Toll-Like Receptor 3. *J Allergy Clin Immunol* (2004) 114(1):174–82. doi: 10.1016/j.jaci.2004.03.049
25. McCurdy JD, Olynych TJ, Maher LH, Marshall JS. Cutting Edge: Distinct Toll-Like Receptor 2 Activators Selectively Induce Different Classes of Mediator Production From Human Mast Cells. *J Immunol* (2003) 170(4):1625–9. doi: 10.4049/jimmunol.170.4.1625
26. Tancowny BP, Karpov V, Schleimer RP, Kulka M. Substance P Primes Lipoteichoic Acid- and Pam3CysSerLys4-Mediated Activation of Human Mast Cells by Up-Regulating Toll-Like Receptor 2. *Immunology* (2010) 131(2):220–30. doi: 10.1111/j.1365-2567.2010.03296.x
27. Supajatura V, Ushio H, Nakao A, Akira S, Okumura K, Ra C, et al. Differential Responses of Mast Cell Toll-Like Receptors 2 and 4 in Allergy and Innate Immunity. *J Clin Invest* (2002) 109(10):1351–9. doi: 10.1172/JCI0214704
28. Tang X, Hu F, Xia X, Zhang H, Zhou F, Huang Y, et al. Mannose-Capped Lipoarabinomannan (ManLAM) Binding TLR2 Activates Mast Cells to Release Exosomes and Induces M2 Polarization of Macrophages. *Xi Bao Yu Fen Zi Mian Yi Xue Za Zhi* (2021) 37(6):481–6.
29. Aoki R, Kawamura T, Goshima F, Ogawa Y, Nakae S, Moriishi K, et al. The Alarmin IL-33 Derived From HSV-2-Infected Keratinocytes Triggers Mast Cell-Mediated Antiviral Innate Immunity. *J Invest Dermatol* (2016) 136(6):1290–2. doi: 10.1016/j.jid.2016.01.030
30. Saluja R, Delin I, Nilsson GP, Adner M. FcepsilonR1-Mediated Mast Cell Reactivity is Amplified Through Prolonged Toll-Like Receptor-Ligand Treatment. *PloS One* (2012) 7(8):e43547. doi: 10.1371/journal.pone.0043547
31. Shin JS, Abraham SN. Glycosylphosphatidylinositol-Anchored Receptor-Mediated Bacterial Endocytosis. *FEMS Microbiol Lett* (2001) 197(2):131–8. doi: 10.1111/j.1574-6968.2001.tb10594.x
32. Marshall JS, Jawdat DM. Mast Cells in Innate Immunity. *J Allergy Clin Immunol* (2004) 114(1):21–7. doi: 10.1016/j.jaci.2004.04.045
33. Malaviya R, Ikeda T, Ross E, Abraham SN. Mast Cell Modulation of Neutrophil Influx and Bacterial Clearance at Sites of Infection Through TNF-Alpha. *Nature* (1996) 381(6577):77–80. doi: 10.1038/381077a0
34. Shin K, Watts GF, Oettgen HC, Friend DS, Pemberton AD, Gurish MF, et al. Mouse Mast Cell Tryptase mMCP-6 is a Critical Link Between Adaptive and Innate Immunity in the Chronic Phase of Trichinella Spiralis Infection. *J Immunol* (2008) 180(7):4885–91. doi: 10.4049/jimmunol.180.7.4885
35. Yang D, Chertov O, Oppenheim JJ. Participation of Mammalian Defensins and Cathelicidins in Anti-Microbial Immunity: Receptors and Activities of Human Defensins and Cathelicidin (LL-37). *J Leukoc Biol* (2001) 69(5):691–7. doi: 10.1189/jlb.69.5.691
36. Wang Z, MacLeod DT, Di Nardo A. Commensal Bacteria Lipoteichoic Acid Increases Skin Mast Cell Antimicrobial Activity Against Vaccinia Viruses. *J Immunol* (2012) 189(4):1551–8. doi: 10.4049/jimmunol.1200471
37. Jimenez M, Cervantes-Garcia D, Cordova-Davalos LE, Perez-Rodriguez MJ, Gonzalez-Espinosa C, Salinas E. Responses of Mast Cells to Pathogens: Beneficial and Detrimental Roles. *Front Immunol* (2021) 12:685865. doi: 10.3389/fimmu.2021.685865
38. Elieh Ali Komi D, Kuebler WM. Significance of Mast Cell Formed Extracellular Traps in Microbial Defense. *Clin Rev Allergy Immunol* (2022) 62(1):160–79. doi: 10.1007/s12016-021-08861-6
39. Brinkmann V, Reichard U, Goosmann C, Fauler B, Uhlemann Y, Weiss DS, et al. Neutrophil Extracellular Traps Kill Bacteria. *Science* (2004) 303(5663):1532–5. doi: 10.1126/science.1092385
40. von Kockritz-Blickwede M, Goldmann O, Thulin P, Heinemann K, Norrby-Teglund A, Rohde M, et al. Phagocytosis-Independent Antimicrobial Activity of Mast Cells by Means of Extracellular Trap Formation. *Blood* (2008) 111(6):3070–80. doi: 10.1182/blood-2007-07-104018
41. Trivedi NH, Guentzel MN, Rodriguez AR, Yu JJ, Forsthuber TG, Arulanandam BP. Mast Cells: Multitalented Facilitators of Protection Against Bacterial Pathogens. *Expert Rev Clin Immunol* (2013) 9(2):129–38. doi: 10.1586/eci.12.95
42. Kearley J, Erjefalt JS, Andersson C, Benjamin E, Jones CP, Robichaud A, et al. IL-9 Governs Allergen-Induced Mast Cell Numbers in the Lung and Chronic Remodeling of the Airways. *Am J Respir Crit Care Med* (2011) 183(7):865–75. doi: 10.1164/rccm.200909-1462OC
43. Bradding P, Arthur G. Mast Cells in Asthma–State of the Art. *Clin Exp Allergy* (2016) 46(2):194–263. doi: 10.1111/cea.12675
44. Pejler G. The Emerging Role of Mast Cell Proteases in Asthma. *Eur Respir J* (2019) 54(4):1–17. doi: 10.1183/13993003.00685-2019
45. Pesci A, Bertorelli G, Gabrielli M, Olivieri D. Mast Cells in Fibrotic Lung Disorders. *Chest* (1993) 103(4):989–96. doi: 10.1378/chest.103.4.989
46. Hoffmann J, Yin J, Kukucka M, Yin N, Saarikko I, Sterner-Kock A, et al. Mast Cells Promote Lung Vascular Remodelling in Pulmonary Hypertension. *Eur Respir J* (2011) 37(6):1400–10. doi: 10.1183/09031936.00043310

47. Liebler JM, Qu Z, Buckner B, Powers MR, Rosenbaum JT. Fibroproliferation and Mast Cells in the Acute Respiratory Distress Syndrome. *Thorax* (1998) 53 (10):823–9. doi: 10.1136/thx.53.10.823
48. Ballarin A, Bazzan E, Zenteno RH, Turato G, Baraldo S, Zanovello D, et al. Mast Cell Infiltration Discriminates Between Histopathological Phenotypes of Chronic Obstructive Pulmonary Disease. *Am J Respir Crit Care Med* (2012) 186(3):233–9. doi: 10.1164/rccm.201112-2142OC
49. Theoharides TC, Donelan JM, Papadopoulou N, Cao J, Kempuraj D, Conti P. Mast Cells as Targets of Corticotropin-Releasing Factor and Related Peptides. *Trends Pharmacol Sci* (2004) 25(11):563–8. doi: 10.1016/j.tips.2004.09.007
50. Murdaca G, Di Gioacchino M, Greco M, Borro M, Paladin F, Petrarca C, et al. Basophils and Mast Cells in COVID-19 Pathogenesis. *Cells* (2021) 10(10):1–13. doi: 10.3390/cells10102754
51. Schaller T, Markl B, Claus R, Sholl L, Hornick JL, Giannetti MP, et al. Mast Cells in Lung Damage of COVID-19 Autopsies: A Descriptive Study. *Allergy* (2022) 77(3). doi: 10.1111/all.15293
52. Cardinal-Fernandez P, Bajwa EK, Dominguez-Calvo A, Menendez JM, Papazian L, Thompson BT. The Presence of Diffuse Alveolar Damage on Open Lung Biopsy Is Associated With Mortality in Patients With Acute Respiratory Distress Syndrome: A Systematic Review and Meta-Analysis. *Chest* (2016) 149(5):1155–64. doi: 10.1016/j.chest.2016.02.635
53. Rios F, Iscar T, Cardinal-Fernandez P. What Every Intensivist Should Know About Acute Respiratory Distress Syndrome and Diffuse Alveolar Damage. *Rev Bras Ter Intensiva* (2017) 29(3):354–63. doi: 10.5935/0103-507X.20170044
54. Tan C, Zheng X, Sun F, He J, Shi H, Chen M, et al. Hypersensitivity may be Involved in Severe COVID-19. *Clin Exp Allergy* (2022) 52(2):324–33. doi: 10.1111/cea.14023
55. Wechsler JB, Butuci M, Wong A, Kamboj AP, Youngblood BA. Mast Cell Activation is Associated With Post-Acute COVID-19 Syndrome. *Allergy* (2022) 77(4):1288–91. doi: 10.1111/all.15188
56. Dheda K, Schwander SK, Zhu B, van Zyl-Smit RN, Zhang Y. The Immunology of Tuberculosis: From Bench to Bedside. *Respirology* (2010) 15(3):433–50. doi: 10.1111/j.1440-1843.2010.01739.x
57. Lyon SM, Rossman MD. Pulmonary Tuberculosis. *Microbiol Spectr* (2017) 5 (1):1–10. doi: 10.1128/9781555819866.ch16
58. Bussi C, Gutierrez MG. Mycobacterium Tuberculosis Infection of Host Cells in Space and Time. *FEMS Microbiol Rev* (2019) 43(4):341–61. doi: 10.1093/femsre/fuz006
59. Ganbat D, Seehase S, Richter E, Vollmer E, Reiling N, Fellenberg K, et al. Mycobacteria Infect Different Cell Types in the Human Lung and Cause Species Dependent Cellular Changes in Infected Cells. *BMC Pulm Med* (2016) 16:19. doi: 10.1186/s12890-016-0185-5
60. Pahari S, Kaur G, Negi S, Aqdas M, Das DK, Bashir H, et al. Reinforcing the Functionality of Mononuclear Phagocyte System to Control Tuberculosis. *Front Immunol* (2018) 9:193. doi: 10.3389/fimmu.2018.00193
61. Heemskerk D, Caws M, Marais B, Farrar J. Tuberculosis in Adults and Children. In: *Tuberculosis in Adults and Children*. London, UK: Springer (2015). doi: 10.1007/978-3-319-19132-4
62. van Leth F, van Crevel R, Brouwer M. Latent Tuberculosis Infection as a Target for Tuberculosis Control. *Future Microbiol* (2015) 10(6):905–8. doi: 10.2217/fmb.15.30
63. Monarrez-Espino J, Enciso-Moreno JA, Laflamme L, Serrano CJ. Serial QuantiFERON-TB Gold In-Tube Assay and Tuberculin Skin Test to Diagnose Latent Tuberculosis in Household Mexican Contacts: Conversion and Reversion Rates and Associated Factors Using Conventional and Borderline Zone Definitions. *Mem Inst Oswaldo Cruz* (2014) 109(7):863–70. doi: 10.1590/0074-0276140085
64. Ratnam S, Ratnam S, Puri BK, Chandrasekhar S. Mast Cell Response During the Early Phase of Tuberculosis: An Electron-Microscopic Study. *Can J Microbiol* (1977) 23(9):1245–51. doi: 10.1139/m77-186
65. Carlos D, de Souza Junior DA, de Paula L, Jamur MC, Oliver C, Ramos SG, et al. Mast Cells Modulate Pulmonary Acute Inflammation and Host Defense in a Murine Model of Tuberculosis. *J Infect Dis* (2007) 196(9):1361–8. doi: 10.1086/521830
66. Munoz S, Hernandez-Pando R, Abraham SN, Enciso JA. Mast Cell Activation by Mycobacterium Tuberculosis: Mediator Release and Role of CD48. *J Immunol* (2003) 170(11):5590–6. doi: 10.4049/jimmunol.170.11.5590
67. Champsi J, Young LS, Bermudez LE. Production of TNF-Alpha, IL-6 and TGF-Beta, and Expression of Receptors for TNF-Alpha and IL-6, During Murine Mycobacterium Avium Infection. *Immunology* (1995) 84(4):549–54.
68. Munoz S, Rivas-Santiago B, Enciso JA. Mycobacterium Tuberculosis Entry Into Mast Cells Through Cholesterol-Rich Membrane Microdomains. *Scand J Immunol* (2009) 70(3):256–63. doi: 10.1111/j.1365-3083.2009.02295.x
69. Carlos D, Frantz FG, Souza-Junior DA, Jamur MC, Oliver C, Ramos SG, et al. TLR2-Dependent Mast Cell Activation Contributes to the Control of Mycobacterium Tuberculosis Infection. *Microbes Infect* (2009) 11(8-9):770–8. doi: 10.1016/j.micinf.2009.04.025
70. Naqvi N, Srivastava R, Naskar P, Puri N. Mast Cells Modulate Early Responses to Mycobacterium Bovis Bacillus Calmette-Guerin by Phagocytosis and Formation of Extracellular Traps. *Cell Immunol* (2021) 365:104380. doi: 10.1016/j.cellimm.2021.104380
71. Gengenbacher M, Kaufmann SH. Mycobacterium Tuberculosis: Success Through Dormancy. *FEMS Microbiol Rev* (2012) 36(3):514–32. doi: 10.1111/j.1574-6976.2012.00331.x
72. Campillo-Navarro M, Leyva-Paredes K, Donis-Maturano L, Rodriguez-Lopez GM, Soria-Castro R, Garcia-Perez BE, et al. Mycobacterium Tuberculosis Catalase Inhibits the Formation of Mast Cell Extracellular Traps. *Front Immunol* (2018) 9:1161. doi: 10.3389/fimmu.2018.01161
73. Torres-Atencio I, Rosero S, Ordonez C, Ruiz M, Goodridge A. Mycobacterial Lipids Induce Calcium Mobilization and Degranulation of Mast Cells. *Am J Respir Crit Care Med* (2018) 198(6):813–6. doi: 10.1164/rccm.201803-0436LE
74. Yan S, Liu R, Mao M, Liu Z, Zhang W, Zhang Y, et al. Therapeutic Effect of Bacillus Calmette-Guerin Polysaccharide Nucleic Acid on Mast Cell at the Transcriptional Level. *PeerJ* (2019) 7:e7404. doi: 10.7717/peerj.7404
75. Queiroz A, Riley LW. Bacterial Immunostat: Mycobacterium Tuberculosis Lipids and Their Role in the Host Immune Response. *Rev Soc Bras Med Trop* (2017) 50(1):9–18. doi: 10.1590/0037-8682-0230-2016
76. Taweevisit M, Poumsuk U. High Mast Cell Density Associated With Granulomatous Formation in Tuberculous Lymphadenitis. *Southeast Asian J Trop Med Public Health* (2007) 38(1):115–9.
77. Caramori G, Lasagna L, Casalini AG, Adcock IM, Casolari P, Contoli M, et al. Immune Response to Mycobacterium Tuberculosis Infection in the Parietal Pleura of Patients With Tuberculous Pleurisy. *PloS One* (2011) 6(7):e22637. doi: 10.1371/journal.pone.0022637
78. Liu QY, Han F, Pan LP, Jia HY, Li Q, Zhang ZD. Inflammation Responses in Patients With Pulmonary Tuberculosis in an Intensive Care Unit. *Exp Ther Med* (2018) 15(3):2719–26. doi: 10.3892/etm.2018.5775
79. Garcia-Rodriguez KM, Bini EI, Gamboa-Dominguez A, Espitia-Pinzon CI, Huerta-Yepez S, Bulfone-Paus S, et al. Differential Mast Cell Numbers and Characteristics in Human Tuberculosis Pulmonary Lesions. *Sci Rep* (2021) 11 (1):10687. doi: 10.1038/s41598-021-89659-6
80. Magalhaes Gde O, Valentim Vda C, Pereira MJ, Nery JA, Illarramendi X, Antunes SL. A Quantitative and Morphometric Study of Tryptase-Positive Mast Cells in Cutaneous Leprosy Lesions. *Acta Trop* (2008) 105(1):62–6. doi: 10.1016/j.actatropica.2007.10.001
81. Montagna NA, de Oliveira ML, Mandarim-de-Lacerda CA, Chimelli L. Leprosy: Contribution of Mast Cells to Epineurial Collagenization. *Clin Neuropathol* (2005) 24(6):284–90.

Conflict of Interest: The authors declare that the research was conducted in the absence of any commercial or financial relationships that could be construed as a potential conflict of interest.

The reviewer RMC declared a past co-authorship with the author MM to the handling editor.

Publisher's Note: All claims expressed in this article are solely those of the authors and do not necessarily represent those of their affiliated organizations, or those of the publisher, the editors and the reviewers. Any product that may be evaluated in this article, or claim that may be made by its manufacturer, is not guaranteed or endorsed by the publisher.

Copyright © 2022 Torres-Atencio, Campble, Goodridge and Martin. This is an open-access article distributed under the terms of the Creative Commons Attribution License (CC BY). The use, distribution or reproduction in other forums is permitted, provided the original author(s) and the copyright owner(s) are credited and that the original publication in this journal is cited, in accordance with accepted academic practice. No use, distribution or reproduction is permitted which does not comply with these terms.

frontiers | Frontiers in Immunology

REVIEW
published: 27 June 2022
doi: 10.3389/fimmu.2022.923265

Regulatory Roles of Phospholipase A_2 Enzymes and Bioactive Lipids in Mast Cell Biology

Yoshitaka Taketomi and Makoto Murakami *

Laboratory of Microenvironmental and Metabolic Health Sciences, Center for Disease Biology and Integrative Medicine, Graduate School of Medicine, The University of Tokyo, Bunkyo-ku, Japan

Lipids play fundamental roles in life as an essential component of cell membranes, as a major source of energy, as a body surface barrier, and as signaling molecules that transmit intracellular and intercellular signals. Lipid mediators, a group of bioactive lipids that mediates intercellular signals, are produced *via* specific biosynthetic enzymes and transmit signals *via* specific receptors. Mast cells, a tissue-resident immune cell population, produce several lipid mediators that contribute to exacerbation or amelioration of allergic responses and also non-allergic inflammation, host defense, cancer and fibrosis by controlling the functions of microenvironmental cells as well as mast cell themselves in paracrine and autocrine fashions. Additionally, several bioactive lipids produced by stromal cells regulate the differentiation, maturation and activation of neighboring mast cells. Many of the bioactive lipids are stored in membrane phospholipids as precursor forms and released spatiotemporally by phospholipase A_2 (PLA_2) enzymes. Through a series of studies employing gene targeting and lipidomics, several enzymes belonging to the PLA_2 superfamily have been demonstrated to participate in mast cell-related diseases by mobilizing unique bioactive lipids in multiple ways. In this review, we provide an overview of our current understanding of the regulatory roles of several PLA_2-driven lipid pathways in mast cell biology.

Keywords: phospholipid, phospholipase A_2, lipid mediator, mast cells, allergy, type 2 immunity

OPEN ACCESS

Edited by:
Frans J. Van Overveld, University College Roosevelt, Netherlands

Reviewed by:
Vineesh Vimala Raveendran, King Faisal Specialist Hospital & Research Centre, Saudi Arabia
Viktor Bugajev, Institute of Molecular Genetics (ASCR), Czechia

***Correspondence:**
Makoto Murakami
makmurak@m.u-tokyo.ac.jp

Specialty section:
This article was submitted to Inflammation, a section of the journal Frontiers in Immunology

Received: *19 April 2022*
Accepted: *30 May 2022*
Published: *27 June 2022*

Citation:
Taketomi Y and Murakami M (2022) Regulatory Roles of Phospholipase A_2 Enzymes and Bioactive Lipids in Mast Cell Biology. Front. Immunol. 13:923265. doi: 10.3389/fimmu.2022.923265

INTRODUCTION

Altered tissue sensitivity to environmental triggers contributes to the development of allergic inflammation, which is often associated with type 2 immunity (1, 2). Allergic diseases have become very common in hygienic countries, with a prevalence that has increased by 2–3-fold within the last two decades. Patients with anaphylaxis, food allergy, asthma, allergic rhinitis, and atopic eczema typically have elevated levels of serum IgE in association with activation of mast cells (3). Development of mast cells in extravascular tissues depends essentially on the stromal cytokine stem cell factor (SCF) and its receptor c-Kit, with various cytokines and adhesion molecules having accessory roles in tissue- or disease-specific contexts (4). Crosslinking of FcεRI, a high affinity IgE receptor on the surface of mast cells, with IgE and antigen (allergen), or exposure to several IgE-independent stimuli such as substance P, which is released from $TRPV1^+$ sensory neurons and acts

on the MRGPR family receptors on mast cells (5), triggers exocytosis of granule contents (*e.g.*, histamine and proteases) and production of various cytokines and chemokines, thereby promoting harmful allergic reactions and also participating in beneficial host defense against invading microorganisms or venom components (6). Mast cells also generate a variety of bioactive lipids called lipid mediators, which take part in fine-tuning of allergic responses by regulating the functions of various cell types. Furthermore, proper maturation and activation of mast cells are positively or negatively affected by various microenvironmental factors, including bioactive or structural lipids. For instance, the CD300 immunoreceptor family binds to structural lipids (*e.g.*, ceramides, sphingomyelin, phosphatidylserine (PS) and phosphatidylethanolamine (PE)) as functional ligands and negatively regulates FcεRI signaling to put a brake on excessive immediate allergic reactions (7, 8).

Lipid mediators, on which we put a specific focus in this article, are produced through specific biosynthetic pathways, are released extracellularly *via* diffusion, specific transporters or extracellular vesicles (EVs), act on specific receptors on target cells, and are rapidly degraded or inactivated within local tissue microenvironments. Individual lipid mediators display pleiotropic functions and can have both offensive and protective effects by acting on distinct receptor subtypes expressed on different cell types. Lipid mediators are categorized into several classes, including eicosanoids derived from ω6 arachidonic acid (AA), such as prostaglandins (PGs) and leukotrienes (LTs); specialized pro-resolving lipid mediators (SPMs) derived from ω3 eicosapentaenoic acid (EPA) or docosahexaenoic acid (DHA), such as resolvins, maresins and protectins; and lysophospholipid-derived mediators, such as lysophosphatidic acid (LPA) and platelet-activating factor (PAF) (9–12). Biosynthesis of these lipid mediators is initiated in many if not all cases by hydrolysis of membrane phospholipids by phospholipase A_2s (PLA_2s). The mammalian genome encodes more than 50 PLA_2-related enzymes, which are classified into several structurally related families, including the cytosolic PLA_2 ($cPLA_2$), Ca^{2+}-independent PLA_2 ($iPLA_2$), secreted PLA_2 ($sPLA_2$), PAF acetylhydrolase (PAF-AH), lysosomal PLA_2, PLA-acyltransferase (PLAAT), and α/β hydrolase (ABHD) families (13). The properties and functions of individual PLA_2s, as revealed by studies using knockout or transgenic mice for individual PLA_2s in combination with comprehensive lipidomics, have been summarized in current reviews (14, 15).

Importantly, genetic and pharmacological studies have provided evidence that several intracellular and extracellular PLA_2s uniquely regulate the maturation and functions of mast cells through driving distinct lipid pathways *in vivo* (16–23). These include (i) $cPLA_2\alpha$-driven generation of AA metabolites by activated mast cells for propagation or sequestration of allergic inflammation, (ii) PAF-AH2-driven constitutive generation of EPA/DHA metabolites for optimization of mast cell activation, (iii) $sPLA_2$-III-driven paracrine PGD_2 circuit for mast cell maturation, (iv) $sPLA_2$-IIA-driven modulation of gut microbiota that indirectly affects mast cells, and (v) miscellaneous PLA_2s whose roles in mast cells are controversial. In this article, we will make an overview of the roles of these PLA_2-driven lipid pathways in mast cell biology.

REGULATORY ROLES OF INTRACELLULAR PLA_2S IN MAST CELL BIOLOGY

Eicosanoid Generation by $cPLA_2\alpha$ in Activated Mast Cells

In general, PLA_2 acts as the most upstream enzyme in the biosynthetic pathways for various lipid mediators derived from membrane phospholipids (**Figure 1**). It is well established that group IVA $cPLA_2$ ($cPLA_2\alpha$ or PLA2G4A), the only PLA_2 subtype that shows a striking substrate specificity for AA-containing phospholipids, is essential for stimulus-coupled release of AA from phospholipids and thereby production of eicosanoids in many cell types including mast cells (24, 25). $cPLA_2\alpha$ has an *N*-terminal C2 domain, which allows translocation of the enzyme from the cytosol to perinuclear, ER and Golgi membranes in response to an increase in cytosolic Ca^{2+} following cell activation (24). In addition, $cPLA_2\alpha$ is phosphorylated by mitogen-activated protein kinases (MAPKs) and possibly other kinases, an event that is essential for full activation of $cPLA_2\alpha$ (25). Phosphatidylinositol-4,5-bisphosphate (PIP_2) and ceramide-1-phosphate (C1P) modulate the subcellular localization and activation of $cPLA_2\alpha$ (26, 27). These properties place $cPLA_2\alpha$ as a central regulator of the stimulus-coupled generation of eicosanoids, a class of AA-derived lipid mediators including PGs and LTs.

Activated mast cells produce LTB_4, LTC_4 and PGD_2 as major AA-derived eicosanoids. Following FcεRI-dependent or -independent activation of mast cells, the AA released by $cPLA_2\alpha$ from membrane phosphatidylcholine (PC) and phosphatidylethanolamine (PE) is converted by the sequential action of 5-lipoxygenase (LOX) and terminal LT synthases to LTs (the 5-LOX pathway), or by that of cyclooxygenases (COXs) and hematopoietic PGD synthase (H-PGDS) to PGD_2 (the COX pathway) (**Figure 2**), with preferential production of PGD_2 by connective-tissue mast cells (CTMCs) and LTC_4 by mucosal mast cells (MMCs) (28–30). After being exported from mast cells *via* the specific transporter MRP1, LTC_4 is converted to LTD_4 and then to LTE_4 by extracellular peptidases; therefore, these three LTs, which have a glutathione-derived cysteine in their structures, are often referred to as cysteinyl LTs (cysLTs) (31). Of the two COX isoforms COX-1 and -2, pre-existing COX-1 is mainly responsible for immediate PGD_2 generation that occurs within a few minutes, while inducible COX-2 is responsible for delayed PGD_2 generation that lasts for several hours (32, 33). IL-3-driven bone marrow-derived mast cells (BMMCs), a relatively immature mast cell population, produce LTC_4 in preference to PGD_2, thus resembling MMCs. Coculture of BMMCs with fibroblasts in the presence of SCF facilitates their maturation toward a CTMC-like phenotype, with an eicosanoid balance shift from LTs to PGD_2 that is accompanied by increased expression of $cPLA_2\alpha$, COX-2, H-PGDS and LTB_4 dehydrogenase (which inactivates LTB_4) and by decreased expression of LTA_4 hydrolase (LTA_4H; LTB_4 synthase) and LTC_4 synthase (LTC_4S) (34, 35).

Following FcεRI-dependent or -independent activation, BMMCs from $cPLA_2\alpha$-deficient (*Pla2g4a*$^{-/-}$) mice fail to produce LTs and PGD_2 as well as PAF, a lysophospholipid-

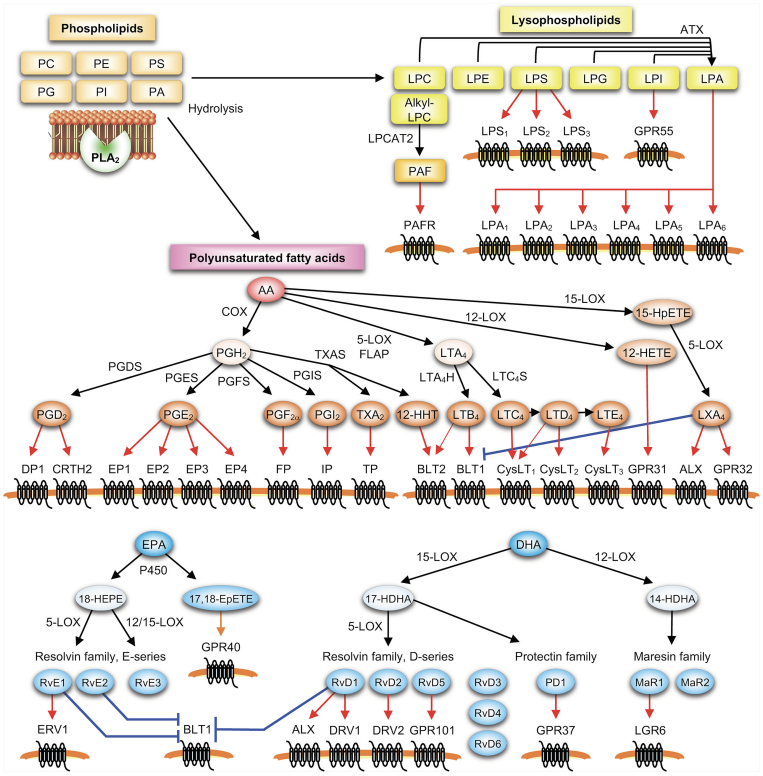


FIGURE 1 | PLA_2-driven lipid mediator pathways. Lysophospholipids (such as lysophosphatidylcholine (LPC), lysophosphatidylethanolamine (LPE), lysophosphatidylserine (LPS), lysophosphatidylglycerol (LPG), lysophosphatidylinositol (LPI) and LPA) and polyunsaturated fatty acids (such as AA, EPA and DHA) released from membrane phospholipids (PC, PE, PS, phosphatidylinositol (PI), phosphatidylglycerol (PG) and phosphatidic acid (PA)) by PLA_2 are metabolized by downstream enzymes into various lipid mediators, which in turn act on their specific receptors on target cells. In the PLA_2-lysophospholipid axis, various lysophospholipids are converted by autotaxin (ATX) into LPA, and alkyl-LPC is converted by LPC acyltransferase 2 (LPCAT2) into PAF. In the PLA_2-PUFA axis, ω6 AA released by PLA_2 is metabolized into prostanoids including PGD_2, PGE_2, $PGF_{2\alpha}$, PGI_2, TXA_2, and 12-hydroxyheptadecatrenoic acid (12-HHT) *via* the COX pathway involving COX-1 or COX-2 and terminal PG synthases (PGDS, PGES, $PGF_{2\alpha}$ synthase (PGFS), PGI_2 synthase (PGIS) and TXA_2 synthase (TXAS)), or into LTB_4 and cysLTs (LTC_4, D_4 and E_4) *via* the 5-LOX pathway involving 5-LOX, its cofactor 5-LOX-activating protein (FLAP), and terminal LT synthases (LTA_4H and LTC_4S). Combined actions of 15-LOX and 5-LOX give rise to lipoxins (*e.g.*, LXA_4), an AA-derived SPM. ω3 PUFAs (*e.g.*, EPA and DHA) are metabolized by LOXs and/or CYP450s into various SPMs including hydroxy-EPA (*e.g.*, 18-HEPE), hydroxy-DHA (*e.g.*, 14- and 17-HDHAs), E- and D-series resolvins (*e.g.*, RvE1-3 and RvD1-6), protectin D1 (PD1), maresins (*e.g.*, MaR1-2), and ω3 epoxides (e.g., 17,18-EpETE).

derived lipid mediator that also participates in allergic responses, with no change (17) or a slight increase (36, 37) in degranulation. *Pla2g4a*$^{-/-}$ mice or WT mice treated with a $cPLA_2\alpha$ inhibitor display reduced asthmatic responses upon pulmonary antigen challenge (16, 38). As in mice lacking $cPLA_2\alpha$, asthmatic responses are attenuated in mice lacking biosynthetic enzymes or receptors for LTs, PGD_2, or PAF (39–45), implying a critical role of the $cPLA_2\alpha$-LT/PGD_2/PAF axis in this pulmonary allergic disease. In contrast, passive cutaneous anaphylaxis (PCA), a model of immediate-type allergic reactions, is not altered in *Pla2g4a*$^{-/-}$ mice, likely due to simultaneous shutdown of the generation of pro-anaphylactic LTC_4 and anti-anaphylactic PGD_2 by mast cells (20).

LTB_4 is a potent chemoattractant for leukocytes, while cysLTs promote microvascular permeability, sustained smooth muscle contraction, and mucus secretion. Among the three cysLT receptors ($CysLT_{1\sim3}$), $CysLT_1$ binds to LTD_4 > LTC_4 > LTE_4, $CysLT_2$ to LTC_4 = LTD_4 > LTE_4, and $CysLT_3$ to LTE_4 as determined by transfection systems, although their specificity *in vivo* is less clear. Besides being produced by mast cells as well as by macrophages, eosinophils and basophils, cysLTs can also activate mast cells to produce contractile PGs *via* a mechanism involving a receptor sensitive to montelukast (46, 47), a $CysLT_1$ antagonist that is now clinically used for treating patients with asthma (48). IL-4-dependent mast cell proliferation requires autocrine/paracrine cysLT signaling *via* $CysLT_1$, and $CysLT_2$ interacts with $CysLT_1$ to dampen cysLT-dependent mitogenic responses of mast cells (49, 50). Recently, cysLTs have attracted attention as critical regulators of group 2 innate lymphoid cells (ILC2s). CysLTs induce $CysLT_1$-dependent production of Th2 cytokines (IL-4, IL-5, and IL-13) by ILC2s in cooperation with the epithelial-derived cytokines IL-25 and IL-33, promoting the expansion of ILC2s, Th2 cells, and eosinophils after allergen challenge (51–53). $CysLT_2$-driven production of IL-33 by type 2 alveolar cells leads to expansion of ILC2s, and pharmacological inhibition of $CysLT_2$ blocks IL-33-driven mast cell activation and

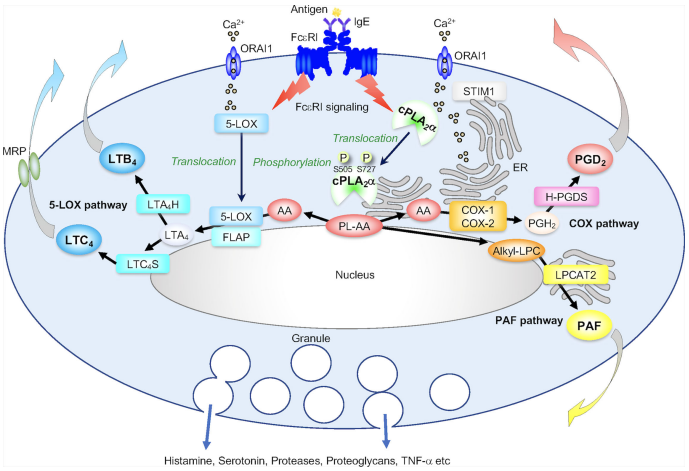


FIGURE 2 | The cPLA$_2$α-eicosanoid axis. (A) The role of cPLA$_2$α in generation of PGD$_2$ and LTs in IgE/antigen (Ag)-activated mast cells. Following FcεRI-dependent signaling that is linked to STIM1/ORAI1-driven Ca^{2+} influx, cPLA$_2$α translocates from the cytosol to the perinuclear, Golgi and ER membranes, where several downstream eicosanoid-biosynthetic enzymes are also located. The activity of cPLA$_2$α is augmented by phosphorylation at Ser^{505} by MAPKs, Ser^{727} by MAPK-activated protein kinases (MAPKAPKs), and possibly other kinases. The AA released from AA-containing phospholipids (PL-AA) by cPLA$_2$α is then metabolized into PGD$_2$ *via* the COX pathway involving COX-1 (or COX-2 if it is induced) and H-PGDS and into LTB$_4$ and LTC$_4$ *via* the 5-LOX pathway involving 5-LOX (which also translocates from the cytosol to the perinuclear membrane in response to Ca^{2+}), FLAP (a cofactor that presents AA to 5-LOX), LTA$_4$H and LTC$_4$S. Alternatively, cPLA$_2$α-generated alkyl-LPC is acetylated by LPCAT2 to PAF. These reactions occur independently of degranulation and cytokine induction.

associated lung inflammation (54). Antigen inhalation leads to expansion of IL-25-producing airway brush cells or tuft cells, which is attenuated by genetic deletion of LTC$_4$S or CysLT$_3$, revealing an importance of the airway LTE$_4$-CysLT$_3$ axis in type 2 inflammation (55). Similarly, cysLTs produced by intestinal tuft cells cooperate with IL-25 to activate ILC2s, and tuft cell-specific deletion of cysLT generation blocks type 2 immune responses against food allergens or helminth infection (56). In the context of atopic dermatitis, tape stripping of the stratus corneum (equivalent to scratching) causes keratinocytes to systemically release IL-33, which synergizes with intestinal tuft cell-derived IL-25 and cysLTs to drive the expansion and activation of ILC2s that produce IL-4, eventually promoting mast cell expansion in the intestine (57). In addition, LTC$_4$ derived from basophils rather than mast cells acts on CysLT$_2$ on natriuretic polypeptide-positive ($Nppb^+$) sensory neurons to elicit itch (58, 59), underscoring a novel mechanism for acute itch flares in atopic dermatitis.

PGD$_2$ exerts pro- and anti-allergic functions through two PGD receptors, DP1 and CRTH2 (DP2), depending on the disease contexts. Global or mast cell-specific deletion of DP1 ameliorates asthma and anaphylaxis, which may be attributable in part to the impaired maturation of mast cells (see below) (20, 43). In contrast, DP1 deficiency increases the migration of antigen-captured dendritic cells into the draining lymph nodes, thereby exacerbating contact hypersensitivity (CHS), a Th1-dependent delayed-type allergic response (60, 61). Global or mast cell-specific deletion of H-PGDS worsens anaphylaxis (20, 62) and food allergy with mast cell hyperplasia (63). The anti-inflammatory action of PGD$_2$ is mediated, at least in part, by its non-enzymatic conversion to 15-deoxy-PGJ$_2$, which acts on the nuclear receptor PPARγ to attenuate pro-inflammatory NF-κB signaling (64). Mast cell-derived PGD$_2$ is involved in ILC2 expansion *via* CRTH2 (65), and CRTH2-deficient mice exhibit reduced pulmonary ILC2 responses and type 2 inflammation, an event that is rescued by transfer of CRTH2-sufficient ILC2s (66). LTE$_4$ enhances the ability of PGD$_2$ to induce ILC2 and Th2 cells (52, 67), implying a synergistic role of the two mast cell-derived eicosanoids in promoting type 2 immunity. Activation of cPLA$_2$α in intestinal tuft cells leads to generation of not only LTC$_4$ (see above) but also PGD$_2$, the latter of which increases mucus secretion by goblet cells to impede pathogen invasion (68). Thus, it seems that mast cells and tuft cells share common characteristics in that they produce both PGD$_2$ (via the cPLA$_2$α/COX-2/H-PGDS pathway) and LTC$_4$ (via the cPLA$_2$α/5-LOX/LTC$_4$S pathway) in response to specific stimuli and participate in fine-tuning allergic responses as well as host defense against pathogens.

Although mast cells produce PGE$_2$ minimally, this pleiotropic eicosanoid is produced by stromal cells surrounding mast cells and plays an anti-allergic role in general by acting on four types of its receptor (EP1–4). During mast cell-fibroblast coculture, the AA released by cPLA$_2$α in mast cells is transferred to adjacent fibroblasts through the transcellular route and then metabolized there by PGE$_2$ synthase (mPGES-1) to PGE$_2$ (17), which acts on stromal EP3 to counteract allergic reaction. As such, mice lacking EP3 display more severe asthma, anaphylaxis, and CHS (20, 69, 70). Paradoxically, however, PGE$_2$ directly elicits mast cell activation *via* EP3 by evoking Ca^{2+} signaling (71). Genetic deletion of mPGES-1 or pharmacological inhibition of COX-1 rather than COX-2 mimics aspirin-exacerbated respiratory disease (AERD) that is characterized by bronchoconstriction,

eosinophilia, and mucus secretion upon exposure to non-steroidal anti-inflammatory drugs (NSAIDs; COX inhibitors), an event that is reversed by EP2 (or to a lesser extent EP1) agonist (72). In this AERD pathology, aspirin-induced mast cell activation and cysLT overproduction depend on the adherent interaction of platelets with granulocytes and thromboxane A_2 (TXA_2) signaling (72, 73). In addition, PGE_2 alleviates mast cell activation (74–76), increases vascular remodeling (77), prevents eosinophilia (78, 79), reduces proliferation of ILC2s and Th2 cells (80, 81), and attenuates atopic dermatitis by reducing TSLP expression (82) *via* EP2 signaling. The mast cell-related eicosanoid network is illustrated in **Figure 3**.

Constitutive Generation of ω3 Epoxides by PAF-AH2 in Mast Cells

PAF-AHs were originally identified as a unique group of PLA_2s having the capacity to hydrolyze and thereby inactivate PAF (83, 84). Plasma-type PAF-AH (PLA2G7 or group VIIA PLA_2) is a secreted protein produced by macrophages, mast cells or other sources, and is now more generally referred to as lipoprotein-associated PLA_2 (Lp-PLA_2), existing as a low-density lipoprotein (LDL)-bound form in human plasma (85). PAF-AH2 (group VIIB PLA_2) is a cytosolic enzyme that shows significant structural homology with Lp-PLA_2. Despite their names, however, there has been no confirmative evidence that Lp-PLA_2 or PAF-AH2 has a protective role against allergic reactions by degrading PAF *in vivo*. Rather, it is now recognized that Lp-PLA_2 and PAF-AH2 preferentially hydrolyze oxidized phospholipids in lipoproteins and cells, respectively. Importantly, PAF-AH2 is abundantly expressed in mast cells and contributes to constitutive (*i.e.*, stimulus-independent) generation of unique epoxy-metabolites of ω3 fatty acids (ω3 epoxides), which prime mast cells to ensure optimal FcεRI-dependent activation (**Figure 4A**) and attenuates pulmonary hypertension by reducing the expression of pro-fibrotic factors (**Figure 4B**) in autocrine and paracrine manners, respectively (18, 19).

Comprehensive lipidomics profiling of BMMCs revealed that unique ω3 epoxides, namely 17,18-epoxyeicosatetraenoic acid (17,18-EpETE) and 19,20-epoxydocosapentaenoic acid (19,20-EpDPE) derived respectively from EPA and DHA, are constitutively released from the cells (18). Unlike the canonical route for eicosanoid biosynthesis, in which the AA released by cPLA$_2\alpha$ from membrane phospholipids is metabolized by downstream enzymes to eicosanoids (see above), these ω3 epoxides are liberated directly by PAF-AH2 from ω3 epoxide-esterified phospholipids pre-existing in cell membranes (**Figure 4A**). Genetic or pharmacological inactivation of PAF-AH2 shuts off the constitutive release of ω3 epoxides from mast cell membranes, resulting in reduced FcεRI signaling and anaphylaxis. Supplementation of *Pafah2*$^{-/-}$ BMMCs with ω3 epoxides fully restores the defective FcεRI-dependent, but not -independent, activation. Mechanistically, ω3 epoxides augment FcεRI-driven activation of mast cells by downregulating Srcin1, a Src-inhibitory protein that counteracts the FcεRI-proximal Src-family tyrosine kinases Fyn and Lyn and thereby dampens FcεRI signaling (18). Transcriptome analysis revealed that genes regulated by ω3 epoxides largely overlap with those regulated by a PPARγ antagonist in *Pafah2*$^{-/-}$ BMMCs, implying that the action of ω3 epoxides may involve the inactivation of PPARγ, a lipid-sensing nuclear receptor that induces Srcin1 expression (18).

In general, ω3 fatty acids including EPA and DHA play beneficial roles in various biological events. These ω3 fatty acids act by themselves on the fatty acid receptors GPR40 or GPR120 (86, 87), or are converted by LOX or cytochrome P450 (CYP450) enzymes to SPMs with potent anti-inflammatory or pro-resolving functions. Indeed, several CYP450 isoforms have the capacity to catalyze the epoxidation of EPA and DHA to yield

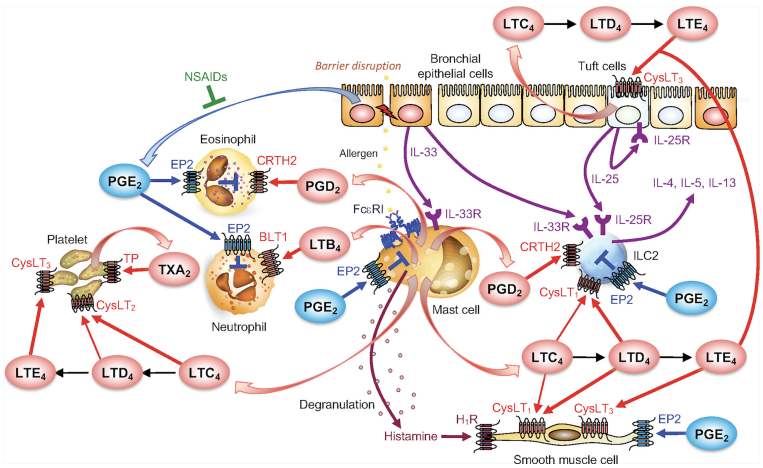


FIGURE 3 | The mast cell-driven eicosanoid network in asthma. PGD_2 and LTs produced by activated mast cells act on various cell types including leukocytes, platelets, bronchial epithelial cells and smooth muscle cells to promote allergic responses. PGE_2, produced by various cells such as bronchial epithelial cells (but not mast cells), dampens allergic responses. NSAIDs (COX inhibitors) blocks PGE_2 production, thereby exacerbates asthma known as AERD. For details, please see the text.

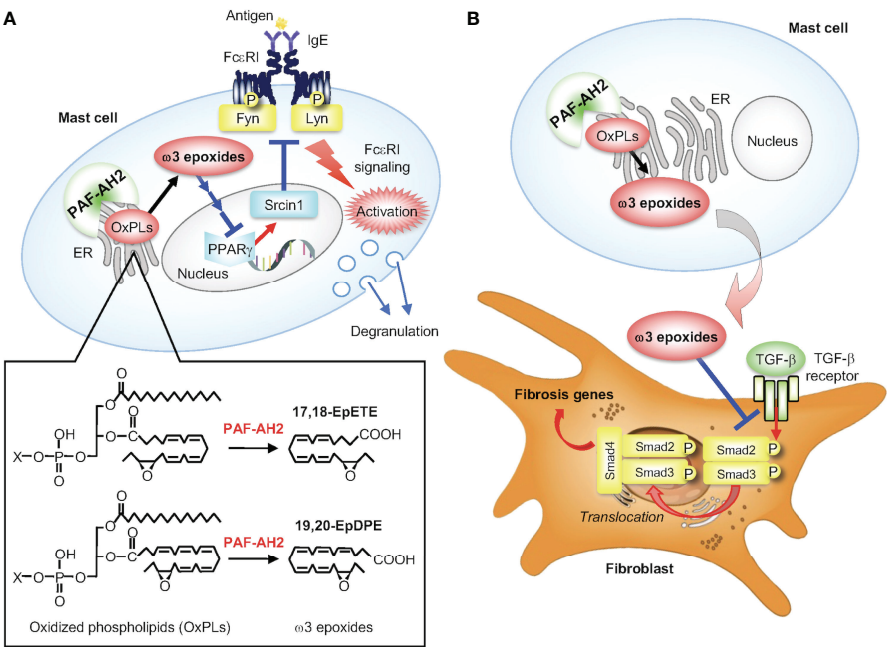


FIGURE 4 | The PAF-AH2-ω3 epoxide axis. **(A)** PAF-AH2-driven constitutive generation of ω3 epoxides in mast cells and their cell-autonomous role in augmentation of FcεRI signaling. PAF-AH2 directly hydrolyzes phospholipids with oxidized fatty acids (ω3 epoxides in this case) to release free ω3 epoxides (17,18-EpETE and 19,20-EpDPE), which act on the nuclear receptor PPARγ (probably indirectly) to suppress the expression of Srcin1, a Src-inhibitory protein. This Srcin1 downregulation eventually leads to increased activation of the FcεRI-proximal Src family kinases Fyn and Lyn, thereby ensuring optimal FcεRI signaling. **(B)** Suppression of pulmonary hypertension by PAF-AH2-derived ω3 epoxides. The ω3 epoxides released from lung mast cells acts on neighboring fibroblasts in a paracrine manner to prevent TGF-β-driven Smad2 phosphorylation, thereby attenuating perivascular fibrosis leading to amelioration of pulmonary hypertension.

ω3 epoxides (88). Individual SPMs act on their specific receptors, such as ERV1/ChemR23 for resolvin E1 (RvE1), DRV1/GPR32 for RvD1, DRV2/GPR18 for RvD2, GPR37 for protectin D1 (PD1), and LGR6 for maresin 1 (MaR1) (89–93), and can limit leukocyte recruitment, induce granulocyte apoptosis, enhance efferocytosis by phagocytes, facilitate the switch from M1 to M2 macrophages, promote the return of non-apoptotic cells to lymphatics and blood vessels, and help tissue repair (11, 94, 95). In this context, it seems strange that ω3 epoxides potentiate (rather than attenuate) mast cell activation and thereby exacerbate allergic responses. It should be noted, however, that the immunosuppressive action of SPMs can be disadvantageous to host defense (11, 94, 95). Conceivably, FcεRI-induced mast cell activation might have evolved originally as a defense system against harmful venom, bacteria, and/or parasites (96, 97), where the ω3 epoxide-mediated optimization of FcεRI signaling may be important for proper elimination of these unfavorable materials from the body and thereby maintenance of a healthy state. In a modern hygienic environment, however, this protective response has been shifting into deleterious outcomes against exposure to environmental allergens, manifesting as allergic diseases.

In contrast to their augmentative role in FcεRI-dependent mast cell activation and anaphylaxis, ω3 epoxides produced by PAF-AH2 in mast cells have a protective role in pulmonary hypertension, a fatal rare disease that causes right heart failure by elevated pulmonary arterial resistance (19). Global or mast cell-specific deletion of PAF-AH2 in mice accelerates vascular remodeling with perivascular fibrosis, resulting in exacerbation of hypoxic pulmonary hypertension. Mechanistically, 17,18-EpETE and 19,20-EpDPE produced by PAF-AH2 in lung mast cells act on stromal fibroblasts in a paracrine manner to suppress their activation by inhibiting TGF-β-driven Smad2 signaling (**Figure 4B**). Administration of ω3 epoxides into mice improves pulmonary hypertension by reducing advanced vascular remodeling harboring perivascular fibrosis in several models. Furthermore, the whole-exome sequencing of patients with pulmonary arterial hypertension identifies two candidate pathogenic variants of the *PAFAH2* gene. Thus, the PAF-AH2–ω3 epoxide axis could be a promising therapeutic target for pulmonary hypertension. In addition, 17,18-EpETE suppresses CHS by inhibiting neutrophil migration through GPR40 (98) Thus, the actions of ω3 epoxides are context-dependent, having detrimental or beneficial effects depending on the diseases.

Plasma-type PAF-AH (PLA2G7/Lp-PLA$_2$) is abundantly expressed in BMMCs, is secreted after FcεRI-dependent activation, and may participate in the degradation of PAF produced by these cells in an autocrine fashion (99). Interestingly, a comprehensive transcriptome analysis of various mast cell populations demonstrated that the expression level of the *Pla2g7* gene in skin mast cells is much lower than that in tongue, tracheal, esophageal and peritoneal mast cells (100).

Although the physiological significance of the low expression of this enzyme in skin mast cells is unclear, it might avoid rapid degradation of PAF produced by these cells or neighboring cells in a local skin niche. In the aforementioned pulmonary hypertension model, *Pla2g7*$^{-/-}$ mice do not display any noticeable phenotype (19), implying the segregated role of the two (plasma-type and intracellular) PAF-AH isoforms in this disease.

REGULATORY ROLES OF EXTRACELLULAR PLA$_2$S IN MAST CELL BIOLOGY

General View of sPLA$_2$s

The sPLA$_2$ family comprises Ca^{2+}-dependent, low-molecular-mass enzymes with a conserved His-Asp catalytic dyad. There are 11 mammalian sPLA$_2$s (catalytically active IB, IIA, IIC, IID, IIE, IIF, III, V, X and XIIA and inactive XIIB), which are structurally subdivided into group I/II/V/X, group III, and group XII branches (101). Individual sPLA$_2$s exhibit distinct tissue distributions and exert their specific functions in lipid mediator-dependent or -independent fashions (102–105). In extracellular milieus, sPLA$_2$s act on the plasma membrane of activated, damaged, or dying cells (rather than that of resting cells) and also on non-cellular phospholipid components, such as dietary food, lipoproteins, lung surfactant, EVs, and membranes of invading microbes, as hydrolytic targets. Although the expression and potential functions of sPLA$_2$s in mast cells had been reported in previous studies (106–113), the results should be interpreted with caution since many of them relied on the strategies employing overexpression or exogenous addition of super-physiologic levels of sPLA$_2$s, which might not precisely reflect pathophysiologic situations *in vivo*. Beyond this caveat, gene targeting studies have provided unequivocal evidence for the involvement of several sPLA$_2$s in the regulation of mast cells in cell-autonomous and non-autonomous ways. Our comprehensive phenotypic screening of various sPLA$_2$ knockout strains, with mast cell-dependent PCA reaction *in vivo* and BMMC functions *ex vivo* as readouts, has revealed that mice null for sPLA$_2$-III and -IIA, but not those for sPLA$_2$-IB, -IID, -IIE, -IIF, -V and -X, displayed notable alterations in the maturation and/or functions of mast cells (20), as described below.

Regulation of Mast Cell Maturation by sPLA$_2$-III Through the Paracrine PGD$_2$ Pathway

Bee venom group III PLA$_2$ (bvPLA$_2$), when injected into mouse skin, directly activates mast cells likely through hydrolysis of membrane phospholipids to give rise to lysophospholipids, whose massive accumulation can cause lysis of all the cells (including mast cells) in the milieu due to their detergent-like nature leading to release of the alarmin IL-33 and thereby activation of ILC2s and then Th2 cells (114). The aggravated Th2 response by bvPLA$_2$ can be considered as a protective mechanism against future exposure to this noxious venom component. Administration of human sPLA$_2$-III, the sole mammalian homolog of bvPLA$_2$, into mouse skin also elicits mast cell activation (20). Endogenous sPLA$_2$-III is stored in and released from secretory granules of mouse and human mast cells. Importantly, mast cell-dependent passive and active anaphylactic responses are markedly reduced in mice lacking sPLA$_2$-III (*Pla2g3*$^{-/-}$) and conversely augmented in mice with transgenic overexpression of human sPLA$_2$-III (*PLA2G3*^{TG}) (20). Notably, mast cells in *Pla2g3*$^{-/-}$ mice are numerically normal but morphologically and functionally immature, indicating that sPLA$_2$-III does not merely act as a mast cell activator, but also facilitates mast cell maturation. In fact, histamine and protease contents in secretory granules, expression of mast cell maturation markers (*e.g.*, histidine decarboxylase (histamine synthase), mast cell proteases, and H-PGDS), and FcεRI-dependent and even -independent activation are considerably lower in *Pla2g3*$^{-/-}$ mast cells than in *Pla2g3*$^{+/+}$ mast cells. These phenotypes are mast cell-autonomous, since BMMCs from *Pla2g3*$^{-/-}$ mice fail to reconstitute the anaphylactic response after their transfer into mast cell-deficient *Kit*$^{W\text{-}sh/W\text{-}sh}$ mice, and since mast cell-specific deletion of sPLA$_2$-III also leads to similar defects in mast cell maturation and anaphylaxis (20, 21). Importantly, the perturbed mast cell maturation and anaphylaxis in *Pla2g3*$^{-/-}$ mice are recapitulated in mice lacking lipocalin-type PGD$_2$ synthase (L-PGDS), which is expressed in stromal fibroblasts, or those lacking the PGD$_2$ receptor DP1, which is induced in maturing mast cells. Thus, sPLA$_2$-III secreted from mast cells hydrolyzes phospholipids in adjacent fibroblasts to release AA, which is then converted by fibroblastic L-PGDS to PGD$_2$ that acts on DP1 on mast cells to promote their proper maturation (**Figure 5A**). This sPLA$_2$-III-L-PGDS-DP1 paracrine circuit highlights a new aspect of PGD$_2$-DP1 signaling in the regulation of mast cell maturation and thereby allergy and provides evidence for the long-standing proposal that sPLA$_2$ acts as a paracrine coordinator of eicosanoid production in tissue microenvironments (20). Since EVs serve as a better hydrolytic target of sPLA$_2$s (115, 116), it is also possible that sPLA$_2$-III may act on mast cell-secreted EVs to release AA, which is incorporated into fibroblasts and utilized for L-PGDS-driven PGD$_2$ generation.

Furthermore, mast cell-specific *Pla2g3*-deficient mice, as well as mast cell-deficient *Kit*$^{W\text{-}sh}$ mice reconstituted with mast cells prepared from global *Pla2g3*$^{-/-}$ mice, display a significant reduction of irritant contact dermatitis (ICD) and an aggravation of Th1-dependent CHS (21). The increased CHS response by sPLA$_2$-III deficiency in mast cells depends, at least in part, on the reduced expression of H-PGDS and thereby reduced production of PGD$_2$ due to immaturity of mast cells. During severe CHS responses, mast cells represent a source of IL-2 and IL-10, which amplify recruitment, maintenance, and function of T$_{reg}$ cells that limit ear swelling and epidermal hyperplasia (117–120). H-PGDS deficiency in mast cells also abrogates the suppressive effect of mast cells on CHS, indicating that, in addition to the cytokines IL-2 and IL-10, the lipid mediator PGD$_2$ serves as another negative regulator of the CHS responses. In support, mice lacking DP1 also display an exacerbation of

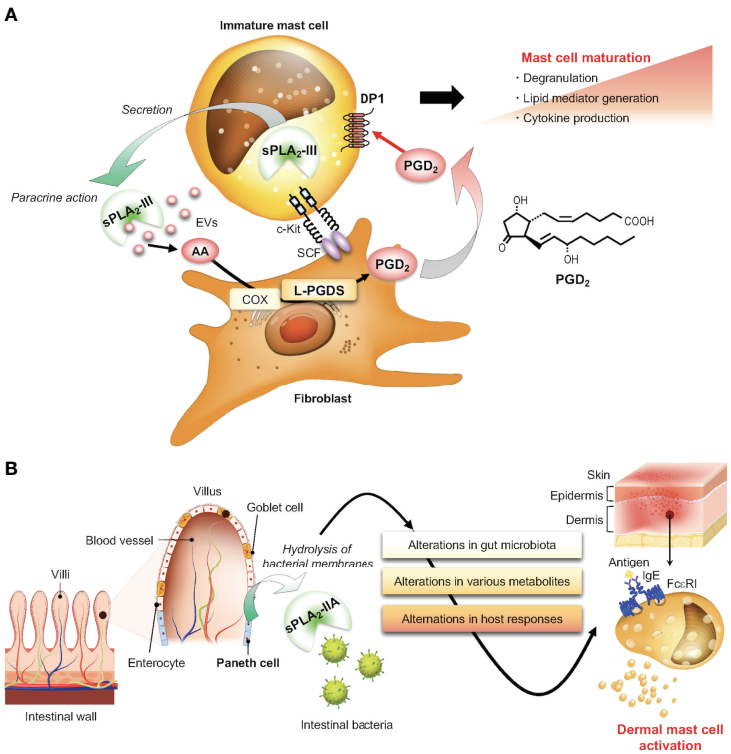


FIGURE 5 | Regulatory roles of sPLA$_2$s in mast cell biology. **(A)** The sPLA$_2$-III-driven paracrine PGD$_2$ circuit for proper mast cell maturation. sPLA$_2$-III secreted from immature mast cells hydrolyzes phospholipids in adjacent fibroblast membranes or possibly in mast cell-derived EVs to release AA. This AA is metabolized by fibroblastic COX/L-PGDS to PGD$_2$, which in turn acts on DP1 on mast cells to promote mast cell maturation. **(B)** Non-canonical action of sPLA$_2$-IIA on mast cells *via* shaping of the gut microbiota. sPLA$_2$-IIA, a potent bactericidal protein, is secreted from intestinal Paneth cells and modulates the gut microbiota. This event has systemic effects on immunity and metabolism, thereby secondarily affecting mast cell activation in distal tissues.

CHS by affecting the expression of IL-10 in dendritic cells (60, 61). Taken together, sPLA$_2$-III, which is secreted from mast cells, promotes mast cell maturation through the lipid-driven functional interaction with stromal fibroblasts, thereby facilitating acute anaphylactic and ICD reactions and limiting delayed CHS response.

sPLA$_2$-IIA Regulates Mast Cells Through Shaping of the Gut Microbiota

sPLA$_2$-IIA (PLA2G2A) is a prototypic sPLA$_2$ that is highly upregulated in various human tissues during inflammation such as rheumatoid arthritis, sepsis, and COVID-19 infection (121–123). While sPLA$_2$-IIA promotes sterile inflammation by mobilizing pro-inflammatory lipid mediators or DAMPs (danger-associated molecular patterns) from EVs as an "inflammatory sPLA$_2$" (115), it also efficiently degrades bacterial membranes (Gram-positive in particular), thereby playing a protective role against bacterial infection as a "bactericidal sPLA$_2$" (124). In the context of mast cell biology, sPLA$_2$-IIA was partially purified from rat mastocytoma RBL-2H3 cells (125), was detected immunohistochemically in secretory granules of rat serosal mast cells (126), triggered histamine release or PGD$_2$ production by rat serosal mast cells when added exogenously at high concentrations (106, 107), and enhanced FcεRI-induced degranulation when overexpressed in RBL-2H3 cells (110, 111). However, as the *Pla2g2a* gene is naturally disrupted in C57BL/6 and 129 strains due to a natural frameshift mutation (127, 128), it had been difficult to evaluate the precise *in vivo* functions of endogenous sPLA$_2$-IIA using a standard knockout strategy. Even in BALB/c mice, a strain that has an intact *Pla2g2a* gene (127), sPLA$_2$-IIA expression is highly restricted to intestinal Paneth cells (129, 130). Although a trace level of *Pla2g2a* mRNA is induced in BALB/c-derived BMMCs after stimulation with SCF plus accessory cytokines *in vitro* (131), there has been no follow-up study showing that sPLA$_2$-IIA is substantially expressed in mouse mast cells *in vivo*. This expression profile of sPLA$_2$-IIA in BALB/c mice is in marked contrast to that in other animal species including humans and rats, in which sPLA$_2$-IIA is expressed or induced in many tissues. Beyond these limitations, sPLA$_2$-IIA-depleted (*Pla2g2a*$^{-/-}$) mice on the BALB/c background are best suited for analyzing the role of endogenous sPLA$_2$-IIA in the intestine. Importantly, this new mouse model has unveiled a previously unrecognized, non-canonical action of intestinal sPLA$_2$-IIA on mast cells *via* shaping of the gut microbiota.

Despite the restricted expression of $sPLA_2$-IIA in the intestine, its genetic deletion unexpectedly leads to unusual changes in mast cell degranulation in distal skin. In a model of carcinogen-induced skin cancer, tumor development is markedly reduced, accompanied by a reduction of degranulated mast cells in the tumor tissue, in *Pla2g2a*$^{-/-}$ mice relative to *Pla2g2a*$^{+/+}$ mice (22). Surprisingly, cohousing of *Pla2g2a*$^{-/-}$ and *Pla2g2a*$^{+/+}$ mice in the same cages, which results in mixing of the microbiota between the genotypes through coprophagia, abolishes the skin cancer-related phenotypes. Of more interest, IgE/antigen-induced PCA is uniquely altered in *Pla2g2a*$^{-/-}$ mice depending on housing conditions; when *Pla2g2a*$^{+/+}$ and *Pla2g2a*$^{-/-}$ mice are housed in two different animal facilities, the PCA response in *Pla2g2a*$^{-/-}$ mice is reduced in one facility, while it is conversely elevated in the other facility, relative to *Pla2g2a*$^{+/+}$ mice (23). Furthermore, in both facilities, the opposite PCA phenotypes in *Pla2g2a*$^{-/-}$ mice are lost when they are cohoused with *Pla2g2a*$^{+/+}$ mice. Thus, the PCA phenotypes in *Pla2g2a*$^{-/-}$ mice are greatly influenced by housing conditions, implying that $sPLA_2$-IIA, primary expressed in intestinal Paneth cells that secrete various antimicrobial peptides, contributes to shaping of the gut microbiota through its bactericidal activity, thereby secondarily affecting mast cell fate and associated allergic reaction in distal skin. Indeed, metagenome analysis of the stool revealed that several bacterial genera such as Gram-positive *Lachnospiraceae* and *Ruminococcaceae* and Gram-negative *Helicobacteraceae* and *Prevotellaceae* are differently distributed in *Pla2g2a*$^{+/+}$ and *Pla2g2a*$^{-/-}$ mice, and there is a better correlation between distinct PCA responses and *Ruminococcaceae* and *Mucispirillum* abundances in the two facilities. The alteration in gut microbiota in *Pla2g2a*$^{-/-}$ BALB/c mice, as well as in *PLA2G2A*-transgenic C57BL/6 mice in which human $sPLA_2$-IIA is overexpressed systemically, also impact the severity of arthritis and psoriasis (22, 132). Thus, $sPLA_2$-IIA acts as a host factor that is primarily expressed in the intestine and contributes to shaping of the gut microbiota, whose disturbance by *Pla2g2a* deletion or overexpression secondarily affects various diseases including those involving mast cells in proximal and distal tissues (**Figure 5B**). This concept opens a new avenue for the action modes of this classical $sPLA_2$ and might be applicable to other $sPLA_2$ isoforms expressed in the gastrointestinal tract or even in other anatomical sites such as the respiratory tract and skin.

Nonetheless, looking back the classical view that $sPLA_2$-IIA is expressed in mast cells of rat and human, mast cell-autonomous roles of $sPLA_2$-IIA should be reconsidered. Related to the observations that forcible overexpression or exogenous addition of $sPLA_2$-IIA resulted in enhanced mast cell degranulation as described above (106–108, 110, 111), $sPLA_2$ inhibitors suppressed degranulation by rat serosal mast cells (107) or LTC_4 production by human lung mast cells (112), although the inhibitors used in those studies were not strictly specific for $sPLA_2$-IIA. Alternatively, $sPLA_2$-IIA released from activated mast cells, like that released from other cells such as platelets, leukocytes and epithelial cells, might contribute to propagation of inflammation by mobilizing lipid mediators from EVs (133), host defense against infection by degrading bacterial membranes (124), or regulation of cellular signaling by acting as a ligand for the $sPLA_2$ receptor PLA2R1 (130, 134).

MISCELLANEOUS ROLES OF OTHER PLA_2S IN MAST CELL BIOLOGY

Several studies have demonstrated the potential roles of $sPLA_2$-V (PLA2G5) and $sPLA_2$-X (PLA2G10) in mast cells. Reportedly, $sPLA_2$-V is released from antigen-activated BMMCs and then acts on neighboring fibroblasts to augment COX-1-dependent PGD_2 biosynthesis (135–137), is localized to the perinuclear area in BMMCs (131), and augments FcεRI-induced PGD_2 and LTC_4 production when overexpressed in RBL-2H3 cells (110, 111). TLR2-induced, COX-2-dependent delayed PGD_2 generation is partially reduced in BMMCs from $sPLA_2$-V-deficient (*Pla2g5*$^{-/-}$) mice, where $sPLA_2$-V may act in cooperation with $cPLA_2\alpha$ (138). In addition, $sPLA_2$-X is detected in BMMCs, and IL-13 induction in response to IL-33 is substantially impaired in BMMCs from $sPLA_2$-X-deficient (*Pla2g10*$^{-/-}$) mice (139). Importantly, *Pla2g5*$^{-/-}$ and *Pla2g10*$^{-/-}$ mice are both protected from airway inflammation induced by allergen challenge through the mechanisms involving ILC2 cells, M2 macrophages, eosinophils, airway epithelial cells, and possibly mast cells (139–145). However, other studies showed that the expression levels of $sPLA_2$-V and -X in BMMCs are rather low and that FcεRI-induced BMMC activation *ex vivo* and PCA reaction *in vivo* are not significantly affected in *Pla2g5*$^{-/-}$ and *Pla2g10*$^{-/-}$ mice (17, 20, 146). To reconcile these inconsistencies, it is necessary to clarify whether these two $sPLA_2$s are expressed in a certain population of mast cells and play specific roles therein under particular pathophysiological conditions.

Several lines of evidence argue the involvement of mast cells in cardiometabolic diseases (147). Since activated mast cells produce PGD_2 and LTB_4, which have been implicated in cardiovascular pathology including atherosclerosis (148, 149), it is likely that $cPLA_2\alpha$ contributes to the disease by supplying these eicosanoids in atherosclerotic plaques. Indeed, global *Pla2g4a*$^{-/-}$ mice are protected from the development of atherosclerosis (150). However, the contribution of $cPLA_2\alpha$ expressed in mast cells to the disease remains unknown and should be confirmed using mast cell-specific *Pla2g4a*$^{-/-}$ mice. Modified or oxidized low-density lipoprotein (LDL) has been shown to induce mast cell activation, resulting in cytokine secretion and subsequent leucocyte recruitment, presumably through TLR4 (151). As a component of modified LDL, the lysophospholipid mediator LPA can induce mast cell activation, resulting in the release of tryptase and chemokines (152). Many LPA species could be detected in the atherosclerotic lesion, where mast cells also reside (152, 153). Since several $sPLA_2$s have the capacity to generate modified LDL with a pro-atherogenic potential *in vitro* (154–157), it is tempting to speculate that LPA produced in LDL by these $sPLA_2$s may contribute to the development of atherosclerosis through activating aortic mast cells. Although several studies using mice overexpressing $sPLA_2$-IIA or those lacking $sPLA_2$-V or $sPLA_2$-X have proposed the potential roles of these $sPLA_2$s in atherosclerosis, none of them has provided evidence that these

$sPLA_2$s generate modified, pro-atherogenic LDL *in vivo* (158–162). Therefore, it is still unclear whether $sPLA_2$s could promote atherosclerosis development by modifying LDL and generating LPA, and if so, which $sPLA_2$ isoform(s) would be truly responsible for this event in the context of mast cell activation.

Group IVD $cPLA_2$ ($cPLA_2\delta$ or PLA2G4D) was initially identified as a keratinocyte-specific $cPLA_2$ isoform that is highly induced during psoriasis (163). It has recently been shown that $cPLA_2\delta$ is expressed in mast cells of psoriatic patients and is released extracellularly *via* mast cell-derived EVs to be transferred into adjacent Langerhans cells (164). The EV-driven $cPLA_2\delta$ captured by Langerhans cells generates neolipid antigens, which are then presented on CD1a to activate lipid-specific CD1a-reactive T cells, leading to induction of the Th17 cytokines IL-17A and IL-22. Although these results have provided a model whereby $cPLA_2\delta$ promotes psoriasis pathology, it remains unclear which lipid metabolites produced by $cPLA_2\delta$ can act as neolipid antigens. Since $cPLA_2\delta$ exhibits PLA_1 activity in preference to PLA_2 activity (165), certain lipid metabolites generated by the PLA_1 reaction might underlie the function of $cPLA_2\delta$. Further, given that $cPLA_2\delta$ is expressed in epidermal keratinocytes rather than in mast cells and that CD1a is present in humans but not in mice, the regulatory roles of $cPLA_2\delta$ in psoriasis or other skin diseases such as atopic dermatitis in the context of mast cells need further exploration.

Mast cells also express group VIA Ca^{2+}-independent PLA_2 ($iPLA_2\beta$, also known as PLA2G6 or PNPLA9). Pharmacologic inhibition of $iPLA_2\beta$ by bromoenol lactone (BEL), a well-known $iPLA_2$ inhibitor, attenuates IgE/antigen-stimulated mast cell exocytosis (166). However, mice deficient in $iPLA_2\beta$ (*Pla2g6*$^{-/-}$) show a normal PCA response *in vivo*, and *Pla2g6*$^{-/-}$ BMMCs exhibit normal degranulation, eicosanoid generation, and cytokine expression *in vitro* (17), arguing against the contribution of $iPLA_2\beta$ to mast cell development and functions. Thus, caution should be exercised when interpreting the results obtained from studies using BEL or other $iPLA_2$ inhibitors. Alternatively, considering that the $iPLA_2$ family includes nine isoforms, some BEL-sensitive $iPLA_2$ isoform(s) other than $iPLA_2\beta$, such as group VIB $iPLA_2\gamma$ (PNPLA8) which is expressed in BMMCs more abundantly than $iPLA_2\beta$ (18), might be involved in the regulation of mast cells.

Interestingly, silencing of adipose triglyceride lipase (ATGL, also referred to as PNPLA2 or $iPLA_2\zeta$), a member of the $iPLA_2$ family that plays an essential role in lipolysis and thereby energy metabolism by hydrolyzing triglycerides stored in lipid droplets (167), results in the reduction of PGD_2 and LTC_4 synthesis more efficiently than silencing of $cPLA_2\alpha$ in human mast cells derived from blood $CD34^+$ progenitors (168). These results suggest that the AA released from triglycerides by ATGL is coupled with eicosanoid synthesis in mast cells, underscoring a functional link between energy homeostasis and eicosanoid signaling. However, given the essential role of $cPLA_2\alpha$ in eicosanoid generation in mast cells as revealed by studies using *Pla2g4a*$^{-/-}$ mice (see above), the following possibilities should also be taken into consideration: (i) mouse and human mast cells might have distinct dependence on $cPLA_2\alpha$ and ATGL; (ii) the AA released by ATGL from lipid droplets might be firstly incorporated into membrane phospholipids by lysophospholipid acyltransferases and then cleaved out by $cPLA_2\alpha$ toward eicosanoid synthesis; or (iii) ATGL-mediated energy supply might be required for appropriate $cPLA_2\alpha$-driven eicosanoid generation. Also, it is important to clarify whether ATGL in mast cells is involved in the regulation of eicosanoid synthesis or other effector functions under certain *in vivo* conditions.

CONCLUDING REMARKS

In this article, we have highlighted current understanding of the pathophysiological roles of several PLA_2s and associated bioactive lipids in mast cell biology, focusing mainly on the findings obtained from studies using gene-manipulated mice in combination with comprehensive lipidomics. As a future prospect, it is important to translate these findings obtained from experimental animals into humans. It is possible that the functions of mast cells may also be affected by other PLA_2s or bioactive lipids not described in this article, by bioenergetics coupled with lipogenesis, lipolysis and fatty acid β-oxidation, and by lipid composition in membrane microdomains that could affect signal potency through FcεRI or other receptors. A full understanding of lipid networks in relation to mast cells, allergy, and other mast cell-dependent biological events should be further elucidated using advanced techniques such as spatiotemporal lipid imaging, untargeted lipidomics, and novel pharmacological tools to manipulate the activity or expression of particular PLA_2 subtypes that would have a potential to sequester allergic or other diseases. Further research will lead to a better understanding of the overall picture of the regulation of mast cells by lipids, hopefully allowing the prophylactic and/or therapeutic application of novel agents that target specific PLA_2-driven lipid pathways to human diseases.

AUTHOR CONTRIBUTIONS

MM and YT wrote the manuscript and prepared Figures. All authors have read and agreed to the published version of the manuscript.

FUNDING

This work was supported by Grants-in-Aid for Scientific Research JP19K22483 and JP20H05691 (to MM) and JP18K06624 (to YT) from Japan Society for the Promotion of Science, and AMED-CREST JP21gm1210013 from the Japan Agency for Medical Research and Development (to MM).

REFERENCES

1. Zheng T, Yu J, Oh MH, Zhu Z. The Atopic March: Progression From Atopic Dermatitis to Allergic Rhinitis and Asthma. *Allergy Asthma Immunol Res* (2011) 3(2):67–73. doi: 10.4168/aair.2011.3.2.67
2. Dainichi T, Kitoh A, Otsuka A, Nakajima S, Nomura T, Kaplan DH, et al. The Epithelial Immune Microenvironment (EIME) in Atopic Dermatitis and Psoriasis. *Nat Immunol* (2018) 19(12):1286–98. doi: 10.1038/s41590-018-0256-2
3. Devereux G. The Increase in the Prevalence of Asthma and Allergy: Food for Thought. *Nat Rev Immunol* (2006) 6(11):869–74. doi: 10.1038/nri1958

4. Gurish MF, Austen KF. Developmental Origin and Functional Specialization of Mast Cell Subsets. *Immunity* (2012) 37(1):25–33. doi: 10.1016/j.immuni.2012.07.003
5. Serhan N, Basso L, Sibilano R, Petitfils C, Meixiong J, Bonnart C, et al. House Dust Mites Activate Nociceptor-Mast Cell Clusters to Drive Type 2 Skin Inflammation. *Nat Immunol* (2019) 20(11):1435–43. doi: 10.1038/s41590-019-0493-z
6. Galli SJ, Tsai M. IgE and Mast Cells in Allergic Disease. *Nat Med* (2012) 18 (5):693–704. doi: 10.1038/nm.2755
7. Izawa K, Yamanishi Y, Maehara A, Takahashi M, Isobe M, Ito S, et al. The Receptor LMIR3 Negatively Regulates Mast Cell Activation and Allergic Responses by Binding to Extracellular Ceramide. *Immunity* (2012) 37 (5):827–39. doi: 10.1016/j.immuni.2012.08.018
8. Kitaura J, Murakami M. Positive and Negative Roles of Lipids in Mast Cells and Allergic Responses. *Curr Opin Immunol* (2021) 72:186–95. doi: 10.1016/j.coi.2021.06.001
9. Shimizu T. Lipid Mediators in Health and Disease: Enzymes and Receptors as Therapeutic Targets for the Regulation of Immunity and Inflammation. *Annu Rev Pharmacol Toxicol* (2009) 49:123–50. doi: 10.1146/annurev.pharmtox.011008.145616
10. Narumiya S, Furuyashiki T. Fever, Inflammation, Pain and Beyond: Prostanoid Receptor Research During These 25 Years. *FASEB J* (2011) 25 (3):813–8. doi: 10.1096/fj.11-0302ufm
11. Serhan CN. Pro-Resolving Lipid Mediators are Leads for Resolution Physiology. *Nature* (2014) 510(7503):92–101. doi: 10.1038/nature13479
12. Kano K, Aoki J, Hla T. Lysophospholipid Mediators in Health and Disease. *Annu Rev Pathol* (2022) 17:459–83. doi: 10.1146/annurev-pathol-050420-025929
13. Murakami M. Novel Functions of Phospholipase A_2s: Overview. *Biochim Biophys Acta Mol Cell Biol Lipids* (2019) 1864(6):763–5. doi: 10.1016/j.bbalip.2019.02.005
14. Murakami M. Lipoquality Control by Phospholipase A_2 Enzymes. *Proc Jpn Acad Ser B Phys Biol Sci* (2017) 93(9):677–702. doi: 10.2183/pjab.93.043
15. Murakami M, Sato H, Taketomi Y. Updating Phospholipase A_2 Biology. *Biomolecules* (2020) 10(10):1457. doi: 10.3390/biom10101457
16. Uozumi N, Kume K, Nagase T, Nakatani N, Ishii S, Tashiro F, et al. Role of Cytosolic Phospholipase A_2 in Allergic Response and Parturition. *Nature* (1997) 390(6660):618–22. doi: 10.1038/37622
17. Ueno N, Taketomi Y, Yamamoto K, Hirabayashi T, Kamei D, Kita Y, et al. Analysis of Two Major Intracellular Phospholipases A_2 (PLA_2) in Mast Cells Reveals Crucial Contribution of Cytosolic $PLA_2\alpha$, Not CA^{2+}-Independent $PLA_2\beta$, to Lipid Mobilization in Proximal Mast Cells and Distal Fibroblasts. *J Biol Chem* (2011) 286(43):37249–63. doi: 10.1074/jbc.M111.290312
18. Shimanaka Y, Kono N, Taketomi Y, Arita M, Okayama Y, Tanaka Y, et al. Omega-3 Fatty Acid Epoxides are Autocrine Mediators That Control the Magnitude of IgE-Mediated Mast Cell Activation. *Nat Med* (2017) 23 (11):1287–97. doi: 10.1038/nm.4417
19. Moriyama H, Endo J, Kataoka M, Shimanaka Y, Kono N, Sugiura Y, et al. Omega-3 Fatty Acid Epoxides Produced by $PAF\text{-}AH^2$ in Mast Cells Regulate Pulmonary Vascular Remodeling. *Nat Commun* (2022) 13(1):3013. doi: 10.1038/s41467-022-30621-z
20. Taketomi Y, Ueno N, Kojima T, Sato H, Murase R, Yamamoto K, et al. Mast Cell Maturation Is Driven *via* a Group III Phospholipase A_2-Prostaglandin D_2-DP1 Receptor Paracrine Axis. *Nat Immunol* (2013) 14(6):554–63. doi: 10.1038/ni.2586
21. Taketomi Y, Endo Y, Higashi T, Murase R, Ono T, Taya C, et al. Mast Cell-Specific Deletion of Group III Secreted Phospholipase A_2 Impairs Mast Cell Maturation and Functions. *Cells* (2021) 10(7):1691. doi: 10.3390/cells10071691
22. Miki Y, Taketomi Y, Kidoguchi Y, Yamamoto K, Muramatsu K, Nishito Y, et al. Group IIA Secreted Phospholipase A_2 Controls Skin Carcinogenesis and Psoriasis by Shaping the Gut Microbiota. *JCI Insight* (2022) 7(2): e152611. doi: 10.1172/jci.insight.152611
23. Taketomi Y, Miki Y, Murakami M. Old But New: Group IIA Phospholipase A_2 as a Modulator of Gut Microbiota. *Metabolites* (2022) 12(4):352. doi: 10.3390/metabo12040352
24. Clark JD, Lin LL, Kriz RW, Ramesha CS, Sultzman LA, Lin AY, et al. A Novel Arachidonic Acid-Selective Cytosolic PLA_2 Contains a Ca^{2+}-Dependent Translocation Domain With Homology to PKC and GAP. *Cell* (1991) 65(6):1043–51. doi: 10.1016/0092-8674(91)90556-e
25. Lin LL, Wartmann M, Lin AY, Knopf JL, Seth A, Davis RJ. $cPLA_2$ is Phosphorylated and Activated by MAP Kinase. *Cell* (1993) 72(2):269–78. doi: 10.1016/0092-8674(93)90666-e
26. Casas J, Gijon MA, Vigo AG, Crespo MS, Balsinde J, Balboa MA. Phosphatidylinositol 4,5-Bisphosphate Anchors Cytosolic Group IVA Phospholipase A_2 to Perinuclear Membranes and Decreases its Calcium Requirement for Translocation in Live Cells. *Mol Biol Cell* (2006) 17(1):155–62. doi: 10.1091/mbc.e05-06-0545
27. Stahelin RV, Subramanian P, Vora M, Cho W, Chalfant CE. Ceramide-1-Phosphate Binds Group IVA Cytosolic Phospholipase A^2 *via* a Novel Site in the C^2 Domain. *J Biol Chem* (2007) 282(28):20467–74. doi: 10.1074/jbc.M701396200
28. Murakami M, Austen KF, Arm JP. The Immediate Phase of C-Kit Ligand Stimulation of Mouse Bone Marrow-Derived Mast Cells Elicits Rapid Leukotriene C_4 Generation Through Posttranslational Activation of Cytosolic Phospholipase A_2 and 5-Lipoxygenase. *J Exp Med* (1995) 182 (1):197–206. doi: 10.1084/jem.182.1.197
29. Murakami M, Matsumoto R, Urade Y, Austen KF, Arm JP. C-Kit Ligand Mediates Increased Expression of Cytosolic Phospholipase A_2, Prostaglandin Endoperoxide Synthase-1, and Hematopoietic Prostaglandin D_2 Synthase and Increased IgE-Dependent Prostaglandin D_2 Generation in Immature Mouse Mast Cells. *J Biol Chem* (1995) 270(7):3239–46. doi: 10.1074/jbc.270.7.3239
30. Murakami M, Austen KF, Bingham CO 3rd, Friend DS, Penrose JF, Arm JP. Interleukin-3 Regulates Development of the 5-Lipoxygenase/Leukotriene C_4 Synthase Pathway in Mouse Mast Cells. *J Biol Chem* (1995) 270(39):22653–6. doi: 10.1074/jbc.270.39.22653
31. Kanaoka Y, Boyce JA. Cysteinyl Leukotrienes and Their Receptors: Cellular Distribution and Function in Immune and Inflammatory Responses. *J Immunol* (2004) 173(3):1503–10. doi: 10.4049/jimmunol.173.3.1503
32. Murakami M, Matsumoto R, Austen KF, Arm JP. Prostaglandin Endoperoxide Synthase-1 and -2 Couple to Different Transmembrane Stimuli to Generate Prostaglandin D_2 in Mouse Bone Marrow-Derived Mast Cells. *J Biol Chem* (1994) 269(35):22269–75. doi: 10.1016/S0021-9258(17)31786-6
33. Murakami M, Bingham CO 3rd, Matsumoto R, Austen KF, Arm JP. IgE-Dependent Activation of Cytokine-Primed Mouse Cultured Mast Cells Induces a Delayed Phase of Prostaglandin D_2 Generation *via* Prostaglandin Endoperoxide Synthase-2. *J Immunol* (1995) 155(9):4445–53.
34. Ogasawara T, Murakami M, Suzuki-Nishimura T, Uchida MK, Kudo I. Mouse Bone Marrow-Derived Mast Cells Undergo Exocytosis, Prostanoid Generation, and Cytokine Expression in Response to G Protein-Activating Polybasic Compounds After Coculture With Fibroblasts in the Presence of c-Kit Ligand. *J Immunol* (1997) 158(1):393–404.
35. Murakami M, Taketomi Y. Secreted Phospholipase A_2 and Mast Cells. *Allergol Int* (2015) 64(1):4–10. doi: 10.1016/j.alit.2014.07.005
36. Fujishima H, Sanchez Mejia RO, Bingham CO3rd, Lam BK, Sapirstein A, Bonventre JV, et al. Cytosolic Phospholipase A_2 is Essential for Both the Immediate and the Delayed Phases of Eicosanoid Generation in Mouse Bone Marrow-Derived Mast Cells. *Proc Natl Acad Sci USA* (1999) 96(9):4803–7. doi: 10.1073/pnas.96.9.4803
37. Nakatani N, Uozumi N, Kume K, Murakami M, Kudo I, Shimizu T. Role of Cytosolic Phospholipase A_2 in the Production of Lipid Mediators and Histamine Release in Mouse Bone-Marrow-Derived Mast Cells. *Biochem J* (2000) 352(Pt 2):311–7. doi: 10.1042/bj3520311
38. Hewson CA, Patel S, Calzetta L, Campwala H, Havard S, Luscombe E, et al. Preclinical Evaluation of an Inhibitor of Cytosolic Phospholipase $A_2\alpha$ for the Treatment of Asthma. *J Pharmacol Exp Ther* (2012) 340(3):656–65. doi: 10.1124/jpet.111.186379
39. Irvin CG, Tu YP, Sheller JR, Funk CD. 5-Lipoxygenase Products are Necessary for Ovalbumin-Induced Airway Responsiveness in Mice. *Am J Physiol* (1997) 272(6 Pt 1):L1053–8. doi: 10.1152/ajplung.1997.272.6.L1053
40. Tager AM, Bromley SK, Medoff BD, Islam SA, Bercury SD, Friedrich EB, et al. Leukotriene B_4 Receptor BLT1 Mediates Early Effector T Cell Recruitment. *Nat Immunol* (2003) 4(10):982–90. doi: 10.1038/ni970

41. Kim DC, Hsu FI, Barrett NA, Friend DS, Grenningloh R, Ho IC, et al. Cysteinyl Leukotrienes Regulate Th2 Cell-Dependent Pulmonary Inflammation. *J Immunol* (2006) 176(7):4440–8. doi: 10.4049/jimmunol.176.7.4440
42. Barrett NA, Rahman OM, Fernandez JM, Parsons MW, Xing W, Austen KF, et al. Dectin-2 Mediates Th2 Immunity Through the Generation of Cysteinyl Leukotrienes. *J Exp Med* (2011) 208(3):593–604. doi: 10.1084/jem.20100793
43. Matsuoka T, Hirata M, Tanaka H, Takahashi Y, Murata T, Kabashima K, et al. Prostaglandin D_2 as a Mediator of Allergic Asthma. *Science* (2000) 287 (5460):2013–7. doi: 10.1126/science.287.5460.2013
44. Shiraishi Y, Asano K, Niimi K, Fukunaga K, Wakaki M, Kagyo J, et al. Cyclooxygenase-2/Prostaglandin D_2/CRTH2 Pathway Mediates Double-Stranded RNA-Induced Enhancement of Allergic Airway Inflammation. *J Immunol* (2008) 180(1):541–9. doi: 10.4049/jimmunol.180.1.541
45. Ishii S, Nagase T, Shindou H, Takizawa H, Ouchi Y, Shimizu T. Platelet-Activating Factor Receptor Develops Airway Hyperresponsiveness Independently of Airway Inflammation in a Murine Asthma Model. *J Immunol* (2004) 172(11):7095–102. doi: 10.4049/jimmunol.172.11.7095
46. Paruchuri S, Jiang Y, Feng C, Francis SA, Plutzky J, Boyce JA. Leukotriene E_4 Activates Peroxisome Proliferator-Activated Receptor γ and Induces Prostaglandin D_2 Generation by Human Mast Cells. *J Biol Chem* (2008) 283(24):16477–87. doi: 10.1074/jbc.M705822200
47. Lazarinis N, Bood J, Gomez C, Kolmert J, Lantz AS, Gyllfors P, et al. Leukotriene E_4 Induces Airflow Obstruction and Mast Cell Activation Through the Cysteinyl Leukotriene Type 1 Receptor. *J Allergy Clin Immunol* (2018) 142(4):1080–9. doi: 10.1016/j.jaci.2018.02.024
48. Henderson WRJr., Tang LO, Chu SJ, Tsao SM, Chiang GK, Jones F, et al. A Role for Cysteinyl Leukotrienes in Airway Remodeling in a Mouse Asthma Model. *Am J Respir Crit Care Med* (2002) 165(1):108–16. doi: 10.1164/ajrccm.165.1.2105051
49. Jiang Y, Kanaoka Y, Feng C, Nocka K, Rao S, Boyce JA. Cutting Edge: Interleukin 4-Dependent Mast Cell Proliferation Requires Autocrine/Intracrine Cysteinyl Leukotriene-Induced Signaling. *J Immunol* (2006) 177 (5):2755–9. doi: 10.4049/jimmunol.177.5.2755
50. Jiang Y, Borrelli LA, Kanaoka Y, Bacskai BJ, Boyce JA. $CysLT_2$ Receptors Interact With CysLT1 Receptors and Down-Modulate Cysteinyl Leukotriene Dependent Mitogenic Responses of Mast Cells. *Blood* (2007) 110(9):3263–70. doi: 10.1182/blood-2007-07-100453
51. Doherty TA, Khorram N, Lund S, Mehta AK, Croft M, Broide DH. Lung Type 2 Innate Lymphoid Cells Express Cysteinyl Leukotriene Receptor 1, Which Regulates TH2 Cytokine Production. *J Allergy Clin Immunol* (2013) 132(1):205–13. doi: 10.1016/j.jaci.2013.03.048
52. Salimi M, Stoger L, Liu W, Go S, Pavord I, Klenerman P, et al. Cysteinyl Leukotriene E_4 Activates Human Group 2 Innate Lymphoid Cells and Enhances the Effect of Prostaglandin D_2 and Epithelial Cytokines. *J Allergy Clin Immunol* (2017) 140(4):1090–100.e11. doi: 10.1016/j.jaci.2016.12.958
53. von Moltke J, O'Leary CE, Barrett NA, Kanaoka Y, Austen KF, Locksley RM. Leukotrienes Provide an NFAT-Dependent Signal That Synergizes With IL-33 to Activate ILC2s. *J Exp Med* (2017) 214(1):27–37. doi: 10.1084/jem.20161274
54. Liu T, Barrett NA, Kanaoka Y, Yoshimoto E, Garofalo D, Cirka H, et al. Type 2 Cysteinyl Leukotriene Receptors Drive IL-33-Dependent Type 2 Immunopathology and Aspirin Sensitivity. *J Immunol* (2018) 200(3):915–27. doi: 10.4049/jimmunol.1700603
55. Bankova LG, Dwyer DF, Yoshimoto E, Ualiyeva S, McGinty JW, Raff H, et al. The Cysteinyl Leukotriene 3 Receptor Regulates Expansion of IL-25-Producing Airway Brush Cells Leading to Type 2 Inflammation. *Sci Immunol* (2018) 3(28):eaat9453. doi: 10.1126/sciimmunol.aat9453
56. McGinty JW, Ting HA, Billipp TE, Nadjsombati MS, Khan DM, Barrett NA, et al. Tuft-Cell-Derived Leukotrienes Drive Rapid Anti-Helminth Immunity in the Small Intestine But are Dispensable for Anti-Protist Immunity. *Immunity* (2020) 52(3):528–41.e7. doi: 10.1016/j.immuni.2020.02.005
57. Leyva-Castillo JM, Galand C, Kam C, Burton O, Gurish M, Musser MA, et al. Mechanical Skin Injury Promotes Food Anaphylaxis by Driving Intestinal Mast Cell Expansion. *Immunity* (2019) 50(5):1262–75.E_4. doi: 10.1016/j.immuni.2019.03.023
58. Voisin T, Perner C, Messou MA, Shiers S, Ualiyeva S, Kanaoka Y, et al. The CysLT2R Receptor Mediates Leukotriene C_4-Driven Acute and Chronic Itch. *Proc Natl Acad Sci USA* (2021) 118(13):E2022087118. doi: 10.1073/pnas.2022087118
59. Wang F, Trier AM, Li F, Kim S, Chen Z, Chai JN, et al. A Basophil-Neuronal Axis Promotes Itch. *Cell* (2021) 184(2):422–40.e17. doi: 10.1016/j.cell.2020.12.033
60. Hammad H, de Heer HJ, Soullie T, Hoogsteden HC, Trottein F, Lambrecht BN. Prostaglandin D_2 Inhibits Airway Dendritic Cell Migration and Function in Steady State Conditions by Selective Activation of the D Prostanoid Receptor 1. *J Immunol* (2003) 171(8):3936–40. doi: 10.4049/jimmunol.171.8.3936
61. Yamamoto Y, Otani S, Hirai H, Nagata K, Aritake K, Urade Y, et al. Dual Functions of Prostaglandin D_2 in Murine Contact Hypersensitivity *via* DP and CRTH2. *Am J Pathol* (2011) 179(1):302–14. doi: 10.1016/j.ajpath.2011.03.047
62. Nakamura T, Fujiwara Y, Yamada R, Fujii W, Hamabata T, Lee MY, et al. Mast Cell-Derived Prostaglandin D_2 Attenuates Anaphylactic Reactions in Mice. *J Allergy Clin Immunol* (2017) 140(2):630–2.e9. doi: 10.1016/j.jaci.2017.02.030
63. Nakamura T, Maeda S, Horiguchi K, Maehara T, Aritake K, Choi BI, et al. PGD_2 Deficiency Exacerbates Food Antigen-Induced Mast Cell Hyperplasia. *Nat Commun* (2015) 6:7514. doi: 10.1038/ncomms8514
64. Trivedi SG, Newson J, Rajakariar R, Jacques TS, Hannon R, Kanaoka Y, et al. Essential Role for Hematopoietic Prostaglandin D_2 Synthase in the Control of Delayed Type Hypersensitivity. *Proc Natl Acad Sci U.S.A.* (2006) 103 (13):5179–84. doi: 10.1073/pnas.0507175103
65. Xue L, Salimi M, Panse I, Mjosberg JM, McKenzie AN, Spits H, et al. Prostaglandin D_2 Activates Group 2 Innate Lymphoid Cells Through Chemoattractant Receptor-Homologous Molecule Expressed on TH2 Cells. *J Allergy Clin Immunol* (2014) 133(4):1184–94. doi: 10.1016/j.jaci.2013.10.056
66. Wojno ED, Monticelli LA, Tran SV, Alenghat T, Osborne LC, Thome JJ, et al. The Prostaglandin D_2 Receptor $CRTH^2$ Regulates Accumulation of Group 2 Innate Lymphoid Cells in the Inflamed Lung. *Mucosal Immunol* (2015) 8(6):1313–23. doi: 10.1038/mi.2015.21
67. Xue L, Barrow A, Fleming VM, Hunter MG, Ogg G, Klenerman P, et al. Leukotriene E_4 Activates Human Th2 Cells for Exaggerated Proinflammatory Cytokine Production in Response to Prostaglandin D_2. *J Immunol* (2012) 188(2):694–702. doi: 10.4049/jimmunol.1102474
68. Xiong Z, Zhu X, Geng J, Xu Y, Wu R, Li C, et al. Intestinal Tuft-2 Cells Exert Antimicrobial Immunity *via* Sensing Bacterial Metabolite N-Undecanoylglycine. *Immunity* (2022) 55(4):686–700.e7. doi: 10.1016/j.immuni.2022.03.001
69. Kunikata T, Yamane H, Segi E, Matsuoka T, Sugimoto Y, Tanaka S, et al. Suppression of Allergic Inflammation by the Prostaglandin E Receptor Subtype EP3. *Nat Immunol* (2005) 6(5):524–31. doi: 10.1038/ni1188
70. Honda T, Matsuoka T, Ueta M, Kabashima K, Miyachi Y, Narumiya S. Prostaglandin E_2-EP3 Signaling Suppresses Skin Inflammation in Murine Contact Hypersensitivity. *J Allergy Clin Immunol* (2009) 124(4):809–18.E2. doi: 10.1016/j.jaci.2009.04.029
71. Morimoto K, Shirata N, Taketomi Y, Tsuchiya S, Segi-Nishida E, Inazumi T, et al. Prostaglandin E_2-EP3 Signaling Induces Inflammatory Swelling by Mast Cell Activation. *J Immunol* (2014) 192(3):1130–7. doi: 10.4049/jimmunol.1300290
72. Liu T, Laidlaw TM, Katz HR, Boyce JA. Prostaglandin E_2 Deficiency Causes a Phenotype of Aspirin Sensitivity That Depends on Platelets and Cysteinyl Leukotrienes. *Proc Natl Acad Sci USA* (2013) 110(42):16987–92. doi: 10.1073/pnas.1313185110
73. Liu T, Garofalo D, Feng C, Lai J, Katz H, Laidlaw TM, et al. Platelet-Driven Leukotriene C_4-Mediated Airway Inflammation in Mice is Aspirin-Sensitive and Depends on T Prostanoid Receptors. *J Immunol* (2015) 194(11):5061–8. doi: 10.4049/jimmunol.1402959
74. Feng C, Beller EM, Bagga S, Boyce JA. Human Mast Cells Express Multiple EP Receptors for Prostaglandin E_2 That Differentially Modulate Activation Responses. *Blood* (2006) 107(8):3243–50. doi: 10.1182/blood-2005-07-2772
75. Safholm J, Manson ML, Bood J, Delin I, Orre AC, Bergman P, et al. Prostaglandin E_2 Inhibits Mast Cell-Dependent Bronchoconstriction in Human Small Airways Through the E Prostanoid Subtype 2 Receptor. *J Allergy Clin Immunol* (2015) 136(5):1232–9.e1. doi: 10.1016/j.jaci.2015.04.002

76. Rastogi S, Willmes DM, Nassiri M, Babina M, Worm M. PGE_2 Deficiency Predisposes to Anaphylaxis by Causing Mast Cell Hyperresponsiveness. *J Allergy Clin Immunol* (2020) 146(6):1387–96.e13. doi: 10.1016/j.jaci.2020.03.046
77. Lundequist A, Nallamshetty SN, Xing W, Feng C, Laidlaw TM, Uematsu S, et al. Prostaglandin E_2 Exerts Homeostatic Regulation of Pulmonary Vascular Remodeling in Allergic Airway Inflammation. *J Immunol* (2010) 184(1):433–41. doi: 10.4049/jimmunol.0902835
78. Sturm EM, Schratl P, Schuligoi R, Konya V, Sturm GJ, Lippe IT, et al. Prostaglandin E_2 Inhibits Eosinophil Trafficking Through E-Prostanoid 2 Receptors. *J Immunol* (2008) 181(10):7273–83. doi: 10.4049/jimmunol.181.10.7273
79. Okano M, Fujiwara T, Haruna T, Kariya S, Makihara S, Higaki T, et al. Prostaglandin E_2 Suppresses Staphylococcal Enterotoxin-Induced Eosinophilia-Associated Cellular Responses Dominantly Through an E-Prostanoid 2-Mediated Pathway in Nasal Polyps. *J Allergy Clin Immunol* (2009) 123(4):868–74.e13. doi: 10.1016/j.jaci.2009.01.047
80. Maric J, Ravindran A, Mazzurana L, Bjorklund AK, Van Acker A, Rao A, et al. Prostaglandin E_2 Suppresses Human Group 2 Innate Lymphoid Cell Function. *J Allergy Clin Immunol* (2018) 141(5):1761–73.e6. doi: 10.1016/j.jaci.2017.09.050
81. Okano M, Sugata Y, Fujiwara T, Matsumoto R, Nishibori M, Shimizu K, et al. E Prostanoid 2 (EP2)/EP4-Mediated Suppression of Antigen-Specific Human T-Cell Responses by Prostaglandin E_2. *Immunology* (2006) 118 (3):343–52. doi: 10.1111/j.1365-2567.2006.02376.x
82. Sawada Y, Honda T, Nakamizo S, Nakajima S, Nonomura Y, Otsuka A, et al. Prostaglandin E_2 (PGE_2)-EP2 Signaling Negatively Regulates Murine Atopic Dermatitis-Like Skin Inflammation by Suppressing Thymic Stromal Lymphopoietin Expression. *J Allergy Clin Immunol* (2019) 144(5):1265–73.e9. doi: 10.1016/j.jaci.2019.06.036
83. Hattori M, Arai H. Intracellular PAF-Acetylhydrolase Type I. *Enzymes* (2015) 38:23–36. doi: 10.1016/bs.enz.2015.09.007
84. Kono N, Arai H. Intracellular Platelet-Activating Factor Acetylhydrolase, Type II: A Unique Cellular Phospholipase A_2 That Hydrolyzes Oxidatively Modified Phospholipids. *Enzymes* (2015) 38:43–54. doi: 10.1016/bs.enz.2015.09.008
85. Tjoelker LW, Wilder C, Eberhardt C, Stafforini DM, Dietsch G, Schimpf B, et al. Anti-Inflammatory Properties of a Platelet-Activating Factor Acetylhydrolase. *Nature* (1995) 374(6522):549–53. doi: 10.1038/374549a0
86. Oh DY, Talukdar S, Bae EJ, Imamura T, Morinaga H, Fan W, et al. GPR120 is an Omega-3 Fatty Acid Receptor Mediating Potent Anti-Inflammatory and Insulin-Sensitizing Effects. *Cell* (2010) 142(5):687–98. doi: 10.1016/j.cell.2010.07.041
87. Oh DY, Walenta E, Akiyama TE, Lagakos WS, Lackey D, Pessentheiner AR, et al. A Gpr120-Selective Agonist Improves Insulin Resistance and Chronic Inflammation in Obese Mice. *Nat Med* (2014) 20(8):942–7. doi: 10.1038/nm.3614
88. Isobe Y, Itagaki M, Ito Y, Naoe S, Kojima K, Ikeguchi M, et al. Comprehensive Analysis of the Mouse Cytochrome P450 Family Responsible for Omega-3 Epoxidation of Eicosapentaenoic Acid. *Sci Rep* (2018) 8(1):7954. doi: 10.1038/s41598-018-26325-4
89. Luangsay S, Wittamer V, Bondue B, De Henau O, Rouger L, Brait M, et al. Mouse ChemR23 is Expressed in Dendritic Cell Subsets and Macrophages, and Mediates an Anti-Inflammatory Activity of Chemerin in a Lung Disease Model. *J Immunol* (2009) 183(10):6489–99. doi: 10.4049/jimmunol.0901037
90. Krishnamoorthy S, Recchiuti A, Chiang N, Yacoubian S, Lee CH, Yang R, et al. Resolvin D1 Binds Human Phagocytes With Evidence for Proresolving Receptors. *Proc Natl Acad Sci USA* (2010) 107(4):1660–5. doi: 10.1073/pnas.0907342107
91. Chiang N, Dalli J, Colas RA, Serhan CN. Identification of Resolvin D_2 Receptor Mediating Resolution of Infections and Organ Protection. *J Exp Med* (2015) 212(8):1203–17. doi: 10.1084/jem.20150225
92. Bang S, Xie YK, Zhang ZJ, Wang Z, Xu ZZ, Ji RR. GPR37 Regulates Macrophage Phagocytosis and Resolution of Inflammatory Pain. *J Clin Invest* (2018) 128(8):3568–82. doi: 10.1172/JCI99888
93. Chiang N, Libreros S, Norris PC, de la Rosa X, Serhan CN. Maresin 1 Activates LGR6 Receptor Promoting Phagocyte Immunoresolvent Functions. *J Clin Invest* (2019) 129(12):5294–311. doi: 10.1172/JCI129448
94. Basil MC, Levy BD. Specialized Pro-Resolving Mediators: Endogenous Regulators of Infection and Inflammation. *Nat Rev Immunol* (2016) 16 (1):51–67. doi: 10.1038/nri.2015.4
95. Serhan CN, Levy BD. Resolvins in Inflammation: Emergence of the Pro-Resolving Superfamily of Mediators. *J Clin Invest* (2018) 128(7):2657–69. doi: 10.1172/JCI97943
96. Metz M, Piliponsky AM, Chen CC, Lammel V, Abrink M, Pejler G, et al. Mast Cells can Enhance Resistance to Snake and Honeybee Venoms. *Science* (2006) 313(5786):526–30. doi: 10.1126/science.1128877
97. Abraham SN, St John AL. Mast Cell-Orchestrated Immunity to Pathogens. *Nat Rev Immunol* (2010) 10(6):440–52. doi: 10.1038/nri2782
98. Nagatake T, Shiogama Y, Inoue A, Kikuta J, Honda T, Tiwari P, et al. The 17,18-Epoxyeicosatetraenoic Acid-G Protein-Coupled Receptor 40 Axis Ameliorates Contact Hypersensitivity by Inhibiting Neutrophil Mobility in Mice and Cynomolgus Macaques. *J Allergy Clin Immunol* (2018) 142 (2):470–84.e12. doi: 10.1016/j.jaci.2017.09.053
99. Nakajima K, Murakami M, Yanoshita R, Samejima Y, Karasawa K, Setaka M, et al. Activated Mast Cells Release Extracellular Type Platelet-Activating Factor Acetylhydrolase That Contributes to Autocrine Inactivation of Platelet-Activating Factor. *J Biol Chem* (1997) 272(32):19708–13. doi: 10.1074/jbc.272.32.19708
100. Dwyer DF, Barrett NA, Austen KFImmunological Genome Project C. Expression Profiling of Constitutive Mast Cells Reveals a Unique Identity Within the Immune System. *Nat Immunol* (2016) 17(7):878–87. doi: 10.1038/ni.3445
101. Lambeau G, Gelb MH. Biochemistry and Physiology of Mammalian Secreted Phospholipases A_2. *Annu Rev Biochem* (2008) 77:495–520. doi: 10.1146/annurev.biochem.76.062405.154007
102. Murakami M, Taketomi Y, Miki Y, Sato H, Hirabayashi T, Yamamoto K. Recent Progress in Phospholipase A_2 Research: From Cells to Animals to Humans. *Prog Lipid Res* (2011) 50(2):152–92. doi: 10.1016/j.plipres.2010.12.001
103. Murakami M, Sato H, Miki Y, Yamamoto K, Taketomi Y. A New Era of Secreted Phospholipase A_2. *J Lipid Res* (2015) 56(7):1248–61. doi: 10.1194/jlr.R058123
104. Murakami M, Yamamoto K, Miki Y, Murase R, Sato H, Taketomi Y. The Roles of the Secreted Phospholipase A_2 Gene Family in Immunology. *Adv Immunol* (2016) 132:91–134. doi: 10.1016/bs.ai.2016.05.001
105. Murakami M, Miki Y, Sato H, Murase R, Taketomi Y, Yamamoto K. Group IID, IIE, IIF and III Secreted Phospholipase A_2s. *Biochim Biophys Acta Mol Cell Biol Lipids* (2019) 1864(6):803–18. doi: 10.1016/j.bbalip.2018.08.014
106. Murakami M, Kudo I, Inoue K. Eicosanoid Generation From Antigen-Primed Mast Cells by Extracellular Mammalian 14-kDa Group II Phospholipase A_2. *FEBS Lett* (1991) 294(3):247–51. doi: 10.1016/0014-5793(91)81440-j
107. Murakami M, Kudo I, Suwa Y, Inoue K. Release of 14-kDa Group-II Phospholipase A_2 From Activated Mast Cells and its Possible Involvement in the Regulation of the Degranulation Process. *Eur J Biochem* (1992) 209 (1):257–65. doi: 10.1111/j.1432-1033.1992.tb17284.x
108. Murakami M, Hara N, Kudo I, Inoue K. Triggering of Degranulation in Mast Cells by Exogenous Type II Phospholipase A_2. *J Immunol* (1993) 151 (10):5675–84.
109. Bingham CO3rd, Fijneman RJ, Friend DS, Goddeau RP, Rogers RA, Austen KF, et al. Low Molecular Weight Group IIA and Group V Phospholipase A_2 Enzymes Have Different Intracellular Locations in Mouse Bone Marrow-Derived Mast Cells. *J Biol Chem* (1999) 274(44):31476–84. doi: 10.1074/jbc.274.44.31476
110. Enomoto A, Murakami M, Valentin E, Lambeau G, Gelb MH, Kudo I. Redundant and Segregated Functions of Granule-Associated Heparin-Binding Group II Subfamily of Secretory Phospholipases A_2 in the Regulation of Degranulation and Prostaglandin D_2 Synthesis in Mast Cells. *J Immunol* (2000) 165(7):4007–14. doi: 10.4049/jimmunol.165.7.4007
111. Murakami M, Koduri RS, Enomoto A, Shimbara S, Seki M, Yoshihara K, et al. Distinct Arachidonate-Releasing Functions of Mammalian Secreted Phospholipase A_2s in Human Embryonic Kidney 293 and Rat Mastocytoma RBL-2H3 Cells Through Heparan Sulfate Shuttling and External Plasma Membrane Mechanisms. *J Biol Chem* (2001) 276(13):10083–96. doi: 10.1074/jbc.M007877200

112. Triggiani M, Giannattasio G, Calabrese C, Loffredo S, Granata F, Fiorello A, et al. Lung Mast Cells Are a Source of Secreted Phospholipases A_2. *J Allergy Clin Immunol* (2009) 124(3):558–65, 65.e1-3. doi: 10.1016/j.jaci.2009.04.035
113. Granata F, Staiano RI, Loffredo S, Petraroli A, Genovese A, Marone G, et al. The Role of Mast Cell-Derived Secreted Phospholipases A_2 in Respiratory Allergy. *Biochimie* (2010) 92(6):588–93. doi: 10.1016/j.biochi.2010.02.030
114. Palm NW, Rosenstein RK, Yu S, Schenten DD, Florsheim E, Medzhitov R. Bee Venom Phospholipase A_2 Induces a Primary Type 2 Response That Is Dependent on the Receptor ST2 and Confers Protective Immunity. *Immunity* (2013) 39(5):976–85. doi: 10.1016/j.immuni.2013.10.006
115. Boudreau LH, Duchez AC, Cloutier N, Soulet D, Martin N, Bollinger J, et al. Platelets Release Mitochondria Serving as Substrate for Bactericidal Group IIA-Secreted Phospholipase A_2 to Promote Inflammation. *Blood* (2014) 124 (14):2173–83. doi: 10.1182/blood-2014-05-573543
116. Kudo K, Miki Y, Carreras J, Nakayama S, Nakamoto Y, Ito M, et al. Secreted Phospholipase A_2 Modifies Extracellular Vesicles and Accelerates B Cell Lymphoma. *Cell Metab* (2022) 34(4):615–33.e8. doi: 10.1016/j.cmet.2022.02.011
117. Grimbaldeston MA, Nakae S, Kalesnikoff J, Tsai M, Galli SJ. Mast Cell-Derived Interleukin 10 Limits Skin Pathology in Contact Dermatitis and Chronic Irradiation With Ultraviolet B. *Nat Immunol* (2007) 8(10):1095–104. doi: 10.1038/ni1503
118. Hershko AY, Suzuki R, Charles N, Alvarez-Errico D, Sargent JL, Laurence A, et al. Mast Cell Interleukin-2 Production Contributes to Suppression of Chronic Allergic Dermatitis. *Immunity* (2011) 35(4):562–71. doi: 10.1016/j.immuni.2011.07.013
119. Dudeck A, Dudeck J, Scholten J, Petzold A, Surianarayanan S, Kohler A, et al. Mast Cells are Key Promoters of Contact Allergy That Mediate the Adjuvant Effects of Haptens. *Immunity* (2011) 34(6):973–84. doi: 10.1016/j.immuni.2011.03.028
120. Reber LL, Sibilano R, Starkl P, Roers A, Grimbaldeston MA, Tsai M, et al. Imaging Protective Mast Cells in Living Mice During Severe Contact Hypersensitivity. *JCI Insight* (2017) 2(9):e92900. doi: 10.1172/jci.insight.92900
121. Boilard E, Lai Y, Larabee K, Balestrieri B, Ghomashchi F, Fujioka D, et al. A Novel Anti-Inflammatory Role for Secretory Phospholipase A_2 in Immune Complex-Mediated Arthritis. *EMBO Mol Med* (2010) 2(5):172–87. doi: 10.1002/emmm.201000072
122. Hamaguchi K, Kuwata H, Yoshihara K, Masuda S, Shimbara S, Oh-ishi S, et al. Induction of Distinct Sets of Secretory Phospholipase A_2 in Rodents During Inflammation. *Biochim Biophys Acta* (2003) 1635(1):37–47. doi: 10.1016/j.bbalip.2003.10.004
123. Snider JM, You JK, Wang X, Snider AJ, Hallmark B, Zec MM, et al. Group IIA Secreted Phospholipase A_2 is Associated With the Pathobiology Leading to COVID-19 Mortality. *J Clin Invest* (2021) 131(19):e149236. doi: 10.1172/JCI149236
124. Weinrauch Y, Abad C, Liang NS, Lowry SF, Weiss J. Mobilization of Potent Plasma Bactericidal Activity During Systemic Bacterial Challenge. Role of Group IIA Phospholipase A_2. *J Clin Invest* (1998) 102(3):633–8. doi: 10.1172/JCI3121
125. Murakami M, Kudo I, Umeda M, Matsuzawa A, Takeda M, Komada M, et al. Detection of Three Distinct Phospholipases A_2 in Cultured Mast Cells. *J Biochem* (1992) 111(2):175–81. doi: 10.1093/oxfordjournals.jbchem.a123733
126. Chock SP, Schmauder-Chock EA, Cordella-Miele E, Miele L, Mukherjee AB. The Localization of Phospholipase A_2 in the Secretory Granule. *Biochem J* (1994) 300(Pt 3):619–22. doi: 10.1042/bj3000619
127. Kennedy BP, Payette P, Mudgett J, Vadas P, Pruzanski W, Kwan M, et al. A Natural Disruption of the Secretory Group II Phospholipase A_2 Gene in Inbred Mouse Strains. *J Biol Chem* (1995) 270(38):22378–85. doi: 10.1074/jbc.270.38.22378
128. MacPhee M, Chepenik KP, Liddell RA, Nelson KK, Siracusa LD, Buchberg AM. The Secretory Phospholipase A_2 Gene is a Candidate for the *Mom1* Locus, a Major Modifier of Apc^{Min}-Induced Intestinal Neoplasia. *Cell* (1995) 81(6):957–66. doi: 10.1016/0092-8674(95)90015-2
129. Mulherkar R, Rao RS, Wagle AS, Patki V, Deo MG. Enhancing Factor, a Paneth Cell Specific Protein From Mouse Small Intestines: Predicted Amino Acid Sequence From RT-PCR Amplified cDNA and its Expression. *Biochem Biophys Res Commun* (1993) 195(3):1254–63. doi: 10.1006/bbrc.1993.2179
130. Schewe M, Franken PF, Sacchetti A, Schmitt M, Joosten R, Bottcher R, et al. Secreted Phospholipases A_2 Are Intestinal Stem Cell Niche Factors With Distinct Roles in Homeostasis, Inflammation, and Cancer. *Cell Stem Cell* (2016) 19(1):38–51. doi: 10.1016/j.stem.2016.05.023
131. Bingham CO3rd, Murakami M, Fujishima H, Hunt JE, Austen KF, Arm JP. A Heparin-Sensitive Phospholipase A_2 and Prostaglandin Endoperoxide Synthase-2 Are Functionally Linked in the Delayed Phase of Prostaglandin D_2 Generation in Mouse Bone Marrow-Derived Mast Cells. *J Biol Chem* (1996) 271(42):25936–44. doi: 10.1074/jbc.271.42.25936
132. Dore E, Joly-Beauparlant C, Morozumi S, Mathieu A, Levesque T, Allaeys I, et al. The Interaction of Secreted Phospholipase A_2-IIA With the Microbiota Alters its Lipidome and Promotes Inflammation. *JCI Insight* (2022) 7(2):e152638. doi: 10.1172/jci.insight.152638
133. Duchez AC, Boudreau LH, Naika GS, Bollinger J, Belleannee C, Cloutier N, et al. Platelet Microparticles are Internalized in Neutrophils *via* the Concerted Activity of 12-Lipoxygenase and Secreted Phospholipase A_2-IIA. *Proc Natl Acad Sci USA* (2015) 112(27):E3564–73. doi: 10.1073/pnas.1507905112
134. Rouault M, Le Calvez C, Boilard E, Surrel F, Singer A, Ghomashchi F, et al. Recombinant Production and Properties of Binding of the Full Set of Mouse Secreted Phospholipases A_2 to the Mouse M-Type Receptor. *Biochemistry* (2007) 46(6):1647–62. doi: 10.1021/bi062119b
135. Reddy ST, Herschman HR. Transcellular Prostaglandin Production Following Mast Cell Activation is Mediated by Proximal Secretory Phospholipase A_2 and Distal Prostaglandin Synthase 1. *J Biol Chem* (1996) 271(1):186–91. doi: 10.1074/jbc.271.1.186
136. Reddy ST, Herschman HR. Prostaglandin Synthase-1 and Prostaglandin Synthase-2 are Coupled to Distinct Phospholipases for the Generation of Prostaglandin D_2 in Activated Mast Cells. *J Biol Chem* (1997) 272(6):3231–7. doi: 10.1074/jbc.272.6.3231
137. Reddy ST, Winstead MV, Tischfield JA, Herschman HR. Analysis of the Secretory Phospholipase A_2 That Mediates Prostaglandin Production in Mast Cells. *J Biol Chem* (1997) 272(21):13591–6. doi: 10.1074/jbc.272.21.13591
138. Kikawada E, Bonventre JV, Arm JP. Group V Secretory PLA_2 Regulates TLR2-Dependent Eicosanoid Generation in Mouse Mast Cells Through Amplification of ERK and $cPLA_2\alpha$ Activation. *Blood* (2007) 110(2):561–7. doi: 10.1182/blood-2006-10-052258
139. Nolin JD, Lai Y, Ogden HL, Manicone AM, Murphy RC, An D, et al. Secreted PLA_2 Group X Orchestrates Innate and Adaptive Immune Responses to Inhaled Allergen. *JCI Insight* (2017) 2(21):e94929. doi: 10.1172/jci.insight.94929
140. Munoz NM, Meliton AY, Arm JP, Bonventre JV, Cho W, Leff AR. Deletion of Secretory Group V Phospholipase A_2 Attenuates Cell Migration and Airway Hyperresponsiveness in Immunosensitized Mice. *J Immunol* (2007) 179(7):4800–7. doi: 10.4049/jimmunol.179.7.4800
141. Giannattasio G, Fujioka D, Xing W, Katz HR, Boyce JA, Balestrieri B. Group V Secretory Phospholipase A_2 Reveals its Role in House Dust Mite-Induced Allergic Pulmonary Inflammation by Regulation of Dendritic Cell Function. *J Immunol* (2010) 185(7):4430–8. doi: 10.4049/jimmunol.1001384
142. Ohta S, Imamura M, Xing W, Boyce JA, Balestrieri B. Group V Secretory Phospholipase A_2 is Involved in Macrophage Activation and is Sufficient for Macrophage Effector Functions in Allergic Pulmonary Inflammation. *J Immunol* (2013) 190(12):5927–38. doi: 10.4049/jimmunol.1203202
143. Yamaguchi M, Samuchiwal SK, Quehenberger O, Boyce JA, Balestrieri B. Macrophages Regulate Lung ILC2 Activation *via* PlA^2g5-Dependent Mechanisms. *Mucosal Immunol* (2018) 11(3):615–26. doi: 10.1038/mi.2017.99
144. Henderson WRJr., Chi EY, Bollinger JG, Tien YT, Ye X, Castelli L, et al. Importance of Group X-Secreted Phospholipase A_2 in Allergen-Induced Airway Inflammation and Remodeling in a Mouse Asthma Model. *J Exp Med* (2007) 204(4):865–77. doi: 10.1084/jem.20070029
145. Henderson WRJr., Ye X, Lai Y, Ni Z, Bollinger JG, Tien YT, et al. Key Role of Group V Secreted Phospholipase A_2 in Th2 Cytokine and Dendritic Cell-Driven Airway Hyperresponsiveness and Remodeling. *PloS One* (2013) 8(2):e56172. doi: 10.1371/journal.pone.0056172
146. Diaz BL, Satake Y, Kikawada E, Balestrieri B, Arm JP. Group V Secretory Phospholipase A_2 Amplifies the Induction of Cyclooxygenase 2 and Delayed Prostaglandin D_2 Generation in Mouse Bone Marrow Culture-Derived Mast Cells in a Strain-Dependent Manner. *Biochim Biophys Acta* (2006) 1761 (12):1489–97. doi: 10.1016/j.bbalip.2006.09.009

147. Shi GP, Bot I, Kovanen PT. Mast Cells in Human and Experimental Cardiometabolic Diseases. *Nat Rev Cardiol* (2015) 12(11):643–58. doi: 10.1038/nrcardio.2015.117
148. Song WL, Stubbe J, Ricciotti E, Alamuddin N, Ibrahim S, Crichton I, et al. Niacin and Biosynthesis of PGD_2 by Platelet COX-1 in Mice and Humans. *J Clin Invest* (2012) 122(4):1459–68. doi: 10.1172/JCI59262
149. Heller EA, Liu E, Tager AM, Sinha S, Roberts JD, Koehn SL, et al. Inhibition of Atherogenesis in BLT1-Deficient Mice Reveals a Role for LTB_4 and BLT1 in Smooth Muscle Cell Recruitment. *Circulation* (2005) 112(4):578–86. doi: 10.1161/CIRCULATIONAHA.105.545616
150. Ii H, Hontani N, Toshida I, Oka M, Sato T, Akiba S. Group IVA Phospholipase A_2-Associated Production of MMP-9 in Macrophages and Formation of Atherosclerotic Lesions. *Biol Pharm Bull* (2008) 31(3):363–8. doi: 10.1248/bpb.31.363
151. Meng Z, Yan C, Deng Q, Dong X, Duan ZM, Gao DF, et al. Oxidized Low-Density Lipoprotein Induces Inflammatory Responses in Cultured Human Mast Cells *via* Toll-Like Receptor 4. *Cell Physiol Biochem* (2013) 31(6):842–53. doi: 10.1159/000350102
152. Bot M, de Jager SC, MacAleese L, Lagraauw HM, van Berkel TJ, Quax PH, et al. Lysophosphatidic Acid Triggers Mast Cell-Driven Atherosclerotic Plaque Destabilization by Increasing Vascular Inflammation. *J Lipid Res* (2013) 54(5):1265–74. doi: 10.1194/jlr.M032862
153. Bot M, Bot I, Lopez-Vales R, van de Lest CH, Saulnier-Blache JS, Helms JB, et al. Atherosclerotic Lesion Progression Changes Lysophosphatidic Acid Homeostasis to Favor its Accumulation. *Am J Pathol* (2010) 176(6):3073–84. doi: 10.2353/ajpath.2010.090009
154. Hanasaki K, Yamada K, Yamamoto S, Ishimoto Y, Saiga A, Ono T, et al. Potent Modification of Low Density Lipoprotein by Group X Secretory Phospholipase A_2 is Linked to Macrophage Foam Cell Formation. *J Biol Chem* (2002) 277(32):29116–24. doi: 10.1074/jbc.M202867200
155. Wooton-Kee CR, Boyanovsky BB, Nasser MS, de Villiers WJ, Webb NR. Group V $Spla_2$ Hydrolysis of Low-Density Lipoprotein Results in Spontaneous Particle Aggregation and Promotes Macrophage Foam Cell Formation. *Arterioscler Thromb Vasc Biol* (2004) 24(4):762–7. doi: 10.1161/01.ATV.0000122363.02961.c1
156. Pruzanski W, Lambeau L, Lazdunsky M, Cho W, Kopilov J, Kuksis A. Differential Hydrolysis of Molecular Species of Lipoprotein Phosphatidylcholine by Groups IIA, V and X Secretory Phospholipases A_2. *Biochim Biophys Acta* (2005) 1736(1):38–50. doi: 10.1016/j.bbalip.2005.07.005
157. Sato H, Kato R, Isogai Y, Saka G, Ohtsuki M, Taketomi Y, et al. Analyses of Group III Secreted Phospholipase A_2 Transgenic Mice Reveal Potential Participation of This Enzyme in Plasma Lipoprotein Modification, Macrophage Foam Cell Formation, and Atherosclerosis. *J Biol Chem* (2008) 283(48):33483–97. doi: 10.1074/jbc.M804628200
158. Ivandic B, Castellani LW, Wang XP, Qiao JH, Mehrabian M, Navab M, et al. Role of Group II Secretory Phospholipase A_2 in Atherosclerosis: 1. Increased Atherogenesis and Altered Lipoproteins in Transgenic Mice Expressing Group IIa Phospholipase A_2. *Arterioscler Thromb Vasc Biol* (1999) 19(5):1284–90. doi: 10.1161/01.atv.19.5.1284
159. Bostrom MA, Boyanovsky BB, Jordan CT, Wadsworth MP, Taatjes DJ, de Beer FC, et al. Group V Secretory Phospholipase A_2 Promotes Atherosclerosis: Evidence From Genetically Altered Mice. *Arterioscler Thromb Vasc Biol* (2007) 27(3):600–6. doi: 10.1161/01.ATV.0000257133.60884.44
160. Boyanovsky B, Zack M, Forrest K, Webb NR. The Capacity of Group V $Spla_2$ to Increase Atherogenicity of $ApoE^{-/-}$ and $LDLR^{-/-}$ Mouse LDL *In Vitro* Predicts its Atherogenic Role In Vivo. *Arterioscler Thromb Vasc Biol* (2009) 29(4):532–8. doi: 10.1161/ATVBAHA.108.183038
161. Zack M, Boyanovsky BB, Shridas P, Bailey W, Forrest K, Howatt DA, et al. Group X Secretory Phospholipase A_2 Augments Angiotensin II-Induced Inflammatory Responses and Abdominal Aortic Aneurysm Formation in apoE-Deficient Mice. *Atherosclerosis* (2011) 214(1):58–64. doi: 10.1016/j.atherosclerosis.2010.08.054
162. Ait-Oufella H, Herbin O, Lahoute C, Coatrieux C, Loyer X, Joffre J, et al. Group X Secreted Phospholipase A_2 Limits the Development of Atherosclerosis in LDL Receptor-Null Mice. *Arterioscler Thromb Vasc Biol* (2013) 33(3):466–73. doi: 10.1161/ATVBAHA.112.300309
163. Chiba H, Michibata H, Wakimoto K, Seishima M, Kawasaki S, Okubo K, et al. Cloning of a Gene for a Novel Epithelium-Specific Cytosolic Phospholipase A_2, $cPLA_2\delta$, Induced in Psoriatic Skin. *J Biol Chem* (2004) 279(13):12890–7. doi: 10.1074/jbc.M305801200
164. Cheung KL, Jarrett R, Subramaniam S, Salimi M, Gutowska-Owsiak D, Chen YL, et al. Psoriatic T Cells Recognize Neolipid Antigens Generated by Mast Cell Phospholipase Delivered by Exosomes and Presented by CD1a. *J Exp Med* (2016) 213(11):2399–412. doi: 10.1084/jem.20160258
165. Ohto T, Uozumi N, Hirabayashi T, Shimizu T. Identification of Novel Cytosolic Phospholipase A_2s, Murine $cPLA_2\delta$, ϵ, and ζ, Which Form a Gene Cluster With $cPLA_2\beta$. *J Biol Chem* (2005) 280(26):24576–83. doi: 10.1074/jbc.M413711200
166. Fensome-Green A, Stannard N, Li M, Bolsover S, Cockcroft S. Bromoenol Lactone, an Inhibitor of Group V1A Calcium-Independent Phospholipase A_2 Inhibits Antigen-Stimulated Mast Cell Exocytosis Without Blocking CA^{2+} Influx. *Cell Calcium* (2007) 41(2):145–53. doi: 10.1016/j.ceca.2006.06.002
167. Zimmermann R, Strauss JG, Haemmerle G, Schoiswohl G, Birner-Gruenberger R, Riederer M, et al. Fat Mobilization in Adipose Tissue is Promoted by Adipose Triglyceride Lipase. *Science* (2004) 306(5700):1383–6. doi: 10.1126/science.1100747
168. Dichlberger A, Schlager S, Maaninka K, Schneider WJ, Kovanen PT. Adipose Triglyceride Lipase Regulates Eicosanoid Production in Activated Human Mast Cells. *J Lipid Res* (2014) 55(12):2471–8. doi: 10.1194/jlr.M048553

Conflict of Interest: The authors declare that the research was conducted in the absence of any commercial and financial relationships that could be construed as a potential conflict of interest.

Publisher's Note: All claims expressed in this article are solely those of the authors and do not necessarily represent those of their affiliated organizations, or those of the publisher, the editors and the reviewers. Any product that may be evaluated in this article, or claim that may be made by its manufacturer, is not guaranteed or endorsed by the publisher.

Copyright © 2022 Taketomi and Murakami. This is an open-access article distributed under the terms of the Creative Commons Attribution License (CC BY). The use, distribution or reproduction in other forums is permitted, provided the original author(s) and the copyright owner(s) are credited and that the original publication in this journal is cited, in accordance with accepted academic practice. No use, distribution or reproduction is permitted which does not comply with these terms.

frontiers | Frontiers in Immunology

ORIGINAL RESEARCH
published: 28 June 2022
doi: 10.3389/fimmu.2022.892239

Spatiotemporal Patterns of Substance P-Bound MRGPRX2 Reveal a Novel Connection Between Macropinosome Resolution and Secretory Granule Regeneration in Mast Cells

Pia Lazki-Hagenbach[1], *Elisabeth Kleeblatt*[1], *Hydar Ali*[2] *and Ronit Sagi-Eisenberg*[1,3*]

[1] Department of Cell and Developmental Biology, Sackler Faculty of Medicine, Tel Aviv University, Tel Aviv, Israel, [2] Department of Basic and Translational Sciences, School of Dental Medicine, University of Pennsylvania, Philadelphia, PA, United States, [3] Sagol School of Neuroscience, Tel Aviv University, Tel Aviv, Israel

OPEN ACCESS

Edited by:
Frans J. Van Overveld, University College Roosevelt, Netherlands

Reviewed by:
Zane Orinska, Forschungszentrum Borstel, Germany
Claudia Gonzalez-Espinosa, Centro de Investigación y de Estudios Avanzados del Instituto Politécnico Nacional, Mexico

***Correspondence:**
Ronit Sagi-Eisenberg
histol3@tauex.tau.ac.il

Specialty section:
This article was submitted to Inflammation, a section of the journal Frontiers in Immunology

Received: 08 March 2022
Accepted: 30 May 2022
Published: 28 June 2022

Citation:
Lazki-Hagenbach P, Kleeblatt E, Ali H and Sagi-Eisenberg R (2022) Spatiotemporal Patterns of Substance P-Bound MRGPRX2 Reveal a Novel Connection Between Macropinosome Resolution and Secretory Granule Regeneration in Mast Cells. Front. Immunol. 13:892239. doi: 10.3389/fimmu.2022.892239

MRGPRX2, the human member of the MAS-related G protein coupled receptors (Mrgprs), serves as the cellular target of human mast cells (MCs) for innate ligands, including neuropeptides and antimicrobial peptides. In addition, MRGPRX2 also functions as the receptor for multiple FDA-approved drugs. As such, MRGPRX2 is a mediator of MC responses in neurogenic inflammation, host defense and pseudoallergy. We analyzed the spatiotemporal patterns of MRGPRX2 following its binding of the neuropeptide substance P (SP). Herein, we show that MRGPRX2 internalizes *via* both endocytosis and macropinocytosis, followed by its distribution between a perinuclear region and the secretory granules (SGs). Further, we show that MRGPRX2-containing macropinosomes undergo resolution by a mechanism that involves dynamin and LC3, giving rise to the incorporation of both LC3 and MRGPRX2 into the SGs. SP then promotes the acidification of the LC3-associated SGs, presumably by stimulating their fusion with lysosomes. Taken together, our results reveal a unique mode of MRGPRX2 trafficking that complements endocytosis and involves macropinocytosis, autophagic machinery-assisted macropinosome resolution and receptor delivery to the SGs.

Keywords: mast cell, MRGPRX2, substance P, endocytosis, autophagy, macropinocytosis, secretory granules

INTRODUCTION

While best known for their involvement in immunoglobulin E (IgE)-triggered allergy (1), mast cells (MCs) are key players in innate immune responses (2–4). Indeed, their strategic location in tissues that interface the external environment, jointly with their IgE-independent responses to multiple stressors, have marked them as sentinel cells and first responders to external insults (5). Both IgE-

Abbreviations: MC, Mast cell; SP, substance P; SG, secretory granule; TGN, trans Golgi network; IgE, immunoglobulin; GPCRs, G protein coupled receptors; Mrgprs, Mas-related G protein coupled receptors; CytD, cytochalasin D; FACS, flow cytometric analyses; MFI, mean fluorescence intensity; NK1, Neurokinin 1; DN, dominant negative; 3-MA, 3-methyladenine: UT, untreated; BF, brightfield; HA, hemagglutinin.

dependent and independent immune responses of the MCs are caused by the release of inflammatory mediators, part of which are pre-stored in cytoplasmic secretory granules (SGs) and released during regulated exocytosis (6, 7). Others, including lipid mediators, cytokines and chemokines are released following their *de novo* synthesis (8). Taken together, these mediators accomplish the important roles played by MCs in health and disease.

In particular intriguing are the responses of a subset of MCs to a variety of ligands, including neuropeptides, antimicrobial peptides and toxins, that share commonly only their positive charge (9, 10). MC responses to this class of stimuli play major roles in host defense and neurogenic inflammation (11–13). Furthermore, included in this class of ligands are multiple FDA-approved drugs, that by triggering MC degranulation cause pseudo-allergic reactions (14). The underlying mechanism(s) of MC activation by these positively charged stimuli has remained enigmatic until the recent identification of the Mas-related G protein coupled receptors (Mrgprs) as their cellular targets (15). This recognition has placed Mrgprs, and in particular MRGPRX2, the human member of this family, at a central position in MC biology.

The cellular functions of G protein coupled receptors (GPCRs) are tightly linked with their cellular positioning. Internalization and post-endocytic trafficking may terminate GPCR signaling or may prolong or diverse it (16–18). Therefore, we have undertaken to decipher the spatiotemporal patterns of MRGPRX2, following its binding of the neuropeptide substance P, that by binding to MRGPRX2 mediates the neuro-immune responses of MCs, such as in itch and pain (12, 19). Here we report on the unique patterns of MRGPRX2 internalization, that involve macropinocytosis and LC3-assisted delivery to the SGs.

MATERIAL AND METHODS

Antibodies and Reagents

Anti-human MRGPRX2 antibody (cat no. 359002) and anti-HA.11 Epitope Tag antibody (cat no. 901513) were from Biolegend (San Diego, CA). Anti-syntaxin 3 antibody (cat no. ab133750), secondary Alexa Fluor® 488 Goat Anti-Rabbit IgG H&L (cat no. ab150077, dilution 1:500) and secondary Alexa Fluor® 647 Goat Anti-Mouse IgG H&L (cat no. ab150115) were from Abcam (Cambridge, UK). Substance P (cat no. S6883), pitstop2 (cat no. SML1169) and saponin (cat no. S4521-25G) were purchased from Sigma-Aldrich (St Louis, MO, USA). Cytochalasin D (cat no. 1233), dynasore (cat no. 2897) and EIPA (cat no. 3378) were from Tocris Bioscience (Minneapolis, MN, USA). Tetramethylrhodamine (TRITC)- labeled 70 kDa dextran was purchased from Thermo Fischer Scientific (cat no. D1818, Waltham, MA, USA).

Plasmids Used in this Study

The following expression plasmids were used in this study: Neuropeptide Y (NPY)–mRFP and NPY Venus were a gift from Dr. U. Ashery (Tel Aviv University, Tel Aviv, Israel), NPY-CFP was a gift from Dr. P. Blinder, (Tel Aviv University, Tel Aviv, Israel). pEGFP-LC3 was a gift from Dr. A. Ashkenazi (Tel Aviv University, Tel Aviv, Israel), originally a gift from Tamotsu Yoshimori (Addgene plasmid # 21073; http://n2t.net/addgene:21073; RRID : Addgene_21073) and LC3-EGFP-mRFP (ptfLC3) was a gift from Dr. R. Pinkas Kramarski (Tel Aviv University, Tel Aviv, Israel), originally a gift from Dr. Tamotsu Yoshimori (Addgene plasmid # 21074; http://n2t.net/addgene:21074; RRID : Addgene_21074). Lifeact-GFP was a gift from Dr. B.-Z. Shilo (Weizmann Institute of Science, Rehovot, Israel) and pcDNA3-EGFP-Rac1-T17N was a gift from Dr. Gary Bokoch (Addgene plasmid # 12982; http://n2t.net/addgene:12982; RRID : Addgene_12982). pcDNA3-EGFP was a gift from Dr. J. Silvio Gutkind (University of California, San Diego, USA).

Cell Culture

RBL cells stably expressing N-terminally tagged hemagglutinin (HA) human MRGPRX2 (RBL-MRGPRX2) were generated as previously described (20). Cells were maintained at 37°C in a humidified incubator with 5% CO_2 in adherent cell cultures in low glucose DMEM (cat no. 01-050-1A, Biological Industries, Beit-Haemek, Israel) supplemented with 10% FBS (cat no. 12657, GIBCO, Grand Island, NY), 2 mM L-Glutamine (cat no. 03-020-1A, Biological Industries), 100 µg/mL streptomycin and 100 U/mL penicillin, 12.5 U/mL nystatin (Biological Industries) and 1 mg/mL of G418 (cat no. A1720, Sigma Aldrich). LAD-2 cells (a kind gift from Dr. A.S. Kirshenbaum and Dr. D. Metcalfe, Laboratory of Allergic Diseases, National Institute of Allergy and Infectious Diseases, National Institutes of Health, Bethesda, MD) were cultured in StemPro-34 (cat no. 10640-019, GIBCO) supplemented with 1x StemPro-34 Nutrient, 2 mM L-Glutamine (cat no. 03-020-1A, Biological Industries), 100 U/mL penicillin and 100 µg/mL streptomycin (cat no. 03-032-1B, Biological Industries), and 100 ng/mL hSCF (cat no. 300-07, Peprotech, Rocky Hill, NJ).

Cell Transfection

Transient transfection of RBL-MRGPRX2 cells was performed as previously described (21). Briefly, RBL-MRGPRX2 cells (1.5×10^7) were transfected with 30-50 µg cDNA by electroporation at 300 V for 20 ms, using an ECM 830 electroporator (BTX, Holliston, Mass, USA). The cells were immediately replated in either 24-well (1×10^5 cells/well) tissue culture dishes for confocal imaging or in 6-well (0.2×10^6 cells/well) tissue culture dishes for flow cytometry experiments containing growth medium and used within 20-24 h after transfection.

Dextran Uptake Assay

RBL-MRGPRX2 cells (1×10^5 cells/well) were incubated with 0.1 mg/mL of TRITC- labeled 70 kDa dextran (D1818, Thermo Fischer Scientific) in Tyrode's buffer (10 mM HEPES [pH 7.4], 130 mM NaCl, 5 mM KCl, 1.4 mM $CaCl_2$, 1 mM $MgCl_2$, 5.6 mM glucose, and 0.1% BSA) for the desired time periods, without or with 10 µM SP, in 24-well dishes at 37°C and 5% CO_2. Where

indicated, cells were preincubated for 30 minutes (min), prior to SP trigger, with vehicle or with the indicated inhibitor(s). Cells were washed three times with ice-cold PBS and fixed for 20 min at room temperature (RT) with 4% paraformaldehyde (catalog no. 15710; Electron Microscopy Sciences, Hatfield, Pa) followed by permeabilization for 15 min with 0.1% Triton X-100, 5% FBS, and 2% BSA diluted in PBS. Subsequently, cells were labeled with mouse anti-HA (1:100 dilution) antibody for 1 hour (h) at RT, followed by three washes and a 1-h incubation with Alexa Fluor® 647 Goat Anti-Mouse IgG H&L secondary antibody (1:500 dilution).

Flow Cytometry Analysis

RBL-MRGPRX2 cells were washed three times in Tyrode's buffer to remove dead, non-adherent cells. RBL-MRGPRX2 (5×10^5) or LAD-2 (6×10^5) cells were stimulated at 37°C and 5% CO_2, in Tyrode's buffer for the desired time periods. Cells were then washed three times with ice-cold PBS containing 0.5% BSA and 2 mM sodium azide (FACS buffer) followed by fixation in 4% paraformaldehyde for 15 min at RT. For analyses of cell surface MRGPRX2, cells were stained for 30 min at RT with anti-human MRGPRX2 antibody (1:300 dilution). Cells were subsequently washed three times and stained with Alexa Fluor® 647-conjugated Goat Anti-Mouse IgG H&L secondary antibody (1:2000 dilution) for 30 min at RT, in the dark. For total receptor expression, cells were washed and fixed for 15 min at RT with 4% paraformaldehyde. Cells were subsequently washed and permeabilized with 0.1% saponin and 10% FBS containing PBS for 15 min at RT, after which the cells were washed and stored in the permeabilization buffer overnight at 4°C. The permeabilized cells were then stained for 30 min at RT with anti-human MRGPRX2 antibody (1:300 dilution), washed three times with the permeabilization buffer and stained with the secondary antibody as above. Cells were washed three times with FACS buffer and analyzed by flow cytometry using a CytoFLEX LX flow cytometer (Beckman Coulter, Indianapolis, IN). A minimum of 10,000 cells was acquired per sample. Cells were gated on single cells and were additionally gated on GFP-positive cells in experiments involving transient transfection with either dominant negative (DN) Rac1-GFP or control GFP. Data was analyzed using the FlowJo™ Software Version 10 (Treestar, Ashland, OR).

Immunostaining and Laser Confocal Microscopy Analysis

RBL-MRGPRX2 (1×10^5) and LAD-2 (0.6×10^5) cells grown on untreated (RBL-MRGPRX2) or fibronectin (cat no. F1141, Sigma Aldrich, St Louis, MO, USA) coated (LAD-2) 12-mm round glass coverslips (thick #1; Thermo Scientific, Menzel-Gläser, Saarbrücken, Germany) were washed three times in Tyrode's buffer, the cells were stimulated as indicated in the same buffer at 37°C and 5% CO_2. The cells were subsequently washed three times with ice-cold PBS and fixed for 20 min at RT with 4% paraformaldehyde (cat no. 15710; Electron Microscopy Sciences, Hatfield, PA) in PBS. Fixed cells were permeabilized for 15 min at RT with 0.1% Triton X-100, 5% FBS, and 2% BSA diluted in PBS. Cells were then incubated for 1 h at RT with the desired primary antibodies followed by three washes and a 1-h incubation with the appropriate secondary antibody (1:500 dilution). After washing, cells were mounted in mounting medium (cat no. E18-18; Golden Bridge Life Science, Mukilteo City, WA) and analyzed with a Leica SP5 or SP8 TCS laser scanning confocal microscope (Leica, Wetzlar, Germany) equipped with a HyD detector and a ×63 oil/1.4 NA objective or a Zeiss LSM 710 confocal microscope equipped with a 63 x1.4 oil Plan-Apochromat objective. Colocalization analysis of NPY-CFP with immunostained MRGPRX2 was quantified as the Manders' correlation coefficient with Costes' automatic threshold using the JaCoP plugin of the extended ImageJ version Fiji (22–24). Three-dimensional reconstructions of z stacks (slice thickness ≤ 0.5μm for both fluorescent channels with ~ 10 slices) were performed by using Imaris software (Bitplane, Zurich, Switzerland). Macropinosomes were defined as circular, phase-bright organelles that dissociated from circular ruffles or peripheral ruffles in cells stimulated with SP. To determine the mean fluorescence intensity (MFI) of macropinosomes, the borderline of each macropinosome was outlined with the segmented line tool, saved as a region of interest (ROI) and the MFI was measured using the extended ImageJ version Fiji. The background MFI was subtracted from the MFI of the macropinosomes for each cell, and the MFIs for at least 20 cells/condition were averaged. Next, the MFI values of four randomly selected regions of interest at the periphery of cells triggered with SP for 30 min were selected, measured, and averaged. This averaged MFI values were used for normalization. The size of macropinosomes was calculated by drawing the borderline of each macropinosome with the segmented line tool, again saved as ROIs. The length of the ROIs was then measured using the extended ImageJ version Fiji (23). To determine the vesicles/cell images were converted into threshold images, the required channels were merged (using the AND or XOR operations of the image calculator) to compare the signal patterns and then analyzed with the ImageJ "analyze particle" macro (23).

Statistical Analysis

Data were analyzed using GraphPad Prism Version 8.3.0 for Windows (GraphPad Software, La Jolla, CA). One-way analysis of variance (ANOVA) with repeated measures followed by Dunnett's post-test or Student's or Welch's t-test was used for comparing means, respectively according to the statistic requirements. Results were considered significant when P values were smaller than 0.05.

RESULTS

MRGPRX2 Internalizes *via* Two Distinct Pathways

Given the profound differences between the human MRGPRX2 and its rodent orthologs, we used the RBL-MRGPRX2 cells (19), that stably express the human MRGPRX2, as our model. We have recently validated the authenticity of this model by demonstrating that the ectopically expressed MRGPRX2 in

RBL cells retains the authentic signaling elicited by the endogenously expressed MRGPRX2 in the human LAD-2 cells (21). Furthermore, unlike naïve RBL cells, RBL-MRGPRX2 cells have acquired responsiveness to MRGPRX2 ligands, this model allows measuring the exclusive responses of MRGPRX2 to ligands, such as SP, that additionally bind to canonical receptors, such as Neurokinin 1 (NK1), that is endogenously expressed in some MCs. Consistent with our previous results (25), flow cytometric analyses (FACS) revealed a reduction in the cell surface expression of MRGPRX2 in response to SP trigger (**Figure 1A** and **Supplementary Figure 1**). However, no significant changes were noted in the total amount of receptor (**Figure 1A**), implying that half of the total amount of the receptor either remains at the plasma membrane or internalizes, but recycles back to the plasma membrane. However, half of the total amount of receptor, which internalizes in response to SP stimulation, is targeted to an internal, non-degradative compartment(s), and is retained intracellularly, without recycling back to the plasma membrane (**Figure 1A**). A similar distribution was also noted for the endogenously expressed MRGPRX2 in LAD-2 cells, in which 40% of the total amount of receptor localized to the cell surface following 30 min of cell stimulation with SP, while 60% of the receptor could only be immunostained after cell permeabilization, implying its retainment in an intracellular compartment (**Figure 1B**).

Further analysis of the first phase of MRGPRX2 internalization in RBL-MRGPRX2 cells revealed that MRGPRX2 endocytosis was sensitive to pitstop2, an inhibitor of both clathrin-dependent endocytosis and clathrin-independent and Arf6-dependent endocytosis (26, 27) (**Figure 1C**). Thus, following a 5-min trigger with SP, 44% of MRGPRX2 internalized in the absence of pitstop2, but only 26% in its presence (**Figure 1C**). However, with increasing time of trigger, pitstop2 became less efficient, whereby approximately 60% of MRGPRX2 internalized following 30 min of SP trigger in the absence of inhibitor and 52% in its presence (**Figure 1C**). MRGPRX2 internalization also displayed a similar pattern of sensitivity to cytochalasin D (CytD), an inhibitor of actin polymerization (28), significantly inhibiting MRGPRX2 internalization following a 5-min trigger with SP, but displaying no inhibition following 30 min SP trigger (**Figure 1D**). Therefore, collectively, these results suggested that another pathway, alternative to endocytosis, exists for MRGPRX2 internalization.

Cell surface expression of MRGPRX2 was also reduced by dynasore, an inhibitor of dynamin, that executes membrane fission events (29) (**Figure 1E**). Furthermore, consistent with the more general role of dynamin in controlling internalization pathways, the inhibitory effect of dynasore was evident also at longer periods of SP trigger (**Figure 1E**).

In agreement with our previous results (21), close inspection of the receptor by high resolution confocal microscopy revealed that in resting cells, the receptor distributed between the plasma membrane and an internal fraction, part of which was perinuclear, reminiscent of the Golgi/TGN, and part resided at

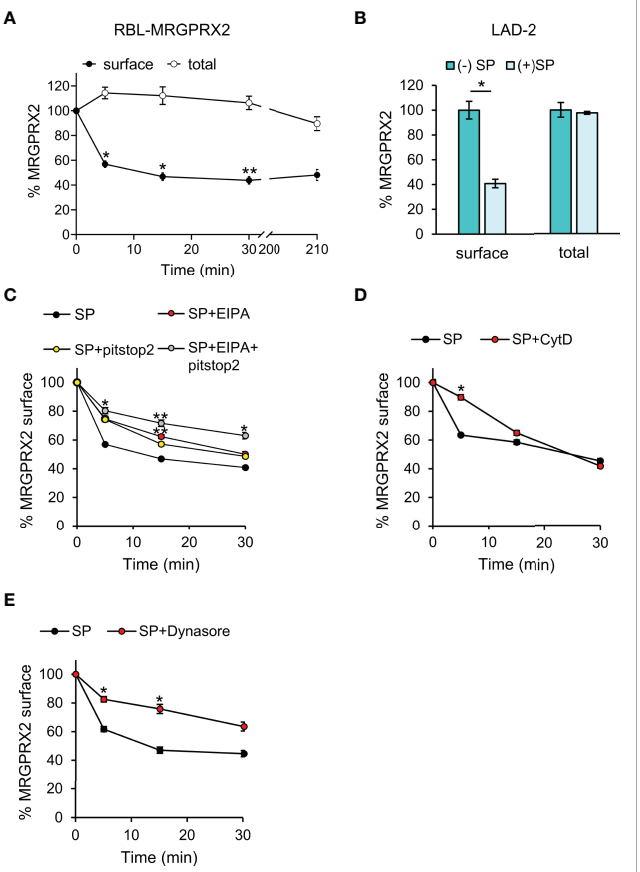


FIGURE 1 | MRGPRX2 internalizes into non-recycling and non-degradative compartment(s). RBL-MRGPRX2 cells **(A, C–E)** or LAD-2 cells **(B)** were incubated for 30 min with either vehicle **(A, B)**, or 20 μM pitstop2, 50 μM EIPA or their combination **(C)**, or 10 μM CytD **(D)**, or 80 μM dynasore **(E)**, as indicated. Cells were subsequently triggered with 10 μM SP for the indicated time periods **(A, C-E)** or for 30 min **(B)** and stained with anti-MRGPRX2 antibodies in the absence (**A**, closed circles, **B–E**) or presence of 0.1% saponin (**A**, open circles, **B**). Cells were analyzed by flow cytometry as described under Materials and Methods. Cell surface and total receptor expression are presented as the percentage of cell surface or total MRGPRX2 expression in the absence of trigger. Data are means ± SEM (n = 5-9). Statistical significance was determined by one–way ANOVA, followed by Dunnett's post-test, for A - C. $^{*}P < 0.05$, $^{**}P < 0.01$, and $P < 0.05$ for 5 min SP vs. 5 min SP +pitstop2, $P < 0.01$ for 5 min SP vs. 5 min SP + EIPA and $P < 0.05$ for 15 min SP vs. 15 min SP + pitstop2. Statistical significance was determined by unpaired two-tailed Student's t-test for B, D and E $^{*}P$[surface (–):SP vs. (+)SP] = 0.0156, $^{*}P$[5 min: SP vs. SP+CytD] = 0.019, $^{*}P$[5 min: SP vs. SP + dynasore] = 0.013, $^{*}P$[15 min: SP vs. SP + dynasore] = 0.019.

vesicles, which we have previously identified as the SGs, based on their labelling with the SG marker, NPY-mRFP (30) (**Figure 2A**). Confocal images of the cells also revealed marked alterations in cell morphology that occurred following their stimulation with SP (**Figure 2A**). The latter included cell flattening and formation of membrane ruffles and macropinosomes, that were identified by brightfield images and confirmed by their proximity to actin ruffles, visualized by the expression of Lifeact-GFP, an actin marker (**Figure 2A**). Furthermore, some of the plasma

membrane-localized receptor concentrated at what appeared like sites of macropinosome formation from the membrane ruffles, and some localized to the macropinosomes (**Figure 2A**). Following a longer period of SP trigger (i.e. 3.5 h), the majority of MRGPRX2 distributed between the perinuclear region and the NPY-mRFP-labelled SGs (**Figure 2A**). Similar results were also observed in the LAD-2 cells, in which at the end of 30 min stimulation by SP, the internalized receptor was detected in the vicinity of macropinosomes and SGs, which were stained by anti-syntaxin 3 antibodies (**Supplementary Figure 2**). In contrast, MRGPRX2 localized to membrane protrusions, associated with actin ruffles, in RBL-MRGPRX2 cells that were triggered by SP for 30 min in the presence of CytD (**Figure 2B**). Quantitative analysis of the confocal images revealed significant increases in

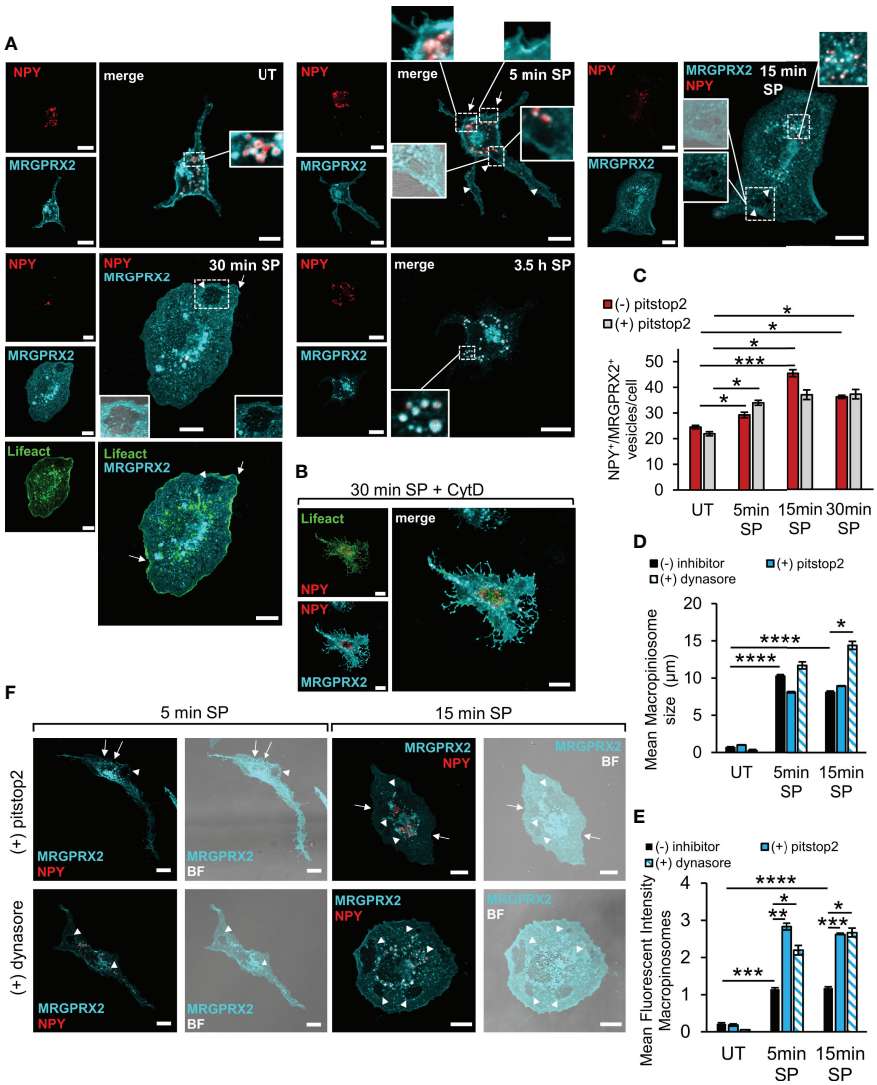


FIGURE 2 | Modes of MRGPRX2 internalization. RBL-MRGPRX2 cells, transiently transfected with NPY-mRFP (red) or NPY-mRFP and Lifeact-GFP (green), as indicated, were either left untreated (UT), or triggered with 10 µM SP for the indicated time periods, in the absence of inhibitor **(A, C–E)**, or following preincubation for 30 min with 10 µM CytD **(B)**, 20 µM pitstop2 **(C, D–F)** or 80 µM dynasore **(D–F)**, as indicated. Cells were immunostained with anti-HA antibodies, followed by Alexa Fluor® 647-conjugated secondary antibodies (pseudo colored cyan). Enlargements correspond to the boxed areas. Macropinosomes are shown by the overlap with the brightfield (BF) image. Arrows point to MRGPRX2 that is localized to cell ruffles. Arrowheads point to macropinosomes. Scale bars = 10µm. The mean number of vesicles/cell that are double positive for NPY-mRFP and MRGPRX2 ($NPY^+/MRGPRX2^+$) **(C)**, the mean size of macropinosomes **(D)**, and the Mean Fluorescent Intensity (MFI) of macropinosome-associated MRGPRX2 **(E)**, were calculated as described under Materials and Methods. Results are the means ± SEM from three independent experiments for dynasore and four independent experiments for pitstop2, each experiment including at least 20 cells/condition. Statistical significance was determined by one–way ANOVA, followed by Dunnett's post-test for C $^*P < 0.05$, $^{**}P < 0.01$ and $^{***}P < 0.001$. Statistical significance was determined by unpaired two-tailed Student's t-test for D, $^{****}P$[UT vs. 5 min SP] = 6.12552E-08, $^{****}P$[UT vs.15 min SP = 1.62931E-07, $^*P$[15 min: SP vs. SP + dynasore] = 0.013, and for E, $^{***}P$[UT vs. 5 min SP] = 0.0001, $^{****}P$[UT vs. 15 min SP] = 2.01147E-05, $^*P$[5 min: SP vs. SP + dynasore] = 0.042, $^{**}P$[5 min: SP vs. SP + pitstop2] = 0.0017, $^*P$[15 min: SP vs. SP + dynasore] = 0.0171, $^{***}P$[15 min: SP vs. SP + pitstop2] = 4.6873E-06).

MRGPRX2 association with the SGs (**Figure 2C**), size of the cellular macropinosomes (**Figure 2D**) and the extent of MRGPRX2 association with macropinosomes (**Figure 2E**), in response to cell triggering with SP.

Imaging of cells that were triggered for 5 min with SP in the presence of pitstop2 demonstrated a significant increase in the amount of macropinosome-associated MRGPRX2 (**Figures 2E, F**), with no significant change in the SG-localized MRGPRX2 (**Figure 2C**). Therefore, these results implied that pitstop2-sensitive endocytosis and macropinocytosis may represent two interchangeable modes of MRGPRX2 internalization, whereby inhibition of one pathway, i.e. endocytosis by pitstop2, shifts the receptor to the alternative macropinocytic pathway.

We also analyzed the influence of dynasore on the distribution of MRGPRX2 and found that in a similar manner to the effect of pitstop2, also dynasore significantly increased the amount of macropinosome-associated MRGPRX2 (**Figures 2E, F**). Furthermore, dynasore significantly increased the mean size of the cellular macropinosomes as well (**Figures 2D, F**).

SP Stimulates Macropinocytosis

To gain direct evidence for the involvement of macropinocytosis in MRGPRX2 internalization, we allowed the cells to take up TRITC-dextran (70 kDa), a commonly used probe for measuring macropinocytosis (31), and compared its location with the location of the internalized MRGPRX2. The results of these experiments revealed that SP stimulated the uptake of TRITC-dextran, which could be completely inhibited by EIPA, a Na^+/H^+ exchange inhibitor, that is known to inhibit macropinocytosis (32, 33) (**Figures 3A, B**). These results therefore demonstrated that SP can stimulate macropinocytosis. Furthermore, MRGPRX2 localized to the same dextran-containing vesicles (**Figures 3A, B**), part of which also contained NPY-Venus (**Figures 3A, C**), revealing a connection between MRGPRX2-positive macropinosomes and the SGs. In sharp contrast to the profound effect of EIPA, the uptake of TRITC-dextran was not affected by pitstop2 (**Figures 3A–C**), indicating that this alternative pathway of MRGPRX2 internalization was insensitive to this inhibitor, consistent with its ability to compensate for MRGPRX2 internalization by endocytosis (**Figure 2E**). Indeed, analysis of the cell surface expression of MRGPRX2 by flow cytometry revealed that EIPA was as potent as pitstop2 in inhibiting MRGPRX2 internalization (**Figure 1B**). Furthermore, combining EIPA with pitstop2 further inhibited internalization, supporting the notion of MRGPRX2 internalization *via* both pitstop2-sensitive endocytosis and EIPA-sensitive macropinocytosis (**Figure 1B**).

To substantiate the role of macropinocytosis in MRGPRX2 internalization even further, we also examined the impact of expression of a dominant negative (DN) mutant of Rac1 [i.e. Rac1(T17N)], a key player of actin rearrangements during macropinocytosis (34, 35), on the internalization of MRGPRX2, using the internalization of dextran as a positive control. Expectedly, DN Rac1 inhibited the uptake of TRITC-dextran (**Figure 3D**) and accordingly significantly reduced the number of internal vesicles that were double positive for dextran and MRGPRX2 (**Figure 3E**) or triple positive for dextran, MRGPRX2 and NPY-CFP (**Figure 3F**), which like NPY-mRFP and NPY-Venus, serves as a SG marker. Finally, DN Rac1 significantly retained the cell surface expression of MRGPRX2 (**Figure 3G**), thus demonstrating its capacity to inhibit SP-stimulated internalization of MRGPRX2.

Trafficking of MRGPRX2 to the SGs Involves the Autophagic Machinery

We have previously shown that early endosomes fuse with the SGs in MCs (36), thus providing a possible mechanism for MRGPRX2 targeting to the SGs. However, our results, showing that inhibition of endocytosis by pitstop2 does not prevent MRGPRX2 targeting to the SGs (**Figure 2C**), strongly suggested that MRGPRX2 can reach the SGs also directly from macropinosomes. Recently, it was demonstrated that cells respond to plasma membrane injury by forming large macropinosomes at the repair site (37). These structures eventually become positive for the autophagy-related LC3B protein, followed by their shrinkage and fusion with lysosomes (37). Given the lysosomal nature of the MC SGs, the previous reports that documented the presence of LC3 on MC SGs (38, 39), and our recent findings on inhibition of MRGPRX2-stimulated secretion by autophagy targeting drugs (21), we were motivated to examine if LC3 plays a role in MRGPRX2 delivery from macropinosomes to the SGs. To this end, we monitored the intracellular distribution of MRGPRX2 in response to SP trigger, in cells that were co-transfected with NPY-mRFP and LC3-GFP. Analysis of the confocal images revealed that the vesicular fraction of MRGPRX2, which increased with the time of SP trigger, indeed resided on NPY-mRFP labelled SGs, however a fraction of the NPY-positive SGs also labelled positive for LC3-GFP (**Figures 4A–E**). A smaller fraction of intracellular MRGPRX2 localized to LC3-GFP-positive, but NPY-mRFP-negative vesicles (**Figure 4F**), that were smaller in size and resided in close proximity to the SGs (**Figures 4A, B**). Consistent with the reports on bone marrow derived MCs (38), these vesicles, that may correspond to autophagosomes, were present also in resting cells (**Figure 4A**). Three-dimensional reconstructions of the confocal images corroborated the existence of three types of vesicles (**Figure 4B**, and **Supplementary Video 1**), and suggested that a fusion event between LC3-positive vesicles and LC3-negative SGs gives rise to the formation of the LC3-positve SGs (**Figure 4C**). This fusion event is fast and therefore restricting the number of LC3-positive and NPY-negative vesicles.

To further decipher the connection between macropinocytosis and MRGPRX2 trafficking to the SGs, we tested the impact of dynasore, that inhibits endocytosis, on the cellular distribution of MRGPRX2 in the LC3-GFP-expressing cells. Consistent with its profound impact on the macropinosomes' size (**Figure 2D**), dynasore significantly inhibited the association of MRGPRX2 with LC3-posivtive as well as LC3-negative SGs

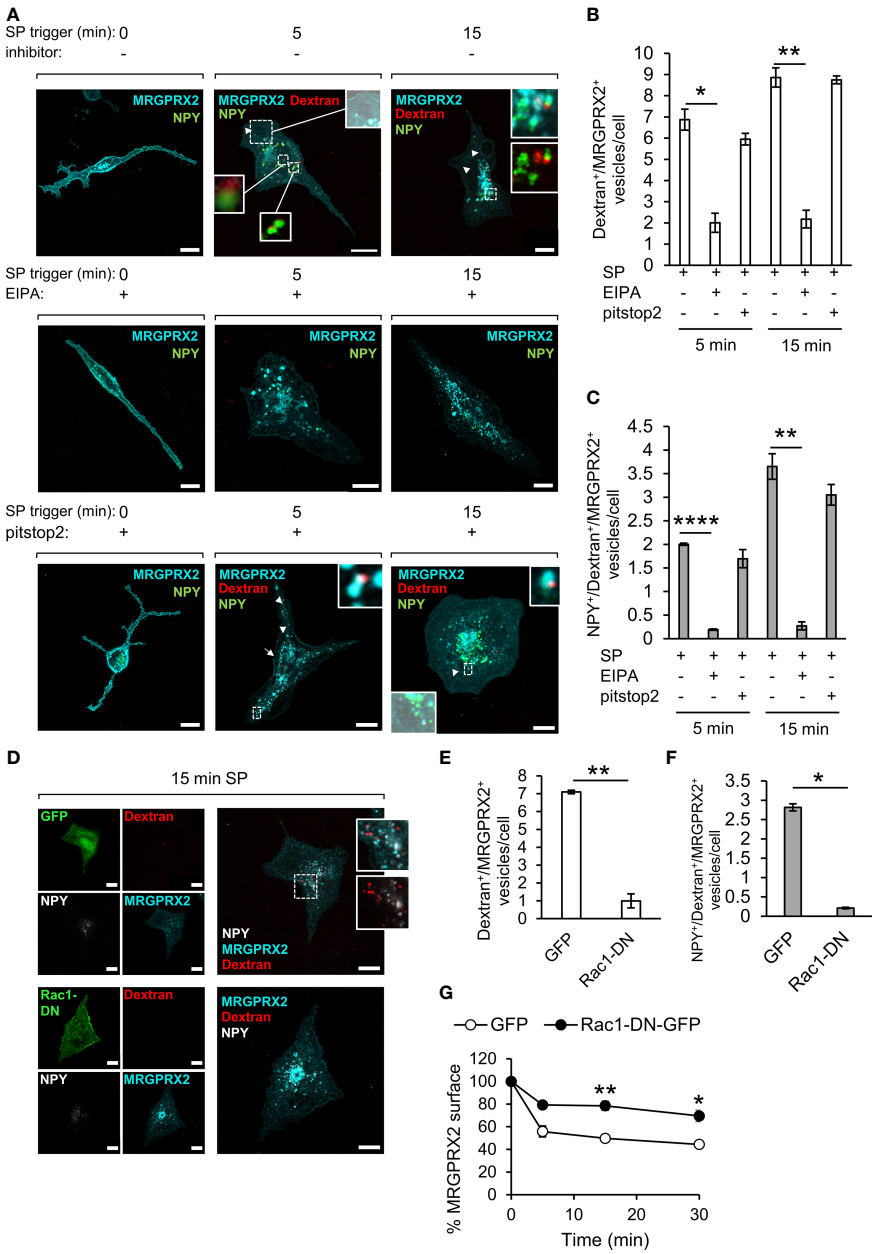


FIGURE 3 | MRGPRX2 internalizes by macropinocytosis. RBL-MRGPRX2 cells, transiently transfected with NPY-Venus (green) **(A)**, or co-transfected with NPY-CFP (pseudo colored white) and either GFP or Rac1-DN-GFP (green) **(D)**, were triggered with 10 µM SP in the presence of 0.1 mg/ml TRITC-Dextran (red) for the indicated time periods, in the presence of vehicle **(A, D)** or following 30 min pre-incubation with either 50 µM EIPA or 20 µM pitstop2, as indicated **(A)**. Cells were immunostained with anti-HA antibodies followed by Alexa Fluor® 647-conjugated secondary antibodies (pseudo colored cyan). Enlargements correspond to the boxed areas. Macropinosomes are shown as the overlap with the brightfield images. Arrows point to MRGPRX2 position at sites of macropinosome formation and arrowheads point to macropinosomes. Scale bars = 10µm. The mean number of vesicles/cell that are double positive for Dextran and MRGPRX2 (Dextran$^+$/MRGPRX2$^+$) **(B, E)**, or triple positive for NPY, Dextran and MRGPRX2 (NPY$^+$/Dextran$^+$/MRGPRX2) **(C, F)**, was calculated for cells that were triggered for the indicated time periods with SP (15 min for **E** and **F**), in the absence or presence of the indicated inhibitors or Rac1-DN. Results are means ± SEM from three **(D–F, G)** or four **(A–C)** independent experiments, with each experiment including 15-20 cells/condition. The effect of Rac1-DN expression on SP-induced internalization of MRGPRX2 was quantified by flow cytometry, by measuring the cell surface amount of MRGPRX2 gated on GFP-positive single cells. Results are presented as the percentage of the amount of cell surface MRGPRX2 in the absence of stimulation by SP **(G)**. Data are means ± SEM of four independent experiments. Statistical significance was determined by unpaired two-tailed Welch's t-test. P values for Dextran$^+$/MRGPRX2$^+$ vesicles/cell: *P[5 min: SP vs. SP+ EIPA] = 0.0271, **P[15 min: SP vs. SP + EIPA] = 0.0026, **P[GFP vs. Rac1-DN-GFP] = 0.009. P values for NPY$^+$/Dextran$^+$/MRGPRX2$^+$ vesicles/cell: **P[15 min: SP vs. SP + EIPA] = 0.01, ****P[5 min: SP vs. 5 min SP + EIPA] = 2.996x10^6, *P[GFP vs. Rac1-DN-GFP] = 0.018. P values for MRGPRX2 surface expression are **P[5 min: SP/GFP vs. SP/Rac1-DN-GFP] = 0.01, *P[15 min: SP/GFP vs. SP/Rac1-DN-GFP] = 0.0358.

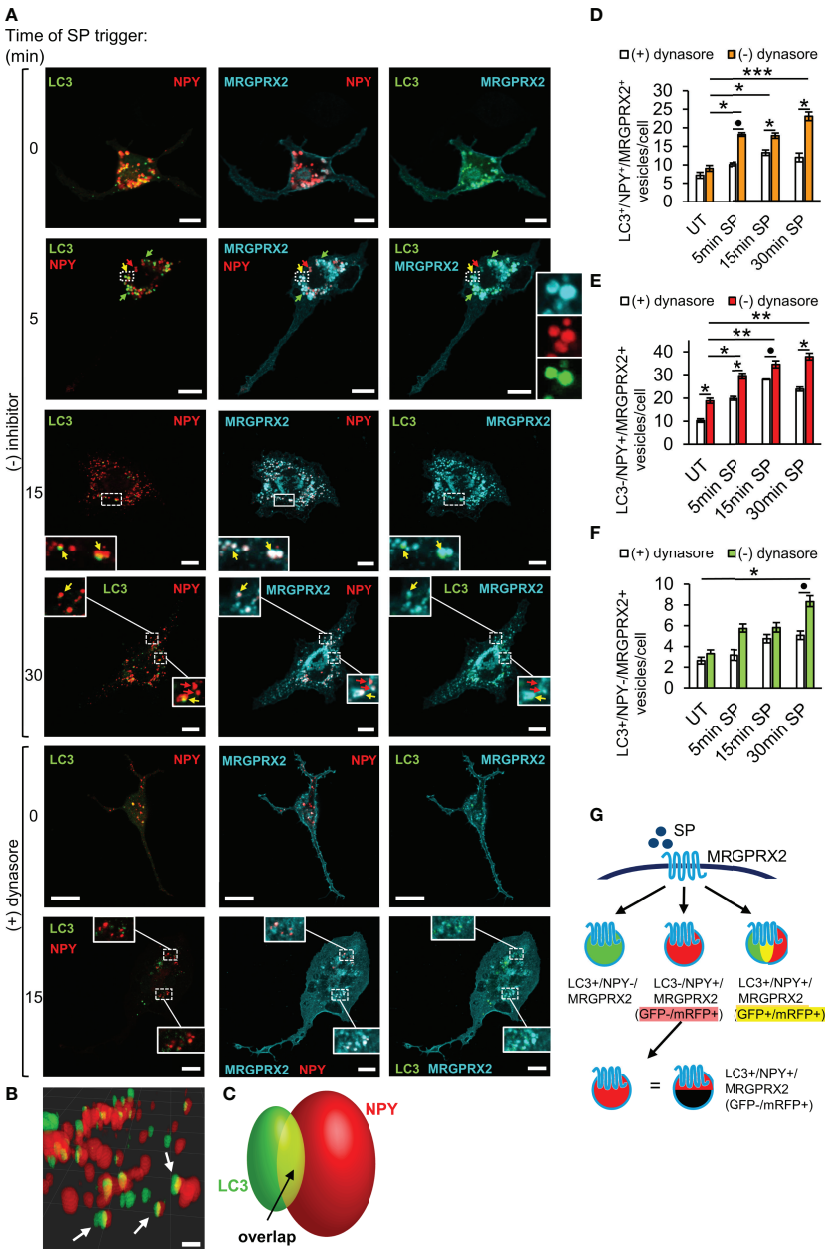


FIGURE 4 | LC3 and dynamin assist MRGPRX2 trafficking to SGs. RBL-MRGPRX2 cells, transiently co-transfected with NPY-mRFP (red) and LC3-GFP (green), were triggered for the indicated time periods with 10 µM SP, in the presence of vehicle or following 30 min pre-incubation with 80 µM dynasore, as indicated **(A)**. Cells were immunostained with anti-HA antibodies followed by Alexa Fluor® 647-conjugated secondary antibodies (pseudo colored cyan). Yellow arrows point to MRGPRX2 that is localized to NPY-mRFP and LC3-positive SGs, red arrows point to NPY-mRFP-positive, but LC3 negative SGs, and green arrows point to LC3 positive, but NPY-mRFP negative vesicles. Enlargements correspond to the boxed areas. Scale bars = 10µm. Confocal images of cells that were activated for 15 min with SP, were 3-dimensionally reconstructed by using Imaris software (scale bars 2 µm) **(B)**. Arrows point to $LC3^+/NPY^+$ vesicles. A scheme of a 3-dimensionally reconstructed $LC3^+/NPY^+$ vesicle is shown in **(C)**, showing that some of the fluorescence of LC3-GFP overlaps with NPY-mRFP (yellow). The average number of $LC3^+/NPY^+/MRGPRX2^+$ **(D)**, $LC3^-/NPY^+/MRGPRX2^+$ **(E)**, or $LC3^+/NPY^-/MRGPRX2^+$ **(F)** vesicles/cell was calculated using the ImageJ software and is presented as the mean ± SEM from three to six independent experiments, with each experiment including at least 20 cells/condition. Statistical significance was determined by one-way ANOVA, followed by Dunnett's post-test, for comparison of UT with different time points of SP trigger in D-F: $^*P < 0.05$, $^{**}P < 0.01$, $^{***}P < 0.001$, or unpaired two-tailed Welch's t-test comparison SP ± dynasore for D, $^*P[LC3^+/NPY^+/MRGPRX2^+$ - 5 min: SP vs. SP + dynasore] = 0.0652, for E, $^*P[LC3^+/NPY^+/MRGPRX2^+$ - 15 min: SP vs. SP + dynasore] = 0.0220, $^*P[LC3^+/NPY^+/MRGPRX2^+$ - 30 min: SP vs. SP + dynasore] = 0.0365, and for F, $^*P[LC3^-/NPY^+/MRGPRX2^+$ - UT: SP vs. SP + dynasore] = 0.0191, $^*P[LC3^-/NPY^+/MRGPRX2^+$ - 5 min: SP vs. SP + dynasore] = 0.0238, $^*P[LC3^-/NPY^+/MRGPRX2^+$ - 15 min: SP vs. SP + dynasore] = 0.1049 and $^*P[LC3^-/NPY^+/MRGPRX2^+$ - 5 min: SP vs. SP + dynasore] = 0.0216. A schematic presentation of the types of vesicles into which MRGPRX2 internalizes in response to SP trigger is shown in **(G)**.

(**Figures 4A, D–F**). These results therefore implicated dynamin in playing a role in the delivery of MRGPRX2 from macropinosomes to the SGs.

GFP fluorescence is pH sensitive. Thus, while LC3-GFP is fluorescent in autophagosomes, this fluorescence quenches in autolysosomes that form following autophagosome fusion with lysosomes. The possibility therefore arises that the LC3-negative SGs (i.e. $LC3^-/NPY^+$) may still contain LC3-GFP, the fluorescence of which is quenched (**Figure 4G**). To address this possibility, we repeated our analyses of MRGPRX2 distribution in cells that were co-transfected with NPY-CFP and LC3-GFP-mRFP, a tandem fluorescent protein that is commonly used to monitor various stages of autophagy due to the pH insensitivity of mRFP. Thus, LC3-GFP-mRFP yields both green and red signals when located in the less acidic autophagosomes and only a red signal when located in the acidic autolysosomes (40). These studies demonstrated the presence of LC3-containing vesicles that were either double positive for GFP and mRFP, or only positive for mRFP (**Figure 5A**). Notably, the amount of both types of LC3-positive vesicles significantly increased in response to SP trigger (**Figure 5B**), indicating that they were formed by a dynamic and trigger-dependent process. Furthermore, with increasing time of SP trigger, the relative amount of GFP-negative/mRFP-positive vesicles increased, suggesting that SP stimulated their acidification, presumably by promoting their fusion with lysosomes (**Figure 5B**). NPY-CFP colocalized with both LC3-GFP-mRFP double positive and LC3-GFP-negative and mRFP-positive vesicles (**Figures 5A, C**), implying that both types of MRGPRX2-associated SGs contain LC3, but differ in their internal pH.

DISCUSSION

While internalization of GPCRs has been historically associated with signal termination, it is currently well established that GPCRs may continue signaling post their internalization. Moreover, their intracellular signaling patterns may differ from their plasma membrane signaling (18, 41). Therefore, deciphering the spatiotemporal regulation of GPCRs is central to understanding their functions. Given the important role played by MRGPRX2 in mediating MC innate immune and neurogenic responses, we have undertaken this study to investigate its route of trafficking in response to the binding of its neuropeptide ligand SP. We have previously shown that SP stimulates MRGPRX2 internalization (25), but the fate of the internalized receptor has not been characterized before. The

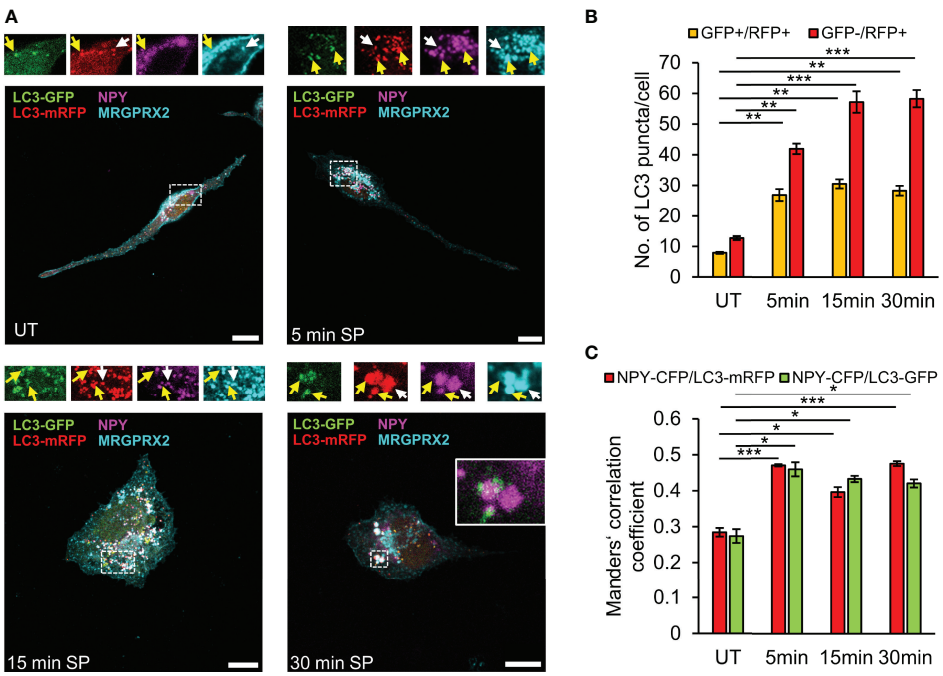


FIGURE 5 | SP stimulates fusion of LC3-positive SGs with lysosomes. RBL-MRGPRX2 cells, transiently co-transfected with NPY-CFP (magenta) and LC3-GFP-mRFP (green and red), were either left untreated (UT) or triggered for the indicated time periods with 10 µM SP. Cells were subsequently immunostained with anti-HA antibodies followed by Alexa Fluor® 647-conjugated secondary antibodies (pseudo colored cyan) **(A)**. Enlargements correspond to the boxed areas. Yellow arrows point to MRGPRX2 that is localized to LC3-positive-SGs ($GFP^+/mRFP^+$), and white arrows point to MRGPRX2 that is localized to LC3-autolysosome-SGs ($GFP^-/mRFP^+$). An example of the merge of NPY-CFP and LC3-GFP is shown in the inset of the 30 min image. Scale bars = 10µm. The average number of double positive $GFP^+/mRFP^+$ vesicles or single $GFP^-/mRFP^+$ vesicles was quantified using the ImageJ software and is presented as the mean ± SEM from five independent experiments, with each experiment including at least 20 cells/condition **(B)**. The extent of colocalization of NPY-CFP with LC3-mRFP or LC3-GFP was quantified (n = 3) and is presented as Mander's correlation coefficient **(C)**. Statistical significance was determined by one-way ANOVA, followed by Dunnett's post-test. *$P < 0.05$, **$P < 0.01$, *** $P < 0.001$.

first important finding that emerged from this study is the recognition that while a fraction of the internalized receptor may recycle back to the plasma membrane, approximately half of internalized MRGPRX2 is retained intracellularly, indicating its trafficking to a neither recycling nor degradative compartment. This pattern of intracellular targeting was not the result of overexpression, because we have previously shown that the level of MRGPRX2 expression in the stably transfected RBL-MRGPRX2 cells is even lower than its endogenous expression in LAD-2 cells (21). Furthermore, similar intracellular retention was also noted in the LAD-2 cells. Second, we demonstrate that MRGPRX2 internalizes *via* two parallel pathways, that can compensate each other, upon inhibition of one of them. Specifically, we show that alongside its internalization by an endocytic pathway, MRGPRX2 internalizes by macropinocytosis. This conclusion is supported by a number of observations, including the location of the receptor in macropinosomes, its colocalization with internalized dextran (70 kDa) and the inhibition of its targeting to macropinosomes by either EIPA or expression of DN Rac1, both known inhibitors of macropinocytosis (33, 35). The endocytic pathway of MRGPRX2 internalization is sensitive to pitstop2, an inhibitor of clathrin-dependent endocytosis and clathrin-independent and Arf6-dependent endocytosis (26, 27), thus implicating either one of these pitstop2-sensitive endocytic pathways in mediating MRGPRX2 internalization. However, the fact that MRGPRX2 internalization is only partially inhibited by the combination of pitstop2 and EIPA raises the possibility that an additional mode of clathrin-independent endocytosis that is resistant to pitstop2, might also be involved.

Macropinocytosis has been associated with innate immune cell surveillance and has been demonstrated to occur in macrophages and dendritic cells in response to microbe associated molecular patterns (42). This concept was recently extended by the finding that macropinocytosis complements endocytosis in internalizing the chemokine GPCR, CCR5 in macrophages (43). Our demonstration that MRGPRX2, a GPCR that mediates a broad spectrum of innate immune responses of MCs, also internalizes by both endocytosis and macropinocytosis strongly supports the recognition of macropinocytosis as a central mechanism in innate immunity. Whether macropinosomes comprise a site of intracellular signaling of MRGPRX2 is presently unknown and is the subject of our future research.

Analysis of the post endocytic trafficking of SP-bound MRGPRX2 revealed that the receptor distributes between a perinuclear region, reminiscent of the Golgi/TGN and the SGs. The latter intriguing location prompted us to investigate the route by which MRGPRX2 reaches the SGs. We have previously shown that MC SGs incorporate endocytic cargo by fusing with early endosomes (34). Thus, SG fusion with endosomes could provide a mechanism for MRGPRX2 targeting to the SGs. However, the finding that inhibition of endocytosis by pitstop2 does not prevent MRGPRX2 delivery to the SGs, suggested the existence of an alternative pathway that connects macropinocytosis, the second mechanism of MRGPRX2 internalization, with the SGs. Motivated to delineate such pathway, we hypothesized that macropinosome resolution may serve as a mechanism of regenerating SGs. We based our hypothesis on parallel mechanisms that exist during phagocytosis, where phagosome fragmentation leads to lysosome reformation (44), or repair of plasma membrane injury, during which LC3-mediated resolution of macropinosomes is linked with fusion with lysosomes (37). Indeed, our results reveal a novel link between macropinosomes, LC3 and the SGs. Specifically, we show that MRGPRX2 internalizes into LC3-positive vesicles that very rapidly acquire the patterns of LC3-GFP-positive-mRFP-positive SGs, followed by the patterns of LC3-GFP-negative-mRFP positive SGs. Furthermore, in the presence of dynasore, that blocks endocytosis, reduction in the amount of MRGPRX2 that is associated with these LC3-positive vesicles is accompanied by an increase in the macropinosome size. Therefore, taken together, our results are compatible with a model, whereby plasma membrane-localized MRGPRX2 internalizes in response to cell trigger by SP by both endocytosis, which may include both clathrin-dependent and clathrin-independent endocytosis, and by macropinocytosis, that may or may not be coupled to SG recapture (**Figure 6**). Endosomes then fuse with the SGs, thereby delivering MRGPRX2 to the SGs, whereas dynamin and LC3 promote the budding of macropinosome-derived vesicles leading to macropinosome resolution (**Figure 6**). These macropinosome-derived vesicles then fuse with NPY-mRFP labelled SGs (type I in our model, **Figure 6**), to form NPY positive and GFP-LC3-positive SGs (type II in the model, **Figure 6**), which then fuse with lysosomes to form NPY-positive/LC3-GFP-negative, but LC3-mRFP-positive, SGs (type III in the model, **Figure 6**). Therefore, this pathway provides not only a mode for incorporation of extracellular or membranal cargo into the SGs, but it may also serve as mechanism of regeneration of SGs by capturing part of the released cargo by macropinocytosis and incorporating it back into the SGs. Alternatively, macropinocytosis might be directly involved in the recapturing of SGs that have partially emptied their content during exocytosis. Macropinosomes may thereby facilitate the internalization of MRGPRX2, and its SG targeting by their subsequent fusion with non-degranulated SGs (**Figure 6**). Consistent with this notion are previous observations that documented LC3 location and release by bone marrow derived MCs (38). We do not presently know if cytosolic LC3 binds to the macropinosomes, in analogy to LC3-associated macropinocytosis during membrane repair (37) or LC3-associated phagocytosis (45), in which case, the LC3-GFP-positive, but NPY-negative vesicles correspond to macropinosome derived vesicles, that fuse with the type I SGs to form type IIa SGs (**Figure 6**), or whether LC3 resides on phagophores or autophagosomes, that respectively engulf or fuse with macropinosome-derived vesicles, prior to their fusion with the SGs to form type IIb SGs (**Figure 6**), in analogy to the biogenesis of lamellar bodies in the lung (46). Future studies will

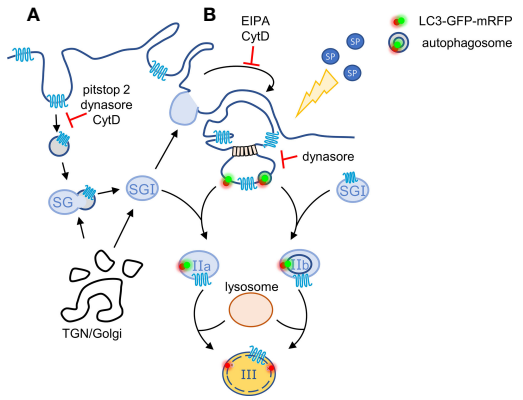


FIGURE 6 | Model for the crosstalk between macropinosomes and the SGs. According to our model, plasma membrane-localized MRGPRX2 internalizes in response to cell stimulation by SP by two parallel mechanisms: **(A)** by endocytosis that is partially sensitive to pitstop2 and **(B)** by macropinocytosis. Endosomes may fuse with the SGs, thereby delivering MRGPRX2 to the SGs, whereas MRGPRX2-containing vesicles bud from macropinosomes by a mechanism that involves dynamin and either the binding of cytosolic or phagophore associated LC3, or fusion with autophagosomes. These vesicles then fuse with TGN-derived SGs (Type I) generating respectively, Type IIa or Type IIb, LC3-positive SGs. The latter then acidify, most likely by their fusion with lysosomes, by a SP-stimulated process, generating Type III SGs.

distinguish between these possibilities. It is interesting to note in this context that autophagy has been implicated in playing a role in FcεRI-mediated exocytosis (38) and we have shown that 3-methyladenine (3-MA), an inhibitor of canonical autophagy, inhibits MRGPRX2-mediated secretion (21). However, while these results implicate canonical autophagy in the mechanism of MC exocytosis, they do not necessarily counteract the possibility of non-canonical autophagy playing a role in MRGRPX2 trafficking.

In summary, deciphering the spatiotemporal regulation of MRGPRX2 is of particular interest given the different ability of MRGPRX2 ligands to stimulate internalization. Thus, it is tempting to speculate that biased ligands, such as AG30/5C (11), that do not stimulate receptor internalization, and therefore restrict MRGPRX2 signaling to the plasma membrane, may confer distinct functions than balanced ligands, such as SP (25), that may stimulate intracellular signaling. Delineating the route of post endocytic trafficking of MRGPRX2 may thus pave the road for the rational design of cell-permeable antagonists that will specifically target undesired and site-specific MRGPRX2 activation. Here we show that SP-bound MRGPRX2 internalizes by two parallel pathways, including endocytosis and macropinocytosis. We also show that the internalized receptor is targeted to internal non-degradative compartments that include the SGs. Further, we uncovered a novel mechanism that connects macropinosomes and SGs and which mediates the delivery of MRGPRX2 to the SGs. Whether the SGs participate in MRGPRX2 signaling or serve as an alternative to endocytic recycling, for the direct coupling of receptor retrieval with exocytosis, are intriguing questions, which we shall address in our future studies.

DATA AVAILABILITY STATEMENT

The original contributions presented in the study are included in the article/**Supplementary Material**. Further inquiries can be directed to the corresponding author.

AUTHOR CONTRIBUTIONS

RS-E and HA conceived the project, PL-H and EK designed and performed the experiments, analysed the data, discussed the results, PL-H prepared the figures and commented on the manuscript, RS-E supervised the project and wrote the manuscript. All authors reviewed the manuscript. All authors contributed to the article and approved the submitted version.

FUNDING

This work was supported by grant 1600/19 from the Israel Science Foundation, founded by the Israel Academy for Sciences (to RS-E), and grant 2017182 by the United States–Israel Binational Science Foundation (to RS-E). PL-H was supported through The American Association of Immunologists Careers in Immunology Fellowship Program. This work was also supported by National Institutes of Health grant R01-AI124182 (to HA).

ACKNOWLEDGMENTS

We thank Drs. U. Ashery, P. Blinder, R. Pinkas Kramarski, A. Ashkenazi, S. Gutkind and B.-Z. Shilo for their generous gifts of cDNAs.

SUPPLEMENTARY MATERIAL

The Supplementary Material for this article can be found online at: https://www.frontiersin.org/articles/10.3389/fimmu.2022.892239/full#supplementary-material

Supplementary Video 1 | RBL-MRGPRX2 cells were transiently transfected with NPY-mRFP, marking SGs, and LC3-GFP. Next day, cells were triggered for 15 min with 10μM SP and imaged using a Zeiss LSM 710 confocal microscope. Three-dimensional reconstructions of z stacks (slice thickness ≤ 0.5μm for both fluorescent channels with ~ 10 slices) were performed by using Imaris software (Bitplane, Zurich, Switzerland).

Supplementary Figure 1 | RBL-MRGPRX2 cells **(A, B)** or LAD-2 cells **(C, D)** were stained with anti-MRGPRX2 antibody followed by Alexa Fluor® 647 secondary antibody (blue lines) or by the secondary antibody (grey lines, control) in the absence **(A, C)** or presence **(B, D)** of 0.1% saponin, and analyzed by flow cytometry.

Supplementary Figure 2 | LAD-2 cells were either left untreated (UT) or triggered with 10 μM SP for 30 min (n = 2 with at least 20 cells/condition per experiment). Cells were immunostained with mouse anti-MRGPRX2 and rabbit anti-syntaxin 3

(STX3) antibodies, followed by Alexa Fluor® 647-conjugated goat anti-mouse secondary antibodies (pseudo colored cyan) and Alexa Fluor® 488-conjugated goat anti-rabbit secondary antibodies (pseudo colored red). Enlargements correspond to the boxed areas. Enlargements correspond to the boxed areas. Macropinosomes are shown by the overlap with the brightfield (BF) image. White arrows point to MRGPRX2 that is localized to macropinosomes. Blue arrows points to STX3 located at the plasma membrane, where it overlaps with MRGPRX2. Arrowheads point to macropinosomes. Scale bars = 10μm.

REFERENCES

1. Blank U, Huang H, Kawakami T. The High Affinity Ige Receptor: A Signaling Update. *Curr Opin Immunol* (2021) 72:51–8. doi: 10.1016/j.coi.2021.03.015
2. Galli SJ, Tsai M. Mast Cells: Versatile Regulators of Inflammation, Tissue Remodeling, Host Defense and Homeostasis. *J Dermatol Sci* (2008) 49(1):7–19. doi: 10.1016/j.jdermsci.2007.09.009
3. Jiménez M, Cervantes-García D, Córdova-Dávalos LE, Pérez-Rodríguez MJ, Gonzalez-Espinosa C, Salinas E. Responses of Mast Cells to Pathogens: Beneficial and Detrimental Roles. *Front Immunol* (2021) 12:685865. doi: 10.3389/fimmu.2021.685865
4. Redegeld FA, Yu Y, Kumari S, Charles N, Blank U. Non-Ige Mediated Mast Cell Activation. *Immunol Rev* (2018) 282(1):87–113. doi: 10.1111/imr.12629
5. Dahlin JS, Maurer M, Metcalfe DD, Pejler G, Sagi-Eisenberg R, Nilsson G. The Ingenious Mast Cell: Contemporary Insights Into Mast Cell Behavior and Function. *Allergy* (2021) 77:83–99. doi: 10.1111/all.14881
6. Wernersson S, Pejler G. Mast Cell Secretory Granules: Armed for Battle. *Nat Rev Immunol* (2014) 14(7):478–94. doi: 10.1038/nri3690
7. Moon TC, Befus AD, Kulka M. Mast Cell Mediators: Their Differential Release and the Secretory Pathways Involved. *Front Immunol* (2014) 5:569. doi: 10.3389/fimmu.2014.00569
8. Mukai K, Tsai M, Saito H, Galli SJ. Mast Cells as Sources of Cytokines, Chemokines, and Growth Factors. *Immunol Rev* (2018) 282(1):121–50. doi: 10.1111/imr.12634
9. Lagunoff D, Martin TW, Read G. Agents That Release Histamine From Mast Cells. *Annu Rev Pharmacol Toxicol* (1983) 23:331–51. doi: 10.1146/annurev.pa.23.040183.001555
10. Ferry X, Brehin S, Kamel R, Landry Y. G Protein-Dependent Activation of Mast Cell by Peptides and Basic Secretagogues. *Peptides* (2002) 23(8):1507–15. doi: 10.1016/S0196-9781(02)00090-6
11. Roy S, Chompunud Na Ayudhya C, Thapaliya M, Deepak V, Ali H. Multifaceted Mrgprx2: New Insight Into the Role of Mast Cells in Health and Disease. *J Allergy Clin Immunol* (2021) 148(2):293–308. doi: 10.1016/j.jaci.2021.03.049
12. Serhan N, Cenac N, Basso L, Gaudenzio N. Mas-Related G Protein-Coupled Receptors (Mrgprs) - Key Regulators of Neuroimmune Interactions. *Neurosci Lett* (2021) 749:135724. doi: 10.1016/j.neulet.2021.135724
13. Ali H. Emerging Roles for Mas-Related G Protein-Coupled Receptor-X2 in Host Defense Peptide, Opioid, and Neuropeptide-Mediated Inflammatory Reactions. *Adv Immunol* (2017) 136:123–62. doi: 10.1016/bs.ai.2017.06.002
14. McNeil BD. Mrgprx2 and Adverse Drug Reactions. *Front Immunol* (2021) 12:676354. doi: 10.3389/fimmu.2021.676354
15. McNeil BD, Pundir P, Meeker S, Han L, Undem BJ, Kulka M, et al. Identification of a Mast-Cell-Specific Receptor Crucial for Pseudo-Allergic Drug Reactions. *Nature* (2015) 519(7542):237–41. doi: 10.1038/nature14022
16. Crilly SE, Puthenveedu MA. Compartmentalized Gpcr Signaling From Intracellular Membranes. *J Membrane Biol* (2021) 254(3):259–71. doi: 10.1007/s00232-020-00158-7
17. Lobingier BT, von Zastrow M. When Trafficking and Signaling Mix: How Subcellular Location Shapes G Protein-Coupled Receptor Activation of Heterotrimeric G Proteins. *Traffic* (2019) 20(2):130–6. doi: 10.1111/tra.12634
18. Eichel K, von Zastrow M. Subcellular Organization of Gpcr Signaling. *Trends Pharmacol Sci* (2018) 39(2):200–8. doi: 10.1016/j.tips.2017.11.009
19. Meixiong J, Dong X. Mas-Related G Protein–Coupled Receptors and the Biology of Itch Sensation. *Annu Rev Genet* (2017) 51(1):103–21. doi: 10.1146/annurev-genet-120116-024723
20. Subramanian H, Kashem SW, Collington SJ, Qu H, Lambris JD, Ali H. Pmx-53 as a Dual Cd88 Antagonist and an Agonist for Mas-Related Gene 2 (Mrgx2) in Human Mast Cells. *Mol Pharmacol* (2011) 79(6):1005–13. doi: 10.1124/mol.111.071472
21. Lazki-Hagenbach P, Ali H, Sagi-Eisenberg R. Authentic and Ectopically Expressed Mrgprx2 Elicit Similar Mechanisms to Stimulate Degranulation of Mast Cells. *Cells* (2021) 10(2):376. doi: 10.3390/cells10020376
22. Schneider CA, Rasband WS, Eliceiri KW. Nih Image to Imagej: 25 Years of Image Analysis. *Nat Methods* (2012) 9(7):671–5. doi: 10.1038/nmeth.2089
23. Schindelin J, Arganda-Carreras I, Frise E, Kaynig V, Longair M, Pietzsch T, et al. Fiji: An Open-Source Platform for Biological-Image Analysis. *Nat Methods* (2012) 9(7):676–82. doi: 10.1038/nmeth.2019
24. Bolte S, Cordelières FP. A Guided Tour Into Subcellular Colocalization Analysis in Light Microscopy. *J Microsc* (2006) 224(Pt 3):213–32. doi: 10.1111/j.1365-2818.2006.01706.x
25. Chompunud NA, Ayudhya C, Amponnawarat A, Ali H. Substance P Serves as a Balanced Agonist for Mrgprx2 and a Single Tyrosine Residue Is Required for β-Arrestin Recruitment and Receptor Internalization. *Int J Mol Sci* (2021) 22(10):5318. doi: 10.3390/ijms22105318
26. von Kleist L, Stahlschmidt W, Bulut H, Gromova K, Puchkov D, Robertson MJ, et al. Role of the Clathrin Terminal Domain in Regulating Coated Pit Dynamics Revealed by Small Molecule Inhibition. *Cell* (2011) 146(3):471–84. doi: 10.1016/j.cell.2011.06.025
27. Dutta D, Williamson CD, Cole NB, Donaldson JG. Pitstop 2 Is a Potent Inhibitor of Clathrin-Independent Endocytosis. *PLoS One* (2012) 7(9):e45799. doi: 10.1371/journal.pone.0045799
28. Casella JF, Flanagan MD, Lin S. Cytochalasin D Inhibits Actin Polymerization and Induces Depolymerization of Actin Filaments Formed During Platelet Shape Change. *Nature* (1981) 293(5830):302–5. doi: 10.1038/293302a0
29. Schmid SL, Frolov VA. Dynamin: Functional Design of a Membrane Fission Catalyst. *Annu Rev Cell Dev Biol* (2011) 27:79–105. doi: 10.1146/annurev-cellbio-100109-104016
30. Azouz NP, Matsui T, Fukuda M, Sagi-Eisenberg R. Decoding the Regulation of Mast Cell Exocytosis by Networks of Rab Gtpases. *J Immunol (Baltimore Md 1950)* (2012) 189(5):2169–80. doi: 10.4049/jimmunol.1200542
31. Li L, Wan T, Wan M, Liu B, Cheng R, Zhang R. The Effect of the Size of Fluorescent Dextran on Its Endocytic Pathway. *Cell Biol Int* (2015) 39(5):531–9. doi: 10.1002/cbin.10424
32. Lin H-P, Singla B, Ghoshal P, Faulkner JL, Cherian-Shaw M, O'Connor PM, et al. Identification of Novel Macropinocytosis Inhibitors Using a Rational Screen of Food and Drug Administration-Approved Drugs. *Br J Pharmacol* (2018) 175(18):3640–55. doi: 10.1111/bph.14429
33. Koivusalo M, Welch C, Hayashi H, Scott CC, Kim M, Alexander T, et al. Amiloride Inhibits Macropinocytosis by Lowering Submembranous Ph and Preventing Rac1 and Cdc42 Signaling. *J Cell Biol* (2010) 188(4):547–63. doi: 10.1083/jcb.200908086
34. Mylvaganam S, Freeman SA, Grinstein S. The Cytoskeleton in Phagocytosis and Macropinocytosis. *Curr Biol CB* (2021) 31(10):R619–r32. doi: 10.1016/j.cub.2021.01.036
35. Fujii M, Kawai K, Egami Y, Araki N. Dissecting the Roles of Rac1 Activation and Deactivation in Macropinocytosis Using Microscopic Photo-Manipulation. *Sci Rep* (2013) 3(1):2385. doi: 10.1038/srep02385
36. Azouz NP, Zur N, Efergan A, Ohbayashi N, Fukuda M, Amihai D, et al. Rab5 Is a Novel Regulator of Mast Cell Secretory Granules: Impact on Size, Cargo, and Exocytosis. *J Immunol* (2014) 192(9):4043–53. doi: 10.4049/jimmunol.1302196
37. Sønder SL, Häger SC, Heitmann ASB, Frankel LB, Dias C, Simonsen AC, et al. Restructuring of the Plasma Membrane Upon Damage by Lc3-Associated Macropinocytosis. *Sci Adv* (2021) 7(27):eabg1969. doi: 10.1126/sciadv.abg1969
38. Ushio H, Ueno T, Kojima Y, Komatsu M, Tanaka S, Yamamoto A, et al. Crucial Role for Autophagy in Degranulation of Mast Cells. *J Allergy Clin Immunol* (2011) 127(5):1267–76.e6. doi: 10.1016/j.jaci.2010.12.1078

39. Nakano H, Ushio H. An Unexpected Role for Autophagy in Degranulation of Mast Cells. *Autophagy* (2011) 7(6):657–9. doi: 10.4161/auto.7.6.15384
40. Kimura S, Noda T, Yoshimori T. Dissection of the Autophagosome Maturation Process by a Novel Reporter Protein, Tandem Fluorescent-Tagged Lc3. *Autophagy* (2007) 3(5):452–60. doi: 10.4161/auto.4451
41. Tsvetanova NG, von Zastrow M. Spatial Encoding of Cyclic Amp Signaling Specificity by Gpcr Endocytosis. *Nat Chem Biol* (2014) 10(12):1061–5. doi: 10.1038/nchembio.1665
42. Canton J. Macropinocytosis: New Insights Into Its Underappreciated Role in Innate Immune Cell Surveillance. *Front Immunol* (2018) 9:2286. doi: 10.3389/fimmu.2018.02286
43. Liu Z, Xu E, Zhao HT, Cole T, West AB. Lrrk2 and Rab10 Coordinate Macropinocytosis to Mediate Immunological Responses in Phagocytes. *EMBO J* (2020) 39(20):e104862. doi: 10.15252/embj.2020104862
44. Lancaster CE, Fountain A, Dayam RM, Somerville E, Sheth J, Jacobelli V, et al. Phagosome Resolution Regenerates Lysosomes and Maintains the Degradative Capacity in Phagocytes. *J Cell Biol* (2021) 220(9):e202005072. doi: 10.1083/jcb.202005072
45. Martinez J, Almendinger J, Oberst A, Ness R, Dillon CP, Fitzgerald P, et al. Microtubule-Associated Protein 1 Light Chain 3 Alpha (Lc3)-Associated Phagocytosis Is Required for the Efficient Clearance of Dead Cells. *Proc Natl Acad Sci USA* (2011) 108(42):17396–401. doi: 10.1073/pnas.1113421108
46. Morishita H, Kanda Y, Kaizuka T, Chino H, Nakao K, Miki Y, et al. Autophagy Is Required for Maturation of Surfactant-Containing Lamellar Bodies in the Lung and Swim Bladder. *Cell Rep* (2020) 33(10):108477. doi: 10.1016/j.celrep.2020.108477

Conflict of Interest: The authors declare that the research was conducted in the absence of any commercial or financial relationships that could be construed as a potential conflict of interest.

Publisher's Note: All claims expressed in this article are solely those of the authors and do not necessarily represent those of their affiliated organizations, or those of the publisher, the editors and the reviewers. Any product that may be evaluated in this article, or claim that may be made by its manufacturer, is not guaranteed or endorsed by the publisher.

Copyright © 2022 Lazki-Hagenbach, Kleeblatt, Ali and Sagi-Eisenberg. This is an open-access article distributed under the terms of the Creative Commons Attribution License (CC BY). The use, distribution or reproduction in other forums is permitted, provided the original author(s) and the copyright owner(s) are credited and that the original publication in this journal is cited, in accordance with accepted academic practice. No use, distribution or reproduction is permitted which does not comply with these terms.

frontiers | Frontiers in Immunology

ORIGINAL RESEARCH
published: 29 June 2022
doi: 10.3389/fimmu.2022.900532

CT-M8 Mice: A New Mouse Model Demonstrates That Basophils Have a Nonredundant Role in Lupus-Like Disease Development

John Tchen[1,2], *Quentin Simon*[1,2], *Léa Chapart*[1,2], *Christophe Pellefigues*[1,2], *Hajime Karasuyama*[3], *Kensuke Miyake*[3], *Ulrich Blank*[1,2], *Marc Benhamou*[1,2], *Eric Daugas*[1,2,4] *and Nicolas Charles*[1,2]*

[1] Université Paris Cité, Centre de Recherche sur l'Inflammation, Institut National de la Santé Et de la Recherche Médicale (INSERM) UMR1149, Centre National de la Recherche Scientifique (CNRS). EMR8252, Faculté de Médecine site Bichat, Paris, France, [2] Université Paris Cité, Laboratoire d'Excellence INFLAMEX, Paris, France, [3] Inflammation, Infection and Immunity Laboratory, TMDU Advanced Research Institute, Tokyo Medical and Dental University (TMDU), Tokyo, Japan, [4] Service de Néphrologie, Hôpital Bichat, Assistance Publique-Hôpitaux de Paris, Paris, France

OPEN ACCESS

Edited by:
Frans J. Van Overveld, University College Roosevelt, Netherlands

Reviewed by:
Zou Xiang, Hong Kong Polytechnic University, Hong Kong SAR, China
Matthias Mack, University Medical Center Regensburg, Germany

***Correspondence:**
Nicolas Charles
nicolas.charles@inserm.fr
orcid.org/0000-0002-5416-5834

Specialty section:
This article was submitted to Inflammation, a section of the journal Frontiers in Immunology

Received: 20 March 2022
Accepted: 30 May 2022
Published: 29 June 2022

Citation:
Tchen J, Simon Q, Chapart L, Pellefigues C, Karasuyama H, Miyake K, Blank U, Benhamou M, Daugas E and Charles N (2022) CT-M8 Mice: A New Mouse Model Demonstrates That Basophils Have a Nonredundant Role in Lupus-Like Disease Development. Front. Immunol. 13:900532. doi: 10.3389/fimmu.2022.900532

Tissue-specific mouse models are essential tools to decipher the role of each cell compartment and/or their expressed genes in the pathophysiology of diseases. Here, we describe a new knock-in mouse model allowing expression of both the fluorescent protein tdTomato and the CRE recombinase selectively in the basophil compartment under the control of the Mcpt8 gene. These "CT-M8" mice did not show any abnormalities in their peripheral distribution of major immune cell populations nor their basophil function. CT-M8 mice allowed the identification of basophils by immunofluorescence and flow cytometry and basophil-specific Cre-mediated floxed gene deletion. Breeding of our CT-M8 mice with the *ROSA26*$^{flox\text{-}stop\text{-}DTA}$ mice led to the generation of basophil-deficient mice with no detectable abnormalities in other cell compartments. These mice were then used to document basophil involvement in systemic lupus erythematosus (SLE) pathophysiology since we previously reported by transient depletion of these cells during the course of an ongoing disease that they support and amplify autoantibody production in two distinct lupus-like mouse models (*Lyn*$^{-/-}$ and pristane-induced). Here, constitutive basophil deficiency prevented pristane-induced lupus-like disease development by limiting autoantibody titers and renal damages. Therefore, basophils have a nonredundant role in pristane-induced lupus-like disease and are involved in both its induction and amplification. This CT-M8 new mouse model will allow us to finely decipher the role of basophils and their expressed genes in health and disease.

Keywords: basophils, mouse model, systemic lupus erythematosus, lupus nephritis, autoimmunity, TH2

INTRODUCTION

Systemic lupus erythematosus (SLE) is an autoimmune disease (AID) affecting mainly women of child-bearing age. SLE can affect different organs, such as skin, lungs, joints, or kidneys. Lupus nephritis is one of the most severe organ manifestations of SLE. It affects 25% to 60% of SLE patients, and about 20% of these patients develop a life-threatening end-stage renal disease (1). SLE is characterized by the presence in the patient's blood of autoreactive antibodies of several isotypes, mainly raised against nuclear antigens such as double-stranded DNA (dsDNA) or ribonucleoproteins (RNPs) (2). Once conjugated to autoantigens and complement factors, the formed immune complexes (ICs) can deposit in target organs where they induce inflammation, leading to organ injury and consequent organ dysfunction. ICs also induce Fc receptor-dependent activation of innate immune cells such as plasmacytoid dendritic cells (pDCs), neutrophils, macrophages, and basophils, which all contribute to an amplification loop of autoantibody production and disease activity (1, 3).

We previously reported that basophils accumulate in secondary lymphoid organs (SLOs) during lupus pathogenesis through mechanisms dependent on IgE, IL-4, prostaglandin D2 (PGD2), and CXCR4. There, they promote autoreactive plasma cell accumulation and consequent autoantibody production (4–6). These findings were validated in several human SLE patient cohorts and multiple lupus-like mouse models. Among these models, basophils were shown to contribute to the pristane-induced lupus-like disease (PIL) (7). In mice with established disease, basophil depletion dampened disease activity by reducing short-lived plasma cell number, serum autoantibody titers, IC deposition in glomeruli, and the proinflammatory environment in the kidneys (4, 6, 7), identifying basophils as promising therapeutic targets in SLE. However, whether basophils are involved in the primary development of the disease remains unknown.

Here, we report the generation of a new mouse model called CT-M8 (*Mcpt8*^{tm1Ics}) that allows the expression of the CRE recombinase (CRE) and the tandem Tomato (tdT) fluorescent protein downstream of the gene of the basophil-specific protease mast cell protease 8 (*Mcpt8*) (8). This model enabled convenient basophil detection by fluorescent microscopy and flow cytometry as well as basophil-specific floxed gene deletion. Breeding of these CT-M8 mice with the ROSA-DTA mice (expressing a loxP site-flanked stop cassette upstream of the gene encoding diphtheria toxin A under the control of the Rosa26 promoter [B6.129P2-Gt(ROSA)26Sortm1(DTA)Lky/J)] (9) allowed the generation of constitutive basophil-deficient mice (*Mcpt8*$^{CT/+}$ *Rosa26*$^{DTA/+}$). In the PIL model, basophil deficiency prevented the accumulation of short-lived plasma cells in SLOs as well as the detection of anti-RNP autoantibodies and IC deposits in the glomeruli of the mice 8 weeks after pristane injection. Overall, this new model of basophil-deficient mice allowed showing that basophils have a nonredundant role in PIL development and might be mandatory in the SLE-like disease course to reach a pathogenic threshold.

MATERIAL AND METHODS

Generation of *Mcpt8*^{tm1Ics} or CT-M8 Mice

The C57BL/6 Mcpt8-Cre-tdTomato or *Mcpt8*^{tm1Ics} or "CT-M8" mice were generated by the Institut Clinique de la Souris (Illkirch, France) from the Phenomin consortium. Briefly, a cassette containing an internal ribosome entry site (IRES), the cDNA encoding the CRE recombinase, a viral Thosea asigna virus 2A (T2A) sequence, and the fluorescent protein tandem Tomato or "tdT" was knocked in together with a Neo resistance (Neo^r) cassette flanked by two FRT sites after the stop codon of the Mcpt8 gene. Chimeric mice were generated by the injection of mutant ES cells into C57BL/6 blastocysts and cross-bred with Flp deleter C57BL/6N females (10) to obtain Neo^r-deleted *Mcpt8*^{tm1Ics} mice (**Figure 1A**).

Mice

C57BL/6J wild-type mice were purchased from Charles River Laboratories (Ecully, France). The Rosa26-loxP-Stop-loxP-DTA C57BL/6J ($R_{26}^{DTA/DTA}$ or $R_{26}^{DTA/+}$) mice (9) were purchased from The Jackson Laboratory through Charles River Laboratories. *Il4*$^{fl/fl}$ C57BL/6J mice were previously described (11). For all experiments, WT, *Mcpt8*$^{CT/CT}$, *Mcpt8*$^{CT/+}$, *Mcpt8*$^{CT/+}$ x *Il4*$^{fl/fl}$, *Il4*$^{fl/fl}$, $R_{26}^{DTA/DTA}$, and *Mcpt8*$^{CT/+}$ × $R_{26}^{DTA/+}$ mice were used on a C57BL/6J, C57BL/6N, or C57BL/6JxN mixed background.

For phenotyping experiments, mice from both sexes in equal proportions were used between 8 and 15 weeks of age. For pristane-induced lupus-like (PIL) disease experiments, 8-week-old female mice of the indicated genotype received a single intraperitoneal injection of 500 µl of pristane (Sigma-Aldrich, Burlington, MA, USA) or phosphate-buffered saline (PBS, Gibco) as a control and were sacrificed 8 weeks later. Mice were maintained under specific pathogen-free conditions in our animal facilities. The study was conducted in accordance with the French and European guidelines and approved by the local ethics committee, comité d'éthique Paris Nord N°121 and the Ministère de l'enseignement supérieur, de la recherche et de l'innovation under the authorization number APAFIS#14115.

Mouse Sample Processing

Mice were euthanized in a regulated CO_2 chamber. Blood was harvested with a heparinized syringe with a 25-G needle by cardiac puncture. Peritoneal lavages were realized by injecting 5 ml of PBS and 2 ml of air into the peritoneal cavity. After 50 rotations, the peritoneal wall was opened and peritoneal lavage was harvested with a pipette. Cervical, axillary, and inguinal lymph nodes were harvested and pooled. Bone marrow was extracted from both femurs, and the spleen was harvested. The left kidney was embedded in OCT (CellPath, Newton, UK) and snap-frozen in liquid nitrogen and kept at −80°C until immunofluorescence analysis. Single-cell suspensions from blood, bone marrow, peritoneal lavage, spleen, or peripheral lymph nodes (LNs) (pooling inguinal, axillary, and cervical LNs) were prepared by mechanical disruption over a 40-µm cell strainer (Falcon, Corning, Corning, NY, USA) when necessary. Blood was centrifuged at 300×*g* for 10 min at room temperature, and

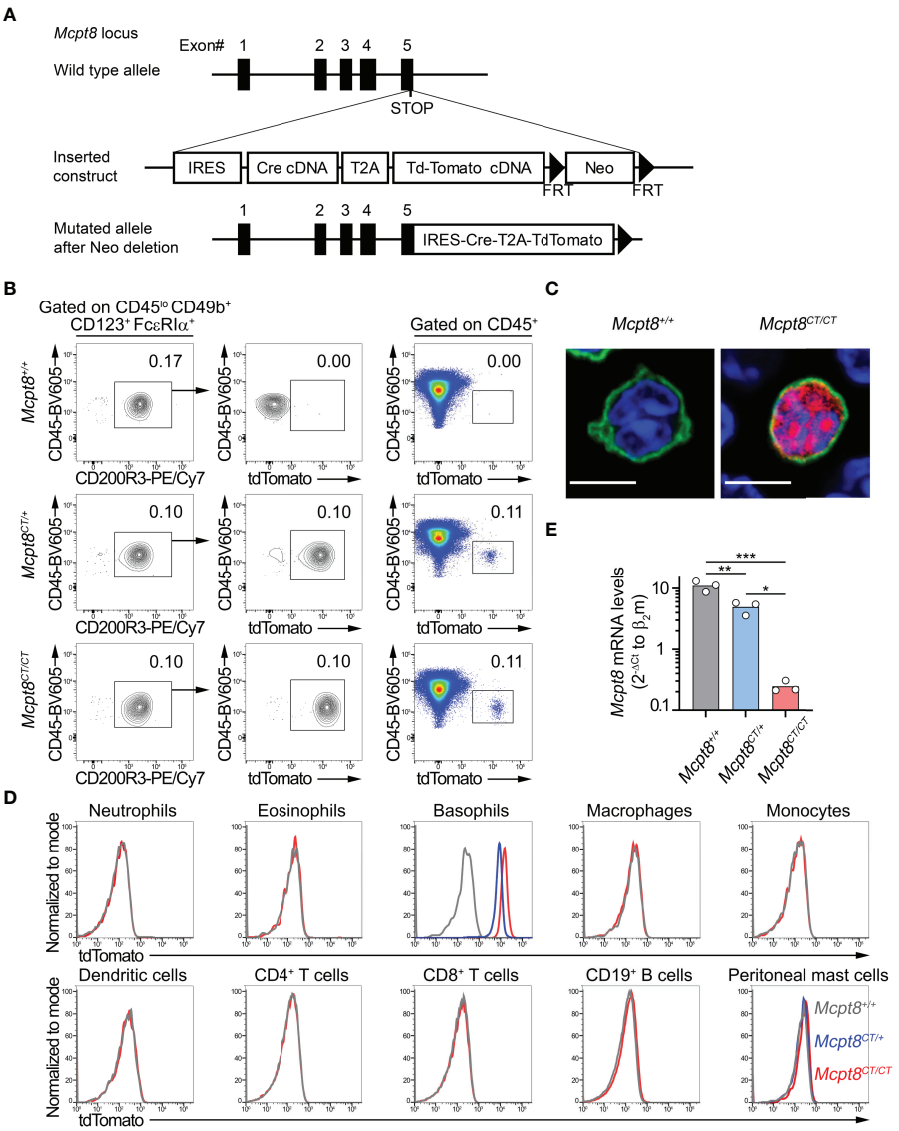


FIGURE 1 | The CT-M8 mice: a new basophil-specific mouse model. **(A)** Schematic representation of Mcpt8-Cre-tdT knock-in targeting constructs to generate the CT-M8 (*Mcpt8*^{tm1Ics}) mice (see *Methods*) where Cre and tandem tomato fluorescent protein are expressed under the control of the basophil-specific Mcpt8 promoter. **(B)** Fluorescence-activated cell sorter (FACS) gating strategy showing tdTomato expression in spleen basophils from *Mcpt8*$^{CT/CT}$ and *Mcpt8*$^{CT/+}$ mice but not in wild-type animals (*Mcpt8*$^{+/+}$). **(C)** Basophil-specific tdTomato expression (red) imaged by confocal microscopy on splenocytes from *Mcpt8*$^{+/+}$ (left) and *Mcpt8*$^{CT/CT}$ (right) mice, stained with anti-IgE antibody (green) and DNA staining (DAPI, blue). Scale bar, 5 µm. Larger fields are shown in **Supplementary Figure S1**. **(D)** Expression of the tdTomato assessed by flow cytometry in the indicated spleen cell types (except for peritoneal mast cells, which are from the peritoneal cavity) defined as described in **Table 1** in *Mcpt8*$^{+/+}$ (grey lines), *Mcpt8*$^{CT/+}$ (blue lines), and *Mcpt8*$^{CT/CT}$ (red lines). One representative set of data out of 4 per genotype is shown. **(E)** Mcpt8 mRNA expression levels were assessed by RT-quantitative PCR on mRNA purified from FACS-sorted bone marrow primary basophils from mice of the indicated genotypes (see *Methods*). Data are expressed as the mean of the $2^{-\Delta Ct}$ values of Mcpt8 relative to the β_2-microglobulin Ct. Individual values are shown inside bars. Statistical analyses were done by one-way ANOVA followed by Tukey's multiple comparisons test. *$p < 0.05$; **$p < 0.01$; ***$p < 0.001$.

plasma was harvested for further analysis. The specimens were incubated for 5 min at room temperature in ACK lysing buffer (150 mM of NH_4Cl, 12 mM of $NaHCO_3$, 1 mM of EDTA, pH 7.4) and neutralized with twice the volume of PBS, and cells were centrifuged (500×*g*, 5 min). This step was repeated three times for blood samples. Cell concentrations were determined with a hemacytometer, and 1–5 million cells per point were used for fluorescence-activated cell sorting (FACS) staining (see below).

Flow Cytometry

Unspecific antibody-binding sites were saturated with a blocking buffer containing 10 µg/ml of anti-CD16/CD32 antibody clone

2.4G2 (BioXcell, Lebanon, NH, USA), and 100 µg/ml of polyclonal rat IgG, polyclonal mouse IgG, and polyclonal Armenian Hamster IgG (Innovative Research, Inc., Novi, MI, USA) in FACS buffer (PBS, 1% bovine serum albumin, 1 mM EDTA, and 0.05% sodium azide). Mouse cells were stained in optimized concentration of fluorophore-conjugated monoclonal antibodies (clone) targeting CD45 (30-F11), FcεRIα (MAR1), CD49b (DX5), IA/IE (M5/114.2), CD200R1 (OX-110), CD200R3 (Ba13), TCRβ (KT3.1.1), CD4 (RM4-4), CD8α (53-6.7), CD11b (M1/70), F4/80 (BM8), CD11c (N418), CD317 (927), Ly6G/Ly6C (Gr1, RB6-8C5), CD19 (6D5), CD117 (2B8), and CD138 (281-2), all from BioLegend, San Diego, CA, USA; and IL-4 (11B11) from BD Biosciences, Franklin Lakes, NJ, USA; IL-6 (MP5-20F3), IL-13 (eBio13A), and CD123 (5B11) from ThermoFisher Scientific, Waltham, MA, USA. Basophils were defined as $CD45^{lo}$ $CD3^-$ $CD19^-$ $CD117^-$ $CD200R3^+$ $CD49b^+$ $FcεRIα^+$ $CD123^+$ cells among $CD45^+$ viable singlets. Peritoneal mast cells were defined as $CD45^+$ $CD3^-$ $CD19^-$ F4/80$^-$ $FcεRIα^+$ $CD117^+$. Other cells were defined as indicated in **Tables 1**, **2**. For all flow cytometry experiments, dead cells were stained in PBS with GHOST 510 viability dye (TONBO, San Diego, CA, USA) and excluded from the analysis. For intracellular cytokine staining, cells were fixed for 30 min at 4°C with fixation buffer and staining was realized in intracellular staining permeabilization wash buffer following the manufacturer's instructions (both buffers from BioLegend, San Diego, CA, USA). Flow cytometry acquisition was realized using a Becton Dickinson 5-laser LSR Fortessa X-20 and data analysis using Flowjo vX (Treestar, BD Biosciences, Franklin Lakes, NJ, USA). For assessment of the CD200R1 expression level, the ratio of the geometric mean fluorescence intensity (gMFI) of CD200R1 to the fluorescence minus one (containing the isotype control) gMFI was calculated and expressed in arbitrary units (A.U.).

Confocal Microscopy

Mouse splenocytes were harvested as described above and resuspended in PBS containing 2% FCS and 2 mM of EDTA. Splenocytes were then depleted from B, NK, and T cells by magnetic selection through the use of biotinylated anti-CD19 (6D5), anti-NK1.1 (PK136), anti-CD8α (53-6.7), anti-CD4 (RM4-5) (BioLegend) and MagniSort™ streptavidin-negative selection beads, following manufacturer's instructions (ThermoFisher Scientific, Waltham, MA, USA). This basophil-enriched cell suspension was then stained with a FITC-conjugated

TABLE 1 | Immune cell populations in *Mcpt8*$^{+/+}$, *Mcpt8*$^{CT/+}$, and *Mcpt8*$^{CT/CT}$ mice.

Population	Defined in $CD45^+$ living singlets as cells	*Mcpt8*$^{+/+}$ (*n* = 4)		*Mcpt8*$^{CT/+}$ (*n* = 4)			*Mcpt8*$^{CT/CT}$ (*n* = 4)		
		Mean	SD	Mean	SD	*p*-value to +/+	Mean	SD	*p*-value to +/+
Spleen									
Basophils	$CD45^{lo}$ $CD49b^+$ $FcεRIα^+$ $CD123^+$ $CD200R3^+$	0.18	0.0483	0.1165	0.0275	*0.8284*	0.224	0.2574	*0.9127*
tdT^+ cells	$CD45^+$ tdT^+	0.0010	0.0007	0.1275	0.0330	***<0.0001***	0.1033	0.0115	***0.0006***
$CD19^+$ B cells	$CD45^+CD19^+$	52.75	4.133	51.18	1.258	*0.6875*	52.15	1.515	*0.9451*
$CD4^+$ T cells	$CD45^+$ $TCRβ^+$ $CD4^+$ $CD8^-$	19.18	1.497	19.58	2.232	*0.9871*	17.65	5.786	*0.8316*
$CD8^+$ T cells	$CD45^+$ $TCRβ^+$ $CD4^-$ $CD8^+$	11.5	1.481	10.98	0.6898	*0.8056*	10.64	1.218	*0.5755*
Neutrophils	$CD45^+$ $TCRβ^-$ $CD19^-$ $Gr1^{hi}$ $CD11b^{hi}$	2.548	0.6401	2.895	0.633	*0.681*	3.113	0.429	*0.3867*
Macrophages	$CD45^+$ $TCRβ^-$ $CD19^-$ Neutro$^-$ $CD11b^{lo}$ F4/80^{hi}	1.015	0.6523	0.98	0.6606	*0.9963*	0.6725	0.4869	*0.7122*
Eosinophils	$CD45^+$ $TCRβ^-$ $CD19^-$ Neutro$^-$ Macro$^-$ $CD11b^+$ SSC^{hi}	0.475	0.1731	0.5525	0.4801	*0.9308*	0.5275	0.1198	*0.9675*
pDCs	$CD45^+$ $TCRβ^-$ $CD19^-$ Neutro$^-$ Macro$^-$ Eosino$^-$ $CD11c^+$ $PDCA1^+$	0.4625	0.3356	0.45	0.3982	*0.9987*	0.395	0.3534	*0.9628*
DCs	$CD45^+$ $TCRβ^-$ $CD19^-$ Neutro$^-$ Macro$^-$ Eosino$^-$ pDC$^-$ $CD11c^+$ $IA\text{-}IE^+$	1.303	0.1406	1.355	0.2063	*0.8999*	1.115	0.152	*0.3059*
Monocytes	$CD45^+$ $TCRβ^-$ $CD19^-$ Neutro$^-$ Macro$^-$ Eosino$^-$ pDC$^-$ DC$^-$ $CD11b^+$	1.618	0.6074	1.828	0.2952	*0.8218*	1.95	0.5311	*0.6636*
Bone marrow									
Basophils	$CD45^{lo}$ $CD49b^+$ $FcεRIα^+$ $CD123^+$ $CD200R3^+$	0.77	0.0828	0.7275	0.1209	*0.8433*	0.6275	0.1135	*0.199*
tdT^+ cells	$CD45^+$ tdT^+	0.0034	0.0036	0.7475	0.1087	***<0.0001***	0.6525	0.1115	***<0.0001***
Neutrophils	$CD45^+$ $TCRβ^-$ $CD19^-$ $Gr1^{hi}$ $CD11b^{hi}$	60.9	5.363	65.88	3.82	*0.4056*	61.8	6.185	*0.9678*
Eosinophils	$CD45^+$ $TCRβ^-$ $CD19^-$ Neutro$^-$ Macro$^-$ $CD11b^+$ SSC^{hi}	4.138	1.325	4.145	2.126	*>0.9999*	4.228	1.646	*0.997*
Blood									
Basophils	$CD45^{lo}$ $CD49b^+$ $FcεRIα^+$ $CD123^+$ $CD200R3^+$	0.3733	0.2515	0.2925	0.1565	*0.8186*	0.2725	0.1162	*0.7355*
tdT^+ cells	$CD45^+$ tdT^+	0.0056	0.0026	0.2875	0.1735	***0.021***	0.2525	0.1112	***0.04***
Neutrophils	$CD45^+$ $TCRβ^-$ $CD19^-$ $Gr1^{hi}$ $CD11b^{hi}$	23.8	6.483	27.45	6.675	*0.6468*	22.2	3.093	*0.9165*
Eosinophils	$CD45^+$ $TCRβ^-$ $CD19^-$ Neutro$^-$ Macro$^-$ $CD11b^+$ SSC^{hi}	2.005	0.8843	1.948	0.9925	*0.9954*	2.1	0.7896	*0.9876*
Peritoneal cavity									
Mast cells	$CD45^+$ F4/80$^-$ $FcεRIα^+$ $CD117^+$	2.313	0.640	2.378	0.726	*0.9879*	2.268	0.218	*0.9938*

Proportions of immune cell populations among $CD45^+$ cells in the indicated compartments were determined by flow cytometry. Cells were defined following the indicated gating strategy; 8- to 15-week-old mice were analyzed. Statistical analysis was done by one-way analysis of variance (ANOVA) followed by Tukey's multiple comparison test. p-values indicated are from comparison to the Mcpt8$^{+/+}$ group. SD, standard deviation.

Bold/Italic values in Table 1 and 2 are the statistically significant values (p<0.05).

TABLE 2 | Immune cell populations in basophil-deficient mice.

Population	Defined in CD45$^+$ living singlets as cells	*Mcpt8*$^{CT/+}$ (*n* = 8–12)		*Mcpt8*$^{CT/+}$*R26-Stop*$^{fl/WT}$*-DTA* (*n* = 5–12)			*Mcpt8*$^{+/+}$ *R26-Stop*$^{fl/fl}$*-DTA* (*n* = 5–12)		
		Mean (% of CD45$^+$)	SD	Mean (% of CD45$^+$)	SD	*p*-value to *Mcpt8*$^{CT/+}$	Mean (% of CD45$^+$)	SD	*p*-value to *Mcpt8*$^{CT/+}$
Spleen									
Basophils	CD45^{lo} CD49b$^+$ FcεRIα$^+$ CD123$^+$ CD200R3$^+$	0.1258	0.032	0.0026	0.001	***<0.0001***	0.1586	0.055	0.1799
tdT$^+$ cells	CD45$^+$ tdT$^+$	0.13	0.040	0.0013	0.002	***<0.0001***	0.0010	0.000	***<0.0001***
CD19$^+$ B cells	CD45$^+$CD19$^+$	40.01	13.67	45.28	11.14	*0.6382*	36.08	7.167	*0.8221*
CD4$^+$ T cells	CD45$^+$ TCRβ$^+$ CD4$^+$ CD8$^-$	24.23	6.822	21.28	4.477	*0.5101*	25.88	2.590	*0.8454*
CD8$^+$ T cells	CD45$^+$ TCRβ$^+$ CD4$^-$ CD8$^+$	14.98	5.007	13.10	2.290	*0.5696*	16.16	2.624	*0.8378*
Neutrophils	CD45$^+$ TCRβ$^-$ CD19$^-$ Gr1^{hi} CD11b^{hi}	3.010	0.922	2.040	1.406	*0.3369*	3.224	1.758	*0.9576*
Macrophages	CD45$^+$ TCRβ$^-$ CD19$^-$ Neutro$^-$ CD11b^{lo} F4/80^{hi}	1.324	0.759	1.975	1.296	*0.4398*	1.732	0.963	*0.7735*
Eosinophils	CD45$^+$ TCRβ$^-$ CD19$^-$ Neutro$^-$ Macro$^-$ CD11b$^+$ SSC^{hi}	0.5400	0.338	0.5125	0.192	*0.9909*	0.8760	0.747	*0.3732*
pDCs	CD45$^+$ TCRβ$^-$ CD19$^-$ Neutro$^-$ Macro$^-$ Eosino$^-$ CD11c$^+$ PDCA1^{hi}	0.2878	0.315	0.1665	0.116	*0.4971*	0.1098	0.051	*0.3235*
DCs	CD45$^+$ TCRβ$^-$ CD19$^-$ Neutro$^-$ Macro$^-$ Eosino$^-$ pDC$^-$ CD11c$^+$ IA-IE$^+$	1.830	0.738	1.209	0.829	*0.2585*	2.662	0.672	*0.1628*
Monocytes	CD45$^+$ TCRβ$^-$ CD19$^-$ Neutro$^-$ Macro$^-$ Eosino$^-$ pDC$^-$ DC$^-$ CD11b^{hi}	1.938	0.319	1.740	0.939	*0.8224*	2.182	0.483	*0.7945*
Bone marrow									
Basophils	CD45^{lo} CD49b$^+$ FcεRIα$^+$ CD123$^+$ CD200R3$^+$	0.7870	0.141	0.0210	0.008	***<0.0001***	0.6957	0.215	*0.3735*
tdT$^+$ cells	CD45$^+$ tdT$^+$	0.8667	0.138	0.0267	0.011	***<0.0001***	0.0080	0.005	***<0.0001***
Neutrophils	CD45$^+$ TCRβ$^-$ CD19$^-$ Gr1^{hi} CD11b^{hi}	47.07	4.794	48.05	5.363	*0.9381*	49.84	6.493	*0.7566*
Eosinophils	CD45$^+$ TCRβ$^-$ CD19$^-$ Neutro$^-$ Macro$^-$ CD11b$^+$ SSC^{hi}	4.575	1.600	5.323	1.788	*0.5082*	4.542	1.055	*0.9987*
Blood									
Basophils	CD45^{lo} CD49b$^+$ FcεRIα$^+$ CD123$^+$ CD200R3$^+$	0.4580	0.234	0.0035	0.003	***<0.0001***	0.5471	0.184	*0.5331*
tdT$^+$ cells	CD45$^+$ tdT$^+$	0.5133	0.174	0.0024	0.001	***<0.0001***	0.0042	0.007	***<0.0001***
Neutrophils	CD45$^+$ TCRβ$^-$ CD19$^-$ Gr1^{hi} CD11b^{hi}	19.03	9.178	14.16	5.145	*0.3562*	14.8	9.194	*0.4710*
Eosinophils	CD45$^+$ TCRβ$^-$ CD19$^-$ Neutro$^-$ Macro$^-$ CD11b$^+$ SSC^{hi}	1.465	0.765	1.585	0.655	*0.9235*	1.219	0.754	*0.7306*
Peritoneal cavity									
Mast cells	CD45$^+$ F4/80$^-$ FcεRIα$^+$ CD117$^+$	1.746	0.724	1.895	0.677	*0.8788*	2.236	0.803	*0.2502*

Proportions of immune cell populations in the indicated compartments were determined by flow cytometry. Cells were defined following the indicated gating strategy; 15- to 25-week-old mice were analyzed. Statistical analysis was done by one-way analysis of variance (ANOVA) followed by Tukey's multiple comparison test. p-values indicated are from comparison to the Mcpt8$^{CT/+}$ group. SD, standard deviation.

Bold/Italic values in Table 1 and 2 are the statistically significant values (p<0.05).

anti-IgE antibody (23G3, Southern Biotech, Birmingham, AL, USA) in FACS buffer, washed, incubated on poly-L-lysine-coated coverslips for 20 min at 37°C, washed in PBS, fixed with a fixation buffer (BioLegend), and permeabilized with PZB. The nuclei were stained with 360 nM of 4′,6-diamidino-2-phenylindole (DAPI) in PZB and washed in PBS. Coverslips were then mounted in Shandon Immu-Mount (ThermoFisher Scientific, Waltham, MA, USA) on superfrost slides (VWR, Radnor, PA, USA) and incubated overnight at 4°C. Image acquisition was realized with a Zeiss, Oberkochen, Germany LSM 780 confocal microscope, and image analysis was done with the Zen 2012 (Blue edition) service pack 2 software.

Ex Vivo Primary Cell Stimulation

Mouse splenocytes were harvested through mechanical disruption over a 40-µm of cell strainer, and red blood cells were lysed as described above. Single-cell suspensions at 2 million cells/ml were cultured in a culture medium (RPMI 1640) with Glutamax and 20 mM of HEPES, 1 mM of Na-pyruvate, and 1× nonessential amino acids (all from Life Technologies); 100 µg/ml of streptomycin and 100 U/ml of penicillin (GE Healthcare, Chicago, IL, USA); and 37.5 µM of β-mercaptoethanol (Sigma-Aldrich, Burlington, MA, USA) supplemented with 20% heat-inactivated fetal calf serum (FCS) (Life Technologies) at 37°C and 5% CO_2. For phorbol-myristate-acetate (PMA) and ionomycin-stimulation experiments, whole splenocytes were stimulated or not with 40 nM of PMA and 800 nM of ionomycin for 4 h in the presence of 2 µg/ml of brefeldin A (all from Sigma-Aldrich, Merck). For other stimulations, splenocytes were enriched in basophils by depleting T, B, and NK cells as described in the confocal microscopy section. CD200R1 upregulation was measured after 2 h of stimulation with 500 ng/ml of anti-IgE antibody (clone RME-1, BioLegend). Anti-IgE-induced IL-4 and IL-6 productions by basophils were quantified by flow cytometry after 4 h of stimulation with 500 ng/ml of anti-IgE antibody in the presence of brefeldin A. At the end of these stimulations, cells were harvested and treated as described in the *Flow Cytometry* section. For IL-3-induced basophil stimulation, cells were stimulated over 24 h with

1 ng/ml of recombinant mouse IL-3 (PeproTech, Rocky Hill, NJ, USA) and IL-4 and IL-6 productions were quantified by ELISA (R&D systems, Minneapolis, MN, USA), normalized to the number of basophils present in each well and expressed in picograms per 1,000 basophils.

Mcpt8 mRNA qPCR Analysis

Single-cell suspensions of bone marrow (BM) cells (in PBS containing 2% FCS and 2 mM of EDTA) were stained with biotin-conjugated anti-Ly6G (1A8) and anti-CD19 (6D5) antibodies (BioLegend, San Diego, CA, USA) before removing positive cells with MagniSort™ streptavidin-negative selection beads following the manufacturer's instructions (ThermoFisher Scientific, Waltham, MA, USA). After this basophil enrichment, primary BM basophils were selected for CD200R3 expression and sorted using a BD FACSMelody™ cell sorter (BD Biosciences, Franklin Lakes, NJ, USA). RNA extraction was performed by using Trizol reagent as described in the manufacturer's protocol (Invitrogen). cDNA was synthesized with SuperScript™ III First-Strand Synthesis System (Invitrogen). Quantitative PCR was performed with SsoAdvanced SYBR green reaction mix (Bio-Rad, Hercules, CA, USA) using the M_B2m_1 KiCqStart™ primer pair for mouse β2-microglobulin as housekeeping gene (Sigma-Aldrich, Merck) and the following primers for Mcpt8 quantification: Forward primer: 5′-GTGGGAAATCCCAGTGAGAA-3′ and Reverse primer: 5′-TCCGAATCCAAGGCATAAAG-3′ (12). Quantitative PCR was performed on the CFX96 Touch Real-Time PCR Detection System (Bio-Rad, Hercules, CA, USA), and, following amplification, Ct values were obtained using the CFX Manager™ software 2.1 (Bio-Rad, Hercules, CA, USA).

TH2 Polarization of Spleen CD4+ T Cells *Ex Vivo*

F(ab')2 anti-CD3 (clone145-2C11 at 10 µg/ml) and anti-CD28 (clone PV-1 at 2 µg/ml) antibodies (BioXcell, Lebanon, NH, USA) were coated overnight at 4°C in 96-well plates (Costar) in sterile-filtered 20-mM carbonate buffer (pH 9.6) containing 2 mM of $MgCl_2$ and 0.01% NaN_3. Wells were washed in PBS before plating the cells. Total spleen $CD4^+$ T cells were sorted by magnetic negative selection following the manufacturer's instructions (STEMCELL Technologies, Vancouver, Canada). $CD4^+$ T cells were then resuspended in a culture medium (same as above) at 0.25 million cells/ml. Two hundred microliters of cell suspension were then added to wells and supplemented with 10 ng/ml of IL-2 and 50 ng/mL of IL-4 (both from BioLegend, San Diego, CA, USA). After 2 days in the culture at 37°C and 5% CO_2, IL-2 and IL-4 were added again at the same concentrations for 3 more days. TH2-polarized $CD4^+$ T cells were then stimulated for 4 h with 40 nM of PMA and 800 nM of ionomycin in the presence of 2 µg/ml of brefeldin A (Sigma-Aldrich, Merck). Flow cytometry analysis was then performed as described above.

Detection of Anti-RNP Autoantibodies

Maxisorp plates (Thermo Scientific) were coated overnight at 4°C with 10 µg/ml of purified RNP complexes (Immunovision, Springdale, AR, USA) diluted in carbonate buffer (100 mM of $NaHCO_3$ and 30 mM of Na_2CO_3, pH 9.6). Plates were washed 3 times in 300 µl of PBS containing 0.05% Tween-20 (PBS-T, Bio-Rad Laboratories) and then saturated for 1 h at room temperature with 200 µl of PBS containing 5% FCS (Gibco, Waltham, MA, USA). Plates were then washed 3 times in 300 µl of PBS-T. All plasma samples were diluted 1:100 in PBS-T containing 5% FCS and 100 µl added to the wells and incubated for 2 h at room temperature. After 5 washes in PBS-T, a secondary antibody goat anti-mouse IgG conjugated to horseradish peroxidase (HRP) (Invitrogen) was diluted in PBS-T at 5% FCS at a final concentration of 500 ng/ml, and 100 µl was added to the wells for 1 h at room temperature. The plates were finally washed 5 times in 300 µl of PBS-T. A total of 100 µl of tetramethylbenzidine (TMB) substrate (ThermoFisher Scientific, Waltham, MA, USA) was added to the wells, incubated at room temperature for at least 20 min, and the reaction was stopped by adding 100 µl of 0.2 N of sulfuric acid solution. Optical density at 450 nm was measured by spectrophotometry (Infinite 200 Pro plate reader, Tecan, Männedorf, Germany). On each plate, similar negative and positive controls were run. Optical density (OD) values were first normalized to the negative controls, and then, the presented results were normalized to the mean of the PBS-injected control mice values and expressed in arbitrary units.

Kidney Immunofluorescence Assays

Acetone-fixed 4 µm cryosections of OCT-embedded kidneys were thawed and blocked in 10% fetal calf serum (FCS) (Gibco, Waltham, MA, USA). Slices were stained with FITC-conjugated anti-mouse C3 (Cedarlane, Burlington, ON, Canada) or Alexa Fluor® 488-conjugated anti-mouse IgG F(ab)'2 (Jackson Immunoresearch, West Grove, PA, USA), or their respective isotype controls, before being mounted in Immunomount (ThermoFisher Scientific, Waltham, MA, USA) and analyzed by fluorescent microscopy (Leica DMR, Leica Microsystems, Wetzlar, Germany). The ratio of specific glomerular fluorescence over tubulointerstitial background was then measured using ImageJ software (NIH), averaging 30 glomeruli per mouse for each sample.

Statistics

Student's unpaired *t*-tests were used to compare the differences of one variable between two groups when distributions were Gaussian and Mann–Whitney *U* tests for nonparametric distributions. When more than two groups were compared, one-way ANOVA coupled with Tukey's multiple comparisons test was used. Statistics were done using Prism v9 software (Graphpad).

RESULTS

CT-M8: A New Basophil-Specific Mouse Model

We aimed at developing a basophil-specific mouse model in which we could both follow basophil localization by immunofluorescence and flow cytometry and express the CRE recombinase selectively in the basophil compartment. To achieve that goal, we took

advantage of the gene encoding for the basophil-specific protease Mcpt8 (8). The strategy described in the *Methods* section and **Figure 1A** led to the generation of *Mcpt8*^{tm1Ics} mice named here "CT-M8" (*Mcpt8*$^{CT/CT}$), standing for CRE recombinase and tdTomato expressions (CT) under the control of *Mcpt8* gene transcription (M8). CT-M8 mice had normal fertility and did not show any dysregulation of their immune cell distribution in lymphoid organs or blood (**Table 1**). As expected, the construct allowed straightforward basophil detection by flow cytometry (**Figure 1B**). Direct tdTomato$^+$ basophil gating on living singlet CD45$^+$ cells was as efficient to detect basophils as a conventional gating strategy for basophils (CD45^{lo} CD49b$^+$ FcεRIα$^+$ CD123$^+$ CD200R3$^+$) (**Figure 1B**; **Table 1**). By confocal microscopy, basophil detection was evident in CT-M8 mice, and tdTomato expression in the spleen was restricted to IgE-bearing cells (**Figure 1C**; **Supplementary Figure S1**). Of note, tdTomato expression in *Mcpt8*$^{CT/+}$ basophils was half that in *Mcpt8*$^{CT/CT}$ basophils (**Figures 1B, D**). Although inserted after the stop codon, the construct inserted into the *Mcpt8* locus led to a drastic reduction of *Mcpt8* mRNA expression as measured by qPCR in bone marrow (BM) basophils isolated from *Mcpt8*$^{CT/CT}$ mice. However, *Mcpt8* mRNA expression was still significantly retained in *Mcpt8*$^{CT/+}$ basophils (**Figure 1E**).

tdTomato expression was strictly restricted to the basophil population in all tested organs (blood, peritoneal lavage, lymph nodes, bone marrow, and spleen) (**Figure 1D**; **Table 1**). Spleen basophils from *Mcpt8*$^{CT/CT}$ and *Mcpt8*$^{CT/+}$ mice produced IL-4 and IL-6 to the same extent as WT (*Mcpt8*$^{+/+}$) basophils after phorbol myristate acetate (PMA) and ionomycin stimulation, demonstrating that construct expression did not alter the maximal abilities of the basophils from CT-M8 mice to produce these cytokines (**Figures 2A–C**). CD200R1 is a recognized mouse basophil activation marker (13, 14). Anti-IgE-mediated basophil activation resulted in similar CD200R1 upregulation on spleen basophils from *Mcpt8*$^{+/+}$ and *Mcpt8*$^{CT/CT}$ mice and to similar IL-4 and IL-6 productions (**Figures 2D–J**). Furthermore, IL-3-mediated activation was as efficient in *Mcpt8*$^{+/+}$ as in *Mcpt8*$^{CT/CT}$ basophils to induce IL-4 and IL-6 productions (**Figures 2K, L**).

Overall, these data demonstrated that the CT-M8 mice (i) allowed convenient and selective basophil detection by microscopy and flow cytometry, (ii) did not show any abnormalities in their immune cell populations, and (iii) had a tdTomato expression restricted to basophils in all the compartments analyzed, and that basophils from these mice, despite an alteration of Mcpt8 expression, exhibited normal

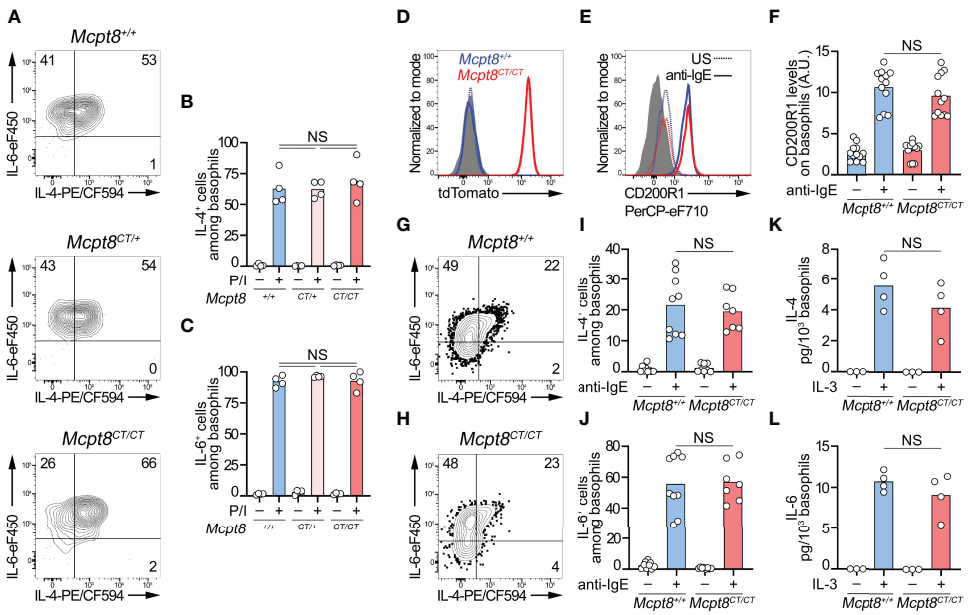


FIGURE 2 | CT-M8 mice have fully functional basophils. **(A–C)** Splenocytes from *Mcpt8*$^{+/+}$, *Mcpt8*$^{CT/+}$, and *Mcpt8*$^{CT/CT}$ mice were stimulated over 4 h with PMA and ionomycin (P/I) in the presence of brefeldin A. Proportions of IL-4$^+$ and IL-6$^+$ basophils were assessed by intracellular flow cytometry staining as depicted in **(A)** and quantified in **(B, C)** (see *Methods*). (**D**–**F**) Splenocytes (depleted of T, B, and NK cells) from *Mcpt8*$^{+/+}$ (blue) and *Mcpt8*$^{CT/CT}$ (red) mice were left unstimulated (US, dotted line) or were stimulated over 2 h with 0.5 µg/ml of anti-IgE antibody (solid line). tdTomato **(D)** and activation marker CD200R1 expression levels **(E)** were assessed in basophils by flow cytometry. Quantification of CD200R1 expression levels on basophils is shown in **(F)**. **(G–J)** T-, B-, and NK-cell-depleted splenocytes from *Mcpt8*$^{+/+}$ (blue) and *Mcpt8*$^{CT/CT}$ (red) mice were stimulated over 4 h with anti-IgE antibody (anti-IgE) in the presence of brefeldin A (see *Methods*). As depicted in **(G, H)**, proportions of IL-4$^+$ **(I)** and IL-6$^+$ **(J)** basophils were assessed by flow cytometry. **(K, L)**. The same cells as in **(G–J)** were stimulated (+) or not (–) over 24 h with 1 ng/ml of mouse IL-3 without brefeldin A (see *Methods*). IL-4 and IL-6 concentrations in the culture supernatant were measured by ELISA and normalized to the number of basophils in each condition. Statistical analyses were done by one-way ANOVA followed by Tukey's multiple comparison tests between the indicated groups. NS, not significant ($p > 0.05$). **(A–J)** Results from at least 3 different mice per group from 3 independent experiments are shown. **(K, L)** Results from 3 different mice are shown.

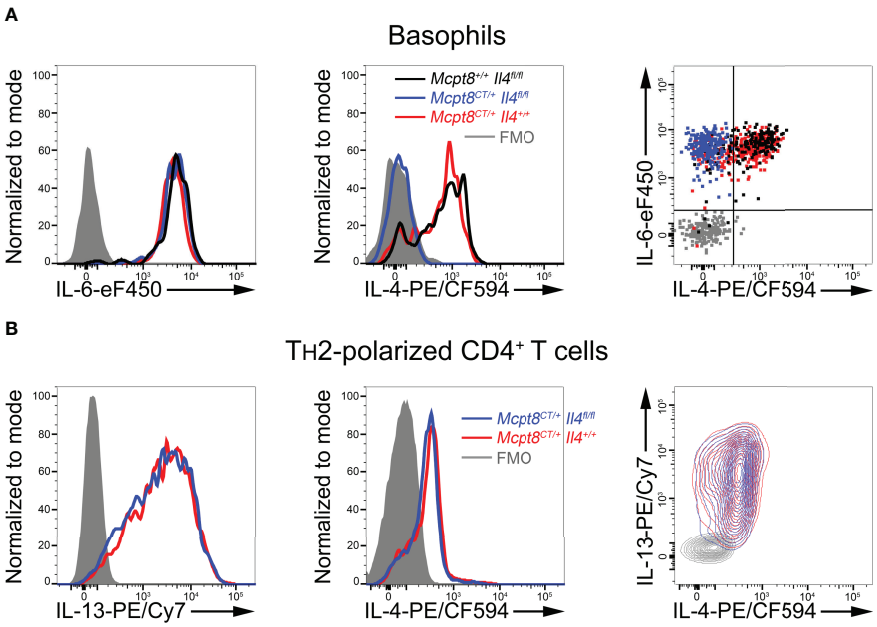


FIGURE 3 | Functional and basophil-specific CRE recombinase expression in CT-M8 mice. **(A)** Splenocytes from *Mcpt8*$^{+/+}$ *Il4*$^{fl/fl}$ (black lines/dots), *Mcpt8*$^{CT/+}$ *Il4*$^{+/+}$ (red lines/dots), and *Mcpt8*$^{CT/+}$ *Il4*$^{fl/fl}$ (blue lines/dots) were stimulated for 4 h with PMA and ionomycin in the presence of brefeldin A (see *Methods*). IL-6 (left) and IL-4 (middle) productions were assessed in basophils by intracellular flow cytometry staining. Productions are also shown together on the right panel as a dot plot. Gray-filled histograms and gray dots represent signals from basophils intracellularly incubated with fluorophore-conjugated isotype controls (fluorescence minus one (FMO)). **(B)** TH2-polarized CD4$^+$ T cells from mice with the indicated genotypes (see *Methods*) were stimulated with PMA and ionomycin for 4 h in the presence of brefeldin **(A)** Productions were assessed by intracellular staining of IL-13 (left) and IL-4 (middle). Productions are also shown together on the right panel as a contour plot. **(A, B)** Representative data from one mouse per genotype are shown. A minimum of 3 mice per genotype were analyzed, showing similar results.

distribution and normal function as assessed after IgE-, IL-3-, and PMA-ionomycin-mediated stimulations.

CRE Expression in CT-M8 Mice Is Basophil-Specific and Functional

We next sought to verify that functional CRE recombinase expression occurred only in basophils and allowed induction of basophil-specific floxed gene recombination. To that end, *Mcpt8*$^{CT/+}$ mice were bred with *Il4*$^{fl/fl}$ mice (11). Unlike IL-6 production, which was not altered, PMA-ionomycin-induced IL-4 production by basophils from *Mcpt8*$^{CT/+}$ *Il4*$^{fl/fl}$ mice was completely abrogated as compared to *Mcpt8*$^{CT/+}$ *Il4*$^{+/+}$ and *Mcpt8*$^{+/+}$ *Il4*$^{fl/fl}$ mice (**Figure 3A**). Thus, CRE recombinase was functional, and its expression was restricted to the basophil compartment since IL-4 production in *in vitro* polarized T helper type 2 (TH2) CD4$^+$ T cells was not impaired in *Mcpt8*$^{CT/+}$ *Il4*$^{fl/fl}$ mice as compared to *Mcpt8*$^{CT/+}$ *Il4*$^{+/+}$ mice (**Figure 3B**).

Next, we bred the CT-M8 mice with the ROSA-DTA mice (9). *Mcpt8*$^{CT/+}$ *Rosa26*$^{DTA/+}$ mice were constitutively basophil-deficient and did not show any other immune cell population defects in homeostatic conditions as compared to *Mcpt8*$^{CT/+}$ *Rosa26*$^{+/+}$ and *Mcpt8*$^{+/+}$ *Rosa26*$^{DTA/DTA}$ mice in all analyzed compartments (**Table 2**; **Figures 4A–C**).

Overall, these results confirmed the basophil-restricted expression of a functional CRE recombinase in CT-M8 mice that allowed generating basophil-specific ablation of selected genes and a constitutive basophil-deficient mouse model.

Basophils Have a Nonredundant Role in Lupus-Like Nephritis Amplification

By accumulating in SLOs during lupus pathogenesis, we previously showed that basophils support the survival of autoreactive antibody-secreting cells, leading to the amplification of autoantibody titers both in lupus-like mouse models and in SLE patient cohorts (4, 6, 7). Pristane (TMPD; 2, 6, 10, 14- tetramethylpentadecane) is a mineral oil able to induce the development of a lupus-like phenotype when injected intraperitoneally (ip) into C57BL/6 mice (15). The resulting PIL was associated with peripheral basophilia and an accumulation of basophils in SLOs. When depleting basophils using different approaches over 14 days in C57BL/6 female mice in established PIL (24 weeks after pristane injection), the accumulation of autoantibody-secreting plasma cells and amplification of autoantibody production were dampened (7). However, these approaches did not allow for evaluating the contribution of basophils to the onset of the disease.

We, therefore, took advantage of our new model of constitutive basophil-deficient mice described above to address this question. Basophil-sufficient (*Mcpt8*$^{CT/CT}$ *Rosa26*$^{+/+}$) and basophil-deficient (*Mcpt8*$^{CT/+}$ *Rosa26*$^{DTA/+}$) female mice were injected ip with pristane at around 8 weeks of age and euthanized for analysis

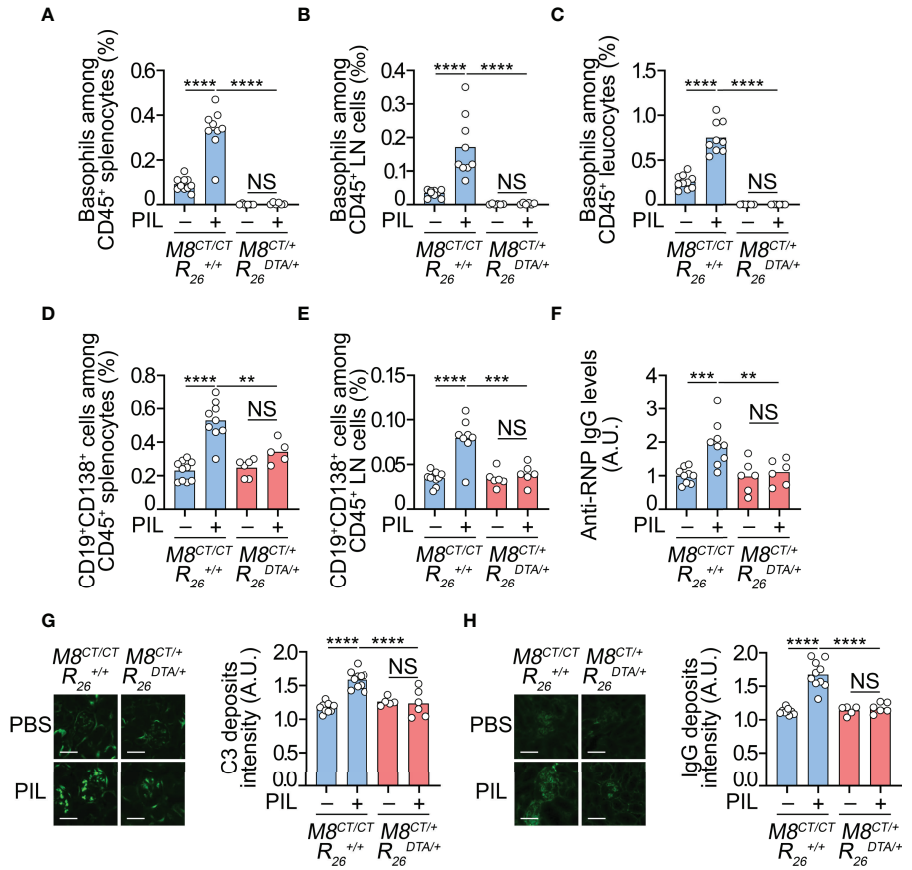


FIGURE 4 | Basophils have a nonredundant role in PIL development. **(A–H)** Eight-week-old *Mcpt8*$^{CT/CT}$ *Rosa26*$^{+/+}$ (basophil sufficient, *M8*$^{CT/CT}$ $R_{26}^{+/+}$) and *Mcpt8*$^{CT/+}$ *Rosa26*$^{DTA/+}$ (basophil deficient, *M8*$^{CT/+}$ $R_{26}^{DTA/+}$) mice were injected ip with PBS or pristane (PIL). Eight weeks later, the mice were euthanized and analyzed. **(A–C)** Basophil accumulation in the spleen **(A)** and peripheral lymph nodes (LNs) (cervical, axillary, and inguinal) **(B)** and blood basophils **(C)** were quantified by flow cytometry, as shown in **Figure 1** and described in the *Methods* section. Basophils were defined as CD45^{lo} CD3^{-} CD19^{-} CD117^{-} CD49b^{+} FcεRIα^{+} tdTomato^{+} cells among CD45^{+} viable singlets. **(D, E)** CD19^{+} CD138^{+} plasma cells were quantified in the spleen **(D)** and peripheral lymph nodes **(E)** of the mice described above. **(F)** Anti-RNP IgG autoantibody titers were quantified by ELISA from plasma samples of indicated mice, as described in the *Methods* section. The O.D. values at 450 nm were determined, and data were normalized to the mean of PBS-injected *Mcpt8*$^{CT/CT}$ *Rosa26*$^{+/+}$ values. A.U., arbitrary units. **(G, H)** Four-micrometer cryosections of kidneys were analyzed by immunofluorescence for C3 **(G)** and IgG **(H)** staining as shown on images (scale bar, 60 µm) and quantified in adjacent bar graphs as A.U., corresponding to the ratio between fluorescence intensity measured in glomeruli to that in interstitial background. **(A–H)** Results are from at least three independent experiments and are presented as individual values in bars representing the mean values. Statistical analyses were done by one-way ANOVA followed by Tukey's multiple comparison tests between the indicated groups. NS, not significant, $p > 0.05$; $^{**}p < 0.01$; $^{***}p < 0.001$; $^{****}p < 0.0001$.

8 weeks after injection. This time point corresponded to an early stage of PIL since neither proteinuria nor other biological parameters evidencing kidney dysfunction (blood urea nitrogen and creatininemia) were detectable (*data not shown*). However, 8 weeks after pristane injection in basophil-sufficient animals, basophil and short-lived plasma cell (CD19^{+}CD138^{+} B cells) accumulation in SLOs (spleen and lymph nodes), peripheral basophilia, and autoantibodies in plasma were detected (**Figures 4A–F**). This was associated with the detection of complement component C3 and IgG deposits in the kidney glomeruli of pristane-injected mice, unlike the glomeruli of PBS-injected control mice, confirming the early development stages of the pristane-induced lupus-like nephritis (**Figures 4G, H**).

As expected, no basophil was detected in basophil-deficient mice (*Mcpt8*$^{CT/+}$ *Rosa26*$^{DTA/+}$) 8 weeks after pristane injection in any of the compartments analyzed (**Figures 4A–C**). No accumulation of CD19^{+}CD138^{+} short-lived plasma cells was detected in SLOs of pristane-injected basophil-deficient mice, suggesting that basophil deficiency prevented PIL development (**Figures 4D, E**). Indeed, no significant increase in antiribonucleoprotein (anti-RNP) antibodies, autoantibodies present in PIL in C57BL/6 mice (6, 7), was measurable in the blood of basophil-deficient mice (**Figure 4F**). Moreover, no significant C3 and IgG deposits in the glomeruli of basophil-deficient mice were detected 8 weeks after pristane injection (**Figures 4G, H**).

Overall, these results demonstrate that basophils have a nonredundant role in PIL development as basophil deficiency sufficed to prevent the onset of autoantibody production and lupus-like nephritis induced by pristane injection.

DISCUSSION

Beyond its role in allergic and parasitic diseases, type 2 immunity is now identified as a key player in the pathophysiology of various autoimmune diseases (16, 17). Several studies have demonstrated its relevance to SLE pathogenesis and identified IgE and basophils as promising therapeutic targets due to their role in amplifying both autoantibody production and tissue damage. Most of these studies are based on a translational approach that allowed us to study and decipher in lupus-like mouse models what was observed in human patients (4, 6, 18–20). The use of a novel mouse model allowing basophil-specific short-term depletion (*Mcpt8*^{DTR} mice (21)) demonstrated that basophil targeting efficiently dampened lupus-like activity in mice with established disease (6). Here, using a new basophil-deficient mouse model, we show that basophils were required to reach a pathogenic threshold in PIL, supporting their nonredundant role in early lupus-like disease development.

Besides specific depletion of basophils, the new CT-M8 mouse model also enables convenient detection of basophils by flow cytometry and confocal microscopy as well as the selective depletion of a floxed gene in the basophil compartment. In particular, our analysis showed that constitutive basophil deficiency in this model did not lead to any identified immunological bias. Likewise, mice rendered IL-4 deficient in the basophil compartment did not impact the ability of TH2-polarized CD4$^+$ T cells from the same mice to produce IL-4. Unexpectedly, *Mcpt8* mRNA expression was dramatically dampened by the insertion of the IRES-based construct after the stop codon site of the Mcpt8 gene. If a knock-in approach would be expected to induce Mcpt8 deficiency (22), the reason explaining this alteration of Mcpt8 expression in our model will need further investigation. Fortunately, Mcpt8 expression was still detected in *Mcpt8*$^{CT/+}$ heterozygous mice, allowing for the generation of Mcpt8-sufficient mice expressing both tdTomato and CRE recombinase only in the basophil compartment. Of note, Mcpt8-reduced expression is known not to induce any significant alteration in basophil function in mouse models of parasite infection (22) or sepsis (12).

To our knowledge, three other mouse models expressing the CRE recombinase selectively in basophils are currently available. Generated in 2010 by Voehringer and colleagues, the "Mcpt8CRE" mouse is a BAC transgenic mouse strain expressing the Cre recombinase inserted behind the start codon of the Mcpt8 gene. Unfortunately, these mice showed a constitutive 90% basophil deficiency, probably due to CRE overexpression preventing its use for floxed gene deletion selectively in basophils (23). The "Basoph8" mice were developed by Locksley and colleagues, who replaced the Mcpt8 gene at the start site by inserting a reporter cassette containing a sequence encoding the yellow fluorescent protein (YFP), followed by an IRES and a sequence encoding humanized Cre recombinase. This mouse strain is effective at basophil-specific Cre-mediated gene deletion and expresses constitutively the YFP in basophils (22). The third one was recently developed by Karasuyama and colleagues and called *Mcpt8*$^{iCre/+}$. This mouse strain expresses the improved Cre (iCre) recombinase inserted to replace the first exon of the Mcpt8 gene and is efficient in basophil-specific Cre-mediated gene deletion but does not express constitutively any fluorescent reporter gene (11).

The advantages of the CT-M8 mice are then similar to the ones of the Basoph8 mouse model (22), but they express another fluorescent protein (tdTomato), allowing distinct breeding strategies for the generation of multiple gene/cell-specific reporter mouse strains. In addition, the CT-M8 mice (in their heterozygous *Mcpt8*$^{CT/+}$ strain) retain significant expression of the *Mcpt8* gene while allowing fully sufficient functional expression of the CRE recombinase.

Mast cells and basophils share immediate common progenitors, and Mcpt8 gene-controlled CRE or DTR expression may be detected at low levels in other cell types including mast cells, granulocyte-macrophage progenitors, T cells, B cells, NK cells, eosinophils, and dendritic cells (23–25). Therefore, both the construct used to generate CT-M8 mice and DTα expression in Mcpt8-expressing cells could have affected immune cell populations other than basophils. However, analysis of CT-M8 mice showed that tdTomato expression was fully restricted to the basophil compartment (**Table 1**). As well, Mcpt8-dependent DTα expression in *Mcpt8*$^{CT/+}$ *R*$_{26}$*-Stop*$^{fl/WT}$*-DTA* mice did not impact any immune cell populations other than basophils (**Table 2**). The very low Mcpt8 mRNA expression levels in the former cell populations, or their progenitors, as compared to mature basophils, may explain the basophil-selectivity observed in the various Mcpt8 gene-based mouse models.

In the present study, basophil deficiency prevented the development of the pristane-induced lupus-like disease. Indeed, our data suggest that basophils are necessary to reach a pathogenic threshold in early PIL. This is evidenced by the ablation of plasmablast accumulation in SLOs, autoantibody production, and glomerular deposition of circulating immune complexes in basophil-deficient mice.

Further investigations will be required to determine the mechanisms by which basophils contribute to autoimmune evolution in the PIL. In this context, our new basophil-specific mouse model will allow selective depletion in the basophil compartment of candidate genes. For instance, it will allow deciphering of the axis of autoreactive IgE and FcεRI-mediated basophil activation in the nonredundant role of basophils in lupus-like pathogenesis. Indeed, autoreactive IgE is highly prevalent in SLE patients with active disease (26), and the basophil activation status correlates strongly with disease activity (4, 6). Furthermore, IgE itself is known to exert an immunoregulatory role in various lupus-like mouse models (4, 18). We will now be able to deplete specifically FcεRI in basophils by breeding CT-M8 mice with *FcεRIγ*$^{fl/fl}$ mice (C57BL/6J-Fcer1g$^{em1Gfng/J}$, *Jax* mice #036592) and demonstrate whether basophil involvement in lupus-like disease amplification depends on FcεRI-mediated signals. The role of

factors produced by basophils during the course of the disease, such as IL-4 or IL-6, could be assessed as well. Although technically challenging, basophil reconstitution of basophil-deficient animals through frequent adoptive transfer of purified basophils during the whole procedure may further help to decipher the non-redundant role of basophils in PIL onset.

The nonredundant role of basophils in lupus-like pathogenesis demonstrated in PIL will need to be validated in other lupus-like mouse models, including spontaneous models. This preclinical development is necessary to determine whether targeting basophils or basophil-activating factors in recently diagnosed SLE patients may be a promising therapeutic strategy to prevent the development of lesions in targeted organs. Several approaches may be envisaged to alter the basophil contribution to lupus nephritis development, including targeting IgE, PTGDRs, or directly basophils through a basophil-specific surface marker that still needs to be identified. Basophils have a deleterious role in various allergic, inflammatory, and autoimmune diseases (16, 27). Identifying therapeutic strategies targeting these cells, their mediators, or the factors involved in their contribution to these diseases may represent a promising area of clinical development.

DATA AVAILABILITY STATEMENT

The raw data supporting the conclusions of this article will be made available by the authors, without undue reservation.

ETHICS STATEMENT

The animal study was reviewed and approved by the comité d'éthique Paris Nord N°121 and the Ministère de l'enseignement supérieur, de la recherche et de l'innovation under the authorization number APAFIS#14115.

AUTHOR CONTRIBUTIONS

JT designed the experiments, conducted the experiments, and wrote the manuscript. NC conceived the project, designed the experiments, conducted the experiments, wrote the manuscript, and directed the project. QS, LC, CP, UB, MB, and ED conducted the experiments, analyzed the data, and/or edited the manuscript. HK and KM provided the *Il4*$^{fl/fl}$ mice and edited the manuscript. NC had full access to all of the data in the study and takes responsibility for the integrity of the data and the accuracy of the data analysis. All authors listed have made a substantial, direct, and intellectual contribution to the work and approved it for publication.

FUNDING

This work was supported by the Fondation pour la Recherche Médicale (FRM) (grant # EQU201903007794) to NC, the French Agence Nationale de la Recherche (ANR) (grants # ANR-19-CE17-0029 BALUMET to NC and ANRPIA-10-LABX-0017 INFLAMEX), by the Centre National de la Recherche Scientifique (CNRS), by Université de Paris, and by the Institut National de la Santé et de la Recherche Médicale (INSERM).

ACKNOWLEDGMENTS

We acknowledge the expert work from the members of the animal core facility (I. Renault and S. Olivré), the flow cytometry core facility (G. Gautier, J. Da Silva, and V. Gratio), and the imaging facility (S. Benadda) of the Centre de Recherche sur l'Inflammation (INSERM UMR1149) and the help from O. Thibaudeau and L. Wingertsmann from the morphology core facility (INSERM UMR1152). We acknowledge as well the expert work from the members of the Institut Clinique de la Souris (Illkirch, France) from the Phenomin consortium for the CT-M8 mouse generation.

SUPPLEMENTARY MATERIAL

The Supplementary Material for this article can be found online at: https://www.frontiersin.org/articles/10.3389/fimmu.2022.900532/full#supplementary-material

REFERENCES

1. Anders HJ, Saxena R, Zhao MH, Parodis I, Salmon JE, Mohan C, et al. Lupus Nephritis. *Nat Rev Dis Primers* (2020) 6(1):7. doi: 10.1038/s41572-019-0141-9
2. Dema B, Charles N. Autoantibodies in SLE: Specificities, Isotypes and Receptors. *Antibod (Basel)* (2016) 5(1):2. doi: 10.3390/antib5010002
3. Dema B, Charles N. Advances in Mechanisms of Systemic Lupus Erythematosus. *Discovery Med* (2014) 17(95):247–55.
4. Charles N, Hardwick D, Daugas E, Illei GG, Rivera J. Basophils and the T Helper 2 Environment can Promote the Development of Lupus Nephritis. *Nat Med* (2010) 16(6):701–7. doi: 10.1038/nm.2159
5. Charles N, Watford WT, Ramos HL, Hellman L, Oettgen HC, Gomez G, et al. Lyn Kinase Controls Basophil GATA-3 Transcription Factor Expression and Induction of Th2 Cell Differentiation. *Immunity* (2009) 30(4):533–43. doi: 10.1016/j.immuni.2009.02.008
6. Pellefigues C, Dema B, Lamri Y, Saidoune F, Chavarot N, Loheac C, et al. Prostaglandin D2 Amplifies Lupus Disease Through Basophil Accumulation in Lymphoid Organs. *Nat Commun* (2018) 9(1):725. doi: 10.1038/s41467-018-03129-8
7. Dema B, Lamri Y, Pellefigues C, Pacreau E, Saidoune F, Bidault C, et al. Basophils Contribute to Pristane-Induced Lupus-Like Nephritis Model. *Sci Rep* (2017) 7(1):7969. doi: 10.1038/s41598-017-08516-7
8. Poorafshar M, Helmby H, Troye-Blomberg M, Hellman L. MMCP-8, the First Lineage-Specific Differentiation Marker for Mouse Basophils. Elevated Numbers of Potent IL-4-Producing and MMCP-8-Positive Cells in Spleens of Malaria-Infected Mice. *Eur J Immunol* (2000) 30(9):2660–8. doi: 10.1002/1521-4141(200009)30:9<2660::AID-IMMU2660>3.0.CO;2-I

9. Voehringer D, Liang HE, Locksley RM. Homeostasis and Effector Function of Lymphopenia-Induced "Memory-Like" T Cells in Constitutively T Cell-Depleted Mice. *J Immunol* (2008) 180(7):4742–53. doi: 10.4049/jimmunol.180.7.4742
10. Birling MC, Dierich A, Jacquot S, Herault Y, Pavlovic G, et al. Highly-Efficient, Fluorescent, Locus Directed Cre and FlpO Deleter Mice on a Pure C57BL/6N Genetic Background. *Genesis* (2012) 50(6):482–9. doi: 10.1002/dvg.20826
11. Shibata S, Miyake K, Tateishi T, Yoshikawa S, Yamanishi Y, Miyazaki Y, et al. Basophils Trigger Emphysema Development in a Murine Model of COPD Through IL-4-Mediated Generation of MMP-12-Producing Macrophages. *Proc Natl Acad Sci U.S.A.* (2018) 115(51):13057–62. doi: 10.1073/pnas.1813927115
12. Piliponsky AM, Shubin NJ, Lahiri AK, Truong P, Clauson M, Niino K, et al. Basophil-Derived Tumor Necrosis Factor can Enhance Survival in a Sepsis Model in Mice. *Nat Immunol* (2019) 20(2):129–40. doi: 10.1038/s41590-018-0288-7
13. Bakocevic N, Claser C, Yoshikawa S, Jones LA, Chew S, Goh CC, et al. CD41 is a Reliable Identification and Activation Marker for Murine Basophils in the Steady State and During Helminth and Malarial Infections. *Eur J Immunol* (2014) 44 (6):1823–34. doi: 10.1002/eji.201344254
14. Torrero MN, Larson D, Hubner MP, Mitre E. CD200R Surface Expression as a Marker of Murine Basophil Activation. *Clin Exp Allergy* (2009) 39(3):361–9. doi: 10.1111/j.1365-2222.2008.03154.x
15. Reeves WH, Lee PY, Weinstein JS, Satoh M, Lu L. Induction of Autoimmunity by Pristane and Other Naturally Occurring Hydrocarbons. *Trends Immunol* (2009) 30(9):455–64. doi: 10.1016/j.it.2009.06.003
16. Charles N. Autoimmunity, IgE and FcepsilonRI-Bearing Cells. *Curr Opin Immunol* (2021) 72:43–50. doi: 10.1016/j.coi.2021.03.003
17. Maurer M, Altrichter S, Schmetzer O, Scheffel J, Church MK, Metz M. Immunoglobulin E-Mediated Autoimmunity. *Front Immunol* (2018) 9:689. doi: 10.3389/fimmu.2018.00689
18. Dema B, Charles N, Pellefigues C, Ricks TK, Suzuki R, Jiang C, et al. Immunoglobulin E Plays an Immunoregulatory Role in Lupus. *J Exp Med* (2014) 211(11):2159–68. doi: 10.1084/jem.20140066
19. Henault J, Riggs JM, Karnell JL, Liarski VM, Li J, Shirinian L, et al. Self-Reactive IgE Exacerbates Interferon Responses Associated With Autoimmunity. *Nat Immunol* (2016) 17(2):196–203. doi: 10.1038/ni.3326
20. Pan Q, Gong L, Xiao H, Feng Y, Li L, Deng Z, et al. Basophil Activation-Dependent Autoantibody and Interleukin-17 Production Exacerbate Systemic Lupus Erythematosus. *Front Immunol* (2017) 8:348. doi: 10.3389/fimmu.2017.00348
21. Wada T, Ishiwata K, Koseki H, Ishikura T, Ugajin T, Ohnuma N, et al. Selective Ablation of Basophils in Mice Reveals Their Nonredundant Role in Acquired Immunity Against Ticks. *J Clin Invest* (2010) 120(8):2867–75. doi: 10.1172/JCI42680
22. Sullivan BM, Liang HE, Bando JK, Wu D, Cheng LE, McKerrow JK, et al. Genetic Analysis of Basophil Function *In Vivo*. *Nat Immunol* (2011) 12 (6):527–35. doi: 10.1038/ni.2036
23. Ohnmacht C, Schwartz C, Panzer M, Schiedewitz I, Naumann R, Voehringer D. Basophils Orchestrate Chronic Allergic Dermatitis and Protective Immunity Against Helminths. *Immunity* (2010) 33(3):364–74. doi: 10.1016/j.immuni.2010.08.011
24. El Hachem C, Hener P, Kirstetter P, Li J, Chan S, Li M. Treatment of MCPT8(DTR) Mice With High- or Low-Dose Diphtheria Toxin Leads to Differential Depletion of Basophils and Granulocyte-Macrophage Progenitors. *Eur J Immunol* (2018) 48(5):861–73. doi: 10.1002/eji.201747351
25. Wanet A, Bassal MA, Patel SB, Marchi F, Mariani SA, Ahmed N, et al. E-Cadherin is Regulated by GATA-2 and Marks the Early Commitment of Mouse Hematopoietic Progenitors to the Basophil and Mast Cell Fates. *Sci Immunol* (2021) 6(56):eaba0178. doi: 10.1126/sciimmunol.aba0178
26. Dema B, Pellefigues C, Hasni S, Gault N, Jiang C, Ricks TK, et al. Autoreactive IgE is Prevalent in Systemic Lupus Erythematosus and is Associated With Increased Disease Activity and Nephritis. *PloS One* (2014) 9(2):e90424. doi: 10.1371/journal.pone.0090424
27. Karasuyama H, Miyake K, Yoshikawa S, Yamanishi Y. Multifaceted Roles of Basophils in Health and Disease. *J Allergy Clin Immunol* (2018) 142(2):370–80. doi: 10.1016/j.jaci.2017.10.042

Conflict of Interest: CP and NC are coinventors of the patent WO2016128565A1 related to the use of PTGDR-1 and PTGDR-2 antagonists for the prevention or treatment of systemic lupus erythematosus. NC holds a patent related to compositions and methods for treating or preventing lupus (W020120710042).

The remaining authors declare that the research was conducted in the absence of any commercial or financial relationships that could be construed as a potential conflict of interest.

Publisher's Note: All claims expressed in this article are solely those of the authors and do not necessarily represent those of their affiliated organizations, or those of the publisher, the editors and the reviewers. Any product that may be evaluated in this article, or claim that may be made by its manufacturer, is not guaranteed or endorsed by the publisher.

Copyright © 2022 Tchen, Simon, Chapart, Pellefigues, Karasuyama, Miyake, Blank, Benhamou, Daugas and Charles. This is an open-access article distributed under the terms of the Creative Commons Attribution License (CC BY). The use, distribution or reproduction in other forums is permitted, provided the original author(s) and the copyright owner(s) are credited and that the original publication in this journal is cited, in accordance with accepted academic practice. No use, distribution or reproduction is permitted which does not comply with these terms.

frontiers | Frontiers in Immunology

ORIGINAL RESEARCH
published: 29 June 2022
doi: 10.3389/fimmu.2022.883605

Immunological Changes of Basophil Hyperreactivity to Sweat in Patients With Well-Controlled Atopic Dermatitis

Tomofumi Numata[1], *Shunsuke Takahagi*[1]*, *Kaori Ishii*[1], *Satoshi Morioke*[1], *Takanobu Kan*[1], *Hayato Mizuno*[1], *Yuhki Yanase*[2], *Tomoko Kawaguchi*[1], *Akio Tanaka*[1] and *Michihiro Hide*[1]

[1] Department of Dermatology, Graduate School of Biomedical & Health Sciences, Hiroshima University, Hiroshima, Japan,
[2] Department of Pharmacotherapy, Graduate School of Biomedical and Health Sciences, Hiroshima University, Hiroshima, Japan

Background: Sweat aggravates atopic dermatitis (AD). In patients with AD, type-I hypersensitivity to sweat may be shown by histamine release from patients' basophils in response to the semi-purified sweat antigen (QR), and the presence of specific immunoglobulin E (IgE) binding to MGL_1304, the component of QR. However, there has been no information on the immunological changes of type-I hypersensitivity to the sweat antigen in patients with well-controlled AD using topical corticosteroids (TCSs) and/or biologics as treatments.

Method: Histamine-releasing tests using patients' basophils and QR and the detection of serum IgE against MGL_1304 and mite allergen Der f 1 were performed in patients with AD who were well controlled by topical TCS with/without dupilumab for 53–96 weeks.

Results: In total, 14 patients were enrolled. Seven patients received TCS therapy alone (TCS group), and seven patients received TCS with dupilumab therapy (dupilumab group). In all participants, the level of specific IgE against MGL_1304 decreased after treatments, but histamine release from basophils in response to QR did not show a statistically significant reduction; rather, it increased. In the dupilumab group, all changes in histamine release induced by QR (increase), the IgE level against MGL_1304 (decrease), and that against Der f 1 (decrease) were statistically significant, whereas the TCS group showed no significant change in any of them.

Conclusion: The well-controlled condition for 53–96 weeks resulted in no reduction of the hyperreactivity of basophils against in patients with AD, even with the treatment with dupilumab. This study suggests persistent basophil hyperreactivity to sweat antigen over a year or longer.

Keywords: atopic dermatitis, sweat antigen, histamine release, basophil, IgE, *Malassezia*, MGL_1304, dupilumab

OPEN ACCESS

Edited by:
Satoshi Tanaka,
Kyoto Pharmaceutical University, Japan

Reviewed by:
Masato Kubo,
Tokyo University of Science, Japan
Mitsunobu Mio,
Shujitsu University, Japan

***Correspondence:**
Shunsuke Takahagi
shunstk@hiroshima-u.ac.jp

Specialty section:
This article was submitted to Inflammation, a section of the journal Frontiers in Immunology

Received: *25 February 2022*
Accepted: *23 May 2022*
Published: *29 June 2022*

Citation:
Numata T, Takahagi S, Ishii K, Morioke S, Kan T, Mizuno H, Yanase Y, Kawaguchi T, Tanaka A and Hide M (2022) Immunological Changes of Basophil Hyperreactivity to Sweat in Patients With Well-Controlled Atopic Dermatitis. Front. Immunol. 13:883605. doi: 10.3389/fimmu.2022.883605

Abbreviations: AD, atopic dermatitis; QR, semi-purified sweat antigen; E1, the 1st evaluation; E2, the 2nd evaluation; TCS, topical corticosteroid; IL, interleukin; HRT, histamine release test; *M.*, *Malassezia*; IGA, Investigator's Global Assessment; HPLC, high-performance liquid chromatography; PBS, phosphate-buffered saline; HRP, horseradish peroxidase.

INTRODUCTION

Atopic dermatitis (AD) is a common chronic inflammatory skin disease, which is characterized by pruritic, eczematous lesions with the fluctuation of remission and relapse (1). It is often associated with high levels of serum immunoglobulin E (IgE) and a personal/family history of atopic diseases (1). The underlying pathogenesis of AD involves complex interactions among immune dysregulation, pruritus, and skin barrier dysfunction (2). The dysregulated immune system skews to a Th2 cell–mediated immune response, by which Th2 cytokines including interleukin (IL)-4 and 13 are activated in the lesions of AD (3). In addition to conventional treatments such as topical corticosteroids (TCSs), topical calcineurin inhibitors, and moisturizers, a monoclonal antibody against the alpha subunit of the IL-4 receptor, dupilumab, has recently emerged to inhibit both IL-4 and IL-13 signaling (4, 5). Its inhibition of the Th2 pathway improves AD skin lesions and skin barrier dysfunction, as well as IgE overproduction (5–7).

Sweat is one of aggravating factors for patients with AD (8, 9). In some patients with AD, type-I hypersensitivity to sweat is detected by the intradermal injection of autologous sweat and histamine release test (HRT) by using autologous sweat (9–11). The major antigen in sweat has been partially purified as the semi-purified sweat antigen (QR) (12). Recently, MGL_1304, a secreted protein by *Malassezia globosa*, has been identified as the histamine-releasing component in QR (13). Specific IgE binding to QR and MGL_1304 are detected in more than half of patients with AD (14). Furthermore, QR and MGL_1304 induce histamine release from basophils in 77% and 62% of patients with AD, respectively (12, 13). Although this large portion of patients with AD show basophil reactivity against QR, there is no information on the prognosis of type-I hypersensitivity to the sweat antigen. In this study, we performed an analysis of the change in basophil hyperreactivity and serum IgE titer against the sweat antigen in patients with AD that was well controlled by treatments with/without dupilumab.

MATERIALS AND METHODS

Study Design

The study protocol is shown in **Figure 1A**. Retrospective analysis for a total of 14 patients with AD was performed on the data obtained from electronic medical records at Hiroshima University Hospital. Participants were diagnosed as AD according to the Japanese guideline of the management of AD (1). They also had type-I hypersensitivity to sweat proven by HRT using QR (12). The type-I hypersensitivity to sweat was diagnosed in cases where anti-human IgE antibody (positive control) and QR induced the net histamine release of >10% and >5%, respectively (15). Two measurements of histamine release in response to QR, and serum IgE levels against MGL_1304 and mite allergen Der f 1 were performed at the first evaluation (E1) and the second one (E2). During the period from E1 to E2, the patients were treated with TCS or TCS with dupilumab but without any other systemic therapies for AD. The patients who entered the study had an Investigator's Global Assessment (IGA) score of 2 or lower for 53–96 weeks, except for transient flares of AD within a month (**Table 1**). The IGA score at E1 was score 4 in five patients, 3 in four patients, 2 in three patients, and 1 in two patients, while the scores at E2 were score 2 in nine patients, 1 in three patients, and 0 in two patients. The change of the IGA score between E1 and E2 was 0 in three patients, −1 in four patients, −2 in six patients, and −3 in one other patient. All patients were advised to cope with sweat by taking a shower or wiping it with towels and to avoid dusty environments during the observation period. No uniform recommendation was given for patients to avoid other allergens during the study period unless the patient had an allergy to a specific antigen. The institutional review board of Hiroshima University Hospital approved the study protocol (approval number: E-2781, E-1716). Informed consent was obtained in the form of opt-out on the website.

HRT Using the Semi-Purified Sweat Antigen, QR

QR was prepared by concanavalin A chromatography, anion-exchange chromatography, and reverse-phase chromatography in reference to histamine release activity from the basophils of patients with AD (12). HRT with basophils obtained from peripheral blood were performed as described previously (11, 16). Briefly, fresh blood was obtained with ethylenediaminetetraacetic acid (EDTA) from each donor by venipuncture. The whole blood was mixed with the same volume of 1% methylcellulose in saline and then allowed to stand at room temperature for 30 min. A supernatant with abundant leukocytes was collected, leaving red blood cells precipitated. After washing with the washing buffer, 136 mM sodium chloride/10 mM 4-(2-hydroxyethyl)-1-piperazineethanesulfonic acid (HEPES)/0.1% glucose/0.03% human serum albumin, the leukocyte fraction containing basophils was suspended in the reaction buffer, 136 mM sodium chloride/10 mM HEPES/0.1% glucose/0.03% human serum albumin/2 mM $CaCl_2$/1 mM $MgCl_2$. The suspended cells were stimulated with 0.33 μg/ml of goat anti-human IgE antibody (Bethyl Laboratories, Inc., TX, USA) or 10 ng/ml QR at 37°C for 40 min. After incubation, the cells and supernatant were separated by centrifugation and mixed with $HClO_4$ to a final concentration of 2.5% to denature excess proteins. After centrifugation, the amounts of histamine extracted in the supernatant were measured using high-performance liquid chromatography (HPLC). The HPLC system consisted of an LC-20A (Shimadzu, Kyoto, Japan) using a VP-ODS column (Shimadzu, Kyoto, Japan) with an RF-10Axl fluorescence detector (Shimadzu, Kyoto, Japan) operating at an emission wavelength of 440 nm and an excitation wavelength of 360 nm. The percentage of histamine release was calculated using the ratio of the amount of histamine in the supernatant to the total amount of histamine in the supernatant and cells. For analysis, the value of histamine release against the sweat antigen was normalized by the maximum release of histamine induced by anti-IgE, namely, (net % of histamine release induced by QR)/(net % of histamine release induced by anti-human IgE)×100 (%).

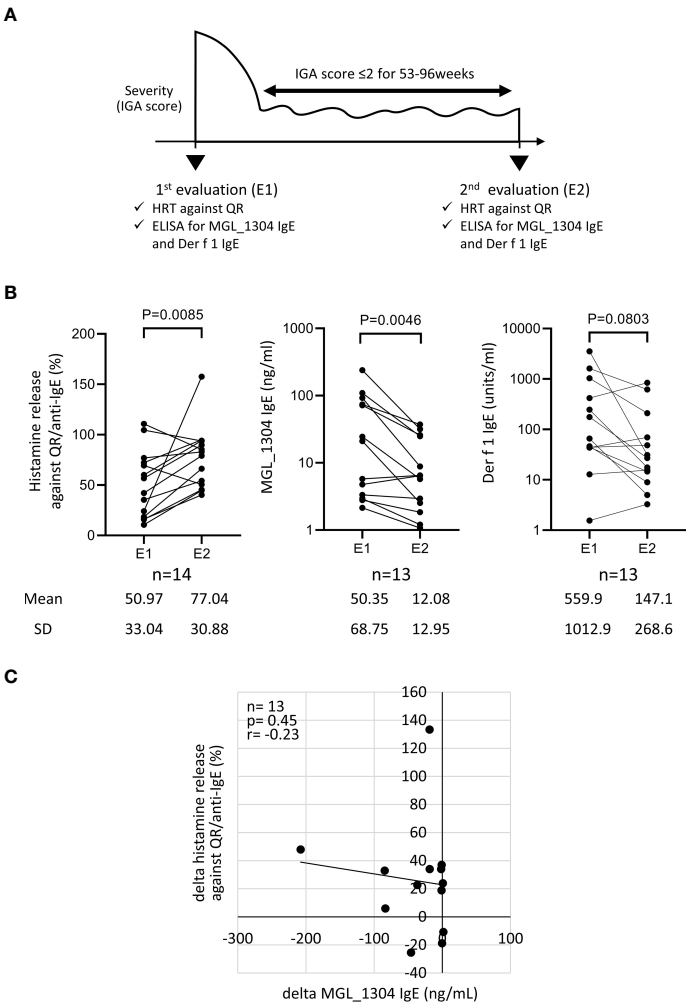


FIGURE 1 | **(A)** Study design. **(B)** Histamine release from basophils in response to the semi-purified sweat antigen (QR) and levels of IgE to MGL_1304 and Der f 1 at E1 and E2 in total participants. **(C)** Correlation of the change of histamine release in response to QR to that of MGL_1304 IgE. Histamine release was expressed as (net % of histamine release induced by QR)/(net % of histamine release induced by anti-human IgE)×100 (%). "delta" means the changes of parameters calculated by the subtraction of values at E1 from those at E2. E1, the 1st evaluation; E2, the 2nd evaluation; HRT, histamine release test; IGA, Investigator's Global Assessment.

Enzyme-Linked Immunosorbent Assay (ELISA) for Specific IgE Against MGL_1304

A 96-well plate was coated with Smith2, a mouse monoclonal antibody against MGL_1304 (13), at 250 ng/well in phosphate-buffered saline (PBS) at 4°C overnight. After blocking, 10 ng/ml of the purified MGL_1304 from cultured *M. globosa* (13) were added in each well at room temperature for 2 h. After washing, the wells were incubated with several concentrations of a human monoclonal IgE against MGL_1304 (BioPorto Diagnostics A/S, Copenhagen, Denmark) (17), for standard reaction at 100 µl, and with 100 µl of patients' sera diluted 1:10 with 10% blocking one solution (Nakalai Tesque, Inc., Tokyo, Japan) at room temperature for 2 h. After washing, each well was incubated with horseradish peroxidase (HRP)–conjugated goat anti-human IgE (Kirkegaard & Perry Laboratories, Inc., Gaithersburg, MD, USA). Color development was achieved by TMB substrate solution and stop solution (SeraCare Life science, Inc., MA, USA), and then absorbance at 450 nm was measured using a microplate spectrophotometer. A standard curve was constructed by plotting the concentrations of a series of standard reactions on the x-axis and absorbance on the y-axis. The concentration of MGL_1304 IgE was calculated in reference to the standard curve.

ELISA for Specific IgE Against House Dust Mite Antigen, Der f 1

A 96-well plate was coated with 100 ng/well of Mite Extract-Df (LSL Co., Tokyo, Japan) in PBS at 4°C overnight. After blocking, the wells were incubated with 100 µl of patients' sera diluted 1:10 with 10% blocking one solution at room temperature for 2 h. For a standard reaction in each experiment, the wells were also incubated with the serial

TABLE 1 | Patients' characteristics.

Sex (male: female)		10:4	
Age, years (range)		44.1 ± 12.9 (21–66)	
Period between E1 and E2, weeks (range)		73.4 ± 16.1 (54–99)	
Period between E1 and the date of achieving IGA score ≤2, weeks (range)		2.0 ± 2.0 (0–6)	
Period between the date of achieving IGA score ≤2 and E2, weeks (range)		69.3 ± 16.3 (53–96)	
Treatments between E1 and E2		TCS, 7	
		TCS with dupilumab, 7	
Number of patients with skin diseases caused by *Malassezia*	Seborrheic dermatitis	0	
	Pityriasis versicolor	0	
	Malassezia folliculitis	3	
Number of patients sensitized to *Malassezia* species	*M. globosa*	14	
	M. restricta	14	
	M. sympodialis	13	
		<E1>	<E2>
Severity of AD (IGA score)	Score 0	None	2 patients
	Score 1	2 patients	3 patients
	Score 2	3 patients	9 patients
	Score 3	4 patients	None
	Score 4	5 patients	None
	Mean score	2.9 ± 1.1	1.5 ± 0.8
Serum IgE, ng/ml		12,169 ± 7,958	4,695 ± 4,928
TARC, pg/ml		4,913 ± 7,724	695 ± 552

Descriptive statistics are shown in mean ± standard deviation. E1, the 1st evaluation; E2, the 2nd evaluation; TCS, topical corticosteroids; IGA, Investigator's Global Assessment; AD, atopic dermatitis; TARC, thymus- and activation-regulated chemokine.

dilution of the standard serum with high titer to Der f 1. The standard serum was obtained from a patient with AD sensitized to Der f 1. The subsequent method was the same as the ELISA for MGL_1304. The concentration of Der f 1 IgE was calculated in reference to the standard curve.

Statistical Analysis

The changes of various parameters between E1 and E2 were calculated by the subtraction of values at E1 from those at E2. The statistical analysis was performed by GraphPad Prism (GraphPad Software, ver. 9.1, San Diego, CA, USA). A p-value of less than 0.05 was considered significant. Groups were compared by using the Wilcoxon matched-pairs signed rank test for paired samples. Correlation was tested with the Spearman's rank test.

RESULTS

Patients

A total of 14 patients with AD (men:women, 10:4) were recruited. Their clinical characteristics are shown in **Table 1**. The observation period from E1 to E2 was 73.4 ± 16.1 weeks (mean ± SD) including 69.3 ± 16.3 weeks in the well-controlled condition of IGA ≤2. During the observation period, seven patients received TCS therapy alone (TCS group), and seven patients received TCS with dupilumab therapy (dupilumab group). As for the sensitization to fungus, it has been reported that the sensitization to the sweat antigen, MGL_1304, is not correlated with *Candida albicans*, which belongs to another fungal genus (13). However, almost all participants were sensitized to more than one species of the *Malassezia* genus.

Basophil Histamine Release in Response to QR and Serum IgE Binding to MGL_1304

The leukocyte fraction in blood was used to analyze histamine release from basophils in response to the sweat antigen. This fraction contained 0.48%–2.11% basophils, while the magnetic isolation of the basophil population achieved a basophil purity of 83.9%–93.6% by negative selection (n=4) (**Supplementary Figure 1A**, **Supplementary Materials and Methods**). The leukocyte fraction showed the same amount of histamine release in response to anti-IgE, QR, and MGL_1304 as the purified basophil fraction in patients with AD and hyperreactivity to QR (**Supplementary Figure 1B**, **Supplementary Material and Methods**). Thus, anti-IgE and the sweat antigen directly activate basophils regardless of the presence of other leukocytes in our HRT assay. The following experiments were performed with the leukocyte fraction containing basophils.

In the analysis of all participants, the level of IgE binding to MGL_1304 was significantly decreased at E2 from that at E1, but no significant reduction was observed in histamine release in response to QR and specific IgE binding to Der f 1 (**Figure 1B**) in the period between E1 and E2. No significant correlation was observed in the change of histamine release in response to QR and that of the level of IgE binding to MGL_1304 ($r=-0.23$, $p=0.45$) (**Figure 1C**). In this study, we calculated histamine release induced by QR with the normalization of maximum

histamine release induced by anti-human IgE stimuli (positive control). However, non-normalized data showed the same tendency in the change of histamine release as normalized data (**Supplementary Figure 2A**). Non-normalized histamine release induced by QR was well correlated with histamine release induced by QR normalized with histamine release by anti-IgE (*r=0.74, p<0.0001*) at least for histamine release to QR (**Supplementary Figure 2B**).

Stratified Analysis by Treatments With/ Without Dupilumab

Patients in the TCS group showed no significant difference between E1 and E2 in histamine release by QR and in the levels of IgE against MGL_1304 and Der f 1 (**Figure 2A**). In the dupilumab group, the levels of IgE against MGL_1304 and Der f 1 decreased, but histamine release in response to QR significantly increased at E2 from that at E1 (**Figure 2B**).

Factors Affecting Histamine Release in Response to QR

To explore reasons why the hyperreactivity of basophils against QR showed no reduction in spite of the decrease of IgE against MGL_1304, we analyzed the relationship of histamine release in response to QR to the length of periods under a well-controlled disease (IGA ≤2), net histamine release in response to the anti-human IgE antibody, and total serum IgE level. There was no significant correlation of the change of histamine release in response to QR to the length of periods under a well-controlled disease (*r=0.44, p=0.11*) (**Figure 3A**). The change of net histamine release in response to QR and the change of net histamine release in response to anti-human IgE antibody were positively correlated (*r=0.63, p=0.018*) (**Figure 3B**). This correlation was significant in the TCS group (*r=0.89, p=0.012*) but not in the dupilumab group (*r=0.50, p=0.27*) (**Supplementary Figure 3A,B**). While most patients enrolled in this study showed an increase of histamine release in response to anti-human IgE and a decrease of total serum IgE at E2 compared to those at E1 (**Figure 3C**), there was no correlation between the change of histamine release against anti-human IgE and that of total IgE (*r=-0.18, p=0.57*).

DISCUSSION

In this study, we performed an investigation of the change of basophil hyperreactivity to sweat in patients who achieved a

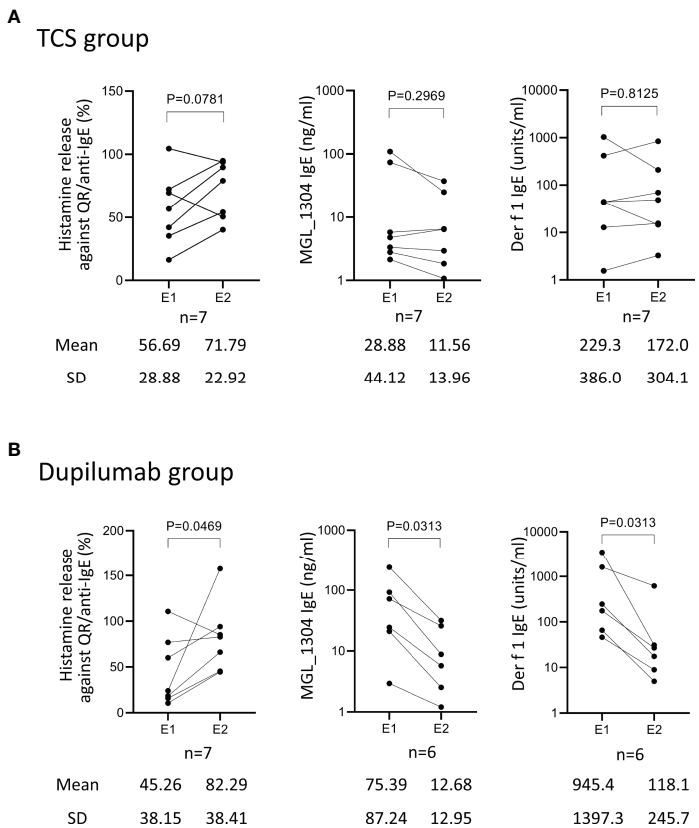


FIGURE 2 | Histamine release from basophils in response to QR, and levels of IgE against MGL_1304 and Der f 1 at E1 and E2 in patients treated with TCS (TCS group) **(A)** and those treated with TCS plus dupilumab (dupilumab group) **(B)**. TCS, topical corticosteroid. Histamine release was expressed as (net % of histamine release induced by QR)/(net % of histamine release induced by anti-human IgE)×100 (%). E1, the 1st evaluation; E2, the 2nd evaluation.

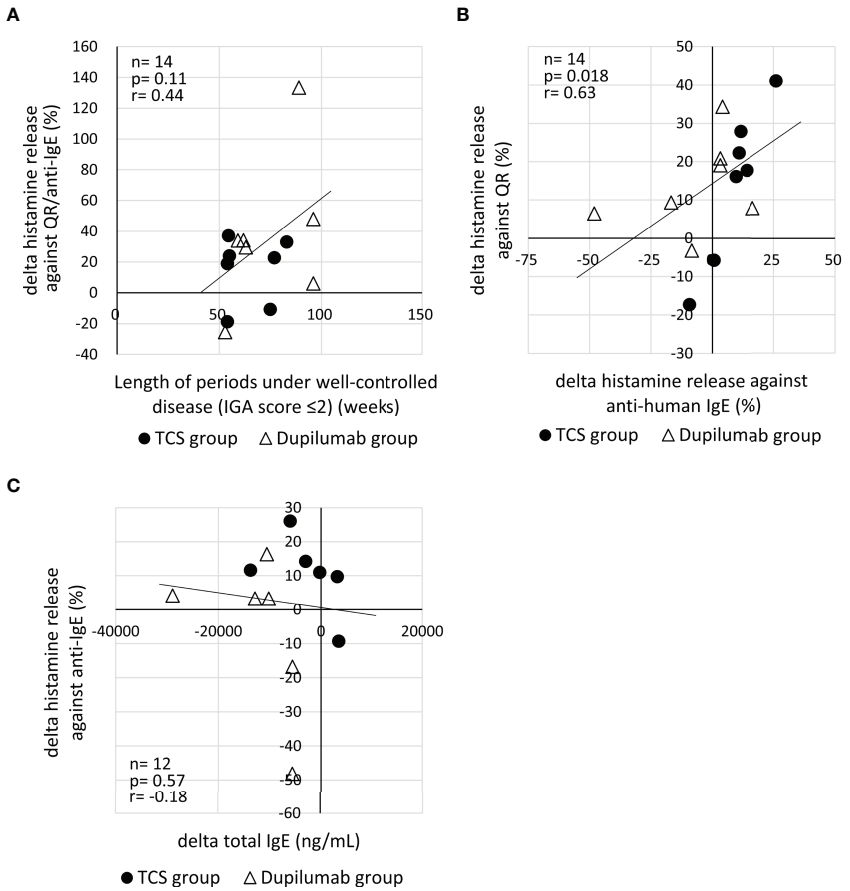


FIGURE 3 | **(A)** Correlation of the change of histamine release in response to QR to the length of periods under a well-controlled disease (IGA ≤2). Histamine release was expressed as (net % of histamine release induced by QR)/(net % of histamine release induced by anti-IgE)×100 (%). **(B)** Correlation between the change of histamine release in response to QR and that of histamine release in response to anti-human IgE. **(C)** Correlation of the change of histamine release in response to anti-human IgE with the change of serum total IgE. "delta" means the changes of parameters calculated by the subtraction of values at E1 from those at E2. E1, the 1st evaluation; E2, the 2nd evaluation; IGA, Investigator's Global Assessment.

good control of AD. The histamine release activity of patients' basophils in response to the semi-purified sweat antigen (QR) was not attenuated in the period of a well-controlled disease with the mean interval of 69 weeks (53–96 weeks) regardless of the use of dupilumab. Patients in the dupilumab group showed a significant reduction of specific IgE against MGL_1304 and Der f 1, whereas those in the TCS group did not. Thus, the suppression of the Th2 pathway by dupilumab reduced both the level of IgE against the sweat antigen and that against the mite antigen but did not result in a decrease of reactivity of basophils in response to the antigen.

The reduction of basophil hyperreactivity has not been observed in sweat allergy in this study but described in a type of food allergy. A previous study on the basophil hyperreactivity to hydrolyzed wheat (Glupearl 19S) sensitized by facial soap revealed a negative conversion of the basophil reactivity over the time of a year or longer by avoiding exposure to the antigen (18), suggesting that basophil hyperreactivity may decrease in food allergy developed by percutaneous sensitization. On the other hand, no significant reduction of histamine release in response to QR in this study implies persistent hyperreactivity of basophils to the sweat antigen in the period of 53–96 weeks. Although sweat allergy has likely developed by percutaneous sensitization, as was the case with Glupearl 19S allergy, the mechanism of sensitization to the sweat antigen in patients with AD may be somewhat different from that of food allergens. The avoidance of contact to food allergens on the skin is easier than that of the sweat antigen. Moreover, food antigens may induce tolerance *via* gastrointestinal uptake.

Several reasons may explain why the hyperreactivity of basophils against QR showed no reduction even in cases with the decrease of anti-MGL_1304 IgE in this study. First, MGL_1304 IgE levels might not have been sufficiently reduced to decrease the hyperreactivity of basophils. In mast cells, the crosslinking of only a few hundred molecules of the high-affinity IgE receptors are sufficient to induce mediator release (19). Second, the basophil function may have been impaired in the IgE receptor–mediated reaction at E1. It has been reported that severe dermatitis reduces the reactivity of basophils to IgE stimulation in patients with AD (20). In this study, AD lesions

became well controlled between E1 and E2 in 9 patients, and the other 5 patients were maintained at a low disease activity (IGA ≤2) over the period. Ten of the total 14 patients showed higher levels of net histamine release from basophils in response to anti-human IgE at E2 compared to E1 (**Figure 3B**). Moreover, 9 of the 10 patients with increased histamine release in response to anti-human IgE also showed increased histamine release in response to QR (**Figure 3B**). This suggests that the maintenance of well-controlled disease activity may restore basophil reactivity *via* the high-affinity IgE receptor, resulting in the increase of histamine release in response to QR. The recovery of impaired basophil function during the time between two evaluations may explain a discrepancy between the change of antigen-specific IgE levels and that of histamine release in response to the sweat antigen. The recovery of basophil function may be partially associated with decrease of total serum IgE because most patients with decreased total IgE showed increased histamine release against anti-human IgE (**Figure 3C**). Further studies are necessary to confirm such possibilities of the basophil dysfunction using other parameters of basophil reactivity, including membrane activation markers and non-IgE receptor-mediated stimuli, such as complement component 5a (C5a) and formyl-methionyl-leucyl-phenylalanine (fMLP).

In this study, type-I hypersensitivity to sweat was assessed by HRT using QR but not evaluated by clinical aggravation due to perspiration. The *in vitro* detection of the hyperreactivity of basophils against the sweat antigen may not always be associated with clinical aggravation by perspiration. Nevertheless, prolonged hyperreactivity of patients' basophils to the semi-purified sweat antigen shown in this study suggests that the extended management of sweat by showering (21, 22) and so on is necessary even after achieving an improvement of AD. The maintenance therapy to preserve a healthy skin barrier should also be taken to avoid flare due to the penetration of the sweat antigen through the damaged epidermis.

This study has a limitation in that a small number of patients were retrospectively involved in this study, and the observation period was only 53–96 weeks, despite many patients suffering from AD for a much longer period of time. Moreover, basophil reactivity was examined using the semi-purified sweat antigen, QR, but not MGL_1304, while the specific IgE was detected against MGL_1304. However, basophil reactivity in response to QR can be regarded as equivalent to that in response to MGL_1304 because MGL_1304 is considered to be identical to the histamine-releasing component in QR (see the reference 13 and **Supplementary Figure 1B**). Furthermore, the amount of MGL_1304 on the skin surface of individual patients was not quantified. Therefore, we cannot exclude the possibility that a difference between the amount of MGL_1304 on the skin surface at E1 and that at E2 may affect basophil reactivity to MGL_1304.

Collectively, this observation for 53–96 weeks showed no reduction of hyperreactivity of basophils against the sweat antigen in patients with AD that was clinically well controlled, even in cases treated with the Th2 pathway inhibitor, dupilumab. Further studies with longer observation periods are needed to determine the prognosis of hyperreactivity of basophils to sweat antigen.

DATA AVAILABILITY STATEMENT

The raw data supporting the conclusions of this article will be made available by the authors, without undue reservation.

ETHICS STATEMENT

The study protocol was reviewed and approved by the institutional review board of Hiroshima University Hospital (approval number: E-2781, E-1716).

AUTHOR CONTRIBUTIONS

TN, ST and MH designed the study. TN, ST, MH, KI, YY, and ToK wrote the manuscript. KI, AT, HM, SM, YY, TaK and ToK contributed to data collection. TN and ST performed the statistical analysis and interpretation of the results. All authors read and approved the final manuscript.

FUNDING

This study was supported by AMED under Grant Number JP19ek0410059 (ST and MH) and by JSPS KAKENHI under Grant Number JP21K08302 (ST), JP21K08346 (MH), and JP20K17319 (KI).

SUPPLEMENTARY MATERIAL

The Supplementary Material for this article can be found online at: https://www.frontiersin.org/articles/10.3389/fimmu.2022.883605/full#supplementary-material

REFERENCES

1. Katoh N, Ohya Y, Ikeda M, Ebihara T, Katayama I, Saeki H, et al. Japanese Guidelines for Atopic Dermatitis 2020. *Allergol Int* (2020) 69(3):356–69. doi: 10.1016/j.alit.2020.02.006
2. Kabashima K. New Concept of the Pathogenesis of Atopic Dermatitis: Interplay Among the Barrier, Allergy, and Pruritus as a Trinity. *J Dermatol Sci* (2013) 70(1):3–11. doi: 10.1016/j.jdermsci.2013.02.001
3. Gittler JK, Shemer A, Suárez-Fariñas M, Fuentes-Duculan J, Gulewicz KJ, Wang CQ, et al. Progressive Activation of T(H)2/T(H)22 Cytokines and Selective Epidermal Proteins Characterizes Acute and Chronic Atopic Dermatitis. *J Allergy Clin Immunol* (2012) 130(6):1344–54. doi: 10.1016/j.jaci.2012.07.012
4. Weidinger S, Beck LA, Bieber T, Kabashima K, Irvine AD. Atopic Dermatitis. *Nat Rev Dis Primers* (2018) 4(1):1. doi: 10.1038/s41572-018-0001-z
5. Gooderham MJ, Hong HC, Eshtiaghi P, Papp KA. Dupilumab: A Review of its Use in the Treatment of Atopic Dermatitis. *J Am Acad Dermatol* (2018) 78(3 Suppl 1):S28–s36. doi: 10.1016/j.jaad.2017.12.022

6. Beck LA, Thaci D, Hamilton JD, Graham NM, Bieber T, Rocklin R, et al. Dupilumab Treatment in Adults With Moderate-to-Severe Atopic Dermatitis. *N Engl J Med* (2014) 371(2):130–9. doi: 10.1056/NEJMoa1314768
7. Hamilton JD, Suarez-Farinas M, Dhingra N, Cardinale I, Li X, Kostic A, et al. Dupilumab Improves the Molecular Signature in Skin of Patients With Moderate-to-Severe Atopic Dermatitis. *J Allergy Clin Immunol* (2014) 134 (6):1293–300. doi: 10.1016/j.jaci.2014.10.013
8. Williams JR, Burr ML, Williams HC. Factors Influencing Atopic Dermatitis-a Questionnaire Survey of Schoolchildren's Perceptions. *Br J Dermatol* (2004) 150(6):1154–61. doi: 10.1111/j.1365-2133.2004.05869.x
9. Takahagi S, Tanaka A, Hide M. Sweat Allergy. *Allergol Int* (2018) 67(4):435–41. doi: 10.1016/j.alit.2018.07.002
10. Adachi K, Aoki T. IgE Antibody to Sweat in Atopic Dermatitis. *Acta dermato-venereologica Supplementum* (1989) 144:83–7. doi: 10.2340/000155551448387
11. Hide M, Tanaka T, Yamamura Y, Koro O, Yamamoto S. IgE-Mediated Hypersensitivity Against Human Sweat Antigen in Patients With Atopic Dermatitis. *Acta Derm Venereol* (2002) 82(5):335–40. doi: 10.1080/000155502320624050
12. Tanaka A, Tanaka T, Suzuki H, Ishii K, Kameyoshi Y, Hide M. Semi-Purification of the Immunoglobulin E-Sweat Antigen Acting on Mast Cells and Basophils in Atopic Dermatitis. *Exp Dermatol* (2006) 15(4):283–90. doi: 10.1111/j.0906-6705.2006.00404.x
13. Hiragun T, Ishii K, Hiragun M, Suzuki H, Kan T, Mihara S, et al. Fungal Protein MGL_1304 in Sweat is an Allergen for Atopic Dermatitis Patients. *J Allergy Clin Immunol* (2013) 132(3):608–15.e4. doi: 10.1016/j.jaci.2013.03.047
14. Hiragun M, Hiragun T, Ishii K, Suzuki H, Tanaka A, Yanase Y, et al. Elevated Serum IgE Against MGL_1304 in Patients With Atopic Dermatitis and Cholinergic Urticaria. *Allergol Int* (2014) 63(1):83–93. doi: 10.2332/allergolint.13-OA-0611
15. Takahagi S, Tanaka T, Ishii K, Suzuki H, Kameyoshi Y, Shindo H, et al. Sweat Antigen Induces Histamine Release From Basophils of Patients With Cholinergic Urticaria Associated With Atopic Diathesis. *Br J Dermatol* (2009) 160(2):426–8. doi: 10.1111/j.1365-2133.2008.08862.x
16. Hide M, Francis DM, Grattan CE, Hakimi J, Kochan JP, Greaves MW. Autoantibodies Against the High-Affinity IgE Receptor as a Cause of Histamine Release in Chronic Urticaria. *N Engl J Med* (1993) 328(22):1599–604. doi: 10.1056/NEJM199306033282204
17. Ishii K, Hiragun M, Hiragun T, Kan T, Kawaguchi T, Yanase Y, et al. A Human Monoclonal IgE Antibody That Binds to MGL_1304, a Major Allergen in Human Sweat, Without Activation of Mast Cells and Basophils. *Biochem Biophys Res Commun* (2015) 468(1-2):99–104. doi: 10.1016/j.bbrc.2015.10.154
18. Hiragun M, Ishii K, Yanase Y, Hiragun T, Hide M. Remission Rate of Patients With Wheat Allergy Sensitized to Hydrolyzed Wheat Protein in Facial Soap. *Allergol Int* (2016) 65(1):109–11. doi: 10.1016/j.alit.2015.07.004
19. Fewtrell C, Metzger H. Larger Oligomers of IgE are More Effective Than Dimers in Stimulating Rat Basophilic Leukemia Cells. *J Immunol* (1980) 125 (2):701–10.
20. Imamura S, Washio K, Mizuno M, Oda Y, Fukunaga A, Nishigori C. Activated Steady Status and Distinctive Fcεri-Mediated Responsiveness in Basophils of Atopic Dermatitis. *Allergol Int* (2021) 70(3):327–34. doi: 10.1016/j.alit.2021.01.005
21. Mochizuki H, Muramatsu R, Tadaki H, Mizuno T, Arakawa H, Morikawa A. Effects of Skin Care With Shower Therapy on Children With Atopic Dermatitis in Elementary Schools. *Pediatr Dermatol* (2009) 26(2):223–5. doi: 10.1111/j.1525-1470.2009.00887.x
22. Murota H, Takahashi A, Nishioka M, Matsui S, Terao M, Kitaba S, et al. Showering Reduces Atopic Dermatitis in Elementary School Students. *Eur J Dermatol EJD* (2010) 20(3):410–1. doi: 10.1684/ejd.2010.0928

Conflict of Interest: TN has received a research grant from Sun pharma and Kyowa-Kirin. ST has received a research grant from Sanofi, Maruho, and Taiho Pharma and an honorarium from Novartis. MH has received a research grant from GlaxoSmithKline, Kaken Pharmaceutical, Mitsubishi-Tanabe, Novartis, Sanofi, and Taiho Pharma, honorarium from Ely-Lilly, Kaken-Pharmaceutical, Kyowa-Kirin, Mitsubishi-Tanabe, MSD, Novartis, Sanofi, Taiho Pharma, Teikoku seiyaku, and Uriach. AT has received a research grant from Maruho, Sanofi, Eisai, and Mitsubishi Tanabe Pharma and an honorarium from Maruho, Torii Pharma, Mitsubishi Tanabe Pharma, Sanofi, and Taiho Pharma.

The remaining authors declare that the research was conducted in the absence of any commercial or financial relationships that could be construed as a potential conflict of interest.

Publisher's Note: All claims expressed in this article are solely those of the authors and do not necessarily represent those of their affiliated organizations, or those of the publisher, the editors and the reviewers. Any product that may be evaluated in this article, or claim that may be made by its manufacturer, is not guaranteed or endorsed by the publisher.

Copyright © 2022 Numata, Takahagi, Ishii, Morioke, Kan, Mizuno, Yanase, Kawaguchi, Tanaka and Hide. This is an open-access article distributed under the terms of the Creative Commons Attribution License (CC BY). The use, distribution or reproduction in other forums is permitted, provided the original author(s) and the copyright owner(s) are credited and that the original publication in this journal is cited, in accordance with accepted academic practice. No use, distribution or reproduction is permitted which does not comply with these terms.

frontiers | Frontiers in Immunology

SYSTEMATIC REVIEW
published: 05 July 2022
doi: 10.3389/fimmu.2022.918305

Mast Cell and Basophil Granule Proteases - *In Vivo* Targets and Function

Lars Hellman[1]*, *Srinivas Akula*[2], *Zhirong Fu*[1] and *Sara Wernersson*[2]

[1] Department of Cell and Molecular Biology, Uppsala University, The Biomedical Center, Uppsala, Sweden, [2] Department of Anatomy, Physiology, and Biochemistry, Swedish University of Agricultural Sciences, Uppsala, Sweden

Proteases are stored in very large amounts within abundant cytoplasmic granules of mast cells (MCs), and in lower amounts in basophils. These proteases are stored in their active form in complex with negatively charged proteoglycans, such as heparin and chondroitin sulfate, ready for rapid release upon MC and basophil activation. The absolute majority of these proteases belong to the large family of chymotrypsin related serine proteases. Three such enzymes are found in human MCs, a chymotryptic enzyme, the chymase, a tryptic enzyme, the tryptase and cathepsin G. Cathepsin G has in primates both chymase and tryptase activity. MCs also express a MC specific exopeptidase, carboxypeptidase A3 (CPA3). The targets and thereby the functions of these enzymes have for many years been the major question of the field. However, the fact that some of these enzymes have a relatively broad specificity has made it difficult to obtain reliable information about the biologically most important targets for these enzymes. Under optimal conditions they may cleave a relatively large number of potential targets. Three of these enzymes, the chymase, the tryptase and CPA3, have been shown to inactivate several venoms from snakes, scorpions, bees and Gila monster. The chymase has also been shown to cleave several connective tissue components and thereby to be an important player in connective tissue homeostasis. This enzyme can also generate angiotensin II (Ang II) by cleavage of Ang I and have thereby a role in blood pressure regulation. It also display anticoagulant activity by cleaving fibrinogen and thrombin. A regulatory function on excessive T_H2 immunity has also been observed for both the chymase and the tryptase by cleavage of a highly selective set of cytokines and chemokines. The chymase also appear to have a protective role against ectoparasites such as ticks, mosquitos and leeches by the cleavage of their anticoagulant proteins. We here review the data that has accumulated concerning the potential *in vivo* functions of these enzymes and we discuss how this information sheds new light on the role of MCs and basophils in health and disease.

Keywords: mast cell, tryptase, chymase, serine protease, CPA3

OPEN ACCESS

Edited by:
Satoshi Tanaka,
Kyoto Pharmaceutical University, Japan

Reviewed by:
Violetta Borelli,
University of Trieste, Italy
Viktor Bugajev,
Institute of Molecular Genetics (ASCR), Czechia

***Correspondence:**
Lars Hellman
Lars.Hellman@icm.uu.se

Specialty section:
This article was submitted to Inflammation, a section of the journal Frontiers in Immunology

Received: *12 April 2022*
Accepted: *08 June 2022*
Published: *05 July 2022*

Citation:
Hellman L, Akula S, Fu Z and Wernersson S (2022) Mast Cell and Basophil Granule Proteases - In Vivo Targets and Function. Front. Immunol. 13:918305. doi: 10.3389/fimmu.2022.918305

INTRODUCTION

Mast cells (MCs) are tissue resident cells that are found primarily in regions of the body in contact with the external world, such as the skin, the tongue, the small intestine, the lungs and in connective tissues surrounding different organs (1). They are also often found close to blood vessels and nerves where they act as sentinel cells, sensing the environment, signaling to other immune cells, and opening the tissues for influx of antibodies, complement and inflammatory cells. To perform these tasks they store massive amounts of physiologically acting substances in cytoplasmic granules, ready for rapid release upon activation of the cell. In these granules we find histamine, heparin and several proteases (2–10). The proteases, which are present in very large amounts can account for up to 35% of the total cellular protein of the MC, and they are stored in their active form in tight complex with negatively charged proteoglycans such as heparin and chondroitin sulfate (3, 4, 9, 11, 12). The absolute majority of these proteases belong to the chymotrypsin related serine protease family of endopeptidases (13). MCs primarily express chymases and tryptases with chymotryptic or tryptic primary cleavage specificities, respectively. The chymase is MC specific and the tryptase is expressed in both MC and basophils. MCs also express a carboxypeptidase named CPA3 that is restricted in its expression to MCs and basophils (14–17). This A/B type exopeptidase belongs to the M14 metallo-carboxypeptidase family. Upon activation MCs also produce and secrete potent lipid mediators, primarily leukotriene C4 (LTC4), and prostaglandin D2 (PGD2) (10, 18–20). Leukotriene B4 (LTB4) is also be produced by MC. However the major producer of this leukotriene seems to be neutrophils and monocytes/macrophages (21).

The transcripts for the granule proteases are the most highly expressed transcripts in the mature MC where the expression levels can be in the range of several percent of the total transcriptome (1, 16, 22). In addition to MC tryptase and chymase, serine proteases belonging to the same family of trypsin/chymotrypsin related serine proteases have in mammals also been identified in basophils, neutrophils, cytotoxic T cells and natural killer (NK) cells but not in B cells, macrophages, red blood cells, platelets or dendritic cells and only at relatively low levels in eosinophils. A very broad spectrum of primary cleavage specificities has been observed for these hematopoietic serine proteases, including chymase, tryptase, asp-ase, elastase and met-ase specificities, which highlights the large flexibility in their active site (23). It is the amino acids of active site pocket that determines the primary specificity and it is primarily three residues that are responsible for this specificity, i.e. the residues 189, 216 and 226, according to the numbering in bovine pancreatic chymotrypsinogen (**Figure 1**) (24).

The genes encoding these hematopoietic serine proteases are organized in four different loci, i.e. the MC chymase locus, the MC tryptase locus, the T cell tryptase locus and the met-ase locus (25, 26). In mammals, these loci are often located on four different chromosomes, indicating that some of them may originate from whole genome duplications, so called tetraploidizations. Two such tertraploidizations have most likely occurred during early vertebrate evolution, which indicate that the original locus was present before these evolutionary important events (27). Interestingly, only one of these loci is present in cartilaginous fish, the T cell tryptase locus, which also is named the granzyme A/K locus. Not any of these loci is present in jawless fish, including lamprey and hagfish, indicating that they appear at the base of jawed vertebrates (25).

Two major subtypes of MCs have been identified in mammals, connective tissue MCs (CTMCs) and mucosal MCs (MMCs) (28–30). They have been named primary based on their tissue distribution. In humans and rodents CTMCs are primarily located in connective tissue of the skin, the tongue and in connective tissue surrounding different organs, whereas MMCs are found in the intestinal mucosa of the duodenum and in primates also in the lung (1, 31, 32). These MC subtypes express different sets of the MC specific proteases. In humans the MMCs are also named MC_T, because they only express the tryptase, whereas the human CTMCs, also named MC_{TC} express four proteases, the tryptase, the chymase, cathepsin G and CPA3 (30). Interestingly, relatively large differences in the number of these proteases and their tissue specificity have been observed between species. As mentioned above human MCs primarily express four such proteases, the chymase, the tryptase, cathepsin G and CPA3 (33, 34). In marked contrast, mouse and rat have a relatively large number of such proteases. Mouse CTMCs express mMCP-5, the evolutionary counterpart of the human chymase, a second chymase named mMCP-4, two tryptases, named mMCP-6 and -7 and the carboxypeptidase CPA3 (1). The name for the human chymase gene and mMCP-5 in the locus annotation is Cma1. Cma1 is also classified as the α-chymase. In rodents a second subfamily of chymases has been identified, a subfamily named ß-chymases. These ß-chymases most likely originate from a relatively early gene duplication of the α-chymase gene. This initial duplication was then most likely followed by several successive duplications. In the mouse chymase locus there are five active such ß-chymases: mMCP-1, mMCP-2, mMCP-4, mMCP-9 and mMCP-10 (**Figure 2**). Mouse CTMCs express one of them, the mMCP-4. Mouse MMCs only express chymases, mMCP-1 and mMCP-2, and no tryptase or CPA3. To this should be added that the evolutionary counterpart of human chymase in mice, the mMCP-5, is per definition no longer a chymase since it lacks chymase activity. During evolution, the origin of mMCP-5 has by mutations of the amino acids surrounding the substrate binding pocket changed its primary specificity from being a chymase to now only accepting smaller aliphatic amino acids and thereby becoming an elastase (**Figure 1**) (35, 36). Interestingly, when the α-

Abbreviations: MC, mast cell; MMC, mucosal mast cell; CTMC, connective tissue mast cell; Ang II, angiotensin II; CPA3, Carboxypeptidase A3; mMCP-1, mouse mast cell protease 1; rMCP-1, rat mast cell protease 1; MC_T, mast cell expressing only the tryptase; MC_{TC} mast cell expressing both the chymase and the tryptase; TSLP, thymic stromal lymphopoietin; AT1, angiotensin receptor 1; ACE, angiotensin converting enzyme; NK cell, natural killer cell; Vch, vascular chymase; TAP, tick anticoagulant protein.

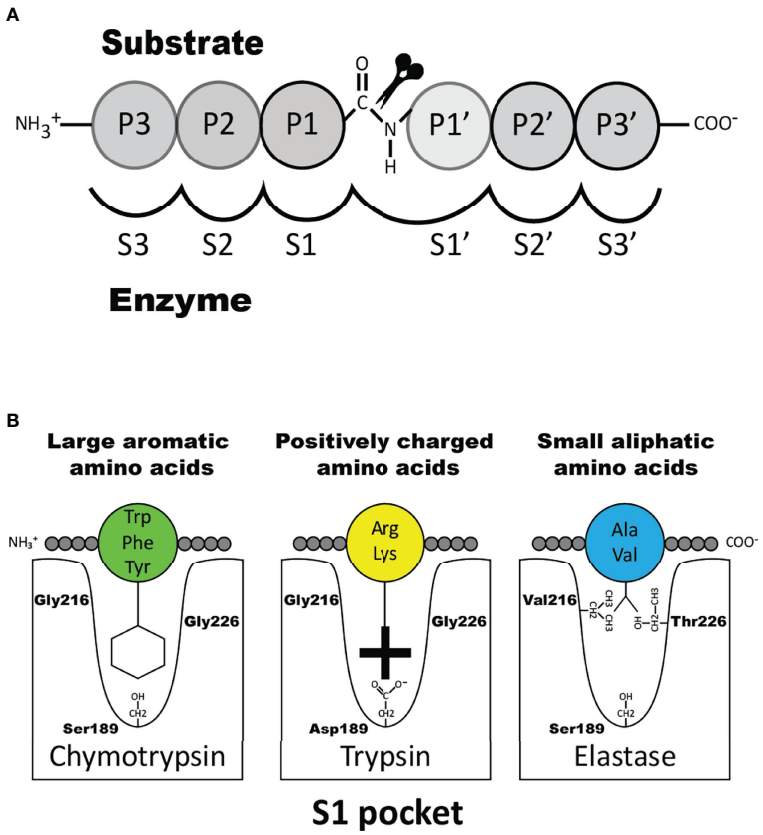


FIGURE 1 | Nomenclature of the amino acids surrounding the cleaved peptide bond and the amino acids forming the active site pocket. Panel **A** shows the amino acids N-terminal from the cleaved bond are termed P1 (where cleavage occurs, depicted by scissors), P2, P3 etc. Amino acids C-terminal of the cleaved bond are termed P1' (adjacent to P1), P2', P3' etc. The corresponding interacting sub-sites in the enzyme are denoted with S. Panel **B** shows the S1 pocket, which is important in determining the primary specificity of the chymotrypsin family. The important residues are shown, which determine chymotrypsin-, trypsin- or elastase-like specificity. Three residues corresponding to positions 189, 216 and 226 in bovine pancreatic chymotrypsinogen has been found to be the amino acids forming the major part of this pocket and thereby giving the primary specificity of the enzyme (24).

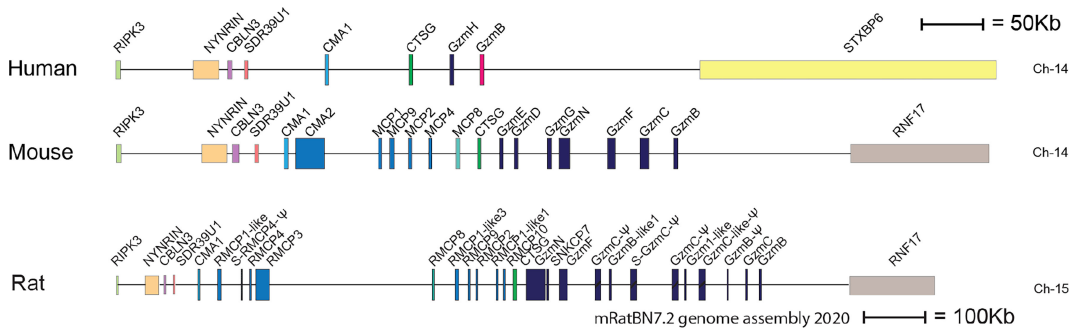


FIGURE 2 | The chymase locus of three mammalian species. An in-scale figure of the chymase locus in three mammalian species; human, mouse and rat. The genes are color coded. Granzymes are shown in dark blue, α-chymases in light blue and β-chymases as blue with a darker tint. mMCP-8-related genes are in cyan, duodenases in red and cathepsin G in green. The general scale bar of 50 kB is valid for most of the genes. However, the rat locus is much larger in size why we have reduced the size to half. For rat we have therefore introduced a 100 kB size marker.

chymase mMCP-5, became an elastase, the ß-chymase mMCP-4 seems to have taken over the role of the α-chymase. mMCP-4 has been found to have an extended cleavage specificity almost identical to the human MC chymase (37). A similar expansion of the number of chymases is also seen in the rat (**Figure 2**). However, here the number of ß-chymases is even higher. Rats have seven ß-chymases: rat (r)MCP-1, rMCP-2, rMCP-3, rMCP-4, rMCP-1-like 1 (also named the vascular chymase (Vch)), rMCP-1 like 2 and rMCP-1 like 3 (**Figure 2**) (25).

This massive increase in protease genes in rodent is primarily seen in one of the four loci encoding the hematopoietic serine proteases, i.e. in the chymase locus (**Figure 2**) (25, 26). This locus encodes in humans only four genes, the MC chymase, cathepsin G and two T cell expressed granzymes, the granzymes B and H. In marked contrast, this locus encodes 15 functional protease genes in mouse and as many as 18 such genes in rat (**Figure 2**). Why rodents seem to need so many more of these genes compared to primates is still an open but very interesting question.

Basophils also express some of these proteases but store them at lower levels compared to MCs. Human basophils express the tryptase and CPA3, whereas mouse basophils express the basophil specific proteases mMCP-8 and mMCP-11 together with CPA3 (34, 38–41).

A number of very diverse functions have been identified for the different hematopoietic serine proteases, including apoptosis induction, blood pressure regulation, inactivation of insect and snake venoms, killing of bacteria and fungi, mobilization or degradation of cytokines and the degradation of connective tissue components (23, 42–47). These MC proteases may act both locally and systemically. However, in the circulation the presence of large amounts of protease inhibitors results in that the chymase rapidly become inactivated upon entering the circulation. The tryptase tetramers do relatively rapidly form monomers after entering the circulation and the monomers are inactive at physiological pH. The activity of these proteases is therefore primarily confined to the area close to the mast cells within the tissue and in there in macromolecular complex with the proteoglycans, and only to a minor extent in the circulation.

The situation for the two tryptases in the mouse, mMCP-6 and mMCP-7, is slightly different. mMCP-6 seems to stay at the site and is not found in the circulation, whereas active tetramers of mMCP-7 are found in relatively high amounts in plasma of mice, but is gone from the circulation 4 hours after MC activation (48). In this review we will try to summarize the evidence that has accumulated on the biological targets for the very abundant MC enzymes and the less abundant basophil proteases and what this new knowledge can tell us about their role in MC and basophil biology. We will first look at the targets for the chymases, where most data have accumulated, followed by the tryptases and CPA3 and finally the basophil specific proteases. By applying an evolutionary approach we aim to identify potential targets that have been conserved among the majority of mammals which would strongly support their evolutionary importance as targets for particular enzymes.

IN VIVO TARGETS FOR THE MC CHYMASES

Angiotensin I and The Regulation of Blood Pressure

Angiotensin I (Ang I) is one of the first potential targets to be identified for the human MC chymase. Ang I is a 10 amino acid inactive peptide originating from cleavage of an elongated N terminus of angiotensinogen by the aspartyl protease renin (49) (**Figure 3**). Angiotensinogen is a member of the serpin family of protease inhibitors mainly produced by the liver but mRNA is also found in many other organs (50, 51). However, no inhibitory activity on proteases has been detected for angiotensinogen (49). Cleavage of Ang I by the human chymase at residue Phe8 results in the eight amino acid peptide Ang II. Ang II, but not Ang I, is a ligand for the G-protein coupled angiotensin receptors 1 and 2 (AT1 and AT2) (52). Most of the classical effects by Ang II is mediated by AT1, involving induction of blood vessel contraction, aldosterone release from the adrenal zona glomerulosa, salt retention in the renal proximal tubules and

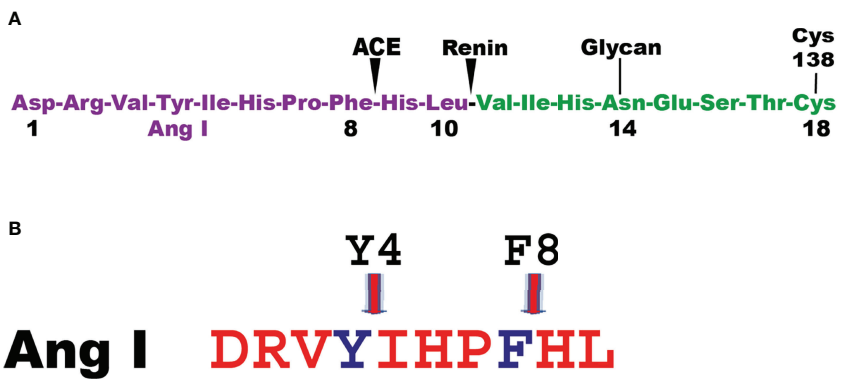


FIGURE 3 | Angiotensin cleavage. Panel **A** shows the N-terminal end of angiotensinogen including the 10 amino acid and the cleavage sites in angiotensinogen for renin and for the angiotensin converting enzyme (ACE). Panel **B** shows the Ang I peptide with the cleavage site for the majority of MC chymase at Phe 8 generating Ang II and for a few additional MC chymases from some species where their chymases also degrade Ang II by cleavage at Tyr 4.

stimulation of the sympathetic nervous system thereby resulting in an increase in blood pressure (52). In some mammals the MC chymase also cleaves after Tyr4 in Ang I and thereby also degrade the peptide (**Figure 3**) (53, 54). The major Ang II generating enzyme in the blood has classically been considered to be the angiotensin converting enzyme (ACE) (**Figure 3**) (52). However, Ang I conversion in the tissues may to a larger extent be dependent on other enzymes including the MC chymases (55). Human, macaque and dog MC chymases, and mouse mMCP-4 seem to almost exclusively generate Ang II from Ang I by cleavage at Phe8 (53, 54). However, the major rat CTMC chymase, rMCP-1, seems to efficiently cleave at both Tyr4 and Phe8 and thereby degrade Ang I (**Figure 3**) (53, 54). A similar situation has been observed for golden hamster, and opossum chymases indicating that not all mammals have MC chymases with Ang I converting function (54). No studies have so far been performed to look for other potential enzymes in these species, which could have this function, except for in the rat (54). In the rat one of the ß-chymases have changed tissue specificity and is now no longer considered to be expressed in MCs, but instead in vascular muscle cells, therefore it has been named rat vascular chymase (Vch) (54, 56, 57). This protease was previously thought to have taken over the role of Ang I converting enzyme from rMCP-1, which also degrades Ang I by cleavage at Tyr4 (53, 56). However, when we recently analyzed the Ang I converting activity of recombinant Vch we found that it was a very poor Ang I converter (54). The question therefore remains if other enzymes in rat, hamster and opossum is responsible for Ang I conversion in these species or if they have alternative strategies to cope with blood pressure drop upon massive MC activation.

To have the MC enzymes involved in blood pressure regulation makes biologically a lot of sense as a massive release of histamine, leukotriene C4 and prostaglandin D2 from MCs upon antigen triggering result in increased blood vessel permeability and outflow of plasma from the vessels leading to a drop in blood pressure (58). In such scenario, the generation of Ang II by MC chymase could be essential for survival to counteract a massive drop in blood pressure that could result in unconsciousness, and severe injuries after fainting.

Matrix Components

The amount of proteolytic enzymes stored in the CTMCs is remarkable. In spite of the fact that the granules already are filled with these enzymes, MCs still seem to constantly synthesize these enzymes. Their mRNA levels are namely exceptionally high even in resting tissue CTMCs (1, 16, 22). It has been proposed that these tissue resident MCs secrete small amounts of these proteases by piece meal degranulation, possibly constantly as a part of normal tissue homeostasis. The human, mouse, macaque, dog and opossum MC chymases have been shown to efficiently cleave fibronectin and at least the human chymase also seems to activate pro-collagenases indicating that they play an active role in connective tissue turnover (43, 44, 47, 59). Findings from mMCP-4 knock out mice support the role of the MC chymase in connective tissue homeostasis where the connective tissue in these mice increase in thickness with increasing age indicating a reduced turnover of the connective tissue components (59). A similar phenomenon has been observed in mice lacking macrophage colony stimulating factor (M-CSF) where these mice lack or have very low numbers of osteoclasts, a type of bone macrophages. These mice develop osteopetrosis with very dense bone that become brittle due to that their bone matrix is not being degraded and resynthesized, which results in small cracks in the bone that are not being sealed (60). So at least two different immune cells may have an important role in general tissue homeostasis, i.e. MCs of connective tissue and macrophages of both bone and connective tissue. Mouse peritoneal macrophages also express high levels of several connective tissue components including fibronectin, proteoglycan 4, syndecan 3 and extracellular matrix protein 1 indicating that they are major players in connective tissue homeostasis (61).

Regulating Intestinal Permeability

During parasite infections MMCs increase in numbers quite dramatically in the intestinal mucosa peaking between one and two weeks after a worm infestation (29, 62). The numbers can increase by 10-50 fold and the majority of these new MCs are located just below the epithelial layer of the intestinal mucosa of the duodenum (29, 62, 63). Injection of the rat MMC-specific protease rMCP-2 has been shown to rapidly affect the permeability of the mucosal layer resulting in outflow of antibodies, complement components and also inflammatory cells, including eosinophils and neutrophils (64, 65). By analyzing the cleavage of a panel of cell adhesion molecules expressed in the intestinal mucosa of rats we found that rMCP-2 effectively cleave several of these components including protocadherin, E-cadherin, cadherin-17 and occludin (66). Interestingly, human MMCs lack chymases, so the question is if primates have alternative strategies to increase intestinal permeability. Injection of rMCP-2 intravenously, not only locally produced, has been shown to result in this increase in intestinal permeability indicating that also chymase originating from CTMC could have this effect. We therefore decided to test the ability of human chymase to cleave the same set of cell adhesion molecules that we used to analyze the activity of rMCP-2. We can here show that the human chymase actually is even more active against these cell adhesion molecules than the MMC-specific rMCP-2. Almost all of the tested targets, including protocadherin, E-cadherin, cadherin-17 and occludin were efficiently cleaved by the human chymase indicating that it may have a similar function as rMCP-2 (**Figure 4**), despite its absence in normal human MMCs.

MCs in Immunity to Bacteria

The role of MCs in the defense against bacterial infection have been controversial due to the initially relatively poor animal models (67). The early MC deficient mouse models, primarily the W/W^v but also the W^{sh}/W^{sh}, that was based on mutations in the stem cell factor receptor, the c-kit, had indicated a clear involvement of MCs in bacterial defense. However, many of these effects and also the role of MCs in autoimmunity could not be confirmed when more stringent MC deficient mouse models became available (67). In these early MC-deficient models there

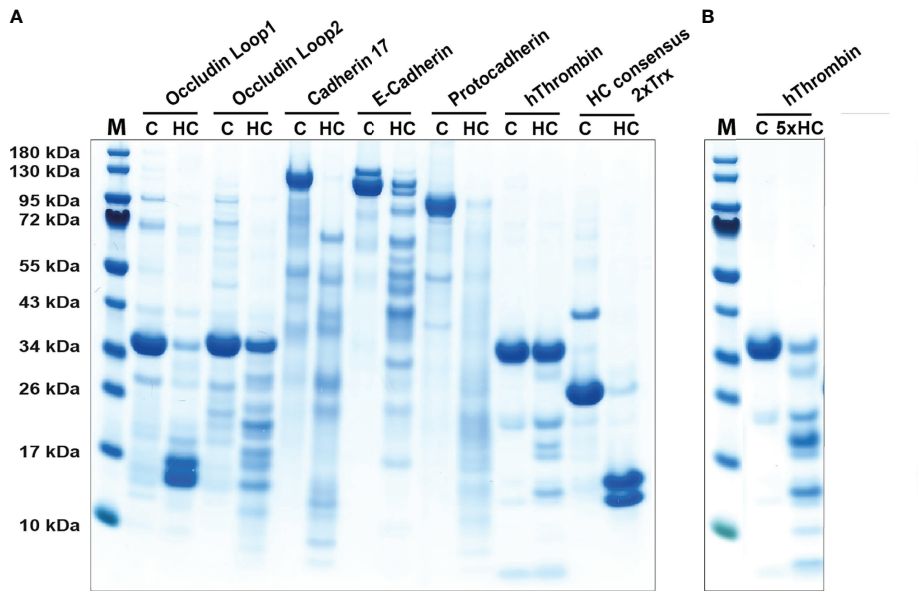


FIGURE 4 | Cleavage of adhesion molecules and thrombin by the human chymase. An SDS-PAGE analysis of a cleavage analysis of a panel of different cell adhesion molecules and of the coagulation factor thrombin by the human MC chymase. C marks the target protein without addition of the chymase, as control, and HC marks the cleavage of the target molecule by the human chymase. As a control for the activity of the human chymase is also a recombinant 2xTrx substrate included, where an optimal cleavage site for this enzyme is inserted between two copies of the *E. coli* redox protein thioredoxin (43). In panel **(A)** forty ng of HC was used in each of the cleavage reactions. In panel **(B)** which is a second cleavage reaction included of thrombin, there we used five times higher amount, or 200 ng, of the human chymase.

were also reduced numbers and activity of neutrophils and also more general effects on hematopoiesis, which turned out to be the major cause of the reduced efficiency to combat bacterial infections in these mice. However, a clear role of MCs has later been seen with the new and improved MC-deficient animal model, including the CPA3-Cre, mMCP-5-Cre and Mcl-1fl/fl mice (67). These new models are considerably better than the kit dependent model, but also these new models have flaws. They also show reduced numbers of basophils (68).

One important example of the importance of MC in bacterial defense when using these new models is the defense against infection by *Escherichia coli* in the urinary bladder. In this type of infections the bacterial clearance has been well documented to be dependent on the mouse MC chymase (mMCP-4) (69). Upon infection by *E. coli*, MCs increase in numbers in the bladder wall and migrate towards the epithelial layer where they release their granules. The granule proteases do in turn cleave adhesion molecules and when mMCP-4 enter the epithelial cells it induces caspase 1 activation and pyroptotic cell death which results in the shedding of the infected epithelial layer of cells lining the bladder inner wall. The bacteria attached to the bladder wall are then flushed out of the bladder resulting in marked reduction in bacterial load and a faster recovery (69). The different MC proteases may have similar functions in the duodenum and the urinary bladder, by cleaving cell adhesion molecules resulting in increased permeability and/or in epithelial shedding. Epithelial shedding seems namely also to be a major defense strategy in the intestinal region during severe bacterial infections, like *Salmonella* infections (70). During severe *Salmonella* infections the infected cells of the epithelial layer are shed to remove the bacteria from the epithelial layer and to inhibit them from reaching deeper into the intestinal tissue (70). Although the involvement of MCs in this intestinal shedding seem very likely, this has to our knowledge not yet been documented. Notably, a recent study has demonstrated a role for both MCs and IgE in the clearance of bacterial infection in the ear of mice. The importance of MCs in this study was linked to protection against secondary lung infection by *Staphylococcus aureus* (71) and there were indications that the MC proteases participated in the defense (71). MC proteases probably also contribute to bacterial clearance by cleavage of many bacterial virulence factors. However, there are so far few documented examples of such potential targets of importance for the bacterial defense.

Many bacteria use adhesion to connective tissue components, primarily fibronectin as one way to attach and avoid being flushed out of a tissue. This attachment is achieved by the production of fibronectin binding proteins by bacteria (72). In at least one study the cleavage of fibronectin by the mouse chymase mMCP-4 have been shown to be of importance for inhibiting bacteria to colonize a tissue and thereby having a beneficial role in bacterial clearance (72).

Regulating coagulation

Granules of rodent CTMCs contain large amounts of heparin and in primates both CTMCs and MMCs contain heparin (73). Heparin is a potent anticoagulant by the activation of anti-thrombin (74). The triggering of MCs results in the release of histamine, leukotrienes, prostaglandins, heparin and proteases. These mediators do in turn trigger the opening of blood vessels, which results in an influx into

the tissue of antibodies, complement, inflammatory cells and blood coagulation components (58, 75). When clotting proteins come in contact with the tissue, coagulation is initiated to seal the leakage of the vessel. The potentially negative effect of coagulation is that the flow of immune components is blocked. To counteract this closure, MC heparin may limit activation of thrombin, one of the key enzymes in the clotting cascade. The MC chymase may also help in this inhibition of coagulation by actively inactivating thrombin by proteolytic cleavage. Cleavage of thrombin by human chymase has been shown previously (76). To further analyze the efficiency of this cleavage we have tested the *in vitro* cleavage of human thrombin with two different concentrations of the chymase (**Figure 4**). We found that considerably more of the enzyme was needed to cleave thrombin compared to the cell adhesion molecules, but still within the physiological range of the enzyme concentration. Hence, degradation of thrombin by the chymase may contribute to the inhibition of coagulation after opening of the vessels for immune mediators and cells. Chymase also efficiently cleave fibrinogen and this effect has also been evolutionary conserved as we have shown that both human and opossum chymase efficiently degrades fibrinogen (47). MCs can thereby have anticoagulant activity by at least three independent mechanisms, heparin and the inactivation of both thrombin and fibrinogen.

Inactivation of Venoms

MCs are most abundant in tissues in close contact with the external world like the skin, the tongue and the intestinal mucosa. Venoms delivered by snake bites, scorpion stings or bee and wasp stings are generally appearing in the skin. Several elegant studies have shown the potent action of the different MC enzymes on these venoms resulting in their inactivation (42, 77–80). The venoms also act directly on the MCs by inducing degranulation (80).

The human MC chymase has been shown to cleave internally in endothelin and sarafotoxin 6B from the Israeli mole viper (78, 81). Interestingly several of these toxins mimic the action of endogenous activators. Some of these toxins show high sequence homology to endothelin, a potent endogenous regulator of blood pressure. Endothelin has been shown to be cleaved by both the human chymase and by CPA3 (81). Chymase cleaves internally in endothelin whereas CPA3 cleaves of a single amino acid in the C-terminal end of this peptide (77, 81). It is the C-terminal trimming, by the removal of the C-terminal tryptophan, that appears to have the major inhibiting effect on the biological activity of endothelin (81).

Regulating Excessive T_H2 Immunity

The default pattern in immune regulation has been considered to be a humoral T_H2 immunity, primarily involving B cells and immunoglobulins. This is an immune response not involving the activation of potentially harmful cytotoxic T cells. However, upon infection with intracellular parasites, including viruses and certain bacteria, like *Mycobacteria*, *Chlamydia* and *Listeria*, the immune system needs to activate a more potent response. However, this will also activate more potentially harmful players to locate and remove the infection including killing the infected cells by inducing apoptosis and subsequent phagocytosis of the infected cells. Antibodies are not sufficient to target infectious agents that hide inside our own cells. The important triggers of this cell mediated T_H1 response are IL-12 and interferons, primarily IFN-α and IFN-ß. T_H1 responses need to be very tightly regulated and very small amounts of IL-12 is apparently sufficient to activate this type of response. Attempts to regulate excessive T_H2 immunity, which occur in allergic patients, by tilting immunity more towards T_H1 immunity has not been successful, primarily due to the high potency of the IL-12. Strikingly, mice injected with 1 ug of IL-12 per day resulted in 100% death at day six due to the potency of the IL-12 (82). The question is if there also is a tight regulation of T_H2 immunity and in that case what cell type would most likely be involved. MCs can produce a large number of cytokines, primarily T_H2 cytokines, so they can potentially enhance an ongoing T_H2 immunity (83). However, do they also have a role in controlling excessive T_H2 immunity? In support of this notion, we found that MC chymase cleaves the T_H2-cytokine IL-33 and exhibits a protective role in a mouse model of allergic asthma, as suggested by the augmented sensitization, airway inflammation and IL-33 levels in mice lacking the chymase mMCP-4 (84). To study the human chymase for its selectivity in degrading cytokines and chemokines we analyzed the activity of the human chymase on a panel of 55 cytokines and chemokines. To our surprise we found that this enzyme was exceptionally restrictive in its cleavage. Only three cytokines were efficiently cleaved by the human chymase, namely IL-18, IL-33 and IL-15 (46). Two of these, IL-18 and IL-33, are classical T_H2 cytokines and the third, IL-15, has recently been shown to be a potent inducer of allergen sensitization, showing that also this cytokine has a potent T_H2 inducing activity (**Figure 5**) (88, 89). This very high selectivity for a small set of T_H2 cytokines, indicated an important role of the chymase in regulating excessive T_H2 immunity (46). We later showed that also the tryptase has a very similar activity, which made the finding even more striking (47). These two MC-specific enzymes combined appear to have a very strong dampening effect on T_H2 immunity. One major function of these abundant MC enzymes seems therefore to act as a potent negative feed-back loop on T_H2 immunity (**Figure 5**). This should be kept in mind when trying to develop anti-allergy drugs by inhibiting the activity of the MC chymase and/or the tryptase. In contrast to what we observed for the human chymase, which did not cleave TNF-α, the mouse counterpart to the human chymase, mMCP-4, has been shown to be a major player in the inactivation of this cytokine *in vivo* (45). The targets for these mast cell enzymes can therefore differ significantly between species, a situation that needs to be kept in mind when using animal models to study the *in vivo* effect of these enzymes.

Role In The Defense Against Ectoparasites

Basophils have been shown to accumulate at the site of tick infestation. However, this happens only after the second contact with the parasite and this accumulation is dependent on adaptive immunity, IgE and the high affinity IgE receptor (FcεRI) (90, 91). Mouse basophils express a protease that is specific for this cell type, the mMCP-8 (39, 62). To study the potential role of this enzyme in the defense against ticks and other ectoparasites we produced a tick anticoagulant protein (TAP) of *Ornithodoros moubata* and

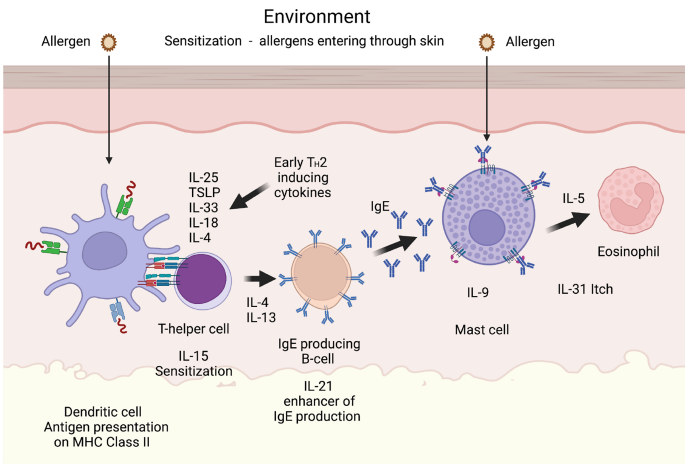


FIGURE 5 | A T_H2 immune response. A number of cytokines have been shown to be potent inducers of T_H2 mediated immunity. The most well characterized are thymic stromal lymphopoietin (TSLP), IL-33, IL-18, IL-25 and IL-4. IL-18 has been shown to be potent inducers of T_H2 mediated immunity when present alone and not in combination with IL-12. Interestingly when present together with IL-12, IL-18 acts instead as an enhancer of T_H1 mediated immunity (85). IL-4 and IL-13 are the only two cytokines known to induce isotype switching in B cells to IgE (86). IL-5 is important for eosinophil infiltration, activation and proliferation, and IL-31 acts as an inducer of itch in skin of atopic dermatitis patients. IL-9 is, in mice, an inducer of mucosal mast cell differentiation (87). Both IL-15 and IL-21 has been found to have T_H2 promoting activity as described in the text. Cleavage of the T_H2 initiating early cytokines would most likely result in a dampening effect on T_H2 mediated immunity.

analyzed its sensitivity for cleavage by the basophil specific protease mMCP-8 and a panel of other hematopoietic serine proteases. In contrast to our expectations, we found that mMCP-8 had no effect on this tick anticoagulants. However, all the connective tissue MC chymases tested, including human-, dog-, rat-, hamster- and opossum chymases did very efficiently degrade this anticoagulant protein, indicating a potent role of the MC chymases in the defense against this ectoparasite (92). We then continued this analysis by analyzing the role of this panel of hematopoietic serine proteases on anticoagulants from two other ectoparasites, leeches and mosquitos. We tested their activity on the thrombin inhibitors hirudin from *Hirudum medicinalis* and on anophelin from the malaria vector *Anopheles gambiae*. Almost an identical pattern of cleavage was seen for these two anticoagulants indicating that the connective tissue MC proteases cleave the anticoagulants of a broad array of different ectoparasites (92). Interestingly, the mucosal MC proteases were in general inactive against these anticoagulant proteins indicating a high selectivity of these proteases in their target specificity (92). Connective tissue MCs are primarily located in the skin which is the primary site of infection for these ectoparasites, indicating a functional adaptation of the cleavage specificity to targets of importance for the particular type and tissue location of the MC. Ticks have been found to have the capacity to counteract this effect of chymases by producing protease inhibitors. One example of such an inhibitor has been found in the saliva of the tick *Ixodes ricinus*, the serpin IRS-2, which is a potent inhibitor of all the MC chymases tested (92, 93).

Other Potential Targets for the MC Chymases

The potential targets for MC proteases as listed above, do most likely not include all the targets of importance for the physiological role of these enzymes. MCs and the different MC proteases have been shown to contribute, positively or negatively, to a number of conditions including arthritis, dermatitis, obesity, atherosclerosis, abdominal aortic aneurysm and cancer (94). This information has been obtained by studies of knock out mice for single and combinations of these proteases or with protease inhibitors. These studies have given a lot of valuable information concerning potential involvements of these proteases in the role of MCs *in vivo* (94). However, to our knowledge no more solid information concerning the most important *in vivo* targets for these proteases in the phenotypic changes that are observed in these studies have been reported. These models give primarily information concerning the importance of MCs or of individual MC proteases in a particular disease or organ function, but they seem to be less suitable for specifying the exact target for the proteases. Combinations of *in vivo* and *in vitro* studies are therefore essential for the fine mapping of the biological function of these proteases as they may have a very complex physiological role in immunity and tissue homeostasis. Surprisingly, the results from knock out mice and from inhibitor studies are also often contradictory as nicely shown in a recent review on the lessons from knockouts and inhibitors into the *in vivo* function of the MC chymase (94). Many of the chymase inhibitors are also affecting the activity of the related cathepsin G that is expressed in high levels in human MCs and the fact that most studies are performed in mice while the inhibitor specificity has been determined for the human chymase, is further complicating these analyses (33, 94). More detailed screenings for potential targets of importance for the biological effects observed are therefore needed before the picture of the role of the various proteases in the observed phenotypes can be obtained.

A summary of the potential targets of the MC chymase is found in **Figure 6**.

IN VIVO TARGETS FOR THE MC TRYPTASES

The target specificity for the tryptases are more restricted than for the chymases. One reason for this is their tetrameric structure. The active sites of tryptase are located in the center of the tetramer making them less accessible for larger substrates (95). The tryptase may also be active in its monomeric form, but this only at a pH lower than the normal physiological pH (96). During inflammatory conditions the pH may drop to 6.0-6.5 and then can the monomeric tryptases also show activity, and the monomers have then a less restrictive active site, potentially allowing larger substrates to enter that active site. However, due to that the most active form of the tryptase is in its tetrameric form most of the potential targets identified for tryptase has been peptides. However, as discussed above the human tryptase has also been shown to cleave a highly selective set of T_H2 cytokines showing that not only peptides can serve as important targets (47). The human tryptase also trims the ends of fibrinogen, most likely resulting in the inability to form a fibrin clot, and that the tryptase may thereby cooperate with the chymase in controlling coagulation (47). The cleavage and activation of the protease activated receptor 2 (PAR-2) by human and mouse mast cell tryptases have been a controversial issue for several years, but seem now to be relatively well documented (95, 97, 98). The human MC tryptase has also been shown to be highly active in detoxifying six different snake venoms (80).

Inactivation of Venoms

Evidence for a prominent role of tryptase in the defense against snake venoms has come from a study of the effect of human skin MC extract and purified human chymase, tryptase and CPA3 on the lethal effect of venom from six different snake species (80). In this study only tryptase, and not chymase or CPA3, had an effect on the survival rate of zebrafish embryos injected with venoms from a number of snake species, indicating that tryptase is the dominant player in the protection against snake venom (80). This study indicates that purified tryptase could be used as a potential treatment for snake bite envenoming. A few of the potential targets of the tryptase in these venoms were identified. One of them was L-amino acid oxidase, an enzyme that act on platelets and induce apoptosis and hemorrhagic effects, but can also induce apoptosis in a number of different cells, the second was a zinc metalloproteinase that induce capillary hemorrhage and myonecrosis (80).

PAR-2 Cleavage

Very recently the role of the mouse mast cell tryptase, mMCP-6, in PAR-2 cleavage and its role in the induction of thymic stromal lymphopoietin (TSLP) expression in mouse skin keratinocytes have been demonstrated (97). In this study, keratinocytes from PAR-2 negative mice did not show this induction of TSLP strongly suggesting that PAR-2 is a target for the mast cell tryptases (97). These findings also suggest that the MC tryptase can be an important trigger of inflammatory cytokines by keratinocytes and possibly also other tissue cells. Interestingly in this study histamine was also found to induce several cytokines and chemokines, although not TSLP but instead several other cytokines and chemokines including IL-6, stem cell factor (SCF) and IL-8 (97).

PAR-2 is also an important component in the blood coagulation system and several coagulation proteases, including FXa and FVIIa, can activate PAR-2 (99).

Histone Modification

The tryptase has been shown to leak out from the granules in small amounts and to enter the nucleus where it can cleave the core histones in their N-terminal tail indicating that the tryptase can have a regulatory role on transcription (100).

Peptide Substrates for the MC Tryptases

A number of peptides have been identified as potential substrates for the MC tryptases including kininogen, vasoactive intestinal peptide (VIP), peptide histidine-methionine (PHM) and calcitonin gene-related peptide (CGRP) indicating that this

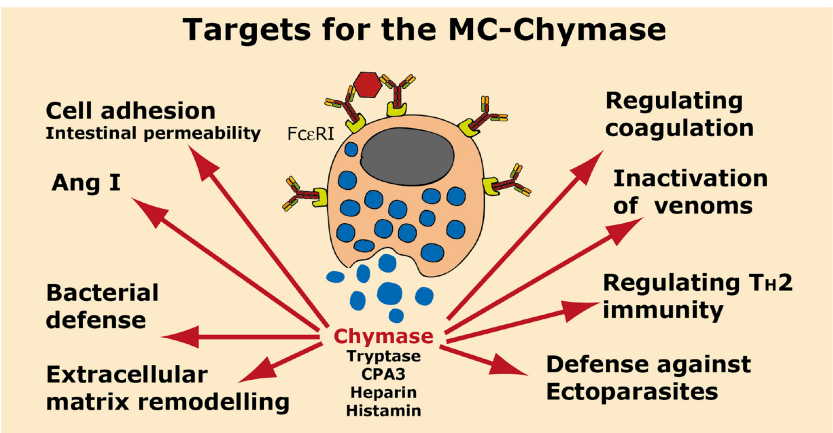


FIGURE 6 | Targets for the human MC-Chymase. A number of potential targets for the human MC chymase is summarized.

MC enzyme can have a potent regulatory function in several tissues (95, 101–103). The degradation of several of these mediators of bronchodilation may lead to increased bronchial responsiveness and may at least partly explain the induction of bronchial hyper-reactivity by tryptase (95).

Regulating Excessive T_H2 Immunity

Due to the remarkable selectivity in the cleavage of cytokines and chemokines by the human chymase, we decided to continue the screening for potential similar activities of the other major granule serine protease of human MCs, the tryptase. The tryptase was found to be even more selective than the chymase. We detected cleavage of only two cytokines out of a panel of 69 different human cytokines and chemokines (47). The two cytokines cleaved by the human tryptase were two additional key T_H2 cytokines, TSLP and IL-21 (**Figure 5**) (47). TSLP has been named a master regulator of T_H2 immunity and IL-21 was recently identified as a potent enhancer of IgE synthesis (104, 105). When we combined the action by both the chymase and the tryptase we found a remarkable selectivity of cytokines cleaved by these two enzymes. All five cytokines cleaved by these two enzymes are key T_H2 cytokines, either directly involved in the induction of a T_H2 cytokine environment, or in sensitization or IgE production. This coordinated action by the two major human MC proteases is in our mind an exceptionally strong indication for a potent role of these two MC proteases and of the MC in controlling excessive T_H2 immunity (**Figure 5**). We will therefore stress the potential danger with using tryptase and chymase inhibitors in the treatment of T_H2 mediated inflammation including asthma, dermatitis and other MC-dependent diseases. The long-term effect may be the increase in T_H2 mediated immunity, by increased sensitization to a broader panel of allergens and an exaggerated allergic inflammation. A clear indication for such an effect was observed in mice lacking the major MC chymase in mice, mMCP-4, which were found to develop exaggerated responses in two models of allergic airway inflammation (84, 106). The lack of both the chymase and the tryptase may here be even more pronounced. Analysis of double knock out mice for both mMCP-4 and mMCP-6, the counterpart of the human tryptase, would therefore be very interesting for its effects on allergen sensitization. However, similar to what was observed for the chymase with TNF-α, there are differences in the cytokines and chemokines cleaved by the MC tryptases in mouse and man. The human tryptase cleaves TSLP and IL-21. The corresponding enzyme in mouse, mMCP-6, does not cleave TSLP, but cleaves IL-21 and also IL- 9, IL-13 and IL-33, indicating that care should be taken when comparing data from human and mouse studies as the exact targets may differ (47).

Interestingly, the tryptases can thereby both induce the expression of certain cytokines, such as TSLP, by acting on PAR-2 on keratinocytes and at the same degrade this cytokine, indication a complex pattern of regulation of cytokines and chemokines by these enzymes.

A summary of the potential targets of the MC tryptase is found in **Figure 7**.

IN VIVO TARGETS FOR THE MC AND BASOPHIL EXPRESSED CPA3

The potential targets for the MC and basophil specific CPA3 have been even more difficult to determine compared to the tryptases due to that it is an exopeptidase and not an endopeptidase. A minor trimming of a C-terminal end of a protein is much more difficult to spot than an internal cleavage, which markedly change the molecular weight of the target. Removing one or a few amino acids of a large protein is often difficult to detect on a gel. The major difficulties in obtaining recombinant CPA3 is another major factor for the low number of potential *in vivo* targets identified for this enzyme. The mouse CPA3 apparently needs co-expression with mMCP-5 for the presence in granules indicating a complex transport through endoplasmic reticulum and Golgi for correct processing and storage (107–109). Production of active mouse and human CPA3 has therefore been very difficult and no active mouse or human recombinant CPA3 are presently available for more detailed

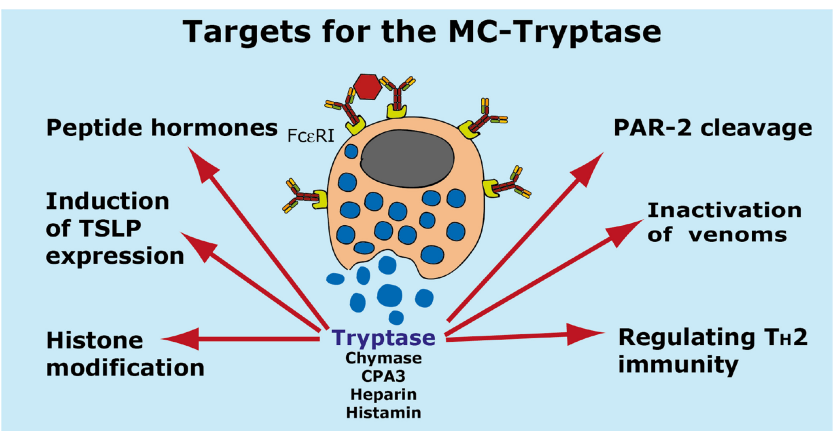


FIGURE 7 | Targets for the human MC-Tryptase. A number of potential targets for the human MC tryptase is summarized.

studies of their potential *in vivo* targets. We have tried with both mammalian and insect cells without success.

The most well documented substrate for the CPA3 is so far endothelin, a potent vasoconstrictor, and the related snake venom component sarafotoxin (77, 81). Endothelins, which are secreted from vascular endothelium, are the most potent vasoconstrictors known (110). They act through two G-protein couplet receptors, ETA and ETB (110). Removing the C-terminal tryptophan results in the inactivation of the 21 amino acid endothelin peptide (81). A few additional peptide hormones have been identified as potential *in vivo* substrates for this enzyme including neurotensin, kinetensin, Leu-enkephalin, neuromedin N and Xenopsin (109, 111–114). However, no more direct functional studies of the *in vivo* effects of these latter targets have been performed as we can see from Pubmed.

Ang I and apolipoprotein B has also been identified as potential targets. CPA3 can remove the C-terminal Leu of Ang I to generate Ang 1-9 (**Figure 3**) (112). CPA3 can also trim apolipoprotein B, a low density lipoprotein (LDL) involved in cholesterol transport (115). This cleavage can promote LDL fusion and thereby plaque formation.

The collected information concerning the biology of CPA3 is thereby relatively limited why additional studies are needed for a better understanding of the role of CPA3 in MC biology and general physiology. However, the difficulty in obtaining recombinant active enzyme is a major hurdle to overcome before additional *in vitro* and *in vivo* studies of this abundant MC and basophil enzyme can be performed. A possible role for CPA3 in regulating T_H2 immunity has not been demonstrated although CPA3 expression has been linked to T_H2 type of asthma in humans (116, 117). We recently found a dampening effect of a CPA inhibitor in a mouse model of allergic asthma, however, the individual role of CPA3 compared to other types of CPAs in this model has not been determined (118).

A summary of the potential targets of the MC CPA3 is found in **Figure 8**.

IN VIVO TARGETS FOR THE BASOPHIL SPECIFIC PROTEASES MMCP-8 AND MMCP-11

Two serine proteases have in mouse been found to be expressed preferentially or almost exclusively in basophils, the proteases mMCP-8 and mMCP-11 (39, 40, 62, 119). Numerous attempts using several methods including phage display, chromogenic and recombinant substrates have failed to obtain information concerning the extended specificity of mMCP-8, why we started to wonder if the protease was inactive. Using whole cell extracts and recombinant mouse proteins have later shown that it is active but highly restrictive in its cleavage pattern. Whole cell extract has led to the identification of tubulin as one potential target (119). However, tubulin is most likely not a biologically important target for this enzyme as tubulin is an intracellular protein and mMCP-8 is most likely only located extracellularly after basophil granule release. Two additional potential targets were recently identified by the screening of a panel of mouse cytokines and chemokines. By using recombinant mMCP-8 on a panel of 52 recombinant mouse cytokines and chemokines we identified mouse PDGF-B and MIP-3a as targets (92). However, a screening in the primary amino acid sequence of these three proteins have not resulted in the identification of a consensus sequence for its cleavage preference (92). The three amino acids that form the substrate binding pocket of mMCP-8 indicate that this protease has a strong preference for negatively charged amino acids in the P1 position (**Figure 1**). Mouse and human granzymes B, which are strict asp-ases, have triplets AGR and TGR, respectively. The arginine in this triplet is responsible for the preference for negatively charged residues in the binding pocket. mMCP-8 and rat rMCP-8, -9 and -10 (all members of the M8 subfamily) have ARR in this pocked (25). This is twice the number of positive charge indicating an even stronger affinity for negatively charged amino acids in the P1 position of substrates (**Figure 1B**) (25). However, this preference for negatively

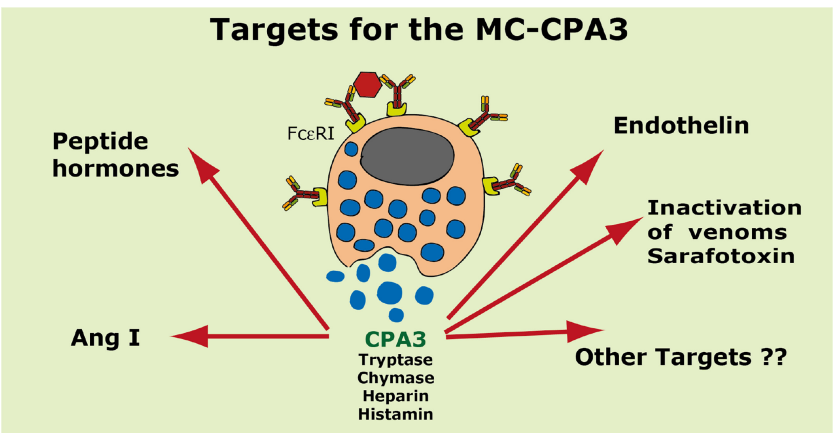


FIGURE 8 | Targets for the human MC-CPA3. A number of potential targets for the human MC carboxypeptidase A3 (CPA3) is summarized.

charged residues in the cleavable position (P1) has not yet been possible to prove definitely.

Cleavage of PDGF-B may have a functional role in controlling excessive fibrosis during a tick infestation (92). However, the role of MIP-3a cleavage depends on the role this cleavage has on the activity of this chemokine. N or C-terminal cleavage can sometimes increase the activity of a cytokine or chemokine and we still do not know if this N or C-terminal cleavage of mouse MIP-3a results in inactivation or activation of this chemokine.

Interestingly also are other potential effects of mMCP-8 and mMCP-11. Both of them have namely been shown to induce inflammation and influx of inflammatory cells upon injection into the skin of mice indicating a complex role in inflammation (40, 119). The targets for these effects are, however, still not known.

A summary of the potential targets of the basophil specific proteases mMCP-8 and mMCP-11 is found in **Figure 9**.

SUMMARY

A number of quite diverse physiological effects have been identified for the very abundant granule proteases of MCs. MCs can act both as inflammatory cells by releasing a number of potent physiologically acting substances such as histamine, prostaglandins, leukotrienes and cytokines, but also act in dampening such reactions by selective cleavage of key T_H2 cytokines. MCs have been shown to produce many of these cytokines and seem now also to be able to trigger keratinocytes, by the action of the tryptase on the protease activated receptor 2 (PAR-2), to produce TSLP. In the same study histamine was able to induce another set of cytokines by these keratinocytes, IL-6, IL-8 and SCF indicating potent effect of both proteases and other granule components in the regulation of cytokines and chemokines by other tissue cells, like the keratinocytes (97).

The MC enzymes can most likely also play an important role in facilitating the influx of inflammatory cells by cleavage of connective tissue components to loosening up the compact connective tissue and also to inhibit coagulation when blood vessels open for influx of antibodies, complement and inflammatory cells. To this should be added the potent effects on numerous venoms from snakes, scorpions, Gila monster and bees (78, 79). The effect on venoms seems to be very complex and involves all three major classes of the mast cell proteases, the chymase, the tryptase and the CPA3. A similar effect may also apply to ectoparasites, by cleavage of their anticoagulants, which are essential for a successful blood meal. Here it is primarily the connective tissue MC chymases that seem to have this role (92). However, the saliva of the ectoparasites is very complex with many different proteins with various biological effects (92). Both tryptase and CPA3 may therefore have effects of other components than only the anticoagulant proteins, which are the prime targets of the connective tissue MC chymases. When it comes to the potential role of the MC proteases in blood pressure regulation we have a similar situation as for the cytokines. One of the MC enzymes, the chymase can generate a blood pressure increasing peptide Ang II, from the precursor Ang I. At the same time another of the MC enzymes, the CPA3, has the opposite effect by inactivating endothelin, the most potent vasoconstrictor known. The question is how these two activities are coordinated during an inflammatory response involving MC activation and degranulation?

The role of the MC proteases in bacterial defense and in autoimmunity has also been controversial. Initially a number of articles appeared in the literature showing potent effects of MCs and also their proteases in the defense against bacterial infection. However, most of these effects did disappear when more stringent MC deficient animal models were used (67). The more stringent models have later shown that MCs do have a role in bacterial clearance, at least in the urinary bladder (69). A

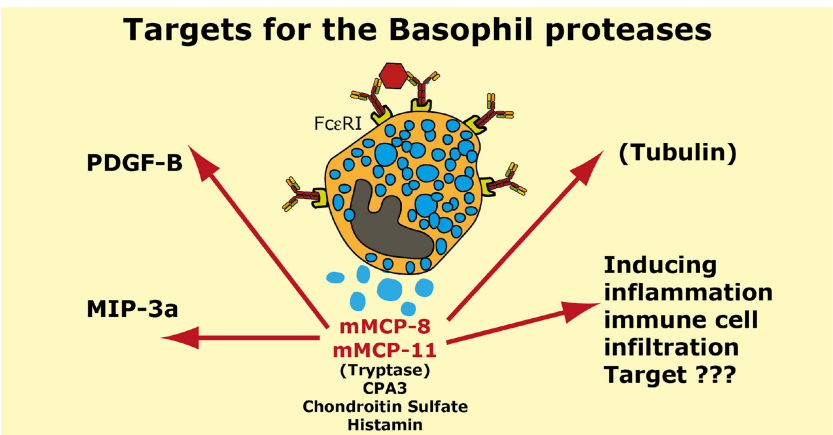


FIGURE 9 | Targets for the mouse basophil proteases mMCP-8 and mMCP-11. A number of potential targets for the mouse basophil proteases mMCP-8 and mMCP-11 is summarized. It is only for mMCP-8 that we so far have any targets identified in mouse PDGF-B, MIP-3a and tubulin. For both mMCP-8 and mMCP-11 we know that they induce inflammation and immune cell infiltration. Human basophils express the MC-tryptase and CPA3. Mouse basophils also express CPA3.

number of bacterial virulence factors are most likely also targets for these MC proteases and for the related neutrophil proteases, including N-elastase, proteinase 3 and cathepsin G, however, to our knowledge no direct evidence for such a role *in vivo* for the MC proteases has been documented.

The analysis of the cleavage activity on the anticoagulants from ticks, leeches and mosquitos by a large panel of hematopoietic serine proteases showed a remarkable specificity of these protease. The connective tissue MC proteases efficiently cleaved these anticoagulants whereas the mucosal MC proteases were inactive (92). This despite the fact that they have a relatively similar cleavage specificity indicating that the difference in specificity is highly relevant for their *in vivo* function (26). The connective tissue proteases sit in the skin where they can encounter the anticoagulant proteins from these ectoparasites whereas the mucosal MC proteases are found at other tissue locations where there is little chance to come in contact with these anticoagulants. Evolution has thereby fine-tuned their specificity to fulfill their function to fit their specific *in vivo* location. The very similar pattern in the cleavage products of fibronectin after cleavage with human, macaque and dog MC chymase also indicate conserved targets over relatively large evolutionary timelines. For some of the targets we see a conservation over several hundred million years involving almost all mammals whereas for others the pattern is more complex as seen for the generation of the blood pressure regulating Ang II. A broad analysis involving MC enzyme from all three extant mammalian lineages, monotremes, marsupials and placental mammals, for a larger panel of potential substrates will be needed to fully understand the role of these MC enzymes in MC biology and how conserved these functions have been during the past 200 million years of mammalian evolution.

DATA AVAILABILITY STATEMENT

The original contributions presented in the study are included in the article/supplementary material. Further inquiries can be directed to the corresponding author.

AUTHOR CONTRIBUTIONS

Conceptualization, LH. Writing original draft, LH. Reviewing and editing, SW, SA, and ZF. All authors contributed to the article and approved the submitted version.

FUNDING

This study was supported by the Knut and Alice Wallenberg Foundation (KAW 2017-0022) to LH and SW, by Konsul Berghs Stiftelse to SA and by the Swedish Heart and Lung Foundation to SW.

REFERENCES

1. Akula S, Paivandy A, Fu Z, Thorpe M, Pejler G, Hellman L. Quantitative in-Depth Analysis of the Mouse Mast Cell Transcriptome Reveals Organ-Specific Mast Cell Heterogeneity. *Cells* (2020) 9(1):1–25. doi: 10.3390/cells9010211
2. Angerth T, Huang RY, Aveskogh M, Pettersson I, Kjellen L, Hellman L. Cloning and Structural Analysis of a Gene Encoding a Mouse Mastocytoma Proteoglycan Core Protein; Analysis of its Evolutionary Relation to Three Cross Hybridizing Regions in the Mouse Genome. *Gene* (1990) 93(2):235–40. doi: 10.1016/0378-1119(90)90230-O
3. Forsberg E, Pejler G, Ringvall M, Lunderius C, Tomasini-Johansson B, Kusche-Gullberg M, et al. Abnormal Mast Cells in Mice Deficient in a Heparin-Synthesizing Enzyme. *Nature* (1999) 400(6746):773–6. doi: 10.1038/23488
4. Ronnberg E, Pejler G. Serglycin: The Master of the Mast Cell. *Methods Mol Biol* (2012) 836:201–17. doi: 10.1007/978-1-61779-498-8_14
5. Ohtsu H, Tanaka S, Terui T, Hori Y, Makabe-Kobayashi Y, Pejler G, et al. Mice Lacking Histidine Decarboxylase Exhibit Abnormal Mast Cells. *FEBS Lett* (2001) 502(1-2):53–6. doi: 10.1016/S0014-5793(01)02663-1
6. Pejler G, Ronnberg E, Waern I, Wernersson S. Mast Cell Proteases: Multifaceted Regulators of Inflammatory Disease. *Blood* (2010) 115 (24):4981–90. doi: 10.1182/blood-2010-01-257287
7. Huang RY, Blom T, Hellman L. Cloning and Structural Analysis of MMCP-1, MMCP-4 and MMCP-5, Three Mouse Mast Cell-Specific Serine Proteases. *Eur J Immunol* (1991) 21(7):1611–21. doi: 10.1002/eji.1830210706
8. Reynolds DS, Stevens RL, Lane WS, Carr MH, Austen KF, Serafin WE. Different Mouse Mast Cell Populations Express Various Combinations of at Least Six Distinct Mast Cell Serine Proteases. *Proc Natl Acad Sci USA* (1990) 87(8):3230–4. doi: 10.1073/pnas.87.8.3230
9. Abe T, Swieter M, Imai T, Hollander ND, Befus AD. Mast Cell Heterogeneity: Two-Dimensional Gel Electrophoretic Analyses of Rat Peritoneal and Intestinal Mucosal Mast Cells. *Eur J Immunol* (1990) 20 (9):1941–7. doi: 10.1002/eji.1830200911
10. Wernersson S, Pejler G. Mast Cell Secretory Granules: Armed for Battle. *Nat Rev Immunol* (2014) 14(7):478–94. doi: 10.1038/nri3690
11. Pejler G, Abrink M, Ringvall M, Wernersson S. Mast Cell Proteases. *Adv Immunol* (2007) 95:167–255. doi: 10.1016/S0065-2776(07)95006-3
12. Ronnberg E, Melo FR, Pejler G. Mast Cell Proteoglycans. *J Histochem Cytochem* (2012) 60(12):950–62. doi: 10.1369/0022155412458927
13. Schwartz LB, Irani AM, Roller K, Castells MC, Schechter NM. Quantitation of Histamine, Tryptase, and Chymase in Dispersed Human T and TC Mast Cells. *J Immunol* (1987) 138(8):2611–5.
14. Irani AM, Goldstein SM, Wintroub BU, Bradford T, Schwartz LB. Human Mast Cell Carboxypeptidase. Selective Localization to MCTC Cells. *J Immunol* (1991) 147(1):247–53.
15. Reynolds DS, Gurley DS, Stevens RL, Sugarbaker DJ, Austen KF, Serafin WE. Cloning of Cdnas That Encode Human Mast Cell Carboxypeptidase a, and Comparison of the Protein With Mouse Mast Cell Carboxypeptidase a and Rat Pancreatic Carboxypeptidases. *Proc Natl Acad Sci U S A* (1989) 86 (23):9480–4. doi: 10.1073/pnas.86.23.9480
16. Lutzelschwab C, Pejler G, Aveskogh M, Hellman L. Secretory Granule Proteases in Rat Mast Cells. Cloning of 10 Different Serine Proteases and a Carboxypeptidase a From Various Rat Mast Cell Populations. *J Exp Med* (1997) 185(1):13–29.
17. Atiakshin D, Kostin A, Trotsenko I, Samoilova V, Buchwalow I, Tiemann M. Carboxypeptidase A3-a Key Component of the Protease Phenotype of Mast Cells. *Cells* (2022) 11(3):1–23. doi: 10.3390/cells11030570
18. Boyce JA. Mast Cells and Eicosanoid Mediators: A System of Reciprocal Paracrine and Autocrine Regulation. *Immunol Rev* (2007) 217:168–85. doi: 10.1111/j.1600-065X.2007.00512.x

19. Heavey DJ, Ernst PB, Stevens RL, Befus AD, Bienenstock J, Austen KF. Generation of Leukotriene C4, Leukotriene B4, and Prostaglandin D2 by Immunologically Activated Rat Intestinal Mucosa Mast Cells. *J Immunol* (1988) 140(6):1953–7.
20. Nakamura T. The Roles of Lipid Mediators in Type I Hypersensitivity. *J Pharmacol Sci* (2021) 147(1):126–31. doi: 10.1016/j.jphs.2021.06.001
21. Peters-Golden M, Henderson WRJr. Leukotrienes. *N Engl J Med* (2007) 357 (18):1841–54. doi: 10.1056/NEJMra071371
22. Akula S, Paivandy A, Fu Z, Thorpe M, Pejler G, Hellman L. How Relevant are Bone Marrow-Derived Mast Cells (Bmmcs) as Models for Tissue Mast Cells? A Comparative Transcriptome Analysis of Bmmcs and Peritoneal Mast Cells. *Cells* (2020) 9(9):1–19. doi: 10.3390/cells9092118
23. Hellman L, Thorpe M. Granule Proteases of Hematopoietic Cells, a Family of Versatile Inflammatory Mediators - an Update on Their Cleavage Specificity, *In Vivo* Substrates, and Evolution. *Biol Chem* (2014) 395 (1):15–49. doi: 10.1515/hsz-2013-0211
24. Schechter I, Berger A. On the Size of the Active Site in Proteases. I. Papain. *Biochem Biophys Res Commun* (1967) 27(2):157–62. doi: 10.1016/S0006-291X(67)80055-X
25. Akula S, Thorpe M, Boinapally V, Hellman L. Granule Associated Serine Proteases of Hematopoietic Cells - an Analysis of Their Appearance and Diversification During Vertebrate Evolution. *PLoS One* (2015) 10(11): e0143091. doi: 10.1371/journal.pone.0143091.eCollection2015
26. Akula S, Fu Z, Wernersson S, Hellman L. The Evolutionary History of the Chymase Locus -a Locus Encoding Several of the Major Hematopoietic Serine Proteases. *Int J Mol Sci* (2021) 22(20):1–25. doi: 10.3390/ijms222010975
27. Sundstrom G, Larsson TA, Brenner S, Venkatesh B, Larhammar D. Evolution of the Neuropeptide Y Family: New Genes by Chromosome Duplications in Early Vertebrates and in Teleost Fishes. *Gen Comp Endocrinol* (2008) 155(3):705–16. doi: 10.1016/j.ygcen.2007.08.016
28. Enerback L. Mast Cells in Rat Gastrointestinal Mucosa. I. Effects of Fixation. *Acta Pathol Microbiol Scand* (1966) 66(3):289–302. doi: 10.1111/apm.1966.66.3.289
29. Lutzelschwab C, Lunderius C, Enerback L, Hellman L. A Kinetic Analysis of the Expression of Mast Cell Protease Mrna in the Intestines of Nippostrongylus Brasiliensis-Infected Rats. *Eur J Immunol* (1998) 28 (11):3730–7. doi: 10.1002/(SICI)1521-4141(199811)28:11<3730::AID-IMMU3730>3.0.CO;2-0
30. Irani AA, Schechter NM, Craig SS, DeBlois G, Schwartz LB. Two Types of Human Mast Cells That Have Distinct Neutral Protease Compositions. *Proc Natl Acad Sci U S A* (1986) 83(12):4464–8. doi: 10.1073/pnas.83.12.4464
31. Erjefalt JS. Mast Cells in Human Airways: The Culprit? *Eur Respir Rev Off J Eur Respir Soc* (2014) 23(133):299–307. doi: 10.1183/09059180.00005014
32. Siddhuraj P, Clausson CM, Sanden C, Alyamani M, Kadivar M, Marsal J, et al. Lung Mast Cells Have a High Constitutive Expression of Carboxypeptidase A3 Mrna That Is Independent From Granule-Stored CPA3. *Cells* (2021) 10(2):1-17. doi: 10.3390/cells10020309
33. Motakis E, Guhl S, Ishizu Y, Itoh M, Kawaji H, de Hoon M, et al. Redefinition of the Human Mast Cell Transcriptome by Deep-CAGE Sequencing. *Blood* (2014) 123(17):e58–67. doi: 10.1182/blood-2013-02-483792
34. Caughey GH. Mast Cell Proteases as Pharmacological Targets. *Eur J Pharmacol* (2016) 778:44–55. doi: 10.1016/j.ejphar.2015.04.045
35. Kunori Y, Koizumi M, Masegi T, Kasai H, Kawabata H, Yamazaki Y, et al. Rodent Alpha-Chymases are Elastase-Like Proteases. *Eur J Biochem FEBS* (2002) 269(23):5921–30. doi: 10.1046/j.1432-1033.2002.03316.x
36. Karlson U, Pejler G, Tomasini-Johansson B, Hellman L. Extended Substrate Specificity of Rat Mast Cell Protease 5, a Rodent Alpha-Chymase With Elastase-Like Primary Specificity. *J Biol Chem* (2003) 278(41):39625–31. doi: 10.1074/jbc.M301512200
37. Andersson MK, Karlson U, Hellman L. The Extended Cleavage Specificity of the Rodent Beta-Chymases Rmcp-1 and Mmcp-4 Reveal Major Functional Similarities to the Human Mast Cell Chymase. *Mol Immunol* (2008) 45 (3):766–75. doi: 10.1016/j.molimm.2007.06.360
38. Jogie-Brahim S, Min HK, Fukuoka Y, Xia HZ, Schwartz LB. Expression of Alpha-Tryptase and Beta-Tryptase by Human Basophils. *J Allergy Clin Immunol* (2004) 113(6):1086–92. doi: 10.1016/j.jaci.2004.02.032
39. Poorafshar M, Helmby H, Troye-Blomberg M, Hellman L. MMCP-8, the First Lineage-Specific Differentiation Marker for Mouse Basophils. Elevated Numbers of Potent IL-4-Producing and MMCP-8-Positive Cells in Spleens of Malaria-Infected Mice. *Eur J Immunol* (2000) 30(9):2660–8. doi: 10.1002/1521-4141(200009)30:9<2660::AID-IMMU2660>3.0.CO;2-I
40. Iki M, Tanaka K, Deki H, Fujimaki M, Sato S, Yoshikawa S, et al. Basophil Tryptase Mmcp-11 Plays a Crucial Role in Ige-Mediated, Delayed-Onset Allergic Inflammation in Mice. *Blood* (2016) 128(25):2909–18. doi: 10.1182/blood-2016-07-729392
41. Charles N, Watford WT, Ramos HL, Hellman L, Oettgen HC, Gomez G, et al. Lyn Kinase Controls Basophil GATA-3 Transcription Factor Expression and Induction of Th2 Cell Differentiation. *Immunity* (2009) 30 (4):533–43. doi: 10.1016/j.immuni.2009.02.008
42. Akahoshi M, Song CH, Piliponsky AM, Metz M, Guzzetta A, Abrink M, et al. Mast Cell Chymase Reduces the Toxicity of Gila Monster Venom, Scorpion Venom, and Vasoactive Intestinal Polypeptide in Mice. *J Clin Invest* (2011) 121(10):4180–91. doi: 10.1172/JCI46139
43. Thorpe M, Yu J, Boinapally V, Ahooghalandari P, Kervinen J, Garavilla LD, et al. Extended Cleavage Specificity of the Mast Cell Chymase From the Crab-Eating Macaque (Macaca Fascicularis): An Interesting Animal Model for the Analysis of the Function of the Human Mast Cell Chymase. *Int Immunol* (2012) 12:771–82. doi: 10.1093/intimm/dxs081
44. Tchougounova E, Lundequist A, Fajardo I, Winberg JO, Abrink M, Pejler G. A Key Role for Mast Cell Chymase in the Activation of Pro-Matrix Metalloprotease-9 and Pro-Matrix Metalloprotease-2. *J Biol Chem* (2005) 280(10):9291–6. doi: 10.1074/jbc.M410396200
45. Piliponsky AM, Chen CC, Rios EJ, Treuting PM, Lahiri A, Abrink M, et al. The Chymase Mouse Mast Cell Protease 4 Degrades TNF, Limits Inflammation, and Promotes Survival in a Model of Sepsis. *Am J Pathol* (2012) 181(3):875–86. doi: 10.1016/j.ajpath.2012.05.013
46. Fu Z, Thorpe M, Alemayehu R, Roy A, Kervinen J, de Garavilla L, et al. Highly Selective Cleavage of Cytokines and Chemokines by the Human Mast Cell Chymase and Neutrophil Cathepsin G. *J Immunol* (2017) 198(4):1474–83. doi: 10.4049/jimmunol.1601223
47. Fu Z, Akula S, Thorpe M, Hellman L. Highly Selective Cleavage of TH2-Promoting Cytokines by the Human and the Mouse Mast Cell Tryptases, Indicating a Potent Negative Feedback Loop on TH2 Immunity. *Int J Mol Sci* (2019) 20(20):1–18. doi: 10.3390/ijms20205147
48. Ghildyal N, Friend DS, Stevens RL, Austen KF, Huang C, Penrose JF, et al. Fate of Two Mast Cell Tryptases in V3 Mastocytosis and Normal BALB/C Mice Undergoing Passive Systemic Anaphylaxis: Prolonged Retention of Exocytosed Mmcp-6 in Connective Tissues, and Rapid Accumulation of Enzymatically Active Mmcp-7 in the Blood. *J Exp Med* (1996) 184(3):1061–73. doi: 10.1084/jem.184.3.1061
49. Shu Z, Wan J, Read RJ, Carrell RW, Zhou A. Angiotensinogen and the Modulation of Blood Pressure. *Front Cardiovasc Med* (2021) 8:645123. doi: 10.3389/fcvm.2021.645123
50. Doolittle RF. Angiotensinogen is Related to the Antitrypsin-Antithrombin-Ovalbumin Family. *Science* (1983) 222(4622):417–9. doi: 10.1126/science.6604942
51. Wu C, Lu H, Cassis LA, Daugherty A. Molecular and Pathophysiological Features of Angiotensinogen: A Mini Review. *N Am J Med Sci (Boston)* (2011) 4(4):183–90. doi: 10.7156/v4i4p183
52. Bader M, Ganten D. Update on Tissue Renin-Angiotensin Systems. *J Mol Med* (2008) 86(6):615–21. doi: 10.1007/s00109-008-0336-0
53. Caughey GH, Raymond WW, Wolters PJ. Angiotensin II Generation by Mast Cell Alpha- and Beta-Chymases. *Biochim Biophys Acta* (2000) 1480(1-2):245–57. doi: 10.1016/S0167-4838(00)00076-5
54. Berglund P, Akula S, Fu Z, Thorpe M, Hellman L. Extended Cleavage Specificity of the Rat Vascular Chymase, a Potential Blood Pressure Regulating Enzyme Expressed by Rat Vascular Smooth Muscle Cells. *Int J Mol Sci* (2020) 21(22):1*21. doi: 10.3390/ijms21228546
55. Takai S, Sakaguchi M, Jin D, Yamada M, Kirimura K, Miyazaki M. Different Angiotensin II-Forming Pathways in Human and Rat Vascular Tissues. *Clin Chim Acta* (2001) 305(1-2):191–5. doi: 10.1016/S0009-8981(01)00379-5
56. Guo C, Ju H, Leung D, Massaeli H, Shi M, Rabinovitch M. A Novel Vascular Smooth Muscle Chymase is Upregulated in Hypertensive Rats. *J Clin Invest* (2001) 107(6):703–15. doi: 10.1172/JCI9997

57. Ju H, Gros R, You X, Tsang S, Husain M, Rabinovitch M. Conditional and Targeted Overexpression of Vascular Chymase Causes Hypertension in Transgenic Mice. *Proc Natl Acad Sci U S A* (2001) 98(13):7469–74. doi: 10.1073/pnas.131147598
58. Nakamura T, Murata T. Regulation of Vascular Permeability in Anaphylaxis. *Br J Pharmacol* (2018) 175(13):2538–42. doi: 10.1111/bph.14332
59. Tchougounova E, Pejler G, Abrink M. The Chymase, Mouse Mast Cell Protease 4, Constitutes the Major Chymotrypsin-Like Activity in Peritoneum and Ear Tissue. A Role for Mouse Mast Cell Protease 4 in Thrombin Regulation and Fibronectin Turnover. *J Exp Med* (2003) 198 (3):423–31. doi: 10.1081/jem.2003067
60. Wiktor-Jedrzejczak W, Bartocci A, Ferrante AWJr., Ahmed-Ansari A, Sell KW, Pollard JW, et al. Total Absence of Colony-Stimulating Factor 1 in the Macrophage-Deficient Osteopetrotic (Op/Op) Mouse. *Proc Natl Acad Sci U S A* (1990) 87(12):4828–32. doi: 10.1073/pnas.87.12.4828
61. Paivandy A, Akula S, Lara S, Fu Z, Olsson AK, Kleinau S, et al. Quantitative in-Depth Transcriptome Analysis Implicates Peritoneal Macrophages as Important Players in the Complement and Coagulation Systems. *Int J Mol Sci* (2022) 23(3):1–24. doi: 10.3390/ijms23031185
62. Lutzelschwab C, Huang MR, Kullberg MC, Aveskogh M, Hellman L. Characterization of Mouse Mast Cell Protease-8, the First Member of a Novel Subfamily of Mouse Mast Cell Serine Proteases, Distinct From Both the Classical Chymases and Tryptases. *Eur J Immunol* (1998) 28(3):1022–33. doi: 10.1002/(SICI)1521-4141(199803)28:03<1022::AID-IMMU1022>3.0.CO;2-1
63. King SJ, Miller HR, Newlands GF, Woodbury RG. Depletion of Mucosal Mast Cell Protease by Corticosteroids: Effect on Intestinal Anaphylaxis in the Rat. *Proc Natl Acad Sci USA* (1985) 82(4):1214–8. doi: 10.1073/pnas.82.4.1214
64. King SJ, Miller HR. Anaphylactic Release of Mucosal Mast Cell Protease and its Relationship to Gut Permeability in Nippostrongylus-Primed Rats. *Immunology* (1984) 51(4):653–60. doi: 10.1073/pnas.82.4.1214
65. Scudamore CL, Thornton EM, McMillan L, Newlands GF, Miller HR. Release of the Mucosal Mast Cell Granule Chymase, Rat Mast Cell Protease-II, During Anaphylaxis is Associated With the Rapid Development of Paracellular Permeability to Macromolecules in Rat Jejunum. *J Exp Med* (1995) 182(6):1871–81. doi: 10.1084/jem.182.6.1871
66. Fu Z, Thorpe M, Hellman L. Rmcp-2, the Major Rat Mucosal Mast Cell Protease, an Analysis of its Extended Cleavage Specificity and its Potential Role in Regulating Intestinal Permeability by the Cleavage of Cell Adhesion and Junction Proteins. *PLoS One* (2015) 10(6):e0131720. doi: 10.1371/journal.pone.0131720
67. Rodewald HR, Feyerabend TB. Widespread Immunological Functions of Mast Cells: Fact or Fiction? *Immunity* (2012) 37(1):13–24. doi: 10.1016/j.immuni.2012.07.007
68. Lilla JN, Chen CC, Mukai K, BenBarak MJ, Franco CB, Kalesnikoff J, et al. Reduced Mast Cell and Basophil Numbers and Function in Cpa3-Cre; Mcl-1fl/Fl Mice. *Blood* (2011) 118(26):6930–8. doi: 10.1182/blood-2011-03-343962
69. Choi HW, Bowen SE, Miao Y, Chan CY, Miao EA, Abrink M, et al. Loss of Bladder Epithelium Induced by Cytolytic Mast Cell Granules. *Immunity* (2016) 45(6):1258–69. doi: 10.1016/j.immuni.2016.11.003
70. Sellin ME, Muller AA, Felmy B, Dolowschiak T, Diard M, Tardivel A, et al. Epithelium-Intrinsic NAIP/NLRC4 Inflammasome Drives Infected Enterocyte Expulsion to Restrict Salmonella Replication in the Intestinal Mucosa. *Cell Host Microbe* (2014) 16(2):237–48. doi: 10.1016/j.chom.2014.07.001
71. Starkl P, Watzenboeck ML, Popov LM, Zahalka S, Hladik A, Lakovits K, et al. Ige Effector Mechanisms, in Concert With Mast Cells, Contribute to Acquired Host Defense Against Staphylococcus Aureus. *Immunity* (2020) 53 (6):1333. doi: 10.1016/j.immuni.2020.11.012
72. Gendrin C, Shubin NJ, Boldenow E, Merillat S, Clauson M, Power D, et al. Mast Cell Chymase Decreases the Severity of Group B Streptococcus Infections. *J Allergy Clin Immunol* (2018) 142(1):120–9.e6. doi: 10.1016/j.jaci.2017.07.042
73. Craig SS, Irani AM, Metcalfe DD, Schwartz LB. Ultrastructural Localization of Heparin to Human Mast Cells of the MCTC and MCT Types by Labeling With Antithrombin III-Gold. *Lab Investigation J Tech Methods Pathol* (1993) 69(5):552–61.
74. Olson ST, Chuang YJ. Heparin Activates Antithrombin Anticoagulant Function by Generating New Interaction Sites (Exosites) for Blood Clotting Proteinases. *Trends Cardiovasc Med* (2002) 12(8):331–8. doi: 10.1016/S1050-1738(02)00183-4
75. Hellman L. Profound Reduction in Allergen Sensitivity Following Treatment With a Novel Allergy Vaccine. *Eur J Immunol* (1994) 24:415–20. doi: 10.1002/eji.1830240222
76. Pejler G, Soderstrom K, Karlstrom A. Inactivation of Thrombin by a Complex Between Rat Mast-Cell Protease 1 and Heparin Proteoglycan. *Biochem J* (1994) 299(Pt 2):507–13. doi: 10.1042/bj2990507
77. Metz M, Piliponsky AM, Chen CC, Lammel V, Abrink M, Pejler G, et al. Mast Cells can Enhance Resistance to Snake and Honeybee Venoms. *Science* (2006) 313(5786):526–30. doi: 10.1126/science.1128877
78. Galli SJ, Metz M, Starkl P, Marichal T, Tsai M. Mast Cells and Ige in Defense Against Lethality of Venoms: Possible "Benefit" of Allergy[]. *Allergo J Int* (2020) 29(2):46–62. doi: 10.1007/s40629-020-00118-6
79. Starkl P, Gaudenzio N, Marichal T, Reber LL, Sibilano R, Watzenboeck ML, et al. Ige Antibodies Increase Honeybee Venom Responsiveness and Detoxification Efficiency of Mast Cells. *Allergy* (2022) 77(2):499–512. doi: 10.1111/all.14852
80. Anderson E, Stavenhagen K, Kolarich D, Sommerhoff CP, Maurer M, Metz M. Human Mast Cell Tryptase is a Potential Treatment for Snakebite Envenoming Across Multiple Snake Species. *Front Immunol* (2018) 9:1532. doi: 10.3389/fimmu.2018.01532
81. Schneider LA, Schlenner SM, Feyerabend TB, Wunderlin M, Rodewald HR. Molecular Mechanism of Mast Cell Mediated Innate Defense Against Endothelin and Snake Venom Sarafotoxin. *J Exp Med* (2007) 204 (11):2629–39. doi: 10.1084/jem.20071262
82. Leonard JP, Sherman ML, Fisher GL, Buchanan LJ, Larsen G, Atkins MB, et al. Effects of Single-Dose Interleukin-12 Exposure on Interleukin-12-Associated Toxicity and Interferon-Gamma Production. *Blood* (1997) 90 (7):2541–8.
83. Wang N, Wang J, Zhang Y, Hu S, Zhang T, Wu Y, et al. Substance P-Induced Lung Inflammation in Mice is Mast Cell Dependent. *Clin Exp Allergy* (2022) 52(1):46–58. doi: 10.1111/cea.13902
84. Waern I, Lundequist A, Pejler G, Wernersson S. Mast Cell Chymase Modulates IL-33 Levels and Controls Allergic Sensitization in Dust-Mite Induced Airway Inflammation. *Mucosal Immunol* (2013) 6(5):911–20. doi: 10.1038/mi.2012.129
85. Nakanishi K. Unique Action of Interleukin-18 on T Cells and Other Immune Cells. *Front Immunol* (2018) 9:763. doi: 10.3389/fimmu.2018.00763
86. Punnonen J, Aversa GG, Cocks BG, McKenzie ANJ, Menon S, Zurawski G, et al. Interleukin-13 Induces Interleukin-4-Independent Igg4 and Ige Synthesis and CD23 Expression by Human B Cells. *Proc Natl Acad Sci USA* (1993) 90:3730–4. doi: 10.1073/pnas.90.8.3730
87. Miller HR, Wright SH, Knight PA, Thornton EM. A Novel Function for Transforming Growth Factor-Beta1: Upregulation of the Expression and the Ige-Independent Extracellular Release of a Mucosal Mast Cell Granule-Specific Beta-Chymase, Mouse Mast Cell Protease-1. *Blood* (1999) 93 (10):3473–86. doi: 10.1182/blood.V93.10.3473.410k01_3473_3486
88. Ruckert R, Herz U, Paus R, Ungureanu D, Pohl T, Renz H, et al. IL-15-Igg2b Fusion Protein Accelerates and Enhances a Th2 But Not a Th1 Immune Response *In Vivo*, While IL-2-Igg2b Fusion Protein Inhibits Both. *Eur J Immunol* (1998) 28(10):3312–20. doi: 10.1002/(SICI)1521-4141(199810)28:10<3312::AID-IMMU3312>3.0.CO;2-I
89. Ruckert R, Brandt K, Braun A, Hoymann HG, Herz U, Budagian V, et al. Blocking IL-15 Prevents the Induction of Allergen-Specific T Cells and Allergic Inflammation In Vivo. *J Immunol* (2005) 174(9):5507–15. doi: 10.4049/jimmunol.174.9.5507
90. Karasuyama H, Miyake K, Yoshikawa S. Immunobiology of Acquired Resistance to Ticks. *Front Immunol* (2020) 11:601504. doi: 10.3389/fimmu.2020.601504
91. Wada T, Ishiwata K, Koseki H, Ishikura T, Ugajin T, Ohnuma N, et al. Selective Ablation of Basophils in Mice Reveals Their Nonredundant Role in Acquired Immunity Against Ticks. *J Clin Invest* (2010) 120(8):2867–75. doi: 10.1172/JCI42680

92. Fu Z, Akula S, Olsson AK, Kervinen J, Hellman L. Mast Cells and Basophils in the Defense Against Ectoparasites: Efficient Degradation of Parasite Anticoagulants by the Connective Tissue Mast Cell Chymases. *Int J Mol Sci* (2021) 22(23):1–15. doi: 10.3390/ijms222312627
93. Chmelar J, Oliveira CJ, Rezacova P, Francischetti IM, Kovarova Z, Pejler G, et al. A Tick Salivary Protein Targets Cathepsin G and Chymase and Inhibits Host Inflammation and Platelet Aggregation. *Blood* (2011) 117(2):736–44. doi: 10.1182/blood-2010-06-293241
94. Pejler G. Novel Insight Into the *In Vivo* Function of Mast Cell Chymase: Lessons From Knockouts and Inhibitors. *J Innate Immun* (2020) 12(5):357–72. doi: 10.1159/000506985
95. Hallgren J, Pejler G. Biology of Mast Cell Tryptase. An Inflammatory Mediator. *FEBS J* (2006) 273(9):1871–95. doi: 10.1111/j.1742-4658.2006.05211.x
96. Fukuoka Y, Schwartz LB. Human Beta-Tryptase: Detection and Characterization of the Active Monomer and Prevention of Tetramer Reconstitution by Protease Inhibitors. *Biochemistry* (2004) 43(33):10757–64. doi: 10.1021/bi049486c
97. Redhu D, Franke K, Aparicio-Soto M, Kumari V, Pazur K, Illerhaus A, et al. Mast Cells Instruct Keratinocytes to Produce Thymic Stromal Lymphopoietin: Relevance of the Tryptase/Protease-Activated Receptor 2 Axis. *J Allergy Clin Immunol* (2022) 149(6):2053–61. doi: 10.1016/j.jaci.2022.01.029
98. Redhu D, Franke K, Kumari V, Francuzik W, Babina M, Worm M. Thymic Stromal Lymphopoietin Production Induced by Skin Irritation Results From Concomitant Activation of Protease-Activated Receptor 2 and Interleukin 1 Pathways. *Br J Dermatol* (2020) 182(1):119–29. doi: 10.1111/bjd.17940
99. Rothmeier AS, Ruf W. Protease-Activated Receptor 2 Signaling in Inflammation. *Semin Immunopathol* (2012) 34(1):133–49. doi: 10.1007/s00281-011-0289-1
100. Melo FR, Vita F, Berent-Maoz B, Levi-Schaffer F, Zabucchi G, Pejler G. Proteolytic Histone Modification by Mast Cell Tryptase, a Serglycin Proteoglycan-Dependent Secretory Granule Protease. *J Biol Chem* (2014) 289(11):7682–90. doi: 10.1074/jbc.M113.546895
101. Imamura T, Dubin A, Moore W, Tanaka R, Travis J. Induction of Vascular Permeability Enhancement by Human Tryptase: Dependence on Activation of Prekallikrein and Direct Release of Bradykinin From Kininogens. *Lab Investigation J Tech Methods Pathol* (1996) 74(5):861–70.
102. Caughey GH, Leidig F, Viro NF, Nadel JA. Substance P and Vasoactive Intestinal Peptide Degradation by Mast Cell Tryptase and Chymase. *J Pharmacol Exp Ther* (1988) 244(1):133–7.
103. Tam EK, Caughey GH. Degradation of Airway Neuropeptides by Human Lung Tryptase. *Am J Respir Cell Mol Biol* (1990) 3(1):27–32. doi: 10.1165/ajrcmb/3.1.27
104. Ozaki K, Spolski R, Feng CG, Qi CF, Cheng J, Sher A, et al. A Critical Role for IL-21 in Regulating Immunoglobulin Production. *Science* (2002) 298 (5598):1630–4. doi: 10.1126/science.1077002
105. Shamji MH, Layhadi JA, Achkova D, Kouser L, Perera-Webb A, Couto-Francisco NC, et al. Role of IL-35 in Sublingual Allergen Immunotherapy. *J Allergy Clin Immunol* (2019) 143(3):1131–42.e4. doi: 10.1016/j.jaci.2018.06.041
106. Waern I, Jonasson S, Hjoberg J, Bucht A, Abrink M, Pejler G, et al. Mouse Mast Cell Protease 4 is the Major Chymase in Murine Airways and has a Protective Role in Allergic Airway Inflammation. *J Immunol* (2009) 183 (10):6369–76. doi: 10.4049/jimmunol.0900180
107. Stevens RL, Qui D, McNeil HP, Friend DS, Hunt JE, Austen KF, et al. Transgenic Mice That Possess a Disrupted Mast Cell Protease 5 Gene Cannot Store Carboxypeptidase a in Their Granules. *FASEB J* (1996) 10:1307–.
108. Feyerabend TB, Hausser H, Tietz A, Blum C, Hellman L, Straus AH, et al. Loss of Histochemical Identity in Mast Cells Lacking Carboxypeptidase a. *Mol Cell Biol* (2005) 25(14):6199–210. doi: 10.1128/MCB.25.14.6199-6210.2005
109. Pejler G, Knight SD, Henningsson F, Wernersson S. Novel Insights Into the Biological Function of Mast Cell Carboxypeptidase a. *Trends Immunol* (2009) 30(8):401–8. doi: 10.1016/j.it.2009.04.008
110. Eroglu E, Kocyigit I, Lindholm B. The Endothelin System as Target for Therapeutic Interventions in Cardiovascular and Renal Disease. *Clin Chim Acta* (2020) 506:92–106. doi: 10.1016/j.cca.2020.03.008
111. Piliponsky AM, Chen CC, Nishimura T, Metz M, Rios EJ, Dobner PR, et al. Neurotensin Increases Mortality and Mast Cells Reduce Neurotensin Levels in a Mouse Model of Sepsis. *Nat Med* (2008) 14(4):392–8. doi: 10.1038/nm1738
112. Goldstein SM, Leong J, Bunnett NW. Human Mast Cell Proteases Hydrolyze Neurotensin, Kinetensin and Leu5-Enkephalin. *Peptides* (1991) 12(5):995–1000. doi: 10.1016/0196-9781(91)90049-U
113. Cochrane DE, Carraway RE, Boucher W, Feldberg RS. Rapid Degradation of Neurotensin by Stimulated Rat Mast Cells. *Peptides* (1991) 12(6):1187–94. doi: 10.1016/0196-9781(91)90193-S
114. Bunnett NW, Goldstein SM, Nakazato P. Isolation of a Neuropeptide-Degrading Carboxypeptidase From the Human Stomach. *Gastroenterology* (1992) 102(1):76–87. doi: 10.1016/0016-5085(92)91786-4
115. Paananen K, Kovanen PT. Proteolysis and Fusion of Low Density Lipoprotein Particles Independently Strengthen Their Binding to Exocytosed Mast Cell Granules. *J Biol Chem* (1994) 269(3):2023–31. doi: 10.1016/S0021-9258(17)42130-2
116. Dougherty RH, Sidhu SS, Raman K, Solon M, Solberg OD, Caughey GH, et al. Accumulation of Intraepithelial Mast Cells With a Unique Protease Phenotype in T(H)2-High Asthma. *J Allergy Clin Immunol* (2010) 125 (5):1046–53.e8. doi: 10.1016/j.jaci.2010.03.003
117. Fricker M, Gibson PG, Powell H, Simpson JL, Yang IA, Upham JW, et al. A Sputum 6-Gene Signature Predicts Future Exacerbations of Poorly Controlled Asthma. *J Allergy Clin Immunol* (2019) 144(1):51–60.e11. doi: 10.1016/j.jaci.2018.12.1020
118. Waern I, Taha S, Lorenzo J, Montpeyo D, Covaleda-Cortes G, Aviles FX, et al. Carboxypeptidase Inhibition by Nvci Suppresses Airway Hyperreactivity in a Mouse Asthma Model. *Allergy* (2021) 76(7):2234–7. doi: 10.1111/all.14730
119. Tsutsui H, Yamanishi Y, Ohtsuka H, Sato S, Yoshikawa S, Karasuyama H. The Basophil-Specific Protease Mmcp-8 Provokes an Inflammatory Response in the Skin With Microvascular Hyperpermeability and Leukocyte Infiltration. *J Biol Chem* (2017) 292(3):1061–7. doi: 10.1074/jbc.M116.754648

Conflict of Interest: The authors declare that the research was conducted in the absence of any commercial or financial relationships that could be construed as a potential conflict of interest.

Publisher's Note: All claims expressed in this article are solely those of the authors and do not necessarily represent those of their affiliated organizations, or those of the publisher, the editors and the reviewers. Any product that may be evaluated in this article, or claim that may be made by its manufacturer, is not guaranteed or endorsed by the publisher.

Copyright © 2022 Hellman, Akula, Fu and Wernersson. This is an open-access article distributed under the terms of the Creative Commons Attribution License (CC BY). The use, distribution or reproduction in other forums is permitted, provided the original author(s) and the copyright owner(s) are credited and that the original publication in this journal is cited, in accordance with accepted academic practice. No use, distribution or reproduction is permitted which does not comply with these terms.

frontiers | Frontiers in Immunology

ORIGINAL RESEARCH
published: 05 July 2022
doi: 10.3389/fimmu.2022.881655

Allergen-Specific IgA Antibodies Block IgE-Mediated Activation of Mast Cells and Basophils

*Yasmeen S. El Ansari[1,2], Cynthia Kanagaratham[1,3], Oliver T. Burton[4], Jenna V. Santos[1], Brianna-Marie A. Hollister[1], Owen L. Lewis[1], Harald Renz[5] and Hans C. Oettgen[1,3]**

[1] Division of Immunology, Department of Pediatrics, Boston Children's Hospital, Boston, MA, United States, [2] Institute of Laboratory Medicine, Philipps University Marburg, Marburg, Germany, [3] Department of Pediatrics, Harvard Medical School, Boston, MA, United States, [4] Laboratory of Lymphocyte Signaling and Development, The Babraham Institute, Cambridge, United Kingdom, [5] Institute of Laboratory Medicine, Universities of Giessen and Marburg Lung Center (UGMLC), Philipps University Marburg, German Center for Lung Research (DZL), Marburg, Germany

Mast cells and basophils have long been implicated in the pathogenesis of IgE-mediated hypersensitivity reactions. They express the high-affinity IgE receptor, FcεRI, on their surface. Antigen-induced crosslinking of IgE antibodies bound to that receptor triggers a signaling cascade that results in activation, leading to the release of an array of preformed vasoactive mediators and rapidly synthesized lipids, as well as the *de novo* production of inflammatory cytokines. In addition to bearing activating receptors like FcεRI, these effector cells of allergy express inhibitory ones including FcγR2b, an IgG Fc receptor with a cytosolic inhibitory motif that activates protein tyrosine phosphatases that suppress IgE-mediated activation. We and others have shown that food allergen-specific IgG antibodies strongly induced during the course of oral immunotherapy (OIT), signal *via* FcγR2b to suppress IgE-mediated mast cell and basophil activation triggered by food allergen challenge. However, the potential inhibitory effects of IgA antibodies, which are also produced in response to OIT and are present at high levels at mucosal sites, including the intestine where food allergens are encountered, have not been well studied. Here we uncover an inhibitory function for IgA. We observe that IgA binds mouse bone marrow-derived mast cells (BMMCs) and peritoneal mast cells. Binding to BMMCs is dependent on calcium and sialic acid. We also found that IgA antibodies inhibit IgE-mediated mast cell degranulation in an allergen-specific fashion. Antigen-specific IgA inhibits IgE-mediated mast cell activation early in the signaling cascade, suppressing the phosphorylation of Syk, the proximal protein kinase mediating FcεRI signaling, and suppresses mast cell production of cytokines. Furthermore, using basophils from a peanut allergic donor we found that IgA binds to basophils and that activation by exposure to peanuts is effectively suppressed by IgA. We conclude that IgA serves as a regulator of mast cell and basophil degranulation, suggesting a physiologic role for IgA in the maintenance of immune homeostasis at mucosal sites.

Keywords: basophils, basophil activation test, allergy, IgE, IgA, oral immunotherapy (OIT)

OPEN ACCESS

Edited by:
Frans J. Van Overveld, University College Roosevelt, Netherlands

Reviewed by:
Monique A. Vogel, Bern University Hospital, Switzerland
Jia-Jie Chen, Shenzhen University, China

***Correspondence:**
Hans C. Oettgen
hans.oettgen@childrens.harvard.edu

Specialty section:
This article was submitted to Inflammation, a section of the journal Frontiers in Immunology

Received: *22 February 2022*
Accepted: *30 May 2022*
Published: *05 July 2022*

Citation:
El Ansari YS, Kanagaratham C, Burton OT, Santos JV, Hollister B-MA, Lewis OL, Renz H and Oettgen HC (2022) Allergen-Specific IgA Antibodies Block IgE-Mediated Activation of Mast Cells and Basophils. Front. Immunol. 13:881655. doi: 10.3389/fimmu.2022.881655

INTRODUCTION

IgE, while present at low concentrations in the serum, is unique in its ability to induce rapid and severe hypersensitivity responses. It is found tightly bound to basophils and mast cells *via* its high affinity-receptor, FcεRI. Upon antigen binding, IgE-FcεRI aggregation triggers a signaling cascade that results in the immediate release of preformed mediators and rapidly synthesized arachidonic acid metabolites followed by the production of pro-inflammatory cytokines. Mast cell mediators rapidly elicit a range of physiological responses including vasodilation and plasma extravasation, leading to tissue edema along with mucus production and smooth muscle constriction, all part of the immediate hypersensitivity response (1, 2). In addition to mediating these rapid physiologic changes, mast cells-via their delayed production of cytokines- serve a second but critical function in allergy as adjuvants for emerging type 2 adaptive immune responses. Mast cell-derived IL-4 drives IgE switching in B cells and promotes the expansion of pro-allergic lymphocytes, including type 2 innate lymphoid cells (ILC2) and Th2 cells, while suppressing the development and function of T regulatory cells (Treg) (3). Thus, the role of mast cells extends beyond driving immediate hypersensitivity reactions to include the induction and regulation of emerging immune responses (4, 5).

To date, a number of regulatory mechanisms that counter IgE-mediated activation of mast cells and basophils in immediate hypersensitivity responses have been described but their individual contributions to controlling allergic reactions in physiologic settings are unclear (6–8). IgE-mediated allergies are typically diagnosed based on skin prick testing or immunoassays. However, positive tests for IgE are not consistently predictive of clinical allergy. Despite being sensitized (e.g. detectable/measurable allergen specific IgE in the blood), some subjects with low to moderate levels of allergen-specific IgE will not experience any symptoms upon allergen exposure. Others will exhibit significant reactions. This is particularly evident in children undergoing testing for food allergies, creating clinical uncertainty that can only be resolved by performing food challenges to reliably establish allergy status (9–11). The absence of symptoms in some allergen IgE-sensitized children constitutes strong evidence for the presence and significant physiologic impact of factors that suppress IgE-mediated activation of mast cells and basophils.

Allergen-specific IgG antibodies have recently received attention as suppressors of allergic reactions to foods in subjects who harbor IgE. It is well established that allergen-specific IgG antibodies can inhibit IgE-mediated mast cell and basophil activation by two distinct mechanisms: 1) steric blockade of antigenic epitopes, or 2) signaling *via* the inhibitory Fc receptor FcγR2b (12, 13). Signals relayed *via* FcγR2b oppose activating input from FcεRI, preventing downstream events that lead to mast cell and basophil degranulation (12, 14). In the setting of allergy, such IgG effects inhibit IgE-mediated immediate hypersensitivity reactions. The suppressive effects of IgG extend beyond immediate hypersensitivity. Studies using mouse models of food allergy have shown that allergen-specific IgG antibodies inhibit cytokine production by activated mast cells and basophils with immunomodulatory consequences for emerging adaptive immune responses including impaired Th2 expansion along with suppression and reprogramming of Tregs (15). Some compelling evidence regarding the relevance of inhibitory functions of IgG in allergy has come from studies showing that the appearance of allergen specific IgG coincides with natural resolution of milk and egg allergies in children (16, 17) and from parallel observations in respiratory allergy where the presence of IgG is inversely correlated with airway symptoms (18). Food-specific IgG antibody titers have recently been found to increase by several logs in patients who have completed oral immunotherapy (OIT). We and others have found that allergen/food specific IgG antibodies efficiently suppress the activation of IgE-sensitized basophils by allergen, which partly explains the food unresponsive state induced by OIT (14, 15, 19).

The most abundant antibody isotype in the intestine, where food allergens are encountered, is IgA. Thus, it would clearly be of interest to understand the effects of allergen specific IgA on IgE-mediated allergic reactions. IgA protects against mucosal pathogens through immune exclusion mechanisms by reducing the motility and adhesive capabilities of enteric pathogens. Strait and colleagues have suggested that IgA interactions might similarly impact the fate of ingested allergens, blocking their uptake and systemic absorption into the bloodstream. Like IgG, food-specific IgA antibodies increase dramatically after OIT (20). Some observations have pointed to correlations between impaired IgA responses and the development of allergic disease. Both high fecal and high salivary IgA have been correlated with a reduced risk of developing IgE associated diseases (21–23). A recent analysis of stool samples from healthy non-allergic individuals revealed a substantial amount of food allergen specific IgA is produced stably over time (24). Given its abundance and protective roles at mucosal surfaces, we hypothesized that IgA, like IgG, might inhibit IgE induced mast cell and basophil activation.

In this study we evaluated this hypothesis by testing the effects of antigen-specific IgA antibodies on IgE-mediated activation of murine mast cells and human basophils. We observed that IgA inhibits IgE-induced activation in an allergen-specific manner, and that IgA binding to murine mast cells was calcium- and sialic acid-dependent.

MATERIALS AND METHODS

Mouse Anti-TNP IgA Production and Purification

Frozen TIB-194 hybridoma cells (ATCC, Manassas, VA) were thawed according to manufacturer's instructions, transferred and diluted with warmed RPMI-1640 (10% FBS, 100U/ml penicillin). Cells were centrifuged at 300 x g for 5 minutes, and the diluted freezing additive was removed and replaced with new media. Cells were propagated by the addition of fresh media approximately every 2-3 days. As cells multiplied, they were transferred into bigger flasks. Culture supernatants were tested by a sandwich ELISA for presence of anti-TNP IgA.

Supernatants were collected and run over a protein L column (ThermoFisher Scientific, Waltham, MA). IgA was then concentrated and dialyzed with Amicon Ultra Centrifugal Filter Devices carrying a 100 kDa cut-off (Millipore Sigma, Darmstadt, Germany) and filter-sterilized with 0.2μM syringe filters (Millex, EMD Millipore, Billerica, MA).

Mast Cell Culture

BALB/cJ mouse bone marrow was cultured in RPMI-1640 media supplemented with 10% fetal bovine serum (Atlanta Biologicals, Lawrenceville, GA), 10mM HEPES buffer, 100 μg/ml streptomycin, 100U/ml penicillin 10μg/ml gentamicin, 1% Minimum Essential Medium non-essential amino acids, 1 mM sodium pyruvate, and 55μm 2-mercaptoethanol, (all from ThermoFisher Scientific, Waltham, MA) in the presence of both 10-20 ng/ml of IL-3 and SCF (Shenandoah Biotechnology, Warwick, PA) for the differentiation into BMMCs. BMMCs were cultured for 4-6 weeks until cultures reached 90% purity. The purity of BMMCs were assessed by flow cytometry ($c\text{-}Kit^+$ $Fc\varepsilon RI\alpha^+$).

For the lysosomal-associated membrane protein 1 (LAMP-1) assay, mouse BMMCs were incubated overnight with anti-TNP IgE (50 ng/ml, BD Biosciences, Franklin Lakes, NJ), and anti-TNP IgA (100 μg/ml, TIB-194 hybridoma, ATCC, Manassas, VA). Cells are then washed with RPMI to remove unbound antibody, and then stimulated for 10 mins at 37°C with TNP BSA (50 ng/ml, Biosearch Technologies, Teddington, UK) while simultaneously being stained with, BV605 anti-c-Kit (Biolegend, San Diego,CA), fixable viability dye eFluor 780 (eBioscience, San Diego, CA), and PE anti-LAMP-1. For antigen specificity experiments, anti-OVA IgA (gifted by Dr. Duane Wesemann), was used alongside anti-TNP IgA.

For imaging experiments, BMMCs were IgE/IgA sensitized as per the conditions above, and stained with NucBlue Live Cell Stain (Thermofisher Scientific, Carlsbad, CA), and anti-mouse Fc block and FITC anti-IgA (BD Biosciences, Franklin Lakes, NJ), or isotype control. Cells were then cytospun onto a slide. Slides were visualized and imaged using an EVOS M7000 microscope (Thermofisher Scientific, Bothell, WA).

For measurements of phospho-Syk, mouse BMMCs were incubated with anti-TNP IgE, and anti-TNP IgA as above, and stimulated at 37°C for zero, one and two minutes. Cells were fixed and stained using Thermofisher Scientific Protocol C: Two-step Protocol for Fixation/Methanol. Cells were stained with mouse PE anti-phospho-Syk (Cell Signaling Technologies, Danvers, MA), in the presence of mouse Fc block and assessed on an LSR Fortessa.

For phospho-Syk/Syk western blots, 10^6 BMMCs were sensitized overnight with anti-TNP IgE, and anti-TNP IgA as described in conditions above. After sensitization, cells were stimulated with 100 ng/mL of TNP-OVA for 0–3 minutes. Cold FACS buffer was used to stop stimulation, and cells were pelleted and lysed with radioimmunoprecipitation assay buffer (Sigma-Aldrich) containing a cocktail of protease and phosphatase inhibitors (MilliporeSigma, Burlington, Mass).Lysed cells were then spun down to collect protein supernatant. Twenty microliters of lysate were resolved on a 4-15% MiniProtean TGX precast gel (Biorad, Hercules, Calif) and electrophoretically transferred to a polyvinylidene fluoride (PVDF) membrane (MilliporeSigma). Membranes were blocked with 5% BSA in tris-buffered saline with 0.05% tween 20 (TBST) for 1 hour. Membranes were probed with primary antibodies overnight, washed with TBST, and then probed with appropriate peroxidase-conjugated secondary antibodies for 1 hour. Membranes were developed with Supersignal chemiluminescent substrate reagent and imaged on an iBright Western Blot scanner (Thermo Fisher Scientific, Waltham, Mass).

Cytokine Release Assay

For the cytokine release assay, BMMCs were stimulated for 6 hours. Supernatants were collected and cytokines were measured using the Cytometric Bead Array (CBA) Mouse/Rat Soluble Protein Master Buffer kit, along with the cytokine flex sets for IL-13, IL-6, and TNF-α according to manufacturer's instructions (BD Biosciences, Franklin Lakes, NJ).

Flow Cytometry and Immunofluorescence IgA Binding Studies on BMMCs, Splenic T Cells and Peritoneal Cells

T cells were purified from a BALB/cJ spleen by MACS sorting using the CD3ε Microbead kit according to manufacturers instructions (Miltenyi Biotec, Bergisch Gladbach, Germany). BMMCs were incubated with 100 μg/ml anti-TNP IgA or anti-TNP OVA in 1X HBSS for 30 minutes at 4°C. Purified T cells were also incubated with 100 μg/ml anti-TNP IgA in 1X HBSS for 30 minutes at 4°C. Mast cells were stained for BV605 anti-c-Kit, PE anti-FcεRI, fixable viability dye eFluor 780 (eBioscience, San Diego, CA), and FITC anti-IgA (BD Biosciences, Franklin Lakes, NJ) in the presence of anti-mouse Fc block (Biolegend, San Diego, CA), in FACS buffer (1X PBS, 10% FBS) at 4°C for 30 minutes. T cells were stained for PE anti-CD3 (eBioscience, San Diego, CA), BV605 anti-CD4 (Biolegend, San Diego, CA), FITC anti-IgA (BD Biosciences, Franklin Lakes, NJ), and fixable viability dye eFluor 780 (eBioscience, San Diego, CA), in FACS buffer.

Peritoneal lavage was isolated from BALB/cJ by injection of 5 ml of 1X HBSS into the peritoneal cavity to dislodge attached cells. Cells were pelleted and resuspended in 1X HBSS containing 100 μg/ml of anti-TNP IgA – incubated for 30 minutes at 4°C. Cells were then washed in FACS buffer and stained with mouse AF700 anti-CD45 (Biolegend, San Diego, CA), APC anti-CD11b (eBioscience, San Diego, CA), BV605 anti-c-Kit (Biolegend, San Diego, CA), PE anti-FcεRIα (Biolegend, San Diego, CA), and FITC anti-IgA (BD Biosciences, Franklin Lakes, NJ.

Deglycosylation and Desialylation of IgA

For removal of N-linked glycans, anti-TNP IgA was incubated with PNGase F (New England Bioscience, Ipswich, MA) at 37°C

for 72 hours according to manufacturer's instructions. For desialylation, anti-TNP IgA was digested with neuraminidase from *Vibrio cholerae* (Sigma, Saint Louis, MO) at 37°C for 24 hours according to manufacturer's instructions. The reactions (control IgA in glycobuffer, and digested IgA in glycobuffer and neuraminidase) were then incubated at 65°C for 10 min. to deactivate the enzymes. Digestion efficacy was assessed by lectin blot analysis.

Human IgA Purification and Anti-Peanut IgA Quantification From Post OIT Sera

As OIT induces a strong food allergen-specific IgA response, we used sera obtained from patients who had undergone peanut OIT as a source of peanut-specific IgA (25). Post OIT sera were pooled from several patients and IgA was purified using an anti-human IgA CaptureSelect affinity column as per manufacturer's instructions (ThermoFisher Scientific, Carlsbad, CA). The IgA-enriched eluate from this column was then run through a Protein G column as per manufacturer's instructions to further deplete it of IgG (ThermoFisher Scientific, Carlsbad, CA). The IgA was concentrated to a volume equivalent to that of the original input serum and dialyzed with Amicon Ultra Centrifugal Filter Devices carrying a 100 kDa cut-off (Millipore Sigma, Darmstadt, Germany) and filter-sterilized with 0.2 µm syringe filters (Millex, EMD Millipore, Billerica, MA). Total IgA and IgG was quantified using the Human IgA and IgG ELISA kits (ThermoFisher Scientific, Carlsbad, CA).

Human Basophil Activation Test

Basophil activation tests (BAT) were performed using the Flow CAST Basophil Activation Test kit (Bühlmann Laboratories, Schönenbuch, Switzerland). 50 µl aliquots of whole blood from peanut allergic patients were pre incubated with 125-1000 µg/ml of purified IgA for 2-4 hours at 37°C in 100 µl of basophil stimulation buffer. Samples were incubated for l5 min at 37°C with $3.6x10^{-4}$ µg/ml of crude peanut extract (CPE) and staining antibodies for human PE anti-CCR3 (Biolegend, San Diego, CA) and FITC anti-CD63 (BD Biosciences, Franklin Lakes, NJ). Anti-FcεRI stimulation was used as a positive control for basophil activation. After red blood cell lysis, cells were washed and assessed for activation by flow cytometry. Basophils were identified as $SSC^{low}CCR3^{+}$ and activated cells identified based on CD63 expression. Around 200 basophils were evaluated for each sample. Peripheral blood from peanut allergic donors was obtained with informed consent under a protocol approved by the Institutional Review Board of Boston Children's Hospital.

Fluorescent Labeling of Human IgA and IgA Binding Studies on Human Cell Types

Human IgA purified from post OIT sera was fluorescently labeled using the Pierce FITC antibody labeling kit (Thermofisher Scientific, Rockford, IL) according to the manufacturer's instructions. For IgA binding experiments, donor whole blood was stained with labeled IgA, along with antibodies to human leukocyte markers PE anti-CCR3, APC anti-FcεR1, AF700 anti-CD3, PE-Cy7 anti-CD16, BV510 anti-CD14 all from (Biolegend, San Diego, CA) for 30 minutes at 37°C.

RESULTS

IgA Antibodies Inhibit IgE-Induced Mouse Mast Cell Degranulation in an Antigen-Specific Manner

In order to evaluate the effects of IgA antibodies on IgE-mediated mast cell activation, we took advantage of the availability of monoclonal hapten-specific IgA antibodies as well as the well-characterized experimental model system of cultured BMMCs in which murine bone marrow cells are incubated with IL-3 and SCF to differentiate to $c\text{-}Kit^{+}$ $Fc\varepsilon RI^{+}$ mast cells. Our own investigations as well as others have shown that IgG antibodies can inhibit IgE-mediated BMMC activation in a manner that is antigen specific and FcγR2b -dependent (e.g. the effect is not observed in $Fc\gamma R2b^{-/-}$ BMMCs) (14, 15). To test the effects of IgA on IgE-mediated mast cell activation, BMMCs were incubated with IgE ± IgA monoclonal antibodies specific for the hapten, trinitrophenyl (TNP) prior to antigen exposure. Cells were then washed to remove unbound antibody, and then stimulated for 10-minutes with (TNP-BSA). LAMP-1, which is extruded to the plasma membrane surface during granule fusion, was measured by flow cytometry as an indicator of mast cell degranulation.

In the absence of anti-TNP IgE, TNP-BSA induced no detectable BMMC degranulation, with LAMP-1 expression only 0.1% ± 0.02% (**Figure 1**). Anti-TNP IgE-sensitized BMMCs exposed to TNP-BSA exhibited a robust induction of surface LAMP-1 on the cell surface (16.9% ± 0.5%). Addition of anti-TNP IgA to these cultures resulted in a marked suppression of IgE-induced LAMP-1 expression (3.5% ± 0.2%) (**Figure 1**). In contrast, incubating anti-TNP IgE sensitized mast cells with IgA directed against an irrelevant antigen, ovalbumin (OVA), did not impair IgE mediated activation (20.5% ± 0.7%), indicating that IgA mediated suppression is antigen specific. While anti-OVA IgA did not suppress TNP-IgE responses, we confirmed that it did still bind to BMMCs in a similar manner to anti-TNP IgA (**Figure S1**).

IgA Binds to Bone Marrow Derived Mouse Mast Cells and Peritoneal Mouse Mast Cells

The observation that IgA antibodies blocked IgE-induced activation of allergen-exposed BMMCs, led us to consider the possibility that IgA might be physically interacting with these mast cells. Surface expression of IgA on $c\text{-}Kit^{+}$ $Fc\varepsilon RI^{+}$ cells was measured by flow cytometry following incubation of BMMCs with anti-TNP IgA for 30 minutes in HBSS. In the presence of IgA, BMMCs uniformly stained with anti-IgA FITC in a dose dependent manner (**Figure 2A**, upper and lower panel), however no IgA binding was observed with purified splenic T cells. Immunofluorescence imaging

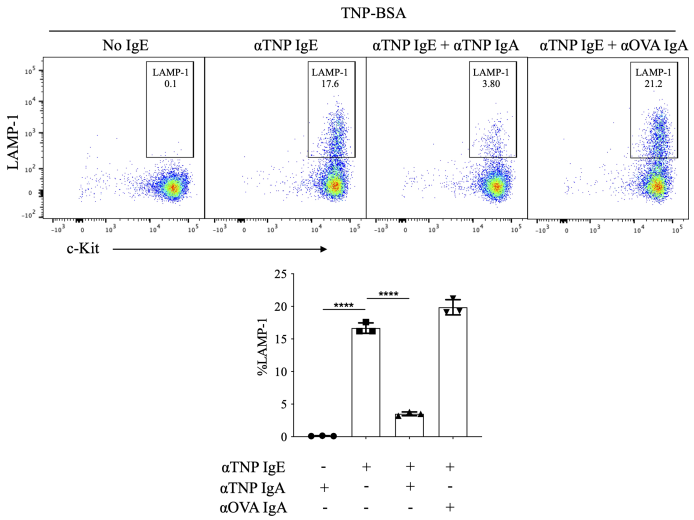


FIGURE 1 | Effects of IgA antibodies on IgE mediated degranulation of bone marrow derived mast cells. Flow cytometry plots from a representative experiment (left) and aggregate data (n=3) bar plots (right) of percent LAMP-1 expression of IgE sensitized BMMCs following antigen exposure. BMMCs were sensitized with anti-TNP IgE (αTNP IgE) (50 ng/ml). Subsequently, some cells were co-incubated with anti-TNP IgA (αTNP IgA) (100 μg/ml) (purified from TIB-194 hybridoma) or anti-OVA IgA [αOVA IgA (100 μg/ml)]. Cells were primed with antibodies overnight, then washed and stimulated with, 50 ng/ml of TNP-BSA for 10 minutes before assessing activation by staining with anti-mouse c-Kit, and LAMP-1. Statistical analysis done by ANOVA. Data shown mean ± SEM of one experiment representative of three independent experiments. ****P < .0001.

of BMMCs, incubated with or without anti-TNP IgA similarly revealed the presence of staining (green) on mast cells incubated with IgA (**Figure 2B**). In order to evaluate IgA binding to primary mast cells, we examined peritoneal lavage cells. Staining for surface IgA after incubation with anti-TNP IgA, revealed IgA binding to CD11b$^-$ c-Kit$^+$ FcεRI$^+$ mast cells isolated from the peritoneum (**Figure 2C**).

IgA Binding to Mast Cells Is Calcium- and Sialic Acid-Dependent

As mast cells do not express any known IgA receptors, we sought to characterize the physical properties of IgA binding to BMMCs. To test calcium dependence, exogenous calcium was chelated by addition of EGTA to BMMC suspensions prior to incubation with IgA. Calcium removal dramatically impaired IgA binding with a decrease in MFI from 3060 ± 13.4 to 961 ± 79.8 (**Figure 3A**), but not IgE binding (**Figure S2**). We similarly observed that BMMCs suspended in calcium-free PBS failed to bind IgA (data not shown).

The abrogated IgA binding after calcium chelation suggested interaction with a calcium dependent receptor. Some such receptors are lectins, leading us to consider that the carbohydrate moieties on IgA might be mediating its interaction with BMMCs. To test this, we treated anti-TNP IgA with either PNGase F to remove all N-linked sugars, or neuraminidase to remove terminal sialic acid residues. Either N-deglycosylation of anti-TNP IgA or the removal of sialic acid rendered the antibody completely unable to bind to BMMCs (**Figure 3C**) without affecting its ability to bind to TNP-OVA (**Figure 3B**). To corroborate this sialic acid dependence of IgA binding to BMMCs, we incubated cells with sialic acid for 30 minutes prior to addition of IgA and observed suppression of IgA binding to undetectable levels (**Figure 3D**). The suppression of this response is dose dependent (data not shown). Using desialylated IgA, we also confirmed a functional requirement for sialic acid in the ability of IgA to suppress IgE-mediated mast cell activation. We observed that while untreated IgA inhibited LAMP-1 induction (of 8.8% ± 0.06% in treated compared to 16.2% ± 1.2% in controls), desialylated anti-TNP IgA was incapable of suppressing IgE-mediated BMMC degranulation (18.3% ± 2.3%) (**Figure 3E**). We could not similarly establish the effects of calcium depletion on the inhibitory function of IgA antibodies since it is not possible to perform mast cell activation assays in the absence of calcium. These experiments reveal that the binding of IgA to BMMCs is dependent both on ambient calcium concentration and on sialylation of the IgA antibodies and that sialyation is also critical for functional inhibition of mast cell activation by IgA.

IgA Inhibits Syk Phosphorylation and Cytokine Production in IgE-Activated Bone Marrow Derived Mast Cells

IgE-antigen receptor crosslinking on BMMCs results in the phosphorylation of the protein tyrosine kinase (PTK) Syk. Activation of a PTK signaling cascade downstream of Syk drives many of the phenotypes of activated mast cells, including degranulation, synthesis of arachidonate-derived lipid mediators and induction of cytokine transcription. In

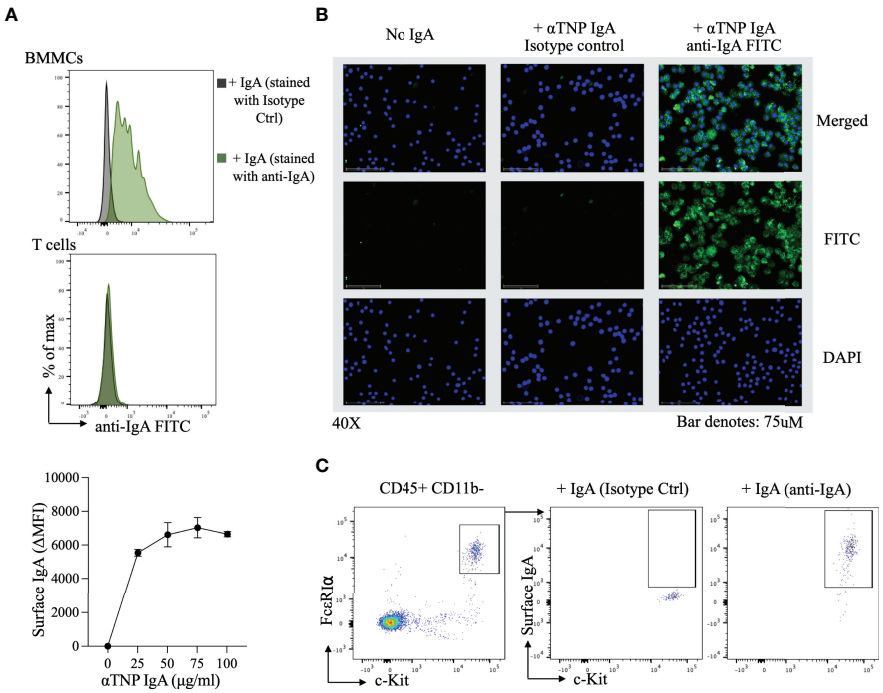


FIGURE 2 | Surface IgA staining on bone marrow derived mast cells and peritoneal mast cells **(A)** *Flow-cytometric evaluation of IgA binding to BMMCs.* Representative histogram of αTNP IgA binding to BMMCs (top) and purified splenic T cells (middle), and a dose response curve of αTNP IgA binding to BMMCs. Mast cells incubated with or without anti-TNP IgA were stained with antibodies for c-Kit, FcεRIα, and IgA and analyzed by flow cytometry. Purified splenic T cells incubated with or without anti-TNP IgA were stained with antibodies for CD3, CD4, and IgA and analyzed by flow cytometry. Data shown is one experiment representative of six independent experiments. **(B)** *Immunofluorescence analysis of IgA binding to BMMCs.* Representative photomicrographs (40x) of BMMCs incubated with or without 100μg/ml of αTNP IgA in HBSS for 30 minutes at 4°C. BMMCs were stained for nucleus (blue), IgA (green), or isotype control (middle), and merged (right). Scale bars: 75 μm. Images were taken using an EVOS M7000 microscope. Data shown is one experiment representative of two independent experiments. **(C)** *Flow-cytometric evaluation of IgA binding to peritoneal mast cells.* Representative flow cytometry plots of IgA staining on peritoneal cavity mast cells, identified by the presence of CD45, c-Kit, FcεRIα. Data shown is one experiment representative of two independent experiments.

order to establish if IgA antibodies block this critical signaling pathway, we evaluated their effects on phosphorylated-Syk (p-Syk), the active signaling form of this PTK. BMMCs loaded with anti-TNP IgE and stimulated with TNP-BSA exhibited rapid increases in p-Syk levels, peaking one minute after stimulation (MFI 298 ± 7.6) and then quickly decreasing (**Figure 4A**). In contrast, allergen-exposed BMMCs sensitized with anti-TNP IgE and also incubated with anti-TNP IgA exhibited attenuated p-Syk induction (176.6 ± 4.7) 1 minute after stimulation. To further validate these results as well as to normalize p-Syk to total Syk, we performed phospho-western blot analysis. This similarly showed Syk phosphorylation detectable as early as 1 minute after stimulation (**Figure 4A**). Quantification of the ratio of signal intensities of phospho-Syk to total Syk revealed that phosphorylation induced by IgE was less at all time points in BMMCs that were also incubated with IgA.

Cytokine production is an important property of activated mast cells and is critical for the generation and tissue recruitment of the effector cells of inflammation as well as for the expansion of type 2 adaptive immune responses. We evaluated the effects of antigen-specific IgA on IgE-induced cytokine production by BMMCs. As expected, IgE-sensitized BMMCs exposed to antigen produce IL-13, TNF-α, and IL-6. Addition of IgA to these IgE-sensitized BMMCs prior to antigen stimulation resulted in a complete suppression of the production of these cytokines (**Figure 4B**). These results indicate that IgA acts early in the FcεRI signaling cascade, inhibiting formation of the most proximal signaling intermediate, p-Syk and that IgA-mediated blockade of mast cell activation extends beyond degranulation to also affect cytokine production.

IgA Antibodies Inhibit the Peanut-Induced Activation of Basophils From Allergic Subjects

Peanut-specific IgG and IgA antibodies are both present in the plasma of subjects with peanut allergy and both of their levels increase after OIT. We have observed that IgE-mediated activation of basophils is potently suppressed by IgG signaling *via* FcγR2b (14). We took advantage of post OIT sera as a source of PN specific IgA to test whether IgA exerts similar protective effects as PN-IgG in peanut allergic patients. IgA was enriched from these patient sera by affinity chromatography and further purified by IgG depletion using Protein G Sepharose, yielding a preparation

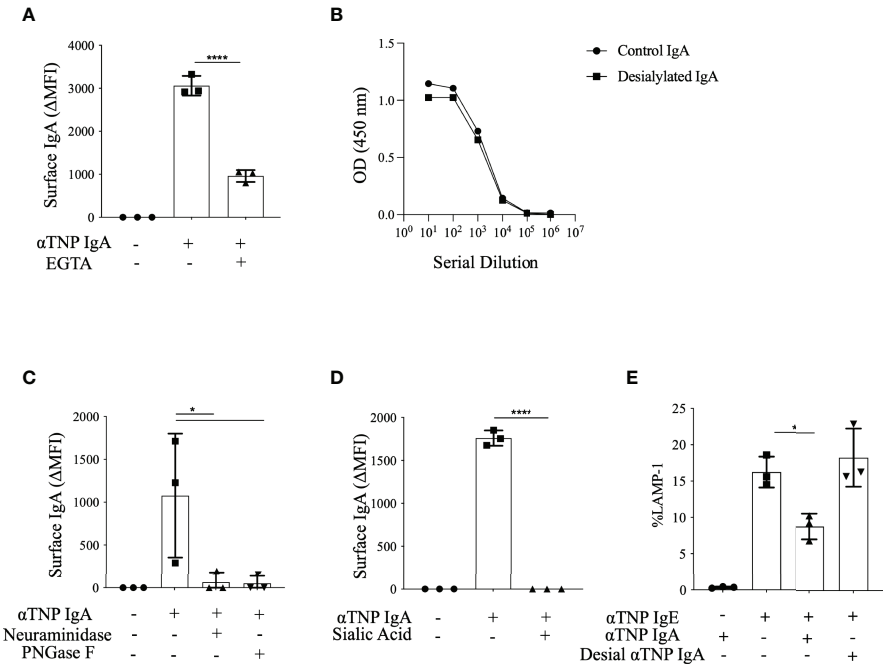


FIGURE 3 | Effects of calcium and sialic acid on IgA binding to BMMCs. **(A)** *Effect of calcium chelation on IgA binding.* Mean fluorescence intensity (MFI) of BMMCs stained with anti-IgA after incubation with anti-TNP IgA in the absence or presence of EGTA. **(B)** *Retention of TNP-OVA binding by desialylated IgA.* Serial dilutions of desialylated or buffer control treated anti-TNP IgA were tested for TNP-OVA binding by ELISA. **(C)** *Analysis of sialic acid requirement for IgA binding*. MFI of BMMCs incubated with untreated anti-TNP IgA, desialylated anti-TNP IgA or N-deglycosylated anti-TNP IgA in HBSS for 30 minutes at 4°C. Mast cells incubated with or without anti-TNP IgA were stained with antibodies for c-Kit, FcεRIα, and IgA and analyzed by flow cytometry. **(D)** *Effects of sialic acid competition on IgA binding to BMMCs.* MFI of BMMCs stained with anti-IgA with or without preincubation with sialic acid **(E)** *Consequences of sialic acid removal on the inhibitory effects of IgA*. Bar plot of percent degranulation across three replicates of LAMP-1 induction in IgE sensitized BMMCs incubated with or without anti-TNP IgA, or desialylated anti-TNP (desial αTNP) IgA as in Figure 3A. Statistical analysis done by one-way analysis of variance (ANOVA). Data shown mean ± SEM of one experiment representative of three independent experiments. *P < .05, and ****P < .0001.

containing 2.5 mg/ml IgA and no detectable IgG. Whole blood samples from a peanut allergic donor (with confirmed IgE mediated allergy to peanut) were pre-incubated for two to four hours with varying concentrations of purified IgA (125-1000 μg/ml). The samples were then stimulated with CPE and expression of CD63 was used to as a marker of basophil activation. Basophil activation was markedly suppressed in the presence of IgA (**Figure 5A**). This inhibitory effect of IgA was dose dependent over a range of IgA amounts from(250-1000 μg/ml) (**Figure 5A**). While IgA has been found to interact with several human cell types, including neutrophils and eosinophils (26, 27), its interaction with mast cells and basophils is incompletely characterized. At least one report has suggested an activating effect of IgA antibodies on basophils (28). We sought to determine if IgA might bind to basophils. We stained whole blood with fluorescently labeled human IgA along with antibodies defining the key leukocyte subsets. As expected, IgA was bound by neutrophils but not by T cells (**Figure 5B**). Basophils also exhibited IgA binding with a unimodal fluorescence shift relative to isotype control. These observations indicate that IgA antibodies, like IgG antibodies, bind to and are capable of inhibiting the activation of antigen stimulated basophils from peanut-allergic subjects.

DISCUSSION

As the most abundant immunoglobulins at mucosal surfaces, IgA antibodies are well-positioned to act as the initial humoral immune sentinels for ingested and inhaled antigens. They have been extensively characterized with respect to their roles in defense in the airway and enteric infection, maintenance of gut microbial homeostasis, and regulation of immune responses (29). Depending on the targeted effector cell and disease model being studied, both pro- and anti-inflammatory properties have been attributed to IgA (26). The physiological functions of IgA in regulating mast cell biology in allergic disease have not been extensively studied.

We took advantage of an array of experimental tools including murine cultured mast cells, primary peritoneal mast cells, human basophils, monoclonal hapten-specific IgA, and polyclonal IgA purified from the sera of peanut allergic subjects to test the hypothesis that antigen-specific IgA antibodies inhibit FcεRI mediated mast cell and basophil activation. We found that IgA binds to mast cells in a manner dependent on calcium and sialic acid and inhibits IgE-induced mast cell degranulation. IgA exerts its function at a receptor-proximal point in the FcεRI-initiated PTK signaling cascade by decreasing phosphorylation of Syk. In addition to blocking degranulation and PTK signaling

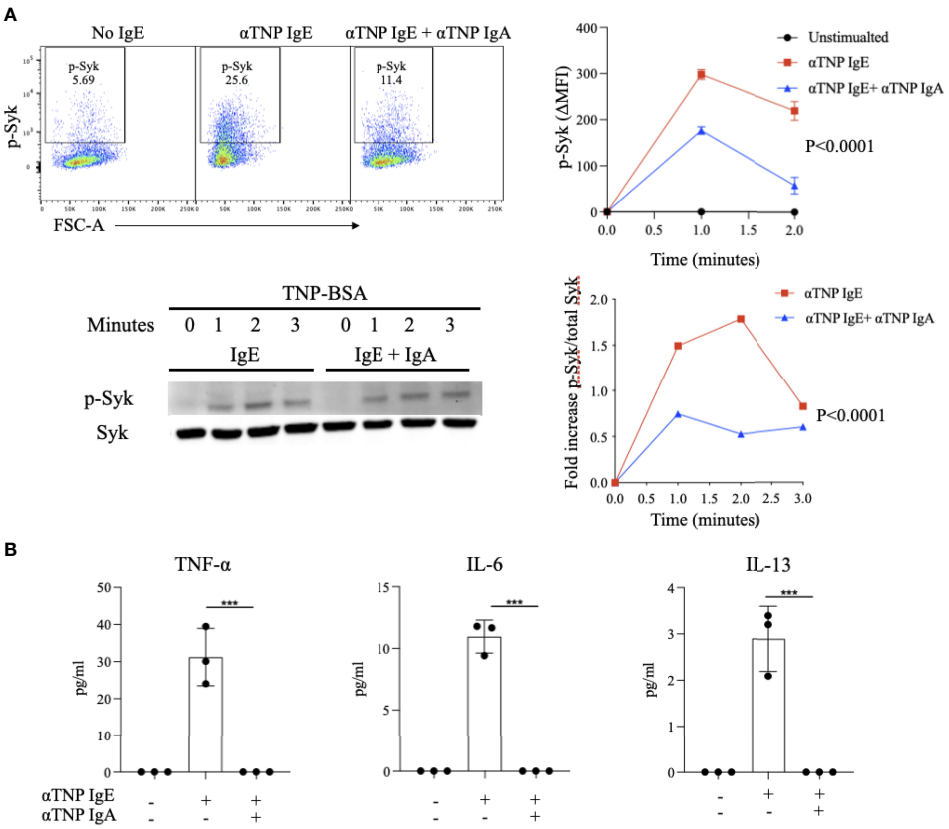


FIGURE 4 | Effect of IgA antibodies on IgE-induced phosphorylation of Syk and on cytokine production by activated bone marrow derived mast cells **(A)** *IgA effects on Syk phosphorylation*. IgE sensitized BMMCs were incubated with or without anti-TNP IgA and stimulated with antigen for up to two minutes followed by measurement of phosphorylated-Syk (phospho-Syk) using flow cytometry (upper panel). Representative Syk phosphorylation blots and compiled ratios of phospho protein/total protein intensities in anti-TNP IgE-sensitized BMMCs or anti-TNP IgE/IgA treated BMMCs (lower panel). This experiment is representative of three replicates. **(B)** *IgA effects on cytokine production*. Cytokine (IL-6, IL-13 and TNF-α) levels in the supernatants of anti-TNP IgE sensitized BMMC incubated with or without anti-TNP IgA and stimulated with TNP-BSA for 6 hours. Statistical analysis done by ANOVA. Data shown mean ± SEM of one experiment representative of three independent experiments. ***P < .001.

pathways, we found that IgA suppresses IgE-induced, cytokine production by mast cells *in vivo*. The relevance of these findings to humans was demonstrated in our confirmation that IgA has suppressive effects on the allergen-induced activation of basophils from peanut allergic subjects.

Our findings provide new insights into regulatory roles IgA might play in allergic disease, most notably its ability to suppress IgE-induced mast cell activation. Strait and colleagues have previously reported that IgA antibodies can suppress IgE-mediated anaphylaxis in mice (20). They showed that the suppressive effect of IgA is observed even in knockout mice lacking the murine IgA receptor, Fcα/μR and conclude that IgA likely confers protection by steric blockade of TNP epitopes on absorbed food allergens rather than by a receptor-mediated inhibitory mechanism. In contrast, some of the observations in our study suggest that IgA mediated inhibition of mast cell activation may in fact be receptor mediated. Specifically, we demonstrate IgA binding to murine mast cells and neutrophils but not lymphocytes, indicating a cellular restriction of IgA interaction suggestive of receptor-mediated binding. We further observed that IgA association with mast cells is calcium-dependent and that both binding and suppressive function of IgA require the presence of sialic acid. These properties are consistent with a receptor-mediated interaction leading us to consider the possibility that a member of the C-type lectin family of receptors might be exerting the inhibitory effect of IgA. However, in our screening experiments using BMMCs from mice with targeted deletions of some of the members of this family known to be expressed on mast cells (including SIGN-R1, CD33, and Siglec F) IgA mediated inhibition of IgE activation remained intact (data not shown). Based on reports that IgA might signal *via* FcγR2b, with Galectin-3 as a binding intermediate (30), we additionally tested IgA's suppressive effects on BMMCs from mice with a targeted deletion of FcγR2b, and found that suppression remained intact (data not shown). Thus, while our results provide some evidence for a receptor-mediated inhibitory effect of antigen-specific IgA on mast cells, further studies will be required to identify the relevant receptor mediating this effect.

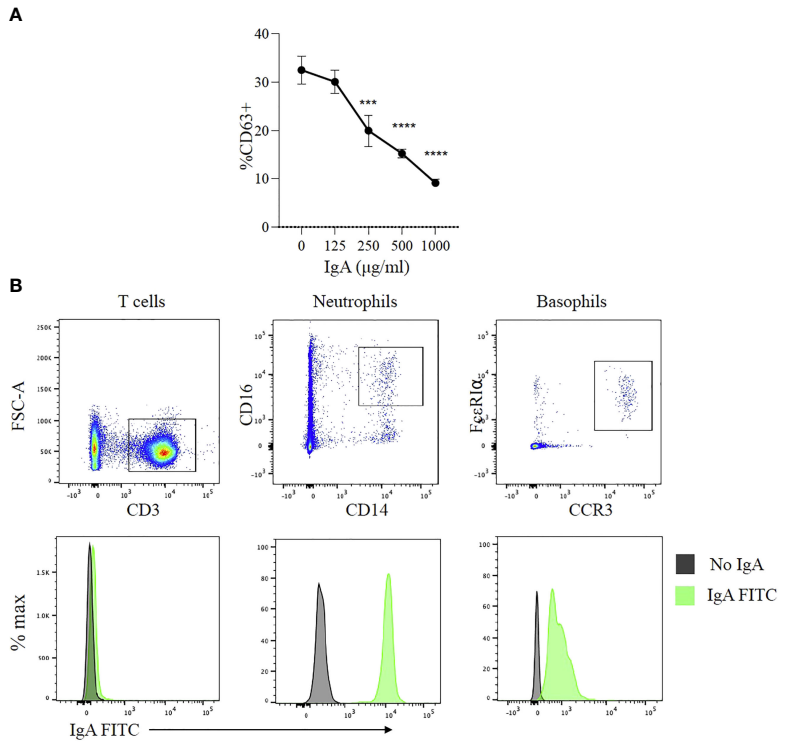


FIGURE 5 | Effects of peanut-specific IgA on basophils from peanut allergic subjects **(A)** *IgA effects on allergen induced degranulation.* Dose response analysis of effects of IgA from peanut allergic subjects on peanut induced activation of basophils from a peanut allergic donor. Data shown from one experiment run in triplicate. Statistical analysis by ANOVA. ***P < .001, ****P < .0001 **(B)** *IgA binding to basophils*. Representative flow cytometry plots showing human IgA purified from post-OIT sera labeled with FITC binding to T cells, neutrophils and basophils from whole blood. T cells were identified by the presence of CD3, neutrophils by CD45, CD14, CD16, and basophils by CCR3 and FcεRI.

Our finding that IgA contained in the serum of subjects with food allergy can suppress peanut-induced activation of basophils from an allergic subject, points to a potential regulatory function of IgA. A role of IgA in food tolerance has previously been suggested by a number of clinical observations. Young children with allergies to cow's milk typically outgrow these allergies later in childhood. The appearance of IgA antibodies specific for cow's milk has been noted to trend in parallel with this resolution of allergy (31). Active induction of food unresponsiveness by OIT is also correlated with the induction of IgA responses. We initially found marked increases in allergen-specific IgA in a trial of OIT for peanut an observation that has subsequently been extended by others to cow's milk and egg OIT (14, 32–35). Murine models have also documented specific IgA responses following food allergen ingestion and OIT (24, 36–38). Despite the consistent observation of association between IgA responses and food tolerance in humans and in murine models of food allergy, neither the direct contributions of IgA to tolerance nor the mechanisms thereof have been established. Immune exclusion, in which IgA antibodies prevent food allergen uptake by intestinal M cells is one proposed mechanism (39). We believe that the findings presented in our current study offer another likely alternative whereby IgA antibodies suppress allergic reactions in a receptor-mediated manner at the effector cell level.

Defining the mechanisms contributing to tolerance of ingested antigens is of critical importance in the field of food allergy. This report provides important new insights in this regard, demonstrating that IgA antibodies, which are known to be physiologically induced after food ingestion and OIT, can block IgE-mediated activation of mast cells and basophils and consequent hypersensitivity reactions. It will be of great interest, going forward to further delineate the mechanisms underlying this effect, and to consider whether the induction of IgA responses or passive administration of allergen-specific IgA might be utilized as therapies.

DATA AVAILABILITY STATEMENT

The original contributions presented in the study are included in the article/**Supplementary Material**. Further inquiries can be directed to the corresponding author.

ETHICS STATEMENT

The studies involving human participants were reviewed and approved by The Institutional Review Board at Boston

Children's Hospital. Written informed consent to participate in this study was provided by the participants' legal guardian/next of kin. The animal study was reviewed and approved by Institutional Animal Care and Use Committee and Animal Research Children's Hospital.

AUTHOR CONTRIBUTIONS

YSE, HR, and HCO designed experiments, interpreted the results, and wrote the paper. Experiments were performed by YSE, OTB, CK and OLL. JS and B-MH recruited peanut allergic patients for the basophil activation tests. All authors contributed to the article and approved the submitted version.

FUNDING

HCO was supported by NIH grant 2R01AI119918-06 and the Food Allergy Science Initiative.

ACKNOWLEDGMENTS

The authors are grateful for Dr. Duane Wesemann and Dr. Teng Zuo for providing αOVA IgA.

SUPPLEMENTARY MATERIAL

The Supplementary Material for this article can be found online at: https://www.frontiersin.org/articles/10.3389/fimmu.2022.881655/full#supplementary-material

Supplementary Figure 1 | Surface anti-OVA IgA staining on bone marrow derived mast cells. Representative histogram of αTNP IgA, and αOVA IgA binding to bone marrow derived mast cells (BMMCs). Mast cells incubated with or without anti-TNP IgA or anti-OVA IgA were stained with antibodies for c-Kit, FcεRIα, and IgA and analyzed by flow cytometry. Data shown representative of one experiment run twice independently.

Supplementary Figure 2 | Effects of calcium on IgE binding to BMMCs. Mean fluorescence intensity (MFI) of BMMCs stained with anti-IgE after incubation with anti-TNP IgE in the absence or presence of EGTA. Data shown representative of one experiment run twice independently.

REFERENCES

1. Renz H, Allen KJ, Sicherer SH, Sampson HA, Lack G, Beyer K, et al. Food Allergy. *Nat Rev Dis Primers* (2018) 4:17098. doi: 10.1038/nrdp.2017.98
2. Oettgen HC. Fifty Years Later: Emerging Functions of IgE Antibodies in Host Defense, Immune Regulation, and Allergic Diseases. *J Allergy Clin Immunol* (2016) 137(6):1631–45. doi: 10.1016/j.jaci.2016.04.009
3. El Ansari YS, Kanagaratham C, Oettgen HC. Mast Cells as Regulators of Adaptive Immune Responses in Food Allergy. *Yale J Biol Med* (2020) 93 (5):711–8.
4. Burton OT, Noval Rivas M, Zhou JS, Logsdon SL, Darling AR, Koleoglou KJ, et al. Immunoglobulin E Signal Inhibition During Allergen Ingestion Leads to Reversal of Established Food Allergy and Induction of Regulatory T Cells. *Immunity* (2014) 41(1):141–51. doi: 10.1016/j.immuni.2014.05.017
5. Nakae S, Ho LH, Yu M, Monteforte R, Iikura M, Suto H, et al. Mast Cell-Derived TNF Contributes to Airway Hyperreactivity, Inflammation, and TH2 Cytokine Production in an Asthma Model in Mice. *J Allergy Clin Immunol* (2007) 120(1):48–55. doi: 10.1016/j.jaci.2007.02.046
6. Bulfone-Paus S, Nilsson G, Draber P, Blank U, Levi-Schaffer F. Positive and Negative Signals in Mast Cell Activation. *Trends Immunol* (2017) 38(9):657–67. doi: 10.1016/j.it.2017.01.008
7. Getahun A, Cambier JC. Of ITIMs, ITAMs, and ITAMis: Revisiting Immunoglobulin Fc Receptor Signaling. *Immunol Rev* (2015) 268(1):66–73. doi: 10.1111/imr.12336
8. Kanagaratham C, El Ansari YS, Lewis OL, Oettgen HC. IgE and IgG Antibodies as Regulators of Mast Cell and Basophil Functions in Food Allergy. *Front Immunol* (2020) 11:603050. doi: 10.3389/fimmu.2020.603050
9. Caubet JC, Sampson HA. Beyond Skin Testing: State of the Art and New Horizons in Food Allergy Diagnostic Testing. *Immunol Allergy Clin North Am* (2012) 32(1):97–109. doi: 10.1016/j.iac.2011.11.002
10. Begin P, Nadeau KC. Diagnosis of Food Allergy. *Pediatr Ann* (2013) 42 (6):102–9. doi: 10.3928/00904481-20130522-10
11. Hogan SP, Wang YH, Strait R, Finkelman FD. Food-Induced Anaphylaxis: Mast Cells as Modulators of Anaphylactic Severity. *Semin Immunopathol* (2012) 34(5):643–53. doi: 10.1007/s00281-012-0320-1
12. Daeron M, Malbec O, Latour S, Arock M, Fridman WH. Regulation of High-Affinity IgE Receptor-Mediated Mast Cell Activation by Murine Low-Affinity IgG Receptors. *J Clin Invest* (1995) 95(2):577–85. doi: 10.1172/JCI117701
13. Tam SW, Demissie S, Thomas D, Daeron M. A Bispecific Antibody Against Human IgE and Human FcgammaRII That Inhibits Antigen-Induced Histamine Release by Human Mast Cells and Basophils. *Allergy* (2004) 59 (7):772–80. doi: 10.1111/j.1398-9995.2004.00332.x
14. Burton OT, Logsdon SL, Zhou JS, Medina-Tamayo J, Abdel-Gadir A, Noval Rivas M, et al. Oral Immunotherapy Induces IgG Antibodies That Act Through FcgammaRIIb to Suppress IgE-Mediated Hypersensitivity. *J Allergy Clin Immunol* (2014) 134(6):1310–7 e6. doi: 10.1016/j.jaci.2014.05.042
15. Burton OT, Tamayo JM, Stranks AJ, Koleoglou KJ, Oettgen HC. Allergen-Specific IgG Antibody Signaling Through FcgammaRIIb Promotes Food Tolerance. *J Allergy Clin Immunol* (2018) 141(1):189–201 e3. doi: 10.1016/j.jaci.2017.03.045
16. Savilahti EM, Rantanen V, Lin JS, Karinen S, Saarinen KM, Goldis M, et al. Early Recovery From Cow's Milk Allergy Is Associated With Decreasing IgE and Increasing IgG4 Binding to Cow's Milk Epitopes. *J Allergy Clin Immunol* (2010) 125(6):1315–21 e9. doi: 10.1016/j.jaci.2010.03.025
17. Caubet JC, Bencharitiwong R, Moshier E, Godbold JH, Sampson HA, Nowak-Wegrzyn A. Significance of Ovomucoid- and Ovalbumin-Specific IgE/IgG(4) Ratios in Egg Allergy. *J Allergy Clin Immunol* (2012) 129(3):739–47. doi: 10.1016/j.jaci.2011.11.053
18. Holt PG, Strickland D, Bosco A, Belgrave D, Hales B, Simpson A, et al. Distinguishing Benign From Pathologic TH2 Immunity in Atopic Children. *J Allergy Clin Immunol* (2016) 137(2):379–87. doi: 10.1016/j.jaci.2015.08.044
19. Santos AF, James LK, Bahnson HT, Shamji MH, Couto-Francisco NC, Islam S, et al. IgG4 Inhibits Peanut-Induced Basophil and Mast Cell Activation in Peanut-Tolerant Children Sensitized to Peanut Major Allergens. *J Allergy Clin Immunol* (2015) 135(5):1249–56. doi: 10.1016/j.jaci.2015.01.012
20. Strait RT, Mahler A, Hogan S, Khodoun M, Shibuya A, Finkelman FD. Ingested Allergens Must Be Absorbed Systemically to Induce Systemic Anaphylaxis. *J Allergy Clin Immunol* (2011) 127(4):982–9 e1. doi: 10.1016/j.jaci.2011.01.034
21. Kukkonen K, Kuitunen M, Haahtela T, Korpela R, Poussa T, Savilahti E. High Intestinal IgA Associates With Reduced Risk of IgE-Associated Allergic Diseases. *Pediatr Allergy Immunol* (2010) 21(1 Pt 1):67–73. doi: 10.1111/j.1399-3038.2009.00907.x
22. Fageras M, Tomicic S, Voor T, Bjorksten B, Jenmalm MC. Slow Salivary Secretory IgA Maturation may Relate to Low Microbial Pressure and Allergic Symptoms in Sensitized Children. *Pediatr Res* (2011) 70(6):572–7. doi: 10.1203/PDR.0b013e318232169e
23. Sandin A, Bjorksten B, Bottcher MF, Englund E, Jenmalm MC, Braback L. High Salivary Secretory IgA Antibody Levels are Associated With Less Late-

Onset Wheezing in IgE-Sensitized Infants. *Pediatr Allergy Immunol* (2011) 22 (5):477–81. doi: 10.1111/j.1399-3038.2010.01106.x
24. Zhang B, Liu E, Gertie JA, Joseph J, Xu L, Pinker EY, et al. Divergent T Follicular Helper Cell Requirement for IgA and IgE Production to Peanut During Allergic Sensitization. *Sci Immunol* (2020) 5(47). doi: 10.1126/sciimmunol.aay2754
25. Schneider LC, Rachid R, LeBovidge J, Blood E, Mittal M, Umetsu DT. A Pilot Study of Omalizumab to Facilitate Rapid Oral Desensitization in High-Risk Peanut-Allergic Patients. *J Allergy Clin Immunol* (2013) 132(6):1368–74. doi: 10.1016/j.jaci.2013.09.046
26. Steffen U, Koeleman CA, Sokolova MV, Bang H, Kleyer A, Rech J, et al. IgA Subclasses Have Different Effector Functions Associated With Distinct Glycosylation Profiles. *Nat Commun* (2020) 11(1):120. doi: 10.1038/s41467-019-13992-8
27. Lamkhioued B, Gounni AS, Gruart V, Pierce A, Capron A, Capron M. Human Eosinophils Express a Receptor for Secretory Component. Role in Secretory IgA-Dependent Activation. *Eur J Immunol* (1995) 25(1):117–25. doi: 10.1002/eji.1830250121
28. Iikura M, Yamaguchi M, Fujisawa T, Miyamasu M, Takaishi T, Morita Y, et al. Secretory IgA Induces Degranulation of IL-3-Primed Basophils. *J Immunol* (1998) 161(3):1510–5.
29. Fagarasan S, Honjo T. Intestinal IgA Synthesis: Regulation of Front-Line Body Defences. *Nat Rev Immunol* (2003) 3(1):63–72. doi: 10.1038/nri982
30. Reljic R, Crawford C, Challacombe S, Ivanyi J. Mouse Monoclonal IgA Binds to the Galectin-3/Mac-2 Lectin From Mouse Macrophage Cell Lines. *Immunol Lett* (2004) 93(1):51–6. doi: 10.1016/j.imlet.2004.01.015
31. Savilahti EM, Savilahti E. Development of Natural Tolerance and Induced Desensitization in Cow's Milk Allergy. *Pediatr Allergy Immunol* (2013) 24 (2):114–21. doi: 10.1111/pai.12004
32. Savilahti EM, Kuitunen M, Savilahti E, Makela MJ. Specific Antibodies in Oral Immunotherapy for Cow's Milk Allergy: Kinetics and Prediction of Clinical Outcome. *Int Arch Allergy Immunol* (2014) 164(1):32–9. doi: 10.1159/000361023
33. Sugimoto M, Kamemura N, Nagao M, Irahara M, Kagami S, Fujisawa T, et al. Differential Response in Allergen-Specific IgE, IgGs, and IgA Levels for Predicting Outcome of Oral Immunotherapy. *Pediatr Allergy Immunol* (2016) 27(3):276–82. doi: 10.1111/pai.12535
34. Wright BL, Kulis M, Orgel KA, Burks AW, Dawson P, Henning AK, et al. Component-Resolved Analysis of IgA, IgE, and IgG4 During Egg OIT Identifies Markers Associated With Sustained Unresponsiveness. *Allergy* (2016) 71(11):1552–60. doi: 10.1111/all.12895
35. Palosuo K, Karisola P, Savinko T, Fyhrquist N, Alenius H, Makela MJ. A Randomized, Open-Label Trial of Hen's Egg Oral Immunotherapy: Efficacy and Humoral Immune Responses in 50 Children. *J Allergy Clin Immunol Pract* (2021) 9(5):1892–901 e1. doi: 10.1016/j.jaip.2021.01.020
36. Maeta A, Katahira R, Matsushima M, Onishi H, Nakamura Y, Takahashi K. Stepwise Oral Immunotherapy for 10 Days in an Egg-White Allergy Mouse Model did Not Ameliorate the Severity of Allergy But Induced the Production of Allergen-Specific IgA. *Biosci Biotechnol Biochem* (2018) 82(12):2176–9. doi: 10.1080/09168451.2018.1517592
37. Wagenaar L, Bol-Schoenmakers M, Giustarini G, Garssen J, Smit JJ, Pieters RHH. Mouse Strain Differences in Response to Oral Immunotherapy for Peanut Allergy. *Immun Inflammation Dis* (2019) 7(1):41–51. doi: 10.1002/iid3.242
38. Frossard CP, Hauser C, Eigenmann PA. Antigen-Specific Secretory IgA Antibodies in the Gut are Decreased in a Mouse Model of Food Allergy. *J Allergy Clin Immunol* (2004) 114(2):377–82. doi: 10.1016/j.jaci.2004.03.040
39. Tordesillas L, Berin MC. Mechanisms of Oral Tolerance. *Clin Rev Allergy Immunol* (2018) 55(2):107–17. doi: 10.1007/s12016-018-8680-5

Conflict of Interest: The authors declare that the research was conducted in the absence of any commercial or financial relationships that could be construed as a potential conflict of interest.

Publisher's Note: All claims expressed in this article are solely those of the authors and do not necessarily represent those of their affiliated organizations, or those of the publisher, the editors and the reviewers. Any product that may be evaluated in this article, or claim that may be made by its manufacturer, is not guaranteed or endorsed by the publisher.

Copyright © 2022 El Ansari, Kanagaratham, Burton, Santos, Hollister, Lewis, Renz and Oettgen. This is an open-access article distributed under the terms of the Creative Commons Attribution License (CC BY). The use, distribution or reproduction in other forums is permitted, provided the original author(s) and the copyright owner(s) are credited and that the original publication in this journal is cited, in accordance with accepted academic practice. No use, distribution or reproduction is permitted which does not comply with these terms.

frontiers | Frontiers in Immunology

REVIEW
published: 06 July 2022
doi: 10.3389/fimmu.2022.923495

Roles of Mast Cells in Cutaneous Diseases

Takafumi Numata[1]*, *Kazutoshi Harada*[1] and *Susumu Nakae*[2,3]*

[1] Department of Dermatology, Tokyo Medical University, Tokyo, Japan, [2] Graduate School of Integrated Sciences for Life, Hiroshima University, Hiroshima, Japan, [3] Precursory Research for Embryonic Science and Technology, Japan Science and Technology Agency, Saitama, Japan

OPEN ACCESS

Edited by:
Satoshi Tanaka,
Kyoto Pharmaceutical University, Japan

Reviewed by:
Elba Mónica Vermeulen,
Instituto de Biología y Medicina Experimental (CONICET), Argentina
Viktor Bugajev,
Institute of Molecular Genetics (ASCR), Czechia

***Correspondence:**
Takafumi Numata
numata@tokyo-med.ac.jp
Susumu Nakae
snakae@hiroshima-u.ac.jp

Specialty section:
This article was submitted to Inflammation, a section of the journal Frontiers in Immunology

Received: 19 April 2022
Accepted: 16 June 2022
Published: 06 July 2022

Citation:
Numata T, Harada K and Nakae S (2022) Roles of Mast Cells in Cutaneous Diseases. Front. Immunol. 13:923495. doi: 10.3389/fimmu.2022.923495

Mast cells are present in all vascularized tissues of the body. They are especially abundant in tissues that are in frequent contact with the surrounding environment and act as potential sources of inflammatory and/or regulatory mediators during development of various infections and diseases. Mature mast cells' cytoplasm contains numerous granules that store a variety of chemical mediators, cytokines, proteoglycans, and proteases. Mast cells are activated *via* various cell surface receptors, including FcεRI, toll-like receptors (TLR), Mas-related G-protein-coupled receptor X2 (MRGPRX2), and cytokine receptors. IgE-mediated mast cell activation results in release of histamine and other contents of their granules into the extracellular environment, contributing to host defense against pathogens. TLRs, play a crucial role in host defense against various types of pathogens by recognizing pathogen-associated molecular patterns. On the other hand, excessive/inappropriate mast cell activation can cause various disorders. Here, we review the published literature regarding the known and potential inflammatory and regulatory roles of mast cells in cutaneous inflammation, including atopic dermatitis, psoriasis, and contact dermatitis GVHD, as well as in host defense against pathogens.

Keywords: skin disease, allergy, autoimmunity, infection, rejection

Abbreviations: ACD, allergic contact dermatitis; AD, atopic dermatitis; BMCMCs, bone marrow-derived cultured mast cells; CBMCs, cord blood-derived mast cells; CHS, contact hypersensitivity; CTMC, connective tissue-type mast cell; Dfb, *Dermatophagoides farina*; DNFB, 1-fluoro-2,4-dinitrobenzene; DST, donor-specific transfusion; EASI, Eczema Area and Severity Index; FITC, fluorescein isothiocyanate; GVHD, graft-versus-host disease; HSV, herpes simplex virus; IL, interleukin; Ig, immunoglobulin; LPP, lichen planopilaris; LPS, lipopolysaccharide; MCPs, mast cell progenitors; MMC, mucosal mast cell; MRGPRX2, mas-related G-protein-coupled receptor X2; NGF, nerve growth factor; PAMP9–20, pro-adrenomedullin peptide 9–20; PGD_2, prostaglandin D2; PRRs, pattern-recognition receptors; RCTs, randomized controlled trials; SCF, stem cell factor; sPLA2-III, group III secreted phospholipase A2; SSSS, staphylococcal scalded skin syndrome; TGF, transforming growth factor; TLR, toll-like receptors; TNCB, 2,4,6-trinitrochlorobenzene; TNF, tumor necrosis factor; Treg, regulatory T cell; TSLP, thymic stromal lymphopoietin.

INTRODUCTION

Mast cells are tissue-resident immune cells that are derived from hematopoietic stem cells (1). First, mast cell progenitors (MCPs) differentiate from hematopoietic stem cells in the bone marrow and/or spleen (shown in mice) and circulate *via* the vascular system (2, 3). The MCPs then infiltrate the local tissues from the blood, where they differentiate into functionally-mature mast cells under the control of the components of the cytokine milieu, such as stem cell factor (SCF), transforming growth factor (TGF)-β, nerve growth factor (NGF), interleukin (IL)-3, IL-4, IL-9, and IL-33 (4–6). Therefore, mast cells are present in all vascularized tissues of the body, and they are especially abundant in tissues that come into frequent contact with the surrounding environment, such as the gastrointestinal tract, skin, and respiratory epithelium (2).

Mature mast cells' cytoplasm contains numerous granules that store a variety of chemical mediators (e.g., histamine), proteoglycans, and proteases. In both rodents and humans, mast cells have been categorized into two types based on their anatomical distribution and the kinds of proteases stored in their granules. In rodents, one type is the mucosal mast cell (MMC), which are located in the mucosa (mucosal epithelium) and whose granules contain tryptase (2). The second type is the connective tissue-type mast cell (CTMC), which are located in connective tissues such as the skin and submucosa and whose granules contain chymase, carboxypeptidases, and tryptase. In humans, one type is termed the TC mast cell (MC_{TC}), whose granules contain tryptase and chymase, while the second type is termed the T mast cell (MC_T), whose granules contain only tryptase (7).

In response to certain stimuli, mast cells release the contents of their granules into the extracellular environment this process is known as degranulation. In one major pathway, degranulation occurs immediately following crosslinking of antigens by antigen-specific immunoglobulin (Ig) E that is bound to FcεRI on mast cells (8). Mobilization of Ca^{2+} is a key process that occurs during degranulation of mast cells after antigen/IgE/FcεRI-crosslinking (9, 10). With or without degranulation, mast cells can also release *de novo*-synthesized inflammatory mediators. In addition, degranulated mast cells are able to replenish their granules, allowing them to undergo repeated degranulation in tissues (11).

Mast cells are able to mount a rapid immunological response by releasing prestored inflammatory mediators, and, owing to their location in the skin and mucosa, they are a part of the front line of defense against pathogens invading the body (12). The released inflammatory mediators bring about increased vascular permeability and fluid accumulation, as well as recruitment and activation of immune cells, including dendritic cells, macrophages, T cells, and B cells (2, 13). However, excessive mast cell activation can rapidly cause death *via* anaphylactic shock. Moreover, inappropriate mast cell activation can cause various diseases such as allergic and autoimmune diseases (14). On the other hand, mast cells play a suppressive role in certain diseases. Thus, they can act not only as pathogenic effector cells but also as suppressor cells in an immune response. Here, we review the published literature regarding the known and potential inflammatory and regulatory roles of mast cells in cutaneous inflammation as well as in host defense.

MAST CELLS IN SKIN INFLAMMATION DURING INFECTION

Toll-like receptors (TLRs), which are pattern-recognition receptors (PRRs), play a crucial role in host defense against various types of pathogens by recognizing pathogen-associated molecular patterns (15). Peptidoglycan (a TLR2 agonist) and lipopolysaccharide (LPS; a TLR4 agonist) are, respectively, components in the cell walls of gram-positive bacteria and mycobacteria, and of gram-negative bacteria. Poly (I:C) (a TLR3 agonist) is a mimic of viral dsRNA. These molecules have been shown to be able to induce cytokine and/or chemokine production by murine and/or human mast cells. In addition, various other peptidoglycans can induce degranulation of murine and/or human mast cells (16–18). Thus, mast cells are important for host defense against viruses and bacteria through PRRs such as TLRs. On the other hand, pathogen-derived antigens/components can promote excessive mast cell activation, resulting in exacerbation of inflammation (**Figure 1**).

Staphylococcus (S.) aureus is a gram-positive bacterium that causes impetigo and staphylococcal scalded skin syndrome (SSSS), primarily in young children (19, 20). Impetigo is a superficial bacterial skin infection that occurs in bullous or non-bullous form. The exfoliative toxin of *S. aureus* cleaves desmoglein 1 and causes bullous impetigo (19). Hematogenous dissemination of exotoxins from the initial site of *S. aureus* infection leads to separation of epidermal keratinocytes and detachment of the superficial epidermis in SSSS (20). *S. aureus* invades and survives in human cord blood-derived mast cells (CBMCs) after internalization (21). *S. aureus* and *S. aureus*-derived peptidoglycan induce degranulation and cytokine production by human CBMCs and mouse bone marrow-derived cultured mast cells (BMCMCs) (16, 17, 21). Mast cells degranulate in response to *S. aureus*-derived δ-toxin, contributing to increased vascular permeability in mice (22). In addition, mast cells are responsible for development of *S. aureus*-mediated skin inflammation accompanied by spongiosis, parakeratosis, and neutrophil infiltration, suggesting that *S. aureus*-stimulated mast cells exacerbate dermatitis such as atopic dermatitis (AD) (22).

Acne vulgaris is a common cutaneous disorder characterized by chronic and recurrent development of multiple inflammatory papules, pustules and nodules, mainly on the face but also on the neck, chest and back. Hyperkeratotic plugs composed of corneocytes in the lower portion of the follicular infundibulum create a new environment that impacts the microbiota and fosters proliferation of a gram-positive bacillus, *Cutibacterium acnes*. IL-17A-producing mast cells were detected in the perifollicular area of acne vulgaris lesions (23). Activated memory/effector $CD4^+$ T cells induced IL-17A production by human mast cells, implying a contribution of mast cells to development of acne vulgaris (23). However, their precise role remains unclear.

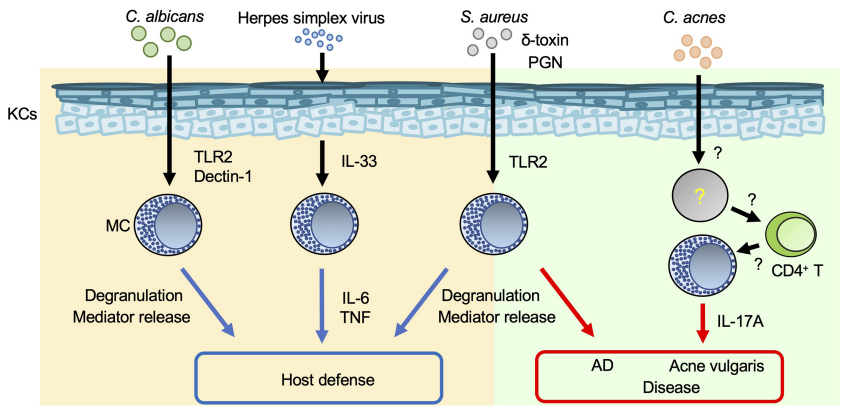


FIGURE 1 | Mast cells in skin inflammation during infection. Mast cells (MCs) are important for host defense against various pathogens. On the other hand, inappropriate MC activation during infection results in aggravation of such skin diseases as AD and acne vulgaris. Blue arrows: appropriate MC activation; red arrows: excessive MC activation.

A fungus, *Candida*, is part of the normal flora of the gastrointestinal tract, oral/nasal cavity, and skin of humans, but it can cause disease when host immunity is compromised or there is an imbalance in the ecological niche. Mast cells reside in various tissues that can be colonized or infected by *Candida* spp., including *Candida* (*C.) albicans* (24). A human mast cell line (HMC-1) degranulated and produced IL-8 in response to *C. albicans*, contributing to enhanced migration of neutrophils (25). Rodent mast cells can phagocytose *C. albicans* and produce nitric oxide, a reactive oxygen species, cytokines and chemokines *via* Dectin-1 and/or TLR2 (26–29). These results suggest that mast cells play a critical role in host defense against *C. albicans* infection, but their precise role in the setting needs to be elucidated.

Dermatophytes are filamentous fungi of the genera *Trichophyton*, *Microsporum*, and *Epidermophyton* that infect the skin, hair, and nails. The yeast and mycelial forms of *Malassezia* are found in the skin scales of patients with pityriasis versicolor (30). MGL_1304, derived from *Malassezia* (*M.*) *globosa*, was identified in human sweat by mass-spectrometric analysis based on the histamine-releasing activity in basophils of patients with AD (31). Serum specific IgE against MGL_1304 was higher in patients with AD and cholinergic urticaria, which is a subtype of chronic urticaria whose symptoms are evoked by sweating, than in normal controls (32). To the best of our knowledge, there are no reports of other types of urticarias that involve MGL_1304. The level of degranulation of a human mast cell line, LAD2, sensitized with sera from patients with AD was greater than with healthy control sera after stimulation with MGL_1304 (32), suggesting that MGL_1304 is a major allergen involved in the exacerbation of AD and cholinergic urticaria *via* induction of mast cell degranulation.

Herpes simplex virus (HSV) is a double-stranded DNA virus and the cause of a common viral infection of epidermal cells that is typically transmitted *via* physical contact (33, 34). HSV can be transmitted even if the source is asymptomatic, but transmission is more likely if the source is symptomatic because the viral titer is much greater when lesions are present (33). Infections by HSV types 1 and 2 are characterized by recurrent, vesicular lesions that are accompanied by pain, tingling, pruritus, and/or burning. Lesions can develop anywhere on the body but occur mainly on the lips (HSV-1) and in the genital area (HSV-2) (33). HSV infections are associated with onset of eczema herpeticum (Kaposi's varicelliform eruption) in patients with AD (35) or erythema multiforme (36). Mast-cell-deficient $Kit^{W}/Kit^{W\text{-}v}$ mice were susceptible to HSV-2 compared with $Kit^{+/+}$ mice (37). HSV-2 induces IL-33 production by keratinocytes, followed by activation of mast cells to produce IL-6 and tumor necrosis factor (TNF) (38), which are crucial for host defense against HSV-2 (37, 38).

MAST CELLS IN CONTACT HYPERSENSITIVITY

Allergic contact dermatitis/contact hypersensitivity (ACD/CHS) develops in response to repeated skin exposure to an allergen. Haptens are generally non-immunogenic, low-molecular-weight chemicals. When haptens are applied to the skin surface, they penetrate the stratum corneum barrier and form chemically-modified, immunogenic neo-antigens by binding with self-proteins (39). Haptens such as 2,4,6-trinitrochlorobenzene (TNCB), oxazalone, 1-fluoro-2,4-dinitrobenzene (DNFB), and fluorescein isothiocyanate (FITC) have long been used experimentally to study CHS in murine models (40). As noted in other reviews (1, 8, 41), the roles of mast cells in the development of acute and chronic CHS have differed with the experimental protocol. In some studies of acute CHS models using mast-cell-deficient and -depleted mice, mast cells (especially mast-cell-derived TNF) were responsible for development of CHS (1, 8, 41–43) (**Figure 2**). In addition, mast-cell-derived IL-25 promoted IL-1β production by dermal

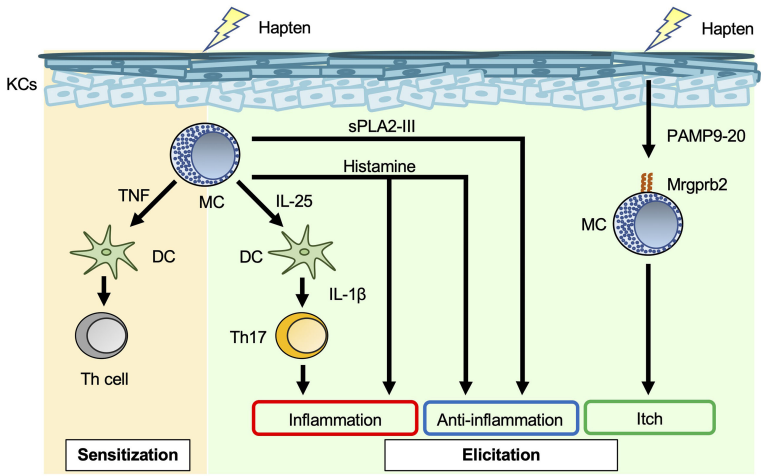


FIGURE 2 | Mast cells in acute contact hypersensitivity. Mast cell (MC)-derived TNF enhances skin dendritic cell (DC) migration to draining LNs, leading to induction of hapten-specific Th-cell expansion in the sensitization phase of contact hypersensitivity (CHS). MC-derived IL-25 induces IL-1β production by dermal DCs, followed by promotion of IL-17 production by Th17 cells in the elicitation phase of CHS. Histamine has dual roles, i.e., inflammatory and anti-inflammatory, in the elicitation phase of CHS. Haptens stimulate keratinocytes (KCs) to produce PAMP9-20, a ligand for Mrgprb2. PAMP9-20 induces itch during CHS.

dendritic cells, which led to exacerbation of Th17-cell-mediated skin inflammation (44). On the other hand, mast cells were not essential for development of acute CHS in certain settings using mast-cell-deficient mice (1, 8, 41). Mast cells can also play a suppressive role in induction of acute CHS in some settings. For example, mast-cell-derived IL-5 was important for expansion of IL-10-producing regulatory B cells, which resulted in suppression of acute CHS (45). Similarly, mast-cell-derived IL-13 inhibited Th1-cell activation by suppressing IL-12 production by skin dendritic cells, which resulted in attenuation of acute CHS (46). Group III secreted phospholipase A2 (sPLA2-III; encoded by *Pla2g3*) released from immature mast cells is important for prostaglandin D2 (PGD_2) production by fibroblasts (47). In turn, fibroblast-derived PGD_2 causes immature mast cells to differentiate into mature mast cells (47). Mast-cell-derived sPLA2-III plays a suppressive role in development of acute CHS, but a promotive role in development of irritant-induced contact dermatitis (48).

Mast cells are a major producer of histamine, which binds to H_1R, H_2R, H_3R, and H_4R. H_1R and H_4R play important roles in allergic diseases, such as urticaria and asthma; H_2R stimulates gastric acid secretion; and H_3R plays a crucial role in the control of sleep–wake behavior (49). H_1R antagonists are widely used to treat pruritic skin inflammation, including urticaria and AD. Mice treated with H_1R antagonists (chlorpheniramine, oxatomide, ketotifen, mequitazine, emedastine, terfenadine and azelastine) showed attenuated acute CHS (50), whereas mice treated with H_1R antagonists (diphenhydramine, homochlorcyclizine, cyproheptadine and cetirizine) showed normal development of acute CHS (50, 51). Mice treated with an H_2R antagonist (cimetidine) showed augmentation of acute CHS (52). In addition, mice deficient in histidine decarboxylase, which is an enzyme involved in histamine synthesis, showed exacerbation of acute CHS (53).

Mas-related G-protein-coupled receptor X2 (MRGPRX2) mRNA is most abundant in human skin, adipose tissue, the bladder, and the colon (54). MRGPRX2 is expressed on human mast cells, and its murine ortholog, Mrgprb2, is specifically expressed on murine CTMCs (55). A new technique based on near-infrared photoimmunotherapy was recently developed for ablation of cancer cells. In that technique, photosensitizer-conjugated monoclonal antibodies specific for a cell surface marker on cancer cells are delivered to the tumor, followed by activation of cytotoxicity (thermotoxicity) by illumination (56). As an extension of that technology, photosensitizer-conjugated monoclonal antibodies specific for MRGPRX2, a cell surface marker on mast cells, were employed to reduce the number of mast cells in the skin (56). MRGPRX2/Mrgprb2 is a promiscuous receptor for cationic ligands, including substance P, compound 48/80, and pro-adrenomedullin peptide 9–20 (PAMP9–20). These ligands induce degranulation of mast cells *via* MRGPRX2/Mrgprb2 (57, 58). PAMP9–20 expression is increased in the inflamed skin lesions of patients with ACD (58). Skin thickness was similarly increased in *Mrgprb2*$^{-/-}$ mice and wild-type mice during acute CHS (58), whereas scratching behavior and the number of inflammatory cells in the skin were significantly reduced in *Mrgprb2*$^{-/-}$ mice (58). Thus, Mrgprb2-mediated mast-cell-activation is somehow involved in induction of itch during acute CHS.

Meanwhile, chronic CHS was induced in rodents by repeated cutaneous exposure to haptens (59–63). Mast cell-deficient/depleted mice showed increased development of chronic CHS (**Figure 3**). In one setting, hapten/hapten-specific IgG1 complexes induced IL-10 production by mast cells by binding

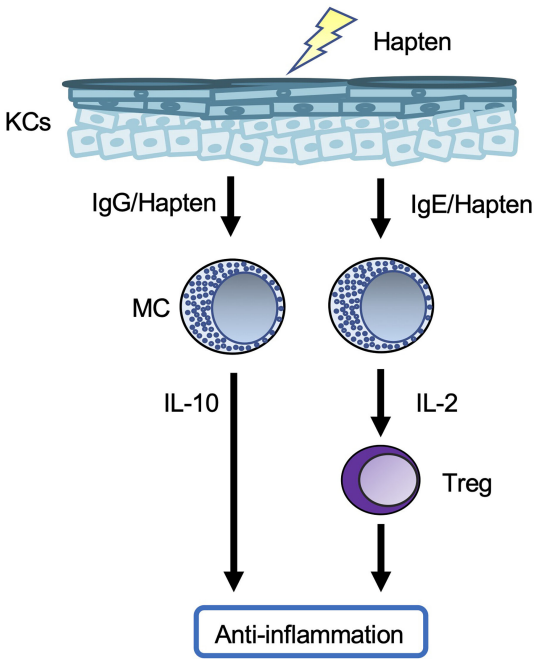


FIGURE 3 | Mast cells in chronic contact hypersensitivity. In one chronic contact hypersensitivity (CHS) setting, crosslinked hapten/hapten-specific IgG complexes stimulate skin mast cells (MCs) to produce IL-10, which leads to suppression of the inflammation. In another chronic CHS setting, crosslinking of hapten/hapten-specific IgE/FcεR1 results in production of IL-2 by splenic MCs, which leads to expansion of Tregs in the spleen. The Tregs migrate from the spleen to local skin lesions, where they suppress the inflammation.

to FcγR on the cells, resulting in IL-10-mediated suppression of chronic CHS (59, 63). In another setting, hapten/hapten-specific IgE/FcεR1 crosslinking induced IL-2 production by mast cells (61). Mast cell-derived IL-2 enhanced regulatory T cell (Treg) expansion, followed by suppression of inflammation during chronic CHS by Tregs (61). Therefore, mast cells have dual roles as both effector cells and regulatory cells in the development of acute and/or chronic CHS induced by certain haptens.

MAST CELLS IN URTICARIA

Mast cell degranulation was observed in the dermis immediately below wheals in various types of inducible urticaria (64). Histamine, which is released by mast cells during IgE-mediated degranulation, is known to be crucial for the pathogenesis of urticaria (65). Increased blood levels of histamine were noted following provocation of inducible urticaria (64). In patients with chronic spontaneous urticaria, more than 200 IgEs, which recognize autoantigens including IL-24, were detected in sera (66). In addition to H_1R antagonists, an anti-human IgE monoclonal antibody (omalizumab) was reported to provide clinical benefit for chronic spontaneous urticaria (67). Moreover, it is known that there is IgE-independent pathogenesis of chronic urticaria (64). The number and proportion of MRGPRX2-positive skin mast cells are increased in the inflamed skin lesions of patients with chronic urticaria compared with the skin of healthy control subjects (68). Intradermal administration of substance P induced greater wheal reactions in patients with chronic spontaneous urticaria than in healthy subjects (69), suggesting that substance P/MRGPRX2-mediated mast cell degranulation is an alternative pathway for induction of chronic spontaneous urticaria. In addition, increased expression of IL-25 and IL-33 on mast cells was observed in lesional skin of patients with chronic spontaneous urticaria (70). IL-25 and IL-33 can modulate many aspects of mast cell function, including proliferation and production of a variety of Th2 cytokines in chronic spontaneous urticaria (64).

MAST CELLS IN ATOPIC DERMATITIS

AD is a chronic, pruritic and inflammatory skin disease that occurs in 15–30% of children and approximately 5% of adults in industrialized nations (71). AD is characterized by barrier disruption, immunological dysfunction and elevated serum IgE. The symptoms of AD, such as recurrent dry, scaly and erythematous lesions and intense pruritus, can place an enormous burden on patients. A significant association was observed between the number of mast cells in AD skin lesions and the disease severity (assessed by the Eczema Area and

Severity Index (EASI) score), although the number of mast cells was not changed by short-term treatment with topical tacrolimus (72).

Filaggrin, a filament-associated protein, is crucial for maintenance of the skin barrier (73). Mutations in the *filaggrin* gene are associated with increased prevalence of ichthyosis vulgaris and AD (73, 74). Mice with mutations in the *filaggrin* gene (Flg^{ft} mice; also called flaky tail mice) spontaneously develop dermatitis that is accompanied by increases in the serum IgE and number of dermal mast cells, thus resembling AD (75).

Topical application of a low-calcemic vitamin-D3-analog MC903 (calcipotriol), which is widely used in the treatment of psoriasis, resulted in development of AD-like dermatitis in mice. MC903-induced dermatitis was dependent on thymic stromal lymphopoietin (TSLP), IL-25 and IL-33 in BALB/c mice (76), and on TSLP, but not IL-25 or IL-33, in C57BL/6 mice (77). Mast cells were involved in TSLP production and induction of skin inflammation in MC903-induced dermatitis (78).

Nc/Nga mice developed AD-like skin inflammation after topical application of an ointment containing *Dermatophagoides farinae* (Dfb) (79). The number of mast cells and histamine level were increased in the inflamed skin of Dfb-treated Nc/Nga mice (79). Although the frequency of scratching was decreased by application of an H4R antagonist (JNJ 7777120) to the skin of wild-type mice after intradermal histamine injection, that same antagonist was ineffective against itching and skin inflammation in Dfb-induced AD-like skin inflammation in NC/Nga mice (80).. Meanwhile, the EASI score was lower for inflammatory AD skin lesions in patients who were treated with an H_4R antagonist (ZPL-3893787) than in those treated with a placebo (81).

Mast cells produce IL-4 and IL-13 (8). Treatment of AD patients with an anti-human IL-4Rα antibody (dupilumab) that inhibits binding of IL-4 and IL-13 to IL-4Rα improved the signs and symptoms of AD (including pruritus), anxiety and depression, as well as the quality of life, compared to placebo controls (82). However, to date, neither meta-analyses and systematic reviews of existing case series nor randomized controlled trials (RCTs) have generated concrete evidence of overall effectiveness of omalizumab for AD (83).

MAST CELLS IN PSORIASIS

Psoriasis is a common chronic skin disease involving systemic inflammation that leads to formation of scaly patches on the skin. The number of mast cells in pruritic lesions was greater than in non-pruritic lesions in psoriasis (84). Activated mast cells were more abundant in psoriatic lesions than in non-lesional psoriatic skin and in healthy subjects, whereas resting mast cells were almost entirely absent in psoriatic skin lesions (85). Importantly, the proportion of resting mast cells gradually normalized in lesional psoriatic skin during etanercept (a TNF inhibitor) therapy (85). These results suggest that mast cells may be involved in the pathogenesis of psoriasis.

Topical application of imiquimod — a TLR7 agonist that is widely used to treat genital warts and actinic keratosis — resulted in development of psoriasis-like dermatitis in mice (86). However, it should be noted that the dermatitis induced in humans by topical imiquimod resembled contact dermatitis rather than psoriasis (87). Expression of *Tlr7* mRNA was constitutively observed and increased in mouse BMCMCs in response to imiquimod, and TLR7 on mast cells was responsible for development of imiquimod-induced dermatitis in mice (88). In those same mice, mast cell activation by imiquimod *via* TLR7 led to TNF production, which in turn promoted skin dendritic

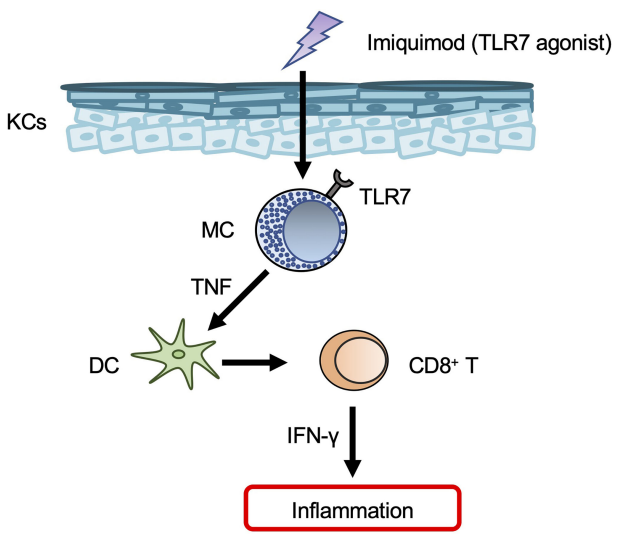


FIGURE 4 | Mast cells in psoriasis. Mast cells (MCs) produce TNF in response to imiquimod *via* TLR7, and TNF then promotes dendritic cell (DC) migration from the skin to draining LNs. The migrated DCs induce $CD8^+$ T-cell expansion in the peripheral blood.

cell migration (88) (**Figure 4**). Imiquimod can induce degranulation of mast cells in humans and mice dependent on human MRGPRX2 and mouse Mrgprb2 (89), although it remains unclear whether imiquimod can bind to MRGPRX2/Mrgprb2. Mrgprb2-dependent mast cell degranulation is crucial for development of imiquimod-induced dermatitis in mice (89).

MAST CELLS IN COLLAGEN SYNTHESIS (WOUND HEALING AND FIBROSIS)

Mast cells activated by tissue injury regulated various phases of skin repair (90). In mice 0.5~1 hour after wounding, the number of degranulated mast cells and the level of vascular permeability were most prominently increased in areas directly adjacent to the wounded skin (91). Moreover, mast cells were involved in neutrophil influx and wound healing in the wounded skin of mice at 12 hours and two to six days after wounding, respectively (91). Thus, mast cells appear to be important for induction of inflammation by increasing vascular permeability and recruiting inflammatory cells to wound sites. Scar width was significantly smaller in mast-cell-deficient $Kit^{W/W\text{-}v}$ mice than in $Kit^{+/+}$ mice at seven and 10 days after wounding (92). In addition, activated mast cells promoted fibroblast expansion (93). These data suggest that mast cells are involved in collagen deposition by activating fibroblasts during remodeling (**Figure 5**).

Systemic sclerosis (scleroderma) is a systemic autoimmune connective tissue disorder characterized by vascular dysfunction and progressive fibrosis of the skin and internal organs, such as the lung and kidney. Mast cell density (mast cells/mm^2) in the papillary and reticular dermis was significantly greater in patients with early progressive systemic sclerosis than in control subjects (94). Histamine and tryptase each enhanced proliferation and collagen synthesis in human skin fibroblasts (95). In aged tight-skin mice, which develop an inherited fibrotic disease resembling scleroderma, mast cells and chymase were responsible for augmentation of fibrosis (96, 97).

Mast cells were detected in lichen planopilaris (LPP), a type of scarring hair loss (cicatricial alopecia) characterized by lymphocytic infiltration in the upper portion of hair follicles (98). The number of IL-17A-positive mast cells was increased in LPP lesions compared with the normal scalp (98). IL-17R is expressed exclusively in follicular epithelial cells in LPP lesions. These observations suggest that mast-cell-derived IL-17A might somehow be involved in the pathogenesis of LPP *via* IL-17R on follicular epithelial cells.

MAST CELLS IN SKIN ALLOGRAFTS AND GRAFT-VERSUS-HOST DISEASE (GVHD)

Long-term acceptance of skin allografts was enabled in mice by injection of anti-CD154 blocking antibody together with allogeneic cells (a process known as donor-specific transfusion; DST) (99). Tregs were important for tolerance to alloantigens in mice (100), and mast cells were increased in the skin allografts of DST-treated mice (99). In addition, in that DST model, Treg-derived IL-9 induced mast cell accumulation and activation in skin allografts, and the accumulated cells suppressed CD8+ T cell-mediated allograft rejection (99).

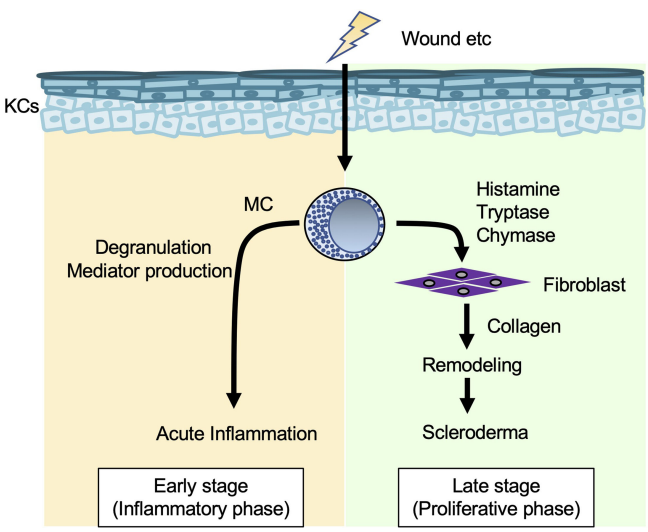


FIGURE 5 | Mast cells in collagen synthesis (wound healing and fibrosis). When the skin is wounded, mast cells (MCs) degranulate and release various mediators that enhance vascular permeability and recruitment of inflammatory cells to injured sites in the early stage (inflammatory phase). In addition, MC-derived histamine, tryptase and chymase induce fibroblasts to produce collagen, which is involved in tissue remodeling and development of scleroderma in the late stage (proliferative phase).

A major side effect of allogeneic hematopoietic stem cell transplantation is graft-versus-host disease (GVHD), in which donor lymphocytes attack the recipient's body as non-self tissues. The number of mast cells was increased in the skin of patients with more severe acute GVHD (101). In GVHD induced by transplantation of $CD8^+$ T cells and T cell-depleted bone marrow cells from C3H.SW mice, the survival rate was significantly higher for irradiated WBB6F1-$Kit^{W/W\text{-}v}$ mice than for irradiated WBB6F1-$Kit^{+/+}$ mice (102). The density of dyskeratotic cells was significantly lower in WBB6F1-$Kit^{W/W\text{-}v}$ mice than in WBB6F1-$Kit^{+/+}$ mice at 14, 21, and 28 days after transplantation, suggesting that mast cells act as effector cells in the development of acute GVHD (102) (**Figure 6**).

On the other hand, development of acute GVHD induced by intravenous injection of either T cell-depleted bone marrow from C57BL/6 mice or $CD4^+$ and $CD8^+$ T cells from FVB mice was significantly greater in irradiated C57BL/6-$Kit^{W\text{-}sh/W\text{-}sh}$ mice than in irradiated C57BL/6 wild-type mice (103). These GVHD reactions were resolved in C57BL/6-$Kit^{W\text{-}sh/W\text{-}sh}$ mice engrafted with wild-type BMCMCs, but not $Il10^{-/-}$ BMCMCs (103). These results indicate that mast-cell-derived IL-10 plays an important role in the inhibition of acute GVHD caused by MHC antigen mismatch.

CONCLUSION

Mast cells act as potential sources of inflammatory and/or regulatory mediators during development of various cutaneous infections and diseases (**Figure 7**). Considerable progress has

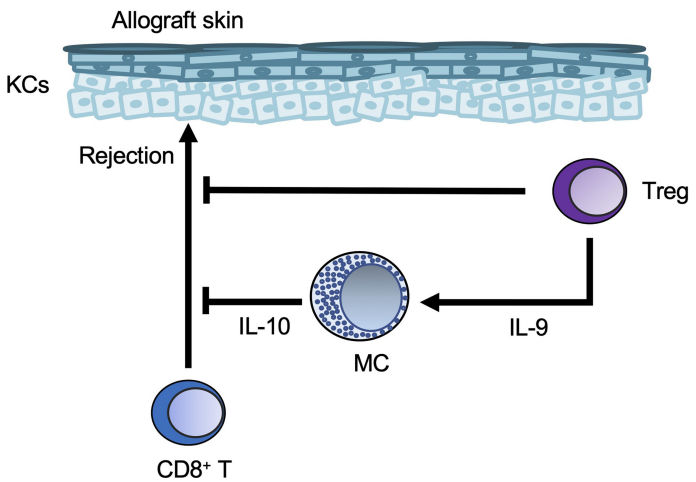


FIGURE 6 | Mast cells in skin allografts. Regulatory T-cell (Treg-)derived IL-9 induces mast cell (MC) accumulation and activation in skin allografts. The Tregs and MCs then suppress CD8+ T-cell-mediated allograft rejection.

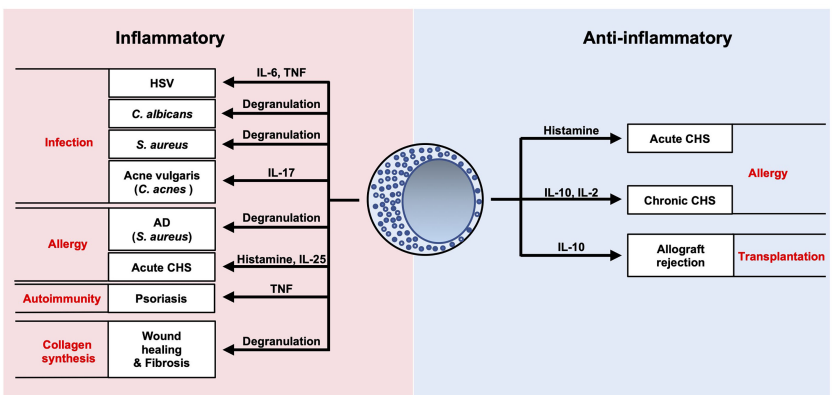


FIGURE 7 | Summary of roles of mast cells in cutaneous diseases. Mast cells are potential sources of inflammatory and/or regulatory mediators during development of various cutaneous infections and diseases.

been made in our understanding of these immune cells in recent years. Further elucidation of the complex interactions of mast cells will potentially lead to novel clinical approaches for various pathological conditions.

AUTHOR CONTRIBUTIONS

TN designed and wrote the manuscript. KH and SN reviewed and revised the manuscript prior to submission. All authors contributed to the article and approved the submitted version.

FUNDING

This work was supported by a Grant-in-Aid for Scientific Research (B)(21H02963 to SN) from the Japan Society for the Promotion of Science, and Precursory Research for Embryonic Science and Technology, Japan Science and Technology Agency (JPMJPR18H6 to SN).

REFERENCES

1. Morita H, Saito H, Matsumoto K, Nakae S. Regulatory Roles of Mast Cells in Immune Responses. *Semin Immunopathol* (2016) 38(5):623–9. doi: 10.1007/s00281-016-0566-0
2. Krystel-Whittemore M, Dileepan KN, Wood JG. Mast Cell: A Multi-Functional Master Cell. *Front Immunol* (2015) 6:620. doi: 10.3389/fimmu.2015.00620
3. Arinobu Y, Iwasaki H, Gurish MF, Mizuno S, Shigematsu H, Ozawa H, et al. Developmental Checkpoints of the Basophil/Mast Cell Lineages in Adult Murine Hematopoiesis. *Proc Natl Acad Sci U.S.A.* (2005) 102(50):18105–10. doi: 10.1073/pnas.0509148102
4. Galli SJ, Grimbaldeston M, Tsai M. Immunomodulatory Mast Cells: Negative, as Well as Positive, Regulators of Immunity. *Nat Rev Immunol* (2008) 8(6):478–86. doi: 10.1038/nri2327
5. Wang Y, Matsushita K, Jackson J, Numata T, Zhang Y, Zhou G, et al. Transcriptome Programming of Il-3-Dependent Bone Marrow-Derived Cultured Mast Cells by Stem Cell Factor (Scf). *Allergy* (2021) 76(7):2288–91. doi: 10.1111/all.14808
6. Ito T, Egusa C, Maeda T, Numata T, Nakano N, Nishiyama C, et al. Il-33 Promotes Mhc Class Ii Expression in Murine Mast Cells. *Immun Inflammation Dis* (2015) 3(3):196–208. doi: 10.1002/iid3.59
7. Irani AA, Schechter NM, Craig SS, DeBlois G, Schwartz LB. Two Types of Human Mast Cells That Have Distinct Neutral Protease Compositions. *Proc Natl Acad Sci U.S.A.* (1986) 83(12):4464–8. doi: 10.1073/pnas.83.12.4464
8. Mukai K, Tsai M, Saito H, Galli SJ. Mast Cells as Sources of Cytokines, Chemokines, and Growth Factors. *Immunol Rev* (2018) 282(1):121–50. doi: 10.1111/imr.12634
9. Turner H, Kinet JP. Signalling Through the High-Affinity Ige Receptor Fc Epsilonri. *Nature* (1999) 402(6760 Suppl):B24–30. doi: 10.1038/35037021
10. Tkaczyk C, Beaven MA, Brachman SM, Metcalfe DD, Gilfillan AM. The Phospholipase C Gamma 1-Dependent Pathway of Fc Epsilon Ri-Mediated Mast Cell Activation Is Regulated Independently of Phosphatidylinositol 3-Kinase. *J Biol Chem* (2003) 278(48):48474–84. doi: 10.1074/jbc.M301350200
11. Burwen SJ. Recycling of Mast Cells Following Degranulation in Vitro: An Ultrastructural Study. *Tissue Cell* (1982) 14(1):125–34. doi: 10.1016/0040-8166(82)90012-x
12. Urb M, Sheppard DC. The Role of Mast Cells in the Defence Against Pathogens. *PloS Pathog* (2012) 8(4):e1002619. doi: 10.1371/journal.ppat.1002619
13. Kunder CA, St John AL, Abraham SN. Mast Cell Modulation of the Vascular and Lymphatic Endothelium. *Blood* (2011) 118(20):5383–93. doi: 10.1182/blood-2011-07-358432
14. Galli SJ, Tsai M. Ige and Mast Cells in Allergic Disease. *Nat Med* (2012) 18(5):693–704. doi: 10.1038/nm.2755
15. Kawasaki T, Kawai T. Toll-Like Receptor Signaling Pathways. *Front Immunol* (2014) 5:461. doi: 10.3389/fimmu.2014.00461
16. Supajatura V, Ushio H, Nakao A, Akira S, Okumura K, Ra C, et al. Differential Responses of Mast Cell Toll-Like Receptors 2 and 4 in Allergy and Innate Immunity. *J Clin Invest* (2002) 109(10):1351–9. doi: 10.1172/jci14704
17. Varadaradjalou S, Féger F, Thieblemont N, Hamouda NB, Pleau JM, Dy M, et al. Toll-Like Receptor 2 (Tlr2) and Tlr4 Differentially Activate Human Mast Cells. *Eur J Immunol* (2003) 33(4):899–906. doi: 10.1002/eji.200323830
18. Orinska Z, Bulanova E, Budagian V, Metz M, Maurer M, Bulfone-Paus S. Tlr3-Induced Activation of Mast Cells Modulates Cd8+ T-Cell Recruitment. *Blood* (2005) 106(3):978–87. doi: 10.1182/blood-2004-07-2656
19. Mannschreck D, Feig J, Selph J, Cohen B. Disseminated Bullous Impetigo and Atopic Dermatitis: Case Series and Literature Review. *Pediatr Dermatol* (2020) 37(1):103–8. doi: 10.1111/pde.14032
20. Liy-Wong C, Pope E, Weinstein M, Lara-Corrales I. Staphylococcal Scalded Skin Syndrome: An Epidemiological and Clinical Review of 84 Cases. *Pediatr Dermatol* (2021) 38(1):149–53. doi: 10.1111/pde.14470
21. Rocha-de-Souza CM, Berent-Maoz B, Mankuta D, Moses AE, Levi-Schaffer F. Human Mast Cell Activation by Staphylococcus Aureus: Interleukin-8 and Tumor Necrosis Factor Alpha Release and the Role of Toll-Like Receptor 2 and Cd48 Molecules. *Infect Immun* (2008) 76(10):4489–97. doi: 10.1128/iai.00270-08
22. Nakamura Y, Oscherwitz J, Cease KB, Chan SM, Muñoz-Planillo R, Hasegawa M, et al. Staphylococcus Δ-Toxin Induces Allergic Skin Disease by Activating Mast Cells. *Nature* (2013) 503(7476):397–401. doi: 10.1038/nature12655
23. Eliasse Y, Leveque E, Garidou L, Battut L, McKenzie B, Nocera T, et al. Il-17 (+) Mast Cell/T Helper Cell Axis in the Early Stages of Acne. *Front Immunol* (2021) 12:740540. doi: 10.3389/fimmu.2021.740540
24. Sakurai A, Yamaguchi N, Sonoyama K. Cell Wall Polysaccharides of Candida Albicans Induce Mast Cell Degranulation in the Gut. *Biosci Microb Food Health* (2012) 31(3):67–70. doi: 10.12938/bmfh.31.67
25. Lopes JP, Stylianou M, Nilsson G, Urban CF. Opportunistic Pathogen Candida Albicans Elicits a Temporal Response in Primary Human Mast Cells. *Sci Rep* (2015) 5:12287. doi: 10.1038/srep12287
26. Trevisan E, Vita F, Medic N, Soranzo MR, Zabucchi G, Borelli V. Mast Cells Kill Candida Albicans in the Extracellular Environment But Spare Ingested Fungi From Death. *Inflammation* (2014) 37(6):2174–89. doi: 10.1007/s10753-014-9951-9
27. De Zuani M, Paolicelli G, Zelante T, Renga G, Romani L, Arzese A, et al. Mast Cells Respond to Candida Albicans Infections and Modulate Macrophages Phagocytosis of the Fungus. *Front Immunol* (2018) 9:2829. doi: 10.3389/fimmu.2018.02829
28. Nieto-Patlán A, Campillo-Navarro M, Rodríguez-Cortés O, Muñoz-Cruz S, Wong-Baeza I, Estrada-Parra S, et al. Recognition of Candida Albicans by Dectin-1 Induces Mast Cell Activation. *Immunobiology* (2015) 220(9):1093–100. doi: 10.1016/j.imbio.2015.05.005
29. Pinke KH, Lima HG, Cunha FQ, Lara VS. Mast Cells Phagocyte Candida Albicans and Produce Nitric Oxide by Mechanisms Involving Tlr2 and Dectin-1. *Immunobiology* (2016) 221(2):220–7. doi: 10.1016/j.imbio.2015.09.004
30. Harada K, Saito M, Sugita T, Tsuboi R. Malassezia Species and Their Associated Skin Diseases. *J Dermatol* (2015) 42(3):250–7. doi: 10.1111/1346-8138.12700
31. Hiragun T, Ishii K, Hiragun M, Suzuki H, Kan T, Mihara S, et al. Fungal Protein Mgl_1304 in Sweat Is an Allergen for Atopic Dermatitis Patients.

J Allergy Clin Immunol (2013) 132(3):608–15.e4. doi: 10.1016/j.jaci.2013.03.047
32. Hiragun M, Hiragun T, Ishii K, Suzuki H, Tanaka A, Yanase Y, et al. Elevated Serum Ige Against Mgl_1304 in Patients With Atopic Dermatitis and Cholinergic Urticaria. *Allergol Int* (2014) 63(1):83–93. doi: 10.2332/allergolint.13-OA-0611
33. Tuddenham S, Hamill MM, Ghanem KG. Diagnosis and Treatment of Sexually Transmitted Infections: A Review. *Jama* (2022) 327(2):161–72. doi: 10.1001/jama.2021.23487
34. Wilkinson DE, Weller SK. The Role of DNA Recombination in Herpes Simplex Virus DNA Replication. *IUBMB Life* (2003) 55(8):451–8. doi: 10.1080/1521654031000161223 7
35. Micali G, Lacarrubba F. Eczema Herpeticum. *N Engl J Med* (2017) 377(7):e9. doi: 10.1056/NEJMicm1701668
36. Kokuba H, Aurelian L, Burnett J. Herpes Simplex Virus Associated Erythema Multiforme (Haem) Is Mechanistically Distinct From Drug-Induced Erythema Multiforme: Interferon-Gamma Is Expressed in Haem Lesions and Tumor Necrosis Factor-Alpha in Drug-Induced Erythema Multiforme Lesions. *J Invest Dermatol* (1999) 113(5):808–15. doi: 10.1046/j.1523-1747.1999.00754.x
37. Aoki R, Kawamura T, Goshima F, Ogawa Y, Nakae S, Nakao A, et al. Mast Cells Play a Key Role in Host Defense Against Herpes Simplex Virus Infection Through Tnf-α and Il-6 Production. *J Invest Dermatol* (2013) 133(9):2170–9. doi: 10.1038/jid.2013.150
38. Aoki R, Kawamura T, Goshima F, Ogawa Y, Nakae S, Moriishi K, et al. The Alarmin Il-33 Derived From Hsv-2-Infected Keratinocytes Triggers Mast Cell-Mediated Antiviral Innate Immunity. *J Invest Dermatol* (2016) 136 (6):1290–2. doi: 10.1016/j.jid.2016.01.030
39. Gefen T, Vaya J, Khatib S, Rapoport I, Lupo M, Barnea E, et al. The Effect of Haptens on Protein-Carrier Immunogenicity. *Immunology* (2015) 144 (1):116–26. doi: 10.1111/imm.12356
40. Gaspari AA, Katz SI, Martin SF. Contact Hypersensitivity. *Curr Protoc Immunol* (2016) 113:4.2.1–7. doi: 10.1002/0471142735.im0402s113
41. Gaudenzio N, Marichal T, Galli SJ, Reber LL. Genetic and Imaging Approaches Reveal Pro-Inflammatory and Immunoregulatory Roles of Mast Cells in Contact Hypersensitivity. *Front Immunol* (2018) 9:1275. doi: 10.3389/fimmu.2018.01275
42. Suto H, Nakae S, Kakurai M, Sedgwick JD, Tsai M, Galli SJ. Mast Cell-Associated Tnf Promotes Dendritic Cell Migration. *J Immunol (Baltimore Md: 1950)* (2006) 176(7):4102–12. doi: 10.4049/jimmunol.176.7.4102
43. Kakurai M, Monteforte R, Suto H, Tsai M, Nakae S, Galli SJ. Mast Cell-Derived Tumor Necrosis Factor Can Promote Nerve Fiber Elongation in the Skin During Contact Hypersensitivity in Mice. *Am J Pathol* (2006) 169 (5):1713–21. doi: 10.2353/ajpath.2006.060602
44. Suto H, Nambu A, Morita H, Yamaguchi S, Numata T, Yoshizaki T, et al. Il-25 Enhances Th17 Cell-Mediated Contact Dermatitis by Promoting Il-1beta Production by Dermal Dendritic Cells. *J Allergy Clin Immunol* (2018) 142 (5):1500–9.e10. doi: 10.1016/j.jaci.2017.12.1007
45. Kim HS, Lee MB, Lee D, Min KY, Koo J, Kim HW, et al. The Regulatory B Cell-Mediated Peripheral Tolerance Maintained by Mast Cell Il-5 Suppresses Oxazolone-Induced Contact Hypersensitivity. *Sci Adv* (2019) 5 (7):eaav8152. doi: 10.1126/sciadv.aav8152
46. Leyva-Castillo JM, Das M, Artru E, Yoon J, Galand C, Geha RS. Mast Cell-Derived Il-13 Downregulates Il-12 Production by Skin Dendritic Cells to Inhibit the T(H)1 Cell Response to Cutaneous Antigen Exposure. *J Allergy Clin Immunol* (2021) 147(6):2305–15.e3. doi: 10.1016/j.jaci.2020.11.036
47. Taketomi Y, Ueno N, Kojima T, Sato H, Murase R, Yamamoto K, et al. Mast Cell Maturation Is Driven *Via* a Group Iii Phospholipase A2-Prostaglandin D2-Dp1 Receptor Paracrine Axis. *Nat Immunol* (2013) 14(6):554–63. doi: 10.1038/ni.2586
48. Taketomi Y, Endo Y, Higashi T, Murase R, Ono T, Taya C, et al. Mast Cell-Specific Deletion of Group Iii Secreted Phospholipase a(2) Impairs Mast Cell Maturation and Functions. *Cells* (2021) 10(7):1691. doi: 10.3390/cells10071691
49. Passani MB, Lin JS, Hancock A, Crochet S, Blandina P. The Histamine H3 Receptor as a Novel Therapeutic Target for Cognitive and Sleep Disorders. *Trends Pharmacol Sci* (2004) 25(12):618–25. doi: 10.1016/j.tips.2004.10.003
50. Inagaki N, Sakurai T, Abe T, Musoh K, Kawasaki H, Tsunematsu M, et al. Characterization of Antihistamines Using Biphasic Cutaneous Reaction in Balb/C Mice. *Life Sci* (1998) 63(11):Pl 145–50. doi: 10.1016/S0024-3205(98)00356-7
51. Griswold DE, Alessi S, Badger AM, Poste G, Hanna N. Differential Sensitivity of T Suppressor Cell Expression to Inhibition by Histamine Type 2 Receptor Antagonists. *J Immunol (Baltimore Md: 1950)* (1986) 137 (6):1811–5.
52. Belsito DV, Kerdel FA, Potozkin J, Soter NA. Cimetidine-Induced Augmentation of Allergic Contact Hypersensitivity Reactions in Mice. *J Invest Dermatol* (1990) 94(4):441–5. doi: 10.1111/1523-1747.ep12874535
53. Garaczi E, Szell M, Janossy T, Koreck A, Pivarcsi A, Buzas E, et al. Negative Regulatory Effect of Histamine in Dnfb-Induced Contact Hypersensitivity. *Int Immunol* (2004) 16(12):1781–8. doi: 10.1093/intimm/dxh179
54. Tatemoto K, Nozaki Y, Tsuda R, Konno S, Tomura K, Furuno M, et al. Immunoglobulin E-Independent Activation of Mast Cell Is Mediated by Mrg Receptors. *Biochem Biophys Res Commun* (2006) 349(4):1322–8. doi: 10.1016/j.bbrc.2006.08.177
55. McNeil BD, Pundir P, Meeker S, Han L, Undem BJ, Kulka M, et al. Identification of a Mast-Cell-Specific Receptor Crucial for Pseudo-Allergic Drug Reactions. *Nature* (2015) 519(7542):237–41. doi: 10.1038/nature14022
56. Plum T, Wang X, Rettel M, Krijgsveld J, Feyerabend TB, Rodewald HR. Human Mast Cell Proteome Reveals Unique Lineage, Putative Functions, and Structural Basis for Cell Ablation. *Immunity* (2020) 52(2):404–16.e5. doi: 10.1016/j.immuni.2020.01.012
57. Babina M, Guhl S, Artuc M, Zuberbier T. Allergic Fcεri- and Pseudo-Allergic Mrgprx2-Triggered Mast Cell Activation Routes Are Independent and Inversely Regulated by Scf. *Allergy* (2018) 73(1):256–60. doi: 10.1111/all.13301
58. Meixiong J, Anderson M, Limjunyawong N, Sabbagh MF, Hu E, Mack MR, et al. Activation of Mast-Cell-Expressed Mas-Related G-Protein-Coupled Receptors Drives Non-Histaminergic Itch. *Immunity* (2019) 50(5):1163–71.e5. doi: 10.1016/j.immuni.2019.03.013
59. Grimbaldeston MA, Nakae S, Kalesnikoff J, Tsai M, Galli SJ. Mast Cell-Derived Interleukin 10 Limits Skin Pathology in Contact Dermatitis and Chronic Irradiation With Ultraviolet B. *Nat Immunol* (2007) 8(10):1095–104. doi: 10.1038/ni1503
60. Dudeck A, Dudeck J, Scholten J, Petzold A, Surianarayanan S, Kohler A, et al. Mast Cells Are Key Promoters of Contact Allergy That Mediate the Adjuvant Effects of Haptens. *Immunity* (2011) 34(6):973–84. doi: 10.1016/j.immuni.2011.03.028
61. Hershko AY, Suzuki R, Charles N, Alvarez-Errico D, Sargent JL, Laurence A, et al. Mast Cell Interleukin-2 Production Contributes to Suppression of Chronic Allergic Dermatitis. *Immunity* (2011) 35(4):562–71. doi: 10.1016/j.immuni.2011.07.013
62. Gimenez-Rivera VA, Siebenhaar F, Zimmermann C, Siiskonen H, Metz M, Maurer M. Mast Cells Limit the Exacerbation of Chronic Allergic Contact Dermatitis in Response to Repeated Allergen Exposure. *J Immunol (Baltimore Md: 1950)* (2016) 197(11):4240–6. doi: 10.4049/jimmunol.1600236
63. Reber LL, Sibilano R, Starkl P, Roers A, Grimbaldeston MA, Tsai M, et al. Imaging Protective Mast Cells in Living Mice During Severe Contact Hypersensitivity. *JCI Insight* (2017) 2(9):e92900. doi: 10.1172/jci.insight.92900
64. Church MK, Kolkhir P, Metz M, Maurer M. The Role and Relevance of Mast Cells in Urticaria. *Immunol Rev* (2018) 282(1):232–47. doi: 10.1111/imr.12632
65. Bracken SJ, Abraham S, MacLeod AS. Autoimmune Theories of Chronic Spontaneous Urticaria. *Front Immunol* (2019) 10:627. doi: 10.3389/fimmu.2019.00627
66. Schmetzer O, Lakin E, Topal FA, Preusse P, Freier D, Church MK, et al. Il-24 Is a Common and Specific Autoantigen of Ige in Patients With Chronic Spontaneous Urticaria. *J Allergy Clin Immunol* (2018) 142(3):876–82. doi: 10.1016/j.jaci.2017.10.035
67. Maurer M, Rosén K, Hsieh HJ, Saini S, Grattan C, Gimenéz-Arnau A, et al. Omalizumab for the Treatment of Chronic Idiopathic or Spontaneous

Urticaria. *N Engl J Med* (2013) 368(10):924–35. doi: 10.1056/NEJMoa1215372
68. Fujisawa D, Kashiwakura J, Kita H, Kikukawa Y, Fujitani Y, Sasaki-Sakamoto T, et al. Expression of Mas-Related Gene X2 on Mast Cells Is Upregulated in the Skin of Patients With Severe Chronic Urticaria. *J Allergy Clin Immunol* (2014) 134(3):622–33.e9. doi: 10.1016/j.jaci.2014.05.004
69. Borici-Mazi R, Kouridakis S, Kontou-Fili K. Cutaneous Responses to Substance P and Calcitonin Gene-Related Peptide in Chronic Urticaria: The Effect of Cetirizine and Dimethindene. *Allergy* (1999) 54(1):46–56. doi: 10.1034/j.1398-9995.1999.00726.x
70. Kay AB, Clark P, Maurer M, Ying S. Elevations in T-Helper-2-Initiating Cytokines (Interleukin-33, Interleukin-25 and Thymic Stromal Lymphopoietin) in Lesional Skin From Chronic Spontaneous ('Idiopathic') Urticaria. *Br J Dermatol* (2015) 172(5):1294–302. doi: 10.1111/bjd.13621
71. Williams H, Flohr C. How Epidemiology Has Challenged 3 Prevailing Concepts About Atopic Dermatitis. *J Allergy Clin Immunol* (2006) 118 (1):209–13. doi: 10.1016/j.jaci.2006.04.043
72. Simon D, Vassina E, Yousefi S, Kozlowski E, Braathen LR, Simon HU. Reduced Dermal Infiltration of Cytokine-Expressing Inflammatory Cells in Atopic Dermatitis After Short-Term Topical Tacrolimus Treatment. *J Allergy Clin Immunol* (2004) 114(4):887–95. doi: 10.1016/j.jaci.2004.05.066
73. Katoh N, Ohya Y, Ikeda M, Ebihara T, Katayama I, Saeki H, et al. Japanese Guidelines for Atopic Dermatitis 2020. *Allergol Int* (2020) 69(3):356–69. doi: 10.1016/j.alit.2020.02.006
74. Gao PS, Rafaels NM, Hand T, Murray T, Boguniewicz M, Hata T, et al. Filaggrin Mutations That Confer Risk of Atopic Dermatitis Confer Greater Risk for Eczema Herpeticum. *J Allergy Clin Immunol* (2009) 124(3):507–13, 13.e1-7. doi: 10.1016/j.jaci.2009.07.034
75. Moniaga CS, Egawa G, Kawasaki H, Hara-Chikuma M, Honda T, Tanizaki H, et al. Flaky Tail Mouse Denotes Human Atopic Dermatitis in the Steady State and by Topical Application With Dermatophagoides Pteronyssinus Extract. *Am J Pathol* (2010) 176(5):2385–93. doi: 10.2353/ajpath.2010.090957
76. Salimi M, Barlow JL, Saunders SP, Xue L, Gutowska-Owsiak D, Wang X, et al. A Role for Il-25 and Il-33-Driven Type-2 Innate Lymphoid Cells in Atopic Dermatitis. *J Exp Med* (2013) 210(13):2939–50. doi: 10.1084/jem.20130351
77. Kim BS, Siracusa MC, Saenz SA, Noti M, Monticelli LA, Sonnenberg GF, et al. Tslp Elicits Il-33-Independent Innate Lymphoid Cell Responses to Promote Skin Inflammation. *Sci Transl Med* (2013) 5(170):170ra16. doi: 10.1126/scitranslmed.3005374
78. Svanberg S, Li Z, Öhlund P, Roy A, Åbrink M. Mast Cells Limit Ear Swelling Independently of the Chymase Mouse Mast Cell Protease 4 in an Mc903-Induced Atopic Dermatitis-Like Mouse Model. *Int J Mol Sci* (2020) 21 (17):6311. doi: 10.3390/ijms21176311
79. Yamada Y, Ueda Y, Nakamura A, Kanayama S, Tamura R, Hashimoto K, et al. Immediate-Type Allergic and Protease-Mediated Reactions Are Involved in Scratching Behaviour Induced by Topical Application of Dermatophagoides Farinae Extract in Nc/Nga Mice. *Exp Dermatol* (2018) 27(4):418–26. doi: 10.1111/exd.13322
80. Kamo A, Negi O, Tengara S, Kamata Y, Noguchi A, Ogawa H, et al. Histamine H(4) Receptor Antagonists Ineffective Against Itch and Skin Inflammation in Atopic Dermatitis Mouse Model. *J Invest Dermatol* (2014) 134(2):546–8. doi: 10.1038/jid.2013.351
81. Werfel T, Layton G, Yeadon M, Whitlock L, Osterloh I, Jimenez P, et al. Efficacy and Safety of the Histamine H(4) Receptor Antagonist Zpl-3893787 in Patients With Atopic Dermatitis. *J Allergy Clin Immunol* (2019) 143 (5):1830–7.e4. doi: 10.1016/j.jaci.2018.07.047
82. Simpson EL, Bieber T, Guttman-Yassky E, Beck LA, Blauvelt A, Cork MJ, et al. Two Phase 3 Trials of Dupilumab Versus Placebo in Atopic Dermatitis. *N Engl J Med* (2016) 375(24):2335–48. doi: 10.1056/NEJMoa1610020
83. Wang HH, Li YC, Huang YC. Efficacy of Omalizumab in Patients With Atopic Dermatitis: A Systematic Review and Meta-Analysis. *J Allergy Clin Immunol* (2016) 138(6):1719–22.e1. doi: 10.1016/j.jaci.2016.05.038
84. Nakamura M, Toyoda M, Morohashi M. Pruritogenic Mediators in Psoriasis Vulgaris: Comparative Evaluation of Itch-Associated Cutaneous Factors. *Br J Dermatol* (2003) 149(4):718–30. doi: 10.1046/j.1365-2133.2003.05586.x
85. Zhang Y, Shi Y, Lin J, Li X, Yang B, Zhou J. Immune Cell Infiltration Analysis Demonstrates Excessive Mast Cell Activation in Psoriasis. *Front Immunol* (2021) 12:773280. doi: 10.3389/fimmu.2021.773280
86. van der Fits L, Mourits S, Voerman JS, Kant M, Boon L, Laman JD, et al. Imiquimod-Induced Psoriasis-Like Skin Inflammation in Mice Is Mediated *Via* the Il-23/Il-17 Axis. *J Immunol (Baltimore Md: 1950)* (2009) 182 (9):5836–45. doi: 10.4049/jimmunol.0802999
87. Garzorz-Stark N, Lauffer F, Krause L, Thomas J, Atenhan A, Franz R, et al. Toll-Like Receptor 7/8 Agonists Stimulate Plasmacytoid Dendritic Cells to Initiate T. *J Allergy Clin Immunol* (2018) 141(4):1320–33.e11. doi: 10.1016/j.jaci.2017.07.045
88. Heib V, Becker M, Warger T, Rechtsteiner G, Tertilt C, Klein M, et al. Mast Cells Are Crucial for Early Inflammation, Migration of Langerhans Cells, and Ctl Responses Following Topical Application of Tlr7 Ligand in Mice. *Blood* (2007) 110(3):946–53. doi: 10.1182/blood-2006-07-036889
89. Hao Y, Peng B, Che D, Zheng Y, Kong S, Liu R, et al. Imiquimod-Related Dermatitis Is Mainly Mediated by Mast Cell Degranulation *Via* Mas-Related G-Protein Coupled Receptor B2. *Int Immunopharmacol* (2020) 81:106258. doi: 10.1016/j.intimp.2020.106258
90. Wulff BC, Wilgus TA. Mast Cell Activity in the Healing Wound: More Than Meets the Eye? *Exp Dermatol* (2013) 22(8):507–10. doi: 10.1111/exd.12169
91. Weller K, Foitzik K, Paus R, Syska W, Maurer M. Mast Cells Are Required for Normal Healing of Skin Wounds in Mice. *FASEB J: Off Publ Fed Am Soc Exp Biol* (2006) 20(13):2366–8. doi: 10.1096/fj.06-5837fje
92. Wulff BC, Parent AE, Meleski MA, DiPietro LA, Schrementi ME, Wilgus TA. Mast Cells Contribute to Scar Formation During Fetal Wound Healing. *J Invest Dermatol* (2012) 132(2):458–65. doi: 10.1038/jid.2011.324
93. Levi-Schaffer F, Kupietzky A. Mast Cells Enhance Migration and Proliferation of Fibroblasts Into an in Vitro Wound. *Exp Cell Res* (1990) 188(1):42–9. doi: 10.1016/0014-4827(90)90275-f
94. Hawkins RA, Claman HN, Clark RA, Steigerwald JC. Increased Dermal Mast Cell Populations in Progressive Systemic Sclerosis: A Link in Chronic Fibrosis? *Ann Intern Med* (1985) 102(2):182–6. doi: 10.7326/0003-4819-102-2-182
95. Garbuzenko E, Nagler A, Pickholtz D, Gillery P, Reich R, Maquart FX, et al. Human Mast Cells Stimulate Fibroblast Proliferation, Collagen Synthesis and Lattice Contraction: A Direct Role for Mast Cells in Skin Fibrosis. *Clin Exp Allergy: J Br Soc Allergy Clin Immunol* (2002) 32(2):237–46. doi: 10.1046/j.1365-2222.2002.01293.x
96. Shiota N, Kakizoe E, Shimoura K, Tanaka T, Okunishi H. Effect of Mast Cell Chymase Inhibitor on the Development of Scleroderma in Tight-Skin Mice. *Br J Pharmacol* (2005) 145(4):424–31. doi: 10.1038/sj.bjp.0706209
97. Everett ET, Pablos JL, Harley RA, LeRoy EC, Norris JS. The Role of Mast Cells in the Development of Skin Fibrosis in Tight-Skin Mutant Mice. *Comp Biochem Physiol A Physiol* (1995) 110(2):159–65. doi: 10.1016/0300-9629(94)00127-f
98. Hobo A, Harada K, Maeda T, Uchiyama M, Irisawa R, Yamazaki M, et al. Il-17-Positive Mast Cell Infiltration in the Lesional Skin of Lichen Planopilaris: Possible Role of Mast Cells in Inducing Inflammation and Dermal Fibrosis in Cicatricial Alopecia. *Exp Dermatol* (2020) 29(3):273–7. doi: 10.1111/exd.13816
99. Lu LF, Lind EF, Gondek DC, Bennett KA, Gleeson MW, Pino-Lagos K, et al. Mast Cells Are Essential Intermediaries in Regulatory T-Cell Tolerance. *Nature* (2006) 442(7106):997–1002. doi: 10.1038/nature05010
100. Hara M, Kingsley CI, Niimi M, Read S, Turvey SE, Bushell AR, et al. Il-10 Is Required for Regulatory T Cells to Mediate Tolerance to Alloantigens in Vivo. *J Immunol* (2001) 166(6):3789–96. doi: 10.4049/jimmunol.166.6.3789
101. Wu KN, Emmons RV, Lisanti MP, Farber JL, Witkiewicz AK. Foxp3-Expressing T Regulatory Cells and Mast Cells in Acute Graft-Versus-Host Disease of the Skin. *Cell Cycle* (2009) 8(21):3601–5. doi: 10.4161/cc.8.21.9999
102. Murphy GF, Sueki H, Teuscher C, Whitaker D, Korngold R. Role of Mast Cells in Early Epithelial Target Cell Injury in Experimental Acute Graft-Versus-Host Disease. *J Invest Dermatol* (1994) 102(4):451–61. doi: 10.1111/1523-1747.ep12373016
103. Leveson-Gower DB, Sega EI, Kalesnikoff J, Florek M, Pan Y, Pierini A, et al. Mast Cells Suppress Murine Gvhd in a Mechanism Independent of Cd4

+Cd25+ Regulatory T Cells. *Blood* (2013) 122(22):3659–65. doi: 10.1182/blood-2013-08-519157

Conflict of Interest: The authors declare that the research was conducted in the absence of any commercial or financial relationships that could be construed as a potential conflict of interest.

Publisher's Note: All claims expressed in this article are solely those of the authors and do not necessarily represent those of their affiliated organizations, or those of the publisher, the editors and the reviewers. Any product that may be evaluated in this article, or claim that may be made by its manufacturer, is not guaranteed or endorsed by the publisher.

Copyright © 2022 Numata, Harada and Nakae. This is an open-access article distributed under the terms of the Creative Commons Attribution License (CC BY). The use, distribution or reproduction in other forums is permitted, provided the original author(s) and the copyright owner(s) are credited and that the original publication in this journal is cited, in accordance with accepted academic practice. No use, distribution or reproduction is permitted which does not comply with these terms.

frontiers | Frontiers in Immunology

TYPE Brief Research Report
PUBLISHED 19 July 2022
DOI 10.3389/fimmu.2022.902652

Check for updates

OPEN ACCESS

EDITED BY
Satoshi Tanaka,
Kyoto Pharmaceutical University, Japan

REVIEWED BY
David Andrew Fulcher,
Australian National University, Australia
Barbara Rogala,
University of Silesia in Katowice, Poland

*CORRESPONDENCE
Martin Metz
martin.metz@charite.de

SPECIALTY SECTION
This article was submitted to Inflammation, a section of the journal Frontiers in Immunology

RECEIVED 23 March 2022
ACCEPTED 29 June 2022
PUBLISHED 19 July 2022

CITATION
Sauer M, Scheffel J, Frischbutter S, Mahnke N, Maurer M, Burmeister T, Krause K and Metz M (2022) STAT3 Gain-of-Function Is Not Responsible for Low Total IgE Levels in Patients With Autoimmune Chronic Spontaneous Urticaria.
Front. Immunol. 13:902652.
doi: 10.3389/fimmu.2022.902652

COPYRIGHT
© 2022 Sauer, Scheffel, Frischbutter, Mahnke, Maurer, Burmeister, Krause and Metz. This is an open-access article distributed under the terms of the Creative Commons Attribution License (CC BY). The use, distribution or reproduction in other forums is permitted, provided the original author (s) and the copyright owner(s) are credited and that the original publication in this journal is cited, in accordance with accepted academic practice. No use, distribution or reproduction is permitted which does not comply with these terms.

STAT3 gain-of-function is not responsible for low total IgE levels in patients with autoimmune chronic spontaneous urticaria

Merle Sauer[1], Jörg Scheffel[1,2], Stefan Frischbutter[1,2], Niklas Mahnke[1,2], Marcus Maurer[1,2], Thomas Burmeister[3], Karoline Krause[1,2] and Martin Metz[1,2]*

[1]Institute of Allergology, Charité - Universitätsmedizin Berlin, Berlin, Germany, [2]Fraunhofer Institute for Translational Medicine and Pharmacology (ITMP), Allergology and Immunology, Berlin, Germany, [3]Department of Hematology, Oncology and Tumor Immunology, Campus Virchow-Klinikum, Charité - Universitätsmedizin Berlin, Berlin, Germany

Background: The pathogenesis of chronic spontaneous urticaria (CSU) has not been clarified entirely. Type IIb autoimmune chronic spontaneous urticaria (CSU^{aiTIIb}) is a distinct subtype of CSU that is often difficult to treat and is connected to low levels of total IgE. Previous findings indicate that an enhanced signal transducer and activator of transcription 3 (STAT3) may be responsible for reduced IgE serum levels.

Objective: Our aim was to investigate a possible underlying gain-of-function mutation or activating polymorphism in *STAT3* that could be responsible for the low levels of IgE in patients with CSU^{aiTIIb}.

Methods: We included 10 patients with CSU^{aiTIIb} and low levels of IgE and sequenced selected single nucleotide polymorphisms (SNP) in *STAT3* associated with common autoimmune diseases. Exon sequencing was performed for the most relevant exons of *STAT3*. To test for a gain-of-function of STAT3, we performed a phospho-specific flow cytometry analysis of STAT3 in peripheral blood mononuclear cells before and after stimulation with interleukin-6.

Results: No differences were found in the prevalence of the tested SNPs between our patients and a control population. Moreover, we could not find any mutations or variants on the tested exons of *STAT3*. The function of STAT3 was also not altered in our patients.

Conclusion: In total, we could not find any evidence for our hypothesis that low IgE in patients with CSU^{aiTIIb} is linked to mutations in *STAT3* or altered activity of STAT3. Thus, it remains to be discovered what causes the low serum levels of IgE in patients with CSU^{aiTIIb}.

KEYWORDS

autoimmune disease, autoreactivity, basophil activation test, chronic spontaneous urticaria, gain-of-function mutation, immunoglobulin E, mast cell, signal transducer and activator of transcription 3

Introduction

Chronic spontaneous urticaria (CSU) is a common mast cell-driven skin disease, characterized by the occurrence of itchy wheals, recurrent angioedema, or both (1). In CSU, total immunoglobulin E (IgE) levels have been found to be elevated in a large proportion of patients (2, 3) and it is thought to play an important role in the pathogenesis of CSU. Despite this, there are some patients who present with low or very low levels of total IgE (4, 5). These patients are especially difficult to treat and are more often non-responders to treatment with Omalizumab, a therapeutic anti-IgE antibody, than those with normal or elevated total IgE (6–9). Moreover, patients with clearly defined type IIb autoimmune CSU (CSU^{aiTIIb}), a subtype of CSU in which IgG autoantibodies against IgE or its high affinity receptor FcεRI are present, express significantly lower levels of total IgE and a higher rate of other autoimmune parameters than those without it (10). It is, as of yet, unclear why this population of CSU patients exhibit such low levels of IgE and others do not.

Several findings from previous studies and observations suggest that enhanced signal transducer and activator of transcription 3 (STAT3) signaling may be responsible for the observed effects in the above-described patients. For example, a loss-of-function mutation in *STAT3* is responsible for the development of the hyper-IgE-syndrome, a condition characterized by extremely high levels of IgE and the development of recurrent infections of the skin, sinusoids and lungs (11). Interestingly, and despite the massively increased IgE levels, mast cell activation and degranulation are reduced in these patients. In contrast, gain-of-function mutations in *STAT3* are not only associated with greatly reduced IgE levels (12) but also with much higher rates of other autoimmune disorders (13–15). Moreover, Luo *et al.* investigated the JAK-STAT3 signaling pathway in CSU and found that in patients with CSU^{aiTIIb}, there is a stronger expression of genes of the JAK-STAT3 signaling pathway, including STAT3 in the skin, compared to healthy subjects (16). Single nucleotide polymorphisms (SNP) in STAT3 have been found to be of relevance in autoimmune diseases (**Table 1**). Especially the incidence of thyroid autoimmune diseases is higher in patients with CSU, in particular CSU^{aiTIIb} (29).

Taking all this together, we hypothesized that gain-of-function mutations or activating polymorphisms in the *STAT3* gene may be present in patients with CSU^{aiTIIb} and low levels of total IgE.

Abbreviations: BAT, Basophil activation test; CSU, Chronic spontaneous urticaria; CSU^{aiTIIb}, Type IIb autoimmune chronic spontaneous urticaria; IgE, Immunoglobulin E; IL-6, Interleukin-6; PBMC, Peripheral blood mononuclear cells; pSTAT3, Phosphorylated signal transducer and activator of transcription; SNP, Single nucleotide polymorphism; STAT3, Signal transducer and activator of transcription 3; UAS, Urticaria activity score.

Methods

Characterization of the patients

We included 10 patients with CSU^{aiTIIb} who had been treated at the Urticaria Reference and Excellence Center (UCARE) (30) at Charitеí - Universitätsmedizin Berlin. All patients provided oral and written informed consent that included the publication of their pseudonymized data. The study was approved by the Ethics Committee of Charitеí - Universitätsmedizin Berlin, Germany.

We selected patients with low total IgE levels and CSU^{aiTIIb}. Less than 40 kU/l was chosen as a cut-off for low IgE levels, as this had previously been reported to be of significance in patients with CSU^{aiTIIb} (10, 31).

As a marker for CSU^{aiTIIb} we chose the basophil activation test (BAT), which is one of three obligatory criteria for defining CSU^{aiTIIb}, as proposed by the European Academy of Allergy and Clinical Immunology (32). The BAT is positive if healthy donor basophils degranulate due to autoantibodies present in the patients' serum. The BAT was performed as previously

described (4). Briefly, the patient's serum was thawed and incubated with fresh basophils taken from a healthy donor. Following washing and centrifugation, cells were stained with CD3, CD193 and the basophil activation markers CD63 and CD203c for measurement in flow cytometry. The BAT was considered positive, if more than 7.77% of the total basophils were both CD63 and CD203c positive. Only patients with a high proportion of double positive basophils were included in the study.

The disease activity of the patients was measured using the 7-day once-daily urticaria activity score (UAS7) (1). Additionally, patients were screened for concomitant recurrent angioedema and presence of autoimmune diseases. Among others, anti-neutrophil cytoplasmic antibodies (ANCA; considered elevated if cANCA ≥10 U/ml, pANCA ≥5 U/ml) and anti-nuclear antibodies (ANA; considered elevated if ≥1:160) were measured in patients' serum.

Single nucleotide polymorphism (SNP) analyses of *STAT3*

Peripheral venous blood was collected from the subjects in an EDTA tube and different SNPs in *STAT3* that were found to be of relevance in other autoimmune diseases (rs1053005, rs3816769, rs6503695, rs9891119, rs744166 and rs1026916; **Table 1**) were analyzed. Cells were lysed and genomic DNA was isolates using Gentra Puregene kit (Cat#158422, QIAGEN, Hilden, Germany) as specified by the manufacturer. PCR products were generated using the HotStarTaq Master Mix kit (Cat#20344, QIAGEN, Hilden, Germany) according to manufacturer's instructions with the primers shown in the **Supplementary Table 1**. The thermocycler protocol was the following: 95°C for 15 min, then 35 cycles of 95°C for 30 s, 63°C for 30 s, 72°C for 30 s. Genotyping of selected SNPs was performed by Sanger sequencing (PlateSeq Service, 96w including sample clean-up, Eurofins Genomics, Ebersberg, Germany) using forward primers (**Supplementary Table 1**). A European (non-Finnish) healthy population taken from the Genome Aggregation Database (gnomAD) v2.1.1 (n=60.146) served as control group (33).

Exon sequencing of *STAT3*

We decided to perform exon sequencing of specific exons of *STAT3* only (exons 10, 11, 13, 14, 21, 22 and 23), as most of the autoimmune-associated gain-of-function variants reported were found here (15). For the exon sequencing, blood was also taken from ten healthy volunteers as controls and to verify the quality of the samples. Genomic DNA was extracted by DNEasy Blood & Tissue Kit (Cat#69506, QIAGEN, Hilden, Germany) as specified by the manufacturer and relevant exons were amplified by PCR using Taq PCR Core Kit (Cat#201225, QIAGEN, Hilden, Germany) according to manufacturer's instructions and using the primers listed in **Supplementary Table 2**. The thermocycler protocol was 5 min at 94°C, followed by 35 cycles of 30 s at 94°C, 30 s at 54 – 58°C (depending on primer pair), 30 s at 72°C, followed by 5 min at 72°C final elongation. Genotyping was performed by Sanger sequencing (PlateSeq Service, 96w including sample clean-up, Eurofins Genomics, Ebersberg, Germany) using forward primers (**Supplementary Table 2**).

Analyses of functional gain-of-function of STAT3

To test functional relevance of possible gain-of-function variants of STAT3, we performed a phospho-specific analysis of STAT3 by flow cytometry before and after stimulation with interleukin-6 (IL-6). The test was performed on peripheral blood mononuclear cells (PBMC) isolated from heparinized blood of four of the patients and of four healthy controls. The PBMCs were stimulated with 20 ng/ml human IL-6 (Cat#200-06-20, PeproTech, Hamburg, Germany) for 15 min at 37°C and stored after fixation and permeabilization with formaldehyde (2%) and addition of 90% ice cold methanol. Before analysis with flow cytometry (MACS Quant, Miltenyi Biotec, Bergisch Gladbach, Germany), the cells were stained with phosphorylated STAT3 (pSTAT3) antibody (Cat#612569, Biolegend, San Diego, CA) in PBS with 1% bovine serum albumin for 30 min at room temperature. The analysis was performed using FlowJo (v.10.6.1, BD Biosciences, Franklin Lakes, NJ) and the

TABLE 1 Selected single nucleotide polymorphisms in *STAT3* associated with common autoimmune diseases.

SNP	Associated autoimmune diseases
rs1053005	Grave's disease and hashimoto thyreoditis (17)
rs3816769	Grave's disease and hashimoto thyreoditis (18), type 1 diabetes (19)
rs6503695	Ankylosing spondylitis (20)
rs9891119	Crohn's disease and ulcerative colitits (21)
rs744166	Crohn's disease and ulcerative colitits (22–24), ankylosing spondylitis (20), grave's disease and hashimoto thyreoditis (17), multiple sclerosis (25–27), psoriatic arthritis (28)
rs1026916	Crohn's disease, ulcerative colitits (27)

10.3389/fimmu.2022.902652

Statistical Package for the Social Science (IBM SPSS version 27; IBM Corp, New York, NY).

Results

Ten patients were included in the study, all of them being female with a median age of 51 years and a median disease duration of one year (Table 2). Median total IgE levels were 8.50 kU/l and all patients had a positive BAT, with a median of 54.1% for CD63/CD203c double positive cells. Eight out of ten patients had concomitant recurrent angioedema and six had either a diagnosed autoimmune disease or elevated levels of ANA or ANCA. The disease activity of the patients differed a lot, ranging from an UAS7 score of 3 up to 35.

The allele frequencies found for the six different SNPs in the *STAT3* gene that we analyzed showed no major differences between the patients and the control group (Table 3).

Exon sequencing was performed for *STAT3* exons 10, 11, 13, 14, 21, 22 and 23. No pathogenic variants or polymorphisms were found in the ten patients. Sequencing performed on controls showed good quality in all of the probes and no differences as compared to the patients' samples.

To test for an enhanced activation of STAT3, we assessed the rate of pSTAT3 after stimulation with IL-6 using phospho-specific flow cytometry. The mean fluorescent intensity (MFI) of pSTAT3 of patients and controls before and after stimulation with IL-6 is depicted in Figure 1A. For this, no significant differences between the groups could be found (Mann-Whitney-U, p=0.89 and p=0.49). Figure 1B shows the MFI for each patient and control individually and indicates the individual ratios. The mean ratio of the MFI of pSTAT3 before and after stimulation with IL-6 was 1.65 (range 1.44-1.97) in the patient group as compared to 1.40 in the control group (range 0.89-1.88) and the ratios also did not differ significantly between the two groups (Mann-Whitney-U, p=0.69).

Discussion

In this study, we examined ten patients with CSU^{aiTIIb} and very low total levels of IgE. We hypothesized that a gain-of-function mutation or activating polymorphism in *STAT3* may be responsible for the very low levels of IgE observed in patients with CSU^{aiTIIb}. However, we could not find any known pathogenic variants at the most common sites of *STAT3*. Moreover, we analyzed the most frequent SNPs in *STAT3* and found that these are not expressed exceptionally more or less compared to the control cohort. Additionally, no substantial increase of STAT3 function as analyzed by phospho-specific flow cytometry was detected. In total, we could not find enough evidence supporting our initial hypothesis.

The study has some limitations that prevent us from drawing definitive conclusions about the role of STAT3 in CSU. First, the number of patients included in the study was quite small. Especially SNP analysis should ideally be done on large patient samples in order to make a statement about the role of the different variants. Furthermore, for future experiments, it would be of interest to also include CSU patients with normal and/or elevated IgE levels and to compare for instance the amount of STAT3 expressed between distinct subtypes of CSU patients.

In addition, we sequenced only the exons of *STAT3* in which most mutations were described. Thus, although we looked at many different aspects of the *STAT3* gene and its function, including phospho-specific flow cytometry of pSTAT3, we cannot rule out that there might be other, possibly not yet discovered, mutations in some of the other exons or even the introns of this gene.

TABLE 2 Patient characteristics.

Patient	Age in years	Disease duration in years	Total IgE in kU/l	CD63 and CD203c positive cells in BAT	UAS7 (0-42)	Concomitant conditions
1	52	7.0	20.90	75.6%	–	Angioedema, ANA elevated (1:160)
2	60	2.0	17.00	64.3%	24	Angioedema, Hashimoto thyroiditis
3	27	8.0	10.10	44.7%*	–	Angioedema, Morbus Basedow
4	66	1.2	6.92	66.7%	14	Angioedema
5	49	1.0	6.30	21.1%	35	Angioedema, ANA elevated (1:160), pANCA elevated (7,2 U/ml)
6	72	0.8	3.25	13.6%	3	Angioedema
7	81	40.0	<2.00	82.2%	21	Angioedema, ANA elevated (1:1280)
8	26	1.0	10.80	33.0%	35	–
9	25	0.8	14.70	70.0%	–	Angioedema, Hashimoto thyroiditis
10	31	0.3	<2.00	43.9%	30	–
Median	**51**	**1.1**	**8.50**	**54.5%**	**24**	

ANA, Anti-nuclear antibodies; ANCA, Anti-neutrophil cytoplasmic antibodies; BAT, Basophil activation test; IgE, Immunoglobulin E; UAS7, 7-day once-daily urticaria activity score.
**For patient 3 the percentage of CD63 positive cells in the BAT is shown only, as no CD203c value was calculated.*

TABLE 3 Allele frequencies of six single nucleotide polymorphisms in *STAT3* in ten patients with CSU^{aiTIIb} compared to controls.

Single nucleotide polymorphism	rs1053005	rs3816769	rs6503695	rs9891119	rs744166	rs1026916
Single nucleotide variant	T-C	T-C	T-C	A-C	A-G	A-G
Minor allele frequency patients (n = 10)	0,25	0,30	0,35	0,30	0,35	0,70
Minor allele frequency controls (n = 60.146)	0,18	0,31	0,30	0,33	0,38	0,67

A European (non-Finnish) healthy population taken from the Genome Aggregation Database (gnomAD) v2.1.1 (n=60.146) served as control group (33).

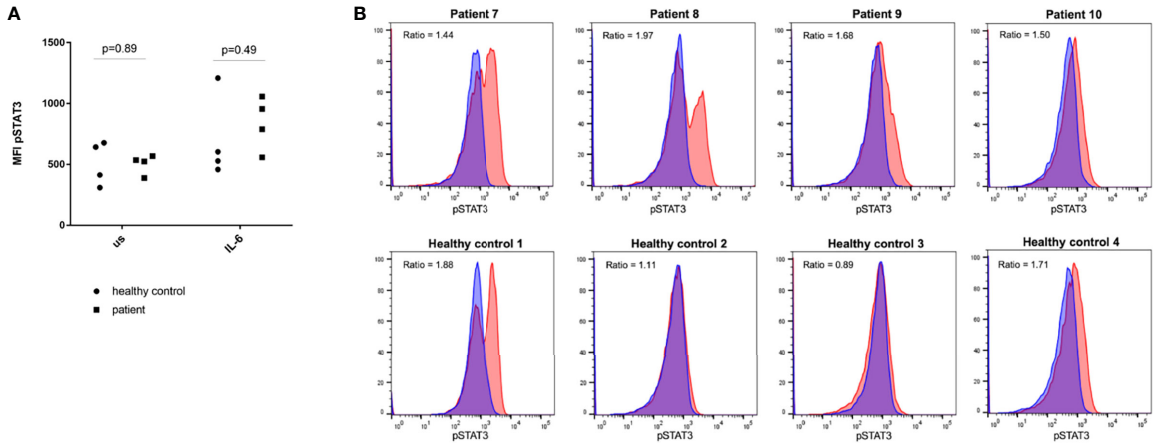


FIGURE 1
Phospho-specific flow cytometry analysis of STAT3 in peripheral blood mononuclear cells of four patients with CSU^{aiTIIb} and four healthy controls. **(A)** shows values of mean fluorescent intensity (MFI) of phosphorylated STAT3 (pSTAT3) for patients compared to healthy controls in unstimulated cells (us) and after stimulation with interleukin-6 (IL-6). For statistical comparison a Mann-Whitney-U test was performed. **(B)** shows the amount of pSTAT3 before (blue) and after (red) stimulation with IL-6 for each individual in a histogram. The ratio of the MFI of pSTAT3 before and after stimulation is indicated.

It therefore remains to be determined what the causes of the low IgE levels in CSU^{aiTIIb} patients are. Potential alternative explanations include effects on T and B cells. For example, increased frequencies of Th2 and Th17 cells have been found in lesional skin of patients with CSU (34). Th1 and Th17 mediated immune pathways, such as IFN-γ and IL-21 have been shown to decrease IgE levels (35). Thus, it can be speculated that the activity of Th17 cells in CSU is responsible for low levels of IgE in CSU. It might therefore be interesting to compare the number of Th17 cells between CSU patients with and without low IgE levels.

Another explanation for low levels of IgE in patients with CSU^{aiTIIb} could be a B-cell defect in these patients, leading to an impaired antibody class switch with imbalanced immunoglobulin production. Recent findings show that CSU patients with low IgE levels often also express lower IgA and IgG levels and higher IgM levels, which supports this hypothesis (4).

A better understanding of the diverse pathogenesis of CSU should be the aim of future studies. Especially in CSU^{aiTIIb}, current treatment options are limited and knowledge about the underlying pathogenesis may help to identify appropriate and optimal therapies for each patient and to decrease the disease burden in patients with CSU.

Data availability statement

The raw data supporting the conclusions of this article will be made available by the authors, without undue reservation.

Ethics statement

The studies involving human participants were reviewed and approved by Ethics Committee of Chariteí - Universitätsmedizin Berlin, Germany. The patients/participants provided their written informed consent to participate in this study.

Author contributions

MS, MMe, and KK substantially contributed to the conception and design of the study, performed analyses and interpretation of the data and drafted the manuscript. MS and NM performed the cellular assays and prepared the blood

samples for the exon sequencing. TB contributed to the methodology of the genetic analyses and performed the preparation of the blood samples for the SNP analyses. JS and SF substantially contributed to the development and interpretation of laboratory tests. JS, SF, TB, and MMa provided critical input to the manuscript. All authors were involved in the final approval of the version to be published.

Funding

This study was funded by intramural grants only. MS was supported by a medical doctoral research stipend funded by Charité and Berlin Institute of Health.

Acknowledgments

We would like to thank all patients for their participation in our study. Furthermore, we thank Daniela Gröger for her excellent technical work.

Conflict of interest

The authors declare that the research was conducted in the absence of any commercial or financial relationships that could be construed as a potential conflict of interest.

Publisher's note

All claims expressed in this article are solely those of the authors and do not necessarily represent those of their affiliated organizations, or those of the publisher, the editors and the reviewers. Any product that may be evaluated in this article, or claim that may be made by its manufacturer, is not guaranteed or endorsed by the publisher.

Supplementary material

The Supplementary Material for this article can be found online at: https://www.frontiersin.org/articles/10.3389/fimmu.2022.902652/full#supplementary-material

References

1. Zuberbier T, Abdul Latiff AH, Abuzakouk M, Aquilina S, Asero R, Baker D, et al. The international EAACI/GA²LEN/EuroGuiDerm/APAAACI guideline for the definition, classification, diagnosis, and management of urticaria. *Allergy* (2021) 77(3):734–66. doi: 10.26416/Aler.6.4.2021.5815

2. Kessel A, Helou W, Bamberger E, Sabo E, Nusem D, Panassof J, et al. Elevated serum total IgE–a potential marker for severe chronic urticaria. *Int Arch Allergy Immunol* (2010) 153(3):288–93. doi: 10.1159/000314370

3. Altrichter S, Fok JS, Jiao Q, Kolkhir P, Pyatilova P, Romero SM, et al. Total IgE as a marker for chronic spontaneous urticaria. *Allergy Asthma Immunol Res* (2021) 13(2):206–18. doi: 10.4168/aair.2021.13.2.206

4. Sauer M, Scheffel J, Frischbutter S, Kolkhir P, Xiang YK, Siebenhaar F, et al. Lower IgA levels in chronic spontaneous urticaria are associated with lower IgE levels and autoimmunity. *Front Immunol* (2021) 12:657211. doi: 10.3389/fimmu.2021.657211

5. Kolkhir P, Kovalkova E, Chernov A, Danilycheva I, Krause K, Sauer M, et al. Autoimmune chronic spontaneous urticaria detection with IgG anti-TPO and total IgE. *J Allergy Clin Immunol Pract* (2021) 9(11):4138–46.e8. doi: 10.1016/j.jaip.2021.07.043

6. Weller K, Ohanyan T, Hawro T, Ellrich A, Sussman G, Koplowitz J, et al. Total IgE levels are linked to the response of chronic spontaneous urticaria patients to omalizumab. *Allergy* (2018) 73(12):2406–8. doi: 10.1111/all.13586

7. Ertas R, Ozyurt K, Atasoy M, Hawro T, Maurer M. The clinical response to omalizumab in chronic spontaneous urticaria patients is linked to and predicted by IgE levels and their change. *Allergy* (2018) 73(3):705–12. doi: 10.1111/all.13345

8. Fok JS, Kolkhir P, Church MK, Maurer M. Predictors of treatment response in chronic spontaneous urticaria. *Allergy* (2021) 76(10):2965–81. doi: 10.1111/all.14757

9. Deza G, Bertolin-Colilla M, Pujol RM, Curto-Barredo L, Soto D, Garcia M, et al. Basophil FcepsilonRI expression in chronic spontaneous urticaria: A potential immunological predictor of response to omalizumab therapy. *Acta Derm Venereol* (2017) 97(6):698–704. doi: 10.2340/00015555-2654

10. Schoepke N, Asero R, Ellrich A, Ferrer M, Gimenez-Arnau A, EHG C, et al. Biomarkers and clinical characteristics of autoimmune chronic spontaneous urticaria: Results of the PURIST study. *Allergy* (2019) 74(12):2427–36. doi: 10.1111/all.13949

11. Tsilifis C, Freeman AF, Gennery AR. STAT3 hyper-IgE syndrome-an update and unanswered questions. *J Clin Immunol* (2021) 41(5):864–80. doi: 10.1007/s10875-021-01051-1

12. Johnson MB, Flanagan SE, Martins TB, Hill HR, Hattersley AT, McDonald TJ. Low IgE is a useful tool to identify STAT3 gain-of-Function mutations. *Clin Chem* (2016) 62(11):1536–8. doi: 10.1373/clinchem.2016.263624

13. Lorenzini T, Dotta L, Giacomelli M, Vairo D, Badolato R. STAT mutations as program switchers: turning primary immunodeficiencies into autoimmune diseases. *J Leukoc Biol* (2017) 101(1):29–38. doi: 10.1189/jlb.5RI0516-237RR

14. Forbes LR, Milner J, Haddad E. Signal transducer and activator of transcription 3: a year in review. *Curr Opin Hematol* (2016) 23(1):23–7. doi: 10.1097/MOH.0000000000000206

15. Chandrasekaran P, Zimmerman O, Paulson M, Sampaio EP, Freeman AF, Sowerwine KJ, et al. Distinct mutations at the same positions of STAT3 cause either loss or gain of function. *J Allergy Clin Immunol* (2016) 138(4):1222–4.e2. doi: 10.1016/j.jaci.2016.05.007

16. Luo XY, Liu Q, Yang H, Tan Q, Gan LQ, Ren FL, et al. OSMR gene effect on the pathogenesis of chronic autoimmune urticaria *via* the JAK/STAT3 pathway. *Mol Med* (2018) 24(1):28. doi: 10.1186/s10020-018-0025-6

17. Xiao L, Muhali FS, Cai TT, Song RH, Hu R, Shi XH, et al. Association of single-nucleotide polymorphisms in the STAT3 gene with autoimmune thyroid disease in Chinese individuals. *Funct Integr Genomics* (2013) 13(4):455–61. doi: 10.1007/s10142-013-0337-0

18. Kotkowska A, Sewerynek E, Domańska D, Pastuszak-Lewandoska D, Brzeziańska E. Single nucleotide polymorphisms in the STAT3 gene influence AITD susceptibility, thyroid autoantibody levels, and IL6 and IL17 secretion. *Cell Mol Biol Lett* (2015) 20(1):88–101. doi: 10.1515/cmble-2015-0004

19. Fung EY, Smyth DJ, Howson JM, Cooper JD, Walker NM, Stevens H, et al. Analysis of 17 autoimmune disease-associated variants in type 1 diabetes identifies 6q23/TNFAIP3 as a susceptibility locus. *Genes Immun* (2009) 10(2):188–91. doi: 10.1038/gene.2008.99

20. Danoy P, Pryce K, Hadler J, Bradbury LA, Farrar C, Pointon J, et al. Association of variants at 1q32 and STAT3 with ankylosing spondylitis suggests genetic overlap with crohn's disease. *PLoS Genet* (2010) 6(12):e1001195. doi: 10.1371/journal.pgen.1001195

21. Yamazaki K, Umeno J, Takahashi A, Hirano A, Johnson TA, Kumasaka N, et al. A genome-wide association study identifies 2 susceptibility loci for crohn's disease in a Japanese population. *Gastroenterology* (2013) 144(4):781–8. doi: 10.1053/j.gastro.2012.12.021

22. Barrett JC, Hansoul S, Nicolae DL, Cho JH, Duerr RH, Rioux JD, et al. Genome-wide association defines more than 30 distinct susceptibility loci for crohn's disease. *Nat Genet* (2008) 40(8):955–62. doi: 10.1038/ng.175

23. Zhang J, Wu J, Peng X, Song J, Wang J, Dong W. Associations between STAT3 rs744166 polymorphisms and susceptibility to ulcerative colitis and crohn's disease: a meta-analysis. *PLoS One* (2014) 9(10):e109625. doi: 10.1371/journal.pone.0109625

24. Polgar N, Csongei V, Szabo M, Zambo V, Melegh BI, Sumegi K, et al. Investigation of JAK2, STAT3 and CCR6 polymorphisms and their gene-gene interactions in inflammatory bowel disease. *Int J Immunogenet* (2012) 39(3):247–52. doi: 10.1111/j.1744-313X.2012.01084.x

25. Jakkula E, Leppä V, Sulonen AM, Varilo T, Kallio S, Kemppinen A, et al. Genome-wide association study in a high-risk isolate for multiple sclerosis reveals associated variants in STAT3 gene. *Am J Hum Genet* (2010) 86(2):285–91. doi: 10.1016/j.ajhg.2010.01.017

26. Lill CM, Schjeide BM, Akkad DA, Blaschke P, Winkelmann A, Gerdes LA, et al. Independent replication of STAT3 association with multiple sclerosis risk in a large German case-control sample. *Neurogenetics* (2012) 13(1):83–6. doi: 10.1007/s10048-011-0305-6

27. Cénit MC, Alcina A, Márquez A, Mendoza JL, Díaz-Rubio M, de las Heras V, et al. STAT3 locus in inflammatory bowel disease and multiple sclerosis susceptibility. *Genes Immun* (2010) 11(3):264–8. doi: 10.1038/gene.2010.10

28. Cénit MC, Ortego-Centeno N, Raya E, Callejas JL, García-Hernandez FJ, Castillo-Palma MJ, et al. Influence of the STAT3 genetic variants in the susceptibility to psoriatic arthritis and behcet's disease. *Hum Immunol* (2013) 74 (2):230–3. doi: 10.1016/j.humimm.2012.10.019

29. Kolkhir P, Altrichter S, Asero R, Daschner A, Ferrer M, Giménez-Arnau A, et al. Autoimmune diseases are linked to type IIb autoimmune chronic spontaneous urticaria. *Allergy Asthma Immunol Res* (2021) 13(4):545–59. doi: 10.4168/aair.2021.13.4.545

30. Maurer M, Metz M, Bindslev-Jensen C, Bousquet J, Canonica GW, Church MK, et al. Definition, aims, and implementation of GA(2) LEN urticaria centers of reference and excellence. *Allergy* (2016) 71(8):1210–8. doi: 10.1111/all.12901

31. de Montjoye L, Darrigade AS, Giménez-Arnau A, Herman A, Dumoutier L, Baeck M. Correlations between disease activity, autoimmunity and biological parameters in patients with chronic spontaneous urticaria. *Eur Ann Allergy Clin Immunol* (2020) 53(2):55–66. doi: 10.23822/EurAnnACI.1764-1489.132

32. Konstantinou GN, Asero R, Ferrer M, Knol EF, Maurer M, Raap U, et al. EAACI taskforce position paper: evidence for autoimmune urticaria and proposal for defining diagnostic criteria. *Allergy* (2013) 68(1):27–36. doi: 10.1111/all.12056

33. Karczewski KJ, Francioli LC, Tiao G, Cummings BB, Alföldi J, Wang Q, et al. The mutational constraint spectrum quantified from variation in 141,456 humans. *Nature* (2020) 581(7809):434–43. doi: 10.1038/s41586-020-2308-7

34. Moy AP, Murali M, Nazarian RM. Identification of a Th2- and Th17-skewed immune phenotype in chronic urticaria with Th22 reduction dependent on autoimmunity and thyroid disease markers. *J Cutan Pathol* (2016) 43(4):372–8. doi: 10.1111/cup.12673

35. Pate MB, Smith JK, Chi DS, Krishnaswamy G. Regulation and dysregulation of immunoglobulin e: a molecular and clinical perspective. *Clin Mol Allergy* (2010) 8:3. doi: 10.1186/1476-7961-8-3

frontiers | Frontiers in Immunology

TYPE Original Research
PUBLISHED 25 July 2022
DOI 10.3389/fimmu.2022.945222

Check for updates

OPEN ACCESS

EDITED BY
Satoshi Tanaka,
Kyoto Pharmaceutical University, Japan

REVIEWED BY
Christophe Pellefigues,
CNRS EMR8252 Centre de Recherche sur l'Inflammation, Spain
William Sewell,
Garvan Institute of Medical Research, Australia

*CORRESPONDENCE
Kumi Izawa
k-izawa@juntendo.ac.jp
Jiro Kitaura
j-kitaura@juntendo.ac.jp

SPECIALTY SECTION
This article was submitted to Inflammation, a section of the journal Frontiers in Immunology

RECEIVED 16 May 2022
ACCEPTED 27 June 2022
PUBLISHED 25 July 2022

CITATION
Kamei A, Izawa K, Ando T, Kaitani A, Yamamoto R, Maehara A, Ide T, Yamada H, Kojima M, Wang H, Tokushige K, Nakano N, Shimizu T, Ogawa H, Okumura K and Kitaura J (2022) Development of mouse model for oral allergy syndrome to identify IgE cross-reactive pollen and food allergens: ragweed pollen cross-reacts with fennel and black pepper. *Front. Immunol.* 13:945222. doi: 10.3389/fimmu.2022.945222

COPYRIGHT
© 2022 Kamei, Izawa, Ando, Kaitani, Yamamoto, Maehara, Ide, Yamada, Kojima, Wang, Tokushige, Nakano, Shimizu, Ogawa, Okumura and Kitaura. This is an open-access article distributed under the terms of the Creative Commons Attribution License (CC BY). The use, distribution or reproduction in other forums is permitted, provided the original author (s) and the copyright owner(s) are credited and that the original publication in this journal is cited, in accordance with accepted academic practice. No use, distribution or reproduction is permitted which does not comply with these terms.

Development of mouse model for oral allergy syndrome to identify IgE cross-reactive pollen and food allergens: ragweed pollen cross-reacts with fennel and black pepper

Anna Kamei[1,2], Kumi Izawa[1]*, Tomoaki Ando[1], Ayako Kaitani[1], Risa Yamamoto[1], Akie Maehara[1], Takuma Ide[1,3], Hiromichi Yamada[1,4], Mayuki Kojima[1,4], Hexing Wang[1,2], Koji Tokushige[1,2], Nobuhiro Nakano[1], Toshiaki Shimizu[1,4], Hideoki Ogawa[1], Ko Okumura[1] and Jiro Kitaura[1]*

[1]Atopy (Allergy) Research Center, Juntendo University Graduate School of Medicine, Tokyo, Japan, [2]Department of Science of Allergy and Inflammation, Juntendo University Graduate School of Medicine, Tokyo, Japan, [3]Department of Otorhinolaryngology, Juntendo University Graduate School of Medicine, Tokyo, Japan, [4]Department of Pediatrics and Adolescent Medicine, Juntendo University Graduate School of Medicine, Tokyo, Japan

Oral allergy syndrome (OAS) is an IgE-mediated immediate food allergy that is localized to the oral mucosa. Pollen food allergy syndrome (PFAS), a pollinosis-associated OAS, is caused by cross-reactivity between food and pollen allergens. However, we need to more precisely understand the underlying pathogenesis of OAS/PFAS. In the present study, we developed a method to comprehensively identify cross-reactive allergens by using murine model of OAS and protein microarray technology. We focused on lip angioedema, which is one of the most common symptoms of OAS, and confirmed that mast cells reside in the tissues inside the lower lip of the mice. Interestingly, when the food allergen ovalbumin (OVA) was injected inside the lower lip of mice with high levels of OVA-specific IgE followed by an intravenous injection of the Evans blue dye, we found immediate dye extravasation in the skin of the neck in a mast cell-dependent manner. In addition, the degree of mast cell degranulation in the oral cavity, reflecting the severity of oral allergic responses, can be estimated by measuring the amount of extravasated dye in the skin. Therefore, we used this model of OAS to examine IgE cross-reactive allergens *in vivo*. Protein microarray analysis showed that serum IgE from mice intraperitoneally sensitized with ragweed pollen, one of the major pollens causing pollinosis, bound highly to protein extracts from several edible plants including black peppercorn and fennel. We confirmed that the levels of black pepper-specific IgE and fennel-specific IgE were significantly higher in the serum from ragweed pollen-sensitized mice than in the serum from non-

sensitized control mice. Importantly, analysis of murine model of OAS showed that the injection of black pepper or fennel extract induced apparent oral allergic responses in ragweed pollen-sensitized mice. These results indicate IgE cross-reactivity of ragweed pollen with black pepper and fennel. In conclusion, we developed mouse model of OAS to identify IgE cross-reactive pollen and food allergens, which will help understand the pathogenesis of OAS/PFAS.

KEYWORDS

oral allergy syndrome (OAS), mouse model, IgE, cross-reactivity, pollen, food, allergen

Introduction

Food allergy is defined as a phenomenon in which adverse reactions are caused by allergen-specific immunological mechanisms following exposure to a given food (1–5). Oral allergy syndrome (OAS) involves the rapid onset of symptoms induced by food allergens in the oral and pharyngeal mucosa, including itching and/or angioedema of the lip, tongue, palate, and throat. In many cases, OAS is an IgE-mediated food allergy that can be induced by any allergen in animal foods such as eggs and milk or plant foods such as fresh fruits and vegetables (6–9). Pollinosis-associated OAS is called pollen food allergy syndrome (PFAS), in which certain fruits and vegetables show cross-reactivity with pollen such as birch pollen (10–13). Food allergens are classified into class I and class II types. Class I food allergens (e.g., milk) are oral allergens that cause sensitization through the gastrointestinal tract, whereas class II food allergens are highly homologous to aeroallergens that cause sensitization through the respiratory tract. Class II food allergens (e.g., vegetables and fruits) are generally heat-labile and easy-to-digest proteins that are structurally similar to pollen homologs. Profilins and Bet v 1-like proteins are class II food allergens that are responsible for OAS. After sensitization with specific pollen, ingestion of certain fruits or vegetables that cross-react with pollen induces IgE-mediated mast cell degranulation in the oral cavity of patients with PFAS (14–18). It has been reported that birch pollen cross-reacts with *Rosaceae* (e.g., apple, pear, and peach) (19–21), mugwort pollen cross-reacts with *Apiaceae* (e.g., celery) (22, 23) or with spice, and ragweed pollen cross-reacts with *Cucurbitaceae* (e.g., melon) (24–27) or with *Musaceae* (e.g., banana) (28, 29) to induce PFAS (30–33).

The spectrum of PFAS symptoms ranges from oropharyngeal symptoms to anaphylactic shock. The reported prevalence of PFAS varies between 2% and 70% according to geographical location. PFAS is generally diagnosed by taking a history from the relevant patients, performing a skin prick test, and measuring serum levels of allergen-specific IgE antibodies (6–17). However, the molecular mechanisms by which aeroallergens show cross-reactivity with food allergens are elusive. In this study, we used murine model of sensitization to ragweed pollen and protein microarray technology (34) to develop methods for the comprehensive identification of foods that may cross-react with ragweed pollen. We identified black pepper and fennel as foods that may cross-react with ragweed pollen using this method and demonstrated IgE cross-reactivity of ragweed pollen with black pepper or fennel using murine model of OAS. Although further examination is required to clarify the clinical significance and molecular mechanisms underlying the cross-reactivity between them, analyses using this newly developed method may clarify the pathogenesis of unexplained cases of OAS/PFAS.

Abbreviations: ANOVA, analysis of variance; APC, allophycocyanin; Cy7, cyanine 7; ELISA, enzyme-linked immunosorbent assay; IL, interleukin; LN, lymph node; OAS, oral allergy syndrome; OVA, ovalbumin; PBS, phosphate-buffered saline; PE, phycoerythrin; PFAS, pollen food allergy syndrome; SD, standard deviation; WT, wild-type.

Material and methods

Mice

All procedures were approved by the Institutional Review Committee of Juntendo University (approval numbers 2020128 and 2020136). Wild-type (WT) and $Kit^{W\text{-}sh/W\text{-}sh}$ (mast cell-deficient) mice with a BALB/c background (aged 8-12 weeks) were used as murine models for OAS (35, 36).

Antibodies and other reagents

The following antibodies were used and were purchased from BioLegend (San Diego, CA): allophycocyanin (APC)/cyanine 7 (Cy7)-conjugated anti-mouse CD45, phycoerythrin/Cy7-conjugated anti-mouse FcεRIα (MAR-1), and APC-conjugated anti-mouse c-Kit. Ragweed pollen was purchased from PolyScience (Niles, IL). 4',6-Diamidino-2-phenylindole

Dihydrochloride (DAPI) was purchased from Dojindo (Kumamoto, Japan). OVA (grade V) was purchased from Sigma-Aldrich (St Louis, MO). Alum was purchased from Thermo Fisher Scientific Inc. (Waltham, MA). Compound 48/80 was purchased from Sigma-Aldrich (St Louis, MO). To prepare fennel extracts, commercially available fennel from Japan (Fruits and vegetables of Otsuru, Fukuoka, Japan) mixed with phosphate-buffered saline (PBS) was ground using a food processor. To prepare the black pepper extracts, commercially available black pepper from Malaysia (S&B Foods Inc., Tokyo, Japan) was ground in a mortar and mixed with PBS. The mixtures were then filtrated into the tube before centrifugation at 20,000g for 10 min. The supernatants were collected and subjected to BCA protein assay (Fujifilm, Tokyo, Japan) to measure protein concentration.

Allergenic protein microarray

Serum from Balb/c mice intraperitoneally injected with 100 μg ragweed pollen plus 2 mg alum or with 2 mg alum alone as a control six times at 1-week intervals was incubated on microarray plates coated with crude allergenic protein extracts from various plants, animals, processed foods, and microorganisms (total 1178 types), including vegetables, fruits, fishes, shellfishes, meats, eggs, cheeses, yogurts, insects, ticks, parasites, bacteria, and fungi (Fukushima Translational Research Project, Fukushima, Japan). After Alexa Fluor 647-conjugated anti-mouse IgE antibody was added to the wells, microarray plates were scanned with a GenePix 4000 B scanner (Molecular Devices, San Jose, CA) and fluorescence intensity was measured. Allergenic protein microarray analysis was performed (Fukushima Translational Research Project, Fukushima, Japan) (34). The relative binding intensity of serum IgE to the respective protein extracts was estimated by subtracting the IgE-binding intensity of serum from mice injected with alum alone from IgE-binding intensity of serum from mice injected with ragweed pollen plus alum.

Measurements for total IgE, ragweed, Fennel, or black pepper-specific IgE, or cytokines using enzyme-linked immunosorbent assay

ELISA kits for total IgE (eBioscience, San Diego, CA), and interleukin-4 (IL-4) and IL-13 (R&D Systems, Minneapolis, MN) were used. Ragweed, fennel, or black pepper-specific IgE was determined using luminescence ELISA as previously described (35, 36). Briefly, ragweed pollen, fennel, or black pepper extract-coated ELISA plates were blocked before adding serial dilutions of serum samples before washing the wells. After biotinylated anti-IgE Ab (R35-118) (BD Pharmingen, San Diego, CA) was added, the plates were incubated and washed. Streptavidin-horseradish peroxidase was added, the plates were incubated and washed. Then, 3,3',5,5'-tetramethylbenzidine substrate solution and stop solution were added (BD Biosciences, San Jose, CA), before measuring the absorbance at a wavelength of 450 nm wavelength using a microplate reader.

Murine model of OAS

The mice were injected with 500 ng compound 48/80 or PBS as a control inside the lower lip just immediately before the intravenous injection of the Evans blue dye. Alternatively, 14 days after intraperitoneal injection of 100 μg OVA plus 2 mg alum twice with a 2-week interval, the mice were given an injection of 2 μg OVA or PBS as a control inside the lower lip right before the intravenous injection of the Evans blue dye. Seven days after intraperitoneal injection of 100 μg ragweed pollen plus 2 mg alum six times with a 1-week interval, the mice were given an injection of 4 μg black pepper extract, 4 μg fennel extract, or PBS as a control inside the lower lip immediately before the intravenous injection of the Evans blue dye. Three days after intranasal injection of 1 mg ragweed pollen for five consecutive days in the first and second week following intraperitoneal injection of 100 μg ragweed pollen plus 2 mg alum three times with a 1-week interval (37–40), the mice were administered an injection of 4 μg fennel extract or PBS as a control inside the lower lip right before the intravenous injection of 0. 2 mL of 0.1% Evans blue dye. The skin of the neck removed 30 min after dye injection was cut into small pieces that were put into 0.3 mL of 1N KOH and left overnight at 37°C with shaking. On the next day, 0.15 mL of 1N phosphoric acid and 0.39 mL of acetone was added to the solution before mixing by inverting. After centrifugation at 700g for 15 min, 0.2 mL of the supernatant was added into each well of 96-well microplate. The amount of extravasated dye was evaluated by measuring the absorbance at a wavelength of 620 nm on 96-well microplate luminometer, as previously described (36, 41–44).

Histological analyses

Histological analyses were performed as previously described (35, 36). Sections of the tissue in the inside of the lower lip of Balb/c mice were stained with both toluidine blue or chloroacetate esterase.

Flow cytometry

Suspension cells were prepared after mincing and digesting the tissue in the inside of the lower tip with 2 mg/ml

collagenase type I (FUJIFILM, Tokyo, Japan) and 0.1 mg/ml DNase I (Roche Diagnostic, Mannheim, Germany) for 1 h at 37 °C. Stained cells were analyzed on a FACSVerse flow cytometer (BD Biosciences, San Jose, CA) and data were analyzed using FlowJo software (Tree Star), as previously described (35, 36).

In vitro analysis of the Th2 response

Single-cell suspensions of cervical lymph node (LN) cells (2×10^6) from mice sensitized intraperitoneally and intranasally with ragweed pollen or from non-sensitized mice were cultured in the presence of 20 μg/mL ragweed pollen, black pepper, or fennel extract or PBS as a control for 4 days to measure the levels of cytokines IL-4 or IL-13 in culture supernatants (35).

Statistical analyses

Data are expressed as mean ± standard deviation (SD). Brown-Forsythe and Welch analysis of variance (ANOVA) with Dunnett T3 multiple comparisons was used in Figures 1F, 2B–D, 3B, C, 4E, 5E, 6F, H, and 7E. Welch's *t*-test was used in Figures 4B, C, F, 5B, C, 6B–D, 7B-D. Spearman's correlation test was used in Figures 4D, 5D, and 6E. $^*p < 0.05$ or $^{**}p < 0.01$ was considered statistically significant.

Results

Development of murine model of pseudo-allergic reaction in oral cavities

We focused on lip angioedema, one of the most common symptoms of OAS, in the development of murine models of OAS. Histological analysis showed that chloroacetate esterase-stained mast cells were distributed in tissues from inside the lower lip of Balb/c mice (Figure 1A) and approximately 70% of the total mast cells were both toluidine blue- and chloroacetate esterase-stained mast cells, corresponding to connective tissue mast cells (Figures 1A, B) (5, 18, 35, 36, 45). Flow cytometric analysis showed that FcεRI$^+$c-Kit$^+$ mast cells resided in the tissues of the lower lip (Figure 1C). Because compound 48/80 is known to degranulate connective tissue mast cells through Mas-related G protein-coupled receptor b2 in mice (41, 46), we investigated whether stimulation with compound 48/80 leads to mast cell degranulation in murine oral cavities. To this end, the mice were intravenously injected with the Evans blue dye immediately after the injection of compound 48/80 or PBS as a control inside the lower lip (Figure 1D). The results showed that injection with compound 48/80, but not with PBS, induced apparent dye extravasation in the skin of the neck (Figure 1E). In sharp contrast, dye extravasation was not observed in mast cell-deficient $Kit^{W\text{-}sh/W\text{-}sh}$ mice treated with compound 48/80 (Figure 1E). Consistent with this, measuring the amount of extravasated dye in the skin showed that an injection of compound 48/80 caused higher amounts of dye extravasation in WT mice as compared to that following PBS injection (Figure 1F). Comparably low amounts of dye extravasation were observed in compound 48/80- and PBS-stimulated $Kit^{W\text{-}sh/W\text{-}sh}$ mice (Figure 1F). Therefore, we developed murine model to evaluate oral pseudo-allergic reactions presumably due to mast cell degranulation.

Development of murine models of IgE- and mast cell-mediated allergic reaction in oral cavities

Next, we developed murine model of IgE- and mast cell-mediated allergic reactions in the oral cavity. WT and $Kit^{W\text{-}sh/W\text{-}sh}$ mice were intraperitoneally injected with OVA plus alum adjuvant twice at 2-week intervals (Figure 2A). We found elevated levels of total IgE and OVA-specific IgE in the serum from immunized mice 2 weeks after the last injection of OVA plus alum. We confirmed that mast cell deficiency did not significantly influence the serum levels of OVA-specific IgE (Figures 2B, C). The mice were intravenously injected with the Evans blue dye immediately after injection of OVA or PBS as a control inside the lower lip (Figure 2A). Notably, the OVA injection induced apparent dye extravasation in the skin of OVA-sensitized WT mice, but not of OVA-sensitized $Kit^{W\text{-}sh/W\text{-}sh}$ mice, whereas PBS injection failed to do so in either mice groups. Consistently, the OVA-challenged WT mice exhibited higher amounts of extravasated dye in the skin than the OVA-challenged $Kit^{W\text{-}sh/W\text{-}sh}$ mice or PBS-challenged WT mice (Figure 2D). Thus, we developed murine model to evaluate oral allergic reactions, which appear to depend on IgE-driven mast cell degranulation.

Identification of foods that may cross-react with ragweed pollen

To identify foods that may cross-react with ragweed pollen, we used murine model of sensitization with ragweed pollen in BALB/c mice as well as protein microarray technology (34). First, the mice were intraperitoneally injected with ragweed pollen plus alum at 1-week intervals (Figure 3A). We observed a gradual increase in the serum levels of total IgE and ragweed-specific IgE after repeated injections (Figures 3B, C). Serum levels of ragweed-specific IgE on day 42 after the sixth injection were significantly higher than those on day 28 after the fourth injection (Figure 3C). We then performed allergenic protein microarray analyses using serum from the mice after the sixth injection with ragweed plus alum or alum alone as a control. A

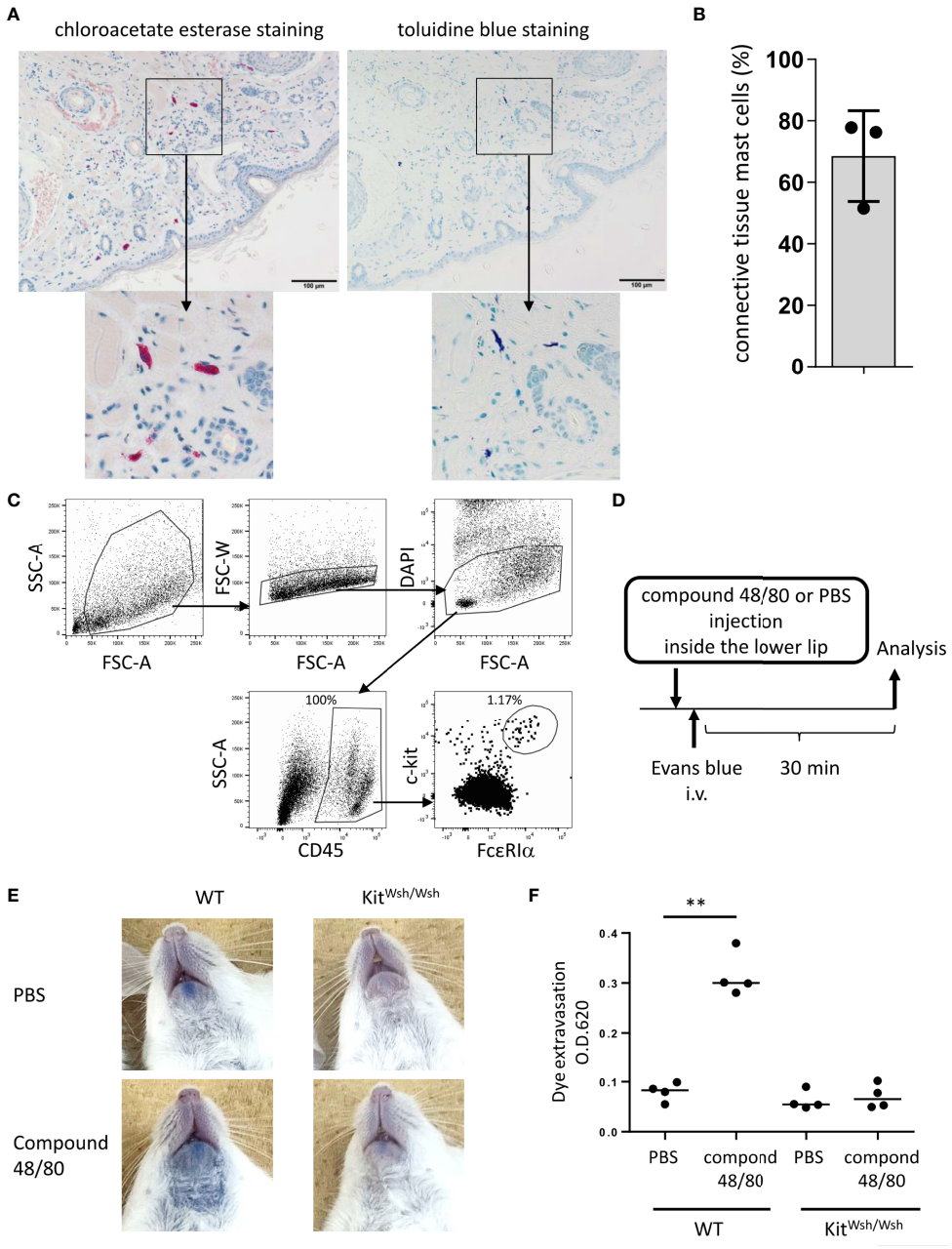


FIGURE 1
Development of murine model of pseudo-allergic reaction in the oral cavity. **(A, B)** Chloroacetate esterase staining or toluidine blue staining of serial tissue sections in the inside of the lower lip from Balb/c mice (n = 3) under steady conditions. **(A)** Chloroacetate esterase-stained (left panel) or toluidine blue-stained (right panel) mast cells are seen. **(B)** The percentage of both chloroacetate esterase- and toluidine blue-stained mast cells among chloroacetate esterase-stained mast cells. The total count was 59, 33, or 45 mast cells in serial tissue sections from three mice. Data are representative of two independent experiments. **(C)** Surface expression levels of FcεRIα and c-Kit among $CD45^+$ hematopoietic cells in the inside tissue of the lower lip from Balb/c mice under steady conditions. $FcεRIα^+c\text{-}Kit^+$ mast cell populations (1.17%) among $CD45^+$ cells (100%) were seen. Data are representative of three independent experiments. **(D)** A schematic representation of murine models of compound 48/80-induced pseudo-allergic reaction in oral cavities. **(E)** Injection of compound 48/80 inside the lower lip caused dye extravasation in the skin from WT mice but not from $Kit^{W\text{-}sh}/^{W\text{-}sh}$ mice. Representative pictures of the neck skin from WT mice injected with compound 48/80 (left/lower) or PBS (left/upper) and from $Kit^{W\text{-}sh}/^{W\text{-}sh}$ mice injected with compound 48/80 (right/lower) or PBS (right/upper) **(F)** Quantification of the Evans blue dye that extravasated into the neck skin from WT or $Kit^{W\text{-}sh}/^{W\text{-}sh}$ mice injected with compound 48/80 or PBS. n =4 per group; data are presented as mean ± SD. Data are representative of two independent experiments. Brown-Forsythe and Welch ANOVA with Dunnett T3 multiple comparisons. $^{**}P < 0.01$.

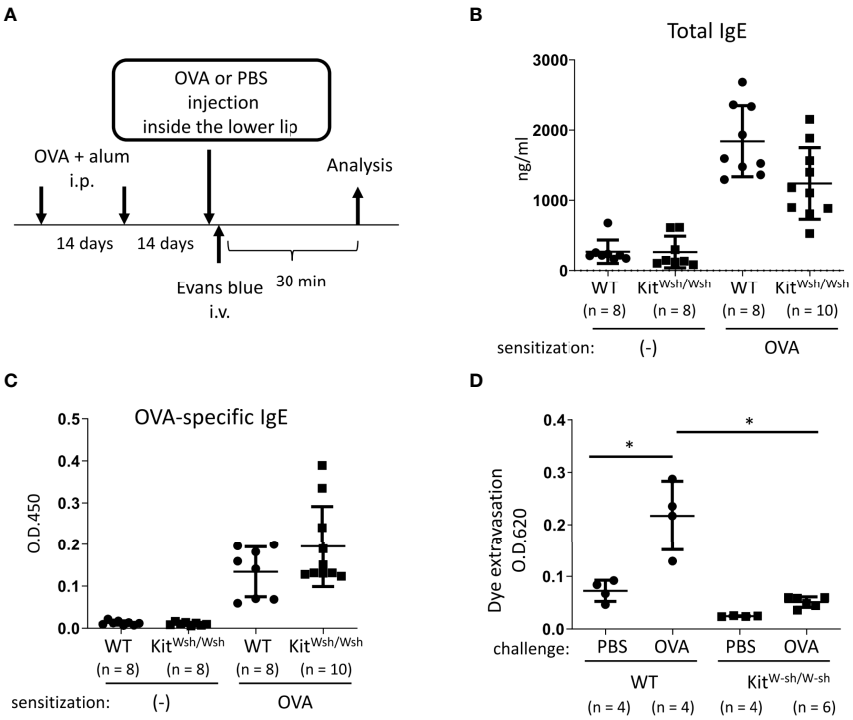


FIGURE 2
Development of murine model of IgE- and mast cell-mediated allergic reaction in oral cavities. **(A)** A schematic representation of murine models of OVA-induced, IgE- and mast cell-dependent allergic reaction in oral cavities. **(B, C)** Serum levels of total IgE **(B)** and OVA-specific IgE **(C)** from WT mice (n = 8) or $Kit^{W\text{-}sh/W\text{-}sh}$ mice (n = 10) intraperitoneally injected with OVA plus alum twice at a 2-week interval or from non-sensitized WT mice (n = 8) or $Kit^{W\text{-}sh/W\text{-}sh}$ mice (n = 8). **(D)** Quantification of the Evans blue dye that extravasated into the neck skin from OVA-sensitized WT mice stimulated by OVA (n = 4) or PBS (n = 4) or $Kit^{W\text{-}sh/W\text{-}sh}$ mice stimulated by OVA (n = 6) or PBS (n = 4). Data are presented as mean ± SD. Data are representative of two independent experiments. Brown-Forsythe and Welch ANOVA with Dunnett T3 multiple comparisons. *$P < 0.05$.

total of 1178 types of crude protein extracts from a variety of plants, animals, processed foods, and microorganisms, including vegetables, fruits, fish, shellfish, meats, eggs, cheeses, yogurts, insects, ticks, parasites, bacteria, and fungi were examined to calculate the relative binding affinity to respective protein extracts of serum IgE from ragweed pollen-sensitized mice versus control mice. All top 22 protein extracts, which were highly bound by serum IgE from the ragweed pollen-sensitized mice, were derived from plants (Table 1). Among them, nine protein extracts, including those ranked first, were derived from ragweed, including *Ambrosia artemisiifoli* (common ragweed), *Ambrosia trifida* (giant ragweed), and *Ambrosia bidentata* (lanceleaf ragweed), a member of the *Asteraceae* family, demonstrating the reliability of this assay. The second- and third-ranked were derived from *Sambucus nigra*, a member of the *Adoxaceae* family, whereas those raked fourth and fourteenth were from fennel, a member of the *Apiaceae* family. *Piper nigrum* (Black peppercorn), *Salvia officinalis* (common sage), *Plantaho asiatica*, *Orthosiphon aristatus* (cumisctin), *Prunus campanulate*, *Ficus pumila*, *Capsicum annuum* (paprika), *Sambucus nigra*, and *Foeniculum vulgare* (fennel) were edible (**Table 1**). In any case, some of the above-described plants may include allergenic proteins that cross-react with ragweed pollen allergens.

Ragweed pollen cross-reacts with black pepper in murine model of OAS

Based on the results of the protein microarray analyses, we investigated whether ragweed pollen cross-reacts with black pepper, which is frequently used as a cooking spice. WT mice, that had been intraperitoneally injected with ragweed pollen plus alum six times weekly, exhibited high levels of ragweed-specific IgE in the serum (Figures 4A, B). Intriguingly, significantly higher levels of black pepper-specific IgE in the serum were also observed in the same ragweed-sensitized mice than in the non-sensitized control mice (Figure 4C). There was no correlation between the serum levels of ragweed-specific IgE and black pepper-specific IgE (Figure 4D). The mice were intravenously injected with the Evans blue dye immediately after the injection of black pepper extract or PBS as a control

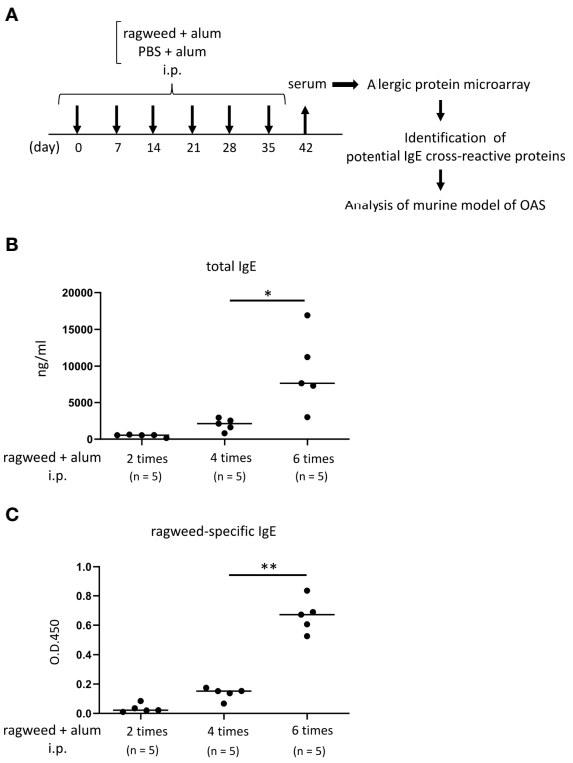


FIGURE 3
Identification of foods that may cross-react with ragweed pollen by using murine model of sensitization with ragweed pollen and allergenic protein microarray technology. **(A)** Allergenic protein microarray analysis was performed using serum from mice given intraperitoneal administration of ragweed pollen plus alum or PBS plus alum as a control, before analysis of murine model of OAS. **(B, C)** Balb/c mice (n = 5) were intraperitoneally injected with ragweed pollen plus alum six times at a 1- week interval. Serum levels of total IgE **(B)** and ragweed-specific IgE **(C)** from Balb/c mice after two, four or six times of intraperitoneal injection of ragweed pollen plus alum. Data are presented as mean ± SD. Data are representative of two independent experiments. Brown-Forsythe and Welch ANOVA with Dunnett T3 multiple comparisons. $*P < 0.05$; $**P < 0.01$.

inside the lower lip. The results showed that significantly higher amounts of dye extravasation were evident in ragweed-sensitized mice injected with black pepper extract but not with PBS (Figure 4E). In accordance with this, histological analyses of the inside of the lower lip revealed frequent distribution of degranulated mast cells in the former mice, but not in the latter mice (Figure 4F). It should be noted that the injection of black pepper extract or PBS did not induce apparent dye extravasation in the non-sensitized control mice (Figure 4E). Collectively, these results indicate that black pepper allergen crosslinked ragweed-specific IgE-bound FcεRI on mast cells, leading to mast cell degranulation inside the lower lip. Thus, we were able to provide evidence of IgE cross-reactivity between ragweed pollen and black pepper in murine model.

Stimulation with fennel extracts did not significantly induce OAS in mice intraperitoneally sensitized with ragweed pollen in murine model

We then examined whether ragweed pollen cross-reacts with fennel, which is frequently used as a cooking spice. Similarly, we used WT mice that received intraperitoneal injections of ragweed pollen plus alum six times weekly (Figure 5A). The results showed that the serum levels of fennel-specific IgE as well as ragweed-specific IgE in ragweed pollen-sensitized mice were higher than those in non-sensitized control mice (Figures 5B, C). There was no correlation between the serum levels of ragweed-specific IgE and fennel-specific IgE (Figure 5D). Although intravenous injection of the Evans blue dye immediately after an injection of fennel extract inside the lower lip did not cause dye extravasation in non-sensitized control mice, similar injections of fennel extracts, but not of PBS, tended to increase the amount of dye extravasation in ragweed pollen-sensitized mice (Figure 5E).

Stimulation with fennel extracts significantly induced OAS in mice intraperitoneally and intranasally sensitized with ragweed pollen in murine model

Since we did not find definite evidence for IgE cross-reactivity between ragweed pollen and fennel *in vivo*, we attempted to use a ragweed pollen-induced allergic rhinitis model (37–40). The mice were administered an intranasal injection of ragweed pollen for five consecutive days in the first and second weeks after intraperitoneal injection of ragweed pollen three times weekly (Figure 6A). The results showed that intranasal administration of ragweed pollen strongly elevated the serum levels of total IgE and ragweed-specific IgE in mice intraperitoneally injected with ragweed pollen (Figures 6B, C). In addition, serum levels of fennel-specific IgE were higher in mice intraperitoneally and intranasally injected with ragweed pollen on day 35 than in non-sensitized control mice. (Figure 6D). There was a weak positive correlation between the serum levels of ragweed-specific IgE and fennel-specific IgE (Figure 6E). Importantly, the intravenous injection of the Evans blue dye immediately after injection of fennel extract, but not of PBS, inside the lower lip induced significant amounts of dye extravasation in mice intraperitoneally and intranasally injected with ragweed pollen on day 35 (Figures 6F, G). When cervical LN cells from these ragweed pollen-administered mice were *ex vivo* stimulated with ragweed pollen, fennel, or black pepper extracts, we found a significant increase in IL-4 and IL13 levels in the culture supernatants of cervical LN cells in response to ragweed pollen, but not to black pepper or fennel extract (Figure 6H) (35).

TABLE 1 Relative binding intensity of serum IgE to the respective protein extracts.

	ID	Classification-1	Classification-2	Allergen	Intensity
1	000981	plant	*Asteraceae*	*Ambrosia artemisiifoli* (common ragweed)	2.64
2	001037	plant	*Adoxaceae*	*Sambucus nigra*	2.27
3	001017	plant	*Adoxaceae*	*Sambucus nigra*	2.23
4	000980	plant	*Apiaceae*	*Foeniculum vulgare* (fennel)	1.90
5	001042	plant	*Asteraceae*	*Ambrosia artemisiifolia* (common ragweed)	1.85
6	000005	plant	*Asteraceae*	*Ambrosia artemisiifolia* (common ragweed)	1.83
7	001022	plant	*Asteraceae*	*Ambrosia artemisiifolia* (common ragweed)	1.78
7	001025	plant	*Asteraceae*	*Ambrosia bidentata* (lanceleaf ragweed)	1.78
9	001045	plant	*Asteraceae*	*Ambrosia bidentata* (lanceleaf ragweed)	1.71
10	000389	plant	*Asteraceae*	*Ambrosia trifida* (giant ragweed)	1.67
10	000505	plant	*Calophyllaceae*	*Calophyllum inophyllum*	1.67
12	000390	plant	*Asteraceae*	*Ambrosia artemisiifolia (ragweed)*	1.58
13	000544	plant	*Piperaceae*	*Piper nigrum* (black peppercorn)	1.57
14	000849	plant	*Lamiaceae*	*Salvia officinalis* (common sage)	1.52
14	001000	plant	*Apiaceae*	*Foeniculum vulgare* (fennel)	1.52
16	000213	plant	*Plantaginaceae*	*Plantago asiatica*	1.40
17	000130	plant	*Lamiaceae*	*Orthosiphon aristatus* (cumisctin)	1.39
18	000225	plant	*Rosaceae*	*Cerasus campanulata*	1.38
18	000210	plant	*Moraceae*	*Ficus pumila*	1.38
18	000834	plant	*Solanaceae*	*Capsicum annuum* (paprika)	1.38
21	000967	plant	*Asteraceae*	*Ambrosia artemisiifolia* (ragweed)	1.35
21	000478	plant	*Malvaceae*	*Gossypium* spp. (cotton linters)	1.35

The relative binding intensity of serum IgE from ragweed-sensitized mice to the respective protein extracts (ID, Classification-1, Classification-2, and Allergen) was estimated by subtracting the IgE-binding intensity of serum from mice injected with alum alone from IgE-binding intensity of serum from mice injected with ragweed pollen plus alum.

Stimulation with fennel extracts induced mast cell-dependent OAS in mice intraperitoneally and intranasally sensitized with ragweed pollen

We then used the same model in WT and $Kit^{W\text{-}sh/W\text{-}sh}$ mice to examine the role of mast cells in these responses (Figure 7A). The results showed that mast cell deficiency did not significantly influence serum levels of total IgE, ragweed-specific IgE, or fennel-specific IgE (Figures 7B-D). However, mast cell deficiency dampened dye extravasation following an injection of fennel extract inside the lower lip in mice intraperitoneally and intranasally injected with ragweed pollen, suggesting that these responses in the oral cavities were induced in an IgE- and mast cell-dependent manner (Figure 7D). Taken together, we were able to provide evidence of IgE cross-reactivity between ragweed pollen and fennel in murine model.

Discussion

OAS/PFAS are frequently caused by IgE cross-reactivity between food and pollen allergens. Indeed, some combinations of cross-reactive pollen and food are well-known by allergologists. Although cross-reactive allergens have been identified by taking a history of patients with suspected OAS/PFAS, detecting allergen-specific IgE in the serum, or performing a skin prick test, unknown combinations of allergens with cross-reactivity may cause unexplained OAS/PFAS (6–17). In the present study, we developed a method to comprehensively identify potential cross-reactive allergens. Analysis of allergenic protein microarray identified several edible plants to which serum IgE from ragweed pollen-sensitized mice can strongly bind. The reliability of this assay was supported by the finding that nine out of 11 extracts derived from ragweed were included in the top 22 extracts that were highly bound by serum IgE from ragweed pollen-sensitized mice. In addition, we developed methods to evaluate the degree of IgE-mediated mast cell degranulation in oral cavities, reflecting the severity of OAS in murine model: immediately after an injection of OVA inside the lower lip in mice with high levels of serum OVA-specific IgE, an intravenous injection of the Evans blue dye induced apparent dye extravasation in the neck skin, of which amounts could be quantitated. Although oral rubbing after an oral challenge was reported to be a symptom of PFAS in murine model (47), the quantitation of extravasated dye seemed to be suitable for evaluating IgE cross-reactivity of allergens of interest *in vivo*. In addition, such murine model

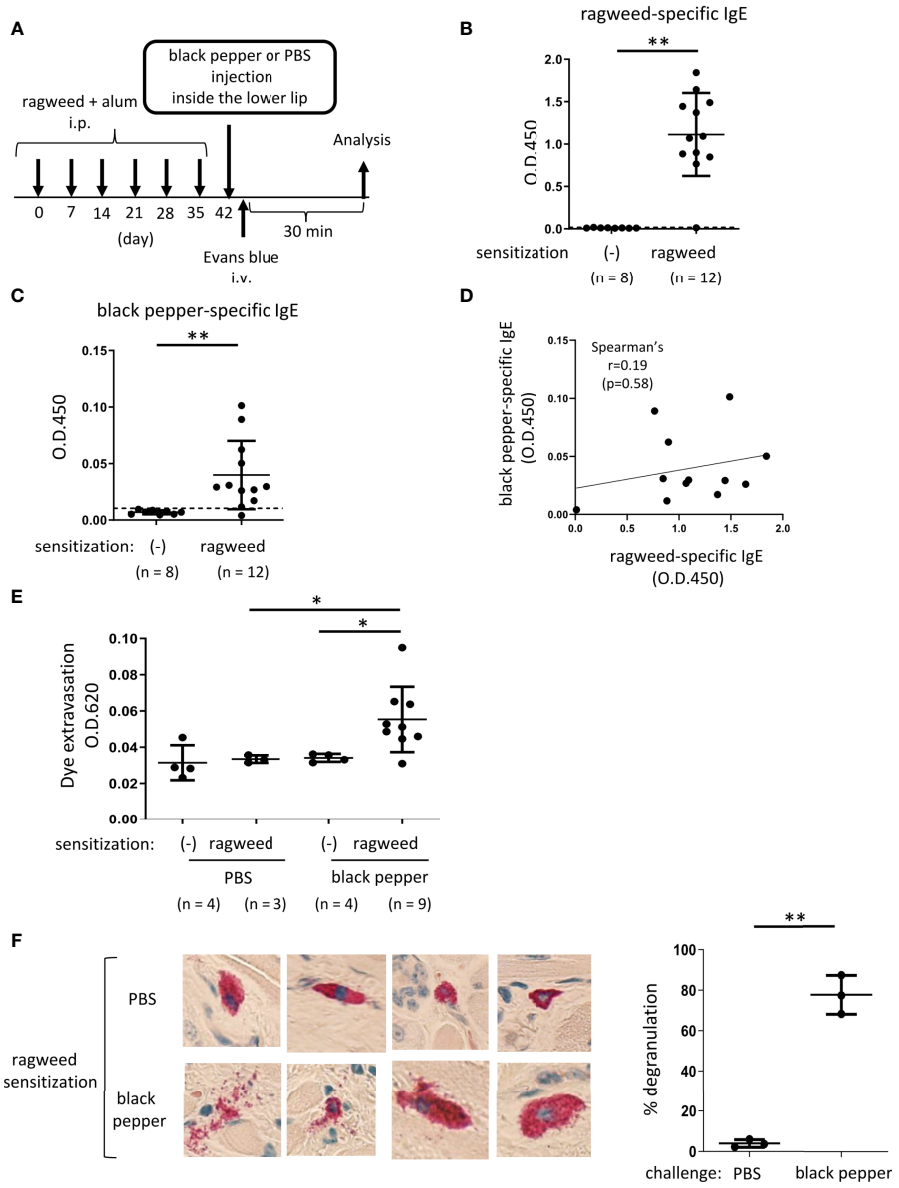


FIGURE 4
Ragweed pollen cross-reacts with black pepper in murine model of OAS. **(A)** A schematic representation of murine model of OAS. WT mice intraperitoneally sensitized with ragweed pollen before stimulation with black pepper or PBS as a control. **(B-D)** Serum levels of ragweed-specific **(B)** and black pepper-specific IgE **(C)** from ragweed-sensitized mice at day 42 (n = 12) or non-sensitized control mice (n = 8). **(B and C)** A positivity threshold (mean + 2SD in non-sensitized mice) is shown as a dotted line. Data are presented as mean ± SD. Data are representative of two independent experiments. Welch's *t*-test. $^{**}P < 0.01$. **(D)** No correlation between serum levels of ragweed-specific IgE and black pepper-specific IgE from ragweed-sensitized mice (n =12). Spearman's correlation test. **(E)** Quantification of the Evans blue dye that extravasated into the neck skin from ragweed-sensitized mice stimulated by black pepper extract (n = 9) or PBS (n = 3) or from non-sensitized control mice stimulated by black pepper extract (n = 4) or PBS (n = 4). Data are presented as mean ± standard deviation. Data are representative of two independent experiments. Brown-Forsythe and Welch ANOVA with Dunnett T3 multiple comparisons. $^{*}P < 0.05$. **(F)** Representative images of images of chloroacetate esterase-stained mast cells in tissue sections in the inside of the lower lip from ragweed-sensitized mice stimulated by black pepper extract (left/lower panel) or PBS (left/upper panel). Percentages of degranulated mast cells were shown (right). n = 3 per each group. Data are presented as mean ± SD. Data are representative of two independent experiments. Welch's *t*-test. $^{**}P < 0.01$.

will be necessary for definite identification of IgE cross-reactive allergens inducing OAS/PFAS, because it is clinically known that IgE cross-reactive allergens do not necessarily cause OAS/PFAS even though IgE cross-reactivity is shown by serological tests (6–17). Accordingly, we were able to test whether an edible plant that potentially cross-reacts with ragweed pollen induces OAS in our murine model. Indeed, an injection of fennel or black pepper extract caused high amounts of dye extravasation in the neck

10.3389/fimmu.2022.945222

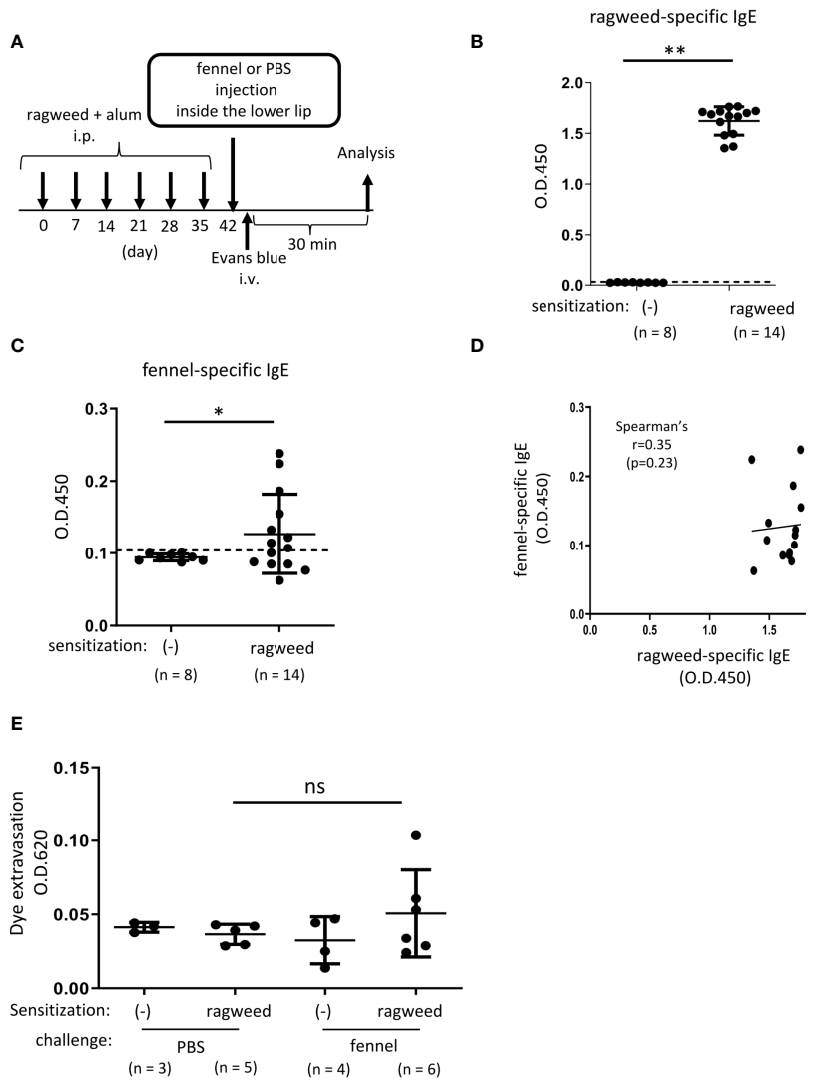


FIGURE 5
Stimulation with fennel extracts did not significantly induce OAS in mice intraperitoneally sensitized with ragweed pollen in murine model. **(A)** A schematic representation of murine model of OAS. WT mice intraperitoneally sensitized with ragweed pollen before stimulation with fennel or PBS as a control. **(B-D)** Serum levels of ragweed-specific IgE **(B)** and fennel-specific IgE **(C)** from mice intraperitoneally sensitized with ragweed pollen at day 42 (n = 14) or non-sensitized control mice (n = 8). **(B, C)** A positivity threshold (mean + 2SD in non-sensitized mice) is shown as a dotted line. Data are expressed as mean ± SD. Data are representative of two independent experiments. Welch's *t*-test. $^{**}P < 0.01$. **(D)** No correlation between serum levels of ragweed-specific IgE and fennel-specific IgE from ragweed-sensitized mice (n = 14). Spearman's correlation test. **(E)** Quantification of the Evans blue dye that extravasated into the neck skin from ragweed-sensitized WT mice stimulated by fennel extract (n = 6) or PBS (n = 5) or from non-sensitized control mice stimulated by fennel extract (n = 4) or PBS (n = 3). Data are expressed as mean ± SD. Data are representative of two independent experiments. Brown-Forsythe and Welch ANOVA with Dunnett T3 multiple comparisons. ns, not significant.

skin of ragweed-sensitized mice but not of non-sensitized control mice. If such an injection induced apparent dye extravasation in control mice, the reaction would presumably be caused by IgE-independent increase in vascular permeability. In the case of an injection of fennel extract, mice intraperitoneally and intranasally injected with ragweed pollen, experiencing allergic rhinitis, exhibited stronger allergic responses in the oral cavity than mice intraperitoneally injected with ragweed pollen, suggesting that the former sensitization method is more appropriate for analyzing IgE

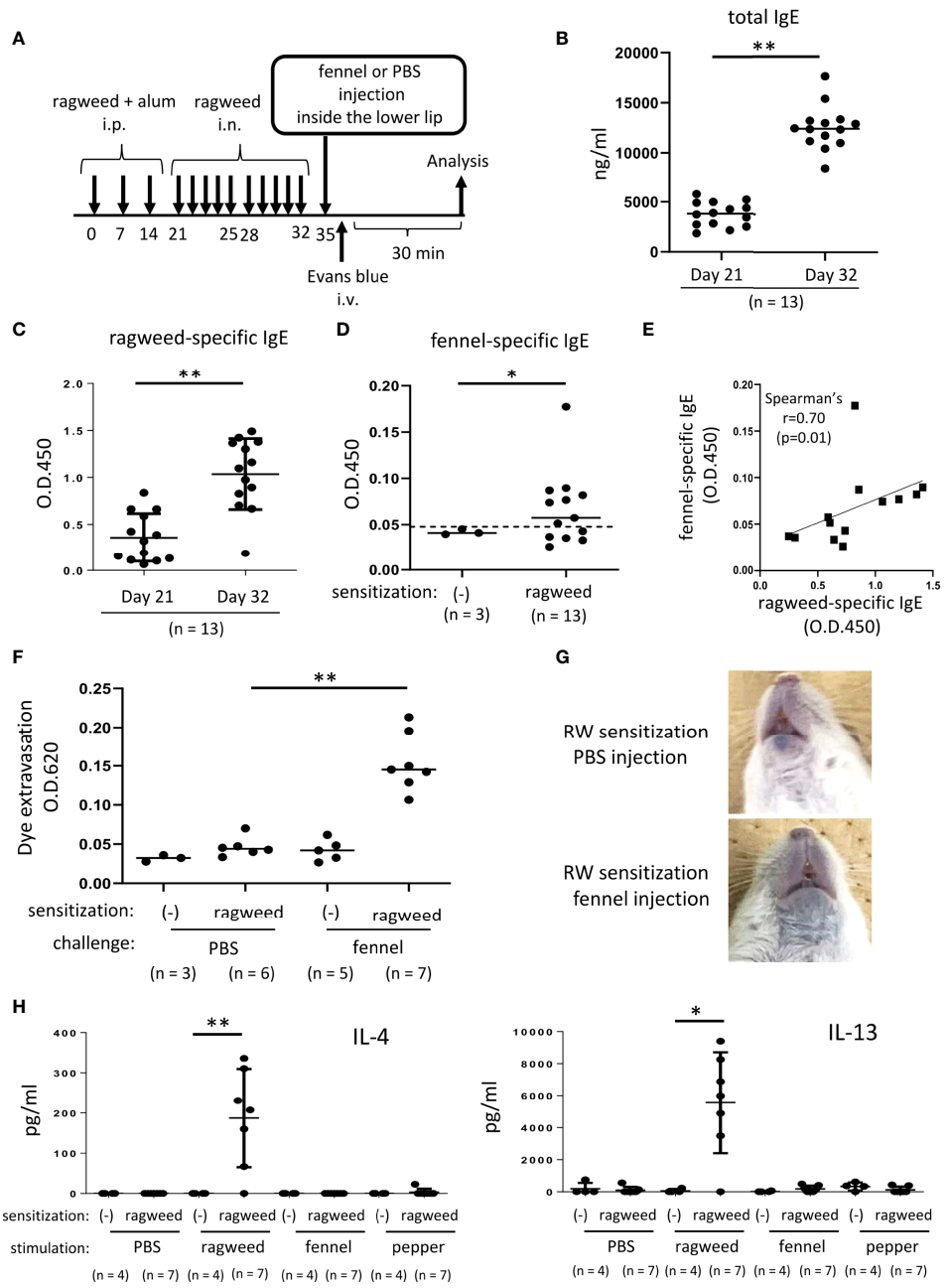


FIGURE 6
Stimulation with fennel extracts induced mast cell-dependent OAS in mice intraperitoneally and intranasally sensitized with ragweed pollen. **(A)** A schematic representation of murine model of OAS. WT mice intraperitoneally and intranasally sensitized with ragweed pollen before stimulation with fennel or PBS as a control. **(B-D)** Serum levels of total IgE **(B)** and ragweed-specific IgE **(C)** from ragweed-sensitized mice (n = 13) at day 21 and at day 32. **(D)** Serum levels of fennel-specific IgE from ragweed-sensitized mice (n = 13) at day 32 or from non-sensitized control mice (n = 3). A positivity threshold (mean + 2SD in non-sensitized mice) is shown as a dotted line. Data are expressed as mean ± SD. Data are representative of two independent experiments. Welch's *t*-test. $*P < 0.05$; $**P < 0.01$. **(E)** A weak positive correlation between serum levels of ragweed-specific IgE and fennel-specific IgE from ragweed-sensitized mice (n = 13). Spearman's correlation test. **(F)** Quantification of the Evans blue dye that extravasated into the neck skin from ragweed-sensitized mice stimulated by fennel extract (n = 7) or PBS (n = 6) or from non-sensitized control mice stimulated by fennel extract (n = 5) or PBS (n = 3). Data are expressed as mean ± SD. Data are representative of two independent experiments. Brown-Forsythe and Welch ANOVA with Dunnett T3 multiple comparisons. $**P < 0.01$. **(G)** Representative pictures of the neck skin from ragweed-sensitized mice stimulated by fennel extracts (lower panel) or PBS (upper panel). Data are representative of two independent experiments. **(H)** Levels of IL-4 (left) and IL-13 (right) in the culture supernatants from cervical LN cells from ragweed-sensitized mice (n = 7) or non-sensitized control mice (n = 4) in response to ragweed pollen, fennel, or black pepper extract. Data are expressed as mean ± SD. Data are representative of two independent experiments. Brown-Forsythe and Welch ANOVA with Dunnett T3 multiple comparisons. $*P < 0.05$; $**P < 0.01$.

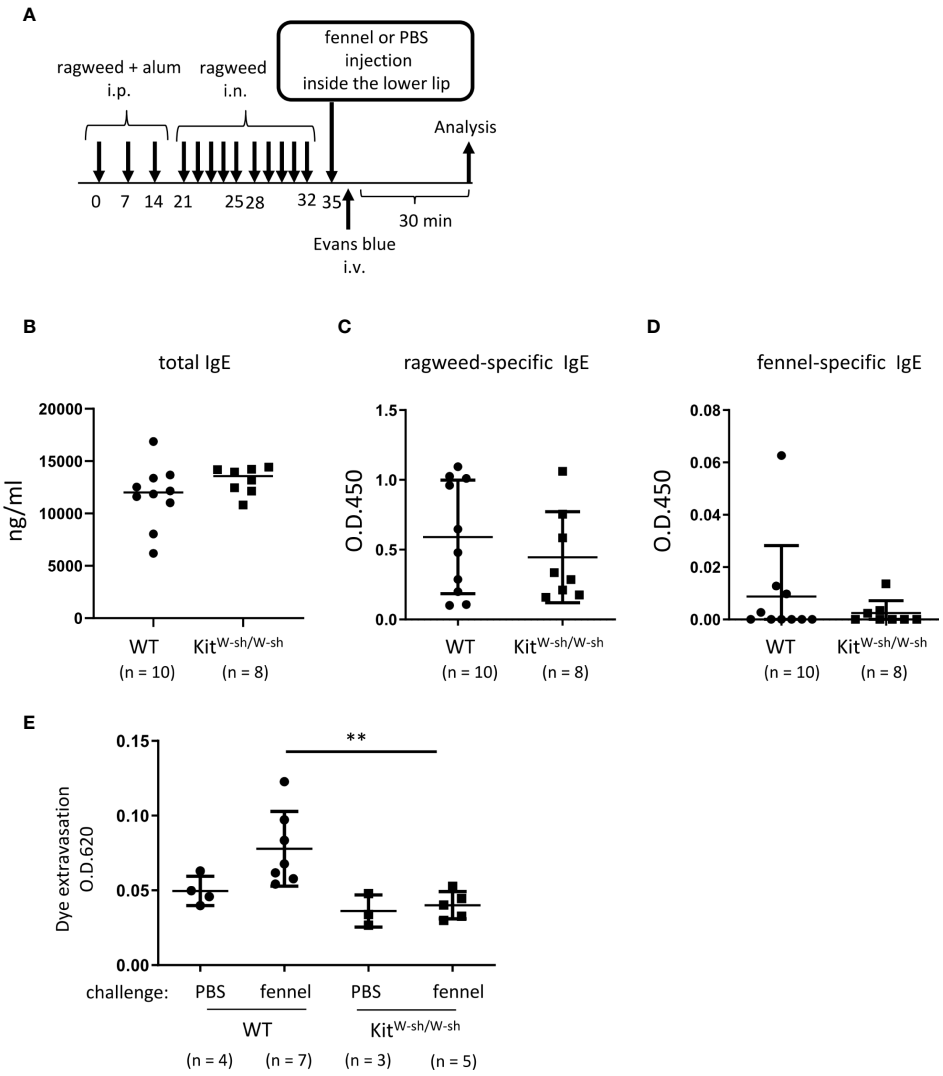


FIGURE 7
Stimulation with fennel extracts induced mast cell-dependent OAS in mice intraperitoneally and intranasally sensitized with ragweed pollen. **(A)** A schematic representation of murine model of OAS. WT or *Kit*$^{W\text{-}sh/W\text{-}sh}$ mice intraperitoneally and intranasally sensitized with ragweed pollen before stimulation with fennel or PBS as a control. **(B-D)** Serum levels of total IgE **(B)**, ragweed-specific IgE **(C)**, or fennel-specific IgE **(D)** from WT (n = 10) or *Kit*$^{W\text{-}sh/W\text{-}sh}$ (n = 8) mice at day 35. **(E)** Quantification of the Evans blue dye that extravasated into the neck skin from ragweed-sensitized WT mice stimulated by fennel extracts (n = 7) or PBS (n = 4) or from *Kit*$^{W\text{-}sh/W\text{-}sh}$ mice stimulated by fennel extracts (n = 5) or PBS (n = 3). Data are expressed as mean ± SD. Data are representative of two independent experiments. **(B-D)** Welch's *t*-test. **(E)** Brown-Forsythe and Welch ANOVA with Dunnett T3 multiple comparisons. $^{**}P < 0.01$.

cross-reactivity in murine model of OAS. In either case, mice were intraperitoneally administered ragweed pollen plus alum to strongly induce ragweed-specific IgE production. In addition, mice were challenged by injection of fennel or black pepper extract inside the lower lip to strongly induce mast cell degranulation in the oral cavity, where exaggerated allergic responses might have been caused. Therefore, our murine model seems useful to identify IgE cross-reactive allergens. However, these sensitization and challenge routes seem not suitable for analyzing the pathophysiology of OAS/PFAS. For this end, we should use a different murine model in which mice are orally challenged with food extract after intranasal sensitization with pollen. In any case, we provided evidence of IgE cross-reactivity of ragweed pollen with black pepper or fennel.

Intriguingly, we found Th2 cytokine production in LN cells from ragweed pollen-sensitized mice only in response to ragweed pollen extract, and not in response to fennel or black

pepper extract, suggesting that T cell reactivity is not the same with ragweed pollen and fennel or black pepper (1, 16). However, it should be noted that the crude extracts of food or pollen contain various allergens with different quantities and stabilities, which may depend on their processing. Accordingly, the analysis of *ex vivo* Th2 responses of LN cells using recombinant allergenic protein available as well as crude extracts of food or pollen in murine model will be useful for understanding the pathogenesis of OAS/PFAS.

Considering that celery-mugwort-spice syndrome is known as PFAS, it may be reasonable to assume that ragweed pollen would cross-react with black pepper, a member of the *Piperaceae* family, and fennel, a member of the *Apiaceae* family (11, 17, 19–22, 48, 49). Our results are also supported by those of a previous report that fennel possibly cross-reacts with mugwort, paprika, ragweed, or black pepper in a case with occupational rhinitis and asthma (50, 51). Nevertheless, our experimental results regarding IgE cross-reactivity will be informative for clinical allergologists and patients with OAS/PFAS. Profilin Amb a 8 or lipid transfer protein Amb a 6, which is known as a ragweed pollen allergen, might be involved in the ragweed-fennel-black pepper association (11, 26, 27, 29, 33). Otherwise, biochemical techniques will be required to identify a specific allergen included in ragweed pollen and clarify how ragweed pollen cross-reacts with fennel or black pepper (6–17). One limitation of this study is that the allergens in ragweed, fennel, or black pepper extracts used were not molecularly defined.

In this allergenic protein microarray analysis, crude protein extracts from various foods, including edible plants, were coated on microarray plates; however, allergens contained in such foods can be quantitatively or qualitatively influenced by cultivar, climates, or chemical treatments. The stability of each allergen can be affected to varying degrees by protein extraction procedures (52). This may explain why melon and banana were not identified as food extract that highly cross-react with serum IgE from ragweed pollen-sensitized mice, notwithstanding that the ragweed-melon-banana association was previously reported as PFAS (24–26, 28). Alternatively, the difference of immune responses between humans and mice may be taken into consideration. In any case, microarray analysis using each recombinant allergenic molecule will lead to more comprehensive and direct identification of IgE cross-reactive molecules (1, 52). Importantly, our analysis using protein microarray technology and murine model of OAS will complement the traditional analysis of serum from patients with OAS/PFAS patients to clarify the molecular mechanisms of the syndrome caused by IgE cross-reactivity. The allergen

In conclusion, we have developed a method to identify cross-reactive allergens using murine model of sensitization to specific allergens and OAS as well as protein microarray technology, which will help understand the pathogenesis of OAS/PFAS.

Data availability statement

The original contributions presented in the study are included in the article/Supplementary Material. Further inquiries can be directed to the corresponding author.

Ethics statement

This study was reviewed and approved by the institutional review boards of Juntendo University (approval numbers 2020128 and 2020136)

Author contributions

AnK performed all the experiments and participated in writing the manuscript. TA, HW, and KT assisted with the *in vitro* experiments. AyK, TI, AM, HY, MK, RY, and NN assisted with the *in vivo* experiments. TS, HO, and KO analyzed the data. KI and JK conceived the project, analyzed the data, and actively participated in manuscript writing. All authors contributed to the article and approved the submitted version.

Funding

This study was supported by JSPS KAKENHI Grant Numbers 17H04217 and 20H03721 and by a Grant-in-Aid for Special Research in Subsidies for ordinary expenses of private schools from The Promotion and Mutual Aid Corporation for Private Schools of Japan.

Acknowledgments

We thank the Laboratory of Morphology and Image Analysis, Research Support Center, Juntendo University Graduate School of Medicine for technical assistance.

Conflict of interest

The authors declare that the research was conducted in the absence of any commercial or financial relationships that could be constructed as a potential conflict of interest.

Publisher's note

All claims expressed in this article are solely those of the authors and do not necessarily represent those of their affiliated organizations, or those of the publisher, the editors and the reviewers. Any product that may be evaluated in this article, or claim that may be made by its manufacturer, is not guaranteed or endorsed by the publisher.

References

1. Valenta R, Hochwallner H, Linhart B, Pahr S. Food allergies: the basics. *Gastroenterology* (2015) 148(6):1120–31.e4. doi: 10.1053/j.gastro.2015.02.006

2. Tordesillas L, Berin MC, Sampson HA. Immunology of food allergy. *Immunity* (2017) 47(1):32–50. doi: 10.1016/j.immuni.2017.07.004

3. Ebisawa M, Ito K, Fujisawa T. Committee for Japanese pediatric guideline for food allergy, the Japanese society of pediatric allergy and clinical immunology, the Japanese society of allergology. Japanese guidelines for food allergy 2017. *Allergol Int* (2017) 66(2):248–64. doi: 10.1016/j.alit.2017.02.001

4. Hagemann PM, Nsiah-Dosu S, Hundt JE, Hartmann K, Orinska Z. Mechanisms of particles in sensitization, effector function and therapy of allergic disease. *Front Immunol* (2019) 10:1174. doi: 10.3389/fimmu.2019.01174

5. Nakano N, Kitaura J. Mucosal mast cells as key effector cells in food allergies. *Cells* (2022) 11(3):329. doi: 10.3390/cells11030329

6. Mari A, Ballmer-Weber BK, Vieths S. The oral allergy syndrome: improved diagnostic and treatment methods. *Curr Opin Allergy Clin Immunol* (2005) 5 (3):267–73. doi: 10.1097/01.all.0000168793.27948.b0

7. Muluk NB, Cingi C. Oral allergy syndrome. *Am J Rhinol Allergy* (2018) 32 (1):27–30. doi: 10.2500/ajra.2018.32.4489

8. Kondo Y, Urisu A. Oral allergy syndrome. *Allergol Int* (2009) 58(4):485–91. doi: 10.2332/allergolint.09-RAI-0136

9. Katelaris CH. Food allergy and oral allergy or pollen-food syndrome. *Curr Opin Allergy Clin Immunol* (2010) 10(3):246–51. doi: 10.1097/ACI.0b013e32833973fb

10. Ma S, Sicherer SH, Nowak-Wegrzyn A. A survey on the management of pollen-food allergy syndrome in allergy practices. *J Allergy Clin Immunol* (2003) 112(4):784–8. doi: 10.1016/s0091-6749(03)02008-6

11. Egger M, Mutschlechner S, Wopfner N, Gadermaier G, Briza P, Ferreira F. Pollen-food syndromes associated with weed pollinosis: an update from the molecular point of view. *Allergy* (2006) 61(4):461–76. doi: 10.1111/j.1398-9995.2006.00994.x

12. Carlson G, Coop C. Pollen food allergy syndrome (PFAS): A review of current available literature. *Ann Allergy Asthma Immunol* (2019) 123(4):359–65. doi: 10.1016/j.anai.2019.07.022

13. Kim M, Ahn Y, Yoo Y, Kim DK, Yang HJ, Park HS, et al. Clinical manifestations and risk factors of anaphylaxis in pollen-food allergy syndrome. *Yonsei Med J* (2019) 60(10):960–8. doi: 10.3349/ymj.2019.60.10.960

14. Valenta R, Kraft D. Type 1 allergic reactions to plant-derived food: a consequence of primary sensitization to pollen allergens. *J Allergy Clin Immunol* (1996) 97(4):893–5. doi: 10.1016/s0091-6749(96)80062-5

15. Breiteneder H, Ebner C. Molecular and biochemical classification of plant-derived food allergens. *J Allergy Clin Immunol* (2000) 106(1 Pt 1):27–36. doi: 10.1067/mai.2000.106929

16. Bohle B. The impact of pollen-related food allergens on pollen allergy. *Allergy* (2007) 62(1):3–10. doi: 10.1111/j.1398-9995.2006.01258.x

17. Alessandri C, Ferrara R, Bernardi ML, Zennaro D, Tuppo L, Giangrieco I, et al. Molecular approach to a patient's tailored diagnosis of the oral allergy syndrome. *Clin Transl Allergy* (2020) 10:22. doi: 10.1186/s13601-020-00329-8

18. Kitaura J, Murakami M. Positive and negative roles of lipids in mast cells and allergic responses. *Curr Opin Immunol* (2021) 72:186–95. doi: 10.1016/j.coi.2021.06.001

19. Biedermann T, Winther L, Till SJ, Panzner P, Knulst A, Valovirta E. Birch pollen allergy in Europe. *Allergy* (2019) 74(7):1237–48. doi: 10.1111/all.13758

20. Mogensen JE, Wimmer R, Larsen JN, Spangfort MD, Otzen DE. The major birch allergen, bet v 1, shows affinity for a broad spectrum of physiological ligands. *J Biol Chem* (2002) 277(26):23684–92. doi: 10.1074/jbc.M202065200

21. Vallier P, Dechamp C, Vial O, Deviller P. A study of allergens in celery with cross-sensitivity to mugwort and birch pollens. *Clin Allergy* (1988) 18(5):491–500. doi: 10.1111/j.1365-2222.1988.tb02899.x

22. Bauer L, Ebner C, Hirschwehr R, Wüthrich B, Pichler C, Fritsch R, et al. IgE cross-reactivity between birch pollen, mugwort pollen and celery is due to at least three distinct cross-reacting allergens: immunoblot investigation of the birch-mugwort-celery syndrome. *Clin Exp Allergy* (1996) 26(10):1161–70. doi: 10.1111/j.1365-2222.1996.tb00503.x

23. Figueroa J, Blanco C, Dumpiérrez AG, Almeida L, Ortega N, Castillo R, et al. Mustard allergy confirmed by double-blind placebo-controlled food challenges: clinical features and cross-reactivity with mugwort pollen and plant-derived foods. *Allergy* (2005) 60(1):48–55. doi: 10.1111/j.1398-9995.2005.00644.x

24. Enberg RN, Leickly FE, McCullough J, Bailey J, Ownby DR. Watermelon and ragweed share allergens. *J Allergy Clin Immunol* (1987) 79(6):867–75. doi: 10.1016/0091-6749(87)90234-x

25. Nagakura KI, Takei M, Sato S, Yanagida N, Ebisawa M. Anaphylaxis to winter melon due to cross-reactivity of sensitization to ragweed pollen. *Pediatr Allergy Immunol* (2022) 33(3):e13764. doi: 10.1111/pai.13764

26. Asero R, Mistrello G, Amato S. The nature of melon allergy in ragweed-allergic subjects: A study of 1000 patients. *Allergy Asthma Proc* (2011) 32(1):64–7. doi: 10.2500/aap.2011.32.3416

27. Rodriguez-Perez R, Crespo JF, Rodríguez J, Salcedo G. Profilin is a relevant melon allergen susceptible to pepsin digestion in patients with oral allergy syndrome. *J Allergy Clin Immunol* (2003) 111(3):634–9. doi: 10.1067/mai.2003.74

28. Anderson LBJr, Dreyfuss EM, Logan J, Johnstone DE, Glaser J. Melon and banana sensitivity coincident with ragweed pollinosis. *J Allergy* (1970) 45(5):310–9. doi: 10.1016/0021-8707(70)90037-7

29. Grob M, Reindl J, Vieths S, Wüthrich B, Ballmer-Weber BK. Heterogeneity of banana allergy: characterization of allergens in banana-allergic patients. *Ann Allergy Asthma Immunol* (2002) 89(5):513–6. doi: 10.1016/S1081-1206(10)62090-X

30. Skypala IJ, Asero R, Barber D, Cecchi L, Diaz Perales A, Hoffmann-Sommergruber K, et al. Non-specific lipid transfer protein allergy across europe. non-specific lipid-transfer proteins: Allergen structure and function, cross-reactivity, sensitization, and epidemiology. *Clin Transl Allergy* (2021) 11(3): e12010. doi: 10.1002/clt2.12010

31. Smeekens JM, Bagley K, Kulis M. Tree nut allergies: Allergen homology, cross-reactivity, and implications for therapy. *Clin Exp Allergy* (2018) 48(7):762–72. doi: 10.1111/cea.13163

32. Fuhrmann V, Huang HJ, Akarsu A, Shilovskiy I, Elisyutina O, Khaitov M, et al. From allergen molecules to molecular immunotherapy of nut allergy: A hard nut to crack. *Front Immunol* (2021) 12:742732. doi: 10.3389/fimmu.2021.742732

33. Reindl J, Anliker MD, Karamloo F, Vieths S, Wüthrich B. Allergy caused by ingestion of zucchini (Cucurbita pepo): characterization of allergens and cross-reactivity to pollen and other foods. *J Allergy Clin Immunol* (2000) 106(2):379–85. doi: 10.1067/mai.2000.107602

34. Hoshino A, Kanegane H, Nishi M, Tsuge I, Tokuda K, Kobayashi I, et al. Identification of autoantibodies using human proteome microarrays in patients with IPEX syndrome. *Clin Immunol* (2019) 203:9–13. doi: 10.1016/j.clim.2019.03.011

35. Uchida S, Izawa K, Ando T, Yamada H, Uchida K, Negishi N, et al. CD300f is a potential therapeutic target for the treatment of food allergy. *Allergy* (2020) 75 (2):471–4. doi: 10.1111/all.14034

36. Izawa K, Yamanishi Y, Maehara A, Takahashi M, Isobe M, Ito S, et al. The receptor LMIR3 negatively regulates mast cell activation and allergic responses by binding to extracellular ceramide. *Immunity* (2012) 37(5):827–39. doi: 10.1016/j.immuni.2012.08.018

37. Haenuki Y, Matsushita K, Futatsugi-Yumikura S, Ishii KJ, Kawagoe T, Imoto Y, et al. A critical role of IL-33 in experimental allergic rhinitis. *J Allergy Clin Immunol* (2012) 130(1):184–94. doi: 10.1016/j.jaci.2012.02.013

38. Kato Y, Akasaki S, Muto-Haenuki Y, Fujieda S, Matsushita K, Yoshimoto T. Nasal sensitization with ragweed pollen induces local-allergic-rhinitis-like symptoms in mice. *PloS One* (2014) 9(8):e103540. doi: 10.1371/journal.pone.0103540

39. Akasaki S, Matsushita K, Kato Y, Fukuoka A, Iwasaki N, Nakahira M, et al. Murine allergic rhinitis and nasal Th2 activation are mediated *via* TSLP- and IL-33-signaling pathways. *Int Immunol* (2016) 28(2):65–76. doi: 10.1093/intimm/dxv055

40. Matsuba-Kitamura S, Yoshimoto T, Yasuda K, Futatsugi-Yumikura S, Taki Y, Muto T, et al. Contribution of IL-33 to induction and augmentation of experimental allergic conjunctivitis. *Int Immunol* (2010) 22(6):479–89. doi: 10.1093/intimm/dxq035

41. Takamori A, Izawa K, Kaitani A, Ando T, Okamoto Y, Maehara A, et al. Identification of inhibitory mechanisms in pseudo-allergy involving Mrgprb2/MRGPRX2-mediated mast cell activation. *J Allergy Clin Immunol* (2019) 143 (3):1231–5. doi: 10.1016/j.jaci.2018.10.034

42. Izawa K, Kaitani A, Ando T, Maehara A, Nagamine M, Yamada H, et al. Differential lipid recognition by mouse versus human CD300f, inhibiting passive cutaneous anaphylaxis, depends on a single amino acid substitution in its immunoglobulin-like domain. *J Invest Dermatol* (2020) 140(3):710–3. doi: 10.1016/j.jid.2019.08.439

43. Shiba E, Izawa K, Kaitani A, Isobe M, Maehara A, Uchida K, et al. Ceramide-CD300f binding inhibits lipopolysaccharide-induced skin inflammation. *J Biol Chem* (2017) 292(7):2924–32. doi: 10.1074/jbc.M116.768366

44. Izawa K, Isobe M, Matsukawa T, Ito S, Maehara A, Takahashi M, et al. Sphingomyelin and ceramide are physiological ligands for human LMIR3/CD300f,

inhibiting FcεRI-mediated mast cell activation. *J Allergy Clin Immunol* (2014) 133 (1):270–3. doi: 10.1016/j.jaci.2013.08.008

45. Tanaka S, Furuta K. Roles of IgE and histamine in mast cell maturation. *Cells* (2021) 10(8):2170. doi: 10.3390/cells10082170

46. McNeil BD, Pundir P, Meeker S, Han L, Undem BJ, Kulka M, et al. Identification of a mast-cell-specific receptor crucial for pseudo-allergic drug reactions. *Nature* (2015) 519(7542):237–41. doi: 10.1038/nature14022

47. Kato Y, Morikawa T, Kato E, Yoshida K, Imoto Y, Sakashita M, et al. Involvement of activation of mast cells *via* IgE signaling and epithelial cell-derived cytokines in the pathogenesis of pollen food allergy syndrome in a murine model. *J Immunol* (2021) 206(12):2791–802. doi: 10.4049/jimmunol.2000518

48. Leitner A, Jensen-Jarolim E, Grimm R, Wüthrich B, Ebner H, Scheiner O, et al. Allergens in pepper and paprika. immunologic investigation of the celery-birch-mugwort-spice syndrome. *Allergy* (1998) 53(1):36–41. doi: 10.1111/j.1398-9995.1998.tb03771.x

49. Asero R. Fennel, cucumber, and melon allergy successfully treated with pollen-specific injection immunotherapy. *Ann Allergy Asthma Immunol* (2000) 84 (4):460–2. doi: 10.1016/S1081-1206(10)62281-8

50. Van der Walt A, Jeebhay MF. Work-related allergy and asthma to inhaled spices: A review. *Curr Allergy Clin Immunol* (2010) 23(4):186–92. doi: 10.13140/2.1.4460.0968

51. Schwartz HJ, Jones RT, Rojas AR, Squillace DL, Yunginger JW. Occupational allergic rhinoconjunctivitis and asthma due to fennel seed. *Ann Allergy Asthma Immunol* (1997) 78(1):37–40. doi: 10.1016/S1081-1206(10)63369-8

52. Hiller R, Laffer S, Harwanegg C, Huber M, Schmidt WM, Twardosz A, et al. Microarrayed allergen molecules: diagnostic gatekeepers for allergy treatment. *FASEB J* (2002) 16(3):414–6. doi: 10.1096/fj.01-0711fje

frontiers | Frontiers in Immunology

ORIGINAL RESEARCH
published: 26 July 2022
doi: 10.3389/fimmu.2022.930945

The Number of MRGPRX2-Expressing Cells Is Increased in Skin Lesions of Patients With Indolent Systemic Mastocytosis, But Is Not Linked to Symptom Severity

Polina Pyatilova[1,2‡], Tameem Ashry[1,2,3‡], Yanyan Luo[1,2‡], Jiajun He[1,2,4‡], Hanna Bonnekoh[1,2‡], Qingqing Jiao[1,2,5‡], Sherezade Moñino-Romero[1,2‡], Man Hu[1,2‡], Jörg Scheffel[1,2‡], Stefan Frischbutter[1,2†], Maud A. W. Hermans[6†], Bradford A. Youngblood[7‡], Marcus Maurer[1,2‡], Frank Siebenhaar[1,2†‡] and Pavel Kolkhir[1,2†‡]*

[1] Institute of Allergology, Charité – Universitätsmedizin Berlin, Corporate Member of Freie Universität Berlin, Humboldt-Universität zu Berlin, and Berlin Institute of Health, Berlin, Germany, [2] Allergology and Immunology, Fraunhofer Institute for Translational Medicine and Pharmacology ITMP, Berlin, Germany, [3] Department of Pathology, College of Medicine, King Saud University, Riyadh, Saudi Arabia, [4] Department of Dermatology, The Affiliated Hospital of Southwest Medical University, Luzhou, China, [5] Department of Dermatology, The First Affiliated Hospital of Soochow University, Suzhou, China, [6] Department of Internal Medicine, Section Allergy and Clinical Immunology, Erasmus University Medical Center, Rotterdam, Netherlands, [7] Allakos Inc., San Carlos, CA, United States

Background: Recently, the expression of the mast cell (MC) receptor Mas-related G protein–coupled receptor X2 (MRGPRX2) has been detected in lesional skin of adult patients with cutaneous mastocytosis. As of yet, little is known about the clinical relevance of MRGPRX2 and its agonists in patients with mastocytosis, including indolent systemic mastocytosis (ISM).

Methods: MRGPRX2 and MRGPRX2 agonists, cortistatin (CST), and major basic protein (MBP) were analyzed in lesional and non-lesional skin of patients with ISM and skin of healthy controls by immunohistochemistry. Co-localization of MRGPRX2 and MRGPRX2-mRNA with the MC marker tryptase was assessed by immunofluorescence microscopy and *in situ* hybridization, respectively. We assessed clinical, demographic, and laboratory data, including mastocytosis activity score (MAS), serum tryptase, and *KIT* D816V allele burden.

Results: The number of MRGPRX2-expressing (MRGPRX2+) cells, MRGPRX2-mRNA+ MCs, and CST-expressing (CST+) and MBP-expressing (MBP+) cells was significantly higher in lesional skin as compared to non-lesional skin and/or skin of healthy controls (all $p < 0.05$). Increased numbers of MRGPRX2+ cells, MRGPRX2-mRNA+ MCs, and CST+ and MBP+ cells were not associated with clinical and laboratory features of ISM, including disease burden, symptom severity, evidence of anaphylaxis, and tryptase levels.

OPEN ACCESS

Edited by:
Satoshi Tanaka,
Kyoto Pharmaceutical University, Japan

Reviewed by:
Mariana C. Castells,
Brigham and Women's Hospital and Harvard Medical School, United States
Nicolas Gaudenzio,
Institut National de la Santé et de la Recherche Médicale (INSERM), France

***Correspondence:**
Pavel Kolkhir
pavel.kolkhir@charite.de

[†]These authors share senior authorship

Specialty section:
This article was submitted to Inflammation, a section of the journal Frontiers in Immunology

Received: 28 April 2022
Accepted: 24 June 2022
Published: 26 July 2022

Citation:
Pyatilova P, Ashry T, Luo Y, He J, Bonnekoh H, Jiao Q, Moñino-Romero S, Hu M, Scheffel J, Frischbutter S, Hermans MAW, Youngblood BA, Maurer M, Siebenhaar F and Kolkhir P (2022) The Number of MRGPRX2-Expressing Cells Is Increased in Skin Lesions of Patients With Indolent Systemic Mastocytosis, But Is Not Linked to Symptom Severity. Front. Immunol. 13:930945. doi: 10.3389/fimmu.2022.930945

Conclusions: Skin lesions of patients with ISM showed high numbers of MRGPRX2+ cells, although they were not linked to symptom severity. Clinical relevance of the MRGPRX2-mediated pathway of MC activation in ISM remains unclear and should be investigated in further studies.

Keywords: MRGPRX2, cortistatin, mastocytosis, mast cell, mRNA, major basic protein (MBP), skin, symptoms

INTRODUCTION

Systemic mastocytosis (SM) is a rare disease characterized by infiltration of clonally derived mast cells (MCs) in bone marrow, skin, the gastrointestinal tract, and other organs. The prevalence of SM in the general population varies from 10 to 17 cases per 100,000 people (1–3). Indolent systemic mastocytosis (ISM) is the most common form of SM found in up to 91% of adult patients and is associated with a favorable prognosis (2, 4, 5). ISM is diagnosed when spleen and liver impairment is absent and no more than one B-finding is present, i.e., >30% MC infiltration in the bone marrow and serum tryptase level >200 ng/ml—signs of dysmyelopoiesis without substantial cytopenias and/or organomegaly (5). Skin involvement has been reported in about 95% of ISM patients, often associated with symptoms including itching, whealing, and flushing (6, 7). Severe anaphylaxis triggered by hymenoptera venom, food, or drug components is observed in half of ISM patients (2).

ISM symptoms can induce a significant impairment of patients' quality of life (4, 8). Avoidance of known symptom triggers and antimediator therapies are not always effective in ISM patients, whereas cytoreductive therapies and non-selective tyrosine kinase inhibitors can be associated with severe adverse effects (9). Although there are some novel drugs in development for ISM, no curative treatment for the disease exists (10). Thus, there is a high unmet need to identify markers associated with disease severity and poor response to treatment and investigate new MC-associated targets for development of effective and safe therapies.

MCs, primary effector cells in mastocytosis, express a wide range of receptors and release a variety of mediators upon activation (10). The best explored pathway of MC activation is linked to allergen-induced IgE crosslinking of the high-affinity FcεRI receptor, which drives IgE-mediated anaphylactic reactions associated with mastocytosis (11). Also, IgE-independent MC activation could lead to clinically relevant reactions, particularly associated with drug intolerance, *via* the Mas-related G protein–coupled receptor X2 (MRGPRX2) on MCs (12). Increased MRGPRX2 expression on skin MCs has been recently reported in patients with maculopapular cutaneous mastocytosis and suggested as a possible driver of mastocytosis pathogenesis (13).

MRGPRX2 is a multiligand receptor expressed by MCs (14), which responds to a broad variety of exogenous and endogenous stimuli, e.g., insect venom, drugs, neuropeptides such as cortistatin (CST) and substance P (SP), eosinophil granule proteins including major basic protein (MBP) and eosinophil cationic protein (ECP), and infections (15–19). Insect venom and quinolone antibiotics are known triggers of anaphylaxis in ISM patients. Mastoparan, an insect venom constituent, and quinolones are also MRGPRX2 agonists that might point toward a contribution of MRGPRX2-mediated MC activation to anaphylaxis development in some ISM patients (14, 20). For example, the MRGPRX2-mediated pathway was hypothesized in a patient with ISM who developed anaphylaxis to ciprofloxacin (21). On the other hand, FcεRI but not MRGPRX2 was overexpressed on bone marrow MCs in patients with clonal MC disorders, mostly ISM, and wasp venom anaphylaxis, compared to those without anaphylaxis (22). Therefore, the role and relevance of MRGPRX2-mediated MC activation and MRGPRX2 agonists in ISM are still unclear and require further investigation.

Here, we assessed whether MRGPRX2 and its agonists, namely, CST and MBP, are expressed in the skin of ISM patients and whether their expression in skin is linked to clinical features and laboratory markers of ISM.

MATERIALS AND METHODS

Study Population

Skin samples (lesional n = 22, non-lesional n = 21) from 22 adult patients with ISM, who participated in a clinical trial (ClinicalTrials.gov identifier: NCT02808793) were included in a *post hoc* analysis to assess expression of MRGPRX2 and MRGPRX2 agonists. All patients were diagnosed in accordance with the 2016 WHO criteria (5). Skin samples of 10 healthy controls (HCs) were included from the biobank of Charité – Universitätsmedizin Berlin (ethics approval EA1/407/16) and further analyzed for CST (n = 10) and MRGPRX2 (n = 8) expression in the skin. All participants signed an informed consent.

Baseline serum tryptase levels (ImmunoCAP) and *KIT* D816V allele burden in blood (allele-specific quantitative polymerase chain reaction/ASO-qPCR) were assessed on a regular basis in Labor Berlin-Charité/Vivantes. Symptoms, i.e., itching, whealing, flushing, diarrhea, abdominal pain, musculoskeletal pain, fatigue, headache, and difficulty

Abbreviations: ASO-qPCR, allele-specific quantitative polymerase chain reaction; bST, baseline serum tryptase; CST, cortistatin; ECP, eosinophil cationic protein; IF, immunofluorescence; IHC, immunohistochemistry; ISH, *iIn situ* hybridization; ISM, indolent systemic mastocytosis; MAS, mastocytosis activity score; MBP, major basic protein; MC, mast cell; MIS, mastocytosis in the skin; MRGPRX2, Mas-related G-protein coupled receptor X2; PB, peripheral blood; SP, substance P; WHO, World Health Organization.

concentrating, as well as total disease activity were assessed using the Mastocytosis Activity Score (MAS) (6). The Questionnaire was completed daily by the patients for at least 1 week. Afterward, total scores and domain scores were calculated. MAS total score ranges <19, 19–34, and >34 were counted as mild, moderate, and severe disease severity, respectively, as described before (6).

The extent of skin involvement was analyzed independently by two experienced physicians. The mastocytosis in the skin (MIS) scoring system was developed. Patients were divided into five groups, due to the number and color intensity of lesions in the most involved region, where 0 is no skin lesions and 5 is very severe skin involvement (**Supplementary Figure 1**). The evidence of anaphylaxis and osteopenia/osteoporosis was retrospectively extracted from the medical files. Patients were under standard dosed H1-antihistamine therapy, but no topical treatment or ultraviolet irradiation was applied.

Immunohistochemistry and Immunofluorescence

CST and MRGPRX2 staining was performed, as described earlier (23). Briefly, after embedding in paraffin *via* standard protocol, 5-µm sections were baked at 60°C for 1 h in an incubator. Deparaffinization and rehydration were performed using regular procedures. Heat-induced antigen retrieval citrate buffer was applied for the staining with anti-CST (sc-393108, A-7; Santa Cruz Biotechnology, Dallas, TX, USA). Enzymatic pretreatment was used for anti-MRGPRX2 (ab167125, Abcam, Cambridge, MA, USA) staining. Further procedures were performed according to the manufacturer's instructions (Dako EnVision+, Peroxidase). Washing steps in between were performed. Finally, slides were stained with Mayer's hematoxylin (ab128990, Abcam). Lack of the primary antibody was used as a negative control.

MBP expression was assessed in skin of ISM patients only. For MBP staining, enzymatically pretreated paraffin sections were incubated with anti-MBP (Bio-Rad, Hercules, CA, USA, MCA5751) at 4°C overnight. Alkaline phosphatase IgG polymer (MP-5402, Vector, Burlingame, CA, USA), detected with Vector Red Substrate Kit (VEC-SK-5100, Biozol, Eching, Germany), was used as a secondary antibody. Other steps were performed as described above. MCs were identified with the use of anti-tryptase (M7052; Dako, Glostrup, Denmark) according to the manufacturer's instructions.

Co-localization of MRGPRX2 with the MC marker tryptase was assessed by immunofluorescence. The sections were prepared, as described above with the use of heat-induced antigen retrieval and incubated with a mixture of anti-MRGPRX2 (LS-A6644; LSBio, Seattle, WA, USA) and anti-tryptase (M7052; Dako) at 4°C overnight. The next day, slides were incubated in a mixture of two fluorescent conjugated secondary antibodies, Alexa Flour 488-conjugated goat anti-mouse and Rhodamine (TRITC)-conjugated goat anti-rabbit, diluted in TBS containing 2% goat normal serum, for 30 min in the dark at room temperature. In between slides were washed three times in TBS. Mounting with preserve reagent including DAPI (00-4959-52; Invitrogen) was applied afterward.

In Situ Hybridization

In situ hybridization (ISH) of MRGPRX2-mRNA was conducted in line with RNAscope Single-Plex Red Chromogen V2.5 protocol and the recommended HybEZ oven and in combination with materials for immunohistochemistry (IHC)/immunofluorescence (IF). ISH was completed prior to any IHC/IF protocol. All tissue was prepared in line with RNAscope FFPE protocol with antigen retrieval being performed for skin at 65°C for 20.5 h up to 21 h maximum in an oven. The remainder of the RNAscope protocol was followed as per the ACDBio manuals (Documents 322452 and 322360-USM). RNAscope negative and positive controls were used to ensure the quality of yield in this approach. IHC/IF tryptase co-staining was conducted after ISH red chromogen development at the step for protein block. Red chromogen was visible using a fluorescence microscope (BZ-X800; Keyence, Itasca, USA), and positive and negative controls were used to calibrate fluorescence excitation to represent the chromogen stain. After adjusting the settings, they were then used for imaging of the entire assay.

Quantitative Histomorphometry

All sections were blinded and assessed independently by two investigators. The number of positive cells was manually counted in at least five horizontally adjacent high-power microscopic fields (HPF) in the upper papillary dermis. Mean values "per HPF" were calculated and further converted to "per mm^2" (CST^+ cells ×200, 0.6 mm^2, $MRGPRX2^+$ cells ×200, 0.42 mm^2, MCs ×400, 0.2 mm^2, and MRGPRX2-$mRNA^+$ MCs ×400, 0.1 mm^2).

Statistical Analysis

We used the Statistical Package for the Social Science (IBM SPSS version 25.0; IBM Corp, New York, NY), R (R Foundation for Statistical Computing), and GraphPad Prism 8 (GraphPad Software, La Jolla, CA). Demographic characteristics of patients with ISM were reported using descriptive statistics. Data distribution was analyzed with the Kolmogorov–Smirnov test. Normally and not normally distributed data were presented as mean ± SD and median (interquartile range), respectively. The Spearman correlation coefficient was applied to assess correlations. Statistically significant differences between groups were calculated using t-test for normally distributed data and the Mann–Whitney U test for non-normally distributed data. Differences between lesional and non-lesional parameters were analyzed with the paired t-test (normally distributed data) or the Wilcoxon signed-rank test (not normally distributed data). For all tests, $P < 0.05$ was considered as statistically significant.

RESULTS

Demographic, Clinical, and Laboratory Characteristics

We studied 22 patients with ISM (72.7% women) and 10 HCs (40.0% women) with mean age of 50.6 ± 9.3 and 51.6 ± 14.2 years, respectively. Skin lesions, i.e., MIS, were present in all ISM

patients. Osteopenia/osteoporosis and anaphylaxis were common signs associated with mastocytosis, present in 70.0% and 42.9% of patients, respectively (**Table 1**). The median baseline serum tryptase level (bST) and *KIT* D816V allele burden were 31.0 (IQR: 21.0–109.5) ng/ml and 1.0 (0.3–2.6)% in the blood of ISM patients, respectively. Disease activity was mild (27.3%, n = 6), moderate (31.8%, n = 7), and severe (40.9%, n = 9), based on the MAS total values. Detailed demographic and clinical characteristics of ISM patients and HCs are presented in **Supplementary Tables 1, 2**.

The Number of MRGPRX2-, CST-, and MBP-expressing Cells is Increased in Lesional Skin of Patients With Indolent Systemic Mastocytosis

The numbers of MRGPRX2+, CST+, and MBP+ cells were assessed in lesional and non-lesional skin of ISM patients and skin of healthy controls by immunohistochemistry.

The number of MRGPRX2-expressing (MRGPRX2+) cells was significantly higher in lesional skin (median [IQR]: 22.3 [2.5–64.8] cells/mm^2) as compared to non-lesional skin (5.2 [1.5–9.0] cells/mm^2, p = 0.001) and skin of HCs (2.9 [1.2–5.2] cells/mm^2, p = 0.03, **Table 2**, **Figures 1A, B**; **Supplementary Figure 2A**). Most cells showed intracellular and/or paranuclear expression. The membrane expression of MRGPRX2 was rarely detected and more frequently observed in patients with ISM compared to HCs.

The mean number of CST-expressing (CST+) cells was significantly higher in lesional skin than non-lesional skin (mean ± SD: 13.8 ± 8.1 vs. 6.7 ± 4.8 cells/mm^2, p = 0.0005). CST+ cells were also more prominent in lesional skin than in skin of HCs (10.7 ± 3.0 cells/mm^2); however, statistical significance was not reached (**Figures 1C, D**; **Supplementary Figure 2B**).

The number of MBP-expressing (MBP+) cells was significantly higher in lesional skin as compared to non-lesional skin (median [IQR]: 0.7 [0.0–3.6] vs. 0.0 [0.0–0.0] cells/mm^2, p = 0.002) (**Figures 1E, F**).

Mean/median, IQR, and range values are summarized in **Table 2**.

The Number of Mast Cells and MRGPRX2-mRNA+ Mast Cells Is Increased in the Skin of Patients With Indolent Systemic Mastocytosis

Next, we performed IF staining and *in situ* hybridization in combination with IF to identify if and how many MCs are MRGPRX2+ and MRGPRX2-mRNA+. Moreover, we compared the percentage of MRGPRX2-mRNA+ MCs in lesional and non-lesional skin.

TABLE 1 | Demographic, clinical, and laboratory characteristics of ISM patients and healthy controls.

Parameter	ISM, n = 22	HCs, n = 10
Age, years, mean ± SD (range)	50.6 ± 9.3 (33.0–65.0)	51.6 ± 14.2 (23.0–68.0)
Gender, female, n/total (%)	16/22 (72.7)	4/10 (40.0)
Anaphylaxis, n/total (%)	9/21 (42.9)	–
Osteoporosis/osteopenia, n/total (%)	14/20 (70.0)	–
Skin lesions (i.e., MIS), n/total (%)	22/22 (100.0)	–
MAS total, mean ± SD (range)	31.4 ± 14.6 (9.0–54.0)	–
Serum baseline tryptase, ng/ml, median (IQR)	31.0 (21.0–109.5)	5.2 (4.2–6.3)
***KIT* D816V in PB, yes,** n/total (%)	21/22 (95.5)	–
***KIT* D816V burden in PB, %,** median (IQR)	1.0 (0.3–2.6)	–

ISM, indolent systemic mastocytosis; HCs, healthy controls; MIS, mastocytosis in the skin; MAS, mastocytosis activity score; PB, peripheral blood; –, not applicable/no information.

TABLE 2 | MRGPRX2 and its agonists in the skin of ISM patients and healthy controls.

Parameter	ISM		HCs	P value
	Lesional (L)	Non-lesional (NL)		
MRGPRX2+ cells/mm^2, median (IQR)	22.3 (2.5–64.8) *n = 22*	5.2 (1.5–9.0) *n = 21*	2.9 (1.2-5.2) *n=8*	0.001 (L vs. HCs) 0.03 (L vs. NL)
MRGPRX2-mRNA+ MCs/mm^2, median (IQR)	12.4 (3.6–21.5) *n = 8*	4.3 (0.3–9.8) *n = 8*	–	0.017
MRGPRX2-mRNA+ MCs in all MCs, %, median (IQR)	15.3 (7.7–23.1) *n = 8*	13.3 (0.6–32.8) *n = 8*	–	NS
MRGPRX2-mRNA+ MCs in all MRGPRX2-mRNA+ cells, %, mean ± SD (range)	32.0 ± 23.8 (2.9–79.1) *n = 8*	19.2 ± 22.5 (0.0–57.0) *n = 8*	–	0.05
CST+ cells/mm^2 Mean ± SD (range)	13.8 ± 8.1 (4.1–30.8) *n = 12*	6.7 ± 4.8 (0.9–19.0) *n = 12*	10.7 ± 3.0 (6.2–17.2) *n = 10*	0.0005 (L vs. NL) 0.009 (NL vs. HCs)
MBP+ cells/mm^2 median (IQR)	0.7 (0.0–3.6) *n = 22*	0.0 (0.0–0.0) *n = 21*	–	0.002

CST, cortistatin; ISM, indolent systemic mastocytosis; HCs, healthy controls; L, lesional skin; NL, non-lesional skin; NS, non-significant; –, no information.

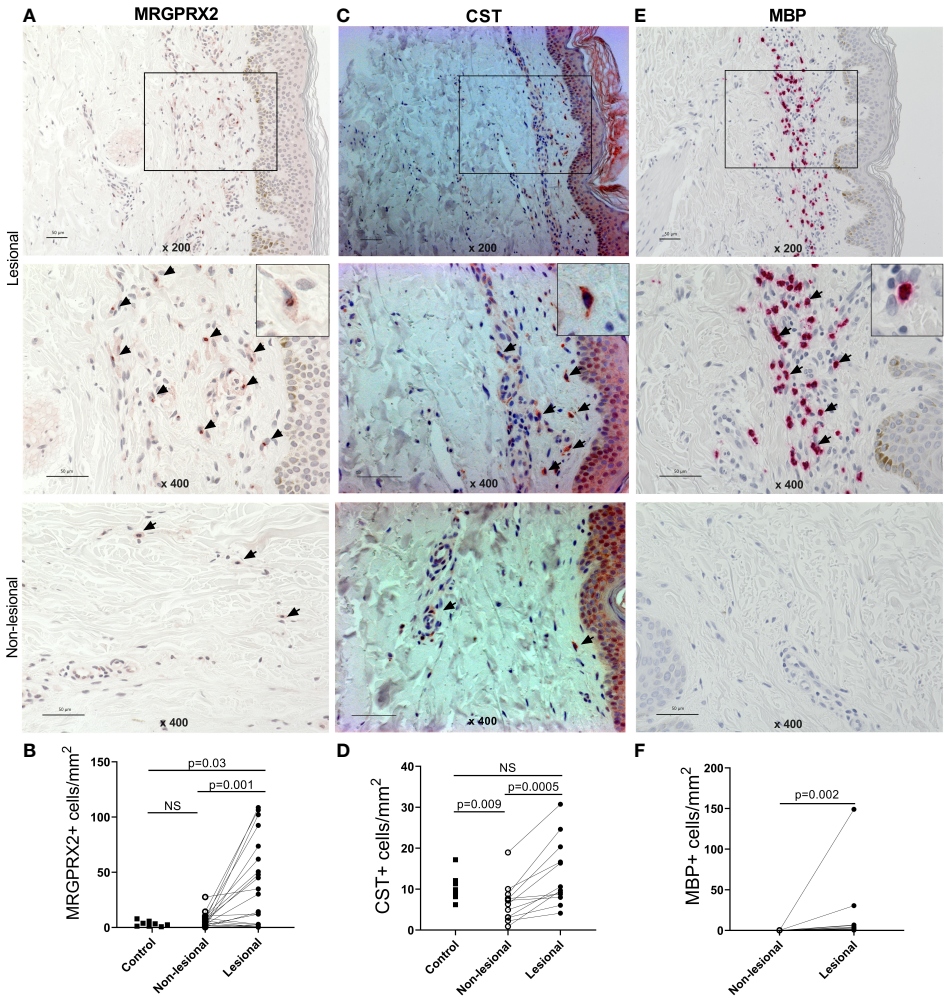


FIGURE 1 | The number of MRGPRX2+, CST+, and MBP+ cells is increased in the lesions of patients with indolent systemic mastocytosis. Immunohistochemical staining of **(A)** MRGPRX2, **(C)** CST, and **(E)** MBP in the lesional and non-lesional skin of patients with ISM #6, #10, and #13, respectively. ×200 magnification of upper picture; ×400 magnification of all other pictures (expressing cells are shown by arrows). Bar = 50 µm. Number of **(B)** MRGPRX2+ cells, **(D)** CST+ cells, and **(F)** MBP+ cells in lesional and non-lesional skin of patients with ISM and skin of healthy controls. $p < 0.05$ was considered significant. The number of patients and controls as well as means/medians are summarized in the **Table 2**. CST, cortistatin; ISM, indolent systemic mastocytosis; MBP, major basic protein; NS, non-significant.

The number of MRGPRX2+ cells strongly correlated with the number of MCs and CST+ and MPB+ cells (**Figures 2A–C**). Double staining for MRGPRX2 and MC tryptase strongly suggests for a colocalization of MRGPRX2 and MCs (**Figure 2D**).

The number of MRGPRX2-mRNA+ MCs in ISM patients was markedly higher in lesional than non-lesional skin (median [IQR]: 12.4 [3.6–21.5] vs. 4.3 [0.3–9.8] cells/mm^2, $p = 0.017$) (**Figures 3A, B**), whereas the overall median percentage of MRGPRX2-mRNA+ MCs in all of MCs was rather low (<16%) and did not differ between lesional and non-lesional skin (**Table 2**; **Figure 3C**). The mean percentage of MRGPRX2-mRNA+ MCs in all of MRGPRX2-mRNA+ cells in ISM patients was significantly higher in lesional skin as compared to non-lesional skin, i.e., 32.0 ± 23.8% and 19.2 ± 22.5%, respectively ($p = 0.05$) (**Table 2**; **Figure 3D**).

Increased Numbers of MRGPRX2+ Cells, MRGPRX2-mRNA+ MCs, and CST+ and MBP+ Cells are Not Associated With Clinical and Laboratory Features of ISM

Finally, we aimed to assess the association of MRGPRX2+ cells, MRGPRX2-mRNA+ MCs, and CST+ and MBP+ cells in the skin with clinical and laboratory characteristics of ISM patients.

There was no link between the numbers of MRGPRX2+ cells, MRGPRX2-mRNA+ MCs, and CST+ and MBP+ cells in lesional skin of ISM patients and disease clinical characteristics, i.e., evidence of anaphylaxis and/or osteopenia/osteoporosis, severity of mastocytosis in the skin (MIS score), and symptom burden as assessed by MAS (**Figure 4**; **Supplementary Figure 3**). Neither the number of MRGPRX2+ cells nor the number or

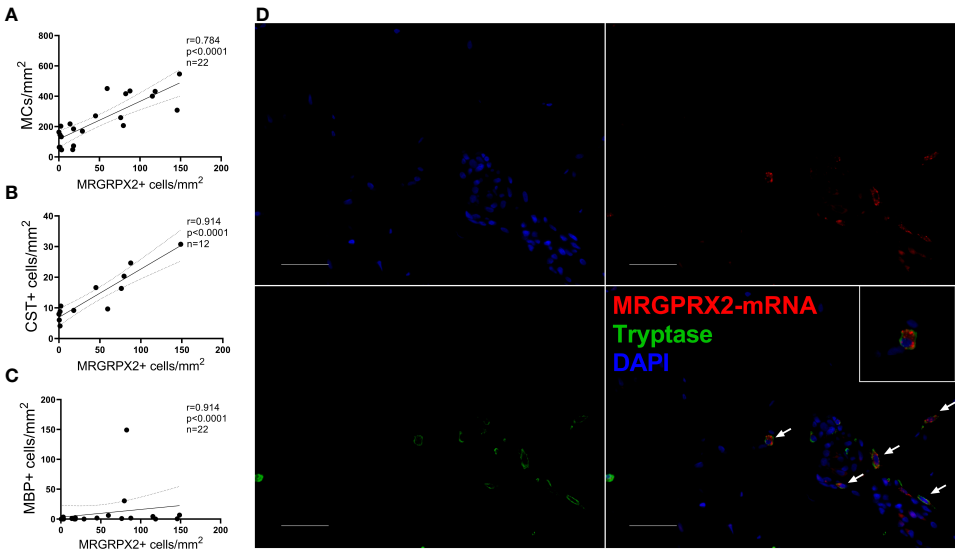


FIGURE 2 | Mast cells express MRGPRX2, and their numbers correlate with numbers of MRGPRX2+ cells in ISM patients. In lesional skin, the number of MRGPRX2+ cells correlates with the number of **(A)** MCs, **(B)** CST+, and **(C)** MBP+ cells. The Spearman correlation coefficient was applied to assess correlations. **(D)** Immunofluorescence staining of lesional skin of a patient with ISM #12 with anti-tryptase (green), anti-MRGPRX2 (red), and DAPI (blue). White arrows indicate some of tryptase-MRGPRX2 double-positive cells. ×400 magnification. Bar = 50 μm. CST, cortistatin; DAPI, 49-6-diamidino-2-phenylindole dihydrochloride; MBP, major basic protein; MC, mast cell.

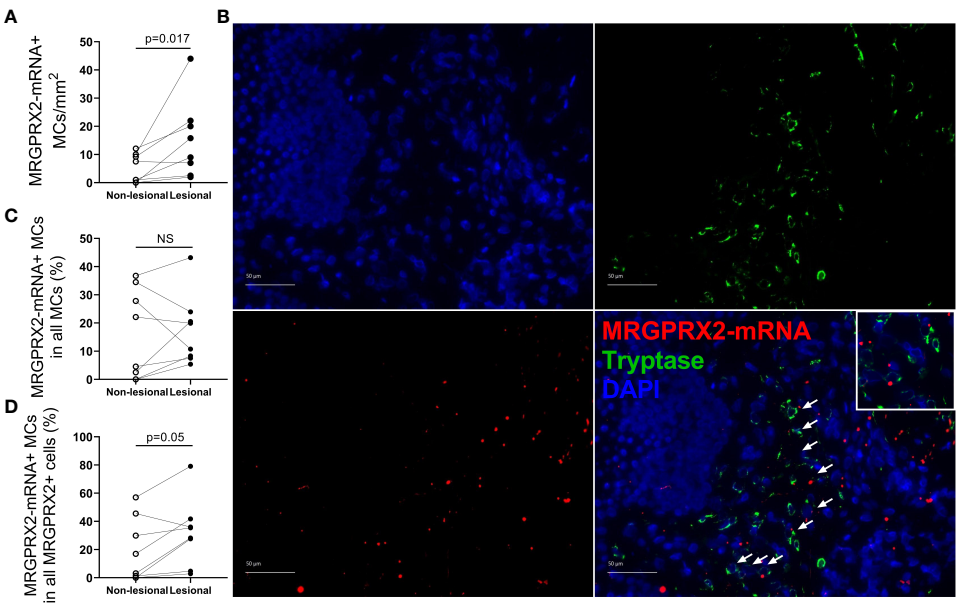


FIGURE 3 | The number of MRGPRX2-mRNA-expressing mast cells is increased in lesional skin of patients with indolent systemic mastocytosis. **(A)** Number of MRGPRX2-mRNA+ MCs in lesional and non-lesional skin of ISM patients. **(B)** *In situ* hybridization (MRGPRX2-mRNA) (red) and immunofluorescence (tryptase) (green) double staining in lesional skin of a patient with ISM #12 (MRGPRX2-mRNA+MCs are shown by white arrows). ×400 magnification. Bar = 50 μm. **(C)** The percentage of MRGPRX2-mRNA+ MCs in all MCs in lesional and non-lesional skin of ISM patients. **(D)** The percentage of MRGPRX2-mRNA+ MCs in all MRGPRX-mRNA+ cells in lesional and non-lesional skin of ISM patients. ISM, indolent systemic mastocytosis; MC, mast cell.

percentage of MRGPRX2-mRNA+ MCs in the skin of ISM patients correlated with any laboratory parameter, including bST, *KIT* D816V allele burden, and alkaline phosphatase levels (**Figure 4**).

DISCUSSION

In this study, we intended to identify whether the presence of MRGPRX2 or its agonists in the skin is associated with certain symptoms, particularly itch and flushing, in patient with ISM. We found that skin lesions of ISM patient hosts markedly increased numbers of MRGPRX2+, CST+, and MPB+ cells and MRGPRX2-mRNA+ MCs, although this increase was not associated with severity of signs and symptoms in ISM patients.

MCs are known to express MRGPRX2, and MC accumulation is a typical finding in mastocytosis in the skin (7). Indeed, overexpression of MRGPRX2 and/or increased numbers of MRGPRX2+ MCs have been described in the lesions of patients with MC-driven disorders, e.g., cutaneous mastocytosis (13), chronic spontaneous urticaria (CSU) (15), and chronic prurigo (23), and correlated with disease severity in the latter. In line with this, the number of MRGPRX2+ cells was increased in our study and correlated with MC numbers as well as numbers of MBP+ cells. MBP, stored in eosinophil granules, has been described to activate human skin MCs *via* MRGPRX2 (15). Eosinophils, *via* cross talk with MCs, are known to contribute to various inflammatory and neoplastic disorders (24). They were identified in lesional skin of most patients with mastocytosis, varying from minimal to severe eosinophil infiltration, with the latter being present after initiation of a wheal-and-flare reaction (Darier's sign) (25). A study by Wedi et al. showed that blood eosinophils express MRGPRX2 but to a lesser extent than MCs (26). We observed elevated numbers of MBP+ cells in lesional skin of ISM patients, although the overall number in the skin was rather low. However, MBP levels exhibited no correlation with signs in ISM patients and were not linked to symptom severity. Whether other cells, e.g., eosinophils or neurons, express MRGPRX2 in the skin of ISM patients should be investigated in further studies. In our study, the number of CST+ cells was also higher in lesional skin of patients with ISM and correlated with the extent of MC accumulation. CST is one of the most potent MRGRPX2 agonists and has been reported to be expressed and released by MCs upon activation (16, 23). This neuropeptide is thought to have both pro- and anti-inflammatory activities (27) and was shown to be upregulated in the skin of patients with chronic prurigo (23), but downregulated in psoriasis (28). In chronic prurigo, proinflammatory properties of CST might be related to autocrine activation of MCs *via* MRGPRX2 (23). In our study, increased numbers of CST+ cells were not associated with ISM symptom severity, including skin symptoms. However, the exact role of CST in the pathophysiology of ISM and its clinical relevance should be assessed in further studies.

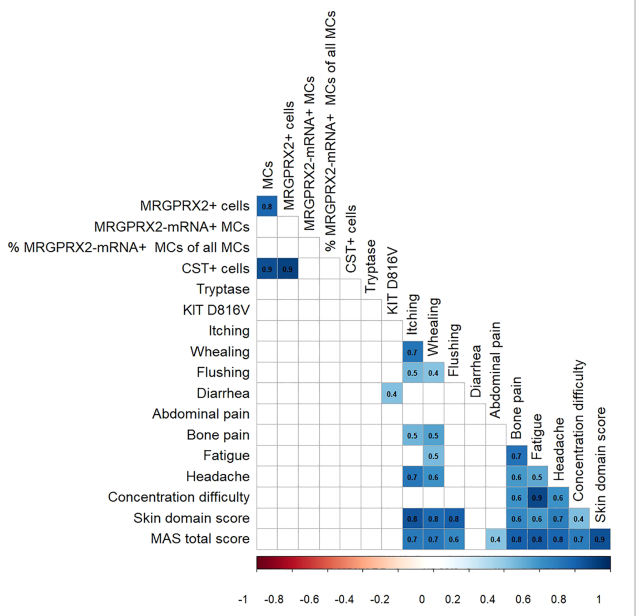


FIGURE 4 | Correlation of MRGPRX2 and its agonists in the skin with the clinical and laboratory parameters in patients with ISM.The color shades represent the value of the Spearman correlation coefficient (r) and the relationship (red and blue are negative and positive r values, respectively). Only statistically significant correlations are shown ($p < 0.05$). CST, cortistatin; MAS, mastocytosis activity score; MC, mast cell.

Despite increased numbers of MRGPRX2+ cells, there was no association of any MRGPRX2-related parameter with clinical or laboratory features of ISM in our cohort of patients. There was no difference in MRGPRX2+ MC burden in the skin in patients with and without anaphylaxis, which is in line with recently published data (22). Whether anaphylaxis in ISM patients is linked to IgE-dependent or MRGPRX2-dependent MC activation or both mechanisms needs to be investigated in further studies. FcεRI- and MRGPRX2-evoked MC degranulation has been recently shown to be fully additive (29).

Finally, we assessed whether MRGPRX2 expression differs between wild-type MCs and MCs with *KIT* D816V mutation using a recently developed human-induced pluripotent stem cell-derived mast cell model (hiPSC-MCs) (30). The surface expression of MRGPRX2 on hiPSC-MCs carrying the *KIT* D816V mutation (hiPSC-MCs$^{KIT\ D816V}$) as assessed by flow cytometry was comparable to the respective wild-type (hiPSC-MCs^{WT}) (data not shown). Thus, we can speculate that the *KIT* D816V mutation does not affect the level of MRGPRX2 surface expression on MCs.

Our study is limited by inclusion of only symptomatic patients and a single-center retrospective design. In most cases, a functional mechanism for the elicitation of symptoms by MRGPRX2 agonists could not be evaluated in detail. The role and relevance of MRGPRX2 and its agonists for the elicitation of anaphylaxis and intolerance reactions to different triggers, e.g., drugs, in ISM should be addressed in future studies.

In conclusion, skin lesions of patients with ISM showed high numbers of MRGPRX2-expressing cells, although the *KIT*

D816V mutation, at least *in vitro*, seems not to affect MRGPRX2 expression by MCs. The expression of MRGPRX2 and its agonists in the skin exhibits no association with signs and symptoms of ISM. Whether other factors, such as a combination of different MRGPRX2 agonists, synergy with the FcεRI-dependent pathway, or MRGPRX2 genetic alterations, are being involved in MC activation in patients with ISM is yet unknown. To answer these questions, further studies should be performed, e.g., functional assays and *in vivo* tests with MRPGRX2 agonists.

DATA AVAILABILITY STATEMENT

The original contributions presented in the study are included in the article/**Supplementary Material**. Further inquiries can be directed to the corresponding author.

ETHICS STATEMENT

The studies involving human participants were reviewed and approved by the Ethics Committee of Charité – Universitätsmedizin Berlin EA1/407/16. The patients/participants provided their written informed consent to participate in this study.

AUTHOR CONTRIBUTIONS

PP, FS, and PK designed the study, interpreted the data, and prepared the manuscript. PP, PK, SM-R, YL, TA, HB, QJ, JH, and MH (8th Author) performed experiments and/or analyzed the data. The study was supervised by PK and FS. All coauthors critically revised and provided substantial input to the manuscript. All authors contributed to the article and approved the submitted version.

FUNDING

This study was in part financially supported by Allakos Inc. The funder was not involved in the study design, collection, analysis, interpretation of data, the writing of this article, or decision to submit it for publication.

SUPPLEMENTARY MATERIAL

The Supplementary Material for this article can be found online at: https://www.frontiersin.org/articles/10.3389/fimmu.2022.930945/full#supplementary-material

REFERENCES

1. Cohen SS, Skovbo S, Vestergaard H, Kristensen T, Moller M, Bindslev-Jensen C, et al. Epidemiology of Systemic Mastocytosis in Denmark. *Br J Haematol* (2014) 166(4):521–8. doi: 10.1111/bjh.12916
2. Zanotti R, Bonifacio M, Isolan C, Tanasi I, Crosera L, Olivieri F, et al. A Multidisciplinary Diagnostic Approach Reveals a Higher Prevalence of Indolent Systemic Mastocytosis: 15-Years' Experience of the GISM Network. *Cancers (Basel)* (2021) 13(24). doi: 10.3390/cancers13246380
3. van Doormaal JJ, Arends S, Brunekreeft KL, van der Wal VB, Sietsma J, van Voorst Vader PC, et al. Prevalence of Indolent Systemic Mastocytosis in a Dutch Region. *J Allergy Clin Immunol* (2013) 131(5):1429–31 e1. doi: 10.1016/j.jaci.2012.10.015
4. Jensen B, Broesby-Olsen S, Bindslev-Jensen C, Nielsen DS. Everyday Life and Mastocytosis From a Patient Perspective-a Qualitative Study. *J Clin Nurs* (2019) 28(7-8):1114–24. doi: 10.1111/jocn.14676
5. Valent P, Akin C, Metcalfe DD. Mastocytosis: 2016 Updated WHO Classification and Novel Emerging Treatment Concepts. *Blood* (2017) 129 (11):1420–7. doi: 10.1182/blood-2016-09-731893
6. Siebenhaar F, Sander B, Ho LHT, Ellrich A, Maurer M, Weller K. Development and Validation of the Mastocytosis Activity Score. *Allergy* (2018) 73(7):1489–96. doi: 10.1111/all.13425
7. Hartmann K, Escribano L, Grattan C, Brockow K, Carter MC, Alvarez-Twose I, et al. Cutaneous Manifestations in Patients With Mastocytosis: Consensus Report of the European Competence Network on Mastocytosis; the American Academy of Allergy, Asthma & Immunology; and the European Academy of Allergology and Clinical Immunology. *J Allergy Clin Immunol* (2016) 137 (1):35–45. doi: 10.1016/j.jaci.2015.08.034
8. Siebenhaar F, von Tschirnhaus E, Hartmann K, Rabenhorst A, Staubach P, Peveling-Oberhag A, et al. Development and Validation of the Mastocytosis Quality of Life Questionnaire: MC-QoL. *Allergy* (2016) 71(6):869–77. doi: 10.1111/all.12842
9. Vaes M, Benghiat FS, Hermine O. Targeted Treatment Options in Mastocytosis. *Front Med (Lausanne)* (2017) 4:110. doi: 10.3389/fmed.2017.00110
10. Kolkhir P, Elieh-Ali-Komi D, Metz M, Siebenhaar F, Maurer M. Understanding Human Mast Cells: Lesson From Therapies for Allergic and Non-Allergic Diseases. *Nat Rev Immunol* (2022) 22(5):294–308. doi: 10.1038/s41577-021-00622-y
11. Bonadonna P, Bonifacio M, Lombardo C, Zanotti R. Hymenoptera Allergy and Mast Cell Activation Syndromes. *Curr Allergy Asthma Rep* (2016) 16(1):5. doi: 10.1007/s11882-015-0582-5
12. Weiler CR. Mastocytosis, Quinolones, MRGPRX2, and Anaphylaxis. *J Allergy Clin Immunol Pract* (2019) 7(6):2091–2. doi: 10.1016/j.jaip.2019.02.015
13. Deepak V, Komarow HD, Alblaihess AA, Carter MC, Metcalfe DD, Ali H. Expression of MRGPRX2 in Skin Mast Cells of Patients With Maculopapular Cutaneous Mastocytosis. *J Allergy Clin Immunol Pract* (2021) 9(10):3841– e1. doi: 10.1016/j.jaip.2021.05.042
14. McNeil BD, Pundir P, Meeker S, Han L, Undem BJ, Kulka M, et al. Identification of a Mast-Cell-Specific Receptor Crucial for Pseudo-Allergic Drug Reactions. *Nature* (2015) 519(7542):237–41. doi: 10.1038/nature14022
15. Fujisawa D, Kashiwakura J, Kita H, Kikukawa Y, Fujitani Y, Sasaki-Sakamoto T, et al. Expression of Mas-Related Gene X2 on Mast Cells is Upregulated in the Skin of Patients With Severe Chronic Urticaria. *J Allergy Clin Immun* (2014) 134(3):622. doi: 10.1016/j.jaci.2014.05.004
16. Robas N, Mead E, Fidock M. MrgX2 Is a High Potency Cortistatin Receptor Expressed in Dorsal Root Ganglion. *J Biol Chem* (2003) 278(45):44400–4. doi: 10.1074/jbc.M302456200
17. Ogasawara H, Furuno M, Edamura K, Noguchi M. Peptides of Major Basic Protein and Eosinophil Cationic Protein Activate Human Mast Cells. *Biochem Biophys Rep* (2020) 21:100719. doi: 10.1016/j.bbrep.2019.100719
18. Kuhn H, Kolkhir P, Babina M, Dull M, Frischbutter S, Fok JS, et al. Mas-Related G Protein-Coupled Receptor X2 and its Activators in Dermatologic Allergies. *J Allergy Clin Immunol* (2021) 147(2):456–69. doi: 10.1016/j.jaci.2020.08.027
19. Subramanian H, Gupta K, Guo Q, Price R, Ali H. Mas-Related Gene X2 (MrgX2) Is a Novel G Protein-Coupled Receptor for the Antimicrobial

Peptide LL-37 in Human Mast Cells: Resistance to Receptor Phosphorylation, Desensitization, and Internalization. *J Biol Chem* (2011) 286(52):44739–49. doi: 10.1074/jbc.M111.277152
20. Arifuzzaman M, Mobley YR, Choi HW, Bist P, Salinas CA, Brown ZD, et al. MRGPR-Mediated Activation of Local Mast Cells Clears Cutaneous Bacterial Infection and Protects Against Reinfection. *Sci Adv* (2019) 5(1):eaav0216. doi: 10.1126/sciadv.aav0216
21. Giavina-Bianchi P, Goncalves DG, Zanandrea A, Borges de Castro R, Garro LS, Kalil J, et al. Anaphylaxis to Quinolones in Mastocytosis: Hypothesis on the Mechanism. *J Allergy Clin Immunol Pract* (2019) 7(6):2089–90. doi: 10.1016/j.jaip.2019.01.059
22. Elst J, De Puysseleyr LP, Ebo DG, Faber MA, Van Gasse AL, van der Poorten MM, et al. Overexpression of FcepsilonRI on Bone Marrow Mast Cells, But Not MRGPRX2, in Clonal Mast Cell Disorders With Wasp Venom Anaphylaxis. *Front Immunol* (2022) 13:835618. doi: 10.3389/fimmu.2022.835618
23. Kolkhir P, Pyatilova P, Ashry T, Jiao Q, Abad-Perez AT, Altrichter S, et al. Mast Cells, Cortistatin, and its Receptor, MRGPRX2, Are Linked to the Pathogenesis of Chronic Prurigo. *J Allergy Clin Immunol* (2022) 149(6):1998–2009.e5. doi: 10.1016/j.jaci.2022.02.021
24. Gotlib J, Akin C. Mast Cells and Eosinophils in Mastocytosis, Chronic Eosinophilic Leukemia, and non-Clonal Disorders. *Semin Hematol* (2012) 49(2):128–37. doi: 10.1053/j.seminhematol.2012.01.007
25. Maehara E, Kido-Nakahara M, Ito T, Uchi H, Furue M. Darier's Sign in Urticaria Pigmentosa-Significance of Perivascular Eosinophilic Infiltration. *Allergol Int* (2018) 67(4):532–4. doi: 10.1016/j.alit.2018.04.006
26. Wedi B, Gehring M, Kapp A. The Pseudoallergen Receptor MRGPRX2 on Peripheral Blood Basophils and Eosinophils: Expression and Function. *Allergy* (2020) 75(9):2229–42. doi: 10.1111/all.14213
27. Delgado-Maroto V, Falo CP, Forte-Lago I, Adan N, Morell M, Maganto-Garcia E, et al. The Neuropeptide Cortistatin Attenuates Experimental Autoimmune Myocarditis *via* Inhibition of Cardiomyogenic T Cell-Driven Inflammatory Responses. *Br J Pharmacol* (2017) 174(3):267–80. doi: 10.1111/bph.13682
28. Li D, He HL, Yao MZ, Chen ML, Chen X. Cortistatin is Dysregulated in Skin Tissue of Patients With Psoriasis Vulgaris and Suppresses Keratinocyte Proliferation *In Vitro*. *Int J Dermatol* (2015) 54(8):e309–14. doi: 10.1111/ijd.12836
29. Babina M, Wang Z, Li Z, Franke K, Guhl S, Artuc M, et al. FcepsilonRI- and MRGPRX2-Evoked Acute Degranulation Responses are Fully Additive in Human Skin Mast Cells. *Allergy* (2022) 77(6):1906–1909. doi: 10.1111/all.15270
30. Luo Y, Fernandez Vallone V, He J, Frischbutter S, Kolkhir P, Monino-Romero S, et al. A Novel Approach for Studying Mast Cell-Driven Disorders: Mast Cells Derived From Induced Pluripotent Stem Cells. *J Allergy Clin Immunol* (2022) 149(3):1060–8 e4. doi: 10.1016/j.jaci.2021.07.027

Conflict of Interest: HB received honoraria (advisory board, speaker) from AbbVie, Novartis, and Sanofi-Aventis, outside of submitted work. JS has no relevant conflict of interest in relation to this work. Outside of it, JS is or recently was advisor for Boehringer Ingelheim. BY is employed by Allakos Inc. MM has no relevant conflict of interest in relation to this work. Outside of it, MM is or recently was a speaker and/or advisor or received institutional research funding from Astria, Allakos, Alnylam, Amgen, Aralez, ArgenX, AstraZeneca, BioCryst, Blueprint, Celldex, Centogene, CSL Behring, Dyax, FAES, Genentech, GIInnovation, GSK, Innate Pharma, Kalvista, Kyowa Kirin, Leo Pharma, Lilly, Menarini, Moxie, Novartis, Pfizer, Pharming, Pharvaris, Roche, Sanofi/Regeneron, Shire/Takeda, Third Harmonic Bio, UCB, and Uriach. FS is or recently was a speaker and/or advisor for and/or has received research funding from Allakos, Blueprint, Celldex, CogentBio, Genentech, Novartis, Moxie, Sanofi/Regeneron, and Uriach. PK has no relevant conflict of interest in relation to this work. Outside of it, PK is or recently was a speaker and/or advisor for Novartis and Roche.

The remaining authors declare that the research was conducted in the absence of any commercial or financial relationships that could be construed as a potential conflict of interest.

Publisher's Note: All claims expressed in this article are solely those of the authors and do not necessarily represent those of their affiliated organizations, or those of the publisher, the editors and the reviewers. Any product that may be evaluated in this article, or claim that may be made by its manufacturer, is not guaranteed or endorsed by the publisher.

‡*ORCID: Polina Pyatilova, orcid.org/0000-0001-5520-2900; Yanyan Luo, orcid.org/0000-0003-2330-6072; Tameem Ashry, orcid.org/0000-0003-0616-7509; Hanna Bonnekoh, orcid.org/0000-0002-3567-0149; Qingqing Jiao, orcid.org/0000-0001-6278-2608; Sherezade Moñino-Romero, orcid.org/0000-0003-3775-2989; Jiajun He, orcid.org/0000-0002-9856-1310; Man Hu, orcid.org/0000-0003-2886-8023; Jörg Scheffel, orcid.org/0000-0002-9365-3785; Stefan Frischbutter, orcid.org/0000-0003-3971-7343; Maud Hermans, orcid.org/0000-0002-1643-8387; Bradford A Youngblood; Marcus Maurer, orcid.org/0000-0002-4121-481X; Frank Siebenhaar, orcid.org/0000-0003-4532-1644; Pavel Kolkhir, orcid.org/0000-0001-5380-8132*

Copyright © 2022 Pyatilova, Ashry, Luo, He, Bonnekoh, Jiao, Moñino-Romero, Hu, Scheffel, Frischbutter, Hermans, Youngblood, Maurer, Siebenhaar and Kolkhir. This is an open-access article distributed under the terms of the Creative Commons Attribution License (CC BY). The use, distribution or reproduction in other forums is permitted, provided the original author(s) and the copyright owner(s) are credited and that the original publication in this journal is cited, in accordance with accepted academic practice. No use, distribution or reproduction is permitted which does not comply with these terms.

frontiers | Frontiers in Immunology

TYPE Systematic Review
PUBLISHED 28 July 2022
DOI 10.3389/fimmu.2022.901851

Check for updates

OPEN ACCESS

EDITED BY
Satoshi Tanaka,
Kyoto Pharmaceutical University, Japan

REVIEWED BY
Chiara Cardamone,
University of Salerno, Italy
Umit Murat Sahiner,
Hacettepe University, Turkey

*CORRESPONDENCE
Marcus Maurer
marcus.maurer@charite.de

SPECIALTY SECTION
This article was submitted to Inflammation, a section of the journal Frontiers in Immunology

RECEIVED 22 March 2022
ACCEPTED 04 July 2022
PUBLISHED 28 July 2022

CITATION
Kulthanan K, Church MK, Grekowitz EM, Hawro T, Kiefer LA, Munprom K, Nanchaipruek Y, Rujitharanawong C, Terhorst-Molawi D and Maurer M (2022) Evidence for histamine release in chronic inducible urticaria – A systematic review. *Front. Immunol.* 13:901851. doi: 10.3389/fimmu.2022.901851

COPYRIGHT
© 2022 Kulthanan, Church, Grekowitz, Hawro, Kiefer, Munprom, Nanchaipruek, Rujitharanawong, Terhorst-Molawi and Maurer. This is an open-access article distributed under the terms of the Creative Commons Attribution License (CC BY). The use, distribution or reproduction in other forums is permitted, provided the original author (s) and the copyright owner(s) are credited and that the original publication in this journal is cited, in accordance with accepted academic practice. No use, distribution or reproduction is permitted which does not comply with these terms.

Evidence for histamine release in chronic inducible urticaria – A systematic review

Kanokvalai Kulthanan[1], Martin K. Church[2,3], Eva Maria Grekowitz[2,3], Tomasz Hawro[2,3,4], Lea Alice Kiefer[2,3], Kanyalak Munprom[1], Yanisorn Nanchaipruek[1], Chuda Rujitharanawong[1], Dorothea Terhorst-Molawi[2,3] and Marcus Maurer[2,3]*

[1]Department of Dermatology, Faculty of Medicine Siriraj Hospital, Mahidol University, Bangkok, Thailand, [2]Institute of Allergology, Charité – Universitätsmedizin Berlin, Corporate Member of Freie Universität Berlin and Humboldt-Universität zu Berlin, Berlin, Germany, [3]Fraunhofer Institute for Translational Medicine and Pharmacology ITMP, Allergology and Immunology, Berlin, Germany, [4]Department of Dermatology, Allergology and Venereology, Institute and Comprehensive Center for Inflammation Medicine, University Medical Center Schleswig-Holstein, Lübeck, Germany

Background: Chronic inducible urticaria (CIndU) constitutes a group of nine different CIndUs in which pruritic wheals and/or angioedema occur after exposure to specific and definite triggers. Histamine released from activated and degranulating skin mast cells is held to play a key role in the pathogenesis of CIndU, but evidence to support this has, as of yet, not been reviewed systematically or in detail. We aim to characterize the role and relevance of histamine in CIndU.

Methods: We systematically searched 3 electronic databases (PubMed, Scopus, and Embase) for studies that reported increased serum or skin histamine concentration (direct evidence) or *in vitro* or *ex vivo* histamine release (indirect evidence) following trigger exposure.

Results: An initial total of 3,882 articles was narrowed down to 107 relevant studies of which 52 were in cold urticaria, 19 in cholinergic urticaria, 14 in heat urticaria, 10 in contact urticaria, 7 each in solar urticaria and vibratory angioedema, 4 each in symptomatic dermographism and aquagenic urticaria, and 3 in delayed pressure urticaria. The results of our review support that histamine has a key pathogenic role in the pathogenesis of all CIndUs, but it is not the sole mediator as evidenced by the often poor relationship between the level of histamine and severity of symptoms and the variable clinical efficacy of H_1-antihistamines.

Conclusions: Histamine released from skin mast cells is a key driver of the development of signs and symptoms and a promising therapeutic target in CIndU.

KEYWORDS

antihistamines, chronic inducible urticaria, histamine, mast cell, wheal

Introduction

Chronic inducible urticaria (CIndU) is a subgroup of chronic urticaria in which recurrent pruritic wheals and/or angioedema occur after exposure to specific and definite triggers (1). There are nine different CIndUs, with a wide spectrum of physical and chemical triggers. Examples of the former are exposure to cold and pressure in cold urticaria (ColdU) and delayed pressure urticaria (DPU), respectively. Examples of the latter are water in aquagenic urticaria (AquaU) and sweat in cholinergic urticaria (CholU). How these triggers cause the occurrence of wheals, angioedema, or both, in patients with CIndUs, is largely unclear (2, 3).

Histamine, released from activated and degranulating skin mast cells, is held to play a key role in the pathogenesis of CIndU. This is supported by several independent lines of evidence. First, the wheals that occur in patients with CIndU share many features of those induced by histamine skin prick testing or intracutaneous injection (4–6). Both occur within minutes of exposure, and they are, in most cases, pruritic and short lived, with resolution after minutes to a few hours (4, 5). Second, immunoglobulin E (IgE) autoantibodies appear to be involved, in some CIndUs, in the activation of skin mast cells (1, 7–10). IgE-mediated activation is a well characterized mechanism of mast cell histamine release and relevant in allergies and chronic spontaneous urticaria (9). Third, H_1-antihistamines (AH_1) protect many, but not all, patients with CIndU from the occurrence of signs and symptoms (11–15). In addition, there is also direct evidence, from *in vivo* studies, as well as indirect evidence, from *in vitro* studies, for histamine release from skin mast cells in CIndU, but this evidence has, as of yet, not been reviewed systematically or in detail.

Here, we review both *in vivo* and *in vitro* evidence for histamine release as a pathogenic driver in CIndU. Our aim is to better characterize the role and relevance of histamine, and, by proxy, those of its receptors and its only relevant source in human skin, mast cells, as mechanisms of the development of signs and symptoms and relevant treatment targets in CIndU.

Materials and methods

Preferred Reporting Items for Systematic Reviews and Meta-Analysis were used in this study (16). We systematically searched 3 electronic databases (PubMed, Scopus, and Embase) for studies that reported direct and/or indirect evidence of histamine release in CIndU and were published before April 2021 (inclusion criteria). Increased serum or skin histamine concentration in patients with CIndU after provocation testing was defined as direct evidence (17), whereas other evidence for histamine release was classified as indirect (18). The advanced search option was used with the Mesh terms "histamine" AND each type of CIndU, for example, "cold urticaria" or "symptomatic dermographism". All articles identified were screened by at least two independent reviewers, and their reference lists were searched for additional reports of relevance. Case reports, case series, randomized controlled trials (RCTs), cohort, case-control, and cross-sectional studies that reported evidence of histamine release in CIndU were included. Owing to the relatively limited number of studies of histamine release in CIndU, case reports and case series were included, aiming to collect data from available published evidence as much as possible.

From each report included in our review, we extracted the number of studied patients, how histamine release was assessed and what the outcome was, as well as the author information and year of publication. Our search identified 3,882 potentially relevant articles (429 from PubMed, 622 from Embase, and 2,831 from Scopus). After the exclusion of 976 duplicates, 2,906 studies were reviewed by title and abstract. Of these, 2617 articles were excluded because they did not fulfill our inclusion criteria. A total of 289 articles underwent full-text review. In the end, 107 studies, consisting of 1 RCT, 10 cohort studies, 9 case-control studies, 35 cross-sectional studies, 6 case series and 46 case reports, were included in our systematic review (Figure 1). Of these 107 studies, 52 were in ColdU, 19 in CholU, 14 in heat urticaria (HeatU), 10 in contact urticaria (ConU), 7 each in solar urticaria (SolU) and vibratory angioedema (VA), 4 each in symptomatic dermographism (SD) and AquaU, and 3 in DPU. Some articles reported multiple types of CIndU. All articles were in English. The quality and risk of bias assessment of included articles in systematic review was determined (Supplementary Table 1).

The rating system developed by de Croon et al. (19) was applied to categorized the levels of evidence for 'association' and 'no association' The Levels of evidence for "association" were categorized as *strong*: 3 studies available that find an association in the same direction or ≥ 4 studies available, of which > 66% find a significant association in the same direction and no more than 25% find an opposite association, *weak*: 2 studies available that find a significant association in the same direction or 3 studies available, of which two find a significant association in the same direction and the third study finds no significant association, *no evidence*: ≤ 1 study available, *inconsistent*: remaining cases. The levels of evidence for "no association" were defined as *strong*: > 4 studies are available, of which >85% find no significant association, *weak*: > four studies are available, of which >75% find no significant association.

Results

Symptomatic dermographism

Two studies provided direct evidence of an increase in blood histamine levels following provocation testing in symptomatic dermographism (SD). In the first, post-provocation blood

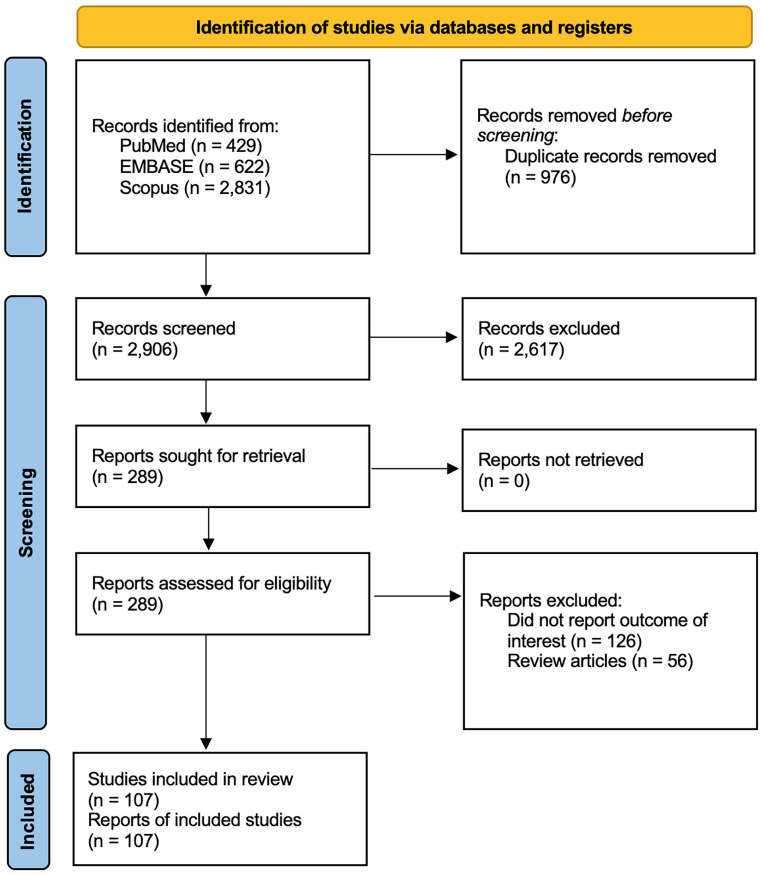


FIGURE 1
Flow diagram of the literature review in this systematic review. One hundred and seven articles met the inclusion criteria and were included in this systematic review (1 randomized controlled trial, 10 cohort studies, 9 case-control studies, 35 cross-sectional studies, 6 case series, and 46 case reports). There were 4 articles with SD, 52 articles with ColdU, 3 articles with DPU, 7 articles with SolU, 19 articles with CholU, 14 articles with HeatU, 7 articles with VA, 4 articles with AquaU, and 10 articles with ConU. Some of articles reported multiple chronic inducible urticaria cases. AquaU, aquagenic urticaria; CholU, cholinergic urticaria; ColdU, cold urticaria; ConU, contact urticaria; DPU, delayed pressure urticaria; HeatU, heat urticaria; SD, symptomatic dermographism; SolU, solar urticaria; VA, vibratory angioedema.

histamine levels were increased in five of ten patients of whom two had markedly higher levels (20) (Supplementary Table 2). In the second, a patient with severe SD showed a marked increase in venous histamine from 18 ng/ml before scratching to a peak of 62 ng/ml two minutes after provocation. Blood histamine levels returned to baseline within 4 minutes (21).

In 1970, Greaves and Sondegaard reported direct evidence for histamine release in SD obtained by the use of fine bore needles to sample the skin in the provocation area of 8 patients and 16 controls (17). Histamine was detected in the basal perfusate of all 8 patients, probably due to whealing in response to needle insertion. None of the controls showed detectable basal histamine. In six of the 8 patients, stroking the skin produced further whealing accompanied by a further rise in skin histamine levels.

As for indirect evidence of histamine release in SD, a systematic review of RCTs and non-RCTs of treatment of SD revealed that first-generation H_1-antihistamines ($fgAH_1$) had variable efficacy and significant side effects, whereas second-generation H_1-antihistamines ($sgAH_1$), in all studies, were effective with a good safety profile and should be the first-line treatment (22).

Cold urticaria

That histamine is released in symptomatic patients with cold urticaria (ColdU) was first suggested by Bram Rose in 1941 who detected elevated blood histamine levels in these patients after cold challenge (20, 23) (Supplementary Table 3). This finding was confirmed by several subsequent studies, including the ones by Dunér et al. (24, 25), who found that blood histamine levels can also be elevated in healthy subjects after cold challenge, Spuzic *et al.* (26), who found plasma histamine to be elevated in

3 of 7 ColdU patients washed with cold water, and others (27–30).

Perhaps the most definitive experiments were performed by Kaplan et al. (18, 31), who showed, in six ColdU patients, that immersion of one hand in cold water caused a rise in plasma histamine of 10-36 ng/ml, peaking at 4 minutes. The results of these reports on blood histamine levels are supported by studies in which histamine skin levels were found to be increased in cold-induced wheals (3). Using skin microdialysis, Andersson et al. (32) showed ice cube-induced increases in skin histamine levels varying from 91 to 550 nM in three patients. Nuutinen et al. (33) reported that of six patients, two had high dialysate histamine levels (621 and 1,269 nM) while the others had lower levels (21 – 100 nM). Kring Tannert et al. (10) also detected, by skin microdialysis, histamine release following cold challenge, which was much reduced after tolerance induction.

In a study with the $sgAH_1$ bilastine, post-provocation skin microdialysis was performed in 20 ColdU patients on three occasions, following treatment for one week each with placebo, bilastine 20, and bilastine 80 mg (12). While only group mean data were reported in the published paper, results for individual patients are presented here.

The results of microdialysis for each patient for the three occasions were remarkably consistent for each showing that the antihistamine, while significantly reducing the critical temperature threshold (CTT), had no effect on histamine release. Several conclusions may be made from the results shown in Figure 2. First, the increases in histamine release at the temperature at which wheals occurred were very variable, from 3 – 222 nM. Second, there is a significant (P = 0.003) relationship between dialysate histamine concentrations and CTTs suggesting that histamine is a major mediator. Third, the regression line intercepts the CTT line at 13°C indicating strongly that there is participation of another mediator in addition to histamine in producing the symptoms. Fourth, the patients with the highest histamine levels are in general less sensitive to 80 mg bilastine, the antihistamine used in this study.

Studies that provided indirect evidence for histamine release in ColdU include those of Juhlin et al. (34), who reported that mast cells in biopsies of ColdU patients show signs of degranulation, and of Kaplan et al. (35), who demonstrated histamine release by *ex vivo* cooling and rewarming of skin biopsies from ColdU patients. One interesting feature of these studies is the wide variability of histamine release, ranging from 14 to 128 ng/ml (3).

Sigler et al. (36) showed that the $fgAH_1$ cyproheptadine can prevent cold-induced hives, and a recent systematic review by Dressler et al. showed that $sgAH_1$ were more effective than placebo in the treatment of patients with ColdU. Standard and high dose treatment were more effective than placebo in terms of the rates of patients who became "symptom free" (37).

Delayed pressure Urticaria

Direct evidence of histamine release in DPU comes from 3 studies. Two of them measured histamine release in skin lesions of DPU patients. Kaplan et al. (3) assessed suction blister fluid obtained at 2-hour intervals from skin sites exposed to pressure and found histamine levels to be increased between 4-10 hours, with peak levels of approximately 30 ng/ml at 6-8 hours (Supplementary Table 4). Czarnetzki et al. (38) reported that mean histamine levels were elevated in wheals induced by pressure. They also reported indirect evidence that peripheral blood leukocytes had significantly increased intracellular histamine levels and increased histamine releasability.

Mijailović et al. (39) reported that pressure challenge on a patient's forearm caused increased histamine levels in blood collected from the draining cubital vein 14 hours later as compared with the contralateral cubital vein and to baseline. Of note, 18 hours after challenge the patient developed systemic anaphylaxis and received adrenaline.

For indirect evidence, a systematic review of treatment of DPU showed that $sgAH_1$ were effective in 3 RCTs. Combining a $sgAH_1$ with montelukast (2 RCTs) or theophylline (1 non-RCT) was more effective than the $sgAH_1$ alone. There are no studies on $sgAH_1$ updosing in DPU (40).

Solar urticaria

Direct evidence for histamine release in solar urticaria (SolU) comes mostly from blood histamine assessment: Two patients with confirmed SolU were challenged and histamine was measured by Soter et al. (41) (Supplementary Table 5) Serum histamine rose from baseline of <0.1 ng/ml to peak levels of 7.0 and 37 ng/ml at 5 minutes. Levels returned to baseline by 20 minutes.

Hawk et al. studied histamine release in four SolU patients provoked by UVB (42). The results showed that two patients had increased histamine levels of 20 ng/ml and 8.5 ng/ml at 2 and 5 minutes after irradiation, respectively while the other two showed smaller increases. Additionally, electron microscopy of skin specimens taken after challenge showed numerous mast cells undergoing exocytotic changes, characteristically seen during histamine release, whereas in some cells no signs of degranulation were found.

Keahey et al. (6) measured venous blood histamine levels in three patients before and after UVA irradiation with various intervals up to 30 min compared with after induction of tolerance by repeated exposure to UVA. The results showed small and variable histamine release, which was reduced by tolerance induction. Watanabe et al. (43) reported increase in venous histamine in two SolU patients when wheals developed approximated 30 minutes after UV irradiation.

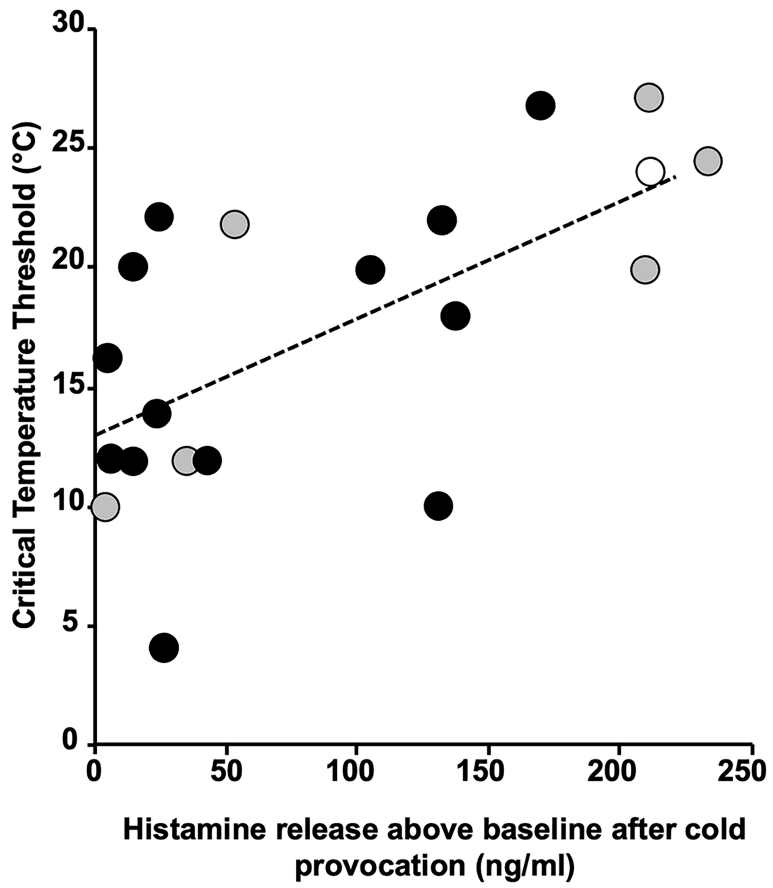


FIGURE 2
Regression plot of critical threshold temperatures against dialysate histamine concentrations. Patients are colour coded as to their responsiveness to 80 mg bilastine, green > 80% inhibition (responders), yellow 30–80% inhibition (partial responders) and red < 30% (nonresponders). The regression line is statistically significant (P = 0.003) and intercepts the critical threshold temperature axis at 13°C.

There is only one study, of Kaplan et al. (3), that performed histamine measurements in the skin. SolU was induced in one patient by ultraviolet (UV) light filtered through window glass for 30 seconds. Histamine levels in suction blisters induced over urticarial lesions and the contralateral non-urticarial skin were 127 ng/ml and 24 ng/ml, respectively.

As for indirect evidence, Baart de Faille et al. (44) reported that histological evaluation revealed higher numbers of mast cells in irradiated specimens, as well as appearance of degranulation 24 hours after irradiation, implying histamine release. Also, AH_1 treatment is of benefit in 35-75% of SolU patients (45–47).

Heat-induced urticaria

Histamine release in heat-induced urticaria (HeatU) was demonstrated by 14 studies, all of which have adopted an *in vivo* approach and showed a homogeneous picture with histamine rising to peak levels in venous blood draining the exposed site within minutes of exposure (14, 20, 48–57) (Supplementary Table 6). Most studies chose exposure temperatures of 40°C, going up to 45°C, with one exception of 56°C due to the high individual threshold of the examined patient (49). These results from venous blood are also supported by a study in which suction blister histamine peaked at 30 minutes after heat challenge, whereas it did not rise in healthy controls (15). Most of the blood studies did not have healthy controls who underwent the same procedures, but those who did showed no rise of histamine levels upon exposure to heat (50). Two studies reported that after successful treatment of HeatU patients with a desensitization protocol, patients remained symptom free and the previously seen rise of histamine could no longer be detected upon exposure to heat (50, 56).

As for indirect evidence, one study examined skin biopsies after heat provocation using electron microscopy, revealing features of mast cell degranulation (58). Also, approximately 60% of patients with HeatU respond to $sgAH_1$, although only few patients achieve complete control (59).

Vibratory angioedema

Vibratory angioedema (VA) is divided into 2 subgroups, hereditary vibratory angioedema (HVA) and acquired vibratory angioedema (AVA), with histamine release being purported to be relevant for both subgroups.

Direct evidence of histamine release in HVA is reported in 3 studies. Metzger et al. (60) and Kaplan et al. (31) studied the same patient whose forearm was applied on a vortex mixer for 4 minutes on different occasions Supplementary Table 7). Venous histamine levels peaked at 22 and 53 ng/ml at 1-3 minutes and declined to baseline at 4-13 minutes. A similar study was reported by Boyden et al. (61), with serum histamine levels peaking at 90 and 130 nmol/l within 5 minutes after challenge in two patients.

Four *in vivo* investigations of histamine release provide direct evidence in AVA, using blood obtained before and after vibratory stimulation for 1-5 min at various intervals. Ting *et al.* (62) reported peak venous blood histamine of 24 ng/ml at 1 minute. Wener et al. (63) detected peak histamine of 18 ng/ml at 5 minutes. Keahey et al. (5) reported 2 patients having peak levels of serum histamine of 1,224 to 9,000 pg/ml at 5 minutes and a secondary rise at 3-4 hours. Zhao et al. (64) reported mean peak serum histamine levels of 9 ng/ml in 3 patients at 30 minutes after stimulation.

As for indirect evidence, three studies demonstrated mast cells in various stages of degranulation at provocation sites, as assessed by immunohistochemistry or electron microscopy (5, 61, 62). Also, VA patients can benefit from AH_1 treatment (65).

Cholinergic urticaria

The first report of direct evidence of histamine release in three patients with cholinergic urticaria (CholU) was by Kaplan et al. in 1975 (18) (Supplementary Table 8). Baseline venous blood histamine levels were ≤1 ng/ml. The first patient had mild symptoms and a peak histamine level of 3 ng/ml during exercise, which returned to baseline within 20 minutes. The second patient had more severe symptoms and a peak histamine level of 25 ng/ml during exercise, which was still elevated (4 ng/ml) at 35 minutes. The third patient had no itch accompanying the skin lesions and showed no detectable histamine release after exercise challenge. Variable elevations of venous blood histamine with exercise were reported in other studies (11, 14, 29, 31, 66–70).

Indirect evidence of histamine release was demonstrated in five recent *in vitro* studies including 84 patients using basophil histamine release tests (71–76). Although $sgAH_1$ are used as first-line treatment for patients with CholU, many patients report only mild to moderate improvement. The addition of AH_2 was effective in some patients with refractory cases of CholU (77). A systematic review by Dressler et al. showed that $fgAH_1$ and $sgAH_1$ are more effective than placebo, with increased doses resulting in higher efficacy compared with placebo (37).

Contact urticaria

Contact urticaria (ConU) may be divided into immunologic and non-immunologic ConU. Among 11 studies reporting direct evidence of histamine release in immunologic ConU, 20 cases were provoked by latex (78–80), and 1 each by limonium tataricum (81), cereal flour extract (82), rice (83), polyvinylpyrrolidone (84), and chlorhexidine (85) Supplementary Table 9). These urticariogenic substances all released histamine from patient leucocytes *in vitro* (78–83).

For *in vivo* results, serum histamine levels were assessed in 2 cases. The histamine levels of the patient with chlorhexidine allergy were measured before and after skin prick test and patch test. The results showed an increase of more than 3-fold and 2-fold after skin prick test and patch test, respectively (85).

In an *in vivo* study of nettle induced non-immunologic contact urticaria, histamine levels rose to 35 ± 240 nM at 15 minutes after challenge and declined rapidly (86).

For indirect evidence of ConU, $sgAH_1$ are effective in controlling both the number and the duration of wheals in most patients with ConU had a good response and relieved the symptoms. In uncontrolled cases, updosing of antihistamines can be helpful (87).

Aquagenic urticaria

In vivo histamine release in AquaU was demonstrated in two studies (67, 88) (Supplementary Table 10). Following skin provocation testing, increased plasma histamine levels were reported in 2 patients. Davis et al. reported peak plasma histamine of 2 ng/ml at 60 minutes after challenge, which returned to baseline within 2 hours (67). Sibbald et al. reported plasma histamine increase of up to 11 ng/ml after challenge (88). Acetone enhanced the plasma histamine increase in response to subsequent challenge, but it did not evoke wheals by itself (88).

As for indirect evidence, two studies demonstrated mast cell degranulation at sites of provocation in one patient each (88, 89). Also, an *in vitro* study of basophils from patients with AquaU, showed histamine release in response to challenge with all of 4 dilutions of human callus extract (90). $FgAH_1$ and $sgAH_1$ lead to benefit in most patients (91–93), and up-dosing can improve the response (94, 95).

Discussion

Our systematic review demonstrates direct and indirect evidence of histamine release in all types of CIndUs and confirms the role of histamine in their pathogenesis. (Supplementary Tables 11, 12).

Comparisons of blood histamine levels before and after challenge was the most common *in vivo* approach and demonstrate the extent and kinetics of skin histamine release. The histamine detection methods used in these studies were various and varied over time. In earlier studies, use of guinea-pig ileum in a superfusion cascade system was frequently used (96, 97). In later studies more sensitive chemical methods were employed, including radioenzyme techniques (98–100) and competitive enzyme immunoassay (57, 101). Skin microdialysis was another *in vivo* method commonly used. Its advantages include that it does not require repeated blood sampling to assess the release of histamine in human skin (102).

Regarding *in vitro* methods, basophil tests were commonly performed to detect histamine release, e.g. by fluorometric assay (103–105), radioenzyme technique (98), enzymatic double-isotopic assay (106), enzyme-linked immunosorbent assay (107), and HPLC (72). Furthermore, demonstration of mast cell degranulation in skin biopsy by some studies provided indirect evidence that histamine might be involved in the development of signs and symptoms of CIndU. Because different studies used different methods with different sensitivity, the levels of histamine released are difficult to compare.

Although the exact pathogenesis of CIndU is still largely unclear (1), mast cell activation and degranulation with subsequent release of proinflammatory mediators are held to be critical and histamine is a main mediator. Other mediators and cytokines with pathogenic relevance in CIndU include tumor necrotic factor-α (108, 109), prostaglandin D_2 (110–112), leukotriene (113), acetylcholine (114), platelet activating factor and interleukins (109, 115). However, the role of mediators other than histamine in each CIndU subtype remains ill defined, and their relevance should be explored in future studies. Treatment with AH_1 in each CIndU can lead to various clinical responses ranging from non-response to complete response (12, 116). (Supplementary Table 11) Thus, it is likely that histamine is not of the same relevance in all CIndUs or in all patients with the same CIndU. Importantly, non-response to an AH_1 does not rule out that histamine is a major CIndU driver, as histamine can also induce skin inflammation and itch *via* H_4 receptors. H_4 receptor antagonists should be assessed for their efficacy in the treatment of patients with CIndU (117). Also, further studies should explore and better define the spectrum and roles of mast cell mediators other than histamine that are involved in the induction of signs and symptoms of each CIndU. Finally, novel targeted therapies are needed and should be developed to improve the management of CIndUs (Supplementary Table 13).

Conclusions

This review supports a key pathogenic role of histamine in all types of CIndUs. However, some points are still unclear, for example, the trigger pathway for histamine release and the relationship between the level of histamine and severity of symptoms.

Our systematic review identified direct and indirect evidence of histamine release by *in vivo* and/or *in vitro* analyses in all types of CIndUs. This should prompt further studies on the role of histamine receptors other than H1R, especially H4R in the pathogenesis of CIndUs.

Data availability statement

The original contributions presented in the study are included in the article/**Supplementary Material**. Further inquiries can be directed to the corresponding author.

Author contributions

KK, MC, and MM contributed to conception and design of the study. KK, KM, and CR built the research strategy. MC, EG, TH, LK, KM, YN, CR, and DT-M performed data extraction. MC, EG, TH, LK, KM, YN, CR, and DT-M wrote the first draft of the manuscript. KK, MC, and MM reviewed the manuscript. All authors contributed to manuscript revision, read, and approved the submitted version.

Conflict of interest

The authors declare that the research was conducted in the absence of any commercial or financial relationships that could be construed as a potential conflict of interest.

Publisher's note

All claims expressed in this article are solely those of the authors and do not necessarily represent those of their affiliated organizations, or those of the publisher, the editors and the reviewers. Any product that may be evaluated in this article, or claim that may be made by its manufacturer, is not guaranteed or endorsed by the publisher.

Supplementary material

The Supplementary Material for this article can be found online at: https://www.frontiersin.org/articles/10.3389/fimmu.2022.901851/full#supplementary-material

References

1. Maurer M, Fluhr JW, Khan DA. How to approach chronic inducible urticaria. *J Allergy Clin Immunol Pract* (2018) 6(4):1119–30. doi: 10.1016/j.jaip.2018.03.007

2. Church MK, Kolkhir P, Metz M, Maurer M. The role and relevance of mast cells in urticaria. *Immunol Rev* (2018) 282(1):232–47. doi: 10.1111/imr.12632

3. Kaplan AP, Horáková Z, Katz SI. Assessment of tissue fluid histamine levels in patients with urticaria. *J Allergy Clin Immunol* (1978) 61(6):350–4. doi: 10.1016/0091-6749(78)90113-6

4. Juhlin L. Cold urticaria with persistent weals. *Br J Dermatol* (1981) 104 (6):705–7. doi: 10.1111/j.1365-2133.1981.tb00759.x

5. Keahey TM, Indrisano J, Lavker RM, Kaliner MA. Delayed vibratory angioedema: Insights into pathophysiologic mechanisms. *J Allergy Clin Immunol* (1987) 80(6):831–8. doi: 10.1016/s0091-6749(87)80273-7

6. Keahey TM, Lavker RM, Kaidbey KH, Atkins PC, Zweiman B. Studies on the mechanism of clinical tolerance in solar urticaria. *Br J Dermatol* (1984) 110(3):327–38. doi: 10.1111/j.1365-2133.1984.tb04639.x

7. Altrichter S, Peter H-J, Pisarevskaja D, Metz M, Martus P, Maurer M. Ige mediated autoallergy against thyroid peroxidase – a novel pathomechanism of chronic spontaneous urticaria? *PloS One* (2011) 6(4):e14794. doi: 10.1371/journal.pone.0014794

8. Gruber BL, Baeza ML, Marchese MJ, Agnello V, Kaplan AP. Prevalence and functional role of anti-ige autoantibodies in urticarial syndromes. *J Invest Dermatol* (1988) 90(2):213–7. doi: 10.1111/1523-1747.ep12462239

9. Kolkhir P, Church MK, Weller K, Metz M, Schmetzer O, Maurer M. Autoimmune chronic spontaneous urticaria: What we know and what we do not know. *J Allergy Clin Immunol* (2017) 139(6):1772–81.e1. doi: 10.1016/j.jaci.2016.08.050

10. Kring Tannert L, Stahl Skov P, Bjerremann Jensen L, Maurer M, Bindslev-Jensen C. Cold urticaria patients exhibit normal skin levels of functional mast cells and histamine after tolerance induction. *Dermatology* (2012) 224(2):101–5. doi: 10.1159/000336572

11. Kato T, Komatsu H, Tagami H. Exercise-induced urticaria and angioedema: Reports of two cases. *J Dermatol* (1997) 24(3):189–92. doi: 10.1111/j.1346-8138.1997.tb02770.x

12. Krause K, Spohr A, Zuberbier T, Church MK, Maurer M. Up-dosing with bilastine results in improved effectiveness in cold contact urticaria. *Allergy* (2013) 68(7):921–8. doi: 10.1111/all.12171

13. Kurtz AS, Kaplan AP. Regional expression of cold urticaria. *J Allergy Clin Immunol* (1990) 86(2):272–3. doi: 10.1016/s0091-6749(05)80076-4

14. McClean SP, Arreaza EE, Lett-Brown MA, Grant JA. Refractory cholinergic urticaria successfully treated with ketotifen. *J Allergy Clin Immunol* (1989) 83 (4):738–41. doi: 10.1016/0091-6749(89)90008-0

15. Neittaanmäki H, Fräki JE. Combination of localized heat urticaria and cold urticaria. release of histamine in suction blisters and successful treatment of heat urticaria with doxepin. *Clin Exp Dermatol* (1988) 13(2):87–91. doi: 10.1111/j.1365-2230.1988.tb00665.x

16. Moher D, Shamseer L, Clarke M, Ghersi D, Liberati A, Petticrew M, et al. Preferred reporting items for systematic review and meta-analysis protocols (Prisma-p) 2015 statement. *Syst Rev* (2015) 4(1):1. doi: 10.1186/2046-4053-4-1

17. Greaves MW, Sondergaard J. Urticaria pigmentosa and factitious urticaria. direct evidence for release of histamine and other smooth muscle-contracting agents in dermographic skin. *Arch Dermatol* (1970) 101(4):418–25. doi: 10.1001/archderm.101.4.418

18. Kaplan AP, Gray L, Shaff RE, Horakova Z, Beaven MA. *In vivo* studies of mediator release in cold urticaria and cholinergic urticaria. *J Allergy Clin Immunol* (1975) 55(6):394–402. doi: 10.1016/0091-6749(75)90078-0

19. de Croon EM, Sluiter JK, Nijssen TF, Dijkmans BA, Lankhorst GJ, Frings-Dresen MH. Predictive factors of work disability in rheumatoid arthritis: A systematic literature review. *Ann Rheum Dis* (2004) 63(11):1362–7. doi: 10.1136/ard.2003.020115

20. Rose B. Studies on blood histamine in cases of allergy: I. blood histamine during wheal formation. *J Allergy* (1941) 12(4):327–34. doi: 10.1016/S0021-8707(41)90260-5

21. Garafalo J, Kaplan AP. Histamine release and therapy of severe dermatographism. *J Allergy Clin Immunol* (1981) 68(2):103–5. doi: 10.1016/0091-6749(81)90166-4

22. Kulthanan K, Ungprasert P, Tuchinda P, Chularojanamontri L, Rujitharanawong C, Kiratiwongwan R, et al. Symptomatic dermographism: A systematic review of treatment options. *J Allergy Clin Immunol Pract* (2020) 8 (9):3141–61. doi: 10.1016/j.jaip.2020.05.016

23. Rose B. Studies on blood histamine in patients with allergy. ii. alterations in the blood histamine in patients with allergic disease. *J Clin Invest* (1941) 20(4):419–28. doi: 10.1172/JCI101237

24. Duner H, Pernow B. Histamine in man under physiological and pathological conditions. *Acta Med Scand* (1960) 168:307–23. doi: 10.1111/j.0954-6820.1960.tb13452.x

25. Dunér H, Pernow B, Sterky G. The histamine concentration of the blood on exposure to cold and heat. *Allergy* (1960) 15(5):417–24. doi: 10.1111/j.1398-9995.1960.tb02869.x

26. Spuzic I, Ivkovic L. Histamine in plasma in the induced urticaria due to cold. *Acta Allergol* (1961) 16:228–31. doi: 10.1111/j.1398-9995.1961.tb02896.x

27. Soter NA, Wasserman SI, Austen KF. Cold urticaria: Release into the circulation of histamine and eosinophil chemotactic factor of anaphylaxis during cold challenge. *N Engl J Med* (1976) 294(13):687–90. doi: 10.1056/nejm197603252941302

28. Bentley-Phillips CB, Black AK, Greaves MW. Induced tolerance in cold urticaria caused by cold-evoked histamine release. *Lancet* (1976) 2(7976):63–6. doi: 10.1016/s0140-6736(76)92285-6

29. Sigler RW, Levinson AI, Evans R3rd, Horakova Z, Kaplan AP. Evaluation of a patient with cold and cholinergic urticaria. *J Allergy Clin Immunol* (1979) 63 (1):35–8. doi: 10.1016/0091-6749(79)90159-3

30. Black AK, Eady RA, Greaves MW, Keahey TM, Sibbald G. Treatment of acquired cold urticaria by prednisone: Dissociation of histamine release and clinical improvement [Proceedings]. *Br J Clin Pharmacol* (1980) 9(1):116p–7p. doi: 10.1111/j.1365-2125.1980.tb04818.x

31. Kaplan AP, Beaven MA. *In vivo* studies of the pathogenesis of cold urticaria, cholinergic urticaria, and vibration-induced swelling. *J Invest Dermatol* (1976) 67 (3):327–32. doi: 10.1111/1523-1747.ep12514352

32. Andersson T, Wårdell K, Anderson C. Human in vivo cutaneous microdialysis: Estimation of histamine release in cold urticaria. *Acta Derm Venereol* (1995) 75(5):343–7. doi: 10.2340/0001555575343347

33. Nuutinen P, Harvima IT, Ackermann L. Histamine, but not leukotriene C4, is an essential mediator in cold urticaria wheals. *Acta Derm Venereol* (2007) 87 (1):9–13. doi: 10.2340/00015555-0185

34. Juhlin L, Shelley WB. Role of mast cell and basophil in cold urticaria with associated systemic reactions. *Jama* (1961) 177:371–7. doi: 10.1001/jama.1961.73040320001004

35. Kaplan AP, Garofalo J, Sigler R, Hauber T. Idiopathic cold urticaria: *In vitro* demonstration of histamine release upon challenge of skin biopsies. *N Engl J Med* (1981) 305(18):1074–7. doi: 10.1056/nejm198110293051808

36. Sigler RW, Evans R3rd, Horakova Z, Ottesen E, Kaplan AP. The role of cyproheptadine in the treatment of cold urticaria. *J Allergy Clin Immunol* (1980) 65 (4):309–12. doi: 10.1016/0091-6749(80)90161-x

37. Dressler C, Werner RN, Eisert L, Zuberbier T, Nast A, Maurer M. Chronic inducible urticaria: A systematic review of treatment options. *J Allergy Clin Immunol* (2018) 141(5):1726–34. doi: 10.1016/j.jaci.2018.01.031

38. Czarnetzki BM, Meentken J, Rosenbach T, Pokropp A. Clinical, pharmacological and immunological aspects of delayed pressure urticaria. *Br J Dermatol* (1984) 111(3):315–23. doi: 10.1111/j.1365-2133.1984.tb04729.x

39. Mijailović BB, Karadaglić DM, Ninković MP, Mladenović TM, Zecević RD, Pavlović MD. Bullous delayed pressure urticaria; pressure testing may produce a systemic reaction. *Br J Dermatol* (1997) 136(3):434–6. doi: 10.1111/j.1365-2133.1997.tb14962.x

40. Kulthanan K, Ungprasert P, Tuchinda P, Chularojanamontri L, Charoenpipatsin N, Maurer M. Delayed pressure urticaria: A systematic review of treatment options. *J Allergy Clin Immunol Pract* (2020) 8(6):2035–49.e5. doi: 10.1016/j.jaip.2020.03.004

41. Soter NA, Wasserman SI, Pathak MA, Parrish JA, Austen KF. Solar urticaria: Release of mast cell mediators into the circulation after experimental challenge. *J Invest Dermatol* (1979) 72(5):282.

42. Hawk JL, Eady RA, Challoner AV, Kobza-Black A, Keahey TM, Greaves MW. Elevated blood histamine levels and mast cell degranulation in solar urticaria. *Br J Clin Pharmacol* (1980) 9(2):183–6. doi: 10.1111/j.1365-2125.1980.tb05831.x

43. Watanabe M, Matsunaga Y, Katayama I. Solar urticaria: A consideration of the mechanism of inhibition spectra. *Dermatology* (1999) 198(3):252–5. doi: 10.1159/000018124

44. Baart de la Faille H, Rottier PB, Baart de la Faille-Kuyper EH. Solar urticaria. a case with possible increase of skin mast cells. *Br J Dermatol* (1975) 92(1):101–7. doi: 10.1159/000144432

45. Haylett AK, Koumaki D, Rhodes LE. Solar urticaria in 145 patients: Assessment of action spectra and impact on quality of life in adults and children. *Photodermatol Photoimmunol Photomed* (2018) 34(4):262–8. doi: 10.1111/phpp.12385

46. Beattie PE, Dawe RS, Ibbotson SH, Ferguson J. Characteristics and prognosis of idiopathic solar urticaria: A cohort of 87 cases. *Arch Dermatol* (2003) 139(9):1149–54 doi: 10.1001/archderm.139.9.1149

47. Du-Thanh A, Debu A, Lalheve P, Guillot B, Dereure O, Peyron JL. Solar urticaria: A time-extended retrospective series of 61 patients and review of literature. *Eur J Dermatol* (2013) 23(2):202–7. doi: 10.1684/ejd.2013.1933

48. Farnam J, Grant JA, Lett-Brown MA, Lord RA, Russell WL, Henry DP. Combined cold- and heat-induced cholinergic urticaria. *J Allergy Clin Immunol* (1986) 78(2):353–7. doi: 10.1016/s0091-6749(86)80089-6

49. Irwin RB, Lieberman P, Friedman MM, Kaliner M, Kaplan R, Bale G, et al. Mediator release in local heat urticaria: Protection with combined H1 and H2 antagonists. *J Allergy Clin Immunol* (1985) 76(1):35–9. doi: 10.1016/0091-6749(85)90801-2

50. Baba T, Nomura K, Hanada K, Hashimoto I. Immediate-type heat urticaria: Report of a case and study of plasma histamine release. *Br J Dermatol* (1998) 138(2):326–8. doi: 10.1046/j.1365-2133.1998.02084.x

51. Atkins PC, Zweiman B. Mediator release in local heat urticaria. *J Allergy Clin Immunol* (1981) 68(4):286–9. doi: 10.1016/0091-6749(81)90153-6

52. Grant JA, Findlay SR, Thueson DO, Fine DP, Krueger GG. Local heat Urticaria/Angioedema: Evidence for histamine release without complement activation. *J Allergy Clin Immunol* (1981) 67(1):75–7. doi: 10.1016/0091-6749(81)90049-x

53. Koro O, Dover JS, Francis DM, Kobza Black A, Kelly RW, Barr RM, et al. Release of prostaglandin D2 and histamine in a case of localized heat urticaria, and effect of treatments. *Br J Dermatol* (1986) 115(6):721–8. doi: 10.1111/j.1365-2133.1986.tb06654.x

54. Higgins EM, Friedmann PS. Clinical report and investigation of a patient with localized heat urticaria. *Acta Derm Venereol* (1991) 71(5):434–6.

55. Skrebova N, Takiwaki H, Miyaoka Y, Arase S. Localized heat urticaria: A clinical study using laser Doppler flowmetry. *J Dermatol Sci* (2001) 26(2):112–8. doi: 10.1016/s0923-1811(00)00162-6

56. Fukunaga A, Shimoura S, Fukunaga M, Ueda M, Nagai H, Bito T, et al. Localized heat urticaria in a patient is associated with a wealing response to heated autologous serum. *Br J Dermatol* (2002) 147(5):994–7. doi: 10.1046/j.1365-2133.2002.04952.x

57. Martín-Muñoz MF, Muñoz-Robles ML, González P, Martín-Esteban M. Immediate heat urticaria in a child. *Br J Dermatol* (2002) 147(4):813–5. doi: 10.1046/j.1365-2133.2002.49055.x

58. Koh YI, Choi IS, Lee SH, Lee JB, Park CH, Hong SN. Localized heat urticaria associated with mast cell and eosinophil degranulation. *J Allergy Clin Immunol* (2002) 109(4):714–5. doi: 10.1067/mai.2002.122462

59. Pezzolo E, Peroni A, Gisondi P, Girolomoni G. Heat urticaria: A revision of published cases with an update on classification and management. *Br J Dermatol* (2016) 175(3):473–8. doi: 10.1111/bjd.14543

60. Metzger WJ, Kaplan AP, Beaven MA, Irons JS, Patterson R. Hereditary vibratory angioedema: Confirmation of histamine release in a type of physical hypersensitivity. *J Allergy Clin Immunol* (1976) 57(6):605–8. doi: 10.1016/0091-6749(76)90012-9

61. Boyden SE, Desai A, Cruse G, Young ML, Bolan HC, Scott LM, et al. Vibratory urticaria associated with a missense variant in Adgre2. *N Engl J Med* (2016) 374(7):656–63. doi: 10.1056/NEJMoa1500611

62. Ting S, Reimann BE, Rauls DO, Mansfield LE. Nonfamilial, vibration-induced angioedema. *J Allergy Clin Immunol* (1983) 71(6):546–51. doi: 10.1016/0091-6749(83)90435-9

63. Wener MH, Metzger WJ, Simon RA. Occupationally acquired vibratory angioedema with secondary carpal tunnel syndrome. *Ann Intern Med* (1983) 98(1):44–6. doi: 10.7326/0003-4819-98-1-44

64. Zhao Z, Reimann S, Wang S, Wang Y, Zuberbier T. Ordinary vibratory angioedema is not generally associated with Adgre2 mutation. *J Allergy Clin Immunol* (2019) 143(3):1246–8.e4. doi: 10.1016/j.jaci.2018.10.049

65. Kulthanan K, Ungprasert P, Tapechum S, Rujitharanawong C, Kiratiwongwan R, Munprom K, et al. Vibratory angioedema subgroups, features, and treatment: Results of a systematic review. *J Allergy Clin Immunol Pract* (2021) 9(2):971–84. doi: 10.1016/j.jaip.2020.09.009

66. Soter NA, Wasserman SI, Austen KF, McFadden ERJr. Release of mast-cell mediators and alterations in lung function in patients with cholinergic urticaria.*N Engl J Med* (1980) 302(11):604–8. doi: 10.1056/nejm198003133021104

67. Davis RS, Remigio LK, Schocket AL, Bock SA. Evaluation of a patient with both aquagenic and cholinergic urticaria. *J Allergy Clin Immunol* (1981) 68(6):479–83. doi: 10.1016/0091-6749(81)90202-5

68. Kaplan AP, Natbony SF, Tawil AP, Fruchter L, Foster M. Exercise-induced anaphylaxis as a manifestation of cholinergic urticaria. *J Allergy Clin Immunol* (1981) 68(4):319–24. doi: 10.1016/0091-6749(81)90158-5

69. Lawrence CM, Jorizzo JL, Kobza-Black A, Coutts A, Greaves MW. Cholinergic urticaria with associated angio-oedema. *Br J Dermatol* (1981) 105(5):543–50. doi: 10.1111/j.1365-2133.1981.tb00797.x

70. Lewis J, Lieberman P, Treadwell G, Erffmeyer J. Exercise-induced urticaria, angioedema, and anaphylactoid episodes. *J Allergy Clin Immunol* (1981) 68(6):432–7. doi: 10.1016/0091-6749(81)90197-4

71. Fukunaga A, Bito T, Tsuru K, Oohashi A, Yu X, Ichihashi M, et al. Responsiveness to autologous sweat and serum in cholinergic urticaria classifies its clinical subtypes. *J Allergy Clin Immunol* (2005) 116(2):397–402. doi: 10.1016/j.jaci.2005.05.024

72. Takahagi S, Tanaka T, Ishii K, Suzuki H, Kameyoshi Y, Shindo H, et al. Sweat antigen induces histamine release from basophils of patients with cholinergic urticaria associated with atopic diathesis. *Br J Dermatol* (2009) 160(2):426–8. doi: 10.1111/j.1365-2133.2008.08862.x

73. Washio K, Fukunaga A, Onodera M, Hatakeyama M, Taguchi K, Ogura K, et al. Clinical characteristics in cholinergic urticaria with palpebral angioedema: Report of 15 cases. *J Dermatol Sci* (2017) 85(2):135–7. doi: 10.1016/j.jdermsci.2016.11.001

74. Kim JE, Jung KH, Cho HH, Kang H, Park YM, Park HJ, et al. The significance of hypersensitivity to autologous sweat and serum in cholinergic urticaria: Cholinergic urticaria may have different subtypes. *Int J Dermatol* (2015) 54(7):771–7. doi: 10.1111/ijd.12549

75. Iijima S, Kojo K, Takayama N, Hiragun M, Kan T, Hide M. Case of cholinergic urticaria accompanied by anaphylaxis. *J Dermatol* (2017) 44(11):1291–4. doi: 10.1111/1346-8138.13951

76. Kozaru T, Fukunaga A, Taguchi K, Ogura K, Nagano T, Oka M, et al. Rapid desensitization with autologous sweat in cholinergic urticaria. *Allergol Int* (2011) 60(3):277–81. doi: 10.2332/allergolint.10-OA-0269

77. Fukunaga A, Washio K, Hatakeyama M, Oda Y, Ogura K, Horikawa T, et al. Cholinergic urticaria: Epidemiology, physiopathology, new categorization, and management. *Clin Auton Res* (2018) 28(1):103–13. doi: 10.1007/s10286-017-0418-6

78. Carrillo T, Cuevas M, Muñoz T, Hinojosa M, Moneo I. Contact urticaria and rhinitis from latex surgical gloves. *Contact Dermatitis* (1986) 15(2):69–72. doi: 10.1111/j.1600-0536.1986.tb01279.x

79. Turjanmaa K, Räsänen L, Lehto M, Mäkinen-Kiljunen S, Reunala T. Basophil histamine release and lymphocyte proliferation tests in latex contact urticaria. *In vitro* tests in latex contact urticaria. *Allergy* (1989) 44(3):181–6. doi: 10.1111/j.1398-9995.1989.tb02259.x

80. Fernández de Corres L, Moneo I, Muñoz D, Bernaola G, Fernández E, Audicana M, et al. Sensitization from chestnuts and bananas in patients with urticaria and anaphylaxis from contact with latex. *Ann Allergy* (1993) 70(1):35–9.

81. Quirce S, García-Figueroa B, Olaguíbel JM, Muro MD, Tabar AI. Occupational asthma and contact urticaria from dried flowers of limonium tataricum. *Allergy* (1993) 48(4):285–90. doi: 10.1111/j.1398-9995.1993.tb00730.x

82. Lezaun A, Igea JM, Quirce S, Cuevas M, Parra F, Alonso MD, et al. Asthma and contact urticaria caused by rice in a housewife. *Allergy* (1994) 49(2):92–5. doi: 10.1111/j.1398-9995.1994.tb00806.x

83. Yamakawa Y, Ohsuna H, Aihara M, Tsubaki K, Ikezawa Z. Contact urticaria from rice. *Contact Dermatitis* (2001) 44(2):91–3. doi: 10.1034/j.1600-0536.2001.440207.x

84. Adachi A, Fukunaga A, Hayashi K, Kunisada M, Horikawa T. Anaphylaxis to polyvinylpyrrolidone after vaginal application of povidone-iodine. *Contact Dermatitis* (2003) 48(3):133–6. doi: 10.1034/j.1600-0536.2003.00050.x

85. Nishioka K, Doi T, Katayama I. Histamine release in contact urticaria. *Contact Dermatitis* (1984) 11(3):191. doi: 10.1111/j.1600-0536.1984.tb00975.x

86. Taskila K, Saarinen JV, Harvima IT, Harvima RJ. Histamine and Ltc4 in stinging nettle-induced urticaria. *Allergy* (2000) 55(7):680–1. doi: 10.1034/j.1398-9995.2000.00635.x

87. Gimenez-Arnau AM, Maibach H. Contact urticaria. *Immunol Allergy Clin North Am* (2021) 41(3):467–80. doi: 10.1016/j.iac.2021.04.007

88. Sibbald RG, Black AK, Eady RA, James M, Greaves MW. Aquagenic urticaria: Evidence of cholinergic and histaminergic basis. *Br J Dermatol* (1981) 105(3):297–302. doi: 10.1111/j.1365-2133.1981.tb01289.x

89. Gimenez-Arnau A, Serra-Baldrich E, Camarasa JG. Chronic aquagenic urticaria. *Acta Derm Venereol* (1992) 72(5):389. doi: 10.1080/00015557238

90. Czarnetzki BM, Breetholt KH, Traupe H. Evidence that water acts as a carrier for an epidermal antigen in aquagenic urticaria. *J Am Acad Dermatol* (1986) 15(4 Pt 1):623–7. doi: 10.1016/s0190-9622(86)70215-6

91. Magerl M, Altrichter S, Borzova E, Giménez-Arnau A, Grattan CE, Lawlor F, et al. The definition, diagnostic testing, and management of chronic inducible

urticarias - the Eaaci/Ga(2) Len/Edf/Unev consensus recommendations 2016 update and revision. *Allergy* (2016) 71(6):780–802. doi: 10.1111/all.12884

92. Fearfield LA, Gazzard B, Bunker CB. Aquagenic urticaria and human immunodeficiency virus infection: Treatment with stanozolol. *Br J Dermatol* (1997) 137(4):620–2. doi: 10.1111/j.1365-2133.1997.tb03798.x

93. Rorie A, Gierer S. A case of aquagenic urticaria successfully treated with omalizumab. *J Allergy Clin Immunol Pract* (2016) 4(3):547–8. doi: 10.1016/j.jaip.2015.12.017

94. Gallo R, Gonçalo M, Cinotti E, Cecchi F, Parodi A. Localized salt-dependent aquagenic urticaria: A subtype of aquagenic urticaria? *Clin Exp Dermatol* (2013) 38 (7):754–7. doi: 10.1111/ced.12147

95. Kılıç M, Taşkın E, Tan M, Gözütok A. Association of cold urticaria with aquagenic urticaria in an adolescent girl: A case report. *Asthma Allergy Immunol* (2020) 18(2):105–9. doi: 10.21911/aai.529

96. Gaddum JH. The technique of superfusion. *Br J Pharmacol Chemother* (1953) 8(3):321–6. doi: 10.1111/j.1476-5381.1953.tb00801.x

97. Vane JR. The use of isolated organs for detecting active substances in the circulating blood. *Br J Pharmacol Chemother* (1964) 23(2):360–73. doi: 10.1111/j.1476-5381.1964.tb01592.x

98. Beaven MA, Jacobsen S, Horáková Z. Modification of the enzymatic isotopic assay of histamine and its application to measurement of histamine in tissues, serum and urine. *Clin Chim Acta* (1972) 37:91–103. doi: 10.1016/0009-8981(72)90419-6

99. Verburg KM, Bowsher RR, Henry DP. A new radioenzymatic assay for histamine using purified histamine n-methyltransferase. *Life Sci* (1983) 32 (25):2855–67. doi: 10.1016/0024-3205(83)90322-3

100. Guilloux L, Hartmann D, Ville G. Enzymatic isotopic assay for human plasma histamine. *Clin Chim Acta* (1981) 116(3):269–75. doi: 10.1016/0009-8981(81)90046-2

101. Meyer J, Gorbach AM, Liu WM, Medic N, Young M, Nelson C, et al. Mast cell dependent vascular changes associated with an acute response to cold immersion in primary contact urticaria. *PloS One* (2013) 8(2):e56773. doi: 10.1371/journal.pone.0056773

102. Baumann KY, Church MK, Clough GF, Quist SR, Schmelz M, Skov PS, et al. Skin microdialysis: Methods, applications and future opportunities–an eaaci position paper. *Clin Trans Allergy* (2019) 9(1):24. doi: 10.1186/s13601-019-0262-y

103. May CD, Lyman M, Alberto R, Cheng J. Procedures for immunochemical study of histamine release from leukocytes with small volume of blood. *J Allergy* (1970) 46(1):12–20. doi: 10.1016/0021-8707(70)90056-0

104. Siraganian RP. An automated continuous-flow system for the extraction and fluorometric analysis of histamine. *Anal Biochem* (1974) 57(2):383–94. doi: 10.1016/0003-2697(74)90093-1

105. Oehling A, Ona J, Trento H, Sanz ML, Domínguez MA. The diagnostic value of the histamine release test in food allergy. *Allergol Immunopathol (Madr)* (1984) 12(6):439–48.

106. Beaven MA. Radiochemical assay procedures for drugs and transmitters. In: LL Iversen and SH Snyder, editors. *Handbook of psychopharmacology*, vol. 1 . New York: Plenum Press (1975). p. 253–90. Biochemical Principles and Techniques in Neuropharmacology.

107. Nishi H, Nishimura S, Higashiura M, Ikeya N, Ohta H, Tsuji T, et al. A new method for histamine release from purified peripheral blood basophils using monoclonal antibody-coated magnetic beads. *J Immunol Methods* (2000) 240(1-2):39–46. doi: 10.1016/s0022-1759(00)00169-1

108. Tillie-Leblond I, Gosset P, Janin A, Dalenne R, Joseph M, Wallaert B, et al. Tumor necrosis factor-alpha release during systemic reaction in cold urticaria. *J Allergy Clin Immunol* (1994) 93(2):501–9. doi: 10.1016/0091-6749(94)90360-3

109. Hermes B, Prochazka AK, Haas N, Jurgovsky K, Sticherling M, Henz BM. Upregulation of tnf-alpha and il-3 expression in lesional and uninvolved skin in different types of urticaria. *J Allergy Clin Immunol* (1999) 103(2 Pt 1):307–14. doi: 10.1016/s0091-6749(99)70506-3

110. Ormerod AD, Kobza Black A, Dawes J, Murdoch RD, Koro O, Barr RM, et al. Prostaglandin D2 and histamine release in cold urticaria unaccompanied by evidence of platelet activation. *J Allergy Clin Immunol* (1988) 82(4):586–9. doi: 10.1016/0091-6749(88)90968-2

111. Heavey DJ, Kobza-Black A, Barrow SE, Chappell CG, Greaves MW, Dollery CT. Prostaglandin D2 and histamine release in cold urticaria. *J Allergy Clin Immunol* (1986) 78(3 Pt 1):458–61. doi: 10.1016/0091-6749(86)90033-3

112. Grandel KE, Farr RS, Wanderer AA, Eisenstadt TC, Wasserman SI. Association of platelet-activating factor with primary acquired cold urticaria. *N Engl J Med* (1985) 313(7):405–9. doi: 10.1056/nejm198508153130702

113. Maltby NH, Ind PW, Causon RC, Fuller RW, Taylor GW. Leukotriene E4 release in cold urticaria. *Clin Exp Allergy* (1989) 19(1):33–6. doi: 10.1111/j.1365-2222.1989.tb02340.x

114. Kaplan AP. Exercise-induced hives. *J Allergy Clin Immunol* (1984) 73(5, Part 2):704–7. doi: 10.1016/0091-6749(84)90310-5

115. Lawlor F, Bird C, Camp RD, Barlow R, Barr RM, Kobza-Black A, et al. Increased interleukin 6, but reduced interleukin 1, in delayed pressure urticaria. *Br J Dermatol* (1993) 128(5):500–3. doi: 10.1111/j.1365-2133.1993.tb00225.x

116. Mellerowicz E, Weller K, Zuberbier T, Maurer M, Altrichter S. Real-life treatment of patients with cholinergic urticaria in German-speaking countries. *J Dtsch Dermatol Ges* (2019) 17(11):1141–7. doi: 10.1111/ddg.13979

117. Thangam EB, Jemima EA, Singh H, Baig MS, Khan M, Mathias CB, et al. The role of histamine and histamine receptors in mast cell-mediated allergy and inflammation: The hunt for new therapeutic targets. *Front Immunol* (2018) 9:1873. doi: 10.3389/fimmu.2018.01873

frontiers | Frontiers in Immunology

TYPE Mini Review
PUBLISHED 29 July 2022
DOI 10.3389/fimmu.2022.932090

Check for updates

OPEN ACCESS

EDITED BY
Satoshi Tanaka,
Kyoto Pharmaceutical University,
Japan

REVIEWED BY
Hydar Ali,
University of Pennsylvania,
United States

*CORRESPONDENCE
Silvia Bulfone-Paus
silvia.bulfone-paus@manchester.ac.uk

SPECIALTY SECTION
This article was submitted to Inflammation, a section of the journal Frontiers in Immunology

RECEIVED 29 April 2022
ACCEPTED 30 June 2022
PUBLISHED 29 July 2022

CITATION
West PW and Bulfone-Paus S (2022) Mast cell tissue heterogeneity and specificity of immune cell recruitment. *Front. Immunol.* 13:932090. doi: 10.3389/fimmu.2022.932090

COPYRIGHT
© 2022 West and Bulfone-Paus. This is an open-access article distributed under the terms of the Creative Commons Attribution License (CC BY). The use, distribution or reproduction in other forums is permitted, provided the original author(s) and the copyright owner(s) are credited and that the original publication in this journal is cited, in accordance with accepted academic practice. No use, distribution or reproduction is permitted which does not comply with these terms.

Mast cell tissue heterogeneity and specificity of immune cell recruitment

Peter W. West and Silvia Bulfone-Paus*

Lydia Becker Institute of Immunology and Inflammation, School of Biological Sciences, Faculty of Biology, Medicine and Health, University of Manchester, Manchester Academic Health Science Centre, Manchester, United Kingdom

Mast cells occupy a unique niche within tissues as long lived perpetrators of IgE mediated hypersensitivity and anaphylaxis, as well as other immune responses. However, mast cells are not identical in different tissues and the impact of this tissue heterogeneity on the interaction with other immune cells and on defined immune responses is still unclear. In this review, we synthesize the characteristics of mast cell heterogeneity in the gut and the skin. Furthermore, we attempt to connect mast cell heterogeneity with functional diversity by exploring differences in mast cell-induced immune cell recruitment in these two model organs. The differential expression of certain receptors on mast cells of different tissues, notably tissue-specific expression patterns of integrins, complement receptors and MRGPRX2, could indicate that tissue environment-dependent factors skew mast cell-immune cell interactions, for example by regulating the expression of these receptors.

KEYWORDS

Mast cells, chemotaxis, cell heterogeneity, chemokines, cytokines, MRGPRX2

Abbreviations: FcεRI, high-affinity IgE receptor; IL, interleukin; MCs, mast cells; MRGPRX2, Mas-related G-protein coupled receptor member X2; TNF, Tumor necrosis factor; TGF, transforming growth factor; SCF, Stem cell factor; VEGF, Vascular endothelial growth factor; NGF, Nerve growth factor; MCP, Monocyte chemoattractant protein; TLR, Toll-like receptor; PGD, Prostaglandin D; LTC, leukotriene C; GM-CSF, Granulocyte-macrophage colony stimulating factor; IFN interferon; CTMC, Connective tissue mast cell; MMC, Mucosal mast cell; EMP, Erythromyeloid progenitor; HSC, hematopoietic stem cell; CSF, Colony stimulating factor; TRAIL, Tumor necrosis factor-related apoptosis-inducing ligand; FGL, Fibrinogen-like protein; MadCAM, mucosal addressin cell adhesion molecule-1; VCAM, vascular cell adhesion molecule; RIG-I, retinoic acid-inducible gene I; MDA-5, melanoma differentiation-associated protein 5; NK, Natural killer; SP, Substance P.

Introduction

Beyond their classical role in IgE-mediated hypersensitivity reactions, mast cells (MCs) are now recognised to have diverse immunological functions (1). Their longevity as tissue-resident cells, particularly at barrier sites in the skin, intestine, lung and around blood vessels makes them uniquely situated to initiate, shape and resolve responses to insults, injury and infections (2). Additionally, we now appreciate MCs exhibit remarkable plasticity and specialisation such that, not only are their phenotype and responses shaped by their specific tissue environment in a steady-state, but also, the particular repertoire of preformed and synthesised mediators they release is context and stimulus-dependent (3). Here, we highlight current understanding of the differing nature of MC-induced immune cells recruitment, drawing on the examples of skin and intestinal MCs as archetypes of the traditional distinction between connective tissue and mucosal MCs.

Mast cell mediator release

MCs of differing type and species produce a vast array of biologically active molecules including proteases, biogenic amines, cytokines, chemokines, growth factors and eicosanoids (4). While some of these products are stored in secretory granules, for near immediate release upon activation, others are newly synthesised and secreted within hours. Secretory granules consist of a dense gel matrix core formed of negatively charged proteoglycans such as heparin and chondroitin sulphate and amines such are histamine and serotonin as well as proteases, which typically, but variably include tryptases, chymases, carboxypeptidase A3, beta-hexosaminidase and cathepsins among others (5). Some cytokines including most notably TNFα, but also IL-4, IL-5, IL-13, IL-16, TGFβ, SCF, and growth factors, VEGF and NGF have been reported to be stored in MC granules in some circumstances (6–10). The release of granules, or their contents is tightly regulated and is an active process requiring calcium signalling, nucleoside catabolism and actin reorganisation (6).

Little is known about the cellular mechanisms of preformed mediator-storage in MCs apart from that of TNFα, which differs even between mice and human MCs, but involves transient exocytosis and re-endocytosis in humans (11). However, multiple different secretory vesicles and degranulation pathways exist suggesting a great deal of complexity in the control of secretion (12, 13). Apart from multigranular exocytosis, MCs also release smaller amounts of granule contents through piecemeal degranulation, kiss-and-run exocytosis, extracellular vesicle release and immune synapse formation. The release of *de novo* synthesised chemokines/cytokines likely differs from secretory granule mechanisms (6).

Whilst MC degranulation induced by FcεR1α crosslinking, C3a, or substance P, results in immediate release, and later *de-novo* synthesis of chemokines/cytokines (14–16), activation of other receptors [reviewed elsewhere (1)] leads to more finely-tuned responses. For example IgE binding, in the absence of antigen-crosslinking, induces the release of IL-6 (17) and increases MCP-1 and CXCL8 release from IL-4-conditioned MCs (18). Weak, low receptor occupancy, FcεR1α-crosslinking favours the production of chemokines, CCL2, CCL3 and CCL4 over cytokine production (19). Toll-Like Receptor (TLR) engagement results in the release of cytokines (*eg* IL-6) and chemokines in the absence of degranulation (1). MC responses are individualised to specific bacteria, where pathogenic *L.monocytogenes* induces degranulation and high levels of CXCL8 and MCP-1 release, while gut commensal *E.coli* induces lower levels of CXCL8 and MCP-1 without degranulation. Skin commensal *S.aureus* on the other hand does not induce CXCL8 or MCP-1 release and induces PGD_2 at much lower levels (3). MC responses to viral infection include TNFα, type I interferon (20, 21), IL-4, IL-13, and chemokine production (22, 23). Purinergic receptor activation of MCs also releases cytokines (IL-6, TNFα, IL-33), leukotrienes, and chemokines (CCL2, CCL7, CXCL2) (24, 25).

The full plethora or MC mediators, cytokines, chemokines and their various roles are extensively reviewed elsewhere (1, 26). Those that induce immune cell recruitment and their cellular targets are listed in Table 1. MC-mediated activities that recruit leukocytes across tissues involves increasing vascular permeability (tryptase, histamine, VEGF, IL-6, CXCL8, LTC_4, PGD_2) (65, 66), upregulating adhesion molecule expression (TNFα) (26), recruitment of neutrophils (TNFα, IL-6, CXCL8, CXCL2) (51) monocyte/macrophages (TNFα, IL-6, CCL2) (67), ILCs (PGD_2) (25), DCs (TNFα, GM-CSF, IL-1β) (68, 69), and CD8+ T-cells, (CCL5, LTB_4) (4, 70). For example TNFα is stored and released by MCs from both skin and gut (71, 72), CCL2 is widely secreted and belongs to the core MC-transcriptional signature (44, 73, 74), and MCs have been shown to be essential for cell recruitment in many murine models (50, 51, 75). Mediator release is influenced by the inflammatory environment, for instance by IL-4, IL-5, IL-9, IL-33 and IFNγ (4, 76–79) which further regulate the expression of MC IL-2, IL-13, IL-9 and IL-25 (25, 29, 80–82). However there are tissue-specific aspects such as intestinal MCs lacking IFNγ (27) and skin MCs not producing LTC_4 (57), which are yet to be fully elucidated.

Mast cell heterogeneity between and within tissues

The traditional categorisation of MCs based on histological findings into connective tissue (CTMC) and mucosal MCs (MMCs) in mice, and the human correlates of tryptase+

TABLE 1 Key mediators and chemoattractants released by mast cells.

Mediator	Role	References
Cytokines		
TNFα	DC migration T-cell proliferation Monocyte Macrophage Activation Neutrophil recruitment	(27, 28)
GM-CSF	DC migration to lymph nodes	(29)
IL-1	Eosinophil recruitment Neutrophil recruitment DC-migration Inflammasome activation	(27, 29)
IL-2	T-regulatory cell recruitment ILC2 proliferation	(30, 31)
IL-4	Eosinophil recruitment Differentiation of T_h0 cells to T_h2	(32, 33)
IL-3	Mixed lymphocyte migration MC and basophil growth and differentiation	(29, 34)
IL-5	Eosinophil migration and survival	(35)
IL-6	Monocyte/Macrophage activation Local Neutrophil recruitment	(27, 29)
IL-9	MC proliferation DC migration T-cell recruitment	(36)
IL-10	CD8+ T-cell recruitment Inhibition of CD4+ T-cell recruitment Inhibition of proinflammatory cytokine production	(37–39)
IL-12	CD4+ Effector T-cell recruitment Th1 response induction Induction if IFNγ in NK, T_h1, and MCs	(26, 40)
IL-16	T-cell recruitment DC migration	(27, 41)
IL-17A	B-cell recruitment (lung)	(42)
IL-18	DC migration	(27, 43)
Chemokines		
CCL1	Monocyte recruitment T-cell recruitment	(44)
CCL2	Neutrophil migration Monocyte migration T-cell recruitment MCp migration	(45)
CCL3	Monocyte recruitment T-cell recruitment	(44)
CCL4	Monocyte recruitment T-cell recruitment	(44)
CCL5	CD8+ T-cell recruitment Eosinophil recruitment Basophil recruitment Monocyte recruitment NK cell recruitment DC recruitment	(44)
CCL7	Monocyte recruitment T-cell recruitment NK cell recruitment Immature DC recruitment Basophil recruitment Eosinophil recruitment Hematopoietic progenitor cell recruitment	(46, 47)

(Continued)

TABLE 1 Continued

Mediator	Role	References
CCL18	Naïve $CD4^+/CD8^+$ T-cell recruitment Memory T-cell recruitment B-cell recruitment Immature DC recruitment	(44, 48)
CCL20	B-cell recruitment Effector memory T-cell recruitment CD11b+ DC recruitment	(44, 49)
CXCL1	Neutrophil recruitment	(50)
CXCL2	Neutrophil recruitment Eosinophil recruitment Basophil recruitment	(44, 50, 51)
CXCL3	Neutrophil recruitment	(44)
CXCL8	CD4+ T-cell recruitment Neutrophil recruitment	(27)
XCL1	DC migration and cross presentation of antigen	(44, 52)
CX3CL1	Monocyte and T-cell recruitment and survival	(53, 54)
Lipid Mediators		
LTB_4	Neutrophil chemotaxis DC chemotaxis MC chemotaxis CD8+ T-cell recruitment	(55, 56)
LTC_4	Eosinophil migration	(57–59)
LTD_4	Eosinophil migration Neutrophil migration	(60)
LTE_4	Eosinophil migration ILC2 migration	(61, 62)
PGD_2	Eosinophil chemotaxis and activation Basophil chemotaxis and activation T_h2 cell recruitment & activation ILC2 migration Vasodilation Increased Vascular Permeability	(57, 63)
PGE_2	DC migration	(64)

(MC_T), tryptase+ and chymase+ (MC_{TC}) and chymase+ (MC_C) is well established (83–86). However, at transcriptional level, protease content exhibits greater tissue-specific heterogeneity both between and within tissues (73, 87). Additionally, while evolutionarily conserved, there are also differences between human and mouse mast cells (88).

One source of tissue heterogeneity is the MC embryonic origin. In both humans and mice, tissue MCs are seeded from MC progenitors originating from both embryonic yolk sac and adult bone marrow (89–91). During embryogenesis in mice, three waves of MCs are seeded successively from early erythromyeloid progenitors (EMPs), late EMPs and foetal hematopoietic stem cells. At birth, early EMPs-derived MCs constitute over 15% of MCs in pleural cavity, adipose tissue and skin, but less than 3% in gut and spleen. In contrast HSC-derived MCs were much higher in gut (>30%) than in skin (~8%) (89). In adult mice early EMP-derived MCs are maintained in the adipose tissue, a likely stem cell niche for MCs (92), but give way to other MC progenitors in skin (89, 90). Although sharing a core MC signature, these cells are transcriptionally distinct. Both embryonic and bone marrow-derived MCs, complete their maturation in peripheral tissues (89, 92). They are therefore subject to tissue-specific cues during that maturation process making them, to some degree, site specific. Additionally, in mice skin MCs are known to undergo *in situ* self-renewal by clonal expansion in the steady-state (93), whereas mucosal MCs are dependent on recruitment of MCp from the circulation (94–96). Nevertheless, both MMCs and CTMCs can be augmented by recruitment of MCp from the circulation during inflammation (93, 97, 98). Given the longevity of MCs this implies that environmental interactions during a lifespan can alter MC set points in the tissue which adds further complexity to MC heterogeneity.

A growing body of transcriptomic work demonstrates that MCs are distinct and highly variable between and within tissues. Indeed, MCs form a distinct transcriptional cluster differing greatly from other granulocytes. Furthermore, comparing between different types of connective tissue MCs, nearly 1000 genes can be differentially expressed (73).

Mouse MCs also display a marked tissue heterogeneity in their receptor profile (87). In both humans and mice TLR4 expression is low in skin, peritoneal and duodenal MCs but higher in colon and lung (99). Similarly, in mice the ATP receptor P_2X_7 is expressed more greatly in MCs from colon or lung rather than skin (24). C5aR1 expression also differs in some circumstances, in humans (100, 101). MRGPR receptor gene expression is a core component of murine foetal derived MCs (89) and tissue-resident MCs (73). However, intriguingly MRGPRX2, a receptor with wide agonist range and a key driver of pseudo-allergic reactions, shows large variation between tissues in humans (102). It is expressed at a high level in human skin, fat and synovial MCs, *i.e.* CTMCs. It is only expressed at low levels in lung and colonic MCs, which are refractory to substance P stimulation (57). Thus, this would suggest a distinct MRGPRX2-mediated response between mucosal and connective tissue.

Single cell RNA sequencing (scRNA-seq) across disease states in eosinophilic oesophagitis revealed a predominant tryptase and amphiregulin positive population of MC_{TC} in the lamina propria during homeostasis with the development of persistent epithelial localised chymase and cathepsin G high expressing MCs, and transient CD117high, ST2high population during active disease. In remission the transient locally proliferative population disappears, while the chymase population remains in the epithelium and the resident lamina propria MCs become CSF1high. These changes exemplify the plastic nature of human MCs which show both acute and chronic phenotypic alterations in response to tissue environment and spatial compartmentalisation. For example, MCs may switch from homeostatic to an inflammatory IL-33-responsive, and end with an IL-13-producing, macrophages supportive phenotype (103). Similar results have been obtained from scRNAseq studies in chronic rhinosinusitis in MC_T cells (CD117low, FcεR1αlow), and MC_{TC} (CD117high, chymase$^+$, cathepsin G$^+$) from the epithelial and sub-epithelial compartments respectively. MC_{TC} expressed ST2, CSF1 and IL-13 in addition to CCL2, CCL3 and CCL4, whereas MC_T expressed TRAIL, FGL2 and IL-17RB. In this tissue, the authors discovered polarised states of a core set of MC genes that distinguished them from proliferative and unpolarised MCs and concluded that the polarised cells are primed to respond either according to a pro-inflammatory (MC_{TC}) or a Th2-skewed pattern (MC_T). Although similarities existed between MC_{TC} in this study and skin MC_{TC}, the authors showed key differences in C5aR1 and MRGPRX2 expression, not only between the two populations but also within the lung (104). The continuous, rather than discrete, nature of human MC heterogeneity in the respiratory tract is supported by evidence from a large number of expressed cell surface proteins which show a continuous distribution in their expression (105).

Despite the marked transcriptomic heterogeneity observed by several authors, proteomic comparisons between two types of human connective tissue MCs, skin and fat, showed remarkably low levels of differentially expressed markers, at least in a quiescent state (102). There was also a remarkable interspecies correlation between mouse and human CTMCs and a common mast cell protein signature (102). Additionally, although mouse peritoneal MCs are reported to express the transcript for TLR4 (89), it was not found among 4620 MC expressed proteins during proteomic analysis (102).

In summary, discussions about the role of MCs in a given tissue drawn from general aspects of MC biology obtained across multiple tissues, cell lines or models are worthwhile and useful commentaries. However, one should challenge those views in light of the well-established tissue-specific heterogeneity of MCs and undertake a bigger effort in investigating MC-driven tissue-specific aspects of immunity.

Mast cell-mediated immune cell recruitment in the gut

Situated throughout the gastro-intestinal tract, MCs are regarded as key in controlling organ homeostasis (106). Contributing to the maintenance of the epithelial barrier, the initiation and modulation of both innate and adaptive immune responses to pathogens, and the cross-talk with the enteric nervous system, MCs regulate tissue homeostasis and disease (107).

Intestine constitutive homing of MCp in mice, *via* transendothelial migration, is controlled by MC α4β7 integrin binding to adhesion molecules MAdCAM-1 and VCAM-1 (96) while chemoattraction is dependent on MC CXCR2 (108). Since germ-free mice have fewer intestinal MCs and express lower levels of CXCR2 ligands, this process is thought to be driven by commensal bacterial interactions with intestinal epithelial cells (109). In humans, intestinal MCs express mainly α2β1 integrin, which is not expressed in other mucosal or connective tissue MCs (110).

MCs play a key role in the acute inflammatory response of the gut (see Figure 1). MC-derived TNFα recruits neutrophils, eosinophils and macrophages (94). Furthermore, human intestinal MCs produce an array of chemokines *de novo* when primed with SCF or IL-4 and activated by FcεRI-receptor crosslinking. These include CCL1, CCL2, CCL3, CCL4, CCL5, CCL18, CCL20, CXCL2, CXCL3, CXCL8 and XCL1 (44). Interestingly, CCL2, but not CXCL8, release by intestinal MCs in response to FcεRIα activation exhibits a diurnal pattern indicating a role for MCs in intestine circadian biology (111). Moreover, in a gut injury mouse model, MC activation and Mcpt5, Mcpt6 and CPA3 protease release, is associated with neutrophil influx and alterations in epithelial barrier integrity. MC stabiliser cromolyn sodium results in preservation of barrier integrity, reduced neutrophil influx associated with significant reductions in TNFα, CCL2, CCL5, IL-1β and CXCL1 (112).

Direct evidence of MC involvement in anti-parasitic immunity of the gut is provided by a number of rodent models. *Trichinella spiralis* infection induces an influx of MC

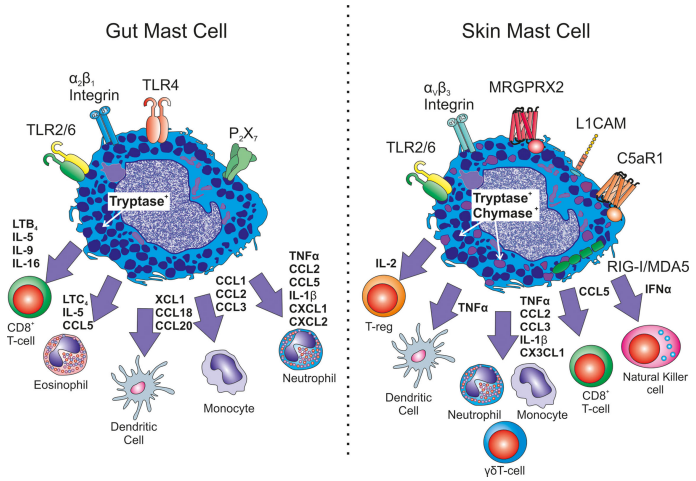


FIGURE 1
Heterogeneity in immune cell recrutiment. Exemplary differences between mucosal gut mast cells and connective tissue skin mast cells are shown. Differences in receptor expression include TLR4, P2X7, L1CAM, C5aR1, MRGPRX2 as well as integrin expression. Different mast cell mediators have been shown to be released with altered down stream consequences for immune cell recruitment in infection or inflammation.

to the gut which transiently alters their protease expression. This is associated with a strong Th_2 immune response, eosinophilia and marked increase in barrier permeability. The MC influx and the transiently-expressed MC-derived Mcpt1 is critical to control worm burden (113). Additionally, Mcpt6 is required for eosinophil recruitment (114). Mice lacking the proteoglycan serglycin, important in granule storage, also exhibit a deficit in worm clearance with lower circulating TNFα, IL-1β, IL-10, IL-13 compared to wild type infected controls (115). Human skin MCs also express these cytokines, and IL-13 downregulates T_h1 responses in mice (116, 117), which raises the prospect that intestinal MCs could be a critical source of these cytokines in anti-parasitic immunity. Additionally Th_2/Th_9 cytokine IL-9, released early during parasitic infections and important for murine worm expulsion (118, 119) is also secreted by MC activated synergistically with LPS (120, 121), although the importance of MC-derived IL-9 in the intestine has not been proven definitively. In this regard, MCs in human gut are also immunoreactive for IL-5 and IL-16 both of which enhance T-cell recruitment and activation (26, 99, 122).

MCs have also been described to limit human colorectal cancers. In murine models MC-derived LTB_4 was found to be critical for CD8+ T-cell recruitment and anti-tumor immunity (123).

Mast cell-mediated immune cell recruitment in the skin

Like the gut, the skin is a barrier exposed to a wide array of environmental insults on a nearly continual basis. However, the skin is generally a less permeable barrier than the gut and as such MCs localise to the upper dermis around eccrine glands and blood vessels and not to the epidermis (124). Therefore, they regularly encounter fewer pathogens unless barrier integrity is disturbed through mechanical (*e.g.* wound or bite) or inflammatory means. This is thought to be a reason why TLR and P_2X_7 expression in skin MCs appears low, and maintains the cells in an unresponsive state (99). Low TLR4 expression might imply a diminished role for skin MCs in human skin Th9 biology (125). To our knowledge IL-9 has not been demonstrated in skin MCs. Nevertheless, skin MCs do respond to lipoteichoic acid, a TLR2 agonist component of commensal gram-positive bacterial cell walls, leading to enhanced responses to pox causing vaccinia virus in mice (126). Similar to recruitment in the gut, the skin microbiome is responsible for MC maturation. In this case through TLR2-dependent SCF production from keratinocytes (127) rather than direct interaction. In humans their adhesion is probably dependent on a different integrin αvβ3 (128). Large amounts of retinoic acid can also overcome the P_2X_7 down regulation in mouse skin MCs (129), emphasising the plasticity of tissue-resident cells.

Like other MCs, skin MCs have been identified to store and release TNFα in response to SP, FcεRI, UVB and calcium ionohpore activation (130–132). There is good evidence from the murine passive cutaneous anaphylaxis model and delayed hypersensitivity reactions in skin, that leukocyte recruitment is dependent on MC-derived TNFα (51, 133), and that $CD8^+$ dendritic cell migration to draining lymph nodes of the skin also relies on MC TNFα (68, 134) (Figure 1). Skin MCs can also exocytose TNFα containing granules which can be transported

to the draining lymph nodes to enhance antigen presentation and antigen specific responses (135). This isn't a phenomenon so far identified in other tissues.

MCs have recently been shown to have antiviral immune activities to dengue virus, a mosquito borne pathogen *via* activation of innate response pathway RIG-I/MDA5 resulting in TNFα, IFNα, CCL5, CXCL12 and CX3CL1 production. These MC-derived cytokines appear to be critical to limiting viral spread to lymph nodes through recruitment of NK and NKT-cells to the infected skin in a mouse model (53). Additionally, MCs form an immune synapse in infected skin with γδT-cells which induced activation through the T-cell receptor (136). There is also evidence that MCs are important in limiting other intradermal viral infections through DC activation (137). MC-derived TNFα and IL-6 have also been shown to be important for protection from cutaneous herpes simplex virus infection (138). In contrast, intestinal MCs are thought to have deficiencies in IFNγ production, and whilst RIG-I might be present in lung mucosal MCs it has not yet been identified in gut MCs (139).

The recently identified MC receptor for substance P MRGPRX2 and its murine homologue mrgprb2 (140, 141) has revealed a surprising dependence of a large degree of skin inflammation and pain on MCs. Green et al. (142) observed that Mrgprb2$^{-/-}$ mice had significantly reduced hypersensitivity to inflammatory pain with not only ablated MC recruitment, but also reduced neutrophil and monocyte recruitment to the affected skin with a reduction in both CCL2 and CCL3 in response to injury or SP treatment of skin tissue. There has been much speculation about the involvement of gut MCs in painful symptoms of disease, however such compelling evidence is still lacking in other tissues and mucosal MCs have low MRGPRX2 expression.

In different murine models and human tissue samples, it has been demonstrated that skin MCs are sources of other cytokines with a likely impact on inflammation and immune activation. These include; IL-1β, which drives inflammasome activation and neutrophil recruitment in the skin (143, 144), an association also present in the gut (112); IL-2, not yet identified in gut MCs, which supresses inflammation in contact-hypersensivity through MC-dependent T-regulatory cell recruitment (30); IL-4 which drives type 2 inflammation in atopic dermatitis (32); IL-10 which as one of the first products of MCs, limit contact hypersensitivity reactions (37, 145) and also has a role in MC intestinal IBD pathology (146).

Conclusions

Despite their heterogeneous origins, functionally, MCs from diverse tissues share a common set of responses including not least to IgE/allergen but also the release of key cytokines and chemokines involved in the initiation of inflammation *i.e.* TNFα, IL-1β, CCL2. MC plasticity then allows further functional differentiation based on the tissue context and lifetime environmental interactions such as pathogen or allergen exposure, or type I/type II inflammation. This plasticity will be shaped by existing heterogeneity in receptor expression such as C5aR1, MRGPRX2 and P_2X_7 which will limit the form of response that the cells can mount to a particular stimulus. For instance skin MCs might be better equipped to release IFNγ than intestinal MCs (27) whereas skin MCs will be more susceptible to neurogenic inflammation (57). Ultimately the application of new multi-omics, single cell and imaging mass cytometry technologies to isolated cells and tissues will reveal an as yet unforeseen level of detail about tissue-specific heterogeneity.

Author contributions

PW and SB-P reviewed literature and wrote the article. All authors contributed to the article and approved the submitted version.

Funding

SBP is the recipient of a grant from MRC DPFS: MR/S036954/1. PW is supported by a GSK research grant. The funder was not involved in the collection of data, analysis, interpretation of data, the writing of this article or the decision to submit it for publication.

Conflict of interest

The authors declare that the review was conducted in the absence of any commercial or financial relationships that could be construed as a potential conflict of interest.

Publisher's note

All claims expressed in this article are solely those of the authors and do not necessarily represent those of their affiliated organizations, or those of the publisher, the editors and the reviewers. Any product that may be evaluated in this article, or claim that may be made by its manufacturer, is not guaranteed or endorsed by the publisher.

References

1. Elieh Ali Komi D, Wöhrl S, Bielory L. Mast cell biology at molecular level: A comprehensive review. *Clin Rev Allergy Immunol* (2020) 58:342–65. doi: 10.1007/S12016-019-08769-2

2. Chan CY, St John AL, Abraham SN. Plasticity in mast cell responses during bacterial infections. *Curr Opin Microbiol* (2012) 15:78–84. doi: 10.1016/j.mib.2011.10.007

3. Garcia-Rodriguez KM, Bahri R, Sattentau C, Roberts IS, Goenka A, Bulfone-Paus S. Human mast cells exhibit an individualized pattern of antimicrobial responses. *Immunity Inflammation Dis* (2020) 8:198–210. doi: 10.1002/IID3.295

4. Bulfone-Paus S, Bahri R. Mast cells as regulators of T cell responses. *Front Immunol* (2015) 6:394. doi: 10.3389/fimmu.2015.00394

5. Vukman KV, Försönits A, Oszvald Á, Tóth E, Buzás EI. Mast cell secretome: Soluble and vesicular components. *Semin Cell Dev Biol* (2017) 67:65–73. doi: 10.1016/j.semcdb.2017.02.002

6. Blank U, Madera-Salcedo IK, Danelli L, Claver J, Tiwari N, Sánchez-Miranda E, et al. Vesicular trafficking and signaling for cytokine and chemokine secretion in mast cells. *Front Immunol* (2014) 5:453. doi: 10.3389/FIMMU.2014.00453

7. de Paulis A, Minopoli G, Arbustini E, de Crescenzo G, Dal Piaz F, Pucci P, et al. Stem cell factor is localized in, released from, and cleaved by human mast cells. *J Immunol* (1999) 163:2799–808. doi: 10.4049/issn.1550-6606

8. Lindstedt KA, Wang Y, Shiota N, Saarinen J, Hyytiäinen M, Hyytiäinen H, et al. Activation of paracrine TGF-β1 signaling upon stimulation and degranulation of rat serosal mast cells: A novel function for chymase. *FASEB J* (2001) 15:1377–88. doi: 10.1096/FJ.00-0273COM

9. Leon A, Buriani A, Dal Toso R, Fabris M, Romanello S, Aloe L, et al. Mast cells synthesize, store, and release nerve growth factor. *Proc Natl Acad Sci U S A* (1994) 91:3739–43. doi: 10.1073/PNAS.91.9.3739

10. Laberge S, Pinsonneault S, Ernst P, Olivenstein R, Ghaffar O, Center DM, et al. Phenotype of IL-16-Producing cells in bronchial mucosa: Evidence for the human eosinophil and mast cell as cellular sources of IL-16 in asthma. *Int Arch Allergy Immunol* (1999) 119:120–5. doi: 10.1159/000024186

11. Olszewski MB, Groot AJ, Dastych J, Knol EF. TNF trafficking to human mast cell granules: Mature chain-dependent endocytosis. *J Immunol* (2007) 178:5701–9. doi: 10.4049/JIMMUNOL.178.9.5701

12. Woska JR, Gillespie ME. SNARE complex-mediated degranulation in mast cells. *J Cell Mol Med* (2012) 16:649. doi: 10.1111/J.1582-4934.2011.01443.X

13. Puri N, Roche PA. Mast cells possess distinct secretory granule subsets whose exocytosis is regulated by different SNARE isoforms. *Proc Natl Acad Sci USA* (2008) 105:2580–5. doi: 10.1073/PNAS.0707854105

14. Kulka M, Sheen CH, Tancowny BP, Grammer LC, Schleimer RP. Neuropeptides activate human mast cell degranulation and chemokine production. *Immunology* (2008) 123:398–410. doi: 10.1111/j.1365-2567.2007.02705.x

15. West PW, Bahri R, Garcia-Rodriguez KM, Sweetland G, Wileman G, Shah R, et al. Interleukin-33 amplifies human mast cell activities induced by complement anaphylatoxins. *Front Immunol* (2021) 11:615236. doi: 10.3389/FIMMU.2020.615236

16. Oliveira SHP, Lukacs NW. Stem cell factor and IgE-stimulated murine mast cells produce chemokines (CCL2, CCL17, CCL22) and express chemokine receptors. *Inflammation Res* (2001) 50:168–74. doi: 10.1007/s000110050741

17. Kalesnikoff J, Huber M, Lam V, Damen JE, Zhang J, Siraganian RP, et al. Monomeric IgE stimulates signaling pathways in mast cells that lead to cytokine production and cell survival. *Immunity* (2001) 14:801–11. doi: 10.1016/S1074-7613(01)00159-5

18. Matsuda K, Piliponsky AM, Iikura M, Nakae S, Wang EW, Dutta SM, et al. Monomeric IgE enhances human mast cell chemokine production: IL-4 augments and dexamethasone suppresses the response. *J Allergy Clin Immunol* (2005) 116:1357–63. doi: 10.1016/J.JACI.2005.08.042

19. Gonzalez-Espinosa C, Odom S, Olivera A, Hobson JP, Cid Martinez ME, Oliveira-dos-Santos A, et al. Preferential signaling and induction of allergy-promoting lymphokines upon weak stimulation of the high affinity IgE receptor on mast cells. *J Exp Med* (2003) 197:1453–65. doi: 10.1084/JEM.20021806

20. Kulka M, Alexopoulou L, Flavell RA, Metcalfe DD. Activation of mast cells by double-stranded RNA: Evidence for activation through toll-like receptor 3. *J Allergy Clin Immunol* (2004) 114:174–82. doi: 10.1016/j.jaci.2004.03.049

21. Lappalainen J, Rintahaka J, Kovanen PT, Matikainen S, Eklund KK. Intracellular RNA recognition pathway activates strong anti-viral response in human mast cells. *Clin Exp Immunol* (2013) 172:121–8. doi: 10.1111/CEI.12042

22. Brown MG, McAlpine SM, Huang YY, Haidl ID, Al-Afif A, Marshall JS, et al. RNA Sensors enable human mast cell anti-viral chemokine production and IFN-mediated protection in response to antibody-enhanced dengue virus infection. *PloS One* (2012) 7:e34055. doi: 10.1371/JOURNAL.PONE.0034055

23. Saluja R, Metz M, Maurer M. Role and relevance of mast cells in fungal infections. *Front Immunol* (2012) 3:146. doi: 10.3389/FIMMU.2012.00146

24. Kurashima Y, Amiya T, Nochi T, Fujisawa K, Haraguchi T, Iba H, et al. Extracellular ATP mediates mast cell-dependent intestinal inflammation through P2X7 purinoceptors. *Nat Commun* (2012) 3:1034. doi: 10.1038/ncomms2023

25. Symowski C, Voehringer D. Interactions between innate lymphoid cells and cells of the innate and adaptive immune system. *Front Immunol* (2017) 8:1422. doi: 10.3389/FIMMU.2017.01422

26. Mukai K, Tsai M, Saito H, Galli SJ. Mast cells as sources of cytokines, chemokines and growth factors. *Immunol Rev* (2018) 282:121. doi: 10.1111/IMR.12634

27. Lorentz A, Schwengberg S, Sellge G, Manns MP, Bischoff SC. Human intestinal mast cells are capable of producing different cytokine profiles: Role of IgE receptor cross-linking and IL-4. *J Immunol* (2000) 164:43–8. doi: 10.4049/jimmunol.164.1.43

28. Summers SA, Chan J, Gan PY, Dewage L, Nozaki Y, Steinmetz OM, et al. Mast cells mediate acute kidney injury through the production of TNF. *J Am Soc Nephrol* (2011) 22:2226–36. doi: 10.1681/ASN.2011020182

29. Burd PR, Thompson WC, Max EE, Mills FC. Activated mast cells produce interleukin 13. *J Exp Med* (1995) 181:1373–80. doi: 10.1084/jem.181.4.1373

30. Hershko AY, Suzuki R, Charles N, Alvarez-Errico D, Sargent JL, Laurence A, et al. Mast cell interleukin-2 production contributes to suppression of chronic allergic dermatitis. *Immunity* (2011) 35:562–71. doi: 10.1016/J.IMMUNI.2011.07.013

31. Roediger B, Kyle R, Yip KH, Sumaria N, Guy TV, Kim BS, et al. Cutaneous immuno-surveillance and regulation of inflammation by group 2 innate lymphoid cells. *Nat Immunol* (2013) 14:564. doi: 10.1038/NI.2584

32. Horsmanheimo L, Harvima IT, Järvikallio A, Harvima RJ, Naukkarinen A, Horsmanheimo M. Mast cells are one major source of interleukin-4 in atopic dermatitis. *Br J Dermatol* (1994) 131:348–53. doi: 10.1111/j.1365-2133.1994.tb08522.x

33. Dubois GR, Bruijnzeel-Koomen CAFM, Bruijnzeel PLB. IL-4-Induced migration of eosinophils in allergic inflammation. *Agents Actions* (1994) 41:C256–7. doi: 10.1007/BF01987660

34. Bacon K, Gearing A, Camp R. Induction of *In vitro* human lymphocyte migration by interleukin 3, interleukin 4, and interleukin 6. *Cytokine* (1990) 2:100–5. doi: 10.1016/1043-4666(90)90003-C

35. Lorentz A, Schwengberg S, Mierke C, Manns MP, Bischoff SC. Human intestinal mast cells produce IL-5 *in vitro* upon IgE receptor cross-linking and *In vivo* in the course of intestinal inflammatory disease. *Eur J Immunol* (1999) 29:1496–503. doi: 10.1002/(SICI)1521-4141(199905)29:05<1496::AID-IMMU1496>3.0.CO;2-5

36. Li J, Chen S, Xiao X, Zhao Y, Ding W, Li XC. IL-9 and Th9 cells in health and diseases–from tolerance to immunopathology. *Cytokine Growth Factor Rev* (2017) 37:47–55. doi: 10.1016/J.CYTOGFR.2017.07.004

37. Grimbaldeston MA, Nakae S, Kalesnikoff J, Tsai M, Galli SJ. Mast cell-derived interleukin 10 limits skin pathology in contact dermatitis and chronic irradiation with ultraviolet b. *Nat Immunol* (2007) 8:1095–104. doi: 10.1038/ni1503

38. Abrams J, Figdor CG, De Waal Malefyt R, Bennett B, De Vries JE. Interleukin 10(IL-10) inhibits cytokine synthesis by human monocytes: An autoregulatory role of IL-10 produced by monocytes. *J Exp Med* (1991) 174:1209–20. doi: 10.1084/JEM.174.5.1209

39. Jinquan T, Larsen CG, Gesser B, Matsushima K, Thestrup-Pedersen K. Human IL-10 is a chemoattractant for CD8+ T lymphocytes and an inhibitor of IL-8-Induced CD4+ T lymphocyte migration. *J Immunol* (1993) 151:4545–51. doi: 10.1016/0923-1811(92)90162-5

40. Zhang X, Niessner A, Nakajima T, Ma-Krupa W, Kopecky SL, Frye RL, et al. Interleukin 12 induces T-cell recruitment into the atherosclerotic plaque. *Circ Res* (2006) 98:524–31. doi: 10.1161/01.RES.0000204452.46568.57

41. Rumsaeng V, Cruikshank WW, Foster B, Prussin C, Kirshenbaum AS, Davis TA, et al. Human mast cells produce the CD4+ T lymphocyte chemoattractant factor, IL-16. *J Immunol* (1997) 159:1904–2910.

42. Halwani R, Al-Kufaidy R, Vazquez-Tello A, Pureza MA, BaHammam AS, Al-Jahdali H, et al. IL-17 enhances chemotaxis of primary human b cells during asthma. *PLoS One* (2014) 9:e114604. doi: 10.1371/JOURNAL.PONE.0114604

43. Yoshimoto T, Nakanishi K. Roles of IL-18 in basophils and mast cells. *Allergol Int* (2006) 55:105–13. doi: 10.2332/ALLERGOLINT.55.105

44. Feuser K, Thon KP, Bischoff SC, Lorentz A. Human intestinal mast cells are a potent source of multiple chemokines. *Cytokine* (2012) 58:178–85. doi: 10.1016/J.CYTO.2012.01.001

45. Wang X, Chen H, Zhang M, Liu Z. Roles of mast cells and monocyte chemoattractant protein-1 in the renal injury of obesity-related glomerulopathy. *Am J Med Sci* (2013) 346:295–301. doi: 10.1097/MAJ.0B013E31827559F8

46. Wakahara S, Fujii Y, Nakao T, Tsuritani K, Hara T, Saito H, et al. Gene expression profiles for fc epsilon RI, cytokines and chemokines upon fc epsilon RI activation in human cultured mast cells derived from peripheral blood. *Cytokine* (2001) 16:143–52. doi: 10.1006/CYTO.2001.0958

47. Cheng JW, Sadeghi Z, Levine AD, Penn MS, von Recum HA, Caplan AI, et al. The role of CXCL12 and CCL7 chemokines in immune regulation, embryonic development, and tissue regeneration. *Cytokine* (2014) 69:277–83. doi: 10.1016/J.CYTO.2014.06.007

48. Tsicopoulos A, Chang Y, Ait Yahia S, De Nadai P, Chenivesse C. Role of CCL18 in asthma and lung immunity. *Clin Exp Allergy* (2013) 43:716–22. doi: 10.1111/CEA.12065

49. Williams IR. CCR6 and CCL20. *Ann N Y Acad Sci* (2006) 1072:52–61. doi: 10.1196/ANNALS.1326.036

50. De Filippo K, Dudeck A, Hasenberg M, Nye E, Van Rooijen N, Hartmann K, et al. Mast cell and macrophage chemokines CXCL1/CXCL2 control the early stage of neutrophil recruitment during tissue inflammation. *Blood* (2013) 121:4930–7. doi: 10.1182/BLOOD-2013-02-486217

51. Biedermann T, Kneilling M, Mailhammer R, Maier K, Sander CA, Kollias G, et al. Mast cells control neutrophil recruitment during T cell-mediated delayed-type hypersensitivity reactions through tumor necrosis factor and macrophage inflammatory protein 2. *J Exp Med* (2000) 192:1441–52. doi: 10.1084/jem.192.10.1441

52. Ohta T, Sugiyama M, Hemmi H, Yamazaki C, Okura S, Sasaki I, et al. Crucial roles of XCR1-expressing dendritic cells and the XCR1-XCL1 chemokine axis in intestinal immune homeostasis. *Sci Rep* (2016) 6:1–11. doi: 10.1038/srep23505

53. St. John AL, Rathore APS, Yap H, Ng ML, Metcalfe DD, Vasudevan SG, et al. Immune surveillance by mast cells during dengue infection promotes natural killer (NK) and NKT-cell recruitment and viral clearance. *Proc Natl Acad Sci USA* (2011) 108:9190–5. doi: 10.1073/PNAS.1105079108

54. Liu WM, Jiang L, Bian C, Liang Y, Xing R, Yishakea M, et al. Role of CX3CL1 in diseases. *Arch Immunol Ther Exp* (2016) 64:371–83. doi: 10.1007/S00005-016-0395-9

55. Subramanian BC, Majumdar R, Parent CA. The role of the LTB4-BLT1 axis in chemotactic gradient sensing and directed leukocyte migration. *Semin Immunol* (2017) 33:16–29. doi: 10.1016/J.SMIM.2017.07.002

56. Taube C, Miyahara N, Ott V, Swanson B, Takeda K, Loader J, et al. The leukotriene B4 receptor (BLT1) is required for effector CD8+ T cell-mediated, mast cell-dependent airway hyperresponsiveness. *J Immunol* (2006) 176:3157–64. doi: 10.4049/JIMMUNOL.176.5.3157

57. Varricchi G, Pecoraro A, Loffredo S, Poto R, Rivellese F, Genovese A, et al. Heterogeneity of human mast cells with respect to MRGPRX2 receptor expression and function. *Front Cell Neurosci* (2019) 13:299/BIBTEX. doi: 10.3389/FNCEL.2019.00299/BIBTEX

58. Kopicky-Burd JA, Kagey-Sobotka A, Peters SP, Dvorak AM, Lennox DW, Lichtenstein LM, et al. Characterization of human synovial mast cells. *J Rheumatol* (1988) 15:1326–33.

59. Busse WW. Leukotrienes and inflammation. *Am J Respir Crit Care Med* (1998) 157:S210–3. doi: 10.1164/ajrccm.157.6.mar-1

60. Komi DEA, Mortaz E, Amani S, Tiotiu A, Folkerts G, Adcock IM. The role of mast cells in IgE-independent lung diseases. *Clin Rev Allergy Immunol* (2020) 58:377–87. doi: 10.1007/s12016-020-08779-5

61. Jin J, Sunusi S, Lu H. Group 2 innate lymphoid cells (ILC2s) are important in typical type 2 immune-mediated diseases and an essential therapeutic target. *J Int Med Res* (2022) 50:1–14. doi: 10.1177/03000605211053156

62. Kastl BC, Pohlman LM. "Basophils, Mast Cells, and Their Disorders," in Schalm's Veterinary Hematology, eds. Brooks M. B., Harr K. E., Seelig D. M., Wardrop K. J. and Weiss D. J., (John Wiley & Sons, Ltd), 373–380. doi: 10.1002/9781119500537.CH47

63. Arima M, Fukuda T. Prostaglandin D2 and TH2 inflammation in the pathogenesis of bronchial asthma. *Korean J Intern Med* (2011) 26:8. doi: 10.3904/KJIM.2011.26.1.8

64. Galli SJ, Nakae S, Tsai M. Mast cells in the development of adaptive immune responses. *Nat Immunol* (2005) 6:135–42. doi: 10.1038/ni1158

65. Kennelly R, B.Conneely J, Bouchier-Hayes D, C. Winter D. Mast cells in tissue healing: From skin to the gastrointestinal tract. *Curr Pharm Des* (2011) 17:3772–5. doi: 10.2174/138161211798357854

66. Ashina K, Tsubosaka Y, Nakamura T, Omori K, Kobayashi K, Hori M, et al. Histamine induces vascular hyperpermeability by increasing blood flow and endothelial barrier disruption *In vivo*. *PLoS One* (2015) 10(7):e0132367. doi: 10.1371/JOURNAL.PONE.0132367

67. Chu Y-T, Wan S-W, Anderson R, Lin Y-S. Mast cell-macrophage dynamics in modulation of dengue virus infection in skin. *Immunology* (2015) 146:163–72. doi: 10.1111/imm.12492

68. Suto H, Nakae S, Kakurai M, Sedgwick JD, Tsai M, Galli SJ. Mast cell-associated TNF promotes dendritic cell migration. *J Immunol* (2006) 176:4102–12. doi: 10.4049/jimmunol.176.7.4102

69. de Vries VC, Pino-Lagos K, Nowak EC, Bennett KA, Oliva C, Noelle RJ. Mast cells condition dendritic cells to mediate allograft tolerance. *Immunity* (2011) 35:550–61. doi: 10.1016/J.IMMUNI.2011.09.012

70. Ott VL, Cambier JC, Kappler J, Marrack P, Swanson BJ. Mast cell–dependent migration of effector CD8+ T cells through production of leukotriene B4. *Nat Immunol 2003 410* (2003) 4:974–81. doi: 10.1038/ni971

71. Bischoff SC, Lorentz A, Schwengberg S, Weier G, Raab R, Manns MP. Mast cells are an important cellular source of tumour necrosis factor α in human intestinal tissue. *Gut* (1999) 44:643–52. doi: 10.1136/GUT.44.5.643

72. Walsh LJ, Trinchieri G, Waldorf HA, Whitaker D, Murphy GF. Human dermal mast cells contain and release tumor necrosis factor α, which induces endothelial leukocyte adhesion molecule 1. *Proc Natl Acad Sci USA* (1991) 88:4220–4. doi: 10.1073/PNAS.88.10.4220

73. Dwyer DF, Barrett NA, Austen KF, Kim EY, Brenner MB, Shaw L, et al. Expression profiling of constitutive mast cells reveals a unique identity within the immune system. *Nat Immunol* (2016) 17:878–87. doi: 10.1038/ni.3445

74. Gordon JR. Monocyte chemoattractant peptide-1 expression during cutaneous allergic reactions in mice is mast cell dependent and largely mediates the monocyte recruitment response. *J Allergy Clin Immunol* (2000) 106:110–6. doi: 10.1067/MAI.2000.107036

75. Dudeck J, Kotrba J, Immler R, Hoffmann A, Voss M, Alexaki VI, et al. Directional mast cell degranulation of tumor necrosis factor into blood vessels primes neutrophil extravasation. *Immunity* (2021) 54:468–83.e5. doi: 10.1016/J.IMMUNI.2020.12.017

76. Bischoff SC, Sellge G, Lorentz A, Sebald W, Raab R, Manns MP. IL-4 enhances proliferation and mediator release in mature human mast cells. *Proc Natl Acad Sci* (1999) 96:8080–5. doi: 10.1073/pnas.96.14.8080

77. Ochi H, De Jesus NH, Hsieh FH, Austen KF, Boyce JA. IL-4 and -5 prime human mast cells for different profiles of IgE-dependent cytokine production. *Proc Natl Acad Sci* (2000) 97:10509–13. doi: 10.1073/pnas.180318697

78. Kearley J, Erjefalt JS, Andersson C, Benjamin E, Jones CP, Robichaud A, et al. IL-9 governs allergen-induced mast cell numbers in the lung and chronic remodeling of the airways. *Am J Respir Crit Care Med* (2011) 183:865–75. doi: 10.1164/rccm.200909-1462OC

79. Bischoff SC, Sellge G, Manns MP, Lorentz A. Interleukin-4 induces a switch of human intestinal mast cells from proinflammatory cells to Th2-type cells. *Int Arch Allergy Immunol* (2001) 124:151–4. doi: 10.1159/000053695

80. Ho LH, Ohno T, Oboki K, Kajiwara N, Suto H, Iikura M, et al. IL-33 induces IL-13 production by mouse mast cells independently of IgE-fc RI signals. *J Leukoc Biol* (2007) 82:1481–90. doi: 10.1189/jlb.0407200

81. Moretti S, Renga G, Oikonomou V, Galosi C, Pariano M, Iannitti RG, et al. A mast cell-ILC2-Th9 pathway promotes lung inflammation in cystic fibrosis. *Nat Commun* (2017) 8:14017. doi: 10.1038/ncomms14017

82. Hepworth MR, Daniłowicz-Luebert E, Rausch S, Metz M, Klotz C, Maurer M, et al. Mast cells orchestrate type 2 immunity to helminths through regulation of tissue-derived cytokines. *Proc Natl Acad Sci USA* (2012) 109:6644–9. doi: 10.1073/PNAS.1112268109

83. Ribatti D. The staining of mast cells: A historical overview. *Int Arch Allergy Immunol* (2018) 176:55–60. doi: 10.1159/000487538

84. Enerbäck L. Mast cells in rat gastrointestinal mucosa. *Acta Pathol Microbiol Scand* (1966) 66:303–12. doi: 10.1111/APM.1966.66.3.303

85. Irani AM, Bradford TR, Kepley CL, Schechter NM, Schwartz LB. Detection of MCT and MCTC types of human mast cells by immunohistochemistry using new monoclonal anti-tryptase and anti-chymase antibodies. *J Histochem Cytochem* (1989) 37:1509–15. doi: 10.1177/37.10.2674273

86. Pejler G, Åbrink M, Ringvall M, Wernersson S. Mast cell proteases. *Adv Immunol* (2007) 95:167–255. doi: 10.1016/S0065-2776(07)95006-3

87. Akula S, Paivandy A, Fu Z, Thorpe M, Pejler G, Hellman L. Quantitative in-depth analysis of the mouse mast cell transcriptome reveals organ-specific mast cell heterogeneity. *Cells* (2020) 9:211. doi: 10.3390/CELLS9010211

88. St. John AL, Rathore APS, Ginhoux F. New perspectives on the origins and heterogeneity of mast cells. *Nat Rev Immunol* (2022), 1–14. doi: 10.1038/s41577-022-00731-2

89. Li Z, Liu S, Xu J, Zhang X, Han D, Liu J, et al. Adult connective tissue-resident mast cells originate from late erythro-myeloid progenitors. *Immunity* (2018) 49:640–53.e5. doi: 10.1016/j.immuni.2018.09.023

90. Gentek R, Ghigo C, Hoeffel G, Bulle MJ, Msallam R, Gautier G, et al. Hemogenic endothelial fate mapping reveals dual developmental origin of mast cells. *Immunity* (2018) 48:1160–71. doi: 10.1016/j.immuni.2018.04.025

91. Wang X, Yang L, Wang YC, Xu ZR, Feng Y, Zhang J, et al. Comparative analysis of cell lineage differentiation during hepatogenesis in humans and mice at the single-cell transcriptome level. *Cell Res* (2020) 30:1109–26. doi: 10.1038/s41422-020-0378-6

92. Grootens J, Ungerstedt JS, Nilsson G, Dahlin JS. Deciphering the differentiation trajectory from hematopoietic stem cells to mast cells. *Blood Adv* (2018) 2:2273–81. doi: 10.1182/bloodadvances.2018019539

93. Weitzmann A, Naumann R, Dudeck A, Zerjatke T, Gerbaulet A, Roers A. Mast cells occupy stable clonal territories in adult steady-state skin. *J Invest Dermatol* (2020) 140:2433–41. doi: 10.1016/j.jid.2020.03.963

94. Albert-Bayo M, Paracuellos I, González-Castro AM, Rodríguez-Urrutia A, Rodríguez-Lagunas MJ, Alonso-Cotoner C, et al. Intestinal mucosal mast cells: Key

modulators of barrier function and homeostasis. *Cells* (2019) 8:135. doi: 10.3390/CELLS8020135

95. Collington SJ, Hallgren J, Pease JE, Jones TG, Rollins BJ, Westwick J, et al. The role of the CCL2/CCR2 axis in mouse mast cell migration *In vitro* and *In vivo*. *J Immunol* (2010) 184:6114–23. doi: 10.4049/JIMMUNOL.0904177

96. Gurish MF, Tao H, Abonia JP, Arya A, Friend DS, Parker CM, et al. Intestinal mast cell progenitors require CD49dbeta7 (Alpha4beta7 integrin) for tissue-specific homing. *J Exp Med* (2001) 194:1243–52. doi: 10.1084/JEM.194.9.1243

97. Zarnegar B, Mendez-Enriquez E, Westin A, Söderberg C, Dahlin JS, Grönvik KO, et al. Influenza infection in mice induces accumulation of lung mast cells through the recruitment and maturation of mast cell progenitors. *Front Immunol* (2017) 8:310. doi: 10.3389/FIMMU.2017.00310

98. Nakano T, Sonoda T, Hayashi C, Yamatodani A, Kanayama Y, Yamamura T, et al. Fate of bone marrow-derived cultured mast cells after intracutaneous, intraperitoneal, and intravenous transfer into genetically mast cell-deficient W/Wv mice. evidence that cultured mast cells can give rise to both connective tissue type and mucosal mast cells. *J Exp Med* (1985) 162:1025–43. doi: 10.1084/JEM.162.3.1025

99. Frossi B, Mion F, Sibilano R, Danelli L, Pucillo CEM. Is it time for a new classification of mast cells? what do we know about mast cell heterogeneity? *Immunol Rev* (2018) 282:35–46. doi: 10.1111/IMR.12636

100. Füreder W, Agis H, Willheim M, Bankl HC, Maier U, Kishi K, et al. Differential expression of complement receptors on human basophils and mast cells. evidence for mast cell heterogeneity and CD88/C5aR expression on skin mast cells. *J Immunol* (1995) 155:3152–60. doi: 10.4049/issn.1550-6606

101. Oskeritzian CA, Zhao W, Min HK, Xia HZ, Pozez A, Kiev J, et al. Surface CD88 functionally distinguishes the MCTC from the MCT type of human lung mast cell. *J Allergy Clin Immunol* (2005) 115:1162–8. doi: 10.1016/j.jaci.2005.02.022

102. Plum T, Wang X, Rettel M, Krijgsveld J, Feyerabend TB, Rodewald HR. Human mast cell proteome reveals unique lineage, putative functions, and structural basis for cell ablation. *Immunity* (2020) 52:404–16.e5. doi: 10.1016/j.immuni.2020.01.012

103. Ben-Baruch Morgenstern N, Ballaban AY, Wen T, Shoda T, Caldwell JM, Kliewer K, et al. Single-cell RNA sequencing of mast cells in eosinophilic esophagitis reveals heterogeneity, local proliferation, and activation that persists in remission. *J Allergy Clin Immunol* (2022) 149:2026–77. doi: 10.1016/J.JACI.2022.02.025

104. Dwyer DF, Ordovas-Montanes J, Allon SJ, Buchheit KM, Vukovic M, Derakhshan T, et al. Human airway mast cells proliferate and acquire distinct inflammation-driven phenotypes during type 2 inflammation. *Sci Immunol* (2021) 6:eabb7221. doi: 10.1126/sciimmunol.abb7221

105. Rönnberg E, Boey DZH, Ravindran A, Säfholm J, Orre AC, Al-Ameri M, et al. Immunoprofiling reveals novel mast cell receptors and the continuous nature of human lung mast cell heterogeneity. *Front Immunol* (2022) 12:804812. doi: 10.3389/FIMMU.2021.804812

106. Bischoff SC, Krämer S. Human mast cells, bacteria, and intestinal immunity. *Immunol Rev* (2007) 217:329–37. doi: 10.1111/J.1600-065X.2007.00523.X

107. Bischoff SC. Mast cells in gastrointestinal disorders. *Eur J Pharmacol* (2016) 778:139–45. doi: 10.1016/J.EJPHAR.2016.02.018

108. Abonia JP, Austen KF, Rollins BJ, Joshi SK, Flavell RA, Kuziel WA, et al. Constitutive homing of mast cell progenitors to the intestine depends on autologous expression of the chemokine receptor CXCR2. *Blood* (2005) 105:4308. doi: 10.1182/BLOOD-2004-09-3578

109. Kunii J, Takahashi K, Kasakura K, Tsuda M, Nakano K, Hosono A, et al. Commensal bacteria promote migration of mast cells into the intestine. *Immunobiology* (2011) 216:692–7. doi: 10.1016/J.IMBIO.2010.10.007

110. Lorentz A, Schuppan D, Gebert A, Manns MP, Bischoff SC. Regulatory effects of stem cell factor and interleukin-4 on adhesion of human mast cells to extracellular matrix proteins. *Blood* (2002) 99:966–72. doi: 10.1182/BLOOD.V99.3.966

111. Baumann A, Feilhauer K, Bischoff SC, Froy O, Lorentz A. IgE-dependent activation of human mast cells and fMLP-mediated activation of human eosinophils is controlled by the circadian clock. *Mol Immunol* (2015) 64:76–81. doi: 10.1016/J.MOLIMM.2014.10.026

112. Karhausen J, Qing M, Gibson A, Moeser AJ, Griefingholt H, Hale LP, et al. Intestinal mast cells mediate gut injury and systemic inflammation in a rat model of deep hypothermic circulatory arrest. *Crit Care Med* (2013) 41:e200. doi: 10.1097/CCM.0B013E31827CAC7A

113. McDermott JR, Bartram RE, Knight PA, Miller HRP, Garrod DR, Grencis RK. Mast cells disrupt epithelial barrier function during enteric nematode infection. *Proc Natl Acad Sci USA* (2003) 100:7761. doi: 10.1073/PNAS.1231488100

114. Shin K, Watts GFM, Oettgen HC, Friend DS, Pemberton AD, Gurish MF, et al. Mouse mast cell tryptase mMCP-6 is a critical link between adaptive and innate immunity in the chronic phase of trichinella spiralis infection. *J Immunol* (2008) 180:4885. doi: 10.4049/JIMMUNOL.180.7.4885

115. Roy A, Sawesi O, Pettersson U, Dagälv A, Kjellén L, Lundén A, et al. Serglycin proteoglycans limit enteropathy in trichinella spiralis-infected mice. *BMC Immunol* (2016) 17:1–13. doi: 10.1186/S12865-016-0155-Y

116. Brink N, Szamel M, Young AR, Wittern KP, Bergemann J. Comparative quantification of IL-1β, IL-10, IL-10r, tnfα and IL-7 mRNA levels in UV-irradiated human skin *In vivo*. *Inflammation Res* (2014) 49:290–6. doi: 10.1007/PL00000209

117. Leyva-Castillo JM, Das M, Artru E, Yoon J, Galand C, Geha RS. Mast cell–derived IL-13 downregulates IL-12 production by skin dendritic cells to inhibit the TH1 cell response to cutaneous antigen exposure. *J Allergy Clin Immunol* (2021) 147:2305–15.e3. doi: 10.1016/J.JACI.2020.11.036

118. Faulkner H, Humphreys N, Renauld JC, Van Snick J, Grencis R. Interleukin-9 is involved in host protective immunity to intestinal nematode infection. *Eur J Immunol* (1997) 27:2536–40. doi: 10.1002/eji.1830271011

119. Faulkner H, Renauld JC, Van Snick J, Grencis RK. Interleukin-9 enhances resistance to the intestinal nematode Trichuris muris. *Infect Immun* (1998) 66:3832–40. doi: 10.1128/IAI.66.8.3832-3840.1998

120. Hültner L, Kölsch S, Stassen M, Kaspers U, Kremer JP, Mailhammer R, et al. In activated mast cells, IL-1 up-regulates the production of several Th2-related cytokines including IL-9. *J Immunol* (2000) 164:5556–63. doi: 10.4049/jimmunol.164.11.5556

121. Stassen M, Arnold M, Hültner L, Müller C, Neudörfl C, Reineke T, et al. Murine bone marrow-derived mast cells as potent producers of IL-9: Costimulatory function of IL-10 and kit ligand in the presence of IL-1. *J Immunol* (2000) 164:5549–55. doi: 10.4049/jimmunol.164.11.5549

122. Theoharides TC, Kempuraj D, Kourelis T, Manola A. Human mast cells stimulate activated T cells: Implications for multiple sclerosis. *Ann N Y Acad Sci* (2008) 1144:74–82. doi: 10.1196/ANNALS.1418.029

123. Bodduluri SR, Mathis S, Maturu P, Krishnan E, Satpathy SR, Chilton PM, et al. Mast cell–dependent CD8+ T-cell recruitment mediates immune surveillance of intestinal tumors in ApcMin/þ mice. *Cancer Immunol Res* (2018) 6:332–47. doi: 10.1158/2326-6066.CIR-17-0424/470586

124. Cowen T, Trigg P, Eady RAJ. Distribution of mast cells in human dermis: Development of a mapping technique. *Br J Dermatol* (1979) 100:635–40. doi: 10.1111/J.1365-2133.1979.TB08066.X

125. Liu J, Harberts E, Tammaro A, Girardi N, Filler RB, Fishelevich R, et al. IL-9 regulates allergen-specific Th1 responses in allergic contact dermatitis. *J Invest Dermatol* (2014) 134:1903–11. doi: 10.1038/JID.2014.61

126. Wang Z, MacLeod DT, Di Nardo A. Commensal bacteria lipoteichoic acid increases skin mast cell antimicrobial activity against vaccinia viruses. *J Immunol* (2012) 189:1551–8. doi: 10.4049/JIMMUNOL.1200471

127. Wang Z, Mascarenhas N, Eckmann L, Miyamoto Y, Sun X, Kawakami T, et al. Skin microbiome promotes mast cell maturation by triggering stem cell factor production in keratinocytes. *J Allergy Clin Immunol* (2017) 139:1205–16.e6. doi: 10.1016/J.JACI.2016.09.019

128. Columbo M, Bochner BS. Human skin mast cells adhere to vitronectin *via* the αvβ3 integrin receptor (CD51/CD61). *J Allergy Clin Immunol* (2001) 107:554. doi: 10.1067/MAI.2001.113238

129. Kurashima Y, Amiya T, Fujisawa K, Shibata N, Suzuki Y, Kogure Y, et al. The enzyme Cyp26b1 mediates inhibition of mast cell activation by fibroblasts to maintain skin-barrier homeostasis. *Immunity* (2014) 40:530–41. doi: 10.1016/J.IMMUNI.2014.01.014

130. Okayama Y, Ono Y, Nakazawa T, Church MK, Mori M. Human skin mast cells produce TNF-alpha by substance p. *Int Arch Allergy Immunol* (1998) 117:48–51. doi: 10.1159/000053571

131. Furuta T, Imajo-Ohmi S, Fukuda H, Kano S, Miyake K, Watanabe N. Mast cell-mediated immune responses through IgE antibody and toll-like receptor 4 by malarial peroxiredoxin. *Eur J Immunol* (2008) 38:1341–50. doi: 10.1002/EJI.200738059

132. Gibbs BF, Wierecky J, Welker P, Henz BM, Wolff HH, Grabbe J. Human skin mast cells rapidly release preformed and newly generated TNF-alpha and IL-8 following stimulation with anti-IgE and other secretagogues. *Exp Dermatol* (2001) 10:312–20. doi: 10.1034/j.1600-0625.2001.100503.x

133. Wershil BK, Wang ZS, Gordon JR, Galli SJ. Recruitment of neutrophils during IgE-dependent cutaneous late phase reactions in the mouse is mast cell-dependent. partial inhibition of the reaction with antiserum against tumor necrosis factor-alpha. *J Clin Invest* (1991) 87:446–53. doi: 10.1172/jci115016

134. Dudeck J, Ghouse SM, Lehmann CH, Hoppe A, Schubert N, Nedospasov SA, et al. Mast-Cell-Derived TNF amplifies CD8(+) dendritic cell functionality and CD8(+) T cell priming. *Cell Rep* (2015) 13:399–411. doi: 10.1016/j.celrep.2015.08.078

135. McLachlan JB, Hart JP, Pizzo SV, Shelburne CP, Staats HF, Gunn MD, et al. Mast cell-derived tumor necrosis factor induces hypertrophy of draining lymph nodes during infection. *Nat Immunol* (2003) 4:1199–205. doi: 10.1038/ni1005

136. Mantri CK, St. John AL. Immune synapses between mast cells and γδ T cells limit viral infection. *J Clin Invest* (2019) 129:1094–108. doi: 10.1172/JCI122530

137. Hackler Y, Siebenhaar F, Löhning M, Maurer M, Muñoz M. Mast cells modulate antigen-specific CD8+ T cell activation during LCMV infection. *Front Immunol* (2021) 12:688347. doi: 10.3389/FIMMU.2021.688347

138. Aoki R, Kawamura T, Goshima F, Ogawa Y, Nakae S, Nakao A, et al. Mast cells play a key role in host defense against herpes simplex virus infection through TNF-α and IL-6 production. *J Invest Dermatol* (2013) 133:2170–9. doi: 10.1038/JID.2013.150

139. Agier J, Pastwińska J, Brzezińska-Błaszczyk E. An overview of mast cell pattern recognition receptors. *Inflammation Res* (2018) 67:737–46. doi: 10.1007/S00011-018-1164-5

140. Kothari R, Dong X. Scratching the surface of itch receptors. *Trends Pharmacol Sci* (2022) 43:168–70. doi: 10.1016/J.TIPS.2021.12.005

141. McNeil BD, Pundir P, Meeker S, Han L, Undem BJ, Kulka M, et al. Identification of a mast-Cell-Specific receptor crucial for pseudo-allergic drug reactions. *Nature* (2015) 519:237–41. doi: 10.1038/nature14022

142. Green DP, Limjunyawong N, Gour N, Pundir P, Dong X. A mast-Cell-Specific receptor mediates neurogenic inflammation and pain. *Neuron* (2019) 101:412–20.e3. doi: 10.1016/j.neuron.2019.01.012

143. Nakamura Y, Kambe N, Saito M, Nishikomori R, Nishikomiri R, Kim Y-G, et al. Mast cells mediate neutrophil recruitment and vascular leakage through the NLRP3 inflammasome in histamine-independent urticaria. *J Exp Med* (2009) 206:1037–46. doi: 10.1084/jem.20082179

144. Nakamura Y, Franchi L, Kambe N, Meng G, Strober W, Núñez G. Critical role for mast cells in interleukin-1β-Driven skin inflammation associated with an activating mutation in the Nlrp3 protein. *Immunity* (2012) 37:85–95. doi: 10.1016/J.IMMUNI.2012.04.013

145. Reber LL, Sibilano R, Starkl P, Roers A, Grimbaldeston MA, Tsai M, et al. Imaging protective mast cells in living mice during severe contact hypersensitivity. *JCI Insight* (2017) 2:1–13. doi: 10.1172/jci.insight.92900

146. Chichlowski M, Westwood GS, Abraham SN, Hale LP. Role of mast cells in inflammatory bowel disease and inflammation-associated colorectal neoplasia in IL-10-Deficient mice. *PLoS One* (2010) 5:e12220. doi: 10.1371/JOURNAL.PONE.0012220

frontiers | Frontiers in Immunology

TYPE Original Research
PUBLISHED 02 August 2022
DOI 10.3389/fimmu.2022.924244

Check for updates

OPEN ACCESS

EDITED BY
Frans J. Van Overveld,
University College Roosevelt,
Netherlands

REVIEWED BY
Nicholas A. Pullen,
University of Northern Colorado,
United States
Naoya Tanabe,
Kyoto University, Japan

*CORRESPONDENCE
Jonas S. Erjefält
jonas.erjefalt@med.lu.se

SPECIALTY SECTION
This article was submitted to Inflammation,
a section of the journal
Frontiers in Immunology

RECEIVED 20 April 2022
ACCEPTED 06 July 2022
PUBLISHED 02 August 2022

CITATION
Siddhuraj P, Jönsson J, Alyamani M, Prabhala P, Magnusson M, Lindstedt S and Erjefält JS (2022) Dynamically upregulated mast cell CPA3 patterns in chronic obstructive pulmonary disease and idiopathic pulmonary fibrosis. *Front. Immunol.* 13:924244. doi: 10.3389/fimmu.2022.924244

COPYRIGHT
© 2022 Siddhuraj, Jönsson, Alyamani, Prabhala, Magnusson, Lindstedt and Erjefält. This is an open-access article distributed under the terms of the Creative Commons Attribution License (CC BY). The use, distribution or reproduction in other forums is permitted, provided the original author(s) and the copyright owner(s) are credited and that the original publication in this journal is cited, in accordance with accepted academic practice. No use, distribution or reproduction is permitted which does not comply with these terms.

Dynamically upregulated mast cell CPA3 patterns in chronic obstructive pulmonary disease and idiopathic pulmonary fibrosis

Premkumar Siddhuraj[1], Jimmie Jönsson[2], Manar Alyamani[1], Pavan Prabhala[3], Mattias Magnusson[3], Sandra Lindstedt[4] and Jonas S. Erjefält[1,5]*

[1]Unit of Airway Inflammation, Department of Experimental Medical Sciences, Lund University, Lund, Sweden, [2]Medetect AB, Lund, Sweden, [3]Division of Molecular Medicine and Gene Therapy, Lund Stem Cell Center, Lund University, Lund, Sweden, [4]Department of Thoracic Surgery, Lund University Skane University Hospital, Lund, Sweden, [5]Department of Allergology and Respiratory Medicine, Lund University, Skane University Hospital, Lund, Sweden

Background: The mast cell-specific metalloprotease CPA3 has been given important roles in lung tissue homeostasis and disease pathogenesis. However, the dynamics and spatial distribution of mast cell CPA3 expression in lung diseases remain unknown.

Methods: Using a histology-based approach for quantitative spatial decoding of mRNA and protein single cell, this study investigates the dynamics of CPA3 expression across mast cells residing in lungs from control subjects and patients with severe chronic obstructive pulmonary disease (COPD) or idiopathic lung fibrosis (IPF).

Results: Mast cells in COPD lungs had an anatomically widespread increase of CPA3 mRNA (bronchioles $p < 0.001$, pulmonary vessels $p < 0.01$, and alveolar parenchyma $p < 0.01$) compared to controls, while granule-stored CPA3 protein was unaltered. IPF lungs had a significant upregulation of both mast cell density, CPA3 mRNA ($p < 0.001$) and protein ($p < 0.05$), in the fibrotic alveolar tissue. Spatial expression maps revealed altered mast cell mRNA/protein quotients in lung areas subjected to disease-relevant histopathological alterations. Elevated CPA3 mRNA also correlated to lung tissue eosinophils, CD3 T cells, and declined lung function. Single-cell RNA sequencing of bronchial mast cells confirmed CPA3 as a top expressed gene with potential links to both inflammatory and protective markers.

Conclusion: This study shows that lung tissue mast cell populations in COPD and IPF lungs have spatially complex and markedly upregulated CPA3

expression profiles that correlate with immunopathological alterations and lung function. Given the proposed roles of CPA3 in tissue homeostasis, remodeling, and inflammation, these alterations are likely to have clinical consequences.

KEYWORDS

mast cells, carboxypeptidase A3, lung, COPD, tryptase

Introduction

Human adult lungs are densely populated with mast cells at healthy baseline conditions (1, 2). These tissue-inherent mast cells are strategically located throughout all lung compartments where they are thought to have important roles for tissue homeostasis and orchestrating tissue inflammation (3–5). Mast cells have also been implicated in major airway diseases like asthma, chronic obstructive pulmonary disease (COPD), and idiopathic pulmonary fibrosis (IPF) (2, 6–9). In disease, mast cells may act in a pro-inflammatory manner by releasing histamine, leukotrienes, prostaglandins, and cytokines. Another important mechanism by which mast cells influence their tissue surroundings is through their specific proteases. Indeed, the large granules in mast cells serve as storage sites for pre-synthesized effector molecules, with the major content being proteases (10, 11). Among these, tryptase and chymase have been the most studied (10–13) and are also used for the classical division of mast cells into "connective tissue-like" mast cells (MC_{TC} cells; containing tryptase and chymase) and "mucosal- like" mast cells (MC_T; lacking chymase) (3–5). Less explored is the mast cell-specific zinc-containing metalloprotease carboxypeptidase A3 (CPA3). Still, this protease is equally abundant as tryptase and chymase and has protease activities regulating both local homeostasis and inflammation (14, 15). Among targets for CPA3-mediated cleavage are neurotensin, kinetensin, endothelin-1, apolipoprotein B, and angiotensin I (16–21). It has also been proposed that CPA3 promotes the formation of the fibrous component of the extracellular matrix during tissue remodeling. It thus seems like CPA3 may have both important protective roles and pathogenic pro-remodeling properties.

As support for involvement in disease, increased CPA3 levels have been reported in cancer and cardiovascular diseases (22), diseases of the gastrointestinal tract (23, 24), and the respiratory system (25–27). Altered expression levels of CPA3 have also been proposed as a diagnostic and prognostic marker in asthma and COPD (25–29). Another recent biomarker example is the proposal to use serum CPA3 to monitor severe COVID-19 (30). Although the link between altered CPA3 expression and many clinical manifestations seems clear, very little is known about what effector functions of CPA3 are operating in respective disease.

To gain further insight into the complex roles of CPA3 in health and disease, it is critical to understand the spatial distribution pattern of the mast cell CPA3 expression, as it occurs inside relevant healthy and diseased tissues. Interestingly, recent data suggest that the content of granule-stored CPA3 protein and CPA3 mRNA expression may already under healthy baseline conditions display distinct patterns across human tissues (31). For example, in a recent study (31), a CPA3 protein^{high}, mRNA^{low} profile in the skin was contrasted by a reversed CPA3 protein^{low}, mRNA^{high} profile in human lungs. This was most dramatic in the alveolar region of normal lungs where the normal chymase-negative alveolar MC_T cells commonly lacked CPA3 protein but had a high constitutive CPA3 mRNA expression (31). Based on this observation, and new understanding of fine-tuned gradual mast cell protease secretion mechanisms (14), it has recently been proposed that mast cells may already at healthy baseline conditions exert important homeostatic functions *via* a basal "pacemaker-like" degranulation through microvesicles (14, 31). To what extent this type of basal CPA3 mRNA expression can be further increased in chronic lung diseases emerges as an important question. Since mast cell phenotypes are strongly influenced by the local microenvironments, another critical issue is how the CPA3 mRNA and protein balance is altered in the key anatomical compartments of diseased lungs.

The present study uses a histological approach that yields spatially resolved quantitative data on mRNA and protein within single cells to study how spatially dictated mast cell CPA3 patterns are altered in patients with severe COPD and IPF. The rationale to study COPD and IPF is that, in contrast to the previous important CPA3 studies in asthma (8, 26, 27), little is known about CPA3 in COPD and IPF. Furthermore, from these diseases, as well as controls, it is possible to obtain large enough tissue samples as part of clinical lung surgery and lung transplantation procedures. After exploring such surgical resections, we reveal here novel intriguing observations on altered mast cell CPA3 expression patterns in patients with COPD and IPF.

Materials and methods

Human lung tissue acquisition and sample processing for histology

Human lung tissue: Human control lung tissue was obtained from nine non-atopic patients undergoing lobectomy due to suspected lung cancer but otherwise lacking any history of respiratory disease. Only patients with solid well-delineated tumors were included and central and distal lung tissue samples were collected as far as possible from the tumor site. Although most of the subjects are former smokers, this procedure has commonly been used to collect non-diseased control lung tissue samples for histological research (32, 33). Corresponding lung tissues were collected from diseased lungs that we excised as part of a lung transplantation (n = 15; nine patients with diagnosed COPD and six confirmed IPF cases). Hence, both the COPD and IPF patients were in the severe category of their respective disease. All COPD patients were in the GOLD 4 severe category and all IPF patients had confirmed progressing lung fibrosis. Basic demographics of the patients are presented in Table 1. All 24 subjects gave their written informed consent, which was approved by the ethical committee in Lund, Sweden (Dnr. LU- 2015/891).

To avoid technical bias inflicted by the variation in fixation times, which commonly occurs in routine clinical pathology laboratories, the excised tissues were prepared at our own research laboratory and histology platform. All tissues were immediately subjected to standardized fixation in buffered 4% formaldehyde (#02176; Histolab, Askim, Sweden) for 24 h ± 4 h at room temperature before being dehydrated in an automated dehydration machine (SAKURA-Tissue-Tek VIP® 6 AI; Sakura Finetek USA, Inc., Torrance, CA, USA) and embedded into paraffin blocks (SAKURA EC350; Sakura Finetek, Inc.). Large multiple cm^2-sized 4-µm paraffin sections were generated, dehydrated, and used for the present high-end quantitative MC protease analysis.

Combined *in situ* hybridization and immunohistochemistry (ISH-IHC) for simultaneous detection of CPA3 mRNA, CPA3, tryptase, and chymase protein across mast cells in human lung sections

Initial visualization of CPA3 mRNA was performed through *in situ* hybridization (ISH) using the RNAscope® Multiplex fluorescence kit V2 assay kit (#323100; Advanced Cell Diagnostics, Hayward, CA, USA) for fluorescent ISH (FISH) and using the RNAscope® 2.5 HD Detection Reagents-RED (#322360, Advanced Cell Diagnostics) for chromogenic ISH (CISH), according to the manufacturer's instructions. Briefly, 4-µm lung tissue sections were baked at 60°C for 1 h and then deparaffinized through a series of alcohol and xylene baths. Afterwards, the slides were incubated with hydrogen peroxide for 10 min at RT and then with mRNA retrieval solution for 15 min at 99°C before dehydration with 99.5% EtOH for 3 min at RT and then evaporation at 60°C for 5 min. After creating a hydrophobic border around each tissue specimen, they were incubated at 40°C for 30 min together with RNAscope Protease Plus and then at the same temperature for 2 h with the CPA3 mRNA probe (#486731). Additional control probes were run in parallel: negative control (DapB, #310043) and positive control probes (PPIB, #486081; Advanced Cell Diagnostics). For fluorescent read-out, tyramide (TSA) amplification was performed with Cyanine 3 (Cy3, NEL744E001KT, Perkin Elmer, Waltham, MA, USA). The slides with fluorescent read-

Table 1. Patient demographics.

Parameter	Lung Controls	COPD Patients	IPF Patients	Overall p-value
Subjects, $n^{\#}$	9[#]	10[#]	6[#]	
Gender, male/female[#]	3/6[#]	6/4[#]	5/1[#]	
Age, years	74 (64–78) [#]	62 (59–64)	60 (53–66) [†]	0.0334
Height, m	1.6 (1.5–1.8)	1.8 (1.6–1.8)	1.8 (1.6–1.8)	0.1347
Body mass index, kg/m^2	32.7 (25.7–60.2)	30.1 (25.7–35.4)	32.5 (29.2–37.0)	0.2727
Smoking status, never/ex/current	2/6/1	0/10/0	4/2/0	
FEV_1, L	1.8 (1.7–2.4)	0.8 (0.6–0.8) [†]	2.0 (1.5–2.5)	0.0002
FEV_1/(F)VC, %	82 (66–121)	78 (71–88) [†]	67 (65–70)	<0.0001
FEV_1, % of predicted	85 (72–95)	22 (18–29) [†]	67 (44–76)	0.0003
DLCO	88 (65–110)	36 (28–43) [†]	29 (24–50) [§]	<0.0001
Corticosteroids (yes/no/unknown)	0/9/0	9/0/1	4/2/0	

Values are median (range) or n. Statistical analysis was performed using Kruskal–Wallis nonparametric test followed by Dunn's multiple comparison post-test. Chronic obstructive pulmonary disease (COPD); Idiopathic pulmonary fibrosis (IPF); FEV_1: forced expiratory volume in 1 s; (F)VC: (forced) vital capacity; diffusing capacity of the lungs for carbon monoxide (DLCO). [#]The mean value of the study group is 68 years. [†]$p = 0.0334$ vs. Lung Controls. [†]$p = 0.0002$ vs. Lung Controls. [†]$p < 0.0001$ vs. Lung Controls. [†]$p = 0.0003$ vs. Lung Controls. [§]$p < 0.0001$ vs. Lung Controls.

out were then blocked with an HRP blocker and placed in PBS awaiting immunofluorescence staining.

After the FISH of CPA3 mRNA in the Cy3/555 nm channel, slides were subjected to subsequent immunofluorescence immunohistochemical staining for mast cell protein targets such as tryptase (TPSAB1/AB1tryptase and TPSB2/B2 tryptase combined in Cy7/750 nm fluorescence channel) and CPA3 (Cy5/640 nm channel). For tryptases (TPSAB1 and TPSB2) and CPA3 immunostaining, sections were incubated (for 1 h) with a cocktail of a mouse anti-human AB1 tryptase/TPSAB1 (#MAB1222A; 0.1 g/0.1 ml, dilution 1:350; Millipore, Solna, Sweden), mouse anti Human B2 tryptase/TPSB2 (#MAB37961; 1 µg/1 µl, dilution 1:500, R&D Abingdon, UK), and a rabbit anti-human CPA3 primary antibody (#HPA0526634, 0.4 mg/ml, dilution 1:500, Atlas antibodies, Bromma, Sweden).

After a washing step, these primary antibodies were detected by a secondary antibody cocktail (incubated for 1 h) with an AlexaFluor 647 Goat anti-Rabbit secondary antibody (#A27040; 2 mg/ml, 1:200; Thermo Fisher Scientific, Göteborg, Sweden) and an Alexa Fluor Cy7 Goat anti-Mouse secondary antibody (#A21037; 2 mg/ml, 1:200; Thermo Fisher Scientific, Göteborg, Sweden). All the primary and secondary antibodies were diluted in antibody diluent (#S0809, Dako). After completion of combined ISH and IF-IHC staining, the slides were incubated with Bisbenzimide-33342 (#A0741; Applichem, Darmstadt, Germany) for DAPI nucleus counterstaining (358 nm) and mounted with Vectashield (#H1400; Vector Laboratories, Inc.) and No. 1 coverslips (ECN 631-1574; VWR, Radnor, PA, USA).

The present antibody against CPA3 and the other primary and secondary antibodies have been validated and used in multiple previous studies (31, 34, 35). Detailed tests also confirmed the specificity of the staining results, i.e., that there was no artifactual cross-reactions and unwanted streptavidin binding, and that the low autofluorescence within mast cells had no or negligible impact on the analyses.

Masson Trichrome staining

The serial lung sections (4 µm thickness) from the different study groups (control, COPD, and IPF) were stained with Masson's trichome (#HT15, Trichrome Stain Kit, MilliporeSigma, Missouri, USA) for evaluation of gross anatomical changes and degree of fibrosis.

Slide digitalization and IF image quantification

The Olympus VS-200 (Shinjuku, Tokyo, Japan) fluorescence virtual microscopy slide scanning platform was used for digitalization of fluorescence-stained tissue sections. The fluorophores corresponding to DAPI (nuclei), Cy3 (CPA3 mRNA), Cy5 (CPA3 protein), and Cy7 (combined AB1 and B2 tryptase) channels were recorded with "locked" exposure time for each channel across all the samples within an experiment. Separate test experiments confirmed minimal bleeding between the fluorescence filter settings. To measure CPA3 protein and mRNA content at the single-cell level, a tryptase-based mast cell mask was created for mast cells using Qupath Software (version 0.3.0). First, the mask for mast cell regions of interest (ROI) was segmented by applying standard intensity threshold for the tryptase channel (Cy7). Secondly, the generated masks for mast cells from the tryptase channel were digitally superimposed to the raw data images in Cy3 and y5 channels to measure CPA3 the mRNA and protein content, respectively. Finally, after ROI size filtration, the intensity values were corrected by subtracting the tissue background fluorescence value.

To compare protease profiles within defined anatomical compartments, the following structures were manually delineated by cursor tracing: large and small airway compartments (i.e., bronchioles), epithelium and subepithelial tissue, large pulmonary vessels, and alveolar parenchymal regions. The ROIs for all compartments were applied to other channels of the same image to extract the single-cell data, as described above. For spatial visualization of mast cell distribution in lung tissue sections, x and y coordinates were extracted during the quantification and superimposed on the original image together with color-coded CPA3 intensity levels. x,y-coordinate-based topographic contour maps and statistical differences in mast cell CPA3 profiles across spatially defined tissue regions were performed using the JMP Software, Version 16, SAS Institute Inc, NC, USA.

Correlations between mast CPA3 parameters and crude immune cell profiles

To get a crude insight into the type of cellular inflammation associated with the present elevated CPA3, comparisons were made to lung tissue content of key immune cells like eosinophils, basophils, T lymphocytes and B lymphocytes. These immune cells were analyzed by pairwise double immunohistochemistry (eosinophils–basophils and T–B lymphocytes) using the following primary cell identification markers: T cells (a mouse anti-human CD3- #M7254; 138 mg/L; dilution 1:50; Clone F7.2.38, DAKO, Glostrup, Denmark), B cells (a mouse anti-human CD20- #M0755; 126 mg/L; dilution 1:200; Clone L26; DAKO, Glostrup, Denmark), basophils (a mouse anti-human proMBP1 #J175 704, 0.5 mg/ml; dilution 1:150; BioLegend, Täby, Sweden), and eosinophils (a mouse anti-human ECP/clone EG2 #mAB593, 1 mg/ml; dilution 1:700; Diagnostic Development, Uppsala, Sweden). As part of the antigen retrieval process, slides were baked at 60°C for 45 min and

pre-treated with low pH heat-induced epitope retrieval (HIER) by a pH6 target retrieval solution (#DM829; Dako, Glostrup, Denmark) in a DAKO PT Link HIER machine (PTlink 200; Dako, Glostrup, Denmark). The immunohistochemical staining was performed in an automated immunohistochemistry robot (Dako Cytomation, Glostrup, Denmark) with Dako wash buffer (#DM831; Dako, Glostrup, Denmark). Briefly, slides were blocked with peroxidase blocking reagent (DAKO-DM821) for 10 min before being incubated with the primary antibody for 1 h, washed, and incubated with a polymer-HRP-labeled secondary ab (#DM822, Envision Flex, Dako, Glostrup, Denmark) for 30 min and brown chromogen development with 3,3′-Diaminobenzidine (# DM827 DAB-Dako, Glostrup, Denmark). Next, the slides were treated with denaturing solution for 5 min (#DNS001L, Biocare, CA, USA) to remove any remaining antibodies for the first target. After the antibody denaturation step, slides were treated with the secondary primary ab for 1 h and polymer-based secondary antibody as above [but with visualization using the green chromogen Vina Green (#BRR807BC, BioCare, CA, USA) for 10 min]. Finally, the slides were counterstained with Mayer's hematoxylin (#01820; Histolab, Askim, Sweden), mounted with pertex (#00840; Histolab), and digitized using a ScanScope Slide Scanning Robot (Aperio Technologies, Vista, CA, USA). The generated 20X high-resolution images were used for computerized quantitative analysis of chromogens (i.e., immunoreactivity). The amount of immunoreactivity for each cell marker was normalized to the total analyzed tissue area and quantified using the Visiomorph software (Visiopharm, Hørsholm, Denmark).

RNA sequencing and single-cell analysis

Cell preparations from bronchial biopsies were subjected to single-cell RNA sequencing using the 10x based Chromium system (10x Genomics, USA). Single-cell RNA sequencing libraries were sequenced on Nextseq500 or Novaseq 6000. Raw data were further analyzed using the bustools kallisto pipeline (36). We used the following parameters to filter out low-quality cells: gene and unique molecular identifier (UMI) minimum 1,000/maximum 75,000; percentage mitochondria, minimum 0% maximum 20%; average number of reads/cells, 25,000. All analyses, including log normalization, scaling, clustering of cells, and identifying cluster marker genes, were performed using python packages. We performed principal component analysis dimensionality reduction with scanpy highly variable genes as input. Unsupervised clustering was performed using the scanpy.tl.umap function, the heatmap was generated using the scanpy.pl.heatmap function. Mast cells were identified by the expression pattern of mast cell marker genes. Two outlying cells not shown in the representative UMAP for space purposes but were included for all relevant analyses.

Data visualization and statistics

All results are presented as median with interquartile range and ranks were compared among samples using the non-parametric Mann–Whitney test. To compare more than two groups of samples, ANOVA test, Kruskal–Wallis test and Dunn's multiple comparisons test was used. Symbols used for indicating statistical significance: ns, not significant, $p > 0.05$, $^{*}p \leq 0.05$, $^{**}p \leq 0.01$, and $^{***}p \leq 0.001$. Calculations and graphs were performed using Prism version 6.01 (GraphPad, San Diego, CA, USA). JMP pro 16 (JMP, Cary, NC, USA) statistical software was used for scatterplots and spatially linked contour maps.

Results

Differential alteration of lung CPA3 patterns in COPD

Our approach for histology-based quantitative analysis of CPA3 expression patterns in individual tissue cells revealed that mast cells in COPD lungs had significant increased CPA3 mRNA expression across the distal lung compartments compared to non-diseased control lungs (Figure 1A). The highest numerical and relative increase was seen in small airways and pulmonary vessels where mean patient CPA3 mRNA expression levels increased threefold and twofold, respectively.

Contrasting the mRNA picture, levels of mast cell granule-stored CPA3 protein was not increased in any of the analyzed compartments compared to controls. On the contrary, there was a trend towards reduced CPA3 protein content in pulmonary vessels (Figure 1B).

Our simultaneous analysis of CPA3 mRNA and protein allowed for single-cell assessment of the mRNA/protein quotient in all individual mast cells. The mean patient values for this quotient were significantly increased in COPD lungs, particularly in small airways ($p < 0.05$) and pulmonary vessels ($p < 0.05$). A trend towards reduction was also seen in the alveolar parenchyma (Figure 1C).

A head-to-head comparison between anatomical sites demonstrated that in COPD, small airway MCs had the highest CPA3 mRNA expression (Figure 2A), whereas small airways and pulmonary vessels were equal at the protein level (Figure 2B). The discrepancy between CPA3 protein and mRNA content within individual mast cells was also examined within small airway compartments in COPD. Here, intraepithelial mast cells had a striking $mRNA^{high}$, $protein^{low}$ profile compared to the reversed pattern in subepithelial cells (Figure 2C). The distinct expression pattern among epithelial and subepithelial MCs is also illustrated in Figures 2D, E.

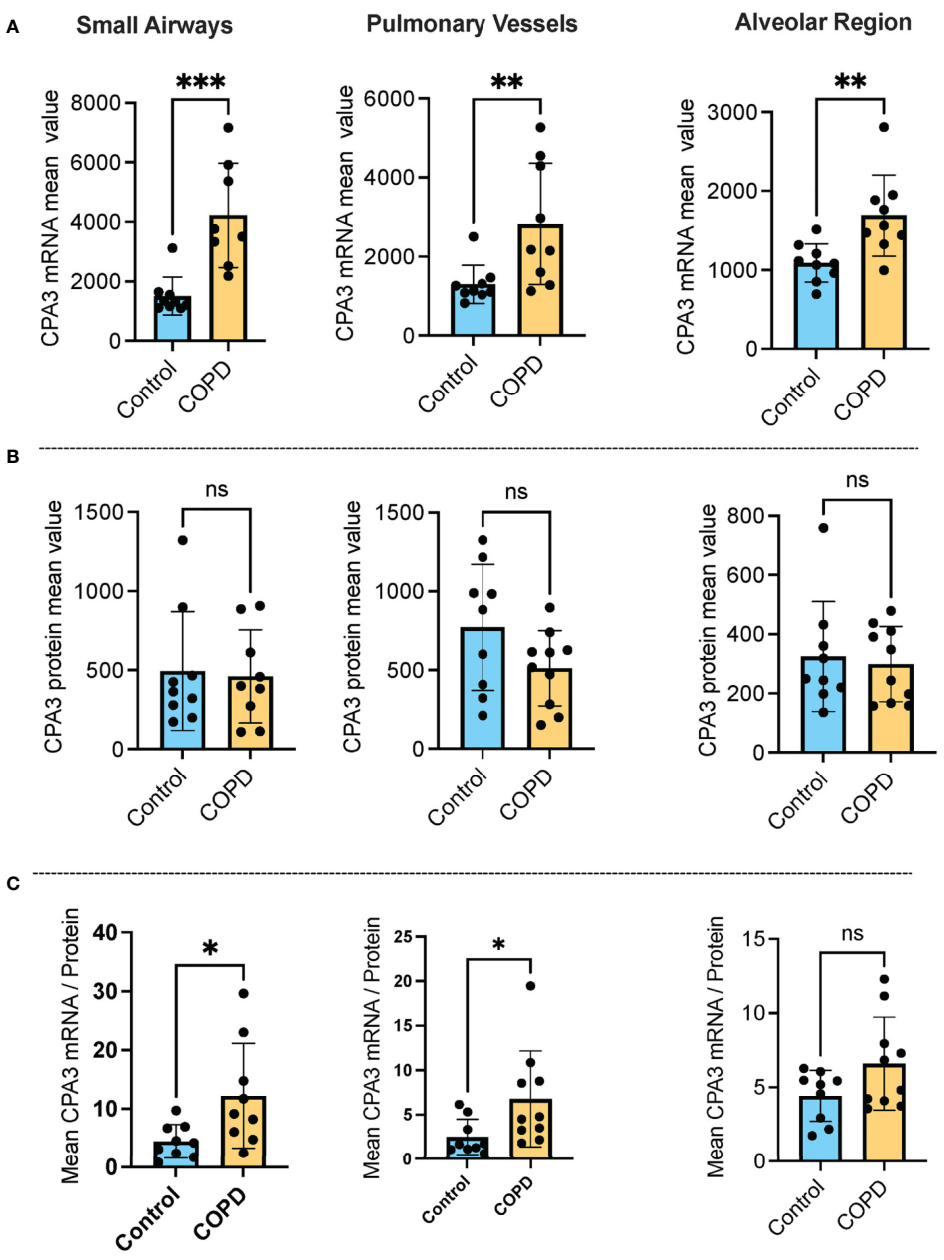


FIGURE 1
Increased mast cell CPA3 mRNA expression across major lung compartments in COPD lungs. **(A–C)** Mean patient values for individual mast cell expression of CPA3 mRNA **(A)**, CPA3 protein **(B)**, and the mean mRNA/protein quotient **(C)** in control subjects and COPD category GOLD 4 patients. In total, >18,000 individual mast cells were analyzed in the control group and >41,000 mast cells were analyzed in the COPD group. Dots denote mean patient values of >1,500 individual mast cells per control tissue and >2,500 mast cells per COPD patient. Statistical significance levels are marked as ns = non-significant, *$p < 0.05$, **$p < 0.01$, and ***$p < 0.001$.

Both CPA3 mRNA and protein increase in IPF lungs

Compared to control lungs, mast cells in IPF lung parenchyma had a more than threefold significant increase in mast cell CPA3 mRNA expression (Figure 3A). Significantly increased levels were also seen in the small airways (Figure 3A). Contrasting the situation in COPD, the increased CPA3 mRNA in the IPF lung parenchyma was also accompanied with elevated CPA3 protein levels (Figure 3B). A weak trend towards increased mast cell CPA3 protein was observed for small airways (Figure 3B). Due to the parallel increased mRNA

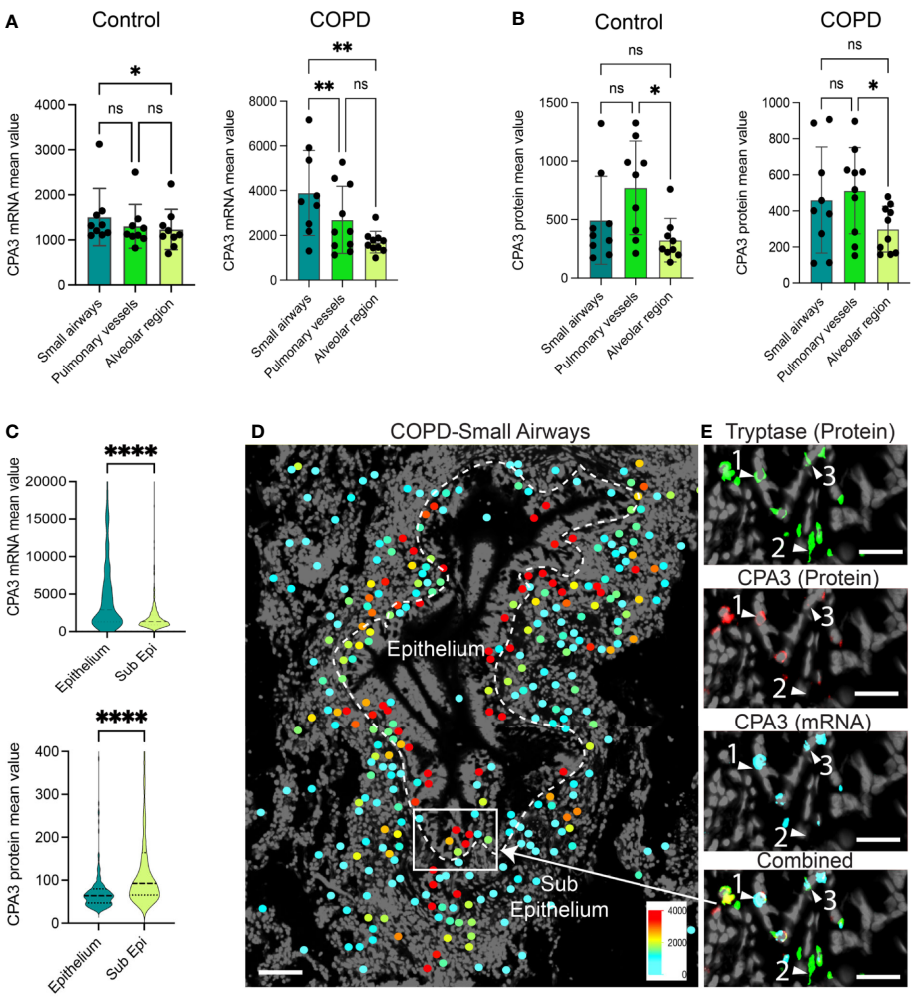


FIGURE 2
Anatomically differentiated mast cell CPA3 expression responses in COPD lungs. **(A, B)** Mean patient values for individual mast cell expression of CPA3 mRNA **(A)** and CPA3 protein **(B)** across anatomical lung compartments in non-diseased controls and COPD lungs. Statistical significance levels are marked as ns = non-significant, *$p < 0.05$, **$p < 0.01$, and ****$p < 0.0001$. **(C)** Raincloud plots illustrating the difference in CPA3 mRNA and protein expression profiles between small airway intraepithelial and sub-epithelial small airway mast cells. **(D)** Zoomed-in region with a small airway where size-filtered mast cell coordinates have been color-coded for CPA3 level (high = red; low = turquoise). Note the foremost red CPA3^{high} profile in the epithelial region. **(E)** Raw fluorescence images of MC markers exemplifying a CPA3 mRNA+protein double-positive mast cell (label 1), CPA3 mRNA and protein double-negative cell (2), and a CPA3 mRNA-positive and protein-negative cell (3) at an epithelial–subepithelial interface. Scale bars: D = 150 µm, E = 40 µm.

and protein expression, the mRNA/protein quotient was not increased in IPF compared to controls (Figure 3C). Interestingly, although CPA3 mRNA and protein had a parallel increase in IPF, their spatial distribution pattern seemed differentially regulated at a microenvironmental level. One example of this type of dynamic expression heterogeneity is shown in Figures 3D, E. The spatial heterogeneity and marked variations in relative proportion of mast cell CPA3 mRNA and protein across tissue microenvironments was confirmed statistically by comparing mean mRNA/protein quotients between spatially distinct lung regions within lung sections/patients (Figure 4).

Head-to-head comparisons reveal disease-relevant distinctions in combined mast cell density and spatial mast cell CPA3 expression patterns

The lungs from IPF, COPD, and control groups were subjected to a normalized MC density assessment and in-depth head-to-head MC CPA3 comparisons to gain further insight into the characteristic features of CPA3 expression in the respective disease.

Looking at two-dimensional scattergrams visualizing CPA3 mRNA and protein patterns across pooled MCs (>50,000 cells/

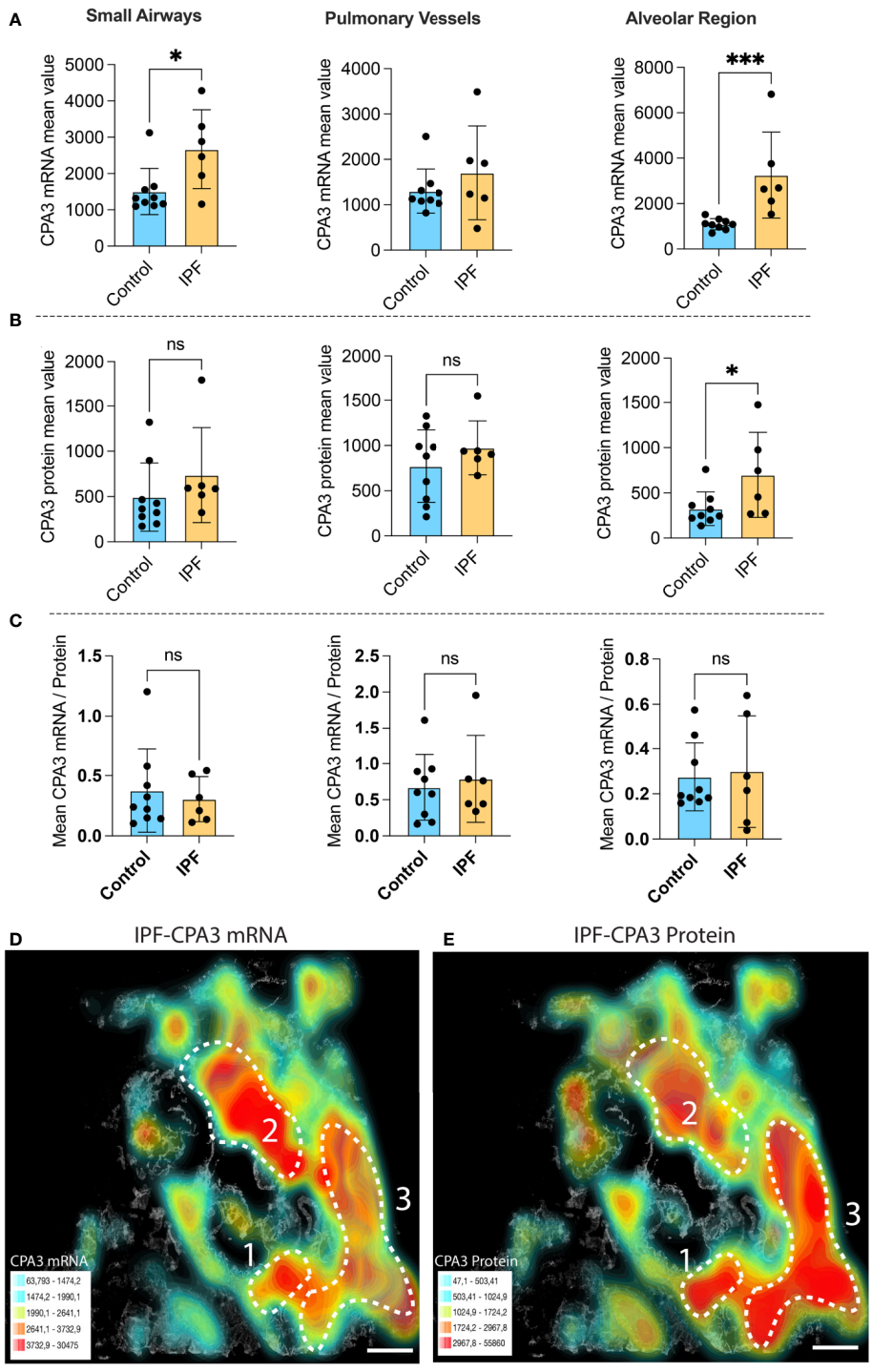


FIGURE 3
The expanded mast cell population in distal IPF lungs has a robust upregulation of both CPA3 mRNA and protein. **(A–C)** Mean patient values for individual mast cell expression of CPA3 mRNA **(A)**, CPA3 protein **(B)**, and the mean mRNA/protein quotient **(C)** across control subjects and COPD patients. A total of >81,000 individual mast cells were analyzed in the IPF disease group, and each dot denotes mean patient values of >12,000 mast cells per IPF patient. Statistical significance levels are indicated as ns = non-significant, *$p < 0.05$, and ***$p < 0.001$. **(D, E)** Low-power micrograph of a representative IPF lung section where a gray-scale background tissue is overlayed with color-coded density maps (high–low is shown as red–turquoise) displaying combined mast cell density and expression levels of CPA3 mRNA **(D)** or CPA3 protein **(E)**. Note that although both the level of protein and mRNA is high, the relative proportion varies across tissue microenvironments, as illustrated by a CPA3 mRNA^{high}, protein^{moderate} profile in region 2 and a CPA3 mRNA^{moderate}, protein^{high} signature in region 3. Scale bars = 1.8 mm.

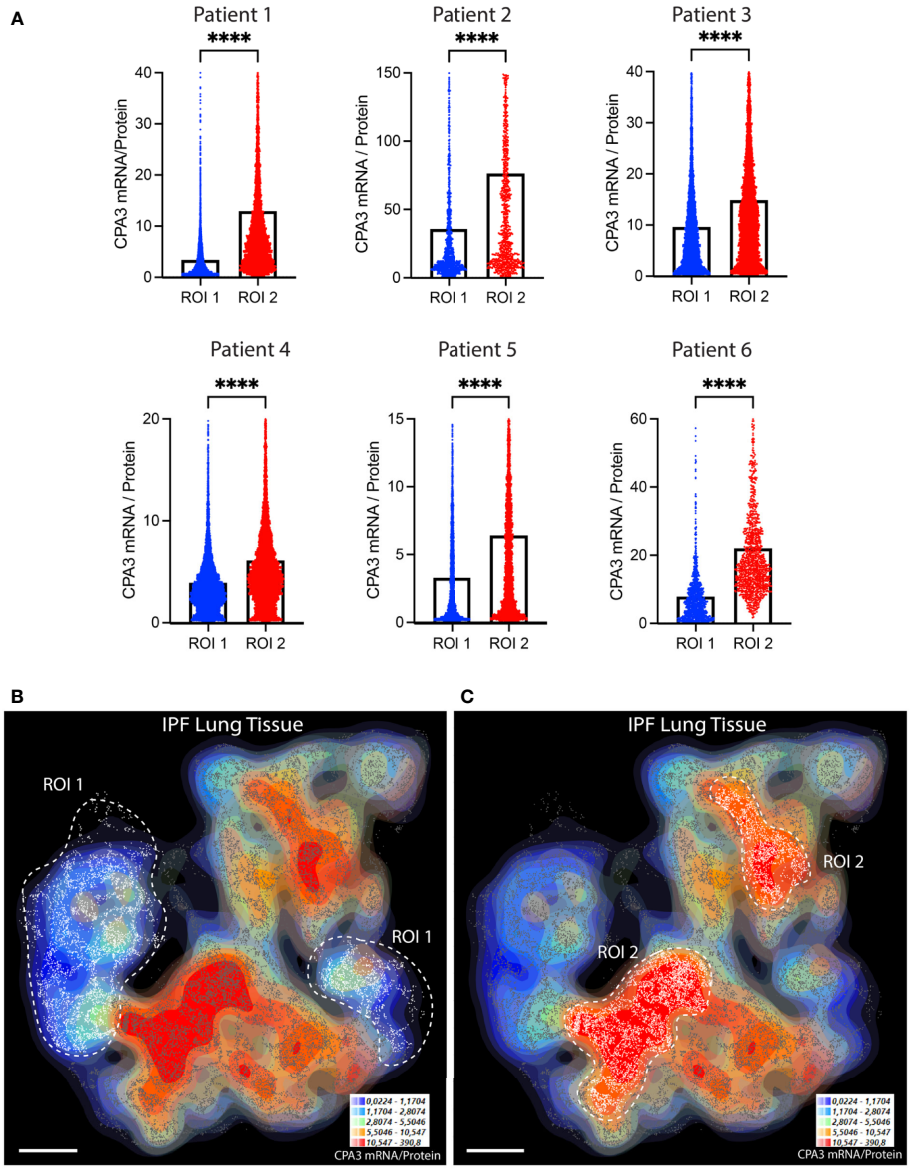


FIGURE 4
The relative proportion of mast cell CPA3 mRNA and stored protein vary significantly between lung tissue microenvironments. **(A)** Quantitative data and violin plots comparing individual mast cell CPA3 mRNA/protein quotients in pre-determined spatial lung section regions of interest (ROIs). Regions with relatively low (ROI type 1) or high (ROIs 2) quotients were selected from computer-generated topographic contour maps visualizing the heterogeneous spatial distribution of mRNA/protein quotients (exemplified for one IPF section in **(B)** and **(C)**; red denotes spatial regions with a high quotient; coordinates for individual mast cells are shown as white-gray dots). Scale bars: **B**, **C** = 3.5 mm. Black bars in A show mean values and statistical analysis was performed by a Mann–Whitney *U* test and where **** denotes a significance level of $p < 0.0001$.

group), IPF parenchymal MCs stood out by having a unique combined protein and mRNA high signature (Figures 5A–C). Interestingly, at this pooled data level, small airway and pulmonary vessel MCs displayed elevated protein compared to controls and COPD (Figures 5A–C), although this was not significantly different at a mean patient level (Figure 3B). The 2D plots also confirmed the elevated mRNA in COPD, albeit visually less clearly than for the mean patient data in Figure 1).

Filtering out only mast cells with a high CPA3 mRNA-high signature demonstrated that in IPF these constituted almost 40% of the total MC pool (contrasting the <5% in non-diseased controls; Figure 5F). In the small airways and pulmonary vessels both COPD and IPF had enriched proportions of CPA3 mRNA-high cells compared to controls, although statistical significance was only reached for COPD (Figures 5D, E).

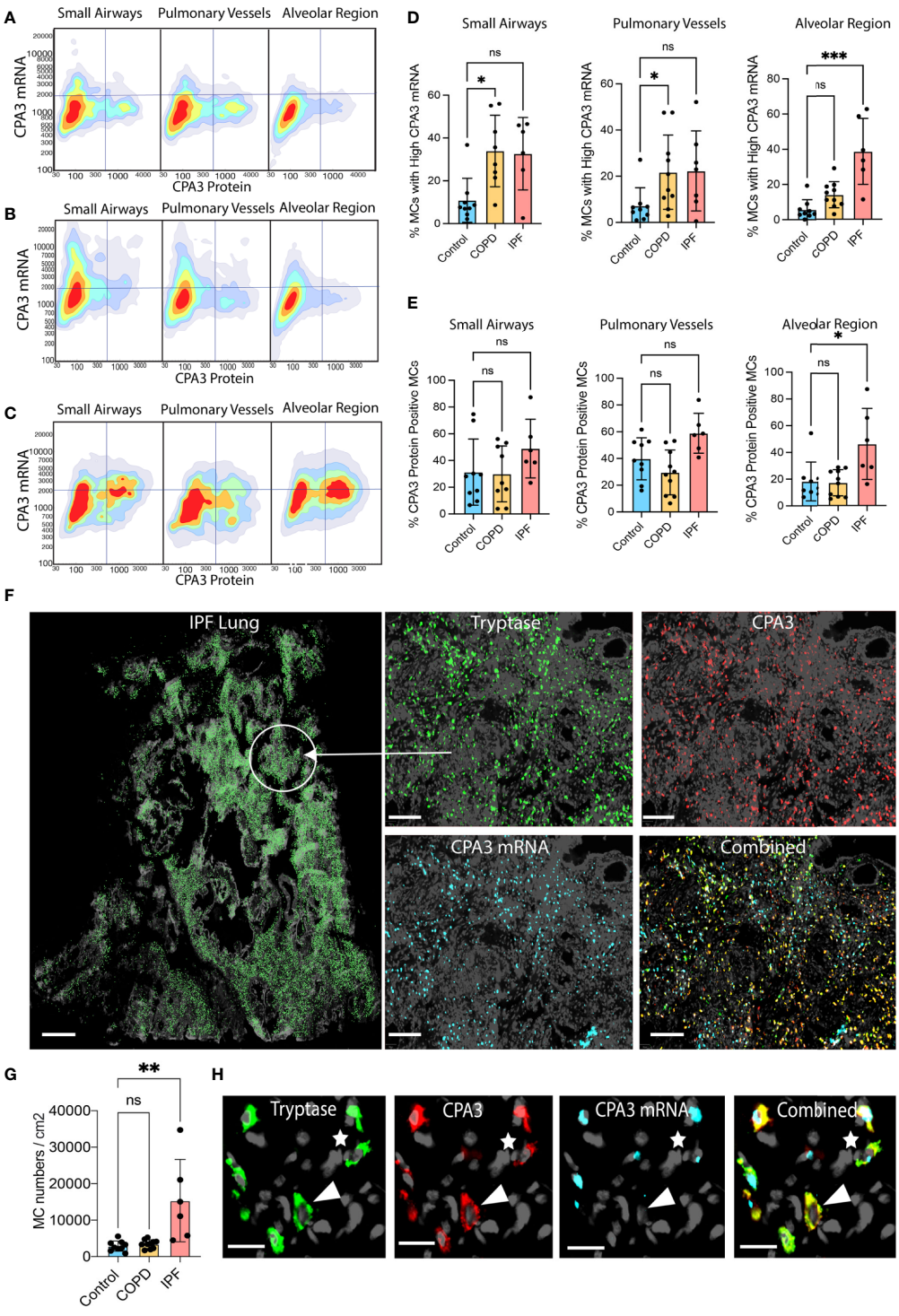


FIGURE 5
Disease-specific small airway and alveolar CPA3 responses in COPD and IPF. **(A–C)** 2D scattergrams showing CPA3 mRNA and protein relationships across pooled mast cells from control lungs (A; *n* = 18,504 pooled MCs), COPD (B; *n* = 41,313), and IPF cases (C; *n* = 81 806). **(D, E)** Mean patient percentage of lung mast cells with a high CPA3-mRNA profile **(D)** or CPA3 protein **(E)** within anatomical regions and disease categories (as defined by a pre-determined locked threshold values). **(F)** Low-power graph exemplifying the very high density of mast cells in distal IPF lung. To visualize individual mast cells, their *x,y* coordinates have been replaced with pseudo-colored green circles (left). The right quartet set of images shows the original fluorescence-based staining in a zoomed-in region. **(G)** Mean patient lung mast cell density levels. Statistical significance levels are marked as ns = non-significant, **p* < 0.05, ***p* < 0.01, ****p* < 0.001. **(H)** Zoomed-in ICH and IHC fluorescence images exemplifying a CPA3mRNA$^-$, protein$^+$ MC (arrowhead) and a CPA3mRNA$^+$, protein$^+$ MC (* uppermost right corner). Scale bars: H = 25 µm, F-left = 1.8 mm, F-right =200 µm.

Apart from CPA3 expression in individual mast cells, the impact of CPA3 in diseased lungs also depends on the total cell mast cell density. Among the present study groups, COPD lungs had no increase in MC density compared to significant baseline mast cell content in controls (Figure 5G). IPF lungs, on the other hand, displayed a striking sevenfold statistical increase (Figure 5G). Representative illustrations of this very high MC density and examples of corresponding CPA3 expressions are presented in Figures 5H, I.

We also performed direct comparisons between color-coded mast cell CPA3 expression maps (providing combined information of MC density and CPA3 expression) and trichrome-stained serial sections (visualizing the structural features and any classical histological features of the lung) (Figures 6A–F). This approach confirmed the various degrees of microscopic emphysema and patchy fibrotic foci in COPD lungs and that patchy distal lung regions had elevated CPA3 expression in association with small airways (examples are shown in Figures 6C, D). As expected, our IPF sections were characterized by classical IPF histopathological features like parenchymal fibrosis, accumulation of distal lung myofibroblasts and honeycombing (Figure 6F) and that these changes were accompanied with a combined striking increase in both MC density and CPA3 expression (Figure 6).

Mast cell CPA3 mRNA correlates to distal lung CD3+ T-lymphocytes and eosinophils

Comparisons were made between mast cell CPA3 parameters and lung tissue compartment infiltration of eosinophils, basophils, CD3+ T lymphocytes, and CD20+ B lymphocytes. Pooled patient data revealed that for mean CPA3mRNA intensity, there was a statistical positive correlation to alveolar parenchymal eosinophils and CD3+T cells (Figures 7C, F). The mean intensity of CPA3 mRNA also correlated to T cells in pulmonary vessel (Figure 7E). No statistical correlation was seen in the other compartments (Figures 7A, B, D), or between any of the immune cells and CPA3 protein.

Mast cell CPA3 parameters correlate to several lung spirometry parameters

With the limited number of patients, correlation analysis between the mast cell CPA3 parameters and lung function was made on pooled patient group data (presented in Table 2). In summary, the strongest correlations to lung mast cell CPA3 were fond for FEV1, FEV1% predicted and FEV1/VC. Across the lung compartments, the most anatomically widespread correlation was found for pulmonary vessel CPA3 (Table 2). Apart from the pooled data, statistically secured correlations between alveolar CPA3 protein/mRNA quotients and FEV1 and FEV1% were also found within the COPD cohort ($r = -0.84$, $p = 0.004$ and $r = -0.69$, $p = 0.04$, respectively).

Single-cell RNA Seq data

Using single-cell RNA Seq on primary cells isolated from healthy bronchial airways, 148 mast cells were identified based on mast cell-specific gene signatures (Figure 8A). Division of the mast cells into $CPA3^{high}$ and $CPA3^{low}$ expressing cells showed a tendency for increased expression of the tryptase genes TPSAB1 and TPSB2 among the CPA3 high MCs (Figure 8B). In addition, statistical analysis further suggested that $CPA3^{high}$ profile MCs could be associated with high expression for the leukotriene-producing enzyme LTC4-S, the granule storage-regulating proteoglycan serglycin, and the MC activity regulatory protein annexin-1 ($p < 0.002$).

Discussion

Carboxypeptidase A3 is one of the most abundant mast cell proteases. It is frequently highlighted in gene expression studies across many diseases. Yet, surprisingly little is known about how the CPA3 mRNA and protein expression patterns are manifested inside diseased patient tissues. Although the present study only involves limited numbers of patients, it offers several new insights into this issue.

Any discussion about disease-modifying functions of mast cells must also consider the mast cell density in the affected organ. In this study, MC density did not increase in the COPD lungs. We have recently shown that in COPD mast cell density in distal lung compartments may not be higher than healthy lungs since an increase in the MC_{TC} population is counteracted by reduced MC_T cells (37). The present observation of increased MC numbers in IPF confirms previous observations of elevated mast cell numbers in fibrotic lungs (38–40) and shows that this increase is mainly confined to the fibrotic alveolar parenchyma, a compartment that, in this study, also displayed the most striking alteration in CPA3 expression.

Despite that mast cells have been implicated in most fibrotic diseases, including IPF (2, 9, 41, 42), little is known about their specific role in disease pathogenesis. From the known properties of MC proteases, these roles may be both protective and destructive. An interesting observation in this regard is the report of higher MC density in biopsies from IPF patients being correlated with a slower decline in lung function (40). On the other hand, a more recent study showed that plasma tryptase is elevated in IPF patients and correlates negatively with lung function (FVC), suggesting a pro-pathogenic role (41).

The present findings suggest that the structural pathologies in both COPD and IPF lungs are associated with an elevated

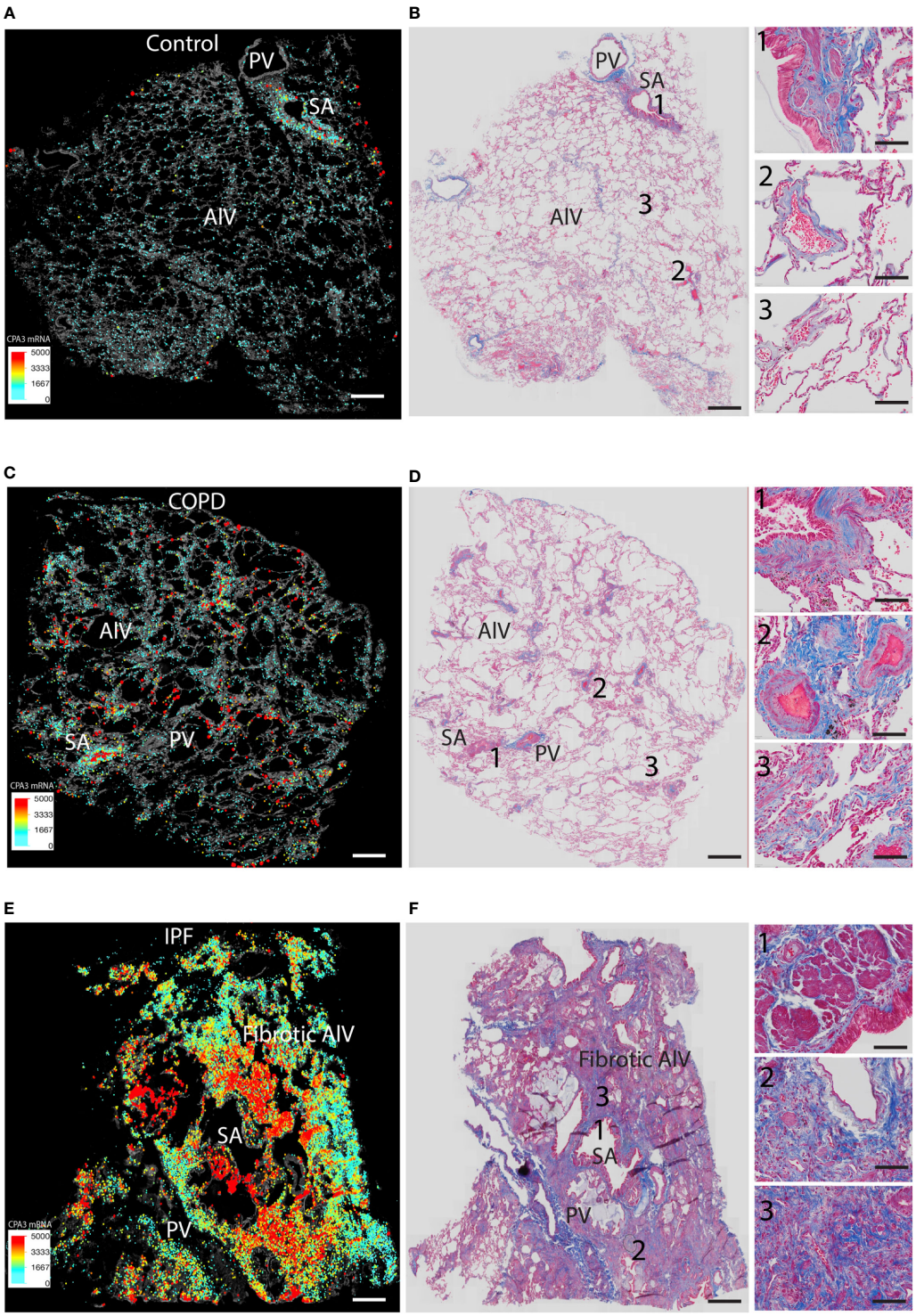


FIGURE 6
Comparisons of density-weighted and spatial CPA3 variations and lung structure in non-diseased control tissue, COPD lungs, and IPF. **(A, C, E)** Low-power section overviews with gray-scale tissue background in control lung **(A)**, COPD **(C)**, and IPF **(D)** where *x,y* coordinates for individual mast cells have been replaced with enlarged dots color and size coded for CPA3mRNA expression levels. **(B, D, E)** Corresponding serial section stained with routine trichrome staining to visualize cells (red) and collagen-rich extracellular matrix (blue) and overall lung structure. SA = small airways; PV = pulmonary vessels; Alv = alveolar parenchyma. The COPD section in **(C, D)** show microscopic emphysema whereas the IPF in E and F displays archetype histopathological IPF features like honeycombing, myofibroblast accumulation, and distal parenchymal fibrosis. Scale bars: **A–F** = 1.8 mm, insets in **B, D, F** = 200 µm.

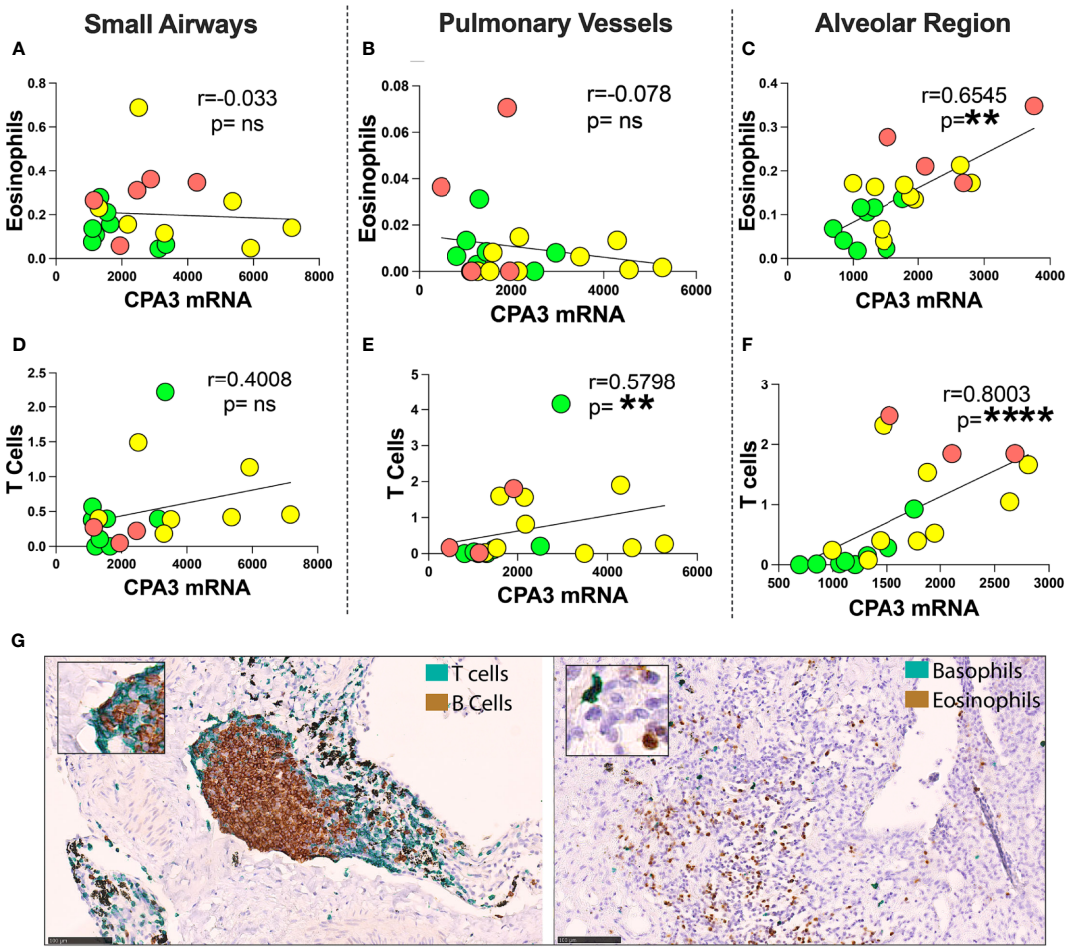


FIGURE 7
Correlation between mean mast cell CPA3 mRNA and eosinophils and CD3+ T lymphocytes. **(A–F)** Scattergrams with pooled mean patient data (green circles = healthy controls, yellow = COD, and red = IPF). Correlation analysis was performed with the non-parametric Spearman´s pairwise correlation test. *r* = correlation coefficient, the *p*-values and significance levels are shown as $^{**}p < 0.01$ and $^{****}p < 0.0001$. **(G)** Bright-field micrographs exemplifying CD3+ T lymphocyte and CD20-positive B lymphocyte double staining (left) and basophil and eosinophil double staining (right) with brown (DAB chromogen) and green (Vina green chromogen). Scale bars = 100 µm. ns, non-significant.

local CPA3 mRNA expression. Importantly, the fact that the MC numbers are significantly elevated in fibrotic regions in IPF further increases the local tissue capacity to generate CPA3. Indeed, the present >300% increase in average MC CPA3 mRNA expression and sevenfold increase in MC density create a situation where the total distal lung capacity of CPA3 release is theoretically >20 times ()! higher compared to the already robust CPA mRNA expression at lung healthy baseline.

A similar theoretical exercise may also be done for COPD lungs, although in contrast to IPF, MC numbers are more modest, and the highest relative CPA increase was found in small airways rather than the alveolar parenchyma. Furthermore, COPD patients differed from IPF since they did not have elevated CPA3 protein.

Interestingly, in another COPD study, increased sputum CPA3 was particularly high in female patients with HRCT-defined emphysema (43). Unfortunately, the limited patient numbers in this study prevented us from exploring how the present CPA3 alterations in COPD relate to degree of emphysema.

It is, however, noteworthy that, as for asthma (34, 44), CPA3 levels in COPD and IPF may be particularly elevated in the subcategory of patients that have a type 2 immunity and eosinophil signature (29, 45). Indeed, the present correlation between pooled patient mast cell CPA3 mRNA and eosinophils supports this possibility. Interestingly, CD3+ T cells also correlated with CPA3 mRNA but not protein. Although larger follow-up studies are needed, from other studied linking luminal CPA3 to steroid sensitivity in asthma, it is tempting to speculate that local tissue content of elevated mast cell CPA3 mRNA may be a general marker of both type 2 immunity and steroid responsiveness.

Taken together, our study agrees with previous data on increased sputum CPA3 in COPD (29, 43, 45) and elevated

Table 2. Correlations between mast cell CPA3 and lung function parameters.

Mast Cell CPA3	Lung Compartments	FEV1	FEV1%	FEV1/VC	DLCO%
CPA3 mRNA	Small Airways	r = −0.4168 p = 0.0602	**r = −0.4508** **p = 0.0403**	r = −0.3449 p = 0.1257	r = −0.3681 p = 0.1459
	Pulmonary Vessels	**r = −0.5092** **p = 0.0155**	**r = −0.513** **p = 0.0146**	**r = −0.5369** **p = 0.0100**	r = −0.2097 p = 0.4036
	Alveolar Region	r = 0.06733 p = 0.7659	r = −0.1672 p = 0.4570	r = 0.06337 p = 0.7794	r = −0.3988 p = 0.1012
CPA3 Protein	Small Airways	r = 0.2748 p = 0.2280	r = 0.2762 p = 0.2256	r = 0.2227 p = 0.3320	r = −0.2038 p = 0.4293
	Pulmonary Vessels	**r = 0.4932** **p = 0.0197**	**r = 0.6736** **p = 0.0006**	**r = 0.6389** **p = 0.0014**	r = 0.1509 p = 0.5500
	Alveolar Region	r = 0.2691 p = 0.2259	r = 0.325 p = 0.1401	r = 0.2632 p = 0.2367	r = −0.2749 p = 0.2695
CPA3 Protein/mRNA	Small Airways	**r = 0.5766** **p = 0.0062**	**r = 0.666** **p = 0.0010**	**r = 0.4727** **p = 0.0305**	r = 0.1694 p = 0.5123
	Pulmonary Vessels	**r = 0.5645** **p = 0.0062**	**r = 0.7234** **p = 0.0001**	**r = 0.6786** **p = 0.0005**	r = 0.1292 p = 0.6094
	Alveolar Region	0.2765 p = 0.2130	**0.4346** **p = 0.0433**	0.2218 p = 0.3211	−0.05685 p = 0.8227

Spearman r non-parametric correlation analysis was performed using Prism (Version 9.3.1). r = correlation coefficient, p = p value. Statistically confirmed correlations (i.e., $p < 0.05$) are marked in bold. FEV_1: forced expiratory volume in 1 s; VC: vital capacity; diffusing capacity of the lungs for carbon monoxide (DLCO).

CPA3 in IPF (39). It is likely that the strikingly increased and strategically localized MC CPA3 mRNA expression revealed in this study will impact pathophysiological and immunopathological processes in COPD and IPF lungs. Interestingly, despite the limited patient numbers, we did observe some correlations between elevated CPA3 parameters and worsening of lung function. What is more difficult to speculate on is whether the net effect of CPA3 release is harmful or protective.

Of potential importance for both IPF and COPD is the capacity of CPA3 to regulate smooth muscle constriction, blood vessel tonus, and vascular flow through proteolytic modification of, e.g., endothelin-1, angiotensin I, apolipoprotein B, and neurotensin (46, 47). The capacity of CPA3 to counteract these mediators would likely be beneficial in lung disease, like the protective actions of CPA3 demonstrated in animal models (14, 47, 48). As further support for a potential protective role in relation to the cardiovascular aspects associated with severe COPD and IPF is the observation that decreased serum CPA3 is associated with risk factors of blood vessel disease and cardiovascular damage (49).

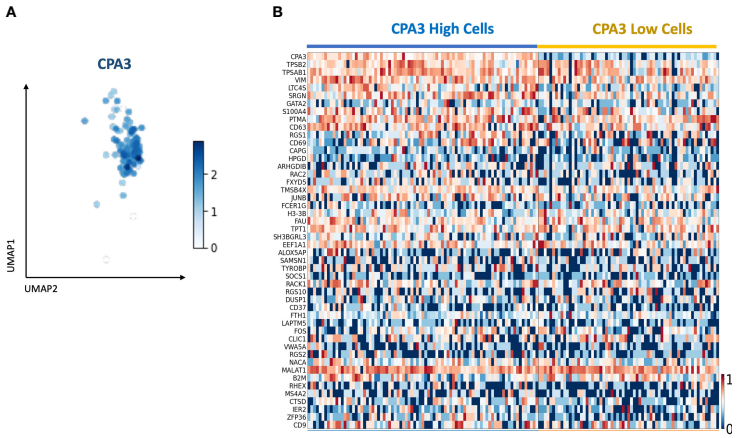


FIGURE 8
Single-cell RNA sequencing identifies a mast cell population with CPA3 high and low gene expression. **(A)** UMAP of the subset of mast cells determined by the expression of commonly known last cell markers (TPSB2, TPSAB1, MS4A2, and CPA3). CPA3 expression is shown. **(B)** Gene expression heatmap showing cells with "high" and "low" CPA3. Cells were considered "high" when CPA3 expression was above 1.5 and "low" when CPA3 expression was below or equal to 1.5. The genes on the *y*-axis are the top 48 upregulated genes within the mast cell population.

Even with the suggested role of CPA3 in protection and homeostasis, the upregulated CPA3 mRNA may also have pro-inflammatory or pathogenic actions. One example of potential relevance for the fibrotic processes in IPF and the small airway remodeling in COPD is the proposed importance of CPA3 for biogenesis of the fibrous component of the extracellular matrix (14, 50). Currently, there are no CPA3 inhibitors in clinical use. Hence, given the multifaceted biological actions of CPA3 protease activity, it thus remains an open question whether pharmaceutical neutralization of CPA3 would have therapeutic benefits or would interfere with homeostatic mechanism for limiting harmful effects of internal pro-inflammatory mediators. More research is needed to identify the tentative good and bad effects of CPA3.

Similar to our recent study on non-diseased lungs (31), the present study shows that also in advanced lung disease, mast cells may have high mRNA expression while displaying a seemingly surprising paucity of granule-stored CPA3 protein. In our study, this phenomenon was most evident in COPD where the mRNA/protein quotient was higher than for controls and IPF patients. The most extreme imbalance was observed in the small airways where intraepithelial and subepithelial mast cells displayed reversed mRNA/protein patterns. Interestingly, a specifically high CPA3 signature in epithelial mast cells have also been reported in type 2 asthma (34).

The discrepancy of CPA3 protein and CPA3 mRNA levels call for cautiousness when predicting biological roles based on only measuring one of these parameters. In this context, the present calculation of mRNA/protein quotients for CPA3 may be a more useful indication of CPA3 turnover in disease than merely study protein or mRNA alone. Especially predicting CPA3 roles based on only CPA3 protein in tissues seems risky, since higher CPA3 levels may merely reflect increased numbers of resting MC_{TC} cells, the subset of mast cells with a high content of co-stored CPA3 and chymase in resting states.

The present observation of striking increases in mRNA/protein quotients in severe disease raises an important question, namely, to what extent is the elevated CPA3 mRNA translated into protein? Furthermore, what is the evidence that CPA3 can be released from mast cells with low content of granule-stored CPA3 but high mRNA expression? Interestingly, recent observations may shed some light into this issue. Firstly, a high mRNA gene expression is coupled to translation and subsequent protein synthesis. Tentatively, a high CPA3 mRNA expression in MCs lacking granule CPA3 may be expected in cells during the refilling phase after degranulation. This could be a possibility in an active disease since we have previously demonstrated that mast cells in COPD, but not in controls, may undergo piecemeal degranulation (37). Classical degranulation, of course, cannot explain the enigmatic high expression of CPA3 and tryptase mRNA already at healthy baseline levels. Here, from new information on the many non-IgE-mediated alternative pathways for degranulation (51, 52), it may be proposed that, as part of a healthy baseline homeostatic regulation, mast cells may constitutively release tryptase and CPA3 directly *via* small secretory vesicles rather than through classical large granules (14, 31). Speculatively, a similar but heightened mode of release may also explain the increased CPA3 mRNA in the present study.

The methodological basis in our study was a histology-based approach using combined ROI masks (in this case, digital mast cell contours) to measure the CPA3 mRNA and protein at a single-cell level directly in routine formalin-fixed paraffin-embedded (FFPE) samples. The high MC numbers in the present large surgical sections, typically 5–12,000 mast cells, provide a robust statistical evaluation for this type of analysis. Naturally, for our approach to be valid, the combined tryptase-chymase ROI masks used for the CPA3 analysis must be mast cell specific. Theoretically, basophils could have affected the measurements since they are known to express tryptase (53, 54). However, both basophil tryptase expression (53, 54) and numbers of basophils (55) are much lower than for mast cells and we have in a recent study showed that they will not be picked up by the staining intensity threshold used for the present computerized tryptase and chymase-based MC segmentation (31).

Another methodological aspect worth noting is that, in contrast to other single-cell staining intensity methods like flow cytometry and high-end single-cell RNA sequencing, the present histology approach analyzes "2-dimensional" cell profiles rather than whole cells. Accordingly, variations in granule and nucleus areas among cell profiles generate some fluctuations of the staining intensity levels. Even so, considering the statistical power of the vast numbers of analyzed mast cells, it seems clear that this phenomenon, which occurs similarly among the sections and study groups, has no relevant impact on the main study conclusions. Another technical perspective is the potential bias of differences in tissue processing. To minimize any such bias, all lung sample tissues in this study were processed at our research laboratory in a consistent fashion, rather than at the routine clinical pathology unit where fixation time, etc. may vary considerably due to logistical issues. Furthermore, the ISH-IHC staining procedures were performed simultaneously for all tissue sections and study groups, resulting in identical processing conditions.

For practical reasons, the patient number was limited in this study. Despite this, given the clear statistical differences between the study groups, it can be argued that the study material is well justified to allow for robust conclusions around the major observations.

Since we used explanted lungs from lung transplantation cases, the COPD and IPF patients were all within the very severe spectrum of their respective disease. Future studies are now needed to explore to what extent the present CPA3 alterations occur earlier during disease progression. That said, in very severe cases, there is patchwork of microenvironments representing different stages of histopathological alterations. Because of their

severe stage, both the COPD and IPF patients were subjected to significant steroid treatment, and it cannot be excluded that this have influenced the results.

The major histology-based exploration was in this study complemented with a single-cell RNAseq analysis. The rationale was to get an exploratory first insight into how a more holistic gene expression profile differs between $CPA3^{high}$ and $CPA3^{low}$ mRNA expressing mast cells. In alignment with recent studies (31, 56), and despite the fact that CPA3 is strongly linked to chymase at a protein level (31), CPA3 mRNA expression seemed to be more linked to the tryptase genes TPSAB1 and TPSB2. However, at a single-cell level, the tryptase gene expression seemed more universal across the analyzed MC pool. Although our study material for single-cell sequencing was limited and only involved mast cells from non-diseased human bronchi, it is interesting that high CPA3 expression seems to correlate with heightened gene expression for LTC4S, an enzyme involved in synthesis of proinflammatory leukotrienes. On the other hand, there was a weak trend among the CPA3 high mast cells to have higher expression of Annexin-1, a phospholipid-binding protein with potent anti-inflammatory properties that in mast cells negatively regulates pro-inflammatory actions (57, 58). While these observations serve as good example of the complex and multifaceted pro- and anti-inflammatory roles of mast cells, further studies are needed to explore how these results compare to broader mast cell pools, including MCs from diseased lungs.

In summary, this study has demonstrated that lung tissue mast cell populations in COPD and IPF-affected lungs have spatially complex and markedly upregulated CPA3 expression profiles that correlate with sites of structural pathologies. Given the assumed roles of CPA3 in regulating tissue homeostasis, remodeling, and inflammation, finding out what impact elevated lung CPA3 has on clinical outcomes emerges as an important field for future research.

Data availability statement

The datasets presented in this study can be found in online repositories. The name of the repository and accession number can be found below: NCBI Gene Expression Omnibus; GSE201772.

Ethics statement

The studies involving human participants were reviewed and approved by Swedish Research Human Ethics Committee in Lund, Sweden. The patients/participants provided their written informed consent to participate in this study.

Author contributions

JE and PS conceived and designed the studies, designed the experiments, interpreted the generated data, and wrote the manuscript. JJ contributed to image digitalization. SL contributed to clinical assessment and collection of surgical material. MM and PP planned, performed, and analyzed the single-cell RNAseq experiments. PS and MA performed immunohistochemical analyses and quantitative computerized image analyses. All authors read, provided feedback, and approved the final version of the manuscript.

Funding

This work was supported by the Swedish Heart and Lung Foundation (20190508) and the Swedish Medical Research Council (VR2017-19). None of the funding sources took part in the planning, execution, or publication of the present study.

Acknowledgments

We thank Daisy Bornesund at the Unit of Airway Inflammation, Department of Experimental Medicine for skillful technical assistance with tissue processing and serial sectioning.

Conflict of interest

Jimmie Jönsson is an employee of Medetect AB. Jonas S Erjefält is founder of Medetect AB.

The remaining authors declare that the research was conducted in the absence of any commercial or financial relationships that could be constructed as a potential conflict of interest.

Publisher's note

All claims expressed in this article are solely those of the authors and do not necessarily represent those of their affiliated organizations, or those of the publisher, the editors and the reviewers. Any product that may be evaluated in this article, or claim that may be made by its manufacturer, is not guaranteed or endorsed by the publisher.

References

1. Andersson CK, Mori M, Bjermer L, Lofdahl CG, Erjefalt JS. Novel site-specific mast cell subpopulations in the human lung. *Thorax*. (2009) 64(4):297–305. doi: 10.1136/thx.2008.101683

2. Erjefalt JS. Mast cells in human airways: the culprit? *Eur Respir Rev* (2014) 23 (133):299–307. doi: 10.1183/09059180.00005014

3. Galli SJ, Kalesnikoff J, Grimbaldeston MA, Piliponsky AM, Williams CM, Tsai M. Mast cells as "tunable" effector and immunoregulatory cells: recent advances. *Annu Rev Immunol* (2005) 23:749–86. doi: 10.1146/annurev.immunol.21.120601.141025

4. Olivera A, Beaven MA, Metcalfe DD. Mast cells signal their importance in health and disease. *J Allergy Clin Immunol* (2018) 142(2):381–93. doi: 10.1016/j.jaci.2018.01.034

5. Gurish MF, Austen KF. The diverse roles of mast cells. *J Exp Med* (2001) 194 (1):F1–5. doi: 10.1084/jem.194.1.F1

6. Bradding P. Human lung mast cell heterogeneity. *Thorax* (2009) 64(4):278–80. doi: 10.1136/thx.2008.106427

7. Bingham CO3rd, Austen KF. Mast-cell responses in the development of asthma. *J Allergy Clin Immunol* (2000) 105(2 Pt 2):S527–34. doi: 10.1016/S0091-6749(00)90056-3

8. Balzar S, Fajt ML, Comhair SA, Erzurum SC, Bleecker E, Busse WW, et al. Mast cell phenotype, location, and activation in severe asthma. data from the severe asthma research program. *Am J Respir Crit Care Med* (2011) 183(3):299–309. doi: 10.1164/rccm.201002-0295OC

9. Cruse G, Bradding P. Mast cells in airway diseases and interstitial lung disease. *Eur J Pharmacol* (2016) 778:125–38. doi: 10.1016/j.ejphar.2015.04.046

10. Wernersson S, Pejler G. Mast cell secretory granules: armed for battle. *Nat Rev Immunol* (2014) 14(7):478–94. doi: 10.1038/nri3690

11. Caughey GH. Mast cell proteases as protective and inflammatory mediators. *Adv Exp Med Biol* (2011) 716:212–34. doi: 10.1007/978-1-4419-9533-9_12

12. Pejler G, Abrink M, Ringvall M, Wernersson S. Mast cell proteases. *Adv Immunol* (2007) 95:167–255. doi: 10.1016/S0065-2776(07)95006-3

13. Hallgren J, Pejler G. Biology of mast cell tryptase. an inflammatory mediator. *FEBS J* (2006) 273(9):1871–95. doi: 10.1111/j.1742-4658.2006.05211.x

14. Atiakshin D, Kostin A, Trotsenko I, Samoilova V, Buchwalow I, Tiemann M. Carboxypeptidase A3-a key component of the protease phenotype of mast cells. *Cells* (2022) 11(3):570. doi: 10.3390/cells11030570

15. Pejler G. The emerging role of mast cell proteases in asthma. *Eur Respir J* (2019) 54(4):1900685. doi: 10.1183/13993003.00685-2019

16. Tanco S, Lorenzo J, Garcia-Pardo J, Degroeve S, Martens L, Aviles FX, et al. Proteome-derived peptide libraries to study the substrate specificity profiles of carboxypeptidases. *Mol Cell Proteomics* (2013) 12(8):2096–110. doi: 10.1074/mcp.M112.023234

17. Bunnett NW, Goldstein SM, Nakazato P. Isolation of a neuropeptide-degrading carboxypeptidase from the human stomach. *Gastroenterology* (1992) 102(1):76–87. doi: 10.1016/0016-5085(92)91786-4

18. Lundequist A, Tchougounova E, Abrink M, Pejler G. Cooperation between mast cell carboxypeptidase a and the chymase mouse mast cell protease 4 in the formation and degradation of angiotensin II. *J Biol Chem* (2004) 279(31):32339–44. doi: 10.1074/jbc.M405576200

19. Scandiuzzi L, Beghdadi W, Daugas E, Abrink M, Tiwari N, Brochetta C, et al. Mouse mast cell protease-4 deteriorates renal function by contributing to inflammation and fibrosis in immune complex-mediated glomerulonephritis. *J Immunol* (2010) 185(1):624–33. doi: 10.4049/jimmunol.0902129

20. Schneider LA, Schlenner SM, Feyerabend TB, Wunderlin M, Rodewald HR. Molecular mechanism of mast cell mediated innate defense against endothelin and snake venom sarafotoxin. *J Exp Med* (2007) 204(11):2629–39. doi: 10.1084/jem.20071262

21. Kovanen PT, Bot I. Mast cells in atherosclerotic cardiovascular disease - activators and actions. *Eur J Pharmacol* (2017) 816:37–46. doi: 10.1016/j.ejphar.2017.10.013

22. Wu B, Tao L, Yang D, Li W, Xu H, He Q. Development of an immune infiltration-related eight-gene prognostic signature in colorectal cancer microenvironment. *BioMed Res Int* (2020) 2020:2719739. doi: 10.1155/2020/2719739

23. Dellon ES, Selitsky SR, Genta RM, Lash RH, Parker JS. Gene expression-phenotype associations in adults with eosinophilic esophagitis. *Dig Liver Dis* (2018) 50(8):804–11. doi: 10.1016/j.dld.2018.03.021

24. Sallis BF, Acar U, Hawthorne K, Babcock SJ, Kanagaratham C, Goldsmith JD, et al. A distinct esophageal mRNA pattern identifies eosinophilic esophagitis patients with food impactions. *Front Immunol* (2018) 9:2059. doi: 10.3389/fimmu.2018.02059

25. Fricker M, Gibson PG, Powell H, Simpson JL, Yang IA, Upham JW, et al. A sputum 6-gene signature predicts future exacerbations of poorly controlled asthma. *J Allergy Clin Immunol* (2019) 144(1):51–60.e11. doi: 10.1016/j.jaci.2018.12.1020

26. Sverrild A, Bergqvist A, Baines KJ, Porsbjerg C, Andersson CK, Thomsen SF, et al. Airway responsiveness to mannitol in asthma is associated with chymase-positive mast cells and eosinophilic airway inflammation. *Clin Exp Allergy* (2016) 46(2):288–97. doi: 10.1111/cea.12609

27. Yan Z, Liu L, Jiao L, Wen X, Liu J, Wang N. Bioinformatics analysis and identification of underlying biomarkers potentially linking allergic rhinitis and asthma. *Med Sci Monit* (2020) 26:e924934. doi: 10.12659/MSM.924934

28. Berthon BS, Gibson PG, Wood LG, MacDonald-Wicks LK, Baines KJ. A sputum gene expression signature predicts oral corticosteroid response in asthma. *Eur Respir J* (2017) 49(6):1700180. doi: 10.1183/13993003.00180-2017

29. Southworth T, Jevnikar Z, McCrae C, Singh D. A sputum 6-gene signature predicts airway inflammation endotypes and exacerbation frequency in chronic obstructive pulmonary disease. *biomark Med* (2022) 16(4):277–89. doi: 10.2217/bmm-2021-0653

30. Soria-Castro R, Meneses-Preza YG, Rodriguez-Lopez GM, Romero-Ramirez S, Sosa-Hernandez VA, Cervantes-Diaz R, et al. Severe COVID-19 is marked by dysregulated serum levels of carboxypeptidase A3 and serotonin. *J Leukoc Biol* (2021) 110(3):425–31. doi: 10.1002/JLB.4HI0221-087R

31. Siddhuraj P, Clausson CM, Sanden C, Alyamani M, Kadivar M, Marsal J, et al. Lung mast cells have a high constitutive expression of carboxypeptidase A3 mRNA that is independent from granule-stored CPA3. *Cells* (2021) 10(2):309. doi: 10.3390/cells10020309

32. Hogg JC, Chu F, Utokaparch S, Woods R, Elliott WM, Buzatu L, et al. The nature of small-airway obstruction in chronic obstructive pulmonary disease. *N Engl J Med* (2004) 350(26):2645–53. doi: 10.1056/NEJMoa032158

33. Roos AB, Sanden C, Mori M, Bjermer L, Stampfli MR, Erjefalt JS. IL-17A is elevated in end-stage chronic obstructive pulmonary disease and contributes to cigarette smoke-induced lymphoid neogenesis. *Am J Respir Crit Care Med* (2015) 191(11):1232–41. doi: 10.1164/rccm.201410-1861OC

34. Dougherty RH, Sidhu SS, Raman K, Solon M, Solberg OD, Caughey GH, et al. Accumulation of intraepithelial mast cells with a unique protease phenotype in T(H)2-high asthma. *J Allergy Clin Immunol* (2010) 125(5):1046–53 e8. doi: 10.1016/j.jaci.2010.03.003

35. Takabayashi T, Kato A, Peters AT, Suh LA, Carter R, Norton J, et al. Glandular mast cells with distinct phenotype are highly elevated in chronic rhinosinusitis with nasal polyps. *J Allergy Clin Immunol* (2012) 130(2):410–20 e5. doi: 10.1016/j.jaci.2012.02.046

36. Melsted P, Booeshaghi AS, Liu L, Gao F, Lu L, Min KHJ, et al. Modular, efficient and constant-memory single-cell RNA-seq preprocessing. *Nat Biotechnol* (2021) 39(7):813–8. doi: 10.1038/s41587-021-00870-2

37. Andersson CK, Mori M, Bjermer L, Lofdahl CG, Erjefalt JS. Alterations in lung mast cell populations in patients with chronic obstructive pulmonary disease. *Am J Respir Crit Care Med* (2010) 181(3):206–17. doi: 10.1164/rccm.200906-0932OC

38. Andersson CK, Andersson-Sjoland A, Mori M, Hallgren O, Pardo A, Eriksson L, et al. Activated MCTC mast cells infiltrate diseased lung areas in cystic fibrosis and idiopathic pulmonary fibrosis. *Respir Res* (2011) 12:139. doi: 10.1186/1465-9921-12-139

39. Overed-Sayer C, Miranda E, Dunmore R, Liarte Marin E, Beloki L, Rassl D, et al. Inhibition of mast cells: a novel mechanism by which nintedanib may elicit anti-fibrotic effects. *Thorax* (2020) 75(9):754–63. doi: 10.1136/thoraxjnl-2019-214000

40. Cha SI, Chang CS, Kim EK, Lee JW, Matthay MA, Golden JA, et al. Lung mast cell density defines a subpopulation of patients with idiopathic pulmonary fibrosis. *Histopathology* (2012) 61(1):98–106. doi: 10.1111/j.1365-2559.2012.04197.x

41. Shimbori C, Upagupta C, Bellaye PS, Ayaub EA, Sato S, Yanagihara T, et al. Mechanical stress-induced mast cell degranulation activates TGF-beta1 signalling pathway in pulmonary fibrosis. *Thorax* (2019) 74(5):455–65. doi: 10.1136/thoraxjnl-2018-211516

42. Overed-Sayer C, Rapley L, Mustelin T, Clarke DL. Are mast cells instrumental for fibrotic diseases? *Front Pharmacol* (2013) 4:174. doi: 10.3389/fphar.2013.00174

43. Esteve-Codina A, Hofer TP, Burggraf D, Heiss-Neumann MS, Gesierich W, Boland A, et al. Gender specific airway gene expression in COPD sub-phenotypes

supports a role of mitochondria and of different types of leukocytes. *Sci Rep* (2021) 11(1):12848. doi: 10.1038/s41598-021-91742-x

44. Wang G, Baines KJ, Fu JJ, Wood LG, Simpson JL, McDonald VM, et al. Sputum mast cell subtypes relate to eosinophilia and corticosteroid response in asthma. *Eur Respir J* (2016) 47(4):1123–33. doi: 10.1183/13993003.01098-2015

45. Winter NA, Gibson PG, McDonald VM, Fricker M. Sputum gene expression reveals dysregulation of mast cells and basophils in eosinophilic COPD. *Int J Chron Obstruct Pulmon Dis* (2021) 16:2165–79. doi: 10.2147/COPD.S305380

46. Hultner L, Ehrenreich H. Mast cells and endothelin-1: a life-saving biological liaison? *Trends Immunol* (2005) 26(5):235–8. doi: 10.1016/j.it.2005.03.007

47. Maurer M, Wedemeyer J, Metz M, Piliponsky AM, Weller K, Chatterjea D, et al. Mast cells promote homeostasis by limiting endothelin-1-induced toxicity. *Nature* (2004) 432(7016):512–6. doi: 10.1038/nature03085

48. Magnusdottir EI, Grujic M, Bergman J, Pejler G, Lagerstrom MC. Mouse connective tissue mast cell proteases tryptase and carboxypeptidase A3 play protective roles in itch induced by endothelin-1. *J Neuroinflammation* (2020) 17 (1):123. doi: 10.1186/s12974-020-01795-4

49. Lewicki L, Siebert J, Kolinski T, Piekarska K, Reiwer-Gostomska M, Targonski R, et al. Mast cell derived carboxypeptidase A3 is decreased among patients with advanced coronary artery disease. *Cardiol J* (2019) 26(6):680–6. doi: 10.5603/CJ.a2018.0018

50. Atiakshin D, Buchwalow I, Tiemann M. Mast cells and collagen fibrillogenesis. *Histochem Cell Biol* (2020) 154(1):21–40. doi: 10.1007/s00418-020-01875-9

51. Blank U, Madera-Salcedo IK, Danelli L, Claver J, Tiwari N, Sanchez-Miranda E, et al. Vesicular trafficking and signaling for cytokine and chemokine secretion in mast cells. *Front Immunol* (2014) 5:453. doi: 10.3389/fimmu.2014.00453

52. Redegeld FA, Yu Y, Kumari S, Charles N, Blank U. Non-IgE mediated mast cell activation. *Immunol Rev* (2018) 282(1):87–113. doi: 10.1111/imr.12629

53. Galli SJ. Mast cells and basophils. *Curr Opin Hematol* (2000) 7(1):32–9. doi: 10.1097/00062752-200001000-00007

54. Varricchi G, Raap U, Rivellese F, Marone G, Gibbs BF. Human mast cells and basophils-how are they similar how are they different? *Immunol Rev* (2018) 282(1):8–34. doi: 10.1111/imr.12627

55. Jogdand P, Siddhuraj P, Mori M, Sanden C, Jonsson J, Walls AF, et al. Eosinophils, basophils, and type 2 immune microenvironments in COPD-affected lung tissue. *Eur Respir J* (2020) 55(5):1900110. doi: 10.1183/13993003.00110-2019

56. Ronnberg E, Boey DZH, Ravindran A, Safholm J, Orre AC, Al-Ameri M, et al. Immunoprofiling reveals novel mast cell receptors and the continuous nature of human lung mast cell heterogeneity. *Front Immunol* (2021) 12:804812. doi: 10.3389/fimmu.2021.804812

57. Costa MB, Mimura KKO, Freitas AA, Hungria EM, Sousa A, Oliani SM, et al. Mast cell heterogeneity and anti-inflammatory annexin A1 expression in leprosy skin lesions. *Microb Pathog* (2018) 118:277–84. doi: 10.1016/j.micpath.2018.03.050

58. Parisi JDS, Correa MP, Gil CD. Lack of endogenous annexin A1 increases mast cell activation and exacerbates experimental atopic dermatitis. *Cells* (2019) 8 (1). doi: 10.3390/cells8010051

frontiers | Frontiers in Immunology

TYPE Original Research
PUBLISHED 05 August 2022
DOI 10.3389/fimmu.2022.885868

Check for updates

OPEN ACCESS

EDITED BY
Satoshi Tanaka,
Kyoto Pharmaceutical University,
Japan

REVIEWED BY
Hao Xu,
University of Southern Mississippi,
United States
Ronit Sagi-Eisenberg,
Tel Aviv University, Israel

*CORRESPONDENCE
Ryo Suzuki
suzukir@p.kanazawa-u.ac.jp

†These authors have contributed equally to this work

SPECIALTY SECTION
This article was submitted to Inflammation, a section of the journal Frontiers in Immunology

RECEIVED 28 February 2022
ACCEPTED 18 July 2022
PUBLISHED 05 August 2022

CITATION
Mishima S, Sakamoto M, Kioka H, Nagata Y and Suzuki R (2022) Multifunctional regulation of VAMP3 in exocytic and endocytic pathways of RBL-2H3 cells.
Front. Immunol. 13:885868.
doi: 10.3389/fimmu.2022.885868

COPYRIGHT
© 2022 Mishima, Sakamoto, Kioka, Nagata and Suzuki. This is an open-access article distributed under the terms of the Creative Commons Attribution License (CC BY). The use, distribution or reproduction in other forums is permitted, provided the original author(s) and the copyright owner(s) are credited and that the original publication in this journal is cited, in accordance with accepted academic practice. No use, distribution or reproduction is permitted which does not comply with these terms.

Multifunctional regulation of VAMP3 in exocytic and endocytic pathways of RBL-2H3 cells

Satomi Mishima†, Marin Sakamoto†, Hikaru Kioka, Yuka Nagata and Ryo Suzuki*

Faculty of Pharmaceutical Sciences, Institute of Medical, Pharmaceutical and Health Sciences, Kanazawa University, Kanazawa, Japan

Mast cells (MCs) are inflammatory cells involved in allergic reactions. Crosslinking of the high-affinity receptor for IgE (FcεRI) with multivalent antigens (Ags) induces secretory responses to release various inflammatory mediators. These responses are largely mediated by soluble N-ethylmaleimide-sensitive factor attachment protein receptors (SNAREs). Vesicle-associated membrane protein 3 (VAMP3) is a vesicular-SNARE that interacts with targeted SNARE counterparts, driving the fusion of MC secretory granules with the membrane and affecting subsequent assembly of the plasma membrane. However, the role of VAMP3 in FcεRI-mediated MC function remains unclear. In this study, we comprehensively examined the role of VAMP3 and the molecular mechanisms underlying VAMP3-mediated MC function upon FcεRI activation. VAMP3 shRNA transduction considerably decreased VAMP3 expression compared with non-target shRNA-transduced (NT) cells. VAMP3 knockdown (KD) cells were sensitized with an anti-DNP IgE antibody and subsequently stimulated with Ag. The VAMP3 KD cells showed decreased degranulation response upon Ag stimulation. Next, we observed intracellular granule formation using CD63-GFP fluorescence. The VAMP3 KD cells were considerably impaired in their capacity to increase the size of granules when compared to NT cells, suggesting that VAMP3 mediates granule fusion and therefore promotes granule exocytosis in MCs. Analysis of FcεRI-mediated activation of signaling events (FcεRI, Lyn, Syk, and intracellular Ca^{2+} response) revealed that signaling molecule activation was enhanced in VAMP3 KD cells. We also found that FcεRI expression on the cell surface decreased considerably in VAMP3 KD cells, although the amount of total protein did not vary. VAMP3 KD cells also showed dysregulation of plasma membrane homeostasis, such as endocytosis and lipid raft formation. The difference in the plasma membrane environment in VAMP3 KD cells might affect FcεRI membrane dynamics and the subsequent signalosome formation. Furthermore, IgE/Ag-mediated secretion of TNF-α and IL-6 is oppositely regulated in the absence of VAMP3, which appears to be attributed to both the activation of FcεRI and defects in VAMP3-mediated membrane fusion. Taken together, these results suggest that enhanced FcεRI-mediated signal transduction in VAMP3 KD cells occurs due to the disruption of plasma

10.3389/fimmu.2022.885868

membrane homeostasis. Hence, a multifunctional regulation of VAMP3 is involved in complex secretory responses in MCs.

KEYWORDS

allergy, mast cell (MC), SNAREs, VAMP3, FcεRI, exocytosis

Introduction

Mast cells (MCs) possess specialized secretory granules, which fuse with the plasma membrane upon immunoglobulin E-receptor (IgE-FcεRI) stimulation with multivalent antigens (Ags), thereby releasing inflammatory mediators (1). During the exocytotic process (e.g., degranulation), secretory granules fuse with each other prior to contact with the plasma membrane. A family of membrane fusion proteins called soluble N-ethyl-maleimide-sensitive factor attachment protein receptors (SNAREs), which are present on both the granule and the plasma membrane, can drive granule secretion by mediating either granule-to-plasma membrane fusion or granule-to-granule fusion (2). This also affects subsequent membrane assembly and remodeling processes. Thus, MC degranulation and retrieval are largely mediated by SNARE proteins (3, 4).

Vesicle-associated membrane protein 3 (VAMP3) is a ubiquitously expressed vesicular-SNARE that interacts with its targeted SNARE counterparts, such as syntaxin homologs 4 or 13 and soluble N-ethylmaleimide-sensitive fusion protein 23 (SNAP23), leading to vesicle fusion and exocytosis (5, 6). In human synovial sarcoma cells, which are synoviocyte models for extensive studies of rheumatoid arthritis and produce inflammatory cytokines (7), VAMP3 and SNAP23 contribute to the IL-1β-induced Ca^{2+}-dependent secretion of inflammatory cytokines (8). Boddul et al. have demonstrated that VAMP3 and SNAP23, but not syntaxin homologs 2, 3, or 4, are involved in the exocytosis of cytokines in inflamed synoviocytes, highlighting the functional importance of VAMP3 and SNAP23 in the exocytosis pathway of inflammatory cytokines (8). In addition, VAMP3, which is present in professional phagocytes such as macrophages, is also associated with the membrane trafficking pathway linking cytokine secretion and phagocytosis of pathogens (9). This association may economize membrane transport and augment the immune response through the delivery of cytokine from the Golgi to the recycling endosome, where VAMP3 is described as a reliable marker of recycling endosomes (9, 10), which would be further discussed in the discussion section. Therefore, VAMP3 and its partner SNAREs are involved in both exocytosis and endosomal recycling. However, these effects are likely to be observed mainly in inflamed tissue models and phagocytes in macrophages (11, 12). Whether it also operates in MCs, particularly the mechanism by which VAMP3 functions in Ag-bound IgE and FcεRI-mediated activation, which is a typical allergic response triggered by MCs, has not been fully elucidated.

Secretory granules in a wide range of hematopoietic cells, including MCs, contain a variety of biologically active inflammatory mediators, such as histamine, proteases, cytokines, and leukotrienes. These mediators are recognized to be differentially packed in different types of secretory granules, and SNAREs are strongly associated with the secretion of distinct granules (1, 13). For example, in the context of the mobilization of human neutrophil granules, which is critical for the innate immune response, Mollinedo et al. reported that specific and tertiary granules that are readily exocytosed upon cell activation contained VAMP1, VAMP2, and SNAP23, whereas azurophilic granules that are mainly mobilized to the phagosome were enriched in VAMP1 and VAMP7. Syntaxin4 in the plasma membrane was indicated to mediate the secretion of both specific/tertiary and azurophilic granules. They performed ultrastructural, co-immunoprecipitation, and functional assays and suggested that at least two SNARE complexes, made up of syntaxin4/SNAP23/VAMP1 and syntaxin4/SNAP23/VAMP2, are involved in the exocytosis of specific and tertiary granules, whereas interactions between syntaxin4 and VAMP1/VAMP7 are involved in the exocytosis of azurophilic granules (14). Furthermore, Puri et al. found that deletion of VAMP8 in MCs profoundly inhibited FcεRI-mediated exocytosis of serotonin and cathepsin D, but had no effect on either histamine or TNF-α release (1). Therefore, although it has been suggested that functionally distinct secretory granule subsets whose function is regulated by different SNARE proteins exist in MCs, considerable uncertainty remains regarding the precise characterization and fusion of each distinct granule subtype and SNARE involvement (1, 15).

Abbreviations: MC, Mast cell; Ag, antigen; Ig, immunoglobulin; FcεRI, high affinity receptor for IgE; DNP, 2,4-dinitrophenyl; HSA, human serum albumin; SNARE, soluble N-ethyl-maleimide-sensitive factor attachment protein receptor; VAMP, vesicle-associated membrane protein; SNAP, soluble N-ethylmaleimide-sensitive fusion protein; KD, knockdown; TNF-α, tumor necrosis factor alpha; IL, interleukin; shRNA, short hairpin RNA; NT, non-target.

Elucidating the characteristic features of SNAREs, including VAMP3, may contribute to understanding the molecular mechanisms underlying MC activation and mediator secretion in response to Ag. Herein, we comprehensively studied the role of VAMP3 in MCs using the VAMP3 knockdown approach in RBL-2H3 cells, a model for MC IgE-mediated responses.

Materials and methods

Cell culture

RBL-2H3 cells were cultured in RPMI 1640 (Nacalai Tesque, Tokyo, Japan) supplemented with 10% FBS, 2 mM L-glutamine, penicillin (100 IU/ml), and streptomycin (100 IU/ml) at 37°C in a humidified 5% CO_2 atmosphere. Cells were sensitized with anti-DNP IgE (1 μg/ml) and stimulated with DNP-HSA (50 ng/ml; Sigma-Aldrich, St Louis, MO, USA). The β-hexosaminidase release assay was performed according to an established method (16). Briefly, the collected supernatant was incubated with *p*-nitrophenyl-N-acetyl-β-D-glucosaminide (2 mM) dissolved in 0.1 M citrate buffer (pH 4.5) for 1 h at 37°C. 0.1 M carbonate buffer (pH 10) was then added to the reaction wells to stop the reaction and develop color. Colorimetric measurements were performed at a wavelength of 405 nm using the Tecan Infinite F50 microplate reader (Tecan, Mannedorf, Switzerland).

Lentivirus infection

Clones of RBL-2H3 cells with stable knockdown of VAMP3 expression were generated using a commercial lentiviral system for the introduction of short hairpin RNAs (shRNAs; Sigma, St. Louis, MO, USA). Sigma Mission non-target shRNA (SHC002) was used to generate the control cell line, and shRNA TRCN0000110516 was used to knockdown VAMP3 expression. Lentiviral particles were added to RBL-2H3 cells for 1 week, and the cells were subsequently cultured in medium containing 1.5 μg/ml puromycin. CD63-GFP and RFP-VAMP3 were transiently transfected by electroporation (CUY21EditII, BEX, Tokyo, Japan) using the pTagGFP2-N and pTagRFP-C vectors. Fluorescent images were obtained using a confocal laser-scanning microscope (LSM710, Carl Zeiss, Oberkochen, Germany). The primer sets used for the construction of GFP-tagged CD63 and RFP-tagged VAMP3 are listed in Supplementary Table 1. Details of the plasmid construction are described in the Supplementary Experimental Procedures.

Immunoblotting

Cells were harvested and lysed in lysis buffer containing protease inhibitors and centrifuged at 14,000 × g for 10 min. The supernatants were mixed with SDS loading buffer followed by heating at 95°C for 5 min and subjected to SDS-PAGE. Membranes were blocked with blocking buffer (BlockPRO Protein-Free Blocking Buffer, Visual Protein Biotechnology Corporation, Taipei, Taiwan) and Western blotting was performed using anti-phospho-FcεRIγ (Y47, clone: γ-pY^{47}) which was produced as previously described (17) and provided as a kind gift from Dr. Juan Rivera from the US National Institutes of Health, anti-phospho Lyn (Y396), anti-phospho Syk (Y519 and Y520), anti-phospho LAT (Y191), anti-phospho Akt (T308), anti-phospho Erk1/2 (T202 and Y204), anti-phospho p38 (T180 and Y182), anti-VAMP3 (clone: N-12, Santa Cruz Biotechnology, Santa Cruz, CA, USA), anti-FcεRβ (clone: JRK), which was a kind gift from Dr. Juan Rivera from the US National Institutes of Health (18), and anti-β-actin (MBL, Nagoya, Japan), followed by staining with the appropriate secondary antibodies. For the immunoprecipitation of FcεRI, supernatants were incubated with goat anti-mouse IgE (Southern Biotech, Birmingham, AL, USA) for 1 h at 4°C followed by incubation with protein A-Sepharose beads (GE Healthcare, Chicago, IL, USA) for 1 h at 4°C. Beads were washed two times with lysis buffer and boiled in SDS sample buffer at a non-reducing condition for 5 min. Images were scanned using Odyssey (LiCOR Biosciences, Lincoln, NE, USA). Band intensity was measured using ImageJ software (NIH Image, Bethesda, MD, USA). Each band intensity was normalized to that of the internal control, and the data are presented as a relative fold change. None of the images shown were modified using nonlinear adjustments.

Immunostaining

Anti-VAMP3 (Proteintech, Chicago, IL) followed by appropriate secondary antibodies, FITC-labeled anti-TNFα (BioLegend, San Diego, CA), and APC-labeled anti-IL-6 (BioLegend, San Diego, CA) were used for immunocytochemistry. The cells were fixed with 4% paraformaldehyde and permeabilized with 0.2% Triton X-100 prior to staining. Fluorescent images were obtained by confocal laser scanning microscopy (CLSM; LSM 710 Carl Zeiss, Oberkochen, Germany). Anti-FcεRIα (Merck Millipore, Temecula, CA, USA) followed by the appropriate secondary antibody and FITC-labeled anti-IgE (BD Biosciences, San Jose, CA) were used for fixed and unpermeabilized cells. Flow cytometry was performed on a FACSVerse flow cytometer (BD Biosciences, San Jose, CA). The fluorescence intensity was analyzed using ImageJ software (NIH Image) and MIPAV software (NIH Image). None of the images shown were modified using nonlinear adjustments.

Flow cytometry

The stimulated cells were fixed with 4% paraformaldehyde. Anti-IgE-fluorescein isothiocyanate (FITC, BD Biosciences) was

used for labeling the fixed/non-permeabilized cells. Flow cytometry was then performed on a FACSVerse flow cytometer (BD Biosciences).

Intracellular Ca^{2+} measurements

IgE-loaded cells were incubated with 2 μM Fluo-4 acetoxymethyl ester (AM, Dojindo Laboratories, Kumamoto, Japan) and 10 μM Fura Red AM (Invitrogen, Carlsbad, CA, USA) for 30 min. The cells were then washed and resuspended in Tyrode's buffer (1.8 mM $CaCl_2$). An LSM710 CLSM was used for ratiometric measurements with 488 nm wavelength light from an Ar laser. The fluorescence of Fluo-4 and Fura Red was detected using a bandpass filter (505–530 nm) and a longpass filter (>560 nm), respectively. Calcium responses were calculated as the ratio of Fluo-4 to Fura Red, normalized as a fold increase relative to the signal in unstimulated cells. Fluorescence images were collected every 5 s, and fluorescence intensity was quantified using LSM 710 software.

Quantitative RT-PCR

The cells were lysed using TRIzol reagent (Invitrogen, Carlsbad, CA, USA). cDNA was synthesized using an RT Reagent Kit (Toyobo, Osaka, Japan). Real-time RT-PCR was performed using SYBR Green Master Mix (Luna Universal qPCR master mix, New England BioLabs, Ipswich, MA, USA) and analyzed using the MX3005P qPCR System (Stratagene, La Jolla, CA, USA). Gene expression was normalized to the internal control *GAPDH* gene, and the results were expressed as fold stimulation over control. Primer sequences used are listed in Supplemental Table 2.

Enzyme-linked immunosorbent assay (ELISA)

The cell supernatants were collected after 3 h (TNF-α) and 9 h (IL-6) of stimulation with DNP-HSA. The release of TNF-α and IL-6 was determined using an ELISA kit (R&D Systems, Minneapolis, MN, USA), according to the manufacturer's instructions. Briefly, supernatants of the samples were placed into 96-well plates coated with anti-rat TNF-α or anti-rat IL-6 antibodies after blocking the Assay Diluent buffer. The plates were washed five times and biotinylated detection antibodies and streptavidin-HRP were added. This was followed by recording the absorbance (optical density (OD)) using a microplate reader.

Statistical analysis

Statistical significance was assessed using GraphPad Prism, version 7.0d (GraphPad Software, San Diego, CA, USA). Statistical differences were determined using Student's t-test (between two groups), one-way analysis of variance (ANOVA) followed by Tukey's or Dunnett's multiple-comparison test as appropriate (for comparing multiple groups or time-dependent changes), or two-way ANOVA (for curves). Statistical significance was set at $p < 0.05$.

Results

VAMP3 is involved in the granule-to-granule membrane fusion in IgE/Ag-activated MC

To explore the role of VAMP3 in MCs, MC functions were analyzed in VAMP3 knockdown (KD) cells in response to Ag stimulation. VAMP3 knockdown (KD) in MCs was performed using shRNA transfection. The VAMP3 KD cells showed a significant decrease in VAMP3 expression at both the mRNA and protein levels (Figures 1A, B). Additionally, we analyzed the off-target effects in VAMP3 KD cells; the expression levels of VAMP7, which is a SNARE family member and has an important function in MC secretory response (19), were not altered in VAMP3 KD cells when compared to that in NT cells (Supplementary Figure 1). The MC degranulation response following Ag stimulation was analyzed by measuring the granule enzyme β-hexosaminidase, which is commonly used as a biomarker of MC degranulation. A time-dependent increase for the β-hexosaminidase secretion, which peaked at 30–60 min following Ag stimulation has previously been reported; therefore, the secretion of preformed mediator is generally assessed within 30–60 min of Ag stimulation (20). Herein, the degranulation response was significantly attenuated in VAMP3 KD cells compared to that in non-targeted shRNA (NT) transduced cells at 30 min after Ag stimulation (Figure 1C). However, when we observed the degranulation response 180 min after Ag stimulation, there were no significant differences between NT and VAMP3 KD cells (Figure 1C). There was a gradual increase in the Ag-induced β-hexosaminidase release in VAMP3 KD cells compared to that in NT cells, which represented a rapid sigmoidal increase. These findings indicate that while VAMP3 indeed contributes to the Ag induced rapid secretion of β-hexosaminidase, certain compensatory or redundant mechanisms appear to be operating at the later time point of the secretion in MC, consistent with previous reports (4, 21). The β-hexosaminidase release in the VAMP3-rescued VAMP3 KD cells was not restored, since the transient expression of VAMP3 in VAMP3

10.3389/fimmu.2022.885868

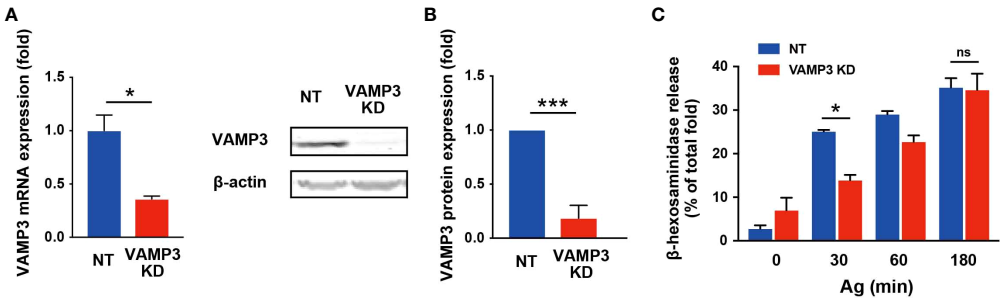


FIGURE 1
VAMP 3 knockdown attenuates β-hexosaminidase release in response to Ag VAMP3-stable KD RBL-2H3 cells were stimulated with IgE/Ag (50 ng/ml). **(A)** VAMP3 expression was analyzed using RT-PCR. **(B)** Expression of VAMP3 protein was confirmed using western blotting. The bar graph shows band density normalized to the loading control and compared to that of NT cells. **(C)** Released β-hexosaminidase was measured in the supernatant and represented as a percentage of total β-hexosaminidase in the cells. NT: control knockdown with a non-targeting shRNA plasmid. Ag: antigen. Data are presented as the mean ± standard error. n = 3 independent experiments **(A–C)**. *p<0.05, ***p<0.001; ns, not significant.

KD cells is limited to a certain population by its low transfection efficiency. Although whole cell population analysis for the β-hexosaminidase release assay was insufficient to estimate the restoration of VAMP3 in our experimental setting, microscopic observation or FACS analysis at single cell levels enabled the analysis of the VAMP3 KD phenotype rescue. To further explore the role of VAMP3 in MC degranulation, we explored granule fusion in VAMP3 KD cells by monitoring the secretory granule marker CD63, which demonstrated that VAMP3 deficiency did not increase granule size, even after Ag stimulation, and this was rescued by the ectopic expression of RFP-VAMP3 positive granules (Figure 2A). In the gain of function experiments, FcεRI surface expression was restored in VAMP3-rescued VAMP3 KD cells (Supplementary Figure 2). Furthermore, we assessed the size of secretory granules expressing VAMP3 in wild-type RBL-2H3 cells by immunostaining with an anti-VAMP3 antibody. As shown in Figure 2B, the size of the VAMP3 positive compartment showed a significant increase 30 min after Ag stimulation, indicating that VAMP3-mediated granule-to-granule fusion occurred during MC degranulation. This increase in size was no longer observed 180 min after Ag stimulation, and the granule size returned to the prestimulation level (Figure 2B). These observations indicate that VAMP3 mediates Ag-induced granule-to-granule fusion during degranulation, thereby contributing to robust degranulation responses in MCs.

VAMP3-deficiency enhances IgE/Ag-induced MC signaling

SNAREs are responsible not only for the exocytotic granule-to-plasma membrane and granule-to-granule fusion, but also contribute to endocytic membrane recycling (12, 22). Thus, VAMP3 KD cells have been hypothesized to be related to the deficiency of plasma membrane assembly. The Lucifer Yellow uptake experiment, which measures endocytosis of Lucifer Yellow dye, clearly demonstrated a dysfunction in endocytosis in VAMP3 KD cells (Supplementary Figure 3). This loss of plasma membrane homeostasis is thought to be reflected by altered FcεRI receptor function in response to exogenous Ag. FcεRI receptor consists of heterotetramer αβγ2-chains, and in response to Ag, Lyn kinase phosphorylates the ITAMs of FcεRIβ (βITAM) and FcεRIγ (γITAM), which initiates a complex signaling cascade involving a series of membrane-associated and cytoplasmic signaling molecules (23, 24). As shown in Figure 3A, FcεRI in MCs was precipitated with an anti-IgE antibody and subjected to immunoblot analysis. Tyrosine phosphorylation of ITAM in the FcεRIβ- and γ-signaling subunits was detected with the anti-phosphotyrosine antibody (clone 4G10), as represented in the left panel in Figure 3A; the phosphorylated Y47 site of ITAM within FcεRIγ is represented in the right panel. The antibody γ-pY^{47} allows the detection of the phosphorylated γ-chain ITAM Y47. The amount of FcεRI β chain used as loading control was detected using anti-FcεRIβ antibody (clone JRK). Tyrosine phosphorylation in both βITAM and γITAM was significantly enhanced in VAMP3 KD cells (Figure 3A). Consistently, subsequent FcεRI signaling molecules including Lyn, Syk, LAT, and ERK1/2 were also significantly activated in the VAMP3 KD cells compared to that in NT cells (Figure 3B). The average Akt and p38 phosphorylation band densities were higher in VAMP3 KD cells compared to that observed in NT cells at the peak time point of phosphorylation. Furthermore, intracellular signaling with Ca^{2+} as a second messenger is important for MC activation, and we observed an upregulation in cellular Ca^{2+} signal propagation following Ag stimulation. VAMP3 KD cells showed a significant and sustained

10.3389/fimmu.2022.885868

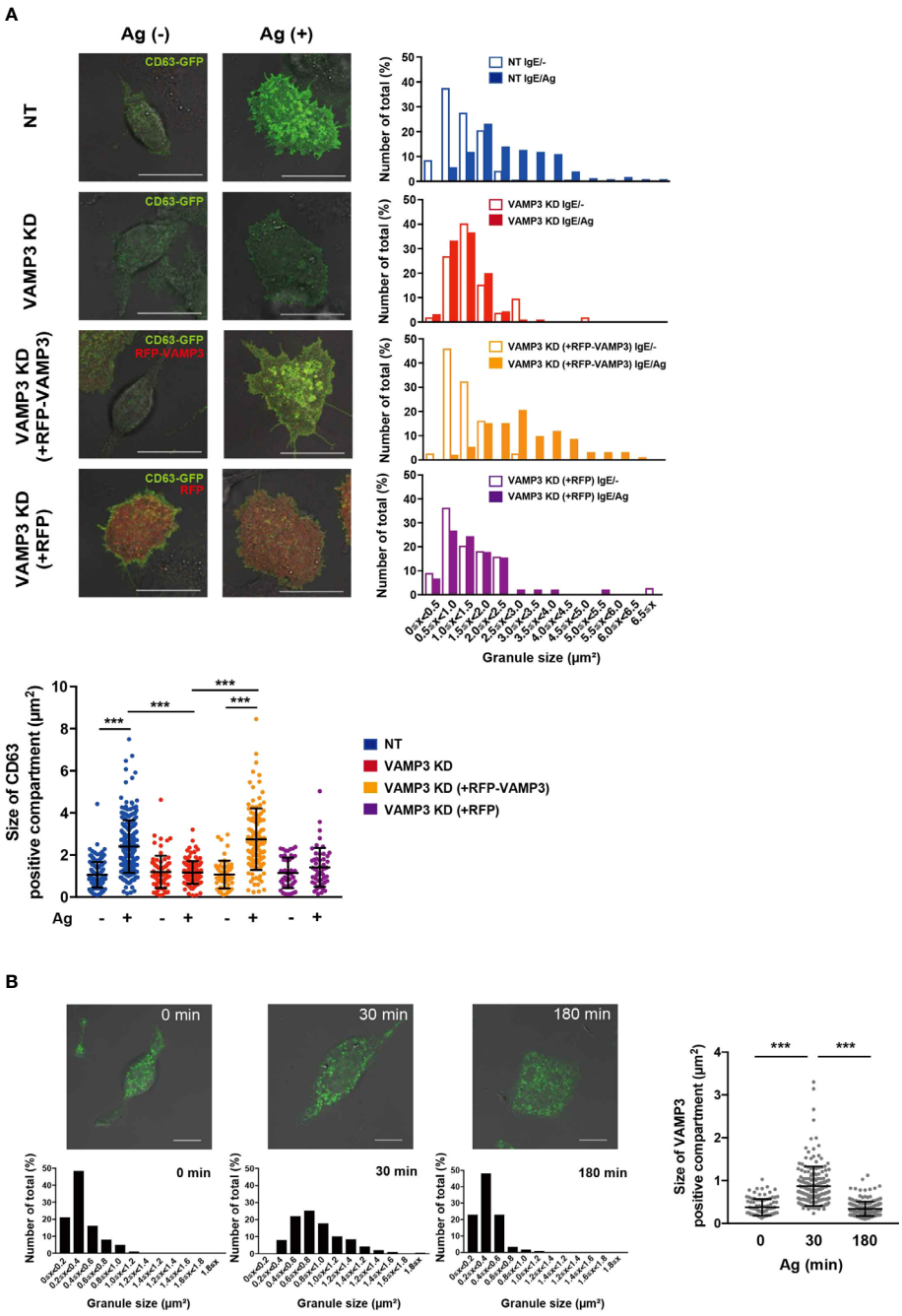


FIGURE 2
VAMP3 mediates granule-to-granule fusions during granule exocytosis VAMP3-mediated granule-to-granule fusion was analyzed using confocal laser scanning microscopy. **(A)** Cultured cells were transfected with GFP-tagged CD63 and/or RFP-tagged VAMP3 and stimulated with Ag (50 ng/ml) for 30 min. Bar graphs show size distribution of the CD63 positive granule; representative images are shown from three independent experiments (magnification ×63, scale bar = 20 μm). Dot plot represents the average size of granules in all analyzed events (granules) counted from 47–236 granules from 3–5 cells/sample from 3 independent experiments. **(B)** IgE/Ag stimulated RBL-2H3 cells were stained for VAMP3. Green indicates Alexa 488-stained VAMP3. Bar graphs represent size distribution of the VAMP3 positive granule analyzed; representative images are shown from three independent experiments (magnification ×63, scale bar = 10 μm). Dot plot represents the average size of granules in all analyzed events (granules) counted from 101–235 granules from 3–5 cells/sample from three independent experiments. NT: control knockdown with a non-targeting shRNA plasmid. Ag: antigen. ***p<0.001.

10.3389/fimmu.2022.885868

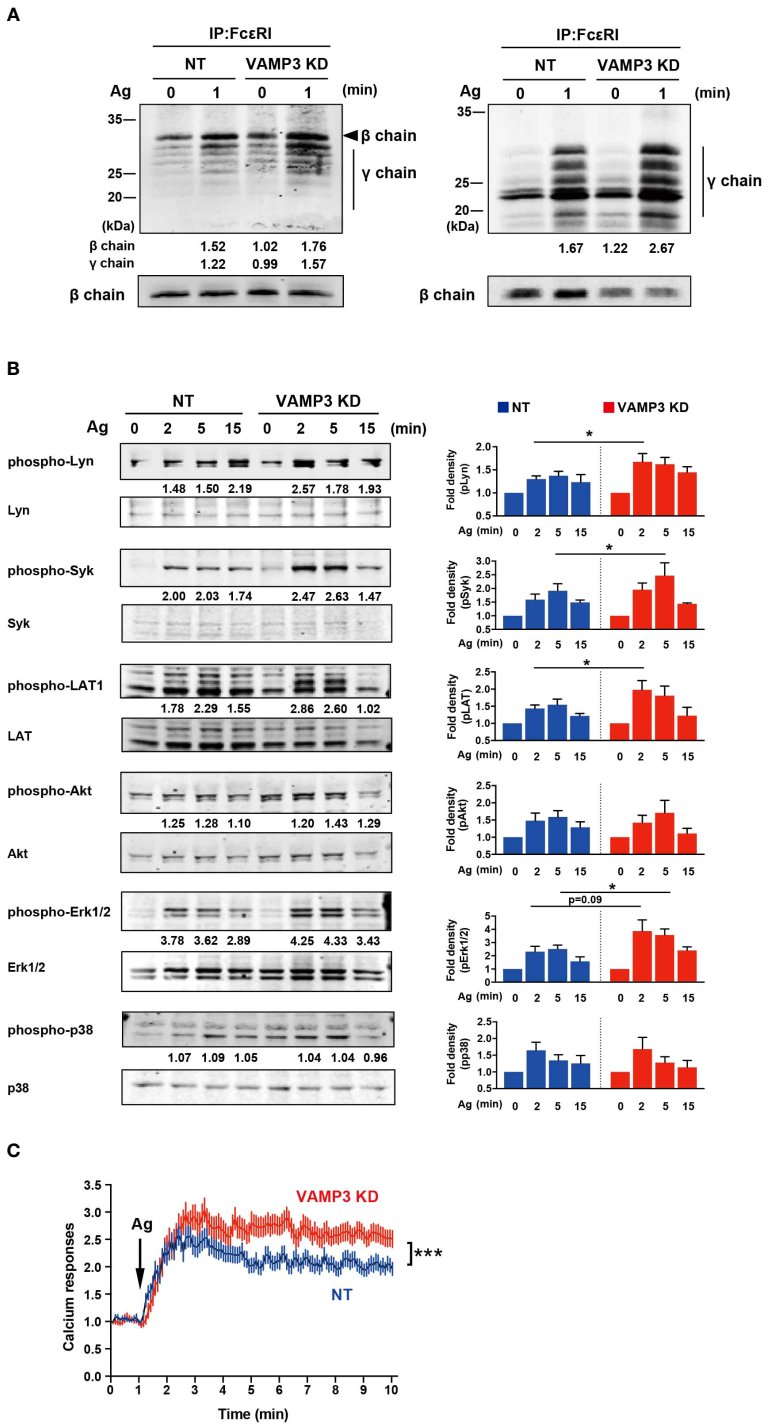


FIGURE 3
FcεRI phosphorylation is upregulated following Ag stimulation FcεRI signaling following Ag stimulation (50 ng/ml) was analyzed, which resulted in enhanced VAMP3 KD. **(A)** FcεRI was precipitated and analyzed by immunoblotting with antibodies specific for tyrosine-phosphorylated proteins (4G10, left panel) and phosphorylated ITAMs of FcεRIγ (right panel). Expression of β-chain was measured as an internal loading control by re-blotting the membranes with anti-β chain antibody JRK. **(B)** A series of protein phosphorylation events triggered by FcεRI crosslinking with the Ag was analyzed. **(C)** Calcium response. Each line represents the mean ± standard error of 51-69 single cells/group from 4 independent experiments. One representative blot of three independent experiments is shown. The band density normalized to that of unstimulated cells is shown below each band **(A, B)**. The P values refer to the differences between two groups that were analyzed using the two-tailed Student's t-test. NT: control knockdown with a non-targeting shRNA plasmid. Ag: antigen. *p<0.05, ***p<0.001.

upregulation of Ca^{2+} signaling throughout the observation period (Figure 3C).

VAMP3 regulates surface expression of FcεRI and membrane homeostasis

The mechanism by which plasma membrane dysfunction caused by VAMP3 elimination led to enhanced FcεRI activation remained unclear. To address this issue, we examined whether a quantitative and/or locational difference existed in FcεRI between NT and VAMP3 KD cells. The total cellular expression of FcεRI α, β, and γ chains did not differ between NT cells and VAMP3 KD cells at both the mRNA and protein levels (Figures 4A, B). Unexpectedly, the cell surface expression of FcεRI showed a significant decrease in VAMP3 KD cells (Figure 4C), despite the cells displaying augmented FcεRI signaling (Figure 3). In addition, FcεRI clustering and subsequent internalization in response to IgE/Ag were observed (Figure 4D). The surface IgE-FcεRI complex was monitored using FACS, which showed a slow rate of internalization of FcεRI in VAMP3 KD cells for up to 5 min (Figure 4D). The slow rate of FcεRI internalization in VAMP3 KD cells existed despite demonstrating augmented Ag-induced FcεRI signaling (Figure 3). Given these contradicting results, we explored the total number of cellular lipid rafts in MCs. Using confocal laser scanning microscopy, a lipid raft marker ganglioside GM1 was detected with the cholera toxin subunit B. Results revealed an enhanced amount of the ganglioside GM1 in VAMP3 KD cells indicating a significant increase in the number of lipid rafts upon VAMP3 elimination (Supplementary Figure 4). Lipid raft enrichment in VAMP3 KD cells might be associated with the enhancement of FcεRI phosphorylation following Ag stimulation as increase in GM1 ganglioside in the plasma membrane is responsible for regulating the activities of several membrane receptors (25, 26). Furthermore, lipid raft microdomains might contribute to FcεRI clustering and its association with signaling molecules in the plasma membrane (27, 28). Based on these observations, we suggest that the enhanced activation of FcεRI in VAMP3 KD cells might occur

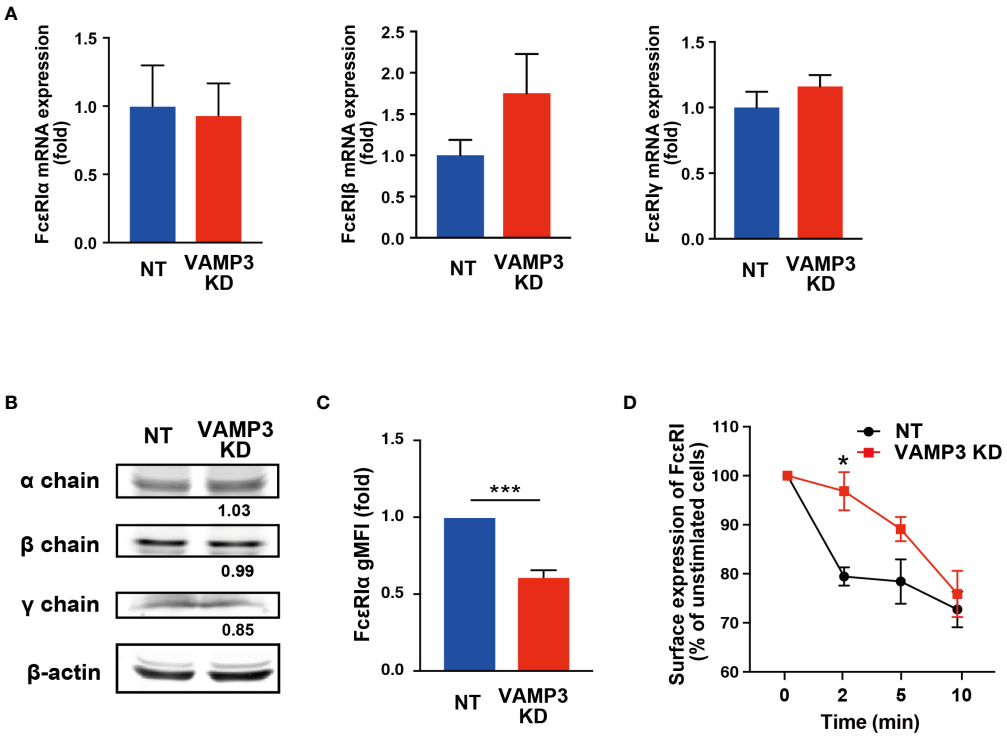


FIGURE 4
No FcεRI upregulation was observed in cell surface expression or internalization The expression of each subunit of FcεRI in VAMP3 KD cells was determined. **(A)** Gene expression was analyzed using quantitative RT-PCR. **(B)** Protein expression was analyzed using western blot analysis. **(C)** Cell surface expression levels of FcεRIα that binds to the IgE Fc region were analyzed using flow cytometry in the cells at steady state. **(D)** Ag-induced time-dependent reduction in cell surface FcεRI-bound IgE was analyzed using flow cytometry. A representative blot is shown for three independent experiments, and the band density normalized to that of unstimulated cells is shown below each band **(B)**. Data are presented from three independent experiments. Three biological repeats were quantified in a single run of PCR in the qPCR analysis. NT: control knockdown with a non-targeting shRNA plasmid. Ag: antigen. gMFI: geometric mean fluorescence intensity. *p<0.05, ***p<0.001; ns, not significant.

due to FcεRI cluster formation in the lipid raft-modified membrane. Although further examination is required, these findings suggest a bifunctional role of VAMP3 in plasma membrane homeostasis and the subsequent activation of MCs.

VAMP3 differentially regulates secretory responses of heterogeneity granules

As discussed above, VAMP3 plays multifunctional roles in membrane homeostasis and signaling events in MCs. To further examine the consequences of VAMP3-mediated regulation of MC signaling, we assessed IgE/Ag-induced cytokine expression and secretion in MCs. IgE/Ag-induced degranulation, which is monitored by β-hexosaminidase release, was significantly attenuated at 30 min in VAMP3 KD cells. This might have occurred due to the granule-to-granule fusion in the degranulation responses. However, a series of FcεRI signaling events following IgE/Ag stimulation was augmented in VAMP3 KD cells. To address the complex regulation of MC functions, we analyzed the mRNA expression of several inflammatory mediators and secretory responses in VAMP3 KD cells. The tested inflammatory cytokines appeared to be differentially regulated in the context of VAMP3 involvement. RT-PCR analysis of the Ag-stimulated cells revealed that the transcription levels of IL-6 were significantly upregulated in VAMP3 KD cells 3 h after Ag stimulation, whereas TNF-α did not show a marked difference (Figure 5A). In addition, IL-2 and IL-13, but not CCL2 and IL-4, were significantly upregulated in VAMP3 KD cells at the peak time point of the expression (Supplementary Figure 5). We further explored time-dependent changes of protein secretion levels of TNF-α and IL-6 following Ag stimulation. The cytokine secretion has been generally observed not only in case of preformed mediator secretion (granule stored), but also in case of the *de novo* synthesized mediators. As shown in Figure 5B, there was a considerably high and sustained secretion of IL-6 up to 9 h following Ag stimulation in VAMP3 KD cells. In contrast, no significant increases were observed in TNF-α in VAMP3 KD cells. VAMP3 elimination attenuated Ag-induced TNF-α secretion from MCs, which is consistent with the results of the β-hexosaminidase release assay (Figure 1C), whereas IL-6 secretion was significantly enhanced in the VAMP3 KD cells (Figure 5B). To investigate the cause of differences in secretory response, we evaluated the distribution of TNF-α and IL-6 in MC granules and found that they exhibited differential distribution (Figure 5C). These data suggest that each granule contains a specific cytokine. The upregulated transcription and extracellular secretion of IL-6 in VAMP3 KD cells appear to be attributed to the enhancement of FcεRI signal transduction as shown in Figure 3, whereas the deficiency of membrane fusion in certain granules and the plasma membrane contributed to the attenuation of robust secretory responses (i.e., β-hexosaminidase, TNF-α). Collectively, these data suggest that a multifunctional regulation of VAMP3 is involved in the complex secretory responses of MCs.

Discussion

We demonstrated that VAMP3 is involved in both IgE/Ag-triggered granule exocytotic process and plasma membrane endocytic mechanism in MCs. VAMP3-mediated granule-to-granule fusion appears to be limited to a distinct granule population, which indicates that VAMP3 could contribute to the heterogeneity of secretory responses in MCs.

VAMP3 KD cells showed a markedly decreased in degranulation responses at 30 min, but not at 180 min, as assessed by β-hexosaminidase release. β-hexosaminidase is a glycolytic enzyme that is commonly recognized as a major component of MC granules, and its secretion is widely used as a marker for MC degranulation triggered by IgE/Ag. For β-hexosaminidase secretion, a time- dependent increase has been reported, which peaked at 30–60 min following Ag stimulation (20); therefore, the secretion of preformed mediator is generally assessed within this time frame. Indeed, we found similar results, wherein VAMP3-mediated regulation of secretory responses was observed 30 min post Ag stimulation (Figure 1). Previous studies have demonstrated that a membrane receptor (an opioid receptor) was recycled within 90 min in an agonist-induced endocytosis in HEK293 cells (29). In MCs, the endocytic recycling under degranulation might be occurring in newly formed secretory granules within 180 min. In addition, Ag-induced enlargement of VAMP3 positive granules were restored to normal levels at 180 min post stimulation, which might be caused by the recycled and/or newly formed secretory granules. Therefore, VAMP3 appears to contribute to the degranulation responses in MCs by mediating granule-to-plasma membrane fusion as well as intracellular granule-to-granule fusion, as indicated in Figure 2. The rescue of VAMP3 KD phenotype expectedly restored the Ag-induced granule fusions; however, whether the Ag-induced β-hexosaminidase release was rescued by VAMP3 remains to be determined. This transient rescue established using shRNA may possibly be achievable in whole cell population.

The endogenous and exogenous VAMP3 could be downregulated by stably expressing the siRNA. Indeed, FACS analysis in Supplementary Figure 2 demonstrated lower GFP-VAMP3 expression efficacy in VAMP3 KD cells [VAMP3 KD (+VAMP3 GFP)] compared with GFP-transfected VAMP3 KD cells [VAMP3 KD (+GFP)]. In this study, we could exclude the possibility for off-target effects of VAMP7 and MC signaling molecules. Development of RNAi-resistant version of VAMP3 would further validate this. For the roles of VAMP3 on the MC signal transduction, the VAMP3 KD cells displayed enhanced susceptibility to exogenous Ag exposure by which the FcεRI

10.3389/fimmu.2022.885868

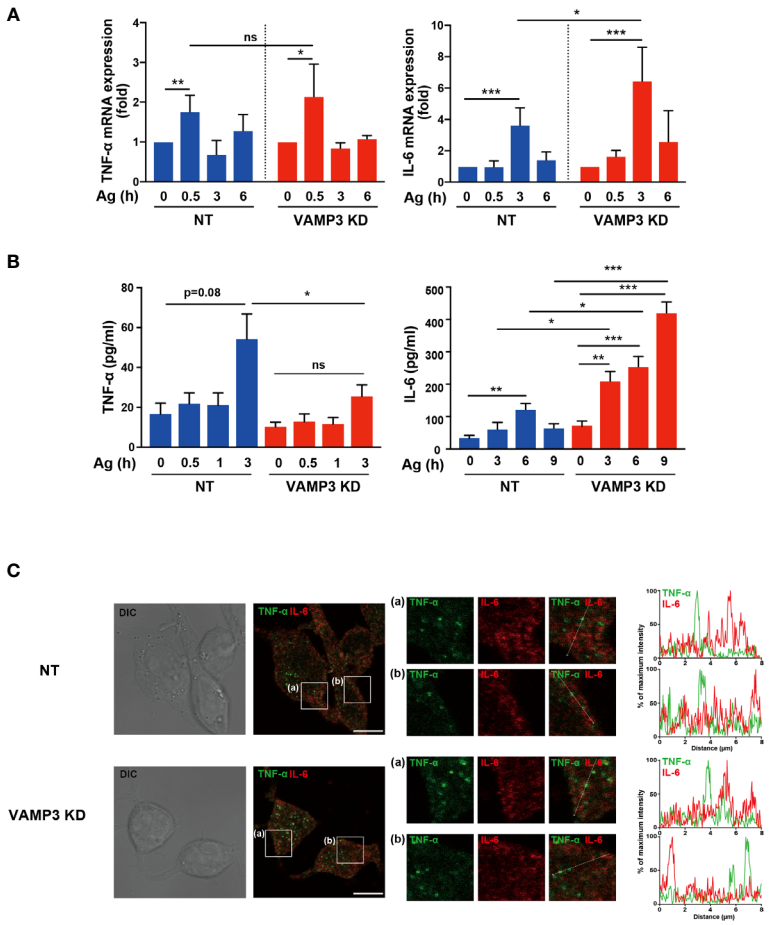


FIGURE 5
Ag-induced release of cytokines are differentially regulated by VAMP3 Ag stimulation (50 ng/ml)-induced cytokine expression and extracellular secretion were analyzed in the cells. **(A)** Time-dependent expression of TNF-α and IL-6 following Ag stimulation were compared to NT cells and VAMP3 KD cells. **(B)** Time-dependent secretion of TNF-α and IL-6 following Ag stimulation were analyzed. The supernatant of each cell type was subjected to ELISA. The qPCR data are presented from three to five independent experiments; three to five independent runs of PCR were performed. **(C)** Intracellular localization of TNF-α and IL-6 were analyzed using confocal microscopy. The large panels show transmitted light image (DIC) and merge image of TNF-α (green) and IL-6 (red) signals. The small panels **(a, b)** are magnified images of the area within the white square in the large panels. Representative images (magnification ×63, scale bar = 10 μm) and line profiles of fluorescence intensity were obtained from three independent experiments. Time-dependent differences were statistically validated using one-way ANOVA followed by multi-group comparisons. Differences between two groups were analyzed using the two-tailed Student's t-test. NT: control knockdown with a non-targeting shRNA plasmid. Ag: antigen. *p<0.05, **p<0.01, ***p<0.001; ns, not significant.

signal events including activation of Src family kinases Lyn, and other critical molecules and messengers (i.e., Syk, LAT1, Akt, MAPKs, Ca^{2+}) were significantly upregulated. Crosslinking of FcεRI with multivalent Ag initiates a series of cellular biochemical events leading to activation, which comprises the rapid release of granule-stored mediators and delays the secretion of *de novo*-synthesized mediators. These processes are coordinated by a complex cascade of signaling events involving the activation and recruitment of signaling molecules and scaffolding proteins in each step (30). Thus, an increase in FcεRI signaling is a relevant feature of the MC allergic response to Ag stimulation. In VAMP3 KD cells, however, the enhanced FcεRI signals did not reflect the major degranulation response monitored by β-hexosaminidase release. This complicated observation, illustrated in Figures 1–3, prompted us to identify the multifunctional roles of VAMP3 in MC activation and secretion. Indeed, VAMP3 has several distinct roles in secretory proteins, exocytic/endocytic pathways, trafficking, and processing of membranes, as described above (8–10). Specifically, the functions of VAMP3 have been well investigated in macrophage phagocytes. VAMP3 mediates TNF-α secretion in macrophages in which VAMP3 delivers cytokine-positive granules to the cell surface at the site of phagocytic cup formation (9). Granular fusion in forming of the phagocytic cup simultaneously allows the rapid release of TNF-α and expands the membrane for phagocytosis (9). Likewise, VAMP3 function

has been known to be required for the efficient phagocytosis of yeast (31, 32). These important SNARE complexes in macrophages also have been found to facilitate cell adhesion, spreading, and persistent cell migration on fibronectin through the delivery of VAMP3-positive membrane with its cargo, to expand the plasma membrane and participate in organizing a specialized adhesive structure called podosome, which plays an important role in macrophage migration (33, 34). Therefore, the role of VAMP3 in MCs is thought to be associated with both membrane endosome process and exocytotic granule release.

In this study, the cellular uptake of Lucifer Yellow dye, which is used to monitor endocytosis, demonstrated significant reduction in the level of endocytosis in VAMP3 KD cells compared to that in NT cells. This observation appears to be consistent with previous studies reporting the involvement of VAMP7 in mediating vesicular transport within the endosomal pathway. VAMP7 plays a role in early endosome to lysosome vesicular trafficking (35). A study using immunoelectron microscopy analysis showed that VAMP7 is primarily concentrated in the trans-Golgi network region of the cells, as well as in late endosomes and transport vesicles that do not contain the mannose-6 phosphate receptor, which is responsible in mediating the transport of newly synthesized lysosomal enzymes to endosomes (35). More recently, Tang BL reported that in autophagy, sytaxin16 and VAMP7 could be involved in the regulation of autophagosome formation and subsequent lysosomal fusion (36). Moreover, syntaxin17 phosphorylation regulates the initiation of autophagy (36, 37). Given these observations and our findings in the present study, further investigations of cell surface FcεRI receptor expression and its functions in the context of internalization were conducted, revealing a significant reduction in MC surface FcεRI in VAMP3 KD cells. Remarkably, in NT cells, FcεRI internalization occurred immediately after Ag stimulation; however, in VAMP3 KD cells, FcεRI internalization showed a significantly slower rate. Ag binding to IgE-bound FcεRI causes cross-linking of IgE–FcεRI complexes. FcεRI dynamics on the plasma membrane determine FcεRI-mediated signal transduction (38). FcεRI behavior in the plasma membrane of MCs has been suggested to correlate with FcεRI signal initiation (39, 40). According to these observations, the slower rate of IgE-FcεRI internalization observed in VAMP3 KD cells suggest that the IgE-FcεRI complex remained on the cell surface in VAMP3 KD cells longer compared to that in NT cells and/or altered its aggregation behavior to a certain degree in VAMP3 KD cells, and this was associated with the enhanced phosphorylation of FcεRI in response to Ag.

To further examine the mechanism underlying the induction of FcεRI activation and subsequent signaling upon VAMP3 elimination, we analyzed lipid raft formation in MCs and observed a considerable increase in the lipid raft domain in VAMP3 KD cells. Lipid rafts are ordered regions of the plasma membrane that are enriched in cholesterol and glycosphingolipids, which play important roles in receptor-mediated signaling (41, 42). Thus, the integrity of lipid rafts significantly impacts cell surface receptor stabilization and is associated with signaling molecules in the membrane. Indeed, in MCs, lipid rafts are crucial for FcεRI function and actin cytoskeleton reorganization (43, 44). Furthermore, lipid raft stability is known to be capable of enhancing FcεRI signaling, possibly by suppressing phosphatase activity, where the lipid raft submembrane location is critical to phosphatase-mediated regulation of Lyn kinase activity that supports activation of FcεRI (28). A more recent study showed that lipid rafts form transient proteins that are protected while in a raft and are subject to dephosphorylation when the raft breaks up; such proteins are found in the non-raft region of the membrane (27, 45). Based on these observations, our findings suggest that the enhancement of lipid rafts in VAMP3 KD cells is likely to be associated with an increase in FcεRI phosphorylation. Even with the significant decrease in surface expression of FcεRI in VAMP3 KD cells, the modified plasma membrane potential in relation to raft integrity is thought to affect FcεRI signal transduction under Ag stimulation, resulting in enhanced distal gene transcription. Although further studies on the coalesced lipid raft domain and the efficacy of FcεRI signal transduction are required, the enhanced FcεRI signaling observed in VAMP3 KD cells could be attributed to the modulated plasma membrane caused by the absence of VAMP3.

MCs contain a variety of inflammatory mediators (e.g., histamine, cytokines, and chemokines) that can be released *via* exocytosis (e.g., degranulation) after activation. Inflammatory cytokines such as TNF-α and IL-6 are considered important contributors to MCs. Trafficking granules in MCs also intersect with endocytic routes to form specialized cytoplasmic granules called secretory lysosomes (46). Some mediators, such as histamine, reach granules *via* specific vesicular monoamine transporters directly from the cytoplasm [reviewed in (46)]. The comprehensive review summarizes the available data on granule biogenesis and signaling events that coordinate the complex steps leading to the release of inflammatory mediators from various vesicular carriers in MCs (46). The endocytic recycling under degranulation (i.e., β-hexosaminidase secretion) might be occurring in newly formed secretory granules within 180 min. For cytokine secretion, this has been generally observed not only in case of preformed mediator secretion (granule stored), but also in case of *de novo* synthesized mediators (47). In this study, detailed analysis of cytokine production and release up to 9 h following stimulation with Ag was performed. Results for the transcription and secretion levels of each cytokine for the selected differential time-courses indicated significantly slower transcriptional regulation of IL-6 compared to that of TNF-α (Figure 5). Furthermore, it has been suggested that inflammatory cytokines are differentially packaged in distinct secretory granules in macrophages (10). Manderson et al. showed that

in macrophages, newly synthesized IL-6 accumulates in the Golgi complex and exits through the tubulovesicular carriers that deliver cargo proteins to the plasma membrane either as the sole labeled cargo or together with TNF-α, utilizing specific SNAREs to fuse with the recycling endosomes. Manderson et al. also demonstrated that there is compartmentalization of the cargo proteins within the recycling endosomes, wherein IL-6 is dynamically segregated from TNF-α and surface recycling transferrin (10). Thereafter, these cytokines are independently secreted, with TNF-α being delivered to phagocytic cups, but not IL-6. Therefore, they concluded that the recycling endosome plays a central role in orchestrating the differential secretion of cytokines during inflammation (10, 46). In MCs, however, precise mechanisms regarding the differential regulation of secretory responses have not been fully elucidated, especially in the context of SNARE involvement. A previous report on the function of VAMPs in MCs demonstrated that VAMP3 colocalizes with TNF-α (48). In our observations, microscopic images showed that IL-6 and TNF-α were distributed in distinct granules in MCs. Therefore, combined with the previous report and our findings, there are distinct granules packaging TNF-α and IL-6. VAMP3 mediated granule to granule fusion appears to be involved in Ag-induced secretion of TNF-α, but not IL-6, as shown in Figure 5. In addition, our RT-PCR analysis of several inflammatory cytokines also indicated differential regulation depending on VAMP3 expression; therefore, there might be a more complicated secretory regulation of cytokines in MCs in the context of SNARE distribution.

While this study indicated the multifunctional regulation of VAMP3 in MCs, there seem to be important limitations in the FcεRI behavior (e.g., formation of FcεRI clusters, interaction with lipid rafts) in Ag-stimulated MCs, which may explain the enhancement of FcεRI signaling in VAMP3 KD cells. In addition, whether VAMP3 is involved in FcεRI transport to the plasma membrane and the FcεRI recycling pathway remains to be seen. Further investigation into this problem may facilitate a deeper understanding of the role of VAMP3 in allergic responses to MC. Additionally, compensation mechanisms involving SNAREs are also involved in SNARE-mediated secretion of inflammatory mediators in MCs, which might lead to complex secretory responses. This study also showed that the marked knockdown of VAMP3 did not result in the complete inhibition of β-hexosaminidase release (Figure 1). A study using VAMP8-deficient mice indicated that VAMP3-containing SNARE complexes were increased in MCs from VAMP8-deficient cells. In VAMP8-deficient MCs, constitutive vesicular trafficking is perturbed by increased SNARE complex formation between VAMP3 and SNAP23 (49). Thus, the orchestrated mechanisms of SNAREs may be responsible for FcεRI-mediated secretory responses in MCs.

In conclusion, our study demonstrates the multifaceted role of VAMP3, which appear to be involved in the heterogeneity of MC secretory responses. The results of this study may provide a foundation for identifying novel therapeutic targets in the treatment of allergic reactions to MCs.

Data availability statement

The original contributions presented in the study are included in the article/Supplementary Material. Further inquiries can be directed to the corresponding author.

Author contributions

SM, MS, HK, and YN contributed by conducting experiments, summarizing data, and/or generating the necessary reagents. YN and RS conceived of and directed the study. SM, MS, HK, YN, and RS participated in the writing of the manuscript. All authors contributed to the article and approved the submitted version.

Funding

This research was funded by JSPS KAKENHI, grant numbers 20K15992 (to YN), 16H05082, and 19H03369 (to RS). This research was also funded by the Uehara Memorial Foundation, the Naito Foundation, and the Takeda Science Foundation (to RS).

Conflict of interest

The authors declare that the research was conducted in the absence of any commercial or financial relationships that could be construed as a potential conflict of interest.

Publisher's note

All claims expressed in this article are solely those of the authors and do not necessarily represent those of their affiliated organizations, or those of the publisher, the editors and the reviewers. Any product that may be evaluated in this article, or claim that may be made by its manufacturer, is not guaranteed or endorsed by the publisher.

Supplementary material

The Supplementary Material for this article can be found online at: https://www.frontiersin.org/articles/10.3389/fimmu.2022.885868/full#supplementary-material

References

1. Puri N, Roche PA. Mast cells possess distinct secretory granule subsets whose exocytosis is regulated by different SNARE isoforms. *Proc Natl Acad Sci USA* (2008) 105:2580–5. doi: 10.1073/pnas.0707854105

2. Lorentz A, Baumann A, Vitte J, Blank U. The SNARE machinery in mast cell secretion. *Front Immunol* (2012) 3:143. doi: 10.3389/fimmu.2012.00143

3. Sander LE, Bolat S, Klempnauer J, Manns MP, Bischoff SC, Lorentz A. Primary human mast cells express specific isoforms of SNARE proteins. *J Allergy Clin Immunol* (2005) 115:S187. doi: 10.1016/j.jaci.2004.12.760

4. Woska JRJr., Gillespie ME. SNARE complex-mediated degranulation in mast cells. *J Cell Mol Med* (2012) 16:649–56. doi: 10.1111/j.1582-4934.2011.01443.x

5. Kean MJ, Williams KC, Skalski M, Myers D, Burtnik A, Foster D, et al. VAMP3, syntaxin-13 and SNAP23 are involved in secretion of matrix metalloproteinases, degradation of the extracellular matrix and cell invasion. *J Cell Sci* (2009) 122:4089–98. doi: 10.1242/jcs.052761

6. Pulido IR, Jahn R, Gerke V. VAMP3 is associated with endothelial weibel–palade bodies and participates in their Ca2+-dependent exocytosis. *Biochim Biophys Acta (BBA) Mol Cell Res* (2011) 1813:1038–44. doi: 10.1016/j.bbamcr.2010.11.007

7. Ribel-Madsen S, Bartels EM, Stockmarr A, Borgwardt A, Cornett C, Danneskiold-Samsøe B, et al. A synoviocyte model for osteoarthritis and rheumatoid arthritis: response to ibuprofen, betamethasone, and ginger extract-a cross-sectional *in vitro* study. *Arthritis* (2012) 2012:505842–. doi: 10.1155/2012/505842

8. Boddul SV, Meng J, Dolly JO, Wang J. SNAP-23 and VAMP-3 contribute to the release of IL-6 and TNFα from a human synovial sarcoma cell line. *FEBS J* (2014) 281:750–65. doi: 10.1111/febs.12620

9. Murray RZ, Kay JG, Sangermani DG, Stow JL. A role for the phagosome in cytokine secretion. *Science* (2005) 310:1492–5. doi: 10.1126/science.1120225

10. Manderson AP, Kay JG, Hammond LA, Brown DL, Stow JL. Subcompartments of the macrophage recycling endosome direct the differential secretion of IL-6 and TNFα. *J Cell Biol* (2007) 178:57–69. doi: 10.1083/jcb.200612131

11. >Zhu J-J, Jiang Z-T, Liu C, Xi Y-F, Wang J, Yang F-F, et al. VAMP3 and SNAP23 as potential targets for preventing the disturbed flow-accelerated thrombus formation. *Front Cell Dev Biol* (2020) 8:576826–. doi: 10.3389/fcell.2020.576826

12. Veale KJ, Offenhäuser C, Whittaker SP, Estrella RP, Murray RZ. Recycling endosome membrane incorporation into the leading edge regulates lamellipodia formation and macrophage migration. *Traffic* (2010) 11:1370–9. doi: 10.1111/j.1600-0854.2010.01094.x

13. Harcha PA, Garcés P, Arredondo C, Fernández G, Sáez JC, van Zundert B. Mast cell and astrocyte hemichannels and their role in alzheimer's disease, als, and harmful stress conditions. *Int J Mol Sci* (2021) 22:1924. doi: 10.3390/ijms22041924

14. Mollinedo F, Calafat J, Janssen H, Martín-Martín B, Canchado J, Nabokina SM, et al. Combinatorial SNARE complexes modulate the secretion of cytoplasmic granules in human neutrophils. *J Immunol* (2006) 177:2831–41. doi: 10.4049/jimmunol.177.5.2831

15. Agarwal V, Naskar P, Agasti S, Khurana GK, Vishwakarma P, Lynn AM, et al. The cysteine-rich domain of synaptosomal-associated protein of 23 kda (snap-23) regulates its membrane association and regulated exocytosis from mast cells. biochimica et biophysica acta. *Mol Cell Res* (2019) 1866:1618–33. doi: 10.1016/j.bbamcr.2019.06.015

16. Suzuki R, Leach S, Liu W, Ralston E, Scheffel J, Zhang W, et al. Molecular editing of cellular responses by the high-affinity receptor for IgE. *Sci (New York NY)* (2014) 343:1021–5. doi: 10.1126/science.1246976

17. Suzuki R, Leach S, Dema B, Rivera J. Characterization of a phospho-specific antibody to the fcε receptor γ chain, reveals differences in the regulation of syk and akt phosphorylation. *Antibodies* (2013) 2:321–37. doi: 10.3390/antib2020321

18. Rivera J, Kinet JP, Kim J, Pucillo C, Metzger H. Studies with a monoclonal antibody to the beta subunit of the receptor with high affinity for immunoglobulin e. *Mol Immunol* (1988) 25:647–61. doi: 10.1016/0161-5890(88)90100-9

19. Sander LE, Frank SP, Bolat S, Blank U, Galli T, Bigalke H, et al. Vesicle associated membrane protein (VAMP)-7 and VAMP-8, but not VAMP-2 or VAMP-3, are required for activation-induced degranulation of mature human mast cells. *Eur J Immunol* (2008) 38:855–63. doi: 10.1002/eji.200737634

20. Rådinger M, Jensen BM, Swindle E, Gilfillan AM. Assay of mast cell mediators. *Methods Mol Biol* (2015) 1220:307–23. doi: 10.1007/978-1-4939-1568-2_19

21. Dressel R, Elsner L, Novota P, Kanwar N, Fischer von Mollard G. The exocytosis of lytic granules is impaired in Vti1b- or Vamp8-deficient CTL leading to a reduced cytotoxic activity following antigen-specific activation. *J Immunol* (2010) 185:1005–14. doi: 10.4049/jimmunol.1000770

22. Hu C, Hardee D, Minnear F. Membrane fusion by VAMP3 and plasma membrane t-SNAREs. *Exp Cell Res* (2007) 313:3198–209. doi: 10.1016/j.yexcr.2007.06.008

23. Rivera J. Molecular adapters in FcεRI signaling and the allergic response. *Curr Opin Immunol* (2002) 14:688–93. doi: 10.1016/S0952-7915(02)00396-5

24. Xiao W, Nishimoto H, Hong H, Kitaura J, Nunomura S, Maeda-Yamamoto M, et al. Positive and negative regulation of mast cell activation by Lyn *via* the FcepsilonRI. *J Immunol (Baltimore Md* (2005) 1950) 175:6885–92. doi: 10.4049/jimmunol.175.10.6885

25. Ledeen RW, Wu G. The multi-tasked life of GM1 ganglioside, a true factotum of nature. *Trends Biochem Sci* (2015) 40:407–18. doi: 10.1016/j.tibs.2015.04.005

26. Kara S, Amon L, Lühr JJ, Nimmerjahn F, Dudziak D, Lux A. Impact of plasma membrane domains on IgG fc receptor function. *Front Immunol* (2020) 11. doi: 10.3389/fimmu.2020.01320

27. Barua D, Goldstein B. A mechanistic model of early fcεri signaling: lipid rafts and the question of protection from dephosphorylation. *PloS One* (2012) 7:e51669. doi: 10.1371/journal.pone.0051669

28. Young RM, Zheng X, Holowka D, Baird B. Reconstitution of regulated phosphorylation of fcεri by a lipid raft-excluded protein-tyrosine phosphatase. *J Biol Chem* (2005) 280:1230–5. doi: 10.1074/jbc.M408339200

29. Tanowitz M, von Zastrow M. A novel endocytic recycling signal that distinguishes the membrane trafficking of naturally occurring opioid receptors. *J Biol Chem* (2003) 278:45978–86. doi: 10.1074/jbc.M304504200

30. Kambayashi T, Koretzky GA. Proximal signaling events in FcεRI-mediated mast cell activation. *J Allergy Clin Immunol* (2007) 119:544–52. doi: 10.1016/j.jaci.2007.01.017

31. Braun V, Fraisier V, Raposo G, Hurbain I, Sibarita J-B, Chavrier P, et al. TI-VAMP/VAMP7 is required for optimal phagocytosis of opsonised particles in macrophages. *EMBO J* (2004) 23:4166–76. doi: 10.1038/sj.emboj.7600427

32. Allen L-AH, Yang C, Pessin JE. Rate and extent of phagocytosis in macrophages lacking vamp3. *J Leukocyte Biol* (2002) 72:217–21. doi: 10.1189/jlb.72.1.217

33. Linder S, Aepfelbacher M. Podosomes: adhesion hot-spots of invasive cells. *Trends Cell Biol* (2003) 13:376–85. doi: 10.1016/S0962-8924(03)00128-4

34. Veale KJ, Offenhäuser C, Lei N, Stanley AC, Stow JL, Murray RZ. VAMP3 regulates podosome organisation in macrophages and together with Stx4/SNAP23 mediates adhesion, cell spreading and persistent migration. *Exp Cell Res* (2011) 317:1817–29. doi: 10.1016/j.yexcr.2011.04.016

35. Advani RJ, Yang B, Prekeris R, Lee KC, Klumperman J, Scheller RH. VAMP-7 mediates vesicular transport from endosomes to lysosomes. *J Cell Biol* (1999) 146:765–76. doi: 10.1083/jcb.146.4.765

36. Tang BL. Syntaxin 16's newly deciphered roles in autophagy. *Cells* (2019) 8:1655. doi: 10.3390/cells8121655

37. Kumar S, Gu Y, Abudu YP, Bruun J-A, Jain A, Farzam F, et al. Phosphorylation of syntaxin 17 by tbk1 controls autophagy initiation. *Dev Cell* (2019) 49:130–44.e6. doi: 10.1016/j.devcel.2019.01.027

38. Nagata Y, Suzuki R. FcεRI: A master regulator of mast cell functions. *Cells* (2022) 11:622. doi: 10.3390/cells11040622

39. Andrews NL, Pfeiffer JR, Martinez AM, Haaland DM, Davis RW, Kawakami T, et al. Small, mobile fcεri receptor aggregates are signaling competent. *Immunity* (2009) 31:469–79. doi: 10.1016/j.immuni.2009.06.026

40. Wilson BS, Oliver JM, Lidke DS. Spatio-temporal signaling in mast cells. *Adv Exp Med Biol* (2011) 716:91–106. doi: 10.1007/978-1-4419-9533-9_6

41. Silveira E Souza AMM, Mazucato VM, Jamur MC, Oliver C. Lipid rafts in mast cell biology. *J Lipids* (2011) 2011:752906–. doi: 10.1155/2011/752906

42. Holowka D, Baird B. Nanodomains in early and later phases of FcεRI signalling. *Essays Biochem* (2015) 57:147–63. doi: 10.1042/bse0570147

43. Sheets ED, Holowka D, Baird B. Membrane organization in immunoglobulin e receptor signaling. *Curr Opin Chem Biol* (1999) 3:95–9. doi: 10.1016/S1367-5931(99)80017-9

44. Holowka D, Sheets ED, Baird B. Interactions between FcεRI and lipid raft components are regulated by the actin cytoskeleton. *J Cell Sci* (2000) 113:1009–19. doi: 10.1242/jcs.113.6.1009

45. Varshney P, Yadav V, Saini N. Lipid rafts in immune signalling: current progress and future perspective. *Immunology* (2016) 149:13–24. doi: 10.1111/imm.12617

46. Blank U, Madera-Salcedo IK, Danelli L, Claver J, Tiwari N, Sánchez-Miranda E, et al. Vesicular trafficking and signaling for cytokine and chemokine secretion in mast cells. *Front Immunol* (2014) 5:453–. doi: 10.3389/fimmu.2014.00453

47. Mukai K, Tsai M, Saito H, Galli SJ. Mast cells as sources of cytokines, chemokines, and growth factors. *Immunol Rev* (2018) 282:121–50. doi: 10.1111/imr.12634

48. Martín-Ávila A, Medina-Tamayo J, Ibarra-Sánchez A, Vázquez-Victorio G, Castillo-Arellano JI, Hernández-Mondragón AC, et al. Protein tyrosine kinase fyn regulates tlr4-elicited responses on mast cells controlling the function of a pp2a-pkcα/β signaling node leading to tnf secretion. *J Immunol* (2016) 196:5075–88. doi: 10.4049/jimmunol.1501823

49. Tiwari N, Wang CC, Brochetta C, Scandiuzzi L, Hong W, Blank U. Increased formation of VAMP-3-containing SNARE complexes in mast cells from VAMP-8 deficient cells. *Inflammation Res* (2009) 58:13–4. doi: 10.1007/s00011-009-0645-y

frontiers | Frontiers in Immunology

TYPE Original Research
PUBLISHED 10 August 2022
DOI 10.3389/fimmu.2022.930979

Check for updates

OPEN ACCESS

EDITED BY
Frans J. Van Overveld,
University College Roosevelt,
Netherlands

REVIEWED BY
Vadim V. Sumbayev,
University of Kent, United Kingdom
Manuel Pedro Pereira,
University Hospital Münster, Germany
Miriam Margareta Düll,
University Hospital Erlangen, Germany

*CORRESPONDENCE
Marcus Maurer
marcus.maurer@charite.de

SPECIALTY SECTION
This article was submitted to Inflammation, a section of the journal Frontiers in Immunology

RECEIVED 28 April 2022
ACCEPTED 20 July 2022
PUBLISHED 10 August 2022

CITATION
Terhorst-Molawi D, Lohse K, Ginter K, Puhl V, Metz M, Hu M, Maurer M and Altrichter S (2022) Mast cells and tryptase are linked to itch and disease severity in mycosis fungoides: Results of a pilot study.
Front. Immunol. 13:930979.
doi: 10.3389/fimmu.2022.930979

COPYRIGHT
© 2022 Terhorst-Molawi, Lohse, Ginter, Puhl, Metz, Hu, Maurer and Altrichter. This is an open-access article distributed under the terms of the Creative Commons Attribution License (CC BY). The use, distribution or reproduction in other forums is permitted, provided the original author(s) and the copyright owner(s) are credited and that the original publication in this journal is cited, in accordance with accepted academic practice. No use, distribution or reproduction is permitted which does not comply with these terms.

Mast cells and tryptase are linked to itch and disease severity in mycosis fungoides: Results of a pilot study

Dorothea Terhorst-Molawi[1,2,3], Katharina Lohse[1,2], Katharina Ginter[1,2], Viktoria Puhl[1,2], Martin Metz[1,2], Man Hu[1,2], Marcus Maurer[1,2]* and Sabine Altrichter[1,2,4]

[1]Institute of Allergology, Charité – Universitätsmedizin Berlin, Corporate Member of Freie Universität Berlin and Humboldt-Universität zu Berlin, Berlin, Germany, [2]Fraunhofer Institute for Translational Medicine and Pharmacology (ITMP), Allergology and Immunology, Berlin, Germany, [3]Institute of Clinical Physiology, Charité – Universitätsmedizin Berlin, Corporate Member of Freie Universität Berlin and Humboldt-Universität zu Berlin, Berlin, Germany, [4]Department of Dermatology and Venerology, Kepler University Hospital, Linz, Austria

Introduction: In mycosis fungoides (MF), the most common cutaneous T-cell lymphoma, itch is a frequent clinical symptom. Whether mast cells (MCs), eosinophils (Eos) or their mediators play a role in MF-associated itch or disease severity is controversially discussed. Here, we explored the role of MC and Eo numbers in the skin as well as blood levels of their mediators in disease severity and itch.

Methods: In 10 patients with MF and 10 matched control subjects we assessed disease severity, itch, and quality of life impairment using dedicated tools such as the mSWAT, ItchyQoL and DLQI. We analyzed skin biopsies and measured serum levels of tryptase, a mast cell mediator, as well as of the eosinophil products eosinophil cationic protein (ECP) and major basic protein (MBP).

Results: The presence of chronic itch, in four of 10 patients, was associated with significantly higher disease severity (mSwat), larger body surface area affected, and stronger QoL impairment (Itchy-Qol, DLQI). Serum levels of tryptase, but not ECP and MBP, were linked with patient-reported disease severity, body surface area affected, and the presence of itch. Three of the four patients with chronic itch, but none of the six patients without, had tryptase levels above >6µg/l. Numbers of MCs in the papillary dermis were higher in MF skin lesions then in non-lesional skin of MF patients and skin of healthy controls.

Discussion: The MC-mediator tryptase, in MF, is linked to disease activity and impact, most prominently to itch. Our findings call for larger studies that explore the role of MCs, tryptase and other MC mediators as drivers of itch and their role in MF pathogenesis.

KEYWORDS

mycosis fungoides, cutaneous T-cell lymphoma, mast cell, eosinophil, tryptase, itch (pruritus)

Introduction

Mycosis fungoides (MF) is the most common form of cutaneous T-cell lymphoma (CTCL). MF is caused by the uncontrolled growth of atypical T-cells, usually $CD4^+$ T-lymphocytes, and associated inflammation in the epidermis. MF most commonly occurs between 50–70 years of age (1), but can affect people of any age. Neoplastic cells in MF typically express CLA and CCR4, exhibiting the phenotype of skin-homing CD4+ T cells (2). The disease can progress through several stages and is characterized by a skin rash, eczematous lesions and often pruritus (1, 3, 4). In the later stages, intradermal tumors can develop, which may spread into the peripheral blood, lymph nodes and other organs (4). In this stage of the disease, the prognosis is poor with a median survival of less than three years. Monitoring of the disease is crucial in the disease management of these patients. However, no readily assessable biomarkers for disease characterization and monitoring have been identified to date (5).

Itch can be a bothersome symptom and affects more than half of the patients with MF. Itch, in MF, is one of the main drivers of quality of life impairment in these patients (6–8). The exact mechanisms of itch induction in MF lesions are not understood. The degranulation of skin mast cells (MC) and subsequent release of histamine could account for pruritus *via* histamine 1 or 4 receptors. Both receptors are found on sensory skin nerves (9). H1 antihistamines are used for the treatment of pruritus in MF, but this treatment has limited effect (10). In a more recent publication, a role of eosinophils for the itch component in MF was proposed (11), but eosinophils have not been described as common infiltrating cells in early disease stages (12).

Mast cells in the skin, the gastrointestinal tract, and the airways (13, 14) are commonly recognized for their role in IgE-dependent and independent immune responses. MC numbers have been reported to be increased in several hematological and solid cancers (15, 16). Depending on the type of malignancy, MCs have been suggested to have pro-tumorigenic functions, protective effects, or serve as bystanders (17). For example, MCs have been linked to prostate, skin and pancreatic cancer progression (18–20), but have been reported to have protective, anti-tumorigenic effects in breast and lung cancer (21, 22). As for MF, earlier reports have shown that MC numbers are increased in skin lesions and linked to tumor stage and level of invasiveness, suggesting that MCs have a pro-tumorigenic role in MF (10, 15, 16). In support of this notion, MC-deficient mice showed markedly decreased tumor growth in experimental cutaneous lymphoma (4).

The role and relevance of MCs in MF are ill characterized. Human skin MCs produce and release a comprehensive range of biologically active mediators (23). In addition, their activation can drive the recruitment of other proinflammatory cells including basophils, neutrophils and eosinophils (Eos). Changes in Eos numbers in the blood and skin have been linked to MF progression (12, 24, 25). The detection of MC and Eos activation in human skin is challenging, and serological markers have been established as surrogate markers for their activation. Tryptase is only produced by MCs and the most abundant secretory serine protease in MC granules. It is released constantly as well as upon MC activation and is used as a marker for MC numbers as well as MC activation (26). For Eos, blood levels of eosinophilic cationic protein (ECP) and major basic protein (MBP) are used as surrogate markers for cell numbers as well as activation.

Taken together, MC and Eos as well as their mediators appear to be linked to pathogenetic features and the course of MF. To address the gap of knowledge regarding their role on itch and disease severity, we explored the link of MCs, Eos and their activation products with MF disease severity, itch severity and quality of life impairment.

Materials and methods

Study participants

In this case-control study, patients with MF were recruited from the Department of Dermatology and Allergy, Charité - Universitätsmedizin Berlin between July 2017 and April 2018. We diagnosed CTCL according to the WHO-EORTC classification for cutaneous lymphomas (27). Patients were required to stop taking local or systemic steroids therapy for the previous two weeks before we performed the tests. We recorded a detailed medical history, took blood samples and biopsies from lesional and non-lesional

Abbreviations: CTCL, cutaneous T-cell lymphoma; ECP, eosinophil cationic protein; Eos, eosinophil granulocytes; MBP, major basic protein; MC, mast cell; MF, Mycosis fungoides.

skin. Supplementary Figure 1 shows a representative patient photo with characteristic skin lesions. We also recruited ten healthy subjects as a control group who underwent identical procedures (except lesional skin biopsy). Demographic and clinical characteristics of the MF patients and healthy controls are shown in Table 1. All 20 participants were skin type II or III according to the classification of Fitzpatrick (28).

The Ethics Committee of the Charité - Universitätsmedizin Berlin approved this study (EA4/124/10). The study is registered in the German Clinical Trials Registry (DRKS-ID: DRKS00004277). Presented data are from subcohorts of the trial "ROBERTIS". Other subcohorts will be presented elsewhere.

Assessment of clinical parameters

We assessed patients' global assessment of disease severity *via* a visual analogue scale (VAS) and a Likert scale (0–3). Physicians also assessed disease severity using a Likert scale (0–3). We evaluated the affected body surface area (BSA) using the patient's palm as a rough reference point for 1%. We determined the skin tumor burden in patients with MF using the modified severity-weighted assessment tool (mSWAT) (29). The mSWAT score is calculated as the sum of affected BSA per body region multiplied by a lesion type-specific weighting factor, with higher values indicating more active disease (30).

Patient-reported outcome measures were applied: All patients assessed itch severity in the last 24 hours, the previous week, and the last month *via* a VAS, as well as itch-related quality of life (QoL) impairment with the help of the ItchyQol questionnaire (31, 32). Patients assessed their skin-related QoL impairment by using the Dermatological Life Quality Index (DLQI) (33).

Serological analyses

At a central laboratory (Labor Berlin GmbH, Berlin, Germany) the following blood parameters were assessed: differential blood count, total IgE serum levels, tryptase.

Eosinophil-related proteins were analyzed using the following ELISAs: Eosinophilic cationic protein (ECP; MyBioSource MBS700481, San Diego, California, USA) and major basic

TABLE 1 Clinical characteristics of study participants.

	MF patients N=10	Healthy controls N=10	P
Age [years]			0.014
Median (IQR),	67.5 (60.5-72)	54.5 (40-63.3)	
Mean (± SD)	66.2 (± 9.8)	51.6 (± 14.2)	
Sex M:F	9:1	6:4	0.30
BMI [kg/m²]			0.39
Median (IQR),	25.6 (24.1-27.2)	24.5 (22.3-27.0)	
Mean (± SD)	26.6 (± 5.1)	24.5 (± 2.9)	
Duration of disease [years]			–
Median (IQR),	9 (5 – 13.8)	N/A	
Mean (± SD)	9.8 (± 5.7)		
Stage of disease (ISCL/EORTC, 2007)			–
MF IA	2	N/A	
MF IB	4	N/A	
MF IIB	4	N/A	
Palpable Lymph nodes [%]	10	N/A	–
Involved Body surface area [%]			–
Median (IQR),	5.8 (1.8-11)	N/A	
Mean (± SD)	7.8 (± 7.69)		
mSWAT [points]			–
Median (IQR),	8 (2.75-16.9)	N/A	
Mean (± SD)	14.42 (± 19.65)		
Concomitant symptoms:			–
Itch [%]	40	N/A	
Fatigue [%]	20	N/A	
Insomnia [%]	20	N/A	

MF, Mycosis fungoides; mSWAT, Modified Severity-Weighted Assessment Tool; BMI, Body mass index; N, Number; IQR, Interquartile range; SD, Standard deviation; Continuous variables were compared using Wilcoxon rank test and categorical variables using Chi2 test.
N/A, not applicable.

protein (MBP; MyBioSource MBS9308460). Determinations were performed according to the manufacturer's instructions.

Histological analyses

For histological analyses, we took two skin-punch biopsies of 6 mm diameter in the study group (lesional and non-lesional) and one biopsy in the control group (only non-lesional). The non-lesional biopsy was taken approx. 6 cm away from the biopsy of the lesional skin. The proximity of both biopsies assures comparability of MC counts as MC numbers have been shown to vary in different parts of the body (34). After collection, tissue biopsies were immediately fixed in 5% buffered formalin overnight and subsequently embedded in paraffin wax as per routine protocol (Department of Pathology, Charité – Universitätsmedizin Berlin). The wax blocks were cut into 5-µm sections and stained with Giemsa (Merck KG, Darmstadt, Germany) for histology. Supplementary Figure 2 shows exemplary stainings.

MCs and Eos were counted by two independent and blinded trained investigators in five or more horizontally adjacent high-power fields (× 400, 0.15 mm2) per skin layer, and mean cell numbers per horizontal layer were calculated. At least three and up to six skin layers were counted per skin sample.

Statistical Analyses

Datasets were small and hence tests for normal distribution (visually *via* QQ plot, computationally *via* Shapiro-Wilk test) missed normal distribution for most values. For descriptive statistics continuous variables were summarized using median and interquartile range as well as mean and standard deviation. Categorical variables are given as number and percentage. Continuous variables were compared using Wilcoxon rank test and categorical variables using Chi2 test. For sets of matched samples, the Wilcoxon signed rank test and for correlations the Spearman correlation was used. Any missing data was excluded for the respective statistical analysis. A p-value below 0.05 was considered statistically significant. All statistics were performed using RStudio Version 3.6.3 and stored in an encrypted Excel sheet on an internal Charité university hospital server. All analyses were exploratory in nature.

Results

Itch is more prevalent in patients with severe MF and drives quality of life impairment

In our analyzed patient cohort, four of 10 MF patients reported regular itching of their lesional skin. MF patients who presented with itch were more severely affected, with significantly higher disease severity scores in the mSwat (p=0.042) and a larger affected body surface area (BSA, p=0.014) compared to patients without itch (Table 2A).

In MF patients with itch, itch-related quality of life was significantly more impaired (Itchy-Qol), but also their overall quality of life impairment as assessed by general patient assessment (VAS, Likert) and DLQI (Table 2A), indicating a substantial higher disease burden in MF patients with concomitant itch.

MF is linked to higher numbers of skin mast cells, but not eosinophils

Mast cell (MC) counts in the papillary dermis of MF skin lesions and non-lesional skin were higher than in the skin of healthy controls (Figure 1), albeit not statistically significantly. Of note, two MF patients showed a 3-4 fold increase in MC numbers in lesional skin. No differences were seen in MC numbers in the lower parts of the dermis of lesional, non-lesional and healthy skin. Eosinophil numbers were very low in virtually all of skin samples, of MF patients and healthy controls (below 1 cell/HPF); only one MF patient displayed higher eosinophil numbers, i.e. cells/mm² (Supplementary Figure 2).

MC and eosinophil numbers did not show significant correlations with any of the assessed clinical markers, like disease severity scores or quality of life scores (see Supplementary Table 1A). Of note, the two patients with highly increased MC numbers in lesional skin had lower total skin involvement (BSA of 1-2%) as compared to the other patients. The MF patient with the lowest MC count in lesional skin was among the patients with the highest BSA score (11%), resulting in a trend towards lower MC numbers as a marker for higher skin involvement in MF (but not disease stage).

When looking at the two subgroups of patients with and without itch, we saw comparable MC and eosinophil numbers in both groups (see Table 2B).

In MF, blood levels of tryptase, but not eosinophil mediators, are linked to disease activity, quality of life impairment, and itch

Overall, blood tryptase levels did not differ between MF patients and healthy controls. Also, MBP and ECP serum levels were comparable (see Supplementary Table 2).

Blood tryptase was to some extent positively correlated with patient-reported disease severity as assessed by VAS (rS=0.53, p=0.1; Figure 2). Patients with more severe disease based on patient or physician global assessment had the highest tryptase levels (Figure 2). Tryptase also correlated with affected body surface area (rS=0.63, p=0.05; Figure 2). Serum ECP and MBP levels did not correlate with any of the assessed disease severity markers (see Supplementary Table 1B).

10.3389/fimmu.2022.930979

TABLE 2A Clinical characteristics of MF patients with and without itch.

		MF with itch N=4	MF without itch N=6	P
General	**Age [years]**			0.28
	Median (IQR)	64.5 (55.8 - 70.2)	68.0 (63.5 - 74.0)	
	Mean (± SD)	61.5 (± 11.7)	69.3 (± 7.7)	
	Sex: Female			0.83
	N [%]	1 (25.0%)	0 (0.0%)	
	BMI [kg/m2]			1.0
	Median (IQR)	25.6 (23.0 – 30.6)	25.6 (24.5 – 26.7)	
	Mean (± SD)	28.1 (± 8.4)	25.6 (± 1.3)	
	Duration of disease [years] Me			0.91
	dian (IQR)	7.0 (5.0 – 11.2)	11.0 (6.0 - 13.8)	
	Mean (± SD)	9.2 (± 6.1)	10.2 (± 6.0)	
	Age at onset [years]			0.48
	Median (IQR)	53.5 (49.0 - 56.8)	57.5 (52.5 - 66.2)	
	Mean (± SD)	52.2 (± 11.5)	59.2 (± 9.6)	
	Palpable Lymph nodes			0.63
	N [%]	4 (100.0%)	4 (66.7%)	
	Stage of disease			0.43
	MF IA	0 (0.0%)	2 (33.3%)	
	MF IB	2 (50.0%)	2 (33.3%)	
	MF IIB	2 (50.0%)	2 (33.3%)	
MF specific disease severity	**mSWAT [points]**			**0.042**
	Median (IQR	**22.1 (10.3 - 40.4)**	**3.5 (2.2 - 8.5)**	
	Mean (± SD)	**28.6 (± 26.2)**	**5.0 (± 4.0)**	
Involved body surface area (BSA)	**BSA [%]**			**0.014**
	Median (IQR	**11.0 (10.4 - 15.0)**	**3.5 (1.2 - 5.4)**	
	Mean (± SD)	**14.4 (± 8.5)**	**3.4 (± 2.3)**	
Patient global assessment (PGA)	**PGA-VAS [0-10 VAS scale]**			**0.025**
	Median (IQR	**6.1 (5.5 - 6.8)**	**0.4 (0.0 - 2.1)**	
	Mean (± SD)	**6.2 (± 1.2)**	**1.5 (± 2.1)**	
	PGA-L [Likert scale]			**0.031**
	Median (IQR)	**1.5 (1.0 - 2.2)**	**0.0 (0.0 - 0.8)**	
	Mean (± SD)	**1.8 (± 1.0)**	**0.3 (± 0.5)**	
Quality of life (Qol) assessment	**PGA-Qol-VAS [0-10 VAS scale]**			**0.013**
	Median (IQR)	**3.5 (2.4 – 5.3)**	**0.2 (0.0 - 0.6)**	
	Mean (± SD)	**4.2 (± 2.7)**	**0.3 (± 0.3)**	
	PGA-Qol-L [Likert scale]			**0.025**
	Median (IQR)	**1.0 (0.8 – 1.5)**	**0.0 (0.0 – 0.0)**	
	Mean (± SD)	**1.2 (± 1.3)**	**0.0 (± 0.0)**	
	DLQI [points]			**0.011**
	Median (IQR)	**5.0 (4.8 – 5.5)**	**0.0 (0.0 – 0.8)**	
	Mean (± SD)	**5.2 (± 1.3)**	**1.2 (± 1.3)**	
	ItchyQoL-t [points]			**0.006**
	Median (IQR)	**2.0 (1.7 – 2.2)**	**1.0 (1.0 – 1.0)**	
	Mean (± SD)	**2.0 (± 0.4)**	**1.0 (± 0.0)**	

Bold numbers mark significant values.
MF, Mycosis fungoides; mSWAT, Modified Severity-Weighted Assessment Tool; BMI, Body mass index; BSA, Body surface area; PGA, Patient global Assessment; QoL, Quality of Life; DLQI, Dermatology Life Quality Index; N, Number; IQR, Interquartile range; SD, Standard deviation; Continuous variables were compared using Wilcoxon rank test and categorical variables using Chi2 test.

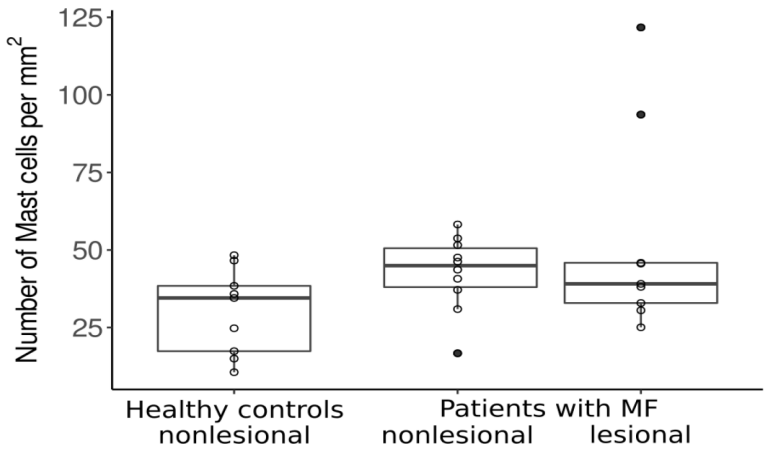


FIGURE 1
Mast cell counts in the papillary dermis of healthy patients and patients with MF. MF, Mycosis fungoides.

Serum tryptase levels were numerically higher in MF patients with itch (Table 2B). Three of the four patients with chronic itch, but none of the six patients without, had tryptase levels above >6µg/l. ECP and MBP levels were not linked to itch (Table 2B; Figure 3).

Discussion

Here, for the first time, we aimed to investigate the possible role of MCs, Eos and their mediators in MF by analyzing both skin and blood samples of patients.

TABLE 2B Histological and serological differences of MF patients with and without itch.

		MF with itch	MF without itch	P
Histological parameters	**MC numbers [per mm^2] (full dermis)**			0.25
	Median (IQR)	18.7 (18.0 - 34.1)	35.1 (29.3 - 52.0)	
	Mean (± SD)	28.5 (± 18.1)	40.4 (± 15.0)	
	MC numbers [per mm^2] (papillary dermis)			0.38
	Median (IQR)	38.1 (31.6 – 41.9)	42.5 (34.4 – 81.7)	
	Mean (± SD)	36.3 (± 10.4)	60.6 (± 37.9)	
	Eos numbers [per mm^2] (full dermis)			0.88
	Median (IQR)	0.4 (0.2 - 0.4)	0.2 (0.2 - 0.2)	
	Mean (± SD)	0.3 (± 0.3)	0.3 (± 0.3)	
	Eos numbers [per mm^2] (papillary dermis)			1.0
	Median (IQR)	0.7 (0.3 – 1.1)	0.6 (0.1 - 1.7)	
	Mean (± SD)	0.8 (± 0.8)	0.9 (± 1.0)	
Serological markers	**Tryptase [µg/l]**			0.16
	Median (IQR)	8.1 (7.0 – 8.5)	5.2 (4.7 - 5.9)	
	Mean (± SD)	7.4 (± 2.1)	5.0 (± 1.2)	
	MBP [ng/ml]			0.35
	Median (IQR)	329.0 (297.6 - 350.0)	428.3 (301.5 - 688.7)	
	Mean (± SD)	318.7 (± 46.4)	694.4 (± 777.2)	
	ECP [ng/ml]			0.17
	Median (IQR)	15.6 (12.2 - 31.9)	11.2 (10.1 - 12.2)	
	Mean (± SD)	28.5 (± 28.8)	14.3 (± 10.4)	

MC, Mast cell; Eos, Eosinophils; MBP, Major Basic Protein; ECP, Eosinophil Cationic Protein; N, Number; IQR, Interquartile range; SD, Standard deviation; Continuous variables were compared using Wilcoxon rank test; Number of patients: Histological parameters "MF with itch", N=3, "MF without itch", N=5 and Serological markers "MF with itch", N=4, "MF without itch", N=6.

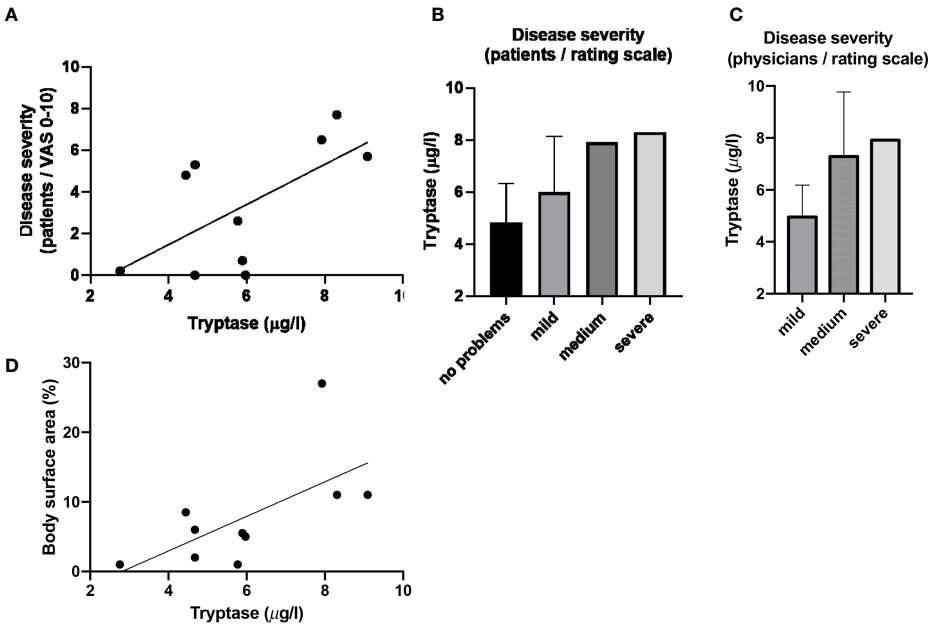


FIGURE 2
Blood tryptase counts correlate with disease severity and affected body surface area. **(A)** Serum Tryptase levels plottet against severity evaluated by patients using VAS (including depiction of linear correlation). **(B)** Tryptase versus disease severity evaluated by patients using rating scale (values given as mean and SD). **(C)** Tryptase versus disease severity evaluated by physicians using rating scale (values given as mean and SD). **(D)** Serum Tryptase levels plotted against affected body surface area (including depiction of linear correlation).

Of our ten MF patients, four had chronic pruritus, which is in line with previous reports that itch in MF is frequent, with up to two thirds of patients affected in some studies (35–37). Our findings also confirm that pruritus, in patients with MF, is linked to poor quality of life. Previous MF studies had shown that itch can significantly affect many aspects of quality of life, including sleep (38) and mental wellbeing (39). In line with these reports, we also saw a significantly stronger quality of life impairment in MF patients with pruritus compared to patients without itch in our study. Interestingly, we found a strong and significant difference regarding higher disease severity assessed by BSA and mSWAT in MF patients with itch, irrespective of their disease stage (see Table 2). To our knowledge, this has not been reported before, as published reports have shown association with advanced disease stages, but not clinical severity (37, 40).

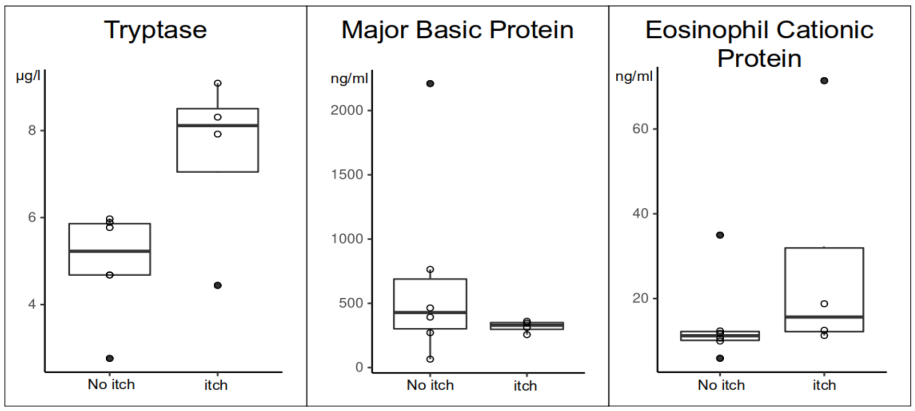


FIGURE 3
Differences of blood tryptase, MBP and ECP levels in MF patients with itch (itch) and without itch (no itch).

The underlying pathomechanisms of pruritus in MF and other cutaneous lymphomas remain unknown. MCs have been suspected to play an important role, since elevated numbers had been reported, especially in patients with more advanced stages and pruritus (4, 41). We also reinforce the evidence that MCs are increased in the skin of patients with MF, in our cohort particularly in lesional skin. Of note, the two patients with markedly elevated levels of MCs in the papillary dermis of lesional skin had low BSA involvement (up to 2%) and a lower mSWAT compared to the other patients. This would rather suggest a protective role of MCs in disease control and would be in contrast to prior publications that have shown that increased MC numbers were linked to tumor stage and advanced level of invasiveness, suggesting that MCs have a pro-tumorigenic role in MF (10, 15, 16). These conflicting data should encourage studies that further investigate the role of MCs in MF, since their presence in MF could not only be seen as a pro-tumorigenic, but also as a mechanism of the innate immune system attempting to control the tumor cells. However, since our cohort was very small, no clear conclusion can be drawn for the role on MCs in MF.

A recent study from Japan showed that the number of eosinophils, but not MCs, in the skin of patients with MF were increased in patients with intense itch (11). In our study, neither the number of eosinophils in the skin of MF patients, nor eosinophil-related mediators were elevated or correlated with disease severity, itch, or BSA. Further studies, ideally in larger and more diverse and multicenter patient populations are needed to better characterize the role of eosinophils and eosinophil-related markers in MF.

Previous reports suggest that MCs may be drivers of itch in MF (41), but that histamine is not the key player (3), suggesting that other inflammatory MC mediators such as cytokines, prostaglandin D2, or proteases including tryptase may importantly contribute to itch in MF (42). Tryptase levels in biological fluids have previously been used as an indicator of MC numbers and activation status (43) and increase with age (44) The recently published data from a large population-based cohort hints at lower reference ranges in adults in comparison with the currently applied upper reference limit (44). Tryptase, in our MF patients, was linked to higher disease severity (reported by both patients and physicians). More importantly, serum tryptase levels were higher in the slightly younger MF patients with itch, and three of the four patients with itch had tryptase levels above >6µg/l, which is higher than the average serum tryptase of healthy individuals (45). Indeed, MC tryptase could not only be a surrogate for MC activation, it has been shown to also directly elicit itching in mice through activation of the proteinase-activated receptor-2 (PAR-2), and that the PAR-2 antagonist FSLLRY, inhibits scratching induced by tryptase (46). We, therefore, propose that tryptase could be a significant pruritogen in MF, and further studies should be conducted to investigate this.

Taken together, our results indicate that itch is an important clinical marker in MF which can be easily assessed using simple questionnaires (7, 32) and could be even explored as a tool for disease severity monitoring. Furthermore, our report suggests that MC and their mediator tryptase play a role in itch in MF.

Due to the lack of efficacy of antihistamines (3), alternative treatments for itch in MF should be explored. Currently, patients with severe itch are treated off-label with substances like aprepitant, naloxone, naltrexone, butorphanol, mirtazapine, gabapentin or thalidomide (47), with limited success and often marked side effects. Newer directed therapies (48, 49) aimed at the inhibition or depletion of skin MCs may help treat pruritus, alongside direct lymphoma targeted therapies (47).

The main limitation of our study is the small patient number of only 10, but these patients were thoroughly investigated clinically, serologically, and histologically. Small numbers limit the meaningfulness of statistical tests, and the low patient numbers is likely to be the main reason for some of our comparisons to not show statistical significance. Also, patients were not followed over time to see whether clinical changes were reflected in changes of the assessed histological or serological markers. Also, healthy controls were somewhat younger, but comparable in the assessed cellular and serological marker. However, they should be better matched in regard to sex, age and localization of the biopsies in future studies which should also include patients with more severe and extensive disease.

Nevertheless, our data encourage further exploration of a possible role of MC and their mediators in driving itch and disease severity in MF.

In conclusion, we demonstrated that itch is an important, easily assessable marker in MF and that MCs and the MC mediator tryptase could play an important pathogenic and pruritogenic role. Of course, further analysis, ideally prospective studies in larger cohorts, need to be undertaken to analyze the pathophysiological roles of MCs and tryptase in MF. The investigation of their role as potential therapeutic targets or as markers for disease severity could improve MF patient management.

Data availability statement

The raw data supporting the conclusions of this article will be made available by the authors, without undue reservation.

Ethics statement

The studies involving human participants were reviewed and approved by Charité. The patients/participants provided their written informed consent to participate in this study.

Author contributions

DT-M has collected patient data, was involved in statistical analysis and drafted the manuscript. KL and VP have collected patient data and performed laboratory analyses. KG performed

statistical analysis and drafted the manuscript. MMe, MH, and MMa were involved in study planning and proof-reading of the manuscript. SA has planned the study, coordinated the study, collected patient data, performed statistical analysis and drafted the manuscript. All authors were involved in proof-reading of the manuscript and provided input. All authors contributed to the aricle and approved the submitted version.

Conflict of interest

DT-M has received research funds and was advisor for Celldex, Novartis, Sanofi and Moxie. MMe is or recently was a speaker and/or advisor for AbbVie, Amgen, ArgenX, AstraZeneca, Bayer, Celldex, Celgene, Escient, Galderma, Grünenthal, GSK, Menlo, Novartis, Pfizer, Pharvaris, Roche, Sanofi-Aventis, Third Harmonic Bio. MMa is or recently was a speaker and/or advisor for and/or has received research funding from Allakos, Aralez, Genentech, GSK, Menarini, Merckle Recordati, Moxie, Novartis, Sanofi, MSD, and Uriach. SA has conducted studies for received research funds/was advisor for Allakos, ALK, AstraZeneca, CSL Behring, LeoPharma, Moxie, Novartis, Sanofi, Takeda, Thermofisher. Published results are part of the study ROBERTIS, funded by AstraZeneca.

The remaining authors declare that the research was conducted in the absence of any commercial or financial relationships that could be construed as a potential conflict of interest.

Publisher's note

All claims expressed in this article are solely those of the authors and do not necessarily represent those of their affiliated organizations, or those of the publisher, the editors and the reviewers. Any product that may be evaluated in this article, or claim that may be made by its manufacturer, is not guaranteed or endorsed by the publisher.

Supplementary material

The Supplementary Material for this article can be found online at: https://www.frontiersin.org/articles/10.3389/fimmu.2022.930979/full#supplementary-material

SUPPLEMENTARY FIGURE 1
Representative photos of a patient with mycosis fungoides. **(A)** An overview of a patient with MF and **(B)** A close-up of the arm, from which both skin biopsies of lesional and non-lesional skin were taken.

SUPPLEMENTARY FIGURE 2
Mast cell numbers are increased in lesional skin of MF patients. Histological pictures of MC in Giemsa stainings are depicted of healthy control skin **(A, B)**, lesional skin **(C, D)** and non-lesional skin **(E, F)** of a representative MF patient. Pictures **(A, C, E)** are shown as 20 fold magnification, pictures **(B, D, F)** in 40 fold magnification of marked area. Arrows point towards MCs.

SUPPLEMENTARY FIGURE 3
Postulated mechanism of pruritus induction in MF patients (1).Higher number of mast cells in the papillary dermis (2). Increased levels of tryptase in the skin (3). Tryptase-induced, PAR-2-mediated pruritus

SUPPLEMENTARY TABLE 1
Correlation of MC numbers in skin with clinical markers of MF. MF, Mycosis fungoides; mSWAT, Modified Severity-Weighted Assessment Tool; BSA, Body surface area; PGA, Patient Global Assessment; QoL, Quality of Life; DLQI, Dermatology Life Quality Index; N, Number; R, Spearman's R; for correlations the Spearman correlation was used

SUPPLEMENTARY TABLE 1
Correlation of serological markers with clinical markers of MF. MF, Mycosis fungoides; MBP, Major Basic Protein; ECP, Eosinophil Cationic Protein; mSWAT, Modified Severity-Weighted Assessment Tool; BSA, Body surface area; PGA, Patient Global Assessment; QoL, Quality of Life; DLQI, Dermatology Life Quality Index; N, Number; R, Spearman's R; for correlations the Spearman correlation was used.

SUPPLEMENTARY TABLE 2
Comparison of serological and histological markers of MF patients and healthy controls. MF, Mycosis fungoides; MC, Mast cell; Eos, Eosinophils; MBP, Major Basic Protein; ECP, Eosinophil Cationic Protein; N, Number; IQR, Interquartile range; SD, Standard deviation; Continuous variables were compared using Wilcoxon rank test.; Number of patients: Serological markers N=10 and Histological parameters N=9.

References

1. Dermatologists B. *Mycosis fungoides - patient information leaflet*. (2019). Available at: https://www.bad.org.uk/pils/mycosis-fungoides/ (Accessed 30th July 2022).

2. Dummer R, Vermeer MH, Scarisbrick JJ, Kim YH, Stonesifer C, Tensen CP, et al. Cutaneous T cell lymphoma. *Nat Rev Dis Primers* (2021) 7(1):61. doi: 10.1038/s41572-021-00296-9

3. Meyer N, Paul C, Misery L. Pruritus in cutaneous T-cell lymphomas: frequent, often severe and difficult to treat. *Acta Derm Venereol* (2010) 90(1):12–7. doi: 10.2340/00015555-0789

4. Rabenhorst A, Schlaak M, Heukamp LC, Förster A, Theurich S, von Bergwelt-Baildon M, et al. Mast cells play a protumorigenic role in primary cutaneous lymphoma. *Blood* (2012) 120(10):2042–54. doi: 10.1182/blood-2012-03-415638

5. Dulmage B, Geskin L, Guitart J, Akilov OE. The biomarker landscape in mycosis fungoides and sézary syndrome. *Exp Dermatol* (2017) 26(8):668–76. doi: 10.1111/exd.13261

6. Holahan HM, Farah RS, Fitz S, Mott SL, Ferguson NN, McKillip J, et al. Health-related quality of life in patients with cutaneous T-cell lymphoma? *Int J Dermatol* (2018) 57(11):1314–9. doi: 10.1111/ijd.14132

7. Ottevanger R, van Beugen S, Evers AWM, Willemze R, Vermeer MH, Quint KD. Quality of life in patients with mycosis fungoides and sézary syndrome: a systematic review of the literature. *J Eur Acad Dermatol Venereol* (2021) 35 (12):2377–87. doi: 10.1111/jdv.17570

8. Sampogna F, Frontani M, Baliva G, Lombardo GA, Alvetreti G, Di Pietro C, et al. Quality of life and psychological distress in patients with cutaneous lymphoma. *Br J Dermatol* (2009) 160(4):815–22. doi: 10.1111/j.1365-2133.2008.08992.x

9. Shim WS, Oh U. Histamine-induced itch and its relationship with pain. *Mol Pain* (2008) 4:29. doi: 10.1186/1744-8069-4-29

10. Misery L. Frontiers in neuroscience pruritus in cutaneous T-cell lymphomas. In: E Carstens, T Akiyama, editors. *Itch: Mechanisms and*

treatment. Boca Raton (FL: CRC Press/Taylor & Francis © 2014 by Taylor & Francis Group, LLC (2014).

11. Shimizu K, Andoh T, Makino T, Yoshihisa Y, Mizawa M, Shimizu T. Mechanisms of itching in mycosis fungoides: grade of itching correlates with eosinophil infiltration and kallikrein 5 expression. *Eur J Dermatol* (2019) 29 (3):268–73. doi: 10.1684/ejd.2019.3560

12. Dalton SR, Chandler WM, Abuzeid M, Hossler EW, Ferringer T, Elston DM, et al. Eosinophils in mycosis fungoides: an uncommon finding in the patch and plaque stages. *Am J Dermatopathol* (2012) 34(6):586–91. doi: 10.1097/DAD.0b013e31823d921b

13. Shelburne CP, Abraham SN. The mast cell in innate and adaptive immunity. *Adv Exp Med Biol* (2011) 716:162–85. doi: 10.1007/978-1-4419-9533-9_10

14. Tsai M, Grimbaldeston M, Galli SJ. Mast cells and immunoregulation/immunomodulation. *Adv Exp Med Biol* (2011) 716:186–211. doi: 10.1007/978-1-4419-9533-9_11

15. Melillo RM, Guarino V, Avilla E, Galdiero MR, Liotti F, Prevete N, et al. Mast cells have a protumorigenic role in human thyroid cancer. *Oncogene* (2010) 29(47):6203–15. doi: 10.1038/onc.2010.348

16. Ribatti D, Ennas MG, Vacca A, Ferreli F, Nico B, Orru S, et al. Tumor vascularity and tryptase-positive mast cells correlate with a poor prognosis in melanoma. *Eur J Clin Invest* (2003) 33(5):420–5. doi: 10.1046/j.1365-2362.2003.01152.x

17. Varricchi G, Galdiero MR, Loffredo S, Marone G, Iannone R, Marone G, et al. Are mast cells MASTers in cancer? *Front Immunol* (2017) 8. doi: 10.3389/fimmu.2017.00424

18. Li L, Dang Q, Xie H, Yang Z, He D, Liang L, et al. Infiltrating mast cells enhance prostate cancer invasion *via* altering LncRNA-HOTAIR/PRC2-androgen receptor (AR)-MMP9 signals and increased stem/progenitor cell population. *Oncotarget* (2015) 6(16):14179–90. doi: 10.18632/oncotarget.3651

19. Strouch MJ, Cheon EC, Salabat MR, Krantz SB, Gounaris E, Melstrom LG, et al. Crosstalk between mast cells and pancreatic cancer cells contributes to pancreatic tumor progression. *Clin Cancer Res* (2010) 16(8):2257–65. doi: 10.1158/1078-0432.CCR-09-1230

20. Weber A, Maurer M. Skin site mast cell numbers correlate with rates of nodular growth, but not incidence, of basal cell carcinoma. *Dermatology* (2005) 211 (3):298–9. doi: 10.1159/000087030

21. Rajput AB, Turbin DA, Cheang MC, Voduc DK, Leung S, Gelmon KA, et al. Stromal mast cells in invasive breast cancer are a marker of favourable prognosis: a study of 4,444 cases. *Breast Cancer Res Treat* (2008) 107(2):249–57. doi: 10.1007/s10549-007-9546-3

22. Welsh TJ, Green RH, Richardson D, Waller DA, O'Byrne KJ, Bradding P. Macrophage and mast-cell invasion of tumor cell islets confers a marked survival advantage in non-small-cell lung cancer. *J Clin Oncol* (2005) 23(35):8959–67. doi: 10.1200/JCO.2005.01.4910

23. Krystel-Whittemore M, Dileepan KN, Wood JG. Mast cell: A multi-functional master cell. *Front Immunol* (2015) 6:620. doi: 10.3389/fimmu.2015.00620

24. Tancrède-Bohin E, Ionescu MA, de la Salmonière P, Dupuy A, Rivet J, Rybojad M, et al. Prognostic value of blood eosinophilia in primary cutaneous T-cell lymphomas. *Arch Dermatol* (2004) 140(9):1057–61. doi: 10.1001/archderm.140.9.1057

25. Terada T. Mycosis fungoides in plaque stage with pronounced eosinophilic infiltration, folliculotropism, and concomitant invasive squamous cell carcinoma. *Int J Clin Exp Pathol* (2013) 6(4):749–56.

26. Payne V, Kam PC. Mast cell tryptase: a review of its physiology and clinical significance. *Anaesthesia* (2004) 59(7):695–703. doi: 10.1111/j.1365-2044.2004.03757.x

27. Willemze R, Cerroni L, Kempf W, Berti E, Facchetti F, Swerdlow SH, et al. The 2018 update of the WHO-EORTC classification for primary cutaneous lymphomas. *Blood* (2019) 133(16):1703–14. doi: 10.1182/blood-2018-11-881268

28. Fitzpatrick TB. The validity and practicality of sun-reactive skin types I through VI. *Arch Dermatol* (1988) 124(6):869–71. doi: 10.1001/archderm.1988.01670060015008

29. Olsen EA, Kim YH, Kuzel TM, Pacheco TR, Foss FM, Parker S, et al. Phase IIb multicenter trial of vorinostat in patients with persistent, progressive, or treatment refractory cutaneous T-cell lymphoma. *J Clin Oncol* (2007) 25 (21):3109–15. doi: 10.1200/JCO.2006.10.2434

30. Olsen EA, Whittaker S, Kim YH, Duvic M, Prince HM, Lessin SR, et al. Clinical end points and response criteria in mycosis fungoides and sézary syndrome: a consensus statement of the international society for cutaneous lymphomas, the united states cutaneous lymphoma consortium, and the cutaneous lymphoma task force of the European organisation for research and treatment of cancer. *J Clin Oncol* (2011) 29(18):2598–607. doi: 10.1200/JCO.2010.32.0630

31. Desai NS, Poindexter GB, Monthrope YM, Bendeck SE, Swerlick RA, Chen SC. A pilot quality-of-life instrument for pruritus. *J Am Acad Dermatol* (2008) 59 (2):234–44. doi: 10.1016/j.jaad.2008.04.006

32. Krause K, Kessler B, Weller K, Veidt J, Chen SC, Martus P, et al. German Version of ItchyQoL: validation and initial clinical findings. *Acta Derm Venereol* (2013) 93(5):562–8. doi: 10.2340/00015555-1544

33. Finlay AY, Khan GK. Dermatology life quality index (DLQI)–a simple practical measure for routine clinical use. *Clin Exp Dermatol* (1994) 19(3):210–6. doi: 10.1111/j.1365-2230.1994.tb01167.x

34. Weber A, Knop J, Maurer M. Pattern analysis of human cutaneous mast cell populations by total body surface mapping. *Br J Dermatol* (2003) 148(2):224–8. doi: 10.1046/j.1365-2133.2003.05090.x

35. Bradford PT, Devesa SS, Anderson WF, Toro JR. Cutaneous lymphoma incidence patterns in the united states: a population-based study of 3884 cases. *Blood* (2009) 113(21):5064–73. doi: 10.1182/blood-2008-10-184168

36. Ku LS, Lo KK. Mycosis fungoides–a retrospective study of 40 cases in Hong Kong. *Int J Dermatol* (2005) 44(3):215–20. doi: 10.1111/j.1365-4632.2004.02362.x

37. Vij A, Duvic M. Prevalence and severity of pruritus in cutaneous T cell lymphoma. *Int J Dermatol* (2012) 51(8):930–4. doi: 10.1111/j.1365-4632.2011.05188.x

38. Hawro T, Hawro M, Zalewska-Janowska A, Weller K, Metz M, Maurer M. Pruritus and sleep disturbances in patients with psoriasis. *Arch Dermatol Res* (2020) 312(2):103–11. doi: 10.1007/s00403-019-01998-7

39. Molloy K, Jonak C, Woei AJF, Guenova E, Busschots AM, Bervoets A, et al. Characteristics associated with significantly worse quality of life in mycosis fungoides/Sézary syndrome from the prospective cutaneous lymphoma international prognostic index (PROCLIPI) study. *Br J Dermatol* (2020) 182 (3):770–9. doi: 10.1111/bjd.18089

40. Green SB, Byar DP, Lamberg SI. Prognostic variables in mycosis fungoides. *Cancer* (1981) 47(11):2671–7. doi: 10.1002/1097-0142(19810601)47:11<2671::AID-CNCR2820471125>3.0.CO;2-X

41. Yamamoto T, Katayama I, Nishioka K. Role of mast cell and stem cell factor in hyperpigmented mycosis fungoides. *Blood* (1997) 90(3):1338–40. doi: 10.1182/blood.V90.3.1338

42. Garcovich S, Maurelli M, Gisondi P, Peris K, Yosipovitch G, Girolomoni G. Pruritus as a distinctive feature of type 2 inflammation. *Vaccines (Basel)* (2021) 9(3):303. doi: 10.3390/vaccines9030303

43. Schwartz LB. Clinical utility of tryptase levels in systemic mastocytosis and associated hematologic disorders. *Leuk Res* (2001) 25(7):553–62. doi: 10.1016/S0145-2126(01)00020-0

44. Slot MC, Claessen LHJ, Bons JAP, Menheere P, Nieuwhof CMG, de Boer D. Tryptase reference ranges are age-dependent in a large population-based cohort. *Allergy* (2022). doi: 10.1111/all.15369

45. Valent P, Sperr WR, Sotlar K, Reiter A, Akin C, Gotlib J, et al. The serum tryptase test: an emerging robust biomarker in clinical hematology. *Expert Rev Hematol* (2014) 7(5):683–90. doi: 10.1586/17474086.2014.955008

46. Ui H, Andoh T, Lee JB, Nojima H, Kuraishi Y. Potent pruritogenic action of tryptase mediated by PAR-2 receptor and its involvement in anti-pruritic effect of nafamostat mesilate in mice. *Eur J Pharmacol* (2006) 530(1-2):172–8. doi: 10.1016/j.ejphar.2005.11.021

47. Ahern K, Gilmore ES, Poligone B. Pruritus in cutaneous T-cell lymphoma: a review. *J Am Acad Dermatol* (2012) 67(4):760–8. doi: 10.1016/j.jaad.2011.12.021

48. Altrichter S, Staubach P, Pasha M, Singh B, Chang AT, Bernstein JA, et al. An open-label, proof-of-concept study of lirentelimab for antihistamine-resistant chronic spontaneous and inducible urticaria. *J Allergy Clin Immunol* (2021) 149 (5):1683–90.e7. doi: 10.1016/j.jaci.2021.12.772

49. Alvarado D, Maurer M, Gedrich R, Seibel SB, Murphy MB, Crew L, et al. Anti-KIT monoclonal antibody CDX-0159 induces profound and durable mast cell suppression in a healthy volunteer study. *Allergy* (2022). doi: 10.1111/all.15262. Epub ahead of print.

frontiers | Frontiers in Immunology

TYPE Review
PUBLISHED 14 September 2022
DOI 10.3389/fimmu.2022.937120

Check for updates

OPEN ACCESS

EDITED BY
Satoshi Tanaka,
Kyoto Pharmaceutical University, Japan

REVIEWED BY
Simon Patrick Hogan,
Michigan Medicine, University of Michigan, United States
Nicholas A. Pullen,
University of Northern Colorado, United States
Nobuhiro Nakano,
Juntendo University, Japan

*CORRESPONDENCE
Yosuke Kurashima
yosukek@chiba-u.jp

SPECIALTY SECTION
This article was submitted to Inflammation, a section of the journal Frontiers in Immunology

RECEIVED 05 May 2022
ACCEPTED 26 July 2022
PUBLISHED 14 September 2022

CITATION
Zhang Z, Ernst PB, Kiyono H and Kurashima Y (2022) Utilizing mast cells in a positive manner to overcome inflammatory and allergic diseases. *Front. Immunol.* 13:937120. doi: 10.3389/fimmu.2022.937120

COPYRIGHT
© 2022 Zhang, Ernst, Kiyono and Kurashima. This is an open-access article distributed under the terms of the Creative Commons Attribution License (CC BY). The use, distribution or reproduction in other forums is permitted, provided the original author(s) and the copyright owner(s) are credited and that the original publication in this journal is cited, in accordance with accepted academic practice. No use, distribution or reproduction is permitted which does not comply with these terms.

Utilizing mast cells in a positive manner to overcome inflammatory and allergic diseases

Zhongwei Zhang[1], Peter B. Ernst[2,3,4], Hiroshi Kiyono[4,5,6,7,8,9,10] and Yosuke Kurashima[1,6,9,10,11,12]*

[1]Department of Innovative Medicine, Graduate School of Medicine, Chiba University, Chiba, Japan, [2]Division of Comparative Pathology and Medicine, Department of Pathology, University of California, San Diego, San Diego, CA, United States, [3]Center for Veterinary Sciences and Comparative Medicine, University of California, San Diego, San Diego, CA, United States, [4]Department of Medicine, School of Medicine and Chiba University-University of California San Diego Center for Mucosal Immunology, Allergy and Vaccine (CU-UCSD), University of California, San Diego, San Diego, CA, United States, [5]Future Medicine Education and Research Organization, Chiba University, Chiba, Japan, [6]Division of Mucosal Immunology, IMSUT Distinguished Professor Unit, The Institute of Medical Science, The University of Tokyo, Tokyo, Japan, [7]Department of Human Mucosal Vaccinology, Chiba University Hospital, Chiba, Japan, [8]HanaVax Inc., Tokyo, Japan, [9]Mucosal Immunology and Allergy Therapeutics, Institute for Global Prominent Research, Chiba University, Chiba, Japan, [10]Research Institute of Disaster Medicine, Chiba University, Chiba, Japan, [11]Institute for Advanced Academic Research, Chiba University, Chiba, Japan, [12]Empowering Next Generation Allergist/immunologist toward Global Excellence Task Force toward 2030 (ENGAGE)-Task Force, Tokyo, Japan

Mast cells (MCs) are immune cells widely distributed in the body, accompanied by diverse phenotypes and functions. Committed mast cell precursors (MCPs) leave the bone marrow and enter the blood circulation, homing to peripheral sites under the control of various molecules from different microenvironments, where they eventually differentiate and mature. Partly attributable to the unique maturation mechanism, MCs display high functional heterogeneity and potentially plastic phenotypes. High plasticity also means that MCs can exhibit different subtypes to cope with different microenvironments, which we call "the peripheral immune education system". Under the peripheral immune education system, MCs showed a new character from previous cognition in some cases, namely regulation of allergy and inflammation. In this review, we focus on the mucosal tissues, such as the gastrointestinal tract, to gain insights into the mechanism underlying the migration of MCs to the gut or other organs and their heterogeneity, which is driven by different microenvironments. In particular, the immunosuppressive properties of MCs let us consider that positively utilizing MCs may be a new way to overcome inflammatory and allergic disorders.

KEYWORDS

mast cells, heterogeneity, inflammation, allergy, tolerance

Introduction

MCs predate the emergence of acquired immunity, since they were first named in 1878, a broad understanding of MCs biology has been published (1). Recently, an investigation of the hematopoietic origin of connective tissue MCs using fate-mapping systems has revealed the dual developmental origin of MCs (2). It was found that most connective tissue MCs (CTMCs) are derived from late erythro-myeloid progenitors (EMPs) produced in the yolk sac at E8.5 (the second transient definitive wave of fetal hematopoiesis), while mucosal MCs (MMCs) seem to come from hematopoietic stem cells (HSCs) in the bone marrow in mice (3). Committed progenitor cells enter the bloodstream, where they are found as lineage-negative Lin^- c-Kit $(CD117)^{hi}$ $Fc\varepsilon RI^+$ $\beta7\text{-integrin}^{hi}$ $ST2^+$ $CD16/32^{hi}$ or $Fc\varepsilon RI^-$ cells (4). In human beings, Lin^- $c\text{-}Kit^{int/hi}$ $Fc\varepsilon RI^+$ $\beta7\text{-integrin}^+$ $CD34^{hi}$ blood cells are considered the immediate precursor of MCs (5). These MCPs travel in the blood circulation and eventually arrive at the peripheral tissues [e.g., skin, respiratory tract, urogenital tract, gastrointestinal tract, etc. (1)] under the stimulation and induction of various factors such as chemokine receptors and adhesion molecules. For example, in the context of microbiota-influence, MCs migrate to the intestinal tract and mature under the regulation of various pathways [e.g., α4β7-MAdCAM-1/VCAM-1 (6, 7), CXC chemokine receptor 2 (CXCR2) (7) sphingosine 1-phosphate (S1P) (8)].

In the process of migration and maturation, MCs of different origins showed distinct preferences in tissue localization (6). For instance, only the adipose and pleural cavity MCs were derived from early EMPs, most of which were replaced by late EMPs during adulthood in mice (3). Late EMPs generate most of the MCs that home to connective tissues, while mucosal MCs mainly derive from fetal hematopoietic stem cells HSCs (3). Diverse tissue preferences also shape remarkable phenotypical and functional heterogeneity, suggesting that MCs may perform various functions in response to different physiological and pathological states (9).

Besides the developmental origin, differences in the tissue microenvironment are also important causes of MC heterogeneity (10). It is clear that MCs in different organs have noticeable differences (11). However, even in the same organ, the microenvironment under different pathological or physiological conditions can produce utterly distinct MC subtypes. Take some examples, in the lung, only MCs of the proximal lung express MRGPRX2, but not of the distal or medial lung (12); in the gut, both CTMCs and MMCs are present and can be transformed into each other in some cases, such as food allergy (13). All this evidence supports the remarkable microenvironment-dependent heterogeneity in MCs.

Different cellular phenotypes bring different functions—one of the representative features of the heterogeneity of MC is regulatory-like properties against inflammation and allergy. In some occasions, MCs have been shown to release cytokines to inhibit and terminate inflammatory and allergic responses (e.g., IL-2 (14) IL-10 (14–16), and TGF-β1 (17), etc.). In addition, MCs interact with regulatory T cells (Tregs) (14, 18–21) and alternatively activated macrophages (AAMΦs) (22) to inhibit inflammatory and allergic responses.

In addition, various MC-derived cytokines [e.g., IL-4, IL-8, IL-13, IL-22, TNF-α, TGF-β1, vascular endothelial growth factor (VEGF), nerve growth factor (NGF), fibroblast growth factor-2 (FGF-2), and platelet-derived growth factor (PDGF)], proteases (tryptase and chymase/chymotrypsin), histamines, lipid mediators [PGD2 and leukotrienes (LTs), etc.] participate in the process of wound healing [e.g., vascular permeability and immune cells recruitment (monocytes and neutrophils), epithelial proliferation and migration, granular formation and remodeling, and scar formation, etc.] (11, 23).

Collectively, MCs play a diverse role in various physiological and pathological processes due to their highly complex heterogeneity. A full understanding of the phenotypic characteristics and functional heterogeneity of MCs in specific diseases will help us create efficient individualized therapy.

Aggregation of mast cells at intestinal mucosal sites

MCs exists in virtually all organs of vertebrates but different widely in their number, phenotype, and function (1). The high heterogeneity is partly attributed to their unique and complex maturation process. Although controversial (11), MCs are believed to have two main origins, bone marrow and yolk sac (2). After leaving the hematopoietic tissue, committed progenitor cells enter the blood, migrate, and colonize the target tissue [e.g., skin, respiratory tract, genitourinary tract, gastrointestinal tract, etc. (1)]. Notably, the exact ontogeny of mice adult MCs has been suggested in recent studies; early EMPs, late EMPs, and fetal HSCs are successively involved in the maturation of fetal MCs (2, 3). Using the inducible runt-related transcription factor1 *(Runx1-icre)* and colony stimulatory factor 1 receptor *(Csf1r-icre)* fate-mapping systems, Zhiqing Li et al. separately traced three waves of hematopoiesis (3). They confirmed that late EMP-derived MCs, as long-lived cells, gradually replace early EMPs and become the main contributors to the adult CTMC pool. Early EMP-derived MCs show a short lifespan in connective tissue, only appearing in adipose tissue and the pleural cavity. Fetal HSC-derived MCs, another possible type of short-lived cells, are mainly located in mucosal tissues and constantly renewed by the bone marrow (3). Therefore, there are at least two ways that MCs mature in mice. However, whether these pathways apply to other mammals, including humans, is not fully understood.

After arriving in the peripheral tissues, MCPs finally differentiate into mature MCs with the stimulation of local cytokines and growth factors in humans (e.g., IL-4 (24), IL-9 (25), IL-33 (26, 27), and TGF-β1 (28), etc.) and mice (e.g., IL-3 (29), IL-4 (28), TGF-β1 (28), and NGF (30), etc.). However, unlike other granulocytic leukocytes (e.g., neutrophils, eosinophils, and basophils), MCs mature in peripheral sites rather than bone marrow. Consequently, there are very few MCPs or mature MCs in bone marrow and blood, so it is relatively difficult to evaluate human MCs. Moreover, the molecular expression necessary for MC migration varies not only during maturation, but also according to cellular charcteristics, such CMMCs or MMCs (31, 32). All of these make it relatively difficult to study human MCs *in vitro*. So far, MCs are studied mainly in rodents (e.g., genetically modified mice) or some malignant MCs cell lines (33, 34). We herein describe some mechanisms by which MCs migrate to the intestinal tract and mature in combination with current findings (Figure 1).

The intestinal mucosa, which is exposed to various foreign components (including microbiota and food components), is one of the primary destinations for MCs and the pool for MCPs (35). MCs have been reported to account for approximately 2% of the cells in the lamina propria of the gastrointestinal tract (36). There is no doubt that integrin α4β7 plays a critical role in the migration of MCs to the intestinal mucosa. MCPs is utterly absent in the small intestine of α4β7-deficient mice (6). Evidence suggests that integrin α4β7 interacts with vascular endothelial molecules, including mucosal addressing protein cell adhesion molecule-1 (MAdCAM-1) and vascular cell adhesion molecule-1 (VCAM1), to facilitate directional migration of MCPs across endothelial cells to the small intestine (6, 7).

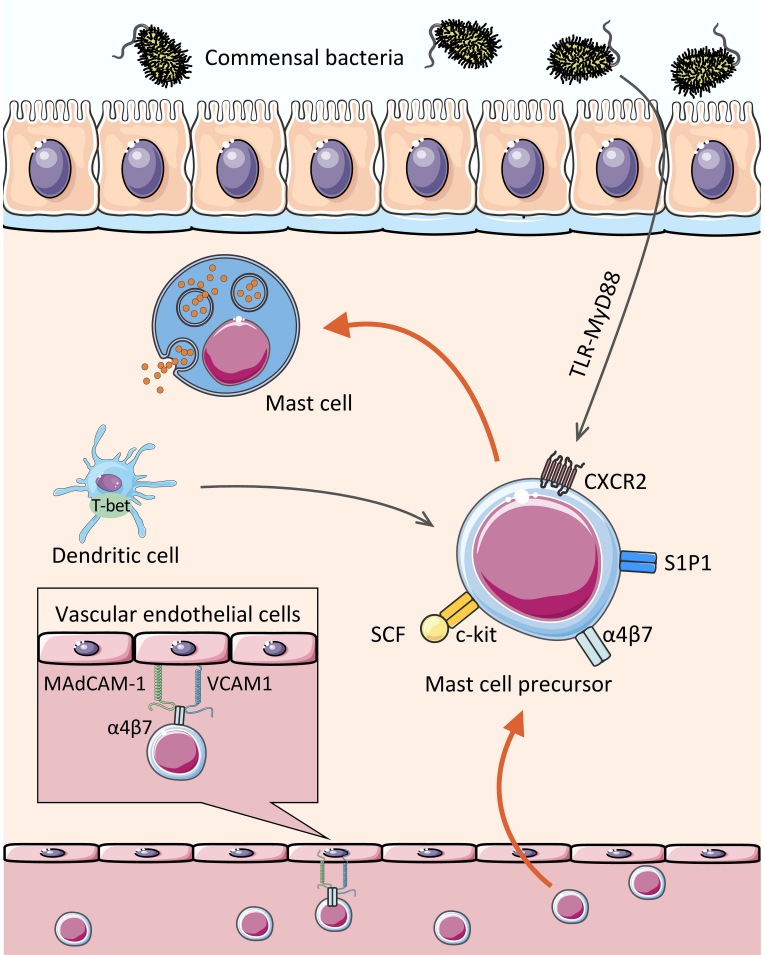


FIGURE 1
Assembly of MCs in the gut. The MCPs leave the hematopoietic tissue, enter the blood stream, migrate and colonize the target tissue. With c-kit, CXCR2, and integrin α4β7 on the cell surface, MCPs bind to MAdCAM-1 and VCAM1 on the vascular endothelial cells, thereby crossing the vascular endothelium and colonizing the intestinal mucosa and submucosa, where they mature. In addition, transcription factor (dendritic cell-derived T-bet), Lipid mediator (sphingosine 1-phosphate), and some intestinal microbiota affect the homing of MCs to the gut.

Like all blood-borne leukocytes, adhesion interactions are not the only requirement for MCPs recruitment to peripheral tissues, but also the migration to target tissues. Stem cell factor (SCF) has chemotactic effects on both mouse (37) and human (38) MCs *in vitro*. *In vivo*, SCF activates the c-kit expressed by MCs (or MCPs) through PI3K, then mediates migration, survival, proliferation, and activation with the help of α4 integrin (39–42). No intestinal MCPs was detected in SCF-deficient mice (6).

CXCR2 also contributes to the migration of MCs. It was experimentally demonstrated that MCs lacking CXCR2 are less able to migrate to the small intestine (7). Although the research of MC migration by CXCR2 is not detailed, the role of CXCR2 has been extensively studied in other cells. For example, in rat cardiogenic endothelial cells, the binding of CXCR2 and its ligand CXCL5 leads to downstream PI3K activation and further cytokine production (43). Another study in which human CXCR2 was stably transfected into lymphoblastic JY cell lines showed that the activation of IL-8 (CXCR2 ligand) induced transient adhesion of α4β7 dependent on VCAM-1 (44). Consequently, it is reasonable to speculate that in the circulatory system, c-kit and CXCR2 expressed by MCPs can interact with their respective ligands to upregulate the affinity of α4β7 integrin with MAdCAM-1 and VCAM-1, and also enhance the expression of VCAM-1 on epithelial cells *via* PI3K pathway (45), which further promotes the migration of MCs (7).

Previous studies have indicated that gut microbiota can mediate the constitutive migration of MCs into the intestine (46). Germ-free (GF) mice showed a lower intestinal MC density and higher blood MCs density compared to SPF (specific pathogen free) mice, followed by an impaired intestinal MCs function and maturity (reduced edema was observed after injecting the degranulation-provoking compound 48/80) (47). In detail, the expression of CXCR2 ligands, e.g., CXCL2, CXCL2, and CXCL5, were significantly reduced in the intestinal epithelial cells of GF mice and MyD88$^{-/-}$ mice compared to the control group (46). Results revealed that the expression of CXCR2 ligands in intestinal epithelial cells induced by intestinal microbiota was at least partially dependent on the Toll-like receptor (TLR) -MyD88 pathway, which promotes MC migration to the intestine. It remains to be seen whether intestinal bacteria directly or indirectly affect MC recruitment *via* their components and metabolites.

Interestingly, intestinal migration of MCs appears to be induced by a combination of gut bacteria, rather than a single bacterial strain. A study based on the Gram-positive *Lactobacillus plantarum* provided partial evidence that a single strain did not seem to mediate MC migration (47). Martin Schwarzer et al. found GF mice showed lower levels of CXCL1 and CXCL2 in the jejunal with fewer and less mature intestinal MCs in comparison to conventional mice after the induction of food allergy. In detail, the susceptibility to allergy symptoms in GF mice was fully restored after they were cohoused with conventional mice. However, similar results were not observed in mice mono-colonized with *L. plantarum* (47). *L. plantarum* was previously shown to aggravate allergic reactions associated with degranulation of MCs (48). Thus, it remains to be determined whether other single strains (e.g., Gram-negative bacteria) or specific bacterial products affect MC migration and maturation.

In addition, T-bet, a Th1-specific T-box transcription factor expressed by leukocytes [e.g., natural killer (NK) cells, dendritic cells (DCs), and CD8$^+$ T cells], seems to mediate the migration of MCPs to the intestinal tract indirectly. Pilar Alcaide et al. found that T-bet$^{-/-}$ mice showed lower number of MCPs homing to the small intestine or lungs (49). It is worth mentioning that T-bet expressing DCs somehow contribute to the migration of MCs since MC itself does not seem to express T-bet during development (49).

Moreover, our previous studies showed that S1P mediates the migration of MCs to the large intestine (8). S1P is a sphingolipid metabolite from platelets and MCs, which is thought to play a role in mediating the migration of lymphocytes from secondary lymphoid organs and the thymus (50). It has been know that MCs express various types of S1P receptors, including type I S1P receptor ($S1P_1$) (8), associated with G_i protein and small GTPases (e.g., Rho and Rac) (51, 52). By administration of FTY720 to mice, a blocker of $S1P_1$-mediated signaling, we found that FTY720 can directly inhibit the migration of MCs, demonstrating the requirement of S1P-$S1P_1$ signaling for MC migration (8).

Heterogeneity of mast cells and the peripheral education system according to the microenvironment

The unique maturation mechanism of MCs also contributes to their astonishing plasticity and heterogeneity, which fully reflects the complex interaction between MCs and microenvironmental signals transmitted by different tissues (10). Traditionally, MCs are classified according to the production of serine proteases, such as trypsin and chymase (11, 53). In mice, MCs are divided into MMCs and CTMCs (11, 53). MMCs, as the name implies, mainly exist in the mucosa (e.g., the intestinal mucosa) and express chymase mMCP-1 and mMCP-2. MMCs are the dominant phenotype in the mucous layer, such as the gut (53). CTMCs can be found in connective tissue (e.g., intestinal submucosa, peritoneum, and skin) (1, 11, 54). CTMCs express chymase mMCP-4, trypsin (mMCP-6 and mMCP7), elastase (mMCP-5), and carboxypeptidase A3, etc. (1, 11, 54). Besides, the cytoplasm of CTMCs contains higher concentrations of heparin proteoglycan, histamine, and prostaglandin D2, while MMCs granules contain almost no heparin proteoglycan and lower levels of histamine (53, 55). Aside from the differences between the anatomic location and

protease composition, MMCs and CTMCs vary in the requirement of T cells-derived cytokines, IL-3, and IL-4 (56) (Figure 2). Similar to mouse MCs, human MCs can be divided into two types: one subtype secretes both tryptase, chymase and carboxypeptidase A3 (MC_{TC}); the other secretes tryptase alone (MC_T) (1). The former is similar to mouse CTMCs, while the latter is equivalent to MMCs. MC_{TC} is mainly distributed in the skin and small intestinal submucosa, and participates in pathological processes, such as urticaria (57). MC_T is mostly expressed in the lung and small intestinal mucosa and is related to asthma and food allergy (1). In the intestine, it is reported that MC_T accounts for approximately 98% of the total MC population in the mucous layer but only 13% of the total MC population in the intestinal submucosa (58), while MC_{TC} accounts for approximately 77% of the MC population in the submucosa (59). Another phenotype, MC_C, has also been mentioned in the intestinal mucosa (60). MC_C seems rich in chymase but deficient in tryptase (60). MC_C accounts for about 7% of the MCs in the intestinal mucosa and 17% in the intestinal submucosa (60); however, MC_C does not seem to be a unique population, given the small number of reports.

With the progression of research, it is currently considered that the existing MC classification system cannot distinguish the highly microenvironment-dependent MC heterogeneity (10, 54). For example, it has been revealed that CTMCs can express different protease phenotypes in different microenvironments within tissue locations in mice. CTMCs in trachea are mMCP-1^+, -2^+, -4 to 7^+, and $CPA3^+$, while those in skin and gut are only mMCP-4 to 7^+, and $CPA3^+$ (61). The ImmGen-project-derived microarray data also indicated that CTMCs subpopulations present more or less tissue-specific genetic programming differences in distinct anatomical locations, such as the skin, tongue, esophagus, trachea, and peritoneal cavity in mice (9). It has been reported that only 110 genes differentially expressed in tongue relative to trachea MCs and 122 in tongue relative to esophagus MCs. However, the difference in gene expression transcripts in peritoneal MCs relative tongue and skin MCs was 612 and 957, respectively (9). As a result, there is a growing call for a new classification method.

The plasticity of MCs in different environments has been well described. The most obvious evidence is that human MCs cultured from progenitor cells that obtained from different sites (e.g., peripheral blood, bone marrow, and cord blood) show significantly different in the expressions of receptors and granular components, and also differ in the response to the cytokines (33, 62, 63). In addition, according to the culture conditions by incubation with IL-1β, IL-4, IL-6, TGF-β1, and lipopolysaccharide in SCF-containing medium, human MCs change the protease expressions from trypsin to chymase (64, 65). In mouse MCs, co-culture with fibroblasts and stimulation with SCF induces the ability to synthesize and store heparin (66). Our previous study found that MCs co-cultured with intestinal-derived fibroblasts produce more heparin and MCPT1 and MCPT2 (10). Skin-derived fibroblasts, on the other hand, had quite different results (i.e., the increased expression of chondroitin sulfate and MCPT4 in MCs) (10, 67). According to our previous studies, there are significant differences between MCs in different organs or tissues. For example, intestinal MCs

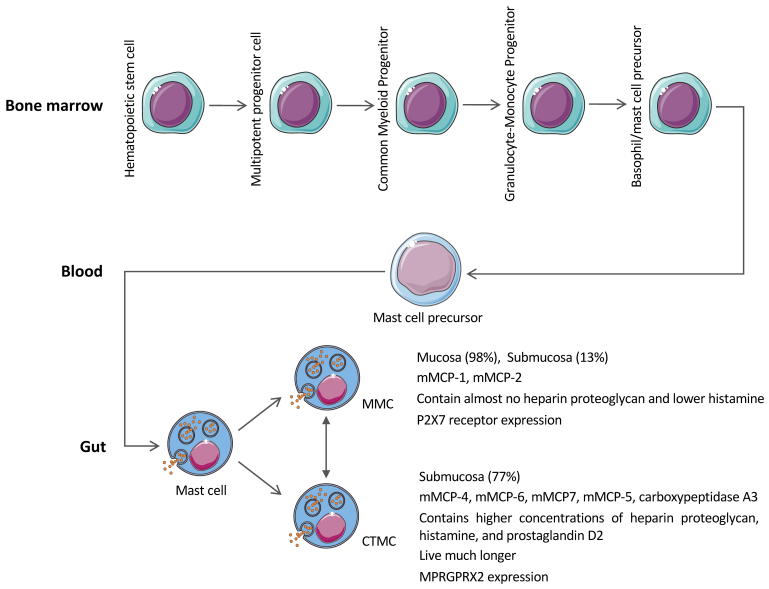


FIGURE 2
Heterogeneity of MCs. MCs mature uniquely, developing them more susceptible to the tissue homeostasis of the peripheral tissue microenvironment, and thus exhibit different subtypes and secrete different mediators to achieve different functions.

expressed high levels of the extracellular ATP receptor P2X7, which mediates the activation of MCs and worsens intestinal inflammation. In contrast, skin MCs expressed lower levels of P2X7; importantly, once the expression of P2X7 is highly induced in skin MCs, chronic inflammation occurs (10, 68). With engaging, different tissue microenvironments can produce distinct MC subtypes, which seem to be required to maintain tissue homeostasis (11). Thus, it is worth mentioning that these series of terminal maturation of MCs may receive the effect of a "peripheral immune education system" dependent on the tissue microenvironment.

The gut serves as a vast repository of agranular Lin^- c-Kit^+ $FcεRIα^-$ $α4β7^+$ IL-33$Rα^+$ $FcγRIII/II^+$ MCPs (69, 70). The gut has almost 10 times more MCPs than the bone narrow in mice (71). With the constantly-changing microenvironment, the intestinal tract is likely to create a range of diverse MC phenotypes. For example, MCs differentiate in different pathological environments and obtain a more tissue- and disease- specific phenotype relative to health conditions, which shows their extreme plasticity. Nematodes, as one of the main drivers of intestinal MCs, not only mediate the migration and expansion of MCs (71), but also induce the change of MC phenotypes. Several studies based on the *Trichinella spiralis* helminth infection model have revealed that MCs have different phenotypes at different stages of the immune response. During nematode infection, MCs in the jejunum move from the submucosa to the epithelium and sequentially expressed mMCP-2, transiently expressed mMCP-9, stopped expressing mMCP-5 to -7, and finally expressed mMCP-1 (72–74). However, in the convalescent stage of infection, MCs returned to their original site and stopped expressing mMCP-1, mMCP-2, and mMCP-5 successively, accompanied by different expression combinations of mMCP-6, -7, and -9 (72–74). The parasite repelling effect of mMCP-1 has been proven (75). In conclusion, the plasticity of MCs has been fully demonstrated by their ability to migrate at different depths in intestinal tissue for the important host defense system.

In addition to parasitic infections, increased MCs in the intestinal mucosa have also been detected in IBD (15, 76), IBS (77, 78), and food allergy (13, 79, 80). In food allergy, inoculation of food antigens leads to a dramatic increase in MMCs (due partly to infiltrating MCPs and CTMCs). Induced by TGF-β1 (81) and the Notch signaling (13) in the inflamed intestine, precursor cells mature and even undergo a reciprocal transformation of CTMCs in the submucosa and/or MMCs in the mucosa, further demonstrating the environment-dependent heterogeneity of MCs (82). Additionally, Chen et al. identified a specific group of MMCs in food allergy named MMC9 (80). MMC9 cells are a group of MMCs of Lin^- c-Kit^+ $FcεRIα^+$ $β_7$-$Integrin^{low}$ $ST2^+$, which can secrete large amounts of IL-9 and IL-13. This population of cells develops from MCPs that migrate to the intestinal mucosa with the help of IL-4. Under the action of IL-3 and SCF, MMC9 has the potential to rapidly develops into granular MCs and drive IgE-mediated food allergy (80, 83).

Crosstalk between MCs and surrounding cells has been widely discussed, which significantly increased the complexity of the terminal differentiation of MCs. For example, studies showed intestinal neurons could be activated by the increased histamine and trypsin secreted from MCs enriched in IBS (77) and IBD gut (76). Correspondingly, intestinal neurons mediated MCs activation by secreting neuronal factors (e.g., substance P, somatostatin, ATP, neuropeptide corticotropin-releasing factor, etc.) that stimulate MC surface receptors (e.g., MRGPRX2, P2X7, etc.) (78). The activation of MCs and their pro-inflammatory and pro-allergic mechanisms were described in more detail elsewhere (11). In addition to intestinal neurons, MCs also crosstalk with other cell types such as Tregs and intestinal epithelial cells to show the identity transformation from pathogenic or allergenic to regulatory, which plays a pivotal role in the fight against allergic responses (14) and inflammation (84). The transformation of MCs from pathogenic to regulatory roles will be discussed in more detail in the next section.

Notably, with the continuous development of technology, more comprehensive methods have been used to detect the phenotypes of different MC populations, such as single-cell RNA sequencing (scRNA-seq). In mice, a study on hematopoietic stem and progenitor cells (HSPCs) in mouse bone marrow showed that E-cadherin could be expressed by early precursors of basophils and MCs, representing the commitment to the lineages (85). Notably, scRNA-seq based on the peritoneal cavity of mice may establish an entirely new developmental trajectory for MCs, given that a discrete group of cells called P1 was found under suitable *in vitro* culture conditions, which have the potential to differentiate into MCs and basophils (86). In human, a study based on scRNA-seq revealed MCs are existed in the human yolk sac. In these human yolk sac-derived MCs, hairy and enhancer of split 1 (HES1), nuclear receptor subfamily 4 group A member 2 (NR4A2), and Kruppel-like factor 1 (KLF1) were detected, which may have non-redundant effects on the differentiation and activation of MCs (87). Another origin of human MCs was also confirmed by scRNA-seq. The analysis of human cord blood identified a group of basophil/eosinophil/MCs progenitors, revealing a close link between MCs and erythroid commitment cells downstream from HSCs (88). In addition, an analysis of nasal polyps in the patients of chronic rhinosinusitis with nasal polyposis detected an intermediate $CD38^{high}CD117^{high}$ MC phenotype distinct from circulating MCPs (12). The same study also confirmed that MRGPRX2 was expressed only in MCs of the proximal lung, but not in the distal or medial lung (12). A high ratio of tumor-suppressive TNF^+/vascular endothelial growth factor A $(VEGFA)^+$ MC phenotype is found in nasopharyngeal cancer in the patients. It seems associated with a better prognosis (89), while another ground glass nodule adenocarcinoma analysis detected pro-inflammatory MCs (90). These results clearly indicated the origin- and microenvironment-dependent heterogeneity of MCs.

Deeper analysis of innovative techniques provide sufficient resolution to fully reveal the heterogeneity of MCs and show the differentiation trajectory and transcriptional heterogeneity of specific cell types in different tissues or disease settings, which helps identify novel putative immune cell subtypes (91).

Mast cells act as the terminator of allergies and inflammation

In pathological reactions, such as allergy and inflammation, MCs and their precursors can recruit and expand in the disease site. For example, Lin^- c-$Kit^{int/hi}$ $Fc\varepsilon RI^+$ $CD34^{hi}$ MCPs are recruited to peripheral tissues mediated by molecules [e.g., α4β7 integrins, VCAM-1 (92, 93)] and cells [e.g., $CD11c^+$ cells (94), $CD4^+$ cells (95)] in acute allergy. IgE (96) and its immune complexes (97) seem to be involved in the survival of MCs and the recruitment of MCPs. Consequently, MCs are closely involved in most allergy and inflammation processes.

Despite having outstanding achievements in innate and adaptive immunity, MCs have a well-deserved reputation as promoters of pathological actions, such as inflammation and allergy. However, as discussed previously, MCs' distinctive migration and maturation patterns contribute to their remarkable plasticity and tissue-microenvironment-dependent heterogeneity. On this basis, we have reason to assume that MCs, as one of the most critical and primary immune cells in damaged tissues, may have positive regulatory functions in inflammation, allergy, tissue regeneration, and tissue repair. It is gratifying to note that there is now accumulating evidence to support the immunoregulatory part of MCs (Table 1).

In the early years, MCs were demonstrated to have immunosuppressive effects. For instance, Hart et al. found that in mice, dermal MCs play an indispensable role in inhibiting systemic contact hypersensitivity (CHS) response to ultraviolet radiation [wavelength 280-320 nm: (UVB)], and that histamine derived by MCs may be a critical factor for the suppression of inflammation (109). Both dermal MC-derived and exogenous histamines inhibited the immune response of UVB-exposed mice (109), through the production of PGE2. PGE2 inhibits the production of IL-12, an inducer of pathogenic Th1 immune responses (110).

In IBD, IL-33 is one of the earliest cytokines released from the necrotic cells of injured tissues (84). IL-33 has been shown to polarize AAMΦs *in vivo*, which requires the participation of MCs (22). AAMΦs have been demonstrated to have the potential to suppress inflammation and promote wound healing (111). Arginase-1 expressed by AAMΦs depletes the extracellular arginine necessary for T cell activation (112). Braune et al. and Fernando et al. found that IL-33 can induce IL-6 and IL-13 secretion by MCs through ST2, which plays a crucial role in AAMΦ polarization (111, 113). Consequently, IL-33 exerts immunosuppressive and anti-inflammatory effects by indirectly promoting AAMΦ polarization, thereby inhibiting the production of IL-17 and IFN-γ by T cells. Moreover, upon IL-33 stimulation, MCs secrete IL-10 and histamine to suppress LPS-mediated monocyte activation, which might be helpful against rheumatoid arthritis (114). Hence, it is plausible to believe that the IL-33/ST2-MC axis plays a positive role in limiting inflammation (115).

$CD4^+CD25^+Foxp3^+$ Treg plays an essential role in immune tolerance. Several studies have shown intricate reciprocal crosstalk between MCs and Tregs. Experiments demonstrated that OX40 on the Treg surface could bind to OX40L expressed on the surface of MCs, subsequently inhibiting IgE-mediated MC degranulation (18). Moreover, TGF-β1 and IL-10 secreted by Tregs were thought to inhibit the expression of FcεRI on the MC surface, which also inhibit the MC degranulation (17, 78, 116). Notably, TGF-β1 reduced the expression of FcεRI subunit proteins α, β, and γ, while IL-10 inhibited only β proteins. TGF-β1 has also been reported to induce the apoptosis of MCs (108).

TABLE 1 The immunoregulatory effect of MCs.

Mediators (Secreted by MC)	Mechanism	Reference
IL-2	Ensures the sustained and stable expression of Foxp3 in Tregs to maintain their development, proliferation, activity, and survival	(14, 98)
IL-10	Inhibits the production of pro-inflammatory and pro-allergy cytokines (TNF-α, IFN-γ, IL-1, IL-13, and IL-6)	(99, 100)
	Inhibits the expression of FcεRI subunit protein β on MCs	(100)
	Inhibits the overactivation and over-proliferation of MCs and promotes MC apoptosis during stable and late inflammatory phases	(101–103)
	Inhibits the proliferation of T cells to inhibit inflammation	(104)
	Prevention of epithelial barrier dysfunction caused by IFN-γ and restoration of the epithelial barrier	(105)
	Inhibits adaptive immunity by suppressing the migration of mature DCs to the lymph nodes in the bladder	(106)
	Induces the production of Tregs and mediates autoantigen tolerance	(20, 107)
Amphiregulin	Boosts the Treg function in colitis and tumors in the tumor-mediated intrinsic immunosuppression vaccination model	(21)
TGF-β1	Inhibits the expression of FcεRI subunit proteins α, β, and γ on MCs and induces MC apoptosis	(8, 17, 108)
	Induces the production of Tregs and mediates autoantigen tolerance	(20, 107)

Research on allotransplantation in experimental mice showed that Treg-derived IL-9 could maintain the tolerance of allografts by affecting MCs (19). IL-9 is a critical factor in promoting the SCF-dependent growth, proliferation, recruitment, and activation of MCs (25), thus Treg-derived IL-9 and SCF synergistically activate hepatic MCs and promote the release of histamine, IL-2, and TGF-β1 in tolerogenic liver allografts. TGF-β1 promoted the generation of γδT cells, and IL-17 released by γδT cells further attracted Tregs and enhanced their immunosuppressive properties (117).

MCs also have inverse impacts on Tregs. MCs secrete TGF-β1, which contribute to Tregs production and mediate autoantigen tolerance (20, 107). Epidermal growth factor (EGF)-like growth factor amphiregulin, which MCs also secrete, directly boosted the Treg function in colitis and tumor vaccination models by activating the EGF receptor (EGFR) on them (21). EGFR is reported to mediate intrinsic immunosuppression in tumors, and EGFR-targeted therapies are widely used for tumors such as colorectal cancer (118) and non-small cell lung cancer (119). Therefore, the immunoregulatory mechanism of MCs may be further applied in tumor therapy.

MCs also seem to ensure the sustained and stable expression of Foxp3 in Treg cells by secreting IL-2, thus maintaining the development, proliferation, activity, and survival of Tregs at sites (98) to sustain their inhibitory function (120). Studies have shown that MC-derived IL-2 in the lung promotes Tregs proliferation and limits allergic airway inflammation (115). In addition, the feasibility of regulating food allergy by inducing Treg cells with a continuous exposure of low concentration of IL-2 has been demonstrated (79).

Our recent research revealed the role of MCs in the regulation of food allergies (14). To delve into the mechanism of a more effective treatment for food allergy-oral allergen desensitization-oral immunotherapy (OIT) from a mucosal immune system perspective, we established a clinically relevant murine model of OIT with an escalating oral dose of ovalbumin (OVA). The OIT protocol induced mucosal desensitized MCs in the intestinal compartment with a low degranulation capacity and IL-4 production but high IFN-γ production, which plays an indispensable role in allergy (14). IL-4 plays a key role in the initiation of food allergy to mediate the isotype switching of IgE, the food-specific-IgE generation from B cells, and the release of MC mediators (e.g., histamine) (121, 122). Moreover, Tomar *et al.* found that IL-4 promotes the development of MMC9 cells, partly through a basic leucine zipper ATF-like transcription factor-dependent pathway (83). Returning to our study, we detected a significant increase in Tregs from the mucosa, peripheral blood, and spleen in OIT treated mice group. In addition, we discovered that the dual synthesis of IL-2 and IL-10 by mucosal desensitized MCs induces Tregs and inhibits allergic symptom (14). In addition, OIT treatment induce desensitization to MCs and reduced their allergenicity by acquiring the regulatory function (Figure 3). It can be expected that elucidation of switch pathway of MCs from allergenic to regulatory properties can lead to the utilization of MCs in a positive manner to overcome the allergy.

IL-10 is a well-known anti-inflammatory cytokine that has been demonstrated to diminish the degree or duration of innate immune or acquired responses (123) by inhibiting the production of pro-inflammatory cytokines [TNF-α, IFN-γ, IL-1, and IL-6 (99)] and chemokines, and also the proliferation of T cells [e.g., $CD4^+$ T cells (123) and $CD8^+$ T cells (123, 124)]. It has been reported that MCs can reduce inflammation, tissue damage, leukocyte infiltration and restore the epithelial barrier function in an IL-10-dependent manner in multiple organs or tissues [e.g., gut (15) bladder (106) and skin (16)] and the antigen-specific T cell immune response caused by *Anopheles* mosquito saliva (125). MC deficiency can increase intestinal

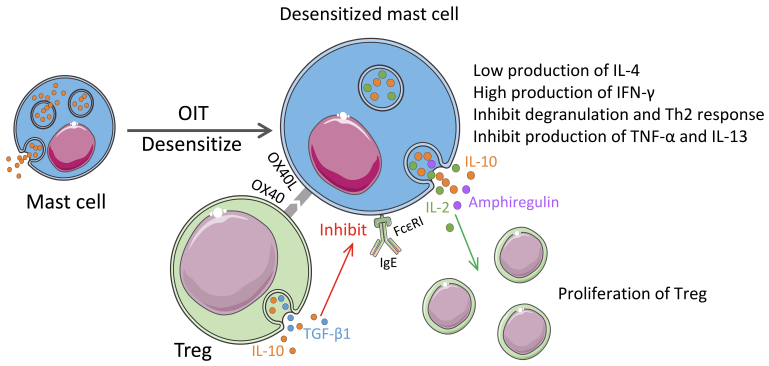


FIGURE 3
Regulatory properties of MCs in the immunotherapy. OIT treatment for food allergy induces desensitization of MCs with the low expression of Th2 cytokines and induces expression of IFN-γ. Desensitized MCs also synthesize IL-2 and IL-10. MC-derived IL-2 and amphiregulin promote proliferation and enhancement of the function of Tregs. Activated Tregs release IL-10 and TGF-β1, and the OX40 on their surface binds to OX40L from MCs, which inhibits the expression of FcεRI on MCs and the release of TNF-α and IL-13, thereby inhibiting the Th2 responses.

permeability in IL10$^{-/-}$ mice and cause spontaneous colitis (15). Artificial IL-10 supplementation prevented IFNγ-induced epithelial barrier dysfunction (105). In addition to the aforementioned Treg, MCs also secrete IL-10. Evidence of the secretion of IL-10 by MCs has been revealed both *in vivo* (14, 16) and *in vitro* (126). In Treg-independent graft-versus-host disease (GVHD), MCs have been found to show an immunosuppressive function by inhibiting T cell proliferation in an IL-10-dependent manner to inhibit inflammation (104). Although the mechanism through which MCs are triggered to produce IL-10 in the disease remains to be determined, it is speculated that endotoxin (LPS) from intestinal bacteria activates TLR4 in MCs, given that LPS has been shown to promote the production of Th2 cytokines by MCs (127). UVB promotes the production of MC-derived IL-10 by increasing the synthesis of vitamin D3 (128) to reduce allergic skin inflammation. Additionally, IL-10 derived from MCs, rather than Tregs, inhibits the migration of mature DCs to the lymph nodes in the bladder, which helps building the "immune privilege" (106).

In addition to their anti-inflammatory and allergic effects, MCs promote tissue repair and wound healing. Studies have shown that depletion of MCs partly inhibits wound healing (129). Furthermore, it has been revealed that IL-33/ST2 promoted the release of IL-13 and IL-22 from MCs (84). IL-13 signaling activates STAT6, which contributes to the survival and migration of epithelial cells and IL-22 can directly promote the production of mucus and the proliferation of epithelial cells (130, 131). Moreover, available evidence suggests that MCs are involved in almost all events of wound healing process (fibroblast migration/proliferation, and remodeling). In the early stage of wound formation, MCs are recruited to the injured site under the action of keratinocyte-derived IL-33, CCL2, and SCF; then they secrete various substances (23, 132). For example, MC produces TNF-α and stimulates DCs to express factor XIIIa, which promotes coagulation (23). Also, MC-derived histamine, lipid mediators [e.g., PGD2 and leukotrienes (LTs), etc.], and VEGF increase the vascular permeability to recruit monocytes and neutrophils (11, 23). Moreover, MCs are essential for the fibrotic process of wound healing. Proteases (e.g., tryptase and chymase), VEGF, IL-4, IL-8, NGF, FGF-2, PDGF, and TGF-β1, which are secreted by MCs, can contribute to angiogenesis, fibrin production, or re-epithelialization (23). At the end of wound healing, the proliferated blood vessels in the tissue degenerate, and the active granulation tissue is remodeled into fiber-rich scar tissue (133). Most studies agree that MCs are involved in this process (134), which might be mediated by gap-junctional intercellular communication between MCs and fibroblasts or myofibroblasts (135). In addition, MCs and zinc have been determined to induce the IL-6 production *via* Zn receptor GPR39 expressed on the cells in the inflammatory tissues such as fibroblasts, macrophages, and DCs (136). IL-6 is essential for wound healing (137).

In summary, although MCs show more inflammatory and allergic properties in the acute phase, they may exhibit more prominent functions during periods of inflammation or chronic inflammation subside to prevent excessive tissue damage and the development of chronic inflammation.

Conclusion

In general, MCs have high plasticity and tissue microenvironment-dependent heterogeneity owing to the distinctive migration and maturation modes. MCs interact with various cells at different physiological and pathological stages to exhibit vastly different functions. Comprehensively, understanding the heterogeneity of human MCs and determining their physiological functions under specific circumstances is a great challenge. Additionally, human MCs are difficult to obtain and isolate, and have poor ability to expand *in vitro* (63). Therefore, rodent MCs are widely used for the time being, which also gives rise to a new question: whether the results observed in these alternative models can be wholly inferred to human MCs. For example, human MCs and mouse MCs sometimes show different responses to the same cytokines or anti-allergic drugs (33, 138). Clinically, due to the profound negative impression that MCs promote inflammation and allergy, until recently, simply inhibiting MCs is still the mainstream way for clinical treatment of allergy and inflammation. Moreover, it is undeniable that MC neutralizing therapies do not seem to have satisfactory therapeutic effects due to the imperfect research at the present stage. According to this review, based on the strong microenvironment-dependent plasticity and heterogeneity of MCs, it appears promising to induce MCs to behave in a manner that regulates and inhibits chronic inflammatory and allergic responses. Accumulating research evidence might have revealed the great potential of MCs in treating disease by proper education in the peripheral tissues to terminate inflammation and allergy.

Author contributions

ZZ and YK conceived the idea for the review. ZZ and YK wrote the manuscript with constructive input from PE and HK. All authors read and approved the final version of the manuscript.

Funding

This work was supported by grants from The Ministry of Education, Culture, Sports, Science, and Technology (MEXT) for LEADER; Japan Agency for Medical Research and Development (AMED) PRIME (20gm6010012h0004/20gm6210024h0001) and

Project Focused on Developing Key Technology for Discovering and Manufacturing Drugs for Next-Generation Treatment and Diagnosis, The next-generation drug discovery and development technology on regulating intestinal microbiome (NeDDTrim) (JP21ae0121040); Japan Society for the Promotion of Science (JSPS) for Grant-in-Aid for Scientific Research S (18H05280) and Scientific Research B (19H03450), Challenging Research (Exploratory) 21K19494], Funds for the Promotion of Joint International Research (18KK0432), Future Medicine Funds at Chiba University, Danone Institute of Japan Foundation, The Naito Foundation, Hoyu Science Foundation, Waksman foundation of Japan, Yamada Science Foundation, The Institute of Medical Science, University of Tokyo (IMSUT) International Joint Research Project K003, and the Chiba University-UC San Diego Center for Mucosal Immunology, Allergy, and Vaccines (cMAV).

Acknowledgments

We thank Mr. Izumi Tanaka for the discussion. Figures were produced using Servier Medical Art (http://smart.servier.com/), licensed under a Creative Common Attribution 3.0 Generic License (https://creativecommons.org/licenses/by/3.0/).

Conflict of interest

HK is director and founder of HanaVax Inc.

The remaining authors declare that the research was conducted in the absence of any commercial or financial relationships that could be construed as a potential conflict of interest.

Publisher's note

All claims expressed in this article are solely those of the authors and do not necessarily represent those of their affiliated organizations, or those of the publisher, the editors and the reviewers. Any product that may be evaluated in this article, or claim that may be made by its manufacturer, is not guaranteed or endorsed by the publisher.

References

1. Galli SJ, Gaudenzio N, Tsai M. Mast cells in inflammation and disease: Recent progress and ongoing concerns. *Annu Rev Immunol* (2020) 38:49–77. doi: 10.1146/annurev-immunol-071719-094903

2. Gentek R, Ghigo C, Hoeffel G, Bulle MJ, Msallam R, Gautier G, et al. Hemogenic endothelial fate mapping reveals dual developmental origin of mast cells. *Immunity* (2018) 48(6):1160–71.e5. doi: 10.1016/j.immuni.2018.04.025

3. Li Z, Liu S, Xu J, Zhang X, Han D, Liu J, et al. Adult connective tissue-resident mast cells originate from late erythro-myeloid progenitors. *Immunity* (2018) 49 (4):640–53.e5. doi: 10.1016/j.immuni.2018.09.023

4. Dahlin JS, Heyman B, Hallgren J. Committed mast cell progenitors in mouse blood differ in maturity between Th1 and Th2 strains. *Allergy* (2013) 68(10):1333–7. doi: 10.1111/all.12223

5. Dahlin JS, Malinovschi A, Ohrvik H, Sandelin M, Janson C, Alving K, et al. Lin- CD34hi CD117int/hi FcepsilonRI+ cells in human blood constitute a rare population of mast cell progenitors. *Blood* (2016) 127(4):383–91. doi: 10.1182/blood-2015-06-650648

6. Gurish MF, Tao H, Abonia JP, Arya A, Friend DS, Parker CM, et al. Intestinal mast cell progenitors require CD49dbeta7 (alpha4beta7 integrin) for tissue-specific homing. *J Exp Med* (2001) 194(9):1243–52. doi: 10.1084/jem.194.9.1243

7. Abonia JP, Austen KF, Rollins BJ, Joshi SK, Flavell RA, Kuziel WA, et al. Constitutive homing of mast cell progenitors to the intestine depends on autologous expression of the chemokine receptor CXCR2. *Blood* (2005) 105 (11):4308–13. doi: 10.1182/blood-2004-09-3578

8. Kurashima Y, Kunisawa J, Higuchi M, Gohda M, Ishikawa I, Takayama N, et al. Sphingosine 1-phosphate-mediated trafficking of pathogenic Th2 and mast cells for the control of food allergy. *J Immunol* (2007) 179(3):1577–85. doi: 10.4049/jimmunol.179.3.1577

9. Dwyer DF, Barrett NA, Austen KF, Immunological Genome Project C. Expression profiling of constitutive mast cells reveals a unique identity within the immune system. *Nat Immunol* (2016) 17(7):878–87. doi: 10.1038/ni.3445

10. Kurashima Y, Amiya T, Fujisawa K, Shibata N, Suzuki Y, Kogure Y, et al. The enzyme Cyp26b1 mediates inhibition of mast cell activation by fibroblasts to maintain skin-barrier homeostasis. *Immunity* (2014) 40(4):530–41. doi: 10.1016/j.immuni.2014.01.014

11. Zhang Z, Kurashima Y. Two sides of the coin: Mast cells as a key regulator of allergy and Acute/Chronic inflammation. *Cells* (2021) 10(7):1615. doi: 10.3390/cells10071615

12. Dwyer DF, Ordovas-Montanes J, Allon SJ, Buchheit KM, Vukovic M, Derakhshan T, et al. Human airway mast cells proliferate and acquire distinct inflammation-driven phenotypes during type 2 inflammation. *Sci Immunol* (2021) 6(56):eabb7221. doi: 10.1126/sciimmunol.abb7221

13. Honjo A, Nakano N, Yamazaki S, Hara M, Uchida K, Kitaura J, et al. Pharmacologic inhibition of notch signaling suppresses food antigen-induced mucosal mast cell hyperplasia. *J Allergy Clin Immunol* (2017) 139(3):987–96.e10. doi: 10.1016/j.jaci.2016.05.046

14. Takasato Y, Kurashima Y, Kiuchi M, Hirahara K, Murasaki S, Arai F, et al. Orally desensitized mast cells form a regulatory network with treg cells for the control of food allergy. *Mucosal Immunol* (2021) 14(3):640–51. doi: 10.1038/s41385-020-00358-3

15. Chichlowski M, Westwood GS, Abraham SN, Hale LP. Role of mast cells in inflammatory bowel disease and inflammation-associated colorectal neoplasia in IL-10-deficient mice. *PLoS One* (2010) 5(8):e12220. doi: 10.1371/journal.pone.0012220

16. Grimbaldeston MA, Nakae S, Kalesnikoff J, Tsai M, Galli SJ. Mast cell-derived interleukin 10 limits skin pathology in contact dermatitis and chronic irradiation with ultraviolet b. *Nat Immunol* (2007) 8(10):1095–104. doi: 10.1038/ni1503

17. Gomez G, Ramirez CD, Rivera J, Patel M, Norozian F, Wright HV, et al. TGF-beta 1 inhibits mast cell fc epsilon RI expression. *J Immunol* (2005) 174 (10):5987–93. doi: 10.4049/jimmunol.174.10.5987

18. Gri G, Piconese S, Frossi B, Manfroi V, Merluzzi S, Tripodo C, et al. CD4 +CD25+ regulatory T cells suppress mast cell degranulation and allergic responses through OX40-OX40L interaction. *Immunity* (2008) 29(5):771–81. doi: 10.1016/j.immuni.2008.08.018

19. Lu LF, Lind EF, Gondek DC, Bennett KA, Gleeson MW, Pino-Lagos K, et al. Mast cells are essential intermediaries in regulatory T-cell tolerance. *Nature* (2006) 442(7106):997–1002. doi: 10.1038/nature05010

20. Belghith M, Bluestone JA, Barriot S, Megret J, Bach JF, Chatenoud L. TGF-beta-dependent mechanisms mediate restoration of self-tolerance induced by antibodies to CD3 in overt autoimmune diabetes. *Nat Med* (2003) 9(9):1202–8. doi: 10.1038/nm924

21. Zaiss DM, van Loosdregt J, Gorlani A, Bekker CP, Grone A, Sibilia M, et al. Amphiregulin enhances regulatory T cell-suppressive function *via* the epidermal growth factor receptor. *Immunity* (2013) 38(2):275–84. doi: 10.1016/j.immuni.2012.09.023

22. Finlay CM, Cunningham KT, Doyle B, Mills KHG. IL-33-Stimulated murine mast cells polarize alternatively activated macrophages, which suppress T cells that mediate experimental autoimmune encephalomyelitis. *J Immunol* (2020) 205(7):1909–19. doi: 10.4049/jimmunol.1901321

23. Komi DEA, Khomtchouk K, Santa Maria PL. A review of the contribution of mast cells in wound healing: Involved molecular and cellular mechanisms. *Clin Rev Allergy Immunol* (2020) 58(3):298–312. doi: 10.1007/s12016-019-08729-w

24. Toru H, Eguchi M, Matsumoto R, Yanagida M, Yata J, Nakahata T. Interleukin-4 promotes the development of tryptase and chymase double-positive human mast cells accompanied by cell maturation. *Blood* (1998) 91 (1):187–95. doi: 10.1182/blood.v91.1.187.187_187_195

25. Matsuzawa S, Sakashita K, Kinoshita T, Ito S, Yamashita T, Koike K. IL-9 enhances the growth of human mast cell progenitors under stimulation with stem cell factor. *J Immunol* (2003) 170(7):3461–7. doi: 10.4049/jimmunol.170.7.3461

26. Iikura M, Suto H, Kajiwara N, Oboki K, Ohno T, Okayama Y, et al. IL-33 can promote survival, adhesion and cytokine production in human mast cells. *Lab Invest* (2007) 87(10):971–8. doi: 10.1038/labinvest.3700663

27. Allakhverdi Z, Smith DE, Comeau MR, Delespesse G. Cutting edge: The ST2 ligand IL-33 potently activates and drives maturation of human mast cells. *J Immunol* (2007) 179(4):2051–4. doi: 10.4049/jimmunol.179.4.2051

28. Macey MR, Sturgill JL, Morales JK, Falanga YT, Morales J, Norton SK, et al. IL-4 and TGF-beta 1 counterbalance one another while regulating mast cell homeostasis. *J Immunol* (2010) 184(9):4688–95. doi: 10.4049/jimmunol.0903477

29. Razin E, Ihle JN, Seldin D, Mencia-Huerta JM, Katz HR, LeBlanc PA, et al. Interleukin 3: A differentiation and growth factor for the mouse mast cell that contains chondroitin sulfate e proteoglycan. *J Immunol* (1984) 132(3):1479–86.

30. Matsuda H, Kannan Y, Ushio H, Kiso Y, Kanemoto T, Suzuki H, et al. Nerve growth factor induces development of connective tissue-type mast cells *in vitro* from murine bone marrow cells. *J Exp Med* (1991) 174(1):7–14. doi: 10.1084/jem.174.1.7

31. Weller CL, Collington SJ, Brown JK, Miller HR, Al-Kashi A, Clark P, et al. Leukotriene B4, an activation product of mast cells, is a chemoattractant for their progenitors. *J Exp Med* (2005) 201(12):1961–71. doi: 10.1084/jem.20042407

32. Ochi H, Hirani WM, Yuan Q, Friend DS, Austen KF, Boyce JA. T Helper cell type 2 cytokine-mediated comitogenic responses and CCR3 expression during differentiation of human mast cells *in vitro*. *J Exp Med* (1999) 190(2):267–80. doi: 10.1084/jem.190.2.267

33. Saito H, Kato A, Matsumoto K, Okayama Y. Culture of human mast cells from peripheral blood progenitors. *Nat Protoc* (2006) 1(4):2178–83. doi: 10.1038/nprot.2006.344

34. McNeil BD, Pundir P, Meeker S, Han L, Undem BJ, Kulka M, et al. Identification of a mast-cell-specific receptor crucial for pseudo-allergic drug reactions. *Nature* (2015) 519(7542):237–41. doi: 10.1038/nature14022

35. Gurish MF, Boyce JA. Mast cells: ontogeny, homing, and recruitment of a unique innate effector cell. *J Allergy Clin Immunol* (2006) 117(6):1285–91. doi: 10.1016/j.jaci.2006.04.017

36. Bischoff SC, Wedemeyer J, Herrmann A, Meier PN, Trautwein C, Cetin Y, et al. Quantitative assessment of intestinal eosinophils and mast cells in inflammatory bowel disease. *Histopathology* (1996) 28(1):1–13. doi: 10.1046/j.1365-2559.1996.262309.x

37. Meininger CJ, Yano H, Rottapel R, Bernstein A, Zsebo KM, Zetter BR. The c-kit receptor ligand functions as a mast cell chemoattractant. *Blood* (1992) 79 (4):958–63. doi: 10.1182/blood.v79.4.958.958

38. Nilsson G, Butterfield JH, Nilsson K, Siegbahn A. Stem cell factor is a chemotactic factor for human mast cells. *J Immunol* (1994) 153(8):3717–23.

39. Lorentz A, Bischoff SC. Regulation of human intestinal mast cells by stem cell factor and IL-4. *Immunol Rev* (2001) 179:57–60. doi: 10.1034/j.1600-065x.2001.790106.x

40. Wang Z, Mascarenhas N, Eckmann L, Miyamoto Y, Sun X, Kawakami T, et al. Skin microbiome promotes mast cell maturation by triggering stem cell factor production in keratinocytes. *J Allergy Clin Immunol* (2017) 139(4):1205–16.e6. doi: 10.1016/j.jaci.2016.09.019

41. Huang B, Lei Z, Zhang GM, Li D, Song C, Li B, et al. SCF-mediated mast cell infiltration and activation exacerbate the inflammation and immunosuppression in tumor microenvironment. *Blood* (2008) 112(4):1269–79. doi: 10.1182/blood-2008-03-147033

42. Tan BL, Yazicioglu MN, Ingram D, McCarthy J, Borneo J, Williams DA, et al. Genetic evidence for convergence of c-kit- and alpha4 integrin-mediated signals on class IA PI-3kinase and the rac pathway in regulating integrin-directed migration in mast cells. *Blood* (2003) 101(12):4725–32. doi: 10.1182/blood-2002-08-2521

43. Chandrasekar B, Melby PC, Sarau HM, Raveendran M, Perla RP, Marelli-Berg FM, et al. (CXCL5) amplifies a proinflammatory cytokine response *via* a phosphatidylinositol 3-kinase-NF-kappa b pathway. *J Biol Chem* (2003) 278 (7):4675–86. doi: 10.1074/jbc.M207006200

44. Sadhu C, Masinovsky B, Staunton DE. Differential regulation of chemoattractant-stimulated beta 2, beta 3, and beta 7 integrin activity. *J Immunol* (1998) 160(11):5622–8.

45. Hallgren J, Jones TG, Abonia JP, Xing W, Humbles A, Austen KF, et al. Pulmonary CXCR2 regulates VCAM-1 and antigen-induced recruitment of mast cell progenitors. *Proc Natl Acad Sci U.S.A.* (2007) 104(51):20478–83. doi: 10.1073/pnas.0709651104

46. Kunii J, Takahashi K, Kasakura K, Tsuda M, Nakano K, Hosono A, et al. Commensal bacteria promote migration of mast cells into the intestine. *Immunobiology* (2011) 216(6):692–7. doi: 10.1016/j.imbio.2010.10.007

47. Schwarzer M, Hermanova P, Srutkova D, Golias J, Hudcovic T, Zwicker C, et al. Germ-free mice exhibit mast cells with impaired functionality and gut homing and do not develop food allergy. *Front Immunol* (2019) 10:205. doi: 10.3389/fimmu.2019.00205

48. Meijerink M, Wells JM, Taverne N, de Zeeuw Brouwer ML, Hilhorst B, Venema K, et al. Immunomodulatory effects of potential probiotics in a mouse peanut sensitization model. *FEMS Immunol Med Microbiol* (2012) 65(3):488–96. doi: 10.1111/j.1574-695X.2012.00981.x

49. Alcaide P, Jones TG, Lord GM, Glimcher LH, Hallgren J, Arinobu Y, et al. Dendritic cell expression of the transcription factor T-bet regulates mast cell progenitor homing to mucosal tissue. *J Exp Med* (2007) 204(2):431–9. doi: 10.1084/jem.20060626

50. Cyster JG. Chemokines, sphingosine-1-phosphate, and cell migration in secondary lymphoid organs. *Annu Rev Immunol* (2005) 23:127–59. doi: 10.1146/annurev.immunol.23.021704.115628

51. Lee MJ, Evans M, Hla T. The inducible G protein-coupled receptor edg-1 signals *via* the g(i)/mitogen-activated protein kinase pathway. *J Biol Chem* (1996) 271(19):11272–9. doi: 10.1074/jbc.271.19.11272

52. Lee MJ, Thangada S, Claffey KP, Ancellin N, Liu CH, Kluk M, et al. Vascular endothelial cell adherens junction assembly and morphogenesis induced by sphingosine-1-phosphate. *Cell* (1999) 99(3):301–12. doi: 10.1016/s0092-8674(00)81661-x

53. Gurish MF, Austen KF. Developmental origin and functional specialization of mast cell subsets. *Immunity* (2012) 37(1):25–33. doi: 10.1016/j.immuni.2012.07.003

54. Frossi B, Mion F, Sibilano R, Danelli L, Pucillo CEM. Is it time for a new classification of mast cells? what do we know about mast cell heterogeneity? *Immunol Rev* (2018) 282(1):35–46. doi: 10.1111/imr.12636

55. Heavey DJ, Ernst PB, Stevens RL, Befus AD, Bienenstock J, Austen KF. Generation of leukotriene C4, leukotriene B4, and prostaglandin D2 by immunologically activated rat intestinal mucosa mast cells. *J Immunol* (1988) 140(6):1953–7.

56. Madden KB, Urban JFJr., Ziltener HJ, Schrader JW, Finkelman FD, Katona IM. Antibodies to IL-3 and IL-4 suppress helminth-induced intestinal mastocytosis. *J Immunol* (1991) 147(4):1387–91.

57. Smith CH, Kepley C, Schwartz LB, Lee TH. Mast cell number and phenotype in chronic idiopathic urticaria. *J Allergy Clin Immunol* (1995) 96 (3):360–4. doi: 10.1016/s0091-6749(95)70055-2

58. Irani AA, Schechter NM, Craig SS, DeBlois G, Schwartz LB. Two types of human mast cells that have distinct neutral protease compositions. *Proc Natl Acad Sci U S A* (1986) 83(12):4464–8. doi: 10.1073/pnas.83.12.4464

59. Irani AM, Bradford TR, Kepley CL, Schechter NM, Schwartz LB. Detection of MCT and MCTC types of human mast cells by immunohistochemistry using new monoclonal anti-tryptase and anti-chymase antibodies. *J Histochem Cytochem* (1989) 37(10):1509–15. doi: 10.1177/37.10.2674273

60. Weidner N, Austen KF. Heterogeneity of mast cells at multiple body sites. fluorescent determination of avidin binding and immunofluorescent determination of chymase, tryptase, and carboxypeptidase content. *Pathol Res Pract* (1993) 189 (2):156–62. doi: 10.1016/S0344-0338(11)80086-5

61. Xing W, Austen KF, Gurish MF, Jones TG. Protease phenotype of constitutive connective tissue and of induced mucosal mast cells in mice is regulated by the tissue. *Proc Natl Acad Sci U S A* (2011) 108(34):14210–5. doi: 10.1073/pnas.1111048108

62. Schmetzer O, Valentin P, Smorodchenko A, Domenis R, Gri G, Siebenhaar F, et al. A novel method to generate and culture human mast cells: Peripheral CD34 + stem cell-derived mast cells (PSCMCs). *J Immunol Methods* (2014) 413:62–8. doi: 10.1016/j.jim.2014.07.003

63. Elst J, Sabato V, van der Poorten MM, Faber M, Van Gasse AL, De Puysseleyr LP, et al. Peripheral blood cultured mast cells: Phenotypic and functional outcomes of different culture protocols. *J Immunol Methods* (2021) 492:113003. doi: 10.1016/j.jim.2021.113003

64. Kirshenbaum AS, Swindle E, Kulka M, Wu Y, Metcalfe DD. Effect of lipopolysaccharide (LPS) and peptidoglycan (PGN) on human mast cell numbers, cytokine production, and protease composition. *BMC Immunol* (2008) 9:45. doi: 10.1186/1471-2172-9-45

65. Gebhardt T, Lorentz A, Detmer F, Trautwein C, Bektas H, Manns MP, et al. Growth, phenotype, and function of human intestinal mast cells are tightly regulated by transforming growth factor beta1. *Gut* (2005) 54(7):928–34. doi: 10.1136/gut.2004.054650

66. Levi-Schaffer F, Austen KF, Gravallese PM, Stevens RL. Coculture of interleukin 3-dependent mouse mast cells with fibroblasts results in a phenotypic change of the mast cells. *Proc Natl Acad Sci U S A* (1986) 83(17):6485–8. doi: 10.1073/pnas.83.17.6485

67. Yamada K, Sato H, Sakamaki K, Kamada M, Okuno Y, Fukuishi N, et al. Suppression of IgE-independent degranulation of murine connective tissue-type mast cells by dexamethasone. *Cells* (2019) 8(2):112. doi: 10.3390/cells8020112

68. Kurashima Y, Amiya T, Nochi T, Fujisawa K, Haraguchi T, Iba H, et al. Extracellular ATP mediates mast cell-dependent intestinal inflammation through P2X7 purinoceptors. *Nat Commun* (2012) 3:1034. doi: 10.1038/ncomms2023

69. Arinobu Y, Iwasaki H, Gurish MF, Mizuno S, Shigematsu H, Ozawa H, et al. Developmental checkpoints of the basophil/mast cell lineages in adult murine hematopoiesis. *Proc Natl Acad Sci U S A* (2005) 102(50):18105–10. doi: 10.1073/pnas.0509148102

70. Chen CC, Grimbaldeston MA, Tsai M, Weissman IL, Galli SJ. Identification of mast cell progenitors in adult mice. *Proc Natl Acad Sci U S A* (2005) 102 (32):11408–13. doi: 10.1073/pnas.0504197102

71. Ernst PB, Petit A, Befus AD, Clark DA, Rosenthal KL, Ishizaka T, et al. Murine intestinal intraepithelial lymphocytes II. Comparison of freshly isolated and cultured intraepithelial lymphocytes. *Eur J Immunol* (1985) 15(3):216–21. doi: 10.1002/eji.1830150303

72. Friend DS, Ghildyal N, Austen KF, Gurish MF, Matsumoto R, Stevens RL. Mast cells that reside at different locations in the jejunum of mice infected with trichinella spiralis exhibit sequential changes in their granule ultrastructure and chymase phenotype. *J Cell Biol* (1996) 135(1):279–90. doi: 10.1083/jcb.135.1.279

73. Friend DS, Ghildyal N, Gurish MF, Hunt J, Hu X, Austen KF, et al. Reversible expression of tryptases and chymases in the jejunal mast cells of mice infected with trichinella spiralis. *J Immunol* (1998) 160(11):5537–45.

74. Shin K, Watts GF, Oettgen HC, Friend DS, Pemberton AD, Gurish MF, et al. Mouse mast cell tryptase mMCP-6 is a critical link between adaptive and innate immunity in the chronic phase of trichinella spiralis infection. *J Immunol* (2008) 180(7):4885–91. doi: 10.4049/jimmunol.180.7.4885

75. Knight PA, Wright SH, Lawrence CE, Paterson YY, Miller HR. Delayed expulsion of the nematode trichinella spiralis in mice lacking the mucosal mast cell-specific granule chymase, mouse mast cell protease-1. *J Exp Med* (2000) 192 (12):1849–56. doi: 10.1084/jem.192.12.1849

76. Bischoff SC. Physiological and pathophysiological functions of intestinal mast cells. *Semin Immunopathol* (2009) 31(2):185–205. doi: 10.1007/s00281-009-0165-4

77. Bischoff SC. Mast cells in gastrointestinal disorders. *Eur J Pharmacol* (2016) 778:139–45. doi: 10.1016/j.ejphar.2016.02.018

78. Wouters MM, Vicario M, Santos J. The role of mast cells in functional GI disorders. *Gut* (2016) 65(1):155–68. doi: 10.1136/gutjnl-2015-309151

79. Bonnet B, Vigneron J, Levacher B, Vazquez T, Pitoiset F, Brimaud F, et al. Low-dose IL-2 induces regulatory T cell-mediated control of experimental food allergy. *J Immunol* (2016) 197(1):188–98. doi: 10.4049/jimmunol.1501271

80. Chen CY, Lee JB, Liu B, Ohta S, Wang PY, Kartashov AV, et al. Induction of interleukin-9-Producing mucosal mast cells promotes susceptibility to IgE-mediated experimental food allergy. *Immunity* (2015) 43(4):788–802. doi: 10.1016/j.immuni.2015.08.020

81. Wright SH, Brown J, Knight PA, Thornton EM, Kilshaw PJ, Miller HR. Transforming growth factor-beta1 mediates coexpression of the integrin subunit alphaE and the chymase mouse mast cell protease-1 during the early differentiation of bone marrow-derived mucosal mast cell homologues. *Clin Exp Allergy* (2002) 32 (2):315–24. doi: 10.1046/j.1365-2222.2002.01233.x

82. Nakano N, Saida K, Hara M, Izawa K, Ando T, Kaitani A, et al. Mucosal mast cell-specific gene expression is promoted by interdependent action of notch and TGF-beta signaling. *J Immunol* (2021) 207(12):3098–106. doi: 10.4049/jimmunol.2100112

83. Tomar S, Ganesan V, Sharma A, Zeng C, Waggoner L, Smith A, et al. IL-4-BATF signaling directly modulates IL-9 producing mucosal mast cell (MMC9) function in experimental food allergy. *J Allergy Clin Immunol* (2021) 147(1):280–95. doi: 10.1016/j.jaci.2020.08.043

84. He Z, Song J, Hua J, Yang M, Ma Y, Yu T, et al. Mast cells are essential intermediaries in regulating IL-33/ST2 signaling for an immune network favorable to mucosal healing in experimentally inflamed colons. *Cell Death Dis* (2018) 9 (12):1173. doi: 10.1038/s41419-018-1223-4

85. Wanet A, Bassal MA, Patel SB, Marchi F, Mariani SA, Ahmed N, et al. E-cadherin is regulated by GATA-2 and marks the early commitment of mouse hematopoietic progenitors to the basophil and mast cell fates. *Sci Immunol* (2021) 6 (56):eaba0178. doi: 10.1126/sciimmunol.aba0178

86. Hamey FK, Lau WWY, Kucinski I, Wang X, Diamanti E, Wilson NK, et al. Single-cell molecular profiling provides a high-resolution map of basophil and mast cell development. *Allergy* (2021) 76(6):1731–42. doi: 10.1111/all.14633

87. Popescu DM, Botting RA, Stephenson E, Green K, Webb S, Jardine L, et al. Decoding human fetal liver haematopoiesis. *Nature* (2019) 574(7778):365–71. doi: 10.1038/s41586-019-1652-y

88. Zheng S, Papalexi E, Butler A, Stephenson W, Satija R. Molecular transitions in early progenitors during human cord blood hematopoiesis. *Mol Syst Biol* (2018) 14(3):e8041. doi: 10.15252/msb.20178041

89. Cheng S, Li Z, Gao R, Xing B, Gao Y, Yang Y, et al. A pan-cancer single-cell transcriptional atlas of tumor infiltrating myeloid cells. *Cell* (2021) 184(3):792–809.e23. doi: 10.1016/j.cell.2021.01.010

90. Lu T, Yang X, Shi Y, Zhao M, Bi G, Liang J, et al. Single-cell transcriptome atlas of lung adenocarcinoma featured with ground glass nodules. *Cell Discovery* (2020) 6:69. doi: 10.1038/s41421-020-00200-x

91. Watcham S, Kucinski I, Gottgens B. New insights into hematopoietic differentiation landscapes from single-cell RNA sequencing. *Blood* (2019) 133 (13):1415–26. doi: 10.1182/blood-2018-08-835355

92. Abonia JP, Hallgren J, Jones T, Shi T, Xu Y, Koni P, et al. Alpha-4 integrins and VCAM-1, but not MAdCAM-1, are essential for recruitment of mast cell progenitors to the inflamed lung. *Blood* (2006) 108(5):1588–94. doi: 10.1182/blood-2005-12-012781

93. Mendez-Enriquez E, Alvarado-Vazquez PA, Abma W, Simonson OE, Rodin S, Feyerabend TB, et al. Mast cell-derived serotonin enhances methacholine-induced airway hyperresponsiveness in house dust mite-induced experimental asthma. *Allergy* (2021) 76(7):2057–69. doi: 10.1111/all.14748

94. Dahlin JS, Feinstein R, Cui Y, Heyman B, Hallgren J. CD11c+ cells are required for antigen-induced increase of mast cells in the lung. *J Immunol* (2012) 189(8):3869–77. doi: 10.4049/jimmunol.1201200

95. Jones TG, Hallgren J, Humbles A, Burwell T, Finkelman FD, Alcaide P, et al. Antigen-induced increases in pulmonary mast cell progenitor numbers depend on IL-9 and CD1d-restricted NKT cells. *J Immunol* (2009) 183(8):5251–60. doi: 10.4049/jimmunol.0901471

96. Mathias CB, Freyschmidt EJ, Caplan B, Jones T, Poddighe D, Xing W, et al. IgE influences the number and function of mature mast cells, but not progenitor recruitment in allergic pulmonary inflammation. *J Immunol* (2009) 182(4):2416–24. doi: 10.4049/jimmunol.0801569

97. Dahlin JS, Ivarsson MA, Heyman B, Hallgren J. IgE immune complexes stimulate an increase in lung mast cell progenitors in a mouse model of allergic airway inflammation. *PLoS One* (2011) 6(5):e20261. doi: 10.1371/journal.pone.0020261

98. Hershko AY, Suzuki R, Charles N, Alvarez-Errico D, Sargent JL, Laurence A, et al. Mast cell interleukin-2 production contributes to suppression of chronic allergic dermatitis. *Immunity* (2011) 35(4):562–71. doi: 10.1016/j.immuni.2011.07.013

99. Fiorentino DF, Zlotnik A, Vieira P, Mosmann TR, Howard M, Moore KW, et al. IL-10 acts on the antigen-presenting cell to inhibit cytokine production by Th1 cells. *J Immunol* (1991) 146(10):3444–51.

100. Mirmonsef P, Shelburne CP, Fitzhugh Yeatman C. 2nd, h. j. chong and j. j. Ryan: Inhibition of kit expression by IL-4 and IL-10 in murine mast cells: role of STAT6 and phosphatidylinositol 3'-kinase. *J Immunol* (1999) 163(5):2530–9.

101. Helmby H, Grencis RK. Contrasting roles for IL-10 in protective immunity to different life cycle stages of intestinal nematode parasites. *Eur J Immunol* (2003) 33(9):2382–90. doi: 10.1002/eji.200324082

102. Bouton LA, Ramirez CD, Bailey DP, Yeatman CF, Yue J, Wright HV, et al. Costimulation with interleukin-4 and interleukin-10 induces mast cell apoptosis and cell-cycle arrest: the role of p53 and the mitochondrion. *Exp Hematol* (2004) 32 (12):1137–45. doi: 10.1016/j.exphem.2004.09.002

103. Bailey DP, Kashyap M, Bouton LA, Murray PJ, Ryan JJ. Interleukin-10 induces apoptosis in developing mast cells and macrophages. *J Leukoc Biol* (2006) 80(3):581–9. doi: 10.1189/jlb.0405201

104. Leveson-Gower DB, Sega EI, Kalesnikoff J, Florek M, Pan Y, Pierini A, et al. Mast cells suppress murine GVHD in a mechanism independent of CD4+CD25+ regulatory T cells. *Blood* (2013) 122(22):3659–65. doi: 10.1182/blood-2013-08-519157

105. Oshima T, Laroux FS, Coe LL, Morise Z, Kawachi S, Bauer P, et al. Interferon-gamma and interleukin-10 reciprocally regulate endothelial junction integrity and barrier function. *Microvasc Res* (2001) 61(1):130–43. doi: 10.1006/mvre.2000.2288

106. Chan CY, St John AL, Abraham SN. Mast cell interleukin-10 drives localized tolerance in chronic bladder infection. *Immunity* (2013) 38(2):349–59. doi: 10.1016/j.immuni.2012.10.019

107. Zhao YB, Yang SH, Shen J, Deng K, Li Q, Wang Y, et al. Interaction between regulatory T cells and mast cells *via* IL-9 and TGF-beta production. *Oncol Lett* (2020) 20(6):360. doi: 10.3892/ol.2020.12224

108. Norozian F, Kashyap M, Ramirez CD, Patel N, Kepley CL, Barnstein BO, et al. TGFbeta1 induces mast cell apoptosis. *Exp Hematol* (2006) 34(5):579–87. doi: 10.1016/j.exphem.2006.02.003

109. Hart PH, Grimbaldeston MA, Swift GJ, Jaksic A, Noonan FP, Finlay-Jones JJ. Dermal mast cells determine susceptibility to ultraviolet b-induced systemic suppression of contact hypersensitivity responses in mice. *J Exp Med* (1998) 187 (12):2045–53. doi: 10.1084/jem.187.12.2045

110. van der Pouw Kraan TC, Boeije LC, Smeenk RJ, Wijdenes J, Aarden LA. Prostaglandin-E2 is a potent inhibitor of human interleukin 12 production. *J Exp Med* (1995) 181(2):775–9. doi: 10.1084/jem.181.2.775

111. Fernando MR, Reyes JL, Iannuzzi J, Leung G, McKay DM. The pro-inflammatory cytokine, interleukin-6, enhances the polarization of alternatively activated macrophages. *PLoS One* (2014) 9(4):e94188. doi: 10.1371/journal.pone.0094188

112. Pesce JT, Ramalingam TR, Mentink-Kane MM, Wilson MS, El Kasmi KC, Smith AM, et al. Arginase-1-expressing macrophages suppress Th2 cytokine-driven inflammation and fibrosis. *PLoS Pathog* (2009) 5(4):e1000371. doi: 10.1371/journal.ppat.1000371

113. Braune J, Weyer U, Hobusch C, Mauer J, Bruning JC, Bechmann I, et al. IL-6 regulates M2 polarization and local proliferation of adipose tissue macrophages in obesity. *J Immunol* (2017) 198(7):2927–34. doi: 10.4049/jimmunol.1600476

114. Rivellese F, Suurmond J, Habets K, Dorjee AL, Ramamoorthi N, Townsend MJ, et al. Ability of interleukin-33- and immune complex-triggered activation of human mast cells to down-regulate monocyte-mediated immune responses. *Arthritis Rheumatol* (2015) 67(9):2343–53. doi: 10.1002/art.39192

115. Morita H, Arae K, Unno H, Miyauchi K, Toyama S, Nambu A, et al. An interleukin-33-Mast cell-Interleukin-2 axis suppresses papain-induced allergic inflammation by promoting regulatory T cell numbers. *Immunity* (2015) 43 (1):175–86. doi: 10.1016/j.immuni.2015.06.021

116. Gillespie SR, DeMartino RR, Zhu J, Chong HJ, Ramirez C, Shelburne CP, et al. IL-10 inhibits fc epsilon RI expression in mouse mast cells. *J Immunol* (2004) 172(5):3181–8. doi: 10.4049/jimmunol.172.5.3181

117. Nakano T, Lai CY, Goto S, Hsu LW, Kawamoto S, Ono K, et al. Immunological and regenerative aspects of hepatic mast cells in liver allograft rejection and tolerance. *PloS One* (2012) 7(5):e37202. doi: 10.1371/journal.pone.0037202

118. Cunningham D, Humblet Y, Siena S, Khayat D, Bleiberg H, Santoro A, et al. Cetuximab monotherapy and cetuximab plus irinotecan in irinotecan-refractory metastatic colorectal cancer. *N Engl J Med* (2004) 351(4):337–45. doi: 10.1056/NEJMoa033025

119. Bonner JA, Harari PM, Giralt J, Azarnia N, Shin DM, Cohen RB, et al. Radiotherapy plus cetuximab for squamous-cell carcinoma of the head and neck. *N Engl J Med* (2006) 354(6):567–78. doi: 10.1056/NEJMoa053422

120. Thornton AM, Donovan EE, Piccirillo CA, Shevach EM. Cutting edge: IL-2 is critically required for the *in vitro* activation of CD4+CD25+ T cell suppressor function. *J Immunol* (2004) 172(11):6519–23. doi: 10.4049/jimmunol.172.11.6519

121. Swain SL, Weinberg AD, English M, Huston G. IL-4 directs the development of Th2-like helper effectors. *J Immunol* (1990) 145(11):3796–806.

122. Bischoff SC, Sellge G, Lorentz A, Sebald W, Raab R, Manns MP. IL-4 enhances proliferation and mediator release in mature human mast cells. *Proc Natl Acad Sci U S A* (1999) 96(14):8080–5. doi: 10.1073/pnas.96.14.8080

123. Moore KW, de Waal Malefyt R, Coffman RL, O'Garra A. Interleukin-10 and the interleukin-10 receptor. *Annu Rev Immunol* (2001) 19:683–765. doi: 10.1146/annurev.immunol.19.1.683

124. Groux H, Bigler M, de Vries JE, Roncarolo MG. Inhibitory and stimulatory effects of IL-10 on human CD8+ T cells. *J Immunol* (1998) 160(7):3188–93.

125. Depinay N, Hacini F, Beghdadi W, Peronet R, Mecheri S. Mast cell-dependent down-regulation of antigen-specific immune responses by mosquito bites. *J Immunol* (2006) 176(7):4141–6. doi: 10.4049/jimmunol.176.7.4141

126. Galli SJ, Kalesnikoff J, Grimbaldeston MA, Piliponsky AM, Williams CM, Tsai M. Mast cells as "tunable" effector and immunoregulatory cells: recent advances. *Annu Rev Immunol* (2005) 23:749–86. doi: 10.1146/annurev.immunol.21.120601.141025

127. Masuda A, Yoshikai Y, Aiba K, Matsuguchi T. Th2 cytokine production from mast cells is directly induced by lipopolysaccharide and distinctly regulated by c-jun n-terminal kinase and p38 pathways. *J Immunol* (2002) 169(7):3801–10. doi: 10.4049/jimmunol.169.7.3801

128. Biggs L, Yu C, Fedoric B, Lopez AF, Galli SJ, Grimbaldeston MA. Evidence that vitamin D(3) promotes mast cell-dependent reduction of chronic UVB-induced skin pathology in mice. *J Exp Med* (2010) 207(3):455–63. doi: 10.1084/jem.20091725

129. Younan GJ, Heit YI, Dastouri P, Kekhia H, Xing W, Gurish MF, et al. Mast cells are required in the proliferation and remodeling phases of microdeformational wound therapy. *Plast Reconstr Surg* (2011) 128(6):649e–58e. doi: 10.1097/PRS.0b013e318230c55d

130. Brand S, Beigel F, Olszak T, Zitzmann K, Eichhorst ST, Otte JM, et al. IL-22 is increased in active crohn's disease and promotes proinflammatory gene expression and intestinal epithelial cell migration. *Am J Physiol Gastrointest Liver Physiol* (2006) 290(4):G827–38. doi: 10.1152/ajpgi.00513.2005

131. Sugimoto K, Ogawa A, Mizoguchi E, Shimomura Y, Andoh A, Bhan AK, et al. IL-22 ameliorates intestinal inflammation in a mouse model of ulcerative colitis. *J Clin Invest* (2008) 118(2):534–44. doi: 10.1172/JCI33194

132. Trautmann A, Toksoy A, Engelhardt E, Brocker EB, Gillitzer R. Mast cell involvement in normal human skin wound healing: expression of monocyte chemoattractant protein-1 is correlated with recruitment of mast cells which synthesize interleukin-4 *in vivo*. *J Pathol* (2000) 190(1):100–6. doi: 10.1002/(SICI)1096-9896(200001)190:1<100::AID-PATH496>3.0.CO;2-Q

133. Nishikori Y, Shiota N, Okunishi H. The role of mast cells in cutaneous wound healing in streptozotocin-induced diabetic mice. *Arch Dermatol Res* (2014) 306(9):823–35. doi: 10.1007/s00403-014-1496-0

134. Ud-Din S, Wilgus TA, Bayat A. Mast cells in skin scarring: A review of animal and human research. *Front Immunol* (2020) 11:552205. doi: 10.3389/fimmu.2020.552205

135. Moyer KE, Saggers GC, Ehrlich HP. Mast cells promote fibroblast populated collagen lattice contraction through gap junction intercellular communication. *Wound Repair Regener* (2004) 12(3):269–75. doi: 10.1111/j.1067-1927.2004.012310.x

136. Nishida K, Hasegawa A, Yamasaki S, Uchida R, Ohashi W, Kurashima Y, et al. Mast cells play role in wound healing through the ZnT2/GPR39/IL-6 axis. *Sci Rep* (2019) 9(1):10842. doi: 10.1038/s41598-019-47132-5

137. Lin ZQ, Kondo T, Ishida Y, Takayasu T, Mukaida N. Essential involvement of IL-6 in the skin wound-healing process as evidenced by delayed wound healing in IL-6-deficient mice. *J Leukoc Biol* (2003) 73(6):713–21. doi: 10.1189/jlb.0802397

138. Saito H, Hatake K, Dvorak AM, Leiferman KM, Donnenberg AD, Arai N, et al. Selective differentiation and proliferation of hematopoietic cells induced by recombinant human interleukins. *Proc Natl Acad Sci U S A* (1988) 85(7):2288–92. doi: 10.1073/pnas.85.7.2288

frontiers | Frontiers in Immunology

TYPE Original Research
PUBLISHED 31 January 2023
DOI 10.3389/fimmu.2023.1006741

Check for updates

OPEN ACCESS

EDITED BY
Satoshi Tanaka,
Kyoto Pharmaceutical University, Japan

REVIEWED BY
Cem Akin,
University of Michigan, United States
Roopesh Singh,
Vanderbilt University Medical Center, United States

*CORRESPONDENCE
Glenn Cruse
gpcruse@ncsu.edu

†These authors have contributed equally to this work

SPECIALTY SECTION
This article was submitted to Inflammation, a section of the journal Frontiers in Immunology

RECEIVED 29 July 2022
ACCEPTED 16 January 2023
PUBLISHED 31 January 2023

CITATION
Hedgespeth BA, Snider DB, Bitting KJ and Cruse G (2023) The exon-skipping oligonucleotide, KitStop, depletes tissue-resident mast cells *in vivo* to ameliorate anaphylaxis. *Front. Immunol.* 14:1006741. doi: 10.3389/fimmu.2023.1006741

COPYRIGHT
© 2023 Hedgespeth, Snider, Bitting and Cruse. This is an open-access article distributed under the terms of the Creative Commons Attribution License (CC BY). The use, distribution or reproduction in other forums is permitted, provided the original author(s) and the copyright owner(s) are credited and that the original publication in this journal is cited, in accordance with accepted academic practice. No use, distribution or reproduction is permitted which does not comply with these terms.

The exon-skipping oligonucleotide, KitStop, depletes tissue-resident mast cells *in vivo* to ameliorate anaphylaxis

Barry A. Hedgespeth[1,2,3,4†], Douglas B. Snider[1,2,3,4†], Katie J. Bitting[1] and Glenn Cruse[1,3*]

[1]Department of Molecular Biomedical Sciences, College of Veterinary Medicine, NC State University, Raleigh, NC, United States, [2]Department of Clinical Sciences, College of Veterinary Medicine, NC State University, Raleigh, NC, United States, [3]Comparative Medicine Institute, North Carolina State University, Raleigh, NC, United States, [4]Comparative Medicine and Translational Research Training Program, North Carolina State University, Raleigh, NC, United States

Introduction: Anaphylaxis represents the most extreme and life-threatening form of allergic disease and is considered a medical emergency requiring immediate intervention. Additionally, some people with mastocytosis experience recurrent episodes of anaphylaxis during normal daily activities without exposure to known triggers. While acute therapy consists primarily of epinephrine and supportive care, chronic therapy relies mostly on desensitization and immunotherapy against the offending allergen, which is a time-consuming and sometimes unsuccessful process. These treatments also necessitate identification of the triggering allergen which is not always possible, and thus highlighting a need for alternative treatments for mast cell-mediated diseases.

Methods: The exon-skipping oligonucleotide KitStop was administered to mice intradermally, intraperitoneally, or systemically at a dose of 12.5 mg/kg. Local mast cell numbers were enumerated via peritoneal lavage or skin histology, and passive systemic anaphylaxis was induced to evaluate KitStop's global systemic effect. A complete blood count and biochemistry panel were performed to assess the risk of acute toxicity following KitStop administration.

Results: Here, we report the use of an exon-skipping oligonucleotide, which we have previously termed KitStop, to safely reduce the severity and duration of the anaphylactic response via mast cell depopulation in tissues. KitStop administration results in the integration of a premature stop codon within the mRNA transcript of the KIT receptor—a receptor tyrosine kinase found primarily on mast cells and whose gain-of-function mutation can lead to systemic mastocytosis. Following either local or systemic KitStop treatment, mice had significantly reduced mast cell numbers in the skin and peritoneum. In addition, KitStop-treated mice experienced a significantly diminished anaphylactic response using a model of passive systemic anaphylaxis when compared with control mice.

Discussion: KitStop treatment results in a significant reduction in systemic mast cell responses, thus offering the potential to serve as a powerful additional treatment modality for patients that suffer from anaphylaxis.

KEYWORDS

mast cell (MC), anaphylaxis, KIT, exon skipping, mast cell depletion

Introduction

Anaphylaxis is a rapid and potentially fatal systemic allergic reaction that occurs following exposure to an allergen (1). The American College of Allergy, Asthma, and Immunology (ACAAI) anaphylaxis working group estimated the lifetime prevalence of anaphylaxis for a person living in the USA to be up to 5% (2); however, more recent reports indicate that anaphylaxis may be experienced much more frequently than previously reported (3, 4). The most common triggers of anaphylaxis include medications (antibiotics, NSAIDs, antineoplastic/cytotoxic drugs, immunomodulators, contrast dyes), bee and wasp venom, and foods such as peanuts, wheat, milk, and soy (5). Following prior immune sensitization by the allergen, future exposures can result in activation of mast cells (MCs) through IgE- or non-IgE-dependent pathways. Activated MCs release a myriad of inflammatory mediators such as histamine, proteases, cytokines, and growth factors, all of which culminates in the development of clinical signs typically associated with anaphylaxis (6). These include skin flushing, pruritus, angioedema, dyspnea, vomiting, diarrhea, hypotension, hypovolemic shock, and cardiovascular collapse; death may also rapidly occur if the patient is not promptly addressed (7). Treatment relies on the acute mitigation of clinical signs with epinephrine and supportive care followed by chronic strategies such as desensitization and immunotherapy to prevent severe future reactions from occurring (7). These chronic therapies rely on the identification of the allergic trigger which is not always possible; in addition, patients must be willing to attend frequent visits to the clinic and are prone to developing side effects associated with these treatments. Absolute contraindications for some chronic therapies include uncontrolled asthma, atopic dermatitis/eczema, and chronic urticaria, leaving these patients with few other options to address their recurrent anaphylaxis (8). As such, additional therapies for treating anaphylaxis and its sequelae are urgently required for patients who are unable to find recourse in currently available treatments.

While countless triggers can result in varying degrees of anaphylaxis, almost all cases are caused in part by the degranulation of MCs. After exiting the bone marrow, hematopoietic progenitor cells migrate throughout the body and, upon reaching their destination within tissues, develop into mature MCs after receiving the appropriate immunostimulatory signals. Primary destinations for these cells include around blood vessels and nerves, within the skin, and at the mucosal surfaces of the respiratory and gastrointestinal tracts (9). The two primary receptors involved in MC function are the high-affinity immunoglobulin E (IgE) receptor, FcεRI, and KIT, a receptor tyrosine kinase also known as CD117 (10). While FcεRI is the primary receptor involved in MC degranulation, KIT is responsible for growth, differentiation, and maturation of MCs *via* binding of its ligand, stem cell factor (SCF) (11). Additionally, the interaction between SCF and KIT are critical for MC proliferation and suppression of apoptosis (12). KIT is initially expressed by most hematopoietic cells but is lost by most during the differentiation process; MCs are one of the few exceptions that retain this receptor for their lifespan (13). Indeed, the gene encoding the KIT protein, *c-Kit*, is considered a proto-oncogene and activating mutations are known to induce the development of cutaneous or systemic mastocytosis—the abnormal accumulation of MCs within tissues (13, 14). Patients suffering from mastocytosis are susceptible to MC activation syndrome (MCAS), a condition characterized by spontaneous, recurrent episodes of systemic anaphylaxis that often do not have a known trigger (15). In addition to antihistamines, treatments aimed at reducing the severity of symptoms experienced by patients suffering from MCAS include glucocorticoids, cytoreductive medications such as interferon-α and cladribine, or tyrosine kinase inhibitors such as masitinib; these are, however, fraught with numerous side effects including cytopenias and increased risk of infections, thereby worsening these patients' already diminished quality of life (15).

Given its relative scarcity among cell types other than MCs as well as its involvement in numerous debilitating MC-related disorders, KIT provides an alluring therapeutic target for anaphylaxis and MCAS. We have previously shown that MC tumors comprising MCs with gain-of-function KIT mutations can successfully be targeted and significantly reduced by the exon-skipping oligonucleotide (ESO) KitStop (16). ESOs belong to a group of antisense oligonucleotides (ASOs) that block binding of the spliceosome to an intron-exon or exon-intron boundary, thus resulting in the skipping of a particular exon of interest. If the skipped exon maintains the reading frame of the mature mRNA transcript, an alternatively spliced product will be generated. KitStop is a 25-mer morpholino ESO that targets the donor splice site of exon 4 of *c-Kit* pre-mRNA; upon its introduction, KitStop induces a frameshift into the mature mRNA open reading frame, resulting in a premature stop codon. This triggers either the nonsense-mediated decay of the KIT mRNA template or the production of a severely truncated peptide and nonfunctional receptor (16). To determine whether a KIT-specific ESO has any effect on the development and severity of anaphylaxis, here we assessed the impact that KitStop has using a well-established mouse model of passive systemic anaphylaxis, as well as compared its efficacy following varying routes of administration.

Materials and methods

Mice

Four to six-week-old female BALB/c mice were purchased from Jackson Laboratories (Bar Harbor, ME) and were maintained at the North Carolina State University laboratory animal facility. Animal care and experimental protocols were conducted with the guidelines of the National Institutes of Health and with the approval of the Institutional Animal Care and Use Committee of North Carolina State University laboratory animal care protocols (17-108-B and 20-223-B).

ESO design

The KitStop ESO was designed to target exon 4 of murine *c-Kit* (GenBank: NM_001329070.1). A region within the splicing donor site was targeted with the following sequence: 5′-AGGACTTA AACAGCACTCACCTGAG-3′. Specificity of the oligonucleotide sequence was confirmed with BLAST search and was purchased

from Gene Tools (Philomath, OR). The unconjugated standard control ASO provided by Gene Tools had the following sequence: 5′-CCTCTTACCTCAGTTACAATTTATA-3′. To facilitate *in vivo* delivery, an octaguanidinium dendrimer was linked to the terminal 3′-N of the standard control and KitStop oligonucleotides (Vivo-Morpholino).

Peritoneal lavage

Peritoneal lavage fluid was collected as described (17). Mice (7 to 10 weeks old) were euthanized and 5 mL of phosphate-buffered saline (PBS) was instilled into the peritoneal cavity. The abdomen was gently massaged, and the fluid was aspirated from the peritoneum before being placed on ice. The fluid was centrifuged at *300 x g* for 5 minutes, the supernatant was discarded, and the cell pellet was resuspended in PBS for further analysis. A sample was collected for total cell enumeration with Trypan Blue staining, as well as mast cell enumeration with Kimura staining.

Qualitative reverse transcription-PCR

RNA from cells in the peritoneal lavage fluid was extracted using the RNeasy Plus Mini kit (QIAGEN) according to the manufacturer's instructions with inclusion of the QIAshredder step. The primers used were designed to amplify exon 4 as well as surrounding exons; their sequences are as follows: forward 50-TCATCGAGTG TGATGGGAAA-30; reverse 50-TCACAGGGGAGATGTTGATG-30. Gel electrophoresis PCR images were acquired using a Licor Odyssey Fc Imaging system.

Flow cytometry

MCs in peritoneal lavage fluid were identified as double-positive for CD117 and FcεRIα. Bone marrow-derived mast cells (BMMCs) were treated with 10 μM of either Vivo-Morpholino standard control ASO or Vivo-Morpholino KitStop ESO for 24 hours before flow cytometric analysis. Cells were stained with the following antibodies on ice for 60 minutes before imaging: fluorescein isothiocyanate (FITC)-conjugated rat anti-mouse CD117 (Clone 2B8; BD Pharmingen) and phycoerythrin (PE)-conjugated anti-mouse FcεRIα (clone MAR-1; eBioscience). Data were acquired using a CytoFLEX (Beckman Coulter) flow cytometer and analyzed with FCS Express version 6 (Denovo Software), or FLOWJO version 10.

Histologic analysis

Skin biopsies were fixed with 10% neutral buffered formalin at 45°C for 24 hours followed by immersion in 70% ethanol until paraffin embedment. Sections were made every 4 μm and stained with either 0.1% toluidine blue or hematoxylin and eosin (H&E). Images were acquired with an Olympus VS200 whole slide scanner at 40X. Images were -visualized using OlyVIA software from the whole slide images (Olympus Life Science).

Passive systemic anaphylaxis model

A model of passive systemic anaphylaxis was generated as previously described (18). In brief, 7 to 10 week-old mice were treated intravenously (retro-orbitally) with standard control ASO or KitStop ESO at a dose of 12.5 mg/kg in 100 μl of PBS. One day after the final oligonucleotide injection, mice were sensitized with an intravenous injection of 3 μg mouse anti-2,4-dinitrophenyl (DNP) monoclonal immunoglobulin (Ig) E (clone SPE-7, Sigma-Aldrich). Mice were challenged on the following day with an intravenous injection of 300 μg DNP conjugated to human serum albumin (DNP-HSA, Sigma-Aldrich) in 200 μL PBS. A rectal temperature measurement was obtained immediately prior to and every 10 minutes after DNP-HSA injection for a total of 90 minutes.

Complete blood count and serum biochemical measurements

Blood was collected from the mice *via* direct cardiac puncture and analyzed at the North Carolina State University Veterinary Clinical Pathology laboratory.

Beta-hexosaminidase degranulation assay

Bone marrow-derived mast cells (BMMCs) were developed from bone marrow obtained from the femurs of 7-12-week-old C57BL/6J mice (The Jackson Laboratory), as described (17). After being in culture for 4 weeks, 0.5 x 10 (6) BMMCs were treated with 10 μM of either Vivo-Morpholino standard control ASO or Vivo-Morpholino KitStop ESO for 24 hours. The cells were concurrently sensitized with 100 ng/mL anti-DNP IgE (SPE7 clone) (Sigma). After 24 hours, the cells were washed with PBS and used to measure β-hexosaminidase release as previously described (19).

Statistical analysis

Results represent mean + individual data points or mean ± SEM. An unpaired Student's t-test was used to evaluate the significance of differences between two datasets. A mixed-effects model (REML) analysis with Sidak's multiple comparisons test was used to determine statistical significance in comparisons of multiple datasets. Data were considered statistically significant if $p \leq 0.05$.

Results

Local KitStop administration reduces KIT expression and MC number *in vivo*

To assess the effect of peritoneal KitStop administration on MC KIT expression as well as total MC number, two intraperitoneal injections of either standard control ASO or KitStop ESO were administered two days apart followed by peritoneal lavage collection two days after the final injection (Figure 1A). No overt adverse effects

10.3389/fimmu.2023.1006741

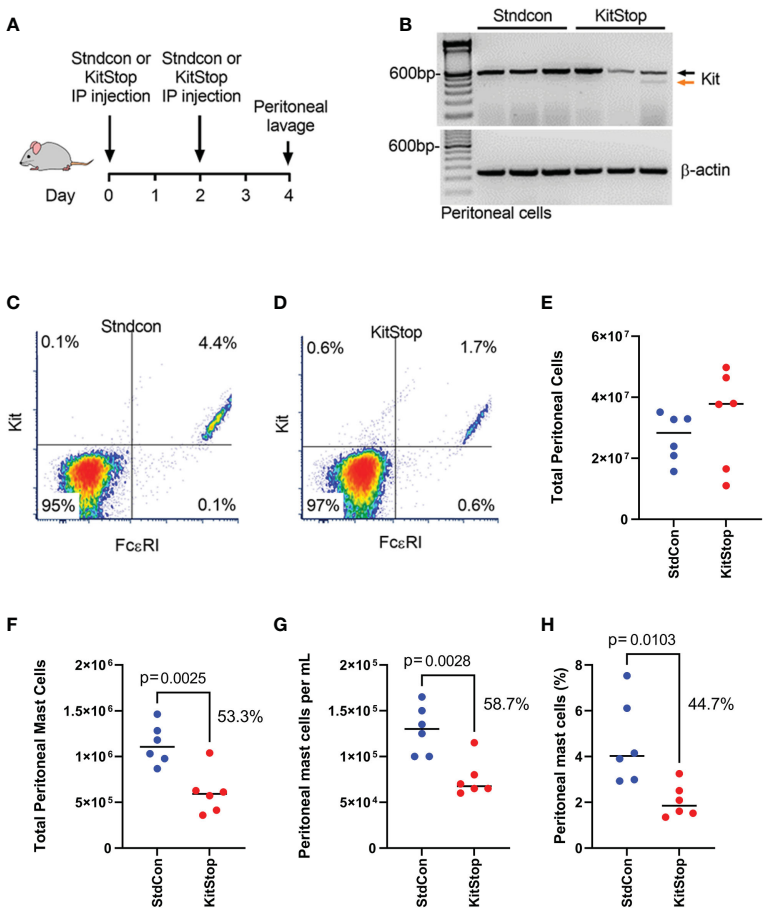


FIGURE 1
KitStop ESO reduces Kit expression in mouse mast cells locally *in vivo*. **(A)** Balb/c mice received 2 intraperitoneal injections of standard control ASO or KitStop ESO 2 days apart. A peritoneal lavage was performed 2 days after the final injection, and cells in the lavage fluid were analyzed for KIT and FcεRI expression. **(B)** RT-PCR of c-Kit expression in cells collected by peritoneal lavage (n=3). Black arrow = full-length c-Kit, orange arrow = alternatively spliced c-Kit. **(C, D)** Representative flow cytometry density plots of peritoneal cells harvested from seven mice treated with standard control ASO **(C)** or KitStop ESO **(D)**. **(E)**Total number of cells enumerated in the peritoneal lavage fluid collected. **(F)** Total number of peritoneal mast cells in peritoneal lavage fluid. **(G)** Number of mast cells per milliliter of peritoneal lavage fluid recovered. **(H)** Percent of mast cells out of all cells recovered from the peritoneal lavage fluid. Each datapoint represent a different mouse and data are combined from at least two independent experiments. P value is from an unpaired t-test.

were observed in either group. Two intraperitoneal injections of KitStop appeared to reduce the overall number of transcripts and induced the expression of a truncated splice variant of *c-Kit* in peritoneal MCs whereas no splice variant was expressed in mice treated with the standard control ASO (Figure 1B). However, while these data suggested that the KitStop ESO worked in this setting, the qualitative reverse transcription PCR data were not reliable for quantitation and demonstrated some variation in appearance between mice. We have shown that KitStop ESO induces nonsense-mediated decay of the truncated KIT mRNA template, which would diminish the truncated variant with this approach (16). We therefore chose to validate the efficacy of the KitStop ESO with another approach directly measuring MC number. The number of peritoneal MCs (those double positive for FcεRIα and KIT) decreased by more than half with KitStop treatment when compared to control mice (Figures 1C, D). The total number of cells collected from the peritoneal lavage was not different between the treatment groups (Figure 1E). However, the total number of MCs, the number of MCs per milliliter of lavage fluid recovered, and overall percentage of peritoneal MCs was significantly lower in the KitStop-treated mice when compared with the standard control ASO treatment (Figures 1F–H).

To evaluate the effect of KitStop on the cutaneous MC population, two intradermal injections of either standard control ASO or KitStop ESO were administered into the dorsal skin of the mice followed by skin biopsy (Figure 2A). Histological evaluation of the skin biopsies revealed normal MC tissue localization and no evidence of overt tissue pathology (Figures 2B, C). The numbers of MCs per mm (2) in the dermis alone (Figure 2D) and full thickness skin sections (Figure 2E) were significantly reduced by nearly 50% in the KitStop-treated mice. Taken together, these data indicate that local administration of KitStop significantly reduces MC KIT expression as well as overall MC number.

Systemic KitStop administration reduces the cutaneous MC population *in vivo*

We next sought to determine the safety and efficacy of KitStop on MCs when administered systemically. Eight intravenous injections of either PBS vehicle control or KitStop ESO were administered to mice; thereafter, ears were harvested for histological assessment (Figure 3A). No adverse effects were observed in either group and no change in body weight occurred for the duration of the treatment course (Figure 3B). There was a significant reduction of the aural cutaneous MC population by 56% in KitStop-treated mice following systemic treatment (Figure 3C). These data indicate that repeated intravenous KitStop administration does not result in a measurable weight change in mice and produces a significant reduction in the cutaneous MC population.

KitStop administration significantly reduces the anaphylactic response while having no overt effect on hematopoietic or biochemical parameters over the 21 day protocol

Having shown that local and systemic KitStop administration is effective at significantly reducing *c-Kit* expression as well as tissue-resident MC numbers, our final aim was to determine KitStop's global effects in a model of passive systemic anaphylaxis. After receiving 8 intravenous injections of either standard control ASO or KitStop ESO, five mice per group were sensitized with intravenous monoclonal IgE specific for 2,4-dinitrophenyl (DNP). On the following day, the mice were challenged with intravenous DNP-HSA and their rectal temperatures were measured every 10 minutes for a total of 90 minutes (Figure 4A). A drop in body temperature of 5-9°C within the first 5-15 minutes is considered a normal systemic anaphylactic response in mice, with recovery to baseline expected to occur within 60-90 minutes (18). In our experiments, KitStop-treated mice experienced a significantly smaller decrease in rectal temperature during the first 10 minutes, with an average reduction of 4°C in contrast to the 6°C decrease experienced by the control mice. This disparity became more significant as time progressed, with a significant difference remaining between the groups until 60 minutes after challenge. Normothermia was achieved more rapidly by KitStop treated mice than control mice, with KitStop treated mice returning to their baseline temperature 30 minutes sooner than control mice (Figure 4B). This effect was unlikely attributable to changes in surface expression of the IgE receptor or mast cell degranulation as there was no significant difference in these criteria following treatment of bone marrow-derived mast cells with either Stndcon ASO or KitStop ESO (Supplemental Figure 1).

Because the KIT receptor is expressed by immature hematopoietic stem cells in addition to MCs, a complete blood count was performed on whole blood from mice that received the same treatment regimen. No differences in erythrocyte, leukocyte, or thrombocyte parameters were noted in either group (Figure 5). To assess the effect that oligonucleotide treatment might have on kidney and liver function, biochemistry panels were performed on serum samples from each mouse. No differences in hepatic or renal function were noted for either group (Figure 6). Two control mice displayed mildly increased hepatocellular enzyme activities, which was likely due to iatrogenic hepatic trauma during the cardiac puncture procedure. In total, these

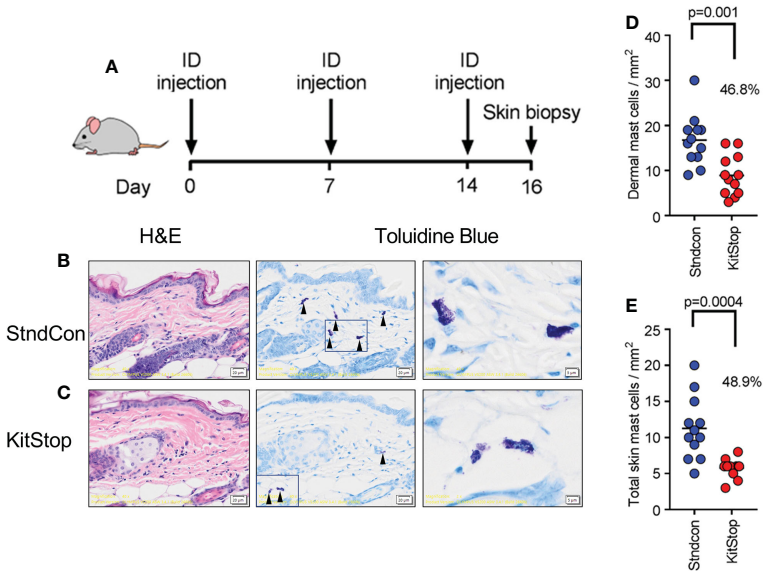


FIGURE 2
Local KitStop ESO administration reduces mouse dorsal skin mast cell numbers *in vivo*. **(A)** Four Balb/c mice were given dorsal intradermal injections of either standard control ASO or KitStop ESO every 7 days for a total of 3 injections. Skin was then biopsied 2 days after the final injection for histological analysis. **(B, C)** In representative sections from standard control ASO (Stndcon; **B**) and KitStop ESO **(C)** treatment groups, MCs were easily identified due to the presence of positive-staining metachromatic granules, which give a deep violet hue (see red arrow heads). Mast cells displayed normal tissue localization with no evidence of pathology. **(D)** Plot of dermal mast cell number per mm2 from toluidine blue stained skin sections taken from standard control ASO (blue) or KitStop ESO (red) treated skin. **(E)** Plot of mast cell number per mm2 from the full thickness skin sections, including dermis and panniculus adiposus surrounding adnexal structures. Each dot represents the average mast cell number per entire specimen. Three specimens were evaluated from each mouse. P values are from an unpaired t-test.

10.3389/fimmu.2023.1006741

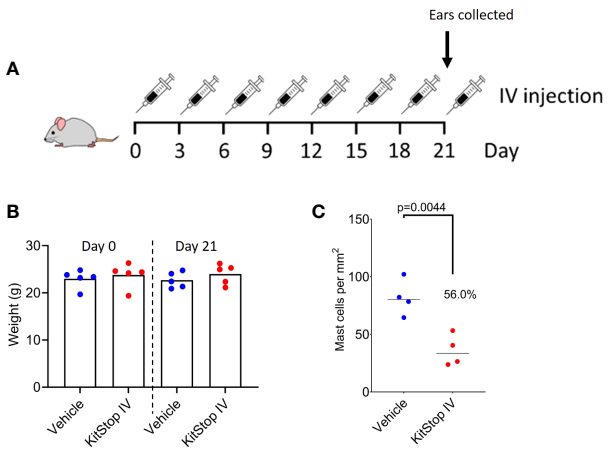


FIGURE 3
Systemic KitStop ESO treatment reduces the number of cutaneous mast cells in ear skin. **(A)** Five Balb/c mice were treated intravenously with PBS vehicle control or KitStop ESO every 3 days for 21 days. Ears were harvested and evaluated histologically with H&E and toluidine blue stains to facilitate counting of tissue MCs. **(B)** No significant changes in body weight were observed between mice treated with PBS vehicle control (blue) or KitStop ESO (red) at the end of the 21-day treatment period. **(C)** The total number of mast cells per mm2 of ear skin was significantly reduced by 56% in KitStop-treated mice. Data shown are the mean ± SEM for each group. P values are from an unpaired t-test.

data indicate that KitStop treatment significantly reduces the severity and duration of the anaphylactic response in a mouse model of passive systemic anaphylaxis, and does not overtly affect hematopoietic stem cell, renal, or hepatic function.

Discussion

Current therapies for people prone to recurrent anaphylaxis, such as those suffering from MCAS, rely heavily on desensitization, immunotherapy, and a variety of medications. Desensitization and immunotherapy treatments require identification of the triggering allergen; however, it is estimated that 30-60% of patients presenting with anaphylaxis have no discernible trigger (20, 21). If desensitization or immunotherapy is elected, the patient must thereafter be able to attend frequent office visits to carry out treatment which can prove burdensome and sometimes unfeasible. Medications such as glucocorticoids, cytoreductive agents, monoclonal antibodies, and tyrosine kinase inhibitors are commonly used, especially in hospital settings after a patient has experienced an anaphylactic reaction in response to other medications (antibiotics, chemotherapeutics) (22). These medications are fraught with adverse effects such as immunosuppression and gastrointestinal upset, resulting in an increased burden on the patient and healthcare system overall. Moreover, patients with severe, uncontrolled allergic conditions such as asthma or atopy may not even be considered for some of the above-mentioned therapies due to their heightened risk for adverse outcomes (8). Our studies suggest that a noteworthy treatment alternative, KitStop, could be considered for patients suffering from recurrent anaphylaxis who may not be eligible or able to undertake other treatments. We demonstrated that KitStop significantly lowers the number of mature MCs within the skin, and as a result, significantly diminishes the duration and severity of the anaphylactic response. Importantly, KitStop does so regardless of administration route (intradermal, intraperitoneal, or intravenous).

The KIT receptor is expressed on immature hematopoietic stem cells as they exit from the bone marrow which helps to promote their migration, differentiation, and maturation. Binding of SCF to KIT induces homodimerization and trans-phosphorylation of various regions of the receptors; phosphorylated residues then serve as docking sites for signaling molecules, thus propagating the signal downstream (23). Upon maturation, nearly all cells cease to express the receptor, though notable exceptions include MCs, melanocytes, and interstitial cells of Cajal (11). This specificity makes the KIT receptor an enticing therapeutic target; however, off-target effects could be possible given the receptor's presence on cells other than MCs. Our studies showed that mice treated with KitStop did not experience any significant changes to their hemogram when compared to control mice, suggesting that hematopoietic stem cells of bone marrow origin were not affected by KitStop. Additionally, biochemical parameters relating to kidney and liver function were unaffected by KitStop treatment. Further studies are required to assess the full safety profile of KitStop as the mice in our study were only treated for a maximum of three weeks whereas human patients would be expected to receive treatments for a longer duration.

Splice-switching antisense oligonucleotides (SSOs) are becoming increasingly more prevalent in the field of biomedical

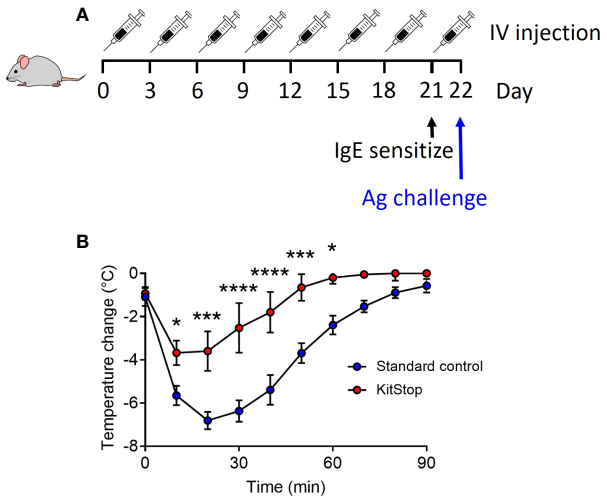


FIGURE 4
Intravenous KitStop ESO treatment reduces mast cell-mediated passive systemic anaphylaxis. **(A)** A standard control ASO or KitStop ESO was administered intravenously to five Balb/c mice every 3 days for a total of 8 doses. After the last dose, mice were sensitized with an intravenous injection of anti-DNP IgE and challenged the following day with DNP-HSA intravenously. **(B)** After antigen challenge, rectal temperatures of mice treated with either standard control ASO (blue) or KitStop ESO (red) were monitored every 10 minutes for 90 minutes as a surrogate for the measurement of the anaphylactic response. Mice that received the KitStop ESO exhibited a significantly less severe and shorter anaphylactic response than control mice. Data shown are the mean ± SEM for each group of five mice. P values were determined by mixed-effects model (REML) analysis with Sidaks multiple comparisons test. *p ≤ 0.05, ***p ≤ 0.001, ****p ≤ 0.0001.

10.3389/fimmu.2023.1006741

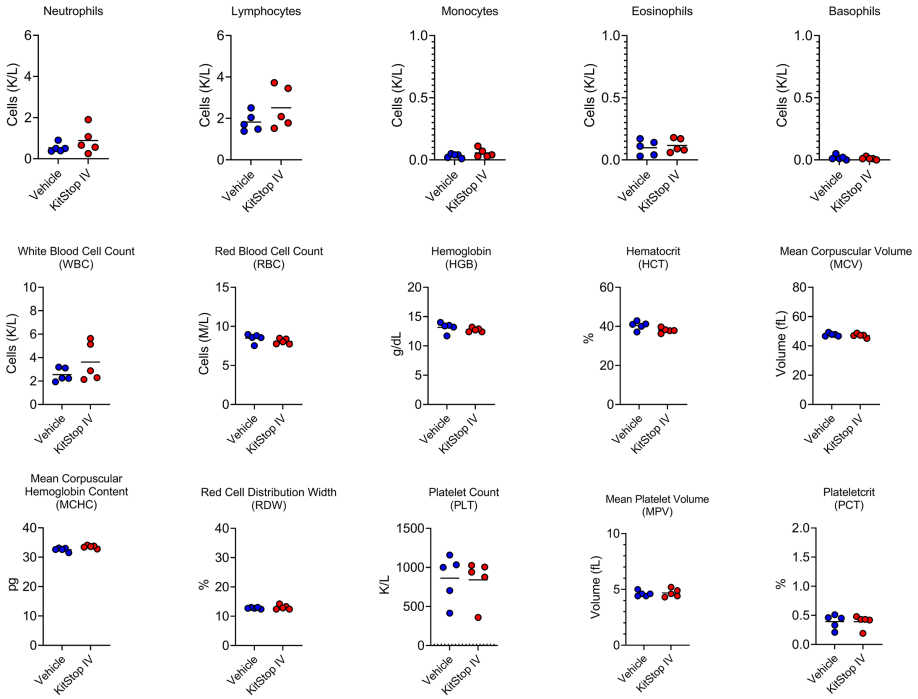


FIGURE 5
Intravenous KitStop treatment does not result in hematopoietic abnormalities. Complete blood count parameters measured from whole blood isolated from Balb/c mice with cardiac puncture after 21 days of either PBS vehicle control (blue) or KitStop ESO (red) treatment administered every 3 days. No significant differences were observed between the groups.

research due to their relative specificity and limited adverse effect profile. Numerous mouse models of human disease have been evaluated to determine the efficacy of SSOs for the treatment of genetic neurodegenerative (24–26), neoplastic (27–30), and cardiovascular (31, 32) diseases. In fact, promising human clinical trials utilizing SSOs have also been conducted in people with Duchenne muscular dystrophy (33, 34) as well as spinal muscular atrophy in children (35, 36). While previous studies have used SSOs to target the high-affinity IgE receptor FcεRI in MCs (19), the present study employs SSO technology to target the KIT receptor in

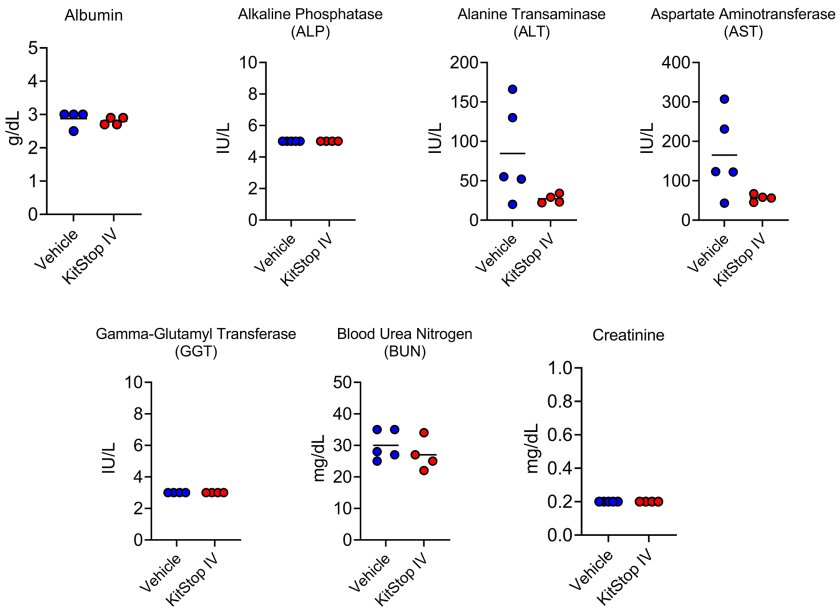


FIGURE 6
Intravenous KitStop ESO administration does not cause organ dysfunction. Serum biochemical parameters for liver and kidney function measured from whole blood isolated from Balb/c mice with cardiac puncture after 21 days of either PBS vehicle control (blue) or KitStop ESO (red) treatment administered every 3 days. No significant differences were observed between the groups.

non-transformed cells, providing yet another tool for the treatment of MC-mediated diseases such as anaphylaxis.

Our study is limited in that a model of passive systemic anaphylaxis was utilized; this model relies on the induction of anaphylaxis due to antibodies from passive sensitization rather than antibodies actively produced in response to antigens as in active models. Future studies are needed to ascertain the effect of KitStop in additional models of anaphylaxis. Additionally, mediators of MC degranulation such as proteases were not measured in the serum of the mice undergoing passive systemic anaphylaxis, because of the timing chosen for the experiments and the focus on body temperature responses over 90 minutes. While a decrease in body temperature is a reliable indicator of an anaphylactic response in mice, future studies should include measurements of products of mast cell degranulation at earlier time-points. While no off-target cellular effects were observed in our study, it is possible that these effects could develop with prolonged administration of KitStop further than 21 days. As such, the possible effect of KitStop on hematopoietic cells, as well as other cells expressing Kit such as melanocytes, neural cells, and germ cells, requires additional investigation utilizing long-term administration.

In conclusion, we have shown that intradermal, intraperitoneal, and intravenous administration of the KitStop ESO targeting exon 4 of the *c-Kit* gene results in the rapid and safe depopulation of MCs within tissues. This translates to a lessened systemic anaphylactic response as well as faster resolution of anaphylaxis in general. KitStop could therefore be considered as a feasible treatment alternative for patients experiencing recurrent episodes of anaphylaxis without the side effects of currently administered treatments.

Data availability statement

The raw data supporting the conclusions of this article will be made available by the authors, without undue reservation.

Ethics statement

The animal studies were approved by the North Carolina State University Institutional Animal Care and Use Committee.

Author contributions

BH, DS, and KB participated in the design and execution of experiments and data analysis. BH wrote the manuscript and prepared the figures. GC conceived the project, designed experiments, analyzed data, procured funding and edited the manuscript. All authors contributed to the article and approved the submitted version.

Funding

Research was supported by the National Institutes of Health (NIH), National Institute of Allergy and Infectious Diseases (NIAID), Award Number R01AI143985 (GC), Department of Molecular Biomedical Sciences, College of Veterinary Medicine, start-up funds (GC), NCSU Center for Human Health and the Environment NIH P30ES025128 (GC), Institutional National Research Service Award from the Office of the Director of National Institutes of Health, NIH T32OD011130 (BH, DS).

Acknowledgments

We would like to thank Cierra Smith for technical assistance. We would also like to thank Greer Arthur and Lauren Ehrhardt-Humbert for training and expert assistance.

Conflict of interest

GC has filed a patent application related to the research reported in this study. An exclusive licensing agreement has been granted to Hoth Therapeutics for this technology. GC has research support from Hoth Therapeutics for a project related to the research reported in this publication and also serves on their Scientific Advisory Board. The terms of this arrangement have been reviewed and approved by NC State University in accordance with its policy on objectivity in research.

The remaining authors declare that the research was conducted in the absence of any commercial or financial relationships that could be constructed as a potential conflict of interest.

Publisher's note

All claims expressed in this article are solely those of the authors and do not necessarily represent those of their affiliated organizations, or those of the publisher, the editors and the reviewers. Any product that may be evaluated in this article, or claim that may be made by its manufacturer, is not guaranteed or endorsed by the publisher.

Supplementary material

The Supplementary Material for this article can be found online at: https://www.frontiersin.org/articles/10.3389/fimmu.2023.1006741/full#supplementary-material

References

1. Sampson HA, Muñoz-Furlong A, Campbell RL, Adkinson NF, Bock SA, Branum A, et al. Second symposium on the definition and management of anaphylaxis: Summary report–second national institute of allergy and infectious Disease/Food allergy and anaphylaxis network symposium. *J Allergy Clin Immunol* (2006) 117():391–7. doi: 10.1016/j.jaci.2005.12.1303

2. Turner PJ, Jerschow E, Umasunthar T, Lin R, Campbell DE, Boyle RJ. Fatal anaphylaxis: Mortality rate and risk factors. *J Allergy Clin Immunol Pract* (2017) 5 (5):1169–78. doi: 10.1016/j.jaip.2017.06.031

3. Poulos LM, Waters A-M, Correll PK, Loblay RH, Marks GB. Trends in hospitalizations for anaphylaxis, angioedema, and urticaria in Australia, 1993-1994 to 2004-2005. *J Allergy Clin Immunol* (2007) 120:878–84. doi: 10.1016/j.jaci.2007.07.040

4. Wood RA, Camargo CA, Lieberman P, Sampson HA, Schwartz LB, Zitt M, et al. Anaphylaxis in America: The prevalence and characteristics of anaphylaxis in the united states. *J Allergy Clin Immunol* (2014) 133(2):461–7. doi: 10.1016/j.jaci.2013.08.016

5. Simons FER, Ardusso LRF, Dimov V, Ebisawa M, El-Gamal YM, Lockey RF, et al. World allergy organization anaphylaxis guidelines: 2013 update of the evidence base. *Int Arch Allergy Immunol* (2013) 162(3):193–204. doi: 10.1159/000354543

6. da Silva EZM, Jamur MC, Oliver C. Mast cell function: A new vision of an old cell. *J Histochem Cytochem* (2014) 62:698–738. doi: 10.1369/0022155414545334

7. Castells M. Diagnosis and management of anaphylaxis in precision medicine. *J Allergy Clin Immunol* (2017) 140():321–33. doi: 10.1016/j.jaci.2017.06.012

8. Pajno GB, Fernandez-Rivas M, Arasi S, Roberts G, Akdis CA, Alvaro-Lozano M, et al. EAACI guidelines on allergen immunotherapy: IgE-mediated food allergy. *Allergy* (2018) 73(4):799–815. doi: 10.1111/all.13319

9. Metz M, Grimbaldeston MA, Nakae S, Piliponsky AM, Tsai M, Galli SJ. Mast cells in the promotion and limitation of chronic inflammation. *Immunol Rev* (2007) 217(1):304–28. doi: 10.1111/j.1600-065X.2007.00520.x

10. Hundley TR, Gilfillan AM, Tkaczyk C, Andrade MV, Metcalfe DD, Beaven MA. Kit and FcεRI mediate unique and convergent signals for release of inflammatory mediators from human mast cells. *Blood* (2004) 104(8):2410–7. doi: 10.1182/blood-2004-02-0631

11. El-Agamy DS. Targeting c-kit in the therapy of mast cell disorders: Current update. *Eur J Pharmacol* (2012) 690:1–3. doi: 10.1016/j.ejphar.2012.06.030

12. Jensen BM, Beaven MA, Iwaki S, Metcalfe DD, Gilfillan AM. Concurrent inhibition of kit- and FcεRI-mediated signaling: Coordinated suppression of mast cell activation. *J Pharmacol Exp Ther* (2008) 324:128–38. doi: 10.1124/jpet.107.125237

13. Cruse G, Metcalfe DD, Olivera A. Functional deregulation of kit: link to mast cell proliferative diseases and other neoplasms. *Immunol Allergy Clin North Am* (2014) 34:219–37. doi: 10.1016/j.iac.2014.01.002

14. Valent P, Akin C, Nedoszytko B, Bonadonna P, Hartmann K, Niedoszytko M, et al. Diagnosis, classification and management of mast cell activation syndromes (MCAS) in the era of personalized medicine. *Int J Mol Sci* (2020) 21(23):E9030. doi: 10.3390/ijms21239030

15. Weiler CR, Austen KF, Akin C, Barkoff MS, Bernstein JA, Bonadonna P, et al. AAAAI mast cell disorders committee work group report: Mast cell activation syndrome (MCAS) diagnosis and management. *J Allergy Clin Immunol* (2019) 144(4):883–96. doi: 10.1016/j.jaci.2019.08.023

16. Snider DB, Arthur GK, Falduto GH, Olivera A, Ehrhardt-Humbert LC, Smith E, et al. Targeting KIT by frameshifting mRNA transcripts as a therapeutic strategy for aggressive mast cell neoplasms. *Mol Ther* (2022) 30(1):295–310. doi: 10.1016/j.ymthe.2021.08.009

17. Jensen BM, Swindle EJ, Iwaki S, Gilfillan AM. Generation, isolation, and maintenance of rodent mast cells and mast cell lines. *Curr Protoc Immunol* (2006) 74:3.23.1–3.23.13. doi: 10.1002/0471142735.im0323s74

18. Doyle E, Trosien J, Metz M. Protocols for the induction and evaluation of systemic anaphylaxis in mice. *Methods Mol Biol* (2013) 1032:133–8. doi: 10.1007/978-1-62703-496-8_10

19. Cruse G, Yin Y, Fukuyama T, Desai A, Arthur GK, Bäumer W, et al. Exon skipping of FcεRIβ eliminates expression of the high-affinity IgE receptor in mast cells with therapeutic potential for allergy. *Proc Natl Acad Sci U S A* (2016) 113(49):14115–20. doi: 10.1073/pnas.1608520113

20. Fenny N, Grammer LC. Idiopathic anaphylaxis. *Immunol Allergy Clin North Am* (2015) 35:349–62. doi: 10.1016/j.iac.2015.01.004

21. Kuhlen JL, Virkud YV. Pathogenesis, newly recognized etiologies, and management of idiopathic anaphylaxis. *Discov Med* (2015) 19(103):137–44.

22. Bilò MB, Martini M, Tontini C, Mohamed OE, Krishna MT. Idiopathic anaphylaxis. *Clin Exp Allergy* (2019) 49:942–52. doi: 10.1111/cea.13402

23. Elieh Ali Komi D, Wöhrl S, Bielory L. Mast cell biology at molecular level: a comprehensive review. *Clin Rev Allergy Immunol* (2020) 58:342–65. doi: 10.1007/s12016-019-08769-2

24. Taniguchi-Ikeda M, Kobayashi K, Kanagawa M, Yu CC, Mori K, Oda T, et al. Pathogenic exon-trapping by SVA retrotransposon and rescue in fukuyama muscular dystrophy. *Nature* (2011) 478(7367):127–31. doi: 10.1038/nature10456

25. Lee JM, Nobumori C, Tu Y, Choi C, Yang SH, Jung HJ, et al. Modulation of LMNA splicing as a strategy to treat prelamin a diseases. *J Clin Invest* (2016) 126(4):1592–602. doi: 10.1172/JCI85908

26. Osorio FG, Navarro CL, Cadiñanos J, López-Mejía IC, Quirós PM, Bartoli C, et al. Splicing-directed therapy in a new mouse model of human accelerated aging. *Sci Transl Med* (2011) 3(106):106ra107. doi: 10.1126/scitranslmed.3002847

27. Bauman JA, Li S-D, Yang A, Huang L, Kole R. Anti-tumor activity of splice-switching oligonucleotides. *Nucleic Acids Res* (2010) 38:8348–56. doi: 10.1093/nar/gkq731

28. Dewaele M, Tabaglio T, Willekens K, Bezzi M, Teo SX, Low DH, et al. Antisense oligonucleotide–mediated MDM4 exon 6 skipping impairs tumor growth. *J Clin Invest* (2016) 126(1):68–84. doi: 10.1172/JCI82534

29. Zammarchi F, de Stanchina E, Bournazou E, Supakorndej T, Martires K, Riedel E, et al. Antitumorigenic potential of STAT3 alternative splicing modulation. *Proc Natl Acad Sci U S A* (2011) 108(43):17779–84. doi: 10.1073/pnas.1108482108

30. Nielsen TO, Sorensen S, Dagnæs-Hansen F, Kjems J, Sorensen BS. Directing HER4 mRNA expression towards the CYT2 isoform by antisense oligonucleotide decreases growth of breast cancer cells *in vitro* and *in vivo*. *Br J Cancer* (2013) 108:2291–8. doi: 10.1038/bjc.2013.247

31. Gedicke-Hornung C, Behrens-Gawlik V, Reischmann S, Geertz B, Stimpel D, Weinberger F, et al. Rescue of cardiomyopathy through U7snRNA-mediated exon skipping in Mybpc3-targeted knock-in mice. *EMBO Mol Med* (2013) 5(7):1060–77. doi: 10.1002/emmm.201202168

32. Gramlich M, Pane LS, Zhou Q, Chen Z, Murgia M, Schötterl S, et al. Antisense-mediated exon skipping: a therapeutic strategy for titin-based dilated cardiomyopathy. *EMBO Mol Med* (2015) 7(5):562–76. doi: 10.15252/emmm.201505047

33. Mendell JR, Goemans N, Lowes LP, Alfano LN, Berry K, Shao J, et al. Longitudinal effect of eteplirsen versus historical control on ambulation in duchenne muscular dystrophy. *Ann Neurol* (2016) 79(2):257–71. doi: 10.1002/ana.24555

34. Voit T, Topaloglu H, Straub V, Muntoni F, Deconinck N, Campion G, et al. Safety and efficacy of drisapersen for the treatment of duchenne muscular dystrophy (DEMAND II): an exploratory, randomised, placebo-controlled phase 2 study. *Lancet Neurol* (2014) 13(10):987–96. doi: 10.1016/S1474-4422(14)70195-4

35. Haché M, Swoboda KJ, Sethna N, Farrow-Gillespie A, Khandji A, Xia S, et al. Intrathecal injections in children with spinal muscular atrophy. *J Child Neurol* (2016) 31 (7):899–906. doi: 10.1177/0883073815627882

36. Chiriboga CA, Swoboda KJ, Darras BT, Iannaccone ST, Montes J, De Vivo DC, et al. Results from a phase 1 study of nusinersen (ISIS-SMNRx) in children with spinal muscular atrophy. *Neurology* (2016) 86(10):890–7. doi: 10.1212/WNL.0000000000002445

Frontiers in Immunology

Explores novel approaches and diagnoses to treat immune disorders.

The official journal of the International Union of Immunological Societies (IUIS) and the most cited in its field, leading the way for research across basic, translational and clinical immunology.

Discover the latest Research Topics

See more →



Frontiers

Avenue du Tribunal-Fédéral 34
1005 Lausanne, Switzerland
frontiersin.org

Contact us

+41 (0)21 510 17 00
frontiersin.org/about/contact